Methods and Principles in Medicinal Chemistry

Edited by
Han van de Waterbeemd and Bernard Testa

WILEY-VCH

Drug Bioavailability

Estimation of Solubility, Permeability, Absorption and Bioavailability

Second, Completely Revised Edition

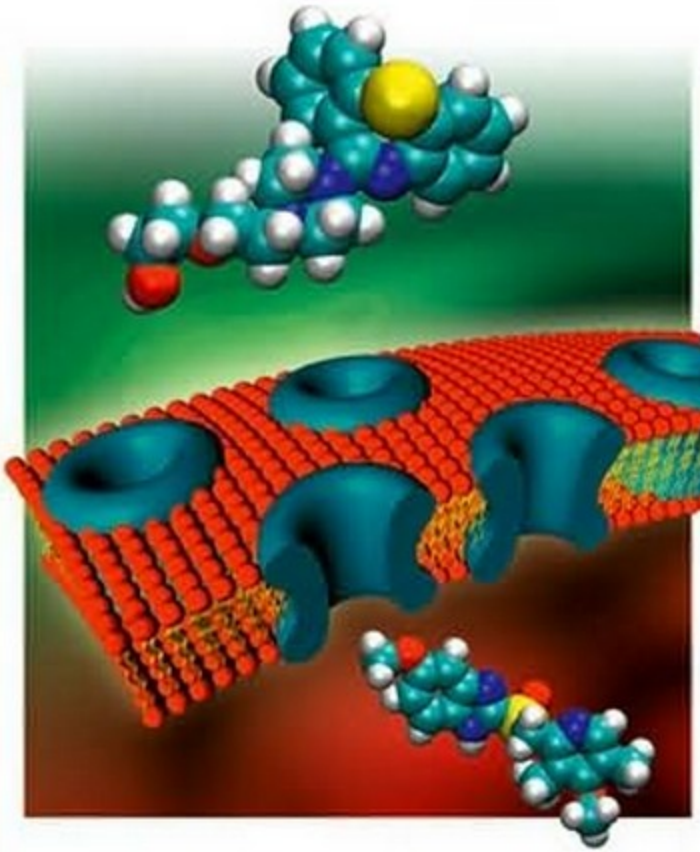

Volume 40

Series Editors:
R. Mannhold,
H. Kubinyi,
G. Folkers

Drug Bioavailability

Edited by
Han van de Waterbeemd
and Bernard Testa

Methods and Principles in Medicinal Chemistry

Drug Bioavailability

Estimation of Solubility, Permeability,
Absorption and Bioavailability

Edited by
Han van de Waterbeemd and Bernard Testa

Second, Completely Revised Edition

WILEY-VCH Verlag GmbH & Co. KGaA

Series Editors

Prof. Dr. Raimund Mannhold
Molecular Drug Research Group
Heinrich-Heine-Universität
Universitätsstrasse 1
40225 Düsseldorf
Germany
mannhold@uni-duesseldorf.de

Prof. Dr. Hugo Kubinyi
Donnersbergstrasse 9
67256 Weisenheim am Sand
Germany
kubinyi@t-online.de

Prof. Dr. Gerd Folkers
Collegium Helveticum
STW/ETH Zurich
8092 Zurich
Switzerland
folkers@collegium.ethz.ch

Volume Editors

Dr. Han van de Waterbeemd
Current address
Rue de la Rasclose 14
66690 Saint André
France
Former address
AstraZeneca
LG DECS-GCS, 50S39
Mereside, Alderley Park
Macclesfield SK10 4TG
United Kingdom

Prof. Dr. Bernard Testa
Univ. Hospital Centre
Pharmacy Dept.-CHUV BH 04
46 Rue du Bugnon
1011 Lausanne
Schweiz

Cover Description
Bioavailability involves the transfer of gut wall membranes in which a drug may encounter metabolising enzymes and transporters limiting or enhancing systemic drug levels.

Library of Congress Card No.:
applied for

British Library Cataloguing-in-Publication Data
A catalogue record for this book is available from the British Library.

Bibliographic information published by the Deutsche Nationalbibliothek
Die Deutsche Nationalbibliothek lists this publication in the Deutsche Nationalbibliografie; detailed bibliographic data are available on the Internet at http://dnb.d-nb.de.

Composition Thomson Digital, Noida, India
Printing Strauss GmbH, Mörlenbach
Bookbinding Litges & Dopf GmbH, Heppenheim
Cover Grafik-Design Schulz, Fußgönheim

Printed in the Federal Republic of Germany
Printed on acid-free paper

ISBN: 978-3-527-32051-6

Contents

List of Contributors

Bertil Abrahamsson
Astra Zeneca R&D
S-43183 Mölndal
Sweden

Gordon L. Amidon
University of Michigan
College of Pharmacy
Department of Pharmaceutical Sciences
Ann Arbor, MI
USA

Pascale Anderle
Laboratory of Experimental Cancer Research
Istituto Oncologico della Svizzera Italiana (IOSI)
Via Vincenzo Vela 6
CH-6500 Bellinzona
Switzerland

Per Artursson
Uppsala University
Department of Pharmacy
BMC, Box 580
SE-751 23 Uppsala
Sweden

Christel A.S. Bergström
Uppsala University
Department of Pharmacy
Pharmaceutical Screening and Informatics
BMC, P.O. Box 580
SE-751 23 Uppsala
Sweden

Michael B. Bolger
6 6th Street
Petaluma, CA 94952
USA

Pierre Bruneau
AstraZeneca Centre de Recherches
Parc Industriel Pompelle
BP 1050
Reims
France

Nicola Colclough
AstraZeneca R&D
Physical and Computational Chemistry
Alderley Park
Macclesfield, Cheshire SK10 4TG
UK

Charles L. Crespi
BD Biosciences-Discovery Labware
6 Henshaw Street
Woburn, MA 01801
USA

Arik S. Dahan
University of Michigan
College of Pharmacy
Department of Pharmaceutical Sciences
Ann Arbor, MI
USA

Andrew M. Davis
AstraZeneca R&D Charnwood
Bakewell Road
Loughborough
Leicestershire LE11 5RH
UK

Robert Fraczkiewicz
42505 10th Street West
Lancaster, CA 93534
USA

Markus Haeberlein
AstraZeneca R&D Södertälje
Medicinal Chemistry
SE-151 85 Södertälje
Sweden

Christopher Kohl
Actelion Pharmaceuticals Ltd
Pharmacokinetics
Gewerbestrasse 16
4123 Allschwil
Switzerland

Hans Lennernäs
Uppsala University
Biopharmaceutics Research Group
Department of Pharmacy
SE-751 23 Uppsala
Sweden

David J. Livingstone
University of Portsmouth
Centre for Molecular Design
Portsmouth
UK

and

ChemQuest
Delamere House
1 Royal Crescent
Sandown
Isle of Wight PO36 8LZ
UK

Chris Logan
AstraZeneca R&D Alderley Park
Clinical Pharmacology and DMPK
Macclesfield, Cheshire SK10 4TG
UK

Viera Lukacova
42505 10th Street West
Lancaster, CA 93534
USA

Kazuya Maeda
The University of Tokyo
Graduate School of Pharmaceutical Sciences
Department of Molecular Pharmacokinetics
7-3-1 Hongo, Bunkyo-ku
Tokyo 113-0033
Japan

Barbara P. Mason
masonphyschem@aol.com

Carsten U. Nielsen
University of Copenhagen
Faculty of Pharmaceutical Sciences
Bioneer:FARMA and Department of Pharmaceutics and Analytical Chemistry
2-Universitetsparken
DK-2100 Copenhagen
Denmark

Ulf Norinder
AstraZeneca R&D Södertälje
Medicinal Chemistry
SE-151 85 Södertälje
Sweden

Niclas Petri
Uppsala University
Biopharmaceutics Research Group
Department of Pharmacy
SE-751 23 Uppsala
Sweden

Linette Ruston
AstraZeneca R&D
Physical and Computational Chemistry
Alderley Park
Macclesfield, Cheshire SK10 4TG
UK

Anna Seelig
University of Basel
Biozentrum
Klingelbergstrasse 70
CH-4056 Basel
Switzerland

Yuichi Sugiyama
The University of Tokyo
Graduate School of Pharmaceutical Sciences
Department of Molecular Pharmacokinetics
7-3-1 Hongo, Bunkyo-ku
Tokyo 113-0033
Japan

Hiroshi Suzuki
The University of Tokyo
Faculty of Medicine
The University of Tokyo Hospital
Department of Pharmacy
7-3-1 Hongo, Bunkyo-ku
Tokyo 113-8655
Japan

Kin Tam
AstraZeneca R&D
Physical and Computational Chemistry
Alderley Park
Macclesfield, Cheshire SK10 4TG
UK

Bernard Testa
University Hospital Centre
Department of Pharmacy
CHUV – BH04
Rue du Bugnon 46
CH-1011 Lausanne
Switzerland

Anna-Lena Ungell
AstraZeneca R&D Mölndal
Discovery DMPK and Bioanalytical Chemistry
Pepperedsleden 1
SE-431 83 Mölndal
Sweden

Arto Urtti
University of Helsinki
Centre for Drug Research
P.O. Box 56 (Viikinkaari 5E)
00014 Helsinki
Finland

Han van de Waterbeemd
Current address
Rue de la Rasclose 14
66690 Saint André
France

Former address
AstraZeneca
LG DECS-GCS
Mereside, Alderley Park
Macclesfield, Cheshire SK10 4TG
UK

Werner Weitschies
University of Greifswald
Institute of Pharmacy
Department of Biopharmaceutics
Friedrich-Ludwig-Jahn-Strasse 17
17487 Greifswald
Germany

Clive G. Wilson
University of Strathclyde
Strathclyde Institute for Biomedical Studies
Department of Pharmaceutical Sciences
Glasgow, Scotland
UK

Guangqing Xiao
Biogen Idec
Drug Metabolism and Pharmacokinetics
14 Cambridge Center
Cambridge, MA 02142
UK

Marjo Yliperttula
University of Helsinki
Division of Biopharmacy and Pharmacokinetics
P.O. Box 56 (Viikinkaari 5E)
00014 Helsinki
Finland

Preface

The processes involved in drug discovery have changed considerably in the past decade. Today we have access to the full human as well as several bacterial genomes offering a rich source of molecular targets to treat diseases. Methods in biology have moved to ultra-high-throughput screening (uHTS) of such precedented and unprecedented targets. Chemistry adapted to this progress by developing methods such as combinational and parallel synthesis allowing the rapid synthesis of hundreds to hundreds of thousands molecules in reasonable quantities, purities and timelines.

Historical data on the fate of potential drugs in development indicate that major reasons for attrition include toxicity, efficacy and pharmacokinetics/drug metabolism. Therefore, in today's drug discovery the evaluation of absorption, distribution, metabolism and excretion (ADME) of drug candidates is performed early in the process. In the last 10 years drug metabolism and physicochemical *in vitro* screening methods have increasingly been introduced. In recent years these methods more and more became medium to high throughput in order to cope with increasing numbers of compounds to evaluate after HTS.

Although HTS seems to be a very efficient approach, it must be stressed that there is also a high cost associated with it. Interest is thus shifting to prediction and simulation of molecular properties, which might hopefully lead to overall more efficient processes.

The next vague of tools will be around computational or *in silico* ADME approaches. These will allow to include ADME into the design of combinational libraries, the evaluation of virtual libraries, as well as in selecting the most promising compounds to go through a battery of *in vitro* screens, possibly even replacing some of these experimental screens. Several of these computational tools are currently under development as will be discussed in this volume.

For reasons of convenience for the patient and compliance to the therapy, most drugs are administered orally. To keep the dose at the lowest possible level, high oral absorption and high bioavailability are prime properties to optimize in a new drug. Drug bioavailability is the outcome of a complex chain of events, and is among others influenced by the drug's solubility, permeability through the gastrointenstinal wall, and its first pass gut wall and liver metabolism. Excluding liver metabolism, all

other factors are characterized by the term oral absorption. Permeability through the gut wall can be favoured or hindered through the effect of various transporter proteins such as P-glycoprotein. Our increased knowledge and understanding of all of these processes involved in permeability, oral absorption and bioavailability will make predictive tools more robust.

A previous volume in our series, edited in 2003 by Han van de Waterbeemd, Hans Lennernäs, and Per Artursson, was dedicated to summarize the current status in the estimation of relevant ADME parameters. This volume emerged as a top-seller in our series indicating the high impact of this topic in modern drug research.

Now, five years later, we are proud to present a complete revision, edited by Han van de Waterbeemd and Bernard Testa, which reflects the enormous developments in this research area. Few chapters were omitted and a new one on "Nanotechnology in Drug Discovery" was added. Some chapters were condensed and merged into others; some other chapters had to be split into two. The majority of chapters remained of high currency and were all comprehensively updated, some by the same and some by new authors such as the chapter on "Prodrugs" by Bernard Testa.

The series editors would like to thank Han van de Waterbeemd and Bernard Testa for their enthusiasm to put together this book and to work with such a fine selection of authors.

September 2008

Raimund Mannhold, Düsseldorf
Hugo Kubinyi, Weisenheim am Sand
Gerd Folkers, Zürich

A Personal Foreword

"*Drug Bioavailability – Estimation of Solubility, Permeability, Absorption and Bioavailability*" was published in 2003 under the editorship of H. van de Waterbeemd, H. Lennernäs and P. Artursson. The book met with such success that it had to be reprinted 4 times. But given the many and fast advances in the field, even this solution was no longer satisfactory. A second, fully revised edition was thus envisaged. Professors Lennernäs and Artursson having too many other commitments, Han van de Waterbeemd found himself alone for the task and approached his colleague and friend Bernard Testa. Having just completed the joint editorship of the 1100-page ADMET volume in "*Comprehensive Medicinal Chemistry II*", we were happy to team up again in an exciting book project. Having decided on an updated content and a logical structure, it was clear that some chapters had to be split into two and rewritten to take latest advances into account. A few chapters could be condensed and merged into others, while yet other chapters remained of high currency and simply needed an in-depth updating. These changes in book structure and chapter contents implied a number of changes in authorship; we are grateful to contributors of the first edition and to our new authors for their enthusiastic cooperation. The final product is thus vastly different from the previous one and, we hope, will be found valuable by afficionados of the first edition as well as by new readers.

May 2008 *Han van de Waterbeemd,* Market Harborough, United Kingdom
Bernard Testa, Lausanne, Switzerland

1
Introduction: The Why and How of Drug Bioavailability Research

Han van de Waterbeemd and Bernard Testa

Abbreviations

ADME	Absorption, distribution, metabolism, and excretion
EMEA	European Agency for the Evaluation of Medicinal Products
FDA	Food and Drug Administration (USA)
NCE	New chemical entity
PD	Pharmacodynamic(s)
P-gp	P-glycoprotein
PK	Pharmacokinetic(s)
R&D	Research and development

Symbols

AUC	Area under the plasma concentration versus time curve
CL	Total plasma clearance
C_{max}	Maximum plasma concentration in blood
F	Fraction of administered dose that reaches the general circulation
M	Amount of drug that reaches the general circulation
t_{max}	Time to reach C_{max}

1.1
Defining Bioavailability

1.1.1
The Biological Context

Before presenting and explaining the content of this book, it is necessary to ponder the concept of bioavailability, more accurately termed oral bioavailability.

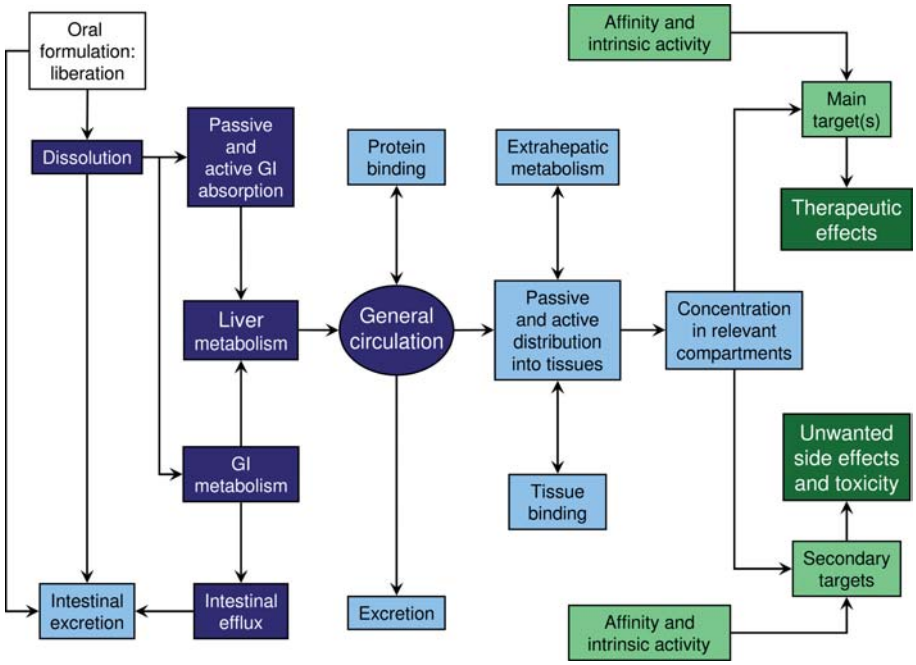

Figure 1.1 A schematic presentation of the fate of a drug in the body following oral administration. Pharmacokinetic processes are in blue, with the components of oral bioavailability in dark blue. Pharmacodynamic processes are in green, with the clinical effects in dark green.

As commonly defined, bioavailability implies the extent and rate at which a drug becomes available in the general circulation [1, 2].

After oral administration, a drug has to overcome a number of hurdles before reaching its sites of action. As schematized in Figure 1.1, a drug must

(a) be liberated from its pharmaceutical form (often a tablet);
(b) be dissolved in the gastrointestinal fluid;
(c) escape metabolism by the intestinal flora;
(d) be absorbed through the intestinal wall by passive and/or active (via transporters) permeation;
(e) escape metabolism in the gut wall;
(f) escape excretion in the intestine lumen by efflux transporters (mainly P-gp);
(g) escape metabolism in the blood while being transported to the liver via the portal vein;
(h) escape metabolism in the liver before reaching the general circulation from which it will be cleared by equilibration in tissues, excretion (mainly urinary), and metabolism (hepatic and extrahepatic).

For clarity, the obstacles a drug must overcome to reach the general circulation are shown in dark blue in Figure 1.1, while other pharmacokinetic (PK) processes are

in light blue. Pharmacodynamic (PD) processes are in green, with clinical effects in dark green.

1.1.2 A Pharmacokinetic Overview

In pharmacokinetic terms [3], bioavailability is described by two parameters, namely, the fraction of the administered dose (F) that reaches the general circulation (see Equations 1.1–1.3) and the rate of this transfer. When the drug is administered by the intravascular route, $F = 1$. When an extravascular route is used, for instance and most often the oral route, $F \leq 1$ due to the mechanisms of loss listed above. These mechanisms, particularly limited absorption (obstacles b, d, and f above) and metabolism (obstacles c, e, g, and h above), are called first-pass effects.

The fraction F of the administered dose that reaches the general circulation is calculated as (Equation 1.1)

$$F = \frac{M}{\text{dose}}, \tag{1.1}$$

where M, the amount of drug that reaches the general circulation, is obtained from Equation 1.2:

$$M = \text{CL} \cdot \text{AUC}. \tag{1.2}$$

In Equation 1.2, CL is the total plasma clearance, namely, the fraction of the volume of distribution cleared per unit of time, and is expressed in volume/time. AUC is the area under the concentration versus time curve and is expressed in (concentration)·(time). In other words (Equation 1.3),

$$F = \frac{\text{CL} \cdot \text{AUC}}{\text{dose}}. \tag{1.3}$$

As far as the rate component of bioavailability is concerned, it is estimated by two parameters, C_{max} and t_{max}. The maximum plasma concentration (C_{max}) is related to (a) total plasma clearance; (b) the fraction of dose that reaches the general circulation without being metabolized; (c) the rate of absorption; and (d) the rates of distribution and elimination . The time to reach C_{max} (t_{max}) depends on (a) the rate of absorption and (b) the rates of distribution and elimination.

After oral administration, bioavailability may be estimated by comparison with either the intravascular route, yielding the absolute bioavailability, or another pharmaceutical form of the drug by the same route, yielding the relative bioavailability.

1.1.3 Specific Issues

In a number of special cases, the above definitions of bioavailability are not directly applicable and singularly complicate the issue [4]. Thus, drugs having active metabolites present a special definitional challenge, particularly prodrugs (i.e., when most or all of the wanted effects are due to an active metabolite). Here, monitoring the

prodrug levels in the general circulation appears pointless due to presystemic metabolic activation. Monitoring the plasma levels of the active metabolite may be more informative, but again there are exceptions such as recent prodrugs designed to undergo *in situ* activation (see Part Five).

Another special case is that of racemic drugs in which all or most of the activity is due to one of the two enantiomers. In such a case, a stereospecific analytic method must be used to monitor the active enantiomer (known as the eutomer).

The thorniest issue with the definition of bioavailability is encapsulated in the question, "Bioavailability at the site of action?" Interestingly, both the Food and Drug Administration (FDA) in the United States and the European Agency for the Evaluation of Medicinal Products (EMEA) define bioavailability in almost identical terms, namely, "the rate and extent to which the active substance or active moiety is absorbed from a pharmaceutical form and becomes available at the *site of action* (italics ours)" [5, 6]. However, both agencies go on to recognize (but here their wordings differ) that in practice the bioavailability of oral medicines can be assessed by monitoring concentrations in the general circulation.

In other words, there are two determinants of a drug's therapeutic efficacy, namely, its intrinsic activity at a target and its bioavailability at the site of action. But given the frequent difficulty of defining that site of action (should it be defined at the organ, tissue, or cellular level?) and the frequent difficulty or impossibility (if only for ethical reasons) of measuring a drug's level at the site of action, the useful definition of bioavailability is indeed based on plasma concentrations. This is certainly the definition clinical pharmacologists work with, and it is the only meaningful definition for drug researchers engaged in drug discovery and development.

Why are bioavailability studies important to drug discovery? There are several good reasons to aim for highest feasible bioavailability in any oral drug project. Poor bioavailability in humans (<30%) results in erratic PK, making a compound difficult to dose to patients. High bioavailability is desired to stave off toxic effects because lesser amounts need to be administered, which also keeps the cost of drugs down.

How is bioavailability studied in drug discovery? Bioavailability is typically assessed *in vivo* in rats during the discovery phase. More advanced compounds (closer to be picked as clinical candidates) will also be studied in the dog and sometimes monkey. If rat and dog give similar results, the average can be used as a first estimate for bioavailability in man. If there is a large difference between the two species, it is better to understand the causes before deciding which of the two species best models humans. *In silico* predictions of oral absorption and bioavailability can help make a better decision and are indeed increasingly used in guiding projects to take the best candidates to the clinic.

1.2 Presentation and Layout of the Book

A few decades ago, pharmacokinetics, drug metabolism, and toxicology of selected clinical candidates were studied mainly during preclinical and clinical develop-

ment. In those days, the mission of medicinal chemistry was to discover and supply very potent compounds, with less attention to their behavior in the body. However, the R&D paradigm in the pharmaceutical industry has undergone dramatic changes since the 1970s and particularly since the mid-1990s, and is now better subdivided into drug discovery and development. A huge number of new chemical entities (NCEs) afforded by combinatorial chemistry and parallel synthesis are screened by high-throughput biological assays. These assays routinely include absorption, distribution, metabolism, and excretion (ADME properties) and ADME-related physicochemical properties (ionization, solubility, partitioning, and permeation).

As schematized in Figure 1.1, solubility, membrane permeation (passive and transporter-mediated), and metabolism are the main factors contributing to oral bioavailability, and hence are of special interest to drug researchers. Such are the focus and the audience of this book, whose first edition, published in 2003, met with considerable success and was reprinted four times [7]. However, progress in recent years has been so fast that the present edition became necessary and is fully updated in structure and content.

This book is organized into five parts according to the processes underlying oral bioavailability and the methodologies and technologies available to researchers. Thus and quite logically, Part One is dedicated to the physicochemical aspects of drug dissolution and solubility, with chapters presenting the industrial and clinical contexts and the prediction of aqueous solubility.

Part Two covers the physicochemical and biological methodologies to assess membrane permeability and oral absorption. Here, the reader begins with physicochemical principles and high-throughput technologies, and moves up the scale of biological complexity toward cell cultures, animal studies, and clinical investigations. As major determinants of bioavailability, transporters and metabolism deserve special attention (Part Three). Here again, biological background is covered explicitly, and so are specific technologies.

Part Four is dedicated to *in silico* tools, which have gained an irreplaceable significance in virtual experimentation by allowing medicinal chemists to predict physicochemical and ADMET properties of projected and existing molecules. Successive chapters present statistical tools, molecular properties, absorption, metabolism, and bioavailability predictions. The book ends with Part Five in which relevant issues in drug development are covered, namely, the biopharmaceutical classification system, prodrug strategy to improve bioavailability, modern biopharmaceutical strategies, and nanotechnologies.

With its logical structure and large number of chapters, this book aims at informing by providing data and examples, and instructing by presenting a conceptual and logical framework. As such, it presents an informative and didactic value even greater than that of the sum of its individual chapters. We do hope that the book will remain useful for many years and thank our contributors for their dedication and enthusiasm.

References

1 van de Waterbeemd, H. and Testa, B. (2007) The why and how of absorption, distribution, metabolism, excretion, and toxicity research, in *ADME-Tox Approaches,* Vol. 5 (eds B. Testa and H. van de Waterbeemd), in *Comprehensive Medicinal Chemistry II* (series eds J.B. Taylor and D.J. Triggle), Elsevier, Oxford, UK, pp. 1–9.

2 Hurst, S., Loi, C.-M., Broadfueher, J. and El-Kattan, A. (2007) Impact of physiological, physicochemical and biopharmaceutical factors in absorption and metabolism mechanisms on the drug oral bioavailability of rats and humans. *Expert Opinion on Drug Metabolism and Toxicology*, **3**, 469–489.

3 Tillement, J.-P. and Tremblay, D. (2007) Clinical pharmacokinetic criteria for drug research: the why and how of absorption, distribution, metabolism, excretion, and toxicity research, in *ADME-Tox Approaches,* Vol. 5 (eds B. Testa and H. van de Waterbeemd), in *Comprehensive Medicinal Chemistry II* (series eds J.B. Taylor and D.J. Triggle), Elsevier, Oxford, UK, pp. 11–30.

4 Balant, L.P., Benet, L.Z., Blume, H., Bozler, G., Breimer, D.D., Eichelbaum, M., Gundert-Remy, U., Hirtz, J., Mutschler, E., Midha, K.K., Rauws, A.G., Ritschel, W.A., Sansom, L.N., Skelly, J.P. and Vollmer, K.-O. (1991) Is there a need for more precise definitions of bioavailability? *European Journal of Clinical Pharmacology*, **40**, 123–126.

5 http://www.accessdata.fda.gov/scripts/cdrh/cfdocs/cfcfr/CFRSearch.cfm?CFRPart=320 (accessed 17 February 2008).

6 http://www.emea.europa.eu/pdfs/human/ewp/140198en.pdf (accessed 10 February 2008).

7 van de Waterbeemd, H., Lennernäs, H. and Artursson, P. (eds) (2003) *Drug Bioavailability*, Wiley-VCH Verlag GmbH, Weinheim.

Part One
Physicochemical Aspects of Drug Dissolution and Solubility

2
Aqueous Solubility in Drug Discovery Chemistry, DMPK, and Biological Assays

Nicola Colclough, Linette Ruston, and Kin Tam

Abbreviations

AZ	AstraZeneca
BCS	Biopharmaceutics Classification System
BNN	Bayesian neural network
CAD	Charged aerosol detector
CD	Candidate drug
CLND	Chemiluminescent nitrogen detection
Clog *P*	Calculated log *P*
DMPK	Drug metabolism and pharmacokinetics
DMSO	Dimethyl sulfoxide
ELSD	Evaporative light scattering detector
HI	Hit identification
HPLC	High-performance liquid chromatography
HTS	High-throughput screening
HTSol	High-throughput solubility
LI	Lead identification
LO	Lead optimization
MLR	Multiple linear regression
PLM	Polarized light microscopy
PLS	Partial least squares
PXRD	Powder X-ray diffraction
QSPR	Quantitative structure–property relationship
SAR	Structure–activity relationship

Symbols

K_{sp}	Solubility product
MX	Salt of acid or base
M^+	Protonated base or cationic counterion to conjugate base

pK_a	Acid dissociation constant
S	Solubility of a compound at a particular pH
S_0	Solubility of a compound in its neutral form/intrinsic solubility
X^-	Conjugate base or anionic counterion to protonated base

2.1 Introduction

Aqueous solubility is one of the key physicochemical properties in drug discovery [1, 2]. High solubility in intestinal fluid provides the concentration gradient that drives the absorption of orally administered drugs and subsequent distribution to the site of action to elicit a pharmacological response. For intravenously administered agents, sufficiently high solubility in plasma is critical to minimize undesirable precipitation in the systematic circulation. Generally, poor aqueous solubility leads to formulation challenges in development, raising costs during this phase. Aqueous solubility data facilitate the interpretation of biological assay results. In particular, poorly soluble compounds can precipitate out of solution during a high-throughput screening (HTS) campaign, thereby giving undesirable false negatives and/or false positives, the latter via binding of the target to aggregates [3, 4]. In the absence of solubility information at the HTS stage, such false hits can go unnoticed and hamper structure–activity relationship (SAR) interpretation. Poor aqueous solubility can lead to problems *in vivo*, such as incomplete absorption following oral administration [5], variable bioavailability, fed/fasting effects [6, 7], and difficulties in establishing a sufficient safety margin following dose escalation studies. Moreover, poor solubility is relatively difficult to modulate in the later stage of a discovery project, where the core structure of the lead series is more or less defined. Enabling formulations, such as nanoparticle technology or polymer dispersion, may provide a solution by particle size reduction, offering an enhanced dissolution rate (Chapter 22). These approaches could show benefits in formulating BCS (Biopharmaceutics Classification System) class II compounds where solubility is low (dose limitation is likely) and permeability is high, and the limiting factor for absorption is the rate of dissolution, rather than the passage across the intestinal barrier [8].

The search for potent chemical series in drug discovery means that for certain biological target types there can be a tendency toward lipophilic and/or planar structures to maximize interactions at the active site. However, the solubilities of these compounds are generally low. On rare occasions, high potency may offset the issue of low solubility because a low dose is sufficient to show the clinical benefit. An example of this is montelukast (leukotriene D receptor antagonist, Clog $P = 8.47$), a very potent compound (0.1 nM) that due to low dose renders solubility no longer an issue [9]. To enable speedy progression of the chemical series of interest along the discovery pipeline, it is important to aim for a good balance of parameters, for example, solubility, exposure, and acceptable toxicity profile, while improving on potency. This translates into a need for physicochemical property assays with greater throughput or more reliable property prediction. The latter will be covered in

Chapter 4. In this chapter, we will focus on the experimental aspect of aqueous solubility and its interplay in discovery chemistry, DMPK, and bioscience assays. Particular emphasis will be placed on the latest technologies for determining aqueous solubility and the use of the solubility data in different phases of drug discovery.

2.1.1 Definition of Aqueous Solubility

Solubility is usually expressed as log S, where S is the saturated compound concentration in mol/l in equilibrium with its most stable crystalline form under certain defined conditions (e.g., physiological pH at room temperature over an extended period of time, typically 24–48 h). This is also known as the thermodynamic solubility. The typical log S values for discovery compounds vary from -3 (1 mM) down to -7 (0.1 μM). In contrast, kinetic solubility refers to the solubility value determined within a defined period of time, which is usually much shorter than 24 h. Since equilibrium conditions are not often achieved in this time frame, the compound is typically not in its most stable crystalline form. Therefore, the kinetic solubility value is normally higher than that obtained from the thermodynamic approach. Despite these caveats, kinetic solubility measurement can be set up in a high-throughput assay format and has been used by some pharmaceutical companies to identify poorly soluble compounds in the very early stage of drug discovery.

A search [10] of the World Drug Index revealed that 62.5% of marketed drugs are ionizable, which implies that these substances can exist in various charged states depending on the pH of the media. For ionizable drugs, solubility is pH dependent, and it is therefore important to understand the solubility in the context of pH. Ionization of a compound can be defined by the acid dissociation constant, pK_a. For the case of monoprotic compounds, the solubility at a given pH can be described by the following equations:

$$\text{base}: \quad S = S_0(1 + 10^{pK_a - pH}), \tag{2.1}$$

$$\text{acid}: \quad S = S_0(1 + 10^{pH - pK_a}), \tag{2.2}$$

where S_0 denotes the solubility of the compound in its neutral form, also referred to as intrinsic solubility. Figure 2.1 shows the pH–solubility profiles generated using Equations 2.1 and 2.2. It can be seen that the solubility of ionizable compounds is limited by the solubility of the neutral form of the compound. Depending on the charge types, solubility increases as pH decreases (base) or increases (acid) until a critical pH is reached, where the salt form and solubility product K_{sp} become solubility limiting (Equations 2.3 and 2.4) [11].

$$MX_{(s)} \rightleftharpoons M^+_{(aq)} + X^-_{(aq)}, \tag{2.3}$$

$$K_{sp} = [M^+_{(aq)}][X^-_{(aq)}]. \tag{2.4}$$

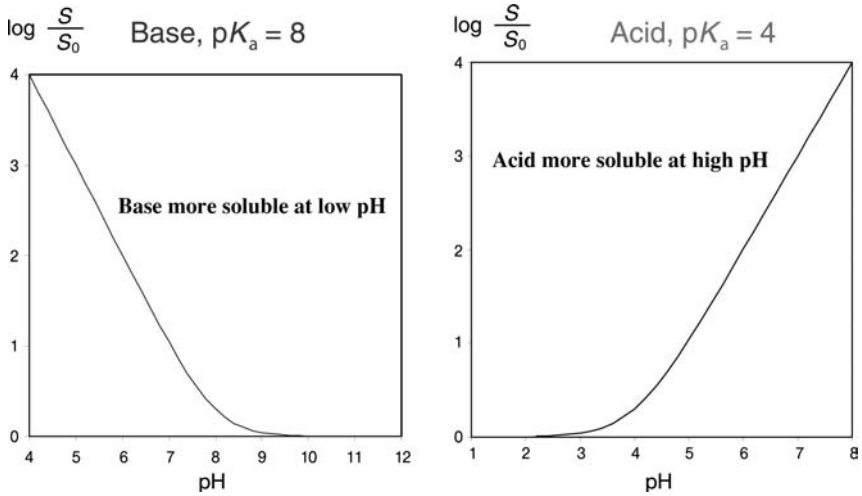

Figure 2.1 Theoretical solubility–pH profiles of a base with pK_a of 8 and an acid with pK_a of 4.

2.1.2
Aqueous Solubility in Different Phases of Drug Discovery

Figure 2.2 shows a schematic diagram of the drug discovery process. The target identification phase seeks to identify the biological target, signaling the start of a discovery project. Solubility evaluation typically begins in the hit identification (HI) phase enabling physicochemical characterization of hits and interpretation of biological and DMPK assay data. In lead identification (LI), solubility data facilitate the selection of "drug-like" lead series that will allow swift identification of a candidate drug (CD). Within the lead optimization (LO) phase, solubility data provide a formulation risk assessment for CDs entering development. Moreover, throughout the HI/LI/LO phases, solubility data are also used extensively as part of molecular design.

2.2
Aqueous Solubility in Hit Identification

In the HI phase of a discovery project, a variety of strategies are employed to identify potential hit series. HTS, focused subset library screening, and fragment library

Figure 2.2 Different phases of drug discovery.

screening represent a selection of the approaches undertaken in trying to find a good hit series. Besides an assessment of potency, it has become increasingly important to simultaneously understand the physicochemical properties of such potential leads to enable rapid identification of quality series most likely to progress quickly to CD delivery. Such front loading of physicochemical property assessment has required the introduction of solubility screens capable of handling the large number of compounds coming out of biological testing during this phase. Various solubility screens have been established in discovery to this end, but all share the common features of requiring compounds to be solubilized in DMSO as the starting point, since this facilitates rapid dispensing from company collections and the use of plate-based automation.

2.2.1
Aqueous Solubility from DMSO Solutions

It is the universally accepted practice within pharmaceutical companies to store compounds both as solids and as solutions in DMSO. Typically, as at AstraZeneca (AZ), a concentration of 10 mM or similar is used. From this, the stock samples are taken for a wide variety of tests including aqueous solubility screens. Using a DMSO solution as the starting point for a solubility assay presents a number of advantages. The automated nature of solution dispensing facilitates the study of a large number of compounds: sample consumption is usually significantly less than that in classic thermodynamic assays where solubility is measured from solid material and where DMSO solution in the aqueous sample is kept low, typically and at the 1% level or less, and there is minimal cosolvent effect [12] (see also Figure 2.3). The use of a DMSO stock solution does, however, mean that the

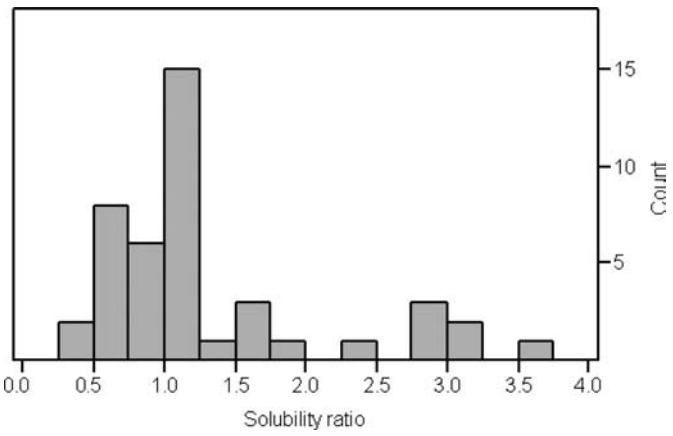

Figure 2.3 The solubility ratios of a set of 43 in-house compounds measured in phosphate buffer at pH 7.4 with and without 1% DMSO by the classic shake-flask method from solid. Compounds span a solubility range from 0.2 µM to 5 mM.

upper end of the dynamic range of the solubility assay is defined by the choice of the stock concentration in the company collection and the final DMSO percentage in the aqueous sample. In the case of AZ, a 10 mM DMSO stock combined with a 1% final cosolvent concentration in the high-throughput solubility (HTSol) assay means the assay upper limit is fixed at 100 μM. This is typically less than can be achieved from a solid-based assay.

Many of the HTSol assays reported in the literature using DMSO solution are "kinetic" HTSol assays. Such assays analyze the aqueous samples after only a short period of agitation with timescales ranging from immediately following precipitation to several minutes. In contrast, "thermodynamic" HTSol assays typically involve agitation for a minimum 24 h period and often longer. Kinetic solubility assays are consequently easier to run and as such are frequently used as a frontline assay to provide an initial ranking of lead series [13, 14]. In addition, kinetic solubility data have been applied to the interpretation of biological assay data where the measurement timescale and precipitation following dilution of a DMSO stock solution into aqueous media more closely mirror the process of biological assay testing [15].

Kinetic solubilities are by definition very time dependent and as such results can be less reproducible than thermodynamic solubility values. The short timescale also means that they are more dependent on the physical form of the initial precipitate. Consequentially, the correlation between kinetic and thermodynamic solubility is generally poor, with the kinetic measurement usually giving higher values [12, 16]. However, an advantage this can bring is that there will be few compounds excluded as false negatives in this phase.

HTSol assays employing DMSO stock solutions vary in the nature of the analysis of aqueous samples. Two approaches are commonly observed: (1) turbidimetric methods, where the formation or loss of precipitate is monitored against concentration, and (2) direct quantification of compound in solution by UV absorption spectroscopy following removal of precipitate by filtration.

2.2.1.1 **Turbidimetric Methods**

Turbidimetric methods rely on the measurement of light scattering from precipitate in solution to determine solubility. The initial approach, described by Lipinski, involves the stepwise addition of aliquots of DMSO stock solution at 1 min intervals to aqueous buffer in a UV cuvette until precipitation occurs when the kinetic solubility limit is achieved [1]. Precipitation is identified by an absorbance increase due to blockage of light by the particles in the range 600–800 nm using a diode array UV spectrometer. Using this approach, Lipinski is able to determine kinetic solubilities in the range 5–65 μg/ml with an upper limit of 0.67% DMSO cosolvent. Other turbidimetric methods have used fixed DMSO compositions (between 0.3 and 5% cosolvent) to avoid any potential cosolvent effects on solubility and have looked for precipitation following serial dilution [13, 14, 17, 18]. Alternative light scattering detection methods have also been used, including nephelometry [14, 17, 18] and flow cytometry [19]. Both make use of the perturbation of a laser beam passed through the sample. Nephelometric detection in a 96-well plate format is more amenable to automation and offers higher throughput than linear flow-through approaches, such

as cytometry, or incremental DMSO addition to a UV cuvette. However, nephelometer readings are very sensitive to plate quality, and the presence of scratches or dust can give rise to erroneously low solubility values.

2.2.1.2 UV Absorption Methods

The alternative method to turbidimetric detection used for measuring solubility in early discovery is to quantify the aqueous supernatant directly via UV absorbance [13, 20, 21]. Typically, DMSO stock solution is added to aqueous buffer such that the final DMSO composition is kept to a minimum (5% or less) and the resulting precipitate is removed by filtration. A UV plate reader is then used to determine the aqueous solubility by comparing the filtrate absorbance against that of a calibration solution prepared in an identical solvent. It is important to match the sample and calibration solutions to prevent solvochromic effects. Care must also be taken in the selection of the filter plate since nonspecific binding of compound can occur with some filter materials leading to erroneously low solubility values [22]. Like nephelometry, the plate-based UV detection approach is amenable to automation.

As with turbidimetric assays, many of the direct UV absorbance assays are set up to determine kinetic solubility. However, the UV absorbance method also lends itself well to thermodynamic solubility determination by extending the period of sample agitation prior to filtration to 24 h or more. This offers a number of advantages. The solubility data generated are less dependent on the physical form of the initial material precipitated from DMSO and are much closer to thermodynamic solubility values determined later in discovery and in early development. As such, it gives more consistent solubility data through the discovery phase and enables a better quality early assessment to be made of the likely difficulties or otherwise of progressing a lead series into development.

It is a version of this latter assay that has been established as our current frontline solubility measurement in the hit identification phase of discovery [23]. The assay uses 10 mM DMSO stock solution, which is diluted into aqueous buffer at pH 7.4 to give a final DMSO composition of 1%. Samples are agitated for 24 h using magnetic stirrer bars prior to plate filtration to remove precipitate. This sample is further diluted and compared against a calibration solution of known concentration also taken from the 10 mM DMSO stock and diluted to the same solvent composition. The assay is based on a 96-well plate format using a UV diode array plate reader. This has enabled full automation of the assay with over 600 compounds measured in each run.

One of the concerns raised with the direct UV absorbance approach is that without HPLC separation the presence of impurities may cause erroneous solubility values to be reported. This is also a concern for turbidimetric methods. However, with strict purity criteria for registration of compounds into the company collection, this has helped to lessen this concern. In addition, for this assay an algorithm has been written that checks the UV spectrum of the sample against that of the calibration. Any significant impurities or decomposition occurring during the 24 h agitation period are readily picked out as a spectral mismatch [23].

To determine how similar solubility values from our high-throughput DMSO-based thermodynamic assay are to classical thermodynamic solubilities measured from solid, a diverse test set of 200 predominantly in-house compounds were compared. In the case of the latter assay as well as starting from solid material, the method included HPLC analysis and separation of undissolved solid from the supernatant via double centrifugation. Figure 2.4 indicates that there is a good correlation between the two methods with most compounds giving solubilities within a factor of 3. Given the potentially different physical forms of the compound generated in the two assays, this seems reasonable. It is noted that the

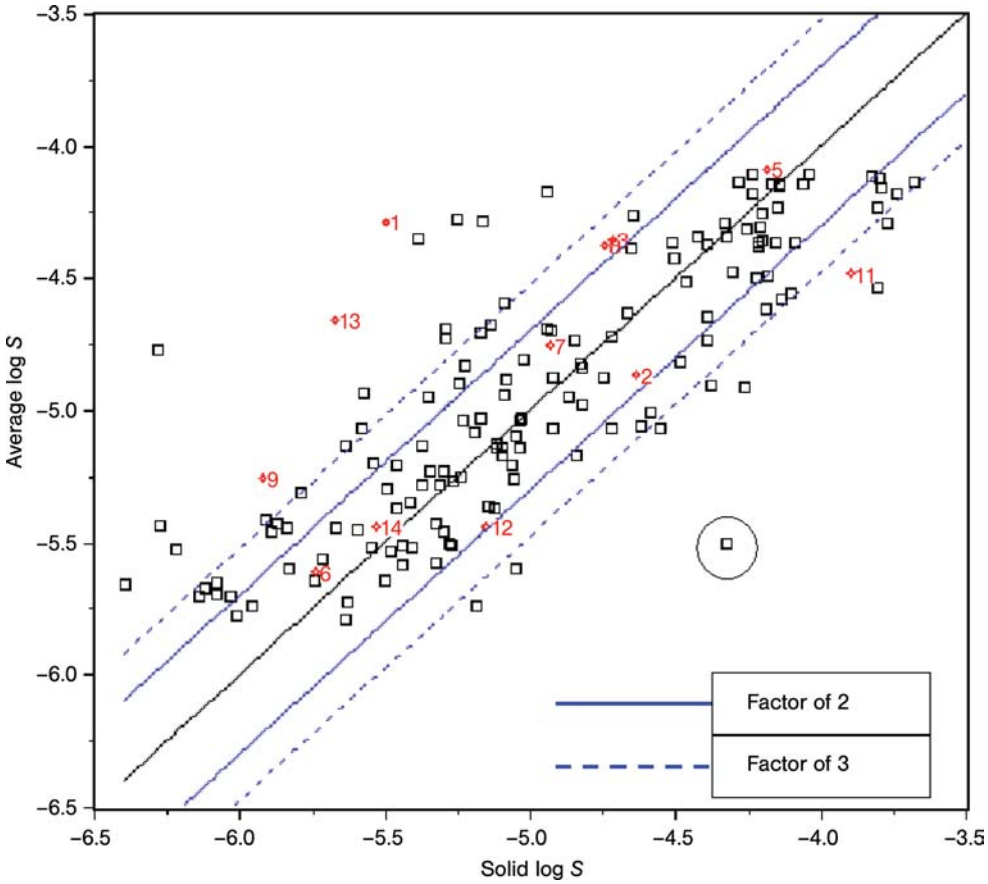

Figure 2.4 Correlation between the solubility of the test set obtained from the solid solubility assay (*x*-axis) and from the high-throughput solubility assay (*y*-axis; average of four experiments). The black line is the 1 : 1 line. Symbol ⊙ represents in-house compounds. Symbol ◇ represents commercial compounds: 1 – disulfiram, 2 – diethylstilbestrol, 3 – griseofulvin, 5 – haloperidol, 6 – mebendazole, 7 – glyburide, 8 – nifedipine, 9 – albendazole, 10 – bumetanide analogue, 11 – loperamide, 12 – astemizole, 13 – nimodipine, 14 – loratadine. Symbol in circle represents the negative outlier as discussed in the text. Reprinted with permission from [23].

effect of different crystalline polymorphs on solubility can typically be within this range [24, 25]. There are a number of outliers in the plot that predominantly fall on the side of greater solubility for the DMSO-based assay. Literature and our own studies suggest that this enhanced solubility effect is unlikely to be caused by the solubilizing effect of 1% DMSO [12]. Figure 2.3 shows the solubility ratios of a set of 43 compounds measured in buffer with and without 1% DMSO by the classic thermodynamic method. The compounds span a solubility range from 0.2 μM to 5 mM. The presence of 1% DMSO has minimal impact on the solubility, with a factor of 3.6 the largest enhancement observed. It is more likely that the enhanced solubility observed for the outliers reflects that the compounds have precipitated from DMSO solution as amorphous material and this has not yet reached true equilibrium with their crystalline form during the 24 h agitation period. Literature indicates that differences in solubility between amorphous and crystalline forms of a compound can be significant [26]. A similar explanation has also been reported for positive outliers observed in an extended agitation solubility study using HPLC–UV analysis [16]. There is one significant negative outlier in Figure 2.4. Further studies ruled out any retention to the filter membrane as a possible explanation. Powder X-ray diffraction on the postsolubility samples for this compound in a scaled-up experiment revealed that the DMSO method had generated a crystalline sample in 24 h whereas the sample from the experiment starting from solid material was predominantly amorphous after this period. This interesting observation highlights that for certain compounds DMSO precipitation conditions can facilitate formation of crystalline material.

2.2.1.3 **Alternative Detection Methodology**

A further recent approach taken to deliver higher throughput kinetic and thermodynamic aqueous solubility measurements from DMSO and solid, respectively, involved changing the assay detection method from UV to one that does not require compound-specific calibration, namely, chemiluminescent nitrogen detection (CLND) [27, 28]. The CLND detector is able to quantify the nitrogen content of the aqueous sample using a generic nitrogen calibration curve, and from the knowledge of the number of nitrogen atoms in the molecule the aqueous concentration and hence the solubility is determined. Eliminating the need for a compound-specific calibration solution reduces assay sample consumption relative to UV methods, and the technique is fast when coupled with direct flow injection onto the detector. However, the sensitivity of the CLND detector to nitrogen necessitates rigorous laboratory housekeeping to avoid contamination of the instrument from nonsample nitrogen sources. Regular recalibration of the CLND detector is required to retain accuracy, and a linear response is not observed for all nitrogen environments; for example, adjacent nitrogen atoms in a molecule are known to be a special class. Care must also be taken if HPLC is not used with the detector to ensure that no nitrogen-containing impurities are present in the sample.

Other universal detectors have been suggested as potential replacements for UV in solubility assays including ELSD and CAD, although at present no specific assay has been reported [29].

2.2.1.4 Application of DMSO-Based Solubility Assays

The advent of fully automated DMSO-based solubility assays has meant that aqueous solubilities can now be determined on HTS output in parallel with biological testing to enable rapid identification of quality hit series from a physicochemical perspective [2]. Figure 2.5 shows an AZ project example where simultaneous solubility and potency measurements highlighted 1 out of 19 hit series as having poor physicochemical properties. A comparison of solubility data with potency data also enables identification of potential false hits, which can be removed to facilitate SAR understanding. Automated DMSO-based solubility assays have also shown benefits in library screening. In relation to this, our thermodynamic HTSol assay described above has been successfully applied to the selection of compounds forming the AZ in-house generic fragment library [23]. Fragments typically show weak binding to molecular targets and so are normally screened at high concentrations. Consequently, good aqueous solubility is one of the key criteria to satisfy in establishing a fragment library. It has been demonstrated that by using a training set of 3234 neutral compounds, a clear relationship could be established between measured solubility and predicted log *P* (Clog *P*) (Figure 2.6) [23]. The use of binning and percentiles in Figure 2.6 enables maximum information to be extracted from data covering a small dynamic range. In particular, multiple percentiles (10, 20, 30, 40, and 50) capture the variation in log *S* and reveal the strength of the trend with Clog *P*. This analysis was applied to all the potential fragment library compounds. Neutral fragments with Clog *P* less than 2.19 were assumed to have acceptable solubility, while those with higher values were submitted for solubility measurement. Only those compounds with solubilities at or above the upper quantification limit for the solubility assay were accepted into the fragment library.

2.3 Aqueous Solubility in Lead Identification and Lead Optimization

In the lead identification and lead optimization phases of discovery, there is greater focus on thermodynamic solubility measurements. Thermodynamic solubility assays are designed to determine the solubility of the stable crystalline form of the compound, since this is the physical form that will be sought in the development phase for orally administered drugs. As such, thermodynamic solubilities provide discovery projects with a better risk assessment of likely formulation issues in development. Thermodynamic solubilities, unlike kinetic solubilities, are less dependent on the initial physical form of the compound and being less time critical also tend to be more reproducible. This is particularly important from a molecular design perspective where chemists are seeking to modify molecular structure to improve solubility.

Classically, thermodynamic solubility is measured using the shake-flask method [21, 30]. This method involves addition of an excess of solid to aqueous buffer at fixed pH. The solution is stirred for a minimum of 24 h prior to separation of the supernatant from undissolved material via centrifugation or filtration followed by

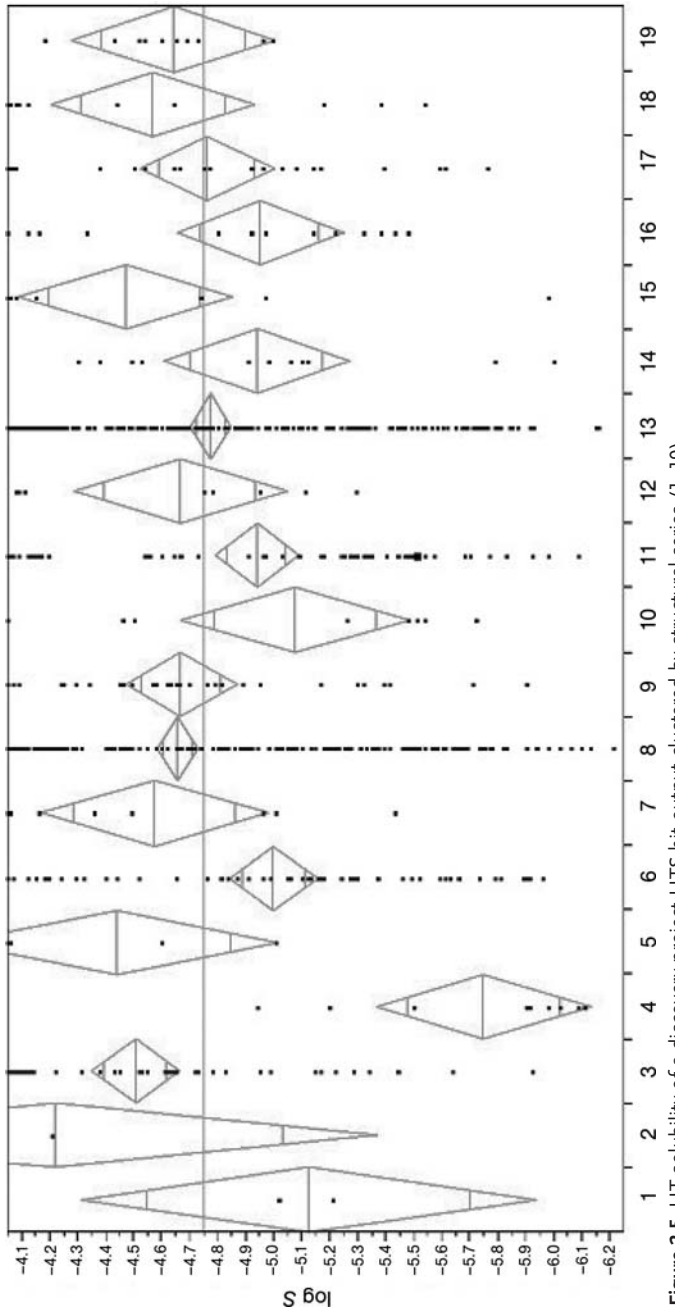

Figure 2.5 HT solubility of a discovery project HTS hit output clustered by structural series (1–19).

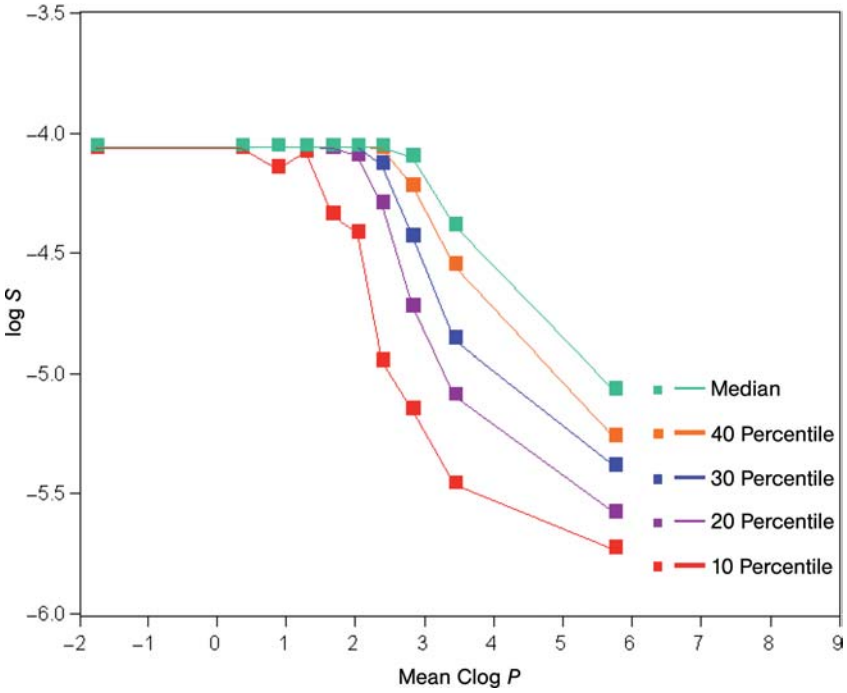

Figure 2.6 Percentiles for solubility for training set fragments as a function of mean Clog *P* for each bin. Data partitioned by Clog *P* into 10 bins each with 356 solubility measurements. Reprinted with permission from [23].

HPLC–UV analysis. The need for weighing out of solid and an analysis via HPLC mean that the method has generally low throughput. However, the increasing demand for thermodynamic solubilities in discovery has led to the development of automation-friendly methods on the basis of the shake-flask approach. Many of these methods make use of DMSO stock solutions as the starting point for the assay, thereby exploiting the automated compound dispensing facilities within pharmaceutical companies. The assays retain the minimum 24 h agitation of the shake-flask method with analysis of supernatant being either via HPLC–UV or direct UV.

2.3.1 Dried-Down Solution Methods

Another approach to increase the throughput of thermodynamic solubility measurement in discovery involves evaporating a DMSO stock solution to dryness at the start of the assay [12, 22, 31]. Aqueous buffer is added to the dried-down solid, which is then agitated for 24 h followed by HPLC–UV or UV analysis of the supernatant. Removal of all the DMSO solvent ensures that the solubility value is not enhanced by

any cosolvent effects. A further advantage of this method is that, as with the classic shake-flask approach, a larger solubility dynamic range can be achieved compared with direct DMSO-based methods. Appropriate selection of DMSO volume to be evaporated coupled with buffer volume selection allows the upper assay limit to be extended by an extra order of magnitude (~1 mM). It should be noted that care must be taken establishing evaporation conditions to avoid loss of volatile or thermally labile compounds. Solubility data using this approach have been reported to give a good correlation with thermodynamic solubility values determined by the classic shake-flask methods [12, 22, 31]. Incidences where differences have been observed are thought to reflect cases where equilibrium with the stable crystalline form has not been achieved by the dried solid method in the 24 h timescale [31].

2.3.2 Solubility from Solid

Many approaches to determine thermodynamic solubility in drug discovery have focused on miniaturizing the classic shake-flask method with solid samples manually weighed and dispensed into 96-well plates or 96-vial arrays [32–34]. The 96-well format enables the use of liquid handling robots to improve throughput. As with the standard shake-flask method, aqueous buffer is added and the solution is agitated for a minimum of 24 h prior to plate filtration or centrifugation to remove the supernatant, which is then analyzed by HPLC–UV or direct UV.

Given the large number of compounds evaluated in discovery for solubility and the small quantities of solid material available, the physical form of the starting solid and that at the end of the agitation period is rarely characterized. Often the starting solid material will be amorphous [35] reflecting the compound purification techniques used by chemists today, which are largely based on preparative HPLC. Recrystallization techniques are generally no longer used.

In all thermodynamic solubility methods, an assumption is made that in the 24 h of agitation the initial form of the compound is able to convert to the stable crystalline form. Evidence indicates that compounds can convert from amorphous to crystalline forms and can also change polymorphs in this period [24, 36]. However, not all compounds are able to equilibrate to the most stable polymorph during this time frame [37]. The question then arises what impact does the initial solid state have on the thermodynamic solubility result reported and how often does the compound convert to its most stable crystalline form in the solubility assay. Pudipeddi *et al.* [24] showed with a data set of 81 compounds that there was little difference in the solubilities of different crystalline polymorphs and that typically the solubility ratio was no greater than 2. Similar observations were made by Hancock *et al.* [26], who showed that the most significant solubility differences occurred between amorphous and crystalline materials. In an attempt to understand how often crystalline material is generated from amorphous samples in thermodynamic solubility assays, we have taken a diverse set of commercial compounds, measured the solubility starting from crystalline and amorphous solids, and compared the solid form by powder X-ray diffraction (PXRD) (Table 2.1). From Figure 2.7, it is apparent that most amorphous

Table 2.1 The aqueous solubility of 16 drug molecules at pH 7.4 measured from crystalline and amorphous solid materials using the shake-flask method (24 h agitation).

Drug name	Crystalline solubility (μM)	Amorphous solubility (μM)	Solubility ratio (amorphous/crystalline)
Disulfiram	2.2	3.2	1.5
Astemizole	3.5	4.3	1.2
Bicalutamide	4.6	6.1	1.3
Ketoconazole	5.2	5.6	1.1
Loperamide	6.6	444.3	67.5
Glyburide	9.5	56.8	6.0
Griseofulvin	15.3	18.0	1.2
Terfenadine	15.7	21.3	1.4
Nifedipine	41.9	882.4	21.1
Haloperidol	52.3	54.7	1.0
Testosterone	57.9	69.0	1.2
Flutamide	92.9	79.8	0.9
Bitolterol	103.0	77.2	0.7
Diazepam	130.0	132.3	1.0
Carbamazepine	428.6	456.2	1.1
Chlorzoxazone	1360.0	1626.2	1.2

compounds reach equilibration with crystalline material in the course of the assay (Figure 2.8). A few positive outliers were seen by PXRD to be amorphous at the end of the experiment (Figure 2.9). Similar observations have been made by Sugano, who examined the solubility of a series of compounds starting from DMSO solution following 20 h of agitation with characterization of the final solid state by polarized light microscopy (PLM) [16]. Indirect evidence also suggests that most compounds are able to generate a stable thermodynamic solubility value in 24 h. For example, subsequent batches of the same compound made in AZ discovery projects show small solubility differences ($\leq$0.44 log units, see Figure 2.10). Moreover, in general, it is observed that there are good correlations between data produced in thermodynamic solubility assays starting from solid, dried DMSO solution [12, 22, 31], and DMSO solution (Figure 2.4).

2.3.3
Thermodynamic Solubility Assays with Solid-State Characterization

More recently in discovery there has been a trend toward developing high-throughput thermodynamic solubility assays, which incorporate a solid-state assessment at the end of the period of agitation. This assessment aids interpretation of the solubility data and is an important consideration when relating the solubility data to molecular structure. Solid-state characterization methods include the use of PLM [16], microscopic analysis [34], PXRD [32, 33], and Raman microscopy [22]. With all these

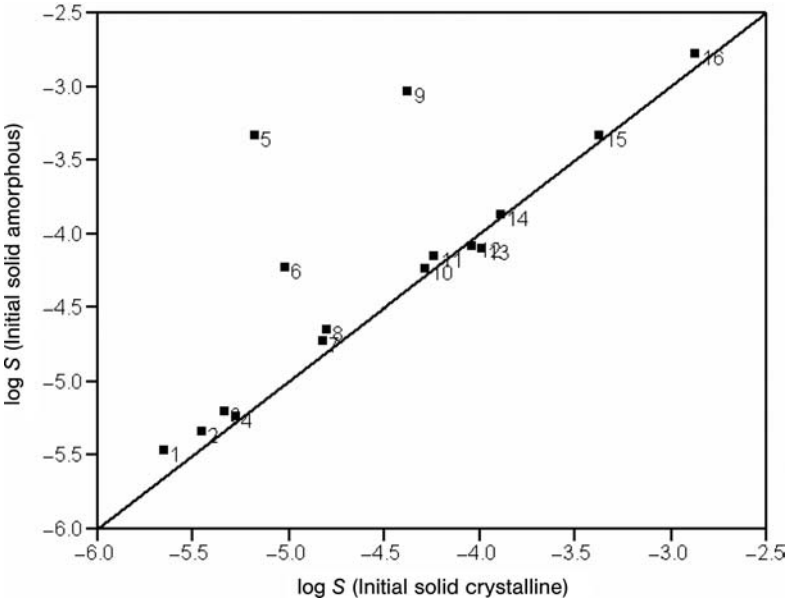

Figure 2.7 Plot of aqueous solubility using amorphous versus crystalline material at pH 7.4 following 24 h agitation. (1) Disulfiram, (2) astemizole, (3) bicalutamide, (4) ketoconazole, (5) loperamide, (6) glyburide, (7) griseofulvin, (8) terfenadine, (9) nifedipine, (10) haloperidol, (11) testosterone, (12) flutamide, (13) bitolterol, (14) diazepam, (15) carbamazepine, (16) chlorzoxazone.

methods having sufficient solid sample postincubation is key. It has been shown that PLM can be applied to a DMSO-based solubility assay with a sample size of 0.6 mg, enabling an amorphous/crystalline interpretation of remaining solid [16]. Direct analysis is made of the solid following centrifugation of the sample solution in a 96-well glass-bottomed plate. A similar interpretation has been reported using microscopic analysis from a solubility assay (PASS) using 0.5–4 mg of sample [34]. In this case, the supernatant is removed following centrifugation and the remaining solid resuspended in silicon oil prior to analysis. More recently, Raman spectroscopic analysis has been added to this assay to enable changes in solid form to be identified [22]. Those thermodynamic solubility assays that characterize the remaining solid by the gold standard method, PXRD, generally require larger amounts of solid than microscopy techniques [32, 33]. A high-throughput thermodynamic solubility assay has been reported including PXRD assessment using 3 mg of solid sample [32]. The sample solution is filtered following 17 h shaking using custom-built nickel filter plates. The nickel filter serves as an effective means of presenting the remaining solid to the PXRD instrument, since it does not give background diffraction in the analysis window.

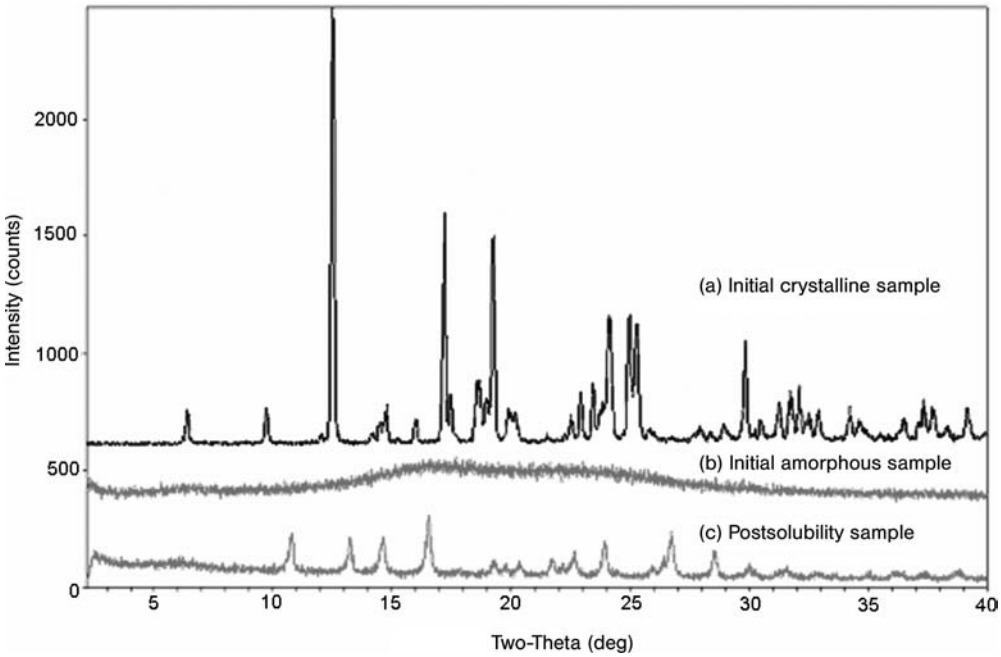

Figure 2.8 PXRD traces of bicalutamide: (a) the initial crystalline sample; (b) the initial amorphous sample; and (c) bicalutamide post-24 h agitation in phosphate buffer from the amorphous sample.

2.3.4
Solubility by Potentiometry

Potentiometry is a further technique used to measure aqueous solubility in discovery, although throughput limitations mean that this technique is used most often later in the LO stage. Potentiometric approaches specifically measure intrinsic solubility, which is the solubility of the neutral form of the molecule [38].

With the potentiometric approach, determination of intrinsic solubility is based upon the measurement of the pH shift caused by compound precipitation during acid–base titration of ionizable compounds. Two commercial potentiometric methods currently available are pSol [30, 39] and Cheqsol [40–42]. In the pSol method developed by Avdeef, a minimum of three titrations in the direction of dissolution are performed. Normal pH versus volume titration plots are reexpressed as Bjerrum plots, that is, average number of bound protons versus pH. The Bjerrum plots enable the shift in compound pK_a to be more readily observed and are used to determine intrinsic solubility (S_0) via Equation 2.5:

$$\log S_0 = \log\left(\frac{C}{2}\right) - (\mathrm{p}K_a^{\mathrm{app}} - \mathrm{p}K_a), \tag{2.5}$$

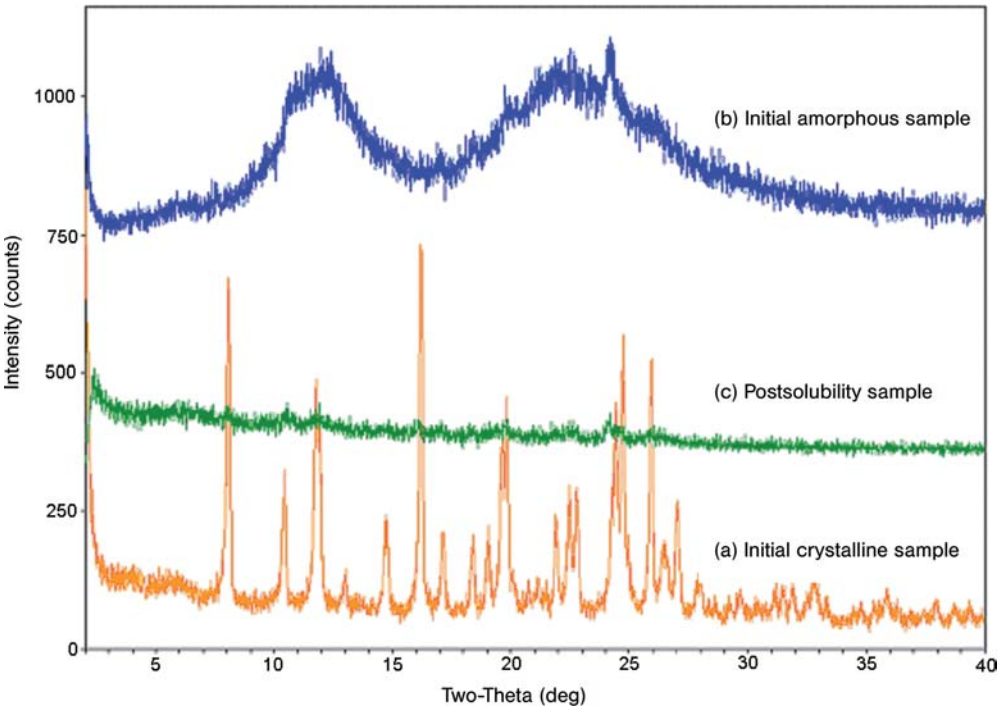

Figure 2.9 PXRD traces of nifedipine: (a) the initial crystalline sample; (b) the initial amorphous sample; and (c) nifedipine post-24 h agitation in phosphate buffer from the amorphous sample.

where S_0 is the intrinsic solubility, C is the total concentration of compound, pK_a^{app} is the measured pK_a in the presence of precipitation, and pK_a is the measured aqueous pK_a (no precipitation).

Intrinsic solubilities determined by pSol have been shown to agree well with values derived by shake-flask methods and have the advantage of requiring less compound since the technique does not require a sample calibration [39]. The time taken for each pSol solubility measurement is compound specific with 3–10 h quoted as typical [39]. Poorly soluble compounds can take longer than this and can be prone to reprecipitation causing outlying titration points. In these circumstances, the manufacturer's recommendation is to repeat the titrations in the presence of cosolvent spanning a range of percentage compositions and extrapolate back to the pure aqueous solubility value. Although this can improve the speed and accuracy of the titration, the need for further titrations generally adds to the overall experiment time. When undertaking the titrations, consideration should also be given to the compound physical form, which is usually not characterized. The initial physical form of the compound supplied may differ from that which is reprecipitated after each titration, and this can affect the solubility reported between the first and subsequent titrations. It should also be noted that since the time the solid spends in equilibrium with the aqueous solution at each pH is very short, there is less

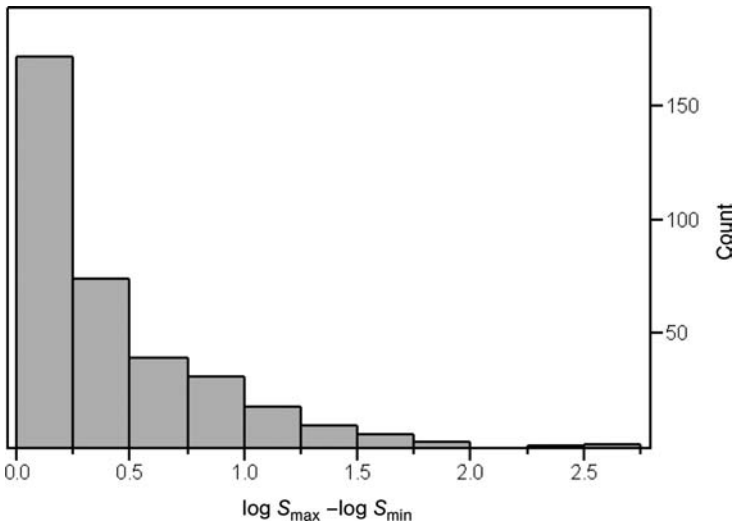

Figure 2.10 Difference between the maximum and minimum log solubility measured for different batches of each compound ($n = 360$). Values greater or less than assay detection limits (over-range values) have been excluded from the analysis. The mean $\log S_{max} - \log S_{min} = 0.44$.

opportunity for the thermodynamically stable form of the compound to be produced in the pSol method than in the 24 h of the classic shake-flask solubility method.

The Cheqsol method uses a similar experimental setup to pSol. However, in contrast to pSol, the Cheqsol method begins with the compound in solution and titration is followed until precipitation is detected by light scattering via a UV spectroscopic probe. At this point, the solution is switched repeatedly between a state of subsaturation and that of supersaturation by the addition of small amounts of acid and base to rapidly generate the point of equilibrium, from which the intrinsic solubility is calculated. As with the pSol technique, determination of the intrinsic solubility requires an accurate measure of the compound aqueous pK_a, and for poorly soluble compounds, titration in cosolvent with extrapolation to the aqueous state is used. The Cheqsol technique has the advantage of being relatively quick to achieve a state of equilibrium with experiment times in the region of 1 h for compounds that do not require cosolvent extrapolation. It has been shown with two compounds, diclofenac and sulindac, that changes in the crystalline polymorphs can occur as a result of the potentiometric cycling in Cheqsol [41, 43]. How the physical forms of the solid generated via Cheqsol compare to those observed in classic shake-flask studies is yet to be established.

2.3.5
Application of Thermodynamic Solubility Data in LI and LO

In LI and LO, thermodynamic solubility data are used to aid the understanding of DMPK data and guide formulation. When solubility is low, DMPK issues arise, such

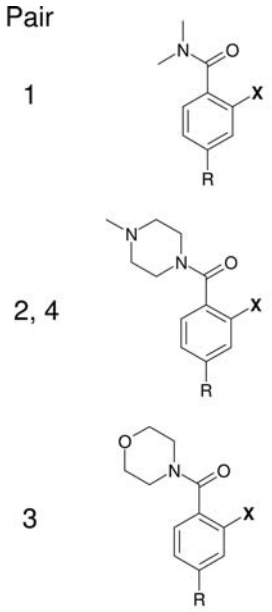

Pair	X	S (μM)	log S	log D	Δlog S	Δlog D
1	H	112	-3.95	2.8	1.36	0.1
	Me	2550	-2.59	2.9		
2	H	42	-4.37	2.5	1.67	0.1
	Me	1950	-2.71	2.6		
3	H	943	-3.02	2.2	>0.54	0.1
	Me	>3300	>-2.48	2.3		
4	H	39	-4.41	2.8	0.7	0.1
	Me	197	-3.7	2.9		

Figure 2.11 Crystalline solubility match pairs showing effects of the *ortho*-methyl substituent.

as poor and variable bioavailability, fed/fasting effects [6], and lack of dose linearity. Poorly soluble molecules can also present significant and time-consuming formulation challenges during development. In trying to address these issues and challenges, solubility data are frequently used as a part of molecular design in discovery. In this respect, thermodynamic solubility data have been successfully applied to local and generic QSPR models using techniques such as BNN, MLR, and PLS [44] and to matched molecular pair analysis to determine substituent effects [45, 46] (Chapter 4). The latter approach has proved particularly useful for identifying novel structural effects on solubility. For example, Figure 2.11 shows a project that was able to improve solubility in a chemical series through incorporation of a single methyl group, not obvious based solely on log *P*, but which is suggestive of an effect on crystal packing. Interpretation of such observations requires that quality solubility data are used, coupled with the knowledge of the solid state to remove any concern about physical form effects. It is to be hoped that the trend toward increased characterization of the solid state earlier in discovery will lead to greater exploitation of solubility data as part of molecular design.

2.4 Conclusions

Aqueous solubility is an important property in discovery that has an impact across chemistry, DMPK, and formulation, and in the interpretation of biological assay results. The difficulties faced in the accurate prediction of solubility mean that measurement of aqueous solubility is essential from early HI onward. Automated approaches based on kinetic solubility and turbidimetric readouts have been developed in response to the high numbers of compounds requiring characterization in HI and also as a result of the desire to better understand biological assay data. However, more recently this demand has switched to high-quality thermodynamic solubilities to enable an early risk assessment of formulation issues in development and to identify quality hit series. Such frontloading of thermodynamic solubility has necessitated modification of the classic shake-flask approach to automation-friendly formats, which offers higher throughputs and can exploit the ease of dispensing provided by DMSO solution. In addition to this, there has also been a growing trend toward increased solid-state characterization of the sample in the solubility experiment during the LO stage of discovery. Such characterization means that there is a better understanding of the discovery solubility data and consequently greater confidence in its use to assess formulation risk when entering development and enhanced application of solubility data in molecular design.

Acknowledgments

We would like to thank our colleagues in the Alderley Park Physical Chemistry group for the AZ physical properties measurements captured in this chapter. In particular, thanks to Mark Timms and June Kenworthy who undertook most of the measurement work in Figures 2.3–2.7. We would also like to thank our computational chemistry colleague, Peter Kenny, for his contribution and valuable discussions on the use of solubility in fragment library design. Thanks also to our pharmaceutical colleagues Rhea Brent, Rebecca Booth, Rod Kittlety, and George Kirk for support around PXRD studies and valuable discussion on solid state and solubility. Thanks also to Trevor Johnstone and Jamie Scott for the preparation of amorphous material, enabling the study in Figure 2.7 to be undertaken.

References

1 Lipinski, C.A., Lombardo, F., Dominy, B.W. and Feeney, P.J. (2001) Experimental and computational approaches to estimate solubility and permeability in drug discovery and development settings. *Advanced Drug Delivery Reviews*, **46**, 3–26.

2 Kerns, E. (2001) High throughput physicochemical profiling for drug discovery. *Journal of Pharmaceutical Sciences*, **90** (11), 1838–1858.

3 Di, L. and Kerns, E.H. (2006) Biological assay challenges from compound solubility: strategies for bioassay

optimisation. *Drug Discovery Today*, **11** (9–10), 446–451.

4 McGovern, S.L., Caselli, E., Grigorieff, N. and Shoichet, B.K. (2002) A common mechanism underlying promiscuous inhibitors from virtual and high-throughput screening. *Journal of Medicinal Chemistry*, **45**, 1712–1722.

5 van de Waterbeemd, H., Smith, D.A., Beaumont, K. and Walker, D.K. (2001) Property-based design: optimization of drug absorption and pharmacokinetics. *Journal of Medicinal Chemistry*, **44**, 1–21.

6 Sunesen, V.H., Vedelsdal, R., Kristensen, H.G., Christrup, L. and Mullertz, A. (2005) Effect of liquid volume and food intake on the absolute bioavailability of danazol, a poorly soluble drug. *European Journal of Pharmaceutical Sciences*, **24**, 297–303.

7 Gu, C.H., Li, H., Levons, J., Lentz, K., Gandhi, R.B., Raghavan, K. and Smith, R.L. (2007) Predicting effect of food on extent of drug absorption based on physicochemical properties. *Pharmaceutical Research*, **24** (6), 1118–1130.

8 Mass, J., Kamm, W. and Hauck, G. (2007) An integrated early formulation strategy – from hit evaluation to preclinical candidate profiling. *European Journal of Pharmaceutics and Biopharmaceutics*, **66**, 1–10.

9 Schmid, E.F. and Smith, D.A. (2007) Pharmaceutical R&D in the spotlight: why is there still unmet medical need? *Drug Discovery Today*, **12**, 998–1006.

10 Comer, J.E.A. (2007) High-throughput measurement of log *D* and pK_a, in *Drug Bioavailability. Methods and Principles in Medicinal Chemistry*, Vol. 8 (eds H. van de Waterbeemd, H. Lennernas and P. Artursson), Wiley-VCH Verlag GmbH, Weinheim, pp. 21–43.

11 Serajuddin, A.T.M. (2007) Salt formation to improve drug solubility. *Advanced Drug Delivery Reviews*, **59**, 603–616.

12 Zhou, L., Yang, L., Tilton, S. and Wang, J. (2007) Development of a high throughput equilibrium solubility assay using miniaturized shake-flask method in early drug discovery. *Journal of Pharmaceutical Sciences*, **96** (11), 3052–3071.

13 Pan, L., Ho, Q., Tsutsui, K. and Takahashi, L. (2001) Comparison of chromatographic and spectroscopic methods used to rank compounds for aqueous solubility. *Journal of Pharmaceutical Sciences*, **90** (4), 521–529.

14 Fligge, T.A. and Schuler, A. (2006) Integration of a rapid automated solubility classification into early validation of hits obtained by high throughput screening. *Journal of Pharmaceutical and Biomedical Analysis*, **42**, 449–454.

15 Popa-Burke, I.G., Issakova, O., Arroway, J.D., Bernasconi, P., Chen, M., Coudurier, L., Galasinski, S., Jadhav, A.P., Janzen, W.P., Lagasca, D., Liu, D., Lewis, R.S., Mohney, R.P., Sepetov, N., Sparkman, D.A. and Hodge, C.N. (2004) Streamlined system for purifying and quantifying a diverse library of compounds and the effect of compound concentration measurements on the accurate interpretation of biological assay results. *Analytical Chemistry*, **76**, 7278–7287.

16 Sugano, K., Kato, T., Suzuki, K., Keiko, K., Sujaku, T. and Mano, T. (2006) High throughput solubility measurement with automated polarized light microscopy analysis. *Journal of Pharmaceutical Sciences*, **95** (10), 2115–2122.

17 Bevan, C. and Lloyd, R.S. (2000) A high-throughput screening method for the determination of aqueous drug solubility using laser nephelometry in micro-titer plates. *Analytical Chemistry*, **72**, 1781–1787.

18 Dehring, K.A., Workman, H.L., Miller, K.D., Mandagere, A. and Poole, S.K. (2004) Automated robotic liquid handling/laser-based nephelometry system for high throughput measurement of kinetic aqueous solubility. *Journal of Pharmaceutical and Biomedical Analysis*, **36**, 447–456.

19 Lilley, M., Shanter, M., Ardiff, M., Ciolkosz, T., Kashdan, M., Aubin, C. and Goodwin, J. A fully automated workstation for testing flow based kinetic solubility of compounds. Poster Presentation, BD

Biosciences, Two Oak Park, Bedford, MA, USA.

20 Chen, T., Shen, H. and Zhu, C. (2002) Evaluation of a method for high throughput solubility determination using a multi-wavelength UV plate reader. *Combinatorial Chemistry & High Throughput Screening*, **5**, 575–581.

21 Avdeef, A. (2001) Pharmacokinetic optimization in drug research, in *Biological, Physicochemical, and Computational Strategies* (eds B. Testa, H. van de Waterbeemd, G. Folkers and R. Guy), Verlag Helvetica Chimica Acta, Zurich, pp. 305–326.

22 Alsenz, J. and Kansy, M. (2007) High throughput solubility measurement in drug discovery and development. *Advanced Drug Delivery Reviews*, **59**, 546–567.

23 Colclough, N., Hunter, A., Kenny, P.W., Kittlety, R.S., Lobedan, L., Tam, K.Y. and Timms, M.A. (2008) High throughput solubility determination with application to selection of compounds for fragment screening. *Bioorganic & Medicinal Chemistry*, **16**, 6611–6616.

24 Pudipeddi, M. and Serajuddin, A.T.M. (2005) Trends in solubility of polymorphs. *Journal of Pharmaceutical Sciences*, **94** (5), 929–939.

25 Yalkowsky, S.H. (1999) *Solubility and Solubilisation in Aqueous Media*, Oxford University Press, Cambridge, pp. 81–115, Table 4.8.

26 Hancock, B. and Parks, M. (2000) What is the true solubility advantage for amorphous pharmaceuticals. *Pharmaceutical Research*, **17** (4), 397–404.

27 Bhattachar, S.N., Welsey, J.A. and Seadeek, S. (2006) Evaluation of the chemiluminescent nitrogen detector for solubility determinations to support drug discovery. *Journal of Pharmaceutical and Biomedical Analysis*, **41**, 152–157.

28 Hill, A. (2007) High-throughput solubility. PhysChem Forum 3, June 2007.

29 Reilly, J. (2007) CAD detector validation and potential for physicochemical measurements. PhysChem Forum 3, June 2007.

30 Glomme, A., Marz, J. and Dressman, J.B. (2005) Comparison of a minaturized shake-flask solubility method with automated potentiometric acid/base titrations and calculated solubilities. *Journal of Pharmaceutical Sciences*, **94** (1), 1–16.

31 Alelyunas, Y. (2006) Exploring the solubility limit of CNS discovery candidates. CHI's Molecular Medicine Tri-Conference, February 21–25, San Francisco, CA.

32 Seadeek, C., Ando, H., Bhattachar, S.N., Heimbach, T., Sonnenberg, J.L. and Blackburn, A.C. (2007) Automated approach to couple solubility with final pH and crystallinity for pharmaceutical discovery compounds. *Journal of Pharmaceutical and Biomedical Analysis*, **43**, 1660–1666.

33 Wyttenbach, N., Alsenz, J. and Grassmann, O. (2007) Miniaturized assay for solubility and residual solid screening (SORESOS) in early drug development. *Pharmaceutical Research*, **24** (5), 888–898.

34 Alsenz, J., Meister, E. and Haenel, E. (2007) Development of a partially automated solubility screening (PASS) assay for early drug development. *Journal of Pharmaceutical Sciences*, **96** (7), 1748–1762.

35 Lipinski, C.A. (2004) Solubility in water and DMSO: issues and potential solutions. *Pharmaceutical Profiling in Drug Discovery*, **1**, 93–125.

36 Buckton, G. (2002) Solid state properties, in *Pharmaceutics: The Science of Dosage Form Design* (ed. M.E. Aulton), Churchill Livingstone, Edinburgh, pp. 141–151.

37 Huang, L.F. and Tong, W.Q. (2004) Impact of solid state properties on developability assessment of drug candidates. *Advanced Drug Delivery Reviews*, **56**, 321–334.

38 Avdeef, A. (2007) Solubility of sparingly-soluble ionizable drugs. *Advanced Drug Delivery Reviews*, **59**, 568–590.

39 Avdeef, A., Berger, C.M. and Brownell, C. (2000) pH-metric solubility. 2. Correlation between the acid–base titration and the

saturation shake-flask solubility–pH methods. *Pharmaceutical Research*, **17** (1), 85–89.

40 Stuart, M. and Box, K. (2005) Chasing equilibrium: measuring the intrinsic solubility of weak acids and bases. *Analytical Chemistry*, **77**, 983–990.

41 Llinas, A., Burley, J.C., Box, K.J., Glen, R.C. and Goodman, J.M. (2007) Diclofenac solubility: independent determination of the intrinsic solubility of three crystal forms. *Journal of Medicinal Chemistry*, **50**, 979–983.

42 Box, K.J., Volgyi, G., Baka, E., Stuart, M., Takacs-Novak, K. and Comer, J.E.A. (2006) Equilibrium versus kinetic measurements of aqueous solubility, and the ability of compounds to supersaturate in solution: a validation study. *Journal of Pharmaceutical Sciences*, **95** (6), 1298–1307.

43 Llinas, A., Box, K.J., Burley, J.C., Glen, R.C. and Goodman, J.M. (2007) A new method for the reproducible generation of polymorphs: two forms of sulindac with very different solubilities. *Journal of Applied Crystallography*, **40**, 379–381.

44 Bruneau, P. (2001) Search for predictive generic model of aqueous solubility using Bayesian neural nets. *Journal of Chemical Information and Computer Sciences*, **41**, 1605–1616.

45 Leach, A.G., Jones, H.D., Cosgrove, D.A., Kenny, P.W., Ruston, L., Macfaul, P., Wood, J.M., Colclough, N. and Law, B. (2006) Matched molecular pairs as a guide in the optimization of pharmaceutical properties: a study of aqueous solubility, plasma protein binding and oral exposure. *Journal of Medicinal Chemistry*, **49** (23), 6672–6682.

46 Haubertin, D.Y. and Bruneau, P. (2007) A database of historically observed chemical replacements. *Journal of Chemical Information and Modeling*, **47**, 1294–1302.

3
Gastrointestinal Dissolution and Absorption of Class II Drugs

Arik S. Dahan and Gordon L. Amidon

Abbreviations

BA/BE	Bioavailability/bioequivalence
BCS	Biopharmaceutics Classification System
CMC	Critical micelle concentration
FDA	Food and Drug Administration
GI	Gastrointestinal
IR	Immediate release
IVIVC	*In vitro–in vivo* correlation
NSAIDs	Nonsteroidal anti-inflammatory drugs

Symbols

A_n	Absorption number
C_S	Equilibrium solubility
D	Diffusion coefficient
D_0	Dose number
D_n	Dissolution number
P_{eff}	Effective permeability
t_{abs}^{-1}	Effective absorption rate constant
t_{Diss}	Dissolution time
t_{res}	Residence time

3.1 Introduction

Modern drug discovery techniques (i.e., advances in *in vitro* high-throughput screening methods, the introduction of combinatorial chemistry) have resulted in

an increase in the number of low water solubility drug substances being selected as drug candidates. According to some estimates, more than 40% of new drug candidates are lipophilic and exhibit poor water solubility [1–3]. With very few exceptions, dissolution of the drug substances in the aqueous gastrointestinal (GI) milieu is a prerequisite for its absorption following oral administration. Hence, low-solubility compounds often suffer from limited oral bioavailability. A great challenge facing the pharmaceutical scientist is making these molecules into orally administered medications with sufficient bioavailability. This chapter reviews the fundamentals of low-solubility, high-permeability drug substances and the intestinal absorption process, including introduction to the Biopharmaceutics Classification System (BCS) focusing on Class II drugs (see Chapter 19). We will discuss the relevant variables affecting the absorption process of these compounds. In addition, this chapter provides a perspective on regulatory issues concerning low-solubility, high-permeability drug substances.

3.2 Drug Absorption and the BCS

The absorption of drugs following oral administration is a cascade of complex events, and the rate and extent of the drug absorption are affected by many factors. These include physicochemical factors (e.g., pK_a, solubility, stability, diffusivity, lipophilicity, surface area, particle size, and crystal form), physiological factors (e.g., GI pH, GI blood flow, gastric emptying, transit time through the different GI segments, and absorption mechanisms), and factors related to the dosage form (e.g., tablet, capsule, solution, suspension, emulsion, and gel) [4, 5].

When Fick's first law is applied to a membrane, the absorption of a drug across the GI mucosal surface under sink conditions can be written as

$$J_W = P_W \times C_W = \frac{dM}{dt} \times \frac{1}{A}, \tag{3.1}$$

where J_W is the mass transport across the GI wall (mass/area/time), P_W is the effective permeability, C_W is the concentration of the drug at the membrane, and A is the surface area. As developed by Amidon *et al.* [6–8], the analysis of this equation reveals that the fundamental events controlling oral drug absorption are the permeability of the drug through the GI membrane, the dissolution of the drug in the GI milieu, and the dose. These key parameters are characterized in the BCS by three dimensionless numbers [7]: absorption number (A_n), dissolution number (D_n), and dose number (D_0). These numbers take into account both physicochemical and physiological parameters and are fundamental to the oral absorption process.

The absorption number (A_n) is the ratio of permeability (P_{eff}) and the intestinal radius (R) multiplied by the residence time (t_{res}), which can be interpreted as the effective absorption rate constant (t_{abs}^{-1}) times the residence time:

$$A_n = \text{absorption number} = \frac{P_{eff}}{R} t_{res} = t_{abs}^{-1} t_{res}. \tag{3.2}$$

The dissolution number (D_n) is the ratio of the residence time and the dissolution time (t_{Diss}), which comprises the equilibrium solubility (C_S), diffusivity (D), density (ρ), the initial particle radius (r_0), and the intestinal residence time (t_{res}):

$$D_n = \text{dissolution number} = \frac{DC_S}{r_0} = \frac{4\pi r_0^2}{(4/3)\pi r_0^3 \rho} t_{res} = \frac{3t_{res}DC_S}{\rho r_0^2} = \frac{t_{res}}{t_{Diss}}. \tag{3.3}$$

Finally, the dose number (D_0) is the ratio of dose to dissolved drug:

$$D_0 = \text{dose number} = \frac{M_0/V_0}{C_S}, \tag{3.4}$$

where C_S is the equilibrium solubility, M_0 is the dose, and V_0 is the volume of water taken with the dose, which is generally set to be 250 ml. This volume was selected based on a typical bioequivalence study that administered an 8 oz (240 ml) glass of water with the oral dosage form. Thus, 250 ml, allowing a small GI residual volume, represents the initial gastrointestinal volume to which an oral dosage form is exposed in the fasting state. This number may be viewed as the number of glasses of water required to dissolve the drug dose.

Based on their solubility and intestinal permeability characteristics, drug substances have been classified into one of the four categories according to the BCS proposed by Amidon *et al.* [6] (Figure 3.1) (see Chapter 19):

- *BCS Class I:* High-solubility, high-permeability drugs. BCS Class I drugs are generally very well absorbed. An immediate release (IR) product of this class is

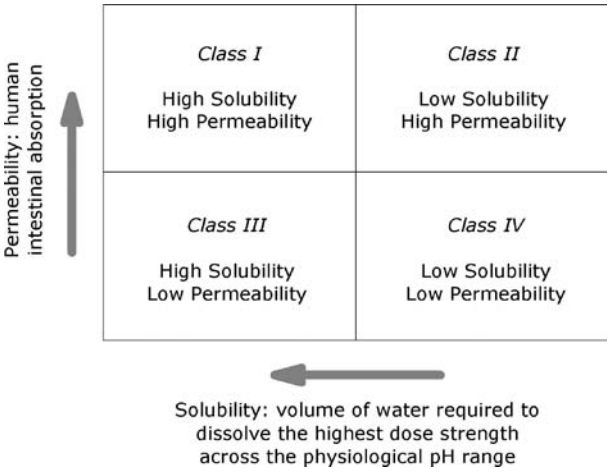

Figure 3.1 The Biopharmaceutics Classification System as defined by Amidon *et al.* [6]. The BCS is a classification of drug substances according to their solubility and permeability properties, in order to stand for the most fundamental view of the drug intestinal absorption process following oral administration.

expected to yield 100% intestinal absorption if at least 85% of the drug is dissolved within 30 min across the physiological pH. Hence, a waiver is granted for bioavailability/bioequivalence (BA/BE) studies of BCS Class I IR drug products.

- *BCS Class II:* Low-solubility, high-permeability drugs. These drugs are the main scope of this chapter. In general, BCS Class II drug products are likely to be limited by the dissolution/solubility rate.
- *BCS Class III:* High-solubility, low-permeability drugs. The intestinal absorption of this class of drugs will be limited by the permeability rate, as the dissolution is likely to occur rapidly. Hence, it has been suggested that as long as the drug product does not contain permeability modifying agents, a waiver for BA/BE studies for this class of drugs should be considered [9–12].
- *BCS Class IV:* Low-solubility, low-permeability drugs. These drugs are characterized by very poor oral bioavailability and tend to exhibit very large inter- and intrasubject variability. Hence, unless the dose is very low, they are generally poor oral drug candidates [1].

This BCS is one of the most significant prognostic tools created to facilitate product development in recent years and has been adopted by the US Food and Drug Administration (FDA) for setting BA/BE standards for drug product approval. The validity and applicability of the BCS have been the subject of extensive research and discussion, and classification of many drugs by the BCS is available in the literature [13–16]. Of particular interest are BCS Class II low-solubility, high-permeability drug substances, which account for the majority of new chemical entities. This chapter will focus on the different aspects of the intestinal absorption process of this class of drugs.

3.3 Class II Drugs

Being low-solubility, high-permeability compounds, Class II drug substances are characterized by high absorption number (A_n) and typically a high dose number (D_0). In these cases, dissolution might play a major role in the rate and extent of the oral absorption. In general, the dissolution of low-solubility drugs is low, that is, $D_n < 1$, while A_n and D_0 are high. In cases where both A_n and D_n are low, the compound will be classified as a Class IV drug [17, 18].

The intestinal absorption of Class II drug substances can be broadly viewed as dissolution limited or solubility limited. The concentration of the drug in the GI tract milieu will be determined by dissolution rate, while the upper limit will be the solubility. The classical example, still relevant today, which illustrates the effect of dissolution number and dose number on the fraction of dose absorbed of highly permeable drugs, is the case of digoxin and griseofulvin. A typical profile of the fraction of dose absorbed as a function of the dissolution number and the dose number for a large absorption number (i.e., highly permeable drug) is shown in

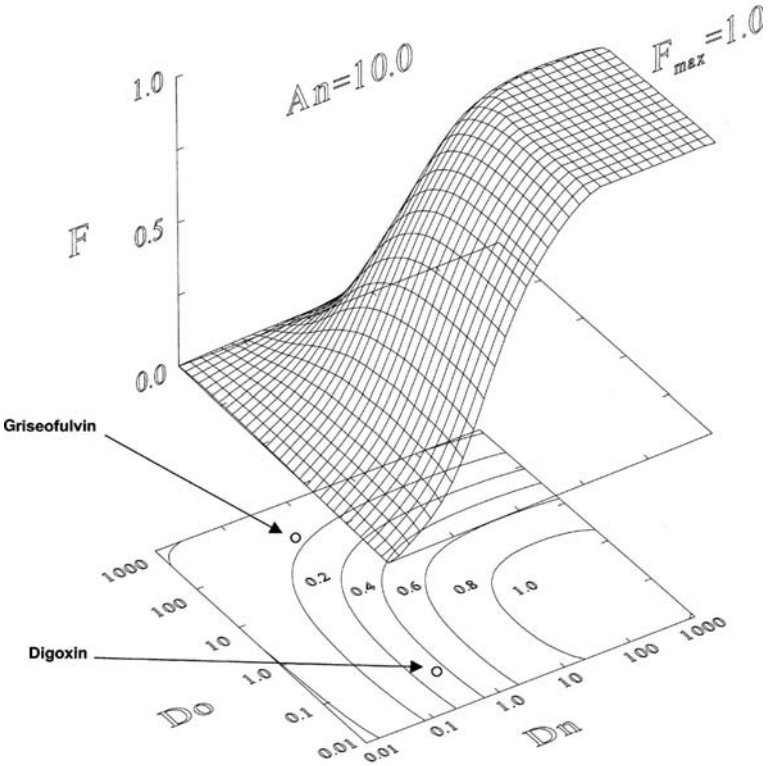

Figure 3.2 Graph of estimated fraction dose absorbed (F) vs dissolution number (D_n) and dose number (D_0) for a high permeability drug [6]. The dose number and the dissolution number of digoxin and griseofulvin are marked in the figure.

Figure 3.2. It can be seen that for high A_n, the critical range of the dose number and the dissolution number is around 1, where sharp changes in the fraction of drug absorbed are obtained due to small changes in D_0 and D_n [6].

Digoxin and griseofulvin have about the same solubility (~20 µg/ml), but a very different dose (0.5 and 500 mg, respectively). Consequently, while digoxin has a very low dose number (0.08), griseofulvin has a dose number, D_0, of 133, which indicates that over 33 l of water is required to dissolve a single griseofulvin dose.

The dose number and the dissolution number of digoxin and griseofulvin are marked in Figure 3.2. It can be seen that for digoxin fraction of drug absorbed is highly dependent upon the dissolution number. A complete intestinal absorption can be expected for digoxin if the drug particle size is small enough (i.e., high D_n); however, digoxin might be a dissolution rate limited drug if the drug particle size is too large (small D_n) [6, 19, 20]. Hence, micronized digoxin powder will lead to a faster dissolution rate, and the intestinal residence time would be sufficient for complete absorption. However, changes in griseofulvin D_n alone would not be sufficient to

influence the fraction of the drug absorbed. Micronization of the drug powder is not expected to improve griseofulvin absorption unless accompanied by reduced dose number, for example, by formulation that enables efficient solubilization in the GI milieu [21, 22]. Without that, griseofulvin absorption will be solubility limited, and complete absorption of the drug cannot be achieved.

3.4 GI Physiological Variables Affecting Class II Drug Dissolution

With very few exceptions, dissolution of the drug substance in the GI tract milieu is a prerequisite for drug absorption following oral administration. For Class II compounds, the rate-limiting factor in their intestinal absorption is dissolution /solubility [23–25]. Hence, in-depth understanding of this process is essential in the oral delivery of low-solubility compounds. Factors governing the dissolution process can be directly identified from the following equation, based on the Nernst–Brunner and Levich modifications of the Noyes–Whitney model [26–28]:

$$\frac{dX_d}{dt} = \frac{A \times D}{h}\left(C_S - \frac{X_d}{V}\right). \tag{3.5}$$

The dissolution rate is a function of the surface area of the solid drug (A), the diffusion coefficient of the drug (D), the effective diffusion boundary layer thickness adjacent to the dissolving surface (h), the saturation solubility of the drug (C_S), the volume of the fluid available for dissolution (V), and the amount of drug already dissolved (X_d). Thus, the rate of dissolution is highly affected by the physicochemical properties of the drug and by many GI physiological factors that will be discussed in this section.

3.4.1 Bile Salts

Bile acids affect both solubility and dissolution by micellization and wetting effects [29, 30]. Hence, they play a significant role in Class II drugs' intestinal absorption, which is a dissolution/solubility rate limited process. The bile fluid is secreted from hepatocytes in the liver and stored and concentrated in the gall bladder before release into the small intestine. The major organic solutes of the bile are bile acids, phospholipids (particularly lecithin), and cholesterol. The bile acids are derivatives of cholesterol in which hydroxyl and carboxylic acid are attached to the steroid moiety, converting it into a powerful natural surfactant. Average typical intestinal concentrations for bile acids and phospholipids are 5 and 0.2 mM, respectively, in the fasting state [31, 32] and 15 and 4 mM, respectively, in the fed state [32]. Above their critical micelle concentration (CMC), these biliary secretions aid in drug dissolution by forming submicron mixed micelles in which the low water-soluble molecule is solubilized and gets to the absorptive membrane of the enterocyte [33–35].

Enhanced solubility of the low water-soluble drug may be obtained by bile salts through the wetting mechanism [36, 37]. This is the main mechanism when the bile salts are present at a level below their CMC [35, 38].

3.4.2 GI pH

BCS II class includes nonionizable substances (e.g., carbamazepine, griseofulvin) and ionizable compounds, either acids (e.g., ibuprofen) or bases (e.g., diazepam). For nonionizable drugs, pH changes along the GI tract would not have an impact on drug solubilization/dissolution. However, the intestinal absorption of BCS Class II ionizable drugs' is highly dependent on pH [30, 39]. Generally, aqueous solubility is directly proportional to the number of hydrogen bonds that can be formed with water, and hence the ionized form exhibits greater aqueous solubility than do the unionized species. The nonionized form has generally better membrane permeability than the ionized species; however, since permeability is not the rate-limiting step for Class II drugs absorption process, this effect is less significant. Hence, for these drugs, an alteration in the degree of conversion of the unionized drug to its ionized form upon dissolution as a function of the pH may dictate the rate of absorption.

Throughout the passage along the GI tract, a drug product experiences a wide pH range. Gastric pH highly depends upon food intake and values from 1 to 8 are reported, while the fasting-state stomach pH is 1.4–2.1 [40–42]. In general, the pH values in the small intestine are higher than those in the stomach, much less dependent upon food intake, and show an upward gradient from the proximal to the distal segments, covering a range of 4.4–7.4 [23, 40, 43].

For BCS Class II weak base drugs (e.g., dipyridamole, ketoconazole), ionization will occur in the gastric acidic environment, leading to a rapid dissolution in the stomach. As the drug is emptying from the stomach to the duodenum, the degree of ionization is significantly reduced due to the elevated pH, with possible precipitation of the drug [44, 45]. This leads to a complicated intestinal absorption pattern controlled by many factors including the extent of supersaturation and solid form of the weak base, pH, fluid volume, viscosity, and bile salts' concentration [30, 46, 47].

For BCS Class II weak acid drugs (e.g., ibuprofen, ketoprofen) with pK_a in the GI physiological range, extensive ionization is expected in the small intestine. As the intestinal pH is on average higher than the pK_a in more than one unit, the apparent solubility of the weak acid increases by 10–100-fold. Thus, the *in vivo* solubility and dissolution of these drugs would be high, presumably behaving more likely as Class I compounds, as discussed in Section 7.1 [38, 48, 49].

3.4.3 GI Transit

The two major components of the GI transit are the gastric residence time, dictated by the gastric emptying, and the small intestinal transit time. In general, the rate of gastric emptying is of significance in cases where dissolution is relatively fast [50]. For

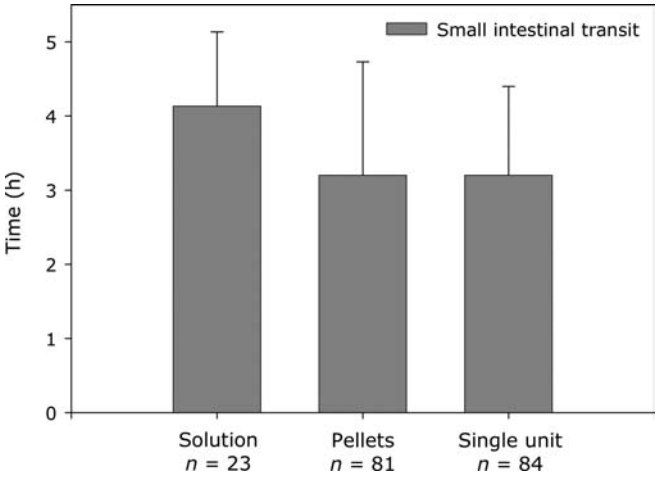

Figure 3.3 Human small intestinal transit time of different pharmaceutical dosage forms measured by γ-scintigraphy [40]. The intestinal transit time is fairly fixed and largely independent of the physical properties of the system or food intake.

BCS Class II drug substances, dissolution rate is expected to be slower than the gastric emptying, and hence this factor is not thought to be significant in their intestinal absorption.

The transit time through the small intestine has the potential to affect Class II intestinal absorption, as increased time in the main absorption site is expected to yield higher absorption. However, the intestinal transit time is fairly fixed and largely independent of food intake (i.e., fasting versus fed states) or the physical properties of the system (Figure 3.3) [40]. On average, the small intestinal transit time is around 3–4 h [51, 52].

3.4.4 Drug Particle Size

The particle size of the drug powder might be an important physical parameter in the dissolution rate, as shown in the case of digoxin (Section 3.3). Smaller particle size will lead to higher surface area available for dissolution, resulting in a faster dissolution rate [53, 54]. Hence, particularly for Class II dissolution rate limited drug substances, the dissolution rate is expected to increase proportionally with an increase in surface area, and the particle size will be a critical formulation variable. The density of particles might also affect the dissolution rate through alteration of the *in vivo* particle dispersion, as greater dispersion leads to improved dissolution [19, 55]. The effect of reduced particle size seems to depend upon food intake. It has been shown that under the fasting state, reduced particle size had a major effect on *in vitro* dissolution and *in vivo* oral absorption of DPC961, a BCS Class II reverse

transcriptase inhibitor, while no effect was observed under the fed state [56]. This may be attributed to the differences in the solubilization capacities in the fed and fasting states. Improved *in vivo* dissolution rate in humans was observed for decreased spironolactone particle size, however, with no influence on the relative bioavailability [57]. The authors suggested that the lack of difference between the bioavailability of the two particle sizes may be related to insufficient washout of particles after perfusion ends, reabsorption of surface active ingredients along the GI tract, relatively small difference in particle size, and the large inter- and intraindividual differences in pharmacokinetic variables [57].

In regard to the drug powder particle size, it is worth noting that it is the effective surface area that is important, that is, the surface area that is available to the dissolution fluid (the wetted surface), and not the actual particle size. This is important in the case of a highly hydrophobic drug in a dissolution medium that has poor wetting properties and in the case of a manufacturing process that changes the particle size during manufacture. In this case, decreased particle size will slow the dissolution rate [58, 59].

3.4.5
Volume Available for Dissolution

The volume of fluids available in the GI tract for drug dissolution depends on the volume of fluids coadministered with the drug, secretions into the GI lumen, and water flux across the gut wall. This factor is of high importance particularly for BCS Class II compounds, as higher volume of available fluids will enable the dissolution of higher amounts of drug. Average fluid volumes approximately representing the usual physiological range are 300–500 ml for the fasting-state stomach (although the volume may be as low as 20–30 ml) and 800–900 ml for the fed-state stomach; 500 ml for the fasting-state small intestine and 900–1000 ml for the fed-state small intestine [23, 60, 61] (although volumes in the upper small intestine in the fed state can reach as much as 1.5 l [62]).

3.5
In Vitro Dissolution Tests for Class II Drugs

As denoted above, the rate-limiting step in the oral absorption of Class II drug substances is often the *in vivo* dissolution [23–25]. Hence, a well-designed dissolution test should be capable of providing adequate *in vitro–in vivo* correlation (IVIVC).

3.5.1
Biorelevant Media

The choice of medium is expected to play a very important role in the dissolution of BCS Class II drug substances. The media used need to closely represent the *in vivo* conditions in the upper GI tract to achieve a meaningful IVIVC. As discussed in this

chapter, Class II drug dissolution depends on a wide variety of parameters, such as surfactants, pH, buffer capacity, ionic strength, and the volume available for dissolution. Class II dissolution test media often fail to produce adequate IVIVC due to composition that does not take into account these essential factors.

Examples of suitable media for simulating the composition of proximal GI tract include simulated gastric fluid (SGF) and surfactant, used to simulate the stomach conditions under the fasting state; long-life milk 3.5% fat, used to simulate the stomach conditions under fed state; fasting-state simulating intestinal fluid (FaSSIF), the medium used to represent fasting state in the proximal small intestine; and fed-state simulating intestinal fluid (FeSSIF), the fed-state proximal small intestine medium [23, 44, 61, 63]. Very good IVIVC was obtained with these media for the low-solubility drugs albendazole, danazol, ketoconazol, atovaquone, and troglitazone [44, 61, 64–66]. For these drugs, fed-state versus fasting-state effects, as well as formulation effects, could be predicted by appropriate dissolution tests, showing the potential of biorelevant dissolution tests to adequately simulate the *in vivo* GI tract milieu composition.

The relationship between the hydrodynamics in the GI tract and that in the current available dissolution tests is another factor that must be considered. It has been reported that, provided an appropriate composition is chosen for the dissolution test, the United States Pharmacopeia (USP) paddle apparatus can be used to reflect variations in hydrodynamic conditions in the upper GI tract [67–69]. However, more data are warranted, as this might insert uncertainty into the interpretation of dissolution tests, even when the composition of the GI milieu is well simulated.

3.5.2 Dynamic Lipolysis Model

One of the approaches to improve the oral bioavailability of Class II drug substances is the utilization of lipid-based drug delivery systems [1, 70, 71]. Enhanced dissolution/solubilization of the coadministered lipophilic drug by stimulation of biliary and pancreatic secretions is a major factor in this phenomenon [72]. Additional mechanisms by which lipid-based formulations might enhance the absorption of lipophilic drugs include presentation of the low water-soluble drug as a solution and hence avoiding the complexities associated with solid state; mild prolongation of GI tract residence time; possible reduced metabolism and efflux activity [73, 74]; and changing the intraenterocyte transport route by stimulation of the lymphatic transport pathway [75, 76].

Following oral administration, the lipidic component of the lipid-based formulation is subjected to enzymatic hydrolysis. Pancreatic lipase, upon complexation with colipase, acts at the surface of the emulsified triglyceride droplets to produce the corresponding 2-monoglyceride and two fatty acids. These amphiphilic lipid digestion products interact with the endogenous bile salts and phospholipids, forming colloidal structures holding different levels of surface activity, which enables the solubilization of the coadministered poorly water-soluble compound and prevents their precipitation in the aqueous GI tract milieu. In most cases, this process, which

maintains the poorly water-soluble drug in solution and prevents its precipitation, is thought to be the primary mechanism by which lipid-based drug delivery systems augment the oral absorption of lipophilic drugs [32, 77]. Owing to the dependence of lipid-based delivery systems' performance on GI processing, a meaningful release test of such formulations will require the presence of lipolytic enzymes that catalyze GI lipid digestion *in vivo* [78].

A dynamic *in vitro* lipolysis model, which provides simulation of the *in vivo* lipid digestion process, has been developed over the past few years [79–81]. This model has been used for assessing different lipid-based delivery systems, and a correlation between *in vitro* dissolution and *in vivo* absorption in the lipolysis model was reported for a number of low water-soluble drugs, including halofantrine [82], griseofulvin [83], and progesterone [84]. Overall, this model looks promising; however, the number of studies evaluating the IVIVC provided by this method is still limited, and a more thorough characterization of the model in different physiological conditions is warranted.

3.6
BCS-Based FDA Guidelines: Implications for Class II Drugs

The current FDA guidelines on waiver of *in vivo* BA/BE studies for BCS Class I drugs in rapid dissolution IR solid oral dosage form are generally considered highly conservative, especially with respect to the class boundaries of solubility, permeability, and dissolution. Thus, the possibility of modifying these boundaries and criteria to allow biowaivers for additional drug products has received increasing attention [24, 85–88].

3.6.1
Potential of Redefining BCS Solubility Class Boundary

Currently, drug substances are classified as high-solubility compounds if the highest strength is soluble in 250 ml or less of aqueous media throughout the pH range of 1.0–7.5. Three factors in this requirement are considered highly conservative and may be reevaluated: (1) the required pH range; (2) the nature of the media; and (3) the volume of the media [86, 88].

Under fasting state, the GI pH varies from 1.4 to 2.1 in the stomach, 4.9–6.4 in the duodenum, 4.4–6.6 in the jejunum, and 6.5–7.4 in the ileum [42, 89]. Hence, it seems reasonable to redefine the BCS class boundary pH range from 1.0–7.5 to 1.4–6.8. Moreover, if a drug product meets the dissolution criterion, that is, not less that 85% dissolved within 30 min, its dissolution process is probably completed during the jejunum, as it generally takes 85 min for a drug to reach the ileum [5, 90]. Thus, it might be reasonable to narrow the pH range requirement even more. This would somewhat ease the requirement for Class II basic drug substances. Many ionizable Class II acidic drugs have low solubility at low pH, but they are highly soluble at higher pH values. For example, most nonsteroidal anti-inflammatory drugs

(NSAIDs) are poorly soluble in the stomach but are highly soluble in the distal intestine, which is the main absorption region of most compounds. These drugs are classified as Class II drugs according to the current solubility definitions. However, their absolute human bioavailability is 90% or higher, thus exhibiting BCS Class I behavior [91]. In the same manner, the NSAID ketoprofen is classified as Class II drug due to low solubility at low pH values; however, it has been demonstrated that this drug behaves in a manner essentially equivalent to Class I drugs and could be considered for a waiver of BA/BE studies [38, 48]. Yazdanian *et al.* [92] evaluated the possible impact of changing the current high-solubility definition on the BCS classification of 18 acidic NSAIDs. While 15 of the 18 drugs were classified as Class II based on the current high-solubility definition, 8 of the 18 could be classified as Class I by considering pH 5 and above. Overall, consideration for an intermediate solubility classification for such compounds, which will take into account only the intestinal relevant pH range, seems warranted.

While the solubility classification is based on the dissolution of the drug in aqueous buffers, the *in vivo* conditions for drug dissolution contain bile salts and phospholipids, even under fasting state. As denoted in Section 3.4.1, these are powerful natural surfactants that aid in the dissolution/solubilization of the drug substances. A medium that more adequately reflects physiological conditions may be more relevant in assessing *in vivo* solubility and dissolution, and potentially, drugs that are classified as Class II according to the current solubility definitions could be classified as Class I under these conditions [66, 86, 88].

Under the fasting state, the physiological volume of the small intestine varies from 50 to 1100 ml with an average of 500 ml [17, 93]. Upon administration, the drug is usually ingested with 250 ml of water that is immediately available to dissolve the solid particles in the stomach. If the drug is not in solution on gastric emptying, it is then exposed to additional fluids in the small intestine. Hence, the dose volume of 250 ml is a conservative estimate of the actual *in vivo* volume available for solubilization and dissolution. However, the wide variability of the small intestinal fluid volume makes an appropriate volume definition difficult to set.

3.6.2
Biowaiver Extension Potential for Class II Drugs

As discussed above, the rate-limiting step in the oral absorption of Class II drug substances is likely to be the *in vivo* dissolution [23–25]. For Class II dissolution rate limited drugs, hence, if *in vivo* dissolution can be estimated *in vitro*, an *in vitro–in vivo* correlation may be established. As discussed in Section 3.5, such media have been developed, and an adequate IVIVC was shown for number of Class II drugs. However, due to the numerous *in vivo* parameters involved, it appears that more research is needed to develop uniform dissolution media reflecting *in vivo* dissolution conditions, to establish an adequate IVIVC, and to asses the risk of bioinequivalence [86, 88]. In addition, the relationship between the hydrodynamics in the currently available dissolution tests and the actual *in vivo* situation is not adequately characterized and might interfere to obtain the correlation.

As discussed in detail above, the intestinal absorption of Class II drug substances may be limited by dissolution rate or solubility rate. In the latter case, when the absorption is limited by the drug equilibrium solubility, an IVIVC is not likely to be obtained. The GI tract drug concentrations in this case will be close to the saturation concentration, and since standard dissolution tests are carried out under sink conditions, they can predict only processes occurring well below the saturation concentration [85]. Hence, at this point, Class II solubility rate limited drugs are probably poor candidates for BA/BE waiver.

3.7 Conclusions

Looking into the future, more BCS Class II drug candidates are likely to be produced, and the delivery of these molecules through the oral route is expected to be a continuing challenge.

In this chapter, we have reviewed the rate and extent of oral absorption of this class of drugs and discussed the numerous factors, physicochemical, physiological, and dosage form, that must be considered in effectively delivering these drug candidates. In-depth comprehension of these factors and their influence on the intestinal absorption process is essential in the effective oral delivery of BCS Class II drug substances.

References

1 Dahan, A. and Hoffman, A. (2006) *Enhancement in Drug Delivery* (eds E. Touitou and B.W. Barry), CRC Press, pp. 111–127.

2 Lipinski, C.A., Lombardo, F., Dominy, B.W. and Feeney, P.J. (2001) Experimental and computational approaches to estimate solubility and permeability in drug discovery and development settings. *Advanced Drug Delivery Reviews*, **46** (1–3), 3.

3 van de Waterbeemd, H., Smith, D.A., Beaumont, K. and Walker, D.K. (2001) Property-based design: optimization of drug absorption and pharmacokinetics. *Journal of Medicinal Chemistry*, **44** (9), 1313–1333.

4 Lennernas, H. (1998) Human intestinal permeability. *Journal of Pharmaceutical Sciences*, **87** (4), 403–410.

5 Yu, L.X., Lipka, E., Crison, J.R. and Amidon, G.L. (1996) Transport approaches to the biopharmaceutical design of oral drug delivery systems: prediction of intestinal absorption. *Advanced Drug Delivery Reviews*, **19** (3), 359.

6 Amidon, G.L., Lennernas, H., Shah, V.P. and Crison, J.R. (1995) A theoretical basis for a biopharmaceutic drug classification: the correlation of *in vitro* drug product dissolution and *in vivo* bioavailability. *Pharmaceutical Research*, **12** (3), 413.

7 Oh, D.M., Curl, R.L. and Amidon, G.L. (1993) Estimating the fraction dose absorbed from suspensions of poorly soluble compounds in humans: a mathematical model. *Pharmaceutical Research*, **10** (2), 264.

8 Sinko, P.J., Leesman, G.D. and Amidon, G.L. (1991) Predicting fraction dose

absorbed in humans using a macroscopic mass balance approach. *Pharmaceutical Research*, **8** (8), 979.

9 Becker, C., Dressman, J.B., Amidon, G.L., Junginger, H.E., Kopp, S., Midha, K.K., Shah, V.P., Stavchansky, S. and Barends, D.M. (2008) Biowaiver monographs for immediate release solid oral dosage forms: pyrazinamide. *Journal of Pharmaceutical Sciences*, **97** (9), 3709–3720.

10 Blume, H.H. and Schug, B.S. (1999) The biopharmaceutics classification system (BCS): Class III drugs – better candidates for BA/BE waiver? *European Journal of Pharmaceutical Sciences*, **9** (2), 117.

11 Cheng, C.L., Yu, L.X., Lee, H.L., Yang, C.Y., Lue, C.S. and Chou, C.H. (2004) Biowaiver extension potential to BCS Class III high solubility-low permeability drugs: bridging evidence for metformin immediate-release tablet. *European Journal of Pharmaceutical Sciences*, **22** (4), 297.

12 Jantratid, E., Prakongpan, S., Amidon, G.L. and Dressman, J. (2006) Feasibility of biowaiver extension to biopharmaceutics classification system class III drug products: cimetidine. *Clinical Pharmacokinetics*, **45** (4), 385–399.

13 Kasim, N.A., Whitehouse, M., Ramachandran, C., Bermejo, M., Lennernäs, H., Hussain, A.S., Junginger, H.E., Stavchansky, S.A., Midha, K.K., Shah, V.P. and Amidon, G.L. (2004) Molecular properties of WHO essential drugs and provisional biopharmaceutical classification. *Molecular Pharmaceutics*, **1** (1), 85–96.

14 Lindenberg, M., Kopp, S. and Dressman, J.B. (2004) Classification of orally administered drugs on the World Health Organization Model list of Essential Medicines according to the biopharmaceutics classification system. *European Journal of Pharmaceutical Sciences*, **58** (2), 265.

15 Takagi, T., Ramachandran, C., Bermejo, M., Yamashita, S., Yu, L.X. and Amidon, G.L. (2006) A provisional biopharmaceutical classification of the top 200 oral drug products in the United States, Great Britain, Spain, and Japan. *Molecular Pharmaceutics*, **3** (6), 631–643.

16 Yang, Y., Faustino, P.J., Volpe, D.A., Ellison, C.D., Lyon, R.C. and Yu, L.X. (2007) Biopharmaceutics classification of selected beta-blockers: solubility and permeability class membership. *Molecular Pharmaceutics*, **4** (4), 608–614.

17 Lobenberg, R. and Amidon, G.L. (2000) Modern bioavailability, bioequivalence and biopharmaceutics classification system. New scientific approaches to international regulatory standards. *European Journal of Pharmaceutics and Biopharmaceutics*, **50** (1), 3–12.

18 Martinez, M.N. and Amidon, G.L. (2002) A mechanistic approach to understanding the factors affecting drug absorption: a review of fundamentals. *Journal of Clinical Pharmacology*, **42** (6), 620–643.

19 Dressman, J. and Fleisher, D. (1986) Mixing-tank model for predicting dissolution rate control or oral absorption. *Journal of Pharmaceutical Sciences*, **75** (2), 109–116.

20 Jounela, A., Pentikainen, P. and Sothmann, A. (1975) Effect of particle size on the bioavailability of digoxin. *European Journal of Clinical Pharmacology*, **8** (5), 365–370.

21 Crison, J.R., Weiner, N.D. and Amidon, G.L. (1997) Dissolution media for *in vitro* testing of water-insoluble drugs: effect of surfactant purity and electrolyte on *in vitro* dissolution of carbamazepine in aqueous solutions of sodium lauryl sulfate. *Journal of Pharmaceutical Sciences*, **86** (3), 384–388.

22 Shah, V.P., Konecny, J.J., Everett, R.L., McCullough, B., Noorizadeh, A.C. and Skelly, J.P. (1989) *In vitro* dissolution profile of water-insoluble drug dosage forms in the presence of surfactants. *Pharmaceutical Research*, **6** (7), 612.

23 Dressman, J.B., Amidon, G.L., Reppas, C. and Shah, V.P. (1998) Dissolution testing as a prognostic tool for oral drug absorption: immediate release dosage forms. *Pharmaceutical Research*, **15** (1), 11.

24 Fagerholm, U. (2007) Evaluation and suggested improvements of the Biopharmaceutics Classification System (BCS). *The Journal of Pharmacy and Pharmacology*, **59**, 751.

25 Wilding, I. (1999) Evolution of the biopharmaceutics classification system (BCS) to oral modified release (MR) formulations; what do we need to consider? *European Journal of Pharmaceutical Sciences*, **8** (3), 157–159.

26 Levich, V. (1962) *Physicochemical Hydrodynamics*, Prentice-Hall, Englewood Cliffs, NJ.

27 Nernst, W. and Brunner, E. (1904) Theorie der reaktionsgeschwindigkeit in heterogenen systemen. *Zeitschrift für Physikalische Chemie*, **47**, 52–110.

28 Noyes, A. and Whitney, W. (1897) The rate of solution of solid substances in their own solutions. *Journal of the American Chemical Society*, **19**, 930–934.

29 Bakatselou, V., Oppenheim, R.C. and Dressman, J.B. (1991) Solubilization and wetting effects of bile salts on the dissolution of steroids. *Pharmaceutical Research*, **8** (12), 1461.

30 Sheng, J.J. (2007) Toward an *in vitro* bioequivalence test. PhD Thesis, University of Michigan, Ann Arbor.

31 Persson, E., Gustafsson, A.-S., Carlsson, A., Nilsson, R., Knutson, L., Forsell, P., Hanisch, G., Lennernas, H. and Abrahamsson, B. (2005) The effects of food on the dissolution of poorly soluble drugs in human and in model small intestinal fluids. *Pharmaceutical Research*, **22** (12), 2141.

32 Porter, C.J.H., Trevaskis, N.L. and Charman, W.N. (2007) Lipids and lipid-based formulations: optimizing the oral delivery of lipophilic drugs. *Nature Reviews. Drug Discovery*, **6** (3), 231.

33 Amidon, G.E., Higuchi, W. and Ho, N. (1982) Theoretical and experimental studies of transport of micelle-solubilized solutes. *Journal of Pharmaceutical Sciences*, **71** (1), 77–84.

34 Granero, G., Ramachandran, C. and Amidon, G.L. (2005) Dissolution and solubility behavior of fenofibrate in sodium lauryl sulfate solutions. *Drug Development and Industrial Pharmacy*, **31** (9), 917–922.

35 Horter, D. and Dressman, J.B. (2001) Influence of physicochemical properties on dissolution of drugs in the gastrointestinal tract. *Advanced Drug Delivery Reviews*, **46** (1–3), 75.

36 Luner, P.E. (2000) Wetting properties of bile salt solutions and dissolution media. *Journal of Pharmaceutical Sciences*, **89** (3), 382–395.

37 Luner, P.E. and Kamp, D.V. (2001) Wetting behavior of bile salt–lipid dispersions and dissolution media patterned after intestinal fluids. *Journal of Pharmaceutical Sciences*, **90** (3), 348–359.

38 Sheng, J.J., Kasim, N.A., Chandrasekharan, R. and Amidon, G.L. (2006) Solubilization and dissolution of insoluble weak acid, ketoprofen: effects of pH combined with surfactant. *European Journal of Pharmaceutical Sciences*, **29** (3–4), 306.

39 Balakrishnan, A., Rege, B.D., Amidon, G.L. and Polli, J.E. (2004) Surfactant-mediated dissolution: contributions of solubility enhancement and relatively low micelle diffusivity. *Journal of Pharmaceutical Sciences*, **93** (8), 2064–2075.

40 Davis, S.S., Hardy, J.G. and Fara, J.W. (1986) Transit of pharmaceutical dosage forms through the small intestine. *Gut*, **27** (8), 886–892.

41 Lindahl, A., Ungell, A.L., Knutson, L. and Lennernäs, H. (1997) Characterization of fluids from the stomach and proximal jejunum in men and women. *Pharmaceutical Research*, **14** (4), 497.

42 Oberle, R. and Amidon, G.L. (1987) The influence of variable gastric emptying and intestinal transit rates on the plasma level curve of cimetidine: an explanation for the double peak phenomenon. *Journal of Pharmacokinetics and Biopharmaceutics*, **15** (5), 529–544.

43 Kalantzi, L., Goumas, K., Kalioras, V., Abrahamsson, B., Dressman, J. and Reppas, C. (2006) Characterization of the human upper gastrointestinal contents under conditions simulating bioavailability/bioequivalence studies. *Pharmaceutical Research*, **23** (1), 165.

44 Galia, E., Nicolaides, E., Hörter, D., Löbenberg, R., Reppas, C. and Dressman, J.B. (1998) Evaluation of various dissolution media for predicting *in vivo* performance of class I and II drugs. *Pharmaceutical Research*, **15** (5), 698.

45 Kalantzi, L., Persson, E., Polentarutti, B., Abrahamsson, B., Goumas, K., Dressman, J. and Reppas, C. (2006) Canine intestinal contents vs. simulated media for the assessment of solubility of two weak bases in the human small intestinal contents. *Pharmaceutical Research*, **23** (6), 1373.

46 Russell, T.L., Berardi, R.R., Barnett, J.L., O'Sullivan, T.L., Wagner, J.G. and Dressman, J.B. (1994) pH-related changes in the absorption of dipyridamole in the elderly. *Pharmaceutical Research*, **11** (1), 136.

47 Zhou, R., Moench, P., Heran, C., Lu, X., Mathias, N., Faria, T.N., Wall, D.A., Hussain, M.A., Smith, R.L. and Sun, D. (2005) pH-dependent dissolution *in vitro* and absorption *in vivo* of weakly basic drugs: development of a canine model. *Pharmaceutical Research*, **22** (2), 188.

48 Granero, G., Ramachandran, C. and Amidon, G.L. (2006) Rapid *in vivo* dissolution of ketoprofen: implications on the biopharmaceutics classification system. *Pharmazie*, **61** (8), 673–676.

49 Jinno, J., Oh, D.M., Crison, J.R. and Amidon, G.L. (2000) Dissolution of ionizable water-insoluble drugs: the combined effect of pH and surfactant. *Journal of Pharmaceutical Sciences*, **89** (2), 268–274.

50 Langguth, P., Lee, K., Spahn-Langguth, H. and Amidon, G.L. (1994) Variable gastric emptying and discontinuities in drug absorption profiles: dependence of rates and extent of cimetidine absorption on motility phase and pH. *Biopharmaceutics & Drug Disposition*, **15** (9), 719–746.

51 Yu, L.X. and Amidon, G.L. (1999) A compartmental absorption and transit model for estimating oral drug absorption. *International Journal of Pharmaceutics*, **186** (2), 119.

52 Yu, L.X., Crison, J.R. and Amidon, G.L. (1996) Compartmental transit and dispersion model analysis of small intestinal transit flow in humans. *International Journal of Pharmaceutics*, **140** (1), 111.

53 Dressman, J.B., Vertzoni, M., Goumas, K. and Reppas, C. (2007) Estimating drug solubility in the gastrointestinal tract. *Advanced Drug Delivery Reviews*, **59** (7), 591.

54 Lobenberg, R., Kramer, J., Shah, V.P., Amidon, G.L. and Dressman, J.B. (2000) Dissolution testing as a prognostic tool for oral drug absorption: dissolution behavior of glibenclamide. *Pharmaceutical Research*, **17** (4), 439.

55 Sinko, C.M., Yee, A.F. and Amidon, G.L. (1990) The effect of physical aging on the dissolution rate of anionic polyelectrolytes. *Pharmaceutical Research*, **7** (6), 648.

56 Aungst, B.J., Nguyen, N.H., Taylor, N.J. and Bindra, D.S. (2002) Formulation and food effects on the oral absorption of a poorly water soluble, highly permeable antiretroviral agent. *Journal of Pharmaceutical Sciences*, **91** (6), 1390–1395.

57 Bonlokke, L., Hovgaard, L., Kristensen, H.G., Knutson, L. and Lennernäs, H. (2001) Direct estimation of the *in vivo* dissolution of spironolactone, in two particle size ranges, using the single-pass perfusion technique (Loc-I-Gut(R)) in humans. *European Journal of Pharmaceutical Sciences*, **12** (3), 239.

58 Kostewicz, E.S., Brauns, U., Becker, R. and Dressman, J.B. (2002) Forecasting the oral absorption behavior of poorly soluble weak bases using solubility and dissolution studies in biorelevant media. *Pharmaceutical Research*, **19** (3), 345.

59 Takano, R., Sugano, K., Higashida, A., Hayashi, Y., Machida, M., Aso, Y. and

Yamashita, S. (2006) Oral absorption of poorly water-soluble drugs: computer simulation of fraction absorbed in humans from a miniscale dissolution test. *Pharmaceutical Research*, **23** (6), 1144.

60 Custodio, J.M., Wu, C.Y. and Benet, L.Z. (2008) Predicting drug disposition, absorption/elimination/transporter interplay and the role of food on drug absorption. *Advanced Drug Delivery Reviews*, **60** (6), 717.

61 Dressman, J.B. and Reppas, C. (2000) *In vitro–in vivo* correlations for lipophilic, poorly water-soluble drugs. *European Journal of Pharmaceutical Sciences*, **11** (Suppl. 2), S73.

62 Fordtran, J. and Locklear, T. (1966) Ionic constituents and osmolality of gastric and small-intestinal fluids after eating. *The American Journal of Digestive Diseases*, **11** (7), 503–521.

63 Macheras, P., Koupparis, M. and Tsaprounis, C. (1986) Drug dissolution studies in milk using the automated flow injection serial dynamic dialysis technique. *International Journal of Pharmaceutics*, **33** (1–3), 125.

64 Galia, E., Horton, J. and Dressman, J.B. (1999) Albendazole generics – a comparative *in vitro* study. *Pharmaceutical Research*, **16** (12), 1871.

65 Nicolaides, E., Symillides, M., Dressman, J.B. and Reppas, C. (2001) Biorelevant dissolution testing to predict the plasma profile of lipophilic drugs after oral administration. *Pharmaceutical Research*, **18** (3), 380.

66 Vertzoni, M., Dressman, J., Butler, J., Hempenstall, J. and Reppas, C. (2005) Simulation of fasting gastric conditions and its importance for the *in vivo* dissolution of lipophilic compounds. *European Journal of Pharmaceutics and Biopharmaceutics*, **60** (3), 413.

67 Scholz, A., Abrahamsson, B., Diebold, S.M., Kostewicz, E., Polentarutti, B.I., Ungell, A.-L. and Dressman, J.B. (2002) Influence of hydrodynamics and particle size on the absorption of felodipine in labradors. *Pharmaceutical Research*, **19** (1), 42.

68 Scholz, A., Kostewicz, E., Abrahamsson, B. and Dressman, J.B. (2003) Can the USP paddle method be used to represent *in-vivo* hydrodynamics? *The Journal of Pharmacy and Pharmacology*, **55**, 443.

69 Sheng, J.J., Sirois, P.J., Dressman, J.B. and Amidon, G.L. (2008) Particle diffusional layer thickness in a USP dissolution apparatus II: a combined function of particle size and paddle speed. *Journal of Pharmaceutical Sciences*, in press.

70 Charman, W.N. (2000) Lipids, lipophilic drugs, and oral drug delivery – some emerging concepts. *Journal of Pharmaceutical Sciences*, **89** (8), 967–978.

71 Gershanik, T. and Benita, S. (2000) Self-dispersing lipid formulations for improving oral absorption of lipophilic drugs. *European Journal of Pharmaceutics and Biopharmaceutics*, **50** (1), 179–188.

72 Fleisher, D., Li, C., Zhou, Y., Pao, L.H. and Karim, A. (1999) Drug, meal and formulation interactions influencing drug absorption after oral administration. Clinical implications. *Clinical Pharmacokinetics*, **36** (3), 233–254.

73 Dintaman, J.M. and Silverman, J.A. (1999) Inhibition of P-glycoprotein by D-α-tocopheryl polyethylene glycol 1000 succinate (TPGS). *Pharmaceutical Research*, **16** (10), 1550.

74 Nerurkar, M.M., Burton, P.S. and Borchardt, R.T. (1996) The use of surfactants to enhance the permeability of peptides through Caco-2 cells by inhibition of an apically polarized efflux system. *Pharmaceutical Research*, **13** (4), 528.

75 Dahan, A. and Hoffman, A. (2005) Evaluation of a chylomicron flow blocking approach to investigate the intestinal lymphatic transport of lipophilic drugs. *European Journal of Pharmaceutical Sciences*, **24** (4), 381–388.

76 Gershkovich, P. and Hoffman, A. (2007) Effect of a high-fat meal on absorption and disposition of lipophilic compounds: the importance of degree of association with

triglyceride-rich lipoproteins. *European Journal of Pharmaceutical Sciences*, **32** (1), 24.

77 Tso, P. (1985) Gastrointestinal digestion and absorption of lipid. *Advances in Lipid Research*, **21**, 143–186.

78 Dahan, A. and Hoffman, A. (2008) Rationalizing the selection of oral lipid based drug delivery systems by an *in vitro* dynamic lipolysis model for improved oral bioavailability of poorly water soluble drugs. *Journal of Controlled Release*, **129** (1), 1–10.

79 Porter, C.J.H. and Charman, W.N. (2001) *In vitro* assessment of oral lipid based formulations. *Advanced Drug Delivery Reviews*, **50** (Suppl. 1), S127.

80 Sek, L., Porter, C.J.H., Kaukonen, A.M. and Charman, W.N. (2002) Evaluation of the *in-vitro* digestion profiles of long and medium chain glycerides and the phase behaviour of their lipolytic products. *The Journal of Pharmacy and Pharmacology*, **54**, 29.

81 Zangenberg, N.H., Mullertz, A., Gjelstrup Kristensen, H. and Hovgaard, L. (2001) A dynamic *in vitro* lipolysis model. II. Evaluation of the model. *European Journal of Pharmaceutical Sciences*, **14** (3), 237.

82 Porter, C.J.H., Kaukonen, A.M., Taillardat-Bertschinger, A., Boyd, B.J., O'Connor, J.M., Edwards, G.A. and Charman, W.N. (2004) Use of *in vitro* lipid digestion data to explain the *in vivo* performance of triglyceride-based oral lipid formulations of poorly water-soluble drugs: studies with halofantrine. *Journal of Pharmaceutical Sciences*, **93** (5), 1110–1121.

83 Dahan, A. and Hoffman, A. (2007) The effect of different lipid based formulations on the oral absorption of lipophilic drugs: the ability of *in vitro* lipolysis and consecutive *ex vivo* intestinal permeability data to predict *in vivo* bioavailability in rats. *European Journal of Pharmaceutics and Biopharmaceutics*, **67** (1), 96.

84 Dahan, A. and Hoffman, A. (2006) Use of a dynamic *in vitro* lipolysis model to rationalize oral formulation development for poor water soluble drugs: correlation with *in vivo* data and the relationship to intra-enterocyte processes in rats. *Pharmaceutical Research*, **23** (9), 2165–2174.

85 Lennernäs, H. and Abrahamsson, B. (2005) The use of biopharmaceutic classification of drugs in drug discovery and development: current status and future extension. *The Journal of Pharmacy and Pharmacology*, **57**, 273.

86 Polli, J.E., Yu, L.X., Cook, J.A., Amidon, G.L., Borchardt, R.T., Burnside, B.A., Burton, P.S., Chen, M.-L., Conner, D.P., Faustino, P.J., Hawi, A.A., Hussain, A.S., Joshi, H.N., Kwei, G., Lee, V.H.L., Lesko, L.J., Lipper, R.A., Loper, A.E., Nerurkar, S.G., Polli, J.W., Sanvordeker, D.R., Taneja, R., Uppoor, R.S., Vattikonda, C.S., Wilding, I. and Zhang, G. (2004) Summary workshop report: biopharmaceutics classification system – implementation challenges and extension opportunities. *Journal of Pharmaceutical Sciences*, **936** 1375–1381.

87 Rinaki, E., Dokoumetzidis, A., Valsami, G. and Macheras, P. (2004) Identification of biowaivers among class II drugs: theoretical justification and practical examples. *Pharmaceutical Research*, **21** (9), 1567.

88 Yu, L.X., Amidon, G.L., Polli, J.E., Zhao, H., Mehta, M.U., Conner, D.P., Shah, V.P., Lesko, L.J., Chen, M.L., Lee, V.H.L. and Hussain, A.S. (2002) Biopharmaceutics classification system: the scientific basis for biowaiver extensions. *Pharmaceutical Research*, **19** (7), 921.

89 Youngberg, C., Berardi, R., Howatt, W., Hyneck, M., Amidon, G., Meyer, J. and Dressman, J. (1987) Comparison of gastrointestinal pH in cystic fibrosis and healthy subjects. *Digestive Diseases and Sciences*, **32** (5), 472–480.

90 Kaus, L.C., Gillespie, W.R., Hussain, A.S. and Amidon, G.L. (1999) The effect of *in vivo* dissolution, gastric emptying rate, and intestinal transit time on the peak concentration and area-under-the-curve of drugs with different gastrointestinal

permeabilities. *Pharmaceutical Research*, **16** (2), 272.

91 Dressman, J. (1997) *Scientific Foundations for Regulating Drug Product Quality* (eds G.L. Amidon, J. Robinson and R. Williams), AAPS Press, pp. 155–168.

92 Yazdanian, M., Briggs, K., Jankovsky, C. and Hawi, A. (2004) The "high solubility" definition of the current FDA guidance on biopharmaceutical classification system may be too strict for acidic drugs. *Pharmaceutical Research*, **21** (2), 293.

93 Lipka, E. and Amidon, G.L. (1999) Setting bioequivalence requirements for drug development based on preclinical data: optimizing oral drug delivery systems. *Journal of Controlled Release*, **62** (1–2), 41.

4
In Silico Prediction of Solubility

Andrew M. Davis and Pierre Bruneau

Abbreviations

ASNN	Associative neutral network
BRNN	Bayesian regularised neural networks
DMSO	Dimethyl sulfoxide
GI	Gastrointestinal
GPs	Gaussian processes
HTS	High-throughput screening
KNNs	*k*-nearest neighbors
LFERs	Linear free-energy relationships
log $D_{7.4}$	logarithm of the distribution coefficient between *n*-octanol and water at pH 7.4
log *P*	logarithm of the partition coefficient of the neutral form of the compound between *n*-octanal and water
LSER	Linear solvation energy relationship
MAD	Maximum absorbable dose
MLR	Multiple linear regression
n	Number of compounds within the training/test set
PCB	Polychlorinated biphenyl
pH	Acidity of solution measured represented as $-\text{logarithm}_{10}$ of the activity of hydronium ions in solution
PLS	Partial least squares
PSA	Polar surface area (dynamic or static – calculated from 2D or 3D structure as defined)
QSAR	Quantitative structure–activity relationship
QSPR	Quantitative structure–property relationship
RMSE	Root mean square error of predictions – average deviation of the predictions from the measured value for a test set
s	Standard error
SD	Sample standard deviation
SVMs	Support vector machines

Symbols

2D	Two-dimensional
3D	Three-dimensional
log P	$\log_{10}$(*n*-octanol–water partition coefficient)
log Sol	$\log_{10}$(solubility measured according to the defined protocol) – usually, on molar scale
MP	Melting point
pK_a	Ionization constant
r	Correlation coefficient
R^2	Coefficient of variation of the fitted multivariate model

4.1 Introduction

Although the pharmaceutical industry has over 100 years of experience in drug discovery, attrition through clinical development remains refractory to our efforts to use experience and modern tools to successfully design drugs. Compound toxicology remains a major cause for uncontrolled attrition. While we seek a detailed understanding of the linkage between molecular mechanisms, *in vivo* toxicity, and adverse drug reactions in humans, increasing focus is now being placed upon exercising control of the simplest of molecular properties, molecular weight, lipophilicity, and drug solubility [1]. Ideally, we would wish to exercise control through the accurate prediction of these properties at the point of design of chemical targets, prior to synthesis; hence, there is an increasing focus upon the development of accurate computational models of these properties. In this chapter, we will focus upon the prediction of one of the most important properties, solubility.

Solubility is widely regarded as one of the most difficult physical properties to predict. But when building predictive solubility models, or in fact any model, one needs to answer a number of questions: what solubility measures are required to be modeled? Do we have a suitable data set on which to build a computational model? What descriptors and what modeling methods should be used? How accurate are the models required to be? What is the influence of the domain of applicability? Do we know when good predictions have been made? In this chapter, we will highlight recent research, in an attempt to answer these key questions in solubility modeling.

4.2 What Solubility Measures to Model?

Solubility is a fundamental compound quality indicator and plays a critical role in many aspects of drug research. Although most research has focused upon modeling solubility in water or aqueous buffered solutions, solubility in other milieu may be equally important.

Oral solid dosage forms need to dissolve with high enough solubility in gastrointestinal (GI) fluids and rapidly enough relative to GI transit time to provide sufficient systemic exposure. The amount of material ultimately absorbed after an oral dose will depend, among other factors, upon the dose, the solid-state form, the rate and extent of dissolution in the gastrointestinal milieu, and the GI transit time, as well as the dissolved drug's inherent permeability.

A number of mathematical models have been developed to describe the interplay of solubility and these physiological parameters to model drug absorption. The most simplistic model is the maximal absorbable dose (MAD) calculation. The MAD calculation combines the amount of drug that can dissolve to form a saturated solution in water equal in volume to the small intestinal volume, with an estimate of the absorption rate and the small intestinal transit time. The maximal absorbable dose is then related to the dose required to achieve the desired therapeutic effect [2]. If the estimated MAD is much greater than the predicted dose to achieve a therapeutic effect, this can give confidence enough to take the drug toward clinical use. Predictions of aqueous solubility may then be useful in predicting the extent of absorption in man.

The MAD calculation penalizes low-solubility compounds, as the predicted maximum absorbable dose, limited by solubility, may be less than the predicted human dose. Low-soluble compounds may result in an acceptable prediction for poorly soluble drugs if the predicted dose is also low. A recent validation study has reported that the MAD calculation underestimates the known human dose range for low aqueous solubility clinical drugs. This is because poorly aqueous soluble drugs often show enhanced solubility in gastric fluids. Measurement of solubility in either aspirated human intestinal fluids or simulated intestinal fluids is often more relevant to poorly soluble lipophilic drugs, as the bile salts, for example, have a significant enhancing effect on solubility [3]. Food may also have a significant solubility-enhancing effect by altering gastric emptying time and affecting the solubility of drugs. Computational models predicting solubility in intestinal fluids may be a promising future area for research.

More sophisticated approaches to predict the extent of oral absorption of drugs use mathematical models based on the known physiology and utilizing simple physicochemical measurements as input. The GastroPlus [4] program is a commercial tool that utilizes an advanced compartmental and transit model, based on the work of Amidon and Yu [5], and allows what–if questions to be posed to enable pharmaceutical optimization (see Chapter 17). For instance, the impact of morphology, formulation, and/or particle size changes, and sensitivity analysis to include errors in parameters on the prediction, can be considered.

Once absorbed, the drug needs to stay in solution as it equilibrates with all the body compartments. For extensively renally cleared drugs, precipitation or crystallization in the kidneys is a particular concern, as it leads to crystalluria [6, 7]. Changes in pH and salt concentrations in the kidneys, the therapeutic dose required, and the rate of renal clearance will affect the risk of crystalluria. Computational models predicting solubility at differing pH values may be useful in the context of renally cleared drugs.

Controlled dissolution from a formulation may be critical for the control of duration of drug action. Extended release formulations are useful for most drug delivery routes.

For instance, fluticasone propionate is dosed topically to the lung via metered dose inhalers or dry-powder inhalers, and its high lipophilicity and low aqueous solubility are important for the drug's pharmacokinetic and pharmacodynamic profile [8, 9]. Models predicting solubility in specific formulations, or models predicting dissolution rate, may be useful in formulation development and drug delivery.

Solubility in nonaqueous solvents is also important in drug discovery. For instance, solubility in DMSO underpins most *in vitro* screening, and HTS depends upon the long-term stability of solutions of compounds in DMSO in screening collections. Although solubility is seldom a limiting factor in chemical synthesis in the drug discovery phase, as drug development progresses, solubility can be a limiting factor in large-scale synthetic processes. Tetko has published one of the first studies describing DMSO solubility models [10]. Published data sets with 20–70 000 cases exist, but they are only categorical in nature. Using common modeling methods such as random forests, recursive partitioning, and linear discriminant analysis produced classification models with 70–80% successful classification of random test sets. Computational models for predicting solubility in DMSO and other nonaqueous solvents are an area for further research throughout the discovery process.

It is apparent from the preceding discussion that there are many choices over solubility measures on which to base a computational model, and data sets and models are sparse beyond solubility in water or aqueous buffered solutions.

4.3 Is the Data Set Suitable for Modeling?

Solubility is a complex property, and this complexity confounds our ability to develop computational models to predict it. Most computational solubility models are empirical QSPR models, trained on solubility data sets either sourced from the literature and corporate databases or generated specifically for the purposes of modeling. Hence, it is not surprising that the quality of the computational model depends on the quality of the data set of experimental measurements used to train the model.

The solubility measure describes the concentration reached in solution, when a pure phase of the material is allowed to dissolve in the solvent for a defined period of time, at a defined temperature (and pressure). Most often for pharmaceutical purposes, the pure phase is a solid, ideally a crystalline solid, and the liquid is water or a buffered aqueous solution, at a controlled temperature (often 25 or 37 °C) and ambient pressure. The purity of the solid can have a large effect on measured solubility. Solubility can be measured in water or in pH-controlled buffers. In water, the extent of solubility for ionizable compounds will depend upon the pK_a values and the nature of the counterion. In pH-controlled aqueous buffered solution, at equilibrium, the solubility will depend upon the compound's intrinsic solubility, its pK_a, and the ionic strength. It may also depend upon the relative solubility of the initial added compound and the solubility of the salt formed by the compound with the buffer salts, with which the solid may equilibrate. In any buffer or solvent system, the measured solubility may depend on the time of sampling, as solubility kinetics

may be important. Sampling at different time points may prove useful not only to define the thermodynamic equilibrium solubility but also sometimes to describe the kinetics of dissolution. The "undissolved" solid may also change its morphology during the experiment. As one solid-state form dissolves and another crystallizes, the solubility measured at the end of an experiment may therefore be the solubility of a form different from the one the experiment began with.

In generating data sets of solubility measurements for modeling purposes, the degree of control of the parameters discussed above will undoubtedly contribute to, or compromise, the accuracy and precision of any predictive model built upon them. Taskinen and Norinder in their recent comprehensive survey [11] of data sources for solubility models commented that inadequate documentation made it difficult to assess whether many data sets represent suitably consistent values regarding thermodynamics or ionization for modeling purposes. For these reasons, an ideal data set for *in silico* modeling would be one from a single laboratory, measured under a consistent and controlled experimental protocol with an understood precision. Ideally, the conditions will be relevant to the end point being optimized and the solid-state form of the compounds being studied should be known before and after the experiment. Most data sets used as the basis for solubility models do not conform to this idealized description. This may contribute to the perceived lack of accuracy and precision of solubility models in general.

Bergström [12] made an interesting discussion about the advantages of the various methods of measuring solubility and permeability. Bergström showed that some methods, such as kinetic measurement of solubility by precipitation of a DMSO solution, by adding increasing amounts of aqueous buffer, can only lead to a qualitative classification in terms of low, intermediate, and high solubility. As a consequence, these results can only be used in classification predictions. On the contrary, if quantitative models are looked for, more labor-intensive and maybe less-automated methods are needed to collect more precise data of solubility and permeability. Bergström emphasizes the need of a database of good, accurate, and reproducible measurements to produce good predictive models. Even if we have a good database, descriptors, and mathematical tools to make a good model, there will remain the problem of applicability of the model to various chemical spaces.

The quality of measured data is often a problem in the research environment where the various batches of a compound show different measured solubility. In an in-house study at AstraZeneca, 75% of repeated measures on the same batch were found to have a standard deviation (SD) of less than 0.29 log unit, whereas the corresponding figure for the interbatch average measurements reached 0.49 log unit and 10% of these interbatch measurements had a variability of more than 0.81 log unit. This discrepancy was tentatively explained by the differences in solid state of the samples issued from different batches. Although an attractive hypothesis, and supported by the data, this suggested explanation is not supported by Delaney [13], who holds that the difference of physical state between compounds is not important to the accuracy of the solubility prediction, and by the recent study of Bergström and coworkers [14], who show that the solubility of poorly soluble compounds is limited more by their weak solvation ability than by their solid state.

4.4
Descriptors and Modeling Methods for Developing Solubility Models

The choice of descriptors is not always clear-cut. The time required to calculate elaborate descriptors by quantum methods is not always justified compared to the results obtained with simpler and more rapidly calculated descriptors. For example, Bergström [12] compared 2D polar surface area (PSA) with 3D PSA and static, instead of dynamic, calculations. No definitive gain was obtained by using the most sophisticated method(s) of calculating PSA descriptors.

There is no such clear-cut judgment about the statistical methods of modeling solubility. There are models as simple as the relationship between log *P* and melting point (MP), established some time ago by Yalkowsky and coworkers, and the very complex linear solvation energy relationships (LSERs). The limitation of the simple Yalkowsky relationship is that it uses two variables, obtained with accuracy only by measurement, and thus the simple relationship turns out to be very complicated when calculated log *P* and MP are used.

Among the recent reviews, the most comprehensive one is by Dearden [15]. In his review, he discusses the fundamentals of aqueous solubility, which lead to the Yalkowsky equation. Dearden also reviews the oldest approaches of predicting aqueous solubility, from a very simple fragment-based approach of 1924 to the numerous approaches post-1990, for which he made an extensive tabular comparison.

Delaney [13] describes the solubilization mechanism as controlled by a double phenomenon: the affinity of the compound for itself and the affinity of the compound for the solvent. The latter effect is simply described either by the log *P* property or by very sophisticated methods such as statistical thermodynamic or quantum mechanical techniques. These very intensive calculation methods have not yet proved their superiority over the simpler and faster methods that tend to mimic the successful log *P* fragment calculator.

The effects of solid-state structure on solubility are even more complicated and so far less successful to calculate, if we exclude some very crude methods of entropy of melting estimation by evaluating the number of rotatable bonds and the symmetry of the molecule. But Delaney estimates that the error on calculation of the compound–compound interaction is small (about half a log unit) compared to the potential error due to the compound–solvent interaction that can be estimated as 2 log units. It is even possible to neglect the variation of the melting points of compounds by using an average value of 125 °C for all compounds without influencing the accuracy of the prediction. This latter argument justifies the use of empirical approaches that neglect the fundamental mechanisms of solubilization but try to correlate the measured values with various calculated descriptors more or less related to the solubility-like parameters accounting for hydrogen bonding or solvent cavity formation. This is reassuring, as the use of solid-state descriptors would first require the *ab initio* prediction of the solid-state structure of compounds, which even for simple compounds is still in its infancy. In this part of his review, Delaney emphasizes the fact that linear methods are suitable for restricted homogeneous series, whereas large

data sets of diverse chemistry should be treated by nonlinear methods. Delaney surveys the various mathematical tools that have been successfully used in the data regression without pointing out a simple method, or a group of methods, which may be better than others. Delaney, similar to many other authors, concludes that the quality of the data is of primary importance and that there are some problems not yet fully solved, such the prediction of charged compounds at various pH values and DMSO solubilities. The influence of the crystal stability on solubility and the success of the Yalkowsky equation have initiated many attempts at predicting the melting point.

A recent publication relates the work of Varnek *et al*. [16] on this subject. The authors have gathered a database of 717 compounds with measured melting points. These compounds were all bromides of nitrogen-containing organic cations. They used associative neural network (ASNN), *k*-nearest neighbors (KNNs), support vector machines (SVMs), and multiple linear regression (MLR). Their validation method was a leave-one-fifth-out method, that is, they built five models on four-fifths of the data using one-fifth of the data reserved for the validation set. The five subvalidation sets were combined to form the internal validation set. Similar to all leave-*n*-out validation methods, these internal validation sets will contain close analogs of the training sets, but it does not seem that there is another good method to validate such models. The results show that there is a slight advantage of using the nonlinear method and that an RMSE of around 40 °C can be achieved.

Nigsch *et al*. [17, 18] made a similar attempt; by using a *k*-nearest neighbors algorithm with a genetic parameter optimization on a training set of 4110 diverse organic molecules and 277 drugs, they obtained an RMSE of 42.2 °C. They explained that the remaining error is due to "the lack of information about the interactions in the liquid state."

4.5 Comparing Literature Solubility Models

The reviews published by Bergström [12] and Delaney [13] in 2005 and Dearden [15] in 2006 give good overviews of the predictive solubility literature.

But the main problem with the multitude of solubility models is how to compare them? The only way to obtain an objective judgment of their predictive power is to test each model using a common external test set. For this purpose, Dearden made a compilation of results from 21 models, whose authors published results of a common test set comprising 20 drugs and pesticides and one PCB, as it was initially used by Yalkowsky and Banerjee to evaluate their own model. A summary of the most homogeneous results from these models is reproduced in Table 4.1.

This comparison is very useful, but one must keep in mind that 20 molecules in a test set does not represent a large chemical space, and although it constitutes a comparative test, it does not prove that the models are predictive for *any* drug-like molecule, as we shall discuss later. Dearden widens his comparative study to 17 commercially available programs able to predict solubility. The comparison was done

Table 4.1 Aqueous solubility prediction studies using the Yalkowsky and Banerjee test set [15].

Author	Year of publication	Compounds in training set	Compounds in test set	Std of training set	Std of test set
Yalkowsky	1992	41	21	0.50	0.79
Klopman	1992	483	21	0.53	1.25
Yalkowsky	1993	41	19	0.39	1.34
Kuhner	1995	694	21	0.38	1.05
Huuskonen	1998	160	21	0.46	1.25
Huuskonen	2000	884	21	0.47	0.63
Huuskonen	2000	675	21	0.52	0.75
Huuskonen	2001	674	21	0.58	0.84
Livingstone	2001	552	21	0.52	0.77
Liu	2001	1033	21	0.70	0.93
Yan	2003	797	21	0.50	0.77
Wegner	2003	1016	21	0.52	0.79
Butina	2003	2688	11	0.61	0.94
Yan	2003	741	21	0.51	0.80
Hou	2004	878	21	0.59	0.64
Delaney	2004	2874	21	0.97	0.78

with a common test set of 122 compounds with accurately measured intrinsic solubility in pure water. In judging the results, one must be careful of the fact that some or even most of the 122 test compounds may have been used on the training set of the software concerned. Keeping in mind this possibility, the standard error of the log Sol of commercial software has a range of 0.47–1.96 with a median at 0.95 log unit. Dearden points out that the best scores, around 0.50, reach the limits of the experimental errors of solubility measurements [18, 19]. A good method to compare the commercially available software is to evaluate the percentage of compounds that are well predicted with an error less than 0.5 log unit and the percentage of compounds that have an acceptable error less than 1 log unit, as shown in Table 4.2.

Schwaighofer *et al*. [19] have done a remarkable work by gathering solubility data on 23 516 compounds from literature sources that after data cleaning led to reliable solubility measurements on 3307 neutral compounds combined with data from about 1100 compounds, mainly electrolytes, which have been measured in-house. They also used data on 704 compounds, which were used by Huuskonen and numerous other researchers. The complete database was used either to predict pure solubility of neutral compounds or to predict solubility at a given pH for neutral compounds and electrolytes. Apart from using a comprehensive database, the main originality of this work is the use of Gaussian process (GP) as the mathematical tool to build the models. GPs are techniques from the field of Gaussian statistics, and similar to the Bayesian regularized neural networks (BRNNs) [20], they have the great advantage to allow an evaluation of the prediction error for the individual predicted solubilities. Their model achieves a performance, as measured by the RMSE, comparable to commercial packages at around 0.6 log unit on neutral compounds,

Table 4.2 Predictive ability of some commercially available software for aqueous solubility, based on a 122-compound test set of drugs [15].

Software	Percentage of compounds predicted within	
	±0.5 log unit	±1.0 log unit
SimulationsPlus	65	91
Admensa	72	87
Pharma Algorithms ADME Boxes	59	87
ChemSilico	60	86
ACDLabs	59	85
ALogS	52	81
PredictionBase	47	81
ESOL	55	79
MOLPRO	62	78
Absolv 2	44	75
QikProp	48	79
SPARC	43	73
Cerius ADME	38	73
WSKOWWIN	41	67
ADMEWORKS Predictor	34	66
AlogP98	38	62
CHEMICALC	23	46

while it is much better on electrolytes with an RMSE of 0.77, compared to well above 1 log unit for commercial packages on the same validation set.

Du-Cuny *et al*. [21] have used a large data set of 2473 compounds likely to be more "drug-like" as they are from their own employer's pharmaceutical company collection. The originalities of their work are

- modeling of intrinsic solubility ($\log 1/S_0$);
- use of 170 structural fragment descriptors and four fragment-based correction factors;
- use of 81 congeneric series indices.

The obtained PLS model gave $R^2 = 0.81$ on an independent test set of 958 compounds. This measure of predictivity is optimistic, since the test set was selected in a manner favorable to good prediction. The initial data set of 2473 compounds was clustered and the singletons were eliminated. Then the remaining data set was randomized and the training set and test set were selected. Therefore, the members of the test set were very likely not too far from members of the training set, thus leading to better prediction statistics. The authors submitted their test set to prediction with a commercial software that led to a poor $R^2 = 0.10$. Although the figure of 0.81 obtained with their model is probably optimistic, the improvement over $R^2 = 0.10$ obtained with WSKOWWIN is large enough to conclude the superiority of the models developed using in-house data over the commercial models.

As Du-Cuny *et al.* [21] have described, it is tempting to derive the intrinsic solubility from a measurement of the solubility at a given pH and measured pK_a and using the Henderson–Hasselbalch equation. Hansen *et al.* [22] followed a reverse path. They built an intrinsic solubility model from intrinsic solubility data and, using a calculated pK_a from a commercial tool, predicted the pH-dependent solubility of a validation set of 27 drugs with experimentally determined pH-dependent solubility profile, to obtain an RMSE of 0.79 log unit. Bergström *et al.* [23] have shown that one must be very cautious in doing this kind of calculation. They measured a set of 25 monoamine compounds. The Henderson–Hasselbalch equation shows a slope of −1 for the relationships of solubility log unit with pH. The Bergström *et al.* measurements reveal that −1 is very rarely observed since the experimental slopes range from −0.5 to −8.6. This is explained by various experimental conditions leading to dimers, aggregates, and micelles and also to the presence of counterions with multi-ionizable sites. The consequences of these observations are that solubility measurements are extremely difficult to obtain with a reproducible and reliable quality.

In his review, Dearden [15] has tabulated the statistical characteristics of nearly 90 models published between 1990 and 2005 in a chronological order. If we exclude two studies showing very low standard error of estimate ($s = 0.08$ and 0.19), which according to Dearden are probably heavily overfitted models, and a model having a very high $s = 2.4$, the remaining reported data of s and RMSE have a mean value of 0.57 log unit, which fits quite well with the generally accepted figure of 0.6 log unit for the experimental error of the solubility measurements. But the data show a remarkable increase with time. Dearden points out that the first studies to use drugs in the training set did not appear until 1998; shortly after, Lipinski *et al.* published their study on the rule-of-5 [24]. If we separate the s and RMSE published before 1998 from the ones published after that year, we observe a clear increase from 0.41 log unit for the pre-1998 data to 0.62 for the post-1998 data. Even after 1998, the increasing trend is shown with an average of 0.49 in 2000 to an average of 0.67 for the models published in 2004. The difference between these two figures is statistically significant at the 0.05 level of a Student t-test. The results for the other years show the trend, although they do not show a statistical difference from each other (Table 4.3).

The reasons for the degradation of modeling performance are unclear. Dearden proposed that there are more and more drugs involved in the modeling process. It is probably true, but there is no fundamental difference between a chemical entity

Table 4.3 Variation of the mean RMSE of the models published between 2000 and 2004.

Year of publication	Mean RMSE	Number of publications
2000	0.49	7
2001	0.62	9
2002	0.60	11
2003	0.65	15
2004	0.67	11

being "drug" and another a "nondrug." Since Dearden's data consider statistics obtained on training sets, the results should at least be stable or should rather improve with the improvement of modeling processes and of the descriptors sets. Any difference explainable by the usual more complex and higher molecular weight of drug-like compounds should be seen only on validation results.

4.6 What Is the Influence of the Domain of Applicability?

As highlighted by Bergström [12], the problem of the applicability domain of a model has not been definitively solved. Stanforth *et al*. [25, 26] have recently addressed this problem by clustering the training set by a *k*-means clustering algorithm in the descriptors space. Then, the distance to domain was evaluated and correlated to the error of the model. Their method compares well with other methods of evaluating the distance to model to estimate the likely error of the prediction. In a similar manner, Bruneau and McElroy [20] set up a method that used the average of the Mahalanobis distances to the three nearest neighbors, calculated in the descriptors space to describe the distance to the models. These authors show a very good dependency of the RMSE of a $\log D_{7.4}$ model on the calculated distance from the model. They also show that the standard deviation of the prediction obtained by sampling a few hundreds of BRNNs is also a very good indication of the likely error of the model.

Bruneau has demonstrated the importance of domain of applicability of solubility models using three training set/test set pairs described by the same set of descriptors and using the same modeling method, Bayesian neural networks with automatic relevance determination variable selection [26]. He defined internal proprietary training and test sets and "public" training and test sets from the literature. A combined data set representing both "public" and "in-house" proprietary data was also constructed. The "public" compounds were on average smaller, less lipophilic, and more soluble than the proprietary drug-like compounds. He showed that similar results were obtained from the "public" model applied to a "public" validation set with an RMSE $= 0.84$ log unit and the so-called "in-house" model applied to "in-house" validation set with an RMSE $= 0.78$ log unit. This would be judged as two equivalent models with similar performance from a publication point of view. But when the validation sets were crossed over, the "public" model gave an RMSE $= 1.0$ on the "in-house" validation set, and the "in-house" model' gave an RMSE $= 1.88$ on the "public" validation set. It is clear that even models with apparently similar performances may give very different results when applied to different data sets. It must be noted that the "in-house" model had much more difficulties in predicting "public" data than the reverse. This was explained by the higher diversity of the "public" database compared to the "in-house" database, which is more series dependent. To solve this, Bruneau combined the training and test set databases and obtained a "mixed" model that when applied to the "public" validation set gave an RMSE $= 0.82$ and when applied to the "in-house" validation set gave an RMSE $= 0.79$. The

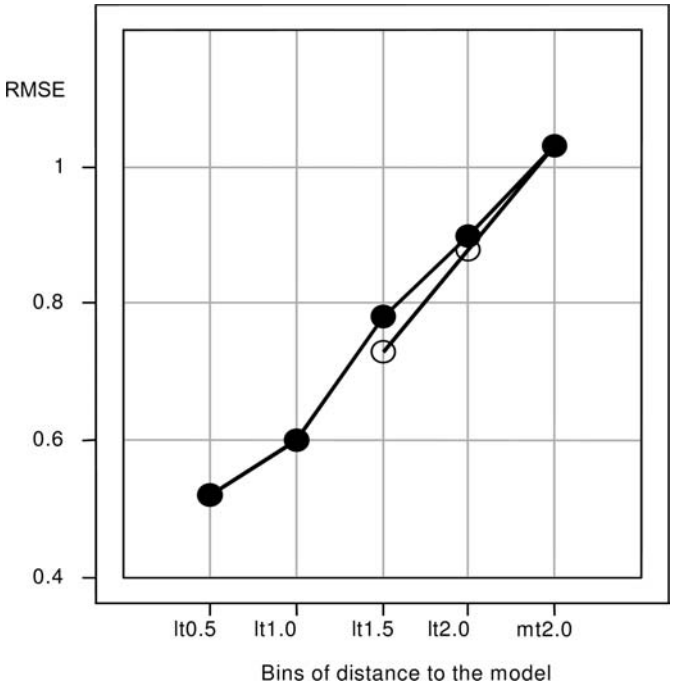

Figure 4.1 Distance-to-model versus RMSE. Solid circles represent "public model" applied to "public" validation set. Open circles represent "public" model applied to "in-house" validation set. The missing open circles correspond to the lack of examples in the corresponding bin. lt0.5, lt1.0, lt1.5, and lt2.0 stand for bins of the Mahalanobis distances of compounds to be tested to the nearest compounds in the training set of less than 0.5, 1.0, 1.5, and 2.0 distance arbitrary units, respectively. mt2.0 stands for bin of the Mahalanobis distances of compounds to be tested to the nearest compounds in the training set of more than 2.0 distance arbitrary units [26].

predictions from the literature model for each test set were then binned by the distance to the training space of the "public" model, and the test set's RMSE values were analyzed per distance bin. It was concluded that once the distance to the training set model space was considered, the literature model now performed similarly on all three test sets, when bins of a similar distance were compared as shown in Figure 4.1.

This analysis is very revealing. It suggests that comparing different computational models on common test sets may not be a very useful exercise. It does tell you which model predicts that particular test set well, but this gives little information on the relative generalizability of the models. The dependence of predictive performance on distance-to-model must be taken into account. As Bruneau states, "It is utopian to expect that a model can predict any structure." This view may undermine many reports in the literature, but the most important consideration is how well does a particular model predict "my test set of interest" or, more importantly, how well does the model predict the next compound I am going to make.

4.7
Can We Tell when Good Predictions Are Made?

Whatever the results of training sets, and test sets, the users ask what is the best model to use? The question is difficult, and even impossible, to answer from the published data on training and validation sets. This is because the performance of any model on any particular test set will heavily depend on the distance of the test set compounds to the training set model space, as well as the inherent predictive poser of the model itself, as has been described in the previous section. The only way to answer this question is for the users to try the models on their own data sets.

The modelers of physical properties face a difficult situation: they are satisfied when their models have an RMSE on validation set of less than the fatidic one order of magnitude, but at the same time the medicinal chemists are frustrated when they use the model in their own projects. The discrepancy of judgments is explained on pure statistical elements. An RMSE of 0.8 log unit on a global model of solubility validated on a validation set spreading from −2 to 8 log unit with an SD of say 5 log units leads to a very satisfactory r^2 of nearly 1, which classified the model as very good. When the medicinal chemist uses the model on his own data, the spread of which is often narrowed to maybe two orders of magnitude with an SD of say 1 log unit, he observes a deceptive r^2 of 0.36. The situation is usually even worse since the series on which the chemist is working might be poorly represented in the training set, and the RMSE of the model on this new series may well be higher than the SD of the measured data leading to an even more disappointing negative r^2. The usual answer to this problem is often a request for "local" models. This approach may sometime be successful, especially when linear regression methods are used, since these methods are able to pick up "local" specificities.

So why cannot we improve the models? Johnson [27] attempts to answer this disturbing question. Although his discussion is centered on QSAR, it has many common points relevant to QSPR, which is used in the field of solubility modeling. He concludes that we should not be led by mere statistics that too often dictates what is good or wrong, but rather by scientific rationale, experimental design, and personal observation.

4.8
Conclusions

The literature and commercial companies abound with computational solubility models. Many data sets have been studied, with many different descriptor sets, and using a multitude of statistical methods. It appears that diverse drug-like data sets are often predicted by our best methods with an RMSE of 0.8–1 log unit. This compares with an error in replicate measurements of approximately 0.5 log unit. A common view is that there is still room for improvement in the computational modeling of solubility. There are a number of suggestions that the quality control of the ideal data set is still lacking. This may be true for some literature data set compilations, but it is

less likely to be the case for proprietary data sets described by large pharmaceutical companies, where a large number of compounds have been measured through single well-controlled assays. There may be further work that could be done to describe the solute–solute interactions in the solid state, but this may be very challenging and may be a minor controlling factor compared to the importance of solvation, which is well described by current QSAR descriptors. Maybe an RMSE of 0.7–0.8, as observed on diverse test sets predicted by a number of models, is the best one should expect to be able to achieve. When distance to the training set model space of the test set is considered, compounds closest to the training sets may be predicted close to the replicate error in measurement. The problem then reduces to keeping the training set space of your computational model close to the compounds you wish to predict and building your computational model to predict to the most relevant end point.

One should always keep in mind that a correlation established on a training set between descriptors and experimental data may not be an indication of causation. Without the causation factor, that is, the descriptors explain the phenomenon that induces the variation in the data, it is unlikely that the model can predict any so far unknown molecular feature. Of course, this is the heart of molecular modeling and this is why the models are so dependent on the distance to the model space. All you can do to gain confidence in your model is to assess the predictivity of your model on your compounds. You can do this by testing the model on compounds synthesized and tested subsequent to the model derivation, with the test set similar to the compound(s) required to be predicted, and consider the effect of distance to model in the prediction errors. Once one has built confidence that the model has some predictive power on similar compounds of interest, a judgment has to be made whether the predictivity achieved has the resolution required for the purpose in hand. If it does have, then all that is left is to hold your breath and make a real prediction. As Niels Bohr said, "Predictions are difficult, especially those of the future." In the end, you have to take your chances that your model really does have enough control of solubility to guide to you to your goal, and this chance is often worth taking than leaving solubility to random chance.

References

1 Leeson, P.D. and Springthorpe, B. (2007) The influence of drug-like concepts on decision-making in medicinal chemistry. *Nature Reviews. Drug Discovery*, **6** (11), 881–890.

2 Johnson, K.C. and Swindell, A.C. (1996) Guidance in the setting of drug particle size specifications to minimize variability in absorption. *Pharmaceutical Research*, **13** (12), 1795–1798.

3 Dressman, J.B., Vertzoni, M., Goumas, K. and Reppas, C. (2007) Estimating drug solubility in the gastrointestinal tract. *Advanced Drug Delivery Reviews*, **59** (7), 591–602.

4 Agoram, B., Gilman, T., Woltosz, W. and Bolger, M. (2001) Application of the ACAT model for simulating the Cp-time profiles of controlled release dosage forms of metoprolol. Proceedings of the 28th

International Symposium on Controlled Release of Bioactive Materials and 4th Consumer & Diversified Products Conference, June 23–27, 2001, San Diego, CA, Vol. 1, pp. 840–841.

5 Yu, L.X., Crison, J.R. and Amidon, G.L. (1996) Compartmental transit and dispersion model analysis of small intestinal transit flow in humans. *International Journal of Pharmaceutics*, **140** (1), 111–118.

6 Stormann, H. and Nigitz, H.P. (1980) Experimental crystalluria induced in rats by sulfamides. *Investigacion Medica Internacional*, **7** (3), 245–250.

7 Merschman, S.A., Rose, M.J., Pearce, G.E.S., Woolf, E.J., Schaefer, B.H., Huber, A.C., Musson, D.G., Petty, K.J., Rush, D.J., Varsolona, R.J. and Matuszewski, B.K. (2005) Characterization of the solubility of a poorly soluble hydroxylated metabolite in human urine and its implications for potential renal toxicity. *Pharmazie*, **60** (5), 359–363.

8 Meibohm, B., Mollmann, H., Wagner, M., Hochhaus, G., Mollmann, A. and Derendorf, H. (1998) The clinical pharmacology of fluticasone propionate. *Reviews in Contemporary Pharmacotherapy*, **9** (8), 535–549.

9 Derendorf, H., Hochhaus, G., Meibohm, B., Mollmann, H. and Barth, J. (1998) Pharmacokinetics and pharmacodynamics of inhaled corticosteroids. *Journal of Allergy and Clinical Immunology*, **101** (4 Pt 2), S440–S446.

10 Balakin, K.V., Savchuk, N.P. and Tetko, I.V. (2006) *In silico* approaches to prediction of aqueous and DMSO solubility of drug-like compounds: trends, problems and solutions. *Current Medicinal Chemistry*, **13** (2), 223–241; Meltzer, P.S., Kallioniemi, A. and Trent, J.M. (2002) Chromosome alterations in human solid tumors, in *The Genetic Basis of Human Cancer* (eds B. Vogelstein and K.W. Kinzler), McGraw-Hill, New York, pp. 93–113.

11 Taskinen, J. and Norinder, U. (2007) *ADME-Tox Approaches*, Vol. 5 (eds B. Testa and H. van de Waterbeemd), in *Comprehensive Medicinal Chemistry II* (series eds D. Triggle and J. Taylor), Elsevier, Oxford, pp. 627–648.

12 Bergström, C.A.S. (2005) Computational models to predict aqueous drug solubility, permeability and intestinal absorption. *Expert Opinion on Drug Metabolism & Toxicology*, **1** (4), 613–627.

13 Delaney, J.S. (2005) Predicting aqueous solubility from structure. *Drug Discovery Today*, **10** (4), 289–295.

14 Bergström, C.A.S., Wassvik, C.M., Johansson, K. and Hubatsch, I. (2007) Poorly soluble marketed drugs display solvation limited solubility. *Journal of Medicinal Chemistry*, **50** (23), 5858–5862.

15 Dearden, J.C. (2006) *In silico* prediction of aqueous solubility. *Expert Opinion on Drug Discovery*, **1** (1), 31–52.

16 Varnek, A., Kireeva, N., Tetko, I.V, Baskin, I.I. and Solov'ev, V.P. (2007) Exhaustive QSPR studies of a large diverse set of ionic liquids: how accurately can we predict melting points? *Journal of Chemical Information and Modeling*, **47** (3), 1111–1122.

17 Nigsch, F., Bender, A., Van Buuren, B., Tissen, J., Nigsch, E. and Mitchell, J.B.O. (2006) Melting point prediction employing *k*-nearest neighbor algorithms and genetic parameter optimization. *Journal of Chemical Information and Modeling*, **46** (6), 2412–2422.

18 Katritzky, A.R., Wang, Y., Sild, S., Tamm, T. and Karelson, M. (1998) QSPR studies on vapor pressure, aqueous solubility, and the prediction of water–air partition coefficients. *Journal of Chemical Information and Computer Sciences*, **38** (4), 720–725.

19 Schwaighofer, A., Schroeter, T., Mika, S., Laub, J., Ter Laak, A., Suelzle, D., Ganzer, U., Heinrich, N. and Mueller, K.-R. (2007) Accurate solubility prediction with error bars for electrolytes: a machine learning approach. *Journal of Chemical Information and Modeling*, **47** (2), 407–424.

20 Bruneau, P. and McElroy, N.R. (2006) Log $D_{7.4}$ modeling using Bayesian regularized neural networks. Assessment and correction of the errors of prediction. *Journal of Chemical Information and Modeling*, **46** (3), 1379–1387.

21 Du-Cuny, L., Huwyler, J., Wiese, M. and Kansy, M. (2008) Computational aqueous solubility prediction for drug-like compounds in congeneric series. *European Journal of Medicinal Chemistry*, **43** (3), 501–512.

22 Hansen, N.T., Kouskoumvekaki, I., Jorgensen, F., Steen, B., Soren, J. and Svava, O. (2006) Prediction of pH-dependent aqueous solubility of druglike molecules. *Journal of Chemical Information and Modeling*, **46** (6), 2601–2609.

23 Bergström, C.A.S., Luthman, K. and Artursson, P. (2004) Accuracy of calculated pH-dependent aqueous drug solubility. *European Journal of Pharmaceutical Sciences*, **22** (5), 387–398.

24 Lipinski, C.A., Lombardo, F., Dominy, B.W. and Feeney, P.J. (1997) Experimental and computational approaches to estimate solubility and permeability in drug discovery and development settings. *Advanced Drug Delivery Reviews*, **23** (1–3), 3–25.

25 Stanforth, R.W., Kolossov, E. and Mirkim, B. (2007) A measure of domain of applicability for QSAR modelling based on intelligent *K*-means clustering. *QSAR & Combinatorial Science*, **26** (7), 837–844.

26 Bruneau, P. (2001) Search for predictive generic model of aqueous solubility using Bayesian neural nets. *Journal of Chemical Information and Computational Sciences*, **41**, 1605–1616.

27 Johnson, S.R. (2008) The trouble with QSAR (or how I learned to stop worrying and embrace fallacy). *Journal of Chemical Information and Modeling*, **48** (1), 25–26.

Part Two
Physicochemical and Biological Studies of Membrane Permeability and Oral Absorption

5
Physicochemical Approaches to Drug Absorption

Han van de Waterbeemd

Abbreviations

1D, 2D, 3D	One-, two-, three-dimensional
ACD	Advanced Chemistry Development (software, vendor)
ADME	Absorption, distribution, metabolism, and excretion
BBB	Blood–brain barrier
BMC	Biopartitioning micellar chromatography
BNN	Bayesian neural networks
Caco-2	Adenocarcinoma cell line derived from human colon
CHIs	Chromatographic hydrophobicity indices
CNS	Central nervous system
DCE	1,2-Dichloroethane
DMPK	Drug metabolism and pharmacokinetics
DMSO	Dimethyl sulfoxide
FaSSIF	Fasting-state simulated artificial intestinal fluid
HB	Hydrogen bonding
HDMs	Hexadecane membranes
HSA	Human serum albumin
HTS	High-throughput screening
IAM	Immobilized artificial membrane
ILC	Immobilized liposome chromatography
IUPAC	International Union of Pure and Applied Chemistry
MAD	Maximum absorbable dose
MEKC	Micellar electrokinetic chromatography
M&S	Modeling and simulation
NMR	Nuclear magnetic resonance
PAMPA	Parallel artificial membrane permeation assay
PASS	Prediction of activity spectra for substances
PBPK	Physiologically based pharmacokinetic modeling
P-gp	P-glycoprotein
PK	Pharmacokinetic(s)

PPB	Plasma protein binding
PSA	Polar surface area (Å^2)
QSAR	Quantitative structure–activity relationship
QSPR	Quantitative structure–property relationship
RP-HPLC	Reversed-phase high-performance liquid chromatography
SPR	Surface plasmon resonance
TLC	Thin-layer chromatography
UWL	Unstirred water layer
WDI	World Drug Index

Symbols

A_D	Cross-sectional area (Å^2)
Brij35	Polyoxyethylene(23)lauryl ether
Clog *P*	Calculated logarithm of the octanol/water partition coefficient (for neutral species)
CLOGP	Daylight/Biobyte computer program for the calculation of log *P*
D	Distribution coefficient (often in octanol/water)
diff(log P^{N-I})	Difference between log P^N and log P^I
Δlog *P*	Difference between log *P* in octanol/water and alkane/water
k_a	Transintestinal rate absorption constant (min^{-1})
K_a	Dissociation constant
Elog *D*	Experimental log *D* based on an HPLC method
log *D*	Logarithm of the distribution coefficient, usually in octanol/water at pH 7.4
log $D_{7.4}$	Logarithm of the distribution coefficient, in octanol/water at pH 7.4
log *P*	Logarithm of the partition coefficient, usually in octanol/water (for neutral species)
log P^I	Logarithm of the partition coefficient of a given compound in its fully ionized form, usually in octanol/water
log P^N	Logarithm of the partition coefficient of a given compound in its neutral form, usually in octanol/water
MW	Molecular weight (Da)
P	Partition coefficient (often in octanol/water)
P_{app}	Permeability constant measured in Caco-2 or PAMPA assay (cm/min)
pK_a	Ionization constant in water
PPB%	Percentage plasma protein binding
S	Solubility (mg/ml)
SITT	Small intestinal transit time (4.5 h = 270 min)
SIWV	Small intestinal water volume (250 ml)
V	Volume (ml or l)
V_{dss}	Volume of distribution at steady state (l/kg)

5.1 Introduction

An important part of the optimization process of potential leads to candidates suitable for clinical trials is the detailed study of the absorption, distribution, metabolism, and excretion (ADME) characteristics of the most promising compounds. Experience has learned that physicochemical properties play a key role in drug metabolism and pharmacokinetics (DMPK) [1–5]. In 1995, 2000, and 2004, specialized but very well-attended meetings were held to discuss the role of log *P* and other physicochemical properties in drug research and lead profiling, and the reader is referred to the proceedings for a highly recommended reading on this subject [4, 6, 7].

The molecular structure is at the basis of physicochemical, DMPK, and safety/toxicity properties as outlined in Figure 5.1. Measurement and prediction of physicochemical properties are relatively easy compared to those of DMPK and safety properties, where biological factors come into play. However, DMPK and toxicity properties depend to a certain extent on the physicochemical properties of compounds as these dictate the degree of access to biological systems such as enzymes and transporters.

The change in work practice toward high-throughput screening (HTS) in biology using combinatorial libraries has also increased the demand for more physicochemical and ADME data. There has been an increasing interest in physicochemical hits and leads profiling in recent years, using both *in vitro* and *in silico* approaches [8–11]. This chapter will review the key physicochemical properties, both how they can be measured and how they can be calculated in some cases. Chemical stability [12] is beyond the scope of this chapter, but is obviously important for a successful drug candidate.

The need and precision of a particular physicochemical property for decision making in a drug discovery project depend on the stage in the drug discovery process (see Figure 5.2). While calculated simple filters may be sufficient in library design,

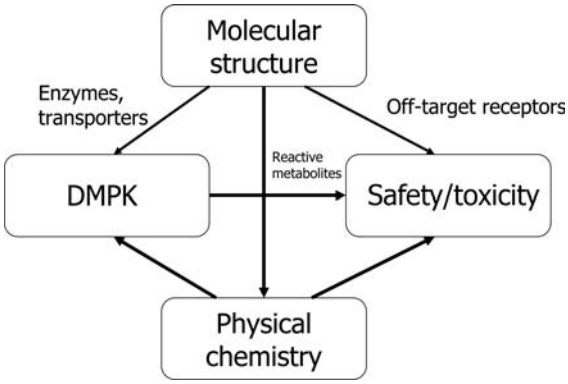

Figure 5.1 Dependency of DMPK and safety/toxicity properties on structural and physicochemical properties.

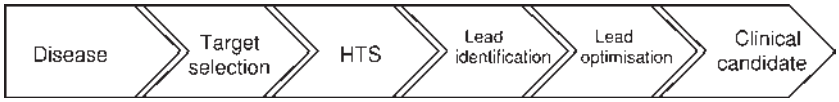

Figure 5.2 The drug discovery process.

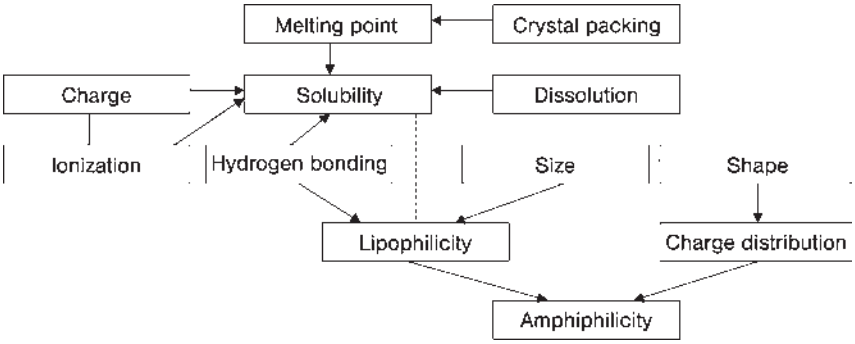

Figure 5.3 Dependencies between various physicochemical properties.

more experimental data are required in lead optimization. Striking the right balance between computational and experimental predictions is an important challenge in cost-efficient and successful drug discovery.

Physicochemical properties are considerably interrelated as visualized in Figure 5.3. The medicinal chemist should bear in mind that modifying one often means changing other physicochemical properties and hence indirectly influencing DMPK and safety profile of the compound.

5.2
Physicochemical Properties and Pharmacokinetics

5.2.1
DMPK

The study of DMPK has changed from a descriptive to a much more predictive science [3]. This is driven by great progress in bioanalytics, development of *in vitro* assays and *in silico* modeling and simulation (M&S), and much better basic understanding of the processes. Thus, and fortunately, ADME-related attrition has lowered from about 40% in 1990 to about 10% in 2005 [13].

5.2.2
Lipophilicity, Permeability, and Absorption

As an example of the role of physicochemical properties in DMPK, the properties relevant to oral absorption are described in Figure 5.4. It is important to note that

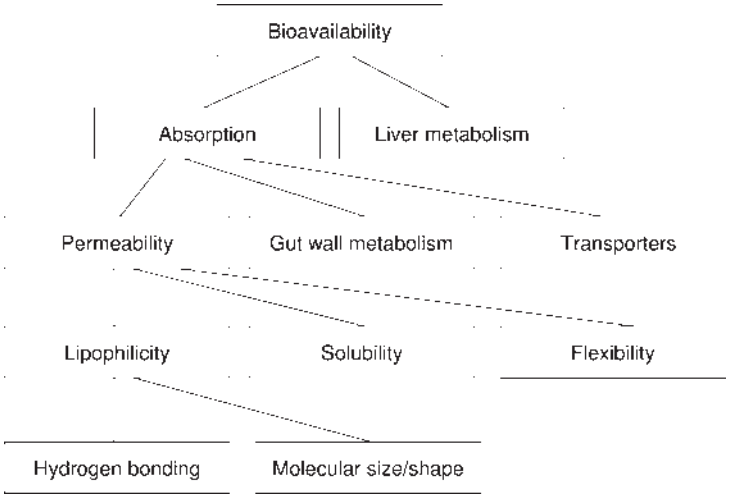

Figure 5.4 Importance of physicochemical properties on permeability, absorption, and bioavailability [16] (copyright Elsevier).

these properties are not independent but closely related to each other. Oral absorption is the percentage of drug taken up from the gastrointestinal lumen into the portal vein blood. The processes involved are a combination of physicochemical and biological processes (transporters, metabolizing enzymes). The transfer process through a membrane without any biological component is often called permeability. It can be mimicked in an artificial membrane such as the PAMPA (parallel artificial membrane permeation assay) setup (see Section 5.8.1). However, *in vivo* permeability cannot be measured in isolation from biological events. All so-called *in vitro* measures for permeability are nothing else than different types of lipophilicity measures. In plotting oral absorption (percentage or fraction) against any "permeability" or lipophilicity scale (see Figure 5.5), one observes a trend indicating that higher permeability or lipophilicity leads to better absorption. Often a plateau is observed too, indicating that such relationships are in fact nonlinear and can be approached by

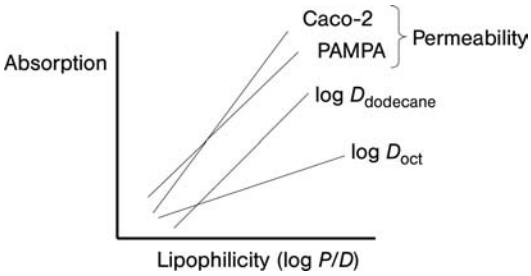

Figure 5.5 Relationships between oral absorption and permeability/lipophilicity. In reality, these relationships are most likely sigmoidal, that is, more complex than these trends indicate.

a sigmoidal function. Several lipophilicity scales can be related to each other via a Collander (Equation 5.1) or an extended Collander relationship (Equation 5.2) by adding a parameter for the difference in hydrogen bonding (HB) between the two solvent systems. The equivalent for relating, for example, PAMPA scales to each other, or PAMPA with Caco-2, has been published as well [14, 15].

$$\log P_1 = a \log P_2 + b, \tag{5.1}$$

$$\log P_1 = p \log P_2 + q\,\mathrm{HB} + r. \tag{5.2}$$

Instead of using surrogate measures for oral absorption with a lipophilicity or permeability assay *in vitro*, oral absorption can also be estimated *in silico* by using human oral absorption data from the literature [16]. These data are rather sparse because oral absorption is not systematically measured in clinical trials. The data are also skewed toward high absorption compounds. In addition, interindividual variability is important, about 15%. Of course, absorption can also depend on dose and formulation. Therefore, early estimates are only rough guides to get the ballpark right.

5.2.3
Estimation of Volume of Distribution from Physical Chemistry

The distribution of a drug in the body is largely driven by its physicochemical properties and in part for some compounds by the contribution of transporter proteins [17]. By using the Oie–Tozer equation and estimates for ionization (pK_a), plasma protein binding (PPB), and lipophilicity ($\log D_{7.4}$), quite robust predictions for the volume of distribution at steady state (V_{dss}), often within twofold of the observed value, can be made [18].

5.2.4
Plasma Protein Binding and Physicochemical Properties

Although the percentage of binding to plasma proteins (PPB%) is an important factor in pharmacokinetics and is a determinant in the actual dosage regimen (frequency), it is not important for the daily dose size [3]. The daily dose is determined by the required free or unbound concentration of drug required for efficacy [3]. Lipophilicity is a major driver of PPB% [19, 20]. The effect of the presence of negative (acids) or positive (bases) charges has different impacts on binding to human serum albumin (HSA), as negatively charged compounds bind more strongly to HSA than would be expected from the lipophilicity of the ionized species at pH 7.4 [19, 20] (see Figure 5.6).

5.3
Dissolution and Solubility

Each cellular membrane can be considered as a combination of physicochemical and biological barriers to drug transport. Poor physicochemical properties may some-

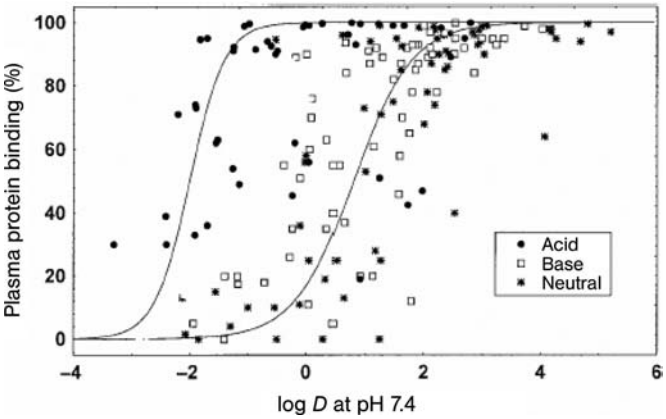

Figure 5.6 Relationships between percentage human plasma protein binding (hPPB%) and octanol/water log $D_{7.4}$ [20]. Note the about 2 log units downshift of the sigmoidal relationship for acids as compared to neutrals and basics (copyright Springer–Kluwer).

times be overcome by an active transport mechanism. Before any absorption can take place at all, the first important properties to consider are dissolution and solubility [21a]. Many cases of solubility-limited absorption have been reported and therefore solubility is now seen as a property to be addressed at early stages of drug discovery [21b]. Only compound in solution is available for permeation across the gastrointestinal membrane. Solubility has long been recognized as a limiting factor in the absorption process leading to the implementation of high-throughput solubility screens in early stages of drug design [22–24, 136, 137]. Excessive lipophilicity is a common cause of poor solubility and can lead to erratic and incomplete absorption following oral administration. Estimates of desired solubility for good oral absorption depend on the permeability of the compound and the required dose, as illustrated in Table 5.1 [137]. The incorporation of an ionizable center, such as an amine or similar function, into a template can bring a number of benefits including water solubility.

The concept of maximum absorbable dose (MAD) relates drug absorption to solubility via Equation 5.3 [25, 26]:

$$\mathrm{MAD} = S \times k_a \times \mathrm{SIWV} \times \mathrm{SITT}, \tag{5.3}$$

where S is the solubility (mg/ml) at pH 6.5, k_a is the transintestinal absorption rate constant (min^{-1}), SIWV is the small intestinal water volume (ml), assumed to be about 250 ml, and SITT is the small intestinal transit time (min), assumed to be 4.5 h = 270 min.

Dissolution testing has been used as a prognostic tool for oral drug absorption [27]. A Biopharmaceutics Classification Scheme (BCS) has been proposed under which drugs can be categorized into four groups according to their solubility and permeability properties [28]. Because both permeability and solubility can be further dissected into more fundamental properties, it has been argued that the principal

Table 5.1 Desired solubility needed for expected doses [137].

Dose (mg/kg)	Permeability (μg/ml)		
	High	**Medium**	**Low**
0.1	1	5	21
1	10	52	210
10	100	520	2100

properties are not solubility and permeability, but rather molecular size and hydrogen bonding [29]. The BCS has been adopted as a regulatory guideline for bioequivalence studies.

5.3.1 Calculated Solubility

As a key first step toward oral absorption, considerable effort went into the development of computational solubility prediction [30–37]. However, partly due to a lack of large sets of experimental data measured under identical conditions, today's methods are not robust enough for reliable predictions [38]. Further fine-tuning of the models can be expected as new high-throughput data become available to construct such models. Models will be approximate since they do not take into account the effect of crystal packing, ionic force, type of buffer, temperature, and so on. Solubility is typically measured in an aqueous buffer only partly mimicking the physiological state. More expensive FaSSIF solutions have been used to measure solubility, which in some cases appear to give better predictions in physiologically based pharmacokinetic (PBPK) modeling than solubility data using a simpler aqueous buffer [39].

5.4 Ionization (pK_a)

For decades, it was assumed that molecules can cross a membrane only in their neutral form. This dogma, based on the pH-partition theory, has been challenged [40, 138]. Using cyclic voltammetry, it was demonstrated that compounds in their ionized form pass into organic phases and might well cross membranes in this ionized form [41].

The importance of drug ionization using cell-based methods such as Caco-2 in the *in vitro* prediction of *in vivo* absorption was discussed [42]. It was observed that when the apical pH used in Caco-2 studies was lowered from 7.4 to 6.0, a better correlation was obtained with *in vivo* data, demonstrating that careful selection of experimental conditions *in vitro* is crucial to have a reliable model. Studies with Caco-2 monolayers also suggested that the ionic species might contribute considerably to overall drug transport [43].

Various ways a charged compound may cross a membrane by a "passive" mechanism have been described [40]. These include ion (trans- and/or paracellular), ion pair, or protein-assisted transport (using the outer surface of a protein spanning a membrane).

Therefore, a continued interest exists in the role of pK_a in oral absorption, which is often related to its effect on lipophilicity and solubility. Medicinal chemists can modulate these properties through structural modifications [44]. Various methods to measure pK_a values have been developed [44–47] and considerable databases are now available.

The difference between the log P of a given compound in its neutral form (log P^N) and its fully ionized form (log P^I) has been termed diff(log P^{N-I}) and contains series-specific information and expresses the influence of ionization on the intermolecular forces and intramolecular interactions of a solute [41, 48, 49].

5.4.1
Calculated pK_a

A number of approaches to predict ionization based on structure have been published (for a review see Ref. [50]), and some of these are commercially available. Predictions tend to be good for structures with already known and measured functional groups. However, predictions can be poor for new innovative structures. Nevertheless, pK_a predictions can still be used to drive a project in the desired direction, and rank order of the compounds is often correct. More recently, training algorithms have also become available, which use in-house data to improve the predictions. This is obviously the way forward.

5.5
Molecular Size and Shape

Molecular size can be a further limiting factor in oral absorption [51]. The Lipinski's rule-of-5 proposes an upper limit of MW 500 as acceptable for orally absorbed compounds [136]. High molecular weight (MW) compounds tend to undergo biliary excretion. High MW is a necessary but not sufficient condition for biliary excretion. Substrates of the excretion transporters must also be anionic, that is, resemble the natural substrates, which are biliary acids. Size and shape parameters are generally not measured but rather calculated. A measured property is the so-called cross-sectional area, which is obtained from surface activity measurements [52].

5.5.1
Calculated Size Descriptors

Molecular weight is often taken as the size descriptor of choice, while it is easy to calculate and is in the chemist's mind. However, other size and shape properties are equally simple to calculate and may offer a better guide to estimate potential for

permeability. Thus far, no systematic work has been reported investigating this in detail. Cross-sectional area A_D obtained from surface activity measurements has been reported as a useful size descriptor to discriminate compounds that can access the brain ($A_D < 80\,Å^2$) from those that are too large to cross the blood–brain barrier (BBB) [52]. Similar studies have been performed to define a cutoff for oral absorption [53].

5.6 Hydrogen Bonding

Molecular size and hydrogen bonding have been unraveled as the two major components of log *P* or log *D* [54–56]. It was found that hydrogen-bonding capacity of a drug solute correlates reasonably well with passive diffusion. $\Delta\log P$, the difference between octanol/water and alkane/water partitioning, was suggested as a good measure for solute hydrogen bonding [55, 57, 58]. However, this involves tedious experimental work, and it appeared that calculated descriptors for hydrogen bonding could most conveniently be assessed, particularly for virtual compounds.

5.6.1 Calculated Hydrogen-Bonding Descriptors

Considerable interest is focused on the calculation of hydrogen-bonding capability in the design of combinatorial libraries for assessing the potential for oral absorption and permeability [16, 59–62]. A number of different descriptors for hydrogen bonding have been discussed [63], one of the simplest being the count of the number of hydrogen bond forming atoms [64].

A simple measure of hydrogen-bonding capacity, originally proposed by van de Waterbeemd and Kansy [65], is the polar surface area (PSA), defined as the sum of the fractional contributions to surface area of all nitrogen and oxygen atoms and hydrogen atoms attached to these. PSA was used to predict the passage of the blood–brain barrier [66–68], flux across a Caco-2 monolayer [69], and human intestinal absorption [70, 71]. The physical explanation is that polar groups are involved in desolvation when they move from an aqueous extracellular environment to the more lipophilic interior of membranes. PSA thus represents, at least, part of the energy involved in membrane transport. PSA depends on conformation, and the original method [65] is based on a single minimum energy conformation. Others [70] have taken into account conformational flexibility and coined a dynamic PSA, in which a Boltzmann-weighted average PSA is computed. However, it was demonstrated that PSA calculated for a single minimum energy conformation is in most cases sufficient to produce a sigmoidal relationship to intestinal absorption, differing very little from the dynamic PSA described above [71]. A fast calculation of PSA as a sum of fragment-based contributions has been published [72], allowing these calculations to be used for large data sets such as combinatorial or virtual libraries. The sigmoidal relationship can be described by $A\% = 100/[1 + (\mathrm{PSA}/\mathrm{PSA}_{50})^{\gamma}]$,

where $A\%$ is percentage of orally absorbed drug, PSA_{50} is the PSA at 50% absorption level, and γ is a regression coefficient [73].

Poorly absorbed compounds have been identified as those with a PSA > 140 Å^2. Considering more compounds, considerably more scatter was found around the sigmoidal curve observed for a smaller set of compounds [71]. This is partly due to the fact that many compounds not only show simple passive diffusion but are also affected by active carriers, efflux mechanisms involving P-glycoprotein (P-gp) and other transporter proteins, and gut wall metabolism. These factors also contribute to the considerable interindividual variability of human oral absorption data. A further refinement in the PSA approach is expected to come from taking into account the strength of the hydrogen bonds, which in principle already is the basis of the HYBOT approach [60–62].

5.7 Lipophilicity

5.7.1 log *P* and log *D*

Octanol/water partition (log *P*) and distribution (log *D*) coefficients are widely used to estimate membrane penetration and permeability, including gastrointestinal absorption [74, 75], BBB crossing [57, 66], and correlations to pharmacokinetic properties [1]. The two major components of lipophilicity are molecular size and hydrogen bonding [54], each of which has been discussed above (see Sections 5.5 and 5.6).

According to published IUPAC recommendations, the terms hydrophobicity and lipophilicity are best described as follows [76]:

- *Hydrophobicity* is the association of nonpolar groups or molecules in an aqueous environment, which arises from the tendency of water to exclude nonpolar molecules.
- *Lipophilicity* represents the affinity of a molecule or a moiety for a lipophilic environment. It is commonly measured by its distribution behavior in a biphasic system, either liquid–liquid (e.g., partition coefficient in 1-octanol/water) or solid–liquid (retention on reversed-phase high-performance liquid chromatography (RP-HPLC) or thin-layer chromatography (TLC) system).

The intrinsic lipophilicity (*P*) of a compound refers only to the equilibrium of the unionized (neutral) drug between the aqueous phase and the organic phase. It follows that the remaining part of the overall equilibrium, that is, the concentration of ionized drug in the aqueous phase, is also of great importance in the overall observed partition ratio. This in turn depends on the pH of the aqueous phase and the acidity or basicity (pK_a) of the charged function. The overall ratio of drug, ionized and unionized, between the phases has been described as the *distribution coefficient* (*D*) to distinguish it from the intrinsic lipophilicity (*P*). The term has become widely used in recent years to

describe, in a single term, the *effective (or net) lipophilicity* of a compound at a given pH taking into account both its intrinsic lipophilicity and its degree of ionization. The distribution coefficient (D) for a monoprotic acid (HA) is defined as

$$D = \frac{[\mathrm{HA}]_{\mathrm{organic}}}{[\mathrm{HA}]_{\mathrm{aqueous}} + [\mathrm{A}^-]_{\mathrm{aqueous}}}, \tag{5.4}$$

where [HA] and [A^-] represent the concentrations of the acid in its unionized and dissociated (ionized) states, respectively. The ionization of the compound in water is defined by its dissociation constant (K_a) as

$$K_a = \frac{[\mathrm{H}^+][\mathrm{A}^-]}{[\mathrm{HA}]}, \tag{5.5}$$

sometimes referred to as the Henderson–Hasselbalch relationship. The combination of Equations 5.4–5.6 gives the pH distribution (or "pH-partition") relationship:

$$D = \frac{P}{1 + (K_a/[\mathrm{H}^+])}, \tag{5.6}$$

more commonly expressed for monoprotic organic *acids* in the form of Equations 5.7 and 5.8:

$$\log\left(\frac{P}{D} - 1\right) = \mathrm{pH} - \mathrm{p}K_a \tag{5.7}$$

or

$$\log D = \log P - \log(1 + 10^{\mathrm{pH} - \mathrm{p}K_a}). \tag{5.8}$$

For monoprotic organic *bases* (BH^+ dissociating to B), the corresponding relationships are

$$\log\left(\frac{P}{D} - 1\right) = \mathrm{p}K_a - \mathrm{pH} \tag{5.9}$$

or

$$\log D = \log P - \log(1 + 10^{\mathrm{p}K_a - \mathrm{pH}}). \tag{5.10}$$

From these equations, it is possible to predict the effective lipophilicity (log D) of an acidic or basic compound at any pH value. The data required to use the relationship in this way are the intrinsic lipophilicity (log P), the dissociation constant (pK_a), and the pH of the aqueous phase. The overall outcome of these relationships is the effective lipophilicity of a compound, at physiological pH, which is approximately the log P value minus one unit of lipophilicity; for every unit of pH, the pK_a value is below (for acids) and above (for bases) pH 7.4. Obviously, for compounds with multifunctional ionizable groups, the relationship between log P and log D, as well as log D as a function of pH, becomes more complex [62, 65, 67]. For diprotic molecules, there are already 12 different possible shapes of log D–pH plots. Ion pairs (salts), zwitterions, and ampholytes are special cases and both measurement of log P/D and their interpretation need special attention [44, 49].

Traditional octanol/water distribution coefficients are still widely used in quantitative structure–activity relationship (QSAR) and in ADME/PK studies. However, alternative solvent systems have been proposed [77]. To cover the variability in biophysical characteristics of different membrane types, a set of four solvents has been suggested, sometimes called the "critical quartet" [78]. The 1,2-dichloroethane (DCE)/water system has been promoted as a good alternative to alkane/water due to its far better dissolution properties [79, 80], but may find little use because of its carcinogenic properties.

Several approaches for higher throughput lipophilicity measurements have been developed in the pharmaceutical industry [47] including automated shake-plate methods [81] and immobilized artificial membranes (IAMs) [82]. A convenient method to measure octanol/water partitioning is based on potentiometric titration, called the pH method [83]. Methods based on chromatography are also widely used and include, for example, chromatographic hydrophobicity indices (CHIs) measured on immobilized artificial membranes [19, 84]. Another chromatography-based method is called Elog *D* giving log *D* values comparable to shake-flask data [85].

5.7.2 Calculated log *P* and log *D*

A number of rather comprehensive reviews on lipophilicity estimation have been published and are recommended for further reading [86–88]. Owing to its key importance, a continued interest is seen to develop good log *P* estimation programs [89–91]. Most log *P* approaches are limited due to a lack of parameterization of certain fragments. For the widely used CLOGP program, a version with the ability to estimate missing fragments has become available [92].

With only few exceptions, most log *P* programs refer to the octanol/water system. Based on Rekker's fragmental constant approach, a log *P* calculation for aliphatic hydrocarbon/water partitioning has been reported [93]. Another more recent approach to alkane/water log *P* and log *D* is based on the program VolSurf [94]. It is believed that these values may afford a better prediction of uptake in the brain. The group of Abraham investigated many other solvent systems and derived equations to predict log *P* from structure for these solvent systems, which are also commercially available [91].

log *D* predictions are more difficult as most approaches rely on the combination of estimated log *P* and estimated pK_a. Obviously, this can lead to error accumulation and errors of 2 log units or more can be found. Some algorithms, however, are designed to learn from experimental data so that the predictions improve over time. An interesting approach is also the combination of a commercial log *D* predictor with proprietary descriptors using a Bayesian neural network (BNN) approach [95].

Often ignored is the fact that log *P*/*D* is a conformation-dependent property [161], which has elegantly been demonstrated with the molecular lipophilicity potential (MLP) descriptor [87]. The MLP algorithm allows to calculate virtual log *P* values in conformational space.

Table 5.2 *In vitro* models for membrane permeability.

Permeability model	References
Solvent/water partitioning	
Octanol/water distribution	[49]
Chromatography	
IAMs	[105–109]
ILC	[111]
MEKC	[113]
BMC	[114]
Vesicles	
Phospholipid vesicles	[129]
Liposome binding	[117, 118]
Transil particles	[120–122]
Fluorosomes	[123]
SPR biosensor	[125, 126]
Colorometric assay	[124]
Artificial membranes	
Impregnated membranes	[69]
PAMPA	[96–102]
Filter IAM	[100–102]
HDM	[103, 104]
Other	
Surface activity	[128]
Cell-based assays	
Caco-2	[73, 75]
MDCK	[150]

5.8 Permeability

An overview of permeability assays is presented in Table 5.2. As discussed earlier in this chapter, these permeability scales are correlated to each other, as well as the various lipophilicity scales, via extended Collander equations.

5.8.1 Artificial Membranes and PAMPA

When screening for absorption by passive membrane permeability, artificial membranes have the advantage of offering a highly reproducible, high-throughput system. Artificial membranes have been compared with Caco-2 cells and found to behave very similar for passive diffusion [69]. This finding was the basis for the development of the parallel artificial membrane permeation assay for rapid prediction of transcellular absorption potential [96–99]. In this system, the permeability through a membrane formed by a mixture of lecithin and an inert organic solvent on a hydrophobic filter support is assessed. While not completely predictive for oral absorption in humans,

PAMPA shows definite trends in the ability of molecules to permeate membranes by passive diffusion, which may be valuable in screening large compound libraries. This system is commercially available [100], but can easily be set up in-house. Further optimization of the experimental conditions has been investigated concluding that predictability increases when a pH of 6.5 or 5.5 is used on the donor side [101, 102]. It was also demonstrated that the effect of a cosolvent such as dimethyl sulfoxide (DMSO) could have a marked effect depending on the nature, basic or acidic, of the compound [102]. Stirring of the donor compartment to limit the contribution of the unstirred water layer (UWL) appears to be important to get meaningful results. There have been so far no reports in the literature about using PAMPA data in a drug discovery project.

A similar system based on polycarbonate filters coated with hexadecane, also called hexadecane membranes (HDMs), has been reported [103, 104]. Thus, this system consists of a 9–10 μm hexadecane liquid layer immobilized between two aqueous compartments. Also, here it was observed that in this setup for lipophilic compounds, the diffusion through the unstirred water layer becomes the rate-limiting step. To mimic the *in vivo* environment permeability, measurements were repeated at different pH values in the range 4–8, and the highest transport value was used for correlation with the percentage absorbed in humans. This gives a sigmoidal dependence, which is better than when taking values measured at a single pH, for example, 6.8.

5.8.1.1 *In Silico* PAMPA

The experimental P_{app} data have been used to build predictive models. However, since PAMPA is already a model, an *in silico* model based on this is a model of a model. The predictability for *in vivo* permeability or absorption of such *in silico* PAMPA model can be questioned (see Equation 5.11), since it is two steps from reality.

$$\text{model} \times \text{model} = \text{random}. \tag{5.11}$$

5.8.2 IAM, ILC, MEKC, and BMC

Immobilized artificial membranes are another means of measuring lipophilic characteristics of drug candidates and other chemicals [105–109]. IAM columns may mimic membrane interactions better than the isotropic octanol/water or other solvent/solvent partitioning system. These chromatographic indices appear to be a significant predictor of passive absorption through the rat intestine [110].

A related alternative is called immobilized liposome chromatography (ILC) [111, 112]. Compounds with the same log *P* were shown to have very different degrees of membrane partitioning on ILC depending on the charge of the compound [112].

Another relatively new lipophilicity scale proposed for use in ADME studies is based on micellar electrokinetic chromatography (MEKC) [113]. A further variant is called biopartitioning micellar chromatography (BMC) and uses mobile phases of Brij35 (polyoxyethylene(23)lauryl ether) [114]. Similarly, the retention factors of 16 beta-blockers obtained with micellar chromatography using sodium dodecyl sulfate

as micelle-forming agent correlate well with permeability coefficients in Caco-2 monolayers and apparent permeability coefficients in rat intestinal segments [115].

Each of these scales produces a lipophilicity index related but not identical to octanol/water partitioning.

5.8.3 Liposome Partitioning

Liposomes, which are lipid bilayer vesicles prepared from mixtures of lipids, also provide a useful tool for studying passive permeability of molecules through lipid. This system, for example, has been used to demonstrate the passive nature of the absorption mechanism of monocarboxylic acids [116]. Liposome partitioning of ionizable drugs can be determined by titration and has been correlated with human absorption [117–119]. Liposome partitioning is only partly correlated with octanol/water distribution and might contain some additional information.

A further partition system based on the use of liposomes, and commercialized under the name Transil [120, 121], has shown its utility as a lipophilicity measure in PBPK modeling [122]. Fluorescent-labeled liposomes, called fluorosomes, are another means of measuring the rate of penetration of small molecules into membrane bilayers [99, 123]. Similarly, a colorometric assay amenable to high-throughput screening for evaluating membrane interactions and penetration has been presented [124]. The platform comprises vesicles of phospholipids and the chromatic lipid-mimetic polydiacetylene. The polymer undergoes visible concentration-dependent red–blue transformations induced through interactions of the vesicles with the studied molecules.

5.8.4 Biosensors

Liposomes have been attached to a biosensor surface, and the interactions between drugs and the liposomes can be monitored directly using surface plasmon resonance (SPR) technology. SPR measures changes in refractive index at the sensor surface caused by changes in mass. Drug–liposome interactions have been measured for 27 drugs and compared with fraction absorbed in humans [125]. A reasonable correlation is obtained, but it is most likely that this method represents just another way of measuring "lipophilicity." The throughput was 100 substances/24 h, but further progress seems possible. In more recent work using this method, it is proposed to use two types of liposomes to separate compounds according to their absorption potential [126].

5.9 Amphiphilicity

The combination of hydrophilic and hydrophobic parts of a molecule defines its amphiphilicity. A program has been described to calculate this property and

calibrated against experimental values obtained from surface activity measurements [127]. These values can possibly be used to predict effect on membranes leading to cytotoxicity or phospholipidosis, but may also contain information, yet not unraveled, on permeability. Surface activity measurements have also been used to make estimates of oral absorption [128].

5.10 Drug-Like Properties

The various properties described above are important for drugs, particularly for those given orally. The important question arises whether such properties of drugs are different from chemicals used in other ways. This has been subject of a number of studies [130, 131, 162]. Using neural networks [132, 133] or a decision tree approach [134], a compound can be predicted as being "drug-like" with an error rate of about 20%. A further approach to predict drug-likeness consists of training of the program PASS [135], which was originally intended to predict activity profiles and thus is suitable to predict potential side effects.

From an analysis of the key properties of compounds in the World Drug Index (WDI), the now well-accepted rule-of-5 has been derived [136, 137]. It was concluded that compounds are most likely to have poor absorption when the molecular weight is more than 500, the calculated octanol/water partition coefficient (Clog *P*) is more than 5, number of H-bond donors is more than 5, and the number of H-bond acceptors is more than 10. Computation of these properties is now available as a simple but efficient ADME screen in commercial software. The rule-of-5 should be seen as a qualitative absorption/permeability predictor [138], rather than a quantitative predictor [139]. The rule-of-5 is not predictive for bioavailability as sometimes mistakenly assumed. An important factor for bioavailability in addition to absorption is liver first-pass effect (metabolism). The property distribution in drug-related chemical databases has been studied as another approach to understand "drug-likeness" [140, 141].

Other attempts have been made to try to define good leads [142, 143]. In general, lead-like properties are lower/fewer than drug-like properties. Thus, MW < 350 and Clog $P < 3$ should be good starting points for leads [142]. A rule-of-3 has been proposed [143] for screening small fragments, which says the good lead fragments have MW < 300, Clog $P < 3$, H-bond donors and acceptors less than 3, and rotatable bonds less than 3.

Similarly, in a study on drugs active as central nervous system (CNS) agents, using neural networks based on Bayesian methods, CNS-active drugs could be distinguished from CNS-inactive ones [144]. A CNS rule of thumb says that if the sum of the nitrogen and oxygen (N + O) atoms in a molecule is less than 5, and if the Clog $P - (N + O) > 0$, then compounds are likely to penetrate the blood–brain barrier [145]. Another "rule" is that the PSA should be less than 90 $Å^2$, the MW should be less than 450, and the log *D* at pH 7.4 should be between 1 and 3 [146]. In designing CNS drugs, it is important to distinguish BBB penetration and CNS efficacy. The CNS efficacy is a subtle balance between permeability, effect of BBB transporters, lipophilicity, and free fraction in blood and brain [147].

These aforementioned analyses point to a critical combination of physicochemical and structural properties [148], which to a large extent can be manipulated by the medicinal chemist. This approach in medicinal chemistry has been called property-based design [2]. Properties in this context mean physicochemical as well as pharmaco- and toxicokinetic properties. These have been neglected for a long time by most medicinal chemists who in many cases in the past had the quest only for strongest receptor binding as ultimate goal. However, this strategy has changed dramatically, and the principles of drug-like compounds are now being used in computational approaches toward the rational design of combinatorial libraries [149] and in decision making on acquisition of outsourced libraries.

5.11
Computation Versus Measurement of Physicochemical Properties

5.11.1
QSAR Modeling

Calculation of many different 1D, 2D, and 3D descriptors for building predictive QSAR models for physicochemical (and ADMET) properties is possible by using a range of commercially available software packages, such as ACD, Sybyl, Cerius2, Molconn-Z, HYBOT, VolSurf, MolSurf, Dragon, MOE, BCUT, and so on. Several descriptor sets are based on quantification of 3D molecular surface properties [151, 152], and these have been explored for the prediction of, for example, Caco-2 permeability and oral absorption [16]. It is pointed out here that a number of these "new" descriptors are often strongly correlated to the more traditional physicochemical properties. An aspect largely neglected so far is the concept of molecular property space that looks at the conformational effects on physicochemical properties [153].

Numerous QSAR tools have been developed [152, 154] and used in modeling physicochemical data. These vary from simple linear to more complex nonlinear models, as well as classification models. A popular approach more recently became the construction of consensus or ensemble models ("combinatorial QSAR") by combining the predictions of several individual approaches [155]. Or, alternatively, models can be built by running the same approach, such as a neural network of a decision tree, many times and combining the output into a single prediction.

To build robust predictive models, good-quality training set and sound test set are required. Criteria for a good set include sufficient coverage of chemical space, good distribution between low- and high-end values of the property studied, and a sufficiently large number of compounds. Models can be global (covering many types of chemistry) or local (project specific). There are many reasons why predictions can fail [156], and medicinal chemists need to be aware of these. There is also a difference between a useful model and a perfect model. The latter does not exist!

In-house physicochemical data collections are growing rapidly through the use of HTS technologies [157]. Therefore, the need for rapidly building and updating is also increasing. Systems for automatic and regular updating of QSAR predictive models have been reported [158] and we expect these to become more widespread. A consequence of regularly updated *in silico* models is that the predicted values will change too. This will require adapted ways of working in projects using more dynamic data generation and interpretation tools.

5.11.2 *In Combo*: Using the Best of Two Worlds

In modern drug discovery, speed and cost control, in addition to high quality, are important. *In silico* virtual screening for drugability [159] is a good first step in library design and compound acquisition. Once compounds have been made for a targeted project, a well-balanced approach using both *in silico* predictions and *in vitro* screening will be a good strategy to guide the program in a cost-efficient manner. New experimental data can be used to update predictive models regularly so that the ongoing projects can benefit from the latest local and global models available [158, 160].

5.12 Outlook

Physical chemistry plays a key role in the behavior of drugs. Measurement of the key properties has been automated and industrialized to high throughput. The data can be and are used to build robust predictive models, which are used in design building in the required compound quality. These can in turn also be used to limit the use of experiments when not strictly needed. This is of course compound saving and more cost-effective. Predictive models for physicochemical, DMPK/ADME, and toxicity/safety properties are thus great tools in virtual screening, prioritization, decision making, and guiding projects [162].

References

1 Smith, D.A., Jones, B.C. and Walker, D.K. (1996) Design of drugs involving the concepts and theories of drug metabolism and pharmacokinetics. *Medicinal Research Reviews*, **16**, 243–266.

2 van de Waterbeemd, H., Smith, D.A., Beaumont, K. and Walker, D.K. (2001) Property-based design: optimisation of drug absorption and pharmacokinetics. *Journal of Medicinal Chemistry*, **44**, 1313–1333.

3 Smith, D.A., van de Waterbeemd, H. and Walker, D.K. (2006) *Pharmacokinetics and Metabolism in Drug Design*, 2nd edn, Wiley-VCH Verlag GmbH, Weinheim.

4 Testa, B., Krämer, S.D., Wunderli-Allensbach, H. and Folkers, G. (eds) (2006) *Biological and Physicochemical*

Profiling in Drug Research, Wiley-VCH Verlag GmbH, Weinheim.

5 Testa, B. and van de Waterbeemd, H. (eds) (2007) *ADME/Tox Approaches*, Vol. 5, in *Comprehensive Medicinal Chemistry*, 2nd edn (series eds J.B Taylor and D.J. Triggle), Elsevier, Oxford.

6 Pliska, V., Testa, B. and van de Waterbeemd, H. (1996) *Lipophilicity in Drug Action and Toxicology*, Wiley-VCH Verlag GmbH, Weinheim.

7 Testa, B., van de Waterbeemd, H., Folkers, G. and Guy, R. (2001) *Pharmacokinetic Optimization in Drug Research*, Wiley-VCH Verlag GmbH, Weinheim.

8 Kerns, E.H. and Di, L. (2004) Physicochemical profiling: overview of the screens. *Drug Discovery Today: Technologies*, **1**, 343–348.

9 van de Waterbeemd, H. (2003) Physicochemical approaches to drug absorption, in *Drug Bioavailability* (eds H. van de Waterbeemd, H. Lennernäs and P. Artursson), Wiley-VCH Verlag GmbH, Weinheim, pp. 3–20.

10 van de Waterbeemd, H. (2006) Physicochemistry, in *Pharmacokinetics and Metabolism in Drug Design*, 2nd edn (eds D.A. Smith, H. van de Waterbeemd and D.K. Walker), Wiley-VCH Verlag GmbH, Weinheim, pp. 1–18.

11 van de Waterbeemd, H. (2006) Property-based lead optimization, in *Biological and Physicochemical Profiling in Drug Research* (eds B. Testa, S.D. Krämer, H. Wunderli-Allensbach and G. Folkers), Wiley-VCH Verlag GmbH, Weinheim, pp. 25–45.

12 Kerns, E.H. and Di, L. (2007) Chemical stability, in *ADME/Tox Approaches*, Vol. 5 (eds B. Testa and H. van de Waterbeemd), in *Comprehensive Medicinal Chemistry*, 2nd edn (series eds J.B Taylor and D.J. Triggle), Elsevier, Oxford, pp. 489–507.

13 Kola, I. and Landis, J. (2004) Can the pharmaceutical industry reduce attrition rates? *Nature Reviews. Drug Discovery*, **3**, 711–716.

14 Avdeef, A. and Tsinman, O. (2006) PAMPA: a drug absorption *in vitro* model. 13. Chemical selectivity due to membrane hydrogen bonding: in combo comparisons of HDM-, DOPC-, and DS-PAMPA models. *European Journal of Pharmaceutical Sciences*, **28**, 43–50.

15 Avdeef, A., Artursson, P., Neuhoff, S., Lazorova, L., Gråsjö, J. and Tavelin, S. (2005) Caco-2 permeability of weakly basic drugs predicted with the double-sink PAMPA pK_a^{flux} method. *European Journal of Pharmaceutical Sciences*, **24**, 333–349.

16 van de Waterbeemd, H. (2007) *In silico* models to predict oral absorption, in *ADME/Tox Approaches*, Vol. 5 (eds B. Testa and H. van de Waterbeemd), in *Comprehensive Medicinal Chemistry*, 2nd edn (series eds J.B Taylor and D.J. Triggle), Elsevier, Oxford, pp. 669–697.

17 van de Waterbeemd, H. (2005) Which *in vitro* screens guide the prediction of oral absorption and volume of distribution? *Basic & Clinical Pharmacology & Toxicology*, **96**, 162–166.

18 Lombardo, F., Obach, R.S., Shalaeva, M.Y. and Gao, F. (2004) Prediction of human volume of distribution values for neutral and basic drugs. 2. Extended data set and leave-class-out statistics. *Journal of Medicinal Chemistry*, **47**, 1242–1250.

19 Valko, K., Nunhuck, S., Bevan, C., Abraham, M.H. and Reynolds, D.P. (2003) Fast gradient HPLC method to determine compounds binding to human serum albumin. Relationships with octanol/water and immobilized artificial membrane lipophilicity. *Journal of Pharmaceutical Sciences*, **92**, 2236–2248.

20 van de Waterbeemd, H., Smith, D.A. and Jones, B.C. (2001) Lipophilicity in PK design: methyl, ethyl, futile. *Journal of Computer-Aided Molecular Design*, **15**, 273–286.

21 Avdeef, A., Voloboy, A. and Foreman, A. (2007) Solubility and dissolution, in *ADME/Tox Approaches*, Vol. 5 (eds B. Testa and H. van de Waterbeemd), in

Comprehensive Medicinal Chemistry, 2nd edn (series eds J.B Taylor and D.J. Triggle), Elsevier, Oxford, pp. 399–423; Stegemann, S., Leveiller, F., Franchi, D., De Jong, H. and Lindén, H. (2007) When poor solubility becomes an issue: from early stage to proof of concept. *European Journal of Pharmaceutical Sciences*, **31**, 249–261.

22 Bevan, C.D. and Lloyd, R.S. (2000) A high-throughput screening method for the determination of aqueous drug solubility using laser nephelometry in microtiter plates. *Analytical Chemistry*, **72**, 1781–1787.

23 Avdeef, A. (2001) High-throughput measurements of solubility profiles, in *Pharmacokinetic Optimization in Drug Research: Biological, Physicochemical and Computational Strategies* (eds B. Testa, H. van de Waterbeemd, G. Folkers and R. Guy), Wiley-VCH Verlag GmbH, Weinheim, pp. 305–325.

24 Avdeef, A. and Berger, C.M. (2001) pH-metric solubility. 3. Dissolution titration template method for solubility determination. *European Journal of Pharmaceutical Sciences*, **14**, 281–291.

25 Johnson, K. and Swindell, A. (1996) Guidance in the setting of drug particle size specifications to minimize variability in absorption. *Pharmaceutical Research*, **13**, 1795–1798.

26 Curatolo, W. (1998) Physical chemical properties of oral drug candidates in the discovery and exploratory development settings. *Pharmaceutical Science & Technology Today*, **1**, 387–393.

27 Dressman, J.B., Amidon, G.L., Reppas, C. and Shah, V.P. (1998) Dissolution testing as a prognostic tool for oral drug absorption: immediate release dosage forms. *Pharmaceutical Research*, **15**, 11–22.

28 Amidon, G.L., Lennernäs, H., Shah, V.P. and Crison, J.R.A. (1995) A theoretical basis for a biopharmaceutic drug classification: the correlation of *in vitro* drug product dissolution and *in vivo* bioavailability. *Pharmaceutical Research*, **12**, 413–420.

29 van de Waterbeemd, H. (1998) The fundamental variables of the bio-pharmaceutics classification system (BCS): a commentary. *European Journal of Pharmaceutical Sciences*, **7**, 1–3.

30 Huuskonen, J. (2001) Estimation of aqueous solubility in drug design. *Combinatorial Chemistry & High Throughput Screening*, **4**, 311–316.

31 McFarland, J.W., Avdeef, A., Berger, C.M. and Raevsky, O.A. (2001) Estimating the water solubilities of crystalline compounds from their chemical structures alone. *Journal of Chemical Information and Computer Sciences*, **41**, 1355–1359.

32 Livingstone, D.J., Ford, M.G., Huuskonen, J.J. and Salt, D.W. (2001) Simultaneous prediction of aqueous solubility and octanol/water partition coefficient based on descriptors derived from molecular structure. *Journal of Computer-Aided Molecular Design*, **15**, 741–752.

33 Bruneau, P. (2001) Search for predictive generic model of aqueous solubility using Bayesian neural nets. *Journal of Chemical Information and Computer Sciences*, **41**, 1605–1616.

34 Liu, R. and So, S.-S. (2001) Development of quantitative structure–property relationship models for early ADME evaluation in drug discovery. 1. Aqueous solubility. *Journal of Chemical Information and Computer Sciences*, **4**, 1633–1639.

35 Taskinen, and Norinder, U. (2007) *In silico* prediction of solubility, in *ADME/Tox Approaches*, Vol. 5 (eds B. Testa and H. van de Waterbeemd), in *Comprehensive Medicinal Chemistry*, 2nd edn (series eds J.B Taylor and D.J. Triggle), Elsevier, Oxford, pp. 627–648.

36 Dearden, J.C. (2006) *In silico* prediction of aqueous solubility. *Expert Opinion on Drug Discovery*, **1**, 31–52.

37 Bergström, C.A.S. (2005) Computational models to predict aqueous drug solubility,

permeability and intestinal absorption. *Expert Opinion on Drug Metabolism and Toxicology*, **1**, 613–627.

38 van de Waterbeemd, H. (2002) High-throughput and *in silico* techniques in drug metabolism and pharmacokinetics. *Current Opinion in Drug Discovery & Development*, **5**, 33–43.

39 Parrott, N., Paquereau, N., Coassolo, P. and Lavé, Th. (2005) An evaluation of the utility of physiologically based models of pharmacokinetics in early drug discovery. *Journal of Pharmaceutical Sciences*, **94**, 2327–2343.

40 Camenisch, G., van de Waterbeemd, H. and Folkers, G. (1996) Review of theoretical passive drug absorption models: historical background, recent development and limitations. *Pharmaceutica Acta Helvetiae*, **71**, 309–327.

41 Caron, G., Gaillard, P., Carrupt, P.A. and Testa, B. (1997) Lipophilicity behavior of model and medicinal compounds containing a sulfide, sulfoxide, or sulfone moiety. *Helvetica Chimica Acta*, **80**, 449–461.

42 Boisset, M., Botham, R.P., Haegele, K.D., Lenfant, B. and Pachot, J.L. (2000) Absorption of angiotensin II antagonists in Ussing chambers, Caco-2, perfused jejunum loop and *in vivo*: importance of drug ionization in the *in vitro* prediction of *in vivo* absorption. *European Journal of Pharmaceutical Sciences*, **10**, 215–224.

43 Palm, K., Luthman, K., Ros, J., Grasjo, J. and Artursson, P. (1999) Effect of molecular charge on intestinal epithelial drug transport: pH-dependent transport of cationic drugs. *The Journal of Pharmacology and Experimental Therapeutics*, **291**, 435–443.

44 Comer, J. (2007) Ionization constants and ionisation profiles, in *ADME/Tox Approaches*, Vol. 5 (eds B. Testa and H. van de Waterbeemd), in *Comprehensive Medicinal Chemistry*, 2nd edn (series eds J.B Taylor and D.J. Triggle), Elsevier, Oxford, pp. 357–397.

45 Saurina, J., Hernandez-Cassou, S., Tauler, R. and Izquierdo-Ridorsa, A. (2000) Spectrophotometric determination of pK_a values based on a pH gradient flow-injection system. *Analytica Chimica Acta*, **408**, 135–143.

46 Jia, Z., Ramstad, T. and Zhong, M. (2001) Medium-throughput pK_a screening of pharmaceuticals by pressure-assisted capillary electrophoresis. *Electrophoresis*, **22**, 1112–1118.

47 Comer, J. and Tam, K. (2001) Lipophilicity profiles: theory and measurement, in *Pharmacokinetic Optimization in Drug Research: Biological, Physicochemical and Computational Strategies* (eds B. Testa, H. van de Waterbeemd, G. Folkers and R. Guy), Wiley-VCH Verlag GmbH, Weinheim, pp. 275–304.

48 Caron, G., Reymond, F., Carrupt, P.A., Girault, H.H. and Testa, B. (1999) Combined molecular lipophilicity descriptors and their role in understanding intramolecular effects. *Pharmaceutical Science & Technology Today*, **2**, 327–335.

49 Caron, G., Scherrer, R.A. and Ermondi, G. (2007) Lipophilicity, polarity and hydrophobicity, in *ADME/Tox Approaches*, Vol. 5 (eds B. Testa and H. van de Waterbeemd), in *Comprehensive Medicinal Chemistry*, 2nd edn (series eds J.B Taylor and D.J. Triggle), Elsevier, Oxford, pp. 425–452.

50 Franczkiewicz, R. (2007) *In silico* prediction of ionisation, in *ADME/Tox Approaches, Vol. 5* (eds B. Testa and H. van de Waterbeemd), in *Comprehensive Medicinal Chemistry*, 2nd edn (series eds J.B Taylor and D.J. Triggle), Elsevier, Oxford, pp. 603–626.

51 Chan, O.H. and Stewart, B.H. (1996) Physicochemical and drug-delivery considerations for oral drug bioavailability. *Drug Discovery Today*, **1**, 461–473.

52 Fischer, H., Gottschlich, R. and Seelig, A. (1998) Blood–brain barrier permeation: molecular parameters governing passive

diffusion. *The Journal of Membrane Biology*, **165**, 201–211.

53 Fischer, H. (1998) Passive diffusion and active transport through biological membranes: binding of drugs to transmembrane receptors. Ph.D. Thesis, University of Basel, Switzerland.

54 van de Waterbeemd, H. and Testa, B. (1987) The parametrization of lipophilicity and other structural properties in drug design. *Advances in Drug Research*, **16**, 85–225.

55 El Tayar, N., Testa, B. and Carrupt, P.A. (1992) Polar intermolecular interactions encoded in partition coefficients: an indirect estimation of hydrogen-bond parameters of polyfunctional solutes. *The Journal of Physical Chemistry*, **96**, 1455–1459.

56 Abraham, M.H. and Chadha, H.S. (1996) Applications of a solvation equation to drug transport properties, in *Lipophilicity in Drug Action and Toxicology* (eds V. Pliska, B. Testa and H. van de Waterbeemd), Wiley-VCH Verlag GmbH, Weinheim, pp. 311–337.

57 Young, R.C., Mitchell, R.C., Brown, Th.H., Ganellin, C.R., Griffiths, R., Jones, M., Rana, K.K., Saunders, D., Smith, I.R., Sore, N.E. and Wilks, T.J. (1988) Development of a new physicochemical model for brain penetration and its application to the design of centrally acting H2 receptor histamine antagonists. *Journal of Medicinal Chemistry*, **31**, 656–671.

58 Von Geldern, T.W., Hoffmann, D.J., Kester, J.A., Nellans, H.N., Dayton, B.D., Calzadilla, S.V., Marsch, K.C., Hernandez, L., Chiou, W., Dixon, D.B., Wu-Wong, J.R. and Opgenorth, T.J. (1996) Azole endothelin antagonists. 3. Using Δlog *P* as a tool to improve absorption. *Journal of Medicinal Chemistry*, **39**, 982–991.

59 Dearden, J.C. and Ghafourian, T. (1999) Hydrogen bonding parameters for QSAR: comparison of indicator variables, hydrogen bond counts, molecular orbital and other parameters. *Journal of Chemical Information and Computer Sciences*, **39**, 231–235.

60 Raevsky, O.A. and Schaper, K.-J. (1998) Quantitative estimation of hydrogen bond contribution to permeability and absorption processes of some chemicals and drugs. *European Journal of Medicinal Chemistry*, **33**, 799–807.

61 Raevsky, O.A., Fetisov, V.I., Trepalina, E.P., McFarland, J.W. and Schaper, K.-J. (2000) Quantitative estimation of drug absorption in humans for passively transported compounds on the basis of their physico-chemical parameters. *Quantitative Structure–Activity Relationships*, **19**, 366–374.

62 van de Waterbeemd, H., Camenisch, G., Folkers, G. and Raevsky, O.A. (1996) Estimation of Caco-2 cell permeability using calculated molecular descriptors. *Quantitative Structure–Activity Relationships*, **15**, 480–490.

63 van de Waterbeemd, H. (2000) Intestinal permeability: prediction from theory, in *Oral Drug Absorption* (eds J.B. Dressman and H. Lennernäs), Dekker, New York, pp. 31–49.

64 Österberg, Th. and Norinder, U. (2000) Prediction of polar surface area and drug transport processes using simple parameters and PLS statistics. *Journal of Chemical Information and Computer Sciences*, **40**, 1408–1411.

65 van de Waterbeemd, H. and Kansy, M. (1992) Hydrogen-bonding capacity and brain penetration. *Chimia*, **46**, 299–303.

66 van de Waterbeemd, H., Camenisch, G., Folkers, G., Chrétien, J.R. and Raevsky, O.A. (1998) Estimation of blood–brain barrier crossing of drugs using molecular size and shape, and H-bonding descriptors. *Journal of Drug Targeting*, **2**, 151–165.

67 Kelder, J., Grootenhuis, P.D.J., Bayada, D.M., Delbressine, L.P.C. and Ploemen, J.-P. (1999) Polar molecular surface as a dominating determinant for oral absorption and brain penetration of

drugs. *Pharmaceutical Research*, **16**, 1514–1519.

68 Clark, D.E. (1999) Rapid calculation of polar molecular surface area and its application to the prediction of transport phenomena. 2. Prediction of blood–brain barrier penetration. *Journal of Pharmaceutical Sciences*, **88**, 815–821.

69 Camenisch, G., Folkers, G. and van de Waterbeemd, H. (1997) Comparison of passive drug transport through Caco-2 cells and artificial membranes. *International Journal of Pharmaceutics*, **147**, 61–70.

70 Palm, K., Luthman, K., Ungell, A.-L., Strandlund, G., Beigi, F., Lundahl, P. and Artursson, P. (1998) Evaluation of dynamic polar molecular surface area as predictor of drug absorption: comparison with other computational and experimental predictors. *Journal of Medicinal Chemistry*, **41**, 5382–5392.

71 Clark, D.E. (1999) Rapid calculation of polar molecular surface area and its application to the prediction of transport phenomena. 1. Prediction of intestinal absorption. *Journal of Pharmaceutical Sciences*, **88**, 807–814.

72 Ertl, P., Rohde, B. and Selzer, P. (2000) Fast calculation of molecular polar surface area as a sum of fragment-based contributions and its application to the prediction of drug transport properties. *Journal of Medicinal Chemistry*, **43**, 3714–3717.

73 Stenberg, P., Norinder, U., Luthman, K. and Artursson, P. (2001) Experimental and computational screening models for the prediction of intestinal drug absorption. *Journal of Medicinal Chemistry*, **44**, 1927–1937.

74 Winiwarter, S., Bonham, N.M., Ax, F., Hallberg, A., Lennernäs, H. and Karlén, A. (1998) Correlation of human jejunal permeability (*in vivo*) of drugs with experimentally and theoretically derived parameters. A multivariate data analysis approach. *Journal of Medicinal Chemistry*, **41**, 4939–4949.

75 Artursson, P. and Karlsson, J. (1991) Correlation between oral drug absorption in humans and apparent drug permeability coefficients in human intestinal epithelial (Caco-2) cells. *Biochemical and Biophysical Research Communications*, **175**, 880–885.

76 van de Waterbeemd, H., Carter, R.E., Grassy, G., Kubinyi, H., Martin, Y.C., Tute, M.S. and Willett, P. (1997) *Pure and Applied Chemistry*, **69**, 1137–1152. and van de Waterbeemd, H., Carter, R.E., Grassy, G., Kubinyi, H., Martin, Y.C., Tute, M.S. and Willett, P. (1998) *Annual Reports in Medicinal Chemistry*, **33**, 397–409.

77 Hartmann, T. and Schmitt, J. (2004) Lipophilicity – beyond octanol/water: a short comparison of modern technologies. *Drug Discovery Today: Technologies*, **1**, 431–439.

78 Leahy, D.E., Morris, J.J., Taylor, P.J. and Wait, A.R. (1991) Membranes and their models: towards a rational choice of partitioning system, in *QSAR: Rational Approaches to the Design of Bioactive Compounds* (eds C. Silipo and A. Vittoria), Elsevier, Amsterdam, pp. 75–82.

79 Steyeart, G., Lisa, G., Gaillard, P., Boss, G., Reymond, F., Girault, H.H., Carrupt, P.A. and Testa, B. (1997) Intermolecular forces expressed in 1,2-dichloroethane–water partition coefficients. A solvatochromic analysis. *Journal of the Chemical Society, Faraday Transactions*, **93**, 401–406.

80 Caron, G., Steyaert, G., Pagliara, A., Reymond, F., Crivori, P., Gaillard, P., Carrupt, P.A., Avdeef, A., Comer, J., Box, K.J., Girault, H.H. and Testa, B. (1999) Structure–lipophilicity relationships of neutral and protonated β-blockers. Part 1. Intra- and intermolecular effects in isotropic solvent systems. *Helvetica Chimica Acta*, **82**, 1211–1222.

81 Hitzel, L., Watt, A.P. and Locker, K.L. (2000) An increased throughput method for the determination of partition coefficients. *Pharmaceutical Research*, **17**, 1389–1395.

82 Faller, B., Grimm, H.P., Loeuillet-Ritzler, F., Arnold, S. and Briand, X. (2005) High-throughput lipophilicity measurement with immobilized artificial membranes. *Journal of Medicinal Chemistry*, **48**, 2571–2576.

83 Avdeef, A. (1993) pH-metric log *P*. II. Refinement of partition coefficients and ionization constants of multiprotic substances. *Journal of Pharmaceutical Sciences*, **82**, 183–190.

84 Valko, K., Du, C.M., Bevan, C.D., Reynolds, D.P. and Abraham, M.H. (2000) Rapid-gradient HPLC method for measuring drug interactions with immobilized artificial membrane: comparison with other lipophilicity measures. *Journal of Pharmaceutical Sciences*, **89**, 1085–1096.

85 Lombardo, F., Shalaeva, M.Y., Tupper, K.A. and Gao, F. (2001) ElogDoct: a tool for lipophilicity determination in drug discovery. 2. Basic and neutral compounds. *Journal of Medicinal Chemistry*, **44**, 2490–2497.

86 Buchwald, P. and Bodor, N. (1998) Octanol–water partition: searching for predictive models. *Current Medicinal Chemistry*, **5**, 353–380.

87 Carrupt, P.A., Testa, B. and Gaillard, P. (1997) Computational approaches to lipophilicity: methods and applications. *Reviews in Computational Chemistry*, **11**, 241–315.

88 Mannhold, R. and van de Waterbeemd, H. (2001) Substructure and whole molecule approaches for calculating log *P*. *Journal of Computer-Aided Molecular Design*, **15**, 337–354.

89 Wildman, S.A. and Crippen, G.M. (1999) Prediction of physicochemical parameters by atomic contributions. *Journal of Chemical Information and Computer Sciences*, **39**, 868–873.

90 Spessard, G.O. (1998) ACD Labs/log *P* dB 3.5 and ChemSketch 3.5. *Journal of Chemical Information and Computer Sciences*, **38**, 1250–1253.

91 Tetko, I. and Livingstone, D.J. (2007) Rule-based systems to predict lipophilicity, in *ADME/Tox Approaches*, Vol. 5 (eds B. Testa and H. van de Waterbeemd), in *Comprehensive Medicinal Chemistry*, 2nd edn (series eds J.B Taylor and D.J. Triggle), Elsevier, Oxford, pp. 649–668.

92 Leo, A.J. and Hoekman, D. (2000) Calculating log *P*(oct) with no missing fragments: the problem of estimating new interaction parameters. *Perspectives in Drug Discovery and Design*, **18**, 19–38.

93 Mannhold, R. and Rekker, R.F. (2000) The hydrophobic fragmental constant approach for calculating log *P* in octanol/water and aliphatic hydrocarbon/water systems. *Perspectives in Drug Discovery and Design*, **18**, 1–18.

94 Caron, G. and Ermondi, G. (2005) Calculating virtual log *P* in the alkane/water system ($\log P^{N}_{alk}$) and its derived parameters $\Delta\log P^{N}_{oct\text{-}alk}$ and $\log D^{pH}_{alk}$. *Journal of Medicinal Chemistry*, **48**, 3269–3279.

95 Bruneau, P. and McElroy, N.R. (2006) log $D_{7.4}$ modeling using Bayesian regularised neural networks. Assessment and correction of errors of prediction. *Journal of Chemical Information and Modeling*, **46**, 1379–1387.

96 Kansy, M., Senner, F. and Gubernator, K. (1998) Physicochemical high throughput screening: parallel artificial membrane permeation assay in the description of passive absorption processes. *Journal of Medicinal Chemistry*, **41**, 1007–1010.

97 Kansy, M., Fischer, H., Kratzat, K., Senner, F., Wagner, B. and Parrilla, I. (2001) High-throughput artificial membrane permeability studies in early lead discovery and development, in *Pharmacokinetic Optimization in Drug Research: Biological, Physicochemical and Computational Strategies* (eds B. Testa, H. van de Waterbeemd, G. Folkers and R., Guy), Wiley-VCH Verlag GmbH, Weinheim, pp. 447–464.

98 Kansy, M., Avdeef, A. and Fischer, H. (2004) Advances in screening for membrane permeability: high resolution

PAMPA for medicinal chemists. *Drug Discovery Today: Technologies*, **1**, 349–355.

99 Sugano, H. (2007) Artificial membrane technologies to assess transfer and permeation of drugs in drug discovery, in *ADME/Tox Approaches, Vol. 5* (eds B. Testa and H. van de Waterbeemd), in *Comprehensive Medicinal Chemistry*, 2nd edn (series eds J.B Taylor and D.J. Triggle), Elsevier, Oxford.

100 Avdeef, A., Strafford, M., Block, E., Balogh, M.P., Chambliss, W. and Khan, I. (2001) Drug absorption *in vitro* model: filter-immobilized artificial membranes. 2. Studies of the permeability properties of lactones in *Piper methysticum* Forst. *European Journal of Pharmaceutical Sciences*, **14**, 271–280.

101 Sugano, K., Hamada, H., Machida, M. and Ushio, H. (2001) High throughput prediction of oral absorption: improvement of the composition of the lipid solution used in parallel artificial membrane permeation assay. *Journal of Biomolecular Screening*, **6**, 189–196.

102 Sugano, K., Hamada, H., Machida, M., Ushio, H., Saitoh, K. and Terada, K. (2001) Optimised conditions of bio-mimetic artificial membrane permeation assay. *International Journal of Pharmaceutics*, **228**, 181–188.

103 Faller, B. and Wohnsland, F. (2001) Physicochemical parameters as tools in drug discovery and lead optimisation, in *Pharmacokinetic Optimization in Drug Research: Biological, Physicochemical and Computational Strategies* (eds B. Testa, H. van de Waterbeemd, G. Folkers and R. Guy), Wiley-VCH Verlag GmbH, Weinheim, pp. 257–274.

104 Wohnsland, F. and Faller, B. (2001) High-throughput permeability pH profile and high-throughput alkane/water log *P* with artificial membranes. *Journal of Medicinal Chemistry*, **44**, 923–930.

105 Yang, C.Y., Cai, S.J., Liu, H. and Pidgeon, C. (1996) Immobilized artificial membranes: screens for drug–membrane interactions. *Advanced Drug Delivery Reviews*, **23**, 229–256.

106 Ong, S., Liu, H. and Pidgeon, C. (1996) Immobilized-artificial-membrane chromatography: measurements of membrane partition coefficient and predicting drug membrane permeability. *Journal of Chromatography A*, **728**, 113–128.

107 Stewart, B.H. and Chan, O.H. (1998) Use of immobilized artificial membrane chromatography for drug transport applications. *Journal of Pharmaceutical Sciences*, **87**, 1471–1478.

108 Ducarne, A., Neuwels, M., Goldstein, S. and Massingham, R. (1998) IAM retention and blood–brain barrier penetration. *European Journal of Medicinal Chemistry*, **33**, 215–223.

109 Reichel, A. and Begley, D.J. (1998) Potential of immobilized artificial membranes for predicting drug penetration across the blood–brain barrier. *Pharmaceutical Research*, **15**, 1270–1274.

110 Genty, M., Gonzalez, G., Clere, C., Desangle-Gouty, V. and Legendre, J.-Y. (2001) Determination of the passive absorption through the rat intestine using chromatographic indices and molar volume. *European Journal of Pharmaceutical Sciences*, **12**, 223–229.

111 Lundahl, P. and Beigi, F. (1997) Immobilized liposome chromatography of drugs for model analysis of drug–membrane interactions. *Advanced Drug Delivery Reviews*, **23**, 221–227.

112 Norinder, U. and Österberg, Th. (2000) The applicability of computational chemistry in the evaluation and prediction of drug transport properties. *Perspectives in Drug Discovery and Design*, **19**, 1–18.

113 Trone, M.D., Leonard, M.S. and Khaledi, M.G. (2000) Congeneric behavior in estimations of octanol–water partition coefficients by micellar electrokinetic chromatography. *Analytical Chemistry*, **72**, 1228–1235.

114 Molero-Monfort, M., Escuder-Gilabert, L., Villanueva-Camanoas, R.M., Sagrado, S. and Medina-Hernandez, M.J. (2001) Biopartitioning micellar chromatography: an *in vitro* technique for predicting human drug absorption. *Journal of Chromatography B*, **753** 225–236.

115 Detroyer, A., VanderHeyden, Y., Cardo-Broch, S., Garcia-Alvarez-Coque, M.C. and Massart, D.L. (2001) Quantitative structure–retention and retention–activity relationships of β-blocking agents by micellar liquid chromatography. *Journal of Chromatography A*, **912**, 211–221.

116 Takagi, M., Taki, Y., Sakane, T., Nadai, T., Sezaki, H., Oku, N. and Yamashita, S. (1998) A new interpretation of salicylic acid transport across the lipid bilayer: implications of pH-dependent but not carrier-mediated absorption from the gastrointestinal tract. *The Journal of Pharmacology and Experimental Therapeutics*, **285**, 1175–1180.

117 Balon, K., Riebesehl, B.U. and Muller, B.W. (1999) Drug liposome partitioning as a tool for the prediction of human passive intestinal absorption. *Pharmaceutical Research*, **16**, 882–888.

118 Balon, K., Riebesehl, B.U. and Muller, B.W. (1999) Determination of liposome partitioning of ionizable drugs by titration. *Journal of Pharmaceutical Sciences*, **88**, 802–806.

119 Avdeef, A., Box, K.J., Comer, J.E.A., Hibbert, C. and Tam, K.Y. (1998) pH-metric log *P* 10. Determination of liposomal membrane–water partition coefficients of ionizable drugs. *Pharmaceutical Research*, **15**, 209–215.

120 Escher, B.I., Schwarzenbach, R.P. and Westall, J.C. (2000) Evaluation of liposome-water partitioning of organic acids and bases. 2. Comparison of experimental determination methods. *Environmental Science & Technology*, **34**, 3962–3968.

121 Loidl-Stahlhofen, A., Eckrt, A., Hartmann, T. and Schottner, M. (2001) Solid-supported lipid membranes as a tool for determination of membrane affinity: high-throughput screening of a physicochemical parameter. *Journal of Pharmaceutical Sciences*, **90**, 599–606.

122 Willmann, S., Lippert, J. and Schmitt, W. (2005) From physicochemistry to absorption and distribution: predictive mechanistic modelling and computational tools. *Expert Opinion on Drug Metabolism and Toxicology*, **1**, 159–168.

123 Melchior, D.L. (2002) A rapid empirical method for measuring membrane bilayer entry equilibration of molecules. *Journal of Pharmaceutical Sciences*, **91**, 1075–1079.

124 Katz, M., Ben-Shlush, I., Kolusheva, S. and Jelinek, R. (2006) Rapid colorometric screening of drug interaction and penetration through lipid barriers. *Pharmaceutical Research*, **23**, 580–588.

125 Danelian, E., Karlén, A., Karlsson, R., Winiwarter, S., Hansson, A., Löfås, S., Lennernäs, H. and Hämäläinen, D. (2000) SPR biosensor studies of the direct interaction between 27 drugs and a liposome surface: correlations with fraction absorbed in humans. *Journal of Medicinal Chemistry*, **43**, 2083–2086.

126 Frostell-Karlsson, A., Widegren, H., Green, C.E., Hämäläinen, M.D., Westerlund, L., Karlsson, R., Fenner, K. and van de Waterbeemd, H. (2005) Biosensor analysis of the interaction between drug compounds and liposomes of different properties: a two-dimensional characterization tool for estimation of membrane absorption. *Journal of Pharmaceutical Sciences*, **94**, 25–37.

127 Fischer, H., Kansy, M. and Bur, D. (2000) CAFCA: a novel tool for the calculation of amphiphilic properties of charged drug molecules. *Chimia*, **54**, 640–645.

128 Suomalainen, P., Johans, C., Soderlund, T. and Kinnunen, P.K. (2004) Surface activity profiling of drugs applied to the prediction of blood–brain barrier

permeability. *Journal of Medicinal Chemistry*, **47**, 1783–1788.

129 Austin, R.P., Davis, A.M. and Manners, C.N. (1995) Partitioning of ionising molecules between aqueous buffers and phospholipid vesicles. *Journal of Pharmaceutical Sciences*, **84**, 1180–1183.

130 Lipinski, C.A. (2005) Filtering in drug discovery. *Annual Reports in Computational Chemistry*, **1**, 155–168.

131 Leeson, P.D., Davis, A.D. and Steele, J. (2004) Drug-like properties: guiding principles for design – or chemical prejudice? *Drug Discovery Today: Technologies*, **1**, 189–195.

132 Ajay, A., Walters, W.P. and Murcko, M.A. (1998) Can we learn to distinguish between drug-like and nondrug-like molecules? *Journal of Medicinal Chemistry*, **41**, 3314–3324.

133 Sadowski, J. and Kubinyi, H. (1998) A scoring scheme for discriminating between drugs and nondrugs. *Journal of Medicinal Chemistry*, **41**, 3325–3329.

134 Wagener, M. and van Geerestein, V.J. (2000) Potential drugs and nondrugs: prediction and identification of important structural features. *Journal of Chemical Information and Computer Sciences*, **40**, 280–292.

135 Anzali, S., Barnickel, G., Cezanne, B., Krug, M., Filimonov, D. and Poroikov, V. (2001) Discriminating between drugs and nondrugs by prediction of activity spectra for substances (PASS). *Journal of Medicinal Chemistry*, **44**, 2432–2437.

136 Lipinski, C.A., Lombardo, F., Dominy, B.W. and Feeney, P.J. (1997) Experimental and computational approaches to estimate solubility and permeability in drug discovery and development settings. *Advanced Drug Delivery Reviews*, **23**, 3–25.

137 Lipinski, C. (2000) Drug-like properties and the causes of poor solubility and poor permeability. *Journal of Pharmacological and Toxicological Methods*, **44**, 235–249.

138 Pagliara, A., Reist, M., Geinoz, S., Carrupt, P.-A. and Testa, B. (1999) Evaluation and prediction of drug permeation. *The Journal of Pharmacy and Pharmacology*, **51**, 1339–1357.

139 Stenberg, P., Luthman, K., Ellens, H., Lee, C.P., Smith, Ph.L., Lago, A., Elliott, J.D. and Artursson, P. (1999) Prediction of the intestinal absorption of endothelin receptor antagonists using three theoretical methods of increasing complexity. *Pharmaceutical Research*, **16**, 1520–1526.

140 Ghose, A.K., Viswanadhan, V.N. and Wendoloski, J.J. (1999) A knowledge-based approach in designing combinatorial or medicinal chemistry libraries for drug discovery. 1. A qualitative and quantitative characterization of known drug databases. *Journal of Combinatorial Chemistry*, **1**, 55–68.

141 Oprea, T.L. (2000) Property distribution of drug-related chemical databases. *Journal of Computer-Aided Molecular Design*, **14**, 251–264.

142 Leeson, P.D. and Davis, A.D. (2004) Time-related differences in the physical property profile of oral drugs. *Journal of Medicinal Chemistry*, **47**, 6338–6348.

143 Carr, R.A.E., Congreve, M., Murray, C.W. and Rees, D.C. (2005) Fragment-based lead discovery: leads by design. *Drug Discovery Today*, **10**, 987–992.

144 Ajay, A., Bemis, G.W. and Murcko, M.A. (1999) Designing libraries with CNS activity. *Journal of Medicinal Chemistry*, **42**, 4942–4951.

145 Norinder, U. and Haeberlein, M. (2002) Computational approaches to the prediction of the blood–brain distribution. *Advanced Drug Delivery Reviews*, **54**, 291–313.

146 van de Waterbeemd, H., Camenisch, G., Folkers, G., Chretien, J.R. and Raevsky, O.A. (1998) Estimation of blood–brain barrier crossing of drugs using molecular size and shape, and H-bonding descriptors. *Journal of Drug Targeting*, **6**, 151–165.

147 Summerfield, S.G., Stevens, A.J., Cutler, L., Del Carmen Osuna, M., Hammond,

B., Tang, S.-P., Hershey, A., Spalding, D.J. and Jeffrey, P. (2006) Improving the *in vitro* prediction of *in vivo* central nervous system penetration: integrating permeability, P-glycoprotein efflux, and free fractions in blood and brain. *The Journal of Pharmacology and Experimental Therapeutics*, **316**, 1282–1290.

148 Blake, J.F. (2000) Chemoinformatics: predicting the physicochemical properties of drug-like molecules. *Current Opinion in Biotechnology*, **11**, 104–107.

149 Matter, H., Baringhaus, K.H., Naumann, T., Klabunde, T. and Pirard, B. (2001) Computational approaches towards the rational design of drug-like compound libraries. *Combinatorial Chemistry & High Throughput Screening*, **4**, 453–475.

150 Irvine, J.D., Takahashi, L., Lockhart, K., Cheong, J., Tolan, J.W., Selick, H.E. and Grove, J.R. (1999) MDCK (Madin–Darby canine kidney) cells: a tool for membrane permeability screening. *Journal of Pharmaceutical Sciences*, **88**, 28–33.

151 Winiwarter, S., Ridderström, M., Ungell, A.-L., Andersson, T.B. and Zamora, I. (2007) Use of molecular descriptors for ADME predictions, in *ADME/Tox Approaches*, Vol. 5 (eds B. Testa and H. van de Waterbeemd), in *Comprehensive Medicinal Chemistry*, 2nd edn (series eds J.B Taylor and D.J. Triggle), Elsevier, Oxford, pp. 531–554.

152 Dudek, A.Z., Arodz, T. and Galvez, J. (2006) Computational methods in developing quantitative structure–activity relationships (QSAR): a review. *Combinatorial Chemistry & High Throughput Screening*, **9**, 213–228.

153 Testa, B., Vistoli, G. and Pedretti, A. (2005) Musings on ADME predictions and structure–activity relations. *Chemistry & Biodiversity*, **2**, 1411–1428.

154 van de Waterbeemd, H. and Rose, S. (2003) Quantitative approaches to structure–activity relationships, in *The Practice of Medical Chemistry*, 2nd edn (ed. C.G. Wermuth), Academic Press, London, pp 351–369; ibid, 3rd edn, 2008, in press.

155 De Cerqueira Lima, P., Golbraikh, A., Oloff, S., Xiao, Y. and Tropsha, A. (2006) Combinatorial QSAR modelling of P-glycoprotein substrates. *Journal of Chemical Information and Modeling*, **46**, 1245–1254.

156 Stouch, T.R., Kenyon, J.R., Johnson, S.R., Chen, X.Q., Doweyko, A. and Li, Y. (2003) *In silico* ADME/Tox: why models fail. *Journal of Computer-Aided Molecular Design*, **17**, 83–92.

157 Saunders, K. (2004) Automation and robotics in ADME screening. *Drug Discovery Today: Technologies*, **1**, 373–380.

158 Cartmell, J., Enoch, S., Krstajic, D. and Leahy, D.E. (2005) Automated QSPR through competitive workflow. *Journal of Computer-Aided Molecular Design*, **19**, 821–833.

159 van de Waterbeemd, H. and Gifford, E. (2003) ADMET *in silico* modelling: towards *in silico* paradise? *Nature Reviews. Drug Discovery*, **2**, 192–204.

160 Smith, D.A. and Cucurull-Sanchez, L. (2007) The adaptive in combo strategy, in *ADME/Tox Approaches, Vol. 5* (eds B. Testa and H. van de Waterbeemd), in *Comprehensive Medicinal Chemistry*, 2nd edn (series eds J.B Taylor and D.J. Triggle), Elsevier, Oxford, pp. 957–969.

161 Vistoli, G., Pedretti, A. and Testa, B. (2008) Assessing drug-likeness: what are we missing? *Drug Discovery Today*, **13**, 285–294.

162 Leeson, P.D. and Springthorpe, B. (2007) The influence of drug-like concepts on decision-making in medicinal chemistry. *Nature Reviews. Drug Discovery*, **6**, 881–890.

6
High-Throughput Measurement of Physicochemical Properties

Barbara P. Mason

Abbreviations

ADME	Absorption, distribution, metabolism, and excretion
BBB	Blood–brain barrier
BSA	Bovine serum albumin
Caco-2	Human colon adenocarcinoma cell line used as a permeation/absorption model
CHI	Chromatography hydrophobicity index
DMSO	Dimethyl sulfoxide
FCS	Fetal calf serum
HEPES	4-(2-hydroxyethyl)-1-piperazineethanesulfonic acid (zwitterionic buffer)
HTS	High-throughput screening
MDCK	Madin–Darby canine kidney
MW	Molecular weight
PAMPA	Parallel artificial membrane permeability assay
PBS	Phosphate buffered saline
RP-HPLC	Reverse-phase high-performance liquid chromatography
TFA	Target factor analysis
UWL	Unstirred water layer

Symbols

$\log D_{\mathrm{pH}}$	Logarithm of the distribution coefficient in octanol/water at pH described in subscript
$\log P$	Logarithm of the partition coefficient in octanol/water
ml	Milliliter
$\mathrm{p}K_{\mathrm{a}}$	Ionization constant in water

p_sK_a	Ionization constant in cosolvent/water
S	Solubility
P_a	Apparent permeability (accounting for UWL effects)
P_e	Effective permeability (not accounting for UWL effects)
%R	Percentage of the compound retained in the membrane

6.1 Introduction

Information about the fundamental properties of a series of compounds, such as permeability, solubility, lipophilicity, and pK_a, is extremely useful to the medicinal chemist in drug discovery. It provides insights into the behavior of compounds, which can be directly applied to planning modifications of structures and scaffolds to improve their behavior. With the introduction and development of high-throughput screening (HTS), combinatorial chemistry, and more recently fragment library approaches, the number of compounds requiring such profiling in some, if not all, physicochemical parameters showed a massive increase while the amount of compound available for study was greatly reduced and very often present as a 10 mM DMSO stock solution. It is, therefore, not a surprise that there have been many significant advances in the technology and methods for measuring these parameters in a high-throughput capacity. It should be noted that this chapter will not make any comment as to the definition of high throughput; where it is feasible to run the methods discussed in microtiter plate format or generate a large number data of points at a time on a given set of compounds, this will be classed as "high throughput." Some background theory and mathematics will be introduced where appropriate, more detailed, explanations and derivations are available, and references to these will be given.

6.2 Positioning of Physicochemical Screening in Drug Discovery

It has always been tempting to drive medicinal chemistry forward on the basis of selectivity and potency alone; however, this has seen the downfall of many projects. While there is a strategic need in drug discovery to identify compounds that will be readily absorbed and distributed around the body, it could be argued that it is more important to identify those series of compounds that *will not*, so that a judicious choice can be made as to whether they are sufficiently potent to make it worth tackling via formulation or to modify the series appropriately. It is prudent to determine which compounds may be prone to these problems as early in the discovery process as possible. Another advantage of screening physicochemical properties early is that it will give invaluable information in sample handling or assistance in the understanding and explanation of outliers in the biological screening assays.

A typical project lifecycle can be described as having five main stages: (i) target identification, (ii) target validation, (iii) high-throughput screening, (iv) hit to lead, and (v) lead optimization. (The exact number, description, and transition from one stage to another are particular to each organization.) Medicinal chemistry typically plays a role in stages (iii)–(v) by providing a huge number of compounds for protein/enzyme 384-well-style assays in HTS, fewer compounds for cell-based functional assays (although the number of compounds being produced at this stage is still significant, particularly in the major pharmaceutical companies) in the hit-to-lead stage, and finally a handful of compounds per project for multiple disease state models in the lead-optimization stage.

6.3 "Fit for Purpose" Versus "Gold Standard"

The challenge then for physical chemists is to provide physicochemical profiling at correct times during this project lifecycle on these varying numbers and quantities of compounds, and to be able to produce data sufficiently quickly, so that lessons can be learnt and judgments are made before the project moves forward. Physicochemical profiling needs to work closely with DMPK and pharmacology to provide a comprehensive data package for the compounds where they have been measured under conditions that are relevant to the assay systems used to generate the potency and selectivity information; in other words, the assays need to be "fit for purpose." Conversely, scientists working on development and preformulation under regulatory guidelines will require a different set of measurements, generated by using recognized, industry standard methods that are capable of producing "gold standard" data.

Advances in instrumentation and computing power have meant that analytical data are both more precise and more reproducible than probably any other measurement made and particularly when compared with biological data. It should be possible with the liquid handling and plate-moving robots available to increase throughput significantly and still provide this high-quality data. This is indeed true; however, the high-quality data presuppose that the samples used for data generation are also of high quality. This is a major assumption, particularly in HTS and library analysis. For any technique, which does not involve a chromatographic separation step, it will not be possible to distinguish an analyte from a contaminant, causing complications in the processing of the data and leading to false positives if its presence is not known. Samples containing highly soluble or highly absorbing impurities, even at relatively low concentration levels, will have a profound effect on the data. To be 100% certain of the accuracy and precision of one's calibration curves, solid material is the starting point of choice. However, this is not a practical option for high-throughput profiling due to the massive pressure that this would place on compound logistics for even a small company. For the majority of high-throughput methods, the compounds are stamped out in microtiter plates and are present as DMSO stock solutions of supposedly known concentration, 10 mM being common.

Although it may appear that to start all assays from a standard 10 mM DMSO stock solution will simplify the profiling processes, there are a number of issues that should be taken into account. The presence of this organic solvent may mask or modify important physical properties that will need to be factored into the information before it can be used for any real benefit. It is very important to ensure that the compound is stable in the solvent and therefore QC checks should be carried out before the assay screens commence to have a time zero point from which to reference. If this is carried out using an HPLC–MS method, then it will have the added benefit of confirming compound purity and validity at the outset. It should also be considered that it is possible that the compounds are not present as 10 mM DMSO stock solutions [1]. This will need to be known and calibration curves adjusted to ensure that any quantitative calculations are correct.

High-throughput physicochemical profiling does have a valid place in drug discovery, and there are four fundamental properties to be measured: aqueous solubility, pK_a, lipophilicity, and permeability [2]. The types of data generated using traditional "gold standard" methods are vital for physicochemical profiling. Such methods include shake-flask log *P*, thermodynamic solubility, and potentiometric pK_a, providing a means by which compounds can be compared and their behavior and characteristics can be described. While these methods are not slow, they cannot be used for many hundreds or even thousands of compounds at a time produced during HTS and hit-to-lead stages because they use much larger quantities of compound than that are typically available and are not always flexible enough to accommodate the varying conditions that a compound will be exposed to as it passes through a long cascade of assays.

6.4 Solubility

Solubility measurements are made to determine an intrinsic property, which influences the absorption potential of a compound [3]. Even though solubility itself does not directly dictate the absorption of a drug, it is important to consider solubility in relation to permeability and potency. In addition, in medicinal chemistry projects, there are other issues to consider that may also be affected by poor solubility, particularly insolubility under screening assay conditions.

6.4.1 "Thermodynamic" Versus "Kinetic"

Traditional "shake-flask" or gold standard solubility methods start from solid material vigorously mixed with an aqueous buffer until equilibrium is reached between undissolved and dissolved materials. This may take only a minute or 72 h or more and is compound specific.

These equilibrium solubility conditions are defined as being "thermodynamic" – the most stable species is in solution at equilibrium and not necessarily the fastest

dissolving. Starting from solid means that forces involved in the crystal lattice need to be overcome before the compound will dissolve. Dissolution is rate limited and therefore a kinetic process, but it needs to occur before the final solubility is reached at true thermodynamic equilibrium.

Assays starting with a compound predissolved in an organic solvent (typically DMSO) tend to have shorter incubation times, do not include time course measurements, and therefore the position of equilibrium is not determined, and for highly soluble species the compound may not be present in excess. This type of measurement is typically referred to as "kinetic."

In the hit-to-lead stage of drug discovery, compounds are generally only available in solvents such as DMSO for a number of reasons:

- Stock solutions allow ease of compound storage and distribution and as such they are particularly amenable to plate-based formats.
- They aid poorly soluble compounds in becoming more accessible to the aqueous environment of bioassays.
- DMSO stock solutions are typically the vehicle of choice for all but a few selected *in vivo* experiments, and subsequently, DMSO is present to some degree in almost all early-stage screens.

Attempting to measure a thermodynamic solubility of compounds which will then be used under these screening conditions, will not necessarily give a useful picture of the compounds' performance. They will not reflect the more "transient" nature of the compound that is present in nonequilibrium systems. The presence of organic solvents changes the dielectric constant of an aqueous solution and thus helps to solvate lipophilic compounds in particular, and will give an increased solubility for some series of compounds across the Biopharmaceutics Classification System (BCS) [4]. This is an important consideration in the ultimate use of the solubility data, and a lack of full solubility of the analyte at the test concentration will lead to an underestimation of the compound's true activity. Measuring the solubility of the compounds in close approximation to the assay conditions to which they will be exposed will be more relevant. Indeed, if sensitivity is not an issue, then the quantities, concentrations, and incubation conditions used should reflect those available in the discovery assays.

Another important consideration is that of batch-to-batch variability. Typically, in medicinal chemistry laboratories, compounds are synthesized in large numbers rather than in large quantities. Should a compound prove to be sufficiently interesting, it is resynthesized and reanalyzed. It is likely that the compounds will have been purified by column chromatography, dried down from organic solvents or freeze-dried. No effort will have been spent on creating homogeneous crystals because the medicinal chemist has other priorities. For each of these resyntheses, these compounds will be complex amorphous solids of unspecified crystal (or noncrystal) form. Furthermore, compounds stored for any length of time, even under "optimum" conditions of temperature, light, humidity, and inert atmosphere, are subject to deterioration. This may be where the sample is decomposing or where the crystal form changes and new polymorphs are formed. These species may have vastly

different lattice energies and it is clear that determining the "true" thermodynamic solubility of each of these batches may, and probably will, give very different data that cannot be used for comparison studies.

6.4.2 Methods of Measuring High-Throughput Solubility

Solubility solution conditions are important. The pH–solubility profile is a function of the intrinsic solubility of the neutral form, with the solubility of the ionized species (protonated for bases and deprotonated for acids) being typically much higher than that of the neutral species. Therefore, pK_a as well as concentration of DMSO present in the final incubated solution needs to be considered.

There are a variety of methods for determining solubility in a relatively high-throughput manner but of these, two methods occur most often. These can be classified as "supernatant concentration" and "precipitate detection."

6.4.3 Supernatant Concentration

The supernatant concentration method uses small volumes of stock solution added to wells containing aqueous buffer in a microtiter filter plate of the type available from Millipore Inc. The solution is incubated for a given amount of time (typically in the range of 1–24 h depending on the requirements of the laboratory) and then filtered or centrifuged. The supernatant is analyzed by UV plate reader or HPLC and the concentration of dissolved species is calculated by reference to a calibration curve. This is often either a three- or a four-point curve prepared from serial dilutions of the stock solution using a solvent such as 80% v/v acetonitrile/water in which the compound is fully soluble.

It is a relatively simple exercise to automate this method using liquid handling robotic hardware, and with integrated plate moving arms, filter manifold systems, plate shakers, centrifuges, and plate readers, the throughput that these types of systems can achieve may only be limited by the plate storage capacity and budget. A UV plate reader such as a Molecular Devices Spectramax 190, reading a scan for each well of a 96-well plate from 200 to 400 nm with 1 nm increments, takes approximately 20 min. For laboratories, where only a single wavelength is required, this is reduced to seconds.

According to Beer's law, path length is a fundamental property of the absorbance of the sample as shown in Equation 6.1:

$$A = Ecl, \tag{6.1}$$

where A is absorbance, c is the concentration, l is the path length, and E is the molar extinction coefficient.

Using a UV plate reader, correction factors for path length are included in the instrument; however, it is critical that the path length is the same in the incubation and calibration samples. The actual path length itself is determined by the depth of

sample in the well, that is, the sample volume. Owing to differences in the solubility of varying samples on the plate, it is likely that the quantity of precipitate present in the wells will vary randomly. It will therefore not be possible to filter a predetermined specified volume of supernatant at the end of the incubation period. For this reason, it is recommended that the samples are filtered into a receiver plate and an aliquot is transferred to a UV plate for analysis.

6.4.4 Measuring Solubility Across a pH Range

The pK_a of a molecule, and therefore the pH of the aqueous environment of the solubility assay, is extremely important. Each group carrying out these measurements will have chosen carefully their incubation conditions. High-throughput platforms give the option of carrying out the solubility measurements at a range of pH values; however, this will bring another level of complexity to the assay. Although it will reduce the number of individual compounds that can be analyzed per plate, it will allow an "on-the-fly" visualization of the effects of pK_a (and therefore % ionized) and pH on the solubility. If a UV plate reader is used, then selecting a single analytical wavelength per compound (λ_{max}, for instance) is not an appropriate option since there may be different molar extinction coefficients for the ionized and neutral species should there be an ionization event at or near the chromophore that causes a spectral change.

Following Beer's law given in Equation 6.1, for a given wavelength, equivalent concentrations of species with a different molar extinction coefficient will not have an equivalent absorbance. Under these circumstances, the use of calibration curves determined from compounds dissolved in organic solvents and therefore present only in the neutral form will not be appropriate for the determination of the concentration of a species that is ionized.

This problem can be overcome by determining a scan of the samples across a range of wavelengths, typically 200–400 nm and selecting the wavelength at which the extinction coefficient is equivalent for all species, the *isosbestic point* (DMSO absorbance will cause interference if scanning is done at wavelengths much lower than 230 nm), to plot the calibration curves and thus calculate the concentration of the analyte present.

To determine the isosbestic point, two calibration samples are required in addition to those of the calibration line. These two will contain sufficient aqueous buffer to cause the pH to shift to the extremes of the pH range of the assay, for example, pH 3 and pH 9, but not enough to cause poorly soluble compounds to precipitate out of solution. As shown in Figure 6.1, the spectra for pH 3 and pH 9 have equivalent absorbances at 315 nm, and therefore this is the isosbestic point and should be chosen for analysis. For situations where there is no clear isosbestic point, a wavelength should be selected from a region of homology.

Setting the concentration in the two spiked solutions to be the same as that of one of the calibration lines will give three spectral lines for qualitative comparison, which will provide additional information about the behavior of the compound. In Figure 6.1, the spectral profiles under purely organic conditions and organic solvent

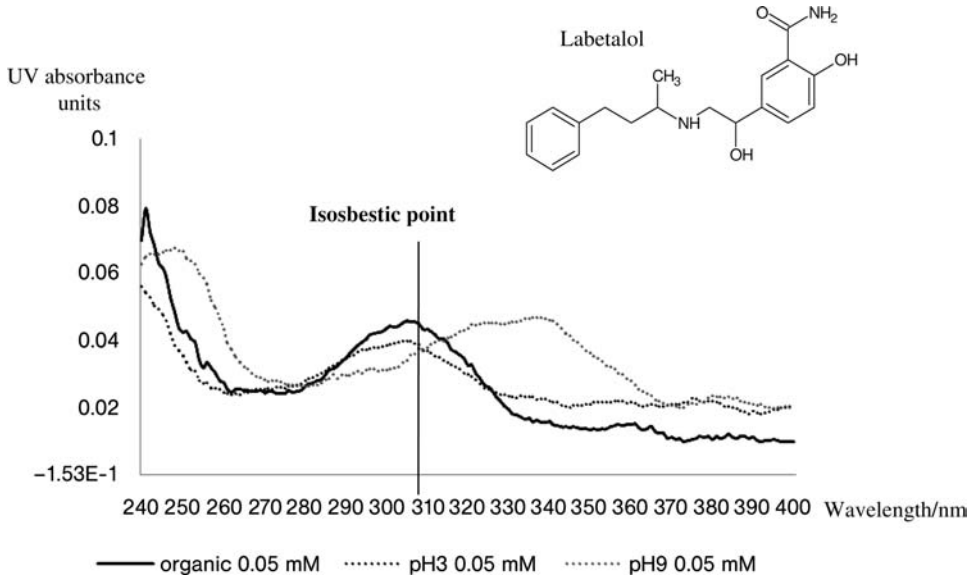

Figure 6.1 Plot of labetalol UV absorbance spectra showing pH 3, pH 9, and organic calibration lines at 0.05 mm.

spiked with pH 9 buffer are equivalent whereas that spiked with pH 3 buffer shows a different profile. This indicates that under basic conditions the compound is in its neutral form, while under acidic conditions it is in its ionized form. Comparison of these calibration spectra with those from the solubility supernatant samples will determine the pH range at which the ionization occurred. Figure 6.2 shows that labetalol has an acidic ionization event between pH 3 and pH 5 and that the acidic

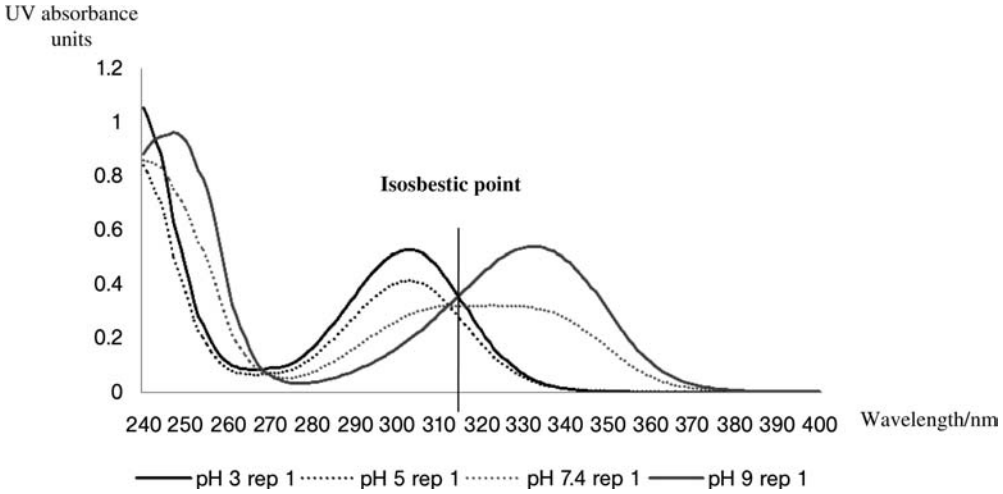

Figure 6.2 Plot of labetalol solubility lines at pH 3, pH 5, pH 7.4, and pH 9.

center is close to the chromophore, in this instance, the phenolic OH group. In situations where there is more than one possible ionization site, this can be extremely helpful in the assignment of pK_a values.

Another major benefit to medicinal chemists of providing pH profile data is the early identification of stability issues – if the solubility and calibration spectra do not match, it will indicate that degradation of the compound may be occurring.

6.4.5
Supernatant Concentration Methods from Solid Material

Methods, which start from DMSO solutions, are relatively easily modified to allow miniaturized shake-flask measurements to be made. A major consideration is the logistics of weighing out the compounds to an accuracy high enough to make the analysis from solid material valid. There are a number of robotic platforms commercially available, which can incorporate automated weighing stations (Zinsser Analytic Inc.) for use with a very large number of compounds. An extra step will be required in the method to transfer an aliquot of the incubation samples to a filter plate to remove the supernatant for analysis, although centrifugation will negate this, and subsequently determine the concentration of the sample against a calibration curve by UV plate reader either at a single wavelength or from a scan, which again depends on whether multiple pH values or HPLC detection is used.

6.4.6
Precipitate Detection

Precipitate detection methods typically use light scattering techniques such as nephelometry, flow cytometry, and turbidity measurements to determine the amount of the precipitate formed during the incubation process. A major advantage with these types of techniques is the availability of particle size distribution and aggregation information.

Bevan [5] measured precipitation in microtiter plates by light scattering directly using a BMG NEPHELOstar plate-based nephelometer. Small volumes of concentrated DMSO stock solutions are added to wells containing aqueous buffer and this is then serially diluted across the wells of the microtiter plate and allowed to equilibrate. The concentration of the resulting precipitate is determined by nephelometry. For compounds that are poorly soluble, the wells are turbid and produce a higher degree of scattering. Plotting turbidity versus concentration will give the maximum concentration dissolved, which is the quoted solubility value.

Dehring *et al*. [6] have used the same nephelometric technology to determine kinetic solubility on a high-throughput robotic platform with good comparison of data with that obtained in a lower throughout method using flow injection analysis (FIA). Fligge and Schuler [7] used a fast nephelometric method in conjunction with liquid chromatography/mass spectrometry (LC/MS) detection method using the same 384-well microtiter plates as used in the LC/MS hit validation without the need for further sample preparation.

6.4.7
Other Methods of Measuring Solubility

Using the Sirius GLpKa instrument and CheqSol technology provides an elegant method for determining the solubility of ionizable molecules by using pH-metric titration. An acid or base titrant is added to precipitate the sample, which is detected by using D-PAS (a quartz fiber dip probe measuring UV absorbance). Small volumes of acid or base are added to the system to cycle the solution between sub- and supersaturated states close to the equilibrium. Equilibrium solubility is calculated using mass and charge balance equations. This method is particularly useful for poorly soluble compounds and reduces the analysis time for equilibrium solubility from potentially greater than 24 h to around 1 h per sample [8]. (For compounds that do not supersaturate, Bjerrum curve analysis is used.) pION Inc. provides the pSol Gemini instrument for measuring equilibrium solubility using an alternative pH-metric titration method whereby titrations are assumed to establish equilibrium typically over a 12 h period. The company has developed a μSol instrument for measuring high-throughput solubility on a Tecan robotic platform from DMSO stock solutions using UV detection.

Recent studies by Seadeek [9] and Sugano [10] discuss how the crystal form and solubility can be monitored together to assess the crystallinity of the precipitate.

6.5
Dissociation Constants, pK_a

It is not easy to find a definition of dissociation constant, pK_a, which is not cumbersome and confusing, and yet the extent of ionization, of which this is a measure, is of fundamental importance. Biologically active molecules tend to be either fully or partially charged at physiological pH with the charged functionality often being required for the biological activity, as well as physicochemical properties such as solubility. Knowledge of the dissociation constant and the protonation equilibria plays an important role in the understanding of absorption, transport, and receptor binding. From the Henderson–Hasselbalch equation given in Equation 6.2,

$$\begin{array}{l} \underset{\text{Protonated base}}{BH^+} \rightleftharpoons H^+ + \underset{\text{Deprotonated(neutral)base}}{B} \\ \underset{\text{Protonated(neutral)acid}}{HA} \rightleftharpoons H^+ + \underset{\text{Deprotonated acid}}{A^-} \end{array} \qquad pK_a = pH + \log_{10}\frac{[\text{protonated}]}{[\text{deprotonated}]}, \tag{6.2}$$

for an aqueous solution of a compound with one ionizable group, the acid dissociation constant, or ionization constant, pK_a, being equal to the pH at which 50% of the compound is in its ionized form (deprotonated for acids and protonated for bases) and 50% is in its neutral form. (This has to be extended using equilibrium equations for multiprotic molecules and Avdeef [11] has shown the derivation of

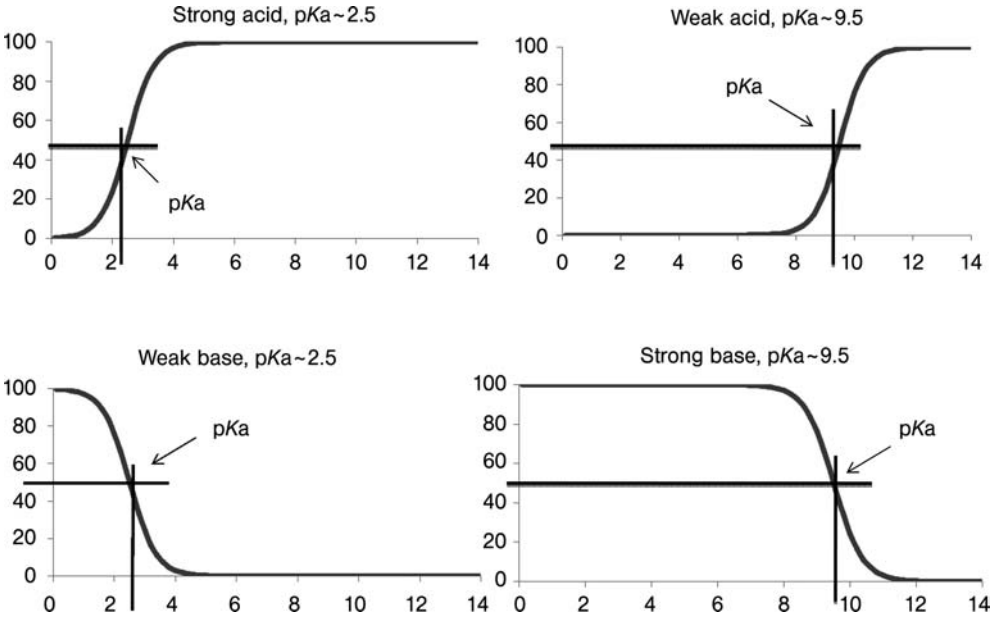

Figure 6.3 Plots of % ionized for a strong acid and weak base with $pK_a \sim 2.5$, weak acid and strong base with $pK_a \sim 9.5$.

these equations.) Rearranging this equation allows the calculation of % ionized as shown in Equation 6.3:

$$\begin{aligned} \%\ \text{Ionized for bases} &= \frac{100}{1+10^{(pK_a-pH)}}; \\ \%\ \text{Ionized for acids} &= \frac{100}{1+10^{(pH-pK_a)}}. \end{aligned} \tag{6.3}$$

Figure 6.3 shows plots of pH versus % ionized for a strong acid and weak base with $pK_a \sim 2.5$ and weak acid and strong bases with $pK_a \sim 9.5$, respectively.

6.5.1 Measuring pK_a

To measure pK_a, the compound is exposed to a changing pH and some characteristics of the molecule that change as a function of pH, for example, solubility, absorbance, and conductivity, are measured. Potentiometric titrimetry in aqueous solution is the traditional method that has been used. pK_a is determined from the shape of a titration curve [12] derived from plotting electromotive force (E or emf) or pH versus the volume of reagent added. The aqueous analyte solution is either preacidified to pH 3 using 0.5 M hydrochloric acid and titrated to pH 12 using 0.3 M potassium hydroxide solution, or prebasified and titrated with acid and monitored using a glass electrode. It is very important for all pK_a measurements to ensure that the ionic strength of the system remains constant so that the activity coefficients of

all the species involved also remain constant. The system is generally maintained under an inert atmosphere to avoid the risk of CO_2 contamination. This method is not amenable to sparingly soluble compounds and highly depends on sample purity. It also needs a relatively large amount of sample, $>5 \times 10^{-4}$ M solution is required to be able to detect a significant change in the shape of the titration curve compared to a blank, and typical sample volumes in the region of 5 ml, although 100 µl volumes are now possible using microelectrodes. The reagent (acid or base) must be added in a stepwise manner, and the protonation equilibria need to be achieved after each addition before measurements can be taken, with 20–40 measurements required in the pH range 3–11. A measurement of this type will take typically 20–40 min per compound. However, this is the most precise method and is generally used for high-quality determinations. Dual-phase potentiometry using direct titration with base followed by back titration with acid in the presence of octanol provides both log *P* and pK_a values. Sirius Analytical's GLpKa instrument allows the automation of this procedure, which reduces the time sufficiently to allow 30–40 titrations per day [13–17].

Owing to increased sensitivity, hybrid potentiometric/UV spectroscopic techniques are useful for reducing the sample concentration required, typically using less than 10^{-5} M solutions. A UV absorbance spectrum is measured at each pH but the samples must have a UV chromophore, which demonstrates a spectral change due to ionization. This means that the ionization site must be part of or in close proximity (up to 4 atoms) to the chromophore. Sirius GLpKa instrument with D-PAS attachment uses a fiber optic dip probe in a titration cell and while the samples are titrated across the pH range, the multiwavelength UV spectra are obtained at each pH. The pK_a values are calculated using target factor analysis (TFA) [16] but again the limiting step is electrode stability. The new Fast D-PAS software allows this technology to be used in a high-throughput mode by making measurements in a linear buffer solution with each titration taking 2 min. This method is particularly suitable for samples that are not stable or are poorly soluble since these measurements can be made before precipitation occurs. It is also possible to determine pK_a using pH gradient titration and this is the principle behind the Sirius Profiler SGA instrument. The samples are injected into a flowing pH gradient created by mixing an acidified and basified buffer together using calibrated syringe pumps ensuring that the pH varies linearly with time. The pH can be determined from the time elapsed eliminating the need to wait for stabilization of an electrode. UV spectroscopy is again used to monitor changes in the absorbance of the compound as a function of pH. This reduces the analysis time to ~4 min per cycle giving a throughput of more than 200 compounds per day.

6.5.2
pK_a Measurements in Cosolvent Mixtures

Poor water solubility is still a problem for all these methods, but it can be overcome to some extent by using a mixture of solvents, although the presence of organic modifiers causes the pH scale to shift and may cause the pK_a to change. The

dissociation equilibria are governed by electrostatic interactions as well as by solute–solvent interactions. As shown in Equation 6.2, during the dissociation of uncharged acids, charged species are created. In this instance, the electrostatic interactions become very important, as the corresponding pK_a increases with decreasing polarity of the solution. During the dissociation of cationic species, there is no change in the number of charges and therefore the permittivity of the solution does not change. In this situation, the solute–solvent interactions are more important than the electrostatic interactions and there is a small error on the pK_a.

Apparent pK_a values measured in the presence of cosolvents are therefore different from those measured in purely aqueous systems and will not give a true indication of the % ionized of the species. One-unit error in pK_a calculation will carry through to a 1-unit error in log D_{pH} if calculated from a measured log P value. This is particularly important where the pK_a is close to the pH of the region of absorption, which can lead to errors in predicting behavior. The Yasuda–Shedlovsky technique uses the measurement of the apparent pK_a (p_sK_a) in a cosolvent mixture and extrapolates back to 100% aqueous. This works well and is well documented [18, 19]; however, it is sample expensive requiring at least three experiments per sample and is therefore not appropriate for a high-throughput setting. Recent work has been published by Völgyi *et al.* [20] demonstrating the use of a universal cosolvent system allowing a single-point measurement against a general calibration curve to determine pK_a in an aqueous environment by using the Yasuda–Shedlovsky plot.

6.5.3
pK_a Measurements based on Separation

Many different types of chromatographic methods have been used to determine pK_a value, such as ion-exchange chromatography, gas chromatography, and RP-HPLC, is well placed for high-throughput analysis. A review by Hardcastle *et al.* [21] explains the theory behind the calculations and the derivation of equations for the determination of pK_a value. It has been demonstrated that the correct determination of pH of the mobile phase is key to the determination of pK_a value of an analyte from chromatographic retention [22, 23]. However, this is the pK_a value of the analyte in the mobile-phase system and not in a purely aqueous environment. The dielectric constant of cosolvent/water mixtures is less than that of water alone and therefore the extent of ionization and the associated ionization equilibria are suppressed:

$$p_sK_a \text{ acids} > pK_a \text{ acids and } p_sK_a \text{ bases} < pK_a \text{ bases.}$$

While this does not give a "true" pK_a value without using the Yasuda–Shedlovsky approach, it does give the dissociation constant for the analyte in the chromatographic system, which will help determine a generic system for the separation of complex mixtures. There are a number of benefits of using chromatographic retentions and capacity factor as a tool for determining pK_a over the potentiometric

methods. Sample requirements are very small and poor aqueous solubility is no longer a problem. Since it is a separation technique, the purity of the compound does not interfere with the analysis, and fast methods significantly reduce analysis time and increase throughput. However, due to stability issues, the pH range of the mobile phase can be limited and therefore the range of pK_a values that can be determined and the precision of the values are not generally as great as those determined by potentiometry.

Capillary electrophoresis has been used for over a decade to determine accurate pK_a values [24, 25] requiring only small amounts of analyte at very low concentrations. It does not require the quantitative determination of the solute or titrant concentrations and since it is a separation technique, impurities do not present a problem, and nonaqueous solvents can be used for poorly soluble compounds [26]. This technique relies solely on migration times. The effective mobility of an ion, m_{eff}, is related to the fraction of ionized species present and therefore the pK_a can be determined, provided the equilibrium is fast with respect to the separation time. A review by Poole *et al.* [27] presents model equations for pK_a determination for compounds with up to three ionization centers. A single peak will be observed for all interconverting species, which will depend on the properties of the electrolyte solution. The weakness of capillary electrophoresis as a high-throughput method is its requirement for multiple buffer systems, since while the analysis is rapid the number of channels available is reduced. There are no special instrument requirements for this system, provided there is an effective thermostating of the column since the equilibrium constants depend on temperature. A commercial instrument is now available from Advanced Analytical [28] using a 96-capillary array separation cassette and diode array detection designed to be used in a 96-well microtiter plate format. Twelve electrolyte solutions of differing pH are used to analyze samples simultaneously allowing a throughput of around 16 samples per hour across a pH range of 2–12. Lišková and Šlampová [29] give details of practical considerations with respect to buffers across the pH range 2–12, and it has been shown that placing the system under pressure during the electrophoretic separation reduces migration times and is good across the pH range 2.5–10.5 [30] as it increases the throughput for nonparallel systems. These methods still rely on the presence of a chromophore since they use UV detection, and due to the very small path lengths, concentrations of about 10 μM are to be recommended to achieve a high enough signal for detection. It is possible to use mass spectrometric detection coupled to capillary electrophoresis, although modification of the electrolytes used will be necessary for compatibility with the mass spectrometer. Wan *et al.* [31] describe a method of simultaneous measurement of a pooled sample comprising 1 μl of 10 mm DMSO stocks of each up to 56 compounds. The presence of 5% DMSO neither did influence the effective mobilities of the samples, and therefore had minimal effect on pK_a values determined, nor did it interfere with peak identification. The use of pressure assistance and volatile buffers meant that the total cycle time for these 56 compounds was less than 150 min, although throughput will depend on the resolution of the mass spectrometer. The main disadvantage of this procedure was that compounds that were too similar in mass (a difference of <2 Da) could be misidentified.

6.6 Lipophilicity

Lipophilicity is the major driving force for binding drugs to a receptor target. If a compound is too lipophilic, it will be retained longer, have a wider distribution and greater nonspecific binding, and potentially be more readily metabolized. It is a means of estimating a molecule's affinity for a lipid, nonaqueous environment. There are many routes by which a drug can be absorbed by passage through membranes and tissues, but transport by passive diffusion is the most common route [32]. For this to occur, the drug must be lipophilic enough to pass from an aqueous environment into the lipid core of the membranes but not so highly lipophilic that it is retained there.

Measurement of lipophilicity is well documented and a large database of measured log *P* values is available [33]. Lipophilicity is defined as the behavior of a compound in a biphasic system, solid/liquid or liquid/liquid, and it is usually expressed by the octanol/water partition coefficient (*P*) or the distribution coefficient (*D*) with octanol and water traditionally forming the biphasic system. Hansch and Fujita [34–36] recommended the use of the partition coefficient logarithm (log *P*) to model the biological partition behavior of drug molecules. An octanol/water system was chosen because it was known that water-saturated *n*-octanol forms into near-spherical clusters: the OH groups of ~16 octanol molecules coordinate around a core of water molecules with the hydrocarbon chains pointing outward. This produces a phase with some of the characteristics of a phospholipid membrane bilayer: the regions where the lipophilic character predominates (as in the core of the lipid membrane) adjacent to a region with a high degree of polar character (e.g., at the membrane surface) [37]. However, an octanol/water system cannot completely model the combination of charge and polarity, which exists in the phospholipid head groups of biological membranes, since it is not sensitive to the hydrogen-bond donor characteristics of the solutes.

6.6.1 log *P* Versus log D_{pH}

The difference between log *P* and log D_{pH} is often a cause for confusion. log *P* is the $\log_{10}$ of the partition coefficient and is the extent to which the *neutral species* has an affinity for the organic environment relative to that of the aqueous environment. log D_{pH} is the $\log_{10}$ of the distribution coefficient and is similar in that it is also a measure of the extent of the affinity for organic over aqueous except that it is *all species present at a given pH* that are measured. For compounds with no ionizable groups or those where the test pH is sufficiently far away from the pK_a of the ionizable groups so that they are in their neutral form, log *P* and log D_{pH} are equivalent. If the test pH of the log D_{pH} assay is changed, the extent of ionization of the molecule will also change. It is therefore imperative that the test pH is always quoted for log *D*, often as a subscript with the nomenclature log D_{pH}. (although, it is not uncommon for the pH value to be found as a superscript with the subscript being used to designate the solvent). This is summarized in Figure 6.4.

$$\text{Partition } (P) = \frac{[\text{ single species in organic phase}]}{[\text{ single species in aqueous phase}]} \qquad \text{Distribution } (D) = \frac{[\text{ unionised + ionised }]_{\text{organic}}}{[\text{ unionised + ionised }]_{\text{aqueous}}}; \text{ where } [\ ] = \text{concentration}$$

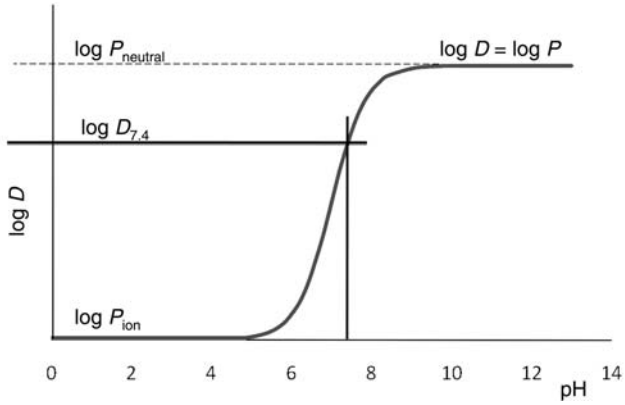

Figure 6.4 Summary of the difference between log P and log D_{pH} with a plot of log D versus pH for a base.

log D_{pH} is arguably a more useful descriptor for ionizable compounds, but, since it depends on pH, values determined at differing pH values should never be compared. A major advantage of log D_{pH} is that it can be measured very easily since no account of the species present is made. It is extremely amenable to high-throughput technologies, and a number of different methods have been studied. Some are true partition experiments while others use validated chromatographic systems that reference retention time and capacity factor to known lipophilicity values and are a good surrogate for log P measurements.

6.6.2 Measuring Lipophilicity

The shake-flask method has been described as the "gold standard" – it has been the method of choice for literature publications against which other methods of lipophilicity determinations have traditionally been calibrated, although other methods, now commonly used, are capable of generating the same quality of data. The shake-flask method starts from solid material incubated in a biphasic solution of aqueous and octanol, and the relative amounts in each layer are determined. There are, however, a number of problems with this method. For example, microemulsions can be formed, which prevent the two layers from separating, and these can be stable for days. The upper and lower ranges that are achievable can cause detection problems; for example, log $D_{7.4} = 4$ contains 10 000 times more samples in the octanol layer causing saturation of the detector, while the quantity present in the aqueous layer may be below the detection limit. Using mass balance equations can accommodate this but the systems must be well validated.

Using potentiometric methods, log *P* is calculated from the difference between the apparent pK_a (p$_s K_a$) values measured in a biphasic system such as octanol/water. The first such method was developed by Sirius Analytical as a basis for its GLpKa instrument. The solid sample is dissolved in a biphasic system, acidified or basified, and titrated with base or acid under controlled conditions. The resulting titration curve is compared with a simulated curve produced from p$_s K_a$ values (and other variables), which are systematically varied until the two curves match as close as possible. This process is known as refinement [38]. The major drawback of this method is that it can be used only for ionizable molecules and is not appropriate for lipophilic weak bases with a low pK_a or weak acids with a high pK_a if the values shift to p$_s K_a$ values outside the measurement range of 2–12. It can, however, be used over a wide range of phase ratios since the pH is measured without phase separation. There are a number of reviews that explain the methodologies and mathematics behind the pH-metric method of determining log *P* [39–41].

6.6.3
High-Throughput log $D_{7.4}$ Measurements

"Miniaturizing" the shake-flask method so that it is transferable to a liquid-handling robotic system is relatively straightforward. The samples can be dispensed into tubes in a microtiter plate format and the two phases are added using any of the standard instruments available. To ensure a thorough mixing of the two phases, the tubes need to be sealed tightly and the plates inverted before, and shaken vigorously during, the incubation period. Once the incubation is complete, the phases need to be allowed to separate fully and this can be achieved most effectively by centrifugation. Using disposable tips and with careful teaching of the aspirate heights, it is possible to sample from the two layers, which are then analyzed and the ratios of the concentration calculated. The use of RP-HPLC analysis allows fast and simple measurements, although it is important to ensure that the octanol and aqueous layers are alternated to avoid a buildup of octanol on the column.

6.6.4
High-Throughput log $D_{7.4}$ Versus Shake-Flask log $D_{7.4}$

In a high-throughput setting, it is beneficial to have a generic method that is applicable to all the compounds being analyzed. If this is not the case, adapting methods can take up valuable time and resources. For this reason, it is most common for the volumes used in the octanol and aqueous layers to be the same. However, in the high-throughput partition experiment detailed above, the samples are present as liquids in DMSO, and adding equal volumes of octanol and water to the sample aliquot will lead to one phase being present in excess. DMSO preferentially partitions into the aqueous layer rather than the octanol and therefore the total volume of DMSO aliquot plus aqueous buffer must be the same as that for the octanol for the two volumes to be equivalent. This assay has been validated by UCB (unpublished data) against the shake-flask method and holds up very well, R^2 is 0.9. Figure 6.5

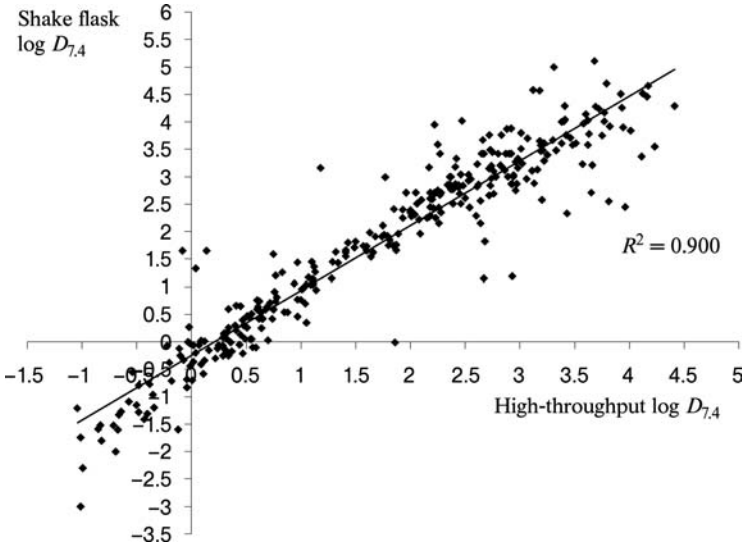

Figure 6.5 Correlation of high-throughput log $D_{7.4}$ measurements from DMSO stock solutions with shake-flask log $D_{7.4}$ measurements from solid material.

shows the correlation between two sets of data for ~300 relatively diverse compounds consisting of commercially available drugs and a range of compounds from a number of medicinal chemistry projects.

There is a loss of correlation at the extremes of the lipophilicity ranges and this can in some way be explained by the presence of DMSO in the high-throughput assay. The relative amount of DMSO present is so low that it will have a negligible effect on the final lipophilicity value. However, for compounds, which are very highly lipophilic, their value may be slightly reduced due to the apparent pulling of the compound into the aqueous layer by the DMSO rather than the compound partitioning into the octanol where it has greater affinity.

6.6.5
Alternative Methods for Determining High-Throughput log D_{pH}

Chromatographic retention time gives a direct measure of the extent of a compound's interaction with the stationary phase. This will therefore relate to its distribution between the two phases. A review by Gocan *et al.* [42] describes the use of chromatography to determine lipophilicity. There are direct methods where sets of compounds with a diverse range of well-characterized lipophilicities are analyzed by RP-HPLC to create a calibration curve constructed from retention times and capacity factors versus lipophilicity against which unknown compounds can be measured [43–47]. This type of approach is good for high throughput in microtiter plate format, and samples are generally from DMSO stock solutions and therefore do not need weighing. It does not depend on the amount of compound injected onto the column

and is not affected by impurities in the sample or the solvent vehicle used. Different types of stationary phase such as immobilized artificial membrane (IAM), human serum albumin (HSA), and α-acid glycoprotein (AGP) [48] can be used depending on the partition and is not restricted to octanol/water partitioning. These methods, however, do not allow direct comparative studies between methods without the use of standards.

Sirius Analytical has developed a commercially available Profiler LDA instrument in which a proprietary stationary phase is coated with octanol. Octanol-saturated mobile phase is recirculated to maintain the octanol content of the stationary phase as constant. This system gives a dynamic range that covers $-1 < \log P < 5$.

Chromatographic hydrophobicity index (CHI) was introduced by Valkó *et al.* in 1997 [49] where an index is derived from the compound's retention time in a fast-gradient RP-HPLC system. The gradient is produced by changing the proportions of buffer and acetonitrile in the mobile phase. The sample is injected onto the column with a low percentage of acetonitrile so that it preferentially binds to the stationary phase. The gradient is then increased until the sample dissolves when the percentage of acetonitrile present in the mobile phase is high enough and the sample will elute from the column. The system is calibrated using retention times for a set of standards with known CHI values. Constants can be used to calculate CHI for the unknown samples, which are normally in the range of 0–100 to give the approximate percentage of acetonitrile required to produce an equal distribution of the compound between mobile and stationary phases.

Using microemulsion electrokinetic chromatography (MEEKC) [50], microemulsions are made from a combination of aqueous buffer, *n*-butanol, heptane, and a surfactant placed inside a fused silica capillary. DMSO stock solutions are diluted with buffer and a highly lipophilic marker, dodecaphenone. This is injected at the anode end of the capillary with a UV detector placed at the cathode end. An electric field is applied, which produces negatively charged droplets of organic solvent. Neutral solutes present in the aqueous phase migrate with the endosmotic flow while those present in the organic phase will migrate at the speed of the charged droplets. This method is suitable only for compounds that are electrically neutral at the pH of the buffer so that bases are run in pH 10 buffer and acids in pH 3 buffer. This method, therefore, does not allow for a single method to be used for all compounds.

6.7 Permeability

It is not uncommon for drug compounds to be able to perform very well in a variety of microtiter plate-based assays, but when transferred to *in vivo* assays, they cannot reach the therapeutic target site. The molecule must permeate through a number of cell membranes made up of phospholipid bilayers, which can increase the passage of highly charged polar molecules. Among the most common means by which a molecule can cross such a membrane are transcellular routes such as passive diffusion, carrier-mediated active transport, and metabolic enzymes, paracellular

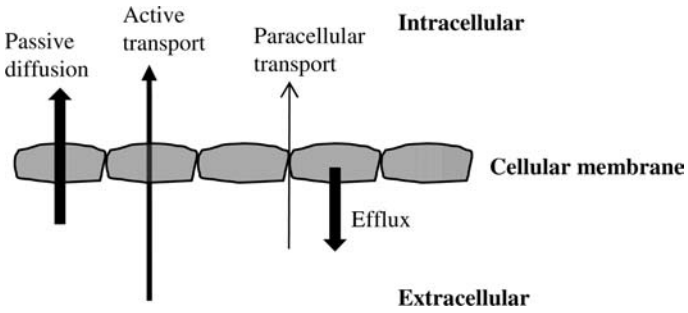

Figure 6.6 Routes by which a drug can cross a membrane.

transport where the molecules diffuse through the tight junctions between the cells, and ATP-dependent efflux mechanisms where the drug is pumped out back, as described in Figure 6.6.

Cultured cells such as Caco-2 (human colon adenocarcinoma) or MDCK (Madin–Darby canine kidney) have long been used to give some measure of the permeation rate. Caco-2 cells express peptide transporters such as PEPT1 [51] and efflux systems such as P-gp [52]. The Caco-2 cell monolayer *in vitro* permeability assay mimics most of the transport pathways in the gastrointestinal tract and has therefore gained broad acceptance as a surrogate marker for estimating *in vivo* drug absorption potential. Krishaa *et al.* [53] and Faassen *et al.* [54] describe in detail the Caco-2 experiment methods. Although these methods remain the key benchmark assays, they are expensive to run, highly variable, and relatively unamenable to a high-throughput environment due to long membrane culture time and the requirement for multiple time point measurements.

The advantage of cell culture models is that they are able to measure active transport processes across the cell membranes and not just the interaction of a drug with a lipid bilayer. They can also be used to study passive and active transport routes; indeed, much of the knowledge as to the active transport mechanisms in the intestine has been derived from cell culture studies. Despite the predominant route being passive diffusion, the research into transport mechanisms indicates that there are a large number of drugs that are used as substrates for active transporter and efflux systems, and it must therefore be appreciated that multiple transport routes may be involved in the intestinal drug transport.

Since the majority of drugs are absorbed by passive diffusion, an assay that measures the rate of permeation through a simple artificial membrane, which mimics this, may be useful; however, how much so as a gastrointestinal tract membrane mimic will be determined by the membrane composition. (Fisher *et al.* [55] provide a review of the molecular parameters that govern passive diffusion.) A major step in the advancement of noncell-based permeability screens designed to overcome many of these issues was the PAMPA (parallel artificial membrane permeability assay) first published by Kansy in 1998 [56] where a concentrated, negatively charged phospholipid bilayer membrane is supported on a filter in a 96-well plate. This technique has been investigated and modified many times and has been widely implemented in

high-throughput screening cascades across the industry and has found favor as a tool for the rank ordering of compounds. PAMPA data are frequently correlated with those from cell-based assays and indeed also with *in vivo* absorption data with some success in terms of R^2 and the numbers of outliers, although how relevant it is to "predict a prediction" remains a matter for individual groups to decide, with similar conclusions being arguably possible from calculated properties such as polar surface area and number of hydrogen-bond donors and acceptors. It is worth noting that there is a lack of published evidence to suggest that PAMPA has been instrumental in the design of a drug candidate or in driving a project forward in the same way as the log *P* or solubility has been on a compound-by-compound basis.

6.7.1
Permeability and Lipophilicity

According to Fick's first law of diffusion, the passive diffusion of a drug across a membrane is directly proportional to the membrane–water partition coefficient, provided the interior of the membrane is homogeneous and the concentration of the drug on the "receiver" side of the membrane is much less than that on the "donor" side of the membrane, although in practice this linearity does not hold over a very wide range of lipophilicities due to issues such as the presence of aqueous pores in oily membranes, membrane retention of lipophilic molecules, pK_a effects, aggregation of the solute, and the unstirred water layer (UWL).

Both lipophilicity values, log *P* and log D_{pH}, are a ratio between two immiscible phases determined once the system has reached equilibrium and is therefore a thermodynamic system. Permeability values, however, are rates of passage through the membranes and conditions are carefully selected to ensure that the system does not reach equilibrium. This is a kinetic system and depends on many variables such as incubation time, membrane composition, stirring rate, pH, and buffer composition. For this reason, it is extremely difficult to make reliable group-to-group comparisons. Although the rank ordering of compounds should be the same, it is unlikely that the absolute values would be the same, making validation of new methods very difficult. As a result, substituting permeability values for lipophilicity values and vice versa should be carried out with caution while correlation of the one with the other has been shown to be reasonably successful [57]. Faller *et al.* [58] have demonstrated the use of PAMPA technology for determining lipophilicity and Chen *et al.* [59] described a variation using polymer-plasticized polyvinylchloride.

6.7.2
Cell-Based Assays

For cell-based assays, all of the instruments used need to be maintained in a sterile environment if growing the cells is to be automated. These assays are labor intensive, expensive, and not generally well suited to high throughput. The cells need to be cultured for around 21 days (depending on the cell line). Bellman *et al.* [60] presented details of a high-throughput Caco-2 cell-based method for measuring permeability

using LC/MS detection. Using 5 μM sample concentration in the donor (apical) wells, the authors measured both apical-to-basolateral (A–B) and basolateral-to-apical (B–A) directions by taking 100 μl samples from both the donor and the acceptor (basolateral) at time $t = 0$ and after 90 min incubation and replacing with 200 μl of 50% acetonitrile/water. A generic HPLC method was used with ESI mass spectrometry detection. They demonstrated that it is possible to measure all the samples in duplicate with a throughput of 20 samples in 24 h. This is an increase in throughput but it still does not satisfy the needs of a department requiring analysis of much greater numbers of compounds.

6.7.3
Noncell-Based Assays: Chromatographic Methods

Chromatography is easily automated and using short retention times hundreds of compounds can be analyzed quickly by methods developed to model intestinal permeability. The stationary phase consists of either immobilized liposomes or immobilized phospholipids. These methods are excellent for screening purposes as they require only small amount of compound, and automation is straightforward. A variety of columns are commercially available and the historical concerns for column stability have been largely overcome. Permeability is related to the retention time of the compound on the stationary phase designed to mimic lipid bilayers [61, 62], which is due to electrostatic interactions between the drug and the lipid surface and partitioning into and across the lipid phase. Retention on the column therefore does not always reflect transport across the membrane [63]. It has been suggested that the correlation from these methods with drug permeability shows no improvement over the use of log *P* [64]. Zhue *et al.* [65] present a good data set with human fraction absorbed, Caco-2 permeability data, and log *P* values for 92 compounds, which are useful for validation studies.

6.7.4
Noncell-Based Assays: Parallel Artificial Membrane Permeability Assay

In contrast to cell-based assays, noncell-based permeability assays using artificial membranes supported on filters are fast, flexible, cheap, and fully automatable. They are therefore ideally placed for use in high throughput. There have been many variations of this assay in terms of the fine details of the experiment and these will be discussed in due course; however, the basic principles remain the same, based on a 96-well microtiter plate format.

A "sandwich" is formed from two plates, a donor plate and a receiver plate. The donor plate is usually of a specially designed geometry, available from pION Inc. for use with its Evolution system and GUT box or from Millipore Inc. These plates are machined to minimize vortexing during shaking so that the buffer solution remains in contact with the lower surface of the receiver plate at all times without the formation of a meniscus. The receiver is a 96-well microfilter plate. The filters are generally 125 μm thick with 0.45 μm pores and 0.3 cm^2 cross-sectional area with 70%

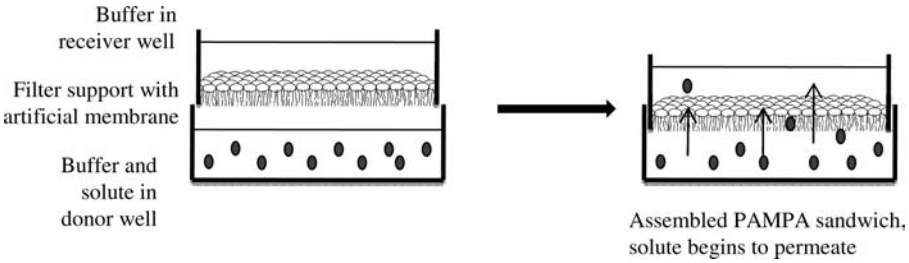

Figure 6.7 Schematic representation of PAMPA system.

porosity onto which is placed a solution of the artificial lipid membrane. BD Biosciences has produced a commercially available PAMPA plate system, which is a 96-well insert with a PVDF filter plate precoated with structured layers of phospholipids and has a matched receiver microplate [66].

The samples as DMSO stock solutions are added to the donor wells and are diluted with buffer. The receiver plate is placed on top of the donor wells, the lipid solution is added carefully to ensure that there is complete coverage of the filter support, and then the buffer solution for the receiver system is added. The resulting sandwich is covered to avoid evaporation and is shaken. Figure 6.7 shows a schematic representation of the construction and incubation of the PAMPA sandwich system.

After the samples have been incubated for the chosen time, the plates are separated and aliquots removed from both donor and receiver wells and the concentration of the solute determined. This is most commonly carried out by using HPLC, LC/MS, or UV plate reader detection.

6.7.4.1 Membrane Composition

There have been many variations in the composition of artificial membranes used in a PAMPA-style analysis and each has been tailored to specific investigations. Sugano *et al.* [67, 68] investigated a variety of phospholipid membrane systems and experimental conditions and were able to show that by modifying the membrane it was possible to improve the predictive power of PAMPA.

Di *et al.* [69] describe the use of a PAMPA for the prediction of passage of a drug across the blood–brain barrier by the modification of the membrane using porcine polar brain lipid and have demonstrated the ability to determine which compounds will be most likely to be CNS positive and CNS negative.

6.7.4.2 Suggestions for PAMPA

The following recommendations are a good starting point for a gastrointestinal, noncell-based artificial membrane permeability assay [70]:

- *Donor wells*: pH 6 and pH 7 (ionization-maintained sink), 5–10 mm bile acid, such as taurocholic acid or glycocholic acid to solubilize lipophilic molecules (binding-maintained sink).
- *Receiver wells*: pH 7.4 phosphate buffer containing 3% w/v bovine serum albumin (BSA) added to receiver wells (binding-maintained sink).

- The artificial membrane composed of phosphatidyl choline, phosphatidylethanolamine, phosphatidylserine, phosphatidylinositol, and cholesterol.
- DMSO final concentration <10%.

In cell-based assays, membrane integrity is monitored using conductivity measurements but is not amenable to high throughput, and alternatives are needed. One approach may be to perform the assay in triplicate, rejecting the data where two points are not in good agreement. This would reduce throughput and does not remove all doubts as to the quality of the data.

Alternatively, a well-validated poorly permeable compound is included in the analyte solutions as an internal standard. A compound such as theophylline has an effective permeability of $\sim 0.12 \times 10^{-6}$ cm/s (exact value will depend on assay conditions). If the compound were seen to be permeating significantly faster than this effective permeability, it could be concluded that the membrane had been compromised. This approach would mean that a detection method based on separation, such as HPLC, would be needed. Upon the inclusion of a second internal standard, which was known to be highly soluble, such as verapamil, effective permeability 16×10^{-6} cm/s would enable monitoring of the incubation time to ensure that equilibrium had not been reached for highly permeable compounds.

A third method of checking the membrane integrity is to monitor the appearance of DMSO in the receiver wells due to damaged membranes by analyzing down to 200 nm. This could be automated, would not result in the need for separation of the analyte before detection, and would not reduce throughput.

6.7.4.3 Considerations in the Calculation of Permeability from PAMPA Data

The equations used to calculate permeability from PAMPA data are derived from Fick's law and assume that equilibrium between the donor and the receiver wells has not been achieved. The equations also assume that the membrane has been fully saturated by the sample upon leaving the donor well before permeation into the receiver well commences. For most compounds, this saturation time is extremely short and does not generally present a problem. Membrane retention also needs to be considered. This will tend to be higher for more lipophilic compounds and has sometimes been seen up to 90%. The consideration, or otherwise, of membrane retention will dictate which set of equations should be used and whether the resulting permeability value is termed the apparent permeability as is used in cell-based determinations or the effective permeability.

Permeability is a kinetic process, and is quoted as a rate. In cell-based assays such as Caco-2, a number of time points are generally taken from both the donor (apical) wells and the receiver (basolateral) wells. Because of this, retention on the membranes is not determined and the permeability values quoted are "apparent," P_a. The main benefit of PAMPA type assays is their usefulness as high-throughput tools and therefore taking time point measurements will create a bottleneck. Measurements of the donor and receiver wells are made at the end of the incubation period and referenced back to the starting concentration of the solute in the donor wells.

Membrane retention values can be determined using mass balance and inclusion of this gives the "effective" permeability, P_e. These are shown in Equations 6.4–6.6:

$$P_e = \frac{-2.303}{At}\frac{V_R V_D}{V_R + V_D}\log_{10}\left[1-\left(\frac{V_R + V_D}{(1-R)V_D}\right)\left(\frac{C_R}{C_D}\right)\right], \tag{6.4}$$

where

$$R = \frac{[C_e-(C_D + C_R)]}{C_e}. \tag{6.5}$$

$$P_a = \frac{V_R V_D}{AtV_R + V_D}\ln\left[1-\left(\frac{C_R}{C_D}\right)\right]. \tag{6.6}$$

Effective permeability (P_e) and apparent permeability (P_a) can be determined using Equations 6.4 and 6.5 and Equation 6.6, respectively, where A is the membrane area (cm^2), t is the incubation time (s), V_R is the volume of the receiver well (cm^3), V_D is the volume of the donor well (cm^3), C_R is the concentration of solute in the receiver well at time t (mol/cm^3), C_D is the concentration of the solute in the donor well at time $t = 0$ (mol/cm^3), and C_e is the concentration of the solute at equilibrium (mol/cm^3).

The distinctions between these two have been discussed here only briefly. Avdeef [71] has published more detailed explanations and derivations of the equations to be used.

6.7.5 Sink Conditions

The term "sink" when referred to *in vitro* permeability systems means any process that significantly lowers the concentration of the neutral species from the receiver wells. *In vivo* sink conditions can be thought of as the continued removal of the permeating species due to the continuous flow of blood. There are three methods of introducing sink conditions into an *in vitro* system:

(1) *Physically-maintained sink conditions:* In cell-based assays, an aliquot is removed for analysis from the receiver wells to make time point measurements. This is replicated in Caco-2 but not in PAMPA.

(2) *Ionization-maintained sink conditions:* Owing to the dependence of ionization on pH, weak acids will be more permeable in a gradient system where the pH of the donor is below that of the acceptor, while weak bases will be more permeable in an iso-pH system. Uncharged species will show the same results using either system. If the pH gradient is wide enough, a neutral compound will become ionized once it reaches the receiver wells.

(3) *Binding-maintained sink conditions:* The presence of serum proteins in the receiver wells, such as 3% w/v BSA, will bind the neutral compound once it crosses the membrane.

The pION Inc. method uses "double-sink" conditions, both ionization and binding maintained.

6.7.6
Unstirred Water Layer

The passive transport of compounds across a membrane is the combination of diffusion through the membrane and the regions of undisturbed solution, the unstirred water layer, on either side of the membrane. The solute samples are present in the bulk solution, which, upon stirring, move through the bulk to the interface of the bulk solution and the UWL. *In vivo*, the gastrointestinal UWL is in the region of 30–100 μm due to an efficient mixing near the surface of the endothelium [72], while in the Caco-2 system it is >1000 μm. Diffusion laws govern the progress of the solute through the UWL that can be reduced in size by increased stirring but will never actually be removed. The UWL is virtually the same for drugs of a comparable size and can be determined by measuring the transport of the compounds from the donor to the receiver wells without addition of the artificial membrane to the filter supports, by determining the stirring rate dependence of the permeability of the compounds (a technique used by pION Inc. in its Gut Box technology, where the shaking of the system can be preset according to desired UWL) or by determining the pH dependence of the effective permeability.

6.7.7
Surface Properties for the Determination of Permeability

Surface tension measurements have been shown to correlate with ADME properties [55, 73–75]. The Kibron Delta8 instrument is a multichannel tensiometer that studies the dependence of surface activity on the solution composition. The technology is based on the determination of the maximum force exerted by surface tension on a wetting probe as it is withdrawn from the liquid/air interface. The main forces acting on the probe are the buoyancy due to the volume of the liquid displaced by the probe and the mass of the meniscus adhering to the probe. The maximum pull force is recorded when the buoyancy force reaches a minimum – just before the meniscus breaks. This instrument uses a microtiter plate-based format and can measure a plate in around 2 min. Across the plate is a series of 8 samples at 12 concentrations, starting from DMSO stock solutions. This allows prediction of the passive diffusion through membranes from plots of the critical micelle concentration versus the concentration of the onset of surface activity (C_o) by calibration against drugs with known permeabilities. This technique can be used for passage through the blood–brain barrier or the gastrointestinal tract [76].

6.8
Data Interpretation, Presentation, and Storage

A major consideration in setting up a high-throughput screen is the data collection, processing, interpretation, and dissemination. It is particularly important to ensure that there is sufficient time and resources dedicated to studying the data. Discrete

numbers are useful for QSAR, QSPR work, correlation, and method validation but they can be overwhelming, particularly for the nonexpert user. A clear and unambiguous method of visualizing the data is needed. This is often done by binning the data as well as providing a numerical value. If this approach is adopted for all of the assays, it is possible to produce the data in a report-style format with expert interpretation, which gives a package of data showing how all the properties of a given series of compounds interrelate. This is particularly useful for reference purposes. Freeman [77] demonstrated how this approach provides a valuable tool for the use of high-throughput physicochemical profiling.

6.9 Conclusions

This chapter has provided only a brief introduction to the field of high-throughput physicochemical screening. It is intended to demonstrate that with ingenuity it is possible to automate or increase throughput of these techniques. High-throughput measurement of physicochemical parameters has a valid place in drug discovery, its exact positioning within the timelines of a project will depend on the individual organization and its particular needs. With careful thought, it is possible to analyze a large number of compounds using very little sample and generate a package of data, which will help to drive projects forward. The assay conditions must be relevant to the individual questions being posed and the data should be "fit for purpose." However, if budgets are generous and compound numbers are high enough, there is a danger that too much data could be generated – a case of diluting the information through shear volume of data – and measurements should not be made "just because they can" be made. Screening for all physicochemical properties is a compromise, high throughput with a low predictive potential or low-throughput with a high predictive potential. However, using multiple data points, pH for instance, rather than large compound numbers and devoting sufficient time to interpretation and education may tip the balance of this compromise toward a higher predictive power.

References

1 Hill, A. High-throughput solubility, http://www.physchem.org.uk/symp03/symp03_ah.pdf.

2 Kerns, E.H. (2001) High-throughput physicochemical profiling for drug discovery. *Journal of Pharmaceutical Sciences*, **90**, 1838–1858.

3 Goodwin, J.J. (2006) Rationale and benefit of using high-throughput solubility screens in drug discovery. *Drug Discovery Today: Technologies*, **3** (1), 67–71.

4 Taub, M.E., Kristensen, L. and Frokjaer, S. (2002) Optimized conditions for MDCK permeability and turbidimetric solubility studies using compounds representative of BCS classes I–IV. *European Journal of Pharmaceutical Sciences*, **15**, 331–340.

5 Bevan, C.D. (2000) A high-throughput screening method for the determination of aqueous drug solubility using laser nephelometry in microtiter plates. *Analytical Chemistry*, **72**, 1781–1787.

6 Dehring, K.A., Workman, H.L., Miller, K.D., Mandagere, A. and Poole, S.K. (2004) Automated robotic liquid handling/laser-based nephelometry system for high-throughput measurement of kinetic aqueous solubility. *Journal of Pharmaceutical and Biomedical Analysis*, **36**, 447–456.

7 Fligge, T.A. and Schuler, A. (2006) Integration of a rapid automated solubility classification into early validation of hits obtained by high-throughput screening. *Journal of Pharmaceutical and Biomedical Analysis*, **42**, 449–454.

8 Llinas, A., Box, K.J., Burley, J.C., Glen, R.C. and Goodman, J.M. (2007) A new method for the reproducible generation of polymorphs: two forms of sulindac with very different solubilities. *Journal of Applied Crystallography*, **40** (2), 379–381.

9 Seadeek, C., Ando, H., Bhattachar, S.N., Heimbach, T., Sonnenberg, J.L. and Blackburn, A.C. (2007) Automated approach to couple solubility with final pH and crystallinity for pharmaceutical discovery compounds. *Journal of Pharmaceutical and Biomedical Analysis*, **43**, 1660–1666.

10 Sugano, K., Kato, T., Keiko, K., Sujaku, T. and Mano, T. (2006) High-throughput solubility measurement with automated polarized light microscopy analysis. *Journal of Pharmaceutical Sciences*, **95** (10), 2115–2122.

11 Avdeef, A. (1992) *Quantitative Structure–Activity Relationships*, **11**, 510–517.

12 Comer, J. (2006) Ionisation constants and ionisation profiles, in *Comprehensive Medicinal Chemistry* (eds D.J. Triggle and J.B. Taylor), Elsevier, Oxford, pp. 357–397.

13 Avdeef, A. (1983) Weighting scheme for regression analysis using pH data from acid base titrations. *Analytica Chimica Acta*, **148**, 237–244.

14 Avdeef, A. (1993) pH-metric log *P* II. Refinement of partition coefficients and ionisation constants of multiprotic substances. *Journal of Pharmaceutical Sciences*, **82**, 183–190.

15 Tam, K.Y. and Takács-Novák, K. (2001) Multiwavelength spectrophotometric determination of acid dissociation constants: a validation study. *Analytica Chimica Acta*, **434**, 157–167.

16 Allen, R.I., Box, K.J., Comer, J.E.A., Peake, C. and Tam, K.Y. (1998) Multiwavelength spectrophotometric determination of acid dissociation constants of ionizable drugs. *Journal of Pharmaceutical and Biomedical Analysis*, **17**, 699–712.

17 Box, K., Bevan, C., Comer, J., Hill, A., Allen, R. and Reynolds, D. (2003) High-throughput measurement of pK_a values in a mixed-buffer linear pH gradient system. *Analytical Chemistry*, **75**, 883–892.

18 Avdeef, A., Comer, J.E.A. and Thomson, S.J. (1993) pH-metric log *P*. 3. Glass electrode calibration in methanol–water, applied to pK_a determination of water-insoluble substances. *Analytical Chemistry*, **65**, 42–49.

19 Takács-Novák, K., Box, K.J. and Avdeef, A. (1997) Potentiometric pK_a determination of water-insoluble compounds: validation study in methanol/water mixtures. *International Journal of Pharmaceutics*, **151**, 235–324.

20 Völgyi, G., Ruiz, R., Comer, J., Bosch, E. and Takács-Novák, K. (2007) Potentiometric and spectrophotometric pK_a determination of water-insoluble compounds: validation study in a new cosolvent system. *Analytica Chimica Acta*, **583**, 418–428.

21 Hardcastle, J.E. and Jano, I. (1998) Determination of dissociation constants of polyprotic acids from chromatographic data. *Journal of Chromatography B*, **717**, 39–56.

22 Canals, I., Portal, J.A., Bosch, E. and Rosés, M. (2000) Retention of ionizable

compounds on HPLC.4. Mobile phase pH measurement in methanol/water. *Analytical Chemistry*, **72**, 1802–1809.

23 Espinosa, S., Bosch, E. and Rosés, M. (2000) Retention of ionizable compounds on HPLC. 5. pH scales and the retention of acids and bases with acetonitrile–water. *Analytical Chemistry*, **72**, 5193–5200.

24 Gluck, S.J., Steele, K.P. and Benko, M.H. (1996) Determination of acidity constants of monoprotic and diprotic acids by capillary electrophoresis. *Journal of Chromatography A*, **745**, 117–125.

25 Ishihama, Y., Oda, Y. and Asakawa, N. (1994) Microscale determination of dissociation constants of multivalent pharmaceuticals by capillary electrophoresis. *Journal of Pharmaceutical Sciences*, **83**, 1500–1507.

26 Barbosa, J., Barron, D., Jimenéz-Lozano, E. and Sanz-Nebot, V. (2001) Comparison between capillary electrophoresis, liquid chromatography, potentiometric and spectrophotometric techniques for evaluation of pK_a values of zwitterionic drugs in acetonitrile–water mixtures. *Analytica Chimica Acta*, **437**, 309–321.

27 Poole, S.K., Patel, S., Dehring, K., Workman, H. and Poole, C.F. (2004) A determination of acid dissociation constants by capillary electrophoresis. *Journal of Chromatography*, **1037**, 445–454.

28 www.combisep.com/systems/pKa_technology.html.

29 Lišková, A. and Šlampová, A. (2007) Measurement of pK_a values of newly synthesized heteroarylaminoethanols by CZE. *European Journal of Pharmaceutical Sciences*, **30**, 375–379.

30 Wan, H., Holmén, A., Någård, M. and Lindberg, W. (2002) Rapid screening of pK_a values of pharmaceuticals by pressure-assisted capillary electrophoresis combined with short-end injection. *Journal of Chromatography A*, **979**, 369–437.

31 Wan, H., Holmén, A., Wang, Lindberg, W., Englund, M., Någård, M.B. and Thompson, R.A. (2003) High-throughput screening of pK_a values of pharmaceuticals by pressure-assisted capillary electrophoresis and mass spectrometry. *Rapid Communications in Mass Spectrometry*, **17**, 2639–3264.

32 Camenisch, G., Folkers, G. and van de Waterbeemd, H. (1996) Review of theoretical passive drug absorption models: historical background, recent developments and limitations. *Pharmaceutica Acta Helvetiae*, **5**, 309–327.

33 Hansch, C. and Leo, A. (1993) MedChem Database, Medicinal Chemistry Project, Pomona, CA.

34 Leo, A. (1993) Calculating log P_{oct} from structures. *Chemical Reviews*, **93**, 1281–1306.

35 Leo, A.J., Hansch, C. and Elkins, D. (1971) Partition coefficients and their uses. *Chemical Reviews*, **71**, 525–616.

36 Hansch, C. and Fujita, T. (1964) ρ–σ–π Analysis. A method for the correlation of biological activity and chemical structure. *Journal of the American Chemical Society*, **86**, 1616–1625.

37 Franks, N.P., Abraham, M.H. and Lieb, W.R. (1993) Molecular organization of liquid *n*-octanol: an X-ray diffraction analysis. *Journal of Pharmaceutical Sciences*, **82**, 466–470.

38 Avdeef, A. (1993) pH-metric log *P*. II. Refinement of partition coefficients and ionization constants of multiprotic substances. *Journal of Pharmaceutical Sciences*, **82**, 183–190.

39 Slater, B., McCormack, A., Avdeef, A. and Comer, J.E.A. (1994) pH-metric log *P*. 4. Comparison of partition coefficients determined by HPLC and potentiometric methods to literature values. *Journal of Pharmaceutical Sciences*, **83** (9), 1280–1283.

40 Caron, G., Gaillard, P., Carrupt, P.-A. and Testa, B. (1997) Lipophilicity behaviour of model and medicinal compounds containing a sulfide, sulfoxide or sulfone moiety. *Helvetica Chimica Acta*, **80**, 449–462.

41 Takács-Novák, K. and Avdeef, A. (1996) Interlaboratory study of log *P* determination by shake-flask and potentiometric methods. *Journal of Pharmaceutical and Biomedical Analysis*, **14**, 1405–1413.

42 Gocan, S., Cimpan, G. and Comer, J. (2006) Lipophilicity measurements by liquid chromatography. *Advances in Chromatography*, **44**, 79–176.

43 Pehourcq, F., Jarry, C. and Bannwarth, B. (2003) Potential of immobilized artificial membrane chromatography for lipophilicity determination of arylpropionic acid non-steroidal anti-inflammatory drugs. *Journal of Pharmaceutical and Biomedical Analysis*, **33**, 137–144.

44 Giaginis, C., Theocharis, S. and Tsantili-Kakoulidou, A. (2007) Octanol/water partitioning simulation by reversed-phase high performance liquid chromatography for structurally divers acidic drugs: effect of *n*-octanol as mobile phase additive. *Journal of Chromatography A*, **1166**, 116–125.

45 Balogh, G.T., Zoltán, S., Forrai, E., Györffy, W. and Lopata, A. (2005) Use of reversed-phase liquid chromatography for determining the lipophilicity of α-aryl-*n*-cyclopropylnitrones. *Journal of Pharmaceutical and Biomedical Analysis*, **39**, 1057–1062.

46 Darrouzin, F., Dallet, P., Dubost, J.-P., Ismaili, L., Pehourcq, F., Bannwarth, B., Matoa, M. and Guillaume, Y.C. (2006) Molecular lipophilicity determination of a huperzine series by HPLC: comparison of C18 and IAM stationary phases. *Journal of Pharmaceutical and Biomedical Analysis*, **41**, 228–232.

47 Plass, M., Valkó, K. and Abraham, M.H. (1998) Determination of solute descriptors of tripeptide derivatives based on high-throughput gradient high-performance liquid chromatography retention data. *Journal of Chromatography A*, **803**, 51–60.

48 Valkó, K. (2004) Application of high-performance liquid chromatography based measurements of lipophilicity to model biological distribution. *Journal of Chromatography A*, **1037**, 299–310.

49 Valkó, K., Bevan, C. and Reynolds, D. (1997) Chromatographic hydrophobicity index by fast-gradient RP-HPLC: a high-throughput alternative to log *P*/log *D*. *Analytical Chemistry*, **69**, 2022–2029.

50 Abraham, M.H., Chadha, H.S., Leitao, R.A.E., Mitchell, R.C., Lambert, W.J., Kaliszan, R. and Masal, H.P. (1997) Determination of solute lipophilicity, as log $P_{octanol}$ and log P_{alkane} using polystyrene divinylbenzene and immobilised artificial membrane stationary phases in reversed-phase high-performance liquid chromatography. *Journal of Chromatography A*, **766**, 35–47.

51 Sekine, T., Watanabe, T., Hosoyamada, M., Kanai, Y. and Endon, H. (1997) Expression cloning and characterization of a novel multispecific organic anion transporter. *The Journal of Biological Chemistry*, **272**, 18526–18529.

52 Ueda, K., Cornwell, M.M., Gottesman, M.M., Pastan, I., Roninson, I.B., Ling, V. and Riordan, J.R. (1986) The MDR1 gene, responsible for multi-drug resistance, codes for P-glycoprotein. *Biochemical and Biophysical Research Communications*, **141**, 956–962.

53 Krishaa, G., Chen, K., Lin, C. and Nomeir, A.A. (2001) Permeability of lipophilic compounds in drug discovery using *in vitro* human absorption model, Caco-2. *International Journal of Pharmaceutics*, **222**, 77–89.

54 Faassen, F., Vogel, G., Sapnings, H. and Vromans, H. (2003) Caco-2 permeability, P-glycoprotein transport ratios and brain penetration of heterocyclic drugs. *International Journal of Pharmaceutics*, **263**, 113–122.

55 Fisher, H., Gottschlich, R. and Seelig, A. (1998) Blood–brain barrier permeation: molecular parameters governing passive diffusion. *The Journal of Membrane Biology*, **165**, 201–211.

56 Kansy, M., Senner, F. and Gubernator, K. (1998) Physicochemical high-throughput screening: parallel artificial membrane permeation assay in the description of passive absorption processes. *Journal of Medicinal Chemistry*, **41**, 1007–1010.

57 Box, K., Comer, J. and Hague, F. (2006) *Pharmaceutical Profiling in Drug Research* (eds B. Testa and S. Krämer), Wiley-VCH Verlag GmbH, Weinheim, pp. 243–257.

58 Faller, B., Grimm, H.P., Loeuilet-Ritzler, F., Arnold, S. and Briand, X. (2005) High-throughput lipophilicity measurement with immobilized artificial membranes. *Journal of Medicinal Chemistry*, **48**, 2571–2576.

59 Chen, Z. and Weber, S.G. (2007) High-throughput method for lipophilicty measurement. *Analytical Chemistry*, **79**, 1043–1049.

60 Bellman, K., Decker, C.J., Jiang, Li., Li, Y., Liu, Z., Sanders, V., Shokri, A., Steel, M. and Worley, J. (2007) AAPS, November.

61 Lundahl, P. and Beigi, F. (1997) Immobilized liposome chromatography of drugs for model analysis of drug–membrane interactions. *Advanced Drug Delivery Reviews*, **23**, 221–227.

62 Yang, C.Y., Cai, S.J., Liu, H. and Pidgeon, C. (1997) Immobilized artificial membranes: screens for drug–membrane interactions. *Advanced Drug Delivery Reviews*, **23**, 229–256.

63 Stenberg, P., Luthman, P. and Artursson, P. (2000) Virtual screening of intestinal drug permeability. *Journal of Controlled Release*, **65**, 231–243.

64 Palm, K., Luthman, K., Ungell, A-L., Strandlund, G., Beigi, F., Lundahl, P. and Artursson, P. (1998) Evaluation of dynamic polar molecular surface area as predictor of drug absorption: comparison with other computational and experimental predictors. *Journal of Medicinal Chemistry*, **41**, 5382–5392.

65 Zhue, C., Jiang, L., Chen, T.-M. and Hwang, K.-K. (2002) A comparative study of artificial membrane permeability assay for high-throughput profiling of drug absorption potential. *European Journal of Medicinal Chemistry*, **37**, 399–407.

66 http://www.bdbiosciences.com/nvCategory.jsp?modeCategory=FULL.

67 Sugano, K., Hamada, H., Machida, M. and Ushio, H. (2001) High-throughput prediction of oral absorption: improvement of the composition of the lipid solution used in parallel artificial membrane permeation assay. *Journal of Biomolecular Screening*, **6**, 189–196.

68 Sugano, K., Hamada, H., Machida, M., Ushio, H., Saitoh, K. and Terrada, K. (2001) Optimized conditions of bio-mimetic artificial membrane permeability assay. *International Journal of Pharmaceutics*, **228**, 181–188.

69 Di, L., Kerns, E., Fan, K., McConnel, O.J. and Carter, G.I. (2003) High-throughput artificial membrane permeability assay for blood–brain barrier. *European Journal of Medicinal Chemistry*, **38**, 223–232.

70 Youdim, K.A., Avdeef, A. and Abbott, N.J. (2003) *In vitro* trans-monolayer permeability calculations: often forgotten assumptions. *Drug Discovery Today*, **8** (21), 997–1003.

71 Avdeef, A. (2003) *Absorption and Drug Development: Solubility, Permeability and Charged State*, John Wiley & Sons, Ltd, Chichester, pp. 139–145.

72 Lennernäs, H. (1998) Human intestinal permeability. *Journal of Pharmaceutical Sciences*, **87**, 403–410.

73 Suomalainen, P., Johnas, C., Söderlund, T. and Kinnunen, P.K.J. (2004) Surface activity profiling of drugs applied to the prediction of blood–brain barrier permeability. *Journal of Medicinal Chemistry*, **47** (7), 1783–1788.

74 Onishi, Y., Hirano, H., Nikata, K., Oosumi, K., Nagakura, M., Tarui, S. and Ishikawa, T. (2003) *Chem-Bio Interface Journal*, **3** (4), 175–193.

75 Seelig, A., Gottschlich, R. and Devant, P.M. (1994) A method to determine the ability of drugs to diffuse through the blood–brain barrier. *Proceedings of*

the National Academy of Sciences of the United States of America, **91**, 6–72.

76 Fisher, H., Seelig, A., Chou, R.C. and van de Waterbeemd, H. (1997) The difference between the diffusion through the blood–brain barrier and the gastro-intestinal membrane. 4th International Conference on Drug Absorption, Edinburgh.

77 Freeman, E. PhysChem measurements: more than just a number, http://www.physchem.org.uk/symp03/symp03_ef.pdf.

7
An Overview of Caco-2 and Alternatives for Prediction of Intestinal Drug Transport and Absorption

Anna-Lena Ungell and Per Artursson

Abbreviations

2/4/A1	Conditionally immortalized cell line derived from fetal rat intestine
ABC	ATP-binding cassette
ATCC	American-type culture collection
BCRP	Breast cancer-resistance protein (ABCG2)
BSA	Bovine serum albumin
Caco-2	Adenocarcinoma cell line derived from human colon
cDNA	Complementary DNA
CYP	Cytochrome P450
DMSO	Dimethyl sulfoxide
ECACC	European Collection of Cell Cultures
ER	Efflux ratio (transport basolateral-to-apical divided by transport a pical-to-basolateral)
hCE-1	Human carboxyesterase-1
hCE-2	Human carboxyesterase-2
HT-29	Pluripotent adenocarcinoma cell line derived from human colon
IEC-18	Rat intestinal epithelial cell line
LLC-PK1	Pig kidney epithelia cell line
MDCK	Madin–Darby canine kidney epithelial cell line
MDR1	Multidrug resistance protein 1 (ABCB1)
MRP	Multidrug resistance-associated protein family 1–6 (ABCC1–6)
MTX	Methotrexate
OATP1B1	Organic anion-transporting polypeptide (SLC21A6; OATP2)
PEPT1	Oligopeptide transporter (solute carrier family 15, member 1 (SLC15A1))
T84	Colon carcinoma cell line derived from human colon

Symbols

Clog P	Predicted octanol/water partitioning coefficient
F_a	Fraction of the oral dose absorbed
P_{app}	Apparent permeability coefficient

7.1 Introduction

One of the limiting factors for the successful therapeutic application of new oral drugs is their transport across one or several membrane(s) into the system, for example, over the intestinal membrane into the systemic circulation, into the cell interior to the target receptor, or into the central nervous system (CNS). The drug transport across a biological membrane can be influenced by a number of factors such as solubility, membrane partitioning, metabolism, and active transport processes [1–3]. To obtain high-quality and useful predictions of the transport processes, highly standardized *in vitro* models, suitable for screening of a large number and variety of drug molecules, are used.

Complementary to experimentally based *in vitro* screening assays are *in silico* predictions of intestinal drug permeability and absorption from molecular structures. These methodologies, which are treated elsewhere in this book, are very time efficient and have a large capacity for virtual screening of entire chemical libraries in early drug discovery. However, they are based on simplistic approximations regarding, for example, membrane partitioning and active transport mechanisms and therefore do not describe the biological complexity of the model in sufficient detail as compared to cell-based *in vitro* models, such as Caco-2 monolayers and alternative cell models, for prediction of intestinal permeability and drug absorption.

7.2 Cell Cultures for Assessment of Intestinal Permeability

Cell culture-based models are the most commonly used methods for studying the mechanisms of passive and active drug transport, and interactions with epithelial proteins, such as transporters and enzymes. These are both simple and quick to use, and still reflect most of the different mechanisms involved in the absorption process. Almost 20 years ago, Caco-2 cells grown on permeable supports were introduced as an experimental tool for mechanistic studies of the intestinal drug transport [4, 5]. At the same time, it was suggested that the Caco-2 model was suitable for screening the intestinal drug permeability and predicting the oral absorption potential of new drug substances [5]. Several factors spurred the development of Caco-2 and similar cell models. These included (1) the awareness that inferior pharmacokinetic properties, including insufficient drug absorption, remained the major reason for the failure of new drug candidates in the clinical

phase [6]; (2) the insight that drug absorption across biological barriers is a fairly complex process involving several pathways and that it can therefore not easily be delineated in experimental animals [7]; and (3) the introduction of combinatorial chemistry in drug discovery [8] .

As with all new techniques that are rapidly embraced by the scientific community, the initial enthusiasm and in some cases uncritical use of Caco-2 cells unraveled the limitations of this *in vitro* [7] and other similar models, for example [9]. A period of critical evaluation followed and today the majority of researchers using these models are aware not only of their advantages but also of their limitations. MDCK (Madin–Darby canine kidney) cells are another well-used cell line, which has been compared with the Caco-2 for the use as intestinal permeability [10]. For the screening of a large number of compounds, these two cell cultures provide extremely useful tools for both preclinical screening and for mechanistic purposes and have routinly been used in the drug industry even for cassette dosing and for analyzing large combinatorial libraries [11, 12].

7.2.1 Caco-2

The main reasons for the popularity of the Caco-2 cell line are that the cells are easy to maintain in culture, and that they develop unusually high degree of differentiation spontaneously under standard culture conditions. The cells exhibit a good reproducibility, robustness, and functional properties of human intestinal epithelial cells. The model has proved capable of predicting the oral absorption of a variety of drug compounds (see Ref. [13]). The Caco-2 cell line originates from a human colon adenocarcinoma [14] and can be obtained from American-type culture collection (ATCC) or the European Collection of Cell Cultures (ECACC). It is a polyclonal cell line, that is, it consists of a heterogeneous population of cells [15], which means that the properties of the cells may change with time in culture. The cells should therefore be used within a limited number of passages, especially for screening purposes over a long period of time. The heterogeneous properties of the cells may be one explanation for the differences in morphology, paracellular permeability, and expression of enzymes and transporters that have been reported from different research groups [16–22]. The cell culture protocol therefore must be standardized and validated by time during screening, and each laboratory has to provide its own standardization [23–25]. Many clones of Caco-2 cells with partly different properties have been derived, but it is beyond the scope of this chapter to cover the vast literature on the physiology of Caco-2 cells.

Caco-2 cells form tight junctions and express many of the brush border enzymes (hydrolases) that are found in the normal small intestine, for example, alkaline phosphatase, sucrase, and amino peptidases [26–29]. Cytochrome P450 (CYP450) isoenzymes and some phase II enzymes (e.g., glutathione-*S*-transferases, sulfotransferase, and glucuronidase) have been identified [29–33] in these cells; however, the level of CYP expression (e.g., CYP3A4) is low in the original cells under standard cell culture conditions [34].

A large number of transport proteins have been identified in Caco-2 cells. Among the efflux transporters, the MDR-1 gene product P-glycoprotein (P-gp) is the most extensively investigated [35–37]. Several different efflux transporters have been identified in the Caco-2 cell line at mRNA level [23, 24, 38–40], and some of these have been verified also at protein and functional levels [41]. Taipalensuu *et al*. showed that the normal Caco-2 cells do not overexpress the efflux transporter P-gp in comparison with human jejunal biopsies [38]. A genetically related protein, BCRP, has also been discussed recently, but this protein seems to be expressed less in cell lines such as Caco-2 than in the human jejunum [38, 39]. The multidrug resistance-related (associated) protein family, MRPs, has also been identified in Caco-2 cells [38–40, 42]. Of the 8 to 10 different MRPs that have been proposed to exist, 6 have been identified in Caco-2 cells, referred to as MRP1–6 [38, 39, 42]. In addition, transport systems for glucose [43, 44], amino acids [45–48], dipeptides [49–51], vitamins [52], and bile acids [53, 54], which are normally found in the small intestinal enterocytes, have been characterized in the Caco-2 model. The expression of the active transport systems is time dependent and may vary with nutritional conditions [55, 56]. Therefore, culture conditions can dramatically alter the biological characteristics and transport properties of Caco-2 cell monolayers [57–60]. As the Caco-2 cell model expresses many important intestinal transporters, it can be used to study not only the passive transport mechanisms but also the mechanisms involving active drug transport. Owing to the complexity of this model of drug transport, there has been reports delineating both pros and cons for the use of it [7, 61–63].

7.2.2 MDCK Cells

The MDCK cell line is also frequently used by pharmaceutical companies to monitor intestinal drug transport, despite the fact that the cell line originates from the dog kidney [10, 64, 65]. An advantage with this cell line as compared to Caco-2 cells is that it differentiates more rapidly. There are two distinct subclones of MDCK cells: MDCK Strain I that forms very tight monolayers and MDCK Strain II that forms monolayers with more leaky tight junctions. Irvine and coworkers reported that the correlation to oral fraction absorbed (F_a) based on 55 different compounds was comparable in the Caco-2 and MDCK model systems [10], although it should be pointed out that due to species differences, the endogenous expression of canine transporters in the renal MDCK monolayers is likely to be very different from that of the human intestinal transporters in Caco-2 cells. Thus, while MDCK monolayers may be useful for estimations of passive epithelial transport, but they may not be applicable to mechanistic studies of human drug transport or for predicting active uptake or efflux across the human intestinal epithelium. In the normal MDCK cell line, a low level of P-gp has been identified [65], while uptake transporters such as renal organic cation transporters have been explored in mechanistic studies [66].

In general, the inherent expression of canine transport proteins in MDCK cells is low. This fact together with the seemingly correct sorting of transport proteins to the right location in the plasma membrane has made these cells a popular choice for the

stable expression of transport proteins of human origin. Furthermore, MDCK cells overexpressing transport proteins maintain cell–cell contact via tight junctions, a feature sometimes lost upon the manipulation of differentiated epithelial cell lines. MDCK cells overexpressing human P-gp (MDR1) have been a useful tool for investigating the contribution of P-gp to transepithelial transport [67–69]. However, it appears that the MDR1-MDCK cells, like many other stably transfected cell lines, tend to form multilayers and in addition, are not as well polarized as MDCK cells [67, 70]. An alternative cell line for assessing P-gp involvement is MDR1-transfected LLC-PK1 (pig kidney) cells [71].

In recent years, it has been recognized that the interplay between uptake and efflux transporters may determine the cellular pharmacokinetics of drugs. Thus, a more hydrophilic drug may require an active uptake mechanism to cross the cell membrane and enter the cell. Only from within the cell will such a molecule become accessible to the binding site(s) of an efflux transporter, such as MRP2. Recently, it was shown that cells overexpressing another efflux protein, ABCG2/BCRP, correctly identified binding to the transport proteins for drugs with a lipophilicity that allowed significant partitioning into the cell membrane (Clog $P > 0.5$) [72]. Since the cell line in question did not express uptake transporters, this result indicates that a log partitioning coefficient above 0.5 was needed for passive membrane permeation and access to the ABC-transporter. Thus, both appropriate uptake and efflux transporters need to be inserted into a cell line to reveal the transport mechanism of more hydrophilic efflux substrates [73]. This was elegantly demonstrated for the rather hydrophilic cholesterol-lowering agent pravastatin (log $P < 0.5$), using MDCK cells overexpressing the pravastatin uptake transporter OATP1B1 and the pravastatin efflux transporter MRP2 [74]. Only in double-transfected cells, an efflux of pravastatin via MRP2 could be observed. Numerous research groups working to better model the interplay between different transport proteins have now constructed a large variety of double-transfected cell lines. Extensions of this technique have resulted in MDCK cells overexpressing as many as four transport proteins [75]. It should be noted that the relative expression levels of multiple transgenes may be difficult to control, which may obscure the goal of obtaining more *in vivo*-like cell cultures. Furthermore, it is often difficult to generate double-transfected cell lines that retain the required differentiated properties including an intact paracellular barrier. Caco-2 cells may therefore remain a viable future alternative in some of these situations, provided sufficiently specific substrates or inhibitors can be identified.

7.2.3 2/4/A1 Cells

As for active drug transport, there is no quantitative relationship between passive drug permeability in Caco-2 cells *in vitro* and drug transport in the human small intestine *in vivo* [76, 77]. Apart from high-permeability drugs that partition into the cell membranes at comparable, rapid speeds *in vitro* and *in vivo*, compounds with intermediate or low permeability have a lower permeability in the Caco-2 model than

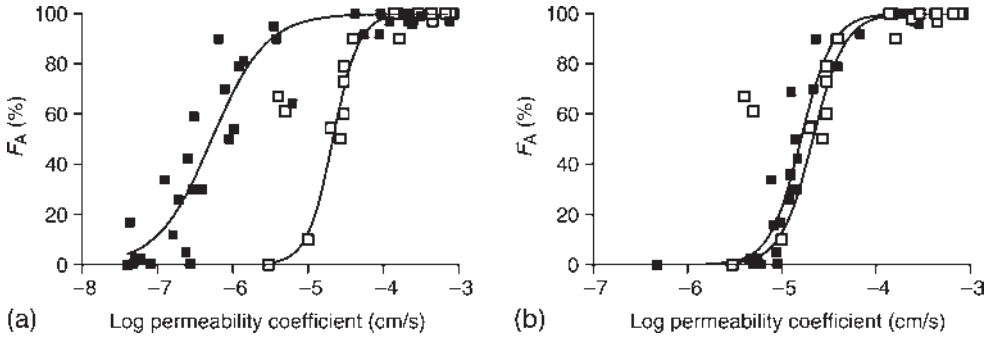

Figure 7.1 Comparison between the permeability coefficients obtained after *in vivo* perfusion of the human jejunum (open symbols) (data compiled from publications by Lennernäs's laboratory [162, 163]) and Caco-2 cells (filled symbols) (data compiled from publications by Artursson's laboratory [84, 164]) (a) and 2/4/A1 cells [84] (b). There is a quantitative overlap in permeability between completely absorbed drugs in Caco-2 cells and in the human jejunum, while the permeabilities for the incompletely absorbed drugs are approximately two orders of magnitude lower in Caco-2 cells than those in the human jejunum. In contrast, the relationship in 2/4/A1 is almost completely overlapping compared to that in the human jejunum for both completely and incompletely absorbed drugs.

in vivo. As shown in Figure 7.1a, this difference increases with a decrease in compound permeability. There are two major reasons for this difference.

First, the paracellular route is tighter in Caco-2 cells than that in the small intestine *in vivo*. Although the average pore radius of the tight junctions in the human small intestine is around 8–13 Å [78], the corresponding radius in Caco-2 cells is lower. As low-permeability drugs are generally more polar than high-permeability drugs, they tend to distribute more slowly into the cell membranes. However, at least a fraction of the drugs are transported through the water pores of the tight junctions, via the paracellular pathway. If this pathway is narrower, as in Caco-2 cells, the permeability will become lower than that *in vivo*. We recently proposed a solution to this problem by exploiting a more leaky cell culture model established from the rat fetal intestine, 2/4/A1 [77, 79]. This cell line, which has paracellular permeability comparable to that of the human small intestinal epithelium *in vivo*, gives a better quantitative relationship with human permeability data generated in the Loc-I-Gut perfusion technique [77] (Figure 7.1b). It is impossible to speculate upon the relative contribution of the paracellular pathway and the possible increased absorptive surface area to the passive transport of low- permeability drugs [80]. Here, we can only conclude that it is possible to mimic human small intestinal permeability to drugs by using a more leaky cell culture model (such as 2/4/A1) than the Caco-2 model. As an alternative, correction factors for the low paracellular permeability in Caco-2 cells and other membrane models have been introduced [81, 82]. Interestingly, the 2/4/A1 cell line seems not to express functional (drug) transporting proteins [83], which makes it an interesting alternative in studies of passive permeability. Indeed, recent data from our laboratory suggest that 2/4/A1 cells better predict the human absorption of intermediate- to low-permeability drugs than do Caco-2 cells [84]. Another advantage of the 2/4/A1 cell line is that a relatively large amount of low-permeability drugs is

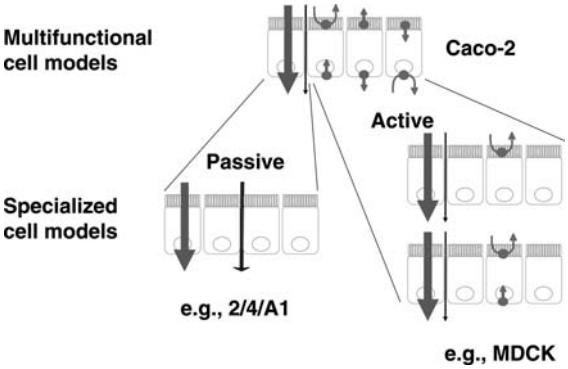

Figure 7.2 Studies of specific drug transport routes in multifunctional cell models such as Caco-2 cells may be complicated, as there is a lack of specific substrates for many drug transporters. Therefore, specialized cell models that accommodate mainly passive (2/4/A1) or selected active (MDCK-MDR1) transport pathways are preferred in some cases.

transported, thus eliminating the need for expensive analysis equipment such as an LC/MS/MS system. However, it must be pointed out that 2/4/A1 cells have poorly differentiated morphology and lack many of the enzyme systems and transporters that are present in Caco-2 cells and in the normal human small intestinal epithelium [83]. Thus, 2/4/A1 cells seem best applicable to investigating passive transport properties of drugs without the consideration of active transport mechanisms. Moreover, the culture conditions are very specific and more demanding than the relatively straightforward procedures used for Caco-2 and MDCK cells, and their use in the pharmaceutical industry has hitherto been limited. A simple serum-free culture procedure for 2/4/A1 cells has recently been developed, but it remains to be seen if this technique will make 2/4/A1 cells a more attractive alternative in drug discovery settings [85, 98] (Figure 7.2).

7.2.4 Other Cell Lines

HT29 is another well-studied human colon carcinoma cell line [15, 28]. When grown under standard culture conditions, the cells form multilayers of undifferentiated cells. However, under modified culture conditions, HT29 cells differentiate into polarized monolayers of absorptive and/or, interestingly, mucus-secreting goblet cells, depending on the chosen conditions. Several permanently differentiated clonal cell lines have been established from HT29 cells. The mucus-layer-producing variants have attracted some interest for two reasons: the mucus layer covering the intestinal epithelium *in vivo* may limit the absorption of some drugs and Caco-2 and MDCK cells lack this barrier. Mucus-producing clones such as HT29-H and HT29-MTX (methotrexate-induced cells) have been used for the development of mucus-layer-containing cell culture models [86–89]. Cocultures of Caco-2 cells and HT29-H

and HT29-MTX have also been investigated, but these have not yet found wide application in drug discovery [88, 90].

Another human colonic cancer cell line is T84, which forms monolayers that are even tighter than those of the Caco-2. It has been described as resembling a colonic crypt cell phenotype. Hence, these cells have been used mainly in studies of epithelial ion secretion and are generally not considered to be adequate for drug transport studies, particularly with respect to carrier-mediated processes [13, 91, 92]. The rat intestinal epithelial cell line IEC-18 has been evaluated as a model to study small intestinal epithelial permeability. This cell line, which forms very leaky monolayers, was proposed to be a better model than the Caco-2 monolayers for evaluating the small intestinal paracellular permeation of hydrophilic molecules [93]. Importantly, the leaky tight junctions of the IEC-18 cells are a result of an undeveloped paracellular barrier lacking the perijunctional actin belt. In addition, the IEC-18 cells have minute expression of transporters [91, 93].

7.3 Correlation to Fraction of Oral Dose Absorbed

Many academic and industrial laboratories have shown that the drug permeability measured in Caco-2 cell monolayers can be used to predict the oral absorption of drugs in humans. Various data sets have therefore been used to establish correlations between Caco-2 permeability and the fraction absorbed orally in humans [5, 18]. Taken together, these studies show good predictability, though with a relatively wide variation in the appearance of correlation profiles between different laboratories [18]. Initially, the good relationship between the passive drug transport across Caco-2 cells and the absorbed fraction after oral administration to humans [5] may be surprising, given that oral drug absorption is influenced by many factors besides drug permeability, such as drug solubility, dissolution, active transport, and, in some cases, presystemic metabolism. The first study with Caco-2 cells was performed under highly controlled conditions on registered drugs that did not have solubility problems and that were largely passively transported. In addition, their metabolism could be accounted for [5]. Similar good results are obtained when the same parameters are strictly controlled in expanded data sets.

However, many drug discovery scientists initially were disappointed when the experimental in-house compounds gave relationships with a much larger scatter than that reported in the original publication [7]. There are several contributing factors to this difference. Discovery compounds have generally been neither characterized nor optimized with regard to chemical stability, metabolism, solubility, or dissolution rate. Another difference is that Caco-2 predictions of oral drug absorption using small data sets for standardization are generally carried out manually by multiple samples at different time points, and full attention is also given to, for example, mass balance issues and the contribution from active transport. Nevertheless, there are several reports describing the usefulness of Caco-2 permeability data also obtained in automated systems, in predictions of oral absorption, for example [94–96], and,

when combined with metabolic stability data, also bioavailability [97]. In the screening setting, binning of permeability values in up to three categories, predicting high, intermediate, and low absorption after oral administration is commonly used. When an analogous series of compounds is tested, permeability ranking is an alternative. Recently, ranking of incompletely absorbed drugs ($F_a < 30\%$) was used to compare the performance of Caco-2 that expresses functional transporters and 2/4/A1 cells that lack functional transport proteins. Both passively and actively transported compounds were included in the study. Both cell lines generated good results,with a slight advantage for 2/4/A1 cells, suggesting that the passive permeability route dominates also in the case of many compounds that are at least partly transported via active transport mechanisms across the intestinal epithelium [98]. Recently, an independent study came to the same conclusion regarding the 2/4/A1 cells [62].

In the drug industry, Caco-2 cells have often been used to rank compounds in analogous compound series and libraries or to estimate F_a in humans early in the screening process. When such data sets are used, Caco-2 cell permeability measurements provide the opportunity to establish structure–permeability relationships for quite different analogous series of drugs. Several examples of the latter case have been published. For example, these include a series of conventional drugs [99–102], peptides, and peptide mimetics [103–107] as well as compounds generated in high-throughput drug discovery [108, 109]. Although most of these structure–permeability relationships have been established for passive membrane permeability, there are also examples of structure–permeability relationships for a series of drugs that are absorbed via an active transport mechanism [110–115].

7.4 Cell Culture and Transport Experiments

Drug absorption experiments are easy to perform in cell culture models, such as Caco-2. Comprehensive step-by-step protocols for the determination of drug permeability and prediction of drug absorption in Caco-2 monolayers has recently been published [25, 116]. The outlined principles are applicable also to the other cell culture models reviewed above. Briefly, the drug is added to the apical (mucosal) side and the appearance of the drug on the basolateral side (serosal) is followed by time. The model also permits experiments to be carried out in the reverse direction, that is, from the basolateral side to the apical side. The monolayers should be agitated during the experiments, not only to produce more reproducible results but also to reduce the effects of aqueous boundary layers adjacent to the epithelial membrane [117]. Without correct stirring conditions being maintained during the experiments, the measured permeability values for rapidly transported compounds will be significantly underestimated. The experiments should preferably be performed under "sink" conditions (e.g., the drug concentration on the receiver side should be less than 10% of the concentration on the donor side during an experiment) to avoid bias by backdiffusion of significant amount of compound from the receiver chamber and

to maintain a "constant" applied drug concentration gradient during the course of the experiment. The following Equation 7.1 is generally used for the calculation of the apparent permeability coefficient (P_{app}):

$$P_{app} = \frac{(dQ/dt)}{(A \times C_{d0})}, \tag{7.1}$$

where dQ/dt is the rate of appearance of drug on the receiver side, C_{d0} is the initial drug concentration on the donor side, and A is the surface area of the filter membrane.

This equation for calculation of P_{app} is easily improved by taking into account the change of donor concentration (C_d) during the experiment, which affects the concentration gradient and the driving force for passive diffusion (Equation 7.2):

$$P_{app} = \frac{k \times V_r}{A}, \tag{7.2}$$

where k is the change in drug concentration in the receiver chamber (C_{r-ti}/C_{d-ti}) per unit time, C_{r-ti} is the concentration on the receiver side at the end of each time interval, C_{d-ti} is the average of the donor concentration determined at the beginning and at the end of each time interval, V_r is the volume of the receiver chamber, and A is the surface area of the filter membrane. By using this method of calculation, a more accurate determination of the P_{app} value is obtained, particularly for rapidly transported drugs where P_{app} values exceed 10×10^{-6} cm/s.

A general equation that does not require sink conditions can also be applied [118, 119] (Equation 7.3). In this "nonsink" analysis, P_{app} is determined by nonlinear curve fitting of

$$C_R(t) = \left[\frac{M}{(V_D + V_R)}\right] + \left\{C_{R,0} - \left[\frac{M}{(V_D + V_R)}\right]\right\} e^{-P_{app}A(1/V_D + 1/V_R)t}, \tag{7.3}$$

where V_D is the volume of the donor compartment, V_R is the volume of the receiver compartment, A is the area of the filter, M is the total amount of substance in the system, $C_{R,0}$ is the concentration of the substance in the receiver compartment at the start of the time interval, and $C_R(t)$ is the concentration of the substance at time t measured from the start of the time interval.

The trend in the industry has been to automate the Caco-2 permeability assay using semi- or fully automated procedures. With such systems throughputs on the order of hundreds of compounds per week are possible. Of particular importance, for good estimation of the permeability coefficient, the compound must be completely dissolved during the transport experiment. Therefore, discovery compounds are often diluted in physiological buffers from stock solutions in DMSO. Twenty-four-well plates with monolayers are usually used for higher analytical precision and compound yield, but 96-well plates for higher throughput are also frequently used. A mixture of several reference compounds is often included on each plate to capture variability between assays by time/passage.

The recovery should be sufficient to assure that reliable P_{app} values are obtained and reported (Equation 7.4). Common limits for recovery are 80–120%. Sometimes,

when lipophilic compounds with assumed high permeability are investigated, a lower recovery may be acceptable. The recovery is calculated according to

$$\text{Recovery}\,[\%] = \frac{\left[C_{\text{D(fin)}} \times V_{\text{D}} + \Sigma(C_{S(t)} \times V_{S(t)}) + C_{\text{R(fin)}} \times V_{\text{R(fin)}}\right] \times 100}{C_{\text{D(0)}} \times V_{\text{D(0)}}}, \tag{7.4}$$

where C_{D} and C_{R} are the concentrations on the donor (D) and receiver (R) sides of the monolayer at the start (0) or end (fin) of the experiment, $C_{S(t)}$ denotes the concentrations of the samples withdrawn at different time points t, and V is used for each of the respective volumes.

7.4.1 Quality Control and Standardization

The variable performance of Caco-2 cells can be minimized by education and training in good cell culture practice [25, 116, 120]. Here, we only note that a major reason for the different results obtained with Caco-2 cells is related to the interval of passage number and ages (time grown on filter) at which the cells are studied. It is therefore important to define a limited number of passages and days that can be used for the experiments. Caco-2 cells obtained from ATCC or from ECACC are normally at passages 20–40. Our experience is that within a predefined and controlled interval of passages, the cells perform very consistently, provided identical cell culture conditions are used. We conclude that in contrast to what is generally believed it is possible to maintain the permeability characteristics of Caco-2 cells over long time periods, at least in the same laboratory.

Another technical limitation of Caco-2 cells is the long culture time required to obtain full differentiation of the cells. It takes 3 weeks to obtain fully differentiated cell monolayers of Caco-2 cells on filter inserts [1, 116, 121]. It has recently been suggested that 2 weeks of culture on filters is sufficient for obtaining a full expression of transporters and integrity [23], but these claims require solid experimental confirmation.

In some screening laboratories, even 2 weeks are considered too long and too demanding to be practical, and culture protocols have been developed to speed up the differentiation process, usually to less than 1 week [122–124]. Today, at least one 3-day system, based on proprietary media supplements and collagen-coated filter inserts, is available (http://www.bdbiosciences.com). Although limited, the published information about the performance of Caco-2 monolayers cultivated under these accelerated protocols suggests that the cells are not fully differentiated and therefore have to be used at a certain time point, for example, on day 3, to obtain reproducible results, as the degree of differentiation may vary from one day to another. Clearly, data from different publications or laboratories should not be mixed without prior harmonization of the experimental protocols. This is underscored by a recent comparative study in which the mRNA expression and function of a number of transport proteins were compared in Caco-2 cells cultivated according to different standard procedures used

in 10 laboratories in the drug industry and universities [125] – although the results were in qualitative agreement, large variations in expression and function were observed between the different laboratories.

7.4.2 Optimizing Experimental Conditions: pH

The pH in the lumen of the GI tract *in vivo* in humans is variable; typically, it is pH 1–2 in the stomach, 5–6.5 in the duodenum and proximal jejunum, 6.5–7.5 in the mid-jejunum, and almost up to 8 in the terminal ileum [126]. In the large bowel, the pH varies between 6.5 and 8 from the colon ascendens to the sigmoideum. This bulk pH will affect the solubility and the degree of ionization of the drug and hence regional differences in the concentration of uncharged drug species, which provides a driving force for the drug absorption. The transport across the rate-limiting barrier of the intestinal epithelial cell membrane is, however, affected by another pH, the so-called microclimate or surface pH, which is up to one pH unit lower in parts of the small intestine compared to the bulk pH adjacent to the epithelial cell surface [127]. In the cell culture models, the pH of the apical solution therefore has a direct impact on the transport experiments, as the solution is in direct contact with the membrane [128]. When only transport in the absorptive direction is considered, the cell-based screening model should reflect the gradient under physiological conditions and reflect the absorption across the jejunum (the main part of absorption of most drugs); thus, a pH of 6.5 should be applied to the apical side while the pH at the basolateral side should be kept at 7.4.

The passive permeability of an ionizable compound will obey the pH partition hypothesis. For weak acids, for example, salicylic acid, the dependence on a pH gradient is complex as both the passive diffusion and the active transport process (which in the case of organic anions may be driven by a proton gradient) will depend on the proton concentration in the apical solution [129]. Similarly, for weak bases such as alfentanil, metoprolol, propranolol, or cimetidine, an apical pH of 6.5 will decrease the passive transport toward the basolateral side [130]. Applying this pH gradient during bidirectional transport studies for weak bases will create an efflux ratio, that is due to unequal concentrations of the uncharged drug species on the apical (pH 6.5) and basolateral (pH 7.4) sides, rather than an active efflux mechanism [129, 131]. In conclusion, in early permeability screening where a pH gradient is often used, it can be difficult to distinguish a passive asymmetric uptake or efflux caused by the pH effect on ionization from a true transporter-mediated uptake or efflux. Thus, caution should be exercised in interpreting efflux data obtained from permeability screening using the recommended pH gradient systems.

7.4.3 Optimizing Experimental Conditions: Concentration Dependence

Optimizing the permeability measurements to avoid adsorption to plastic, filters, or accumulation within the cell monolayer seems highly relevant for increasing the

predictivity of the screening model in the early screening of highly lipophilic drugs [132]. In general, DMSO solutions are the most commonly used vehicle in the early stages. As the available amount of the compounds is small at this stage, only low concentrations of the drug can be used and the influence of carrier-mediated transport (uptake or efflux) may be overemphasized compared to the *in vivo* situation. This could, for instance, result in a falsely low permeability to compounds that are substrates for efflux transporters at the intestinal membrane as after oral drug administration, these transporters could become saturated at the higher (therapeutic) concentrations obtained in the gut after dissolution of the dosage form.

7.4.4
Optimizing Experimental Conditions: Solubility and BSA

The adsorption of compounds to plastic surfaces and accumulation of compounds within the cell membrane are related to the lipophilicity of the compound. Highly lipophilic drugs most likely have high intrinsic permeabilities, but it may be difficult to make a correct determination due to low recoveries in the *in vitro* system. Many authors have suggested using BSA to improve sink conditions and to reduce the adsorption phenomenon [128, 133, 134]. The effect of the presence of BSA will be determined by both the protein-binding capacity of the drug to be tested and its intrinsic permeability, that is, a high protein-binding and a high-permeability value will increase the impact of BSA in the basolateral chamber. Recently, a new promising methodology was presented that may account for the effect of protein binding on the drug permeability through an indirect procedure [135]. Using this approach, good corrections for the changes in unbound drug concentration were obtained for a small set of drugs, and further studies are needed to show on the general applicability of the methodology. There are several positive factors that favor the use of BSA in the basolateral medium. First, it mimics the *in vivo* situation where the circulating blood provides an excellent base for sink conditions due to a large volume and content of albumin [136]. Second, serum albumin hinders adsorption onto plastic surfaces and filters and thereby reduces the loss of compound in the experimental system, as well as in the different steps of dilution before the analysis of drug content. Third, the accumulation of a lipophilic drug within the cell monolayer is reduced due to maintained sink conditions. Fourth, it seems to be more generally applicable as a solubilizer of lipophilic drugs than detergents such as Cremophor [137].

7.5
Active Transport Studies in Caco-2 Cells

Drug transport studies in Caco-2 cells grown on permeable supports are easy to perform under controlled conditions. This makes it possible to extract information about specific transport processes that would be difficult to obtain in more complex models such as those based on whole tissues from experimental animals. When the mRNA expression of drug transporting proteins in Caco-2 cells was compared with

that in various segments of the human intestine and colon in two independent studies [23, 24], fairly good correlations were obtained. Recently, these studies were expanded to incorporate expression comparisons of transport proteins between human intestinal, liver, and kidney tissues and their respective organotypic cell lines [39]. Again, a good correlation was obtained for Caco-2 cells and the human jejunum while the corresponding comparisons for human liver and kidney gave poor results. Furthermore, comparisons with expression data from rat intestine, increased the scatter significantly, indicating that human cell lines such as Caco-2 are more representative of human than of rat organs with respect to transporter expression [39]. The latter finding is supported by differences in transport parameters for the human ABC transporters MDR1 and MRP2 in human Caco-2 cells and canine MDCK cells [138]. Differences between the Caco-2 and MDCK cell lines have also been reported with regard to the activity of peptide transporters [139].

It can be argued that the abundant expression of transport proteins in Caco-2 cells may obscure the study of a specific transporter, especially if the transporter lacks a specific substrate, as in the case of most efflux transporters of the ABC transporter family [140]. However, the expression of multiple transport systems in Caco-2 may be an advantage in the study of (1) the interplay between several transporters, for example, Refs [141, 142]; (2) the interplay between drug metabolism and drug transport [143–148], and (3) the relative contribution of passive and active transport mechanisms to the overall transport of a drug, for example, Refs [98, 149] . Recently, a large number of new inhibitors and substrates for specific transporters were identified among registered drugs, using efficient screening methods, for example, Refs [72, 150, 151]; but, additional studies are needed to investigate their specificities with regard to the broad collection of drug-transporting proteins.

7.6
Metabolism Studies using Caco-2 Cells

Cell culture models can be used to evaluate the importance of metabolism in gut membranes, both with respect to oxidative metabolism via the cytochrome P450 system and phase-II reactions [30–34, 143, 152]. In general, CYP3A4 activity in the parent clone of Caco-2 is very low or absent. Therefore, if a compound is metabolized by CYP450 3A4 in the intestinal membrane, permeability for that compound across Caco-2 cell monolayers will overpredict the absorbed fraction. Since CYP3A4 is the dominating drug-metabolizing enzyme of the human small intestine, a variety of approaches have been described to enhance its functional activity in Caco-2 cells. For example, Caco-2 cells have been transfected with cDNA encoding for CYP3A4 [153, 154]. Another approach is to treat the Caco-2 cells with dihydroxyvitamin D3 that induces an increased activity of the enzyme [155, 156]. Significant induction of CYP3A4 activity and expression has also been reported in CYP3A4-transfected cells by incubation with 12-*O*-tetradecanoylphorbol-13-acetate and sodium butyrate [157].

The inherent enzymatic activity seems low also in other cell lines used for screening, such as MDCK and LLC-PK1 cells [158]. Both MDCK and LLC-PK1 cells have been transfected with CYP3A4 and MDR1 for studying the concert action between drug metabolism and secretion via efflux transporters [158].

Expression levels and activities of enzymes within the gut should be compared with the levels in the different cellular models before starting screening programs. In addition, the presence of the correct enzyme at the brush border membrane or intracellularly in the cellular models is important if the influence of enzymatic degradation on total transport across the intestinal membrane is evaluated. Caco-2 cells are often used for evaluation of prodrug activation as a model for intestinal bioactivation [159, 160]. A report by Imai *et al.*, however, indicates that in the case of Caco-2 cells, the main carboxyl esterase is identified as the hCE-1 and corresponds to the hepatic variant, while in the human intestine the most abundant carboxyl esterase is the hCE-2 [161]. As the specificity of these two enzymes differs, it was suggested that prediction of human intestinal absorption using Caco-2 cells should be performed carefully in the case of ester- and amide-containing drugs such as prodrugs. In addition, if transfected cell lines such as the MDCK-MDR1 are used in studies of prodrug transport, it is important to know if the cells can activate the drug once it has entered the cell. This is especially important if the drug formed is evaluated to be a potential substrate for the MDR1 efflux mechanism. Thus, without prior knowledge of the enzymes involved, studies can be misleading.

There are also successful studies of metabolism during transport using Caco-2 cells. Hubatsch *et al.* have reported a study of metabolism of a tripeptide (anti-HIV) by brush border enzyme dipeptidylpeptidase IV, and the dipeptide thus formed was then transported via PEPT1. These data gave helpful knowledge regarding both prodrug activation and transport of the inactive dipeptide via the PEPT1 [147].

7.7 Conclusions

We conclude that Caco-2 cell cultures remain a versatile and general model to study drug transport mechanisms and screening of drug permeability. Especially important is to have consistency. Ensured high quality during culturing and transport experiments is recommended, as differences can cause major variability among the data acquired. Alternative models that express fewer drug transport pathways may be preferable in situations where specific drug transport mechanisms are to be identified. Therefore, such alternative models to Caco-2 cells are developed in many laboratories for the investigation of, for example, drug transport by specific transport proteins.

Acknowledgment

This work was supported by grants from the Swedish Research Council, the Swedish Governmental Agency for Innovation Systems, and AstraZeneca.

References

1 Ungell, A.-L. (1997) *In vitro* absorption studies and their relevance to absorption from the GI tract. *Drug Development and Industrial Pharmacy*, **23**, 879–892.

2 Ungell, A.-L. and Abrahamsson, B. (2001) Biopharmaceutical support in candidate drug selection, in *Pharmaceutical Preformulation and Formulation. A Practical Guide from Candidate Drug Selection to Commercial Dosage Formulation* (ed. M. Gibson), Interpharm Press.

3 Lipinski, C.A. (2000) Drug-like properties and the causes of poor solubility and poor permeability. *Journal of Pharmacological and Toxicological Methods*, **44**, 235–249.

4 Wilson, G., Hassan, I.F., Dix, C.J., Williamson, I., Shah, R., MacKay, M. and Artursson, P. (1990) Transport and permeability properties of human Caco-2 cells: an *in vitro* model of the intestinal epithelial barrier. *Journal of Controlled Release*, **11**, 25–40.

5 Artursson, P. and Karlsson, J. (1991) Correlation between oral drug absorption in humans and apparent drug permeability coefficients in human intestinal epithelial (Caco-2) cells. *Biochemical and Biophysical Research Communications*, **175**, 880–885.

6 Prentis, R.A., Lis, Y. and Walker, S.R. (1988) Pharmaceutical innovation by the seven UK-owned pharmaceutical companies (1964–1985). *British Journal of Clinical Pharmacology*, **25**, 387–396.

7 Artursson, P. and Borchardt, R.T. (1997) Intestinal drug absorption and metabolism in cell cultures: Caco-2 and beyond. *Pharmaceutical Research*, **14**, 1655–1658.

8 Floyd, C., Leblanc, C. and Whittaker, M. (1999) Combinatorial chemistry as a tool for drug discovery. *Progress in Medicinal Chemistry*, **36**, 91–168.

9 Gumbleton, M. and Audus, K.L. (2001) Progress and limitations in the use of *in vitro* cell cultures to serve as a permeability screen for the blood brain barrier. *Journal of Pharmaceutical Sciences*, **90**, 1681–1698.

10 Irvine, J.D., Takahashi, L., Lockhart, K., Cheong, J., Tolan, J.W., Selick, H.E. and Grove, J.R. (1999) MDCK (Madin–Darby canine kidney) cells: a tool for membrane permeability screening. *Journal of Pharmaceutical Sciences*, **88**, 28–33.

11 Stevenson, C., Augustijns, P. and Hendren, R. (1999) Use of Caco-2 cells and LC/MS/MS to screen a peptide combinatorial library for permeable structures. *International Journal of Pharmaceutics*, **15**, 103–115.

12 Taylor, E.W., Gibbons, J.A. and Braeckman, R.A. (1997) Intestinal absorption screening of mixture from combinatorial libraries in the Caco-2 model. *Pharmaceutical Research*, **14**, 572–577.

13 Hillgren, K.M., Kato, A. and Borchardt, R.T. (1995) *In vitro* systems for studying intestinal drug absorption. *Medicinal Research Reviews*, **15**, 83–109.

14 Fogh, J., Fogh, J.M. and Orfeo, T. (1977) One hundred and twenty-seven cultured human cell lines producing tumors in nude mice. *Journal of the National Cancer Institute*, **59**, 221–225.

15 Artursson, P. (1991) Cell cultures as models for drug absorption across the intestinal mucosa. *Critical Reviews in Therapeutic Drug Carrier Systems*, **8**, 305–330.

16 Artursson, P., Neuhoff, S., Matsson, P. and Tavelin, S. (2007) Passive permeability and active transport models for the prediction of oral absorption, in *ADME/Tox Approaches, Vol. 5* (eds B. Testa and H. van de Waterbeemd), in *Comprehensive Medicinal Chemistry*, 2nd edn (series eds J.B Taylor and D.J. Triggle), Elsevier, Oxford, pp. 259–278.

17 Hidalgo, I.J. and Li, J. (1996) Carrier-mediated transport and efflux mechanisms in Caco-2 cells. *Advanced Drug Delivery Reviews*, **22**, 53–66.

18 Artursson, P., Palm, K. and Luthman, K. (2001) Caco-2 monolayers in experimental and theoretical predictions of drug transport. *Advanced Drug Delivery Reviews*, **46**, 27–43.

19 Hidalgo, I.J., Raub, T.J. and Borchardt, R.T. (1989) Characterization of the human colon carcinoma cell line (Caco-2) as a model for intestinal epithelial permeability. *Gastroenterology*, **96**, 736–749.

20 Walter, E. and Kissel, T. (1995) Heterogeneity in the human intestinal cell line Caco-2 leads to differences in transepithelial transport. *European Journal of Pharmaceutical Sciences*, **3**, 215–230.

21 Delie, F. and Rubas, W.A. (1997) Human colonic cell line sharing similarities with enterocytes as a model to examine oral absorption: advantages and limitations of the Caco-2 model. *Critical Reviews in Therapeutic Drug Carrier Systems*, **14**, 221–286.

22 Hidalgo, I.J. (2001) Assessing the absorption of new pharmaceuticals. *Current Topics in Medicinal Chemistry*, **1**, 385–401.

23 Seithel, A., Karlsson, J., Hilgendorf, C., Björquist, A. and Ungell, A.-L. (2006) Variability in mRNA expression of ABC- and SLC-transporters in human intestinal cells: comparison between human segments and Caco-2 cells. *European Journal of Pharmaceutical Sciences*, **28**, 291–299.

24 Englund, G., Rorsman, F., Rönnblom, A., Karlbom, U., Lazorova, L., Gråsjö, J., Kindmark, A. and Artursson, P. (2006) Regional levels of drug transporters along the human intestinal tract: co-expression of ABC and SLC transporters and comparison with Caco-2 cells. *European Journal of Pharmaceutical Sciences*, **29**, 269–277.

25 Hubatsch, I., Ragnarsson, E. and Artursson, P. (2007) Determination of drug permeability and prediction of drug absorption in Caco-2 monolayers. *Nature Protocols*, **2**, 2111–2119.

26 Pinto, M., Robin-Léon, S., Appay, M.D., Kedinger, M., Triadou, N., Dussaulx, E., Lacroix, B., Simon- Assman, P., Haffen, K., Fogh, J. and Zweibaum, A. (1983) Enterocyte-like differentiation and polarization of the human colon carcinoma cell line Caco-2 in culture. *Biology of the Cell*, **47**, 323–330.

27 Hauri, H.-P., Sterchi, E.E., Bienz, D., Fransen, J.A.M. and Marxer, A. (1985) Expression and intracellular transport of microvillus hydrolases in human intestinal epithelial cells. *Journal of Cell Biology*, **101**, 838–851.

28 Chantret, I., Barbat, A., Dussaulx, E., Brattain, M.G. and Zweibaum, A. (1988) Epithelial polarity, villin expression, and enterocytic differentiation of cultured human colon carcinoma cells: a survey of twenty cell lines. *Cancer Research*, **48**, 1936–1942.

29 Howell, D., Kenny, A.J. and Turner, J. (1992) A survey of membrane peptidases in two human colonic cell lines, Caco-2 and HT29. *Biochemical Journal*, **284**, 595–601.

30 Gervot, L., Carrie're, V., Costet, P., Cugnenc, P.-H., Berger, A., Beaune, P.H. and de Waziers, I. (1996) CYP3A5 is the major cytochrome P450 3A expressed in human colon and colonic cell lines. *Environmental Toxicology and Pharmacology*, **2**, 381–388.

31 Bjorge, S., Hamelehle, K.L., Homa, R., Rose, S.-E., Turluck, D.A. and Wright, D.S. (1991) Evidence for glucuronide conjugation of *p*-nitrophenol in the Caco-2 cell model. *Pharmaceutical Research*, **8**, 1441–1443.

32 Carriére, V., Chambaz, J. and Rousset, M. (2001) Intestinal responses to xenobiotics. *Toxicology In Vitro*, **15**, 373–378.

33 Baranczyk-Kuzma, A., Garren, J.A., Hidalgo, I.J. and Borchardt, R.T. (1991) Substrate specificity and some properties of phenol sulphotransferase from human intestinal Caco-2 cells. *Life Sciences*, **49**, 1197–1206.

34 Pruesaritanont, T., Gorham, L.M., Hochman, J.H., Tran, L.O. and Vyas, K.P. (1996) Comparative studies of drug metabolising enzymes in dog, monkey, and human small intestine, and in Caco-2 cells. *Drug Metabolism and Disposition*, **24**, 634–642.

35 Hunter, J., Jepson, M.A., Tsuruo, T., Simmons, N.L. and Hirst, B.H. (1993) Functional expression of P-glycoprotein in apical membranes of human intestinal epithelial Caco-2 cells: kinetics of vinblastine secretion and interaction with modulators. *Journal of Biological Chemistry*, **268**, 14991–14997.

36 Hunter, J., Hirst, B.H. and Simmons, N.L. (1993) Drugs absorption limited by P-glycoprotein-mediated secretory drug transport in human intestinal epithelial Caco-2 cell layers. *Pharmaceutical Research*, **10**, 743–749.

37 Hunter, J. and Hirst, B.H. (1997) Intestinal secretion of drugs: the role of P-glycoprotein and related drug efflux systems in limiting oral drug absorption. *Advanced Drug Delivery Reviews*, **25**, 129–157.

38 Taipalensuu, J., Törnblom, H., Lindberg, G., Einarsson, C., Sjöqvist, F., Melhus, H., Garberg, P., Sjöström, B., Lundgren, B. and Artursson, P. (2001) Correlation of gene expression of ten drug efflux proteins of the ATP-binding cassette transporter family in normal human jejunum and inhuman intestinal epithelial Caco-2 cell monolayers. *Journal of Pharmacology and Experimental Therapeutics*, **299**, 164–170.

39 Hilgendorf, C., Ahlin, G., Seithel, A., Artursson, P., Ungell, A.-L. and Karlsson, J. (2007) Expression of 36 drug transporter genes in human intestine, liver and kidney and in organotypic cell lines. *Drug Metabolism and Disposition*, **35**, 1333–1340.

40 Luo, F., Paranjpe, P., Guo, A., Rubin, E. and Sinko, P. (2002) Intestinal transport of irinotecan in Caco-2 cells and MDCK II cells overexpressing efflux transporters Pgp, cMOAT, and MRP1. *Drug Metabolism and Disposition*, **30**, 763–770.

41 Stephens, R.H., O'Neill, C.A., Warhurst, A., Carlson, G.L., Rowland, M. and Warhurst, G. (2001) Kinetic profiling of P-glycoprotein-mediated drug efflux in rat and human intestinal epithelia. *Journal of Pharmacology and Experimental Therapeutics*, **296**, 584–591.

42 Kool, M., Haas, M., de Scheffer, G.L., Scheper, R.J., van Eijk, M.J.T., Juijn, J.A., Baas, F. and Borst, P. (1997) Analysis of expression of cMoat (MRP2), MRP3, MRP4, and MRP5, homologues of the multidrug resistance-associated protein gene (MRP1), in human cancer cell lines. *Cancer Research*, **57**, 3537–3547.

43 Blais, A., Bissonnette, P. and Berteloot, A. (1987) Common characteristics for Na^+-dependent sugar transport in Caco-2 cells and human fetal colon. *Journal of Membrane Biology*, **99**, 113–125.

44 Riley, S.A., Warhurst, G., Crowe, P.T. and Turnberg, L.A. (1066) Active hexose transport across cultured human Caco-2 cells: characterisation and influence of culture conditions. *Biochimica et Biophysica Acta*, **1991**, 175–182.

45 Hidalgo, I.J. and Borchardt, R.T. (1990) Transport of large neutral amino acid, phenylalanine, in a human intestinal cell line: Caco-2. *Biochimica et Biophysica Acta*, **1028**, 25–30.

46 Hu, M. and Borchardt, R.T. (1992) Transport of a large neutral amino acid in a human intestinal epithelial cell line (Caco-2): uptake and efflux of phenylalanine *Biochimica et Biophysica Acta*, **1135**, 233–244.

47 Nicklin, P., Irwin, B., Hassan, I., Williamson, I. and MacKay, M. (1992) Permeable support type influence the

transport of compounds across Caco-2 cells. *International Journal of Pharmaceutics*, **83**, 197–209.

48 Nicklin, P.L., Irwin, W.J., Hassan, I.F. and MacKay, M. (1992) Proline uptake by monolayers of human intestinal absorptive (Caco-2) cells *in vitro*. *Biochimica et Biophysica Acta*, **1104**, 283–292.

49 Thwaites, D.T., McEwan, G.T.A., Hirst, B.H. and Simmons, N.L. (1995) H^+-coupled-methylaminoisobutyric acid transport in human intestinal Caco-2 cells. *Biochimica et Biophysica Acta*, **1234**, 111–118.

50 Brandsch, M., Miyamoto, Y., Ganapathy, V. and Leibach, F.H. (1994) Expression and protein C dependent regulation of peptide/H + co-transport system in the Caco-2 human colon carcinoma cell line. *Biochemical Journal*, **299**, 253–260.

51 Ganapathy, M.E., Brandsch, M., Prasad, P.D., Ganapathy, V. and Leibach, F.H. (1995) Differential recognition of b-lactam antibiotics by intestinal and renal peptide transporters, PEPT1 and PEPT2. *Journal of Biological Chemistry*, **270**, 25672–25677.

52 Dix, C.J., Hassan, I.F., Obray, H.Y., Shah, R. and Wilson, G. (1990) The transport of vitamin B12 through polarized monolayers of Caco-2 cells. *Gastroenterology*, **98**, 1272–1279.

53 Hidalgo, I.J. and Borchardt, R.T. (1990) Transport of bile acids in a human intestinal epithelial cell line, Caco-2. *Biochimica et Biophysica Acta*, **1035**, 97–103.

54 Annaba, F., Sarwar, Z., Kumar, P., Saksena, S., Turner, J.R., Dudeja, P.K., Gill, R.K. and Alrefai, W.A. (2008) Modulation of ileal bile acid transporter (ASBT) activity by depletion of plasma membrane cholesterol: association with lipid rafts. *American Journal of Physiology. Gastrointestinal and Liver Physiology*, **294**, G489–497.

55 Hu, M. and Borchardt, R.T. (1990) Mechanism of L-α-methyldopa transport through a monolayer of polarized human intestinal epithelial cells (Caco-2). *Pharmaceutical Research*, **7**, 1313–1319.

56 Peters, W.H.N. and Roelofs, H.M.J. (1989) Time-dependent activity and expression of glutathione S-transferases in the human colon adenocarcinoma cell line Caco-1. *Biochemical Journal*, **264**, 613–616.

57 Yu, H., Cook, T.J. and Sinko, P.J. (1997) Evidence for diminished functional expression of intestinal transporters in Caco-2 cell monolayers at high passages. *Pharmaceutical Research*, **14**, 757–762.

58 Walter, E., Kissel, T., Reers, M., Dickneite, G., Hoffmann, D. and Stuber, W. (1995) Transepithelial transport properties of peptidomimetic thrombin inhibitors in monolayers of a human intestinal cell line (Caco-2) and their correlation to *in vivo* data. *Pharmaceutical Research*, **12**, 360–365.

59 Anderle, P., Niederer, E., Rubas, W., Hilgendorf, C., Spahn-Langguth, H., Wunderli-Allenspach, H., Merkle, H.P. and Langguth, P. (1998) P-glycoprotein (P-gp) mediated efflux in Caco-2 cell monolayers: the influence of culturing conditions and drug exposure on P-gp expression levels. *Journal of Pharmaceutical Sciences*, **87**, 757–762.

60 Nuti, S.L., Mehdi, A. and Rao, S.U. (2000) Activation of the human P-glycoprotein ATPase by trypsin. *Biochemistry*, **39**, 3424–3432.

61 Ungell, A.-L. and Karlsson, J. (2003) Cell cultures in drug discovery: an industrial perspective, in *Drug Bioavailability – Estimation of Solubility, Permeability and Absorption* (eds H. van de Waterbeemd, H. Lennernäs and P. Artursson), Wiley, pp. 90–131.

62 Fagerholm, U. (2007) Prediction of human pharmacokinetics – gastrointestinal absorption. *Journal of Pharmacy and Pharmacology*, **59**, 905–916.

63 Balimane, P.V. and Chong, S. (2005) Cell culture-based models for instestinal

permeability: a critique. *Drug Discovery Today*, **10**, 335–343.

64 Cho, M.J., Thompson, D.P., Cramer, C.T., Vidmar, T.J. and Scieszka, J.F. (1989) The Madin–Darby canine kidney (MDCK) epithelial cell monolayer as a model cellular transport barrier. *Pharmaceutical Research*, **6**, 71–77.

65 Horio, M., Chin, K.-V., Currier, S.J., Goldenberg, S., Wiliams, C., Pasatan, I., Gottesman, M.M. and Handler, J. (1989) Transepithelial transport of drugs by the multidrug transporter in cultured Madin–Darby canine kidney cell epithelia. *Journal of Biological Chemistry*, **264**, 14880–14884.

66 Shu, Y., Bello, C.L., Mangravite, L.M., Feng, B. and Giacomini, K.M. (2001) Functional characteristics and steroid hormone-mediated regulation of an organic cation transporter in Madin–Darby Canine Kidney cells. *Journal of Pharmacology and Experimental Therapeutics*, **299**, 392–398.

67 Lentz, K.A., Polli, J.W., Wring, S.A., Humphreys, J.E. and Polli, J.E. (2000) Influence of passive permeability on apparent P-glycoprotein kinetics. *Pharmaceutical Research*, **17**, 1456–1460.

68 Smith, B.J., Doran, A.C., Mclean, S., Tingley, F.D., III, O'Neil, C.A. and Kajiji, S.M. (2001) P-glycoprotein efflux at the blood-brain barrier mediates differences in brain disposition and pharmacodynamics between two structurally related neurokinin-1 receptor antagonists. *Journal of Pharmacology and Experimental Therapeutics*, **298**, 1252–1259.

69 Schipper, N.G.M., Österberg, T., Wrange, U., Westberg, C., Sokolowski, A., Rai, R., Young, W. and Sjöström, B. (2001) *In vitro* intestinal permeability of factor Xa inhibitors: influence of chemical structure on passive transport and susceptibility to efflux. *Pharmaceutical Research*, **18**, 1735–1741.

70 Hämmerle, S.P., Rothen-Rutishauser, B., Kramer, S.D., Gunthert, M. and Wunderli- Allenspach, H. (2000) P-glycoprotein in cell cultures: a combined approach to study expression, localisation, and functionality in the confocal microscope. *European Journal of Pharmaceutical Sciences*, **12**, 69–77.

71 Lecureur, V., Sun, D., Hargrove, P., Schuetz, E.G., Kim, R.B., Lan, L.B. and Schuetz, J.D. (2000) Cloning and expression of murine sister of P-glycoprotein reveals a more discriminating transporter than MDR1/P-glycoprotein. *Molecular Pharmacology*, **57**, 24–35.

72 Matsson, P., Englund, G., Ahlin, G., Bergström, C.A., Norinder, U. and Artursson, P. (2007) A global drug inhibition pattern for the human ATP-binding cassette transporter breast cancer resistance protein (ABCG2). *Journal of Pharmacology and Experimental Therapy*, **323**, 19–30.

73 Cui, Y., Konig, J. and Keppler, D. (2001) Vectorial transport by double transfected cells expressing the human uptake transporter SLC21A8 and the apical export pump ABCC2. *Molecular Pharmacology*, **60**, 934–943.

74 Sasaki, M., Suzuki, H., Ito, K., Abe, T. and Sugiyama, Y. (2002) Transcellular transport of organic anions across a double-transfected Madin–Darby canine kidney II cell monolayer expressing both human organic aniontransporting polypeptide (OATP2/SLC21A6) and multidrug resistance associated protein 2 (MRP2/ABCC2). *Journal of Biological Chemistry*, **277**, 6497–6503.

75 Kopplow, K., Letschert, K., König, J., Walter, B. and Keppler, D. (2005) Human hepatobiliary transport of organic anions analyzed by quadriple-transfected cells. *Molecular Pharmacology*, **68**, 1031–1038.

76 Lennernäs, H., Palm, K., Fagerholm, U. and Artursson, P. (1996) Comparison between active and passive drug transport in human intestinal epithelial (Caco-2) cells *in vitro* and human jejunum *in vivo*,

International Journal of Pharmaceutics, **127**, 103–107.

77 Tavelin, S., Milovic, V., Ocklind, G., Olsson, S. and Artursson, P. (1999) A conditionally immortalized epithelial cell line for studies of intestinal drug transport. *Journal of Pharmacology and Experimental Therapeutics*, **290**, 1212–1221.

78 Fine, K.D., Santa Ana, C.A., Porter, J.L. and Fordtran, J.S. (1995) Effect of changing intestinal flow rate on a measurement of intestinal permeability. *Gastroenterology*, **108**, 983–989.

79 Paul, E.C.A., Hochman, J. and Quaroni, A. (1993) Conditionally immortalized intestinal epithelial cells. Novel approach for study of differentiated enterocytes. *American Journal of Physiology*, **265**, C266–C278.

80 Artursson, P. and Tavelin, S. (2003) Studies of membrane permeability and oral absorption 6: Caco-2 and emerging alternatives for prediction of intestinal drug transport: a general overview, in *Drug Bioavailability – Estimation of Solubility, Permeability and Absorption* (eds H. van de Waterbeemd, H. Lennernäs and P. Artursson), Wiley, pp. 72–89.

81 Tanaka, Y., Taki, Y., Sakane, T., Nadai, T., Sezaki, H. and Yamashita, S. (1995) Characterization of drug transport through tight-junctional pathway in Caco-2 monolayer: comparison with isolated rat jejunum and colon. *Pharmaceutical Research*, **12**, 523–528.

82 Sugano, K., Takata, N., Machida, M., Saitoh, K. and Terada, K. (2002) Prediction of passive intestinal absorption using bio-mimetic artificial membrane permeation assay and the paracellular pathway model. *International Journal of Pharmaceutics*, **241**, 241–251.

83 Tavelin, S., Taipalensuu, J., Hallböök, F., Vellonen, K., Moore, V. and Artursson, P. (2003) An improved cell culture model based on 2/4/a1 cell monolayers for studies of intestinal drug transport. Characterization of transport routes. *Pharmaceutical Research*, **20**, 373–381.

84 Tavelin, S., Taipalensuu, J., Söderberg, L., Morrison, R., Chong, S. and Artursson, P. (2003) Prediction of the oral absorption of low permeability drugs using small intestinal-like 2/4/A1 cell monolayers. *Pharmaceutical Research*, **20**, 397–405.

85 Nakai, D., Hubatsch, I., Bergström, C., Ekegren, J., Larhed, M. and Artursson, P. (2008) Structure–permeability relationship for a series of HIV-protease inhibitors in intestinal epithelial (2/4/A1) cells (in preparation).

86 Wikman, A., Karlsson, J., Carlstedt, I. and Artursson, P. (1993) A drug absorption model based on the mucus layer producing human intestinal goblet cell line HT29-H. *Pharmaceutical Research*, **10**, 843–852.

87 Karlsson, J., Wikman, A. and Artursson, P. (1993) The mucus layer as a barrier to drug absorption in monolayers of human intestinal epithelial HT29-H goblet cells. *International Journal of Pharmaceutics*, **99**, 209–218.

88 Hilgendorf, C., Spahn-Langguth, H., Regård, C.G., Lipka, E., Amidon, G.L. and Langguth, P. (2001) Caco-2 versus Caco-2/HT29-MTX co-cultured cell lines: permeabilities via diffusion, inside- and outside-directed carrier mediated transport. *Journal of Pharmaceutical Sciences*, **89**, 63–75.

89 Behrens, I., Stenberg, P., Artursson, P. and Kissel, T. (2001) Transport of lipophilic drug molecules in a new mucus-secreting cell culture model based on HT29-MTX cells. *Pharmaceutical Research*, **18**, 1138–1145.

90 Wikman-Larhed, A. and Artursson, P. (1995) Co-cultures of human intestinal goblet (HT29-H) and absorptive (Caco-2) cells for studies of drug and peptide absorption. *European Journal of Pharmaceutical Sciences*, **3**, 171–183.

91 Laboisse, C.L., Jarry, A., Bou- Hanna, C., Merlin, D. and Vallette, G. (1994)

Intestinal cell culture models. *European Journal of Pharmaceutical Sciences*, **2**, 36–38.

92 Brayden, D.J. (1997) Human intestinal epithelial cell monolayers as prescreens for oral drug delivery. *Pharmceutical News*, **4**, 11–15.

93 Duizer, E., Penninks, A.H., Stenhuis, W.H. and Groten, J.P. (1997) Comparison of permeability characteristics of the human colonic Caco-2 and rat small intestinal IEC-18 cell lines. *Journal of Controlled Release*, **49**, 39–49.

94 Pickett, S.D., McLay, I.M. and Clark, D.E. (2000) Enhancing the hit-to-lead properties of lead optimization libraries. *Journal of Chemical Information and Computer Sciences*, **40**, 263–272.

95 Stevenson, C., Augustijns, P. and Hendren, R. (1999) Use of Caco-2 cells and LC/MS/MS to screen a peptide combinatorial library for permeable structures. *International Journal of Pharmaceutics*, **15**, 103–115.

96 McKenna, J.M., Halley, F., Souness, J.E., McLay, I.M., Pickett, S.D., Collis, A.J., Page, K. and Ahmed, I. (2002) An algorithm-directed two-component library synthesized via solid-phase methodology yielding potent and orally bioavailable p38 MAP kinase inhibitors. *Journal of Medicinal Chemistry*, **45**, 2173–2184.

97 Mandagere, A.K., Thompson, T.N. and Hwang, K.K. (2002) Graphical model for estimating oral bioavailability of drugs in humans and other species from their Caco-2 permeability and *in vitro* liver enzyme metabolic stability rates. *Journal of Medicinal Chemistry*, **45**, 304–311.

98 Matsson, P., Bergström, C.A.S., Tavelin, S., Nagahara, N., Norinder, U. and Artursson, P. (2005) Exploring the role of different drug transport routes in permeability screening. *Journal of Medicinal Chemistry*, **48**, 604–613.

99 Liang, E., Proudfoot, J. and Yazdanian, M. (2000) Mechanisms of transport and structure-permeability relationship of sulfasalazine and its analogs in Caco-2 cell monolayers. *Pharmaceutical Research*, **17**, 1168–1174.

100 Ekins, S., Durst, G.L., Stratford, R.E., Thorner, D.A., Lewis, R., Loncharich, R.J. and Wikel, J.H. (2001) Three-dimensional quantitative structure–permeability relationship analysis for a series of inhibitors of rhinovirus replication. *Journal of Chemical Information and Computer Sciences*, **41**, 1578–1586.

101 Palanki, M.S., Erdman, P.E., Gayo-Fung, L.M., Shevlin, G.I., Sullivan, R.W., Goldman, M.E., Ransone, L.J., Bennett, B.L., *et al.* (2000) Inhibitors of NF-kappaB and AP-1 gene expression: SAR studies on the pyrimidine portion of 2-chloro-4-trifluoromethylpyrimidine-5-[N-(30,50-bis(trifluoromethyl)phenyl) carboxamide]. *Journal of Medicinal Chemistry*, **43**, 3995–4004.

102 Proudfoot, J.R., Betageri, R., Cardozo, M., Gilmore, T.A., Glynn, S., Hickey, E.R., Jakes, S., Kabcenell, A., *et al.* (2001) Nonpeptidic, monocharged, cell permeable ligands for the p56lck SH2 domain. *Journal of Medicinal Chemistry*, **44**, 2421–2431.

103 Conradi, R.A., Hilgers, A.R., Ho, N.F. and Burton, P.S. (1991) The influence of peptide structure on transport across Caco-2 cells. *Pharmaceutical Research*, **8**, 1453–1460.

104 Conradi, R.A., Hilgers, A.R., Burton, P.S. and Hester, J.B. (1994) Epithelial cell permeability of a series of peptidic HIV protease inhibitors: amino-4 Caco-2 and emerging alternatives for prediction of intestinal drug transport: a general overview terminal substituent effects. *Journal of Drug Targeting*, **2**, 167–171.

105 Burton, P.S., Conradi, R.A., Ho, N.F., Hilgers, A.R. and Borchardt, R.T. (1996) How structural features influence the biomembrane permeability of peptides. *Journal of Pharmaceutical Sciences*, **85**, 1336–1340.

106 Werner, U., Kissel, T. and Stuber, W. (1997) Effects of peptide structure on transport properties of seven thyrotropin releasing hormone (TRH) analogues in a human intestinal cell line (Caco-2). *Pharmaceutical Research*, **14**, 246–250.

107 Goodwin, J.T., Conradi, R.A., Ho, N.F. and Burton, P.S. (2001) Physicochemical determinants of passive membrane permeability: role of solute hydrogen-bonding potential and volume. *Journal of Medicinal Chemistry*, **44**, 3721–3729.

108 Ellens, C., Lee, P., Smith, P.L., Lago, A., Elliott, J.D. and Artursson, P. (1999) Prediction of the intestinal absorption of endothelin receptor antagonists using three theoretical methods of increasing complexity. *Pharmaceutical Research*, **16**, 1520–1526.

109 Schipper, N.G., Österberg, T., Wrange, U., Westberg, C., Sokolowski, A., Rai, R., Young, W. and Sjöström, B. (2001) *In vitro* intestinal permeability of factor Xa inhibitors: influence of chemical structure on passive transport and susceptibility to efflux. *Pharmaceutical Research*, **18**, 1735–1741.

110 Brandsch, M., Knutter, I.I., Thunecke, F., Hartrodt, B., Born, I.I., Borner, V., Hirche, F., Fischer, G. *et al*. (1999) Decisive structural determinants for the interaction of proline derivatives with the intestinal H+/peptide symporter. *European Journal of Biochemistry*, **266**, 502–508.

111 Friedrichsen, G., Jakobsen, P., Taub, M. and Begtrup, M. (2001) Application of enzymatically stable dipeptides for enhancement of intestinal permeability. Synthesis and *in vitro* evaluation of dipeptide-coupled compounds. *Bioorganic and Medicinal Chemistry*, **9**, 2625–2632.

112 Nielsen, C., Andersen, R., Brodin, B., Frokjaer, S., Taub, M. and Steffansen, B. (2001) Dipeptide model prodrugs for the intestinal oligopeptide transporter. Affinity for and transport via hPepT1 in the human intestinal Caco-2 cell line. *Journal of Controlled Release*, **11**, 129–138.

113 Våben, ø J., Lejon, T., Nielsen, C.U., Steffansen, B., Chen, W., Ouyang, H., Borchardt, R.T. and Luthman, K. (2004) Phe-Gly dipeptidomimetics designed for the di-/tripeptide transporters PEPT1 and PEPT2: synthesis and biological investigations. *Journal of Medicinal Chemistry*, **12** (47), 1060–1069.

114 Våben, ø J., Nielsen, C.U., Ingebrigtsen, T., Lejon, T., Steffansen, B. and Luthman, K. (2004) Dipeptidomimetic ketomethylene isosteres as pro-moieties for drug transport via the human intestinal di-/tripeptide transporter hPEPT1: design, synthesis, stability, and biological investigations. *Journal of Medicinal Chemistry*, **47**, 4755–4765.

115 Hubatsch, I., Arvidsson, P.I., Seebach, D., Luthman, K. and Artursson, P. (2007) Beta- and gamma-di- and tripeptides as potential substrates for the oligopeptide transporter hPepT1. *Journal of Medicinal Chemistry*, **21**, 5238–5242.

116 Tavelin, S., Gråsj, ö J., Taipalensuu, J., Ocklind, G. and Artursson, P. (2002) Applications of epithelial cell culture in studies of drug transport. *Methods in Molecular Biology (Clifton, N.J.)*, **188**, 233–272.

117 Karlsson, J. and Artursson, P. (1991) A method for the determination of cellular permeability coefficients and aqueous boundary layer thickness in monolayers of intestinal epithelial (Caco-2) cells grown in permeable filter chambers. *International Journal of Pharmaceutics*, **71**, 51–64.

118 Palm, K., Luthman, K. and Artursson, P. (1999) Effect of molecular charge on drug transport across intestinal epithelial Caco-2 cell monolayers. *Journal of Pharmacology and Experimental Therapeutics*, **291**, 435–443.

119 Nagahara, N., Tavelin, S. and Artursson, P. (2004) Contribution of the paracellular route to the pH-dependent epithelial

permeability to cationic drugs. *Journal of Pharmaceutical Sciences*, **93**, 2972–2984.

120 Hidalgo, I.J. (2001) Assessing the absorption of new pharmaceuticals. *Current Topics in Medicinal Chemistry*, **1**, 385–401.

121 Artursson, P. (1990) Epithelial transport of drugs I. A model for studying the transport of drugs (β-blocking agents) over an intestinal epithelial cell line (Caco-2). *Journal of Pharmaceutical Sciences*, **79**, 476–482.

122 Chong, S., Dando, S.A. and Morrison, R.A. (1997) Evaluation of biocoat intestinal epithelium differentiation environment (3-day cultured Caco-2 cells) as an absorption screening model with improved productivity. *Pharmaceutical Research*, **14**, 1835–1837.

123 Liang, E., Chessic, K. and Yazdanian, M. (2000) Evaluation of an accelerated Caco-2 cell permeability model. *Journal of Pharmaceutical Sciences*, **89**, 336–345.

124 Yamashita, S., Konishi, K., Yamazaki, Y., Taki, Y., Sakane, T., Sezaki, H. and Furuyama, Y. (2002) New and better protocols for a short-term Caco-2 cell culture system. *Journal of Pharmaceutical Sciences*, **91**, 669–679.

125 Hayeshi, R., Hilgendorf, C., Artursson, P., Augustijns, P., Brodin, B., Fischer, K., Hovenkamp, E., Korjamo, T., Masungi, C., Maubon, N., Mols, R., Monkkonen, J., Müllertz, A., O'Driscoll, C., Oppers - Tiemissen, H.M., Ragnarsson, E., Rooseboom, M. and Ungell, A.-L. (2008) Comparison of drug transporter gene expression and functionality in Caco-2 cells from 10 different laboratories. *European Journal of Pharmaceutical Sciences*, (in press).

126 Fallingborg, J., Christensen, L.A., Ingelman-Nielsen, M., Jacobsen, B.A., Abildgaard, K. and Rasmussen, H.H. (1989) PH-profile and regional transit times of the normal gut measured by radiotelemetry device. *Alimentary Pharmacology & Therapeutics*, **3**, 605–613.

127 Lucas, M.L. (1983) Determination of acid surface pH *in vivo* in rat proximal jejunum. *Gut*, **24**, 734–739.

128 Yamashita, S., Furubayashi, T., Kataoka, M., Sakane, T., Sezaki, H. and Tokuda, H. (2000) Optimized conditions for prediction of intestinal drug permeability using Caco-2 cells. *European Journal of Pharmaceutical Sciences*, **10**, 195–204.

129 Neuhoff, S., Ungell, A.-L., Zamora, I. and Artursson, P. (2005) pH-dependent passive and active transport of acidic drugs across Caco-2 cell monolayers. *European Journal of Pharmaceutical Sciences*, **25**, 211–220.

130 Palm, K., Luthman, K., Ros, J., Grasjo, J. and Artursson, P. (1999) Effect of molecular charge on intestinal epithelial drug transport: pH dependent transport of cationic drugs. *Journal of Pharma-cology and Experimental Therapeutics*, **291**, 435–443.

131 Neuhoff, S., Ungell, A.-L., Zamora, I. and Artursson, P. (2003) pH dependent bi-directional transport of weak basic drugs across Caco-2 monolayers. Implications for drug/drug interactions. *Pharmaceutical Research*, **20**, 1141–1148.

132 Krishna, G., Chen, K.-J., Lin, C.-C. and Nomeir, A.A. (2001) Permeability of lipophilic compounds in drug discovery using *in-vitro* human absorption model, Caco-2. *International Journal of Pharmaceutics*, **222**, 77–89.

133 Walgren, R.A. and Walle, T. (1999) The influence of plasma binding on absorption/exsorption in the Caco-2 model of human intestinal absorption. *Journal of Pharmacy and Pharmacology*, **51**, 1037–1040.

134 Neuhoff, S., Artursson, P., Zamora, I. and Ungell, A.-L. (2006) Impact of extracellular protein binding on passive and active drug transport across Caco-2 cells. *Pharmaceutical Research*, **23**, 350–359.

135 Katneni, K., Charman, S.A. and Porter, C.J. (2008) Use of plasma proteins as solubilizing agents in *in vitro* permeability

experiments: correction for unbound drug concentration using the reciprocal permeability approach. *Journal of Pharmaceutical Sciences*, **97**, 209–224.

136 Diem, K. and Lentner, C. (eds) (1970) *Scientific Tables*, 7th edn, Ciba-Geigy Limited, Basel, Switzerland.

137 Neuhoff, S., Artursson, P. and Ungell, A.-L. (2007) Advantages and disadvantages of using bovine serum albumin and Cremophor EL as extracellular additives during transport studies of lipophilic compounds across Caco-2 monolayers. *Journal of Drug Delivery Science and Technology*, **17**, 259–266.

138 Tang, F., Horie, K. and Borchardt, R.T. (2002) Are MDCK cells transfected with the human MRP2 gene a good model of the human intestinal mucosa? *Pharmaceutical Research*, **19**, 773–779.

139 Putnam, W.S., Pan, L., Tsutsui, K., Takahashi, L. and Benet, L.Z. (2002) Comparison of bidirectional cephalexin transport across MDCK and caco-2 cell monolayers: interactions with peptide transporters. *Pharmaceutical Research*, **19**, 27–33.

140 Litman, T., Druley, T.E., Stein, W.D. and Bates, S.E. (2001) From MDR to MXR: new understanding of multidrug resistance systems, their properties and clinical significance. *Cellular and Molecular Life Sciences*, **58**, 931–959.

141 Wenzel, U., Meissner, B., Doring, F. and Daniel, H. (2001) PEPT1-mediated uptake of dipeptides enhances the intestinal absorption of amino acids via transport system b + 0. *Journal of Cellular Physiology*, **186**, 251–259.

142 Luo, F., Paranjpe, P., Guo, A., Rubin, E. and Sinko, P. (2002) Intestinal transport of irinotecan in Caco-2 cells and MDCK II cells overexpressing efflux transporters Pgp, cMOAT, and MRP1. *Drug Metabolism and Disposition*, **30**, 763–770.

143 Raeissi, S.D., Hidalgo, I.J., Segura-Aguilar, J. and Artursson, P. (1999) Interplay between CYP3A-mediated metabolism and polarized efflux of terfenadine and its metabolites in intestinal epithelial Caco-2 (TC7) cell monolayers. *Pharmaceutical Research*, **16**, 625–632.

144 Hochman, J., Chiba, M., Yamazaki, M., Tang, C. and Lin, J. (2001) P-glycoprotein-mediated efflux of indinavir metabolites in Caco-2 cells expressing cytochrome P450 3. *Journal of Pharmacology and Experimental Therapeutics*, **298**, 323–330.

145 Cummins, C.L., Jacobsen, W. and Benet, L.Z. (2002) Unmasking the dynamic interplay between intestinal P-glycoprotein and CYP3A4. *Journal of Pharmacology and Experimental Therapeutics*, **300**, 1036–1045.

146 Paine, M.F., Leung, L.Y., Lim, H.K., Liao, K., Oganesian, A., Zhang, M.Y., Thummel, K.E. and Watkins, P.B. (2002) Identification of a novel route of extraction of sirolimus in human small intestine: roles of metabolism and secretion. *Journal of Pharmacology and Experimental Therapeutics*, **301**, 174–186.

147 Hubatsch, I., Lazorova, L., Vahlne, A. and Artursson, P. (2005) The orally active antiviral tripeptide GPGamide is a prodrug that is activated by CD26 before transport across the intestinal epithelium. *Antimicrobial Agents Chemotherapy*, **49**, 1087–1092.

148 Flanagan, S.D., Takahashi, L.H., Liu, X. and Benet, L.Z. (2002) Contributions of saturable active secretion, passive transcellular, and paracellular diffusion to the overall transport of furosemide across adenocarcinoma (Caco-2) cells. *Journal of Pharmaceutical Sciences*, **91**, 1169–1177.

149 Hirano, H., Kurata, A., Onishi, Y., Sakurai, A., Saito, H., Nakagawa, H., Nagakura, M., Tarui, S., Kanamori, Y., Kitajima, M. and Ishikawa, T. (2006) High-speed screening and QSAR analysis of human ATP-binding cassette transporter ABCB11 (bile salt export pump) to predict drug-induced intrahepatic cholestasis. *Molecular Pharmacology*, **3**, 252–265.

150 Pedersen, J., Matsson, P., Bergström, C.A.S., Norinder, U., Hoogstraate, J. and Artursson, P. (2008) Prediction and identification of drug interactions with human ATP-binding cassette transporter multidrug-resistance associated protein 2 (MRP2; ABCC2), *Journal of Medicinal Chemistry*, **51**, 3275–3287.

151 Ahlin, G., Karlsson, J.E., Pedersen, J., Gustavsson, L., Larsson, R., Matsson, P., Norinder, U., Bergström, C.A.S. and Artursson P. (2008) Structural requirements for drug inhibition of the human organic cation transport protein OCT1 (SLC22A1). *Journal of Medical Chemisty*, (submitted).

152 Walle, U.K., Galijatovic, A. and Walle, T. (1999) Transport of the flavonoid chrysin and its conjugated metabolites by the human intestinal cell line Caco-2. *Biochemical Pharmacology*, **58**, 431–438.

153 Crespi, C.L., Penman, B.W. and Hu, M. (1996) Development of Caco-2 cells expressing high levels of cDNA-derived cytochrome P450 3A4. *Pharmaceutical Research*, **16**, 1635–1641.

154 Korjamo, T., Honkakoski, P., Toppinen, M.R., Niva, S., Reinisalo, M., Palmgren, J.J. and Mönkkönen, J. (2005) Absorption properties and P-glycoprotein activity of modified Caco-2 cell lines. *European Journal of Pharmaceutical Sciences*, **26**, 266–279.

155 Schmiedlin-Ren, P., Thummel, K.E., Fisher, J.M., Paine, M.F., Lown, K.S. and Watkins, P.B. (1997) Expression of enzymatically active CYP3A4 by Caco-2 cells grown on extracellular matrix-coated permeable supports in the presence of 1-alpha, 25-dihydroxyvitamin D3. *Molecular Pharmacology*, **51**, 741–754.

156 Engman, H.A., Lennernäs, H., Taipalensuu, J., Charlotta, O., Leidvik, B. and Artursson, P. (2001) CYP3A4, CYP3A5, and MDR1 in human small and large intestinal cell lines suitable for drug transport studies. *Journal of Pharmaceutical Sciences*, **90**, 1736–1751.

157 Cummins, C.L., Mangravite, L.M. and Benet, L.Z. (2001) Characterizing the expression of CYP3A4 and efflux transporters (P-gp, MRP, and MRP2) in CYP3A4-transfected Caco-2 cells after induction with sodium butyrate and the phorbol ester 12-Otetradecanoylphorbol-13-acetate. *Pharmaceutical Research*, **18**, 1102–1109.

158 Brimer, C., Dalton, J.T., Zhu, Z., Schuetz, J., Yasuda, K., Vanin, E., Relling, M.V., Lu, Yi. and Schuetz, E.G. (2000) Creation of polarized cells coexpressing CYP3A4, NADPH cytochrome P450 reductase and MDR1/P-glycoprotein. *Pharmaceutical Research*, **17**, 803–810.

159 Gelder, van J., Annaert, P., Naesens, L., Clercq, E. de., Van den Mooter, G., Kinget, R. and Augustijns, P. (1999) Inhibition of intestinal metabolism of the antiviral ester prodrug bis(POC)-PMPA by nature-identical fruit extracts as a strategy to enhance its oral absorption: an *in vitro* study. *Pharmaceutical Research*, **16**, 1035–1040.

160 Augustijns, P., Annaert, P., Heylen, P., Van den Mooter, G. and Kinget, R. (1998) Drug absorption studies of prodrugs esters using the Caco-2 model: evaluation of ester hydrolysis and transepithelial transport. *International Journal of Pharmaceutics*, **166**, 45–53.

161 Imai, T., Imoto, M., Sakamoto, H. and Hashimoto, M. (2005) Identification of esterases expressed in Caco-2 cells and effects of their hydrolyzing activity in predicting human intestinal absorption. *Drug Metabolism and Disposition*, **33**, 1185–1190.

162 Winiwarter, S., Bonham, N.M., Ax, F., Hallberg, A., Lennernäs, H. and Karlen, A. (1998) Correlation of human jejunal permeability (*in vivo*) of drugs with experimentally and theoretically derived parameters. A multivariate data analysis approach. *Journal of Medicinal Chemistry*, **41**, 4939–4949.

163 Lennernäs, H., Knutson, L., Knutson, T., Hussain, A., Lesko, L., Salmonson, T. and Amidon, G. (2002) The effect of amiloride on the *in vivo* effective permeability of amoxicillin in human jejunum: experience from a regional perfusion technique. *European Journal of Pharmaceutical Sciences*, **15**, 271–277.

164 Stenberg, P., Norinder, U., Luthman, K. and Artursson, P. (2001) Experimental and computational screening models for the prediction of intestinal drug absorption. *Journal of Medicinal Chemistry*, **44**, 1927–1937.

8
Use of Animals for the Determination of Absorption and Bioavailability

Chris Logan

Abbreviations

ADME/PK	Absorption, distribution, metabolism, and excretion/pharmacokinetics
AUC	Area under the plasma concentration–time curve
Caco-2	Adenocarcinoma cell line derived from human colon
DMPK	Drug metabolism and pharmacokinetics
GIT	Gastrointestinal tract
HPLC	High-pressure liquid chromatography
hpv	Hepatic portal vein
HTS	High-throughput screen
i.v.	Intravenous
i.t.	Intratracheal
MDCK	Madin–Darby canine kidney cells
PAMPA	Parallel artificial membrane permeation assay
P_{app}	Apparent permeability coefficient
PB/PK	Physiologically based pharmacokinetics
PK	Pharmacokinetics
p.o.	Oral (per os)

Symbols

$C_{min,ss}$	Minimum plasma concentration at steady state
f_u	Fraction unbound in plasma
k	Elimination rate constant
log D	Logarithm of the distribution coefficient in octanol/water (usually at pH 7.4)
τ	(Tau) dosing interval
V_d	Volume of distribution

8.1 Introduction

This chapter will review some of the important methods for carrying out *in vivo* absorption and bioavailability studies, as well as attempt to provide an overview of how the information may be used in the drug discovery process. The chapter is aimed at medicinal chemists and thus will focus on the use of animals in discovery phase absorption, distribution, metabolism, and excretion/pharmacokinetic (ADME/PK) studies, rather than the design of studies that are for regulatory submission or part of a development safety package.

8.1.1 ADME/PK in Drug Discovery

The need to carry out ADME/PK studies prior to the start of drug development has only recently become widely accepted. The very high failure rate of drug development has been well known for a long time, but the key publication of Prentis *et al.* in 1988 [1] highlighted that a significant proportion of the failures (39%) for the seven major UK pharmaceutical companies could be attributed to "inappropriate pharmacokinetics." In a more recent report [2], the failure rate attributed to the same cause was 25%. Whether this apparent improvement is due to the variability in the reporting system or a very rapid change due to the incorporation of DMPK into discovery is not clear. However, it is often very difficult to attribute a failure to a single cause; is the failure due to the toxicity of the compound or to poor PK, which leads to excessive exposures at the peak concentrations that are necessary to achieve the required pharmacological effect over the whole dosing period? Our own experience, like that of others [3], is that there are often several aspects that contribute to the decision not to progress a development project.

Nonetheless, it is now generally accepted that it is worthwhile "frontloading" projects with ADME/PK and toxicology information in order to improve the chances of compounds achieving registration and becoming "best in class" [4].

The incorporation of ADME/PK into the discovery process has required a complete reevaluation of the approach to the science. Drug discovery can be seen as a cyclical process (Figure 8.1), with chemists making compounds that are screened for biological activity. The biological data are fed back to the chemists who use it to improve the design of the next compounds, which are then used to initiate the next revolution of the cycle. The incorporation of ADME/PK in to drug discovery means that there is now a second, often orthogonal, make/test cycle. For this cycle to be productive, it is essential for it to operate at the same rate as the biological testing, otherwise the chemistry will have moved on, and the ADME/PK data will have been generated on compounds that are no longer of interest.

Of course, as the generation of biological information has moved toward high-throughput approaches, ADME/PK is also needed to aspire to similar expectations. This has led to significant automation and simplification of the ADME screens, as will be seen elsewhere in this book. Even so, few projects have had ready access to truly

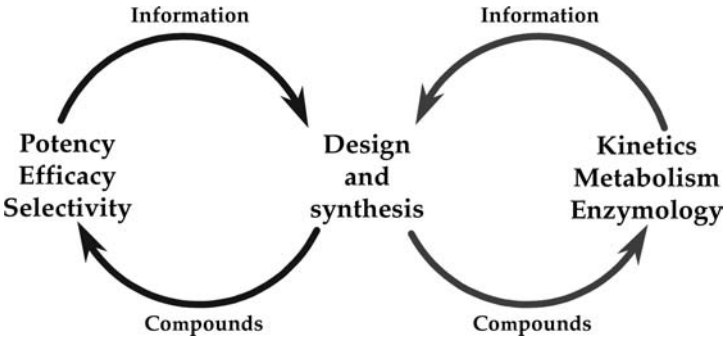

Figure 8.1 Research optimization process.

high-throughput screening (HTS) ADME/PK, and so it is more usual for DMPK considerations to be taken on when projects are at the "hit-to-lead" stage or later [4].

8.1.2
The Need for Prediction

As ADME/PK has become incorporated into drug discovery, it has become necessary to reconsider the purpose of the studies. If the science is really going to reduce the attrition rate in development, then it is essential for the studies to allow predictions of the PK in man to be made. This means predicting the likely size and frequency of the dose. A review of the top 10 medicines of 1999 (Table 8.1) shows all of them to be once-a-day compounds. It is clear that to be "best in class" and to be able to maintain that position as follow-up compounds come along, it seems probable that a compound will need to be suitable for once-a-day dosing.

Although the pressure to screen large numbers of compounds quickly has led to the rapid development of *in silico* and *in vitro* assays, the sheer number and complexity of the processes involved in determining the disposition of any particular compound mean that *in vivo* studies are still required to provide assurance that the important processes are modeled with sufficient accuracy [4–6], and, indeed, that the potential contribution of processes for which there are no good *in vitro* models (e.g., biliary secretion) are adequately assessed.

Although prediction of ADME/PK in man may be the primary purpose for the preclinical studies, it is also important that potential new drugs have acceptable properties in toxicology species. Without these it can be very difficult to generate adequate safety margins to allow studies in man to start. It is also likely that the development safety assessment program will be difficult and hence slow.

8.2
Consideration of Absorption and Bioavailability

There are two methods of dosing that are of primary interest to medicinal chemists: the oral and intravenous routes. Oral is important because it is generally the most

Table 8.1 The top 10 best-selling drugs in 1999.

Product	Indications	1999 sales [$billion]	Percentage of global sales	Launched	Dosing regime
Losec (omeprazole)	Duodenal ulcer Gastroesophageal reflux *Helicobacter* infections	5.7	1.9	1989 – UK and US	Once daily, except when used as part of combination therapy
Zocor (simvastatin)	Hypercholesterolemia Hyperlipoproteinemia Hypertriglyceridemia	3.9	1.3	1989 – UK 1991 – US	Once daily
Lipitor (atorvastatin)	Atherosclerosis Dyslipidemia Hypercholesterolemia	3.8	1.3	1997 – UK and US	Once daily
Norvasc (amlodipine besilate)	Hypertension	3.0	1.0	1990 – UK 1992 – US	Once daily
Prozac (fluoxetine)	Depression Obsessive–compulsive disorders Panic Post-traumatic stress disorder	2.9	1.0	1988 – US 1989 – UK	Once daily
Ogastro (lansoprazole)	Duodenal ulcer	2.3	0.8	1994 – UK	Once daily, except when used as part of combination therapy for *H. pylori* and for hypersecretory conditions. Twice-daily when dose $\geq$20 mg
	Gastroesophageal reflux *Helicobacter* infections			1995 – US	

Seroxat (paroxetine)	Depression Obsessive–compulsive disorders Panic Post-traumatic stress disorder	2.1	0.7	1991 – UK 1993 – US	Once daily
Zoloft (sertraline)	Depression Obsessive–compulsive disorders Panic Post-traumatic stress disorder	2.0	0.7	1996 – EU and US	Once daily
Claritin (loratadine)	Allergy Rhinitis	2.0	0.7	1989 – UK 1993 – US	Once daily
Zyprexa (olanzapine)	Bipolar disorders Gilles de la Tourette's syndrome Psychotic disorders	1.9	0.6	1996 – UK and US	Once daily

Data from Scrip 2001 Yearbook, 17th edition, Table 2.7, p. 69. Sales of top 10 products worldwide 1999.

convenient method of administration for patients and the one most likely to result in high patient compliance. Again, this is confirmed by inspection of Table 8.1, showing the best-selling drugs in 1999. All of the top 10 compounds are for oral administration. Thus, oral administration is likely to be the desired route for any compound to be developed. However, intravenous dosing is also important because it allows determination of both rate of clearance and volume of distribution. These two are usually the primary parameters that determine the half-life. Clearance can be modulated in a series of compounds by altering rates of metabolism, while altering partition properties may change volume. Thus, it is important for medicinal chemists to know how these two parameters vary within their chemical series in order to be able to optimize the chemistry.

The important stages in delivering a drug to its desired target after an oral dose can be summarized as shown in Figure 8.2. Initially the formulation has to be swallowed and survive the transition to the site of absorption – the gastrointestinal tract (GIT). The time required for this to happen will depend on the stomach-emptying time, which in turn will be a function of the fed/fasting state of the subject or animal that is being studied (see for example Ref. [7]). This kind of information can only be obtained from *in vivo* studies.

Once in the GIT, when the drug has been released from the formulation into solution, the process of absorption may begin. In this phase, the compound has to pass across the wall of the GIT. This can be either by passive diffusion, which is commonly thought to be the most predominant route for the majority of drugs with molecular weights below 1000 Da, or it can be by paracellular absorption, or by active uptake. The paracellular route avoids passing through the cells, and instead the drug gains access to the portal blood by either passing through the tight junctions between the cells or through the nonrestrictive junctions. This method of

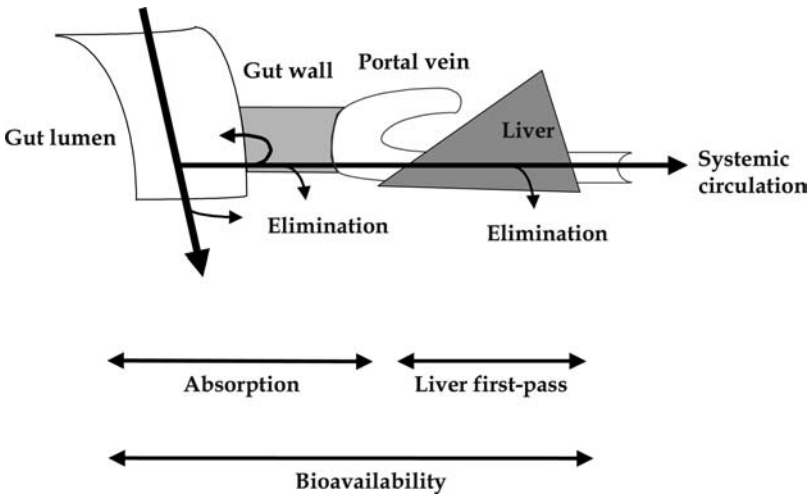

Figure 8.2 Absorption and bioavailability.

absorption can be important for compounds of a smaller size (and hence lower molecular weight) and higher polarity than the norm. Active uptake mechanisms are most common for naturally occurring compounds such as sugars, amino acids, and di- and tripeptides.

The compound in the portal blood is transported to the liver, which usually is the major site of metabolism for pharmaceuticals. In the liver, there is usually one, or more, of three principal fates for the drug: either metabolism; excretion into the bile; or return to the blood for distribution to the other tissues of the body. These other tissues may also be sites of metabolism or, particularly in the case of the kidney, sites of excretion.

There is often confusion as to the meaning of absorption, as opposed to bioavailability. For the purposes of this chapter, absorption will be taken to mean the processes that are involved in transferring the drug in solution from the site of administration to the venous blood. In the case of oral absorption, this will be to the hepatic portal vein (see Figure 8.2). Bioavailability is the ratio of the AUC after administration by the route of interest and after administration of the same amount of drug direct into the systemic circulation, usually by intravenous injection. Thus, bioavailability, after oral dosing, differs from absorption by also including the effects due to such processes as metabolism and/or biliary secretion during the first pass of the compound through the liver.

Bioavailability is an important parameter in drug-screening cascades. It gives a good indication of the efficiency of the delivery of the compound to the systemic circulation by the chosen route. It can only be measured *in vivo* but, as will be described below, it can be predicted for man using a number of methods.

Measurement of absorption can be complicated by efflux mechanisms. It is clear that many compounds are actively transported back into the GIT, into the bile, or into the urine by efflux proteins. In the case of those in the GIT, these may have an impact on the apparent absorption of a compound. Some understanding of the substrate specificity for one of these proteins, P-glycoprotein, is becoming apparent [8, 9], but currently the understanding is limited. At the moment, there are no published reliable methods either *in vivo* or *in vitro* for predicting the importance of efflux mechanisms for a particular compound in man [10–12].

Absorption studies can be carried out using a variety of dosing routes, and although this chapter will focus on oral dosing, analogous stages can be envisioned after other methods of dosing.

8.3 Choice of Animal Species

The main preclinical species used for pharmacokinetic studies are the rat, mouse, and dog. An examination of the Biosys database for 2000 and 2001 shows that of the abstracted papers, 6334 mapped to the subject heading "Pharmacokinetics." Of these, the vast majority (70%) were studies on humans. Studies on rats constituted 14% of the reports, mice 7.5%, and dogs 3.4% (Table 8.2). Nonhuman primates can

Table 8.2 Numbers of pharmacokinetic studies by animal.

Species	Total number of studies[a]	Percentage[a]
All species	6334	100
Human	4411	69.6
Rat	862	13.6
Mouse	478	7.5
Dog	215	3.4
Rabbit	199	3.1
Guinea pig	38	0.6
Hamster	23	0.4
Nonhuman primate	21	0.3[b]

Numbers of papers abstracted into Biosys Previews and mapped to the subject heading Pharmacokinetics.

[a] Numbers given against individual species sum to more than the total given for all studies as some studies included more than one species.

[b] Many primate studies are on human antibodies that cannot be tested with other species due to problems of antigenicity.

also be important pharmacokinetic models, but ethical and practical considerations severely limit studies in these animals such that, with in the same period, they represented less than 0.5% of the abstracted reports on PK.

The initial choice of the rat as the primary species for pharmacokinetic studies arose because of their use in pharmacology and toxicology studies. However, there is now such a large database of information about the relative pharmacokinetics of the same compounds in rats and man that, as described below, useful predictions to man can be made.

The importance of the mouse as a species for pharmacokinetics will probably increase as genetically modified mice become more important in producing humanized models for *in vivo* pharmacology. The mouse presents a particular challenge to pharmacokineticists because of the very small volumes of blood that can be obtained and the difficulties this presents for bioanalysis. However, there are now published methods for obtaining repetitive samples from mice [13], and this means that, provided a statistically appropriate experimental design is used (essentially a Latin Square – see Ref. [14]), the numbers of animals used in a study can be limited. This same approach can be used for studies in larger animals when the analytical method requires plasma samples that are so large that a complete PK profile cannot be determined in a single animal.

8.4 Methods

There are a number of important methods that are worthy of discussion before consideration of how the data are used to predict human ADME/PK.

8.4.1 Radiolabels

An approach that can be used in determining ADME/PK parameters that is simple to execute and gives confidence that the whole dose is accounted for is to use a radiolabel. This has been the standard approach for development ADME studies for many years. The common isotopes used are ^{14}C or ^{3}H (tritium).

Of course, it is important to ensure that the site of labeling is chosen carefully so that it is not readily lost by metabolism. For example, CH_3-N and CH_3-O groups, although perhaps amenable to simple synthetic approaches, are often major sites of metabolism and could lead to significant portions of the dose being converted to $^{14}CO_2$ or $^{3}H_2O$. Even though it is possible to trap and count the exhaled gas, from a practical point of view, these kinds of labels are the poor choices.

The incorporation of ^{14}C into compounds at a suitable site often requires extensive and complicated syntheses and thus a relatively long time. This usually means that ^{14}C-labeled compounds are unsuitable for studies to be carried out during discovery. There are, however, very rapid methods for incorporating ^{3}H into compounds. The newer methods, generally involving metal-catalyzed exchange reactions [15–18], in our experience, mean that suitable labels can often be prepared in 2 or 3 weeks. These timescales make the approach viable for discovery support. Additionally, and importantly, these methods can lead to *specific* incorporation of tritium.

There is a general prejudice among drug metabolism scientists against using tritiated compounds. This is because such labels have often given rise to the formation of $^{3}H_2O$. Tritiated water has a remarkably long half-life in the body of between 6 and 9 days [19–22], and this is probably much longer than the half-life of the compound of interest or its metabolites. In any studies, significant production of $^{3}H_2O$ is an unwanted complication. However, we have found that *specifically* labeled compounds often lose only small amounts of radioactivity as $^{3}H_2O$, and most of this can be readily removed by freeze–drying the samples. Hence, it is usually possible to gain comprehensive information about the fate of the bulk of the dose. We have often found the use of a ^{3}H-labeled compound has significantly improved our knowledge of a compound, and hence its chemical series, and given clear information on the major pathways of clearance or extent of absorption. This then allows the data from *in vitro* screens to be used with greater confidence.

8.4.2 *Ex Vivo* Methods for Absorption

8.4.2.1 Static Method

There are several approaches to estimating absorption using *in vitro* methods, notably, Caco-2 and MDCK cell-based methods or using methods that assess passive permeability, for example, the parallel artificial membrane permeation assay (PAMPA) method. These are reviewed elsewhere in this book. The assays are very useful and usually have an important role in the screening cascades for drug

discovery projects. However, as discussed below, the cell-based assays are not without their drawbacks, and it is often appropriate to use *ex vivo* and/or *in vivo* absorption assays.

The simplest *ex vivo* assay consists of isolating segments of the GIT in an anesthetized rat, while leaving the blood and nervous supply intact as far as possible [23]. Hence, the segments continue to receive a blood supply, and any absorbed compound is carried away. The compound of interest is injected into segments, and at the end of the study the isolated segments are collected and analyzed for remaining compound. Absorption is estimated by loss. By injecting the compound into different segments at different times, a time course for the loss may be established. The approach has the advantage of simplicity, but suffers from the need to obtain good recoveries from what is often a difficult matrix to analyze. For poorly absorbed compounds – often the ones for which reliable estimation of absorption is needed – the method is unable to accurately determine small differences.

8.4.2.2 **Perfusion Methods**

Because of these problems, perfusion assays have been developed. Success in predicting absorption in man using *in-situ* single-pass perfusion of the rat intestine has been reported [24–26]. In this model, the animal is anesthetized and a segment of the gut is exposed and cannulated. A formulation of the drug is perfused through the gut segment, and the concentration before and after perfusion is determined. This approach has the advantage of being able to make several estimations of the concentration of the perfusate and of allowing measurements to be made from a cleaner matrix.

For a series of rennin inhibitors, a good correlation between the measured membrane permeability and $\log D$ was found ($r^2 = 0.8$). The model has been validated against a human perfusion model [10], as well as being extended by including molecular weight as a third parameter [27]. A further development of the model is to chronically cannulate the animals so that they can be allowed to recover [28]. This model should minimize any effects of the anesthetic on the absorption process.

Using the single-pass *in-situ* absorption model in the anesthetized rat, a study of nine compounds found a good correlation between rat and man as to whether compounds were subject to active uptake or absorbed by simple passive diffusion [29].

However, because of the significant surgical alterations that are necessary, studies using isolated perfused gut loops do not always accurately predict the results in whole animals, and there can be significant advantages in whole animal models for absorption.

8.4.3
In Vivo Methods

There are several possible *in vivo* approaches to the determination of the absorption of a compound after oral dosing. Probably the simplest and most direct is to use a

radiolabel. For the vast majority of studies, this means either a ^{14}C or ^{3}H label. The approach used can be quite simple: the labeled version of the drug is administered to an animal that is then housed in a "metabolism cage" for the separate, and complete, collection of both urine and feces. The samples of excreta are collected for as long as is necessary to obtain a full recovery of radioactivity. They are then analyzed for radioactive content. At its simplest, it can usually be assumed that, after an oral dose, at least all of the radioactivity that appears in the urine must have been absorbed, thus giving an assessment of the minimum absorption of the compound. Collecting the feces and subjecting them to chromatographic analysis with radiodetection can refine the study. This allows the identification of the proportion of the dose that has been absorbed but then excreted in the bile as metabolites (as opposed to the dose that has not been absorbed and has passed straight through the GIT as the parent compound). This approach should be supported with further studies to ensure that the parent compound is not metabolized directly in the GIT by the microflora. However, it is possible to be misled if the parent compound is absorbed but excreted unchanged in the bile.

Another refinement, that avoids the necessity of developing suitable fecal extraction and chromatographic methods, is to dose the radiolabeled compound by both the i.v. and p.o. routes in two separate studies. Knowing that, by definition, the whole of the i.v. dose must have been bioavailable; a comparison of the proportion of the dose in the urine after the two different routes allows estimation of the percent absorbed. An analogous approach can be used without the use of a radiolabel, when the urine from the two studies is analyzed either for the parent compound or, more usually, for a major common metabolite. Assuming quantitatively identical clearance after both the i.v. and p.o. doses, the ratio of the amounts of analyte in the two experiments gives the absorption.

8.5
In Vivo Methods for Determining Bioavailability

8.5.1
Cassette Dosing

Cassette dosing or "*N* into 1" dosing was one of the first techniques used to enhance the throughput of ADME/PK studies. It has the advantage of reducing the number of animals used and increasing the number of compounds that can be tested in a set time. This method involves dosing each animal with several compounds at the same time [30]. The selectivity and sensitivity of analytical methods now available, usually HPLC/mass spectrometry [31], mean that it is possible to analyze for each of the compounds in the presence of others [32, 33]. Although reports on cassettes of up to 22 compounds have been made [34], it is more usual to limit the number to between 3 and 6. There are significant benefits to this approach, as animals are only dosed once and the same number of plasma samples is collected as would be for a single compound study. However, the dose levels must be limited in order to

minimize possible stress to the animals and possible compound–compound interactions.

The potential for the metabolites that are formed to have the same masses as other parent compounds is another factor that limits the number of compounds that may be included in the cassette, as does the potential for drug–drug interactions [35]. Other limitations are the total dose that can be administered without saturating important pathways of metabolism or distribution and the solubility of the compounds in the dosing formulation. However, there is a balance to be achieved as, if the dose of each component given is very low, it is likely that the analytical method will not have sufficient sensitivity to provide an accurate assessment of the pharmacokinetics.

Nonetheless, the approach can provide – both routinely and rapidly – large amounts of pharmacokinetic or other distribution information on several compounds without significantly increasing the burden on the animals, while also minimizing the number of animals used. It is common to include a compound of known pharmacokinetics that acts as a control in each of these studies. This can help in identifying when the coadministered compounds have changed the kinetics. However, such marker compounds will not necessarily highlight problems with compounds that are subject to different clearance mechanisms [35].

8.5.2 Semisimultaneous Dosing

An approach that can bring benefits by reducing variability and increasing the speed of generating results is to use "semisimultaneous dosing" pharmacokinetic studies [36]. In these studies, animals are dosed by the two different routes of interest, a short period apart: often 4–6 h and usually less than 48 h. Blood samples are collected in the usual way following the dosing and analyzed for the parent compound. The pharmacokinetic profiles are then constructed, subtracting out, if necessary, any part of the profile from the first dose that is still present during the profile from the second dose [37]. These studies allow both profiles to be determined in the same animals at essentially the same time ("semisimultaneous"). This has the advantage of reducing variability in the pharmacokinetic profiles from the two doses and allowing a more reliable comparison of the two profiles. To ensure that there is not a significant increase in the number of samples that are taken to determine the two profiles, the samples can be withdrawn through an indwelling catheter or the total number of venepunctures restricted to the same number that would be used for single-dosing studies. The total amount of blood taken need not be significantly greater than is taken in a normal pharmacokinetic study, and so there is little increase in the stress on the animals. These studies have the advantage of eliminating a second procedure for the animals, while retaining the advantage of a crossover design with little chance for significant alteration in the factors that control the pharmacokinetics between the two doses. The approach also generates information more rapidly than when there is a "washout" period between the two doses.

The original proposal of the approach, supported by a Monte Carlo simulation study [36], has been further validated with both preclinical [38, 39] and clinical

studies [40]. It has been shown to be robust and accurate and is not highly dependent on the models used to fit the data. The method can give poor estimates of absorption or bioavailability in two sets of circumstances: (i) when the compound shows nonlinear pharmacokinetics, which may happen when the plasma protein binding is nonlinear, or when the compound has cardiovascular activity that changes blood flow in a concentration-dependent manner; or (ii) when the rate of absorption is slow, and hence "flip-flop" kinetics are observed, that is, when the apparent terminal half-life is governed by the rate of drug input.

8.5.3
Hepatic Portal Vein Cannulation

The use of hepatic portal vein-cannulated animals can be helpful in determining specific causes of poor bioavailability. After oral dosing, the total bioavailability of a compound is normally calculated as

$$\text{Bioavailability} = \frac{\text{AUC}_{\text{po}}}{\text{AUC}_{\text{iv}}} \times \frac{\text{Dose}_{\text{iv}}}{\text{Dose}_{\text{po}}}, \tag{8.1}$$

where AUC is the area under the drug concentration–time curve to infinite time and p.o. and i.v. indicate oral or intravenous routes. The oral bioavailability can also be considered from the perspective of loss at different stages of the process of reaching the systemic circulation, that is,

$$F_{\text{oral}} = (1-f_{\text{G}})(1-f_{\text{H}})(1-f_{\text{abs}}), \tag{8.2}$$

where f_{abs} is the fraction not absorbed from the GIT, and f_{G} and f_{H} are the fractions of drug cleared (e.g., metabolized) in the gut wall and the liver, respectively. It is possible to measure the relative contributions of these processes by carrying out dosing and or sampling of the hepatic portal vein [41] in addition to the normal methods of p.o. and i.v. dosing coupled with i.v. sampling. Thus,

$$f_{\text{G}} = \frac{1-\text{AUC}_{\text{po}}}{\text{AUC}_{\text{hpv}}} \tag{8.3}$$

and

$$f_{\text{H}} = \frac{1-\text{AUC}_{\text{hpv}}}{\text{AUC}_{\text{iv}}}. \tag{8.4}$$

These multiple input experiments can be carried out in a crossover fashion.

8.6
Inhalation

There are many ways of administering compounds to man or preclinical safety species, and it is not possible to review them all within the scope of this chapter. However, the inhalation route is worthy of some consideration as it can be important.

This is usually when the target organ is the lung, in diseases such as asthma or chronic obstructive pulmonary disorder (COPD), or when the lung may be a suitable route of administration for the systemic delivery of macromolecular peptide or protein biopharmaceuticals – compounds that would neither survive passage through, nor be absorbed from, the GIT [42, 43]. The absorption of these molecules is thought to occur by diffusion in the conducting airways [44] and by diffusion and transcytosis in the alveolar region of the lungs [42]. Even with the lower metabolic activity in the lung [45], direct administration can be a useful way of delivering compounds to their site of action, while limiting systemic side effects.

However, it is rarely possible to carry out inhalation studies during the research phase. Compared with intratracheal (i.t.) dosing, inhalation dosing is perhaps physiologically more similar to the clinical dosing method, is noninvasive, results in lower dose rates, and may well provide more even and representative distribution within the lungs. Nonetheless, i.t. instillation is often a worthwhile alternative as it allows accurately quantified doses to be administered and does not require the complex dosing systems needed in inhalation studies. Inhalation dosing invariably leads to significant oral exposure, either due to direct ingestion of the aerosol or by the animal grooming particles from its pelt after dosing has finished (see Ref. [46] and references cited therein). Although, i.t. administration has been shown to produce a very nonuniform distribution within the lungs, it has also been possible to obtain remarkably consistent, dose-proportional absorption over a wide range of doses (up to two and four orders of magnitude) [47], suggesting that absorption from the lung will not necessarily be saturated. Compounds given by the i.t. route can give rise to pharmacokinetics that closely mimic those of an i.v. dose [48, 49] with apparently very rapid and extensive absorption. However, i.t. dosing can also give indications of differing rates of absorption from the lung, depending on the compound and its physicochemical properties [45, 47, 50] or formulation [51, 52]. It has been reported that for a series of drugs, the absorption after aerosol administration was approximately twice as fast as through i.t. dosing [53], suggesting that absorption from the deeper alveolar region may be more rapid than that from the tracheobronchial region of the lung.

Although the usual animal model for i.t. studies is the rat [45, 47, 48, 54], studies on dogs [50, 54], rabbits [49], and guinea pigs [55] have also been reported.

A detailed review of i.t. dosing has recently been published [46], which provides practical details of the technique.

8.7 Relevance of Animal Models

8.7.1 Models for Prediction of Absorption

Measurement of the fraction absorbed, as described elsewhere in this book, can be carried out using *in vitro* systems. However, for Caco-2 cells, for example, the

relationship between the apparent rate of permeability that is measured and the percentage of the dose absorbed in man is often very steep. Thus, small changes in the measured rate of permeation may result in a compound with low human absorption being predicted to have good absorption [6, 56]. Other model systems, such as those based on the use of gut tissue in Ussing chambers, are highly dependent on the supply of good-quality tissue. Because of these kinds of issues, *in vivo* models can have significant advantages over the *in vitro* systems. Although the rate of absorption can be highly variable, the extent has often been shown to be similar between species including man (see for example Ref. [57] and references cited therein), and this similarity has recently been analyzed and the correlation between percentage dose absorbed in rat and man shown to be reliable and quantitative [58]. The relationship was analyzed for a group of 64 drugs, which covered a wide range of physical properties (acids, bases, neutrals, and zwitterions) and molecular weights (138–1202 Da). Also included were compounds for which absorption may involve carrier-mediated mechanisms. Excluded were compounds thought to be unstable in the GIT or which are affected by particle size or are polymorphic. The ratio between percent absorbed in human and rat was found to be very close to 1, with a correlation coefficient of 0.97.

The other principal preclinical PK model – the dog – is not thought to be such a useful model for prediction of absorption in man because of larger pore size and greater pore frequency in the paracellular pathway of dog compared with rat [59].

8.7.2
Models for Prediction of Volume

Estimation of the volume of distribution in man may be carried out in a number of ways. These methods have recently been reviewed by Obach *et al.* [60], who carried out a wide-ranging evaluation of a large number of different ways of predicting the human pharmacokinetics of 50 compounds that entered development at Pfizer. One of the simplest methods was reported to be the most reliable. It is based on the assumption that the free fraction of drug in the plasma in dog and human and the volume of distribution are proportional, that is, free $V_{d(human)} =$ free $V_{d(dog)}$. This allows a prediction for V_d in man to be generated:

$$V_{d(\text{predicted in man})} = f_{u(man)} \times V_{d(dog)}/f_{u(dog)} \tag{8.5}$$

Both human and dog volumes are in units of L kg^{-1}, and f_u is the fraction of the drug unbound in plasma. The method was found to predict within twofold for about 80% of the compounds, which spanned about three orders of magnitude in their V_d. Although the dog has been recommended as the best model for predicting volume in man [60], there are also reports indicating that the rat may also be a suitable model [61].

8.8 Prediction of Dose in Man

8.8.1 Allometry

One of the most frequently used methods for predicting human pharmacokinetics from animal data is allometry. This technique was initially used to explain the relationship between body size and organ weights in animals [62–67]. The approach is based on finding a correlation between a physiological and the pharmacokinetic parameter of interest. Generally, the relationship takes the form of

$$y = a \times B^x, \tag{8.6}$$

where y is the dependent variable, for example, clearance; B is the independent variable, for example, body weight, brain size or maximum life span; and a and x are the allometric coefficient and exponent, respectively.

The allometric coefficient and exponent are determined empirically and are not thought to have any physiological correlate.

The drawback of this approach is that it is essentially empirical and does not allow for differences in metabolic clearance between the species, that is, it assumes that clearance is proportional to blood flow. This works well for compounds that are highly extracted in the liver and/or where passive renal clearance is the major pathway [5, 68]. An approach for compounds that are actively secreted into the urine has also been proposed [69], though the precise values of some of the physiological scaling factors have been questioned [70].

Unfortunately, when clearance is largely metabolic and low, allometry can significantly overpredict the human value [71]. Recent investigations have attempted to address this by combining allometric approaches with *in vitro* metabolism data [5].

A recent debate on allometric scaling has suggested that a great deal of further work is necessary before allometry can be used with confidence in a prospective manner. It is claimed that it is not possible to know in advance when allometry will not be suitable, and indeed the accuracy of the predictions may not be as reliable as assumed [72–74].

8.8.2 Physiologically Based Pharmacokinetics

Another method of predicting human pharmacokinetics is physiologically based pharmacokinetics (PB/PK). The normal pharmacokinetic approach is to try to fit the plasma concentration–time curve to a mathematical function with one, two, or three compartments, which are really mathematical constructs necessary for curve fitting, and do not necessarily have any physiological correlates. In PB-PK, the model consists of a series of compartments that are taken to actually represent different tissues [75–77] (Figure 8.3). In order to build the model, it is necessary to know the size and perfusion rate of each tissue, the "partition coefficient" of the compound

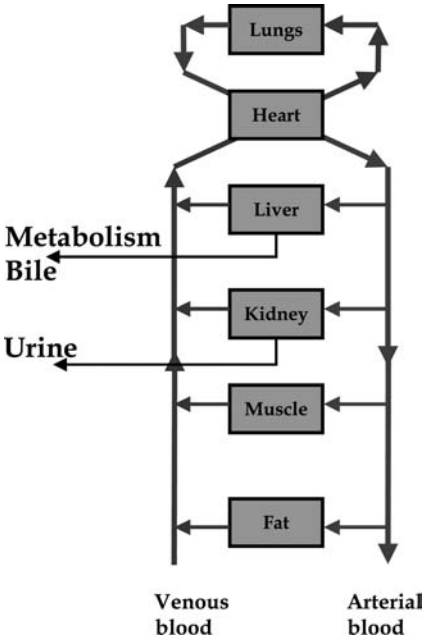

Figure 8.3 Physiological pharmacokinetic model.

between each tissue and blood, and the rate of clearance of the compound in each tissue. Although different sources of errors in the models have been described [78–80], these kinds of models are extremely appealing to kineticists because they lead to a fuller understanding of the factors that determine the pharmacokinetics of any compound. However, they require many experimental determinations to be made for each compound, and thus they are unlikely to become the method of choice during the routine design, make/test cycle (see Figure 8.1).They may however, become an important contributor to the decision about the suitability of a compound to progress into development.

8.8.3
Prediction of Human Dose

As stated in the Section 8.1, one of the principal purposes of carrying out DMPK studies during the discovery phase is to reduce the failure rate during development. For DMPK, this logically means predicting the pharmacokinetics that will be observed and hence the dose that will be required in man when clinical studies are carried out.

It is possible to predict the steady-state minimum plasma concentration (Figure 8.4) using the equation

$$C_{\mathrm{min,ss}} = \frac{f_{\mathrm{a}} \cdot \mathrm{Dose}}{V(\mathrm{e}^{k\tau}-1)}, \tag{8.7}$$

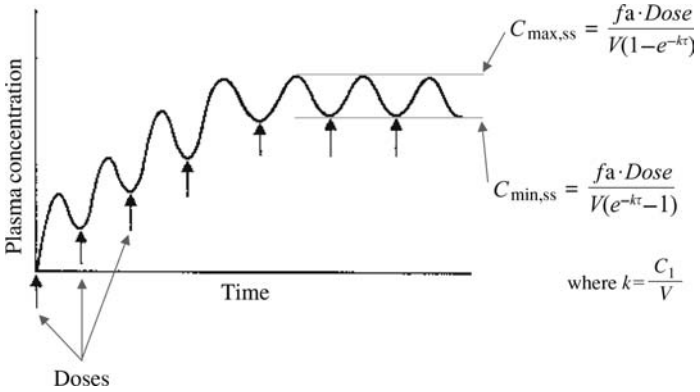

Figure 8.4 Dose prediction.

where $C_{min,ss}$ is the minimum plasma concentration at steady state; f_a is the fraction absorbed in man; Dose is the dose (in mg kg^{-1}); V is the volume of distribution at steady state (in l kg^{-1}); k is the elimination constant (this is given by clearance divided by volume); and τ is the dosing interval given in h^{-1}.

The equation is an approximation, adapted from that for intravenous dosing [81], corrected by addition of a term for absorption. Essentially it assumes instantaneous absorption of the dose, but for compounds with reasonable physicochemical and PK properties that are expected to be suitable for once-a-day dosing, this approximation makes little difference to the predicted value of $C_{min,ss}$. Use of the relationship can provide a simple approach for estimating the required dose in man for a compound in the discovery phase.

Equation 8.7 can be rearranged to allow the prediction of the dose and dose interval, provided that the following can be estimated: human potency, absorption, clearance, and volume.

Estimation of the potency can be made in several ways and will be highly dependent on the nature of the target. If a purified system is used, it is normal to correct for the effect of plasma protein binding (which can be measured directly in human plasma) as it is usual for the effect to be proportional to the unbound concentration [82]. This can be used to set a value for the minimum plasma concentration at steady state.

As described above, it will be normal to assume that the dose interval is 24 h, that is, once-a-day dosing. Absorption can be estimated with good confidence in the rat (see Section 8.1). Clearance is the sum of the predicted hepatic, renal, biliary, and extrahepatic clearance. Hepatic clearance can be derived from *in vitro* studies with the appropriate human system, using either microsomes or hepatocytes. We prefer to use an approach based on that described by Houston and Carlile [83]. Renal clearance can be predicted allometrically (see Section 8.8.1). The other two potential methods of clearance are difficult to predict. To minimize the risks, animal studies can be used to select compounds that show little or no potential for clearance by these routes. As volume can be predicted from that measured in the dog, after correction for human

and dog plasma protein binding (see Section 8.2), it is possible to make predictions for all of the important parameters necessary.

We believe that this approach brings together the best combination of *in vitro*, *in vivo*, and allometric approaches and can provide useful estimates of likely human doses, provided that sufficient attention is paid to the errors associated with all of the measurements [4].

8.9 Conclusions

The purpose of this chapter has been to illustrate the potential role of animal studies in ADME/PK in drug discovery. Given that one of the major objectives for ADME/PK is to predict PK in man, it must be concluded that much work is still to be done in the development of reliable and accurate models. Although, quite rightly, many studies have focused on *in silico* and *in vitro* approaches, there is still a general agreement that, with current knowledge, we are still highly dependent on animal models [3, 5, 6, 84]. Indeed, their use in predicting important parameters such as absorption and volume of distribution has been highlighted in this chapter.

References

1 Prentis, R.A., *et al.* (1988) Pharmaceutical innovation by the seven UK-owned pharmaceutical companies (1964–1985). *British Journal of Clinical Pharmacology*, **25**, 387–396.

2 McAuslane, N. (1999) Accelerating preclinical development by successful integration into drug discovery. Vision in Business, Conference 25–26 February, Nice, France.

3 Eddershaw, P.J., Beresford, A.P. and Bayliss, M.K. (2000) ADME/PK as part of a rational approach to drug discovery. *Drug Discovery Today*, **5**, 409–414.

4 Davis, A.M., Dixon, J., Logan, C.J. and Payling, D.W. (2002) Accelerating the process of drug discovery, in *Pharmacokinetic Challenges in Drug Discovery* (eds O. Pelkonen, A. Baumann and A. Reichel), Springer, Berlin, pp. 1–32.

5 Lavé, T., Coassolo, P. and Reigner, B. (1999) Prediction of hepatic metabolic clearance based on interspecies allometric scaling techniques and *in vitro–in vivo* correlations. *Clinical Pharmacokinetics*, **36**, 211–321 and references cited therein.

6 van de Waterbeemd, H., Smith, D.A., Beaumont, K. and Walker, D.A. (2001) Property based design: optimisation of drug absorption and pharmacokinetics. *Journal of Medicinal Chemistry*, **44**, 1313–1333.

7 Davis, S.S., Hardy, J.G. and Fara, J.W. (1986) Transit of pharmaceutical dosage forms through the small intestine. *Gut*, **27**, 886–892.

8 Seelig, A. (1998) How does P-glycoprotein recognise its substrates? *International Journal of Clinical Pharmacology and Therapeutics*, **36**, 50–54.

9 Seelig, A. and Landwojtowicz, E. (2000) Structure–activity relationship of P-glycoprotein substrates and modifiers. *European Journal of Pharmaceutical Sciences*, **12**, 31–40.

10 Fagerholm, U., Johansson, M. and Lennernäs, H. (1996) Comparison between permeability coefficients in rats

and human jejunum. *Pharmaceutical Research*, **13**, 1336–1341.

11 Schwarz, U.I., Gramatté, T., Krappweis, J., Berndt, A., Oertel, R., von Richter, O. and Kirch, W. (1999) Unexpected effect of verapamil on oral bioavailability of the beta-blocker talinolol in humans. *Clinical Pharmacology and Therapeutics*, **65**, 283–290.

12 Sanderström, R., Knutson, L., Knutson, T., Jannson, B. and Lennernäs, H. (1999) The effect of ketoconazole on jejunal permeability and CYP 3A4 metabolism of *R/S* verapamil in humans. *British Journal of Clinical Pharmacology*, **48**, 180–189.

13 Hem, A., Smith, A.J. and Solberg, P. (1998) Saphenous vein puncture for blood sampling of the mouse, rat, hamster, gerbil, guinea-pig, ferret and mink. *Laboratory Animals*, **32**, 364–368 and http://www.uib.no/vivariet.

14 Cochran, W.G. and Cox, G.M. (1964) *Experimental Designs*, 2nd edn, John Wiley and Sons, Inc.

15 Kingston, L.P., Lockley, W.J.S., Mather, A.N., Spink, E., Thompson, S.P. and Wilkinson, D.J. (2000) Parallel chemistry investigations of orthodirected hydrogen isotope exchange between substituted aromatics and isotopic water: novel catalysis by cyclooctadienyliridium(I) pentan-1,3- dionates. *Tetrahedron Letters*, **41**, 2705–2708.

16 Kingston, L.P., Lockley, W.J.S., Mather, A.N., Spink, E., Thompson, S.P. and Wilkinson, D.J. (2000) Hydrogen isotope labelling: novel applications of parallel chemistry techniques. International Isotope Society Symposium, June 2000, Dresden.

17 Shu, A.Y.L., Saunders, D., Levinson, S.H., Landvatter, S.W., Mahoney, A., Senderoff, S.G., Mack, J.F. and Heys, J.R. (1999) Direct tritium labelling of multifunctional compounds using organoiridium catalysis 2. *Journal of Labelled Compounds & Radiopharmaceuticals*, **42**, 797–807.

18 Chen, W., Garnes, K.T., Levinson, S.H., Saunders, D., Senderoff, S.G., Shu, A.Y.L., Villani, A.J. and Heys, J.R. (1997) Direct tritium labelling of multifunctional compounds using organoiridium catalysis. *Journal of Labelled Compounds & Radiopharmaceuticals*, **39**, 291–298.

19 Trivedi, A., Galeriu, D. and Richardson, R.B. (1997) Dose contribution from metabolized organically bound tritium after acute tritiated water intakes in humans. *Health Physics*, **73**, 579–586.

20 Foy, J.M. and Schnieden, H. (1960) Estimation of total body water (virtual tritium space) in the rat, cat, rabbit, guinea-pig, and man, and of the biological half-life of tritium in man. *The Journal of Physiology*, **154**, 169–176.

21 Wylie, K.F., Bigler, W.A. and Grove, G.R. (1963) Biological half-life of tritium. *Health Physics*, **9**, 911–914.

22 Cawley,C.N., Spitzberg, D.B., Cale, W.G., Jr and Fenyves, E.J. (1978) A model to estimate the biological halflife of tritium in man. *Proceedings of Summer Computer Simulation Conference*, 629–635.

23 Doluisio, J.T., Billups, N.F., Dillert, L.W., Sugita, E.T. and Swintosky, J.V. (1969) Drug absorption I: an *in situ* rat gut technique yielding realistic absorption techniques. *Journal of Pharmaceutical Sciences*, **58**, 1196–1200.

24 Amidon, G.L., Lennernäs, H., Shah, V.P. and Crison, J. (1995) A theoretical basis for a biopharmaceutical drug classification: the correlation of *in vitro* drug product dissolution and *in vivo* bioavailability. *Pharmaceutical Research*, **12**, 413–420.

25 Steffansen, B., Lepist, E.-I., Frökjaer, S., Taub, M. and Lennernäs, H. (1999) Stability, metabolism and transport of D-ASP(OBZL) – a model prodrug with affinity for the oligopeptide transporter. *European Journal of Pharmaceutical Sciences*, **8**, 67–73.

26 Abrahamsson, B., Alpsten, M., Hugosson, M., Jonsson, U.E., Sundgren, M., Svenheden, A. and Tolli, J. (1993) Absorption, gastrointestinal transit, and tablet erosion of felodipine extended

release (ER) tablets. *Pharmaceutical Research*, **10**, 709–714.

27 Artursson, P., Ungell, A.-L. and Löfroth, J.-E. (1993) Selective paracellular permeability in two models of intestinal absorption: cultured monolayers of human intestinal epithelial cells and rat intestinal segments. *Pharmaceutical Research*, **10**, 1123–1129.

28 Poelma, F.G.J. and Tukker, J.J. (1987) Evaluation of the chronically isolated internal loop in the rat for the study of drug absorption kinetics. *Journal of Pharmaceutical Sciences*, **76**, 433–436.

29 Amidon, G.L., Sinko, P.J. and Fleisher, D. (1988) Estimating human oral fraction dose absorbed: a correlation using rat intestinal membrane permeability for passive and carrier-mediated compounds. *Pharmaceutical Research*, **5**, 651–654.

30 Toon, S. and Rowland, M. (1983) Structure–pharmacokinetic relationships among the barbiturates in the rat. *The Journal of Pharmacology and Experimental Therapeutics*, **225**, 752–763.

31 Bryant, M.S., Korfmacher, W.A., Wang, S., Nardo, C., Nomeir, A.A. and Lin, C.-C. (1997) Pharmacokinetic screening for the selection of new drug discovery candidates is greatly enhanced through the use of liquid chromatography–atmospheric pressure ionization tandem mass spectrometry. *Journal of Chromatography. A*, **777**, 61–66.

32 Berman, J., Halm, K., Adkinson, K. and Shaffer, J. (1997) Simultaneous pharmacokinetic screening of a mixture of compounds in the dog using API LC/MS/MS analysis for increased throughput. *Journal of Medicinal Chemistry*, **40**, 827–829.

33 Olah, T.V., McLoughlin, D.A. and Gilbert, J.D. (1997) The simultaneous determination of mixtures of drug candidates by liquid chromatography/atmospheric pressure chemical ionisation mass spectrometry as an *in vivo* drug screening procedure. *Rapid Communications in Mass Spectrometry*, **11**, 17–23.

34 Shaffer, J.E., Adkison, K.K., Halm, K., Hedeen, K. and Berman, J. (1999) Use of '*N*-in-One' dosing to create an *in vivo* pharmacokinetics database for use in developing structure–pharmacokinetic relationships. *Journal of Pharmaceutical Sciences*, **88**, 313–318.

35 White, R.E. and Manitpisitkul, P. (2001) Pharmacokinetic theory of cassette dosing in drug discovery screening. *Drug Metabolism and Disposition*, **29**, 957–966.

36 Karlsson, M.O. and Bredberg, U. (1990) Bioavailability estimation by semi-simultaneous drug administration: a Monte Carlo simulation study. *Journal of Pharmacokinetics and Biopharmaceutics*, **18**, 103–120.

37 Gabrielsson, J. and Weiner, D. (1997) *Pharmacokinetic and Pharmacodynamic Data Analysis: Concepts and Applications*, 2nd edn, Swedish Pharmaceutical Society, Swedish Pharmaceutical Press, Stockholm, pp. 412–418.

38 Karlsson, M.O. and Bredberg, U. (1989) Estimation of bioavailability on a single occasion after semisimultaneous drug administration. *Pharmaceutical Research*, **6**, 817–821.

39 Bredberg, U. and Karlsson, M.O. (1991) *In vivo* evaluation of the semisimultaneous method for bioavailability estimation using controlled intravenous infusion as an 'extravascular' route of administration. *Biopharmaceutics & Drug Disposition*, **12**, 583–597.

40 Karlsson, M.O. and Lindberg-Freijs, A. (1990) Comparison of methods to calculate cyclosporine A bioavailability from consecutive oral and intravenous doses. *Journal of Pharmacokinetics and Biopharmaceutics*, **18**, 293–311.

41 Griffiths, R., Lewis, A. and Jeffrey, P. (1996) Models for drug absorption *in situ* and in conscious animals, in *Models for Assessing Drug Absorption and Metabolism* (eds R.T. Borchard, P.L. Smith and G. Wilson), Plenum Press, New York, pp. 67–84.

42 Patton, J.S. and Platz, R.M. (1992) Routes of delivery: case studies – (2) Pulmonary

delivery of peptides and proteins for systemic action. *Advanced Drug Delivery Reviews*, **8**, 179–196.

43 Byron, P.R. (1990) Determinants of drug and polypeptide bioavailability from aerosols delivered to the lung. *Advanced Drug Delivery Reviews*, **5**, 107–132.

44 Taylor, A.E. and Gaar, K.A. (1970) Estimation of pore radii of pulmonary and alveolar membranes. *The American Journal of Physiology*, **218**, 1133–1140.

45 Chanoine, F., Grenot, C., Heidmann, P. and Junien, J.L. (1991) Pharmacokinetics of butixocort 21-proprionate, budesonide, and beclomethazone diproprionate in the rat after intratrachael, intravenous and oral treatments. *Drug Metabolism and Disposition*, **19**, 546–553.

46 Driscoll, K.E., Costa, D.L., Hatch, G., Henderson, R., Oberdorster, G., Salem, H. and Schlesinger, R.B. (2000) Intratracheal instillation as an exposure technique for the evaluation of respiratory tract toxicity: uses and limitations. *Toxicological Sciences*, **55**, 24–35.

47 Enna, S.J. and Schanker, L.S. (1972) Absorption of saccharides and urea from the rat lung. *The American Journal of Physiology*, **222**, 409–414.

48 Lizio, R., Klenner, T., Borchard, G., Romeis, P., Sarlikiotis, A.W., Reissmann, T. and Lehr, C.-M. (2000) Systemic delivery of the GnRH antagonist cetrorelix by intratracheal instillation in anaesthetized rats. *European Journal of Pharmaceutical Sciences*, **9**, 253–258.

49 Irazuzta, J.E., Ahmad, U., Gancayaco, A., Ahmed, S.T., Zhang, J. and Anand, K.J.S. (1996) Intratracheal administration of fentanyl: pharmacokinetics and local tissue effects. *Intensive Care Medicine*, **22**, 129–133.

50 Bennett, D.B., Tyson, E., Nerenberg, C.A., Mah, S., de Groot, J.S. and Teitelbaum, Z. (1994) Pulmonary delivery of detirelix by intratracheal instillation and aerosol inhalation in the briefly anaesthetized dog. *Pharmaceutical Research*, **11**, 1048–1054.

51 Smith, S.A., Pillers, D.-A.M., Gilhooly, J.T., Wall, M.A. and Olsen, G.D. (1995) Furosemide pharmacokinetics following intratracheal instillation in the guinea pig. *Biology of the Neonate*, **68**, 191–199.

52 Klyashchitsky, B.A. and Owen, A.J. (1999) Nebulizer-compatible liquid formulations for aerosol pulmonary delivery of hydrophobic drugs: glucocorticoids and cyclosporine. *Journal of Drug Targeting*, **7**, 79–99.

53 Schanker, L.S., Mitchell, E.W. and Brown, R.A., Jr (1986) Species comparison of drug absorption from the lung after aerosol inhalation or intratracheal injection. *Drug Metabolism and Disposition*, **14**, 79–88.

54 Leusch, A., Eichhorn, B., Müller, G. and Rominger, K.-L. (2001) Pharmacokinetics and tissue distribution of the anti-cholinergics tiotropium and ipratropium in the rat and the dog. *Biopharmaceutics & Drug Disposition*, **22**, 199–212.

55 Trnovec, T., Durisova, M., Bezek, S., Kallay, Z., Navarova, J., Tomcikova, O., Kettner, M., Faltus, F. and Erichleb, M. (1984) Pharmacokinetics of gentamicin administered intratracheally or as an inhalation aerosol to guinea pigs. *Drug Metabolism and Disposition*, **12**, 641–614.

56 Stewart, B.H., Chan, O.H., Lu, R.H., Reyner, E.L., Schmid, H.L., Hamilton, H.W., Steinbaugh, B.A. and Taylor, M.D. (1995) Comparison of intestinal permeabilities determined in multiple *in vitro* and *in situ* models: relationship to absorption in humans. *Pharmaceutical Research*, **12**, 693–699.

57 Clarke, B. and Smith, D.A. (1984) Pharmacokinetics and toxicity testing. *CRC Critical Reviews in Toxicology*, **12**, 343–385.

58 Chiou, W.L. and Barve, A. (1998) Linear correlation of the fraction of oral dose absorbed of 64 drugs between humans and rats. *Pharmaceutical Research*, **15**, 1792–1795.

59 He, Y.-L., Murby, S., Warhurst, G., Gifford, L., Walker, D., Ayrton, J., Eastmond, R. and Rowland, M. (1998) Species differences in

size discrimination in the paracellular pathway reflected by oral bioavailability of poly(ethylene glycol) and D-peptides. *Journal of Pharmaceutical Sciences*, **87**, 626–633.

60 Obach, R.S., Baxter, J.G., Liston, T.E., Silber, M., Jones, B.C., MacIntyre, F., Rance, D.J. and Wastall, P. (1997) The prediction of human pharmacokinetic parameters from preclinical and *in vitro* metabolism data. *The Journal of Pharmacology and Experimental Therapeutics*, **283**, 46–58.

61 Bachman, K., Pardoe, D. and White, D. (1996) Scaling basic toxicokinetic parameters from rat to man. *Environmental Health Perspectives*, **104**, 400–407.

62 Dedrick, R.L., Bishoff, K.B. and Zaharko, D.S. (1970) Interspecies correlation of plasma concentration history of methotrexate (NSC-740). *Cancer Chemotherapy Reports Part 1*, **54**, 95–101.

63 Mordenti, J. (1986) Man vs. beast: pharmacokinetic scaling in mammals. *Journal of Pharmaceutical Sciences*, **75**, 1028–1040.

64 Boxenbaum, H. (1982) Interspecies scaling, allometry, physiological time, and the ground plan of pharmacokinetics. *Journal of Pharmacokinetics and Biopharmaceutics*, **10**, 201–227.

65 Boxenbaum, H. (1984) Interspecies pharmacokinetic scaling and the evolutionary-comparative paradigm. *Drug Metabolism Reviews*, **15**, 1071–1121.

66 Boxenbaum, H. and DiLea, C. (1995) First-time-in-human dose selection: allometric thoughts and perspectives. *Journal of Clinical Pharmacology*, **35**, 957–966.

67 Mahmood, I. and Balian, J.D. (1996) Interspecies scaling: a comparative study for the prediction of clearance and volume using two or more species. *Life Sciences*, **59**, 579–585.

68 Jezequel, S.G. (1994) Fluconazole: interspecies scaling and allometric relationships of pharmacokinetic properties. *Journal of Pharmacy and Pharmacology*, **46**, 196–199.

69 Mahmood, I. (1998) Interspecies scaling of renally secreted drugs. *Life Sciences*, **63**, 2356–2371.

70 Ward, K.W., Proksch, P.D., Gorycki, P.D., Yu, C.-P., Ho, M.Y.K., Bush, B.D., Levy, M.A. and Smith, B.R. (2002) SB-242235, a selective inhibitor of p-38 mitogen-activated protein kinase. II: *in vitro* and *in vivo* metabolism studies and pharmacokinetic extrapolation to man. *Xenobiotica*, **32**, 235–250.

71 Boxenbaum, H. and D'Souza, R.W. (1990) Interspecies pharmacokinetic scaling, biological design and neoteny, in *Advances in Drug Research*, Vol. 19 (ed. B. Testa), Academic Press Ltd, London, pp. 139–196.

72 Bonate, P.L. and Howard, D. (2000) Critique of prospective allometric scaling: does the emperor have clothes? *Journal of Clinical Pharmacology*, **40**, 335–340.

73 Mahmood, I. (2000) Prospective allometric scaling: does the emperor have clothes? *Journal of Clinical Pharmacology*, **40**, 341–344.

74 Bonate, P.L. and Howard, D. (2000) Rebuttal to Mahmood. *Journal of Clinical Pharmacology*, **40**, 345–346.

75 Himmelstein, K.J. and Lutz, R.J. (1979) A review of the applications of physiologically based pharmacokinetic modelling. *Journal of Pharmacokinetics and Biopharmaceutics*, **7**, 127–145.

76 Rowland, M. (1984) Physiologic pharmacokinetic models: relevance, experience and future trends. *Drug Metabolism Reviews*, **15**, 55–74.

77 Balant, L.P. and Gex-Fabry, M. (1990) Review: physiological pharmacokinetic modelling. *Xenobiotica*, **20**, 1241–1257.

78 Jang, J.-Y., Droz, P.O. and Chung, H.K. (1999) Uncertainties in physiologically based pharmacokinetic models caused by several input parameters. *International Archives of Occupational and Environmental Health*, **72**, 247–254.

79 Khor, S.P. and Mayersohn, M. (1991) Potential error in the measurement of tissue to blood distribution coefficients in

physiological pharmacokinetic modeling: residual tissue blood. 1. Theoretical considerations. *Drug Metabolism and Disposition*, **19**, 478–485.

80 Khor, S.P., Bozigian, H. and Mayersohn, M. (1991) Potential error in the measurement of tissue to blood distribution coefficients in physiological pharmacokinetic modeling: residual tissue blood. 2. Distribution of phencyclidine in the rat. *Drug Metabolism and Disposition*, **19**, 486–490.

81 Rowland, M. and Tozer, T.N. (1994) *Clinical Pharmacokinetics: Concepts and Applications*, 3rd edn, Lippincott, Williams & Wilkins, Philadelphia, USA pp. 99.

82 Ross, E.M. (1995) Pharmacodynamics: mechanism of drug action and the relationship between drug concentration and effect, in *Goodman and Gilman's The Pharmacological Basis of Therapeutics*, 9th edn (eds J.G. Hardman, L.E. Limbird and A.G. Gilman), McGraw-Hill, New York, pp. 29–41.

83 Houston, J.B. and Carlile, D.J. (1997) Prediction of hepatic clearance from microsomes, hepatocytes and liver slices. *Drug Metabolism Reviews*, **29**, 891–922.

84 Balant, L.P. and Gex-Fabry, M. (2000) Modelling during drug development. *European Journal of Pharmaceutics and Biopharmaceutics*, **50**, 13–26.

9
In Vivo Permeability Studies in the Gastrointestinal Tract of Humans

Niclas Petri and Hans Lennernäs

Abbreviations

BCRP	Breast cancer-resistant protein
CYP3A4	Cytochrome P450 3A4
HBD	Number of hydrogen-bond donors
hPEPT1	Oligopeptide carrier for di- and tripeptides
LNAA	Large neutral amino acid
MRP	Multidrug-resistant protein family
P-gp	P-glycoprotein
PSA	Polar surface area

Symbols

CL_{int}	Intrinsic clearance
Clog *P*	Logarithm of the calculated octanol/water partition coefficient (for neutral species)
P_{eff}	Effective intestinal permeability
F	Bioavailability
F_a	Fraction dose absorbed
E_G	Gut wall extraction
E_H	Hepatic extraction
log $D_{6.5}$	Logarithm of the distribution coefficient in octanol/water at pH 6.5
MW	Molecular weight
Q_h	Hepatic blood flow

9.1 Introduction

The predominant way of delivering drugs to the systemic circulation to generate pharmacological and clinical effects is the oral route. Self-administration of drugs to

the gastrointestinal (GI) tract is considered to be safe, efficient, and easily accessible with minimal discomfort to the patient in comparison with other routes of drug administration. The design and composition of the pharmaceutical dosage formulation, as well as the physicochemical properties of the drug itself, will certainly affect *in vivo* performance and hence the therapeutic outcome. Bioavailability (F) of drugs after oral administration is determined by several factors such as solubility and dissolution, transit time, GI stability, intestinal permeability, and first-pass extraction in the gut and/or by the liver [1–4]. Among these factors, effective intestinal permeability (P_{eff}) is a major determinant of fraction dose absorbed (F_a) [1, 3, 5]. It is a recognized fact that some drugs may be transported by multiple mechanisms, passive diffusion, and various carrier-mediated transporters via both absorptive and secretory routes (Figure 9.1) [1, 3, 6–8]. The expression and functional activity of intestinal transport proteins and enzymes are currently under examination, and the future will reveal the extent to which various transporters contribute to intestinal absorption and presystemic metabolism of drugs (Figure 9.1) [9]. Undoubtedly, such knowledge will increase our understanding of the mechanisms underlying the variability between individuals and regulation of responses to drugs, from both genomic and nongenomic perspectives [9, 10]. In spite of the fact above, the *in vivo*

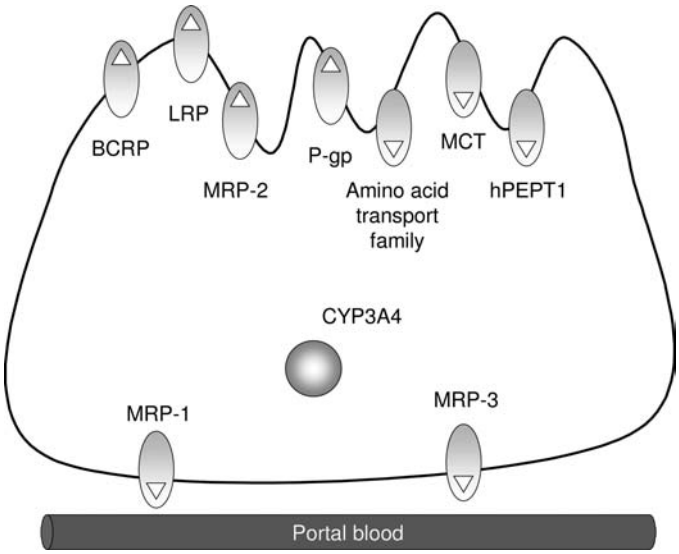

Figure 9.1 P_{eff} of drugs *in vivo* may be affected by several parallel transport mechanisms in both absorptive and secretory directions. A few of the most important transport proteins that may be involved in the intestinal transport of drugs and their metabolites across intestinal epithelial membrane barriers in humans are displayed. P-gp, P-glycoprotein; BCRP, breast cancer-resistant protein; LRP, lung-resistant protein; MRP1–5, multidrug-resistant protein family; hPEPT1, oligopeptide carrier for di- and tripeptides; MCT, $H^{(+)}$-monocarboxylic acid cotransporter. CYP3A4 is an important intracellular oxidation CYP P450 enzyme; approximately 50–60% of all used drugs are substrates for this enzyme.

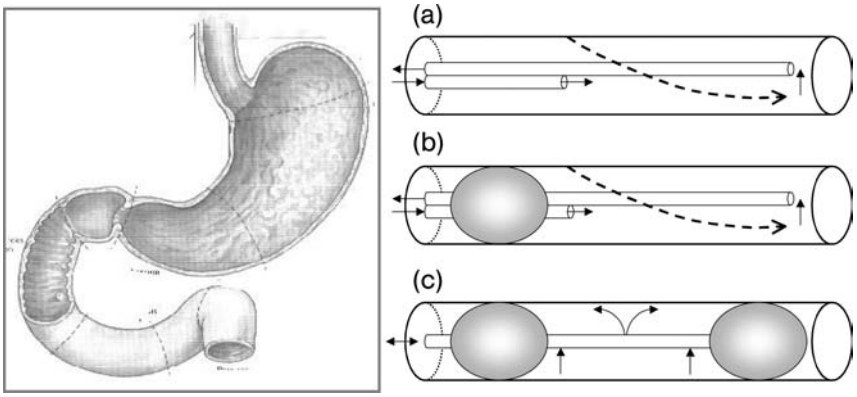

Figure 9.2 Schematic diagram of three different perfusion methodologies for human use: (a) open; (b) semiopen; and (c) double balloon. For the open and semiopen, the hydrodynamics is best described by the parallel-tube model (see the dotted line for the concentration profile over the intestinal length). The well-stirred model is the best hydrodynamic model for the double-balloon perfusion technique.

measured drug transport permeability (P_{eff}) represents the total transport (i.e., the macroscopic transport rate) of all parallel processes.

Direct measurements of intestinal absorption, secretion, and metabolism of drugs in humans are possible by using regional intestinal perfusion techniques [6, 11, 12]. In general, three different clinical tools have been employed in the small intestine: (i) a triple-lumen tube including a mixing segment, (ii) a multilumen tube with a proximal occluding balloon, and (iii) a multilumen tube (Loc-I-Gut) with two balloons occluding a 10 cm long intestinal segment (Figure 9.2) [5, 6, 11, 13–15] . The advantages and disadvantages of various intestinal perfusion techniques are discussed elsewhere [3, 16]. In Figure 9.3, the complete Loc-I-Gut concept is displayed [11, 13]. This intestinal perfusion technique has been widely applied to investigate drug absorption, presystemic metabolism, drug dissolution, *in vitro–in vivo* correlation, drug–drug interactions, variability between individuals, GI physiology, and disease mechanisms (Figure 9.4) [3, 11, 16–36]. The Loc-I-Gut approach makes it possible to investigate and predict integrated *in vivo* processes in the human intestine, where genetic, biochemical, physiological, pathophysiological, and environmental influences may all affect the transport/metabolism of drugs [3, 11]. In addition, the Loc-I-Gut technique has been used to establish an *in vivo* human permeability database for the proposed Biopharmaceutical Classification System (BCS) for oral immediate-release products (Figure 9.5) [1, 31, 37]. Human *in vivo* P_{eff} values obtained under physiological conditions provide the basis for establishing *in vitro–in vivo* correlations, which can be used to make predictions about oral absorption as well as to set bioequivalence standards for drug approval [1, 16, 21, 28, 29, 31]. Recently, this single-pass perfusion approach has been used for measurements of the expression and function of enzymes and transporters in human-shed (harvested) enterocytes in

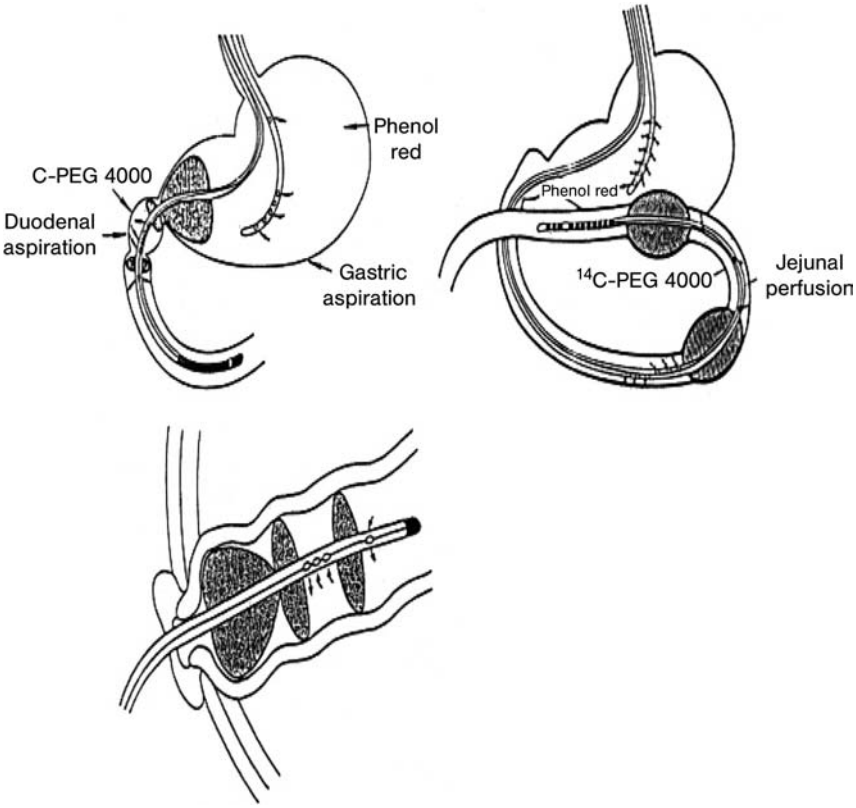

Figure 9.3 The total Loc-I-Gut concept. Left: a perfusion system of the duodenal segment. Center: the tube system with double balloons allows a segmental single-pass perfusion of jejunum. Below: a perfusion system of the small intestinal stomi.

combination with measurements related to transport and presystemic metabolism in the same individuals [38, 39]. This body of data clearly indicates that our understanding of intestinal absorption, secretion, and metabolism of drugs has been significantly increased through the application of intestinal perfusion techniques. The purpose of this chapter is to describe how human *in vivo* perfusion studies continue to provide important information on oral drug delivery and help summarize reports based on these techniques.

9.2
Definitions of Intestinal Absorption, Presystemic Metabolism, and Absolute Bioavailability

The most useful pharmacokinetic variable for describing the quantitative aspects of all processes influencing the absorption (fraction dose absorbed, F_a) and first-pass

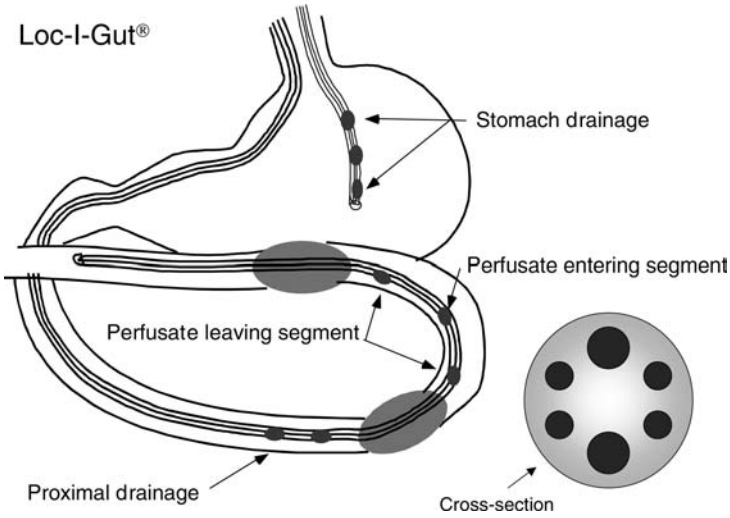

Figure 9.4 Loc-I-Gut is a perfusion technique for the proximal region of the human jejunum. The multichannel tube is 175 cm long and is made of polyvinyl chloride with an external diameter of 5.3 mm. It contains six channels and is provided distally with two 40 mm long, elongated latex balloons, placed 10 cm apart, each separately connected to one of the smaller channels. The two wider channels in the center of the tube are for infusion and aspiration of perfusate. The two remaining peripheral smaller channels are used for administration of marker substances and/or for drainage. At the distal end of the tube, a tungsten weight aids the passage of the tube into the jejunum. The balloons are filled with air when the proximal balloon has passed through the ligament of Treitz. Gastric suction is performed using a separate tube. ^{14}C-PEG 4000 is used as a volume marker to detect water flux across the intestinal barrier.

metabolism and excretion (E_G and E_H) in the gut and liver is the absolute bioavailability (F) [40]. This pharmacokinetic parameter defines the fraction of the dose that reaches the systemic circulation and is used in the evaluation of the pharmacological profile and safety of oral pharmaceutical products in various clinical situations. Bioavailability depends on three major factors: F_a, the first-pass extraction of the drug in the gut wall (E_G), and the liver (E_H) (Equation 9.1) [2–4, 15, 35]:

$$F = F_a \cdot (1-E_G) \cdot (1-E_H). \quad (9.1)$$

Several factors may affect F_a and E_G of drugs. These can be divided into three general categories: (i) pharmaceutical factors; (ii) physicochemical factors of the drug molecule itself; and (iii) physiological, genetic, biochemical, and pathophysiological factors in the intestine [3, 5–8, 11, 15, 27, 32, 41–46]. According to scientific and regulatory definitions, F_a is the fraction of the dose transported (absorbed) across the apical cell membrane into the cellular space of the enterocyte [3, 11, 16, 25–31, 47, 48]. Once the drug has reached the intracellular site, it may be subjected to CYP P450 metabolism, predominantly by CYP3A4, as well as other enzymatic steps [2–4, 15, 34, 35, 38, 49]. The enzymatic capacity of the small intestine to metabolize drugs can be expressed in pharmacokinetic terms as E_G [40]. It is important to emphasize that CYP3A4 is not expressed in the colon [50, 51] and that drug metabolism by colonic microflora

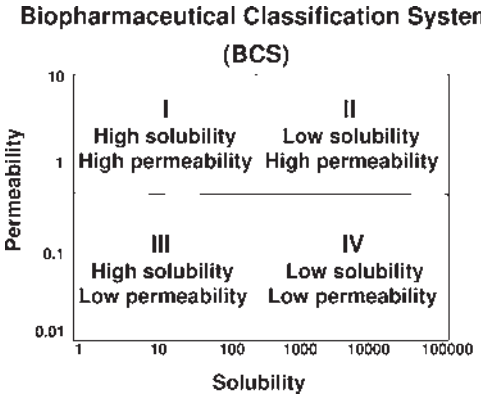

Figure 9.5 The Biopharmaceutics Classification System provides a scientific basis for predicting intestinal drug absorption and identifying the rate-limiting step based on primary biopharmaceutical properties such as solubility and P_{eff}. The BCS divides drugs into four different classes based on these two parameters. Drug regulation aspects related to *in vivo* performance of pharmaceutical dosage forms have been the driving force in the development of BCS. BCS-based guidelines for industry are mainly used to indicate when bioavailability/bioequivalence (BA/BE) studies can be replaced by *in vitro* bioequivalence testing (www.fda.gov/cder/guidance/3618fnl.htm).

may play a crucial role in colonic drug absorption, especially with regard to drugs given in extended-release dosage forms, which may be subjected to predominantly hydrolytic and other reductive reactions [52, 53]. The fraction that escapes metabolism in the small intestine ($1 - E_G$) may undergo additional metabolism and/or biliary secretion in the liver (E_H) before reaching the systemic circulation. E_H depends on blood flow (Q_h), protein binding (f_u), and the intrinsic clearance of enzymes and/or transporters (CL_{int}) [40]. Recently, it has also been recognized that membrane transport into hepatocytes must be included in models for predicting and explaining liver extraction.

9.3 Methodological Aspects of *In Vitro* Intestinal Perfusion Techniques

Clinical studies of P_{eff}, secretion, and metabolism of various compounds such as drugs, environmental pollutants, and nutrients are rarely performed *in vivo* in humans even if experimental techniques are available (Figures 9.2–9.4) [3, 11, 13, 16, 17, 24–31]. Direct measurements of compound transport and metabolism in mesenteric and portal veins in humans are not possible for obvious reasons. Perfusion techniques, however, present great possibilities to measure intestinal processes. Over the past 70 years, different *in vivo* intestinal perfusion techniques have been developed and the importance of this work has been clearly demonstrated [3, 5, 6, 11, 13–16, 25–31]. The fundamental principle of an *in vivo* intestinal perfusion experiment is that P_{eff} is calculated from the rate at which the compound disappears

from the perfused intestinal segment. The accurate determination of P_{eff} requires knowledge of the hydrodynamics, perfusion rate, and surface area of the perfused intestinal segment [3, 11, 16, 25–31]. Fluid hydrodynamics depends on the perfusion technique applied, flow rate, and GI motility [11, 30]. The major advantages of using P_{eff} as the absorption parameter are that first it is possible to measure regardless of the transport mechanism(s) across the intestinal mucosa; second, it predicts F_a; and finally, it can be used to assess *in vitro–in vivo* correlations that validate the use of different intestinal absorption models [21, 22, 28, 29] commonly applied in drug discovery and preclinical development (Figure 9.6). Such *in vivo* studies of intestinal absorption and function provide a fully comprehensive profile of the integrated response to drugs in humans, by taking genetic, biochemical, physiological, pathological, and environmental factors into account [54]. We have established a good correlation between P_{eff} determined *in vitro* and historical data on F_a for a large number of structurally diverse drugs (Figures 9.7 and 9.8).

The enterocyte is the most common cell type (>90%) in the small intestinal barrier, which also contains a significant number of lymphocytes, mast cells, and macrophages. The intestinal P_{eff} for passive transcellular diffusion is considered to reflect the diffusion across the complex apical membrane into the cytosol, which is situated close to the cytoplasmic leaflet of the apical enterocyte membrane [3, 5, 7, 11, 16, 25–31, 47, 49, 55]. Consequently, intestinal perfusion models that measure the disappearance of the drug from the perfused segment directly describe its quantitative uptake into epithelial cells. The apical enterocyte membrane is very complex and is thought to represent the rate-limiting step in diffusion across this barrier. In addition, it has been speculated that the exofacial leaflet is responsible for the low permeability of the apical membrane [47, 55, 56]. Molecular dynamics simulations have identified four separate regions in the membrane, although the biological membrane containing multiple components may be considered more complex [56]. More studies are required to establish the role of bilayer asymmetry and membrane proteins in determining the unique permeability properties of the barrier imposed by the epithelial apical membrane [47, 55, 56].

Assessing the effect of intestinal metabolism on P_{eff} as a membrane transport rate parameter is a methodological issue [7, 26, 34, 35, 49]. An evaluation of its influence has to include a study to establish which enzyme(s) is (are) involved and the site of metabolism in relation to the site of the measurements. Intracellular metabolism in the enterocyte, for example, by CYP3A4 and di- and tripeptidases, does not occur in the vicinity of the outer leaflet of the apical membrane and is therefore not considered to affect P_{eff} determined by the disappearance approach (single-pass perfusion) [7, 15, 26, 34, 35, 38, 49]. However, drug metabolism in the lumen and/or at the brush border will directly interfere with the determination of P_{eff} because in this case the drug is metabolized before it is absorbed [57, 58]. It has also been suggested that intracellular metabolism may indirectly affect P_{eff} by providing a further sink boundary condition across the apical membrane. However, we have shown that specific inhibition of enterocyte CYP3A4 by ketoconazole does not change the P_{eff} of *R*/*S*-verapamil, which suggests that sink condition *in vivo* is provided by the highly perfused mesenteric blood vessels (Figure 9.9) [34, 35].

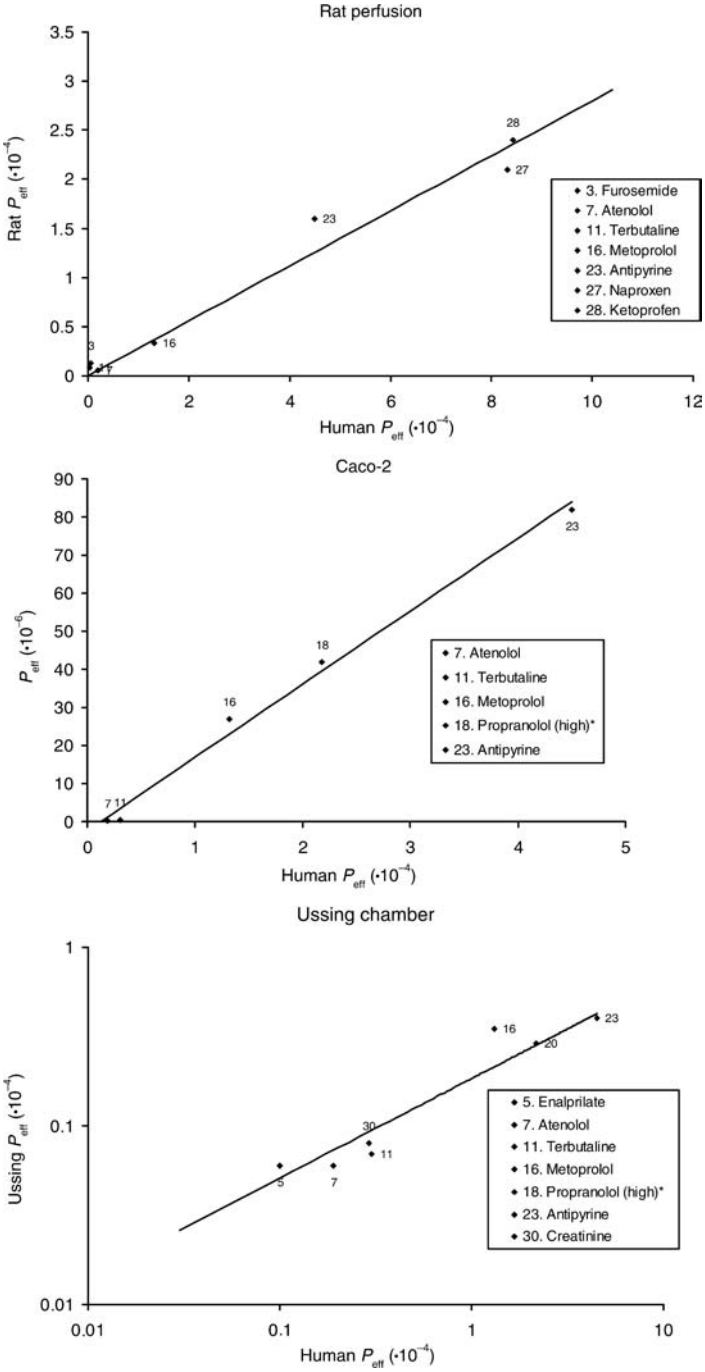
Rat perfusion
Rat P_{eff} ($\cdot 10^{-4}$)
Human P_{eff} ($\cdot 10^{-4}$)
3. Furosemide
7. Atenolol
11. Terbutaline
16. Metoprolol
23. Antipyrine
27. Naproxen
28. Ketoprofen
Caco-2
P_{eff} ($\cdot 10^{-6}$)
Human P_{eff} ($\cdot 10^{-4}$)
7. Atenolol
11. Terbutaline
16. Metoprolol
18. Propranolol (high)*
23. Antipyrine
Ussing chamber
Ussing P_{eff} ($\cdot 10^{-4}$)
Human P_{eff} ($\cdot 10^{-4}$)
5. Enalprilate
7. Atenolol
11. Terbutaline
16. Metoprolol
18. Propranolol (high)*
23. Antipyrine
30. Creatinine

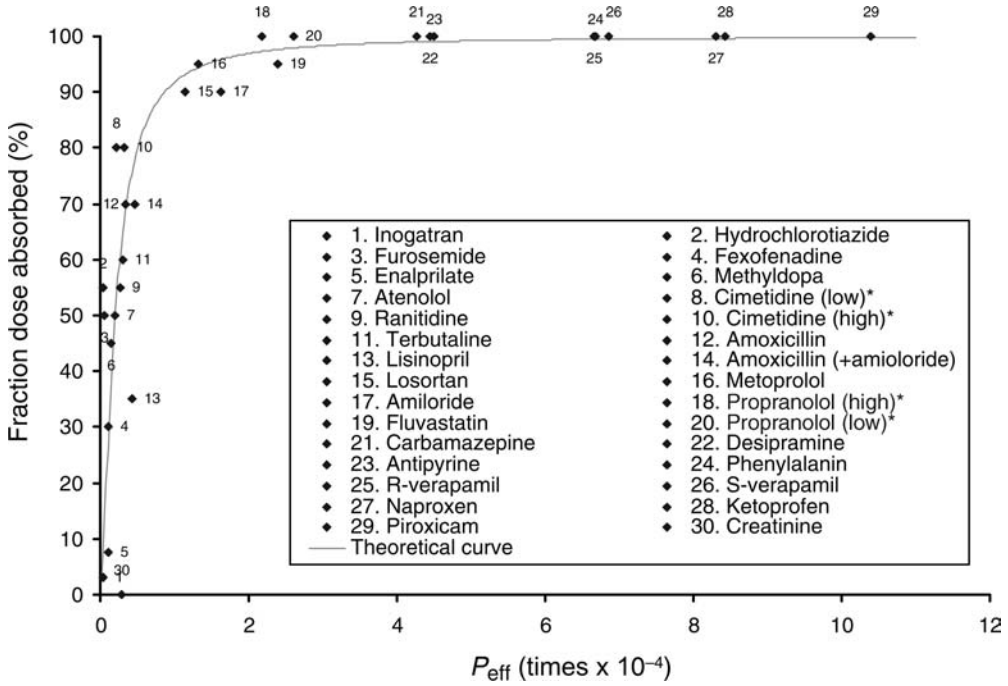

Figure 9.7 *In vivo* P_{eff} values in humans can be determined using Loc-I-Gut. These values correlate closely to F_a of oral doses for a large number of drugs from different pharmacological classes and which are thus structurally diverse.

9.4
Paracellular Passive Diffusion

Enterocytes are connected by negatively charged tight junctions, and the intracellular space formed is considered to be the paracellular route [59, 60]. The available surface area for paracellular intestinal absorption has been estimated to be about 0.01% of the total surface area of the small intestine [59, 60]. The quantitative importance of the paracellular route for macroscopic intestinal absorption of hydrophilic compounds

Figure 9.6 Human *in vivo* permeability is one of the cornerstones of the BCS. Correlation of these measurements with fraction dose absorbed and permeability values from other permeability models make it feasible to classify drugs according to BCS and to define bioequivalence regulation for pharmaceutical product approval. These human *in vivo* P_{eff} values were determined using a regional double-balloon perfusion approach (Loc-I-Gut) (Figure 9.4). The use of P_{eff} as the absorption parameter has several important advantages. First, it is possible to measure P_{eff} regardless of transport mechanism (s) across the intestinal mucosa, and second, it predicts F_a and can be used to assess *in vitro–in vivo* correlations that validate the use of different intestinal absorption models [21, 22, 28, 29] commonly applied in discovery and preclinical development.

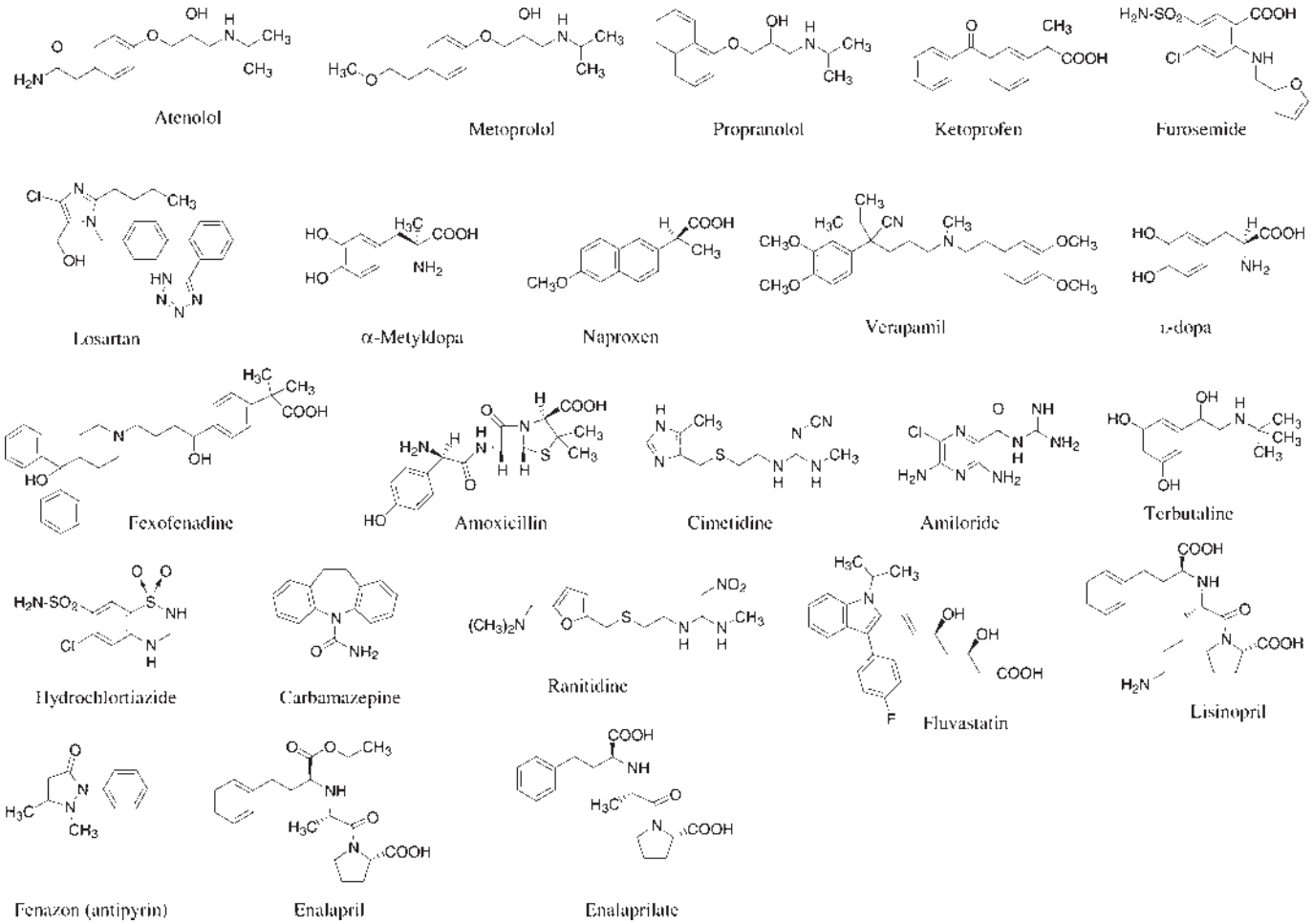

Figure 9.8 Chemical structures of drugs for which human *in vivo* P_{eff} values have been determined.

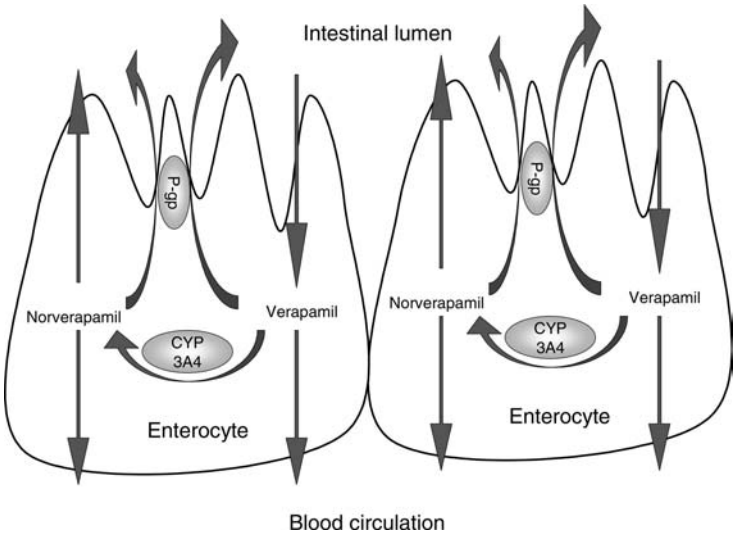

Figure 9.9 Schematic illustration of P-gp transport and CYP3A4 metabolism of *R*/*S*-verapamil in the human jejunum. It is assumed that the drug has to be absorbed before it can be metabolized by CYP3A4 inside the human enterocyte. Both parent drug and its formed metabolite, *R*/*S*-norverapamil, may be transported into the blood circulation as well as back into the intestinal lumen.

in vivo is not yet fully clear. Several *in vitro* investigations have demonstrated that the paracellular route is important for intestinal absorption of various hydrophilic compounds [48, 61–63]. However, *in vivo* studies have suggested that this route contributes only slightly to overall intestinal absorption of drugs [20, 23, 25, 27, 64, 65]. Other *in vitro* studies have suggested that the tight junctions between enterocytes are regulated by nutrients to induce solvent drag and thereby increase intestinal absorption [62, 66–68].

In our assessment of the paracellular hypothesis, we have assumed that water transport during solvent drag is largely paracellular. On the basis of this assumption, we have suggested that compounds with a molecular weight (MW) of over approximately 200 Da (radius > 4.0 Å) are too large to traverse the intercellular space between enterocytes and are therefore not sensitive to solvent drag in terms of quantitative absorption [20, 23, 25, 27]. This hypothesis is supported by our observation that in humans, small hydrophilic compounds such as urea (MW 60 Da, molecular radius 2.6 Å) and creatinine (MW 113 Da, molecular radius 7.2–8.0 Å) are affected by solvent drag, whereas other hydrophilic compounds with an MW more than 180 Da, such as D-glucose (MW 180 Da), antipyrine (MW 188 Da), L-dopa (MW 197 Da), terbutaline (MW 225 Da), atenolol (MW 266 Da), and enalaprilate (MW 348 Da) remain unaffected [20, 23, 25, 27]. Further evidence to support the hypothesis that fairly hydrophilic drugs undergo passive transcellular transport includes the observations that atenolol (logarithm of the distribution coefficient in octanol/water at pH 6.5 ($\log D_{6.5}$) < −2, molecular polar surface area (PSA) 88 Å^2, number of hydrogen-bond

donors (HBD) 4) inhibits the efflux mediated by P-glycoprotein (P-gp) and that terbutaline (log $D_{6.5} < -1.3$, PSA 76 Å^2, HBD 4) is extensively metabolized in the gut wall during first-pass extraction following oral administration. Both these compounds have been suggested to be largely absorbed by the paracellular route due to their hydrophilic properties [61]. However, atenolol has been reported to decrease the basal apical transport of celiprolol, a P-gp substrate that does not undergo CYP3A4 metabolism, in Caco-2 cells [69]. This transport inhibition arises due to competition for the binding sites of P-gp, which are suggested to be located at the transmembrane region of P-gp. Terbutaline undergoes extensive sulfate conjugation after oral administration, which appears to predominately occur in the gut wall [70, 71]. This particular conjugation enzyme is located in the cytosolic fraction of the enterocyte, indicating that terbutaline is transported via the transcellular route despite its hydrophilic properties and low P_{eff}. Our human *in vivo* perfusion data together with the evidence accumulated from studies on atenolol and terbutaline support the hypothesis that small and fairly hydrophilic drugs are mainly absorbed via the transcellular route if passive diffusion is the predominant intestinal absorption mechanism. In addition, Soergel suggests that the intestinal mucosa is nearly impermeable to paracellular transport of hexoses, while Amelsberg *et al*. hypothesize that paracellular absorption in mammals is unlikely to make a major contribution to small intestinal absorption of bile acids (i.e., of MW 500–600 Da) [60, 72].

9.5 Transcellular Passive Diffusion

Previously, the unstirred water layer (UWL) adjacent to the intestinal lining was considered to be the rate-limiting step for intestinal P_{eff} of high-permeability compounds [27, 73]. However, several *in vivo* studies clearly report that the thickness of this UWL is significantly less than what was previously assumed, since there is an instantaneous mixing of intestinal fluids [43, 74]. For example, in 1995, Fagerholm and Lennernäs observed no significant changes in estimated P_{eff} of two high-permeability compounds, D-glucose (10×10^{-4} cm/s) and antipyrine (4×10^{-4} cm/s), or UWL thickness over a fourfold range of perfusion rates (1.5–6.0 ml/min) when using the Loc-I-Gut technique in humans [73]. It is thus currently accepted that the epithelial membrane controls the transport rate for both low- and high-permeability compounds regardless of the transport mechanism *in vivo* [43, 73, 74].

The main intestinal absorption mechanism for drugs *in vivo* is considered to be passive transcellular membrane diffusion with the rate-limiting step imposed by the apical membrane [3, 27, 36, 61, 75]. As most drugs are fairly lipophilic in nature, this mode of absorption is most frequent. For instance, in a pharmacokinetic database of 472 drugs, 235 (50%) had a log *P* value of more than 2 and 379 (80%) had a log *P* value of more than 0 [76]. Even if a drug is a substrate for an intestinal transport protein, passive diffusion will probably be the main absorption mechanism if the drug has suitable lipophilic physicochemical properties. However, intestinal carrier-mediated membrane transport will dominate for hydrophilic drugs and polar metabolites if

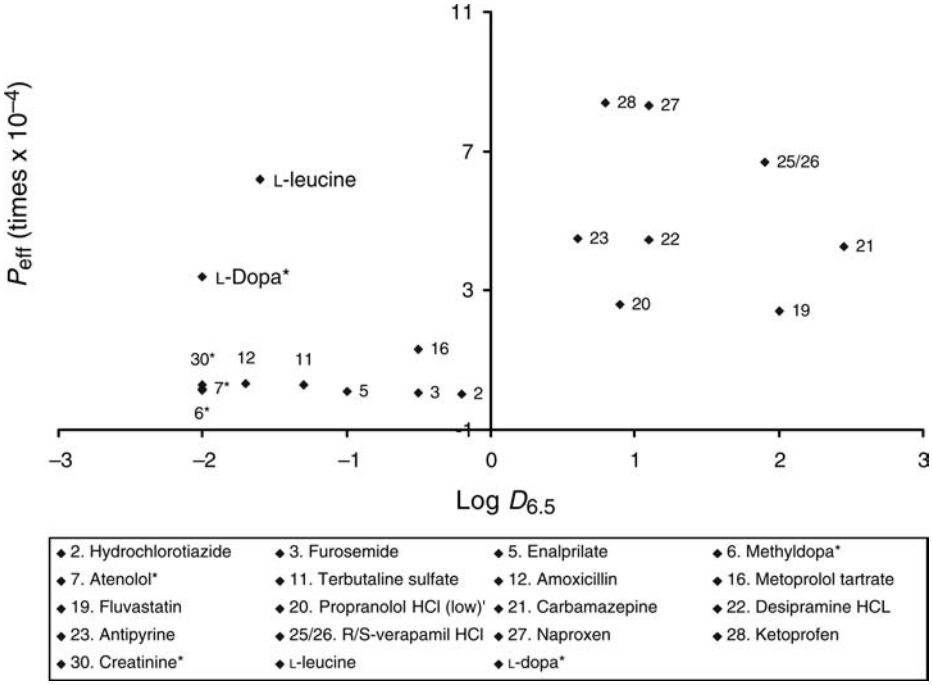

Figure 9.10 Correlation between *in vivo* P_{eff} determined using the Loc-I-Gut technique in humans and the octanol/buffer pH 6.5 partitioning coefficients for a large number of drugs. Drugs with octanol/buffer pH 6.5 partitioning coefficients higher than zero are highly permeable and well absorbed in humans ($F_a > 90\%$).

they are substrates for any transporter, since passive membrane diffusion is then expected to be slow for such compounds [31, 36].

In a detailed multivariate data analysis report on the relationship between compound structure and permeability, we have shown that the *in vivo* jejunal human P_{eff} for 22 compounds with diverse structures, as determined by the Loc-I-Gut technique, correlated well with both experimentally determined lipophilicity values using a pH-metric technique and calculated molecular descriptors [36] (Figures 9.8, 9.10 and 9.11). Seven of the compounds were omitted from the final analysis as their transport was either carrier mediated (amoxicillin, D-glucose, L-leucine, L-dopa, and α-methyldopa) or mediated via the paracellular route (urea and creatinine). The remaining 15 drugs were included in the multivariate analysis for passive membrane diffusion even if some (verapamil, losartan, furosemide, and fluvastatin) have been considered to be substrates for efflux proteins, such as P-gp and multidrug-resistant protein (MRP), located in the enterocyte membrane [7, 36, 46, 77]. The relationships shown in Figures 9.7, 9.10 and 9.11 strongly suggest that the dominant intestinal absorption mechanism for these drugs is probably passive transcellular diffusion, which is supported by the fact that for these drugs, there is a linear relationship between the fraction dose absorbed and the clinical dose range. The theoretical

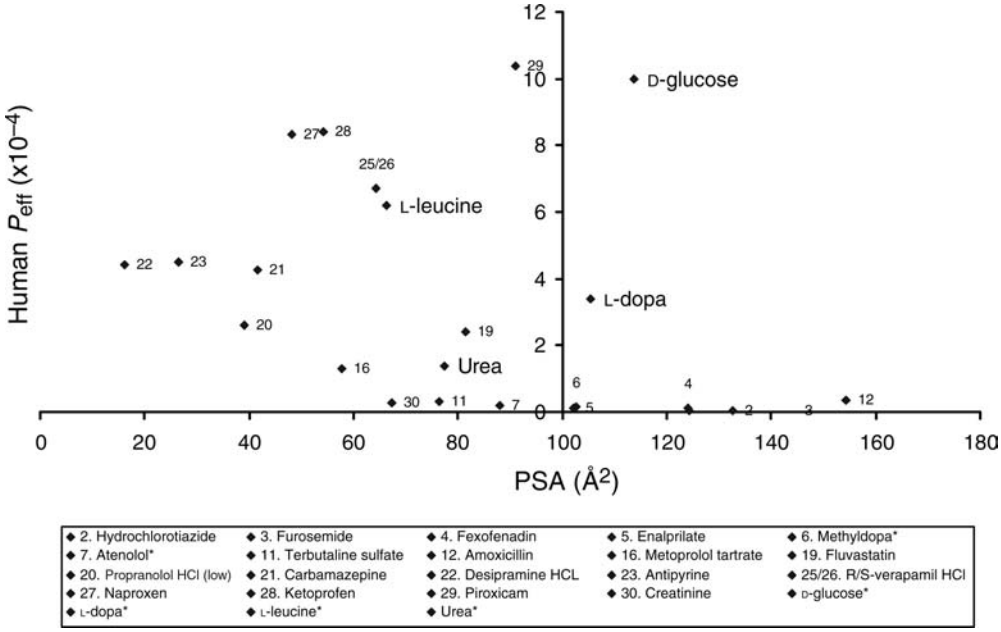

Figure 9.11 Correlation between *in vivo* P_{eff} determined using the Loc-I-Gut technique in humans and the PSA for a large number of drugs. Drugs with PSA less than 100 Å^2 are highly permeable and well absorbed in humans ($F_a > 90\%$).

models based on these *in vivo* permeability data from healthy volunteers can be used to predict passive intestinal membrane diffusion in humans for compounds that fit into the defined property space [36]. We used one of the models obtained from this multivariate analysis to predict the log P_{eff} values for an external validation set consisting of 34 compounds. A good correlation was found with the absorption data of these compounds, which, together with the observation that *in vivo* intestinal absorption of many drugs is dominated by passive diffusion [36], further validates our *in vivo* permeability data set.

In accordance with its polar nature, furosemide (log $D_{6.5}$ −0.5, PSA 124 Å^2, HBD 4) has a low jejunal P_{eff} of 0.05 ± 0.014 cm/s (as measured using the Loc-I-Gut technique) and is classified as a low-permeability compound according to the BCS [1, 16]. Interestingly, after oral administration, absorption and bioavailability (35–75%) of furosemide are highly variable [78, 79]. Several hypotheses have been advanced to account for this high variability, such as active intestinal secretion, low passive diffusion, and highly pH-dependent dissolution and permeability [80]. The data shown in Figures 9.10 and 9.11 suggest that drugs with octanol/buffer partitioning coefficients higher than zero and a PSA less than 100 Å^2 will be highly permeable ($P_{eff} > \approx 1.0 \times 10^{-4}$ cm/s and $F_a > 90\%$) across the human jejunum. The data further imply a strong influence of pH on physicochemical properties that will most certainly alter passive P_{eff} *in vivo*. At pH 7.4, 6.5, and 5.5, the experimentally determined

partitioning coefficients for furosemide were −0.9, −0.5, and 0.4, respectively [36]. In addition, uncharged furosemide has an experimentally determined partitioning coefficient (i.e., log *P* value) of 2.53 ± 0.01. Finally, a recent *in vitro* study shows that active intestinal secretion is important for the transport of furosemide across a Caco-2 monolayer [80]. However, these *in vitro* results must be confirmed *in vivo* before any conclusions regarding the mechanisms underlying the intestinal absorption of furosemide in humans are drawn.

9.6 Carrier-Mediated Intestinal Absorption

Most nutrient absorption occurs in the proximal jejunum. Accordingly, a very large number of carrier proteins, channels, and enzymes are expressed in this highly absorptive part of the GI tract. Carrier-mediated intestinal absorption of drugs is the dominant absorption mechanism of any drug with a reasonably high affinity for any intestinal transport protein, whereas passive permeability plays a relatively small role due to the polar nature of the compound [3, 27, 36, 61, 75]. The intestinal epithelium is polarized, and many transport proteins are located and maintained in the apical membrane due to the tight junctions, which prevent the diffusion of proteins within the membrane. Tight junctions also prevent backflow of nutrients from the basal side of the enterocytes into the gut lumen.

The oral bioavailability of poorly absorbed drugs has been increased by targeting them at nutrient transport systems [7]. Two nutrient absorption mechanisms, the oligopeptide carrier and the amino acid transport family, are among the most important that may be utilized for drug transport in the absorptive direction. These proteins are expressed to any significant degree only in the small intestine and therefore drugs that are mainly absorbed via these carriers will not be absorbed in the colon. By using the Loc-I-Gut technique in the proximal jejunum in humans, we investigated the transport of six drugs (amoxicillin, cephalexin, enalapril, lisinopril, α-methyldopa, and L-dopa) that are substrates for either of these proteins [3, 16, 31, 81, 82].

The oligopeptide carrier, hPEPT1, is a symport carrier, which transports a substrate with a proton across the apical enterocyte membrane. The oligopeptide carrier gains access to protons on the substrate via a sodium carrier, the Na^+/H^+ exchanger, located in the brush border membrane of enterocytes [83]. In humans, the intestinal absorption of amoxicillin decreases from an average value of 72 ± 9 to 45 ± 11% as a consequence of an increase in the oral dose from 500 to 3000 mg [84]. These data confirm that hPEPT1 has a high transport capacity, as amoxicillin is well absorbed despite administration of such large doses. The *in vivo* jejunal P_{eff} for amoxicillin has been reported to be 0.4×10^{-4} cm/s at a concentration of 300 mg/l (0.82 mm), which corresponds to an oral dose of 1200 mg [31]. This jejunal P_{eff} value predicts an F_a value of less than 90%, which classifies amoxicillin as a low-permeability drug according to the BCS. A study by Winiwarter *et al.* in 1999 showed that P_{eff} measured *in vivo* was higher than that predicted for amoxicillin from its physicochemical properties (log $D_{6.5}$ −1.7, logarithm of the calculated octanol/water partition coefficient

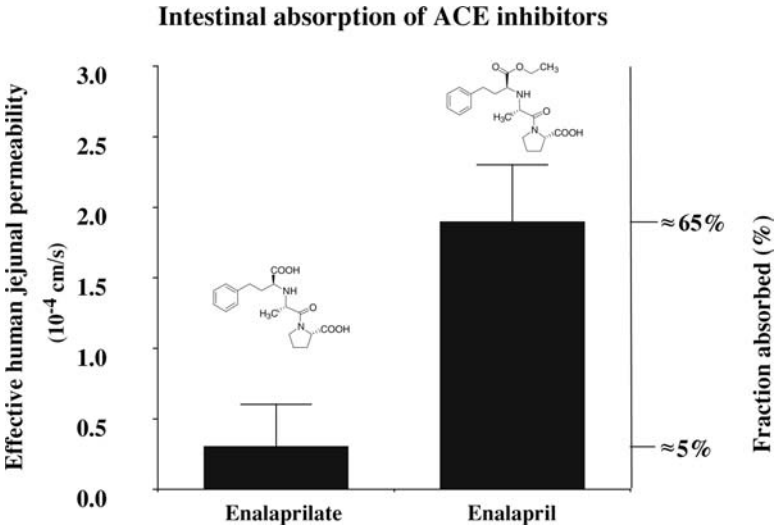

Figure 9.12 The effective permeability (P_{eff}, mean ± SD) of enalapril and enalaprilate in human jejunum *in vivo*. The P_{eff} values predict the fraction dose absorbed for both drugs obtained in pharmacokinetic studies in humans. The higher jejunal P_{eff} of enalapril is most likely due to significantly higher transport through the peptide carrier.

(for neutral species) (Clog P) = 0.33, PSA 154 Å^2, MW 365 Da) [36]. This observation supports previous pharmacokinetic reports and suggests that the intestinal absorption of amoxicillin is higher (about 50–75%) than that expected for a compound of its low lipophilic and amphoteric nature [84, 85]. The large variability in *in vivo* P_{eff} values for amoxicillin between individuals may be due to polymorphism in the expression of hPEPT1. In addition, nutritional status may contribute to the variability, since it has been reported that transcription of the PEPT1 gene may be activated by dietary amino acids and dipeptides [86]. It has also been reported that the integrated response to a certain stimulus may increase PEPT1 activity by translocation from a preformed cytoplasmic pool [87]. We have reported that both diacid and active forms of enalaprilate have low P_{eff} and, consequently, low F_a in humans (Figure 9.12). The prodrug approach of esterifying enalaprilate to enalapril increased *in vivo* P_{eff}, as well as F_a, after oral administration (Figure 9.12). This is most likely due to the higher transport activity of hPEPT1 with the esterified prodrug enalapril than with the diacid form, enalaprilate [88]. In the human jejunum, we determined *in vivo* P_{eff} for amoxicillin, cephalexin, enalapril, and lisinopril. These compounds have physicochemical properties that predict low passive diffusion across the human intestine. It has also been shown that in Caco-2 cells *in vitro* permeability is low, which is in accordance with the poor expression of hPEPT1 in that absorption model. Passive diffusion is low due to the polar nature of the compounds [89]. However, P_{eff} *in vivo* has been reported to be significantly higher. This is in accordance with a higher

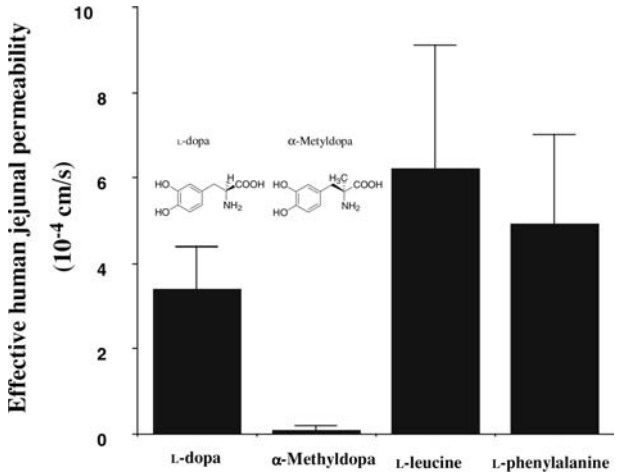

Figure 9.13 The effective permeabilities (P_{eff}, mean ± SD) of L-dopa, α-methyldopa, L-leucine, and L-phenylalanine in human jejunum *in vivo*. The P_{eff} values are determined using a single-pass perfusion technique in human jejunum *in vivo* at the following concentrations: 2.5, 6.7, 40, and 0.06 mm for L-dopa, α-methyldopa, L-leucine, and L-phenylalanine, respectively.

expression of hPEPT1, which is the main mechanism for intestinal absorption of these drugs.

P_{eff} for drugs transported by the amino acid transporter for large neutral amino acid (LNAA) was determined *in vivo* in healthy volunteers for L-dopa and α-methyldopa. α-Methyldopa was classified as a low-P_{eff} drug ($0.1 \pm 0.1 \times 10^{-4}$ cm/s at a perfusate concentration of 6.0–6.5 mm) (Figure 9.13) [16, 36, 81]. The corresponding *in vivo* P_{eff} for L-dopa was about 30 times higher ($3.4 \pm 1.0 \times 10^{-4}$ cm/s at a luminal concentration of 2.0–2.5 mm) (Figure 9.13) [3, 16, 36]. The difference in *in vivo* P_{eff} between α-methyldopa and L-dopa is probably due to a lower affinity of the LNNA transporter for α-methyldopa in addition to lower transport capacity of the LNNA transporter for α-methyldopa. The low *in vivo* P_{eff} of α-methyldopa indicates that passive diffusion for this compound is also low, which is in accordance with its physicochemical properties (MW 211 Da, log $D_{6.5} < -2$, PSA 103 Å^2, HBD 5) [36]. Figure 9.13 illustrates that a small change in the chemical structure of a substrate for the LNAA transporter significantly alters its *in vivo* permeability. This is due to the narrow substrate specificity of this carrier protein. Two nutrient substrates for this carrier family, L-leucine and L-phenylalanine, have high *in vivo* P_{eff} in humans even if in our study, they were determined at very different perfusate concentrations (Figure 9.13). This observation confirms that the amino transport family also exhibits high *in vivo* transport capacity in the human jejunum.

The rate and extent of intestinal absorption of cimetidine have been widely discussed, and F_a for this drug has been estimated at around 75% [90, 91]. It has been reported that cimetidine is a substrate for both P-gp and/or organic cation transporters (OCNT1 and OCNT2) [82, 92]. We determined the human jejunal *in vivo*

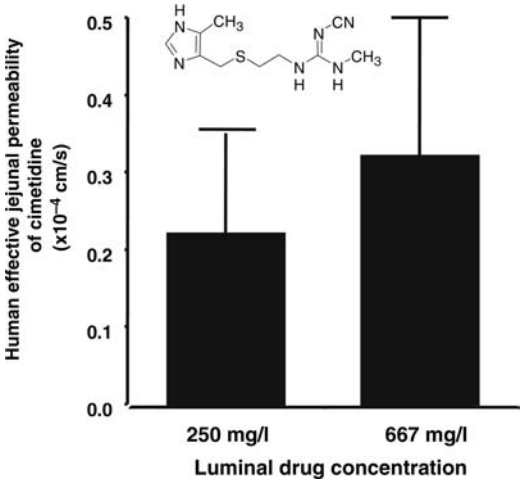

Figure 9.14 The effective permeabilities (P_{eff}, mean ± SD) of cimetidine in human jejunum at two clinically relevant luminal concentrations. The rate and extent of intestinal absorption of cimetidine have been widely discussed, and F_a for this drug has been estimated at around 75% [90, 91]. It has been reported that cimetidine is a substrate for both P-gp and/or organic cation transporters (OCNT1 and OCNT2) [82, 92]. We determined the human jejunal *in vivo* P_{eff} at two different clinically relevant concentrations to investigate saturation in any carrier-mediated transport across the intestinal epithelium. No difference in P_{eff} values between the two concentrations was noted, and, together with the observation that human permeability *in vivo* is similar to permeability in the Caco-2 model (with low expression of carrier proteins), this suggests that passive diffusion is the dominant mechanism even for cimetidine [82].

P_{eff} at two different clinically relevant concentrations to investigate saturation in any carrier-mediated transport across the intestinal epithelium (Figure 9.14). No difference in P_{eff} between the two concentrations was noted, and, together with the observation that human permeability *in vivo* is similar to permeability in the Caco-2 model (with low expression of carrier proteins), this suggests that passive diffusion is the dominant mechanism even for cimetidine [82]. If, on the other hand, organic cation transporters dominated, human intestinal *in vivo* permeability would be expected to be significantly higher than the Caco-2 permeability as the expression of both OCNT1 and OCNT2 is higher in the human small intestine than in the Caco-2 model [82].

9.7 Jejunal Transport and Metabolism

Cytochrome P450 (EC 1.14.14.1) enzymes are well known for their ability to metabolize the majority of drugs, detoxify environmental pollutants, and activate some classes of carcinogens [93]. The most highly expressed subfamily is CYP3A, which includes the isoforms CYP3A4, CYP3A5, CYP3A7, and CYP3A43 [93, 94]. The most abundant isoform is CYP3A4, which accounts for 30% of the total P450 content

in the liver and about 70% of the total P450 content in the intestine [93–95]. The CYP3A4 isoform is one of the most important enzymes for oxidative drug metabolism. About 50–60% of clinically used drugs are metabolized by this particular isoenzyme [93, 96]. Despite the higher enzymatic capacity in the liver than in the small intestine, it has been shown that the human intestine contributes significantly to the first-pass extraction of drugs metabolized by CYP3A4 [4, 97–99]. The apical recycling hypothesis has been proposed to account for this high level of gut wall extraction, despite a relatively low intestinal CYP3A4 activity compared to that in the liver. This hypothesis suggests that P-gp and CYP3A4 act synergistically to prolong the intracellular residence time and thereby repeatedly expose the drug to the CYP3A4 enzyme [49, 77, 100, 101]. In addition, the process may support the active transport of formed metabolites toward the intestinal lumen, which may prevent product inhibition of the enzyme [102–104]. Further evidence to support the metabolism–efflux interplay is provided by the close vicinity of P-gp and CYP3A4 in the enterocyte [100, 105] and by the overlapping substrate specificity [106]. However, the validity of this elegant hypothesis *in vivo* is uncertain as CYP3A4 substrates, such as midazolam and felodipine, undergo extensive gut wall metabolism even though they are not subjected to any intestinal efflux [46, 107].

The intestinal epithelium has a carrier-mediated efflux system for limiting the uptake of xenobiotics, which is in turn mediated by ATP-binding cassette (ABC) transport proteins [3, 7, 108–110]. These proteins are also expressed in numerous cell types in tissues such as the liver, kidney, testes, placenta, and blood–brain barrier and may play a role in the pharmacokinetics of drugs [108]. The multidrug resistance transporter gene MDR1 (HUGO nomenclature: ATP-binding cassette transporter gene ABCB1) encodes P-gp and is the most extensively studied, but other multidrug transporters such as multidrug-resistant protein family (MRP1–6) and breast cancer-resistant protein (BCRP) are also under investigation [46, 111, 112]. Under normal circumstances, these proteins restrict the entry and increase the excretion of agents from the cells where they are expressed [108]. Despite extensive research on the effect of efflux proteins on intestinal drug absorption, relatively few examples in humans have been reported [6, 107, 113, 114]. One notable example of their clinical significance, however, was reported in 1999 by Greiner *et al.*, who showed that the plasma concentration time profile (i.e., bioavailability) of oral digoxin was significantly lower during rifampin treatment, a finding that was attributed to increased expression of intestinal P-gp [8]. It has also been shown that a polymorphism in exon 26 (C34 35T) can result in decreased intestinal expression of P-gp, along with increased oral bioavailability of digoxin [115, 116]. Similarly, atorvastatin (80 mg once a day) has been shown to affect the steady-state pharmacokinetics of digoxin in humans [117]. C_{max} and plasma AUC have been reported to increase by 20 and 15%, respectively. Renal clearance was unaffected, which suggests that this drug–drug interaction is due to increased intestinal absorption and/or decreased biliary secretion of digoxin, mediated through P-gp inhibition [117]. This was also confirmed *in vitro* using Caco-2 cells, where atorvastatin decreased digoxin secretion by 58%, equivalent to the extent of inhibition observed with verapamil, a well-known P-gp inhibitor [117, 118]. Recently, several clinical studies have also claimed that inhibition of intestinal efflux

(especially of P-gp) was the major cause of increased bioavailability when certain drugs were coadministered [100, 119]. In many of these studies, however, it is likely that inhibition of CYP3A4 accounts for most of the increased bioavailability, whereas the role of cellular efflux *in vivo* at the intestinal level remains unclear. The reason for this overinterpretation of the role of enterocyte efflux activity on intestinal drug absorption may be due to the overlapping specificities of both substrates and inhibitors for both CYP3A4 and P-gp [106]. Additional factors may include saturation of the efflux carrier due to high drug concentration in the intestinal lumen and/or a fairly high passive permeability component [34, 35].

Direct *in vivo* assessment of the quantitative importance of gut wall metabolism and transport of drugs and metabolites in humans is difficult and has consequently not been attempted often [3, 6, 11, 12, 15, 16, 23, 25–32, 34, 35, 81]. The most direct *in vivo* approach to investigating these processes in drugs with variable and incomplete bioavailability has been shown to be single-pass intestinal perfusion or an instillation approach (Figure 9.2) [3, 6, 11, 12, 15, 16, 25–32, 34, 35, 81]. In general, traditional pharmacokinetic studies are limited in their capacity to distinguish intestinal extraction from hepatic extraction, as discussed by Lin *et al*. [120]. However, measured values of metabolic extraction of *R*/*S*-verapamil in the human gut (≈50%) and liver (≈50%), using the steady-state single-pass perfusion approach and the instillation technique, have been reported to be similar [15, 34, 35] and are also in agreement with findings from traditional pharmacokinetic studies [2, 121].

A single-pass perfusion approach using the Loc-I-Gut technique was applied for a direct *in vivo* assessment in the human jejunum. *R*/*S*-Verapamil ($\log D_{6.5}$ 2.7, octanol/H_2O, pH 7.4, MW 455 Da) was used as the model compound for CYP3A4- and P-gp-mediated local intestinal kinetics [2, 34, 35, 122] (Figures 9.7 and 9.9). P_{eff} values for both enantiomers at each concentration used (4.0, 40, 120, and 400 mg/l) were 2.5×10^{-4}, 4.7×10^{-4}, 5.5×10^{-4}, and 6.7×10^{-4} cm/s, respectively (Figure 9.15) [34, 35]. The luminal concentration in the upper part of the small intestine after oral administration of a 100 mg dose of verapamil in an immediate-release dosage form is expected to reach 400 mg/l [1, 34, 35]. The three other perfusate concentrations represent fractions of the dose when 30, 10, and 1%, respectively, remain to be absorbed [34, 35]. The increase in *in vivo* jejunal P_{eff} of *R*/*S*-verapamil, along with its increased luminal perfusate concentration, is in accordance with a saturable efflux mechanism mediated by P-gp (Figure 9.15). Furthermore, there was no difference in P_{eff} between the *R*- and *S*-forms of verapamil at any luminal concentration, which suggests that efflux transport cannot discriminate between the two forms of verapamil. However, the measured *in vivo* jejunal P_{eff} ($>2.0 \times 10^{-4}$ cm/s) was sufficient at all four perfusate concentrations to predict complete intestinal F_a following oral dosing (Figures 9.7 and 9.15) [34, 35]. Together with the fact that P_{eff} and F_a are excellent, as predicted from the physicochemical properties of *R*/*S*-verapamil, this suggests that passive diffusion is the dominating transport mechanism for this drug in the human intestine [34–36].

Ketoconazole, a well-known potent inhibitor of CYP3A4 metabolism and a less potent P-gp modulator, acutely inhibited CYP3A4 metabolism but did not affect the P_{eff} of *R*/*S*-verapamil when they were coperfused through the human jejunal

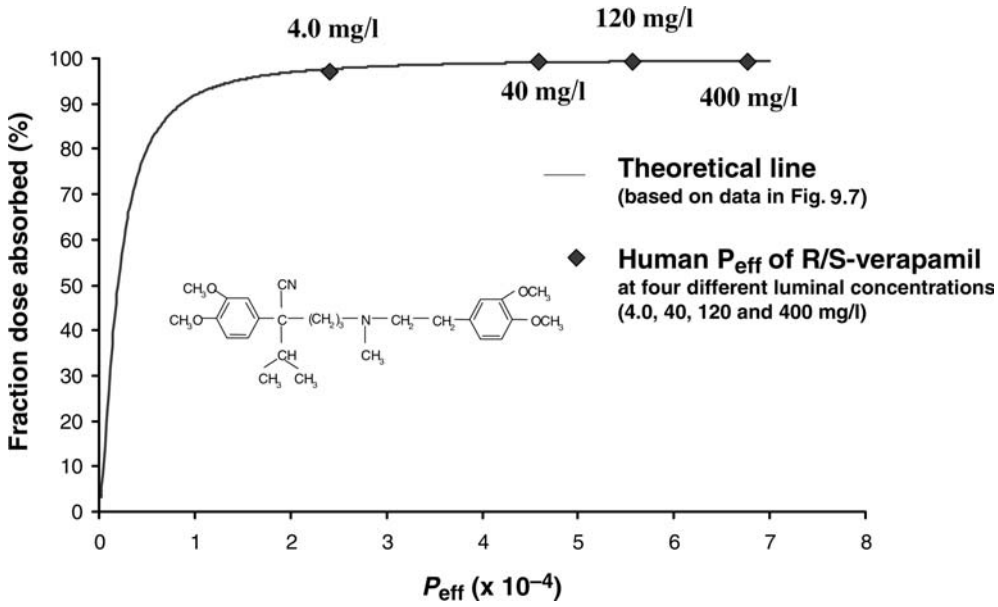

Figure 9.15 The effective permeability (P_{eff}, mean ± SD) of *R*/*S*-verapamil in human jejunum at two clinically relevant luminal concentrations. P_{eff} for both enantiomers at each of the concentrations (4.0, 40, 120, and 400 mg/l) was 2.5×10^{-4}, 4.7×10^{-4}, 5.5×10^{-4}, and 6.7×10^{-4} cm/s, respectively (Figure 9.15) [34, 35]. The luminal concentration in the upper part of the small intestine after oral administration of a 100 mg dose of verapamil in an immediate-release dosage form [1, 34, 35] is expected to reach 400 mg/l. The three other perfusate concentrations represent fractions of the dose when 30, 10, and 1%, respectively, remain to be absorbed. The increased *in vivo* jejunal P_{eff} of *R*/*S*-verapamil along with its increased luminal perfusate concentration is in accordance with a saturable efflux mechanism mediated by P-gp. However, the measured *in vivo* jejunal P_{eff} (>2.0×10^{-4} cm/s) was sufficient at all four perfusate concentrations to predict complete intestinal F_a following oral administration.

segment at 40 mg/l (ketoconazole) and 120 mg/l (*R*/*S*-verapamil)(Figures 9.9 , 9.15, and 9.16) [35]. This confirms that *in vivo*, ketoconazole is a less potent inhibitor of P-gp than CYP3A4 in humans and that even if a significant proportion of verapamil is transported by passive diffusion, increased P_{eff} would be expected for P-gp inhibition [35, 123–125]. It also demonstrates that intracellular metabolism has no effect on apical drug permeability (Figures 9.9 and 9.16). In this regard, it has been proposed that intracellular CYP3A4 metabolism may provide a more pronounced concentration gradient across the apical enterocyte membrane, which theoretically should increase P_{eff} [120, 126, 127]. Since verapamil is transported mainly via passive diffusion and is subjected to extensive CYP3A4 metabolism in the gut, it is considered to be a good model drug to investigate this issue in humans [2, 15, 34–36]. However, inhibition of small intestinal metabolism did not result in decreased jejunal P_{eff}. In addition, if intracellular CYP3A4 metabolism had a pronounced effect on jejunal P_{eff}, *S*-verapamil would have been expected to have significantly higher

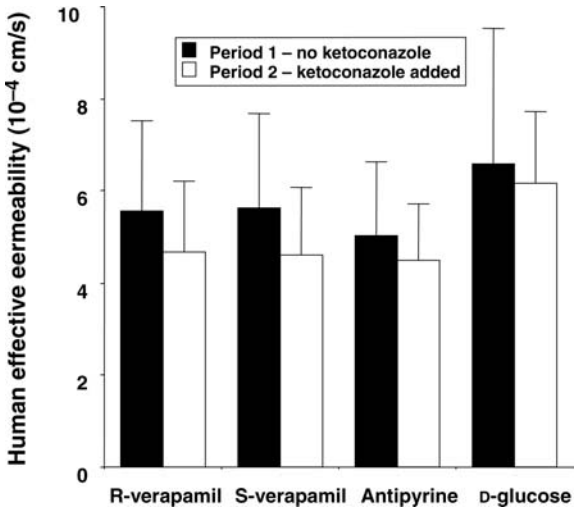

Figure 9.16 The absence of an acute effect of ketoconazole on P_{eff} (mean ± SD) of *R*/*S*-verapamil, antipyrine, and D-glucose in humans. The data suggest that the extensive intracellular metabolism in the human enterocyte mediated by CYP3A4 on substrates such as *R*/*S*-verapamil has no direct or indirect effect on P_{eff} in humans. In addition, the similarity in P_{eff} values between *R*- and *S*-verapamil further supports the hypothesis that intracellular metabolism has no effect on P_{eff}, as stereoselective CYP3A4 metabolism (*S*-verapamil is more readily metabolized) is not reflected in *in vivo* P_{eff}.

P_{eff}, as it is more extensively metabolized than *R*-verapamil in the gut wall. However, we have shown with the Loc-I-Gut technique that the human jejunal P_{eff} for *S*- and *R*-verapamil are identical, though *S*-verapamil was subjected to a significantly higher degree of intestinal first-pass metabolism [35]. Altogether, this suggests that extensive CYP3A4 metabolism in enterocytes in humans does not affect drug permeability across the apical membrane by increasing the concentration gradient across the apical enterocyte membrane (Figures 9.9 and 9.15). A more plausible explanation is that the concentration gradient *in vivo* across the intestinal barrier is provided by extensive mesenteric blood flow. This emphasizes an important methodological aspect of intestinal perfusion techniques in which P_{eff}, based on the disappearance rate from a perfused segment, is not affected by extensive intracellular metabolism.

Jejunal permeability and intestinal and hepatic extraction of fluvastatin, a drug completely metabolized by CYP2C9, were investigated in humans by using the Loc-I-Gut technique [32]. It was shown that the contribution of the intestine to the total first-pass effect is negligible for fluvastatin. This observation is consistent with the observation that CYP2C enzymes are expressed at low levels in enterocytes [8, 128]. When tested at clinically relevant concentrations *in vitro* using Caco-2 cells, the efflux ratio of fluvastatin was approximately 5 and was probably mediated by MRP2. The human *in vivo* P_{eff} was high ($2.4 \pm 1.4 \times 10^{-4}$ cm/s), which demonstrates that despite significant *in vitro* intestinal efflux, fluvastatin is completely absorbed across the intestine *in vivo* (Figure 9.7) [3, 16, 32]. This is most likely due to the significant

contribution of passive P_{eff} to the overall absorption of fluvastatin, which is in accordance with its lipophilic properties (acid pK_a 4.3, log $D_{6.5}$ 2.0, PSA 81 Å^2, HBD 3) (Figures 9.10 and 9.11) [32, 36]. A similar pattern has been shown for many drugs. For instance, jejunal P_{eff} for cyclosporine, a well-known CYP3A4 and P-gp substrate, has been reported to be high and predicts complete intestinal absorption even if the drug is subjected to significant efflux in *in vitro* cell models [2, 15, 34, 35, 129, 130]. Altogether, these directly determined *in vivo* human P_{eff} values suggest that in humans, drugs with a high passive P_{eff} contribution to the overall absorption rate will be completely absorbed from the gut even if they are substrates (such as verapamil, fluvastatin, losartan, and cyclosporine) for one and/or several efflux transporters. The values also suggest that drugs with a sufficiently high lipophilicity will be absorbed from the gut mainly by passive transcellular diffusion. Finally, *in vivo* data suggest that for many drugs, the effect of intestinal active efflux on F_a is limited even if they are efflux substrates, which is in accordance with the limited number of reports supporting its clinical significance [8, 115, 116]. This may be due to a high contribution of passive diffusion, as well as due to the fact that these efflux proteins located in the intestine may be easily saturated owing to high concentrations adjacent to the intestinal membrane of the orally administered drug.

Model drugs and direct *in vivo* methods are needed to perform accurate investigations of the clinical significance and the pharmacogenetics of transporters and their influence on pharmacokinetics. Such model compounds should not be metabolized, which would make the assessment of the role of transporter possible. For instance, digoxin and fexofenadine have been suggested to be model compounds to assess the phenotype for P-gp significance [8, 115, 116, 131]. We investigated the effect of ketoconazole on the measured P_{eff} for fexofenadine because concomitant oral administration of these drugs led to an increase in C_{max} and AUC, which is consistent with inhibition of P-gp-mediated transport [132, 133]. Fexofenadine has indeed been shown to be a substrate for P-gp in Caco-2 and L-MDR1 cells, and its disposition is altered in knockout mice lacking the gene for Mdr1a [134, 135]. It was therefore expected that ketoconazole would increase jejunal P_{eff} and plasma AUC of fexofenadine when added to the jejunal perfusion, but this did not occur. On the contrary, jejunal P_{eff} remained low (0.1–0.2 $\times$ 10^{-4} cm/s) and variable, which, according to the BCS, classifies it among the low-permeability compounds (Figures 9.5 and 9.7) [1]. The reported absence of an effect of ketoconazole on fexofenadine permeability means that further *in vivo* studies are needed to fully understand the interaction between fexofenadine and ketoconazole. It also means that we must increase our understanding of transport mechanisms before we can conclude that fexofenadine is an appropriate *in vivo* probe for P-gp activity in humans. Our understanding of the expression of transporters and their functional activity in different human tissues is at a nascent stage, and there is a need for more *in vivo* pharmacokinetic data to validate *in vitro* methods of studying both quantitative and qualitative aspects of drug transport [107].

Glaeser *et al.* have shown that the majority of shed human enterocytes collected from an intestinal perfusion were still functionally active and did not show signs of apoptosis [38]. On the basis of a validation of the Loc-I-Gut system for the study of

gene expression during perfusion, changes in mRNA levels in shed enterocytes before and after perfusion of a 10 cm long jejunal segment were studied in parallel to P_{eff}, metabolism of selected compounds in the gut wall, and the excretion of their metabolites back into the lumen (Figure 9.4) [39]. Sulforaphane and quercetin-3,4′-diglucoside were rapidly effluxed back into the lumen as sulforaphane-glutathione and quercetin-3′-glucuronide conjugates, respectively. Gene expression analysis in exfoliated enterocytes showed a 1.8 ± 0.5-fold (range 1.1–2.3) induction of glutathione transferase A1 (GST) mRNA and a 2.1 ± 1.3-fold (range 0.7–4.0) induction of UDP-glucuronosyl transferase 1A1 (UGT1A1) mRNA after only 90 min exposure to these two compounds. The technique demonstrates its applicability to the study of intracellular process and their relationships to changes in gene expression (Figure 9.4) [38, 39].

9.8 Regional Differences in Transport and Metabolism of Drugs

Regional differences in transport and metabolism of drugs, especially in the colon, have not been investigated thoroughly in humans by using intestinal perfusion techniques. Therefore, there is a need to develop clinical techniques that make it possible to directly investigate the transport and metabolism *in vivo* of drugs in various regions of the GI tract. This would certainly improve our understanding of regional differences in the transport and metabolism of drugs, an understanding that is crucial for the development of orally controlled release systems, which have received increased attention as they create new therapeutic opportunities. In addition, regional absorption and metabolism may also influence the local effect of a drug, which is targeted at a certain region where diseases such as inflammatory bowel disease (IBD) and colon cancer are localized [136].

Investigations of regional differences in permeability and metabolism have been performed by using various animal models [22, 29, 75, 102, 109, 112, 137]. Animal tissues, mainly rat specimens, are widely used in the Ussing chamber to investigate transport of drugs across specific regions of the intestine [29, 75, 138], whereas studies in human tissues are few due to the limited availability of tissue specimens.

Regional differences in functional activity of P-gp have only been reported in a few cases and are mainly based on animal studies [22, 75, 109, 112, 137]. For instance, one of the few systemic kinetic analyses of efflux activity showed that marked differences exist along the different regions of the rat GI tract [112]. Maximal transporter activity varied over a fourfold to fivefold range in the order ileum > jejunum > colon. Earlier studies have claimed that MDR1 mRNA levels should be highest in the human colon [129]. Recent investigations, however, indicate that P-gp is more readily expressed in the small intestine than in the colorectal region [50, 109]. Interestingly, in 2002, Nakamura *et al.* reported that MDR1, MRP1, and CYP3A mRNA levels were higher in human duodenal tissue than in normal colorectal and colorectal adenocarcinoma tissues [50]. However, reported levels of MDR1 mRNA and P-gp-mediated efflux activity in the small intestine and colon are inconsistent, which may be

attributed to differences in species, methodology and study designs in the various reports [107, 109, 112, 129, 137, 144].

It has also been shown *in vitro* by using rat small intestinal and colonic tissues in an Ussing chamber that low-permeability drugs (BCS classes III–IV) have an even lower permeability in the colon, whereas high-permeability drugs (BCS classes I–II) show a slightly higher permeability in the colon when passive diffusion is the dominant mechanism (Figure 9.5) [75]. This P_{eff} pattern has also been shown to be relevant for small and large intestinal specimens from humans using the Ussing chamber model [104]. A regional difference in permeability for five different compounds has been reported from a study that applied an open triple-lumen tube and perfused an 80 cm long segment of human jejunum and ileum (Figure 9.2) [139]. P_{eff} for hydrochlorotiazide, atenolol, furosemide, and cimetidine, all of which are classified as low-permeability drugs according to the BCS, decreased in the ileum in comparison with the jejunum [3, 139]. This *in vivo* observation is in agreement with the regional Ussing chamber studies in rats for low-permeability compounds [75]. Salicylic acid, which is highly permeable, was well absorbed throughout the small intestine. The small intestinal regional permeability pattern has also been demonstrated for ranitidine (low permeability) and paracetamol and griseofulvin (two high-permeability compounds) by using a similar open intestinal perfusion technique [140–142]. *In vivo* permeability measurements of drugs in the colonic/rectal region in humans are difficult, which probably explains the limited amount of published data. However, we developed and validated a new technique for the perfusion of a defined and closed segment in the colon/rectum [143]. We observed that the permeability of antipyrine in the rectal region was high and D-glucose was not absorbed, which is in accordance with the fact that passive diffusion is the dominant drug absorption mechanism in this specific intestinal region. However, we found the present technique valuable for studying drug absorption from the human rectum, which encouraged us to investigate the influence of a penetration enhancer, sodium caprate, on the rectal absorption of phenoxymethyl penicillin and antipyrine [12]. The data suggest that sodium caprate alone has a limited effect on the permeability *in vivo* across the rectal epithelium when it is presented in a solution. Interestingly, there was a correlation between P_{eff} for sodium caprate and the individual plasma AUC and C_{max} of phenoxymethyl penicillin, which indicates that the permeability of the enhancer in the tissue upon which it should act is crucial to achieving an effect.

9.9 Conclusions

We have emphasized the need for more *in vivo* studies to deconstruct the dynamic interplay between mechanisms of drug transport and metabolism in the human intestine. There is also a need to further develop *in vivo* techniques to directly measure these processes in various regions along the GI tract in humans and to relate the findings to physiological/pathophysiological conditions.

This will increase our knowledge of the important transport mechanisms and will provide *in vivo* data leading to the development and validation of rapid and more reliable *in vitro* intestinal models.

References

1 Amidon, G.L., Lennernäs, H., Shah, V.P. and Crison, J.R. (1995) A theoretical basis for a biopharmaceutic drug classification: the correlation of *in vitro* drug product dissolution and *in vivo* bioavailability. *Pharmaceutical Research*, **12**, 413–420.

2 Fromm, M.F., Busse, D., Kroemer, H.K. and Eichelbaum, M. (1996) Differential induction of prehepatic and hepatic metabolism of verapamil by rifampin. *Hepatology*, **24**, 796–801.

3 Lennernäs, H. (1998) Human intestinal permeability. *Journal of Pharmaceutical Sciences*, **87**, 403–410.

4 Wu, C.Y., Benet, L.Z., Hebert, M.F., Gupta, S.K., Rowland, M. *et al.* (1995) Differentiation of absorption and first-pass gut and hepatic metabolism in humans: studies with cyclosporine. *Clinical Pharmacology and Therapeutics*, **58**, 492–497.

5 Csáky, T.Z. (1984) Methods for investigation of intestinal permeability, in *Pharmacology of Intestinal Permeability I*, Springer, Berlin, pp. 91–112.

6 Gramatte, T., Oertel, R., Terhaag, B. and Kirch, W. (1996) Direct demonstration of small intestinal secretion and site-dependent absorption of the beta-blocker talinolol in humans. *Clinical Pharmacology and Therapeutics*, **59**, 541–549.

7 Zhang, Y. and Benet, L.Z. (2001) The gut as a barrier to drug absorption: combined role of cytochrome P450 3A and P-glycoprotein. *Clinical Pharmacokinetics*, **40**, 159–168.

8 Greiner, B., Eichelbaum, M., Fritz, P., Kreichgauer, H.P., von Richter, O. *et al.* (1999) The role of intestinal P-glycoprotein in the interaction of digoxin and rifampin. *The Journal of Clinical Investigation*, **104**, 147–153.

9 Roden, D.M. and George, A.L.J. (2002) The genetic basis of variability in drug responses. *Nature Reviews. Drug Discovery*, **1**, 37–44.

10 Evans, W.E. and Relling, M.V. (1999) Pharmacogenomics: translating functional genomics into rational therapeutics. *Science*, **286**, 487–491.

11 Lennernäs, H., Ahrenstedt, O., Hällgren, R., Knutson, L., Ryde, M. *et al.* (1992) Regional jejunal perfusion, a new *in vivo* approach to study oral drug absorption in man. *Pharmaceutical Research*, **9**, 1243–1251.

12 Lennernäs, H., Gjellan, K., Hallgren, R. and Graffner, C. (2002) The influence of caprate on rectal absorption of phenoxymethylpenicillin: experience from an *in-vivo* perfusion in humans. *The Journal of Pharmacy and Pharmacology*, **54**, 499–508.

13 Knutson, L., Odlind, B. and Hallgren, R. (1989) A new technique for segmental jejunal perfusion in man. *The American Journal of Gastroenterology*, **84**, 1278–1284.

14 Phillips, S.F. and Summerskill, W.H. (1966) Occlusion of the jejunum for intestinal perfusion in man. *Mayo Clinic Proceedings*, **41**, 224–231.

15 von Richter, O., Greiner, B., Fromm, M.F., Fraser, R., Omari, T. *et al.* (2001) Determination of *in vivo* absorption, metabolism, and transport of drugs by the human intestinal wall and liver with a novel perfusion technique. *Clinical Pharmacology and Therapeutics*, **70**, 217–227.

16 Lennernäs, H. (1997) Human jejunal effective permeability and its correlation with preclinical drug absorption models. *The Journal of Pharmacy and Pharmacology*, **49**, 627–638.

17 Ahrenstedt, O., Knutson, L., Nilsson, B., Nilsson-Ekdahl, K., Odlind, B. *et al*. (1990) Enhanced local production of complement components in the small intestines of patients with Crohn's disease. *The New England Journal of Medicine*, **322**, 1345–1349.

18 Bonlokke, L., Hovgaard, L., Kristensen, H.G., Knutson, L. and Lennernäs, H. (2001) Direct estimation of the *in vivo* dissolution of spironolactone, in two particle size ranges, using the single-pass perfusion technique (Loc-I-Gut) in humans. *European Journal of Pharmaceutical Sciences*, **12**, 239–250.

19 Bonlokke, L., Christensen, F.N., Knutson, L., Kristensen, H.G. and Lennernäs, H. (1997) A new approach for direct *in vivo* dissolution studies of poorly soluble drugs. *Pharmaceutical Research*, **14**, 1490–1492.

20 Fagerholm, U., Borgstrom, L., Ahrenstedt, O. and Lennernäs, H. (1995) The lack of effect of induced net fluid absorption on the *in vivo* permeability of terbutaline in the human jejunum. *Journal of Drug Targeting*, **3**, 191–200.

21 Fagerholm, U., Johansson, M. and Lennernäs, H. (1996) Comparison between permeability coefficients in rat and human jejunum. *Pharmaceutical Research*, **13**, 1336–1342.

22 Fagerholm, U., Lindahl, A. and Lennernäs, H. (1997) Regional intestinal permeability in rats of compounds with different physicochemical properties and transport mechanisms. *The Journal of Pharmacy and Pharmacology*, **49**, 687–690.

23 Fagerholm, U., Nilsson, D., Knutson, L. and Lennernäs, H. (1999) Jejunal permeability in humans *in vivo* and rats *in situ*: investigation of molecular size selectivity and solvent drag. *Acta Physiologica Scandinavica*, **165**, 315–324.

24 Knutson, L., Ahrenstedt, O., Odlind, B. and Hallgren, R. (1990) The jejunal secretion of histamine is increased in active Crohn's disease. *Gastroenterology*, **98**, 849–854.

25 Lennernäs, H., Ahrenstedt, O. and Ungell, A.L. (1994) Intestinal drug absorption during induced net water absorption in man: a mechanistic study using antipyrine, atenolol and enalaprilat. *British Journal of Clinical Pharmacology*, **37**, 589–596.

26 Lennernäs, H., Crison, J.R. and Amidon, G.L. (1995) Permeability and clearance views of drug absorption: a commentary. *Journal of Pharmacokinetics and Biopharmaceutics*, **23**, 333–343.

27 Lennernäs, H. (1995) Does fluid flow across the intestinal mucosa affect quantitative oral drug absorption? Is it time for a reevaluation? *Pharmaceutical Research*, **12**, 1573–1582.

28 Lennernäs, H., Palm, K., Fagerholm, U. and Artursson, P. (1996) Comparison between active and passive drug transport in human intestinal epithelial (Caco-2) cells *in vitro* and human jejunum *in vivo*. *International Journal of Pharmaceutics*, **127**, 103–107.

29 Lennernäs, H., Nylander, S. and Ungell, A.L. (1997) Jejunal permeability: a comparison between the Ussing chamber technique and the single-pass perfusion in humans. *Pharmaceutical Research*, **14**, 667–671.

30 Lennernäs, H., Lee, I.D., Fagerholm, U. and Amidon, G.L. (1997) A residence-time distribution analysis of the hydrodynamics within the intestine in man during a regional single-pass perfusion with Loc-I-Gut: *in vivo* permeability estimation. *The Journal of Pharmacy and Pharmacology*, **49**, 682–686.

31 Lennernäs, H., Knutson, L., Knutson, T., Hussain, A., Lesko, L. *et al*. (2002) The effect of amiloride on the *in vivo* effective permeability of amoxicillin in human jejunum: experience from a regional

perfusion technique. *European Journal of Pharmaceutical Sciences*, **15**, 271–277.

32 Lindahl, A., Sandstrom, R., Ungell, A.L., Abrahamsson, B., Knutson, T.W. *et al.* (1996) Jejunal permeability and hepatic extraction of fluvastatin in humans. *Clinical Pharmacology and Therapeutics*, **60**, 493–503.

33 Lindahl, A., Ungell, A.L., Knutson, L. and Lennernäs, H. (1997) Characterization of fluids from the stomach and proximal jejunum in men and women. *Pharmaceutical Research*, **14**, 497–502.

34 Sandstrom, R., Karlsson, A., Knutson, L. and Lennernäs, H. (1998) Jejunal absorption and metabolism of *R*/*S*-verapamil in humans. *Pharmaceutical Research*, **15**, 856–862.

35 Sandstrom, R., Knutson, T.W., Knutson, L., Jansson, B. and Lennernäs, H. (1999) The effect of ketoconazole on the jejunal permeability and CYP3A metabolism of (*R*/*S*)-verapamil in humans. *British Journal of Clinical Pharmacology*, **48**, 180–189.

36 Winiwarter, S., Bonham, N.M., Ax, F., Hallberg, A., Lennernäs, H. *et al.* (1998) Correlation of human jejunal permeability (*in vivo*) of drugs with experimentally and theoretically derived parameters. A multivariate data analysis approach. *Journal of Medicinal Chemistry*, **41**, 4939–4949.

37 CDER (2000) Waiver of *in vivo* bioavailability and bioequivalence studies for immediate-release solid oral dosage forms based on a biopharmaceutics classification system. Food and Drug Administration.

38 Glaeser, H., Drescher, S., van der Kuip, H., Behrens, C., Geick, A. *et al.* (2002) Shed human enterocytes as a tool for the study of expression and function of intestinal drug-metabolizing enzymes and transporters. *Clinical Pharmacology and Therapeutics*, **71**, 131–140.

39 Petri, N., Tannergren, C., Holst, B., Bao, Y. *et al.* (2003) Absorption/metabolism of sulforaphane and quercetin, and regulation of phase II enzymes in human jejunum *in vivo* and in Caco-2 cells. *Drug Metabolism and Disposition: The Biological Fate of Chemicals*, **31**, 805–813.

40 Rowland, M. and Tozer, T.N. (1995) *Clinical Pharmacokinetics: Concepts and Applications*, 3rd edn, Williams & Wilkins, Media, PA.

41 Dressman, J.B., Amidon, G.L., Reppas, C. and Shah, V.P. (1998) Dissolution testing as a prognostic tool for oral drug absorption: immediate release dosage forms. *Pharmaceutical Research*, **15**, 11–22.

42 Komiya, I., Park, J.Y., Kamani, A. and Higuchi, W.I. (1980) Quantitative mechanistic studies in simultaneous fluid flow and intestinal absorption using steroids as model solutes. *International Journal of Pharmaceutics*, **4**, 249–262.

43 Levitt, M.D., Furne, J.K., Strocchi, A., Anderson, B.W. and Levitt, D.G. (1990) Physiological measurements of luminal stirring in the dog and human small bowel. *The Journal of Clinical Investigation*, **86**, 1540–1547.

44 Oberle, R.L., Chen, T.S., Lloyd, C., Barnett, J.L., Owyang, C. *et al.* (1990) The influence of the interdigestive migrating myoelectric complex on the gastric emptying of liquids. *Gastroenterology*, **99**, 1275–1282.

45 Sandberg, A., Abrahamsson, B. and Sjogren, J. (1991) Influence of dissolution rate on the extent and rate of bio-availability of metoprolol. *International Journal of Pharmaceutics*, **68**, 167–177.

46 Suzuki, H. and Sugiyama, Y. (2000) Role of metabolic enzymes and efflux transporters in the absorption of drugs from the small intestine. *European Journal of Pharmaceutical Sciences*, **12**, 3–12.

47 Lande, M.B., Donovan, J.M. and Zeidel, M.L. (1995) The relationship between membrane fluidity and permeabilities to water, solutes, ammonia, and protons.

The Journal of General Physiology, **106**, 67–84.

48 Artursson, P. (1990) Epithelial transport of drugs in cell culture. I. A model for studying the passive diffusion of drugs over intestinal absorptive (Caco-2) cells. *Journal of Pharmaceutical Sciences*, **79**, 476–482.

49 Benet, L.Z. and Cummins, C.L. (2001) The drug efflux–metabolism alliance: biochemical aspects. *Advanced Drug Delivery Reviews*, **50** (Suppl. 1), S3–S11.

50 Nakamura, T., Sakaeda, T., Ohmoto, N., Tamura, T., Aoyama, N. *et al.* (2002) Real-time quantitative polymerase chain reaction for MDR1, MRP1, MRP2, and CYP3A-mRNA levels in Caco-2 cell lines, human duodenal enterocytes, normal colorectal tissues, and colorectal adenocarcinomas. *Drug Metabolism and Disposition: The Biological Fate of Chemicals*, **30**, 4–6.

51 de Waziers, I., Cugnenc, P.H., Yang, C.S., Leroux, J.P. and Beaune, P.H. (1990) Cytochrome P 450 isoenzymes, epoxide hydrolase and glutathione transferases in rat and human hepatic and extrahepatic tissues. *The Journal of Pharmacology and Experimental Therapeutics*, **253**, 387–394.

52 Lindahl, A., Borestrom, C., Landin, A., Ungell, A.L. and Abrahamsson, B. (2001) *In vitro* metabolism in the colonic lumen. EUFEPS World Conference on Drug Absorption and Drug Delivery Benefiting from the New Biology and Informatics, Copenhagen.

53 Goldin, B.R. (1990) Intestinal microflora: metabolism of drugs and carcinogens. *Annals of Medicine*, **22**, 43–48.

54 Alabaster, V., *In Vivo* Pharmacology Training Group (2002) The fall and rise of *in vivo* pharmacology. *Trends in Pharmacological Sciences*, **23**, 13–18.

55 Lande, M.B., Priver, N.A. and Zeidel, M.L. (1994) Determinants of apical membrane permeabilities of barrier epithelia. *The American Journal of Physiology*, **267**, C367–374.

56 Mouritsen, O.G. and Jorgensen, K. (1998) A new look at lipid-membrane structure in relation to drug research. *Pharmaceutical Research*, **15**, 1507–1519.

57 Krondahl, E., Orzechowski, A., Ekstrom, G. and Lennernäs, H. (1997) Rat jejunal permeability and metabolism of mu-selective tetrapeptides in gastro-intestinal fluids from humans and rats. *Pharmaceutical Research*, **14**, 1780–1785.

58 Langguth, P., Bohner, V., Heizmann, J., Merkle, H.P., S.W. *et al.* (1997) The challenge of proteolytic enzymes in intestinal peptide delivery. *Journal of Controlled Release*, **46**, 29–57.

59 Madara, J.L. and Pappenheimer, J.R. (1987) Structural basis for physiological regulation of paracellular pathways in intestinal epithelia. *The Journal of Membrane Biology*, **100**, 149–164.

60 Soergel, K.H. (1993) Showdown at the tight junction. *Gastroenterology*, **105**, 1247–1250.

61 van de Waterbeemd, H., Smith, D.A., Beaumont, K. and Walker, D.K. (2001) Property-based design: optimization of drug absorption and pharmacokinetics. *Journal of Medicinal Chemistry*, **44**, 1313–1333.

62 Pappenheimer, J.R. and Reiss, K.Z. (1987) Contribution of solvent drag through intercellular junctions to absorption of nutrients by the small intestine of the rat. *The Journal of Membrane Biology*, **100**, 123–136.

63 Smith, D.A., Jones, B.C. and Walker, D.K. (1996) Design of drugs involving the concepts and theories of drug metabolism and pharmacokinetics. *Medicinal Research Reviews*, **16**, 243–266.

64 Nilsson, D., Fagerholm, U. and Lennernäs, H. (1994) The influence of net water absorption on the permeability of antipyrine and levodopa in the human jejunum. *Pharmaceutical Research*, **11**, 1540–1547.

65 Uhing, M.R. and Kimura, R.E. (1995) The effect of surgical bowel manipulation and

anesthesia on intestinal glucose absorption in rats. *The Journal of Clinical Investigation*, **95**, 2790–2798.

66 Sadowski, D.C. and Meddings, J.B. (1993) Luminal nutrients alter tight-junction permeability in the rat jejunum: an *in vivo* perfusion model. *Canadian Journal of Physiology and Pharmacology*, **71**, 835–839.

67 Fine, K.D., Santa Ana, C.A., Porter, J.L. and Fordtran, J.S. (1994) Mechanism by which glucose stimulates the passive absorption of small solutes by the human jejunum *in vivo*. *Gastroenterology*, **107**, 389–395.

68 Pappenheimer, J.R., Dahl, C.E., Karnovsky, M.L. and Maggio, J.E. (1994) Intestinal absorption and excretion of octapeptides composed of D amino acids. *Proceedings of the National Academy of Sciences of the United States of America*, **91**, 1942–1945.

69 Karlsson, J., Kuo, S.M., Ziemniak, J. and Artursson, P. (1993) Transport of celiprolol across human intestinal epithelial (Caco-2) cells: mediation of secretion by multiple transporters including P-glycoprotein. *British Journal of Pharmacology*, **110**, 1009–1016.

70 Walle, U.K., Pesola, G.R. and Walle, T. (1993) Stereoselective sulphate conjugation of salbutamol in humans: comparison of hepatic, intestinal and platelet activity. *British Journal of Clinical Pharmacology*, **35**, 413–418.

71 Nyberg, L. (1984) Pharmacokinetic parameters of terbutaline in healthy man. An overview. *European Journal of Respiratory Diseases Supplement*, **134**, 149–160.

72 Amelsberg, A., Schteingart, C.D., Ton-Nu, H.T. and Hofmann, A.F. (1996) Carrier-mediated jejunal absorption of conjugated bile acids in the guinea pig. *Gastroenterology*, **110**, 1098–1106.

73 Fagerholm, U. and Lennernäs, H. (1995) Experimental estimation of the effective unstirred water layer thickness in the human jejunum, and its importance in oral drug absorption. *European Journal of Pharmaceutical Sciences*, **3**, 247–253.

74 Anderson, B.W., Levine, A.S., Levitt, D.G., Kneip, J.M. and Levitt, M.D. (1988) Physiological measurement of luminal stirring in perfused rat jejunum. *The American Journal of Physiology*, **254**, G843–G848.

75 Ungell, A.L., Nylander, S., Bergstrand, S., Sjoberg, A. and Lennernäs, H. (1998) Membrane transport of drugs in different regions of the intestinal tract of the rat. *Journal of Pharmaceutical Sciences*, **87**, 360–366.

76 Jack, D.B. (1992) *Handbook of Clinical Pharmacokinetic Data*, Macmillan Publishers Ltd, Basingstoke.

77 Johnson, B.M., Charman, W.N. and Porter, C.J. (2001) The impact of P-glycoprotein efflux on enterocyte residence time and enterocyte-based metabolism of verapamil. *The Journal of Pharmacy and Pharmacology*, **53**, 1611–1619.

78 Hammarlund-Udenaes, M. and Benet, L.Z. (1989) Furosemide pharmacokinetics and pharmacodynamics in health and disease – an update. *Journal of Pharmacokinetics and Biopharmaceutics*, **17**, 1–46.

79 Ponto, L.L. and Schoenwald, R.D. (1990) Furosemide (frusemide). A pharmacokinetic/pharmacodynamic review (Part I). *Clinical Pharmacokinetics*, **18**, 381–408.

80 Flanagan, S.D., Takahashi, L.H., Liu, X. and Benet, L.Z. (2002) Contributions of saturable active secretion, passive transcellular, and paracellular diffusion to the overall transport of furosemide across adenocarcinoma (Caco-2) cells. *Journal of Pharmaceutical Sciences*, **91**, 1169–1177.

81 Lennernäs, H., Nilsson, D., Aquilonius, S.M., Ahrenstedt, O., Knutson, L. *et al.* (1993) The effect of L-leucine on the absorption of levodopa, studied by regional jejunal perfusion in man. *British*

Journal of Clinical Pharmacology, **35**, 243–250.

82 Sun, D., Lennernäs, H., Welage, L.S., Barnett, J., Landowaki, C.P. *et al.* (2002) A comparison of human and Caco-2 gene expression profiles for 12,000 genes and the permeabilities of 26 drugs in the human intestine and Caco-2 cells. *Pharmaceutical Research*, (in press).

83 Adibi, S.A. (1997) The oligopeptide transporter (Pept-1) in human intestine: biology and function. *Gastroenterology*, **113**, 332–340.

84 Paintaud, G., Alvan, G., Dahl, M.L., Grahnen, A., Sjovall, J. *et al.* (1992) Nonlinearity of amoxicillin absorption kinetics in human. *European Journal of Clinical Pharmacology*, **43**, 283–288.

85 Chulavatnatol, S. and Charles, B.G. (1994) Determination of dose-dependent absorption of amoxycillin from urinary excretion data in healthy subjects. *British Journal of Clinical Pharmacology*, **38**, 274–277.

86 Shiraga, T., Miyamoto, K., Tanaka, H., Yamamoto, H., Taketani, Y. *et al.* (1999) Cellular and molecular mechanisms of dietary regulation on rat intestinal H^+/peptide transporter PepT1. *Gastroenterology*, **116**, 354–362.

87 Thamotharan, M., Bawani, S.Z., Zhou, X. and Adibi, S.A. (1999) Hormonal regulation of oligopeptide transporter pept-1 in a human intestinal cell line. *The American Journal of Physiology*, **276**, C821–C826.

88 Swaan, P.W., Koops, B.C., Moret, E.E. and Tukker, J.J. (1998) Mapping the binding site of the small intestinal peptide carrier (PepT1) using comparative molecular field analysis. *Receptors & Channels*, **6**, 189–200.

89 Chu, X.Y., Sanchez-Castano, G.P., Higaki, K., Oh, D.M., Hsu, C.P. *et al.* (2001) Correlation between epithelial cell permeability of cephalexin and expression of intestinal oligopeptide transporter. *The Journal of Pharmacology and Experimental Therapeutics*, **299**, 575–582.

90 Grahnen, A. (1985) The impact of time dependent phenomena on bioequivalence studies, in *Topics in Pharmaceutical Sciences*, Elsevier, Amsterdam, pp. 179–190.

91 Grahnen, A., von Bahr, C., Lindstrom, B. and Rosen, A. (1979) Bioavailability and pharmacokinetics of cimetidine. *European Journal of Clinical Pharmacology*, **16**, 335–340.

92 Collett, A., Higgs, N.B., Sims, E., Rowland, M. and Warhurst, G. (1999) Modulation of the permeability of H2 receptor antagonists cimetidine and ranitidine by P-glycoprotein in rat intestine and the human colonic cell line Caco-2. *The Journal of Pharmacology and Experimental Therapeutics*, **288**, 171–178.

93 Guengerich, F.P. (1999) Cytochrome P-450 3A4: regulation and role in drug metabolism. *Annual Review of Pharmacology and Toxicology*, **39**, 1–17.

94 Eichelbaum, M. and Burk, O. (2001) CYP3A genetics in drug metabolism. *Nature Medicine*, **7**, 285–287.

95 Paine, M.F., Khalighi, M., Fisher, J.M., Shen, D.D., Kunze, K.L. *et al.* (1997) Characterization of interintestinal and intraintestinal variations in human CYP3A-dependent metabolism. *The Journal of Pharmacology and Experimental Therapeutics*, **283**, 1552–1562.

96 Shimada, T., Yamazaki, H., Mimura, M., Inui, Y. and Guengerich, F.P. (1994) Interindividual variations in human liver cytochrome P-450 enzymes involved in the oxidation of drugs, carcinogens and toxic chemicals: studies with liver microsomes of 30 Japanese and 30 Caucasians. *The Journal of Pharmacology and Experimental Therapeutics*, **270**, 414–423.

97 Regardh, C.G., Edgar, B., Olsson, R., Kendall, M., Collste, P. *et al.* (1989) Pharmacokinetics of felodipine in patients with liver disease. *European*

Journal of Clinical Pharmacology, **36**, 473–479.

98 Paine, M.F., Shen, D.D., Kunze, K.L., Perkins, J.D., Marsh, C.L. *et al.* (1996) First-pass metabolism of midazolam by the human intestine. *Clinical Pharmacology and Therapeutics*, **60**, 14–24.

99 Thummel, K.E., O'Shea, D., Paine, M.F., Shen, D.D., Kunze, K.L. *et al.* (1996) Oral first-pass elimination of midazolam involves both gastrointestinal and hepatic CYP3A-mediated metabolism. *Clinical Pharmacology and Therapeutics*, **59**, 491–502.

100 Watkins, P.B. (1997) The barrier function of CYP3A4 and P-glycoprotein in the small bowel. *Advanced Drug Delivery Reviews*, **27**, 161–170.

101 Ito, K., Kusuhara, H. and Sugiyama, Y. (1999) Effects of intestinal CYP3A4 and P-glycoprotein on oral drug absorption – theoretical approach. *Pharmaceutical Research*, **16**, 225–231.

102 Lampen, A., Zhang, Y., Hackbarth, I., Benet, L.Z., Sewing, K.F. *et al.* (1998) Metabolism and transport of the macrolide immunosuppressant sirolimus in the small intestine. *The Journal of Pharmacology and Experimental Therapeutics*, **285**, 1104–1112.

103 Hochman, J.H., Chiba, M., Nishime, J., Yamazaki, M. and Lin, J.H. (2000) Influence of P-glycoprotein on the transport and metabolism of indinavir in Caco-2 cells expressing cytochrome P-450 3A4. *The Journal of Pharmacology and Experimental Therapeutics*, **292**, 310–318.

104 Berggren, S., Lennernäs, P., Ekelund, M., Westrom, B., Hoogstraate, J. *et al.* (2002) Regional difference in permeability and metabolism of ropivacaine and its CYP 3A4 metabolite PPX in human intestine. *Drug Metabolism and Disposition: The Biological Fate of Chemicals* (in press).

105 Cummins, C.L., Mangravite, L.M. and Benet, L.Z. (2001) Characterizing the expression of CYP3A4 and efflux transporters (P-gp, MRP1, and MRP2) in CYP3A4-transfected Caco-2 cells after induction with sodium butyrate and the phorbol ester 12-*O*-tetradecanoylphorbol-13- acetate. *Pharmaceutical Research*, **18**, 1102–1109.

106 Wacher, V.J., Wu, C.Y. and Benet, L.Z. (1995) Overlapping substrate specificities and tissue distribution of cytochrome P450 3A and P-glycoprotein: implications for drug delivery and activity in cancer chemotherapy. *Molecular Carcinogenesis*, **13**, 129–134.

107 Tucker, G.T., Houston, J.B. and Huang, S.M. (2001) Optimizing drug development: strategies to assess drug metabolism/transporter interaction potential – towards a consensus. *British Journal of Clinical Pharmacology*, **52**, 107–117.

108 Klein, I., Sarkadi, B. and Varadi, A. (1999) An inventory of the human ABC proteins. *Biochimica et Biophysica Acta*, **1461**, 237–262.

109 Makhey, V.D., Guo, A., Norris, D.A., Hu, P., Yan, J. *et al.* (1998) Characterization of the regional intestinal kinetics of drug efflux in rat and human intestine and in Caco-2 cells. *Pharmaceutical Research*, **15**, 1160–1167.

110 Martin, C., Berridge, G., Higgins, C.F., Mistry, P., Charlton, P. *et al.* (2000) Communication between multiple drug binding sites on P-glycoprotein. *Molecular Pharmacology*, **58**, 624–632.

111 Jonker, J.W., Smit, J.W., Brinkhuis, R.F., Maliepaard, M., Beijnen, J.H. *et al.* (2000) Role of breast cancer resistance protein in the bioavailability and fetal penetration of topotecan. *Journal of the National Cancer Institute*, **92**, 1651–1656.

112 Stephens, R.H., O'Neill, C.A., Warhurst, A., Carlson, G.L., Rowland, M. *et al.* (2001) Kinetic profiling of P-glycoprotein-mediated drug efflux in rat and human intestinal epithelia. *The Journal of Pharmacology and Experimental Therapeutics*, **296**, 584–591.

113 Schwarz, U.I., Gramatte, T., Krappweis, J., Oertel, R. and Kirch, W. (2000) P-glycoprotein inhibitor erythromycin increases oral bioavailability of talinolol in humans. *International Journal of Clinical and Pharmacology and Therapeutics (Munchen)*, **38**, 161–167.

114 Gramatte, T. and Oertel, R. (1999) Intestinal secretion of intravenous talinolol is inhibited by luminal *R*-verapamil. *Clinical Pharmacology and Therapeutics*, **66**, 239–245.

115 Hoffmeyer, S., Burk, O., von Richter, O., Arnold, H.P., Brockmoller, J. *et al.* (2000) Functional polymorphisms of the human multidrug-resistance gene: multiple sequence variations and correlation of one allele with P-glycoprotein expression and activity *in vivo*. *Proceedings of the National Academy of Sciences of the United States of America*, **97**, 3473–3478.

116 Sakaeda, T., Nakamura, T., Horinouchi, M., Kakumoto, M., Ohmoto, N. *et al.* (2001) MDR1 genotype-related pharmacokinetics of digoxin after single oral administration in healthy Japanese subjects. *Pharmaceutical Research*, **18**, 1400–1404.

117 Boyd, R.A., Stern, R.H., Stewart, B.H., Wu, X., Reyner, E.L. *et al.* (2000) Atorvastatin coadministration may increase digoxin concentrations by inhibition of intestinal P-glycoprotein-mediated secretion. *Journal of Clinical Pharmacology*, **40**, 91–98.

118 Bogman, K., Peyer, A.K., Torok, M., Kusters, E. and Drewe, J. (2001) HMG-CoA reductase inhibitors and P-glycoprotein modulation. *British Journal of Pharmacology*, **132**, 1183–1192.

119 Floren, L.C., Bekersky, I., Benet, L.Z., Mekki, Q., Dressler, D. *et al.* (1997) Tacrolimus oral bioavailability doubles with coadministration of ketoconazole. *Clinical Pharmacology and Therapeutics*, **62**, 41–49.

120 Lin, J.H., Chiba, M. and Baillie, T.A. (1999) Is the role of the small intestine in first-pass metabolism overemphasized? *Pharmacological Reviews*, **51**, 135–158.

121 Fromm, M.F., Dilger, K., Busse, D., Kroemer, H.K., Eichelbaum, M. *et al.* (1998) Gut wall metabolism of verapamil in older people: effects of rifampicin-mediated enzyme induction. *British Journal of Clinical Pharmacology*, **45**, 247–255.

122 Loo, T.W. and Clarke, D.M. (2001) Defining the drug-binding site in the human multidrug resistance P-glycoprotein using a methanethiosulfonate analog of verapamil, MTS-verapamil. *The Journal of Biological Chemistry*, **276**, 14972–14979.

123 Zhang, Y., Hsieh, Y., Izumi, T., Lin, E.T. and Benet, L.Z. (1998) Effects of ketoconazole on the intestinal metabolism, transport and oral bioavailability of K02, a novel vinylsulfone peptidomimetic cysteine protease inhibitor and a P450 3A, P-glycoprotein dual substrate, in male Sprague–Dawley rats. *The Journal of Pharmacology and Experimental Therapeutics*, **287**, 246–252.

124 von Moltke, L.L., Greenblatt, D.J., Duan, S.X., Harmatz, J.S. and Shader, R.I. (1994) *In vitro* prediction of the terfenadine–ketoconazole pharmacokinetic interaction. *Journal of Clinical Pharmacology*, **34**, 1222–1227.

125 Gibbs, M.A., Thummel, K.E., Shen, D.D. and Kunze, K.L. (1999) Inhibition of cytochrome P-450 3A (CYP3A) in human intestinal and liver microsomes: comparison of Ki values and impact of CYP3A5 expression. *Drug Metabolism and Disposition: The Biological Fate of Chemicals*, **27**, 180–187.

126 Paine, M.F., Leung, L.Y., Lim, H.K., Liao, K., Oganesian, A. *et al.* (2002) Identification of a novel route of extraction of sirolimus in human small intestine: roles of metabolism and secretion. *The Journal of Pharmacology and Experimental Therapeutics*, **301**, 174–186.

127 Li, L.Y., Amidon, G.L., Kim, J.S., Heimbach, T., Kesisoglou, F. *et al.* (2002) Intestinal metabolism promotes regional differences in apical uptake of indinavir: coupled effect of P-glycoprotein and cytochrome P450 3A on indinavir membrane permeability in rat. *The Journal of Pharmacology and Experimental Therapeutics*, **301**, 586–593.

128 Obach, R.S., Zhang, Q.Y., Dunbar, D. and Kaminsky, L.S. (2001) Metabolic characterization of the major human small intestinal cytochrome P450s. *Drug Metabolism and Disposition: The Biological Fate of Chemicals*, **29**, 347–352.

129 Fricker, G., Drewe, J., Huwyler, J., Gutmann, H. and Beglinger, C. (1996) Relevance of P-glycoprotein for the enteral absorption of cyclosporin A: *in vitro–in vivo* correlation. *British Journal of Pharmacology*, **118**, 1841–1847.

130 Lown, K.S., Mayo, R.R., Leichtman, A.B., Hsiao, H.L., Turgeon, D.K. *et al.* (1997) Role of intestinal P-glycoprotein (mdr1) in interpatient variation in the oral bioavailability of cyclosporine. *Clinical Pharmacology and Therapeutics*, **62**, 248–260.

131 Hamman, M.A., Bruce, M.A., Haehner-Daniels, B.D. and Hall, S.D. (2001) The effect of rifampin administration on the disposition of fexofenadine. *Clinical Pharmacology and Therapeutics*, **69**, 114–121.

132 Davit, B., Reynolds, K., Yuan, R., Ajayi, F., Conner, D. *et al.* (1999) FDA evaluations using *in vitro* metabolism to predict and interpret *in vivo* metabolic drug–drug interactions: impact on labeling. *Journal of Clinical Pharmacology*, **39**, 899–910.

133 Simpson, K. and Jarvis, B. (2000) Fexofenadine: a review of its use in the management of seasonal allergic rhinitis and chronic idiopathic urticaria. *Drugs*, **59**, 301–321.

134 Cvetkovic, M., Leake, B., Fromm, M.F., Wilkinson, G.R. and Kim, R.B. (1999) OATP and P-glycoprotein transporters mediate the cellular uptake and excretion of fexofenadine. *Drug Metabolism and Disposition: The Biological Fate of Chemicals*, **27**, 866–871.

135 Soldner, A., Christians, U., Susanto, M., Wacher, V.J., Silverman, J.A. *et al.* (1999) Grapefruit juice activates P-glycoprotein-mediated drug transport. *Pharmaceutical Research*, **16**, 478–485.

136 Farrell, R.J., Murphy, A., Long, A., Donnelly, S., Cherikuri, A. *et al.* (2000) High multidrug resistance (P-glycoprotein 170) expression in inflammatory bowel disease patients who fail medical therapy. *Gastroenterology*, **118**, 279–288.

137 Sababi, M., Borga, O. and Hultkvist-Bengtsson, U. (2001) The role of P-glycoprotein in limiting intestinal regional absorption of digoxin in rats. *European Journal of Pharmaceutical Sciences*, **14**, 21–27.

138 Ussing, H.H. (1966) Anomalous transport of electrolytes and sucrose through the isolated frog skin induced by hypertonicity of the outside bathing solution. *Annals of the New York Academy of Sciences*, **137**, 543–555.

139 Sutcliffe, F.A., Riley, S.A., Kaser-Liard, B., Turnberg, L.A. and Rowland, M. (1988) Absorption of drugs from the human jejunum and ileum. *British Journal of Clinical Pharmacology*, **26**, 206P–207P.

140 Gramatte, T. (1994) Griseofulvin absorption from different sites in the human small intestine. *Biopharmaceutics & Drug Disposition*, **15**, 747–759.

141 Gramatte, T. and Richter, K. (1994) Paracetamol absorption from different sites in the human small intestine. *British Journal of Clinical Pharmacology*, **37**, 608–611.

142 Gramatte, T., el Desoky, E. and Klotz, U. (1994) Site-dependent small intestinal absorption of ranitidine. *European Journal of Clinical Pharmacology*, **46**, 253–259.

143 Lennernäs, H., Fagerholm, U., Raab, Y., Gerdin, B. and Hallgren, R. (1995)

Regional rectal perfusion: a new *in vivo* approach to study rectal drug absorption in man. *Pharmaceutical Research*, **12**, 426–432.

144 Brady, J.M., Cherrington, N.J., Hartley, D.P., Buist, S.C., Li, N. and Klaassen, C.D. (2002) Distribution and chemical induction of multiple drug resistance genes in rats. *Drug Metabolism and Disposition: The Biological Fate of Chemicals*, **30**, 838–844.

Part Three
Role of Transporters and Metabolism in Oral Absorption

10
Transporters in the Gastrointestinal Tract

Pascale Anderle and Carsten U. Nielsen

Abbreviations

ABC	ATP-binding cassette
ATP	Adenosine 5′-triphosphate
CDX	Caudal-type homeobox transcription factor
CNT	Concentrative nucleoside transporter
ENT	Equilibrative nucleoside transporter
EMT	Epithelial–mesenchymal transition
GIT	Gastrointestinal tract
GO	Gene ontology
NCE	New chemical entity
PEPT1	Di/tri-peptide transporter 1
PMT	Pharmacogenetics of Membrane Transporters Project
QSAR	Quantitative structure–activity relationship
SAR	Structure–activity relationship
SLC	Solute carriers (SLCs)

10.1
Introduction

In 1992, Beauchamp *et al*. published a paper on the synthesis of 18 amino acid esters of the antiherpetic drug, acyclovir [1]. These esters were synthesized as potential prodrugs intended for oral administration, and were less potent than the parent compound with respect to *in vitro* antiviral activity against herpes simplex virus type 1 (HSV-1). However, 10 of the prodrugs produced greater amounts of the parent drug in the urine of rats used in the study. The L-amino acid esters were better prodrugs than the corresponding D- or D,L-isomers, suggesting the involvement of a stereo-

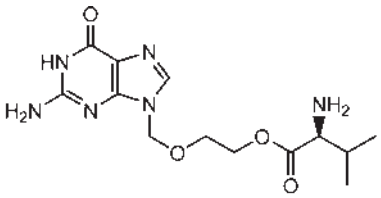

I. Valaciclovir

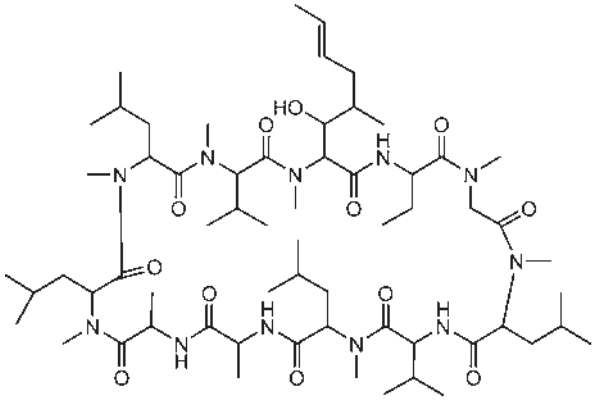

II. Cyclosporine A

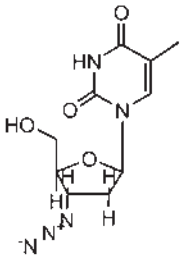

III. AZT

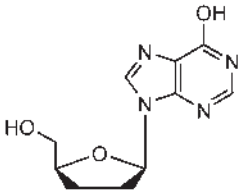

IV. 2',3'-dideoxyinosine

Figure 10.1 Chemical structures of some selected compounds involved in active drug absorption.

selective transporter. The L-valyl ester was the best prodrug (cf. Figure 10.1 (**I**)),[1)] and in 1998 de Vrueh and coworkers showed that the responsible transporter was the di/tripeptide transporter also termed PEPT1 (SLC15A1) [2]. This illustrated the impact of targeting transporters, although the discovery of valaciclovir as a PEPT prodrug

1) In the following text, roman numbers refer to the chemical structures throughout, as illustrated in Figure 10.1.

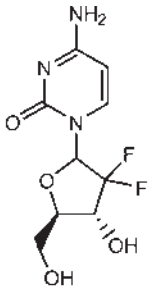

V. Gemcitabine

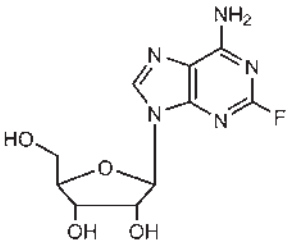

VI. Fludarabine

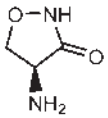

VII. D-cycloserine

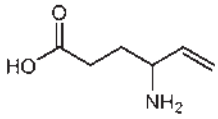

VIII. Vigabatrin

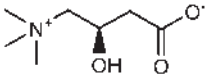

IX. L-carnitine

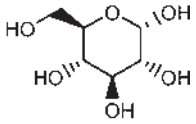

X. Glucose

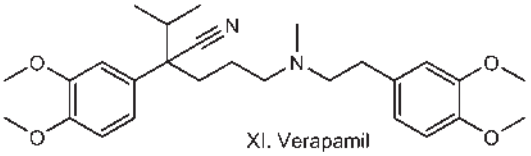

XI. Verapamil

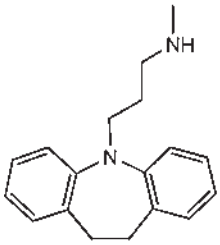

XII. Desipramine

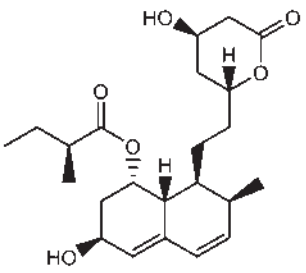

XIII. Pravastatin

Figure 10.1 (*Continued*)

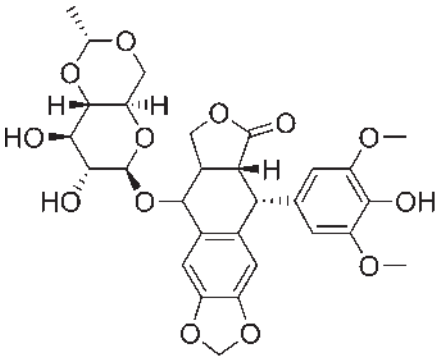

XV. Etoposide

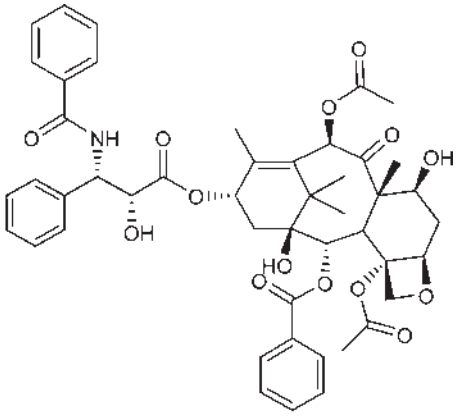

XVI. Paclitaxel

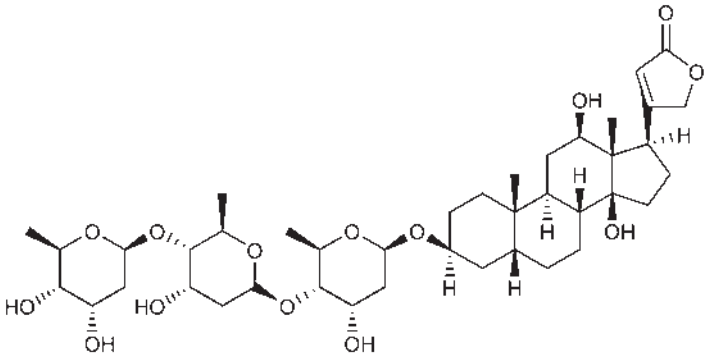

XVII. Digoxin

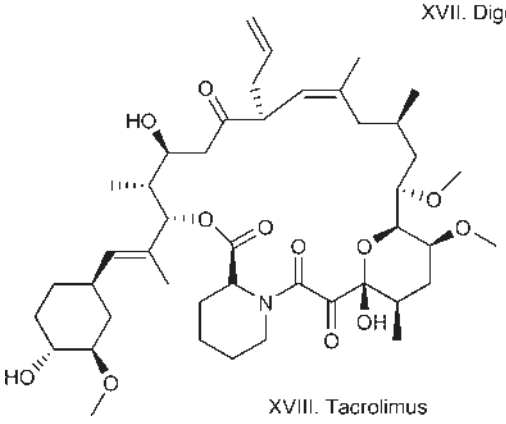

XVIII. Tacrolimus

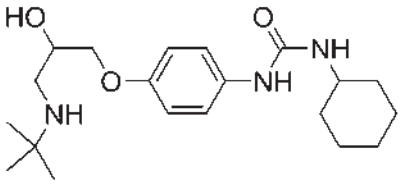

XIX. Talinolol

Figure 10.1 (*Continued*)

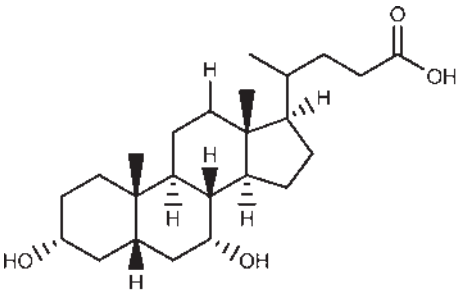

XX. Chenodeoxycholic acid

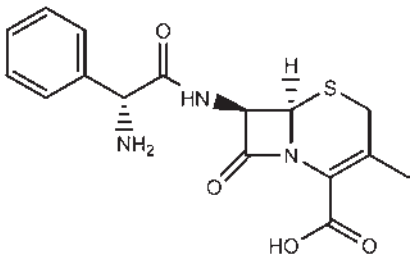

XXI. Cephalexin

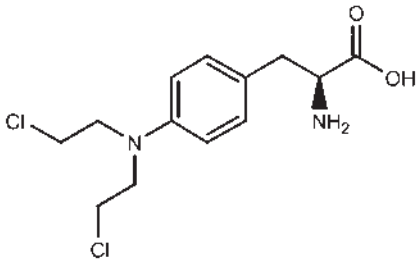

XXII. Melphalan

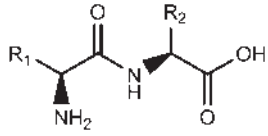

XXIII. Dipeptide backbone

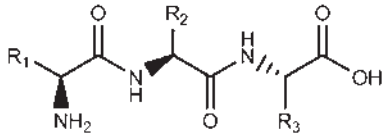

XXIV. Tripeptide Backbone

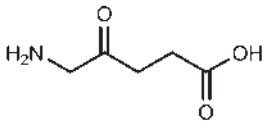

XXV. δ-amino levulinic acid

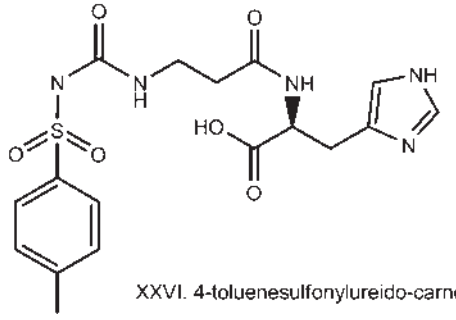

XXVI. 4-toluenesulfonylureido-carnosine

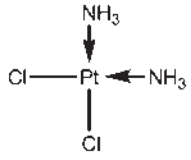

XXVII: Cisplatin

Figure 10.1 (*Continued*)

seems to have been serendipitous. Nevertheless, over the past two decades, an increased focus has been on transporters – absorptive as well as efflux – in relation to drug absorption.

The aim of this chapter is to provide an overview of transporters present in the gastrointestinal tract, their role in intestinal drug absorption, and their relevance as a drug delivery target to the medicinal chemist. Drug discovery is a multidisciplinary process, which we would like to illustrate in this chapter. We will cover elements of prodrug design, structure–activity relations, expression profiles, transporter genomics, and regulation and briefly mention methods for studying these elements all in specific relation to the relevance of active transport in the gastrointestinal tract (GIT) for drug absorption or pathophysiological conditions. In addition, in the context of pathophysiological states of the intestine, we will discuss the role of transporters not only as drug carriers but also as direct drug targets.

In the previous edition of this book, the chapter on transporters in the gastrointestinal tract described the various transporters and their families in general. In this edition, we will focus on selected transporters that have proven relevant to the medicinal chemist or pharmaceutical scientist in general. The chapter is structured in the following manner: Section 10.2 provides an overview of active transporters present along the intestine and their influence on drug absorption, Section 10.3 deals with transporters and their genomics, Section 10.4 discusses structural features for targeting intestinal transporters, and Section 10.5 illustrates the altered expression of transporters in diseased staten of the intestine. We will outline at the end of each section, the impact on medical chemistry and how these various aspects affect the work of the medical chemists.

10.2
Active Transport Along the Intestine and Influence on Drug Absorption

Transporters in the intestine generally fall into two distinct groups. One group consists of absorptive transporters belonging to the solute carrier (SLC) family and a second group consists of drug efflux transporters of the ATP-binding cassette (ABC) family (ABC transporters). In general, active transporters are transporters where the translocation of substrate is linked to the ATP consumption, whereas transporters where the translocation of substrate is down the concentration gradient of the substrate or coupled to the influx of ion such as Na^+ or H^+ are termed carriers. Transporters are often referred to as drug transporters, which in the context of drug discovery or development is certainly an appropriate term. However, it is important to remember that the normal function of transporters is to move nutrients or xenobiotic waste products across the cell membrane. In Table 10.1, a number of relevant intestinal drug transporters are listed. In Figure 10.2, a few examples of the localization of transporters in the apical and basolateral membranes are shown. The distribution of different transporters is part of the cellular polarization of cellular components, and the asymmetric distribution gives rise to polarized transport across the intestine. Certain drug compounds and xenobiotic natural products are exported

Table 10.1 List of relevant transporters for intestinal absorption and/or diseased states of the intestine.

Transporter family	Transporter[a]	Source[b]: Expression	Source[c]: SNP	Xenobiotic substrates[d]
Peptides				
SLC15A	*SLC15A/PEPT1*	Small intestine, all three segments [3, 4]	[61, 62]	β-Lactam antibiotics (e.g., cephalexin), various amino acid and dipeptide prodrugs (e.g., valaciclovir) [2, 8–10]
	CDH17/HPT1	Small intestine, colon [3, 4]	N/A	Valaciclovir [6, 12, 204]
Nucleosides				
SLC28A	*SLC28A1/CNT1*	Small intestine, all three segments [3, 4]	[64]	Azidothymidine, cemcitabine [20–22]
	SLC28A2/CNT2	Small intestine, all three segments [3, 4]	[65]	2′,3′-dideoxyinosine [23]
	SLC28A3/CNT3	Small intestine, duodenum, and jejunum [3, 4]	[66]	Gemcitabine, cladribine, and fludarabine [17]
SLC29A	*SLC29A1/ENT1*	Small intestine, duodenum, and jejunum [3, 4]	PMT	Cladribine, cytarabine, and gemcitabine [205]
	SLC29A2/ENT2	Colon [3, 4, 16]	[67]	AZT, gemcitabine [205]
	SLC29A3/ENT3	Small intestine, duodenum, and jejunum [3, 4]	N/A	cf. ENT2 [206]
Amino acids				
SLC3A	SLC3A1/rBAT	Small intestine [207]	[208–210]	Gabapentin [28]
	SLC3A2/4F2HC	Intestine [4]	[68]	
SLC6A	*SLC6A14/ATB$^{0,+}$*	Colon [29]	[211]	D-Serine, L-carnitine [29]
SLC7A	SLC7A5/LAT1	Duodenum [58]	[68]	Gabapentin [205]
	SLC7A9/b0,+AT	cf. SLC3A1	[212, 213]	Gabapentin [205]
SLC1A	SLC1A1/EAAT3	Duodenum [4]	[214, 215]	N/A

(*Continued*)

Table 10.1 (*Continued*)

Transporter family	Transporter[a]	Source[b]: Expression	Source[c]: SNP	Xenobiotic substrates[d]
	SLC1A5/ATB0	Ileum [216]	[217]	N/A
SLC36A	*SLC36A1/PAT1*	Whole GIT [25]	N/A	GABA, vigabatrin, D-cycloserine [26, 27]
Monosaccharides				
SLC5A	*SLC5A1/SGLT1*	Small intestine [4]	[218]	Phloridzin(I) [95]
SLC2A	*SLC2A5/GLUT5*	Small intestine [4]	N/A	N/A
Organic cations				
SLC22A	SLC22A4/OCTN1	Small and large intestines [3, 4, 16]	[219, 220]	Quinidine, verapamil [30]
	SLC22A5/OCTN2	Small and large intestines [3, 4, 16]	[221]	Cephaloridine [30]
Organic anions				
SLCO2B1	*OATP2B1*	Jejunum, colon [3]	[222]	Pravastatin [32]
Monocarboxylates				
SLC16A	*SLC16A1/MCT1*	Jejunum, colon [3, 4]	N/A	Cefdinir, pravastatin, and valproic acid [35, 36]
	SLC16A8/MCT3	Duodenum [3, 4]	N/A	N/A
	SLC16A3/MCT5	Duodenum, jejunum [3, 4]	N/A	N/A
MRP/MDR (efflux) transporters				
ABC	*ABCB1/MDR1*	Jejunum, colon [3]	[69–71]	Vinblastine, doxorubicin, etoposide, paclitaxel, and dioxine [38]
	ABCC1/MRP1	Jejunum, colon [3]	[73]	Doxorubicin, etoposide, vincristine, and methotrexate [152]
	ABCC2/MRP2	Jejunum [3]	[72, 73]	Methotrexate, etoposide, doxorubicin, cisplatin, and vincristine [152]

	ABCC3/MRP3	Jejunum, colon [3]	[72]	Methotrexate, etoposide, doxorubicin, cisplatin, and vincristine
	ABCC5/MOAT-C	Jejunum, colon [3]	[72, 73]	6-Mercaptopurine, 6-thioguanine [152]
	ABCG2/BCRP	Jejunum, colon [3]	[70]	Doxorubicin, daunorubicin, mitoxantrone, and topotecan [152]
Miscellaneous				
SLC19A	*SLC19A1/RFC1*	Small and large intestines [223]	[224]	Methotrexate [205]
SLC10A	*SLC10A2/ASBT*	Duodenum, ileum [16]	[225]	Bumetanide [205]
Additional, relevant transporters				
SLC5A	SLC5A8	Tumor suppression [161]	N/A	N/A
SLC26A	SLC26A3	Tumor suppression [160, 165]	N/A	N/A
SLC16	SLC16A3/MCT4	Invasion, migration [168]	N/A	N/A

[a] In italics are transporters even more relevant and/or more is known about their involvement in drug and nutrient absorption.
[b] Nonexhaustive list of references regarding expression of the gene in the gut or its specific role in cancer.
[c] Nonexhaustive list of studies on single-nucleotide polymorphisms of the gene; N/A, no relevant reference could be found; PMT, pharmacogenetics of membrane transporters; http://www.pharmgkb.org.
[d] Nonexhaustive list of xenobiotic compounds transported by the protein.

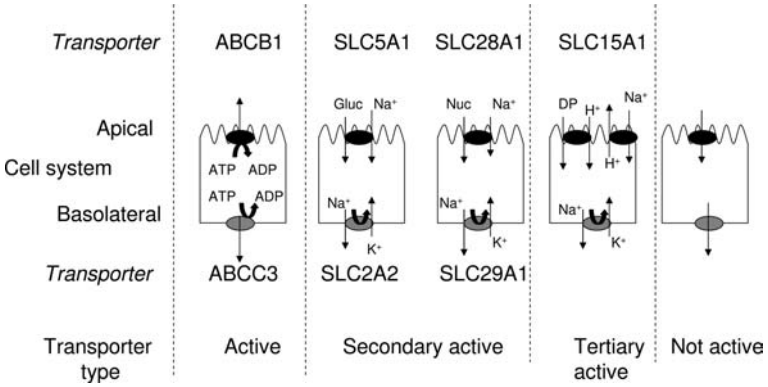

Figure 10.2 Illustration of the various forms of transporters and carriers working in an intestinal epithelial cell. Gluc, glucose; Nuc, nucleotide; DP, dipeptides; and ABC, ATP-binding cassette family transporter; SLC5A1, sodium-dependent glucose transporter; SLC2A2, glucose transporter 2; SLC28A1, concentrative nucleotide transporter 1; SLC29A1, equilibrative transporter 1; and SLC15A1, di/tripeptide transporter.

or effluxed from the epithelial cell by the apical localized ABCB1 (also termed P-glycoprotein (P-gp), and MDR1) and the basolateral localized ABCC3. Glucose is transported across the apical membrane by SLC5A1 (SGLT1) in a sodium-dependent manner, and the cellular efflux is mediated by SLC2A2 (GLUT2), which is not coupled to any other driving force. Nucleoside or nucleoside drugs are transported into the epithelial cell by SLC28A1 (CNT1) and effluxed by SLC29A1 (ENT1). Di/tripeptides and some peptidomimetic drugs are transported into the cell by SLC15A1 (PEPT1) and transported from the cell to the blood circulation by a transporter, which has as yet not been cloned.

In the following section, selected transporters relevant to drug absorption will be discussed along with known drug–drug interactions caused by transporters. The transporters will be discussed according to their natural substrates as indicated in Table 10.1.

10.2.1 Peptide Transporters

In the human intestinal cells, two di/tripeptide transporter genes have been detected by quantitative PCR methods (see Table 10.1): *SLC15A1* (*PEPT1*) (see Figure 10.2) and liver–intestine cadherin *CDH17* (*HPT1*). *PEPT1* is highly expressed in the small intestine, that is, duodenum, jejunum, and ileum and in healthy tissue absent in the colon, whereas *HPT1* is highly expressed in both small and large intestines [3, 4]. So far, the consensus in the literature has been that PEPT1 was the major peptide transporter for dietary uptake of amino acids in the form of di/tripeptides and also in terms of intestinal drug absorption [5–7]. PEPT1 has been shown to mediate the oral bioavailability of some β-lactam antibiotics and a number of amino acid and dipeptide

prodrugs [2, 8–10]. PEPT1 is discussed thoroughly in this chapter, since it remains one of most studied intestinal absorptive transporters in drug delivery and oral bioavailability. The intestinal expression of *HPT1* is higher than that of *PEPT1* [3, 4], and *HPT1* expression has in a study been correlated with the bioavailability of valaciclovir [6, 7, 11, 12]. However, since HPT1 belongs to the cadherin superfamily of calcium-dependent, cell–cell adhesion proteins and only has one transmembrane segment [13], its role as a transporter has not been fully resolved. Although not normally referred to a as peptide transporter, ABCB1 has been shown to transport peptides containing a varying number of amino acids from 3 to at least 11 (cyclosporine A (**II**) [14, 15]), thereby *de facto* acting as a peptide transporter. In the apical membrane, the transport direction is out of the cell, as opposed to PEPT1, which is inward directed and coupled to influx of protons, as illustrated in Figure 10.2. However, at the basolateral membrane, the transport direction of both an ABC transporter and a peptide transporter would be from the cell into the circulation.

10.2.2 Nucleoside Transporters

Transporters for nucleosides are present both in the apical (concentrative nucleoside transporters (CNTs)) and in the basolateral membrane of epithelial cells (equilibrative nucleoside transporters (ENTs)). *CNT2* is expressed primarily in the human duodenum and jejunum and to a much higher degree than *CNT1*, *CNT3*, *ENT2*, and *ENT2* [3, 4]. In the ileum, both *CNT1* and *CNT2* are expressed, whereas *ENT2* is expressed in the colon [16]. It has to be noted that human samples are often obtained from patients, and their medications may to some extent alter the expression profile of the investigated transporters, as exemplified in Section 5.4, where PEPT1 is expressed in the colon due to inflammation of the tissue. In the human intestinal epithelium, nucleoside transporters are responsible for the uptake of dietary nucleosides from the intestinal lumen and the regulation of adenosine concentrations on cells' surface. The nucleoside transporters accept a variety of drug molecules structurally related to nucleosides and they may thus be highly relevant from a drug delivery and drug discovery point of view. ENT1 and ENT2 transport both purine and pyrimidine nucleosides, although the substrate affinities in general are lower than those for the CNTs. The concentrative nucleoside transporters CNT1, CNT2, and CNT3 transport uridine and certain uridine analogues, but are otherwise in general (except for a modest transport of adenosine by CNT1) selective for pyrimidine (CNT1) and purine (CNT2) nucleosides, with CNT3 being nonselective for purine and pyrimidine nucleosides [17, 18]. The differences in purine and pyrimidine substrate recognition are also observed with pyrimidine and purine antiviral and anticancer nucleoside drugs. For example, CNT1 transports 3′-azido-3′-deoxythymidine (AZT) (**III**), 2′,3′-dideoxycytidine, and cemcitabine, whereas CNT2 carries 2′,3′-dideoxyinosine (**IV**) [19–23]. CNT3 translocates pyrimidine anticancer nucleoside structures such as 5-fluorouridine, 5-fluoro-2′-deoxyuridine, zebularine, gemcitabine (**V**), and purine nucleoside struc-

tures such as cladribine and fludarabine (**VI**) [17]. Although the concentrative nucleoside transporters have micromolar affinities for the proteotypical substrate uridine, they are interesting for targeting intestinal cells.

10.2.3 Amino Acid Transporters

Several amino acid transporters are present at both apical and basolateral membranes. They have overlapping substrate specificities, different affinities, and capacities and utilize different ions such as Na^+, H^+, and Cl^- for driving force (for a review on the physiology of intestinal amino acid, see Ref. [24]). Moreover, amino acid transporters are affected by a number of diseases such as Hartnup disorder and other absorptive pathological states. Recently, Kim *et al*. detected 12 genes for amino acid transport in the human intestine, where *EAAT3*, *LAT3*, *4F2HC*, and *PROT* were highest expressed [4]. The gene of a proton-coupled amino acid transporter, *PAT1*, has recently been cloned [25]. On the basis of Northern blot, this transporter is expressed in segments from the stomach to the latter parts of the colon, and the PAT1 protein localizes in the apical membrane [25]. PAT1 has millimolar affinity for its substrates (Pro, Gly, Ala, and GABA) and has been shown in *in vitro* studies to be involved in intestinal absorption of D-cycloserine (**VII**) and vigabatrin (**VIII**) [26, 27]. Thus, PAT1 seems to be a drug delivery target for some clinically relevant GABA-related drugs. However, gabapentin is not transported by PAT1 but may be transported by system b ($rBAT/b^{0,+}AT$, SLC3A1/SLC7A9), which transports neutral and dibasic amino acids in a sodium-independent manner [28]. Another amino acid transporter that seems to be interesting from a pharmaceutical point of view is $SLC6A14/ATB^{0,+}$ [29]. This transporter is located in the apical membrane of colonocytes but is not expressed in the small intestine. The transport of amino acid is coupled to Na^+ and Cl^-, and SLC6A14 has been suggested to be relevant to the intestinal absorption of D-serine, carnitine (**IX**), and nitric oxide synthase inhibitors as well as the γ-glutamyl ester of acyclovir [29].

Amino acid transporters seem to hold a great potential for intestinal absorption of drugs and drug candidates. However, overall, the information on the impact of these transporters in terms of mediating oral bioavailability of amino acid mimetics is rather limited, and systematic investigations using both *in vitro* and *in vivo* data are highly anticipated.

10.2.4 Monosaccharide Transporters

In the intestine, primarily two glucose (**X**) transporter genes are detected: *SGLT1* and *GLUT5* [4]. SGLT1 is located in the apical membrane of the small intestinal enterocytes and operates in a sodium-coupled way, whereas GLUT5 is located in the basolateral membrane (cf. Figure 10.2). SLGT1 has been suggested as a target not only for inhibiting the uptake of glucose but also for intestinal transport of glycoside-bond-containing substrate mimics.

10.2.5
Organic Cation Transporters

The organic cation transporters *OCNT1* (*SLC22A4*) and *OCNT2* (*SLC22A5*) are widely expressed in both small and large intestines [3, 4, 16]. *OCT1* (*SLC22A1*) is expressed in the jejunum and colon, whereas *OCT3* (*SLC22A3*) is expressed only in the jejunum [3]. OCNT1 seems to be located in the luminal membrane and transports compounds such as L-carnitine (**IX**), stachydrine, and the organic cations tetraethylammonuim (TEA), quinidine, pyrilamine, and verapamil (**XI**) [30]. OCNT2 is a Na^+-dependent, high-affinity transporter for L-carnitine, acetyl-L-carnitine, and the zwitterionic β-lactam antibiotic cephaloridine, but can also function alternatively as a polyspecific and Na^+-independent cation transporter [30]. OCT1 is localized in the basolateral membrane and transports tetraethylammonium as well as drugs such as desipramine (**XII**), acyclovir, and ganciclovir [31].

10.2.6
Organic Anion Transporters

OATP transporters, *SLCO1C1*, *SLCO2B1*, *SLCO3A1*, *SLCO4A1*, and *SLCO4C1* have been found in the jejunum, and also in the colon, with the exception of *SLCO3A1* [3]. OATP-B (SLCO2B1) accepts bile salts, as well as pravastatin (**XIII**) and sulfate conjugates of steroid hormones, and is localized in the apical membrane of enterocytes [32].

10.2.7
Monocarboxylate Transporters

Monocarboxylate cotransporters (MCTs) transport monocarboxylates such as acetate, propionate, lactate, and pyruvate in a proton-coupled manner or by exchanging one monocarboxylate for another [33]. In the intestine, *MCT1* and *MCT5* have been detected [3], and in another study *MCT3* was detected at a level similar to *MCT5* [4]. *MCT1* is expressed in both small and large intestines [3, 34], whereas *MCT5* was not found in the colon [3]. MCT1 is located in the apical membrane of epithelial cells, whereas MCT3 is located in the basolateral membrane [33]. MCT1 has been suggested to be involved in intestinal transport of the cephalosporin cefdinir, whereas pravastatin (**XIII**) and valproic acid (**XIV**) inhibit the cellular uptake of lactate *in vitro* [35, 36].

10.2.8
ABC Transporters

Some of the intestinal transporters that have received most attention in drug discovery and development are undoubtedly the ATP-binding cassette transport proteins and especially ABCB1 (for reviews see Refs [37–39]). There are numerous publications on these transporters, and we are, thus, able to give only a small glance

on the impact of efflux transporters on drug delivery, drug disposition, pharmacological therapy, metabolism, cancer therapy, and cancer development. Overall, in terms of drug bioavailability, efflux transporters in the intestine limit the intestinal absorption of a wide range of drugs. In the human jejunum and colon, *ABCB1*, *ABCC1* (*MRP1*), *ABCC3* (*MRP3*), and *ABCC4-6* (*MRP4-6*), as well as *ABCG2* (*BCRP*), are expressed [3]. *ABCB4* (*BSEP*) is expressed in the colon, and *ABCB4* and *ABCC2* (*MRP2*) are expressed in the jejunum [3]. The efflux transporters are located in different membranes of the enterocytes, with ABCB1, ABCC2, and ABCG2 located in the apical membrane and ABCC1 and ABCC3 located in the basolateral membrane [38].

ABCB1 has an extremely broad substrate specificity with a preference for lipophilic and cationic compounds; however, these general structural features are by no means restrictive. This is illustrated by the diversity in the substrates identified for ABCB1, including anticancer drug substances such as vinblastine, doxorubicin, etoposide (**XV**), and paclitaxel (**XVI**), cardiac drug substances such as digoxin (**XVII**) and some β-blockers, endogenous compounds such as steroid hormones and bile salts, HIV drugs such as indinavir and saquinavir, fluoroquinolones such as sparfloxacin, and immunosuppressive drugs such as cyclosporine A (**II**) and tacrolimus (**XVIII**) [38]. In general, ABCB1 substrates are thus amphipathic compounds with a molecular weight ranging from approximately 300 to 2000 Da. It has been suggested that ABCB1 binds substrates through an "induced-fit mechanism," where the shape and size of the substrate change the packing of the transmembrane segments to accommodate the substrate [40, 41]. There is some evidence that ABCB1 is functioning in conjunction with metabolizing enzymes. ABCB1 may thus play a dual role in limiting oral bioavailabilities of drug substrates, that is, by reducing their absorption and delivering them to metabolic enzymes or exporting metabolites. In the liver and intestine, this dual function is present in metabolic active cells. Phase-I enzymes such as cytochrome P450 and phase-II enzymes such as gluthathione-*S*-tranferases are key factors in limiting drug bioavailability. There is also some degree of overlapping substrate specificity between CYP3A4 and ABCB1 [42–44]. It is therefore important to consider both the efflux properties and the metabolic properties of drug candidates.

Digoxin (**XVII**) is a typical substrate for ABCB1, and it has been shown in P-gp knockout mice that intestinal efflux and plasma elimination of digoxin are decreased along with increased brain accumulation [45–47]. Coadministration of other ABCB1 substrates alters the pharmacokinetics of digoxin, as seen with an increased bioavailability after coadministration with talinolol (**XIX**) [48]. Other drug–drug interactions caused by intestinal efflux transporter are known for immunosuppressants such as tacrolimus and cyclosporin A, as well as talinolol [39]. It is important to remember that a large degree of overlapping substrate specificity exists between different ABC transporters, and an analysis of the impact of individual transporters on limiting intestinal absorption is perhaps less important than evaluating the combined impact on intestinal absorption of ABC transporters. Moreover, the oral bioavailability is in addition to intestinal absorption a result of many other processes involving ABC transporters. Nevertheless, efflux transporters are important for the

medicinal chemist, as they are involved in absorption, metabolism, and disposition of many diverse molecular structures.

10.2.9
Bile Acid Transporters

The apical localized sodium-dependent bile acid transporter (ASBT) is expressed in the human duodenum and ileum and is barely detectable in colon [16]. ASBT transports bile acids such as glycodeoxycholate and chenodeoxycholic acid (**XX**) [49, 50]. Few examples exist where the bile acid scaffold has been used as a promoiety for a prodrug approach. ASBT has micromolar affinities for the natural substrates, and the studies on ASBT are too few to make a general statement on the potential and role of this transporter in drug absorption [49, 50].

10.3
Transporters and Genomics

10.3.1
Introduction to Genomics Technologies

The analysis of the human genome sequence suggested the presence of 406 genes encoding ion channels and 883 genes encoding transporters, of which 350 are proposed intracellular transporters [51]. Most of the time, though, it is still unknown which transporters are involved in the uptake of a given drug. Therefore, knowing the expression of transporters along the intestine could help identify relevant drug carriers in the intestine.

The transport activity of drug carriers can be affected in many different ways. Thus, with respect to drug design, different questions have to be addressed: Which transporters can be utilized in the intestine for oral drug absorption? Can the expression of these transporters be affected by either disease states or type of nutrition, age, and sex? Is it possible that in a population, various genotypes exist with different transport activities and substrate specificities?

In recent years, various high-throughput technologies have been developed that are being used to address these questions. While expression arrays, such as Serial Analysis of Gene Expression (SAGE) and Massively Parallel Signature Sequencing (MPSS), are applied to measure the messenger RNA levels, genomic arrays are being used to look for potential amplifications and deletions in the genome, and the so-called single-nucleotide polymorphism (SNP) arrays are being used to perform genotyping of samples.

Using such a genome-wide approach allows not only the study of transporter genes but also can provide some insights into the regulation of transporter genes. Nowadays, commercially available gene chips contain the information of all currently annotated genes. Therefore, in one single experiment, changes of expression patterns of any gene can be analyzed and correlated to a reference gene.

It is important to note that RNA may not always correlate with the expression of encoded proteins. Use of proteomic techniques increasingly serves to resolve discrepancies between mRNA levels and expressed proteins. However, proteomics of integral membrane proteins still remains a challenge; moreover, comparing mRNA levels in similar tissues from different subjects is likely to provide an indication of protein levels. Any polymorphism that affects protein structure and function could also lead to false interpretations if the array fails to measure the functional polymorphism.

10.3.2
Gene Expression Profiling Along the Intestine and in Caco-2 Cells

Even though the transport activity can be influenced at various levels, the first step in elucidating the relevance of membrane transporters in drug absorption is studying the expression of these proteins. Various studies using a genome-wide approach have been done in recent years addressing this question. Some studies have been done using the mouse as a model system to assess the situation in humans. However, many times, *in vitro* systems are being used to perform high-throughput screening to assess the absorption rate of a given drug. The cell line of choice is usually Caco-2. As a consequence, different studies have been performed to characterize its genomic expression profile and to correlate it to the situation in humans. It is though important to note that the Caco-2 cells have significant higher transepithelial electrical resistances than the human intestinal mucosa. And as a consequence, a high correlation of the expression levels of transporters between the Caco-2 cells and the human intestinal mucosa may provide a reasonable prediction, but it may also overestimate the contribution of active transport in oral drug absorption due to the contribution of the paracellular route. In the following section, we will discuss some relevant examples of genomic profiling of the intestinal mucosa and the Caco-2 cell system.

10.3.2.1 **Profiling of the Intestinal Mucosa**

Bates *et al*. studied the expression profile of different gastrointestinal segments in mouse, that is, stomach, duodenum, jejunum, ileum, cecum, proximal colon, and distal colon using an 8.6 k cDNA chip [52]. Genes encoding transport proteins fell into three anatomical patterns: expression throughout the GIT (such as several ion channel and pumps and the polymeric immunoglobulin receptor), expression predominantly in the small intestine (such as intestinal fatty acid-binding protein and apolipoprotein A-IV, C-TI, and C-III), and expression in the colon (such as aquaporin 8, involved in water transport, and carbonic anhydrases). Moreover, when classifying all genes represented on the chip into functional groups, the authors concluded that genes encoding proteins, functioning in intermediary metabolism, transport, and cell–cell communication, have the most dynamically regulated expression profiles. However, the limited set of transporter genes investigated narrows the ability of this study for assessing global transport capacity. On the basis of their functional classification, 181 genes out of the 8638 mouse genes represented on the

chip were defined as genes encoding proteins with transport functions, whereas Venter *et al*. suggested that there are 1289 transporters/ion channels in the human genome [51]. Thus, only a fraction of membrane transporter genes has been analyzed in this study.

Similar to Bates *et al*., we also investigated the expression of transporter genes along the mouse intestine [52, 53]. Using the Affymetrix technology, we could measure the genomic profile of 853 transporter genes. In contrast to Bates *et al*., we could not observe that the class of transporters was significantly regulated compared to other GO classes; however, the subclass carriers, and in particular their daughter classes "antiporters" and "symporters," were significantly regulated [52, 53]. Both are classes in which typical transporters involved in drug delivery can be found. Figure 10.3 shows an overview of changes of expression of transporter groups in mice according to the GO system along the intestine [53]. Although some

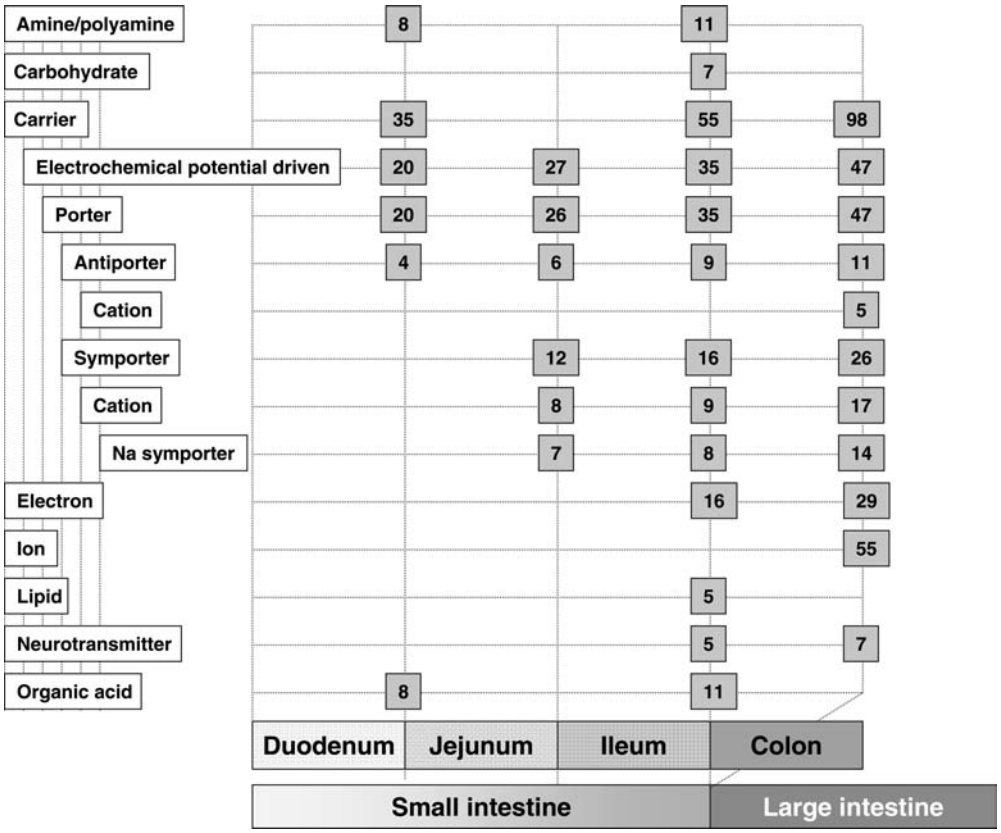

Figure 10.3 Overview of classes according to Gene Ontology (www.geneontology.org), which were significantly changed along the mouse intestine ($p \leq 0.05$). Gray boxes indicate the number of genes for each significant change between two adjoining regions. For a comparison with changes in humans see Ref. [53].

single transporters of a given group may be significantly different between the intestinal segments, the groups they are classified into may not be significantly altered.

Interestingly, the small intestine and the colon revealed that a similar number of genes were more highly expressed in either the small intestine or the large intestine. However, small intestinal transporters were clearly more overexpressed. The majority of differentially expressed transporters were members of the solute carrier super family. The most pronounced change (fold changes > 300), however, was observed for fatty acid-binding protein 1 (Fabp1). Among the solute carriers being more than 20 times overexpressed in the small intestine were the neurotransmitter transporter Slc6a19, the sulfate transporter pendrin-like protein 1 (Slc26a6), L-type amino acid transporter 2 (Slc7a8), facilitated glucose transporter 2 (Slc2a2), and the concentrative nucleoside transporter 2 (Slc28a2, CNT2). The Y(+)L-type amino acid transporter 1 (Slc7a7), the concentrative nucleoside transporter cotransporter (Slc28a3), and the B(0,+)-type amino acid transporter 1 (Slc7a9) were more than 10 times overexpressed. In the colon, the most overexpressed transporter was the neurotransmitter transporter Slc6a14, which was more than 200 times overexpressed in the colon than in the small intestine. The neurotransmitter transporter Slc6a14 and the facilitated glucose transporter 1 (Slc2a1) were more than 10 times overexpressed. By comparing our genomic data with the literature, we could confirm that most of the transporters were similarly expressed in humans. In conclusion, differences in absorption of drugs involving transporters along the intestine can be expected. Different intestinal segments need to be targeted depending on the structure of the compound when trying to imply active uptake systems.

10.3.2.2 **Profiling of Caco-2 Cells**

The first study analyzing the expression profiles of Caco-2 cells using microarrays was done by Mariadason *et al.*, in particular, investigating the influence of postconfluent differentiation in Caco-2 cells on mRNA expression profile [54]. They observed that consistent with cell differentiation, the expression profile reflected a more specialized phenotype. Specifically, Caco-2 cell differentiation was accompanied by coordinated downregulation of genes involved in cell cycle progression and DNA synthesis, which reflected the concomitant reduction in cell proliferation. This study investigated changes of expression profiles only in confluent cells. In any comparison with other studies, the degree of confluence must be considered as an important determinant of mRNA profiles. In a similar study, Fleet *et al.* analyzed the changes in genomic profiles upon differentiation in a subclone of the Caco-2 parental line, the so-called Caco-2 BBE cells [55]. In contrast to Mariadason *et al.*, they observed a significant number of transporter genes being regulated upon differentiation [54]. Even though a comparison between the expression changes observed by Fleet *et al.* and Mariadason *et al.* revealed a rather poor correlation, both studies identified overall the same major pathways that are likely to play a role in the differentiation process [54, 55]. Also, both concluded similarly that the Caco-2 cells express a very complex molecular signature that consists of features of a colonocyte, an enterocyte, and a tumor cell. Similar to these two studies, we analyzed with a home-made oligo array the expression of about

750 genes encoding transporter and channel proteins in differentiated and undifferentiated Caco-2 cells, human small intestine, and colon [56]. In summary, studying only transporter and channel genes, we observed nevertheless a similar trend, namely, that Caco-2 cells have the characteristics of colonocytes, small intestinal enterocytes, and tumor cells. Our results were in general in accordance with the study by Sun and coworkers [57, 58]. They compared the mRNA expression profile of the human duodenum and Caco-2 cells. In contrast to Bates *et al.*, they used the GeneChip U95A by Affymetrix, which contains 12 559 gene sequence tags including in total 443 transporters, ion channels, and metabolic enzymes [52]. The expressions of 26, 38, and 44% of these 443 genes, of which 170 are transporters or ion channels, were detectable in 4-day-old Caco-2 cells, 16-day-old Caco-2 cells, and human duodenum, respectively. Moreover, they compared permeability values in Caco-2 cells and human duodenum of various carrier-mediated and passively absorbed drugs. The *in vivo*/*in vitro* drug permeability measurements correlated well for passively absorbed drug, whereas the correlation coefficient decreased for carrier-mediated drugs. In general, the observed permeability of carrier-mediated drugs was higher in human duodenum than in Caco-2 cells. Most of the transporters expressed in the human duodenum were also expressed in Caco-2 cells. However, it has to be noted that a limited set of drugs has been tested, which are actively transported by only a fraction of transporters that are expressed in the intestine. In addition, the *in vitro* permeability rates in Caco-2 cells have been compared with the ones in the upper jejunum, whereas the expression levels have been compared with the ones in the duodenum.

The findings of each of the genomic studies discussed above contribute to a better assessment of the Caco-2 cells as a model system to study active transport in the human intestine. Having such a vast amount of data available certainly increases our understanding. However, it also requires new strategies to deal with such an immense amount of data to exploit them appropriately. Calcagno *et al*. developed an *in silico* approach to exploit publicly available data sets to assess the Caco-2 model system [59]. They combined genomic results from nine different labs that used different microarray platforms. Consequently, they could increase the robustness of their resulting findings. In their *in silico* approach, using principal component analysis, they showed that the Caco-2 cells express a transport protein profile that to some extent represents not only the absorptive enterocytes but also the colonocytes. However, the profile of the metastatic cell line SW620 differed significantly.

Clearly, genome-wide studies contribute to a better understanding why differences in absorption along the intestine, and between *in vitro* and *in vivo* situations, can be expected. These studies could on the one hand confirm that the most widely used *in vitro* system to study drug absorption, namely, the Caco-2 cells, may not always be very accurate in predicting uptake rates for a new compound. On the other hand, it has to be noted that compared to other *in vitro* systems, which are being used to study transport in liver and kidney, the Caco-2 cells correlate certainly the best with the *in vivo* system with respect to the mRNA expression of transporters [3].

From a medical chemistry point of view, genome-wide expression studies can be exploited to design drugs in such a way that highly expressed transporter proteins can

be better exploited. Moreover, these studies provide information not only about transporter systems but also about other groups of proteins, such as enzymes. Such information could be exploited when designing prodrugs, for instance. A very famous example is certainly valaciclovir (**I**) (cf. below).

10.3.3 Intestinal Transporters and the Influence of Genotypes

So far we have only discussed the fact that in-depth knowledge of the expression of membrane transporters provides crucial information so as to select new, putative targets for active uptake. However, many times the activity of these proteins can be altered in different individuals due to mutations in the genome. Single-nucleotide polymorphisms account many times for differences in activity in individuals. In recent years, many studies have focused on this aspect and have genotyped a variety of genes including transporter genes. For instance, the UCSF "Pharmacogenetics of Membrane Transporters Project" (PMT) focuses mainly on the identification of sequence variants in genes encoding selected membrane transport proteins and the functional characterization of these variants (http://pharmacogenetics.ucsf.edu/index.html). The resulting data of this project are regularly deposited in the PharmGKB database (http://www.pharmgkb.org/), a publicly available database that serves as a genotype–phenotype resource focused on pharmacogenetics and pharmacogenomics. The database contains not only the genotype information of single genes but also the results obtained with SNP arrays. Similar to the classical expression oligo arrays, these arrays identify differences between samples of a vast number of genes with respect to SNPs [60]. So far, no study has been published with the SNP array technology focusing on transporter genes.

As mentioned above, interindividual differences in absorption rate can be explained by SNPs in membrane transporters. However, SNPs in other genes, which are involved in the regulation of transporter genes, could also contribute to interindividual differences. Therefore, the exploitation of array data will be very important to assess the influence of the various genotypes in drug absorption.

In recent years, various studies have been published showing the effects of mutations in the DNA of transporters. Many times, such mutations can account for diseases (cf. Table 10.1). In the following section, however, we will focus on studies in which transporters relevant to oral drug absorption have been sequenced and their genetic variants phenotypically characterized.

In the context of the PMT Project, we have genotyped all 23 exons and adjoining intronic regions of *SLC15A1* in 247 individuals, the so-called Coriell collection (i.e., 100 Caucasians, 100 African–Americans, 30 Asian–Americans – equal numbers of Chinese, Japanese, and Southeast Asians–, 10 Mexican–Americans, and 7 Pacific Islanders) [61]. Overall, significant differences between ethnic populations could be observed. Of 38 SNPs detected, 21 occurred in the intronic and noncoding region and 17 in the exonic, coding regions, of which 9 were nonsynonymous. Eight nonsynonymous SNPs were functionally characterized in transient-transfected Cos7 ad CHO cells. None of the variants had altered transport activity, except the low-frequency

PEPT1-F28Y. It showed a significant reduction of cephalexin (**XXI**) uptake. Altered pH dependence of substrate transport suggested a role of F28Y in H^+-driven translocation. In a similar study, Zhang *et al.* sequenced *SLC15A1* in 44 different individuals and found 13 SNPs in the coding region confirming our findings [62]. In addition to our data, they found another low-frequency SNP with altered transport activity, the PEPT1-P586L. In conclusion, genetic factors could possibly introduce some systematic variability for drugs critically dependent on PEPT1 activity for intestinal absorption. However, other factors acting on PEPT1 transport activity are more likely to cause interindividual variability, recently studied with valaciclovir in human subjects [63]. Alternative splicing cannot yet be ruled out as a clinically relevant variable. Overall, however, PEPT1 displays remarkable low genetic variability. This finding is important for drug therapy with peptoid drugs and for exploiting PEPT1 in prodrug design for improved bioavailability.

Various members of the nucleoside transporter families SLC28 and SLC29 have also been genotyped and their variants functionally characterized. Regarding *CNT1*, a total of 58 coding region haplotypes were identified in the same collection of individuals as the one used for *SLC15A1* (e.g., Coriell collection) [64]. The translated protein of 44 haplotypes contained at least one amino acid variant. More than half of the coding region haplotypes were population specific. Phenotypic studies of 15 protein-altering *CNT1* variants in *Xenopus laevis* oocytes revealed that all variant transporters took up [3H]thymidine with the exception of CNT1-Ser546Pro, a rare variant, and CNT1– 1153del, a single bp deletion, found at a frequency of 3% in the African–American population. The anticancer nucleoside analogue gemcitabine (**VI**) had a reduced affinity for CNT1-Val189Ile (a common CNT1 variant found at a frequency of 26%) compared to reference CNT1. These data suggest that common genetic variants of *CNT1* may contribute to variation in systemic and intracellular levels of anticancer nucleoside analogues. The same group also analyzed the family member *CNT2* in a very similar setup [65]. Six nonsynonymous variants were identified, and all were able to transport guanosine. The four common variants were further characterized with the antiviral nucleoside analogue drug ribavirin. No differences were observed among the four common variants in the uptake kinetics. However, variant CNT2-F355S F355S (3% allele frequency in the African–American sample) exhibited a change in specificity for the naturally occurring nucleosides, which according to the authors may have implications for nucleoside homeostasis. The third member of the SLC28 family has been genotyped by another group. The authors of this study also used the Coriell collection but only the Caucasians [66]. In summary, they identified different variants; however, these variants do not seem to have either an altered transport activity or transport specificity.

In addition, in the context of PMT, members of the equilibrative nucleoside transporter family have been investigated. So far, only *ENT2* has been completely genotyped and its protein product functionally characterized. Similar to *CNT3*, different variants were observed; however, only five haplotypes were sufficient to describe the entire sample set. Thus, the authors suggested that the low overall genetic diversity in *SLC29A2* makes it unlikely that variation in the coding region contributes significantly to clinically observed differences in drug response [67].

Similarly, Kuhne *et al.* analyzed *LAT1* (*SLC7A5*), *LAT2* (*SLC7A8*), and *4F2HC* (*SLC3A2*) and concluded that even though various SNPs are found in these sequences, genetic variation in the genes *4F2HC*, *LAT1*, and *LAT2* does not appear to be a major cause of interindividual variability in pharmacokinetics and of adverse reactions to melphalan (**XXII**) [68].

One of the best-studied transporter proteins is certainly the ABCB1. Many groups have sequenced this gene and studied the impact of the mutations on the transport activity of its protein product [69–71]. While Tang *et al.* analyzed a collection of 261 individuals of three distinct Asian groups (i.e., 104 Chinese, 93 Malay, and 68 Indian), Kroetz *et al.* used the Coriell collection as described above [69, 71]. Tang *et al.* selected four sites in the 5′ noncoding region and six sites in the coding regions as possible sites for SNPs based on publicly available data and verified them in their population [71]. Only three in the coding region and one in the 5′-flanking region could be confirmed. All three coding SNPs (exon 12 1236C > T, exon 21 2677G > T/A, and exon 26 3435C > T) were present in high frequency in each ethnic group, and the derived haplotype profiles exhibited distinct differences between the groups. In summary, fewer haplotypes were observed in the Malays ($n = 6$) compared to the Chinese ($n = 10$) and Indians ($n = 9$). Three major haplotypes (>10% frequency) were observed in the Malays and Chinese; of these, two were observed in the Indians.

In contrast to this study, Kroetz *et al.* sequenced the whole exonic region and the adjoining intronic regions of the gene in a more heterogeneous sample [69]. Considering only the variants used in the previous haplotype analysis by Tang *et al.*, they could find 7 of the 10 haplotypes in their relatively small Asian–American sample [71]. Overall, they identified 48 variant sites, including 30 novel variants and 13 codings for amino acid changes, resulting in 64 statistically inferred haplotypes. As with respect to the impact of various haplotypes on the transport activity of the protein product, the results published so far remain inclusive. Thus, further functional studies are still needed.

As far as the ABCC family members are concerned, only genotype studies have mainly been done so far. Thus, functional data regarding the influence of the different variants found are still missing. Briefly, Saito *et al.* screened entire genomic regions of 48 Japanese individuals and identified 81 SNPs in the *ABCC1* gene, 41 in *ABCC2*, 30 in *ABCC3*, 230 in *ABCC4*, 76 in *ABCC5*, 58 in CFTR, 102 in *ABCC8*, and 70 in *ABCC9* [72]. In contrast, Leschziner *et al.* sequenced only the exon regions of *ABCC1*, *ABCC2*, and *ABCC5* in 47 Caucasion individuals finding 61 SNPs in *ABCC1*, 41 in *ABCC2*, and 34 in *ABCC5* [73]. Overall, the authors concluded that the patterns of linkage disequilibrium (LD) across these drug transporter genes demonstrated large regions of high LD and low haplotype diversity, an important information for the search of a functional variants.

In summary, various important intestinal drug carriers have been characterized regarding their genetic variability and the impact on transport activity. For a good part, the genetic variability does not seem to be the major player in the interindividual variability in drug absorption. However, many times the genetic variation can contribute to an altered transport activity, which in some ethnic populations might be more relevant than in others. Thus, having a catalog of all known SNPs and

relevant haplotypes and their functional characteristics is the first step in estimating the impact of genetic variability on interindividual differences in drug absorption. Many times mutations in the sequence lead to changes in the structure of transporters and as a consequence to an altered functionality. Thus, predicting the impact of such mutations on the structure will be one of the major challenges for medical chemistry. On the one hand, for some established drugs, individualized drug therapy should be applied to account for the differences in drug transport. Moreover, an in-depth knowledge of all mutations and prediction of their possible impact on the transport activity can be exploited to avoid targets drug delivery targets for which different genotypes are expected to show alterations in drug transport.

10.4 Structural Requirements for Targeting Absorptive Intestinal Transporters

The discovery process has traditionally had a preference for evaluating new chemical entities (NCEs) with respect to their pharmacologic potency and selectivity against the selected drug targets. Intestinal transporters are generally not drug targets but could be classified as drug delivery targets [7]. The aim of exploiting a drug delivery target is most often to increase the intestinal absorption of the drug candidate to increase the oral bioavailability or modify the metabolic or stability profile of the drug candidate. Another strategy could be to target a given segment in the intestine in which the transporter of choice is highest expressed.

A lot of structure–activity information has been accumulated over the last two decades for various intestinal transporters. However, the two most studied transporters in terms of quantitative structure–activity relationship (QSAR) are SLC15A1 [74–80] and ABCB1 (for references see Ref. [81]), which will be the topic of Chapter 18. In the following section, the focus will be on strategies for increasing intestinal absorption of drug candidates by targeting intestinal peptide transporters.

10.4.1 Strategies for Increasing Drug Absorption Targeting Transporters

Different strategies for targeting intestinal transporters to increase intestinal permeability have been described:

(a) design of prodrugs targeting the transporter,
(b) substrate mimicry, and
(c) the use of a formulation approach.

A prodrug is composed of an active drug and a promoiety (or transport moiety) and is by definition a pharmacologically inactive compound. As mentioned in the Section "Introduction," an example of a prodrug targeting an intestinal transporter is valaciclovir (**I**). The prodrug has a bioavailability of 63% in rats compared to 15–21% of the parent drug acyclovir due to the transport activity of PEPT1 [1, 2]. A quite similar example is valganciclovir, which is also a substrate for PEPT1 [82],

where the oral bioavailability in human is increased from approximately 6 to 61% [83]. It has to be noted that other transporters also have been suggested to participate in the intestinal absorption of valaciclovir and valganciclovir such as HPT1 and the Na^+/Cl^--coupled amino acid transporter $ATB^{0,+}$ [11, 84]. Several examples exist where the promoiety itself is not a substrate for the transporter and often valine is used [85–89]. Prodrugs designed to use the transport activity of PEPT1 have also been designed by using natural or modified di- or tripeptidomimetic substrate as a promoiety for transporter recognition [90–92]. Prodrugs may also be used to circumvent the transport of efflux transporters and instead utilize an absorptive transport system as in the case of the Val-Val-saquinavir prodrug [91]. Assessing the uptake of a prodrug by a given carrier is many times difficult due to the involvement of other mechanisms of transport.

Another way of exploiting transporters is to optimize intestinal absorption by using QSAR-based database mining to select an NCE, which could be a substrate for an appropriate absorptive transporter or alternatively not substrate for efflux mechanisms [93, 94]. Substrate mimicry is also a possibility in the case of inhibition of transport activity, which maybe relevant not only for efflux transporters. Phloridzin is an inhibitor of the sodium-coupled glucose transporter SGLT1 (SLC5A1), which is located in the apical membrane of enterocytes (cf. Figure 10.2). Poly(gamma-glutamic acid) (gamma-PGA) modified with phloridzin (PGA–PRZ) has been suggested as a novel oral antidiabetic drug [95]. PGA–PRZ was able to decrease glucose transport from the mucosal to serosal side of the everted rat small intestine, and its inhibitory effect was as strong as that of intact phloridzin [95]. After oral administration of PGA–PRZ to rats before glucose administration, the glucose-induced hyperglycemic effect was significantly suppressed, which was not observed in the case of phloridzin administration. These results suggest that the gamma-PGA–phloridzin conjugates have potential as oral antidiabetic drugs due to the interaction with SLC5A1.

As with respect to a formulation approach, the use of pharmaceutical excipient Eudragit L100-55 decreased the pH *in situ* in ileal, closed loops of rats and increased the disappearance of cefadroxil and cefixime from the loop. The plasma concentration after oral administration was increased significantly by coadministration of Eudragit L100-55, whereas a proton-nonreleasing analogous polymer, Eudragit RSPO, did not have any effect. These results indicate that improvement of intestinal absorption of peptide mimetics via PEPT1 is possible by increasing the driving force for PEPT1 transport activity through coadministration of a proton-releasing polymer [96]. As far as ABCB1 is concerned, lipid excipients and surfactants such as Cremophor, Tween 20 and 80, sucrose monolaurate, and Pluronic block copolymers or other ABCB1 substrates/inhibitors have been shown to inhibit ABCB1-mediated efflux of drugs such as cyclosporin A, paclitaxel, ciliprolol, digoxin, and HIV inhibitors [97, 98]. Such pharmaceutical excipients may increase the intestinal permeability (or decrease metabolism) by inhibiting the ABCB1-mediated intestinal apical efflux, but these may also be the cause of drug–drug interactions in a multidrug dosage regimen. Collectively, lipid-based drug delivery system may not only increase solubility of a given drug but also modulate the transport activity of efflux transporters

such as ABCB1. Another strategy may be to develop a formulation capable of releasing the drug in intestinal segments where transporter expression is high (for absorptive transporter) or low (for efflux transporter).

Various strategies for exploitation or limitation of the impact of transporters are available for the discovery and development of drug candidates. Most often, the impact of transporters has been realized retrospectively. However, as knowledge increases on transporter expression and function, genomics of transporter, SAR, and protein structure, the basis for a rational design of substrates or inhibitors of transporter activity is enhanced.

10.4.2
Changing the Substrate: SAR Established for PEPT1

The number and variation in the structure of possible combinations of natural dipeptides (**XXIII**) and tripeptides (**XXIV**) indicate that the structural requirements for binding to PEPT1 are relatively flexible in terms of charge, size, and chemical structure. In general, affinity of natural di/tripeptides for PEPT1 is stereochemically specific for peptides composed of L-enantiomers [99–101]. β-Lactam antibiotics also have a chiral center and therefore exist in both D- and L-forms, and stereoselective uptake of cephalexin (**XXI**) and loracarbef has been demonstrated, with the L-enantiomers displaying the highest affinity for PEPT1 [101]. However, it must be emphasized that di- or tripeptides containing a D-configured amino acid may have a high affinity for PEPT1 after side chain (R_1, R_2, or R_3) derivatization, especially using hydrophobic derivatives [102–104].

The presence of a peptide bond was originally thought to be a prerequisite for transport via PEPT1 [105]. However, Temple *et al.* demonstrated PEPT1-mediated transport of the peptide mimic 4-aminophenylacetic acid (4-APAA), and Doring *et al.* showed that ϖ-amino fatty acids, such as δ-amino levulinic acid (δ-ALA) (**XXV**), are substrates transported by PEPT1 [106–108]. δ-ALA is a Gly-Gly mimetic, in which the amide bond is replaced by a ketomethylene amide bond bioisoster. Vabeno and coworkers investigated the amide bond isosteres ketomethylene, (*R*)- and (*S*)-hydroxyethylidene, and (*R*)- and (*S*)-hydroxyethylene and found that the ketomethylene amide bond isoster had the highest potential as a bioisoster with respect to PEPT1 affinity [109, 110]. Valaciclovir (**I**) is another example of a PEPT1 substrate lacking an amide bond. As shown by Brandsch *et al.*, the peptide bond oxygen atom may be replaced by sulfur in Ala-Ψ[CS-N]-Pro, a modification of Ala-Pro, without abolishing transport by PEPT1 [111]. Very interestingly, the study of Brandsch *et al.* showed that dipeptides in *cis* and *trans* conformations around the peptide bond have different affinities and that PEPT1 selectively transports dipeptides in the *trans* conformation. This was later confirmed using naturally occurring dipeptides [112]. The transporter does also accept some dipeptides with a *N*-methylated peptide bond exemplified by Gly-Sar and some tripeptides with *N*-methylated amide bond; however, *N*-methylation does not seem to be a general stabilization approach, since the affinity for PEPT1 is not retained for all the investigated compounds [113, 114].

In general, the highest affinity for PEPT1 is observed for compounds having free amino-terminal and carboxyl-terminal groups. Yet, acetylating the N-terminus of Phe-Tyr to give an amide highly decreased, but did not abolish, the affinity for PEPT1, and the N-terminal modification of L-carnosine to 4-toluenesulfonylureido-carnosine (**XXVI**) also retained a medium affinity for PEPT1 [6, 12, 115]. The C-terminus is not absolutely essential for affinity, since C-terminal amidation of Phe-Tyr retained an affinity (although lowered) for PEPT1 [6, 12]. Moreover, single amino acid modified in the C-terminus with piperidide, thiazolidide, anilide, 4-nitroanilide, 4-chloroanilide, or 4-phenylanilide has in some cases been shown to retain affinity for PEPT1 [116].

Absolute affinities (K_i-values) for natural di- and tripeptides are normally in the range of 0.1–3 mM. To evaluate relevant affinity values, Brandsch and coworkers have proposed the following classification: $K_i < 0.5$ mM is high affinity, $0.5 < K_i < 5$ is medium affinity, and $K_i > 5$ is low affinity, and values above 15 mm seem to be irrelevant [5]. The latter is probably based on the observation made with β-lactam antibiotics where the oral bioavailability seems to be at least partly mediated via PEPT1-mediated transport, and a threshold of 15 mm was proposed [8].

The impact of the above in terms of drug discovery and development suggests the seeming wide possibilities for substrate mimicry and prodrug design. Even though most dipeptides and tripeptides studied so far are substrates for PEPT1, a number of examples exist where affinity and translocation are absent, for example, observed for Lys-Lys, Trp-Trp, Arg-Arg, and Arg-Lys.

10.4.3
Methods for Investigating Affinity and Translocation

The initial evaluation of novel compounds synthesized for targeting a transporter will normally have to be based on the following assays, to get the desired information needed to verify if the compound indeed is a substrate for the transporter and if this results in an increased intestinal permeability:

(a) investigation of the affinity for the transporter,
(b) investigation of translocation of the compound by the transporter,
(c) transport across an *in vitro* culture model of the intestine or across animal intestinal tissues.

Subsequently, *in vivo* animal studies are necessary to investigate the oral bioavailability.

When studying drug candidates or prodrugs of PEPT1, the affinity is often assessed by competition experiments using nonhydrolyzable peptides such as Gly-Sar (which has a methylated peptide bond) or L-carnosine (β-Ala-His). The affinity is expressed as the IC_{50} value (the concentration of compound, substrate or inhibitor, which causes a 50% inhibition of the uptake). The compounds can thus be described in terms of their IC_{50} value or, more meaningful, their K_i value, since the IC_{50} value depends on the Gly-Sar concentration used. When the concentration of the substrate is much lower than K_m, IC_{50} approaches K_i [117, 118]. The basic outline of an affinity study has been performed in different *in vitro* systems using epithelial cell

lines such as Caco-2 cells or in cell lines using transient and stable transfection with *PEPT1 cDNA* such as LLC-PK1 cells, HeLa cells, Chinese Hamster Ovary (CHO) cells, and Cos7 cells [11, 61]. Expression systems such as Xenopus laevis oocytes have also been applied extensively to study PEPT1 [119]. The methylotrophic yeast, *Pichia pastoris*, has also been used for heterogonous expression of the rabbit intestinal peptide transporter Pept1 [120]. However, care must be taken, as pointed out by Brandsch and coworkers, when comparing affinities obtained in different laboratories due to the different protocols used where pH, different *in vitro* systems, different isoforms, and different isotopes are employed [5].

It must be emphasized that compounds, which are characterized only by their K_i or IC_{50} affinity values, are not necessarily transported by PEPT1, and the only information this parameter yields is that the compound competes for binding to the transporter. The ability of a compound to be translocated by PEPT1 can be studied using radiolabeled compounds or by the two-electrode voltage clamp technique [121–123]. However, it is often expensive to get new compounds radiolabeled, and the two-electrode voltage clamp technique is not suitable for low or medium high-throughput screening. Recently, an assay based on the measurement of membrane depolarization resulting from the cotransport of protons with PEPT1 substrates in MDCK/PEPT1 has been described [124–126]. Membrane potential changes are tracked with a voltage-sensitive fluorescent indicator (FLIPR membrane potential assay kit from Molecular Devices). This allows the investigation of translocation via PEPT1 of a reasonable number of compounds per experimental day. The last step in the *in vitro* characterization is to assess the intestinal permeability, and this may be performed in cell culture models such as Caco-2 cells or MDCK/PEPT1 cells or in intestinal animal tissues [127, 128]. The compound is applied to one side of the epithelium, and samples are taken at the opposite side at various time points postaddition. Transepithelial flux across the intestinal epithelium is determined when the flux across the cells is in steady state; this occurs within 30–60 min, depending on the tissue.

During all investigations, stability and metabolism are an issue, especially for prodrugs, which in nature must be biolabile. Today's analytical tools allow a careful analysis of compounds present after the various types of experiments, thus leading to solid interpretations of transporter interactions before going into *in vivo* studies.

10.4.4
Quantitative Structure–Activity Relations for Binding of Drug to Transporters

In Part IV of this book, "Computational Approaches to Drug Absorption and Bioavailability," computational models for studying drug absorption and bioavailability are described in detail. Chapter deals with quantitative structure–activity relations for ABCB1. Computation-based QSAR models are pursued to gain insight into how steric, electrostatic, hydrophobic, and hydrogen-bonding interactions influence biological activity and to derive predictive 3D QSAR models for designing and forecasting the activity of drug candidates targeting intestinal transporters. The following section discusses some studies of absorptive transporters with a focus on PEPT1. Several

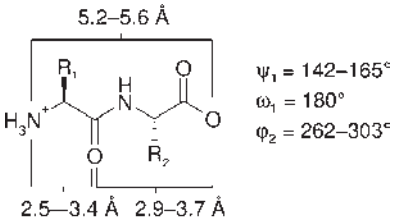

Figure 10.4 Geometrical data for the bioactive conformation of PEPT1 dipeptide substrates proposed by Gebauer *et al.* The dipeptides conformation is defined by backbone torsion angles $\psi_1 = 142°–165°$, $\omega_1 = 180°$, and $\varphi_2 = 262°–303°$ and the distance between the N-terminus and the C-terminus, $d_{N–C} = 5.2–5.6$ Å [77].

models for ligand binding to PEPT1 have been suggested [74–77, 79, 80, 107, 129, 130]. The term ligand is used here since the computational methods published for PEPT1 are based on affinity values and these may not reflect actual translocation, complicating the interpretation of the impact of proposed models on drug design. An extract of the work by Gebauer *et al.* and Biegel *et al.* using comparative molecular field analysis (CoMFA) and comparative molecular similarity indices analysis (CoMSIA) studies is mentioned in the following section [76, 77]. Part of the bioactive conformation is indicated for dipeptides in Figure 10.4.

The model by Gebauer *et al.* describes two electrostatic fields (E_1 and E_2) that represented favorable interactions with the positive N-terminal charge (E_1) and the negative C-terminal charge (E_2) [77]. Derivatization of the N-terminus to give an amide functionality (neutral nitrogen) reduces the interaction in E_1, whereas the introduction of an N-terminal β-amino acid results in misplaced orientation of the positive charge (as in 4-toluenesulfonylureido-carnosine). The removal of the C-terminal carboxyl group results in a dramatic decrease in affinity, while its replacement with an electron-rich aromatic moiety is accepted. Two large cavities were described where L-configured R1 and R2 side chains, respectively, interact favorably. Three disfavored steric areas were also identified, mainly representing steric clash for (i) Pro-Xaa dipeptides, (ii) the R1 side chain/amino group (D-configuration), and (iii) the R2 side chain/hydrogen (D-configuration) . Two areas were described where lipophilicity contributes favorably, one of which partly coincided with the R2 steric cavity indicating that a bulky hydrophobic R2 side chain is favorable. There was no lipophilic contribution overlapping the R1 pocket, suggesting no specific preference in this position. Moreover, two areas where hydrophilicity contributes favorably were described, mainly representing the charged N- and C-termini, in agreement with the electrostatic fields. Three areas were suggested that represent the presence of H-bond acceptor sites in the "binding pocket." These areas represent favorable interactions with H-bond donors, that is, the positively charged α-amino group (L-configuration). Three areas were identified where interaction with H-bond donors were unfavorable, such as the imino hydrogens of Pro-Xaa, an N-terminal amide hydrogen, or the α-amino group

(D-configuration). One area represents the presence of H-bond donor sites in the "binding pocket," meaning that interactions with H-bond acceptors are favorable. It is usually the C-terminal carboxyl group (L-configuration) and the H-bond donor field that are closely related to the E_2 field. A CoMFA-based model highly depends on the initial chosen conformation for subsequent alignment. However, Andersen *et al.* used an approach based on VolSurf descriptors, which are alignment independent, and correlated the VolSurf descriptors of a set of tripeptides with their experimental binding affinity for PEPT [74]. Larsen *et al.* recently expanded this approach to integrate VolSurf, GRIND, and MOE descriptors into a hierarchical PLS model for prediction of affinity for PEPT1 [129].

Substrate-based QSAR models have been proposed for the following absorptive transporters: ENT1 [131], SERT [132], CNT1, and CNT2 [133] and others (see Ref. [93])

The use of QSAR models is of great potential to the work of medicinal chemists since it allows the virtual synthesis and screening of novel drug candidates targeting intestinal transporters. Furthermore, it allows QSAR-based data mining to identify putative ligands in publicly accessible databases or company databases. Moreover, potential drug–drug interactions caused by transporters may be identified [134]. However, the models need to be predictable and able to distinguish between inhibitors or substrates.

10.5
Transporters and Diseased States of the Intestine

10.5.1
Intestinal Diseases

Transporters can affect in various ways the well functioning of our body. Many times an altered transport rate of important nutrients due to, for instance, mutations in the sequence can provoke diseases (cf. Table 10.1). In addition, changes in our body state due to, for example, infection and inflammation can affect the regulation of transporters [135]. Edinger reviewed very extensively how the control of cell growth and cell survival is regulated by nutrient transporter expression, which is very important in carcinogenesis [136]. This shows that changes in expression of transporters need to be considered in drug design when targeting transporters as drug carriers. These findings also show clearly that in some specific cases, transporters can serve as direct drug targets. In the following section, we will mainly focus on the regulation and role of transporters in typical intestinal diseases such as colon cancer and chronic inflammatory diseases, that is, inflammatory bowel disease (IBD) and Crohn's disease. In the following paragraphs, we will give a brief introduction into carcinogenesis and especially colon carcinogenesis. We will show how chronic inflammation is linked to tumor development in the colon and what role transporters play in these diseases.

10.5.2 Basic Mechanisms in Cancer and Specifically in Colon Carcinogenesis

10.5.2.1 Basic Mechanisms

Tumor development is recognized as a multistep process. Carcinogenesis is generally considered to consist of three major stages: tumor initiation, promotion, and progression, which is certainly an oversimplification of the mechanisms involved. Tumor initiation is a rapid and irreversible process that includes exposure of a single cell or multiple cells to a carcinogen and involves DNA alterations. In contrast to the initiation phase, tumor promotion is considered to be a lengthier and reversible process, in which actively proliferating neoplastic cells accumulate. The final stage, tumor progression, involves the growth of tumor that has invasive and metastatic potential [137]. The initiation process can persist in otherwise normal tissue indefinitely until the occurrence of a second type of stimulation, which can result from the exposure of initiated cells to chemical irritants. The cancer cell genotype can be summarized as a manifestation of six essential alterations in cell physiology: self-sufficiency in growth signals, insensitivity to growth inhibitory signals, evasion of apoptosis, limitless replicative potential, sustained angiogenesis and tissue invasion, and metastasis [138]. Each of these changes is acquired during tumor development. Hanahan and Weinberg suggest in their work that most of the time all six characteristics are shared by most, if not all, types of cancers [138].

The causal relationship between inflammation, innate immunity, and cancer is now widely accepted. Normal inflammation is self-limiting because the production of proinflammatory cytokines is followed by that of anti-inflammatory cytokines. In tumors, the inflammatory process persists. Chronic inflammation seems to be due to persistence of the initiating factors or failure of mechanisms that are required to resolve the inflammatory response [139]. The strongest association of chronic inflammation with malignant diseases is in colon carcinogenesis in patients with inflammatory bowel diseases such as chronic ulcerative colitis and Crohn's disease.

Thus far, cancer research has focused mainly on understanding the biology of tumor cell proliferation [138], and, as a result, most anticancer therapies target proliferative mechanisms within the tumor cell compartment. Evidently, the outcome of a cancer depends not solely upon the tumor's proliferative capacity but largely upon the most harmful process in tumor development, that is, the invasion of tumor cells into the surrounding tissue [140]. At this invasive front, the tumor cells undergo the so-called epithelial–mesenchymal transition (EMT) resulting in a reduced proliferative and increased migratory capacity.

EMT, as well as tumor initiation, development, and metastasis formation, does not occur only through genetic and epigenetic changes within tumor cells. It is becoming increasingly clear that signals generated by the surrounding host tissue, that is, the tumor stroma, influence tumor cells [141–145]. However, very little is known about how tumor cells respond to their microenvironment. Conversely, it is well established that tumor cells themselves influence the stroma. They can, for example, stimulate the surrounding healthy tissue to form blood vessels, which provide the tumor with oxygen and other nutrients [146]. Often, the tumor tissue also provokes an inflammatory

response that is comparable to the inflammation observed in wounding and tissue repair [139]. Most important, tumor cells can subvert the functions of normal leukocytes, fibroblasts, and endothelial cells and utilize them to their own advantage [147], which has led to the notion of tumor–stroma cross talk [148].

These observations suggest that targeting reactive stroma in addition to tumor cells may provide a potentially powerful means to control cancer growth and dissemination. Thus, finding ways to exploit tumor–stroma cross talk for new therapeutic strategies has taken center stage in cancer research [149]. One advantage of targeting stromal cells is that these cells are not genetically as unstable as cancer cells and are consequently less likely to develop drug resistance [148].

10.5.2.2 **Colon Cancer**

Colon cancer is one of the main causes of cancer mortality in Western societies [150]. About 15–20% of colorectal tumors are causally determined by inheritance of genetic alterations such as the hereditary nonpolyposis colorectal cancer (HNPCC) and the syndrome familial adenomatous polyposis (FAP) [151, 152]. Microsatellite instability, a characteristic of HNPCC, is caused by mutations in the genes essential for mismatch repair. The loss of mismatch repair has several consequences: most crucially, the loss of proofreading and correction of small deletions and insertions. FAP is a rare autosomal dominant syndrome caused by an inherited mutation in the *APC* gene. The disease is characterized by the development of multiple colorectal adenomas, numbering from a few polyps to several thousands.

Mutations at the *APC* locus are a common and early somatic event in polyps and cancer; that is, for some individuals, the first hit is the germline mutation, whereas for others, it is a somatic event. *APC* can also be silenced by hypermethylation. In general, this finding suggests that, although inheriting mutated copy of *APC* is associated with a highly penetrant phenotype, there are, nonetheless, both genetic and environmental influences that modify that penetrance. Other key players in colon carcinogenesis are the oncogene *KRAS*, and, besides *APC*, two other tumor suppressor genes, namely, *SMAD4* and *TP53* [150]. Potter *et al.* proposed that there are at least four separate molecular pathways involved in colon carcinogenesis that have some events in common: (1) APC–β-catenin–Tcf–MYC pathway associated with the adenoma–carcinoma sequence; (2) the HNPCC pathway characterized by the loss of DNA mismatch repair (by inherited or acquired mutation or methylation) that results in microsatellite instability in the tumors; (3) the ulcerative colitis dysplasia–carcinoma sequence that is usually not associated with *APC* mutation or polyp formation; and (4) hypermethylation silencing of the estrogen receptor gene, which may be part of a wider pattern of gene-specific hypermethylation – common in sporadic tumors [152] .

10.5.3
Transporters and Colon Cancer

Membrane transporters play key roles in cancer drug therapy. In fact, the effectiveness of cancer chemotherapy may often depend on the relative transport capacities of

tumor cells. Some transporters can affect the entry of drugs into cells and others drug exit. In particular, various ABC transporters such as ABCB1 mediate energy-dependent efflux of drugs and thereby play major roles in the development of drug resistance [153]. Most of the current chemotherapeutics such as folate antagonists, pyrimidine and purine antimetabolites, alkylating drugs, platinum agents, and DNA topoisomerase-targeting drugs act upon proliferation, while microtubule-targeting compounds additionally interfere with the migratory activity of cells. Some ABC transporters pump out a wide variety of substances of various classes (e.g., ABCB1, ABCC1, and ABCC3), while others specifically transport microtubule-targeting compounds (ABCB4 and ABCB11), thus, playing potentially a crucial role in affecting the efficacy of drugs that target cell migration [153]. Studies indicate that there might be a correlation between induction of ABCA5 and ABCB1 expression and the differentiation state of human colon tumor [154]. As far as active uptake is concerned, SLC31A1 (CTR1, copper transporter), concentrative nucleoside transporters (SLC28A family), and folate/thiamine transporters (SLC19 family) have been shown, for instance, to transport cisplatin (**XXVII**), antimetabolites, and antifolates, respectively [20, 155, 156]. While most of the time, these influx carriers are responsible for increased chemosensitivity (i.e., susceptibility of tumor cells to the cell-killing effects of chemotherapy drugs), they may also be responsible for resistance (i.e., ability of cancer cells to become resistant to the effects of the chemotherapy drugs). For instance, patients with elevated SLC28A3 levels had lower response to fludarabine therapy suggesting that resistance to fludarabine might be related to intracellular membrane localization of the SLC38A3 protein product due to increased degradation of drugs in intracellular compartments [157]. Di Pietro *et al.* showed a differential expression of transporters in colon cancer compared to healthy mucosa [158]. We have studied the influence of transporters on chemosensitivity and resistance in a genome-wide approach in a panel of 60 cell lines including colon cancer cell lines used by the National Cancer Institute [159, 160]. By correlating gene expression with the potencies of 119 anticancer drugs, we could identify new transporter–drug interactions responsible for either chemoresistance or sensitivity. Positive correlations (chemo-sensitivity) were observed between folate carriers (e.g., SLC19A1, A2, and A3) and folate analogue drugs, nucleoside transporters (e.g., SLC29A1) and nucleoside analogues, and amino acid transporters (e.g., SLC38A2) and amino acid-type drugs. Among 40 ABC transporter genes tested, 3 showed strong negative correlation (chemoresistance) with several drugs using validated array data *ABCB1, ABCC3*, and *ABCB5* (a novel putative drug resistance factor) ($p < 0.001$). For ABCB1, all known substrates (19 drugs) yielded significant negative correlations.

Clearly, transporters play a significant role in cancer therapy. However, in-depth knowledge about the activity of these transporters in colon cancer and more specifically in the various subpopulations of tumor cells is lacking.

Besides the role of drug carriers in cancer, some membrane transporters have been demonstrated to act as tumor suppressor genes and be silenced by DNA methylation in colon cancer, and some transporters have been shown to be involved in EMT. As a consequence, membrane transporters may be differentially expressed between

proliferating and migrating invasive tumor cells. Both aspects will be addressed in more detail later.

In summary, very little is still known about the mechanisms involved in the uptake of chemotherapeutics in solid tumors. Even less is known about the role of transporters in drug delivery with respect to the heterogeneity of a tumor. Understanding the activity of transporters within a tumor may contribute to a more efficient and specific drug therapy. Targeting the microenvironment promises new and successful strategies for drug development. As a consequence, exploiting stroma-specific transporters as drug carriers may allow targeting stromal cells and, thus, interfering with the tumor-stroma cross talk. Moreover, very little has been done to understand the role of transporters in cancer not only as simple drug carriers but also as tumor suppressor genes.

10.5.3.1 Transporters as Tumor Suppressor Genes

Some solute carriers also seem to act as tumor suppressor genes in colon cancer such *SLC5A8* and *SLC26A3* [161–163].

Searching for genes that are aberrantly methylated at high frequency in human colon cancer, Li *et al*. found the transporter SLC5A8 [162]. Transfection of *SLC5A8* suppressed colony growth in each of three SLC5A8-deficient cell lines tested, but it showed no suppressive effect on any of the early events, detectable in colon adenomas, and even on earlier microscopic colonic aberrant crypt foci. Similarly, in a follow-up study, Ueno *et al*. showed in gastric cancer that aberrant methylation and histone deacetylation were associated with silencing of SLC5A8 [164].

Similar to SLC5A8, the glutamate transporter SLC1A2 has been shown to be silenced in glial cells by DNA methylation leading to the hypothesis that malfunctioning or the loss of SLC1A2 in glial may contribute to a certain extent to the progression of malign brain tumors termed glioma [165]. As far as SLC26A3, an anion exchanger, also called DRA (downregulated in adenoma), is concerned, Schweinfest *et al*. described that this transporter is downregulated in colon adenomas and carcinomas compared to healthy mucosa [166]. Later, transfection studies in colon cancer cell lines suggested that this transporter acts as tumor suppressor. Moreover, mutation studies revealed that the loss of the anion transport is not linked to its tumor suppressor function [161].

10.5.3.2 Role of Transporters in the Tumor–Stroma Interaction

Expression of Transporters During EMT Some studies have led to the hypothesis that transporters may be differentially expressed between proliferating and migrating invasive tumor cells and play a role in EMT, such as the zinc transporter LIV-1 [167, 168]. An interesting example in this context is the role of the monocarboxylate transporter MCT4 (SLC16A3) in migration and metastasis formation. A recent study showed that increased expression of CD147, an accessory β-subunit of MCT4, is coupled to the upregulation of MCT4 and that silencing of MCT4 resulted in decreased migration of metastatic cancer cells. CD147 has been shown to induce

MMPs in fibroblasts and cancer cells [169]. There are indications that transporters may be regulated by factors originating from the microenvironment [170].

However, very little is known about the regulation of transporters. Thus, the chemosensitivity and chemoresistance for a given carrier-mediated chemotherapeutic drug may be influenced by the microenvironment and may change significantly during EMT. This aspect has never been addressed so far.

Regulation of PEPT1 and HPT1 in Cancers of the GIT The regulation of PEPT1 is influenced by many different factors such as chemically synthesized dipeptides, leptin, EGF, insulin, and high-protein meal or prolonged fasting. However, only very recently, a direct regulation via a transcription factor-binding site has been identified. Shimakura *et al*. suggested that the transcription factor CDX2 regulates PEPT1 through the functional interaction with SP1 [171]. *In vitro* experiments in Caco-2 cells showed that the mutation of the SP1-binding site diminished the effect of CDX2, and the coexpression of SP1 and CDX2 had synergistically transactivated the PEPT1 promoter. Moreover, Nduati *et al*. presented in their very recent study evidence that the interaction of CDX2 and phosphorylated CREB (CREB) transcription factors is essential for leptin-induced PEPT1 regulation ([172], cf. below).

CDX2 plays a crucial role in the differentiation of healthy intestinal absorptive cells [173, 174]. Clearly, in tumor development, the expression and activity of CDX2 are affected over time [173]. However, opinions about whether CDX2 expression is lost completely or is only in a subset of poorly differentiated tumor cells differ. The mechanisms involved are still subject of ongoing research [173]. Witek *et al*. even suggested that in 80% of the tumors they analyzed the expression of CDX2 was increased [175].

In a very recent study, CDX2 expression has been shown to be adaptable and strongly influenced by the microenvironment. As a consequence, the authors suggest that CDX2 expression might be relevant during the process of metastatic dissemination when the gene is transiently turned down. In line with these findings, Gross *et al*. reported shortly afterwards that CDX2 decreased mobility and dissemination of colon cancer cells [176]. It has already been shown that PEPT1 expression is increased in chronically inflamed colon mucosa (cf. below), a typical diseased state in which the microenvironment plays a significant role (cf. below). In addition, PEPT1 is highly expressed in Caco-2 cells, a colon cancer-derived cell line [177]. As a result, one could assume that the regulation of PEPT1 in colon cancer, which in many respects is a situation of a not-healing wound, could be differently expressed compared to the healthy colon. Nevertheless, to our knowledge, the regulation of PEPT1 expression in human colon cancer has never really been investigated. We have tested the expression in laser dissected, differentiated colon tumor cells and could not observe any expression of *PEPT1* (unpublished data). This leads to the conclusion that the regulation of PEPT1 in colon cancer may mainly be under the control of other factors than CDX2 and the ones active in chronic inflammation (cf. below). While neoplastic processes in the colon do not seem to affect PEPT1 expression, some studies suggest that

PEPT1 expression is increased in cells of the stomach undergoing metaplasia, that is, gastric mucosal cells differentiating into a more intestinal phenotype [178]. Using a mouse model, Mutoh *et al*. demonstrated that CDX2 induced not only morphological but also functional absorptive enterocytes in the intestinal metaplastic mucosa *in vivo*, suggesting that CDX2 is necessary and sufficient by itself to specify the development of intestinal absorptive enterocytes [179]. Thus, the regulation of PEPT1 could take place in metaplastic cells of the stomach under the control of CDX2.

Similar to *PEPT1*, *HPT1* (*CDH17*) is expressed in the small intestine, metaplastic cells in gastric carcinoma, and in Caco-2 cells [180]. However, in contrast to *PEPT1*, it is also expressed in colon and colon carcinoma [181–183]. Very interestingly, while overexpression of this gene in gastric cancer is associated with lymph node metastasis, its reduced expression in colon cancer is linked to the progression of colon carcinoma and lymph node metastasis [183, 184]. *CDH17* and its protein product seem to be mostly expressed in differentiated tumor cells and are downregulated in tumoral dedifferentiation [182, 183]. Similar to PEPT1, Hinoi *et al*. reported that the regulation of CDH17 seems to be under the control of CDX2 [181]. The authors actually discovered this link by applying microarray analysis. They compared the expression profiles of HT29 cells with minimal endogenous CDX2 expression and HT29 cells engineered to express exogenous CDX2. CDH17 was strongly induced in the engineered cells. Moreover, immunoprecipitation assays suggested the presence of two CDX2 responsive elements in the 5′-flanking region of CDH17. Testing the expressions of CDX2 and CDH17 in patient samples, the authors observed a close correlation. In addition, in CDX2 knockout mice, they observed a suppression of CDH17 expression in polyps arising in the proximal colon [181]. Ko *et al*. observed that in intestinal metaplasia and adenocarcinoma of the stomach CDX2 colocalizes with liver–intestine cadherin [185].

Still further investigations are necessary to elucidate the expressions of PEPT1 and CDH17 and their roles in cancers and especially colon cancer. As far as the design of new drugs using PEPT1 as a carrier is concerned, understanding the differences of regulation of this transporter between colon cancer and chronic inflammatory diseases of the large intestine will be very important. Regarding CDH17, still further studies are needed to elucidate its role as a peptide transporter and, thus, as a potential drug carrier.

In summary, we have elucidated that various factors can interfere with the expression of transporters in tumors. In addition, the regulation of transporters may be influenced by the microenvironment. Even though chronic inflammation and tumor formation have many similarities, by using PEPT1 as an example, we have seen that the expression of transporters may differ. Thus, knowing the expression pattern and regulation of transporters in these situations is very important when exploiting transporters as drug carriers. Moreover, the expression of transporters may serve as a readout for active transcription factors in these situations and, thus, serve as an indicator for the design of new drugs. Figure 10.5 presents an overview of the role of transporters in cancer.

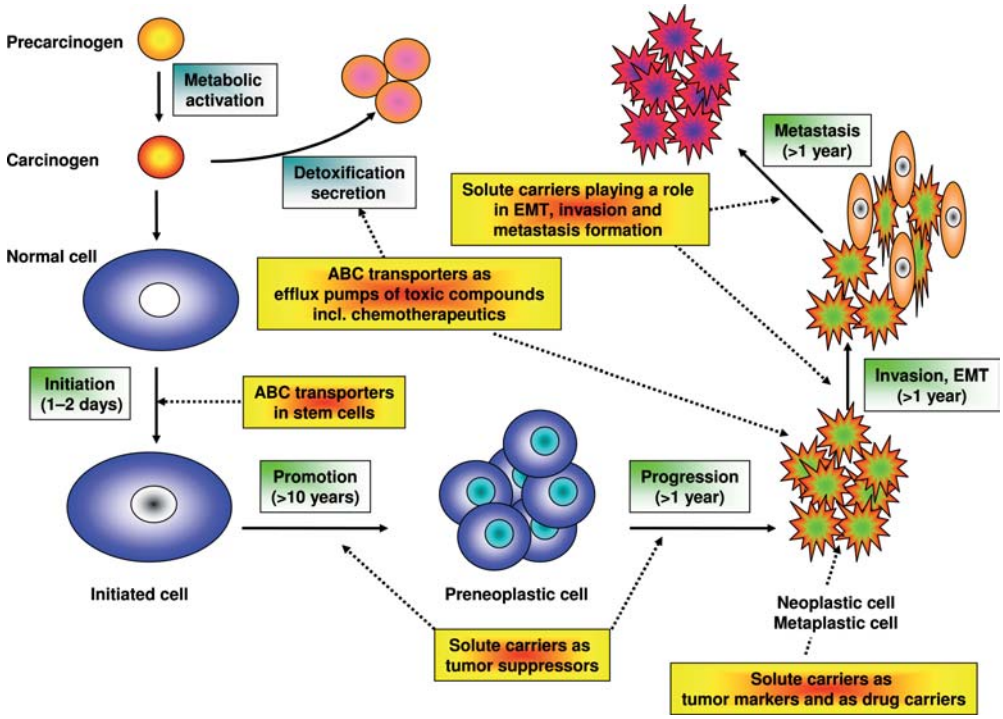

Figure 10.5 Overview of the role of transporters in cancer.

10.5.3.3 Role of Transporters in Intestinal Stem Cells

Various studies indicated that ABC transporters are expressed in stem cells, which led to the hypothesis that they are expressed in tumor-initiating cells [186, 187]. It has been shown in colon cancer that cells expressing CD133+ have such a cancer-initiating potential [188, 189]. Monzani *et al.* observed in melanoma, a coexpression of ABCG2 and CD133+ [190]. Interestingly, CD133+ is strongly expressed in Caco-2 cells and is not downregulated upon differentiation [191]. We observed that compared to other colon cancer cell lines with different stages of differentiation (i.e., T84, HT29, LS174T, SW480, and HCT116), differentiated Caco-2 and HT29 cells had the highest *CD133* expression, while the expression in SW480 cells, cells with mesenchymal characteristics, was lowest (unpublished data). Frank *et al.* showed that ABCB5 is a molecular marker for a distinct subset of chemoresistant, stem cell phenotype-expressing tumor cells among melanoma bulk populations [192]. However, the expression and the role of ABC transporters in cancer-initiating cells in solid tumors have never directly been shown.

In conclusion, various studies indicate that transporters could be exploited in solid tumors when targeting tumor-initiating cells. However, there is still a significant lack of information available regarding their expression and role in these cells. In addition, to date it is still unclear which models may be most appropriate when studying these aspects in such cells. Thus, for the design of new drugs, medical

chemistry has to take into account that most probably chemotherapeutics are subjected to secretion.

10.5.4
Role of PEPT1 in Inflammatory Bowel Disease

Intestinal epithelial and subepithelial cells are an integrated part of the immune system, being a primary barrier and detection zone for pathogens. In a study by Merlin *et al.*, it has been suggested that PEPT1 could be involved in mediating the signal between pathogen invasion and immune response via transport of bacteria-derived *n*-formyl peptides such as formyl-Met-Leu-Phe (fMLP) [118]. The PEPT1-mediated transport of fMLP induced basolateral to apical neutrophil migration in a neutrophil/Caco-2-BBE cell model [118]. In both rat jejunum *in vivo* and *in vitro* cell culture studies, the PEPT1-mediated fMLP transport induced inflammation-like responses, without inducing inflammation in normal rat colon, which does not express *Pept1* [193, 194]. PEPT1 is not normally expressed in the colon, but, under pathophysiological conditions such as chronic ulcerative colitis and Crohn's disease, colonic expression of PEPT1 is observed [193, 194]. Furthermore, *n*-formyl-peptides transported via PEPT1 induced cell surface expression of MHC class 1 in HT-29-Cl.19A cells [194]. However, a recent study in rats indicated that induced colitis does not alter the bioavailability of Pept1 substrates such as cephalexin and valaciclovir [189]. In rabbit, small intestinal inflammation decreases the transport via Pept1; however, this seems to be due to an altered affinity for the substrate rather than altered mRNA expression [196]. After 80% colonic resection in rats, upregulation of *Pept1* expression is observed, and the induction of intestinal inflammation using fMLP causes a damage of the intestinal epithelium indicating a role for PEPT1 in the generation of this disease state [72, 195, 197, 198]. Also, small bowel resection in humans, causing small bowel syndrome, leads to upregulation of PEPT1 in the colon and may be part of an adaptional process to increase dietary nitrogen absorption [195]. In another study, the long-term effects of treating rats with sublethal concentrations of the endotoxin lipopolysaccharide (LPS) was evaluated [199]. LPS is an important component of the outer membrane of Gram-negative bacteria, and, when injected in rats, it increases levels of proinflammatory cytokines such as tumor necrosis factor-α (TNF-α) and interleukin (IL) 1β along with decreasing levels of *Pept1* mRNA and protein in the small intestinal enterocytes [58]. Administration of dexamethasone (0.1 mg/100 g body weight), which decreased the amount of Il-1β and TNF-α in the small intestinal mucosa, could counteract the effect of LPS on Pept1 expression [199]. However, in Caco-2/BBE cells and in mice intestine, it was shown that interleukin IL-1β does not increase Gly-Sar uptake via PEPT1, although the amount of *Pept1* mRNA is increased in the colon and decreased in the small intestine [200]. On the other hand, TNF-α and interferon-γ upregulated Pept1 activity in mouse proximal and distal colon, but they had no effect on the *Pept1* mRNA in the small intestine [200]. TNF-α is able to stimulate the EGF receptor, and the long-term activation results in a decreased expression of *PEPT1* mRNA and its protein product, whereas short-term activation increases PEPT1-mediated uptake in Caco-2 cells [201, 202]. Another

hormone likely to be involved in the regulation of PEPT1 in the colon during inflammation is leptin. Leptin is an adipocyte-secreted hormone that is present at increased levels in the colon during IBD, where the cells express and release leptin on the apical membrane [203]. Recently, Nduati *et al.* have shown by promoter studies that leptin increases *PEPT1* mRNA expression and its protein product in Caco-2 BBE cells by transcriptional activation that depends on the CDX2-binding sites located −579 and −562 in the *PEPT* promoter [172]. Their results indicate that the signaling pathway leading to leptin transcriptional activation of the *PEPT* gene is via increased cAMP levels and subsequent activation of PKA that translocates into the nucleus and increases the level of phosphorylated CREB. This is then followed by binding of CDX2 and pCREB to the promoter [172].

Taken together, PEPT1 seems to play an important role in intestinal inflammation, especially in the colon, and may thus be a novel anti-inflammatory drug target for the medicinal chemist. This is stressed by the recent findings that the tripeptide Lys-Pro-Val, due to the intracellular accumulation via PEPT1, inhibits the activation of NF-κB and MAP kinase inflammation and reduces proinflammatory cytokine secretion in DSS- and TNBS-induced colitis in mice [204].

10.6 Summary and Outlook

Drug absorption has traditionally been thought to occur predominantly via passive transcellular and paracellular transport mechanisms. However, recent studies indicate that carrier-mediated drug transport may play a more important role than previously appreciated. Clearly, the bioavailability of a given drug can be increased by targeting transporters as drug carriers. We have presented a couple of examples for which the design of a prodrug – which is taken up actively – significantly contributed to an improvement of the bioavailability. Yet, the mechanisms of uptake are actually still unknown or only partially elucidated.

Knowing the expression of transporter genes is a first step in elucidating the role of transporters in absorption. With the rise of new high-throughput technologies, significant knowledge of this aspect could be obtained. Yet, information on the protein expression and the functional activity of transporters is still needed. In addition, the influence of genotypes on drug absorption needs further investigation. However, it has become clear that the knowledge gained from genotyping and phenotyping studies can contribute to a more individualized and improved treatment.

Making an increasing amount of genomics and proteomics data publicly available will certainly deepen our understanding of how transporters are regulated and which factors are important. Consequently, drug design can be adjusted accordingly. Besides their role as drug and nutrient carriers, transporters also seem to play other important roles in diseased states of the intestine. Thus, transporters on the one hand should be considered when trying to reduce chemoresistance or improve sensitivity. On the other hand, they could also be exploited in the future as direct drug targets to treat these diseases.

References

1 Beauchamp, L.M., Orr, G.F., de Miranda, P., Burnette, T. and Krenitsky, T.A. (1992) Amino acid ester prodrugs of acyclovir. *Antiviral Chemistry & Chemotherapy*, **3**, 157–164.

2 de Vrueh, R.L., Smith, P.L. and Lee, C.P. (1998) Transport of L-valine-acyclovir via the oligopeptide transporter in the human intestinal cell line, Caco-2. *The Journal of Pharmacology and Experimental Therapeutics*, **286** (3), 1166–1170.

3 Hilgendorf, C., Ahlin, G., Seithel, A., Artursson, P., Ungell, A.L. and Karlsson, J. (2007) Expression of thirty-six drug transporter genes in human intestine, liver, kidney, and organotypic cell lines. *Drug Metabolism and Disposition: The Biological Fate of Chemicals*, **35** (8), 1333–1340.

4 Kim, H.R., Park, S.W., Cho, H.J., Chae, K.A., Sung, J.M., Kim, J.S., Landowski, C.P., Sun, D., Abd El-Aty, A.M., Amidon, G.L. *et al.* (2007) Comparative gene expression profiles of intestinal transporters in mice, rats and humans. *Pharmacological Research*, **56** (3), 224–236.

5 Brandsch, M., Knutter, I. and Leibach, F.H. (2004) The intestinal H+/peptide symporter PEPT1: structure–affinity relationships. *European Journal of Pharmaceutical Sciences*, **21** (1), 53–60.

6 Meredith, D. and Boyd, C.A. (2000) Structure and function of eukaryotic peptide transporters. *Cellular and Molecular Life Sciences*, **57** (5), 754–778.

7 Nielsen, C.U., Brodin, B., Jorgensen, F.S., Frokjaer, S. and Steffansen, B. (2002) Human peptide transporters: therapeutic applications. *Expert Opinion on Therapeutic Patents*, **12**, 1329–1350.

8 Bretschneider, B., Brandsch, M. and Neubert, R. (1999) Intestinal transport of beta-lactam antibiotics: analysis of the affinity at the H+/peptide symporter (PEPT1), the uptake into Caco-2 cell monolayers and the transepithelial flux. *Pharmaceutical Research*, **16** (1), 55–61.

9 Dantzig, A.H. (1998) Oral absorption of beta-lactams by intestinal peptide transport proteins. *Advanced Drug Delivery Reviews*, **23**, 63–76.

10 Han, H., de Vrueh, R.L., Rhie, J.K., Covitz, K.M., Smith, P.L., Lee, C.P., Oh, D.M., Sadee, W. and Amidon, G.L. (1998) 5′-Amino acid esters of antiviral nucleosides, acyclovir, and AZT are absorbed by the intestinal PEPT1 peptide transporter. *Pharmaceutical Research*, **15** (8), 1154–1159.

11 Landowski, C.P., Han, H.K., Lee, K.D. and Amidon, G.L. (2003) A fluorescent hPept1 transporter substrate for uptake screening. *Pharmaceutical Research*, **20** (11), 1738–1745.

12 Meredith, D., Temple, C.S., Guha, N., Sword, C.J., Boyd, C.A., Collier, I.D., Morgan, K.M. and Bailey, P.D. (2000) Modified amino acids and peptides as substrates for the intestinal peptide transporter PepT1. *European Journal of Biochemistry*, **267** (12), 3723–3728.

13 Dantzig, A.H., Hoskins, J.A., Tabas, L.B., Bright, S., Shepard, R.L., Jenkins, I.L., Duckworth, D.C., Sportsman, J.R., Mackensen, D., Rosteck, P.R., Jr, *et al.* (1994) Association of intestinal peptide transport with a protein related to the cadherin superfamily. *Science*, **264** (5157), 430–433.

14 Gao, J., Sudoh, M., Aube, J. and Borchardt, R.T. (2001) Transport characteristics of peptides and peptidomimetics: I. N-methylated peptides as substrates for the oligopeptide transporter and P-glycoprotein in the intestinal mucosa. *The Journal of Peptide Research*, **57** (4), 316–329.

15 Tamai, I. and Safa, A.R. (1991) Azidopine noncompetitively interacts with vinblastine and cyclosporin A binding to P-glycoprotein in multidrug resistant

cells. *The Journal of Biological Chemistry*, **266** (25), 16796–16800.

16 Meier, Y., Eloranta, J.J., Darimont, J., Ismair, M.G., Hiller, C., Fried, M., Kullak-Ublick, G.A. and Vavricka, S.R. (2007) Regional distribution of solute carrier mRNA expression along the human intestinal tract. *Drug Metabolism and Disposition: The Biological Fate of Chemicals*, **35** (4), 590–594.

17 Ritzel, M.W., Ng, A.M., Yao, S.Y., Graham, K., Loewen, S.K., Smith, K.M., Hyde, R.J., Karpinski, E., Cass, C.E., Baldwin, S.A., *et al*. (2001) Recent molecular advances in studies of the concentrative Na + -dependent nucleoside transporter (CNT) family: identification and characterization of novel human and mouse proteins (hCNT3 and mCNT3) broadly selective for purine and pyrimidine nucleosides (system cib). *Molecular Membrane Biology*, **18** (1), 65–72.

18 Ritzel, M.W., Ng, A.M., Yao, S.Y., Graham, K., Loewen, S.K., Smith, K.M., Ritzel, R.G., Mowles, D.A., Carpenter, P., Chen, X.Z. *et al*. (2001) Molecular identification and characterization of novel human and mouse concentrative Na +-nucleoside cotransporter proteins (hCNT3 and mCNT3) broadly selective for purine and pyrimidine nucleosides (system cib). *The Journal of Biological Chemistry*, **276** (4), 2914–2927.

19 Huang, Q.Q., Yao, S.Y., Ritzel, M.W., Paterson, A.R., Cass, C.E. and Young, J.D. (1994) Cloning and functional expression of a complementary DNA encoding a mammalian nucleoside transport protein. *The Journal of Biological Chemistry*, **269** (27), 17757–17760.

20 Mackey, J.R., Mani, R.S., Selner, M., Mowles, D., Young, J.D., Belt, J.A., Crawford, C.R. and Cass, C.E. (1998) Functional nucleoside transporters are required for gemcitabine influx and manifestation of toxicity in cancer cell lines. *Cancer Research*, **58** (19), 4349–4357.

21 Mackey, J.R., Yao, S.Y., Smith, K.M., Karpinski, E., Baldwin, S.A., Cass, C.E. and Young, J.D. (1999) Gemcitabine transport in xenopus oocytes expressing recombinant plasma membrane mammalian nucleoside transporters. *Journal of the National Cancer Institute*, **91** (21), 1876–1881.

22 Ritzel, M.W., Yao, S.Y., Huang, M.Y., Elliott, J.F., Cass, C.E. and Young, J.D. (1997) Molecular cloning and functional expression of cDNAs encoding a human Na + -nucleoside cotransporter (hCNT1). *The American Journal of Physiology*, **272** (2 Pt 1), C707–C714.

23 Ritzel, M.W., Yao, S.Y., Ng, A.M., Mackey, J.R., Cass, C.E. and Young, J.D. (1998) Molecular cloning, functional expression and chromosomal localization of a cDNA encoding a human Na + /nucleoside cotransporter (hCNT2) selective for purine nucleosides and uridine. *Molecular Membrane Biology*, **15** (4), 203–211.

24 Broer, S. (2008) Amino acid transport across mammalian intestinal and renal epithelia. *Physiological Reviews*, **88** (1), 249–286.

25 Chen, Z., Fei, Y.J., Anderson, C.M., Wake, K.A., Miyauchi, S., Huang, W., Thwaites, D.T. and Ganapathy, V. (2003) Structure, function and immunolocalization of a proton-coupled amino acid transporter (hPAT1) in the human intestinal cell line Caco-2. *The Journal of Physiology*, **546** (Pt 2), 349–361.

26 Abbot, E.L., Grenade, D.S., Kennedy, D.J., Gatfield, K.M. and Thwaites, D.T. (2006) Vigabatrin transport across the human intestinal epithelial (Caco-2) brush-border membrane is via the H +-coupled amino-acid transporter hPAT1. *British Journal of Pharmacology*, **147** (3), 298–306.

27 Thwaites, D.T., Armstrong, G., Hirst, B.H. and Simmons, N.L. (1995) D-cycloserine transport in human intestinal epithelial (Caco-2) cells: mediation by a H(+)-coupled amino acid transporter. *British Journal of Pharmacology*, **115** (5), 761–766.

28 Wagner, C.A., Lang, F. and Broer, S. (2001) Function and structure of heterodimeric amino acid transporters. *American Journal of Physiology – Cell Physiology*, **281** (4), C1077–C1093.

29 Ganapathy, M.E. and Ganapathy, V. (2005) Amino acid transporter $ATB^{0,+}$ as a delivery system for drugs and prodrugs. *Current Drug Targets. Immune, Endocrine and Metabolic Disorders*, **5** (4), 357–364.

30 Koepsell, H., Lips, K. and Volk, C. (2007) Polyspecific organic cation transporters: structure, function, physiological roles, and biopharmaceutical implications. *Pharmaceutical Research*, **24** (7), 1227–1251.

31 Koepsell, H. and Endou, H. (2004) The SLC22 drug transporter family. *Pflugers Archiv: European Journal of Physiology*, **447** (5), 666–676.

32 Ito, K., Suzuki, H., Horie, T. and Sugiyama, Y. (2005) Apical/basolateral surface expression of drug transporters and its role in vectorial drug transport. *Pharmaceutical Research*, **22** (10), 1559–1577.

33 Halestrap, A.P. and Meredith, D. (2004) The SLC16 gene family – from monocarboxylate transporters (MCTs) to aromatic amino acid transporters and beyond. *Pflugers Archiv: European Journal of Physiology*, **447** (5), 619–628.

34 Englund, G., Rorsman, F., Ronnblom, A., Karlbom, U., Lazorova, L., Grasjo, J., Kindmark, A. and Artursson, P. (2006) Regional levels of drug transporters along the human intestinal tract: co-expression of ABC and SLC transporters and comparison with Caco-2 cells. *European Journal of Pharmaceutical Sciences*, **29** (3–4), 269–277.

35 Tamai, I., Takanaga, H., Maeda, H., Sai, Y., Ogihara, T., Higashida, H. and Tsuji, A. (1995) Participation of a proton-cotransporter, MCT1, in the intestinal transport of monocarboxylic acids. *Biochemical and Biophysical Research Communications*, **214** (2), 482–489.

36 Tsuji, A., Tamai, I., Nakanishi, M., Terasaki, T. and Hamano, S. (1993) Intestinal brush-border transport of the oral cephalosporin antibiotic, cefdinir, mediated by dipeptide and monocarboxylic acid transport systems in rabbits. *The Journal of Pharmacy and Pharmacology*, **45** (11), 996–998.

37 Calcagno, A.M., Kim, I.W., Wu, C.P., Shukla, S. and Ambudkar, S.V. (2007) ABC drug transporters as molecular targets for the prevention of multidrug resistance and drug–drug interactions. *Current Drug Delivery*, **4** (4), 324–333.

38 Chan, L.M., Lowes, S. and Hirst, B.H. (2004) The ABCs of drug transport in intestine and liver: efflux proteins limiting drug absorption and bioavailability. *European Journal of Pharmaceutical Sciences*, **21** (1), 25–51.

39 Takano, M., Yumoto, R. and Murakami, T. (2006) Expression and function of efflux drug transporters in the intestine. *Pharmacology & Therapeutics*, **109** (1–2), 137–161.

40 Loo, T.W., Bartlett, M.C. and Clarke, D.M. (2003) Substrate-induced conformational changes in the transmembrane segments of human P-glycoprotein. Direct evidence for the substrate-induced fit mechanism for drug, binding. *The Journal of Biological Chemistry*, **278** (16), 13603–13606.

41 Loo, T.W. and Clarke, D.M. (1999) The transmembrane domains of the human multidrug resistance P-glycoprotein are sufficient to mediate drug binding and trafficking to the cell surface. *The Journal of Biological Chemistry*, **274** (35), 24759–24765.

42 Benet, L.Z., Izumi, T., Zhang, Y., Silverman, J.A. and Wacher, V.J. (1999) Intestinal MDR transport proteins and P-450 enzymes as barriers to oral drug delivery. *Journal of Controlled Release*, **62** (1–2), 25–31.

43 Wacher, V.J., Silverman, J.A., Zhang, Y. and Benet, L.Z. (1998) Role of P-glycoprotein and cytochrome P450 3A in limiting oral absorption of peptides and

peptidomimetics. *Journal of Pharmaceutical Sciences*, **87** (11), 1322–1330.

44 Wacher, V.J., Wu, C.Y. and Benet, L.Z. (1995) Overlapping substrate specificities and tissue distribution of cytochrome P450 3A and P-glycoprotein: implications for drug delivery and activity in cancer chemotherapy. *Molecular Carcinogenesis*, **13** (3), 129–134.

45 Kawahara, M., Sakata, A., Miyashita, T., Tamai, I. and Tsuji, A. (1999) Physiologically based pharmacokinetics of digoxin in mdr1a knockout mice. *Journal of Pharmaceutical Sciences*, **88** (12), 1281–1287.

46 Mayer, U., Wagenaar, E., Beijnen, J.H., Smit, J.W., Meijer, D.K., van Asperen, J., Borst, P. and Schinkel, A.H. (1996) Substantial excretion of digoxin via the intestinal mucosa and prevention of long-term digoxin accumulation in the brain by the mdr1a P-glycoprotein. *British Journal of Pharmacology*, **119** (5), 1038–1044.

47 Stephens, R.H., Tanianis-Hughes, J., Higgs, N.B., Humphrey, M. and Warhurst, G. (2002) Region-dependent modulation of intestinal permeability by drug efflux transporters: *in vitro* studies in mdr1a(−/−) mouse intestine. *The Journal of Pharmacology and Experimental Therapeutics*, **303** (3), 1095–1101.

48 Westphal, K., Weinbrenner, A., Giessmann, T., Stuhr, M., Franke, G., Zschiesche, M., Oertel, R., Terhaag, B., Kroemer, H.K. and Siegmund, W. (2000) Oral bioavailability of digoxin is enhanced by talinolol: evidence for involvement of intestinal P-glycoprotein. *Clinical Pharmacology and Therapeutics*, **68** (1), 6–12.

49 Balakrishnan, A. and Polli, J.E. (2006) Apical sodium dependent bile acid transporter (ASBT, SLC10A2): a potential prodrug target. *Molecular Pharmacology*, **3** (3), 223–230.

50 Balakrishnan, A., Wring, S.A. and Polli, J.E. (2006) Interaction of native bile acids with human apical sodium-dependent bile acid transporter (hASBT): influence of steroidal hydroxylation pattern and C-24 conjugation. *Pharmaceutical Research*, **23** (7), 1451–1459.

51 Venter, J.C., Adams, M.D., Myers, E.W., Li, P.W., Mural, R.J., Sutton, G.G., Smith, H.O., Yandell, M., Evans, C.A., Holt, R.A., *et al.* (2001) The sequence of the human genome. *Science*, **291** (5507), 1304–1351.

52 Bates, M.D., Erwin, C.R., Sanford, L.P., Wiginton, D., Bezerra, J.A., Schatzman, L.C., Jegga, A.G., Ley-Ebert, C., Williams, S.S., Steinbrecher, K.A. *et al.* (2002) Novel genes and functional relationships in the adult mouse gastrointestinal tract identified by microarray analysis. *Gastroenterology*, **122** (5), 1467–1482.

53 Anderle, P., Sengstag, T., Mutch, D.M., Rumbo, M., Praz, V., Mansourian, R., Delorenzi, M., Williamson, G. and Roberts, M.A. (2005) Changes in the transcriptional profile of transporters in the intestine along the anterior–posterior and crypt-villus axes. *BMC Genomics*, **6** (1), 69.

54 Mariadason, J.M., Arango, D., Corner, G.A., Aranes, M.J., Hotchkiss, K.A., Yang, W. and Augenlicht, L.H. (2002) A gene expression profile that defines colon cell maturation *in vitro*. *Cancer Research*, **62** (16), 4791–4804.

55 Fleet, J.C., Wang, L., Vitek, O., Craig, B.A. and Edenberg, H.J. (2003) Gene expression profiling of Caco-2 BBe cells suggests a role for specific signaling pathways during intestinal differentiation. *Physiological Genomics*, **13** (1), 57–68.

56 Anderle, P., Rakhmanova, V., Woodford, K., Zerangue, N. and Sadee, W. (2003) Messenger RNA expression of transporter and ion channel genes in undifferentiated and differentiated Caco-2 cells compared to human intestines. *Pharmaceutical Research*, **20** (1), 3–15.

57 Landowski, C.P., Anderle, P., Sun, D., Sadee, W. and Amidon, G.L. (2004) Transporter and ion channel gene expression after Caco-2 cell,

differentiation using 2 different microarray technologies. *AAPS Journal*, **6** (3), e21.

58 Sun, D., Lennernäs, H., Welage, L.S., Barnett, J.L., Landowski, C.P., Foster, D., Fleisher, D., Lee, K.D. and Amidon, G.L. (2002) Comparison of human duodenum and Caco-2 gene expression profiles for 12,000 gene sequences tags and correlation with permeability of 26 drugs. *Pharmaceutical Research*, **19** (10), 1400–1416.

59 Calcagno, A.M., Ludwig, J.A., Fostel, J.M., Gottesman, M.M. and Ambudkar, S.V. (2006) Comparison of drug transporter levels in normal colon, colon cancer, and Caco-2 cells: impact on drug disposition and discovery. *Molecular Pharmacology*, **3** (1), 87–93.

60 Gentalen, E. and Chee, M. (1999) A novel method for determining linkage between DNA sequences: hybridization to paired probe arrays. *Nucleic Acids Research*, **27** (6), 1485–1491.

61 Anderle, P., Nielsen, C.U., Pinsonneault, J., Krog, P.L., Brodin, B. and Sadee, W. (2006) Genetic variants of the human dipeptide transporter PEPT1. *The Journal of Pharmacology and Experimental Therapeutics*, **316** (2), 636–646.

62 Zhang, E.Y., Fu, D.J., Pak, Y.A., Stewart, T., Mukhopadhyay, N., Wrighton, S.A. and Hillgren, K.M. (2004) Genetic polymorphisms in human proton-dependent dipeptide transporter PEPT1: implications for the functional role of Pro586. *The Journal of Pharmacology and Experimental Therapeutics*, **310** (2), 437–445.

63 Phan, D.D., Chin-Hong, P., Lin, E.T., Anderle, P., Sadee, W. and Guglielmo, B.J. (2003) Intra- and interindividual variabilities of valacyclovir oral bioavailability and effect of coadministration of an hPEPT1 inhibitor. *Antimicrobial Agents and Chemotherapy*, **47** (7), 2351–2353.

64 Gray, J.H., Mangravite, L.M., Owen, R.P., Urban, T.J., Chan, W., Carlson, E.J., Huang, C.C., Kawamoto, M., Johns, S.J., Stryke, D. *et al.* (2004) Functional and genetic diversity in the concentrative nucleoside transporter, CNT1, in human populations. *Molecular Pharmacology*, **65** (3), 512–519.

65 Owen, R.P., Gray, J.H., Taylor, T.R., Carlson, E.J., Huang, C.C., Kawamoto, M., Johns, S.J., Stryke, D., Ferrin, T.E. and Giacomini, K.M. (2005) Genetic analysis and functional characterization of polymorphisms in the human concentrative nucleoside transporter, CNT2. *Pharmacogenetics and Genomics*, **15** (2), 83–90.

66 Damaraju, S., Zhang, J., Visser, F., Tackaberry, T., Dufour, J., Smith, K.M., Slugoski, M., Ritzel, M.W., Baldwin, S.A., Young, J.D. *et al.* (2005) Identification and functional characterization of variants in human concentrative nucleoside transporter 3, hCNT3 (SLC28A3), arising from single nucleotide polymorphisms in coding regions of the hCNT3 gene. *Pharmacogenetics and Genomics*, **15** (3), 173–182.

67 Owen, R.P., Lagpacan, L.L., Taylor, T.R., De LaCruz, M., Huang, C.C., Kawamoto, M., Johns, S.J., Stryke, D., Ferrin, T.E. and Giacomini, K.M. (2006) Functional characterization and haplotype analysis of polymorphisms in the human equilibrative nucleoside transporter, ENT2. *Drug Metabolism and Disposition: The Biological Fate of Chemicals*, **34** (1), 12–15.

68 Kuhne, A., Kaiser, R., Schirmer, M., Heider, U., Muhlke, S., Niere, W., Overbeck, T., Hohloch, K., Trumper, L., Sezer, O. *et al.* (2007) Genetic polymorphisms in the amino acid transporters LAT1 and LAT2 in relation to the pharmacokinetics and side effects of melphalan. *Pharmacogenetics and Genomics*, **17** (7), 505–517.

69 Kroetz, D.L., Pauli-Magnus, C., Hodges, L.M., Huang, C.C., Kawamoto, M., Johns, S.J., Stryke, D., Ferrin, T.E., DeYoung, J., Taylor, T. *et al.* (2003) Sequence diversity

and haplotype structure in the human ABCB1 (MDR1, multidrug resistance transporter) gene. *Pharmacogenetics*, **13** (8), 481–494.

70 Smith, N.F., Figg, W.D. and Sparreboom, A. (2006) Pharmacogenetics of irinotecan metabolism and transport: an update. *Toxicology In Vitro*, **20** (2), 163–175.

71 Tang, K., Ngoi, S.M., Gwee, P.C., Chua, J.M., Lee, E.J., Chong, S.S. and Lee, C.G. (2002) Distinct haplotype profiles and strong linkage disequilibrium at the MDR1 multidrug transporter gene locus in three ethnic Asian populations. *Pharmacogenetics*, **12** (6), 437–450.

72 Saito, S., Iida, A., Sekine, A., Miura, Y., Ogawa, C., Kawauchi, S., Higuchi, S. and Nakamura, Y. (2002) Identification of 779 genetic variations in eight genes encoding members of the ATP-binding cassette, subfamily C (ABCC/MRP/CFTR). *Journal of Human Genetics*, **47** (4), 147–171.

73 Leschziner, G., Zabaneh, D., Pirmohamed, M., Owen, A., Rogers, J., Coffey, A.J., Balding, D.J., Bentley, D.B. and Johnson, M.R. (2006) Exon sequencing and high resolution haplotype analysis of ABC transporter genes implicated in drug resistance. *Pharmacogenetics and Genomics*, **16** (6), 439–450.

74 Andersen, R., Jorgensen, F.S., Olsen, L., Vabeno, J., Thorn, K., Nielsen, C.U. and Steffansen, B. (2006) Development of a QSAR model for binding of tripeptides and tripeptidomimetics to the human intestinal di-/tripeptide transporter hPEPT1. *Pharmaceutical Research*, **23** (3), 483–492.

75 Bailey, P.D., Boyd, C.A., Bronk, J.R., Collier, I.D., Meredith, D., Morgan, K.M. and Temple, C.S. (2000) How to make drugs orally active: a substrate template for peptide transporter PepT1. *Angewandte Chemie*, **39** (3), 505–508.

76 Biegel, A., Gebauer, S., Hartrodt, B., Brandsch, M., Neubert, K. and Thondorf, I. (2005) Three-dimensional quantitative structure–activity relationship analyses of beta-lactam antibiotics and tripeptides as substrates of the mammalian H+/peptide cotransporter PEPT1. *Journal of Medicinal Chemistry*, **48** (13), 4410–4419.

77 Gebauer, S., Knutter, I., Hartrodt, B., Brandsch, M., Neubert, K. and Thondorf, I. (2003) Three-dimensional quantitative structure–activity relationship analyses of peptide substrates of the mammalian H+/peptide cotransporter PEPT1. *Journal of Medicinal Chemistry*, **46** (26), 5725–5734.

78 Swaan, P.W., Koops, B.C., Moret, E.E. and Tukker, J.J. (1998) Mapping the binding site of the small intestinal peptide carrier (PepT1) using comparative molecular field analysis. *Receptors & Channels*, **6** (3), 189–200.

79 Swaan, P.W. and Tukker, J.J. (1997) Molecular determinants of recognition for the intestinal peptide carrier. *Journal of Pharmaceutical Sciences*, **86** (5), 596–602.

80 Vabeno, J., Nielsen, C.U., Steffansen, B., Lejon, T., Sylte, I., Jorgensen, F.S. and Luthman, K. (2005) Conformational restrictions in ligand binding to the human intestinal di-/tripeptide transporter: implications for design of hPEPT1 targeted prodrugs. *Bioorganic and Medicinal Chemistry*, **13** (6), 1977–1988.

81 Winiwarter, S. and Hilgendorf, C. (2008) Modeling of drug–transporter interactions using structural information. *Current Opinion in Drug Discovery & Development*, **11** (1), 95–103.

82 Sugawara, M., Huang, W., Fei, Y.J., Leibach, F.H., Ganapathy, V. and Ganapathy, M.E. (2000) Transport of valganciclovir, a ganciclovir prodrug, via peptide transporters PEPT1 and PEPT2. *Journal of Pharmaceutical Sciences*, **89** (6), 781–789.

83 Jung, D. and Dorr, A. (1999) Single-dose pharmacokinetics of valganciclovir in HIV- and CMV-seropositive subjects. *Journal of Clinical Pharmacology*, **39** (8), 800–804.

84 Umapathy, N.S., Ganapathy, V. and Ganapathy, M.E. (2004) Transport of amino acid esters and the amino-acid-based prodrug valganciclovir by the amino acid transporter ATB(0, +). *Pharmaceutical Research*, **21** (7), 1303–1310.

85 Bueno, A.B., Collado, I., de Dios, A., Dominguez, C., Martin, J.A., Martin, L.M., Martinez-Grau, M.A., Montero, C., Pedregal, C., Catlow, J. *et al*. (2005) Dipeptides as effective prodrugs of the unnatural amino acid (+)-2-aminobicyclo[3.1.0]hexane-2,6-dicarboxylic acid (LY354740), a selective group II metabotropic glutamate receptor agonist. *Journal of Medicinal Chemistry*, **48** (16), 5305–5320.

86 Landowski, C.P., Song, X., Lorenzi, P.L., Hilfinger, J.M. and Amidon, G.L. (2005) Floxuridine amino acid ester prodrugs: enhancing Caco-2 permeability and resistance to glycosidic bond metabolism. *Pharmaceutical Research*, **22** (9), 1510–1518.

87 Li, F., Hong, L., Mau, C.I., Chan, R., Hendricks, T., Dvorak, C., Yee, C., Harris, J. and Alfredson, T. (2006) Transport of levovirin prodrugs in the human intestinal Caco-2 cell line. *Journal of Pharmaceutical Sciences*, **95** (6), 1318–1325.

88 Perkins, E.J. and Abraham, T. (2007) Pharmacokinetics, metabolism, and excretion of the intestinal peptide transporter 1 (SLC15A1)-targeted prodrug (1*S*,2*S*,5*R*,6*S*)-2-[(2′*S*)-(2-amino) propionyl]aminobicyclo[3.1.0.]hexen-2,6-di carboxylic acid (LY544344) in rats and dogs: assessment of first-pass bioactivation and dose linearity. *Drug Metabolism and Disposition: The Biological Fate of Chemicals*, **35** (10), 1903–1909.

89 Song, X., Lorenzi, P.L., Landowski, C.P., Vig, B.S., Hilfinger, J.M. and Amidon, G.L. (2005) Amino acid ester prodrugs of the anticancer agent gemcitabine: synthesis, bioconversion, metabolic bioevasion, and hPEPT1-mediated transport. *Molecular Pharmacology*, **2** (2), 157–167.

90 Anand, B.S., Patel, J. and Mitra, A.K. (2003) Interactions of the dipeptide ester prodrugs of acyclovir with the intestinal oligopeptide transporter: competitive inhibition of glycylsarcosine transport in human intestinal cell line-Caco-2. *The Journal of Pharmacology and Experimental Therapeutics*, **304** (2), 781–791.

91 Jain, R., Duvvuri, S., Kansara, V., Mandava, N.K. and Mitra, A.K. (2007) Intestinal absorption of novel-dipeptide prodrugs of saquinavir in rats. *International Journal of Pharmaceutics*, **336** (2), 233–240.

92 Thorn, K., Andersen, R., Christensen, J., Jakobsen, P., Nielsen, C.U., Steffansen, B. and Begtrup, M. (2007) Design, synthesis, and evaluation of tripeptidic promoieties targeting the intestinal peptide transporter hPEPT1. *ChemMedChem*, **2** (4), 479–487.

93 Chang, C. and Swaan, P.W. (2006) Computational approaches to modeling drug transporters. *European Journal of Pharmaceutical Sciences*, **27** (5), 411–424.

94 Ekins, S., Johnston, J.S., Bahadduri, P., D'Souza, V.M., Ray, A., Chang, C. and Swaan, P.W. (2005) *In vitro* and pharmacophore-based discovery of novel hPEPT1 inhibitors. *Pharmaceutical Research*, **22** (4), 512–517.

95 Ikumi, Y., Kida, T., Sakuma, S., Yamashita, S. and Akashi, M. (2008) Polymer–phloridzin conjugates as an anti-diabetic drug that inhibits glucose absorption through the Na^+/glucose cotransporter (SGLT1) in the small intestine. *Journal of Controlled Release*, **125** (1), 42–49.

96 Nozawa, T., Toyobuku, H., Kobayashi, D., Kuruma, K., Tsuji, A. and Tamai, I. (2003) Enhanced intestinal absorption of drugs by activation of peptide transporter PEPT1 using proton-releasing polymer. *Journal of Pharmaceutical Sciences*, **92** (11), 2208–2216.

97 Chen, M.L. (2008) Lipid excipients and delivery systems for pharmaceutical development: a regulatory perspective. *Advanced Drug Delivery Reviews*, **60** (6), 768–777.

98 Constantinides, P.P. and Wasan, K.M. (2007) Lipid formulation strategies for enhancing intestinal transport and absorption of P-glycoprotein (P-gp) substrate drugs: *in vitro*/*in vivo* case studies. *Journal of Pharmaceutical Sciences*, **96** (2), 235–248.

99 Tamura, K., Bhatnagar, P.K., Takata, J.S., Lee, C.P., Smith, P.L. and Borchardt, R.T. (1996) Metabolism, uptake, and transepithelial transport of the diastereomers of Val-Val in the human intestinal cell line, Caco-2. *Pharmaceutical Research*, **13** (8), 1213–1218.

100 Tamura, K., Lee, C.P., Smith, P.L. and Borchardt, R.T. (1996) Metabolism, uptake, and transepithelial transport of the stereoisomers of Val-Val-Val in the human intestinal cell line, Caco-2. *Pharmaceutical Research*, **13** (11), 1663–1667.

101 Wenzel, U., Thwaites, D.T. and Daniel, H. (1995) Stereoselective uptake of beta-lactam antibiotics by the intestinal peptide transporter. *British Journal of Pharmacology*, **116** (7), 3021–3027.

102 Nielsen, C.U., Andersen, R., Brodin, B., Frokjaer, S., Taub, M.E. and Steffansen, B. (2001) Dipeptide model prodrugs for the intestinal oligopeptide transporter. Affinity for and transport via hPepT1 in the human intestinal Caco-2 cell line. *Journal of Controlled Release*, **76** (1–2), 129–138.

103 Taub, M.E., Larsen, B.D., Steffansen, B. and Frokjaer, S. (1997) Beta-carboxylic acid esterified D-Asp-Ala retains a high affinity for the oligopeptide transporter in Caco-2 monolayers. *International Journal of Pharmaceutics*, **146**, 205–212.

104 Taub, M.E., Moss, B.A., Steffansen, B. and Frokjaer, S. (1998) Oligopeptide transporter mediated uptake and transport of D-Asp(OBzl)-Ala, D-Glu (OBzl)-Ala, and D-Ser(Bzl)-Ala in filter-grown Caco-2 monolayers. *International Journal of Pharmaceutics*, **174**, 223–232.

105 Mathews, D.M. and Adibi, S.A. (1976) Peptide absorption. *Gastroenterology*, **71** (1), 151–161.

106 Doring, F., Walter, J., Will, J., Focking, M., Boll, M., Amasheh, S., Clauss, W. and Daniel, H. (1998) Delta-aminolevulinic acid transport by intestinal and renal peptide transporters and its physiological and clinical implications. *The Journal of Clinical Investigation*, **101** (12), 2761–2767.

107 Doring, F., Will, J., Amasheh, S., Clauss, W., Ahlbrecht, H. and Daniel, H. (1998) Minimal molecular determinants of substrates for recognition by the intestinal peptide transporter. *The Journal of Biological Chemistry*, **273** (36), 23211–23218.

108 Temple, C.S., Stewart, A.K., Meredith, D., Lister, N.A., Morgan, K.M., Collier, I.D., Vaughan-Jones, R.D., Boyd, C.A., Bailey, P.D. and Bronk, J.R. (1998) Peptide mimics as substrates for the intestinal peptide transporter. *The Journal of Biological Chemistry*, **273** (1), 20–22.

109 Vabeno, J., Lejon, T., Nielsen, C.U., Steffansen, B., Chen, W., Ouyang, H., Borchardt, R.T. and Luthman, K. (2004) Phe-Gly dipeptidomimetics designed for the di-/tripeptide transporters PEPT1 and PEPT2: synthesis and biological investigations. *Journal of Medicinal Chemistry*, **47** (4), 1060–1069.

110 Vabeno, J., Nielsen, C.U., Ingebrigtsen, T., Lejon, T., Steffansen, B. and Luthman, K. (2004) Dipeptidomimetic ketomethylene isosteres as pro-moieties for drug transport via the human intestinal di-/tripeptide transporter hPEPT1: design, synthesis, stability, and biological investigations. *Journal of Medicinal Chemistry*, **47** (19), 4755–4765.

111 Brandsch, M., Thunecke, F., Kullertz, G., Schutkowski, M., Fischer, G. and Neubert, K. (1998) Evidence for the absolute conformational specificity of the

intestinal H + /peptide symporter, PEPT1. *The Journal of Biological Chemistry*, **273** (7), 3861–3864.

112 Brandsch, M., Knutter, I., Thunecke, F., Hartrodt, B., Born, I., Borner, V., Hirche, F., Fischer, G. and Neubert, K. (1999) Decisive structural determinants for the interaction of proline derivatives with the intestinal H + /peptide symporter. *European Journal of Biochemistry*, **266** (2), 502–508.

113 Addison, J.M., Burston, D. and Matthews, D.M. (1972) Evidence for active transport of the dipeptide glycylsarcosine by hamster jejunum *in vitro*. *Clinical Science*, **43** (6), 907–911.

114 Andersen, R., Nielsen, C.U., Begtrup, M., Jorgensen, F.S., Brodin, B., Frokjaer, S. and Steffansen, B. (2006) *In vitro* evaluation of *N*-methyl amide tripeptidomimetics as substrates for the human intestinal di-/tri-peptide transporter hPEPT1. *European Journal of Pharmaceutical Sciences*, **28** (4), 325–335.

115 Nielsen, C.U., Supuran, C.T., Scozzafava, A., Frokjaer, S., Steffansen, B. and Brodin, B. (2002) Transport characteristics of L-carnosine and the anticancer derivative 4-toluenesulfonylureido-carnosine in a human epithelial cell line. *Pharmaceutical Research*, **19** (9), 1337–1344.

116 Borner, V., Fei, Y.J., Hartrodt, B., Ganapathy, V., Leibach, F.H., Neubert, K. and Brandsch, M. (1998) Transport of amino acid aryl amides by the intestinal H + /peptide cotransport system, PEPT1. *European Journal of Biochemistry*, **255** (3), 698–702.

117 Cheng, Y. and Prusoff, W.H. (1973) Relationship between the inhibition constant (K1) and the concentration of inhibitor which causes 50 per cent inhibition (I_{50}) of an enzymatic reaction. *Biochemical Pharmacology*, **22** (23), 3099–3108.

118 Merlin, D., Steel, A., Gewirtz, A.T., Si-Tahar, M., Hediger, M.A. and Madara, J.L. (1998) hPepT1-mediated epithelial transport of bacteria-derived chemotactic peptides enhances neutrophil–epithelial interactions. *The Journal of Clinical Investigation*, **102** (11), 2011–2018.

119 Ganapathy, M.E., Prasad, P.D., Mackenzie, B., Ganapathy, V. and Leibach, F.H. (1997) Interaction of anionic cephalosporins with the intestinal and renal peptide transporters PEPT 1 and PEPT 2. *Biochimica et Biophysica Acta*, **1324** (2), 296–308.

120 Doring, F., Theis, S. and Daniel, H. (1997) Expression and functional characterization of the mammalian intestinal peptide transporter PepT1 in the methylotropic yeast *Pichia pastoris*. *Biochemical and Biophysical Research Communications*, **232** (3), 656–662.

121 Amasheh, S., Wenzel, U., Boll, M., Dorn, D., Weber, W., Clauss, W. and Daniel, H. (1997) Transport of charged dipeptides by the intestinal H + /peptide symporter PepT1 expressed in Xenopus laevis oocytes. *The Journal of Membrane Biology*, **155** (3), 247–256.

122 Knutter, I., Hartrodt, B., Theis, S., Foltz, M., Rastetter, M., Daniel, H., Neubert, K. and Brandsch, M. (2004) Analysis of the transport properties of side chain modified dipeptides at the mammalian peptide transporter PEPT1. *European Journal of Pharmaceutical Sciences*, **21** (1), 61–67.

123 Kottra, G. and Daniel, H. (2001) Bidirectional electrogenic transport of peptides by the proton-coupled carrier PEPT1 in Xenopus laevis oocytes: its asymmetry and symmetry. *The Journal of Physiology*, **536** (Pt 2), 495–503.

124 Faria, T.N., Timoszyk, J.K., Stouch, T.R., Vig, B.S., Landowski, C.P., Amidon, G.L., Weaver, C.D., Wall, D.A. and Smith, R.L. (2004) A novel high-throughput pepT1 transporter assay differentiates between substrates and antagonists. *Molecular Pharmacology*, **1** (1), 67–76.

125 Herrera-Ruiz, D., Faria, T.N., Bhardwaj, R.K., Timoszyk, J., Gudmundsson, O.S., Moench, P., Wall, D.A., Smith, R.L. and Knipp, G.T. (2004) A novel hPepT1 stably

transfected cell line: establishing a correlation between expression and function. *Molecular Pharmacology*, **1** (2), 136–144.

126 Vig, B.S., Stouch, T.R., Timoszyk, J.K., Quan, Y., Wall, D.A., Smith, R.L. and Faria, T.N. (2006) Human PEPT1 pharmacophore distinguishes between dipeptide transport and binding. *Journal of Medicinal Chemistry*, **49** (12), 3636–3644.

127 Balimane, P.V., Chong, S., Patel, K., Quan, Y., Timoszyk, J., Han, Y.H., Wang, B., Vig, B. and Faria, T.N. (2007) Peptide transporter substrate identification during permeability screening in drug discovery: comparison of transfected MDCK-hPepT1 cells to Caco-2 cells. *Archives of Pharmacal Research*, **30** (4), 507–518.

128 Smith, P.L. (1996) Methods for evaluating intestinal permeability and metabolism *in vitro*. *Pharmceutical Biotechnology*, **8**, 13–34.

129 Larsen, S.B., Jorgensen, F.S. and Olsen, L. (2008) QSAR models for the human H (+)/peptide symporter, hPEPT1: affinity prediction using alignment-independent descriptors. *Journal of Chemical Information and Modeling*, **48** (1), 233–241.

130 Swaan, P.W., Stehouwer, M.C. and Tukker, J.J. (1995) Molecular mechanism for the relative binding affinity to the intestinal peptide carrier. Comparison of three ACE-inhibitors: enalapril, enalaprilat, and lisinopril. *Biochimica et Biophysica Acta*, **1236** (1), 31–38.

131 Zhu, Z. and Buolamwini, J.K. (2008) Constrained NBMPR analogue synthesis, pharmacophore mapping and 3D-QSAR modeling of equilibrative nucleoside transporter 1 (ENT1) inhibitory activity. *Bioorganic and Medicinal Chemistry*, **16** (7), 3848–3865.

132 Kharkar, P.S., Reith, M.E. and Dutta, A.K. (2008) Three-dimensional quantitative structure–activity relationship (3D QSAR) and pharmacophore elucidation of tetrahydropyran derivatives as serotonin and norepinephrine transporter inhibitors. *Journal of Computer-Aided Molecular Design*, **22** (1), 1–17.

133 Chang, C., Swaan, P.W., Ngo, L.Y., Lom, P.Y., Patil, S.D., Unadkat, J.D. (2004) Molecular requirements of the nucleotide transporters hCNT1, hCNT2, and hENT1. *Molecular Pharmacology*, **65**, 558–570.

134 Ekins, S., Ecker, G.F., Chiba, P. and Swaan, P.W. (2007) Future directions for drug transporter modelling. *Xenobiotica; The Fate of Foreign Compounds in Biological Systems*, **37** (10–11), 1152–1170.

135 Petrovic, V., Teng, S. and Piquette-Miller, M. (2007) Regulation of drug transporters during infection and inflammation. *Molecular Interventions*, **7** (2), 99–111.

136 Edinger, A.L. (2007) Controlling cell growth and survival through regulated nutrient, transporter expression. *The Biochemical Journal*, **406** (1), 1–12.

137 Surh, Y.J. (2003) Cancer chemoprevention with dietary phytochemicals. *Nature Reviews. Cancer*, **3** (10), 768–780.

138 Hanahan, D. and Weinberg, R.A. (2000) The hallmarks of cancer. *Cell*, **100** (1), 57–70.

139 Coussens, L.M. and Werb, Z. (2002) Inflammation and cancer. *Nature*, **420** (6917), 860–867.

140 Thiery, J.P. and Sleeman, J.P. (2006) Complex networks orchestrate epithelial–mesenchymal transitions. *Nature Reviews. Molecular Cell Biology*, **7** (2), 131–142.

141 Bhowmick, N.A. and Moses, H.L. (2005) Tumor–stroma interactions. *Current Opinion in Genetics & Development*, **15** (1), 97–101.

142 Bhowmick, N.A., Neilson, E.G. and Moses, H.L. (2004) Stromal fibroblasts in cancer initiation and progression. *Nature*, **432** (7015), 332–337.

143 De Wever, O. and Mareel, M. (2003) Role of tissue stroma in cancer cell invasion. *The Journal of Pathology*, **200** (4), 429–447.

144 Liotta, L.A. and Kohn, E.C. (2001) The microenvironment of the tumour–host interface. *Nature*, **411** (6835), 375–379.

145 Tlsty, T.D. and Hein, P.W. (2001) Know thy neighbor: stromal cells can contribute oncogenic signals. *Current Opinion in Genetics & Development*, **11** (1), 54–59.

146 Elenbaas, B. and Weinberg, R.A. (2001) Heterotypic signaling between epithelial tumor cells and fibroblasts in carcinoma formation. *Experimental Cell Research*, **264** (1), 169–184.

147 Sugiyama, Y., Farrow, B., Murillo, C., Li, J., Watanabe, H., Sugiyama, K. and Evers, B.M. (2005) Analysis of differential gene expression patterns in colon cancer and cancer stroma using microdissected tissues. *Gastroenterology*, **128** (2), 480–486.

148 Mueller, M.M. and Fusenig, N.E. (2004) Friends or foes – bipolar effects of the tumour stroma in cancer. *Nature Reviews. Cancer*, **4** (11), 839–849.

149 Micke, P. and Ostman, A. (2004) Tumour–stroma interaction: cancer-associated fibroblasts as novel, targets in anti-cancer therapy? *Lung Cancer* **45 (**Suppl. 2), S163–S175.

150 Fodde, R., Smits, R. and Clevers, H. (2001) APC, signal transduction and genetic instability in colorectal cancer. *Nature Reviews. Cancer*, **1** (1), 55–67.

151 Berlau, J., Glei, M. and Pool-Zobel, B.L. (2004) Colon cancer risk factors from nutrition. *Analytical and Bioanalytical Chemistry*, **378** (3), 737–743.

152 Potter, J.D. (1999) Colorectal cancer: molecules and populations. *Journal of the National Cancer Institute*, **91** (11), 916–932.

153 Gottesman, M.M., Fojo, T. and Bates, S.E. (2002) Multidrug resistance in cancer: role of ATP-dependent transporters. *Nature Reviews. Cancer*, **2** (1), 48–58.

154 Ohtsuki, S., Kamoi, M., Watanabe, Y., Suzuki, H., Hori, S. and Terasaki, T. (2007) Correlation of induction of ATP binding cassette transporter A5 (ABCA5) and ABCB1 mRNAs with differentiation state of human colon tumor. *Biological & Pharmaceutical Bulletin*, **30** (6), 1144–1146.

155 Ishida, S., Lee, J., Thiele, D.J. and Herskowitz, I. (2002) Uptake of the anticancer drug cisplatin mediated by the copper, transporter Ctr1 in yeast and mammals. *Proceedings of the National Academy of Sciences of the United States of America*, **99** (22), 14298–14302.

156 Matherly, L.H., Hou, Z. and Deng, Y. (2007) Human reduced folate carrier: translation of basic biology to cancer etiology and therapy. *Cancer Metastasis Reviews*, **26** (1), 111–128.

157 Zhang, J., Visser, F., King, K.M., Baldwin, S.A., Young, J.D. and Cass, C.E. (2007) The role of nucleoside transporters in cancer chemotherapy with nucleoside drugs. *Cancer Metastasis Reviews*, **26** (1), 85–110.

158 di Pietro, M., Sabates Bellver, J., Menigatti, M., Bannwart, F., Schnider, A., Russell, A., Truninger, K., Jiricny, J. and Marra, G. (2005) Defective DNA mismatch repair determines a characteristic transcriptional profile in proximal colon cancers. *Gastroenterology*, **129** (3), 1047–1059.

159 Huang, Y., Anderle, P., Bussey, K.J., Barbacioru, C., Shankavaram, U., Dai, Z., Reinhold, W.C., Papp, A., Weinstein, J.N. and Sadee, W. (2004) Membrane transporters and channels: role of the transportome in cancer chemosensitivity and chemoresistance. *Cancer Research*, **64** (12), 4294–4301.

160 Scherf, U., Ross, D.T., Waltham, M., Smith, L.H., Lee, J.K., Tanabe, L., Kohn, K.W., Reinhold, W.C., Myers, T.G., Andrews, D.T. *et al.* (2000) A gene expression database for the molecular pharmacology of cancer. *Nature Genetics*, **24** (3), 236–244.

161 Chapman, J.M., Knoepp, S.M., Byeon, M.K., Henderson, K.W. and Schweinfest, C.W. (2002) The colon anion transporter, down-regulated in adenoma, induces growth suppression that is abrogated by E1A. *Cancer Research*, **62** (17), 5083–5088.

162 Li, H., Myeroff, L., Smiraglia, D., Romero, M.F., Pretlow, T.P., Kasturi, L.,

Lutterbaugh, J., Rerko, R.M., Casey, G., Issa, J.P. *et al.* (2003) SLC5A8, a sodium transporter, is a tumor suppressor gene silenced by methylation in human colon aberrant crypt foci and cancers. *Proceedings of the National Academy of Sciences of the United States of America*, **100** (14), 8412–8417.

163 Schweinfest, C.W., Spyropoulos, D.D., Henderson, K.W., Kim, J.H., Chapman, J.M., Barone, S., Worrell, R.T., Wang, Z. and Soleimani, M. (2006) slc26a3 (dra)-deficient mice display chloride-losing diarrhea, enhanced colonic proliferation, and distinct up-regulation of ion transporters in the colon. *The Journal of Biological Chemistry*, **281** (49), 37962–37971.

164 Ueno, M., Toyota, M., Akino, K., Suzuki, H., Kusano, M., Satoh, A., Mita, H., Sasaki, Y., Nojima, M., Yanagihara, K. *et al.* (2004) Aberrant methylation and histone deacetylation associated with silencing of SLC5A8 in gastric cancer. *Tumour Biology: The Journal of the International Society for Oncodevelopmental Biology and Medicine*, **25** (3), 134–140.

165 Zschocke, J., Allritz, C., Engele, J. and Rein, T. (2007) DNA methylation dependent silencing of the human glutamate transporter EAAT2 gene in glial cells. *Glia*, **55** (7), 663–674.

166 Schweinfest, C.W., Henderson, K.W., Suster, S., Kondoh, N. and Papas, T.S. (1993) Identification of a colon mucosa gene that is down-regulated in colon, adenomas and adenocarcinomas. *Proceedings of the National Academy of Sciences of the United States of America*, **90** (9), 4166–4170.

167 Kiemer, A.K., Takeuchi, K. and Quinlan, M.P. (2001) Identification of genes involved in epithelial–mesenchymal transition and tumor progression. *Oncogene*, **20** (46), 6679–6688.

168 Yamashita, S., Miyagi, C., Fukada, T., Kagara, N., Che, Y.S. and Hirano, T. (2004) Zinc transporter LIVI controls epithelial–mesenchymal transition in zebrafish gastrula organizer. *Nature*, **429** (6989), 298–302.

169 Gallagher, S.M., Castorino, J.J., Wang, D. and Philp, N.J. (2007) Monocarboxylate transporter 4 regulates maturation and trafficking of CD147 to the plasma membrane in the metastatic breast cancer cell line MDA-MB-231. *Cancer Research*, **67** (9), 4182–4189.

170 Ho, E.A. and Piquette-Miller, M. (2006) Regulation of multidrug resistance by pro-inflammatory cytokines. *Current Cancer Drug Targets*, **6** (4), 295–311.

171 Shimakura, J., Terada, T., Shimada, Y., Katsura, T. and Inui, K. (2006) The transcription factor Cdx2 regulates the intestine-specific expression of human peptide transporter 1 through functional interaction with Sp1. *Biochemical Pharmacology*, **71** (11), 1581–1588.

172 Nduati, V., Yan, Y., Dalmasso, G., Driss, A., Sitaraman, S. and Merlin, D. (2007) Leptin transcriptionally enhances peptide transporter (hPepT1) expression and activity via the cAMP-response element-binding protein and Cdx2 transcription factors. *The Journal of Biological Chemistry*, **282** (2), 1359–1373.

173 Guo, R.J., Suh, E.R. and Lynch, J.P. (2004) The role of Cdx proteins in intestinal development and cancer. *Cancer Biology & Therapy*, **3** (7), 593–601.

174 Suh, E. and Traber, P.G. (1996) An intestine-specific homeobox gene regulates proliferation and differentiation. *Molecular and Cellular Biology*, **16** (2), 619–625.

175 Witek, M.E., Nielsen, K., Walters, R., Hyslop, T., Palazzo, J., Schulz, S. and Waldman, S.A. (2005) The putative tumor suppressor Cdx2 is overexpressed by human colorectal adenocarcinomas. *Clinical Cancer Research*, **11** (24 Pt 1), 8549–8556.

176 Gross, I., Duluc, I., Benameur, T., Calon, A., Martin, E., Brabletz, T., Kedinger, M., Domon-Dell, C. and Freund, J.N. (2008) The intestine-specific homeobox gene Cdx2 decreases mobility and antagonizes

dissemination of colon cancer cells. *Oncogene*, **27** (1), 107–115.

177 Ganapathy, M.E., Brandsch, M., Prasad, P.D., Ganapathy, V. and Leibach, F.H. (1995) Differential recognition of beta-lactam antibiotics by intestinal and renal peptide transporters, PEPT 1 and PEPT 2. *The Journal of Biological Chemistry*, **270** (43), 25672–25677.

178 Terada, T., Shimada, Y., Pan, X., Kishimoto, K., Sakurai, T., Doi, R., Onodera, H., Katsura, T., Imamura, M. and Inui, K. (2005) Expression profiles of various transporters for oligopeptides, amino acids and organic ions along the human digestive tract. *Biochemical Pharmacology*, **70** (12), 1756–1763.

179 Mutoh, H., Satoh, K., Kita, H., Sakamoto, H., Hayakawa, H., Yamamoto, H., Isoda, N., Tamada, K., Ido, K. and Sugano, K. (2005) Cdx2 specifies the differentiation of morphological as well as functional absorptive enterocytes of the small intestine. *The International Journal of Developmental Biology*, **49** (7), 867–871.

180 Grotzinger, C., Kneifel, J., Patschan, D., Schnoy, N., Anagnostopoulos, I., Faiss, S., Tauber, R., Wiedenmann, B. and Gessner, R. (2001) LI-cadherin: a marker of gastric metaplasia and neoplasia. *Gut*, **49** (1), 73–81.

181 Hinoi, T., Lucas, P.C., Kuick, R., Hanash, S., Cho, K.R. and Fearon, E.R. (2002) CDX2 regulates liver intestine-cadherin expression in normal and malignant colon epithelium and intestinal metaplasia. *Gastroenterology*, **123** (5), 1565–1577.

182 Kwak, J.M., Min, B.W., Lee, J.H., Choi, J.S., Lee, S.I., Park, S.S., Kim, J., Um, J.W., Kim, S.H. and Moon, H.Y. (2007) The prognostic significance of E-cadherin and liver intestine-cadherin expression in colorectal cancer. *Diseases of the Colon and Rectum*, **50** (11), 1873–1880.

183 Takamura, M., Ichida, T., Matsuda, Y., Kobayashi, M., Yamagiwa, S., Genda, T., Shioji, K., Hashimoto, S., Nomoto, M., Hatakeyama, K. *et al.* (2004) Reduced expression of liver–intestine cadherin is associated with progression and lymph node metastasis of human colorectal carcinoma. *Cancer Letters*, **212** (2), 253–259.

184 Ko, S., Chu, K.M., Luk, J.M., Wong, B.W., Yuen, S.T., Leung, S.Y. and Wong, J. (2004) Overexpression of LI-cadherin in gastric cancer is associated with lymph node metastasis. *Biochemical and Biophysical Research Communications*, **319** (2), 562–568.

185 Ko, S., Chu, K.M., Luk, J.M., Wong, B.W., Yuen, S.T., Leung, S.Y. and Wong, J. (2005) CDX2 co-localizes with liver–intestine cadherin in intestinal metaplasia and adenocarcinoma of the stomach. *The Journal of Pathology*, **205** (5), 615–622.

186 Dean, M., Fojo, T. and Bates, S. (2005) Tumour stem cells and drug resistance. *Nature Reviews. Cancer*, **5** (4), 275–284.

187 Zhou, S., Schuetz, J.D., Bunting, K.D., Colapietro, A.M., Sampath, J., Morris, J.J., Lagutina, I., Grosveld, G.C., Osawa, M., Nakauchi, H. *et al.* (2001) The ABC transporter Bcrp1/ABCG2 is expressed in a wide variety of stem cells and is a molecular determinant of the side-population phenotype. *Nature Medicine*, **7** (9), 1028–1034.

188 O'Brien, C.A., Pollett, A., Gallinger, S. and Dick, J.E. (2007) A human colon cancer cell capable of initiating tumour growth in immunodeficient mice. *Nature*, **445** (7123), 106–110.

189 Radeva, G., Buyse, M., Hindlet, P., Beaufils, B., Walker, F., Bado, A. and Farinotti, R. (2007) Regulation of the oligopeptide transporter, PEPT-1, in DSS-induced rat colitis. *Digestive Diseases and Sciences*, **52** (7), 1653–1661.

190 Monzani, E., Facchetti, F., Galmozzi, E., Corsini, E., Benetti, A., Cavazzin, C., Gritti, A., Piccinini, A., Porro, D., Santinami, M. *et al.* (2007) Melanoma contains CD133 and ABCG2 positive cells with enhanced tumourigenic potential.

European Journal of Cancer, **43** (5), 935–946.

191 Florek, M., Haase, M., Marzesco, A.M., Freund, D., Ehninger, G., Huttner, W.B. and Corbeil, D. (2005) Prominin-1/CD133, a neural and hematopoietic stem cell marker, is expressed in adult human differentiated cells and certain types of kidney cancer. *Cell and Tissue Research*, **319** (1), 15–26.

192 Frank, N.Y., Margaryan, A., Huang, Y., Schatton, T., Waaga-Gasser, A.M., Gasser, M., Sayegh, M.H., Sadee, W. and Frank, M.H. (2005) ABCB5-mediated doxorubicin transport and chemoresistance in human malignant melanoma. *Cancer Research*, **65** (10), 4320–4333.

193 Buyse, M., Tsocas, A., Walker, F., Merlin, D. and Bado, A. (2002) PepT1-mediated fMLP transport induces intestinal inflammation *in vivo*. *American Journal of Physiology – Cell Physiology*, **283** (6), C1795–C1800,

194 Merlin, D., Si-Tahar, M., Sitaraman, S.V., Eastburn, K., Williams, I., Liu, X., Hediger, M.A. and Madara, J.L. (2001) Colonic epithelial hPepT1 expression occurs in inflammatory bowel disease: transport of bacterial peptides influences expression of MHC class 1 molecules. *Gastroenterology*, **120** (7), 1666–1679.

195 Ziegler, T.R., Fernandez-Estivariz, C., Gu, L.H., Bazargan, N., Umeakunne, K., Wallace, T.M., Diaz, E.E., Rosado, K.E., Pascal, R.R., Galloway, J.R. *et al.* (2002) Distribution of the H + /peptide transporter PepT1 in human intestine: up-regulated expression in the colonic mucosa of patients with short-bowel syndrome. *The American Journal of Clinical Nutrition*, **75** (5), 922–930.

196 Sundaram, U., Wisel, S. and Coon, S. (2005) Mechanism of inhibition of proton: dipeptide co-transport during chronic enteritis in the mammalian small intestine. *Biochimica et Biophysica Acta*, **1714** (2), 134–140.

197 Shi, B., Song, D., Xue, H., Li, J. and Li, N. (2006) Abnormal expression of the peptide transporter PepT1 in the colon of massive bowel resection rat: a potential route for colonic mucosa damage by transport of fMLP. *Digestive Diseases and Sciences*, **51** (11), 2087–2093.

198 Shi, B., Song, D., Xue, H., Li, N. and Li, J. (2006) PepT1 mediates colon damage by transporting fMLP in rats with bowel resection. *The Journal of Surgical Research*, **136** (1), 38–44.

199 Shu, H.J., Takeda, H., Shinzawa, H., Takahashi, T. and Kawata, S. (2002) Effect of lipopolysaccharide on peptide transporter 1 expression in rat small intestine and its attenuation by dexamethasone. *Digestion*, **65** (1), 21–29.

200 Vavricka, S.R., Musch, M.W., Fujiya, M., Kles, K., Chang, L., Eloranta, J.J., Kullak-Ublick, G.A., Drabik, K., Merlin, D. and Chang, E.B. (2006) Tumor necrosis factor-alpha and interferon-gamma increase PepT1 expression and activity in the human colon carcinoma cell line Caco-2/bbe and in mouse intestine. *Pflugers Archiv: European Journal of Physiology*, **452** (1), 71–80.

201 Nielsen, C.U., Amstrup, J., Nielsen, R., Steffansen, B., Frokjaer, S. and Brodin, B. (2003) Epidermal growth factor and insulin short-term increase hPepT1-mediated glycylsarcosine uptake in Caco-2 cells. *Acta Physiologica Scandinavica*, **178** (2), 139–148.

202 Nielsen, C.U., Amstrup, J., Steffansen, B., Frokjaer, S. and Brodin, B. (2001) Epidermal growth factor inhibits glycylsarcosine transport and hPepT1 expression in a human intestinal cell line. *American Journal of Physiology – Gastrointestinal and Liver Physiology*, **281** (1), G191–G199.

203 Sitaraman, S., Liu, X., Charrier, L., Gu, L.H., Ziegler, T.R., Gewirtz, A. and Merlin, D. (2004) Colonic leptin: source of a novel proinflammatory cytokine involved in, IBD. *The FASEB Journal*, **18** (6), 696–698.

204 Dalmasso, G., Charrier-Hisamuddin, L., Thu Nguyen, H.T., Yan, Y., Sitaraman, S. and Merlin, D. (2008) PepT1-mediated tripeptide KPV uptake reduces intestinal inflammation. *Gastroenterology*, **134** (1), 166–178.

205 Landowski, C.P., Sun, D., Foster, D.R., Menon, S.S., Barnett, J.L., Welage, L.S., Ramachandran, C. and Amidon, G.L. (2003) Gene expression in the human intestine and correlation with oral valacyclovir pharmacokinetic parameters. *The Journal of Pharmacology and Experimental Therapeutics*, **306** (2), 778–786.

206 Shin, H.C., Landowski, C.P., Sun, D. and Amidon, G.L. (1999) Transporters in the GI Tract, vol. 18, WILEY-VCH Verlag GmbH, Weinheim.

207 Baldwin, S.A., Beal, P.R., Yao, S.Y., King, A.E., Cass, C.E. and Young, J.D. (2004) The equilibrative nucleoside transporter family, SLC29. *Pflugers Archiv: European Journal of Physiology*, **447** (5), 735–743.

208 Palacin, M. (1994) A new family of proteins (rBAT and 4F2hc) involved in cationic and zwitterionic amino acid transport: a tale of two proteins in search of a transport function. *The Journal of Experimental Biology*, **196**, 123–137.

209 Bisceglia, L., Purroy, J., Jimenez-Vidal, M., d'Adamo, A.P., Rousaud, F., Beccia, E., Penza, R., Rizzoni, G., Gallucci, M., Palacin, M. *et al.* (2001) Cystinuria type I: identification of eight new mutations in SLC3A1. *Kidney International*, **59** (4), 1250–1256.

210 Botzenhart, E., Vester, U., Schmidt, C., Hesse, A., Halber, M., Wagner, C., Lang, F., Hoyer, P., Zerres, K. and Eggermann, T. (2002) Cystinuria in children: distribution and frequencies of mutations in the SLC3A1 and SLC7A9 genes. *Kidney International*, **62** (4), 1136–1142.

211 Gasparini, P., Calonge, M.J., Bisceglia, L., Purroy, J., Dianzani, I., Notarangelo, A., Rousaud, F., Gallucci, M., Testar, X., Ponzone, A. *et al.* (1995) Molecular genetics of cystinuria: identification of four new mutations and seven polymorphisms, and evidence for genetic heterogeneity. *American Journal of Human Genetics*, **57** (4), 781–788.

212 Durand, E., Boutin, P., Meyre, D., Charles, M.A., Clement, K., Dina, C. and Froguel, P. (2004) Polymorphisms in the amino acid transporter solute carrier family 6 (neurotransmitter transporter) member 14 gene contribute to polygenic obesity in French Caucasians. *Diabetes*, **53** (9), 2483–2486.

213 Brauers, E., Schmidt, C., Zerres, K. and Eggermann, T. (2006) Functional characterization of SLC7A9 polymorphisms assumed to influence the cystinuria phenotype. *Clinical Nephrology*, **65** (4), 262–266.

214 Schmidt, C., Tomiuk, J., Botzenhart, E., Vester, U., Halber, M., Hesse, A., Wagner, C., Lahme, S., Lang, F., Zerres, K. *et al.* (2003) Genetic variations of the SLC7A9 gene: allele distribution of 13 polymorphic sites in German cystinuria patients and controls. *Clinical Nephrology*, **59** (5), 353–359.

215 Deng, X., Shibata, H., Takeuchi, N., Rachi, S., Sakai, M., Ninomiya, H., Iwata, N., Ozaki, N. and Fukumaki, Y. (2007) Association study of polymorphisms in the glutamate transporter genes SLC1A1, SLC1A3, and SLC1A6 with schizophrenia. *American Journal of Medical Genetics B. Neuropsychiatric Genetics*, **144** (3), 271–278.

216 Dickel, D.E., Veenstra-VanderWeele, J., Cox, N.J., Wu, X., Fischer, D.J., Van Etten-Lee, M., Himle, J.A., Leventhal, B.L., Cook, E.H., Jr. and Hanna, G.L. (2006) Association testing of the positional and functional candidate gene SLC1A1/EAAC1 in early-onset obsessive–compulsive disorder. *Archives of General Psychiatry*, **63** (7), 778–785.

217 Avissar, N.E., Ryan, C.K., Ganapathy, V. and Sax, H.C. (2001) Na(+)-dependent neutral amino acid transporter ATB(0) is a rabbit epithelial cell brush-border protein.

American Journal of Physiology – Cell Physiology, **281** (3), C963–C971.

218 Larriba, S., Sumoy, L., Ramos, M.D., Gimenez, J., Estivill, X., Casals, T. and Nunes, V. (2001) ATB(0)/SLC1A5 gene. Fine localisation and exclusion of association with the intestinal phenotype of cystic fibrosis. *European Journal of Human Genetics*, **9** (11), 860–866.

219 Martin, M.G., Turk, E., Lostao, M.P., Kerner, C. and Wright, E.M. (1996) Defects in Na + /glucose cotransporter (SGLT1) trafficking and function cause glucose–galactose malabsorption. *Nature Genetics*, **12** (2), 216–220.

220 Urban, T.J., Brown, C., Castro, R.A., Shah, N., Mercer, R., Huang, Y., Brett, C.M., Burchard, E.G. and Giacomini, K.M. (2008) Effects of genetic variation in the novel organic cation transporter, OCTN1, on the renal clearance of gabapentin. *Clinical Pharmacology and Therapeutics*, **83** (3), 416–421.

221 Urban, T.J., Yang, C., Lagpacan, L.L., Brown, C., Castro, R.A., Taylor, T.R., Huang, C.C., Stryke, D., Johns, S.J., Kawamoto, M. *et al.* (2007) Functional effects of protein sequence polymorphisms in the organic cation/ergothioneine transporter OCTN1 (SLC22A4). *Pharmacogenetics and Genomics*, **17** (9), 773–782.

222 Wang, Y., Ye, J., Ganapathy, V. and Longo, N. (1999) Mutations in the organic cation/carnitine transporter OCTN2 in, primary carnitine deficiency. *Proceedings of the National Academy of Sciences of the United States of America*, **96** (5), 2356–2360.

223 Kivisto, K.T. and Niemi, M. (2007) Influence of drug transporter polymorphisms on pravastatin pharmacokinetics in humans. *Pharmaceutical Research*, **24** (2), 239–247.

224 Nguyen, T.T., Dyer, D.L., Dunning, D.D., Rubin, S.A., Grant, K.E. and Said, H.M. (1997) Human intestinal folate transport: cloning, expression, and distribution of complementary RNA. *Gastroenterology*, **112** (3), 783–791.

225 Lu, Y., Kham, S.K., Foo, T.C., Hany, A., Quah, T.C. and Yeoh, A.E. (2007) Genotyping of eight polymorphic genes encoding drug-metabolizing enzymes and transporters using a customized oligonucleotide array. *Analytical Biochemistry*, **360** (1), 105–113.

226 Wang, W., Xue, S., Ingles, S.A., Chen, Q., Diep, A.T., Frankl, H.D., Stolz, A. and Haile, R.W. (2001) An association between genetic polymorphisms in the ileal sodium-dependent bile acid transporter gene and the risk of colorectal adenomas. *Cancer Epidemiology, Biomarkers & Prevention*, **10** (9), 931–936.

11
Hepatic Transport

Kazuya Maeda, Hiroshi Suzuki, and Yuichi Sugiyama

Abbreviations

4-MU	4-Methylumberiferone
ABC	ATP binding cassette
BCRP	Breast cancer resistance protein
BSEP	Bile salt export pump
BSP	Bromosulfophthalein
CCK-8	Cholecystokinin octapeptide
CMV	Canalicular membrane vesicle
DHEAS	Dehydroepiandrosterone sulfate
DNP-SG	2,4-Dinitrophenyl-*S*-glucuronide
$E_2$17βG	Estradiol-17β-glutathione
EHBR	Eisai hyperbilirubinemic rat
E-sul	Estrone-3-sulfate
M3G	Morphine-3-glucuronide
MATE	Multidrug and toxic compound extrusion
MDR	Multidrug resistance
MPP^+	1-Methyl-4-phenylpyridinium
MRP	Multidrug resistance-associated protein
NTCP	Na^+-taurocholate cotransporting polypeptide
OAT	Organic anion transporter
OATP	Organic anion transporting polypeptide
OCT	Organic cation transporter
OST	Organic solute transporter
PFIC	Primary familial intrahepatic cholestasis
PG	Prostaglandin
P-gp	P-glycoprotein
SLC	Solute carrier
SNP	Single nucleotide polymorphism
TBuMA	Tributylmethylammonium
TEA	Tetraethylammonium

11.1 Introduction

The liver plays an important role in determining the oral bioavailability of drugs. Drug molecules absorbed into the portal vein are taken up by hepatocytes and then metabolized and/or excreted into the bile in an unchanged form. For hydrophilic drugs, several transporters located on the sinusoidal membrane are responsible for the hepatic uptake [1–3]. Biliary excretion of drugs is also mediated by the primary active transporters, referred to as ATP-binding cassette (ABC) transporters, located on the bile canalicular membrane [3, 4]. Very recently, the importance of sinusoidal efflux mediated by MRP family transporters in the hepatic transport of substrates has also emerged [3, 5, 6]. The functional changes in these uptake and efflux transporters caused by genetic polymorphisms and drug–drug interactions sometimes greatly affect the hepatic availability and clearance of drugs. Now, several *in vitro* experimental systems and methodologies for predicting the *in vivo* hepatic clearance and the contribution of each transporter to the overall hepatic clearance have been developed. In this chapter, we will review the molecular mechanisms of hepatobiliary transport of clinically used drugs and also focus on the quantitative prediction of *in vivo* drug disposition from *in vitro* data.

Please note that the nomenclature of drug transporters (ABC and SLC (solute carrier) family) has recently been established by the HUGO Gene Nomenclature Committee (http://www.gene.ucl.ac.uk/nomenclature/). ABC family transporters are classified into 7 groups (ABCA–ABCG) and each group consists of several isoforms, whereas SLC family transporters are classified into 47 groups (SLC1–SLC47). Exceptionally, the gene symbol of OATP (organic anion transporting polypeptide) family transporters is *SLCO* (previously named as *SLC21*). This grouping is based on the gene homology. Until then, the researchers who first succeeded in the molecular cloning of novel transporters usually put a name to the cloned transporter as they liked, so it is often observed that one transporter has several names. For example, OATP1B1 is also called as OATP-C, OATP2, LST-1, and SLC21A6. We briefly mention the aliases of each transporter frequently used previously in each section. The name of genes is italicized (e.g., *MDR1*), whereas the name of proteins is designated without italicizing (e.g., MDR1). Moreover, all letters of the transporter name in humans are capitalized (e.g., OAT1), whereas only the first letter of the transporter name in rodents is capitalized and the subsequent letters are written by lowercase (e.g., Oat1).

11.2 Hepatic Uptake

Many compounds are efficiently taken up into hepatocytes in a Na^+-dependent and -independent manner, and the effect of various inhibitors on the uptake of substrates is different depending on substrates. Now, so many transporters have been identified in the basolateral membrane of hepatocytes such as NTCP (Na^+-taurocholate cotransporting polypeptide), OATPs, and OATs (organic anion transporters)

for organic anion transport and OCTs (organic cation transporters) for organic cation transport. Major uptake transporters in basolateral membrane are listed in Table 11.1.

11.2.1 NTCP (*SLC10A1*)

NTCP is expressed exclusively in the basolateral membrane of the liver and responsible for the hepatic uptake of several kinds of bile acids in a Na^+-dependent fashion [7, 8]. NTCP generally accepts several kinds of unconjugated and conjugated bile acids including clinically used bile acids for the treatment of cholestatic disorders such as chenodeoxycholate, ursodeoxycholate, and its conjugates with glycine and taurine [9–11]. Regarding the bile acid transport, Mita *et al*. [12] have demonstrated that NTCP-mediated uptake clearances of 10 different bile acids were well correlated between human NTCP and rat Ntcp and their clearances increased in the rank order of taurine-conjugated bile acids > glycine-conjugated bile acids > unconjugated bile acids, suggesting no species differences in the properties of bile acid recognition by NTCP between rats and humans. NTCP can also transport non-bile acid compounds such as dehydroepiandrosterone sulfate (DHEAS), bromosulfophthalein (BSP), and estrone-3-sulfate (E-sul) [13]. Rat Ntcp can also accept thyroid hormones and α-amanitin (mushroom toxin) [14, 15]. Interestingly, Ho *et al*. [16] have shown that rosuvastatin is also a substrate of human NTCP, but not rat Ntcp, and that NTCP accounted for approximately 35% of the rosuvastatin uptake in human hepatocytes judging from the difference in the uptake clearance in the presence and absence of Na^+ ion. These evidences reminded us of the possible contribution of NTCP to the hepatic uptake of non-bile acid types of drugs. In general, Na^+-dependent uptake of anions is considered to be mainly mediated by NTCP; however, the presence of unidentified Na^+-dependent transporters for anionic drugs (e.g., bumetanide) has also been suggested [17].

11.2.2 OATP (*SLCO*) Family Transporters

Although several bile acids are mainly transported into hepatocytes by NTCP in a Na^+-dependent manner, many organic anions are also taken up in a Na^+-independent manner. OATP family transporters are one of the key players for the Na^+-independent hepatic uptake of anions [18–20]. The number of cloned isoforms belonging to OATP family is currently 11, 13, and 12 in humans, rats, and mice, respectively. It should be noted that OATP subtypes in humans do not always genetically correspond to those in rodents. In rats, Oatp1a1 (Oatp1) [21], Oatp1a4 (Oatp2) [22], and Oatp1b2 (Oatp4) [23] are largely responsible for the hepatic uptake, whereas in humans, OATP1B1 (OATP-C/OATP2/LST-1) [24–26] and OATP1B3 (OATP8/LST-2) [27, 28] may be the most important hepatic uptake transporters. Different from other OATP transporters, OATP1B1 and OATP1B3 are exclusively expressed in the liver and can accept a wide variety of organic anions including clinically important drugs such as HMG-CoA

Table 11.1 Major uptake transporters expressed in the basolateral membrane of human liver.

Transporter	Gene symbol	Chromosome	Reference accession (mRNA)	Amino acids	Transmembrane domains	Tissue distribution	Cellular localization	Substrates
OATP1B1	*SLCO1B1*	12p12	NM_006446	691	12	Liver	Basal	Glutathione conjugates (LTC_4), glucuronide conjugates ($E_2$17βG, bilirubin glucuronide), sulfate conjugates (E-sul, DHEAS), bile acids (taurocholate, glycocholate), bilirubin, and several drugs (pravastatin, valsartan, and temocaprilat)
OATP1B3	*SLCO1B3*	12p12	NM_019844	702	12	Liver	Basal	Glutathione conjugates (LTC_4), glucuronide conjugates ($E_2$17βG, bilirubin glucuronide), sulfate conjugates (DHEAS), bile acids (taurocholate, glycocholate), and several drugs (CCK-8, telmisartan, fexofenadine, and digoxin)
OATP2B1	*SLCO2B1*	11q13	NM_007256	709	12	Liver, intestine, and so on	Basal (liver), apical (intestine)	E-sul, DHEAS, pravastatin, rosuvastatin, glybenclamide, benzylpenicillin, and so on
NTCP	*SLC10A1*	14q24	NM_003049	348	7	Liver	Basal	Bile acids, DHEAS, BSP, and E-sul
OAT2	*SLC22A7*	6p21	NM_006672, NM_153320	546/548	12	Liver	Basal	α-Ketoglutarate, salicylate, methotrexate, zidovudine, 5-fluorouracil, and so on
OCT1	*SLC22A1*	6q26	NM_003057, NM_153187	554/506	12	Liver, kidney	Basal	TEA, TBuMA, MPP^+, acyclovir, ganciclovir, famotidine, metformin, and so on

reductase inhibitors (statins) and several kinds of anticancer drugs. The list of reported substrates for OATP1B1 and OATP1B3 are shown in Table 11.2. Because of their high homologies (80% in amino acids), their substrate specificities overlap each other, but some compounds are specifically recognized by specific transporter. For example, digoxin and cholecystokinin octapeptide (CCK-8) can be transported specifically by OATP1B3 but not by OATP1B1 [29, 30]. In another example, though valsartan, olmesartan, and telmisartan are in the same category of drugs, angiotensin II receptor antagonists, valsartan and olmesartan can be transported by both OATP1B1 and OATP1B3, whereas telmisartan is specifically recognized by OATP1B3 as a substrate [31–34]. Thus, the substrate specificities of OATP1B1 and OATP1B3 are very broad and similar, but sometimes strictly distinct from each other. For the endogenous compounds, OATP1B1 plays a predominant role in Na^+-independent hepatic uptake of several bile acids and steroid conjugates. OATP1B1 can accept bilirubin and its glucuronides as a substrate and support the hepatobiliary transport of bilirubin in combination with MRP2 [35, 36], although a contradictory result has also been published [37].

Other OATP family transporters such as OATP1A2 (OATP-A), OATP2B1 (OATP-B), OATP3A1 (OATP-D), and OATP4A1 (OATP-E) have been reported to be expressed in the liver [20]. OATP1A2 accepts a wide variety of compounds including some type II cations (bulky hydrophobic compounds) such as *N*-(4,4-azo-*n*-pentyl)-21-deoxyajmalinium, rocuronium, and *N*-methylquinine [29, 38]. However, because OATP1A2 is mainly expressed in the brain and its hepatic expression is minimal, it is still unknown whether OATP1A2 is involved in the hepatic uptake of type II cations. OATP2B1 is expressed in various tissues and its strongest expression is in the liver [29]. OATP2B1 can transport several kinds of drugs such as glibenclamide, pravastatin, atorvastatin, and pitavastatin, but its contribution to their hepatic uptake is minor or unknown because of the overlapped substrate specificities of OATP1B1 and OATP1B3 [39–42]. Other transporters are expressed ubiquitously and their substrates are almost limited to endogenous compounds (thyroid hormones, prostaglandins (PGs)), so they may not be involved in the hepatic transport of drugs [20, 43].

11.2.3
OAT (*SLC22*) Family Transporters

Though many OAT family proteins are expressed mainly in the kidney and are involved in the active renal secretion of anions, OAT2 (SLC22A7) is expressed predominantly in the basolateral membrane of the liver [44]. Human OAT2 can accept various structurally unrelated drugs (e.g., bumetanide, zidovudine, tetracycline, erythromycin, theophylline, 5-fluorouracil, methotrexate, ranitidine, paclitaxel, and allopurinol) as well as endogenous compounds (e.g., cAMP, α-ketoglutarate, L-ascorbate, prostaglandin E_2 (PGE_2), $PGF_{2\alpha}$, DHEAS, and E-sul) [45]. Though some compounds are also substrates of OATP transporters, the averaged molecular weight of substrates for OAT2 tends to be smaller than that of OATPs. The relative contribution of OAT2 to the overall *in vivo* hepatic uptake of substrates has not been

Table 11.2 Substrates of OATP1B1 and OATP1B3.

	OATP1B1	OATP1B3
Endogenous compounds		
E-sul (estrone-3-sulfate)	0.094&5.34[a]; 0.0675&7[a]; 12.5; 0.458 [35, 151, 251]	+ [29]
$E_2$17βG	3.7–8.2 [24, 252]	5.4 [27]
PGE_2	+ [26, 252]	NT [29]
TXB_2 (thromboxane B_2)	+ [26]	
LTC_4	+ [26, 29]	+ [27, 29]
LTE_4 (leukotriene E_4)	+ [26]	
Triiodothyronine	2.7 [26, 28]	6.4 [28]
Thyroxine	3 [25, 26]	+ [29]
Taurocholate	10–33.8 [25, 26, 35]	5.8 [28]
Glycocholate	+ [29]	+ [29]
Cholate	11.4 [35]	NT [35]
DHEAS	21.5 [29, 35]	>30 [29, 35]
Bilirubin	0.0076 [35, 36]	0.0391 [36]
Bilirubin glucuronide	0.10 (mono), 0.28 (bis) [35]	0.5 (mono), NT (bis) [35]
Tauroursodeoxycholate	7.47 [9]	15.9 [9]
Glycoursodeoxycholate	5.17 [9]	24.7 [9]
Taurolithocholate sulfate	+ [177]	
Exogenous compounds		
DPDPE ([D-penicillamine (2,5)]-enkephalin)	+ [29]	+ [29]
BQ-123 (endothelin antagonist)	+ [29]	+ [29]
Pravastatin	13.7–85.7 [25, 163, 188]	
Cerivastatin	+ [188, 209]	
Fluvastatin	1.4–3.5 [181, 253]	7 [253]
Atorvastatin	12.4 [188]	
Rosuvastatin	4–8.5 [16]	9.8 [16]
Pitavastatin	3 [151]	3.25 [151]
Caspofungin	+ [254]	NT [254]
Demethylphalloin	17 [255]	7.5 [255]
Troglitazone sulfate	+ [256]	NT [256]
Rifampicin	1.5–13 [206, 257]	2.3 [206]
Arsenic	+ [258]	
Atrasentan	+ [259]	+ [259]
Bosentan	44 [219]	141 [219]
Ro 48-5033 (metabolite of bosentan)	60 [219]	166 [219]
Valsartan	1.39 [31]	18.2 [31]
Olmesartan	12.8–42.6 [33, 34]	44.2–71.8 [33, 34]
Enalapril	262 [260]	+ [260]
Methotrexate	+ [28]	24.7 [28]
Temocapril	+ [190]	
Temocaprilat	+ [190]	
DADLE ([D-Ala2, D-Leu5]-enkephalin)	+ [261]	
Microcystin-LR	7 [262]	9 [262]

Table 11.2 (*Continued*)

	OATP1B1	OATP1B3
SN-38 (active metabolite of irinotecan)	+ [263]	NT [263]
Fexofenadine	+ [92]	108 [92, 161]
Bromosulfophthalein	0.14–0.3 [29, 35]	0.4–3.3 [27, 29]
Deltorphin II	NT [29]	+ [29]
Ouabain	NT [29]	+ [29]
Digoxin	NT [29]	+ [29]
Fluo-3		+ [176]
Docetaxel	NT [264]	+ [264]
Paclitaxel	NT [264]	6.79 [264]
CCK-8 (cholecystokinin octapeptide)	NT [30]	11.1 [30]
Telmisartan	NT [32]	21.7 (1% HSA)[b] [32]
Telmisartan glucuronide	NT [179]	118 (1% HSA)[b] [179]
Benzylpenicillin	+ [252]	
Bamet-R2 (*cis*-diammine-chloro-cholylglycinate-platinum (II))	10 [265]	
Bamet-UD2 (*cis*-diammine-bisursodeoxycholate-platinum (II))	9.7 [265]	
TR-14035 (α4β1/α4 β7 integrin dual antagonist)	7.5 [266]	5.3 [266]
CDCA-NBD (7-nitrobenz-2-oxa-1,3-diazole chenodeoxycholate)	17 [267]	10 [267]
CA-NBD (7-nitrobenz-2-oxa-1,3-diazole cholate)	+ [267]	+ [267]
DCA-NBD (7-nitrobenz-2-oxa-1,3-diazole deoxycholate)	+ [267]	+ [267]
LCA-NBD (7-nitrobenz-2-oxa-1,3-diazole lithocholate)	+ [267]	+ [267]
UDCA-NBD (7-nitrobenz-2-oxa-1,3-diazole ursodeoxycholate)	+ [267]	+ [267]

The value represents the K_m values (unit: μM). +: significant uptake was observed.
NT: significant uptake was not observed.

[a]The K_m values for the high- and low-affinity site.

[b]The K_m values determined in the presence of 1% human serum albumin (HSA).

explained yet. OAT3 (SLC22A8) is detected in male rat liver [46] and transports organic anions such as ochratoxin A, E-sul, benzylpenicillin, DHEAS, and pravastatin [45]; however, its hepatic expression is minimal in mice and humans [47]. Indeed, the hepatic uptake of E-sul and *p*-aminohippurate was not different between wild-type and Oat3 knockout mice [48]. Recently, OAT5 (SLC22A10) and OAT7 (SLC22A9) have been reported to be exclusively expressed in the human liver [49, 50]. The substrate of human OAT5 has not been identified yet. OAT7 is located on the basolateral

membrane of human hepatocytes and accepts E-sul and DHEAS in a Na^+-independent manner [50]. Interestingly, OAT7-mediated transport of E-sul was transstimulated by short-chain (C3–C5) fatty acids, which implies that substrates of OAT7 are taken up in exchange for butyrate in hepatocytes [50]. However, the role of these novel OATs in the pharmacokinetics of drugs has not been demonstrated so far.

11.2.4
OCT (*SLC22*) Family Transporters

It has been shown that OCT1 (SLC22A1) and OCT3 (SLC22A3) are confirmed to express in the basolateral membrane of human hepatocytes [51, 52]. OCT1 is predominantly expressed in the liver [51], while OCT3 is expressed in several tissues such as kidney, heart, placenta, and brain [52]. OCT1 accepts type I cations, which consist of small hydrophilic compounds including tetraethylammonium (TEA), tributylmethylammonium (TBuMA), and procainamide, as well as anionic and uncharged compounds (e.g., prostaglandins) [52]. Rat Oct1 transports several endogenous compounds (choline, dopamine, serotonin, adrenaline, noradrenaline, and histamine) as well as exogenous compounds (cimetidine and 1-methyl-4-phenylpyridinium (MPP^+; neurotoxin)) [52]. Human OCT1 can transport not only endogenous and model compounds but also various marketed drugs such as antiviral drugs (acyclovir, ganciclovir), H_2-blockers (famotidine, ranitidine), and metformin [52]. The importance of OCT1 in the *in vivo* disposition of substrates has been explained by using Oct1 knockout mice [53]. By comparing the hepatic uptake of compounds between wild-type and Oct1 (−/−) mice, the uptake of TEA, metaiodobenzylguanidine (anticancer drug), and MPP^+ is mainly mediated by Oct1 [53]. However, the hepatic uptake of cimetidine and choline are not affected by knockdown of Oct1 gene [53], though they are also substrates of rat Oct1 [54]. Thus, it is possible that the uptake of cimetidine into isolated rat hepatocytes is mediated by unknown transporters other than Oct1 [55]. A series of biguanides, which are cationic and frequently used for the treatment of diabetes, is transported by Oct1 and the hepatic uptake of metformin has been drastically decreased in Oct1 (−/−) mice compared to wild-type mice (Figure 11.1) [56]. Moreover, the significant increase in serum lactic acid was observed in Oct1 (−/−) mice after administration of metformin, though its time profile of plasma concentration was similar (Figure 11.1) [57]. This suggests that metformin-induced lactic acidosis is dominated by its intrahepatic concentration and Oct1-mediated transport is a rate-limiting step in hepatic uptake of metformin. Human OCT3 also accepts several compounds such as cimetidine, dopamine, epinephrine, norepinephrine, and atropine [52], but its function in liver has not been explained yet.

11.3
Biliary Excretion

In the canalicular membrane, several ABC transporters such as MDR1 (multidrug resistance 1), MRP2 (multidrug resistance-associated protein 2), BSEP (bile salt

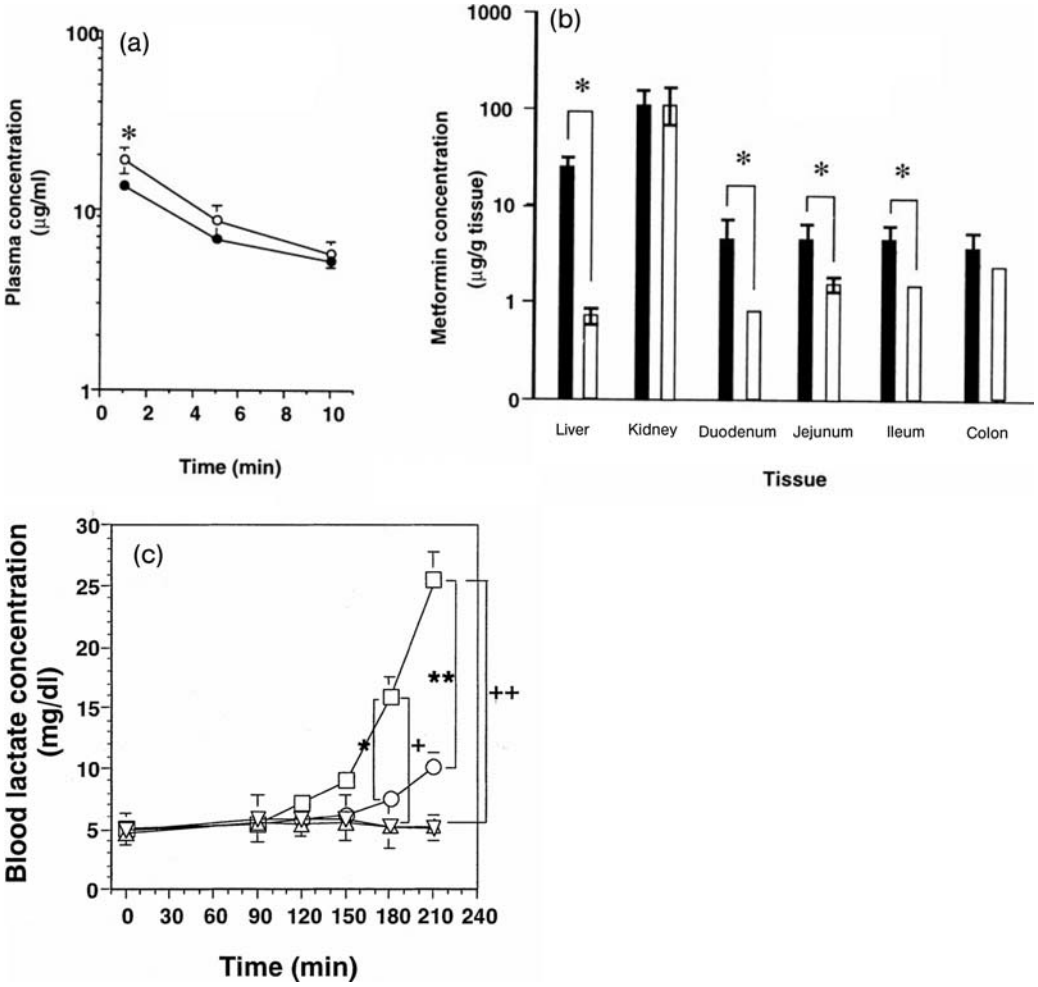

Figure 11.1 Impact of OCT1 on the pharmacokinetics and subsequent toxicological effect of metformin [56, 57]. (a) Plasma concentration profile and (b) tissue distribution of metformin in Oct1 (−/−) (open symbols) and wild-type mice (closed symbols) at 10 min after the i.v. administration of 5.0 mg/kg metformin. (c) Time profile of lactate concentration in wild-type and Oct1 (−/−) mice during intravenous infusion of 150 mg/h/kg metformin. The whole blood lactate concentration in wild-type (□) and Oct1 (−/−) mice (○) was compared with that in saline-treated wild-type (▽) and Oct1 (−/−) mice (△).

export pump), and BCRP (breast cancer resistance protein) are expressed and are involved in the biliary excretion of endogenous and exogenous compounds. Recently, novel SLC transporter, MATE (multidrug and toxic compound extrusion) may also play roles in biliary excretion of cationic compounds. Major efflux transporters in canalicular membrane are listed in Table 11.3.

Table 11.3 Major efflux transporters expressed in the bile canalicular membrane of human liver.

Transporter	Gene symbol	Chromosome	Reference accession (mRNA)	Amino acids	Transmembrane domains	Tissue distribution	Cellular localization	Substrates
MDR1	*ABCB1*	7q21	NM_000927	1280	12	Liver, brain, kidney, intestine, and so on	Apical	Neutral and cationic hydrophilic drugs such as anticancer drugs (CPT-11, doxorubicin, and vinblastine, etc.), digoxin, dexamethasone, loperamide, phenytoin, and so on, and fexofenadine (zwitterion)
MRP2	*ABCC2*	10q24	NM_000392	1545	17	Liver, kidney, and intestine	Apical	Glutathione conjugates (DNP-SG, LTC_4), glucuronide conjugates (bilirubin glucuronide, and $E_2$17βG), and several anionic drugs (pravastatin, temocaprilat, SN-38, and methotrexate)
BCRP	*ABCG2*	4q22	NM_004827	655	6	Various organs	Apical	Mitoxantrone, topotecan, E-sul, DHEAS, imatinib, pitavastatin, and so on
BSEP	*ABCB11*	2q24	NM_003742	1321	12	Liver	Apical	Bile acids, doxorubicin, fexofenadine, and pravastatin
MATE1	*SLC47A1*	17p11	NM_018242	570	12	Liver, kidney, and skeletal muscle	Apical	Cationic compounds (TEA, MPP^+, cimetidine, metformin, creatinine, guanidine, etc.)

11.3.1
MDR1 (P-glycoprotein; *ABCB1*)

MDR1, also known as P-glycoprotein (P-gp), is expressed in various tissues such as liver, kidney, intestine, placenta, and blood–brain barrier and is responsible for the limited intestinal absorption and brain distribution of drugs and enhanced clearance in the liver and kidney. Humans have only one *MDR1* gene, while in rodents, there are two types of *Mdr1* genes, *Mdr1a* and *Mdr1b*, which are expressed in a tissue-specific manner [58–60]. For example, only *Mdr1a* is expressed in the brain and intestine in mice, whereas both *Mdr1a* and *Mdr1b* are expressed in the liver and kidney [58]. MDR1 can accept a wide variety of structurally diverse compounds, most of which are basic or uncharged, and relatively hydrophobic [61]. But organic anions such as fexofenadine and estradiol-17β-glucuronide ($E_2$17βG) are also reported to be recognized by MDR1 as a substrate [62–64]. The information about substrates of MDR1, Mdr1a, and Mdr1b has been published [61].

The direct evidence of the important role of Mdr1 in the hepatic transport of drugs has come from several studies demonstrating the comparison of the biliary excretion between normal and *Mdr1* gene knockout mice. Since Mdr1b is induced in Mdr1a (−/−) mice [65], we had better use Mdr1a/1b double knockout mice rather than Mdr1a (−/−) mice for the analyses [66, 67]. For example, typical type I cations, such as TBuMA and azidoprocainamide methoiodide, and type II cations, such as vecuronium, are excreted into bile via MDR1 [68]. In particular, the role of MDR1 may be emphasized for vecuronium as more than 40% of the administered dose is excreted into bile, largely mediated by Mdr1 [68]. Digoxin is proven to be excreted into bile mainly via Mdr1 [69]. In mice, 45% of the dose is excreted into bile in an unchanged form. The biliary clearance of digoxin in wild-type mice is about 2.7-fold more than that in Mdr1a (−/−) mice. Mdr1 is also responsible for the biliary excretion of doxorubicin and vinblastine [70]. Though the fraction of dose excreted into bile in an unchanged form of doxorubicin and vinblastine is only 13 and 5%, respectively, due to the extensive metabolism, the excreted amount of unchanged doxorubicin and vinblastine into bile in wild-type mice is three- to fivefold more than that in Mdr1a (−/−) mice.

MDR3, a homologue of MDR1, is responsible for the biliary excretion of phospholipids, and a hereditary defect in this gene results in the acquisition of progressive familial intrahepatic cholestatis type 3 (PFIC3) [71].

11.3.2
MRP2 (*ABCC2*)

While MDR1 accepts many kinds of neutral and cationic compounds, MRP2 is thought to be the transporter responsible for the biliary excretion of many organic anions including conjugated metabolites. Originally, the importance of MRP2 in the biliary excretion of several drugs has been explained by comparing the *in vivo* biliary clearance and *in vitro* uptake into the bile canalicular membrane vesicles (CMVs) between wild-type and Mrp2-hereditary deficient rats such as Eisai hyperbilirubinemic rats (EHBRs) and GY/TR$^-$ rats [72, 73]. MRP2 can recognize a

wide variety of endogenous and exogenous compounds including clinically important drugs such as HMG-CoA reductase inhibitors (statins), angiotensin II receptor antagonist (valsartan and olmesartan), methotrexate, temocaprilat, BQ-123 (cyclic peptide for the endothelin antagonist), and cefodizime [74]. Interestingly, the substrate specificities of MRP2 are very similar to those of OATPs, which do not share homology with MRP2; therefore, the efficient hepatobiliary transport of organic anions is thought to be realized with the cooperation of hepatic uptake transport mediated by OATP transporters and biliary efflux via MRP2. Using this transport system, pravastatin can undergo efficient enterohepatic circulation, which leads to its retention in the liver, a pharmacological target of statins, and avoidance of excessive systemic exposure [75]. It is also reported that the impaired biliary excretion of S3025 (1-[2-(4-chlorophenyl)-cyclopropylmethoxy]-3,4-dihydroxy-5-(3-imidazo-[4,5]b pyridine-1-3-yl-3-[4-carboxy]-phenyl-acryloyloxy)-cyclohexancarboxylic acid), a chlorogenic acid derivative, in Mrp2-deficient rats resulted in the prolonged pharmacological action (the inhibition of hepatic glucose production) compared to wild-type rats [76]. MRP2 can also transport many kinds of conjugates with glutathione, glucuronate, and sulfate (e.g., 2,4-dinitrophenyl-*S*-glutathione (DNP-SG), leukotriene C_4 (LTC_4), acetaminophen glucuronide, and lithocholate-3-sulfate) [74]. Several endogenous compounds are also reported to be transported via MRP2 [74]. For example, reduced glutathione is excreted into the bile mainly via MRP2, which is the driving force of the bile salt-independent bile flow [77, 78]. Bilirubin glucuronide is physiologically pumped out by MRP2, and a hereditary defect in MRP2 expression results in the acquisition of Dubin–Johnson syndrome in humans, which exhibits hyperbilirubinemia due to a lack in its biliary excretion [79]. It was suggested that OATP1B1 and MRP2 play important roles in the detoxification of bilirubin. The species difference in the transport function of MRP2 has been investigated. Ishizuka *et al.* [80] have demonstrated that transport activity of temocaprilat (an Mrp2 substrate) into canalicular membrane vesicles prepared from several species was largely different. Niinuma *et al.* [81] have reported that the transport activity per milligram membrane vesicle protein is virtually identical in humans and rats for glucuronide conjugates, but the transport activity of non-conjugated organic anions and glutathione conjugates in humans was 10–20% of that in rats. Ninomiya *et al.* [82] have compared the substrate specificities and their transport activity of MRP2 among four different species, rats, mice, monkey, and dogs, and concluded that their substrate specificities are similar; however, their intrinsic transport activity differs from one species to another due to not only the difference in the K_m and V_{max} values but also the qualitatively different mode of substrate and modulator recognition exhibited by different species. Zimmermann *et al.* [83] have also indicated the species difference in the modulation of transport by other compounds between human and mouse MRP2.

Recently, Mrp2 knockout mice have been established and we can directly evaluate the role of Mdr1, Mrp2, and Bcrp in pharmacokinetics of drugs in mice without considering the species difference in rat and mouse Mrp2 when using EHBRs or GY/TR$^-$ rats [84]. Previous reports have demonstrated the biliary excretion of

glucuronides and sulfates of 4-methylumbelliferone (4-MU), hermol, and acetoaminophen in Mrp2 knockout mice [85]. As a result, the biliary excretion of only 4-MU glucuronide was reduced. This is distinct from the results from rats, showing that biliary excretion of sulfates is shared by Mrp2 and Bcrp, whereas excretion of glucuronides is mainly determined by Mrp2 in rats [86–89]. In other examples, the biliary excretion of fexofenadine in EHBRs was not changed compared to wild-type mice [90], whereas the biliary excretion in Mrp2 knockout mice was partly decreased, though the part of clearance mediated by unidentified transporters is still remained [91, 92]. However, the disposition of irinotecan and its active metabolite, SN-38, was not changed by the knockout of Mrp2 [93], while biliary excretion of irinotecan and SN-38 was reduced in Mrp2-deficient rats [94]. We cannot say which one is a better model for predicting the role of MRP2 in the disposition of drugs in humans, Mrp2-deficient rats or Mrp2-knockout mice.

11.3.3 BCRP (*ABCG2*)

BCRP is sometimes called "half transporter" since it has 6 putative transmembrane domains, whereas other ABC transporters have 12 or 17 transmembrane domains, and it functions as homodimer [95, 96]. The domain organization of BCRP is also unique because ABC region is located in the N-terminus, whereas ABC region of other ABC transporters is located in the C-terminus. Since BCRP was cloned from drug-resistant cancer cells, various kinds of anticancer drugs (mitoxantrone, anthracyclines (doxorubicin and daunorubicin), etoposide, camptothecins, indolocarbazoles, methotrexate, and imatinib) are originally recognized as substrates of BCRP mostly by observing the drug resistance in BCRP-overexpressing cells [95, 96]. Currently, the transport studies have revealed that BCRP can transport many compounds with different physicochemical properties such as sulfate and glucuronide conjugates (E-sul, DHEAS, 4-MU sulfate, and 4-MU glucuronide), antibiotics (ciprofloxacin, erythromycin, rifampicin, and nitrofurantoin), flavonoids (genistein, quercetin), carcinogens (2-amino-1-methyl-6-phenolimidazo(4,5-b)pyridine (PhIP)), sulfasalazine, and cimetidine [95, 96]. The substrate specificity of BCRP overlaps that of P-gp and MRP2. Recently, the role of BCRP in the biliary excretion of compounds has been clarified in the use of Bcrp (−/−) mice. Regarding the biliary excretion, in the case of pitavastatin, interestingly its biliary excretion was not changed in EHBRs compared to wild-type rats [97], unlike pravastatin, which is excreted into the bile predominantly by Mrp2 [98]. However, biliary excretion of pitavastatin was drastically decreased in Bcrp (−/−) mice, suggesting that pitavastatin may be excreted into the bile mainly via Bcrp [97]. However, the biliary excretion of rosuvastatin partially decreased in both Bcrp (−/−) mice and Mrp2-deficient EHBRs (in-house unpublished data). Therefore, the important transporters for the biliary excretion might be different among three unmetabolized statins. The biliary clearance of fluoroquinolones (grepafloxacin, ulifloxacin, ciprofloxacin, and ofloxacin) was also decreased in Bcrp (−/−) mice [99].

11.3.4
BSEP (*ABCB11*)

BSEP mediates the biliary excretion of unconjugated bile salts such as taurocholate, glycocholate, and cholate as well as conjugated bile salts with glycine and taurine [10, 100, 101]. Mita *et al.* [12] have demonstrated that BSEP-mediated uptake clearances of 10 different bile acids were well correlated between human and rat BSEP, and their clearances of taurine-conjugated bile acids were larger than glycine-conjugated and unconjugated bile acids. Thus, BSEP is responsible for the formation of the bile salt-dependent bile flow [10, 100, 101]. Its hereditary defect results in the acquisition of PFIC2, a potentially lethal disease that requires liver transplantation [102]. Hayashi *et al.* [103] have demonstrated that two mutations of BSEP frequently observed in PFIC2 patients, E297G and D482G, resulted in impaired membrane trafficking, whereas the transport functions of these mutants remained largely unchanged. They also demonstrated that 4-phenylbutyrate enhances the cell surface expression and the transport capacity of wild-type and mutated BSEP [104], which suggests that 4-phenylbutyrate has a potential to improve cholestatic diseases by the enhanced redistribution of internalized BSEP to the cell surface. The inhibition of BSEP function by some drugs sometimes results in the drug-induced cholestasis [105]. Recent reports have indicated that BSEP also transports non-bile acid substrates such as doxorubicin, pravastatin, and fexofenadine [92, 106, 107], though its impact on their pharmacokinetics remains to be cleared.

11.3.5
MATE1 (*SLC47A1*)

Very recently, MATE1 has been cloned as a mammalian homologue of bacterial multidrug resistance conferring MATE family [108, 109]. It is supposed to be a cation–proton antiporter that operates in both directions. In humans, two isoforms, MATE1 (highly expressed in the liver, kidney, and skeletal muscle) [109] and MATE2-K (mainly expressed in the kidney) [110], have been identified, while in rodents, Mate1 (mainly expressed in the kidney and placenta) [111, 112] and Mate2 (testis-specific) [113] have been cloned so far. MATE1 can transport several organic cations such as TEA, MPP^+, cimetidine, metformin, creatinine, guanidine, procainamide, cisplatin, oxaliplatin, paraquat, and topotecan [109, 114–116]. Interestingly, acyclovir and ganciclovir (uncharged) and E-sul (anion) are also recognized by MATE1 as a substrate [115]. However, so far the role of MATE1 in the biliary excretion of drugs has not been explained yet.

11.4
Sinusoidal Efflux

Recently, some MRP family transporters such as MRP1, 3, 4, and 6 are located on the basolateral membrane and involved in the sinusoidal efflux of certain compounds

and their conjugates from hepatocytes to blood circulation. Clarifying the role of these transporters in the pharmacokinetics of drugs has just started with the aid of knockout mice. Major efflux transporters in basolateral membrane are listed in Table 11.4.

11.4.1 MRP3 (*ABCC3*)

MRP3 is expressed in a wide range of tissues including liver, intestine, and kidney and it is confirmed to be localized on the basolateral membrane of human liver [5, 6]. Rat Mrp3 is expressed at low level in normal liver and its expression markedly increases in EHBR (Mrp2-deficient rat) [117]. Later, human MRP3 is also induced by several cholestatic disorders [118–120], suggesting that the physiological role of MRP3 has been believed to provide protection to hepatocytes from intrahepatic toxins such as bile acids and bilirubin only under pathological conditions. However, MRP3 is highly expressed in the liver under normal condition in mice [121] and is not largely upregulated in Mrp2 (−/−) mice and under cholestatis conditions [84, 93, 121] compared to humans and rats, maybe due to the little room for upregulation. MRP3 expression is also detected in human liver under physiological condition [118, 122, 123], so at least in humans and mice, MRP3 can partly modulate the hepatic transport of several substrates even under physiological condition. The substrate specificities of MRP3 is narrower compared to MRP2, but several organic anions such as DHEAS, bilirubin glucuronide, methotrexate, LTC_4, and $E_2$17βG can be substrates of MRP3 [6]. Recently, Mrp3 knockout mice have been established [121, 124]. The serum levels of bilirubin glucuronide in Mrp3 (−/−) mice was lower than those of the wild-type mice under cholestatic condition induced by bile duct ligation, but bile acid homeostasis was not modified by knockout of Mrp3 in mice [121, 124]. As far as the transport of xenobiotics is concerned, Mrp3 (−/−) mice cannot excrete morphine-3-glucuronide (M3G) from the liver to the blood, which is the major hepatic elimination route for morphine, leading to the increased concentration of M3G in the liver and bile and 50-fold reduction in its plasma level (Figure 11.2) [125]. Also, the hepatic basolateral efflux clearance of glucuronide conjugates of 4-MU, acetaminophen, and harmol was drastically decreased and that of sulfate conjugates of these three compounds was partly decreased in perfused liver of Mrp3 (−/−) mice [126]. Recently, the biliary excretion rate and the hepatic clearance of non-metabolized drug, fexofenadine were increased in Mrp3 (−/−) mice compared to the wild-type mice [92, 127], suggesting the significant role of Mrp3 in the pharmacokinetics of certain kinds of substrate drugs.

11.4.2 MRP4 (*ABCC4*)

Similar to MRP3, MRP4 is a multispecific efflux transporter expressed in a wide variety of tissues such as the liver, kidney, and brain [5, 6]. Interestingly, MRP4 is localized in the basolateral membrane of human liver [128], whereas it is localized in

Table 11.4 Major efflux transporters expressed in the basolateral membrane of human liver.

Transporter	Gene symbol	Chromosome	Reference accession (mRNA)	Amino acids	Transmembrane domains	Tissue distribution	Cellular localization	Substrates
MRP3	*ABCC3*	17q22	NM_003786	1527	17	Liver, intestine, and kidney	Basal	Bile acids (taurocholate, glycocholate), glucuronide conjugates ($E_2$17βG, E3040-glu), sulfate conjugates (taurolithocholate-3-sulfate), methotrexate, and fexofenadine
MRP4	*ABCC4*	13q32	NM_005845	1325	12	Liver, kidney, and brain	Basal (liver, BCSFB), apical (kidney, BBB)	$E_2$17βG, cAMP, cGMP, 6-mercaptopurine, folate, prostaglandins, and so on
OSTα/β		3q29/15q22	NM_152672/ NM_178859	340/128	7/1	Liver, intestine	Basal	Bile acids
MRP1	*ABCC1*	16p13	NM_004996, NM_019862, NM_019898, NM_019899, NM_019900	1531/1472/ 1475/1416/1466	17	Various organs	Basal	Glutathione conjugates (LTC_4, ethacrynic acid-SG), GSH, GSSG, glucuronide conjugates (bilirubin glucuronide, $E_2$17βG), vincristine, daunorubicin, methotrexate, and so on
MRP5	*ABCC5*	3q27	NM_005688	1437	12	Various organs	Basal	cGMP, cAMP, folate, and methotrexate
MRP6	*ABCC6*	16p13	NM_001171	1503	17	Liver, kidney	Basal	BQ-123, LTC_4, ethylmaleimide-SG, and DNP-SG

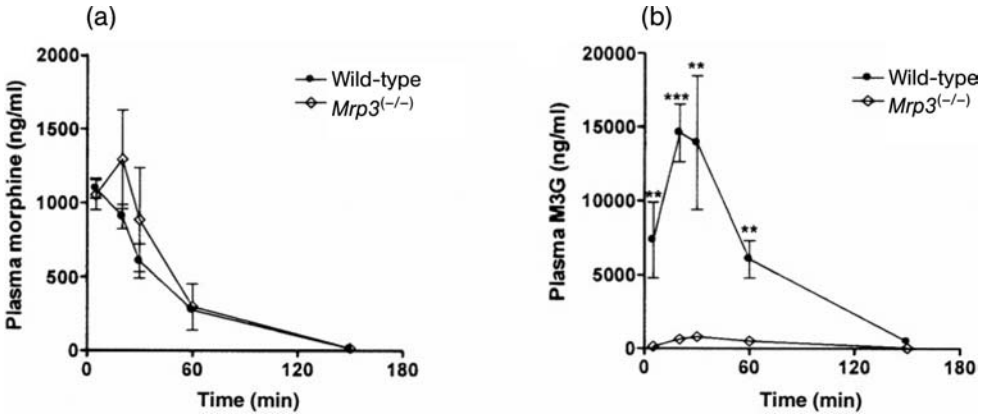

Figure 11.2 Impact of Mrp3 on the pharmacokinetics of morphine [125]. Wild-type mice (closed circle) and Mrp3 (−/−) mice (open circle) received a dose of 15 mg of morphine per kg i. p., and plasma concentrations of morphine (a) and morphine-3-glucuronide (b) were determined at the indicated time points.

the apical membrane of kidney and brain capillary endothelial cells [129–133]. The substrate specificity of MRP4 is broad and it can accept several endogenous compounds including prostaglandins, bile acids, sulfated steroids, and uric acid [5, 6]. Especially, glutathione stimulated the MRP4-mediated bile acid transport and it is cotransported with bile acids [128, 134]. It is worth noting that MRP4 also accepts relatively small compounds such as nucleoside analogues (cGMP, cAMP, adefovir, tenofovir, azidothymidine (AZT), and zidovudine) [5, 6]. Similar to MRP3, MRP4 is also upregulated under cholestatic condition [135, 136], and after the bile duct ligation, serum bile acid concentration was fourfold lower in Mrp4 (−/−) mice compared to wild-type mice, while serum bilirubin level was the same as the control mice [135], suggesting that MRP4 modulates the bile acids but not bilirubin. Also, the hepatic basolateral efflux clearance of sulfate conjugates of 4-MU, acetaminophen, and harmol was partly decreased, but that of glucuronide conjugates was not changed in perfused liver of Mrp4 (−/−) mice [126]. The importance of MRP4 in the pharmacokinetics of drugs is still unknown.

11.4.3 Other Transporters

In the basolateral membrane of liver, MRP1 (ABCC1), MRP5 (ABCC5), and MRP6 (ABCC6) are also localized [137]. The detailed information about these transporters is found in other review article [137]. The expression of MRP1 and MRP5 is very low under normal condition, but severe liver injury induces MRP1 and MRP5 [138, 139], implying that these transporters might be involved in the protection of liver. MRP6 transports LTC_4, DNP-SG, and BQ-123 [140, 141], and the hereditary deficiency of MRP6 gene causes the pseudoxanthoma elasticum, though its molecular mechanism

has not been clarified yet [142–144]. Ostα/Ostβ (organic solute transporter) heterodimer expressed in the kidney, small intestine, and liver is thought to be involved in the efflux transport of some compounds including taurocholate, E-sul, digoxin, PGE_2, and DHEAS [100]. This transporter is also upregulated under the cholestatic conditions through the transactivation of FXR by bile acids [145–147]. Previous reports suggested that OATP family transporters can transport bidirectionally, implying that OATPs can also work as an efflux transporter of anions [148, 149], but its *in vivo* role has not yet been elucidated.

11.5 Prediction of Hepatobiliary Transport of Substrates from *In Vitro* Data

11.5.1 Prediction of Hepatic Uptake Process from *In Vitro* Data

Hepatic transport properties can be investigated by several *in vitro* methods. To evaluate the hepatic uptake of compounds, isolated hepatocytes are very useful. Now, we can purchase several batches of human cryopreserved hepatocytes from several commercial sources. Shitara *et al.* [150] have indicated that we clearly observed the time-dependent saturable uptake of $E_2$17βG (OATP substrate) and taurocholate (NTCP substrate) in human cryopreserved hepatocytes, though the change in uptake clearance before and after cryopreservation exhibited a large interbatch variability among five preparations of human hepatocytes probably due to both the interindividual difference of intrinsic transport activity and the artifact caused by the different condition of isolation and cryopreservation of hepatocytes. Thus, in our usual case, before investigating the transport properties of several compounds using human cryopreserved hepatocytes, we prescreened the uptake clearance of $E_2$17βG and taurocholate in many batches and selected at least three batches of hepatocytes with large transport activity in advance [151]. Cultured hepatocytes can also be used due to the easy handling; however, we must keep in mind that several reports have indicated that long-term (>1 day) culture on collagen-coated dish results in the drastic reduction of the mRNA and protein levels of several transporters and uptake activity of organic anions such as pravastatin [152–154].

Based on the pharmacokinetic theory, the hepatic uptake intrinsic clearance can be estimated simply by scaling up the uptake clearance in hepatocytes *in vivo*. By multiplying the uptake clearance per unit cell number by cell number per gram of liver (e.g., 1.25×10^8 cells/g liver (rat)), it was possible to extrapolate the *in vitro* uptake data to the *in vivo* intrinsic uptake clearance. Miyauchi *et al.* [155] have demonstrated that the uptake clearance of 15 drugs in isolated hepatocytes correlated well with that estimated by *in situ* multiple indicator dilution (MID) method, though *in situ* clearance appeared to reach an upper limit possibly because the diffusion of compounds in unstirred water layer became the rate-determining process. Kato *et al.* [156] have also showed that the uptake clearance of four types of endothelin antagonists obtained from integration plot analysis after i.v. administration of compounds in rats is almost

comparable to that calculated from the uptake clearance in isolated rat hepatocytes assuming the well-stirred model. These evidences suggested that isolated hepatocytes are a good model for predicting the hepatic uptake clearance.

11.5.2
Prediction of the Contribution of Each Transporter to the Overall Hepatic Uptake

The transport property of each transporter can be evaluated by using several kinds of gene expression systems (e.g., mammalian cells, *Xenopus* oocytes). However, there are many transporters expressed on the same membrane and their substrate specificities often overlap one another. In this case, all of the transporters that can transport one compound are not always important for the overall hepatic uptake if their relative contribution is very minor compared to that of other major transporters. Therefore, it is essential to know the quantitative contribution of each transporter to the hepatic uptake to show the importance of each transporter in *in vivo* condition. When the function and/or expression level of one transporter caused by genetic polymorphisms, pathophysiological conditions, and transporter-mediated drug–drug interactions is changed, the information about the contribution is necessary to predict the change in the *in vivo* pharmacokinetics from *in vitro* data.

Kouzuki *et al*. [157, 158] have proposed a method using reference compounds to determine the contribution of rat Oatp1a1 and Ntcp to the hepatic uptake of bile acids and organic anions. This concept is originally established in the field of metabolic enzymes by Crespi *et al*. [159] and they named it "relative activity factor (RAF)" method. In this method, they checked the transport activity of both test compounds and the reference compounds, which should be specific substrates for single transporters, in short-term cultured rat hepatocytes and transporter-expressing COS-7 cells. Then, they estimated the contribution from the following equations:

$$\text{Contribution}(\%) = \frac{R_{\text{COS}}}{R_{\text{hep}}} \times 100, \tag{11.1}$$

$$R_{\text{cos}} = \frac{\text{CL}_{\text{uptake,COS(test)}}}{\text{CL}_{\text{uptake,COS(reference)}}} \tag{11.2}$$

$$R_{\text{hep}} = \frac{\text{CL}_{\text{uptake,hep(test)}}}{\text{CL}_{\text{uptake,hep(reference)}}} \tag{11.3}$$

where $\text{CL}_{\text{uptake,COS(test)}}$ and $\text{CL}_{\text{uptake,COS(reference)}}$ represent the uptake clearances of test compounds and reference compounds in transporter-transfected COS-7 cells, respectively, and $\text{CL}_{\text{uptake,hep(test)}}$ and $\text{CL}_{\text{uptake,hep(reference)}}$ represent the uptake clearances of test compounds and reference compounds in isolated rat hepatocytes, respectively. To estimate the contribution of rat Oatp1a1 and Ntcp, they used taucholate for Ntcp and $E_2$17βG for Oatp1a1 as reference compounds. As a result, rat Ntcp was responsible for the hepatic uptake of bile acids. However, some organic anions were partially taken up via Oatp1a1, but the hepatic uptake of other anions such as pravastatin and DNP-SG could not be explained by Oatp1a1-mediated

transport, suggesting that uptake transporters other than Oatp1a1 are involved in their uptake. Now, other hepatic uptake transporters such as Oatp1a4, Oatp1b2, and Oat2 have also been characterized and they can accept various kinds of anions [22, 23, 160]. Therefore, $E_2$17βG can no longer be used as a reference compound for Oatp1a1, but their concept can be applied to estimate the relative contribution.

Hirano *et al*. [151] have applied this concept to human hepatocytes to estimate the relative contribution of OATP1B1 and OATP1B3 to the hepatic uptake of $E_2$17βG and pitavastatin, a novel HMG-CoA reductase inhibitor, in cryopreserved human hepatocytes. They used E-sul for OATP1B1 and CCK-8 for OATP1B3 as reference compounds (Figure 11.3a). As with the previous method, they calculated the ratio of the uptake clearance of reference compounds in human hepatocytes to that in expression systems and defined as "R_{act}" for OATP1B1 and 1B3, and by multiplying the R_{act} value by the uptake clearance of test compounds (CL_{test}), we could estimate the uptake clearance of test compounds mediated by specific transporter in human liver. Assuming that the hepatic uptake clearance (CL_{hep}) could be explained by OATP1B1- and OATP1B3-mediated transport, the following equation should be correct:

$$CL_{hep} = R_{act,OATP1B1} \times CL_{test,OATP1B1} + R_{act,OATP1B3} \times CL_{test,OATP1B3}. \quad (11.4)$$

They have demonstrated that both pitavastatin and $E_2$17βG were taken up mainly by OATP1B1 in three independent batches of human hepatocytes and that the observed uptake clearance in human hepatocytes was almost comparable to the sum of the estimated clearance mediated by OATP1B1 and 1B3.

They also confirmed their results by two different approaches [42, 151]. One is to directly estimate the ratio of the expression level of OATP1B1, 1B3, and 2B1 in human hepatocytes to that in expression systems by comparing the band density of Western blot analysis and estimated their contributions using that ratio instead of R_{act} value shown above [42, 151] (Figure 11.3b). The other approach is to estimate the inhibitable portion of the uptake of test compounds in human hepatocytes in the presence of specific inhibitor for each transporter [42] (Figure 11.3c). We used E-sul as a specific inhibitor for OATP1B1. The uptake of pitavastatin was completely inhibited by 100 microM E-sul, indicating the major role of OATP1B1 in their hepatic uptake (Figure 11.4a), whereas that of telmisartan was not inhibited by E-sul (Figure 11.4b). Each approach has both advantages and disadvantages, and so we recommend that users compare the results obtained from different methods and validate their results. Though some anionic drugs shared the same pharmacokinetic properties in which they are efficiently accumulated in the liver, the relative contribution of each transporter depends on individual substrates. According to our estimation, valsartan and olmesartan are taken up via both OATP1B1 and OATP1B3, while fexofenadine and telmisartan are transported predominantly by OATP1B3 [31–33, 161].

Gene silencing techniques such as antisense, ribozyme, and RNA interference (RNAi) are also powerful tools to determine the transport activity of a specific protein. Hagenbuch *et al*. [162] have investigated the effect of coinjection of transporter (Ntcp or Oatp1a1)-specific antisense oligonucleotide on the uptake of BSP and taurocholate

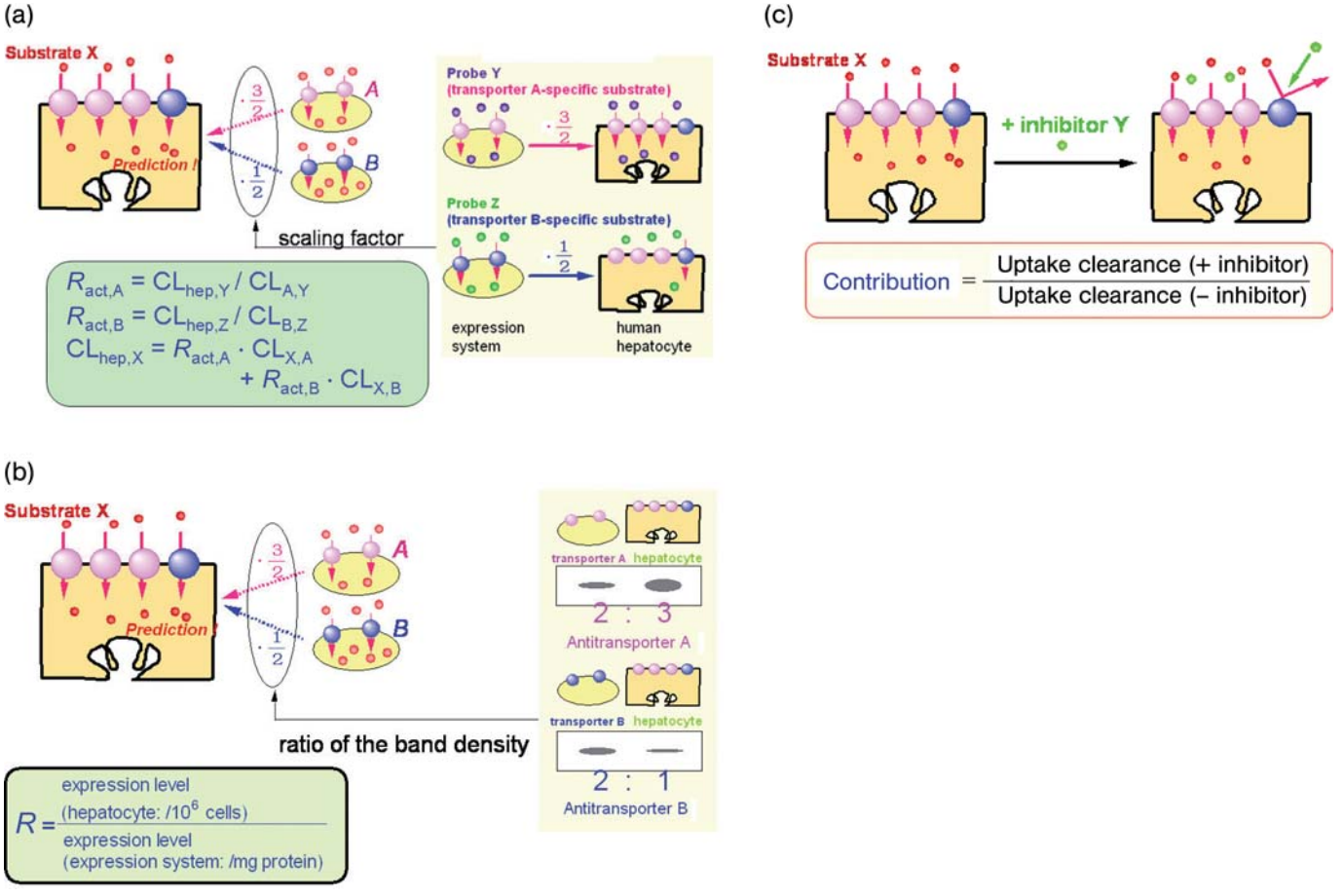

Figure 11.3 Schematic diagram of the methods for estimating the contribution of each transporter to the overall hepatic uptake [250] (a) using reference compounds; (b) using the relative expression levels estimated from Western blot analysis; and (c) using transporter-specific inhibitors. The details are described in the Section 11.5.2.

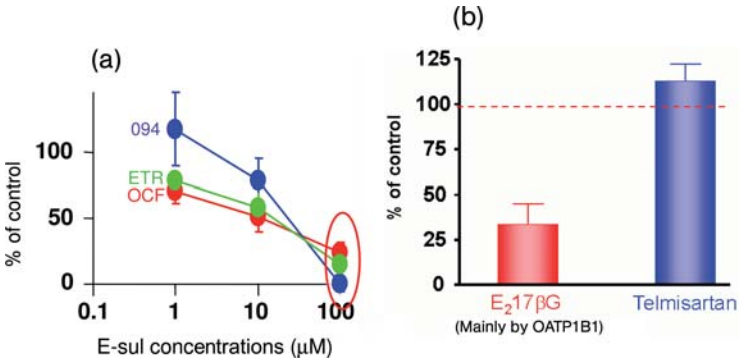

Figure 11.4 The inhibitory effect of E-sul on the hepatic uptake of pitavastatin (a) and $E_2$17βG and telmisartan (b) [32, 42]. (a) The transport of pitavastatin (0.1 microM) into human hepatocytes was determined in the presence or absence of E-sul at the designated concentrations. Three different independent batches of human hepatocytes were used in this study. The values are expressed as a percentage of the uptake of pitavastatin in the absence of E-sul. (b) Saturable uptake of telmisartan into human hepatocytes was determined after the subtraction of nonsaturable uptake (evaluated as the uptake clearance of 40 microM telmisartan) from the uptake of 0.1 microM telmisartan in the presence or absence of E-sul (30 microM). The incubation buffer contains 0.3% human serum albumin to avoid the nonspecific adsorption of telmisartan.

in the *Xenopus* oocytes injected with total rat liver mRNA. They succeeded in the significant reduction of the expression level of target transporter specifically and concluded that Na^+-dependent and independent uptakes of taurocholate were almost accounted for by Ntcp and Oatp1a1, respectively, while only half of the BSP uptake could be explained by Oatp1a1. Nakai *et al.* [163] took the same approach to show the importance of OATP1B1 to the hepatic uptake of pravastatin and $E_2$17βG in humans by adding antisense oligonucleotide to human liver poly(A) mRNA-injected oocytes. Recently, some groups have succeeded in constructing small interference RNAs (siRNAs) that can efficiently decrease the expression level of specific transporters such as MDR1 and MRP2 [164, 165]. However, it is fairly difficult to apply these gene-silencing techniques to the primary cultured hepatocytes because long-term culture dramatically decreases the expression level of several transporters [152–154], though generally it takes a few days to knockdown the protein by the depletion of mRNA expression, and the optimization of the culture condition will be required for this analysis.

11.5.3 Prediction of Hepatic Efflux Process from *In Vitro* Data

One of the popular experimental systems to investigate the hepatic efflux process is canalicular membrane vesicle (CMV). It is difficult to evaluate the transport activity of efflux transporters in cell systems because substrates cannot easily access the intracellular compartment, so CMV system is often used to rapidly determine the ATP-dependent efflux transport of substrates across bile canalicular membrane.

Aoki *et al.* [166] have compared the *in vitro* transport clearance of nine substrates in rat CMVs, defined as the initial velocity for the ATP-dependent uptake divided by the substrate concentration of the incubation medium with *in vivo* biliary excretion clearance defined as the biliary excretion rate normalized by protein unbound concentration in rat liver at steady state, and found a significant correlation between *in vitro* and *in vivo* clearance, suggesting that *in vivo* biliary excretion clearance can be predicted from the *in vitro* transport study using CMVs. Some transporter-specific inhibitors for efflux transporters may be useful to understand the contribution of each efflux transporter to the overall biliary excretion. Ko143 preferentially inhibits the BCRP-mediated transport [167], while PSC833 and LY335979 inhibit the MDR1-mediated transport more potently than the transport via other efflux transporters [168, 169]. By evaluating the effect of transporter-specific inhibitors on the ATP-dependent transport of test compounds in human CMVs, the relative contribution of each transporter to the biliary excretion might be clarified. Recently, LeCluyse *et al.* [170] have demonstrated that a collagen-sandwich culture enables the hepatocytes to form bile canalicular pocket between the adjacent cells and depletion with Ca^{2+} from the incubation medium rapidly disrupts the bile canaliculi [171]. The advantage of this culture configuration is that the polarity and the expression level of uptake and efflux transporters are well retained for several days unlike the normal culture on the rigid collagen and that biliary excretion of compounds can be evaluated in intact cell systems by differential cumulative uptake in the monolayers preincubated with Ca^{2+}-containing buffer and Ca^{2+}-free buffer [171, 172]. Liu *et al.* [173] have found that the *in vitro* biliary clearance of five compounds (inulin, salicylate, methotrexate, [D-pen^{2,5}] enkephalin, and taurocholate) in rat hepatocytes calculated by the amount excreted into bile canalicular pocket divided by the area under the incubation medium concentration–time profile was well correlated with their *in vivo* intrinsic biliary clearance, suggesting that this system is useful for the prediction of *in vivo* biliary excretion of compounds. Recently, Bi *et al.* [174] have evaluated the biliary excretion of several substrates for various efflux transporters in sandwich-cultured cryopreserved human hepatocytes. By scaling up the *in vitro* biliary excretion clearance by multiplying the clearance per cell to the cell number per gram liver, it is possible that *in vivo* clearance may be estimated in humans from *in vitro* data. Ghibellini *et al.* [175] have recently succeeded in the extrapolation of human *in vivo* biliary clearance of three compounds estimated by gamma scintigraphy and direct aspiration of duodenal secretions from *in vitro* biliary clearance in sandwich-cultured human hepatocytes.

11.5.4
Utilization of Double (Multiple) Transfected Cells for the Characterization of Hepatobiliary Transport

A brand-new approach to evaluate the uptake and efflux processes simultaneously is to use double-transfected cells that express both uptake and efflux transporters (Figure 11.5). Originally, Cui *et al.* and Sasaki *et al.* established OATP1B3/MRP2 and OATP1B1/MRP2 double transfectants, respectively [176, 177]. If a compound is a bisubstrate of uptake and efflux transfectants, basal-to-apical transcellular transport

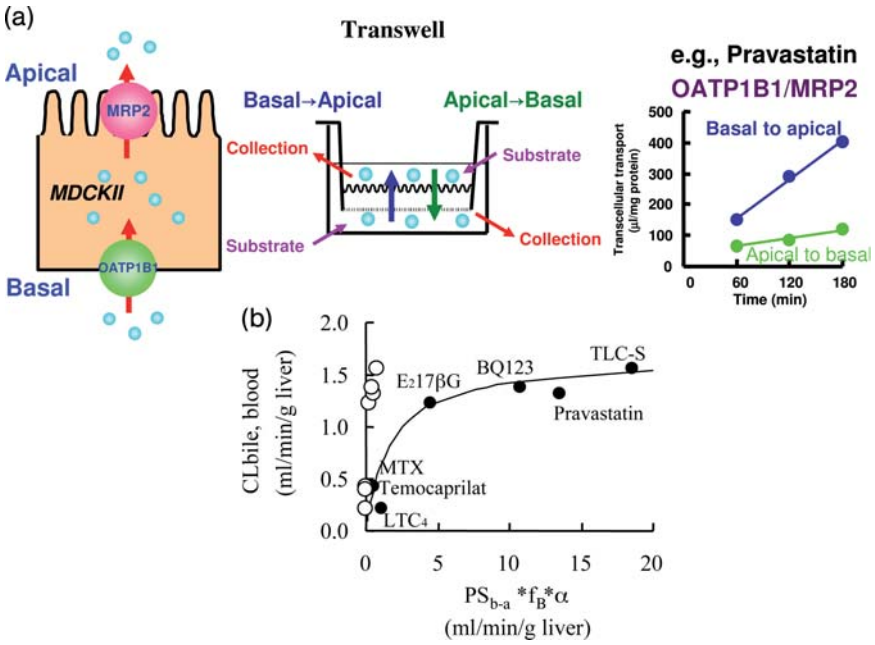

Figure 11.5 Vectorial transcellular transport of drugs in double-transfected cells. (a) The double-transfected cells expressing OATP1B1 (uptake transporter) on the basal side and MRP2 (efflux transporter) on the apical side have been established. If a compound is a bisubstrate of uptake and efflux transporters such as pravastatin, its basal-to-apical transcellular transport is significantly higher compared to the apical-to-basal transport [177]. (b) Prediction of *in vivo* biliary clearance of several bisubstrates of rat Oatp1b2 and Mrp2 from their *in vitro* transcellular transport clearance in rat Oatp1b2/Mrp2 double transfectant [178].

was significantly greater than that in the opposite direction. Therefore, this system is suitable for the high-throughput screening of bisubstrates. To extrapolate the *in vivo* biliary excretion clearance from *in vitro* experiments, Sasaki *et al.* [178] have measured the basal-to-apical transcellular transport clearances of seven bisubstrates in rat Oatp1b2/Mrp2 double transfectants and their *in vivo* biliary clearances ($CL_{bile,blood}$) calculated from the biliary excretion rate normalized by blood concentration at steady state. They proposed that the *in vivo* and *in vitro* clearance can be well described as the following equation:

$$CL_{bile,blood} = \frac{Q_H \cdot f_B \cdot \alpha \cdot PS_{b\to a}}{Q_H + f_B \cdot \alpha \cdot PS_{b\to a}}, \tag{11.5}$$

where Q_H, f_B, and $PS_{b\to a}$ represent the hepatic blood flow rate, protein unbound fraction of the compounds in blood, and transcellular transport clearance in double transfectants corrected by the fact that 1 g of liver contains 160 mg protein, respectively. And, α means the scaling factor to predict *in vivo* clearance from *in vitro* results quantitatively. When α was 17.9, all data were well fitted to the theoretical curve

described as Equation 11.5 (Figure 11.5). Now, we constructed several kinds of double-transfected cells such as human and rat NTCP/BSEP and (OATP1B1 or OATP1B3)/(MRP2, MDR1, or BCRP) double-transfected cells and the methodology for extrapolating the *in vivo* clearance from *in vitro* data will be constructed and validated [12, 64, 179, 180]. Kopplow *et al.* [181] have established the quadruple-transfected cells expressing OATP1B1, OATP1B3, OATP2B1, and MRP2 to screen the transcellular transport of organic anions in human hepatocytes. Very recently, Nies *et al.* [182] have constructed OCT1/MDR1 double transfectant and observed the transcellular transport of cationic plant alkaloid, berberine. To construct a set of double transfectants to mimic the transcellular transport in each organ is important for the understanding of the involvement of transporters in the pharmacokinetics of drugs.

11.6 Genetic Polymorphism of Transporters and Its Clinical Relevance

Genetic polymorphism of transporters is one of the important factors for determining the interindividual difference in the pharmacokinetics and subsequent pharmacological action of substrate drugs. Recently, many mutations including single nucleotide polymorphisms (SNPs) have been identified in several transporters and their impact on the drug transport has been rapidly analyzed by *in vitro* and clinical studies. Excellent reviews about genetic polymorphisms of transporters have been published and we only mention some of the examples here.

The reported mutations in *MDR1* gene observed in humans are more than 100 sites [183]. One of the most famous SNPs is C3435T (Ile1145Ile) in exon 26, which is a synonymous mutation. Its frequency in Japanese and Caucasians is 42.0 and 54.2%, respectively. Hoffmeyer *et al.* [184] have reported that the protein expression level of MDR1 in duodenum in subjects with C3435T mutation was significantly smaller and the plasma AUC after oral administration of digoxin was increased compared to subjects without C3435T mutation. This mutation is closely linked to G2677T (Ala893Ser) and C1236T (Gly412Gly), and extensive clinical studies to observe the effects of these SNPs or haplotypes on the pharmacokinetics of several kinds of MDR1 substrates have been performed. Overall, C3435T tended to increase the plasma AUC of MDR1 substrates, though contradictory results have also come out [185]. There is no evidence showing SNPs in *MDR1* affected the biliary excretion of drugs.

SLCO1B1 (gene product: OATP1B1) has more than 40 naturally occurring mutations and A388G (Asn130Asp) and T521C (Val174Ala) are the most famous and frequent SNPs among them [186]. The allele frequency in each ethnicity (A388G: Asian = 64%, African-American = 74%, and Caucasian = 40%; T521C: Asian 16%, Caucasian = 14%, and African-American = 1%) may lead to racial difference in the pharmacokinetics of OATP1B1 substrate drugs. Nishizato *et al.* [187] have first demonstrated that T521C is highly linked to A388G, and they found a haplotype named *SLCO1B1**15 in Japanese, and that plasma AUC of orally administered

Table 11.5 The effect of *SLCO1B1* polymorphisms on the clinical pharmacokinetics of drugs.

Drugs	Mutations in *SLCO1B1*	Reference
Pravastatin	*1b/*1b < *1b/*15	[187]
	*1a/*1b or *1b/*1b < *1a/*1a < *1a/*5	[268]
	−11187 G/G < G/A	[269]
	521 T/T < T/C	
	*15B noncarriers < carriers	
	*17 noncarriers < carriers	
	*1b/*1b < *1a/*1a	[190]
	*1b/*15 < *1a/*15	
	*17 noncarriers < carriers	[270]
	*1a/*1a < *1a/*15 < *15/*15	[271]
	*15 or *17 noncarriers < carriers	[272]
Pitavastatin	*1b/*1b < *1a/*1a or *1a/*1b < *1a/*15 or *1b/*15	[273]
	*1b/*1b < *1b/*15 < *15/*15	[274]
Rosuvastatin	521 T/T < T/C < C/C (whites)	[275]
	*15 noncarriers < *15 heterozygotes < *15 homozygotes	[276]
	521 T/T < C/C	[277]
Simvastatin	521 T/T or T/C < C/C (acid form)	[278]
Atorvastatin	521 T/T or T/C < C/C	[277]
Fluvastatin	521 T = C	[279]
Repaglinide	521 T/T < T/C < C/C	[192]
Nateglinide	521 T/T < T/C, T/T < C/C	[280]
Fexofenadine	521 T/T < T/C < C/C	[281]
Valsartan	*1b/*1b < *1a/*1a (trend)	[190]
	*1b/*15 < *1a/*15 (trend)	
Temocapril	*1b/*1b < *1a/*1a (trend)	[190]
	*1b/*15 < *1a/*15 (trend)	
Pioglitazone	521 T = C	[282]
Rosiglitazone	521 T = C	[282]
Atrasentan	521 T/T < T/C < C/C	[259]
Mycophenolic acid	No relationship (*1a, *1b, *15)	[283]
Irinotecan	*1a or *1b < *15 (SN-38)	[193]
	*1a/*1a < *1b/*15+*15/*15 (irinotecan)	[284]
	*1a/*1a. < *1b/*15+*15/*15 (SN-38)	
	*1a/*1a > *1b/*15+*15/*15 (SN-38glu)	
Ezetimibe	*1a < *15	[285]
Talinolol	*1b < *1a (trend)	[286]
Torsemide	521 T/T < T/C < C/C	[287]

pravastatin is significantly higher in subjects with *15 alleles compared to *1b alleles (A388G). After that, several clinical studies supported this finding. The results of clinical studies investigating the relationship between SNPs in *SLCO1B1* and pharmacokinetics of drugs are summarized in Table 11.5. In most cases, T521C mutation is thought to decrease the transport function of OATP1B1, which results in the reduction of hepatic clearance [186]. These outcomes are supported by *in vitro* studies demonstrating that cells expressing *15 mutant showed the decrease in the

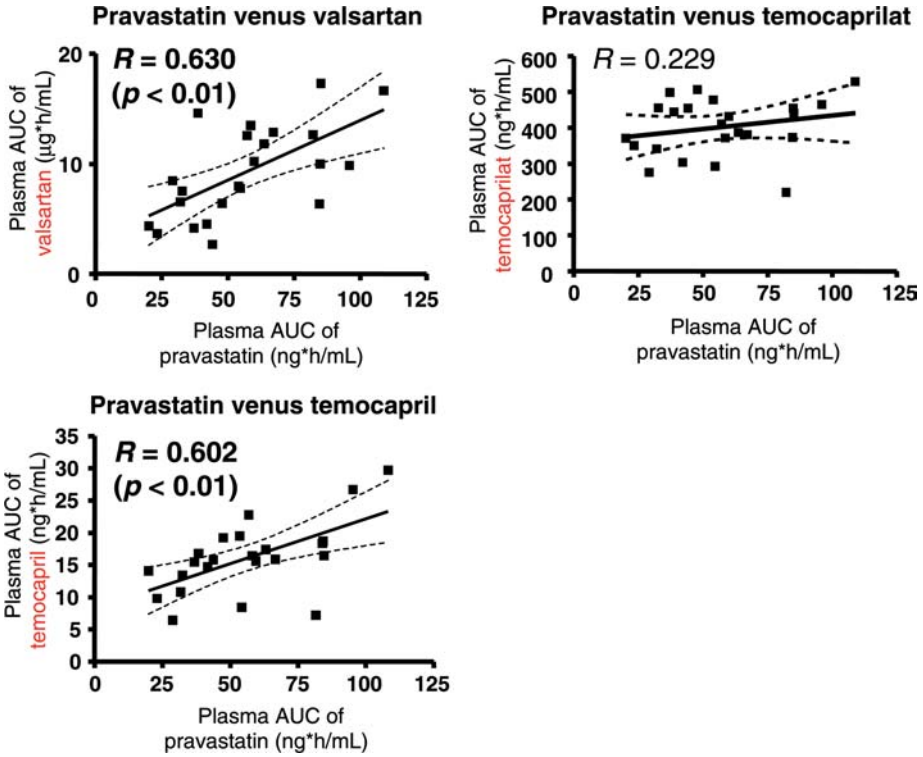

Figure 11.6 The correlation between the plasma AUC of pravastatin in each subject and that of valsartan, temocapril, and temocaprilat [190]. Each point represents AUC values of three drugs for each subject after oral administration of pravastatin (10 mg), valsartan (40 mg), or temocapril (2 mg). Solid lines represent fitted lines calculated by linear regression analysis and dotted lines represent 95% confidence intervals of correlations.

transport activity compared to wild-type OATP1B1 [16, 188, 189]. On the other hand, the subjects with *SLCO1B1**1b alleles showed the lower plasma AUC of pravastatin, valsartan, and temocapril than those with *SLCO1B1**1a alleles, and the plasma AUC of pravastatin in each subject was correlated well with that of valsartan and temocapril (Figure 11.6), which suggested that the clearance mechanism of pravastatin may be shared with valsartan and temocapril and *SLCO1B1**1b may increase the transport function in human liver, though *in vitro* analyses do not simply explain this clinical outcome [190]. Recently, some reports have mentioned that T521C mutation may relate to the pharmacological and toxicological actions of substrate drugs such as decrease in cholesterol-lowering effect of pravastain [191], increase in the reduction of blood glucose level by repaglinide [192], and increased frequency of neutropenia expression induced by irinotecan [193] (Figure 11.7). Other major hepatic OATP transporter, *SLCO1B3* (gene product: OATP1B3) has two frequent SNPs, T334G (Ser112Ala) and G699A (Met233Ile), but currently we have no reports showing these SNPs affected the transport function of substrates [194, 195].

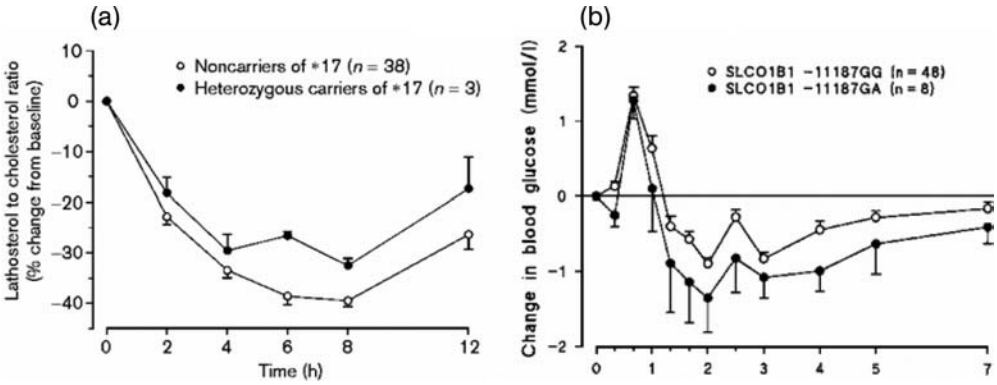

Figure 11.7 Impact of *SLCO1B1* mutations on the pharmacological effects of pravastatin and repaglinide. (a) Plasma lathosterol/cholesterol ratio after single oral administration of 40 mg pravastatin in healthy subjects with or without *SLCO1B1**17 (G-11187A + Asn130Asp + Val174Ala) allele [191]. (b) Change in blood glucose level after single oral administration of 0.25 mg repaglinide in healthy subjects with or without G-11187A mutation in *SLCO1B1* [192].

BCRP has also one frequent SNP, C421A (Gln141Lys). This mutation is more frequently observed in Asians (~35%) than Caucasians (10%). Clinical studies indicated that C421A mutation decreased the total clearance of diflomotecan, rosuvastatin, and sulfasalazine [196–198]. BCRP is expressed in the small intestine as well as the liver and it is difficult to identify whether these clinical outcomes come from a decrease in the transport function in the small intestine or in the liver. However, the pharmacokinetics of diflomotecan was changed after both i.v. and p.o. administration, which indicates that this may be caused partly by the decrease of its biliary excretion mediated by BCRP [198]. *In vitro* analyses revealed that the transport function normalized by the protein expression level of BCRP C421A mutant is apparently normal [199], but another report showed that C421A mutation significantly decreased the protein expression level of BCRP in human placenta [200]. Thus, the decreased function by C421A mutation is thought to be caused by its decreased expression.

In the case of MRP2, though some SNPs are found in coding region, recent studies have indicated the impact of SNPs in the upstream regions on the toxicological aspects of drugs. For example, two kinds of haplotypes (-1774delG, G-1549A and C-24T) of *MRP2* increased the frequency of drug-induced hepatitis [201]. Other report has demonstrated that C-24T mutation increased the frequency of diclofenac-induced hepatotoxicity [202]. These may be caused by the decrease in hepatic clearance of toxicants, which results in the high exposure of toxicants in liver. A-1019G mutation in *MRP2* has also reported to decrease the frequency of severe diarrhea related to irinotecan [203], which suggested that A-1019G may decrease the biliary excretion of SN-38, an active metabolite of irinotecan, and decreased the exposure of SN-38 in the intestine. Very recently, mutations in *OCT1* have been reported to result in the increase in plasma concentration of metformin and subsequent attenuation of its glucose-lowering effect [204, 205].

11.7
Transporter-Mediated Drug–Drug Interactions

11.7.1
Effect of Drugs on the Activity of Uptake Transporters Located on the Sinusoidal Membrane

Recently, several reports have suggested that the inhibition of hepatic uptake transporters by coadministered drugs results in the decrease in the hepatic clearance and increase in the plasma concentration of victim drugs. For example, antituberculosis agents (rifamycin SV and rifampicin) reduced the clearance of BSP and also induced hyperbilirubinemia due to the inhibition of OATP1B1-mediated bilirubin uptake [206]. These results may be accounted for by considering the fact that the Ki values of rifamycin SV are 2 and 3 microM for OATP1B1 and OATP1B3, respectively, whereas those of rifampicin are 17 and 5 microM for these transporters, and that the peak unbound plasma concentrations of rifamycin SV and rifampicin may be 5–10 microM [206]. The fact that rifamycin SV induces a more potent increase in plasma unconjugated bilirubin concentrations than rifampicin may also be accounted for by these kinetic considerations. The interaction between cerivastatin and gemfibrozil has also been highlighted because of the appearance of severe side effects including rhabdomyolysis and death (Figure 11.8) [207]. This led to the withdrawal of cerivastatin from the market. On the other hand, after coadministration of cyclosporin A, the plasma concentration of cerivastatin was increased 3.8-fold (Figure 11.8) [208]. *In vitro* experiments revealed that cyclosporin A potently inhibited the uptake of cerivastatin in human hepatocytes and OATP1B1-expressing MDCKII cells with Ki values of 0.280–0.685 microM and 0.238 microM, respectively [209]. In contrast, cerivastatin metabolism mainly mediated by CYP2C8 and 3A4 was not affected by cyclosporin A at concentrations up to 30 microM [209]. These results suggest that the inhibition of cerivastatin uptake into hepatocytes results in an increased blood concentration of cerivastatin, which may lead to the severe side effects (Figure 11.8) [209]. According to the recent clinical studies, coadministration of cyclosporin A also increased the plasma concentration of several OATP1B1 substrate drugs such as other non-metabolized statins, pravastatin (5–7.9-fold) [210], rosuvastatin (7.1-fold) [211] and pitavastatin (4.5-fold) [212], repaglinide (4-fold) [213], and bosentan (30-fold) [214], which indicates that we pay attention to the drug interaction between cyclosporin A and OATP1B1 substrates in clinical situations. However, gemfibrozil and its glucuronide also have the potency to inhibit OATP1B1-mediated uptake with a Ki value of 4–72 and 24 microM, respectively [215]. Though Shitara *et al.* [215] have concluded that the main mechanism of this drug interaction is the inhibition of CYP2C8-mediated cerivastatin metabolism by gemfibrozil glucuronide (Figure 11.8), gemfibrozil is thought to slightly inhibit the OATP1B1-mediated uptake because it increased the plasma AUC of non-metabolized statins such as pravastatin (2.02-fold) [216], pitavastatin (1.45-fold) [217], and rosuvastatin (1.88-fold) [218], which is lower than that of cerivastatin (4.36-fold) [207]. Several compounds are recognized as bisubstrates of both metabolic enzymes and transporters

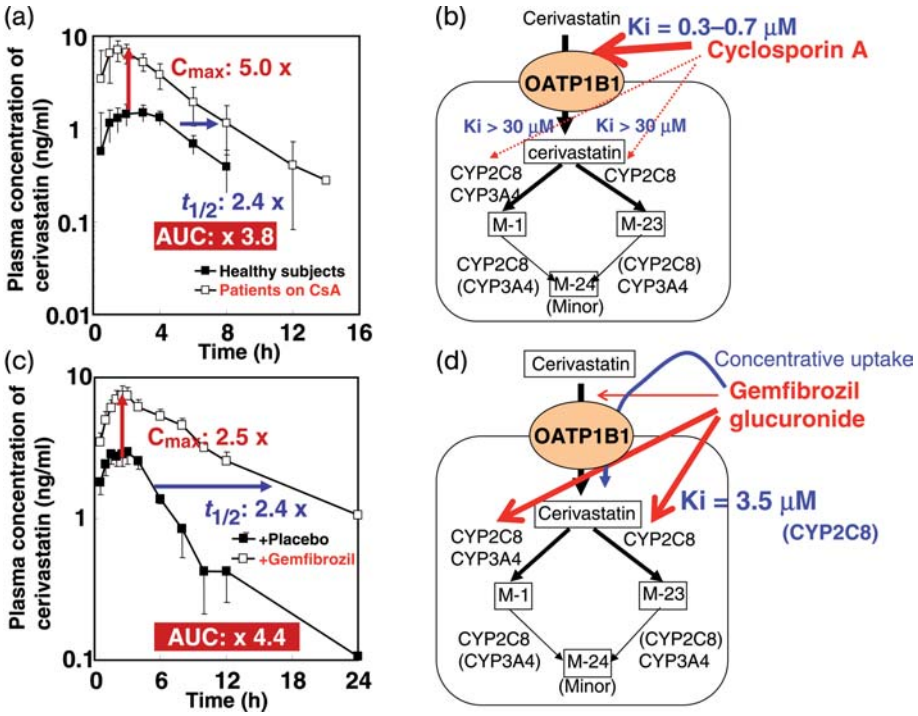

Figure 11.8 Drug–drug interaction between cerivastatin and cyclosporin A and between cerivastatin and gemfibrozil. (a, b) Cyclosporin A increased the plasma concentration of cerivastatin, which is mainly caused by the inhibition of OATP1B1-mediated uptake of cerivastatin by cyclosporin A [208, 209]. (c, d) Gemfibrozil increased the plasma concentration of cerivastatin, mainly caused by the inhibition of CYP2C8-mediated metabolism of cerivastatin by gemfibrozil glucuronide, which may be concentrated in hepatocytes, and partly caused by its inhibition of OATP1B1-mediated uptake [207, 215].

such as atorvastatin, bosentan, and repaglinide [188, 192, 219, 220]. In that case, we should consider the rate-limiting step of overall clearance to predict the drug–drug interaction. Figure 11.9 shows the effects of the coadministration of itraconazole (CYP3A4 inhibitor) and cyclosporin A (CYP3A4 and OATP1B1 inhibitor) on the pharmacokinetics of three different types of statins [210, 221–224]. Pravastatin is a substrate of OATP1B1 [25, 163, 188], but not metabolized, whereas simvastatin uptake is thought to occur without any aid of transporters due to the high lipophilicity of simvastatin lactone. However, atorvastatin is taken up into the liver by OATP1B1 [188, 220] and subsequently metabolized by CYP3A4. Cyclosporin A inhibited the hepatic clearance of these statins, but the inhibition of CYP3A4 by itraconazole greatly affected the plasma AUC of simvastatin, and modestly changed that of pravastatin and atorvastatin, though both simvastatin and atorvastatin are substrates of CYP3A4. This apparent discrepancy can be explained by the rate-limiting step of overall clearance of two statins. For hydrophilic atorvastatin, OATP1B1 is

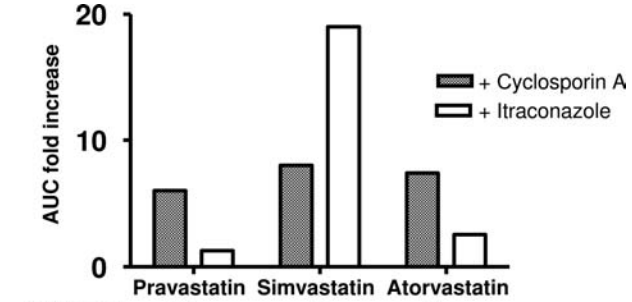

	Pravastatin	Simvastatin	Atorvastatin
OATP1B1	Yes	No	Yes
CYP3A4	No	Yes	Yes
BA	0.18	<0.05 (acid)	0.13
Fh	0.29		0.42
Fa*Fg	0.62		0.31

Figure 11.9 Different effects of itraconazole and cyclosporin A on the plasma AUC of pravastatin, simvastatin, and atorvastatin [210, 221–224]. The fold-increase in the plasma AUC of statins was expressed after coadministration of cyclosporin A or itraconazole. The data were obtained from the previous literature. The details are described in the Section 11.7.1. BA: bioavailability, $F_a{}^*F_g$: fraction of dose absorbed from the small intestine to the portal vein, F_h: hepatic availability.

involved in its hepatic uptake, and overall intrinsic clearance is solely determined by the uptake clearance. Thus, the decrease in the hepatic clearance of atorvastatin was almost the same as that of pravastatin. However, hydrophobic simvastatin can permeate the membrane passively, so the overall intrinsic clearance approximates the metabolic intrinsic clearance, thus the inhibition of CYP3A4 greatly decreased the hepatic clearance of simvastatin. Recently, Ki values of several drugs for OATP1B1 and OATP1B3 have been published [42, 92]. Comparing the Ki values with the maximum unbound plasma concentration at the inlet to the liver in humans, OATP1B1 may be inhibited by several drugs such as cyclosporin A, indinavir, ritonavir, rifamycin SV, rifampicin, and clarithromycin [42], whereas OATP1B3 may also be inhibited by cyclosporin A and rifampicin [92]. Bilirubin is also a substrate of OATP1B1 [35, 36], so the inhibition of OATP1B1 causes the hyperbilirubinemia. Campbell *et al.* [225] have shown that the potency of several compounds that inhibited OATP1B1-mediated transport was correlated well with the incidence of drug-induced hyperbilirubinemia. In another example, clearance of theophylline was decreased after coadministration of erythromycin, which is thought to be partly caused by inhibition of OAT2-mediated uptake of theophylline by erythromycin [226, 227].

The drug-induced change in the expression levels of transporters also modifies the pharmacokinetics of substrate drugs. Though detailed mechanisms have not been explained yet, after repetitive dosing of rifampicin, efavirenz, and ritonavir + saquinavir, the plasma concentration of pravastatin was decreased [228–230]. Because all compounds are PXR ligands, OATP1B1 may be induced by PXR-mediated mechanism and uptake clearance of substrate drugs may be increased.

11.7.2
Effect of Drugs on the Activity of Efflux Transporters Located on the Bile Canalicular Membrane

A variety of inhibitory effects of drugs on the function of efflux transporters in the bile canalicular membrane have also been reported. Though much of the severe drug-induced cholestasis results from immune reactions, part may also be caused by the inhibition of BSEP [11, 231]. Cyclosporin A, rifamycin SV rifampicin, and glibenclamide were reported to *cis*-inhibit the BSEP function in BSEP-expressing membrane vesicles [105]. Bosentan (endothelin antagonist) also often causes cholestasis in humans. The bosentan-induced cholestasis was reported to be reproduced in rats, and bosentan and its metabolite (Ro-47-8634) could inhibit the BSEP-mediated taurocholate transport with Ki values of 12 and 8.5 microM, respectively [105]. Though the predicted plasma concentration of bosentan does not reach its Ki value, its inhibition of the BSEP-mediated efflux of bile acids may contribute to the expression of cholestasis. Troglitazone was withdrawn from the market due to the expression of lethal hepatotoxicity. Though detailed mechanisms have not been clarified, troglitazone and its sulfate potently inhibited the BSEP function [232]. Male rats were shown to have higher troglitazone sulfate levels than those in female rats (due to a higher sulfotransferase activity in male rats), thus more profound cholestasis seen in males after troglitazone administration might be caused by an inhibition of BSEP by troglitazone sulfate [233].

Several experimental systems to check the inhibition potency of bile acid transport have been characterized. Using sandwich-cultured human hepatocytes, bosentan, cyclosporin A, CI-1034 (endothelin-A receptor antagonist), glyburide, erythromycin estolate, and troleandomycin could inhibit the taurocholate efflux to the bile pocket [234]. Moreover, Mita *et al.* [235] constructed NTCP/BSEP double-transfected cells and some cholestasis-induced compounds inhibited both the NTCP-mediated uptake and the BSEP-mediated efflux of taurocholate. Then, they have found fluorescent bile acids whose transcellular transport was clearly observed, which may be used for the rapid identification of inhibitors of NTCP and BSEP in drug screening process [235].

Previous reports have suggested that BSEP may be transinhibited by Mrp2 substrates such as $E_2$17βG by comparing the inhibitory effect of Mrp2 substrates on BSEP function in isolated bile canalicular membrane vesicles in normal and Mrp2-deficient EHBRs and in membrane vesicles expressing only BSEP and those expressing both BSEP and MRP2 [236, 237]. The finding that MRP2 substrates with a cholestatic nature do not cause cholestasis in EHBRs might be consistent with this hypothesis [238].

Regarding the drug–drug interaction, SN-38 is formed in hepatocytes following the hydrolysis of irinotecan and then excreted into the bile. The severe diarrhea is one of the dose-limiting toxicity for irinotecan. One of the reasons for that toxicity is the high exposure of SN-38 in the intestine. Because SN-38 is excreted into bile mainly via MRP2 [94, 239, 240], Horikawa *et al.* [241] have proposed that inhibition of the biliary excretion of SN-38 by pronebecid, an inhibitor for MRP2, causes a reduction in the incidence of diarrhea but does not affect plasma concentration of SN-38. Thus, it is possible to control adverse reactions of irinotecan by utilizing the drug–drug interaction mediated by efflux transporter, MRP2.

Drug interaction between digoxin and quinidine has been reported previously [242]. Quinidine reduced both renal and biliary excretion of digoxin. The Ki value of quinidine for MDR1-mediated efflux was assumed to be 5 microM [243]. However, the maximum unbound plasma concentration of quinidine at the inlet to the liver is estimated to be 4 microM, which suggests that quinidine may inhibit the MDR1-mediated efflux of digoxin due to the similar concentration to Ki value and possible accumulation of quinidine into hepatocytes [244].

11.7.3
Prediction of Drug–Drug Interaction from *In Vitro* Data

If the unbound drug concentrations in plasma (In) are higher than the Ki values for transporters, transporter function may be significantly decreased [244]. To predict the potency of drug–drug interaction quantitatively, the estimation of the inhibitor concentration at the interacting site (e.g., vicinity of transporters) should be needed. To avoid the false-negative prediction, Ito *et al.* [245] have proposed the equation for the calculation of the maximum unbound concentration of inhibitor at the inlet to the liver. For the accurate prediction, physiologically based pharmacokinetic models for both substrates and inhibitors should be constructed, and the plasma concentration–time profiles of substrates and inhibitors can be simulated [75]. The possible target sites of drug interaction in the liver are uptake and efflux processes. However, it is fairly difficult to discriminate which processes are responsible for its interaction.

Ueda *et al.* [246] have established the quantitative prediction method for alteration in pharmacokinetics of drugs caused by the inhibition of uptake as well as efflux transport. They tried to predict the drug–drug interaction between methotrexate and probenecid (Figure 11.10). In this strategy, the inhibitory effect of probenecid for the hepatic uptake of methotrexate was evaluated by using the isolated rat hepatocytes and that for its biliary excretion was examined by bile CMVs. The degree of inhibition of the uptake and efflux processes *in vivo* was comparable to that predicted from *in vitro* experiments. Then, R values $(= 1 + \frac{\mathrm{In}}{\mathrm{Ki}})$ for uptake (R_{uptake}) and efflux process ($R_{\mathrm{excretion}}$) could be calculated. The net degree of inhibition (R_{net}) can be described by the following equation:

$$R_{\mathrm{net}} \leq R_{\mathrm{uptake}} \times R_{\mathrm{excretion}}. \tag{11.6}$$

They showed that the degree of the reduction in the hepatic clearance was overestimated by a simple calculation of the product of the reduction in the hepatic uptake and biliary excretion (Equation 11.6) and this method is useful to avoid the false-negative predictions [246].

11.8
Concluding Remarks

The information summarized in this chapter describes how transporters play an important role in the hepatobiliary excretion of drugs, which is also one of the

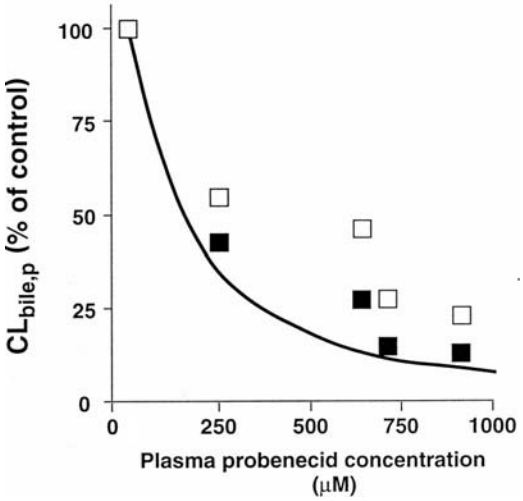

Figure 11.10 Extrapolation of the drug interaction involving both hepatic uptake and biliary excretion processes from *in vitro* data [246]. *Y*-axis represents the biliary excretion clearance of methotrexate in the presence of several concentrations of probenecid with respect to circulating plasma. Open square shows the $CL_{bile,p}$ values of methotrexate observed *in vivo*. Closed square and solid line represent the predicted $CL_{bile,p}$ values derived from intrinsic biliary excretion clearance estimated by using the unbound concentration of the inhibitor in the liver and in the plasma, respectively.

determinants for the bioavailability of drugs. The several *in vitro* systems may be useful for identifying the substrates and inhibitors for each transporter with desired transport properties during the screening of drug candidates. By utilizing these *in vitro* data, we can construct the physiologically-based pharmacokinetic (PBPK) model to predict the time-dependent whole-body pharmacokinetics *in vivo* by integrating the kinetic parameters for each transporter and metabolic enzyme and physiological parameters such as blood flow rate and protein unbound fraction of drugs in plasma into the model. Because especially in humans, it is impossible to measure the concentration in each tissue and the site of actions, it is useful to predict the pharmacological and toxicological effects of drugs by PBPK modeling [75]. Also, with the aid of positron emission tomography (PET) or single-photon emission computed tomography (SPECT), we can obtain the detailed data on tissue distribution directly in humans. Some reports have succeeded in quantifying the drug concentration in human brain [247, 248]. In the field of metabolic enzymes, a set of "probe drug," which is a specific substrate of each enzyme, has been established and metabolic activities of specific P450s can be directly estimated in human *in vivo* condition by measuring the metabolites in the blood and urine after administration of several kinds of probe drugs ("cocktail approach") [249]. To establish a set of clinically applicable probe drug and evaluation method for each transporter is important for the phenotyping of transporter function in humans. Utilizing these tools, more accurate prediction of the transport function and pharmacokinetics of drugs will be realized in future.

References

1 Pauli-Magnus, C. and Meier, P.J. (2006) Hepatobiliary transporters and drug-induced cholestasis. *Hepatology (Baltimore, Md.)*, **44**, 778–787.

2 Shitara, Y., Horie, T. and Sugiyama, Y. (2006) Transporters as a determinant of drug clearance and tissue distribution. *European Journal of Pharmaceutical Sciences*, **27**, 425–446.

3 Annaert, P., Swift, B., Lee, J.K. and Brouwer, K.L.R. (2007) Drug transport in the liver, in *Drug Transporters* (eds G. You and M.E. Morris), John Wiley & Sons, Inc., New Jersey, pp. 359–410.

4 Choudhuri, S. and Klaassen, C.D. (2006) Structure, function, expression, genomic organization, and single nucleotide polymorphisms of human ABCB1 (MDR1), ABCC (MRP), and ABCG2 (BCRP) efflux transporters. *International Journal of Toxicology*, **25**, 231–259.

5 Kruh, G.D., Belinsky, M.G., Gallo, J.M. and Lee, K. (2007) Physiological and pharmacological functions of Mrp2, Mrp3 and Mrp4 as determined from recent studies on gene-disrupted mice. *Cancer Metastasis Reviews*, **26**, 5–14.

6 Borst, P., de Wolf, C. and van de Wetering, K. (2007) Multidrug resistance-associated proteins 3, 4, and 5. *Pflugers Archiv: European Journal of Physiology*, **453**, 661–673.

7 Hagenbuch, B. and Meier, P.J. (1994) Molecular cloning, chromosomal localization, and functional characterization of a human liver Na+/bile acid cotransporter. *The Journal of Clinical Investigation*, **93**, 1326–1331.

8 Hagenbuch, B., Stieger, B., Foguet, M., Lubbert, H. and Meier, P.J. (1991) Functional expression cloning and characterization of the hepatocyte Na+/bile acid cotransport system. *Proceedings of the National Academy of Sciences of the United States of America*, **88**, 10629–10633.

9 Maeda, K., Kambara, M., Tian, Y., Hofmann, A.F. and Sugiyama, Y. (2006) Uptake of ursodeoxycholate and its conjugates by human hepatocytes: role of Na(+)-taurocholate cotransporting polypeptide (NTCP), organic anion transporting polypeptide (OATP) 1B1 (OATP-C), and oatp1B3 (OATP8). *Molecular Pharmaceutics*, **3**, 70–77.

10 Eloranta, J. and Kullak-Ublick, G. (2007) Bile acid transporters, in *Drug Transporters* (eds G. You and M. Morris), John Wiley & Sons, Inc., New Jersey, pp. 201–222.

11 Meier, P.J. and Stieger, B. (2002) Bile salt transporters. *Annual Review of Physiology*, **64**, 635–661.

12 Mita, S., Suzuki, H., Akita, H., Hayashi, H., Onuki, R., Hofmann, A.F. and Sugiyama, Y. (2006) Vectorial transport of unconjugated and conjugated bile salts by monolayers of LLC-PK1 cells doubly transfected with human NTCP and BSEP or with rat Ntcp and Bsep. *American Journal of Physiology. Gastrointestinal and Liver Physiology*, **290**, G550–G556.

13 Meier, P.J., Eckhardt, U., Schroeder, A., Hagenbuch, B. and Stieger, B. (1997) Substrate specificity of sinusoidal bile acid and organic anion uptake systems in rat and human liver. *Hepatology (Baltimore, Md.)*, **26**, 1667–1677.

14 Friesema, E.C., Docter, R., Moerings, E.P., Stieger, B., Hagenbuch, B., Meier, P.J., Krenning, E.P., Hennemann, G. and Visser, T.J. (1999) Identification of thyroid hormone transporters. *Biochemical and Biophysical Research Communications*, **254**, 497–501.

15 Gundala, S., Wells, L.D., Milliano, M.T., Talkad, V., Luxon, B.A. and Neuschwander-Tetri, B.A. (2004) The hepatocellular bile acid transporter Ntcp facilitates uptake of the lethal mushroom toxin alpha-amanitin. *Archives of Toxicology*, **78**, 68–73.

16 Ho, R.H., Tirona, R.G., Leake, B.F., Glaeser, H., Lee, W., Lemke, C.J., Wang, Y. and Kim, R.B. (2006) Drug and bile acid transporters in rosuvastatin hepatic

uptake: function, expression, and pharmacogenetics. *Gastroenterology*, **130**, 1793–1806.

17 Petzinger, E., Blumrich, M., Bruhl, B., Eckhardt, U., Follmann, W., Honscha, W., Horz, J.A., Muller, N., Nickau, L., Ottallah-Kolac, M., Platte, H.D., Schenk, A., Schuh, K., Schulz, K. and Schulz, S. (1996) What we have learned about bumetanide and the concept of multispecific bile acid/drug transporters from the liver. *Journal of Hepatology*, **24** (Suppl. 1), 42–46.

18 Niemi, M. (2007) Role of OATP transporters in the disposition of drugs. *Pharmacogenomics*, **8**, 787–802.

19 Smith, N.F., Figg, W.D. and Sparreboom, A. (2005) Role of the liver-specific transporters OATP1B1 and OATP1B3 in governing drug elimination. *Expert Opinion on Drug Metabolism and Toxicology*, **1**, 429–445.

20 Hagenbuch, B. and Meier, P.J. (2004) Organic anion transporting polypeptides of the OATP/SLC21 family: phylogenetic classification as OATP/SLCO superfamily, new nomenclature and molecular/functional properties. *Pflugers Archiv: European Journal of Physiology*, **447**, 653–665.

21 Jacquemin, E., Hagenbuch, B., Stieger, B., Wolkoff, A.W. and Meier, P.J. (1994) Expression cloning of a rat liver Na(+)-independent organic anion transporter. *Proceedings of the National Academy of Sciences of the United States of America*, **91**, 133–137.

22 Noe, B., Hagenbuch, B., Stieger, B. and Meier, P.J. (1997) Isolation of a multispecific organic anion and cardiac glycoside transporter from rat brain. *Proceedings of the National Academy of Sciences of the United States of America*, **94**, 10346–10350.

23 Cattori, V., Hagenbuch, B., Hagenbuch, N., Stieger, B., Ha, R., Winterhalter, K.E. and Meier, P.J. (2000) Identification of organic anion transporting polypeptide 4 (Oatp4) as a major full-length isoform of the liver-specific transporter-1 (rlst-1) in rat liver. *FEBS Letters*, **474**, 242–245.

24 Konig, J., Cui, Y., Nies, A.T. and Keppler, D. (2000) A novel human organic anion transporting polypeptide localized to the basolateral hepatocyte membrane. *American Journal of Physiology. Gastrointestinal and Liver Physiology*, **278**, G156–G164.

25 Hsiang, B., Zhu, Y., Wang, Z., Wu, Y., Sasseville, V., Yang, W.P. and Kirchgessner, T.G. (1999) A novel human hepatic organic anion transporting polypeptide (OATP2). Identification of a liver-specific human organic anion transporting polypeptide and identification of rat and human hydroxymethylglutaryl-CoA reductase inhibitor transporters. *The Journal of Biological Chemistry*, **274**, 37161–37168.

26 Abe, T., Kakyo, M., Tokui, T., Nakagomi, R., Nishio, T., Nakai, D., Nomura, H., Unno, M., Suzuki, M., Naitoh, T., Matsuno, S. and Yawo, H. (1999) Identification of a novel gene family encoding human liver-specific organic anion transporter LST-1. *The Journal of Biological Chemistry*, **274**, 17159–17163.

27 Konig, J., Cui, Y., Nies, A.T. and Keppler, D. (2000) Localization and genomic organization of a new hepatocellular organic anion transporting polypeptide. *The Journal of Biological Chemistry*, **275**, 23161–23168.

28 Abe, T., Unno, M., Onogawa, T., Tokui, T., Kondo, T.N., Nakagomi, R., Adachi, H., Fujiwara, K., Okabe, M., Suzuki, T., Nunoki, K., Sato, E., Kakyo, M., Nishio, T., Sugita, J., Asano, N., Tanemoto, M., Seki, M., Date, F., Ono, K., Kondo, Y., Shiiba, K., Suzuki, M., Ohtani, H., Shimosegawa, T., Iinuma, K., Nagura, H., Ito, S. and Matsuno, S. (2001) LST-2, a human liver-specific organic anion transporter, determines methotrexate sensitivity in gastrointestinal cancers. *Gastroenterology*, **120** 1689–1699.

29 Kullak-Ublick, G.A., Ismair, M.G., Stieger, B., Landmann, L., Huber, R.,

Pizzagalli, F., Fattinger, K., Meier, P.J. and Hagenbuch, B. (2001) Organic anion-transporting polypeptide B (OATP-B) and its functional comparison with three other OATPs of human liver. *Gastroenterology*, **120**, 525–533.

30 Ismair, M.G., Stieger, B., Cattori, V., Hagenbuch, B., Fried, M., Meier, P.J. and Kullak-Ublick, G.A. (2001) Hepatic uptake of cholecystokinin octapeptide by organic anion-transporting polypeptides OATP4 and OATP8 of rat and human liver. *Gastroenterology*, **121**, 1185–1190.

31 Yamashiro, W., Maeda, K., Hirouchi, M., Adachi, Y., Hu, Z. and Sugiyama, Y. (2006) Involvement of transporters in the hepatic uptake and biliary excretion of valsartan, a selective antagonist of the angiotensin II AT1-receptor, in humans. *Drug Metabolism and Disposition: The Biological Fate of Chemicals*, **34**, 1247–1254.

32 Ishiguro, N., Maeda, K., Kishimoto, W., Saito, A., Harada, A., Ebner, T., Roth, W., Igarashi, T. and Sugiyama, Y. (2006) Predominant contribution of OATP1B3 to the hepatic uptake of telmisartan, an angiotensin II receptor antagonist, in humans. *Drug Metabolism and Disposition: The Biological Fate of Chemicals*, **34**, 1109–1115.

33 Yamada, A., Maeda, K., Kamiyama, E., Sugiyama, D., Kondo, T., Shiroyanagi, Y., Nakazawa, H., Okano, T., Adachi, M., Schuetz, J.D., Adachi, Y., Hu, Z., Kusuhara, H. and Sugiyama, Y. (2007) Multiple human isoforms of drug transporters contribute to the hepatic and renal transport of olmesartan, a selective antagonist of the angiotensin II AT1-receptor. *Drug Metabolism and Disposition: The Biological Fate of Chemicals*, **35**, 2166–2176.

34 Nakagomi-Hagihara, R., Nakai, D., Kawai, K., Yoshigae, Y., Tokui, T., Abe, T. and Ikeda, T. (2006) OATP1B1, OATP1B3, and mrp2 are involved in hepatobiliary transport of olmesartan, a novel angiotensin II blocker. *Drug Metabolism and Disposition: The Biological Fate of Chemicals*, **34**, 862–869.

35 Cui, Y., Konig, J., Leier, I., Buchholz, U. and Keppler, D. (2001) Hepatic uptake of bilirubin and its conjugates by the human organic anion transporter SLC21A6. *The Journal of Biological Chemistry*, **276**, 9626–9630.

36 Briz, O., Serrano, M.A., MacIas, R.I., Gonzalez-Gallego, J. and Marin, J.J. (2003) Role of organic anion-transporting polypeptides, OATP-A, OATP-C and OATP-8, in the human placenta-maternal liver tandem excretory pathway for foetal bilirubin. *The Biochemical Journal*, **371**, 897–905.

37 Wang, P., Kim, R.B., Chowdhury, J.R. and Wolkoff, A.W. (2003) The human organic anion transport protein SLC21A6 is not sufficient for bilirubin transport. *The Journal of Biological Chemistry*, **278**, 20695–20699.

38 van Montfoort, J.E., Hagenbuch, B., Fattinger, K.E., Muller, M., Groothuis, G.M., Meijer, D.K. and Meier, P.J. (1999) Polyspecific organic anion transporting polypeptides mediate hepatic uptake of amphipathic type II organic cations. *The Journal of Pharmacology and Experimental Therapeutics*, **291**, 147–152.

39 Satoh, H., Yamashita, F., Tsujimoto, M., Murakami, H., Koyabu, N., Ohtani, H. and Sawada, Y. (2005) Citrus juices inhibit the function of human organic anion-transporting polypeptide OATP-B. *Drug Metabolism and Disposition: The Biological Fate of Chemicals*, **33**, 518–523.

40 Kobayashi, D., Nozawa, T., Imai, K., Nezu, J., Tsuji, A. and Tamai, I. (2003) Involvement of human organic anion transporting polypeptide OATP-B (SLC21A9) in pH-dependent transport across intestinal apical membrane. *The Journal of Pharmacology and Experimental Therapeutics*, **306**, 703–708.

41 Grube, M., Kock, K., Oswald, S., Draber, K., Meissner, K., Eckel, L., Bohm, M., Felix, S.B., Vogelgesang, S., Jedlitschky, G., Siegmund, W., Warzok, R. and Kroemer,

H.K. (2006) Organic anion transporting polypeptide 2B1 is a high-affinity transporter for atorvastatin and is expressed in the human heart. *Clinical Pharmacology and Therapeutics*, **80**, 607–620.

42 Hirano, M., Maeda, K., Shitara, Y. and Sugiyama, Y. (2006) Drug–drug interaction between pitavastatin and various drugs via OATP1B1. *Drug Metabolism and Disposition: The Biological Fate of Chemicals*, **34**, 1229–1236.

43 Mikkaichi, T., Suzuki, T., Tanemoto, M., Ito, S. and Abe, T. (2004) The organic anion transporter (OATP) family. *Drug Metabolism and Pharmacokinetics*, **19**, 171–179.

44 Sun, W., Wu, R.R., van Poelje, P.D. and Erion, M.D. (2001) Isolation of a family of organic anion transporters from human liver and kidney. *Biochemical and Biophysical Research Communications*, **283**, 417–422.

45 Rizwan, A.N. and Burckhardt, G. (2007) Organic anion transporters of the SLC22 family: biopharmaceutical, physiological, and pathological roles. *Pharmaceutical Research*, **24**, 450–470.

46 Kusuhara, H., Sekine, T., Utsunomiya-Tate, N., Tsuda, M., Kojima, R., Cha, S.H., Sugiyama, Y., Kanai, Y. and Endou, H. (1999) Molecular cloning and characterization of a new multispecific organic anion transporter from rat brain. *The Journal of Biological Chemistry*, **274**, 13675–13680.

47 Cha, S.H., Sekine, T., Fukushima, J.I., Kanai, Y., Kobayashi, Y., Goya, T. and Endou, H. (2001) Identification and characterization of human organic anion transporter 3 expressing predominantly in the kidney. *Molecular Pharmacology*, **59**, 1277–1286.

48 Sweet, D.H., Miller, D.S., Pritchard, J.B., Fujiwara, Y., Beier, D.R. and Nigam, S.K. (2002) Impaired organic anion transport in kidney and choroid plexus of organic anion transporter 3 (Oat3 (Slc22a8)) knockout mice. *The Journal of Biological Chemistry*, **277**, 26934–26943.

49 Eraly, S.A. and Nigam, S.K. (2002) Novel human cDNAs homologous to Drosophila Orct and mammalian carnitine transporters. *Biochemical and Biophysical Research Communications*, **297**, 1159–1166.

50 Shin, H.J., Anzai, N., Enomoto, A., He, X., Kim do, K., Endou, H. and Kanai, Y. (2007) Novel liver-specific organic anion transporter OAT7 that operates the exchange of sulfate conjugates for short chain fatty acid butyrate. *Hepatology (Baltimore, Md.)*, **45**, 1046–1055.

51 Gorboulev, V., Ulzheimer, J.C., Akhoundova, A., Ulzheimer-Teuber, I., Karbach, U., Quester, S., Baumann, C., Lang, F., Busch, A.E. and Koepsell, H. (1997) Cloning and characterization of two human polyspecific organic cation transporters. *DNA and Cell Biology*, **16**, 871–881.

52 Koepsell, H., Lips, K. and Volk, C. (2007) Polyspecific organic cation transporters: structure, function, physiological roles, and biopharmaceutical implications. *Pharmaceutical Research*, **24**, 1227–1251.

53 Jonker, J.W., Wagenaar, E., Mol, C.A., Buitelaar, M., Koepsell, H., Smit, J.W. and Schinkel, A.H. (2001) Reduced hepatic uptake and intestinal excretion of organic cations in mice with a targeted disruption of the organic cation transporter 1 (Oct1 [Slc22a1]) gene. *Molecular and Cellular Biology*, **21**, 5471–5477.

54 Grundemann, D., Liebich, G., Kiefer, N., Koster, S. and Schomig, E. (1999) Selective substrates for non-neuronal monoamine transporters. *Molecular Pharmacology*, **56**, 1–10.

55 Nakamura, H., Sano, H., Yamazaki, M. and Sugiyama, Y. (1994) Carrier-mediated active transport of histamine H2 receptor antagonists, cimetidine and nizatidine, into isolated rat hepatocytes: contribution of type I system. *The Journal of Pharmacology and Experimental Therapeutics*, **269**, 1220–1227.

56 Wang, D.S., Jonker, J.W., Kato, Y., Kusuhara, H., Schinkel, A.H. and

Sugiyama, Y. (2002) Involvement of organic cation transporter 1 in hepatic and intestinal distribution of metformin. *The Journal of Pharmacology and Experimental Therapeutics*, **302**, 510–515.

57 Wang, D.S., Kusuhara, H., Kato, Y., Jonker, J.W., Schinkel, A.H. and Sugiyama, Y. (2003) Involvement of organic cation transporter 1 in the lactic acidosis caused by metformin. *Molecular Pharmacology*, **63**, 844–848.

58 Croop, J.M., Raymond, M., Haber, D., Devault, A., Arceci, R.J., Gros, P. and Housman, D.E. (1989) The three mouse multidrug resistance (mdr) genes are expressed in a tissue-specific manner in normal mouse tissues. *Molecular and Cellular Biology*, **9**, 1346–1350.

59 Gottesman, M.M. and Pastan, I. (1993) Biochemistry of multidrug resistance mediated by the multidrug transporter. *Annual Review of Biochemistry*, **62**, 385–427.

60 Schinkel, A.H. (1997) The physiological function of drug-transporting P-glycoproteins. *Seminars in Cancer Biology*, **8**, 161–170.

61 Lin, J.H. and Yamazaki, M. (2003) Role of P-glycoprotein in pharmacokinetics: clinical implications. *Clinical Pharmacokinetics*, **42**, 59–98.

62 Cvetkovic, M., Leake, B., Fromm, M.F., Wilkinson, G.R. and Kim, R.B. (1999) OATP and P-glycoprotein transporters mediate the cellular uptake and excretion of fexofenadine. *Drug Metabolism and Disposition: The Biological Fate of Chemicals*, **27**, 866–871.

63 Huang, L., Hoffman, T. and Vore, M. (1998) Adenosine triphosphate-dependent transport of estradiol-17beta (beta-D-glucuronide) in membrane vesicles by MDR1 expressed in insect cells. *Hepatology (Baltimore, Md.)*, **28**, 1371–1377.

64 Matsushima, S., Maeda, K., Kondo, C., Hirano, M., Sasaki, M., Suzuki, H. and Sugiyama, Y. (2005) Identification of the hepatic efflux transporters of organic anions using double-transfected Madin–Darby canine kidney II cells expressing human organic anion-transporting polypeptide 1B1 (OATP1B1)/multidrug resistance-associated protein 2, OATP1B1/multidrug resistance 1, and OATP1B1/breast cancer resistance protein. *The Journal of Pharmacology and Experimental Therapeutics*, **314**, 1059–1067.

65 Cordon-Cardo, C., O'Brien, J.P., Boccia, J., Casals, D., Bertino, J.R. and Melamed, M.R. (1990) Expression of the multidrug resistance gene product (P-glycoprotein) in human normal and tumor tissues. *The Journal of Histochemistry and Cytochemistry*, **38**, 1277–1287.

66 Schinkel, A.H., Smit, J.J., van Tellingen, O., Beijnen, J.H., Wagenaar, E., van Deemter, L., Mol, C.A., van der Valk, M.A., Robanus-Maandag, E.C., te Riele, H.P.,*et al.* (1994) Disruption of the mouse mdr1a P-glycoprotein gene leads to a deficiency in the blood–brain barrier and to increased sensitivity to drugs. *Cell*, **77**, 491–502.

67 Schinkel, A.H., Mayer, U., Wagenaar, E., Mol, C.A., van Deemter, L., Smit, J.J., van der Valk, M.A., Voordouw, A.C., Spits, H., van Tellingen, O., Zijlmans, J.M., Fibbe, W.E. and Borst, P. (1997) Normal viability and altered pharmacokinetics in mice lacking mdr1-type (drug-transporting) P-glycoproteins. *Proceedings of the National Academy of Sciences of the United States of America*, **94**, 4028–4033.

68 Smit, J.W., Schinkel, A.H., Weert, B. and Meijer, D.K. (1998) Hepatobiliary and intestinal clearance of amphiphilic cationic drugs in mice in which both mdr1a and mdr1b genes have been disrupted. *British Journal of Pharmacology*, **124**, 416–424.

69 Kawahara, M., Sakata, A., Miyashita, T., Tamai, I. and Tsuji, A. (1999) Physiologically based pharmacokinetics of digoxin in mdr1a knockout mice. *Journal of Pharmaceutical Sciences*, **88**, 1281–1287.

70 van Asperen, J., van Tellingen, O. and Beijnen, J.H. (2000) The role of mdr1a P-glycoprotein in the biliary and intestinal secretion of doxorubicin and vinblastine in mice. *Drug Metabolism and Disposition: The Biological Fate of Chemicals*, **28**, 264–267.

71 Oude Elferink, R.P. and Paulusma, C.C. (2007) Function and pathophysiological importance of ABCB4 (MDR3 P-glycoprotein). *Pflugers Archiv: European Journal of Physiology*, **453**, 601–610.

72 Buchler, M., Konig, J., Brom, M., Kartenbeck, J., Spring, H., Horie, T. and Keppler, D. (1996) cDNA cloning of the hepatocyte canalicular isoform of the multidrug resistance protein, cMrp, reveals a novel conjugate export pump deficient in hyperbilirubinemic mutant rats. *The Journal of Biological Chemistry*, **271**, 15091–15098.

73 Ito, K., Suzuki, H., Hirohashi, T., Kume, K., Shimizu, T. and Sugiyama, Y. (1997) Molecular cloning of canalicular multispecific organic anion transporter defective in EHBR. *The American Journal of Physiology*, **272**, G16–G22.

74 Nies, A.T. and Keppler, D. (2007) The apical conjugate efflux pump ABCC2 (MRP2). *Pflugers Archiv: European Journal of Physiology*, **453**, 643–659.

75 Shitara, Y. and Sugiyama, Y. (2006) Pharmacokinetic and pharmacodynamic alterations of 3-hydroxy-3-methylglutaryl coenzyme A (HMG-CoA) reductase inhibitors: drug–drug interactions and interindividual differences in transporter and metabolic enzyme functions. *Pharmacology & Therapeutics*, **112**, 71–105.

76 Herling, A.W., Schwab, D., Burger, H.J., Maas, J., Hammerl, R., Schmidt, D., Strohschein, S., Hemmerle, H., Schubert, G., Petry, S. and Kramer, W. (2002) Prolonged blood glucose reduction in mrp-2 deficient rats (GY/TR$^-$) by the glucose-6-phosphate translocase inhibitor S 3025. *Biochimica et Biophysica Acta*, **1569**, 105–110.

77 Fernandez-Checa, J.C., Takikawa, H., Horie, T., Ookhtens, M. and Kaplowitz, N. (1992) Canalicular transport of reduced glutathione in normal and mutant Eisai hyperbilirubinemic rats. *The Journal of Biological Chemistry*, **267**, 1667–1673.

78 Paulusma, C.C., van Geer, M.A., Evers, R., Heijn, M., Ottenhoff, R., Borst, P. and Oude Elferink, R.P. (1999) Canalicular multispecific organic anion transporter/multidrug resistance protein 2 mediates low-affinity transport of reduced glutathione. *The Biochemical Journal*, **338** (Pt 2), 393–401.

79 Elferink, R.O. and Groen, A.K. (2002) Genetic defects in hepatobiliary transport. *Biochimica et Biophysica Acta*, **1586**, 129–145.

80 Ishizuka, H., Konno, K., Shiina, T., Naganuma, H., Nishimura, K., Ito, K., Suzuki, H. and Sugiyama, Y. (1999) Species differences in the transport activity for organic anions across the bile canalicular membrane. *The Journal of Pharmacology and Experimental Therapeutics*, **290**, 1324–1330.

81 Niinuma, K., Kato, Y., Suzuki, H., Tyson, C.A., Weizer, V., Dabbs, J.E., Froehlich, R., Green, C.E. and Sugiyama, Y. (1999) Primary active transport of organic anions on bile canalicular membrane in humans. *The American Journal of Physiology*, **276**, G1153–G1164.

82 Ninomiya, M., Ito, K., Hiramatsu, R. and Horie, T. (2006) Functional analysis of mouse and monkey multidrug resistance-associated protein 2 (Mrp2). *Drug Metabolism and Disposition: The Biological Fate of Chemicals*, **34**, 2056–2063.

83 Zimmermann, C., van de Wetering, K., van de Steeg, E., Wagenaar, E., Vens, C. and Schinkel, A.H. (2008) Species-dependent transport and modulation properties of human and mouse multidrug resistance protein 2 (MRP2/Mrp2, ABCC2/Abcc2). *Drug Metabolism and Disposition: The Biological Fate of Chemicals*, **36**, 631–640.

84 Chu, X.Y., Strauss, J.R., Mariano, M.A., Li, J., Newton, D.J., Cai, X., Wang, R.W.,

Yabut, J., Hartley, D.P., Evans, D.C. and Evers, R. (2006) Characterization of mice lacking the multidrug resistance protein MRP2 (ABCC2). *The Journal of Pharmacology and Experimental Therapeutics*, **317**, 579–589.

85 Zamek-Gliszczynski, M.J., Nezasa, K., Tian, X., Kalvass, J.C., Patel, N.J., Raub, T.J. and Brouwer, K.L. (2006) The important role of Bcrp (Abcg2) in the biliary excretion of sulfate and glucuronide metabolites of acetaminophen, 4-methylumbelliferone, and harmol in mice. *Molecular Pharmacology*, **70**, 2127–2133.

86 Takenaka, O., Horie, T., Kobayashi, K., Suzuki, H. and Sugiyama, Y. (1995) Kinetic analysis of hepatobiliary transport for conjugated metabolites in the perfused liver of mutant rats (EHBR) with hereditary conjugated hyperbilirubinemia. *Pharmaceutical Research*, **12**, 1746–1755.

87 Xiong, H., Turner, K.C., Ward, E.S., Jansen, P.L. and Brouwer, K.L. (2000) Altered hepatobiliary disposition of acetaminophen glucuronide in isolated perfused livers from multidrug resistance-associated protein 2-deficient TR(-) rats. *The Journal of Pharmacology and Experimental Therapeutics*, **295**, 512–518.

88 Ogasawara, T. and Takikawa, H. (2001) Biliary excretion of phenolphthalein glucuronide in the rat. *Hepatology Research*, **20**, 221–231.

89 Zamek-Gliszczynski, M.J., Hoffmaster, K.A., Humphreys, J.E., Tian, X., Nezasa, K. and Brouwer, K.L. (2006) Differential involvement of Mrp2 (Abcc2) and Bcrp (Abcg2) in biliary excretion of 4-methylumbelliferyl glucuronide and sulfate in the rat. *The Journal of Pharmacology and Experimental Therapeutics*, **319**, 459–467.

90 Tahara, H., Kusuhara, H., Fuse, E. and Sugiyama, Y. (2005) P-glycoprotein plays a major role in the efflux of fexofenadine in the small intestine and blood–brain barrier, but only a limited role in its biliary excretion. *Drug Metabolism and Disposition: The Biological Fate of Chemicals*, **33**, 963–968.

91 Tian, X., Zamek-Gliszczynski, M.J., Li, J., Bridges, A.S., Nezasa, K., Patel, N.J., Raub, T.J. and Brouwer, K.L. (2008) Multidrug resistance-associated protein 2 is primarily responsible for the biliary excretion of fexofenadine in mice. *Drug Metabolism and Disposition: The Biological Fate of Chemicals*, **36**, 61–64.

92 Matsushima, S., Maeda, K., Hayashi, H., Debori, Y., Schinkel, A.H., Schuetz, J.D., Kusuhara, H. and Sugiyama, Y. (2008) Involvement of multiple efflux transporters in hepatic disposition of fexofenadine. *Molecular Pharmacology*, **73**, 1474–1483.

93 Vlaming, M.L., Mohrmann, K., Wagenaar, E., de Waart, D.R., Elferink, R.P., Lagas, J.S., van Tellingen, O., Vainchtein, L.D., Rosing, H., Beijnen, J.H., Schellens, J.H. and Schinkel, A.H. (2006) Carcinogen and anticancer drug transport by Mrp2 *in vivo*: studies using Mrp2 (Abcc2) knockout mice. *The Journal of Pharmacology and Experimental Therapeutics*, **318**, 319–327.

94 Chu, X.Y., Kato, Y., Niinuma, K., Sudo, K.I., Hakusui, H. and Sugiyama, Y. (1997) Multispecific organic anion transporter is responsible for the biliary excretion of the camptothecin derivative irinotecan and its metabolites in rats. *The Journal of Pharmacology and Experimental Therapeutics*, **281**, 304–314.

95 Mao, Q. and Unadkat, J.D. (2005) Role of the breast cancer resistance protein (ABCG2) in drug transport. *The Aaps Journal*, **7**, E118–E133.

96 Robey, R.W., Polgar, O., Deeken, J., To, K.K.W. and Bates, S.E. (2007) Breast cancer resistance protein, in *Drug Transporters* (eds G. You and M.E. Morris), John Wiley & Sons, Inc., New Jersey, pp. 319–358.

97 Hirano, M., Maeda, K., Matsushima, S., Nozaki, Y., Kusuhara, H. and Sugiyama, Y. (2005) Involvement of BCRP (ABCG2) in

the biliary excretion of pitavastatin. *Molecular Pharmacology*, **68**, 800–807.

98 Yamazaki, M., Kobayashi, K. and Sugiyama, Y. (1996) Primary active transport of pravastatin across the liver canalicular membrane in normal and mutant Eisai hyperbilirubinemic rats. *Biopharmaceutics & Drug Disposition*, **17**, 607–621.

99 Ando, T., Kusuhara, H., Merino, G., Alvarez, A.I., Schinkel, A.H. and Sugiyama, Y. (2007) Involvement of breast cancer resistance protein (ABCG2) in the biliary excretion mechanism of fluoroquinolones. *Drug Metabolism and Disposition: The Biological Fate of Chemicals*, **35**, 1873–1879.

100 Alrefai, W.A. and Gill, R.K. (2007) Bile acid transporters: structure, function, regulation and pathophysiological implications. *Pharmaceutical Research*, **24**, 1803–1823.

101 Stieger, B., Meier, Y. and Meier, P.J. (2007) The bile salt export pump. *Pflugers Archiv: European Journal of Physiology*, **453**, 611–620.

102 Strautnieks, S.S., Bull, L.N., Knisely, A.S., Kocoshis, S.A., Dahl, N., Arnell, H., Sokal, E., Dahan, K., Childs, S., Ling, V., Tanner, M.S., Kagalwalla, A.F., Nemeth, A., Pawlowska, J., Baker, A., Mieli-Vergani, G., Freimer, N.B., Gardiner, R.M. and Thompson, R.J. (1998) A gene encoding a liver-specific ABC transporter is mutated in progressive familial intrahepatic cholestasis. *Nature Genetics*, **20**, 233–238.

103 Hayashi, H., Takada, T., Suzuki, H., Akita, H. and Sugiyama, Y. (2005) Two common PFIC2 mutations are associated with the impaired membrane trafficking of BSEP/ABCB11. *Hepatology (Baltimore, Md.)*, **41**, 916–924.

104 Hayashi, H. and Sugiyama, Y. (2007) 4-Phenylbutyrate enhances the cell surface expression and the transport capacity of wild-type and mutated bile salt export pumps. *Hepatology (Baltimore, Md.)*, **45**, 1506–1516.

105 Fattinger, K., Funk, C., Pantze, M., Weber, C., Reichen, J., Stieger, B. and Meier, P.J. (2001) The endothelin antagonist bosentan inhibits the canalicular bile salt export pump: a potential mechanism for hepatic adverse reactions. *Clinical Pharmacology and Therapeutics*, **69**, 223–231.

106 Lecureur, V., Sun, D., Hargrove, P., Schuetz, E.G., Kim, R.B., Lan, L.B. and Schuetz, J.D. (2000) Cloning and expression of murine sister of P-glycoprotein reveals a more discriminating transporter than MDR1/P-glycoprotein. *Molecular Pharmacology*, **57**, 24–35.

107 Hirano, M., Maeda, K., Hayashi, H., Kusuhara, H. and Sugiyama, Y. (2005) Bile salt export pump (BSEP/ABCB11) can transport a nonbile acid substrate, pravastatin. *The Journal of Pharmacology and Experimental Therapeutics*, **314**, 876–882.

108 Omote, H., Hiasa, M., Matsumoto, T., Otsuka, M. and Moriyama, Y. (2006) The MATE proteins as fundamental transporters of metabolic and xenobiotic organic cations. *Trends in Pharmacological Sciences*, **27**, 587–593.

109 Otsuka, M., Matsumoto, T., Morimoto, R., Arioka, S., Omote, H. and Moriyama, Y. (2005) A human transporter protein that mediates the final excretion step for toxic organic cations. *Proceedings of the National Academy of Sciences of the United States of America*, **102**, 17923–17928.

110 Masuda, S., Terada, T., Yonezawa, A., Tanihara, Y., Kishimoto, K., Katsura, T., Ogawa, O. and Inui, K. (2006) Identification and functional characterization of a new human kidney-specific H+/organic cation antiporter, kidney-specific multidrug and toxin extrusion 2. *Journal of the American Society of Nephrology*, **17**, 2127–2135.

111 Ohta, K.Y., Inoue, K., Hayashi, Y. and Yuasa, H. (2006) Molecular identification and functional characterization of rat multidrug and toxin extrusion type transporter 1 as an organic cation/H+

antiporter in the kidney. *Drug Metabolism and Disposition: The Biological Fate of Chemicals*, **34**, 1868–1874.

112 Hiasa, M., Matsumoto, T., Komatsu, T. and Moriyama, Y. (2006) Wide variety of locations for rodent MATE1, a transporter protein that mediates the final excretion step for toxic organic cations. *American Journal of Physiology. Cell Physiology*, **291**, C678–C686.

113 Hiasa, M., Matsumoto, T., Komatsu, T., Omote, H. and Moriyama, Y. (2007) Functional characterization of testis-specific rodent multidrug and toxic compound extrusion 2, a class III MATE-type polyspecific H+/organic cation exporter. *American Journal of Physiology. Cell Physiology*, **293**, C1437–C1444.

114 Yokoo, S., Yonezawa, A., Masuda, S., Fukatsu, A., Katsura, T. and Inui, K. (2007) Differential contribution of organic cation transporters, OCT2 and MATE1, in platinum agent-induced nephrotoxicity. *Biochemical Pharmacology*, **74**, 477–487.

115 Tanihara, Y., Masuda, S., Sato, T., Katsura, T., Ogawa, O. and Inui, K. (2007) Substrate specificity of MATE1 and MATE2-K, human multidrug and toxin extrusions/H(+)-organic cation antiporters. *Biochemical Pharmacology*, **74**, 359–371.

116 Chen, Y., Zhang, S., Sorani, M. and Giacomini, K.M. (2007) Transport of paraquat by human organic cation transporters and multidrug and toxic compound extrusion family. *The Journal of Pharmacology and Experimental Therapeutics*, **322**, 695–700.

117 Hirohashi, T., Suzuki, H., Ito, K., Ogawa, K., Kume, K., Shimizu, T. and Sugiyama, Y. (1998) Hepatic expression of multidrug resistance-associated protein-like proteins maintained in Eisai hyperbilirubinemic rats. *Molecular Pharmacology*, **53**, 1068–1075.

118 Konig, J., Rost, D., Cui, Y. and Keppler, D. (1999) Characterization of the human multidrug resistance protein isoform MRP3 localized to the basolateral hepatocyte membrane. *Hepatology (Baltimore, Md.)*, **29**, 1156–1163.

119 Scheffer, G.L., Kool, M., de Haas, M., de Vree, J.M., Pijnenborg, A.C., Bosman, D.K., Elferink, R.P., van der Valk, P., Borst, P. and Scheper, R.J. (2002) Tissue distribution and induction of human multidrug resistant protein 3. *Laboratory Investigation; A Journal of Technical Methods and Pathology*, **82**, 193–201.

120 Zollner, G., Fickert, P., Silbert, D., Fuchsbichler, A., Marschall, H.U., Zatloukal, K., Denk, H. and Trauner, M. (2003) Adaptive changes in hepatobiliary transporter expression in primary biliary cirrhosis. *Journal of Hepatology*, **38**, 717–727.

121 Zelcer, N., van de Wetering, K., de Waart, R., Scheffer, G.L., Marschall, H.U., Wielinga, P.R., Kuil, A., Kunne, C., Smith, A., van der Valk, M., Wijnholds, J., Elferink, R.O. and Borst, P. (2006) Mice lacking Mrp3 (Abcc3) have normal bile salt transport, but altered hepatic transport of endogenous glucuronides. *Journal of Hepatology*, **44**, 768–775.

122 Belinsky, M.G., Bain, L.J., Balsara, B.B., Testa, J.R. and Kruh, G.D. (1998) Characterization of MOAT-C and MOAT-D, new members of the MRP/cMOAT subfamily of transporter proteins. *Journal of the National Cancer Institute*, **90**, 1735–1741.

123 Kiuchi, Y., Suzuki, H., Hirohashi, T., Tyson, C.A. and Sugiyama, Y. (1998) cDNA cloning and inducible expression of human multidrug resistance associated protein 3 (MRP3). *FEBS Letters*, **433**, 149–152.

124 Belinsky, M.G., Dawson, P.A., Shchaveleva, I., Bain, L.J., Wang, R., Ling, V., Chen, Z.S., Grinberg, A., Westphal, H., Klein-Szanto, A., Lerro, A. and Kruh, G.D. (2005) Analysis of the *in vivo* functions of Mrp3. *Molecular Pharmacology*, **68**, 160–168.

125 Zelcer, N., van de Wetering, K., Hillebrand, M., Sarton, E., Kuil, A., Wielinga, P.R., Tephly, T., Dahan, A.,

Beijnen, J.H. and Borst, P. (2005) Mice lacking multidrug resistance protein 3 show altered morphine pharmacokinetics and morphine-6-glucuronide antinociception. *Proceedings of the National Academy of Sciences of the United States of America*, **102**, 7274–7279.

126 Zamek-Gliszczynski, M.J., Nezasa, K., Tian, X., Bridges, A.S., Lee, K., Belinsky, M.G., Kruh, G.D. and Brouwer, K.L. (2006) Evaluation of the role of multidrug resistance-associated protein (Mrp) 3 and Mrp4 in hepatic basolateral excretion of sulfate and glucuronide metabolites of acetaminophen, 4-methylumbelliferone, and harmol in Abcc3−/− and Abcc4−/− mice. *The Journal of Pharmacology and Experimental Therapeutics*, **319**, 1485–1491.

127 Tian, X., Swift, B., Zamek-Gliszczynski, M.J., Belinsky, M., Kruh, G. and Brouwer, K.L. (2008) Impact of basolateral Mrp3 (Abcc3) and Mrp4 (Abcc4) on the hepatobiliary disposition of fexofenadine in perfused mouse livers. *Drug Metabolism and Disposition: The Biological Fate of Chemicals*, **36**, 911–915.

128 Rius, M., Nies, A.T., Hummel-Eisenbeiss, J., Jedlitschky, G. and Keppler, D. (2003) Cotransport of reduced glutathione with bile salts by MRP4 (ABCC4) localized to the basolateral hepatocyte membrane. *Hepatology (Baltimore, Md.)*, **38**, 374–384.

129 Chen, C. and Klaassen, C.D. (2004) Rat multidrug resistance protein 4 (Mrp4, Abcc4): molecular cloning, organ distribution, postnatal renal expression, and chemical inducibility. *Biochemical and Biophysical Research Communications*, **317**, 46–53.

130 Leggas, M., Adachi, M., Scheffer, G.L., Sun, D., Wielinga, P., Du, G., Mercer, K.E., Zhuang, Y., Panetta, J.C., Johnston, B., Scheper, R.J., Stewart, C.F. and Schuetz, J.D. (2004) Mrp4 confers resistance to topotecan and protects the brain from chemotherapy. *Molecular and Cellular Biology*, **24**, 7612–7621.

131 Nies, A.T., Jedlitschky, G., Konig, J., Herold-Mende, C., Steiner, H.H., Schmitt, H.P. and Keppler, D. (2004) Expression and immunolocalization of the multidrug resistance proteins, MRP1-MRP6 (ABCC1-ABCC6), in human brain. *Neuroscience*, **129**, 349–360.

132 Smeets, P.H., van Aubel, R.A., van Wouterse, A.C., den Heuvel, J.J. and Russel, F.G. (2004) Contribution of multidrug resistance protein 2 (MRP2/ABCC2) to the renal excretion of p-aminohippurate (PAH) and identification of MRP4 (ABCC4) as a novel PAH transporter. *Journal of the American Society of Nephrology*, **15**, 2828–2835.

133 van Aubel, R.A., Smeets, P.H., Peters, J.G., Bindels, R.J. and Russel, F.G. (2002) The MRP4/ABCC4 gene encodes a novel apical organic anion transporter in human kidney proximal tubules: putative efflux pump for urinary cAMP and cGMP. *Journal of the American Society of Nephrology*, **13** 595–603.

134 Rius, M., Thon, W.F., Keppler, D. and Nies, A.T. (2005) Prostanoid transport by multidrug resistance protein 4 (MRP4/ABCC4) localized in tissues of the human urogenital tract. *The Journal of Urology*, **174**, 2409–2414.

135 Mennone, A., Soroka, C.J., Cai, S.Y., Harry, K., Adachi, M., Hagey, L., Schuetz, J.D. and Boyer, J.L. (2006) Mrp4−/− mice have an impaired cytoprotective response in obstructive cholestasis. *Hepatology (Baltimore, Md.)*, **43**, 1013–1021.

136 Denk, G.U., Soroka, C.J., Takeyama, Y., Chen, W.S., Schuetz, J.D. and Boyer, J.L. (2004) Multidrug resistance-associated protein 4 is up-regulated in liver but down-regulated in kidney in obstructive cholestasis in the rat. *Journal of Hepatology*, **40**, 585–591.

137 Borst, P., Evers, R., Kool, M. and Wijnholds, J. (1999) The multidrug resistance protein family. *Biochimica et Biophysica Acta*, **1461**, 347–357.

138 Ros, J.E., Libbrecht, L., Geuken, M., Jansen, P.L. and Roskams, T.A. (2003)

High expression of MDR1, MRP1, and MRP3 in the hepatic progenitor cell compartment and hepatocytes in severe human liver disease. *The Journal of Pathology*, **200**, 553–560.

139 Donner, M.G., Warskulat, U., Saha, N. and Haussinger, D. (2004) Enhanced expression of basolateral multidrug resistance protein isoforms Mrp3 and Mrp5 in rat liver by LPS. *Biological Chemistry*, **385**, 331–339.

140 Belinsky, M.G., Chen, Z.S., Shchaveleva, I., Zeng, H. and Kruh, G.D. (2002) Characterization of the drug resistance and transport properties of multidrug resistance protein 6 (MRP6, ABCC6). *Cancer Research*, **62**, 6172–6177.

141 Ilias, A., Urban, Z., Seidl, T.L., Le Saux, O., Sinko, E., Boyd, C.D., Sarkadi, B. and Varadi, A. (2002) Loss of ATP-dependent transport activity in pseudoxanthoma elasticum-associated mutants of human ABCC6 (MRP6). *The Journal of Biological Chemistry*, **277**, 16860–16867.

142 Bergen, A.A., Plomp, A.S., Schuurman, E.J., Terry, S., Breuning, M., Dauwerse, H., Swart, J., Kool, M., van Soest, S., Baas, F., ten Brink, J.B. and de Jong, P.T. (2000) Mutations in ABCC6 cause pseudoxanthoma elasticum. *Nature Genetics*, **25**, 228–231.

143 Le Saux, O., Urban, Z., Tschuch, C., Csiszar, K., Bacchelli, B., Quaglino, D., Pasquali-Ronchetti, I., Pope, F.M., Richards, A., Terry, S., Bercovitch, L., de Paepe, A. and Boyd, C.D. (2000) Mutations in a gene encoding an ABC transporter cause pseudoxanthoma elasticum. *Nature Genetics*, **25**, 223–227.

144 Ringpfeil, F., Lebwohl, M.G., Christiano, A.M. and Uitto, J. (2000) Pseudoxanthoma elasticum: mutations in the MRP6 gene encoding a transmembrane ATP-binding cassette (ABC) transporter. *Proceedings of the National Academy of Sciences of the United States of America*, **97**, 6001–6006.

145 Landrier, J.F., Eloranta, J.J., Vavricka, S.R. and Kullak-Ublick, G.A. (2006) The nuclear receptor for bile acids, FXR, transactivates human organic solute transporter-alpha and -beta genes. *American Journal of Physiology. Gastrointestinal and Liver Physiology*, **290**, G476–G485.

146 Lee, H., Zhang, Y., Lee, F.Y., Nelson, S.F., Gonzalez, F.J. and Edwards, P.A. (2006) FXR regulates organic solute transporters alpha and beta in the adrenal gland, kidney, and intestine. *Journal of Lipid Research*, **47**, 201–214.

147 Boyer, J.L., Trauner, M., Mennone, A., Soroka, C.J., Cai, S.Y., Moustafa, T., Zollner, G., Lee, J.Y. and Ballatori, N. (2006) Upregulation of a basolateral FXR-dependent bile acid efflux transporter OSTalpha-OSTbeta in cholestasis in humans and rodents. *American Journal of Physiology. Gastrointestinal and Liver Physiology*, **290**, G1124–G1130.

148 Mahagita, C., Grassl, S.M., Piyachaturawat, P. and Ballatori, N. (2007) Human organic anion transporter 1B1 and 1B3 function as bidirectional carriers and do not mediate GSH-bile acid cotransport. *American Journal of Physiology. Gastrointestinal and Liver Physiology*, **293**, G271–G278.

149 Li, L., Meier, P.J. and Ballatori, N. (2000) Oatp2 mediates bidirectional organic solute transport: a role for intracellular glutathione. *Molecular Pharmacology*, **58**, 335–340.

150 Shitara, Y., Li, A.P., Kato, Y., Lu, C., Ito, K., Itoh, T. and Sugiyama, Y. (2003) Function of uptake transporters for taurocholate and estradiol 17beta-D-glucuronide in cryopreserved human hepatocytes. *Drug Metabolism and Pharmacokinetics*, **18**, 33–41.

151 Hirano, M., Maeda, K., Shitara, Y. and Sugiyama, Y. (2004) Contribution of OATP2 (OATP1B1) and OATP8 (OATP1B3) to the hepatic uptake of pitavastatin in humans. *The Journal of Pharmacology and Experimental Therapeutics*, **311**, 139–146.

152 Jigorel, E., Le Vee, M., Boursier-Neyret, C., Bertrand, M. and Fardel, O. (2005)

Functional expression of sinusoidal drug transporters in primary human and rat hepatocytes. *Drug Metabolism and Disposition: The Biological Fate of Chemicals*, **33**, 1418–1422.

153 Ishigami, M., Tokui, T., Komai, T., Tsukahara, K., Yamazaki, M. and Sugiyama, Y. (1995) Evaluation of the uptake of pravastatin by perfused rat liver and primary cultured rat hepatocytes. *Pharmaceutical Research*, **12**, 1741–1745.

154 Rippin, S.J., Hagenbuch, B., Meier, P.J. and Stieger, B. (2001) Cholestatic expression pattern of sinusoidal and canalicular organic anion transport systems in primary cultured rat hepatocytes. *Hepatology (Baltimore, Md.)*, **33**, 776–782.

155 Miyauchi, S., Sawada, Y., Iga, T., Hanano, M. and Sugiyama, Y. (1993) Comparison of the hepatic uptake clearances of fifteen drugs with a wide range of membrane permeabilities in isolated rat hepatocytes and perfused rat livers. *Pharmaceutical Research*, **10**, 434–440.

156 Kato, Y., Akhteruzzaman, S., Hisaka, A. and Sugiyama, Y. (1999) Hepatobiliary transport governs overall elimination of peptidic endothelin antagonists in rats. *The Journal of Pharmacology and Experimental Therapeutics*, **288**, 568–574.

157 Kouzuki, H., Suzuki, H., Ito, K., Ohashi, R. and Sugiyama, Y. (1998) Contribution of sodium taurocholate co-transporting polypeptide to the uptake of its possible substrates into rat hepatocytes. *The Journal of Pharmacology and Experimental Therapeutics*, **286**, 1043–1050.

158 Kouzuki, H., Suzuki, H., Ito, K., Ohashi, R. and Sugiyama, Y. (1999) Contribution of organic anion transporting polypeptide to uptake of its possible substrates into rat hepatocytes. *The Journal of Pharmacology and Experimental Therapeutics*, **288**, 627–634.

159 Crespi, C.L. and Penman, B.W. (1997) Use of cDNA-expressed human cytochrome P450 enzymes to study potential drug–drug interactions. *Advances in Pharmacology (San Diego, Calif.)*, **43**, 171–188.

160 Sekine, T., Cha, S.H., Tsuda, M., Apiwattanakul, N., Nakajima, N., Kanai, Y. and Endou, H. (1998) Identification of multispecific organic anion transporter 2 expressed predominantly in the liver. *FEBS Letters*, **429**, 179–182.

161 Shimizu, M., Fuse, K., Okudaira, K., Nishigaki, R., Maeda, K., Kusuhara, H. and Sugiyama, Y. (2005) Contribution of OATP (organic anion-transporting polypeptide) family transporters to the hepatic uptake of fexofenadine in humans. *Drug Metabolism and Disposition: The Biological Fate of Chemicals*, **33**, 1477–1481.

162 Hagenbuch, B., Scharschmidt, B.F. and Meier, P.J. (1996) Effect of antisense oligonucleotides on the expression of hepatocellular bile acid and organic anion uptake systems in Xenopus laevis oocytes. *The Biochemical Journal*, **316** (Pt 3), 901–904.

163 Nakai, D., Nakagomi, R., Furuta, Y., Tokui, T., Abe, T., Ikeda, T. and Nishimura, K. (2001) Human liver-specific organic anion transporter, LST-1, mediates uptake of pravastatin by human hepatocytes. *The Journal of Pharmacology and Experimental Therapeutics*, **297**, 861–867.

164 Materna, V., Stege, A., Surowiak, P., Priebsch, A. and Lage, H. (2006) RNA interference-triggered reversal of ABCC2-dependent cisplatin resistance in human cancer cells. *Biochemical and Biophysical Research Communications*, **348**, 153–157.

165 Nieth, C., Priebsch, A., Stege, A. and Lage, H. (2003) Modulation of the classical multidrug resistance (MDR) phenotype by RNA interference (RNAi). *FEBS Letters*, **545**, 144–150.

166 Aoki, J., Suzuki, H. and Sugiyama, Y. (2000) Quantitative prediction of *in vivo* biliary excretion clearance across the bile canalicular membrane from *in vitro* transport studies with isolated membrane vesicles. Millennial World Congress of

Pharmaceutical Sciences, April 16–20, San Francisco, p. 92.

167 Allen, J.D., van Loevezijn, A., Lakhai, J.M., van der Valk, M., van Tellingen, O., Reid, G., Schellens, J.H., Koomen, G.J. and Schinkel, A.H. (2002) Potent and specific inhibition of the breast cancer resistance protein multidrug transporter *in vitro* and in mouse intestine by a novel analogue of fumitremorgin C. *Molecular Cancer Therapeutics*, **1**, 417–425.

168 Dantzig, A.H., Shepard, R.L., Cao, J., Law, K.L., Ehlhardt, W.J., Baughman, T.M., Bumol, T.F. and Starling, J.J. (1996) Reversal of P-glycoprotein-mediated multidrug resistance by a potent cyclopropyldibenzosuberane modulator, LY335979. *Cancer Research*, **56**, 4171–4179.

169 Kusunoki, N., Takara, K., Tanigawara, Y., Yamauchi, A., Ueda, K., Komada, F., Ku, Y., Kuroda, Y., Saitoh, Y. and Okumura, K. (1998) Inhibitory effects of a cyclosporin derivative, SDZ PSC, 833, on transport of doxorubicin and vinblastine via human P-glycoprotein. *Japanese Journal of Cancer Research: Gann.*, **89**, 1220–1228.

170 LeCluyse, E.L., Audus, K.L. and Hochman, J.H. (1994) Formation of extensive canalicular networks by rat hepatocytes cultured in collagen-sandwich configuration. *The American Journal of Physiology*, **266**, C1764–C1774.

171 Liu, X., LeCluyse, E.L., Brouwer, K.R., Lightfoot, R.M., Lee, J.I. and Brouwer, K.L. (1999) Use of Ca2+ modulation to evaluate biliary excretion in sandwich-cultured rat hepatocytes. *The Journal of Pharmacology and Experimental Therapeutics*, **289**, 1592–1599.

172 Hoffmaster, K.A., Turncliff, R.Z., LeCluyse, E.L., Kim, R.B., Meier, P.J. and Brouwer, K.L. (2004) P-glycoprotein expression, localization, and function in sandwich-cultured primary rat and human hepatocytes: relevance to the hepatobiliary disposition of a model opioid peptide. *Pharmaceutical Research*, **21**, 1294–1302.

173 Liu, X., Chism, J.P., LeCluyse, E.L., Brouwer, K.R. and Brouwer, K.L. (1999) Correlation of biliary excretion in sandwich-cultured rat hepatocytes and *in vivo* in rats. *Drug Metabolism and Disposition: The Biological Fate of Chemicals*, **27**, 637–644.

174 Bi, Y.A., Kazolias, D. and Duignan, D.B. (2006) Use of cryopreserved human hepatocytes in sandwich culture to measure hepatobiliary transport. *Drug Metabolism and Disposition: The Biological Fate of Chemicals*, **34**, 1658–1665.

175 Ghibellini, G., Vasist, L.S., Leslie, E.M., Heizer, W.D., Kowalsky, R.J., Calvo, B.F. and Brouwer, K.L. (2007) *In vitro–in vivo* correlation of hepatobiliary drug clearance in humans. *Clinical Pharmacology and Therapeutics*, **81**, 406–413.

176 Cui, Y., Konig, J. and Keppler, D. (2001) Vectorial transport by double-transfected cells expressing the human uptake transporter SLC21A8 and the apical export pump ABCC2. *Molecular Pharmacology*, **60**, 934–943.

177 Sasaki, M., Suzuki, H., Ito, K., Abe, T. and Sugiyama, Y. (2002) Transcellular transport of organic anions across a double-transfected Madin-Darby canine kidney II cell monolayer expressing both human organic anion-transporting polypeptide (OATP2/SLC21A6) and Multidrug resistance-associated protein 2 (MRP2/ABCC2). *The Journal of Biological Chemistry*, **277**, 6497–6503.

178 Sasaki, M., Suzuki, H., Aoki, J., Ito, K., Meier, P.J. and Sugiyama, Y. (2004) Prediction of *in vivo* biliary clearance from the *in vitro* transcellular transport of organic anions across a double-transfected Madin–Darby canine kidney II monolayer expressing both rat organic anion transporting polypeptide 4 and multidrug resistance associated protein 2. *Molecular Pharmacology*, **66**, 450–459.

179 Ishiguro, N., Maeda, K., Saito, A., Kishimoto, W., Matsushima, S., Ebner, T., Roth, W., Igarashi, T. and Sugiyama, Y.

(2008) Establishment of a set of double transfectants co-expressing organic anion transporting polypeptide 1B3 (OATP1B3) and hepatic efflux transporters for the characterization of the hepatobiliary transport of telmisartan acylglucuronide. *Drug Metabolism and Disposition: The Biological Fate of Chemicals*, **36**, 796–805.

180 Mita, S., Suzuki, H., Akita, H., Stieger, B., Meier, P.J., Hofmann, A.F. and Sugiyama, Y. (2005) Vectorial transport of bile salts across MDCK cells expressing both rat Na+-taurocholate cotransporting polypeptide and rat bile salt export pump. *American Journal of Physiology. Gastrointestinal and Liver Physiology*, **288**, G159–G167.

181 Kopplow, K., Letschert, K., Konig, J., Walter, B. and Keppler, D. (2005) Human hepatobiliary transport of organic anions analyzed by quadruple-transfected cells. *Molecular Pharmacology*, **68**, 1031–1038.

182 Nies, A.T., Herrmann, E., Brom, M. and Keppler, D. (2008) Vectorial transport of the plant alkaloid berberine by double-transfected cells expressing the human organic cation transporter 1 (OCT1, SLC22A1) and the efflux pump MDR1 P-glycoprotein (ABCB1). *Naunyn-Schmiedeberg's Archives of Pharmacology*, **376**, 449–461.

183 Kerb, R. (2006) Implications of genetic polymorphisms in drug transporters for pharmacotherapy. *Cancer Letters*, **234**, 4–33.

184 Hoffmeyer, S., Burk, O., von Richter, O., Arnold, H.P., Brockmoller, J., Johne, A., Cascorbi, I., Gerloff, T., Roots, I., Eichelbaum, M. and Brinkmann, U. (2000) Functional polymorphisms of the human multidrug-resistance gene: multiple sequence variations and correlation of one allele with P-glycoprotein expression and activity *in vivo*. *Proceedings of the National Academy of Sciences of the United States of America*, **97**, 3473–3478.

185 Pauli-Magnus, C. and Kroetz, D.L. (2004) Functional implications of genetic polymorphisms in the multidrug resistance gene MDR1 (ABCB1). *Pharmaceutical Research*, **21**, 904–913.

186 Konig, J., Seithel, A., Gradhand, U. and Fromm, M.F. (2006) Pharmacogenomics of human OATP transporters. *Naunyn-Schmiedeberg's Archives of Pharmacology*, **372**, 432–443.

187 Nishizato, Y., Ieiri, I., Suzuki, H., Kimura, M., Kawabata, K., Hirota, T., Takane, H., Irie, S., Kusuhara, H., Urasaki, Y., Urae, A., Higuchi, S., Otsubo, K. and Sugiyama, Y. (2003) Polymorphisms of OATP-C (SLC21A6) and OAT3 (SLC22A8) genes: consequences for pravastatin pharmacokinetics. *Clinical Pharmacology and Therapeutics*, **73**, 554–565.

188 Kameyama, Y., Yamashita, K., Kobayashi, K., Hosokawa, M. and Chiba, K. (2005) Functional characterization of SLCO1B1 (OATP-C) variants, SLCO1B1*5, SLCO1B1*15 and SLCO1B1*15+C1007G, by using transient expression systems of HeLa and HEK293 cells. *Pharmacogenetics and Genomics*, **15**, 513–522.

189 Iwai, M., Suzuki, H., Ieiri, I., Otsubo, K. and Sugiyama, Y. (2004) Functional analysis of single nucleotide polymorphisms of hepatic organic anion transporter OATP1B1 (OATP-C). *Pharmacogenetics*, **14**, 749–757.

190 Maeda, K., Ieiri, I., Yasuda, K., Fujino, A., Fujiwara, H., Otsubo, K., Hirano, M., Watanabe, T., Kitamura, Y., Kusuhara, H. and Sugiyama, Y. (2006) Effects of organic anion transporting polypeptide 1B1 haplotype on pharmacokinetics of pravastatin, valsartan, and temocapril. *Clinical Pharmacology and Therapeutics*, **79**, 427–439.

191 Niemi, M., Neuvonen, P.J., Hofmann, U., Backman, J.T., Schwab, M., Lutjohann, D., von Bergmann, K., Eichelbaum, M. and Kivisto, K.T. (2005) Acute effects of pravastatin on cholesterol synthesis are associated with SLCO1B1 (encoding

OATP1B1) haplotype *17. *Pharmacogenetics and Genomics*, **15**, 303–309.

192 Niemi, M., Backman, J.T., Kajosaari, L.I., Leathart, J.B., Neuvonen, M., Daly, A.K., Eichelbaum, M., Kivisto, K.T. and Neuvonen, P.J. (2005) Polymorphic organic anion transporting polypeptide 1B1 is a major determinant of repaglinide pharmacokinetics. *Clinical Pharmacology and Therapeutics*, **77**, 468–478.

193 Han, J.Y., Lim, H.S., Shin, E.S., Yoo, Y.K., Park, Y.H., Lee, J.E., Kim, H.T. and Lee, J.S. (2008) Influence of the organic anion-transporting polypeptide 1B1 (OATP1B1) polymorphisms on irinotecan-pharmacokinetics and clinical outcome of patients with advanced non-small cell lung cancer. *Lung Cancer (Amsterdam, Netherlands)*, **59**, 69–75.

194 Tsujimoto, M., Hirata, S., Dan, Y., Ohtani, H. and Sawada, Y. (2006) Polymorphisms and linkage disequilibrium of the OATP8 (OATP1B3) gene in Japanese subjects. *Drug Metabolism and Pharmacokinetics*, **21**, 165–169.

195 Smith, N.F., Marsh, S., Scott-Horton, T.J., Hamada, A., Mielke, S., Mross, K., Figg, W.D., Verweij, J., McLeod, H.L. and Sparreboom, A. (2007) Variants in the SLCO1B3 gene: interethnic distribution and association with paclitaxel pharmacokinetics. *Clinical Pharmacology and Therapeutics*, **81**, 76–82.

196 Yamasaki, Y., Ieiri, I., Kusuhara, H., Sasaki, T., Kimura, M., Tabuchi, H., Ando, Y., Irie, S., Ware, J., Nakai, Y., Higuchi, S. and Sugiyama, Y. (2008) Pharmacogenetic characterization of sulfasalazine disposition based on NAT2 and ABCG2 BCRP) gene polymorphisms in humans. *Clinical Pharmacology and Therapeutics* **84**, 95–103.

197 Zhang, W., Yu, B.N., He, Y.J., Fan, L., Li, Q., Liu, Z.Q., Wang, A., Liu, Y.L., Tan, Z.R., Fen, J., Huang, Y.F. and Zhou, H.H. (2006) Role of BCRP 421C>A polymorphism on rosuvastatin pharmacokinetics in healthy Chinese males. *Clinica Chimica Acta; International Journal of Clinical Chemistry*, **373**, 99–103.

198 Sparreboom, A., Gelderblom, H., Marsh, S., Ahluwalia, R., Obach, R., Principe, P., Twelves, C., Verweij, J. and McLeod, H.L. (2004) Diflomotecan pharmacokinetics in relation to ABCG2 421C>A genotype. *Clinical Pharmacology and Therapeutics*, **76**, 38–44.

199 Kondo, C., Suzuki, H., Itoda, M., Ozawa, S., Sawada, J., Kobayashi, D., Ieiri, I., Mine, K., Ohtsubo, K. and Sugiyama, Y. (2004) Functional analysis of SNPs variants of BCRP/ABCG2. *Pharmaceutical Research*, **21**, 1895–1903.

200 Kobayashi, D., Ieiri, I., Hirota, T., Takane, H., Maegawa, S., Kigawa, J., Suzuki, H., Nanba, E., Oshimura, M., Terakawa, N., Otsubo, K., Mine, K. and Sugiyama, Y. (2005) Functional assessment of ABCG2 (BCRP) gene polymorphisms to protein expression in human placenta. *Drug Metabolism and Disposition: The Biological Fate of Chemicals*, **33**, 94–101.

201 Choi, J.H., Ahn, B.M., Yi, J., Lee, J.H., Nam, S.W., Chon, C.Y., Han, K.H., Ahn, S.H., Jang, I.J., Cho, J.Y., Suh, Y., Cho, M.O., Lee, J.E., Kim, K.H. and Lee, M.G. (2007) MRP2 haplotypes confer differential susceptibility to toxic liver injury. *Pharmacogenetics and Genomics*, **17**, 403–415.

202 Daly, A.K., Aithal, G.P., Leathart, J.B., Swainsbury, R.A., Dang, T.S. and Day, C.P. (2007) Genetic susceptibility to diclofenac-induced hepatotoxicity: contribution of UGT2B7, CYP2C8, and ABCC2 genotypes. *Gastroenterology*, **132**, 272–281.

203 de Jong, F.A., Scott-Horton, T.J., Kroetz, D.L., McLeod, H.L., Friberg, L.E., Mathijssen, R.H., Verweij, J., Marsh, S. and Sparreboom, A. (2007) Irinotecan-induced diarrhea: functional significance of the polymorphic ABCC2 transporter protein. *Clinical Pharmacology and Therapeutics*, **81**, 42–49.

204 Shu, Y., Sheardown, S.A., Brown, C., Owen, R.P., Zhang, S., Castro, R.A.,

Ianculescu, A.G., Yue, L., Lo, J.C., Burchard, E.G., Brett, C.M. and Giacomini, K.M. (2007) Effect of genetic variation in the organic cation transporter 1 (OCT1) on metformin action. *The Journal of Clinical Investigation*, **117**, 1422–1431.

205 Shu, Y., Brown, C., Castro, R.A., Shi, R.J., Lin, E.T., Owen, R.P., Sheardown, S.A., Yue, L., Burchard, E.G., Brett, C.M. and Giacomini, K.M. (2008) Effect of genetic variation in the organic cation transporter 1, OCT1, on metformin pharmacokinetics. *Clinical Pharmacology and Therapeutics*, **83**, 273–280.

206 Vavricka, S.R., Van Montfoort, J., Ha, H.R., Meier, P.J. and Fattinger, K. (2002) Interactions of rifamycin SV and rifampicin with organic anion uptake systems of human liver. *Hepatology (Baltimore, Md.)*, **36**, 164–172.

207 Backman, J.T., Kyrklund, C., Neuvonen, M. and Neuvonen, P.J. (2002) Gemfibrozil greatly increases plasma concentrations of cerivastatin. *Clinical Pharmacology and Therapeutics*, **72**, 685–691.

208 Muck, W., Mai, I., Fritsche, L., Ochmann, K., Rohde, G., Unger, S., Johne, A., Bauer, S., Budde, K., Roots, I., Neumayer, H.H. and Kuhlmann, J. (1999) Increase in cerivastatin systemic exposure after single and multiple dosing in cyclosporine-treated kidney transplant recipients. *Clinical Pharmacology and Therapeutics*, **65**, 251–261.

209 Shitara, Y., Itoh, T., Sato, H., Li, A.P. and Sugiyama, Y. (2003) Inhibition of transporter-mediated hepatic uptake as a mechanism for drug–drug interaction between cerivastatin and cyclosporin A. *The Journal of Pharmacology and Experimental Therapeutics*, **304**, 610–616.

210 Regazzi, M.B., Iacona, I., Campana, C., Raddato, V., Lesi, C., Perani, G., Gavazzi, A. and Vigano, M. (1993) Altered disposition of pravastatin following concomitant drug therapy with cyclosporin A in transplant recipients. *Transplantation Proceedings*, **25**, 2732–2734.

211 Simonson, S.G., Raza, A., Martin, P.D., Mitchell, P.D., Jarcho, J.A., Brown, C.D., Windass, A.S. and Schneck, D.W. (2004) Rosuvastatin pharmacokinetics in heart transplant recipients administered an antirejection regimen including cyclosporine. *Clinical Pharmacology and Therapeutics*, **76**, 167–177.

212 Hasunuma, T., Nakamura, M., Yachi, T., Arisawa, N., Fukushima, K. and Iijima, H. (2003) The drug–drug interactions of pitavastatin (NK-104), a novel HMG-CoA reductase inhibitor and cyclosporine. *Journal of Clinical Therapy Medicine*, **19**, 381–389.

213 Kajosaari, L.I., Niemi, M., Neuvonen, M., Laitila, J., Neuvonen, P.J. and Backman, J.T. (2005) Cyclosporine markedly raises the plasma concentrations of repaglinide. *Clinical Pharmacology and Therapeutics*, **78**, 388–399.

214 Treiber, A., Schneiter, R., Delahaye, S. and Clozel, M. (2004) Inhibition of organic anion transporting polypeptide-mediated hepatic uptake is the major determinant in the pharmacokinetic interaction between bosentan and cyclosporin A in the rat. *The Journal of Pharmacology and Experimental Therapeutics*, **308**, 1121–1129.

215 Shitara, Y., Hirano, M., Sato, H. and Sugiyama, Y. (2004) Gemfibrozil and its glucuronide inhibit the organic anion transporting polypeptide 2 (OATP2/OATP1B1:SLC21A6)-mediated hepatic uptake and CYP2C8-mediated metabolism of cerivastatin: analysis of the mechanism of the clinically relevant drug–drug interaction between cerivastatin and gemfibrozil. *The Journal of Pharmacology and Experimental Therapeutics*, **311**, 228–236.

216 Kyrklund, C., Backman, J.T., Neuvonen, M. and Neuvonen, P.J. (2003) Gemfibrozil increases plasma pravastatin concentrations and reduces pravastatin

renal clearance. *Clinical Pharmacology and Therapeutics*, **73**, 538–544.

217 Mathew, P., Cuddy, T. and Tracewell, W.G. (2004) An open-label study on the pharmacokinetics (PK) of pitavastatin (NK-104) when administered concomitantly with fenofibrate or gemfibrozil in healthy volunteers (abstract PI-115). *Clinical Pharmacology and Therapeutics*, **75**, 33.

218 Schneck, D.W., Birmingham, B.K., Zalikowski, J.A., Mitchell, P.D., Wang, Y., Martin, P.D., Lasseter, K.C., Brown, C.D., Windass, A.S. and Raza, A. (2004) The effect of gemfibrozil on the pharmacokinetics of rosuvastatin. *Clinical Pharmacology and Therapeutics*, **75**, 455–463.

219 Treiber, A., Schneiter, R., Hausler, S. and Stieger, B. (2007) Bosentan is a substrate of human OATP1B1 and OATP1B3: inhibition of hepatic uptake as the common mechanism of its interactions with cyclosporin A, rifampicin, and sildenafil. *Drug Metabolism and Disposition: The Biological Fate of Chemicals*, **35**, 1400–1407.

220 Lau, Y.Y., Okochi, H., Huang, Y. and Benet, L.Z. (2006) Multiple transporters affect the disposition of atorvastatin and its two active hydroxy metabolites: application of *in vitro* and *ex situ* systems. *The Journal of Pharmacology and Experimental Therapeutics*, **316**, 762–771.

221 Asberg, A., Hartmann, A., Fjeldsa, E., Bergan, S. and Holdaas, H. (2001) Bilateral pharmacokinetic interaction between cyclosporine A and atorvastatin in renal transplant recipients. *American Journal of Transplantation*, **1**, 382–386.

222 Ichimaru, N., Takahara, S., Kokado, Y., Wang, J.D., Hatori, M., Kameoka, H., Inoue, T. and Okuyama, A. (2001) Changes in lipid metabolism and effect of simvastatin in renal transplant recipients induced by cyclosporine or tacrolimus. *Atherosclerosis*, **158**, 417–423.

223 Mazzu, A.L., Lasseter, K.C., Shamblen, E.C., Agarwal, V., Lettieri, J. and Sundaresen, P. (2000) Itraconazole alters the pharmacokinetics of atorvastatin to a greater extent than either cerivastatin or pravastatin. *Clinical Pharmacology and Therapeutics*, **68**, 391–400.

224 Neuvonen, P.J., Kantola, T. and Kivisto, K.T. (1998) Simvastatin but not pravastatin is very susceptible to interaction with the CYP3A4 inhibitor itraconazole. *Clinical Pharmacology and Therapeutics*, **63**, 332–341.

225 Campbell, S.D., de Morais, S.M. and Xu, J.J. (2004) Inhibition of human organic anion transporting polypeptide OATP 1B1 as a mechanism of drug-induced hyperbilirubinemia. *Chemico-Biological Interactions*, **150**, 179–187.

226 Kobayashi, Y., Sakai, R., Ohshiro, N., Ohbayashi, M., Kohyama, N. and Yamamoto, T. (2005) Possible involvement of organic anion transporter 2 on the interaction of theophylline with erythromycin in the human liver. *Drug Metabolism and Disposition: The Biological Fate of Chemicals*, **33**, 619–622.

227 Jonkman, J.H. and Upton, R.A. (1984) Pharmacokinetic drug interactions with theophylline. *Clinical Pharmacokinetics*, **9**, 309–334.

228 Fichtenbaum, C.J., Gerber, J.G., Rosenkranz, S.L., Segal, Y., Aberg, J.A., Blaschke, T., Alston, B., Fang, F., Kosel, B. and Aweeka, F. (2002) Pharmacokinetic interactions between protease inhibitors and statins in HIV seronegative volunteers: ACTG Study A5047. *AIDS (London, England)*, **16**, 569–577.

229 Gerber, J.G., Rosenkranz, S.L., Fichtenbaum, C.J., Vega, J.M., Yang, A., Alston, B.L., Brobst, S.W., Segal, Y. and Aberg, J.A. (2005) Effect of efavirenz on the pharmacokinetics of simvastatin, atorvastatin, and pravastatin: results of AIDS Clinical Trials Group 5108 Study. *Journal of Acquired Immune Deficiency Syndromes*, **39**, 307–312.

230 Kyrklund, C., Backman, J.T., Neuvonen, M. and Neuvonen, P.J. (2004) Effect of

rifampicin on pravastatin pharmacokinetics in healthy subjects. *British Journal of Clinical Pharmacology*, **57**, 181–187.

231 Bohan, A. and Boyer, J.L. (2002) Mechanisms of hepatic transport of drugs: implications for cholestatic drug reactions. *Seminars in Liver Disease*, **22**, 123–136.

232 Funk, C., Ponelle, C., Scheuermann, G. and Pantze, M. (2001) Cholestatic potential of troglitazone as a possible factor contributing to troglitazone-induced hepatotoxicity: *in vivo* and *in vitro* interaction at the canalicular bile salt export pump (Bsep) in the rat. *Molecular Pharmacology*, **59**, 627–635.

233 Funk, C., Pantze, M., Jehle, L., Ponelle, C., Scheuermann, G., Lazendic, M. and Gasser, R. (2001) Troglitazone-induced intrahepatic cholestasis by an interference with the hepatobiliary export of bile acids in male and female rats. Correlation with the gender difference in troglitazone sulfate formation and the inhibition of the canalicular bile salt export pump (Bsep) by troglitazone and troglitazone sulfate. *Toxicology*, **167**, 83–98.

234 Kostrubsky, V.E., Strom, S.C., Hanson, J., Urda, E., Rose, K., Burliegh, J., Zocharski, P., Cai, H., Sinclair, J.F. and Sahi, J. (2003) Evaluation of hepatotoxic potential of drugs by inhibition of bile-acid transport in cultured primary human hepatocytes and intact rats. *Toxicological Sciences*, **76**, 220–228.

235 Mita, S., Suzuki, H., Akita, H., Hayashi, H., Onuki, R., Hofmann, A.F. and Sugiyama, Y. (2006) Inhibition of bile acid transport across Na+/taurocholate cotransporting polypeptide (SLC10A1) and bile salt export pump (ABCB 11)-coexpressing LLC-PK1 cells by cholestasis-inducing drugs. *Drug Metabolism and Disposition: The Biological Fate of Chemicals*, **34**, 1575–1581.

236 Akita, H., Suzuki, H., Ito, K., Kinoshita, S., Sato, N., Takikawa, H. and Sugiyama, Y. (2001) Characterization of bile acid transport mediated by multidrug resistance associated protein 2 and bile salt export pump. *Biochimica et Biophysica Acta*, **1511**, 7–16.

237 Stieger, B., Fattinger, K., Madon, J., Kullak-Ublick, G.A. and Meier, P.J. (2000) Drug- and estrogen-induced cholestasis through inhibition of the hepatocellular bile salt export pump (Bsep) of rat liver. *Gastroenterology*, **118**, 422–430.

238 Huang, L., Smit, J.W., Meijer, D.K. and Vore, M. (2000) Mrp2 is essential for estradiol-17beta(beta-D-glucuronide)-induced cholestasis in rats. *Hepatology (Baltimore, Md.)*, **32**, 66–72.

239 Chu, X.Y., Kato, Y. and Sugiyama, Y. (1997) Multiplicity of biliary excretion mechanisms for irinotecan, CPT-11, and its metabolites in rats. *Cancer Research*, **57**, 1934–1938.

240 Chu, X.Y., Kato, Y., Ueda, K., Suzuki, H., Niinuma, K., Tyson, C.A., Weizer, V., Dabbs, J.E., Froehlich, R., Green, C.E. and Sugiyama, Y. (1998) Biliary excretion mechanism of CPT-11 and its metabolites in humans: involvement of primary active transporters. *Cancer Research*, **58**, 5137–5143.

241 Horikawa, M., Kato, Y. and Sugiyama, Y. (2002) Reduced gastrointestinal toxicity following inhibition of the biliary excretion of irinotecan and its metabolites by probenecid in rats. *Pharmaceutical Research*, **19**, 1345–1353.

242 Angelin, B., Arvidsson, A., Dahlqvist, R., Hedman, A. and Schenck-Gustafsson, K. (1987) Quinidine reduces biliary clearance of digoxin in man. *European Journal of Clinical Investigation*, **17**, 262–265.

243 Adachi, Y., Suzuki, H. and Sugiyama, Y. (2001) Comparative studies on *in vitro* methods for evaluating *in vivo* function of MDR1 P-glycoprotein. *Pharmaceutical Research*, **18**, 1660–1668.

244 Shitara, Y., Sato, H. and Sugiyama, Y. (2005) Evaluation of drug–drug interaction in the hepatobiliary and

renal transport of drugs. *Annual Review of Pharmacology and Toxicology*, **45**, 689–723.

245 Ito, K., Iwatsubo, T., Kanamitsu, S., Ueda, K., Suzuki, H. and Sugiyama, Y. (1998) Prediction of pharmacokinetic alterations caused by drug–drug interactions: metabolic interaction in the liver. *Pharmacological Reviews*, **50**, 387–412.

246 Ueda, K., Kato, Y., Komatsu, K. and Sugiyama, Y. (2001) Inhibition of biliary excretion of methotrexate by probenecid in rats: quantitative prediction of interaction from *in vitro* data. *The Journal of Pharmacology and Experimental Therapeutics*, **297**, 1036–1043.

247 Takano, A., Kusuhara, H., Suhara, T., Ieiri, I., Morimoto, T., Lee, Y.J., Maeda, J., Ikoma, Y., Ito, H., Suzuki, K. and Sugiyama, Y. (2006) Evaluation of *in vivo* P-glycoprotein function at the blood–brain barrier among MDR1 gene polymorphisms by using 11C-verapamil. *Journal of Nuclear Medicine*, **47**, 1427–1433.

248 Sasongko, L., Link, J.M., Muzi, M., Mankoff, D.A., Yang, X., Collier, A.C., Shoner, S.C. and Unadkat, J.D. (2005) Imaging P-glycoprotein transport activity at the human blood–brain barrier with positron emission tomography. *Clinical Pharmacology and Therapeutics* **77**, 503–514.

249 Fuhr, U., Jetter, A. and Kirchheiner, J. (2007) Appropriate phenotyping procedures for drug metabolizing enzymes and transporters in humans and their simultaneous use in the "cocktail" approach. *Clinical Pharmacology and Therapeutics*, **81**, 270–283.

250 Maeda, K. and Sugiyama, Y. (2007) *In vitro–in vivo* scale-up of drug transport activities, in *Drug Transporters* (eds G. You and M.E. Morris), John Wiley & Sons, Inc., New Jersey, pp. 557–588.

251 Tamai, I., Nozawa, T., Koshida, M., Nezu, J., Sai, Y. and Tsuji, A. (2001) Functional characterization of human organic anion transporting polypeptide B (OATP-B) in comparison with liver-specific OATP-C. *Pharmaceutical Research*, **18**, 1262–1269.

252 Tamai, I., Nezu, J., Uchino, H., Sai, Y., Oku, A., Shimane, M. and Tsuji, A. (2000) Molecular identification and characterization of novel members of the human organic anion transporter (OATP) family. *Biochemical and Biophysical Research Communications*, **273**, 251–260.

253 Noe, J., Portmann, R., Brun, M.E. and Funk, C. (2007) Substrate-dependent drug–drug interactions between gemfibrozil, fluvastatin and other organic anion-transporting peptide (OATP) substrates on OATP1B1, OATP2B1, and OATP1B3. *Drug Metabolism and Disposition: The Biological Fate of Chemicals*, **35**, 1308–1314.

254 Sandhu, P., Lee, W., Xu, X., Leake, B.F., Yamazaki, M., Stone, J.A., Lin, J.H., Pearson, P.G. and Kim, R.B. (2005) Hepatic uptake of the novel antifungal agent caspofungin. *Drug Metabolism and Disposition: The Biological Fate of Chemicals*, **33**, 676–682.

255 Meier-Abt, F., Faulstich, H. and Hagenbuch, B. (2004) Identification of phalloidin uptake systems of rat and human liver. *Biochimica et Biophysica Acta*, **1664**, 64–69.

256 Nozawa, T., Sugiura, S., Nakajima, M., Goto, A., Yokoi, T., Nezu, J., Tsuji, A. and Tamai, I. (2004) Involvement of organic anion transporting polypeptides in the transport of troglitazone sulfate: implications for understanding troglitazone hepatotoxicity. *Drug Metabolism and Disposition: The Biological Fate of Chemicals*, **32**, 291–294.

257 Tirona, R.G., Leake, B.F., Wolkoff, A.W. and Kim, R.B. (2003) Human organic anion transporting polypeptide-C (SLC21A6) is a major determinant of rifampin-mediated pregnane X receptor activation. *The Journal of Pharmacology and Experimental Therapeutics*, **304**, 223–228.

258 Lu, W.J., Tamai, I., Nezu, J., Lai, M.L. and Huang, J.D. (2006) Organic anion

transporting polypeptide-C mediates arsenic uptake in HEK-293 cells. *Journal of Biomedical Science*, **13**, 525–533.

259 Katz, D.A., Carr, R., Grimm, D.R., Xiong, H., Holley-Shanks, R., Mueller, T., Leake, B., Wang, Q., Han, L., Wang, P.G., Edeki, T., Sahelijo, L., Doan, T., Allen, A., Spear, B.B. and Kim, R.B. (2006) Organic anion transporting polypeptide 1B1 activity classified by SLCO1B1 genotype influences atrasentan pharmacokinetics. *Clinical Pharmacology and Therapeutics*, **79**, 186–196.

260 Liu, L., Cui, Y., Chung, A.Y., Shitara, Y., Sugiyama, Y., Keppler, D. and Pang, K.S. (2006) Vectorial transport of enalapril by Oatp1a1/Mrp2 and OATP1B1 and OATP1B3/MRP2 in rat and human livers. *The Journal of Pharmacology and Experimental Therapeutics*, **318**, 395–402.

261 Nozawa, T., Tamai, I., Sai, Y., Nezu, J. and Tsuji, A. (2003) Contribution of organic anion transporting polypeptide OATP-C to hepatic elimination of the opioid pentapeptide analogue [D-Ala2, D-Leu5]-enkephalin. *The Journal of Pharmacy and Pharmacology*, **55**, 1013–1020.

262 Fischer, W.J., Altheimer, S., Cattori, V., Meier, P.J., Dietrich, D.R. and Hagenbuch, B. (2005) Organic anion transporting polypeptides expressed in liver and brain mediate uptake of microcystin. *Toxicology and Applied Pharmacology*, **203**, 257–263.

263 Nozawa, T., Minami, H., Sugiura, S., Tsuji, A. and Tamai, I. (2005) Role of organic anion transporter OATP1B1 (OATP-C) in hepatic uptake of irinotecan and its active metabolite, 7-ethyl-10-hydroxycamptothecin: *in vitro* evidence and effect of single nucleotide polymorphisms. *Drug Metabolism and Disposition: The Biological Fate of Chemicals*, **33**, 434–439.

264 Smith, N.F., Acharya, M.R., Desai, N., Figg, W.D. and Sparreboom, A. (2005) Identification of OATP1B3 as a high-affinity hepatocellular transporter of paclitaxel. *Cancer Biology & Therapy*, **4**, 815–818.

265 Briz, O., Serrano, M.A., Rebollo, N., Hagenbuch, B., Meier, P.J., Koepsell, H. and Marin, J.J. (2002) Carriers involved in targeting the cytostatic bile acid-cisplatin derivatives *cis*-diammine-chloro-cholylglycinate-platinum(II) and *cis*-diammine-bisursodeoxycholate-platinum (II) toward liver cells. *Molecular Pharmacology*, **61**, 853–860.

266 Tsuda-Tsukimoto, M., Maeda, T., Iwanaga, T., Kume, T. and Tamai, I. (2006) Characterization of hepatobiliary transport systems of a novel alpha4beta1/alpha4beta7 dual antagonist, TR-14035. *Pharmaceutical Research*, **23**, 2646–2656.

267 Yamaguchi, H., Okada, M., Akitaya, S., Ohara, H., Mikkaichi, T., Ishikawa, H., Sato, M., Matsuura, M., Saga, T., Unno, M., Abe, T., Mano, N., Hishinuma, T. and Goto, J. (2006) Transport of fluorescent chenodeoxycholic acid via the human organic anion transporters OATP1B1 and OATP1B3. *Journal of Lipid Research*, **47**, 1196–1202.

268 Mwinyi, J., Johne, A., Bauer, S., Roots, I. and Gerloff, T. (2004) Evidence for inverse effects of OATP-C (SLC21A6) 5 and 1b haplotypes on pravastatin kinetics. *Clinical Pharmacology and Therapeutics*, **75**, 415–421.

269 Niemi, M., Schaeffeler, E., Lang, T., Fromm, M.F., Neuvonen, M., Kyrklund, C., Backman, J.T., Kerb, R., Schwab, M., Neuvonen, P.J., Eichelbaum, M. and Kivisto, K.T. (2004) High plasma pravastatin concentrations are associated with single nucleotide polymorphisms and haplotypes of organic anion transporting polypeptide-C (OATP-C, SLCO1B1). *Pharmacogenetics*, **14**, 429–440.

270 Niemi, M., Arnold, K.A., Backman, J.T., Pasanen, M.K., Godtel-Armbrust, U., Wojnowski, L., Zanger, U.M., Neuvonen, P.J., Eichelbaum, M., Kivisto, K.T. and Lang, T. (2006) Association of genetic polymorphism in ABCC2 with hepatic

multidrug resistance-associated protein 2 expression and pravastatin pharmacokinetics. *Pharmacogenetics and Genomics*, **16**, 801–808.

271 Ho, R.H., Choi, L., Lee, W., Mayo, G., Schwarz, U.I., Tirona, R.G., Bailey, D.G., Michael Stein, C. and Kim, R.B. (2007) Effect of drug transporter genotypes on pravastatin disposition in European- and African-American participants. *Pharmacogenetics and Genomics*, **17**, 647–656.

272 Igel, M., Arnold, K.A., Niemi, M., Hofmann, U., Schwab, M., Lutjohann, D., von Bergmann, K., Eichelbaum, M. and Kivisto, K.T. (2006) Impact of the SLCO1B1 polymorphism on the pharmacokinetics and lipid-lowering efficacy of multiple-dose pravastatin. *Clinical Pharmacology and Therapeutics*, **79**, 419–426.

273 Chung, J.Y., Cho, J.Y., Yu, K.S., Kim, J.R., Oh, D.S., Jung, H.R., Lim, K.S., Moon, K.H., Shin, S.G. and Jang, I.J. (2005) Effect of OATP1B1 (SLCO1B1) variant alleles on the pharmacokinetics of pitavastatin in healthy volunteers. *Clinical Pharmacology and Therapeutics*, **78**, 342–350.

274 Ieiri, I., Suwannakul, S., Maeda, K., Uchimaru, H., Hashimoto, K., Kimura, M., Fujino, H., Hirano, M., Kusuhara, H., Irie, S., Higuchi, S. and Sugiyama, Y. (2007) SLCO1B1 (OATP1B1, an uptake transporter) and ABCG2 (BCRP, an efflux transporter) variant alleles and pharmacokinetics of pitavastatin in healthy volunteers. *Clinical Pharmacology and Therapeutics*, **82**, 541–547.

275 Lee, E., Ryan, S., Birmingham, B., Zalikowski, J., March, R., Ambrose, H., Moore, R., Lee, C., Chen, Y. and Schneck, D. (2005) Rosuvastatin pharmacokinetics and pharmacogenetics in white and Asian subjects residing in the same environment. *Clinical Pharmacology and Therapeutics*, **78**, 330–341.

276 Choi, J.H., Lee, M.G., Cho, J.Y., Lee, J.E., Kim, K.H. and Park, K. (2008) Influence of OATP1B1 genotype on the pharmacokinetics of rosuvastatin in Koreans. *Clinical Pharmacology and Therapeutics*, **83**, 251–257.

277 Pasanen, M.K., Fredrikson, H., Neuvonen, P.J. and Niemi, M. (2007) Different effects of SLCO1B1 polymorphism on the pharmacokinetics of atorvastatin and rosuvastatin. *Clinical Pharmacology and Therapeutics*, **82**, 726–733.

278 Pasanen, M.K., Neuvonen, M., Neuvonen, P.J. and Niemi, M. (2006) SLCO1B1 polymorphism markedly affects the pharmacokinetics of simvastatin acid. *Pharmacogenetics and Genomics*, **16**, 873–879.

279 Niemi, M., Pasanen, M.K. and Neuvonen, P.J. (2006) SLCO1B1 polymorphism and sex affect the pharmacokinetics of pravastatin but not fluvastatin. *Clinical Pharmacology and Therapeutics*, **80**, 356–366.

280 Zhang, W., He, Y.J., Han, C.T., Liu, Z.Q., Li, Q., Fan, L., Tan, Z.R., Zhang, W.X., Yu, B.N., Wang, D., Hu, D.L. and Zhou, H.H. (2006) Effect of SLCO1B1 genetic polymorphism on the pharmacokinetics of nateglinide. *British Journal of Clinical Pharmacology*, **62**, 567–572.

281 Niemi, M., Kivisto, K.T., Hofmann, U., Schwab, M., Eichelbaum, M. and Fromm, M.F. (2005) Fexofenadine pharmacokinetics are associated with a polymorphism of the SLCO1B1 gene (encoding OATP1B1). *British Journal of Clinical Pharmacology*, **59**, 602–604.

282 Kalliokoski, A., Neuvonen, M., Neuvonen, P.J. and Niemi, M. (2008) No significant effect of SLCO1B1 polymorphism on the pharmacokinetics of rosiglitazone and pioglitazone. *British Journal of Clinical Pharmacology*, **65**, 78–86.

283 Miura, M., Satoh, S., Inoue, K., Kagaya, H., Saito, M., Inoue, T., Suzuki, T. and Habuchi, T. (2007) Influence of SLCO1B1, 1B3, 2B1 and ABCC2 genetic polymorphisms on mycophenolic acid

pharmacokinetics in Japanese renal transplant recipients. *European Journal of Clinical Pharmacology*, **63**, 1161–1169.

284 Xiang, X., Jada, S.R., Li, H.H., Fan, L., Tham, L.S., Wong, C.I., Lee, S.C., Lim, R., Zhou, Q.Y., Goh, B.C., Tan, E.H. and Chowbay, B. (2006) Pharmacogenetics of SLCO1B1 gene and the impact of *1b and *15 haplotypes on irinotecan disposition in Asian cancer patients. *Pharmacogenetics and Genomics*, **16**, 683–691.

285 Oswald, S., Scheuch, E., Cascorbi, I. and Siegmund, W. (2006) A LC-MS/MS method to quantify the novel cholesterol lowering drug ezetimibe in human serum, urine and feces in healthy subjects genotyped for SLCO1B1. *Journal of Chromatography B: Analytical Technologies in the Biomedical and Life Sciences*, **830**, 143–150.

286 Bernsdorf, A., Giessmann, T., Modess, C., Wegner, D., Igelbrink, S., Hecker, U., Haenisch, S., Cascorbi, I., Terhaag, B. and Siegmund, W. (2006) Simvastatin does not influence the intestinal P-glycoprotein and MPR2, and the disposition of talinolol after chronic medication in healthy subjects genotyped for the ABCB1, ABCC2 and SLCO1B1 polymorphisms. *British Journal of Clinical Pharmacology*, **61**, 440–450.

287 Vormfelde, S.V., Toliat, M.R., Schirmer, M., Meineke, I., Nurnberg, P. and Brockmoller, J. (2007) The polymorphisms Asn130Asp and Val174Ala in OATP1B1 and the CYP2C9 Allele*3 independently affect torsemide pharmacokinetics and pharmacodynamics. *Clinical Pharmacology and Therapeutics*, **83**, 815–817.

12
The Importance of Gut Wall Metabolism in Determining Drug Bioavailability

Christopher Kohl

Abbreviations

ACAT	Advanced compartmental absorption and transit
AUC	Area under the curve
CES	Carboxylesterase
CYP	Cytochrome P450
FDA	Food and Drug Administration
NAT	*N*-Acetyltransferase
NCE	New chemical entity
PAMPA	Parallel artificial membrane permeability assay
PBPK	Physiologically-based pharmacokinetics
QSAR	Quantitative structure–activity relationship
SULT	Sulfotransferase
TMF	Transport, metabolism, and blood flow
UGT	UDP glucuronyltransferase

Symbols

CL	Clearance
CL/F	Oral clearance
CL_h	Hepatic clearance
CL_{int}	Intrinsic clearance
$CL_{int,g}$	Intestinal intrinsic clearance
CL_{perm}	Permeability clearance
D	Dose
f_{abs}	Fraction absorbed
F	Oral bioavailability
F_g	Fraction escaping gut wall extraction
F_h	Fraction escaping liver extraction

F_l	Fraction escaping lung extraction
$f_{u,b}$	Fraction unbound in blood
h	Hour
k_a, k_{01}	Absorption rate constant
ima	Drug administration into the superior mesenteric artery
ip	Drug administration into the portal vein
IV	Drug administration via a peripheral vein
min	Minutes
ml	Milliliters
po	Drug administration via the oral route
Q_g	Gut mucosal blood flow
Q_h	Liver blood flow
Q_{villi}	Blood flow supplying the villi of the intestinal mucosa

12.1 Introduction

Over the past 15 years, the intestinal tract and its drug-metabolizing capacity have attracted increasing attention from the biomedical community. A number of clinical reports have surmised claims of a substantial contribution of gut wall first-pass metabolism to the limited oral bioavailability of well-established drugs such as cyclosporine, midazolam, nifedipine, and verapamil [1]. These clinical observations have been supplemented by elegant *in vitro* studies using molecular biology and biochemical approaches to identify the abundance and substrate selectivity of drug-metabolizing enzymes located in the mucosa of the gastrointestinal tract. Furthermore, physiologically based mathematical models have been refined in an attempt to predict the gut wall first-pass effect of drugs and NCE from *in vitro* data [2–5]. In this chapter, we will explain the physiological context that applies to such models, describe the enzymes thought to be most important for gut wall metabolism, and review the utility and appropriateness of the approaches most commonly used. We will also critically appraise the evidence hitherto available that highlights the relative relevance of gut wall metabolism in comparison to hepatic metabolism (Figure 12.1).

12.2 Physiology of the Intestinal Mucosa

To assess the impact of drug metabolism in the gut wall on oral bioavailability and develop adequate models for gut wall metabolism, it is necessary to understand the physiology of the intestinal mucosa.

The greatest activity of drug-metabolizing enzymes in the gut wall is located in the epithelium of the mucosa, its superficial lining that faces the lumen of the bowel. The mucosal epithelium consists of a single layer of enterocytes lining both the crypts and the villi. The apical membrane of the enterocytes extends in numerous projections (microvilli) forming the brush border membrane and increasing its surface area

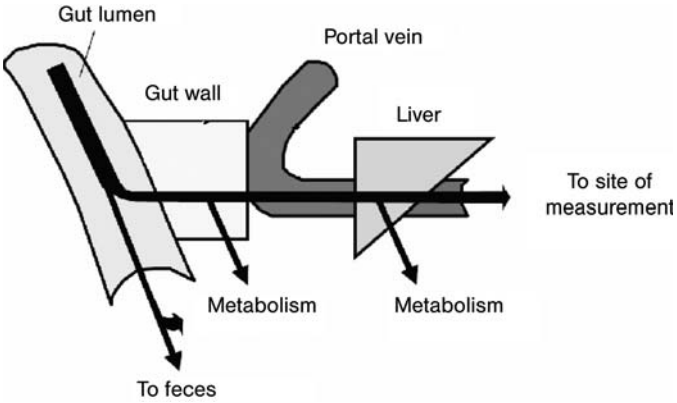

Figure 12.1 Schematic representation of gut wall and liver first-pass effects.

20-fold. These enterocytes have a programmed life span and are continuously generated in the depth of the crypts. During their maturation, they migrate to the tip of the villi, and it is here the highest activity of drug-metabolizing enzymes is found. The time the crypt cells take to mature and ascend to the tip of the villi is about 2–6 days, and one to two enterocytes are renewed per 100 cells and hour. The blood supply of the villus is provided by arterioles that pass to the tip of the villus (see Figure 12.2). Here, they spread into many small capillaries, which then drain into a villus venule. In the villus, afferent arterioles and efferent venules are in very close vicinity to each other (within 20 μm) so that passive diffusion of oxygen, nutrients, and drugs can occur while effectively bypassing the capillary network at the villus tip where the majority of drug-metabolizing enzymatic activity is located. This phenomenon is called countercurrent exchange and could have implications for the impact of metabolism in the gut wall after IV dosing [6].

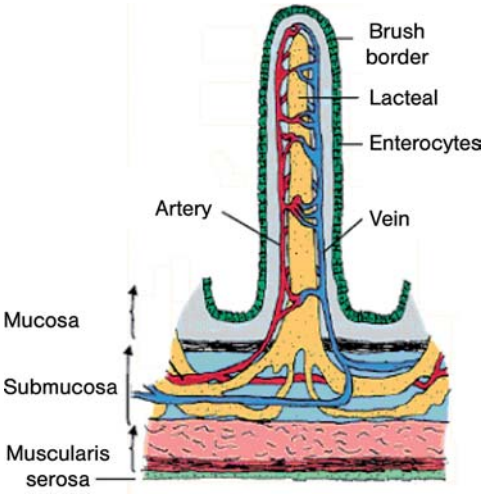

Figure 12.2 Cross section of a villus in the human mucosa of the small intestine.

The small intestine and the proximal half of the colon are supplied with blood by the superior mesenteric artery. The blood flow through the superior mesenteric artery is about 12% of cardiac output (500–700 ml/min in humans). Within the walls of the small intestine, the mesenteric circulation is organized in in-series and in-parallel relationships. The circulation of the mucosa is in series with the submucosa from which the mucosal vessels originate, but it is in parallel with the muscularis layer of the gut wall. Hence, it is important to consider the mucosal blood flow only and not the total intestinal blood flow when estimating intestinal clearance or intestinal extraction (see below). The structure of the mesenteric circulation makes an internal redistribution of intestinal blood flow possible without necessitating changes in the overall blood supply of the organ. The blood flow to each layer of the intestinal wall is constantly adapted to the metabolic demands and activity status prevailing. During absorption, blood flow increases by 30–130%, but the hyperemia is limited to the exposed segment of the intestine. During exercise, sympathetic vasoconstriction can shut off the intestinal blood supply for limited time spans in favor of a redistribution of blood to skeletal muscle and heart. Conversely, after meal intake, the blood flow to the small intestine is increased, and, as the portal vein is in series with the superior mesenteric artery, hepatic blood flow is also increased. As we will see later, increased blood flow may well influence the extent of oral bioavailability. The blood flow supplying the intestinal mucosa can be estimated at 248 ml/min [7].

12.3 Drug-Metabolizing Enzymes in the Human Mucosa

As outlined above, the main drug-metabolizing activity in the gut wall with respect to phase I and phase II enzymes is located in the enterocytes at the tip of the villi. Enzymatic activities of colonocytes, the cells lining the colon, are generally lower; however, the expression of apical efflux transport proteins such as P-glycoprotein in colonocytes is significant and exceeds than that in enterocytes (see Chapter 10).

12.3.1 Cytochrome P450

The predominant CYP in human enterocytes has been found to be CYP3A4 taking up about 80% of all intestinal CYP. The CYP3A4 expression appears to slightly decrease along the length of the small intestine, reaching very low levels in the colonocytes of the large intestine (only about 1/40 of those in the small intestine). The abundance of CYP2C9 equating to about 15% of all intestinal CYP follows a similar pattern. Prototypical substrates of CYP2D6 and CYP2C19, such as metoprolol [8] and omeprazol [9], are also metabolized in the intestinal mucosa. Considerable activity of CYP3A5 has been detected in the gut wall of some individuals within the human population [10] with CYP3A5 expression being higher in the colon than that of CYP3A4 [1]. CYP3A5 appears to metabolize the same substrates as CYP3A4 [11], but it is less prone to inhibition [12, 13] and it may express regioselectivity differently from CYP3A4 [14]. For instance, CYP3A5

metabolizes alprazolam to similar amounts at the 4- and 1′-positions, whereas CYP3A4 favors the 4-position by about 10-fold [14]. The large between-subject variability in the expression levels of CYP3A5 is thought to contribute to the largely varying oral clearance (CL/*F*) values across the patient population seen with many CYP3A4 substrates [15]. This is seen in the case of the immunosuppressant tacrolimus where oral clearance is faster depending on the number of CYP3A51 alleles carried [11].

The percentage contributions to the overall intestinal CYP protein are as follows: CYP3A4 80%, CYP2C9 15%, CYP2C19 2.9%, CYP2J2 1.4%, and CYP2D6 1% [10]. Table 12.1 gives a survey of CYPs identified in the human intestinal tract and examples of some drugs metabolized by them. The oral bioavailability is quoted in this table to help make assumptions regarding the propensity of these drugs toward first-pass metabolism in general and gut wall first-pass metabolism in particular.

12.3.2 Glucuronyltransferase

The major isozymes of the UGT family expressed in the gut wall are UGT1A1, UGT1A3, UGT1A4, UGT1A8, UGT1A9, UGT1A10, and UGT2B7 [58]. Of these, UGT1A8 and UGT1A10 are selectively expressed with the intestinal wall. Table 12.2 gives an exemplary survey of drugs predominantly cleared via glucuronidation (contribution to total CL > 50%) and the UGT isozymes involved.

UGT expression data assessing the abundance along the intestine appear to be less robust compared to CYP data, but several UGT isozymes are expressed along the whole length of the gastrointestinal tract (Figure 12.3, [80]). There is no general trend in terms of the regional activity. Some of the intestinal UGT activities are in the range of those in the liver, for example, for ezetimibe [68] and mycophenolic acid [81], when CL_{int} values are compared on the basis of milligram microsomal protein. If these values are scaled up to the whole organs, however, gastrointestinal glucuronidation rarely exceeds 5% of that of the liver [58].

12.3.3 Sulfotransferase

Studies investigating the expression and activities of SULT in human gut are scarce. One recent study found that the sulfotransferases SULT1A1, 1A3, 1E1, and 2A1 are abundant in the cytosol of the gut wall mucosa [82]. SULT1A3 appears to be not expressed in the liver. In the ileum, higher expression levels (on the basis of ng SULT/mg of cytosolic protein) compared to the liver were found for SULT1A1, SULT1A3, and SULT1B1 [82]. Table 12.3 gives drug examples metabolized by gut wall SULT.

12.3.4 Other Enzymes

About a decade ago, microsomal esterases were classified into four families (CES1–4) based on their sequence homology [95]. Of these, only CES2 is expressed in the

Table 12.1 Drug examples found to be metabolized in the gut wall by CYP.

Drug	CYP isozyme	Metabolic routes	Oral *F* (%)
Alfentanil	3A4	N-Dealkylation (noralfentanil, *N*-phenylpropionamide) [16]	42 ± 15 [17]
Alprazolam	3A4	Hydroxylation (1′-hydroxy, 4-hydroxy) [18]	80–100 [19]
Bufuralol	2D6	Hydroxylation (1′-hydroxy) [18, 20]	46 [20]
Buspirone	3A4	N-Dealkylation (1-pyrimidylpiperazine), hydroxylation (6-hydroxy) [21, 22]	3.9 [23]
Cyclosporin	3A4	AM1-, AM9-, AM4-N-oxidation [24]	22 [25]
Cisapride	3A4	N-Dealkylation (norcisapride), hydroxylation (2-hydroxy, 4-hydroxy) [26]	42 ± 11 [27]
Diclofenac	2C9	Hydroxylation (4′-hydroxy) [28]	54 ± 2 [29]
Erythromycin	3A4	N-Dealkylation [30]	35 ± 2 [29]
Ethinylestradiol	3A4	Hydroxylation (2-hydroxy) [31]	51 ± 9 [29]
Felodipine	3A4	Ring oxidation [32]	15 ± 8 [29]
Flunitrazepam	3A4, 2C19	N-Dealkylation (Norflunitrazepam), hydroxylation (3-hydroxy) [18, 33]	≥80 [34]
Flurazepam	3A4	N-Dealkylation [35]	30–60 [36]
Indinavir	3A4	N-Dealkylation, hydroxylation (*trans*-indan-OH) [37]	60–65 [38]
Lovastatin	3A4	Hydroxylation (6′-exo-methylene, 6′-hydroxy, 3″-hydroxy) [39]	<5 [29]
Metoprolol	2D6	O-Demethylation, hydroxylation [40, 41]	38 ± 14 [29]
Midazolam	3A4	Hydroxylation (1′-hydroxy, 4-hydroxy) [42]	44 ± 17 [29]
Nicardipine	3A4	Ring oxidation [32]	18 ± 11 [29]
Nifedipine	3A4	Ring oxidation [43]	50 ± 13 [29]
Omeprazole	3A4, 2C19	Hydroxylation (CYP2C19), S-oxidation (CYP3A4) [44]	53 ± 29 [29]
Propafenone	3A4, 2D6	N-Dealkylation (CYP3A4), hydroxylation (CYP2D6) [45]	5–50 [29]
Quinidine	3A4	Hydroxylation (3*S*-hydroxy), N-oxidation [46]	71–81 [47]
Rifabutin	3A4	O-Dealkylation (27-*O*-demethyl), hydroxylation (20-hydroxy, 31-hydroxy, 32-hydroxy) [48]	20 [49]
Saquinavir	3A4	Hydroxylations [50]	4 [29]
Tacrolimus	3A4	O-Demethylation [51]	16 ± 7 [29]
Terfenadine	3A4	Hydroxylation, N-dealkylation [52]	<5 [29]
Testosterone	3A4	Hydroxylation (6β-hydroxy) [53]	2–4 [54]
Tolbutamide	2C9	Hydroxylation (4-methyl-hydroxy) [55]	93 ± 10 [36]
Triazolam	3A4	Hydroxylation (1′-hydroxy, 4-hydroxy) [42]	44 [29]
Verapamil	3A4, 2C8	N-, O-dealkylation [56, 57]	22 ± 8 [29]

human small intestine, in contrast to the liver that contains enzymes of both CES1 and CES2 families [96]. Interestingly, the CES activity in the human intestine exhibits no significant proximal-to-distal gradient, in contrast to CYP [96]. Both CES1 and CES2 also cleave amides [95], as evident by their considerable butanilicaine and isocarboxazid hydrolase activity (Figure 12.4).

Table 12.2 Drug examples found to be metabolized in the gut wall by UGT.

Drug	UGT isozyme	Metabolic routes	Oral *F* (%)
Codeine	2B4, 2B7	6-*O*-Glucuronide [59]	50 ± 7 [60]
Morphine	2B4, 2B7	3-*O*-Glucuronide, 6-*O*-glucuronide [59]	24 ± 12 [61]
	1A3	3-*O*-glucuronide [62]	
	1A8	3-*O*-glucuronide, 6-*O*-glucuronide [63]	
Naloxone	2B7	3-*O*-Glucuronide [64]	2 [58]
	1A8	3-*O*-Glucuronide [63]	
Zidovudin	2B7	5′-*O*-Glucuronide [59]	75 ± 15 [65]
Paracetamol	1A1, 1A6, 1A9, 1A10	Phenolic *O*-glucuronide [66]	89 ± 4 [67]
Ezetimibe	1A1, 1A3, 2B15	Phenolic 4′-*O*-glucuronide [68]	35–60 [69]
Rac-ketoprofen	1A3, A9, 1A10, 2B7	Acyl glucuronide [70]	85 ± 21 [71]
Mycophenolic Acid (sodium salt)	1A8, 1A9	Phenolic 7-*O*-glucuronide [72], acyl glucuronide (minor) [73]	72 [74]
	2B7	Acyl glucuronide (minor) [73]	
Raloxifene	1A1, 1A8	4′-*O*-Glucuronide (major), 6-*O*-glucuronide (minor) [75]	2 [76]
	1A10	4′-*O*-glucuronide [75]	
Resveratrol	1A6, 1A8, 1A10	4′-*O*-Glucuronide, 3-*O*-glucuronide [77]	<5 [78]
	1A1	3-*O*-Glucuronide [79]	
	1A9	4′-*O*-Glucuronide [79]	

The wide distribution of esterase activity in the mucosa of stomach, small intestine, and colon has been exploited in designing numerous ester prodrugs [97–101]. Examples of successful ester prodrugs hydrolyzed, at least in part, in the gastrointestinal mucosa are ramipril [102], simvastatin [103], and bacampicillin [104].

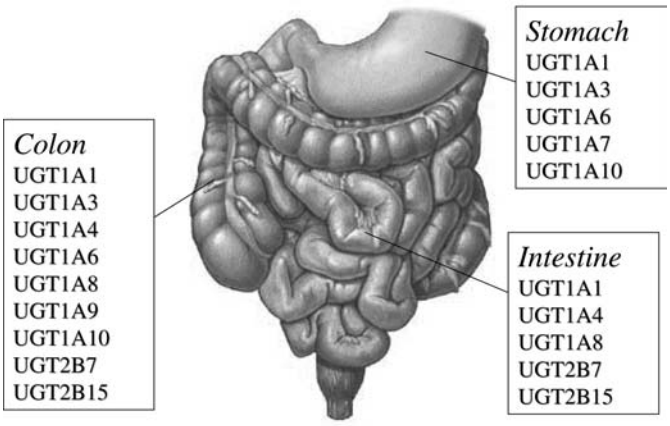

Figure 12.3 Distribution of UGT isozymes in the human gastrointestinal mucosa.

Table 12.3 Drug examples found to be metabolized in the gut wall by SULT.

Drug	SULT isozyme	Metabolic routes	Oral *F* (%)
Paracetamol	1A1 [83]	4-*O*-Sulfate	89 ± 4 [67]
Minoxidil	1A1 [83]	1-*N*-Sulfate	95 [36]
Dobutamine	1A3 [84]	Phenolic sulfate	No data
Apomorphine	1A3 [84]	Phenolic sulfate	<4 [85]
	1A1 [86]	Phenolic sulfate	
Ethinylestradiol	1E1 [82]	3-*O*-Sulfate	51 ± 9 [29]
Tibolone	2A1 [87]	17-*O*-Sulfate [88]	No data
Terbutaline	1A1, 1A3 [89, 90]	Catechol-*O*-sulfate	10–15 [91]
Isoproterenol	1A3 [84, 92]	Catechol-*O*-sulfate	No data
Salbutamol	1A1 [83], 1A3 [93]	4-*O*-Sulfate	49 [94]

In addition, the activation of the anticancer drug irinotecan to its activeprincipal SN-38 occurs by CES2 [105–107], and its gastrointestinal toxicity has been associated with local SN-38 liberation in the gut mucosa [106].

The human Caco-2 cell line has been shown to be of limited value as an *in vitro* model for the absorption and enzymatic cleavage of ester prodrugs in the gut wall mucosa because the expression pattern of CES1 and CES2 resembles more closely to the liver rather than the intestine [107].

For CES, there appear to be no regional differences in the small intestine for the *N*-acetyltransferase (NAT) activity [108]. The presence of both NAT isozymes has been demonstrated in the human gut mucosa by using the prototypical substrates *p*-aminobenzoic acid (NAT1) and sulfamethazine (NAT2) [109, 110]. The active metabolites 5-aminosalicylic acid and sulfapyridine of the prodrug sulfasalazine undergo extensive presystemic acetylation in the small intestine [111].

Alcohol dehydrogenases (ADHs), epoxide hydrolase (hydratase), *S*-methyltransferase, thiopurine methyltransferase, and glutathione *S*-transferases (GSTs) are also expressed in the gastrointestinal mucosa [29], but they are of relatively minor importance for the metabolism of drugs and will not be considered here.

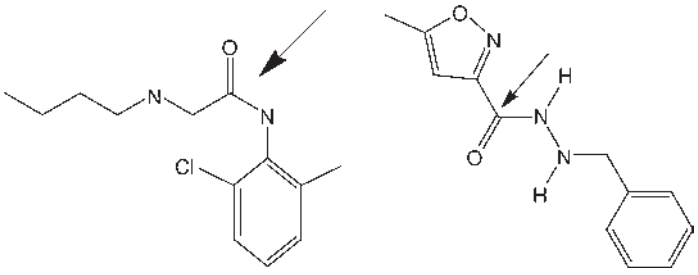

Figure 12.4 Chemical structures of butanilicaine (left) and isocarboxazid (right). The arrow indicates the site of hydrolysis.

12.4 Oral Bioavailability

The FDA definition given in CFR 21.320.1 refers to bioavailability as "the rate and extent to which the active drug ingredient or therapeutic moiety is absorbed from a drug product and becomes available at the site of action." This phrasing has led to a considerable confusion and sometimes misinterpretation of published data [19], and, as a consequence, the terms oral bioavailability and oral absorption are often used interchangeably in the scientific literature [112]. However, in the context of a more mechanistic interpretation of pharmacokinetic data, the separation of the two expressions is desired.

We will refer to oral absorption as the "movement of drug across the outer mucosal membranes of the GI tract" [112], whereas oral bioavailability is "that fraction of the dose that reaches the general circulation unchanged" [113]. The general circulation is defined experimentally in terms of a blood vessel in the peripheral circulation.

As in humans ethical constraints limit sampling sites to peripheral blood vessels, "absorption" cannot directly be estimated. Hence, the "absorption rate" (k_a, k_{01}) as calculated from peripheral plasma concentration data by compartmental or noncompartmental models reflects rather an "oral bioavailability rate," unless any gut wall and liver first-pass elimination is ruled out [112].

The oral bioavailability F consists of the fractions that survive the various barriers posed by successive organs [114]:

$$F = f_{\text{abs}} \cdot F_{\text{g}} \cdot F_{\text{h}} \cdot F_{\text{l}}, \tag{12.1}$$

where f_{abs} is the fraction absorbed from the intestinal lumen and F_{g}, F_{h}, and F_{l} are the fractions escaping extraction in the intestinal mucosa, liver, and lung, respectively. Unfortunately, standard PK sampling regimes do not allow the estimation of f_{abs}. However, the estimation of the product of $f_{\text{abs}} \cdot F_{\text{g}}$ is possible in the preclinical setting after administration of an oral and intraportal dose according to

$$f_{\text{abs}} \cdot F_{\text{g}} = \frac{D^{\text{ip}}}{D^{\text{po}}} \cdot \frac{\text{AUC}^{\text{po}}}{\text{AUC}^{\text{ip}}}, \tag{12.2}$$

where D^{ip} and D^{po} are the intraportal and oral dose, respectively, and AUC^{po} and AUC^{ip} denote the AUC after oral and intraportal administration [113] (see Figure 12.5).

f_{abs} can be estimated according to Equation 12.3 by administering a dose into the superior (cranial) mesenteric artery (D^{ima}) and relating the AUC measured from peripheral vein sampling (AUC^{ima}) to the AUC measured after an oral dose (AUC^{po}):

$$f_{\text{abs}} = \frac{D^{\text{ima}}}{D^{\text{po}}} \cdot \frac{\text{AUC}^{\text{po}}}{\text{AUC}^{\text{ima}}}. \tag{12.3}$$

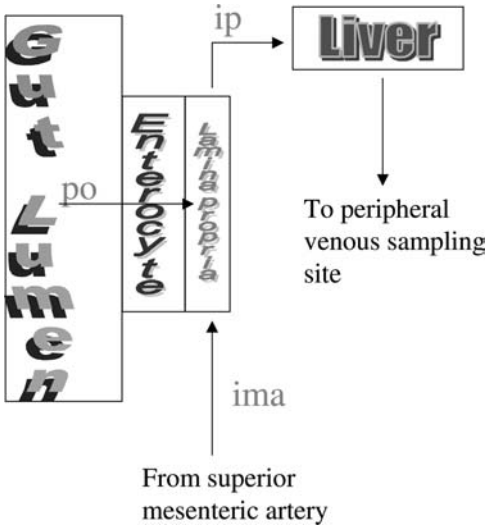

Figure 12.5 Schematic diagram of relative location of administration and sampling sites (for abbreviations see text).

Finally, F_g is derived experimentally from peripheral venous plasma concentrations after dosing to the hepatic portal vein and the superior mesenteric artery, respectively, according to Equation 12.4:

$$F_g = \frac{D^{ip}}{D^{ima}} \cdot \frac{AUC^{ima}}{AUC^{ip}}. \tag{12.4}$$

As these experimental approaches are clearly not applicable to clinical testing, indirect approaches have been used to delineate $f_{abs} \cdot F_g$ [115–118], often making assumptions not necessarily valid (e.g., $f_{abs} = 1$) or using PBPK models not entirely adequate [2].

12.4.1 *In Vivo* Approaches to Differentiate Between Intestinal and Hepatic First-Pass Metabolism

Owing to ethical constraints, the direct assessment of intestinal metabolism occurring in humans *in vivo* can only be undertaken at rare occasions, as it requires access to hepatic portal blood. For instance, transumbilical portal vein catherization can be justified only in patients requiring portal venous system radiography or regional cancer chemotherapy [118]. If the fraction absorbed is known, the extent of intestinal metabolism can then be estimated from drug and metabolite measurements in hepatic portal blood. This way, Lund *et al.* have demonstrated the almost complete hydrolysis of pivampicillin to ampicillin by the gut wall [119]. Mahon *et al.* found higher concentrations of mono- and didesethyl metabolites of flurazepam in the portal venous blood compared to hepatic venous or peripheral arterial blood following duodenal flurazepam administration to two intensive care patients [120].

The evaluation of the extent of drug metabolism in the intestinal wall can also be carried out in patients with a portocaval anastomosis where portal blood (i.e., all the venous return from the stomach, small intestine, and colon) bypasses the liver. In these "anhepatic" patients, no hepatic first-pass metabolism should occur. Comparing AUC after duodenal administration of a drug dose during the "anhepatic phase" and another dose given after the liver is in place will make it possible to calculate $f_{abs} \times F_g$ (Equation 12.1). Unless a further IV dose can be administered, F_g can be estimated only under the assumption that absorption is complete ($f_{abs} = 1$). Other assumptions to be made are linear pharmacokinetics, negligible enterocytic metabolism following drug supply via the mesenteric artery (i.e., after IV administration), and no differential influence of the general anesthesia on intestinal and hepatic clearance [4]. The few drugs that have been investigated in anhepatic patients include propranolol [121], midazolam [122], and cyclosporin [123]. For propranolol, no significant gut wall metabolism was detected suggesting that the low oral bioavailability is rather a result of extensive hepatic first-pass metabolism [121]. In the case of midazolam, however, Paine *et al.* were able to show very significant gut mucosal metabolism (mean intestinal first-pass extraction fraction of 43%) and estimated F_g as 0.57 ± 0.27 [122]. Similarly, Watkins and coworkers found unambiguously the primary cyclosporine metabolites in the hepatic portal vein and systemic blood of anhepatic patients during liver transplantation and concluded that these metabolites were of intestinal mucosal origin [123], assuming that other organs, such as the lungs, did not contribute to extrahepatic metabolism.

Another way to estimate presystemic metabolism in the gut wall is more amenable to routine clinical practice and involves drug administration via intravenous and oral routes. In addition to the assumptions outlined for anhepatic patients, this method assumes an average liver blood that does not change during treatment and uses a simple PBPK model to estimate F_g according to Equation 12.5:

$$F_g = \frac{F}{f_{abs} \cdot F_h}, \tag{12.5}$$

where F is determined from the experimental data after IV and po administration, f_{abs} is assumed to be 1, and F_h is estimated from the IV data according to (12.6), correcting total CL for renal CL and assuming that all nonrenal CL is hepatic.

$$F_h = 1 - \frac{CL_h}{Q_h}. \tag{12.6}$$

With this method, Tateishi *et al.* estimated F_g of midazolam as 0.53 ± 0.22, which is in good agreement with the anhepatic data [124].

The indirect approach by po/IV comparison can be refined by interaction studies attempting to selectively inhibit or induce gut wall metabolism. Grapefruit juice is assumed to selectively cause a mechanism-based inhibition of gut wall CYP3A enzymes, and Kupferschmidt *et al.* have used this method to derive F_g of 0.69 ± 0.31 for midazolam [125]. Similarly, Benet and coworkers have extended the original work on cyclosporin by Watkins' group [123] through interaction studies with the CYP3A4 inducer rifampin [126, 127] and the CYP3A4 inhibitor ketoconazole [128]. Other

CYP3A4 substrates whose poor oral bioavailability has been ascribed to extensive intestinal (next to hepatic) first-pass extraction are verapamil and nifedipine. In both cases, the IV/po approach combined with administration of the inducer rifampin was used to argue for extensive gut wall extraction [129, 130]. The results of the former trial have been confirmed using St John's wort as an inducer and controling absorption by jejunal single-pass perfusion [131]. Alfentanil, metabolized almost exclusively by CYP3A4, exhibited substantial gut wall extraction ($F_g = 0.56 \pm 0.18$) as adjudged from IV/po studies and coadministration of rifampin (CYP3A4 induction), troleandomycin (CYP3A4 inhibition), or grapefruit juice [17].

In summary, recent clinical studies have indicated that the small intestine contributes substantially to the overall first-pass metabolism of CYP3A4 substrates such as cyclosporin, nifedipine, midazolam, verapamil, and alfentanil. Much of the evidence has been derived indirectly from comparisons of areas under the plasma concentration curves (AUCs) after IV and po administrations and additional studies investigating the effect of coadministered CYP3A4 inhibitors and inducers. The absence of well-established clinical inhibitors/inducers for non-CYP3A enzymes may help rationalize the relative lack of clinical studies indicating significant involvement of other drug-metabolizing enzymes in gut wall first-pass extraction. Clearly, some of the assumptions made in those indirect studies have not yet been tested. For instance, it is often assumed that the systemic clearance of a drug after an IV dose reflects only hepatic elimination and that metabolism of the systematically available drug by intestinal enzymes is negligible. Only then can hepatic extraction be calculated directly from the observed total CL after IV administration and the reported values of hepatic blood flow. This allows then the indirect estimation of F_g according to Equation 12.5. Owing to the potential countercurrent exchange and plasma protein binding, the fraction of the systemically available drug metabolized by the intestine may indeed not be as great as that which occurs during absorption. However, it appears unrealistic to neglect completely the intestinal metabolism of drugs when delivered from the systemic circulation. For instance, Paine *et al.* [122] estimated F_g of midazolam in anhepatic patients after IV administration as 0.92 (0.75–1). The neglect of the contribution of the intestinal mucosa to total clearance after IV administration may hence lead to an overestimation of the gut wall first-pass effect. Further uncertainties include the variability in hepatic blood flow and f_{abs} [115]. In this context, it should also be borne in mind that the clinical methods available allow only a realistic (i.e., without assumption regarding f_{abs}) estimation of the product $f_{abs} \times f_g$.

The obvious clinical limitations in directly assessing gut wall metabolism in humans underline the importance of modeling approaches. These will be briefly reviewed in Section 12.4.3.

12.4.2
In Vitro Approaches to Estimate Intestinal Metabolism

Owing to the limitations of the methods available to study intestinal metabolism in a clinical setting (see Section 12.4.1), *in vitro* approaches with human systems give important, often the only information accessible on the intestinal metabolism of a drug or an NCE. Human *in vitro* systems suitable for the determination of gut

mucosal CL_{int} values serving as input parameters for computational models (see Section 12.4.3) comprise whole-tissue models (Ussing chamber, precision-cut intestinal slices), cellular models (shed enterocytes), and subcellular fractions (gut mucosal microsomes).

Complete human intestinal mucosal sheets can be investigated in the Ussing diffusion chamber. This experimental setup makes it possible not only to investigate mucosal metabolism in different gut segments along the length of the intestine but also to conduct vectorial transport of drug and metabolites formed *in situ* [132]. If carried out competently, experiments with Ussing preparations can be characterized by high metabolic activity, good activity of transport proteins, and high tissue viability including membrane integrity. Issues are the supply of suitable, fresh human tissue, and the need for rapid, but careful, tissue preparation including the removal of muscle layers and serosa.

Precision-cut human mucosal slices are prepared with a Krumdieck tissue slicer [132]. A study comparing precision-cut slices and intestinal sheets in the Ussing chamber found comparable utility of both approaches to assess intestinal metabolism [132]. Formation rates of midazolam 1′-hydroxylation (CYP3A4/5), diclofenac 4′-hydroxylation (CYP2C9), bufuralol hydroxylation (CYP2D6), 7-hydroxycoumarin sulfation, and glucuronidation were found to be constant for up to 4 h in both precision-cut slices and Ussing chamber setup [132].

Shed enterocytes constitute a very elegant cellular *in vitro* model of human gut metabolism [133]. About 15–30 million enterocytes are shed per minute into the lumen of the gastrointestinal tract, and these cells can be collected by segmental jejunal perfusion from healthy volunteers. The majority of shed enterocytes collected this way were nonapoptotic and metabolically fully competent. Obstacles to more widespread use of this tool are the still very limited availability and very high price.

Gut mucosal microsomes are the most widespread *in vitro* tool because of their ease to use, commercial availability, and their amenability to long-term storage. Over the past decade, considerable improvements in the preparation methods of intestinal microsomes have been made resulting in a better preservation of CYP activity. Intestinal microsomes prepared by enterocyte elution [134] appear to have generally higher activities compared to those prepared from mucosal scrapings [135].

12.4.3
Computational Approaches to Estimate and to Predict Human Intestinal Metabolism

The lack of generally applicable direct methods to measure intestinal metabolism in humans (see Section 12.4.1) emphasizes the need for reliable computational models to differentiate intestinal metabolism from hepatic first-pass metabolism. Historically, the well-stirred (venous equilibrium) model has been adapted to the gut [1, 29] and used for these predictions according to Equation 12.7:

$$F_g = \frac{Q_g}{(f_{u,b} \cdot CL_{int,g}) + Q_g}, \tag{12.7}$$

where Q_g represents the mucosal blood flow, $f_{u,b}$ the unbound fraction in blood, and $CL_{int,g}$ the intestinal intrinsic clearance. It has been questioned whether the

well-stirred model is adequate for intestinal first-pass metabolism, because the drug is not delivered by the blood to the mucosa, and the influence of plasma protein binding on the vectorial movement of drug from the intestinal lumen to the vasculature is unknown [2, 4, 5]. This approach has been defended by pointing out that mucosal blood flow and plasma protein binding do influence the residence time in enterocytes by drawing drug away from the metabolizing enzymes [29]. However, the main argument against the "intestinal well-stirred model" is its poor predictivity [2, 4, 5]. Tummel *et al.* [29] predicted F_g of 12 CYP3A4 substrates and found up to 15-fold prediction errors with a trend for overpredicting F_g [5]. The poor predictivity has been confirmed by Yang *et al.*, particularly when $f_{u,b}$ was included in the model [4]. Some of the apparent inadequacy of the well-stirred gut model can possibly be explained by the limitations of the "measured" data (see Section 12.4.1) and the use of suboptimal intestinal microsomal data to estimate $CL_{int,g}$ (see Section 12.4.2). It has also been put forward that an intestinal parallel-tube model should better reflect mucosal physiology, as less stirring of the blood is expected compared to that of the liver [5].

To overcome the shortcomings of the intestinal well-stirred model, Yang *et al.* proposed the "Q_{gut} model" [4]. This model maintains the basic equation of the well-stirred model, but expands the flow term into a hybrid of both permeability through the enterocyte membrane defined by CL_{perm} and villous blood flow (Q_{villi}) according to Equation 12.8:

$$Q_{gut} = \frac{Q_{villi} \cdot CL_{perm}}{Q_{villi} + CL_{perm}}. \tag{12.8}$$

CL_{perm} can be derived from *in vitro* permeability experiments (Caco-2, MDCK cells, and PAMPA) or *in silico* from polar surface area and the number of hydrogen-bond donors [4]. Yang *et al.* found a clear superiority of the Q_{gut} model over the well-stirred model in terms of accuracy and precision, particularly when plasma protein binding was ignored [4]. This simplified the model to (12.9):

$$F_g = \frac{Q_{villi}}{Q_{villi} + CL_{int,g} \cdot (1 + (Q_{villi}/CL_{prem}))}. \tag{12.9}$$

The Q_{gut} model can be regarded as the minimal version of the TMF (transport, metabolism, and blood flow) model proposed by Mizuma [2, 136]. An intestinal permeability term was also incorporated by Fagerholm into his approach to predict gut wall first-pass extraction [5]. Instead of relying on scaling factors to convert *in vitro* CL_{int} into *in vivo* CL_{int} and on assumptions regarding blood flow values, Fagerholm used verapamil as a reference compound with known mucosal extraction and known *in vitro* CL_{int}. Using his method, Fagerholm predicted the first-pass *in vivo* gut wall extraction of midazolam, bromocriptine, nifedipine, and diltiazem with little error [5].

These simple models based on the assumption of a single intestinal compartment have been refined to the advanced compartmental absorption and transport model that allows transit and differential expression of enzymes and transporters down the length of the gastrointestinal tract including pH, fluid, and blood flow differences [3]. The ACAT model is based on a series of integrated differential equations and has been implemented in the commercial software Gastroplus (see Chapter 17).

12.5
Clinical Relevance of Gut Wall First-Pass Metabolism

Gut wall metabolism as a major determinant for poor oral bioavailability is still a matter of debate within the scientific community [1, 115, 117]. In general, the metabolic capacity of the intestinal tract appears inferior to that of the liver, but for a number of drug molecules such as midazolam, nifedipine, verapamil, tacrolimus, and saquinavir, gastrointestinal first-pass elimination is substantial. This appears to be particularly true for CYP3A substrates, though the total intestinal CYP3A amount is only about 1% of that in the liver [10]. However, it has been argued that drug exposure to the enterocytic metabolizing enzymes is probably greater than that in the liver where it is limited by fast blood flow and the impact of binding to blood components [4]. In contrast, all drug absorbed into the enterocyte could be freely accessible to drug-metabolizing enzymes, limited only by the flux through the cell and assuming negligible intracellular binding. The higher substrate accessibility might result in more likely enzyme saturation in the mucosa, but this could be offset by recycling and dilution via efflux transport proteins. On the other hand, saturation of intestinal efflux transporters following oral dosing and high luminal concentrations is also a realistic possibility. Owing to experimental limitations, clinically relevant gut wall first-pass metabolism is often discovered only after studies utilizing the complete inhibition of intestinal CYP3A following the ingestion of grapefruit juice are done. In this setting, significant increases in oral exposure have been observed for midazolam [125], buspirone [137], felodipine [138], lovastatin [139], simvastatin [140], cyclosporin [25], nifedipine [141], and cisapride [142]. It is tempting to speculate that detection of clinically relevant intestinal metabolism of non-CYP3A substrates has been hindered by missing gut-selective inhibitors of those enzymes.

Still, from a pharmaceutical industry perspective, drug candidate attrition rates owing to an unexpectedly high gastrointestinal first-pass effect are low, because the majority of intestinal metabolic liabilities will have been readily detected in systems geared toward hepatic metabolism.

References

1 Thummel, K.E. and Shen, D.E. (2002) The role of the gut mucosa in metabolically based drug–drug interactions. *Drugs and the Pharmaceutical Sciences*, **116**, 359–385.

2 Mizuma, T., Tsuji, A. and Hayashi, M. (2004) Does the well-stirred model assess the intestinal first-pass effect well? *The Journal of Pharmacy and Pharmacology*, **56**, 1597–1599.

3 Agoram, B., Woltosz, W.S. and Bolger, M.B. (2001) Predicting the impact of physiological and biochemical processes on oral drug bioavailability. *Advanced Drug Delivery Reviews*, **50** (Suppl. 1), S41–S67.

4 Yang, J., Jamei, M., Rowland Yeo, K., Tucker, G.T. and Rostami-Hodjegan, A. (2007) Prediction of intestinal first-pass metabolism. *Current Drug Metabolism*, **8**, 676–684.

5 Fagerholm, U. (2007) Prediction of human pharmacokinetics – gut-wall metabolism. *The Journal of Pharmacy and Pharmacology*, **59**, 1335–1343.

6 Jacobson, E.D. (1982) Physiology of the mesenteric circulation. *The Physiologist*, **25**, 439–443.

7 Hulten, L., Lindhagen, J. and Lundgren, O. (1977) Sympathetic nervous control of intramural blood flow in the feline and human intestines. *Gastroenterology*, **72**, 41–48.

8 Madani, S., Paine, M.F., Lewis, L., Thummel, K.E. and Shen, D.D. (1999) Comparison of CYP2D6 content and metoprolol oxidation between microsomes isolated from human livers and small intestines. *Pharmaceutical Research*, **16**, 1199–1205.

9 Klotz, U. (2006) Clinical impact of CYP2C19 polymorphism on the action of proton pump inhibitors: A review of a special problem. *International Journal of Clinical Pharmacology and Therapeutics*, **44**, 297–302.

10 Paine, M.F., Hart, H.L., Ludington, S.S., Haining, R.L., Rettie, A.E. and Zeldin, D.C. (2006) The human intestinal cytochrome P450 "pie". *Drug Metabolism and Disposition: The Biological Fate of Chemicals*, **34**, 880–886.

11 Daly, A.K. (2006) Significance of the minor cytochrome P450 3A isoforms. *Clinical Pharmacokinetics*, **45**, 13–31.

12 Gibbs, M.A., Thummel, K.E., Shen, D.D. and Kunze, K.L. (1999) Inhibition of cytochrome P-450 3A (CYP3A) in human intestinal and liver microsomes: comparison of Ki values and impact of CYP3A5 expression. *Drug Metabolism and Disposition: The Biological Fate of Chemicals*, **27**, 180–187.

13 Soars, M.G., Grime, K. and Riley, R.J. (2006) Comparative analysis of substrate and inhibitor interactions with CYP3A4 and CYP3A5. *Xenobiotica; The Fate of Foreign Compounds in Biological Systems*, **36**, 287–299.

14 Galetin, A., Brown, C., Hallifax, D., Ito, K. and Houston, J.B. (2004) Utility of recombinant enzyme kinetics in prediction of human clearance: impact of variability, CYP3A5, and CYP2C19 on CYP3A4 probe substrates. *Drug Metabolism and Disposition: The Biological Fate of Chemicals*, **32**, 1411–1420.

15 Lin, Y.S., Dowling, A.L.S., Quigley, S.D., Farin, F.M., Zhang, J., Lamba, J., Schuetz, E.G. and Thummel, K.E. (2002) Co-regulation of CYP3A4 and CYP3A5 and contribution to hepatic and intestinal midazolam metabolism. *Molecular Pharmacology*, **62**, 162–172.

16 Labroo, R.B., Thummel, K.E., Kunze, K.L., Podoll, T., Trager, W.F. and Kharasch, E.D. (1995) Catalytic role of cytochrome P4503A4 in multiple pathways of alfentanil metabolism. *Drug Metabolism and Disposition: The Biological Fate of Chemicals*, **23**, 490–496.

17 Kharasch, E.D., Walker, A., Hoffer, C. and Sheffels, P. (2004) Intravenous and oral alfentanil as *in vivo* probes for hepatic and first-pass cytochrome P-450 3A activity: noninvasive assessment by use of papillary miosis. *Clinical Pharmacology and Therapeutics*, **76**, 452–466.

18 Galetin, A. and Houston, J.B. (2006) Intestinal and hepatic metabolic activity of five cytochrome P450 enzymes: impact on prediction of first-pass metabolism. *The Journal of Pharmacology and Experimental Therapeutics*, **318**, 1220–1229.

19 Zhao, Y.H., Le, J., Abraham, M.H., Hersey, A., Eddershaw, P.J., Luscombe, C.N., Boutina, D., Beck, G. *et al.* (2001) Evaluation of human intestinal absorption data and subsequent derivation of a quantitative structure–activity relationship (QSAR) with the Abraham descriptors. *Journal of Pharmaceutical Sciences*, **90**, 749–784.

20 Dayer, P., Balant, L., Courvoisier, F., Kupfer, A., Kubli, A., Gorgia, A. and Fabre, J. (1982) The genetic control of bufarolol metabolism in man. *European Journal of*

Drug Metabolism and Pharmacokinetics, **7**, 73–77.

21 Laine, K., Ahokoski, O., Huupponen, R., Haenninen, J., Palovaara, S., Ruuskanen, J., Bjoerklund, H., Anttila, M. and Rouru, J. (2003) Effect of the novel anxiolytic drug deramclicane on the pharmacokinetics and pharmacodynamics of the CYP3A4 probe drug buspirone. *European Journal of Clinical Pharmacology*, **59**, 761–767.

22 Dockens, R., Salazar, D.E., Fulmor, I.E., Wehling, M., Arnold, M.E. and Croop, R. (2006) Pharmacokinetics of a newly identified active metabolite of buspirone after administration of buspirone over its therapeutic dose range. *Journal of Clinical Pharmacology*, **46**, 1308–1312.

23 Jann, M.W. (1988) Buspirone: an update on a unique anxiolytic agent. *Pharmacotherapy*, **8**, 100–116.

24 Kronbach, T., Fischer, V. and Meyer, U. (1988) Cyclosporine metabolism in human liver: identification of a cytochrome P-450III gene family as the major cyclosporine-metabolizing enzyme explains interactions of cyclosporine with other drugs. *Clinical Pharmacology and Therapeutics*, **43**, 630–635.

25 Ducharme, M.P., Warbasse, L.H. and Edwards, D.J. (1995) Disposition of intravenous and oral cyclosporine after administration with grapefruit juice. *Clinical Pharmacology and Therapeutics*, **57**, 485–491.

26 Pearce, R.E., Gotschall, R.R., Kearns, G.L. and Leeder, J.S. (2001) Cytochrome P-450 involvement in the biotransformation of cisapride and racemic norcisapride *in vitro*: differential activity of individual human CYP3A isoforms. *Drug Metabolism and Disposition: The Biological Fate of Chemicals*, **29**, 1548–1554.

27 Van Peer, A., Embrechts, L., Woestenborgs, R. *et al* Pharmacokinetics of cisapride and its bioavailability after oral and rectal administration in six healthy male volunteers. FDA Clinical Pharmacology Biopharmaceutics Review (s), pp. 27–28, see http://www.fda.gov/cder/foi/nda/pre96/020210_S000_Cisapride_IOPHARMR.pdf.

28 Laepple, F., von Richter, O., Fromm, M.F., Richter, T., Thon, K.P. Wisser, H., Griese, E.-U., Eichelbaum, M. and Kivistoe, K.P. (2003) Differential expression and function of CYP2C isoforms in human intestine and liver. *Pharmacogenetics*, **13**, 565–575.

29 Tummel, K.E., Kunze, K.L. and Shen, D.D. (1997) Enzyme-catalyzed processes of first-pass hepatic and intestinal drug extraction. *Advanced Drug Delivery Reviews*, **27**, 99–127.

30 Watkins, P.B., Wrighton, S.A., Maurel, P., Schuetz, E.G., Mendez-Picon, G., Parker, G.A. and Guzelian, P.S. (1985) Identification of an inducible form of cytochrom-450 in human liver. *Proceedings of the National Academy of Sciences of the United States of America*, **83**, 6310–6314.

31 Guengerich, F.P. (1988) Oxidation of 17α-ethynylestradiol by human liver cytochrome P-450. *Molecular Pharmacology*, **33**, 500–508.

32 Guengerich, F.P., Brian, W.R., Iwasaki, M., Sari, M.-A., Baarnhielm, C. and Berntsson, P. (1991) Oxidation of dihydropyridine calcium channel blocker and analogues by human liver cytochrome P-450 IIIA4. *Journal of Medicinal Chemistry*, **34**, 1838–1844.

33 Kilicarslan, T., Haining, R.L., Rettie, A.E., Busto, U., Tyndale, R.F. and Sellers, E.M. (2001) Flunitrazepam metabolism by cytochrome P450 2C19 and 3A4. *Drug Metabolism and Disposition: The Biological Fate of Chemicals*, **29**, 460–465.

34 Cano, J.P., Soliva, M., Hartmann, D., Ziegler, W.H. and Amrein, R. (1977) Bioavailability from various galenic formulations of flunitrazepam. *Arzneim Forsch*, **27**, 2383–2388.

35 Mahon, M.A., Inaba, T. and Stone, R.M. (1977) Metabolism of flurazepam by the small intestine. *Clinical Pharmacology and Therapeutics*, **22**, 228–233.

36 Klotz, U. (1988) Tabellen mit pharmakokinetischen Daten, in *Einführung in die Pharmakokinetik* (ed. U. Klotz), Govi-Verlag, Frankfurt/Main.

37 Chiba, M., Nishime, J.A., Neway, W., Lin, Y. and Lin, J.H. (2000) Comparative *in vitro* metabolism of indinavir in primates – a unique stereoselective hydroxylation in monkey. *Xenobiotica; The Fate of Foreign Compounds in Biological Systems*, **30**, 117–129.

38 Yeh, K.C., Stone, J.A., Carides, A.D., Rolan, P., Woolf, E. and Ju, W.D. (1999) Simultaneous investigation of indinavir nonlinear pharmacokinetics and bioavailability in healthy volunteers using stable isotope labelling technique: study design and model-independent data analysis. *Journal of Pharmaceutical Sciences*, **88**, 568–573.

39 Wang, R.W., Kari, P.H., Lu, A.Y.H., Thomas, P.E., Guengerich, F.P. and Vyas, K.P. (1991) Biotransformation of lovastatin. IV. Identification of cytochrome P450 3A proteins as the major enzymes responsible for oxidative metabolism of lovastatin in rat and human liver microsomes. *Archives of Biochemistry and Biophysics*, **290**, 355–361.

40 Gut, J., Catin, T., Dayer, P., Kronbach, T., Zanger, U. and Meyer, U.A. (1986) Debrisoquine/sparteine-type polymorphism of drug oxidation. *The Journal of Biological Chemistry*, **261**, 11734–11743.

41 Otton, S.V., Crewe, H.K., Lennard, M.S., Tucker, G.T. and Woods, H.F. (1988) Use of quinidine inhibition to define the role of the sparteine/debrisoquine cytochrome P-450 in metoprolol oxidation by human liver microsomes. *The Journal of Pharmacology and Experimental Therapeutics*, **247**, 242–247.

42 Kronbach, T., Mathys, D., Umeno, M., Gonzalez, F.J. and Meyer, U.A. (1989) Oxidation of midazolam and triazolam by human liver cytochrome P-450IIIA4. *Molecular Pharmacology*, **36**, 89–96.

43 Guengerich, F.P., Martin, M.V., Beaune, P.H., Kremers, P., Wolff, T. and Waxman, W.J. (1986) Characterization of rat and human liver microsomal cytochrome P-450 forms involved in nifedipine oxidation, a prototype for genetic polymorphism in oxidative drug metabolism. *The Journal of Biological Chemistry*, **261**, 5051–5060.

44 Brynne, N., Bottiger, Y., Hallen, B. and Bertilsson, L. (1999) Tolterodine does not affect the human *in vivo* metabolism of the probe drugs caffeine, debrisoquine and omeprazole. *British Journal of Clinical Pharmacology*, **47**, 145–150.

45 Hemryck, A., De Vriendt, C. and Belpaire, F.M. (2000) Effect of selective serotonin reuptake inhibitors on the oxidative metabolism of propafenone. *Journal of Clinical Psychopharmacology*, **20**, 428–434.

46 Nielsen, T.B., Buur Rasmussen, B., Flinois, J.-P., Beaune, P. and Brøsen, K. (1999) *In vitro* metabolism of quinidine: the (3S)-3-hydroxylation of quinidine is a specific marker reaction for cytochrome P-450 3A4 activity in human liver microsomes. *The Journal of Pharmacology and Experimental Therapeutics*, **289**, 31–37.

47 Greenblatt, D.J., Pfeifer, H.J., Ochs, H.R., Franke, K., MacLaughlin, D.S., Smith, T.W. and Koch-Weser, J. (1977) Pharmacokinetics of quinidine in humans after intravenous, intramuscular and oral administration. *The Journal of Pharmacology and Experimental Therapeutics*, **202**, 365–378.

48 Iatsimirskaia, E., Tulebaev, S., Storozhuk, E., Utkin, I., Smith, D., Gerber, N. and Koudriakova, T. (1997) Metabolism of rifabutin in human enterocyte and liver microsomes: kinetic parameters, identification of enzyme systems, and drug interactions with macrolides and antifungal agents. *Clinical Pharmacology and Therapeutics*, **61**, 554–562.

49 Skinner, M.H. and Blaschke, T.F. (1995) Clinical pharmacokinetics of rifabutin. *Clinical Pharmacokinetics*, **28**, 115–125.

50 Fitzsimmons, M.E. and Collins, J.M. (1997) Selective biotransformation of the human immunodeficiency virus protease inhibitor saquinavir by human small intestinal cytochrome P-450 3A4. *Drug Metabolism and Disposition: The Biological Fate of Chemicals*, **25**, 256–266.

51 Sattler, M., Guengerich, F.P., Yun, C.-H., Christians, U. and Sewing, K.-F. (1992) Cytochrome P-450 3A enzymes are responsible for the biotransformation of FK506 and rapamycin in man and rat. *Drug Metabolism and Disposition: The Biological Fate of Chemicals*, **20**, 753–761.

52 Ling, K.-H.J., Leeson, G.A., Burmaster, S.D., Hook, R.H., Reith, M.K. and Cheng, L.K. (1995) Metabolism of terfenadine associated with CYP3A4 activity in human hepatic microsomes. *Drug Metabolism and Disposition: The Biological Fate of Chemicals*, **23**, 631–636.

53 Patki, K.C., von Moltke, L.L. and Greenblatt, D.J. (2003) *In vitro* metabolism of midazolam, triazolam, nifedipine, and testosterone by human liver microsomes and recombinant cytochromes P-450: role of CYP3A4 and CYP3A5. *Drug Metabolism and Disposition: The Biological Fate of Chemicals*, **31**, 938–944.

54 Täuber, U., Schröder, K., Dusterberg, B. and Matthes, H. (1986) Absolute bioavailability of testosterone after oral administration of testosterone–undecanoate and testosterone. *European Journal of Drug Metabolism and Pharmacokinetics*, **11**, 145–149.

55 Inoue, K., Yamazaki, H., Imiya, K., Akasaka, S., Guengerich, F.P. and Shimada, T. (1997) Relationship between CYP2C9 and CYP2C19 genotypes and tolbutamide methyl hydroxylation and *S*-mephenytoin 4′-hydroxylation activities in livers of Japanese and Caucasian populations. *Pharmacogenetics*, **7**, 103–113.

56 Kroemer, H.K., Gautier, J.-C., Beaune, P., Henderson, C., Wolff, R. and Eichelbaum, M. (1993) Identification of P450 enzymes involved in metabolism of verapamil in humans. *Naunyn-Schmiedeberg's Archive of Pharmacology*, **348**, 332–337.

57 Busse, D., Cosme, J., Beaune, Kroemer, H.K. and Eichelbaum, M. (1995) Cytochromes of the P450 2C subfamily are the major enzymes involved in the O-demethylation of verapamil in humans. *Naunyn-Schmiedeberg's Archive of Pharmacology*, **353**, 116–121.

58 Ritter, J.K. (2007) Intestinal UGTs as potential modifiers of pharmacokinetics and biological responses to drugs and xenobiotics. *Expert Opinion on Drug Metabolism and Toxicology*, **3**, 93–107.

59 Court, M.H., Krishnaswamy, S., Hao, Q., Duan, S.X., Patten, C.J., von Moltke, L.L. and Greenblatt, D.J. (2003) Evaluation of 3′-azido-3′deoxythymidine, morphine, and codeine as probe substrates for UDP-glucuronosyltransferase 2B7 (UGT2B7) in human liver microsomes: specificity and influence of the UGT2B72 polymorphism. *Drug Metabolism and Disposition: The Biological Fate of Chemicals*, **31**, 1125–1133.

60 Quiding, H., Anderson, P., Bondesson, U., Boreus, L.O. and Hynning, P.A. (1986) Plasma concentrations of codeine and its metabolite, morphine, after single and repeated oral administration. *European Journal of Clinical Pharmacology*, **30**, 673–677.

61 Glare, P.A. and Walsh, T.D. (1991) Clinical pharmacokinetics of morphine. *Therapeutic Drug Monitoring*, **13**, 1–23.

62 Green, M.D., King, C.D., Mojarrabi, B., Mackenzie, P.I. and Tephly, T.R. (1998) Glucuronidation of amines and other xenobiotics catalyzed by expressed human UDP-glucuronosyltransferase 1A3. *Drug Metabolism and Disposition: The Biological Fate of Chemicals*, **26**, 507–512.

63 Cheng, Z., Radominska-Panya, A. and Tephly, T.R. (1999) Studies on the substrate specificity of human intestinal UDP-glucuronosyl transferases 1A8 and

1A10. *Drug Metabolism and Disposition: The Biological Fate of Chemicals*, **27**, 1165–1170.

64 Di Marco, A., D'Antoni, M., Attaccalite, S., Carotenuto, P. and Laufer, R. (2005) Determination of drug glucuronidation and UDP-glucuronosyltransferase selectivity using a 96-well radiometric assay. *Drug Metabolism and Disposition: The Biological Fate of Chemicals*, **33**, 812–819.

65 Moore, K.H.P., Raasch, R.H., Brouweer, K.L.R., Opheim, K., Cheeseman, S.H., Eyster, E., Lemon, S.M. and van der Horst, C.M. (1995) Pharmacokinetics and bioavailablity of zidovudine and its glucuronidated metabolite in patients with human immunodeficiency virus infection and hepatic disease (AIDS Clinical Trials Group Protocol 062). *Antimicrobial Agents and Chemotherapy*, **39**, 2732–2737.

66 Court, M.H., Duan, S.X., von Moltke, L.L., Greenblatt, D.J., Patten, C.J., Miners, J.O. and Mackenzie, P.I. (2001) Inter-individual variability in acetaminophen glucuronidation by human liver microsomes: identification of relevant acetaminophen UDP-glucuronosyltransferase isoforms. *The Journal of Pharmacology and Experimental Therapeutics*, **299**, 998–1006.

67 Rawlins, M.D., Henderson, D.B. and Hijab, A.R. (1977) Pharmacokinetics of paracetamol (acetaminophen) after intravenous and oral administration. *European Journal of Clinical Pharmacology*, **11**, 283–286.

68 Ghosal, A., Hapangama, N., Yuan, Y., Achanfuo-Yeboah, J., Iannucci, R., Chowdhury, S., Alton, K., Patrick, J.E. and Zbaida, S. (2004) Identification of human UDP-glucuronosyltransferase enzyme(s) responsible for the glucuronidation of ezetimibe (Zetia). *Drug Metabolism and Disposition: The Biological Fate of Chemicals*, **32**, 314–320.

69 Kosoglou, T., Statkevich, P., Johnson-Levonas, A.O., Paolini, J.F., Bergman, A.J. and Alton, K.B. (2005) Ezetimibe: a review of its metabolism, pharmacokinetics and drug interactions. *Clinical Pharmacokinetics*, **44**, 467–494.

70 Sabolovic, N., Heydel, J.-M., Li, X., Little, J.M., Humbert, A.-C., Radominska-Pandya, A. and Magdalou, J. (2004) Carboxyl nonsteroidal anti-inflammatory drugs are efficiently glucuronidated by microsomes of the human gastrointestinal tract. *Biochimica et Biophysica Acta*, **1675**, 120–129.

71 Geisslinger, G., Menzel, S., Wissel, K. and Brune, K. (1995) Pharmacokinetics of ketoprofen enantiomers after different doses of the racemate. *British Journal of Clinical Pharmacology*, **40**, 73–75.

72 Bernard, O. and Guillemette, C. (2004) The main role of UGT1A9 in the hepatic metabolism of mycophenolic acid and the effect of naturally occurring variants. *Drug Metabolism and Disposition: The Biological Fate of Chemicals*, **32**, 775–778.

73 Bernard, O., Tojcic, J., Journault, K., Perusse, L. and Guillemette, C. (2006) Influence of nonsynonymous polymorphisms of UGT1A8 and UGT2B7 metabolizing enzymes on the formation of phenolic and acyl glucuronides of mycophenolic acid. *Drug Metabolism and Disposition: The Biological Fate of Chemicals*, **34**, 1539–1545.

74 Staats, C.E. and Tett, S.E. (2007) Clinical pharmacokinetics and pharmaco-dynamics of mycophenolate in solid organ transplant recipients. *Clinical Pharmacokinetics*, **46**, 13–58.

75 Kemp, D.C., Fan, P.W. and Stevens, J.C. (2002) Characterization of raloxifene glucuronidation *in vitro*: contribution of intestinal metabolism to presystemic clearance. *Drug Metabolism and Disposition: The Biological Fate of Chemicals*, **30**, 694–700.

76 Snyder, K.R., Sparano, N. and Malinowski, J.M. (2000) Raloxifene hydrochloride. *American Journal of Health-System Pharmacy*, **57**, 1669–1678.

77 Sabolovic, N., Humbert, A.C., Radominska-Pandya, A. and Magdalou, J. (2006) Resveratrol is efficiently glucuronidated by UDP-glucuronosyltransferases in the human gastrointestinal tract and in Caco-2 cells. *Biopharmaceutics & Drug Disposition*, **27**, 181–189.

78 Walle, T., Hsieh, F., Delegge, M.H., Oatis, J.E., Jr. and Walle, U.K. (2004) High absorption but very low bioavailability of resveratrol in humans. *Drug Metabolism and Disposition: The Biological Fate of Chemicals*, **32**, 1377–1382.

79 Brill, S.S., Furimsky, A.M., Ho, M.N., Furniss, M.J., Li, Y., Green, A.G., Bradford, W.W., Green, C.E., Kapetanovic, I.M. and Iyer, L.V. (2006) Glucuronidation of trans-resveratrol by human liver and intestinal microsomes. *The Journal of Pharmacy and Pharmacology*, **58**, 469–479.

80 Tukey, R.H. and Strassburg, C.P. (2000) Human UDP-glucuronyltransferases: metabolism, expression, and disease. *Annual Review of Pharmacology and Toxicology*, **40**, 581–616.

81 Bowalgaha, K. and Miners, J.O. (2001) The glucuronidation of mycophenolic acid by human liver, kidney and jejunum microsomes. *British Journal of Clinical Pharmacology*, **52**, 605–609.

82 Teubner, W., Meinl, W., Florian, S., Kretzschmar, M. and Glatt, H. (2007) Identification and localization of soluble sulfotransferases in the human gastrointestinal tract. *The Biochemical Journal*, **404**, 207–215.

83 Pacifici, G.M. (2004) Inhibition of human liver and duodenum sulfotransferases by drugs and dietary chemicals: a review of the literature. *International Journal of Clinical Pharmacology and Therapeutics*,, **42**, 488–495.

84 Dajani, R., Cleasby, A., Neu, M., Wonacott, A.J., Jhoti, H., Hood, A.M., Modi, S., Hersey, A., *et al.* (1999) X-ray crystal structure of human dopamine sulfotransferase, SULT1A3. Molecular modelling and quantitative structure–activity relationship analysis demonstrate a molecular basis for sulfotransferase substrate specificity. *The Journal of Biological Chemistry*, **274**, 37862–36868.

85 Gancher, S.T., Nutt, J.G. and Woodward, W.R. (1991) Absorption of apomorphine by various routes in parkinsonism. *Movement Disorders*, **6**, 212–216.

86 Vietri, M., Vaglini, F., Pietrabissa, A., Spisni, R., Mosca, F. and Pacifici, G.M. (2002) Sulfation of *R*(−)-apomorphine in the human liver and duodenum, and its inhibition by mefenamic acid, salicylic acid and quercetin. *Xenobiotica; The Fate of Foreign Compounds in Biological Systems*, **32**, 587–594.

87 Falany, J.L. and Falany, C.N. (2007) Interactions of the human cytosolic sulfotransferases and steroid sulfatase in the metabolism of tibolone and raloxifene. *The Journal of Steroid Biochemistry and Molecular Biology*, **107**, 202–210.

88 Vos, R.M.E., Krebbers, S.F.M., Verhoeven, C.H.J. and Delbressine, L.P.C. (2002) The *in vivo* human metabolism of tibolone. *Drug Metabolism and Disposition: The Biological Fate of Chemicals*, **30**, 106–112.

89 Pacifici, G.M. (2005) Sulfation of drugs, in *Human Cytosolic Sulfotransferases* (eds G.M. Pacifici and M.W.H. Coughtrie), CRC Press, Boca Raton, London.

90 Pacifici, G.M., Eligi, M. and Giuliani, L. (1993) (+)- and (−)- terbutaline are sulphated at a higher rate in human intestine than liver. *European Journal of Clinical Pharmacology*, **45**, 483–487.

91 Karabey, Y., Sahin, S., Oener, L. and Hincal, A.A. (2003) Bioavailability file: terbutaline. *FABAD Journal of Pharmaceutical Sciences*, **28**, 149–160.

92 Hartman, A.P., Wislon, A.A., Wislon, H.M., Aberg, G., Falany, C.N. and Walle, T. (1998) Enantioselective sulfation of β2-

receptor agonists by the human intestine and the recombinant M-form. *Chirality*, **10**, 800–803.

93 Boulton, D.W. and Fawcett, J.P. (2001) The pharmacokinetics of levosalbutamol: what are the clinical implications? *Clinical Pharmacokinetics*, **40**, 23–40.

94 Mizuma, T., Kawashima, K., Sakai, S., Sakaguchi, S. and Hayashi, M. (2005) Differentiation of organ availability by sequential and simultaneous analyses: intestinal conjugative metabolism impacts on intestinal availability in humans. *Journal of Pharmaceutical Sciences*, **94**, 571–575.

95 Satoh, T. and Hosokawa, M. (1998) The mammalian carboxylesterases: from molecules to functions. *Annual Review of Pharmacology and Toxicology*, **38**, 257–288.

96 Taketani, M., Shii, M., Ohura, K., Ninomiya, S. and Imai, T. (2007) Carboxylesterase in the liver and small intestine of experimental animals and human. *Life Sciences*, **81**, 924–932.

97 Inoue, M., Morikawa, M., Tsuboi, M., Yamada, T. and Sugiura, M. (1979) Hydrolysis of ester-type drugs by the purified esterase from human intestinal mucosa. *Japanese Journal of Pharmacology*, **29**, 17–25.

98 Inoue, M., Morikawa, M., Tsuboi, M. and Sugiura, M. (1979) Studies of human intestinal esterase. IV. Application to the development of ester prodrugs of salicylic acid. *Journal of Pharmacobio-Dynamics*, **2**, 229–236.

99 Inoue, M., Morikawa, M., Tsuboi, M., Ito, Y. and Sugiura, M. (1980) Comparative study of human intestinal and hepatic esterases as related to enzymatic properties and hydrolizing activity for ester-type prodrugs. *Japanese Journal of Pharmacology*, **30**, 529–535.

100 Lund-Pero, M., Jeppson, B., Arneklo-Nobin, B., Sjogren, H.O., Holmgren, K. and Pero, R.W. (1994) Non-specific steroidal esterase activity and distribution in human and other mammalian tissues. *Clinica Chimica Acta; International Journal of Clinical Chemistry*, **224**, 9–20.

101 Hojring, N. and Svensmark, O. (1976) Carboxylesterases with different substrate specificity in human brain extracts. *Journal of Neurochemistry*, **27**, 525–528.

102 Vree, T.B., Dammers, E., Ulc, I., Horkovics-Kovats, S., Ryska, M. and Merkx, I. (2003) Lack of male–female differences in disposition and esterase hydrolysis of ramipril to ramiprilat in healthy volunteers after a single oral dose. *The Scientific Word Journal*, **3**, 1332–1343.

103 Vree, T.B., Dammers, E., Ulc, I., Horkovics-Kovats, S., Ryska, M. and Merkx, I. (2001) Variable plasma/liver and tissue esterase hydrolysis of simvastatin in healthy volunteers after a single oral dose. *Clinical Drug Investigation*, **21**, 643–652.

104 Magni, L. and Ekstroem, B. (1985) Hydroylsis of bacampicillin in the human gastrointestinal tract. Recent Advances in Chemotherapy, Proceedings of the International Congress of Chemotherapy, 14th Antimicrobial Section 1, 708–709.

105 Zhang, W., Xu, G. and McLeod, H.L. (2002) Comprehensive evaluation of carboxylesterase-2 expression in normal human tissues using tissue array analysis. *Applied Immunohistochemistry & Molecular Morphology*, **10**, 374–380.

106 Khanna, R., Morton, C.L., Danks, M.K. and Potter, P.M. (2000) Proficient metabolism of irinotecan by a human intestinal carboxylesterase. *Cancer Research*, **60**, 4725–4728.

107 Imai, T. (2006) Human carboxylesterase isozymes: catalytic properties and rational drug design. *Drug Metabolism and Pharmacokinetics*, **21**, 173–185.

108 Hickman, D., Chaudrasena, G. and Unadkat, J. (1995) Longitudinal distribution of arylamine *N*-acetyltransferases along the human small intestine. *ISSX Proceedings*, **8**, 250.

109 Pacifici, G.M., Franchi, M., Bencini, C., Repetti, F., di Lascio, N. and Muraro, G.B.

(1988) Tissue distribution of drug metabolizing enzymes in humans. *Xenobiotica; The Fate of Foreign Compounds in Biological Systems*, **18**, 849–856.

110 Prueksaritanont, T., Gorham, L.M., Hochman, J.H., Tran, L.O. and Vyas, K.P. (1996) Comparative studies of drug metabolizing enzymes in dog, monkey, and human small intestines, and in Caco-2 cells. *Drug Metabolism and Disposition: The Biological Fate of Chemicals*, **24**, 634–642.

111 Ilett, K.F., Tee, L.B.G., Reeves, P.T. and Minchin, K.F. (1990) Metabolism of drugs and other xenobiotics in the gut lumen and wall. *Pharmacology & Therapeutics*, **46**, 67–93.

112 Chiou, W.L. (2001) The rate and extent of oral bioavailability versus the rate and extent of oral absorption: clarification and recommendation of terminology. *J Pharmacokinetics and Pharmacodynamics*, **28**, 3–6.

113 Kwan, K.C. (1997) Oral bioavailability and first-pass effects. *Drug Metabolism and Disposition: The Biological Fate of Chemicals*, **25**, 1329–1336.

114 Wilkinson, G.R. (1987) Clearance approaches in pharmacology. *Pharmacological Reviews*, **39**, 1–47.

115 Lin, J.H., Chiba, M. and Baillie, T.A. (1999) Is the role of the small intestine in first-pass metabolism, overemphasized? *Pharmacological Reviews*, **51**, 135–157.

116 Kwon, Y. and Inskeep, P.B. (1996) Theoretical considerations on two equations for estimating the extent of absorption after oral administration of drugs. *Pharmaceutical Research*, **13**, 566–569.

117 Kato, M., Chiba, K., Hisaka, A., Ishigami, M., Kayama, M., Mizuno, N., Nagata, Y., Takaluwa, S. *et al.* (2003) The intestinal first-pass metabolism of substrates of CYP3A4 and P-glycoprotein – quantitative analysis based on information from the literature. *Drug Metabolism and Pharmacokinetics*, **18**, 365–372.

118 Ilett, K.F. and Davies, D.S. (1982) *In vivo* studies of gut wall metabolism, in Presystemic Drug Elimination, Clinical Pharmacology and Therapeutics, Vol. 1 (eds C.F. George, D.G. Shand and A.G. Renwick), Butterworth, London.

119 Lund, B., Kampmann, J.P., Lindahl, F. and Hansen, J.M. (1976) Pivampicillin and ampicillin in bile, portal and peripheral blood. *Clinical Pharmacology and Therapeutics*, **19**, 587–591.

120 Mahon, W.A., Inaba, T. and Stone, R.M. (1977) Metabolism of flurazepam by the small intestine. *Clinical Pharmacology and Therapeutics*, **22**, 228–233.

121 Shand, D.G. and Rangno, R.E. (1972) The disposition of propranolol. 1. Elimination during oral absorption in man. *Pharmacology*, **7**, 159–168.

122 Paine, M.F., Shen, D.D., Kunze, K.L., Perkins, J.D., Marsh, C.L., McVicar, J.P., Barr, D.M., Gillies, B.S. and Thummel, K.E. (1996) First-pass metabolism of midazolam by the human intestine. *Clinical Pharmacology and Therapeutics*, **60**, 14–24.

123 Kolars, J.C., Awni, W.M., Merion, R.M. and Watkins, P.B. (1991) First-pass metabolism of cyclosporin by the gut. *Lancet*, **338**, 1488–1490.

124 Tateishi, T., Watanabe, M., Nakura, H., Asoh, M., Shirai, H., Mizorogi, Y., Kobayashi, S., Thummel, K.E. and Wilkinson, G.R. (2001) CYP3A activity in European American and Japanese men using midazolam as an *in vivo* probe. *Clinical Pharmacology and Therapeutics*, **69**, 333–339.

125 Kupferschmidt, H.H.T., Ha, H.R., Ziegler, W.H., Meier, P.J. and Kraehenbuehl, S. (1995) Interaction between grapefruit juice and midazolam in humans. *Clinical Pharmacology and Therapeutics*, **58**, 20–28.

126 Hebert, M.F., Roberts, J.P., Prueksaritanont, T. and Benet, L.Z. (1992) Bioavailability of cyclosporine with concomitant rifampin administration is markedly less than predicted by

hepatic enzyme induction. *Clinical Pharmacology and Therapeutics*, **52**, 453–457.

127 Wu, C.-Y., Benet, L.Z., Hebert, M.F., Gupta, S.K., Rowland, M., Gomez, D.Y. and Wacher, V.J. (1995) Differentiation of absorption and first-pass gut and hepatic metabolism in humans: studies with cyclosporine. *Clinical Pharmacology and Therapeutics*, **58**, 492–497.

128 Gomez, D.Y., Wacher, S.J., Tomlanovich, S.J., Hebert, M.F. and Benet, L.Z. (1995) The effects of ketoconazole on the intestinal metabolism and, bioavailability of cyclosporine. *Clinical Pharmacology and Therapeutics*, **58**, 15–19.

129 Fromm, M.F., Busse, D., Kroemer, H.K. and Eichelbaum, M. (1996) Differential induction of prehepatic and hepatic metabolism of verapamil by rifampin. *Hepatology*, **24**, 796–801.

130 Holtbecker, N., Fromm, M.F., Kroemer, H.K., Ohnhaus, E.E. and Heidemann, H. (1996) The nifedipine–rifampin interaction. Evidence for induction of gut wall metabolism. *Drug Metabolism and Disposition: The Biological Fate of Chemicals*, **24**, 1121–1123.

131 Tannergren, C., Engman, H., Knutson, L., Hedeland, M., Bondesson, U. and Lennernaes, H. (2004) St John's wort decreases the bioavailability of *R*- and *S*-verapamil thorugh induction of the first-pass metabolism. *Clinical Pharmacology and Therapeutics*, **75**, 298–309.

132 van de Kerkhof, G., Ungell, A.-L.B., Sjöberg, Å.K., de Jager, M.H., Hilgendorf, C., de Graaf, I.A.M. and Groothuis, G.M.M. (2006) Innovative methods to study human intestinal drug metabolism *in vitro*: precision-cut slices compared with Ussing chamber preparations. *Drug Metabolism and Disposition: The Biological Fate of Chemicals*, **34**, 1893–1902.

133 Glaeser, H., Drescher, S., van der Kuip, H., Behrens, C., Geick, A., Burk, O., Dent, J., Somogyi, A. *et al.* (2002) Shed human enterocytes as a tool for the study of expression and function of intestinal drug-metabolizing enzymes and transporters. *Clinical Pharmacology and Therapeutics*, **71**, 131–140.

134 Zhang, Q.-Y., Dunbar, D., Ostrowska, A., Zeisloft, S., Yang, J. and Kaminsky, L.S. (1999) Characterization of human small intestinal cytochromes P-450. *Drug Metabolism and Disposition: The Biological Fate of Chemicals*, **27**, 804–809.

135 Paine, M.F., Khalighi, M., Fisher, J.M., Shen, D.D., Kunze, K.L., Marsh, C.L., Perkins, J.D. and Thummel, K.D. (1997) Characterization of interintestinal and intraintestinal variations in human CYP3A-dependent metabolism. *The Journal of Pharmacology and Experimental Therapeutics*, **283**, 1552–1562.

136 Mizuma, T. (2002) Kinetic impact of presystemic intestinal metabolism on drug absorption: experiment and data analysis for the prediction of *in vivo* absorption from *in vitro* data. *Drug Metabolism and Pharmacokinetics*, **17**, 496–506.

137 Lilja, J.J., Kivisto, K.T., Backman, J.T., Lamberg, T.S. and Neuvonen, P.J. (1998) Grapefruit juice substantially increases plasma concentrations of buspirone. *Clinical Pharmacology and Therapeutics*, **64**, 655–660.

138 Lown, K.S., Bailey, D.G., Fontana, R.J., Janardan, S.K., Adair, C.H., Fortlage, L.A., Brown, M.B., Guo, W. and Watkins, P.B. (1997) Grapefruit juice increases felodipine oral bioavailability in humans by decreasing intestinal CYP3A protein expression. *The Journal of Clinical Investigation*, **99**, 2545–2553.

139 Kantola, T., Kivisto, K.T. and Neuvonen, P.J. (1998) Grapefruit juicegreatly increases serum concentrations of lovastatin and lovastatin acid. *Clinical Pharmacology and Therapeutics*, **63**, 397–402.

140 Lilja, J.J., Kivisto, K.T. and Neuvonen, P.J. (1998) Grapefruit juice–simvastatin interaction: effect on serum concentrations of simvastatin, simvastatin acid,

and HMG-CoA reductase inhibitors. *Clinical Pharmacology and Therapeutics*, **64**, 477–483.

141 Rashid, T.J., Martin, U., Clarke, H., Waller, D.G., Renwick, A.G. and George, C.F. (1995) Factors affecting the absolutebioavailabilityofnifedipine. *British Journal of Clinical Pharmacology*, **40**, 51–58.

142 Kivisto, K.T., Lilja, J.J., Backman, J.T. and Neuvonen, P.J. (1999) Repeated consumption of grapefruit juice considerably increases plasma concentrations of cisapride. *Clinical Pharmacology and Therapeutics*, **66**, 448–453.

13
Modified Cell Lines

Guangqing Xiao and Charles L. Crespi

Abbreviations

ASBT	Apical sodium-dependent bile acid transporter (also designated as SLC10A2)
BCRP	Breast cancer resistance protein (also designated as ABCG2)
Caco-2	Human colon adenocarcinoma cell line used as absorption model
cDNA	Complementary deoxyribonucleic acid
CYP	Cytochrome P450
CYP-OR	Cytochrome P450:NADPH oxidoreductase
LLC-PK_1	Porcine kidney cell line used as absorption model
MCT	Monocarboxylate transporter (also designated as SLC16)
MDCK	Madin–Darby canine kidney cell line used as absorption model
MDR1	Multidrug resistance protein 1 (also designated P-gp and ABCB1)
MRP1	Multidrug resistance associated protein 1 (also designated ABCC1)
MRP2	Multidrug resistance associated protein 2 (also designated ABCC2)
OATP	Organic anion transporting polypeptide (also designated as SLCO or SLC21)
PEPT	Peptide transporter (also designated as SLC15)
TEER	Transepithelial electrical resistance

13.1
Introduction

The extent of oral absorption of a drug depends on physical properties of the drug (e.g., solubility and membrane permeability) and its interaction with various enzymatic processes of an organism. The two most prominent enzymatic systems are drug metabolic enzymes and drug transporters. Both metabolic enzymes and transporters exist as many related forms that generally have distinct, yet potentially overlapping, substrate specificities.

The action of drug metabolizing enzymes may decrease oral bioavailability by metabolizing a portion of the drug that has been absorbed before it enters circulation. Human drug metabolizing enzymes have been extensively studied for decades and are now well characterized. Metabolic enzyme-specific substrate, inhibitor, and antibody *in vitro* probe reagents as well as authentic standards are available for most of the major enzymes. These allow the establishment of the relative and absolute amounts of metabolism by individual enzymes and prediction of drug–drug interactions. In addition, a number of *in vivo* probes are available. *In vivo* studies are essential to validate predictive models based upon *in vitro* measurements.

There are a number of drug transporters that are expressed in various tissues including the intestine. Intestinal drug transporters can either increase or decrease oral bioavailability depending on whether the transporter facilitates or impedes drug uptake into the enterocyte (which is generally regarded as rate limiting). The impact of transporters on drug bioavailability and drug disposition has been investigated extensively in the last few years. However, the research is still hampered by the lack of comprehensive set of reagents (specific substrates and inhibitors) and standards. As with the metabolic enzymes, the goal for drug transporters is to develop predictive *in vitro* models.

To conduct basic research and address the need for reagents and standards, cell lines have been modified so that the function of metabolizing enzymes and transporters can be examined individually. These cell lines can serve as a source of active protein to validate a chemical as a substrate or inhibitor or as a source of protein to validate the specificity of an antibody. For this approach to be robust for establishing specificity (and to minimize false-negative findings), all of the key proteins need to be available and active in the system. However, as specific probes are being identified and developed, useful mechanistic studies can be performed on transporters and substrates/inhibitors, which are currently available.

There is also a need for cell systems that express a multiplicity of metabolic enzymes and transporters to assess drug disposition *in vivo*. Cell line modification through cDNA expression can be used to add missing functions to cells that are known to express only a subset of needed enzymes or transporters known to be present *in vivo*. Cell lines can also be modified by deleting a natively expressed transporter so that the cell lines are more selective for other transporters. In both ways, the *in vitro* testing models can be improved.

This chapter describes some of the modified mammalian cell-based systems that have been developed to express intestinal cytochrome P450 enzymes and intestinal transporters. The reader should be aware that other experimental systems, such as transporter expression and drug uptake studies in *Xenopus laevis* oocytes and baculovirus expression system, have shown considerable promise [1–3].

13.2 Cell/Vector Systems

Modified mammalian cell systems for the study of the role of transporters and/or metabolism in oral absorption consists of two main components, the cell line and the

vector bearing a cDNA encoding the protein of interest. The cell line serves two roles: first, to support an adequate expression of the cDNA and second, to provide a barrier function that is generally critical in transporter function assays.

The key function of the vector is to introduce the cDNA under the control of a strong promoter and, if a stable cell line is to be developed, also to introduce resistance to a compound that is otherwise toxic to the host cell. This facilitates selection (only vector-bearing cells grown in special media) of a minority of cells that have incorporated the vector. There are many adequate expression vectors available from a number of commercial suppliers. Several classes of vector systems appear appropriate for transporter expression as integrating, episomal, retroviral, Vaccinia virus-, and Adenovirus-based systems have all been used successfully in studies referenced in this chapter.

Analysis of cytochrome P450 function is most commonly performed by analyzing metabolite formation in culture. This presents an analytical challenge, as during the drug discovery/lead optimization phases, radiolabeled compounds or authentic metabolite standards are generally not available. Although the extent of metabolism could theoretically be measured by the loss of parent compound, the extent of the loss is generally less than 20%, which is difficult to detect reliably and provides a very narrow dynamic range to rank compounds.

Bidirectional transport assay is most commonly performed to determine transporter function by analyzing rates of drug transport through cell monolayers grown on membrane support systems (e.g., microporous polycarbonate or polyethylene terephthalate membrane-containing cell culture inserts). Typically, efflux transporters such as MDR1 are preferentially expressed on the apical face of the cell and the apparent permeability of an MDR1 substrate is substantially higher in the basolateral-to-apical direction compared to that in the apical-to-basolateral direction. In the transport assay, rates of drug permeation are measured in two directions. Figure 13.1 provides a diagram of the assay. A polarization ratio is calculated as the apparent permeability in the basolateral-to-apical direction divided by the apparent permeability in the apical-to-basolateral direction. Presumably, polarization ratios greater than unity imply an active efflux transport. However, in practice, polarization ratios greater than 2 are used as an indictor for solid active efflux transport due to experimental errors. The parent compound is the analyte in these assays, and automation-compatible membrane insert systems (24-well) have been available for a number of years. More recently, 96-well insert systems have been introduced.

Alternatively, the transporter function can be analyzed by accumulation or efflux assay. Accumulation assay is generally used to determine substrate accumulation rate into the cells mediated by uptake transporters, whereas efflux assay is generally used to determine substrate efflux rate of the cells mediated by efflux transporters. For efflux assay, cells are preincubated with the substrate.

For efflux transporters, however, the functional interaction between the drug and the transporter occurs in the intracellular space. Some substrates, particularly the negatively charged MRP2 substrates, have very low permeability and in the absence of an uptake transporter may not give detectable transport. In these cases, double-transfected cell lines have been developed so that compounds with low permeability

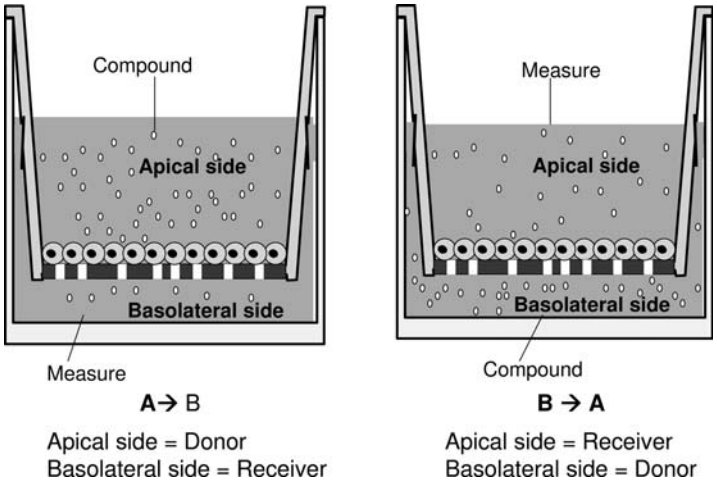

Figure 13.1 Schematic diagram of drug transport assay in cell monolayers cultured on a culture insert containing permeable membrane.

can get in cells via uptake transporters [4]. Another system that has been analyzed uses membrane vesicles prepared from transfected (and control) cells [5]. Generally, studies with membrane vesicles require the use of radiolabeled substrate material, which is generally not available for all compounds in a drug discovery/lead optimization program.

Two properties determine the usefulness of a cell line as a particular host for cDNA expression. These are

(1) The extent to which the cell line supports an appropriate functional expression of the cDNA. The level of expression achieved is determined by interactions of the vector/expressed protein with the cell. These interactions include the strength of the promoter (weaker promoters can be compensated for by using a vector that is present at high copy number), the adequacy of the selective agent (not all agents are toxic to all cells), the stability of the expressed protein (some proteins may be rapidly degraded in some cells), and whether the expressed protein exerts any deleterious effect on the viability of host cells (some efflux transporters could deplete the cell of essential components, such as GSH). If cytochromes P450 are to be expressed, the necessary redox partners (oxidoreductase (OR) and cytochrome b_5) also need to be expressed natively in the host cell (coexpression is also an option). Finally, for bidirectional transport assay, transporters must be expressed in a polarized manner in the host cell (i.e., preferentially either on the basolateral side or apical side of the cell).

(2) The extent to which the cell line is appropriate for drug metabolism and transport studies. If drug bidirectional transport studies are to be performed, the cell line needs to form monolayers with tight cell–cell junctions. If cell–cell junctions are loose, background (or nontransporter-dependent) paracellular drug transport

will be high. In addition, if a panel of cells expressing individual transporters is being developed, expression of any native drug metabolism enzymes or transporters should be low as these native processes introduce background to the system.

Three cell lines, Caco-2, MDCK, and LLC-PK_1, have been most commonly used for cDNA expression. All three of these cell lines have very low levels of oxidative drug metabolism, although variants of Caco-2 and LLC-PK_1, cultured under appropriate conditions, have been reported to express significant levels of CYP3A subfamily enzymes [6–8]. Beside MDR1, Caco-2 cells have been reported to express a significant number of uptake and efflux transporters, such as MRP2-6, BCRP, OATP1A2, OATP2B1, OCT1, MCT1, and PEPT1 [9–13]. It should be noted that mRNA expression levels may change in different Caco-2 clones [12, 13], so transporter levels should be carefully characterized in a particular Caco-2 cell clone.

Owing to the overlapped substrate selectivity of transporters expressed in Caco-2 cells, a particular transporter can be knocked out by using RNAi technology to improve assay selectivity [14].

Using putative MDR1 substrates, MDCK cells express substantially higher levels of native efflux transporters than those of LLC-PK_1 cells. Everything else being equal, the LLC-PK_1 model is preferred because it forms high-quality monolayers and has low levels of native transporters.

13.3 Expression of Individual Metabolic Enzymes

Most interest has focused on oxidative enzymes of the cytochrome P450 (CYP) class, which are expressed not only in the liver to the highest degree but also in the intestine to a significant degree. Conjugating enzymes are also expressed in the intestine [15, 16]. Human intestine appears to be relatively rich in CYP3A4 (which is also abundant in the liver), and intestinal CYP3A4 can significantly contribute to the first-pass metabolism of drugs such as midazolam, cyclosporin A, and verapamil [17]. Human intestine has also been reported to contain lower levels of CYP2C9, CYP2C19, CYP2D6, and CYP1A1 [18, 19]. However, because of low abundance, it appears unlikely that the presence of these enzymes in the intestine significantly reduces oral bioavailability (relative to the impact on first-pass metabolism in the liver).

Catalytic activity of CYP enzymes requires functional coupling with its redox partners, cytochrome P450:NADPH oxidoreductase and cytochrome b_5. Measurable levels of these two proteins are natively expressed in most mammalian cell lines. Therefore, introduction of only the CYP cDNA is generally needed for detectable catalytic activity. However, the levels of expression of the redox partner proteins may be low and may not support maximal CYP catalytic activity; therefore, enhancement of OR levels may be desirable. This approach has been used successfully with an Adenovirus expression system in LLC-PK_1 cells [20].

Because of its importance in first-pass metabolism, there has been a considerable interest in introducing CYP3A4 into cell systems. This protein is normally not expressed in cell lines and was introduced into Caco-2 cells with the goal of improving this common screening model. The first reported expression of a drug-metabolizing enzyme in a drug permeability model was of CYP3A4 in Caco-2 cells [21]. CYP3A4 catalytic activities were increased about 100-fold relative to control cells but still well below than that found in the intestine. However, it was noted that expression of CYP3A4 markedly reduced the proliferative capacity of the Caco-2 cells (relative to CYP2A6-expressing and control cells). Nonetheless, expression of CYP3A4 did not alter transepithelial electrical resistance (TEER) values or the permeability of model compounds. Coexpressing OR did not substantially elevate CYP3A4 catalytic activity (on a milligram cellular protein basis) [22]. However, 4-fold and 16-fold higher catalytic activities were obtained using the same expression system with MDCK and LLC-PK_1 cells as hosts [23]. Similarly, high levels of expression were obtained in the LLC-PK_1 model using an Adenovirus vector [20].

Levels of CYP3A4 activity in LLC-PK_1 models appear to be comparable to those found in human intestine [23], and a significant first-pass effect has been observed as CYP3A4 substrates pass through monolayers. For example, in the LLC-PK_1 model, up to 19% of nifedipine was metabolized as it passed through the monolayer. The LLC-PK_1/CYP3A4 systems appear to be a reasonable model for assessing the extent of any first-pass effect during permeation through the intestine. However, given the modest amount of metabolite formed for nifedipine (an excellent CYP3A4 substrate), there appears to be little reason to adopt these cells as an "improved" screening model. Alternative approaches, such as measuring the rates of parent compound loss in CYP3A4 microsomal incubations, should be as informative and easier to implement.

Over the last few years, the impact of interplay between intestinal metabolic enzymes and transporters on drug first-pass bioavailability has been reported. CYP3A4-transfected Caco-2 was originally developed to evaluate the first-pass metabolism [21]. Since it coexpresses both CYP3A4 and MDR1, the cell line has provided a pivotal experiment model to investigate the influence of interplay between CYP3A4 and MDR1 on drug metabolic extent and extraction ratio of K77 and sirolimus, substrates of both CYP3A4 and MDR1 [24, 25]. The results indicate that inhibition of intestinal apical efflux transporters MDR1 and metabolic enzyme CYP3A4 was synergistic, both reducing drug metabolic extent and extraction ratio. The results also suggested that, by dosing substrates at the basolateral membrane side, CYP3A4-transfected Caco-2 cells could be used to assess the interplay between CYP3A4 and MDR1 in hepatocytes [24–26]. It is expected that the extent of metabolism in intestine could also be affected by the interplay between other apical efflux transporters and enzymes [26]. However, the research is limited by the availability of appropriate experiment models.

It has been reported that the CYP3A4 activity in CYP3A4-transfected Caco-2 cells can be stabilized and improved by adding 5-azacytidine in the culture medium. Cell monolayer normal growth was not affected by the treatment [22].

13.4
Expression of Transporters

13.4.1
Efflux Transporters

The identities and roles of many drug transporters are discussed in other chapters in this volume and are not extensively reintroduced here. The goal is to develop a comprehensive panel of cells expressing individual, functional transporters as research reagents. To simplify data interpretation, the set of transporters should be expressed in the same host cell line and the abundance of functional proteins in the cell line should be known relative to the corresponding *in vivo* values. However, useful mechanistic data can be obtained from less comprehensive systems.

As stated earlier, there are many drug transporters expressed in the intestine [27, 28]. Although the expression levels of some transporters have been examined, the protein levels remain to be further defined and the methods need to be standardized. The export proteins MDR1, MRP1, MRP2, and BCRP have been of particular interest because they are expressed at relatively high levels in the intestine [27, 28] and are known to function to efflux drugs.

The most extensively studied protein is MDR1, natively expressed in Caco-2 cells. MDCK and LLC-PK_1 cells expressing high levels of cDNA-derived human (and rodent) MDR1 have been developed in several laboratories [29, 30]. The development of these cell lines has been facilitated by the fact that MDR1 expression confers resistance to cytotoxic drugs such as vinblastine. This allows direct growth selection of cells expressing high levels of MDR1. MRP2 and BCRP have been successfully expressed in MDCK cells [31, 32]. Like MDR1, MRPs and BCRP expression can confer resistance to cytotoxic drugs that can facilitate isolation of cells expressing high levels of functional protein. Many MRP2 and BCRP substrates have very poor permeability and when added to the extracellular space cannot reach the active site of the transporter. The issue of substrate access to the MRP2 and BCRP active site has been addressed by coexpressing one or multiple uptake transporters, such as OATP1B1 or OATP1B3, which allows an efficient access to the substrate within the intracellular space [4, 33, 34]. These cell lines were developed primarily to address drug clearance in hepatocytes. Although the expression level ratio of the transporters may be different from that under physiological conditions, the substrate transport rank order would not be affected (absolute transport values are affected) since drug uptake is generally the rate-determining step. This has been demonstrated by *in vivo* results showing that the uptake across the sinusoidal membrane determined the biliary clearance of BQ123 [35]. Results from MDCK cell line coexpressing rat Oatp4 and Mrp2 also suggested that Oatp2-mediated uptake across basolateral membrane was the rate-determining process for the transcellular transport of $E_2$17βG and pravastatin [36]. That protein expression level ratio is not critical in determining transport rank order was further confirmed by the good correlation between the transport activity in human and rat double-transfected cell lines, and close prediction of *in vivo* biliary clearance from *in vitro* results obtained from double-transfected cell line [36].

An alternative method to overcome this issue is to perform uptake studies by using membrane vesicles prepared from cDNA-expressing and control cells [5]. Vesicle preparation and vesicle assays are, however, labor intensive. BCRP, MRPs, and BSEP inside-out vesicles prepared from insect cells by using baculovirus system are currently available from BD Biosciences, Solvo, and GenoMembrane.

MDR1-expressing cells have been used extensively to study the extent and rates of drug transport. Generally, a larger polarization ratio (rate of drug permeation basolateral to apical divided by the rate of drug permeation apical to basolateral) in MDR1-expressing cells relative to control cells (or MDR1 cells incubated in the presence of an MDR1 inhibitor) is considered an evidence for active transport by MDR1. Polarization ratio values are determined by both the drug transporting activity of MDR1 in the system for transporting the drug of interest and the intrinsic permeability of the molecule. Compounds with higher intrinsic permeability give lower polarization ratios. In addition, because transport processes are saturable, polarization ratios tend to decrease with increasing drug concentration. Therefore, care must be taken in interpreting the significance of polarization ratio values.

There is a need to develop a framework to better understand the conditions under which efflux transporters will significantly modulate oral bioavailability. Although it is clear that transport by MDR1 can reduce oral bioavailability, many successful, orally bioavailable drugs are *in vitro* substrates for efflux transporters such as MDR1 (e.g., digoxin, fexofenadine, cyclosporin A, and erythromycin). One *in vivo* indication of role of MDR1 in oral bioavailability has been pharmacokinetic drug–drug interactions between MDR1 inhibitors and nonmetabolized MDR1 substrates such as digoxin and fexofenadine. Another *in vivo* manifestation may be nonproportional pharmacokinetics. For example, the high-affinity MDR1 substrate UK-343 664 (K_m 7.3 μM) shows no systemic exposure at doses below 10 mg. Between 30 and 800 mg, the systemic exposure increased about 250-fold [37]. It seems reasonable that there is a region defined by drug dose, drug permeability, efflux enzyme affinity, and efflux enzyme activity where efflux transport will reduce oral bioavailability. Given that transporters are saturable, drugs administered at low doses and/or drugs with low intrinsic permeability are most likely to have lower oral bioavailability reduced by the action of efflux transporters. Similarly, drugs with low concentration, low permeability, and high affinity to efflux transporters generally have difficulties to cross the blood–brain barrier. Published data for more drug compounds are needed to define the combination of conditions that allow MDR1 to significantly reduce oral bioavailability.

Owing to the potentially profound impact of intestinal efflux transporters on drug bioavailability [26], a clear priority remains to build up a panel of intestinal efflux transporters that are expressed individually in modified cell lines. These research tools will be instrumental in identifying and validating selective probe transporter substrates and inhibitors. The availability of such probes will allow a better understanding of the influence of transporters on *in vivo* pharmacokinetics. A similar set of probes has been instrumental in increasing our understanding of the role cytochrome P450 plays in human pharmacokinetics and in avoiding issues associated with these enzymes.

In addition, the availability of specific probes for transporters will help generate data for creating transporter structure–activity models for the transporters [38] and thus provide the ability to rationally design around any transporter-related issues associated with a drug candidate series. In addition, specific probe substrates (and inhibitors) provide a means to relate the levels of transporter function *in vitro* to the levels of transporter function *in vivo*. A quantitative understanding of this relationship is key to developing accurate *in vitro* to *in vivo* extrapolation models. At present, a number of relatively selective probes have been reported but there are major gaps in terms of overall coverage and the degree of specificity. There is also a need to define the conditions (dose, intrinsic permeability, efflux transporter activity, and affinity) that efflux transport requires to significantly limit oral bioavailability. This will permit the analysis of transport and pharmacokinetic parameters for more compounds such as UK-343 664.

13.4.2 Uptake Transporters

Uptake transporters expressed in intestine can function to increase drug bioavailability. Drugs with low intrinsic permeability achieve acceptable oral bioavailability because they are substrates for uptake transporters that normally function in nutrient uptake. Compared to efflux transporters, less is known about intestinal drug uptake transporters. So far, the most prominent example is the peptide transporter, PEPT1, which is active toward peptidomimetic antibiotics such as cephalexin, the antiviral agent valacyclovir [39], and other drugs. Caco-2 cell is a suitable model for intestinal peptide transport studies since it expresses the intestinal peptide transporter PEPT1, but not the renal peptide transporter PEPT2 [40]. H^+/peptide transport activity was also observed in MDCK, but not in LLC-PK_1 [41]. Further studies indicated that, in addition to PEPT1 expressing at the apical membranes, a different peptide transporter expresses natively at the basolateral membranes of both Caco-2 and MDCK monolayers [42, 43]. Recombinant human PEPT1 has also been expressed in Chinese hamster ovary cells and MDCK cells [44, 45].

The reabsorption of conjugated bile acids is mediated by ASBT, which is localized on the apical membrane of ileal enterocytes in mammals. ASBT is a drug target not only to lower plasma cholesterol level but also to improve intestinal permeability [46]. Although available monolayer cell lines do not express ASBT, it has been expressed in MDCK cells [47]. Human intestine also expresses multiple MCT isoforms [48]. These MCTs are responsible for the absorption of short-chain fatty acid. Expression of MCT in Caco-2 allows it to be an appropriate model to study short-chain fatty acid transport [9, 49, 50].

In addition to the above uptake transporters that predominately express in the intestine, uptake transporters that function in other tissues also express in the intestine. For example, brain transporter OATP1A2, hepatic transporter OATP1B1, and OATP1B3 have been detected in human intestine [51]. In the intestine, OATP1A2 is localized on the apical membrane, and is the key uptake transporter for fexofenadine [51] and levofloxacin [12]. OATP1A2 was reported to be natively expressed in

Caco-2 cells and was thought to be the transporter for levofloxacin uptake in Caco-2 cells [12].

13.5 Summary and Future Perspectives

Intestinal transporters and metabolic enzymes influence drug oral bioavailability. The function of these transporters and enzymes has been investigated by using cell lines that either natively express or are modified to express transporters and drug metabolic enzymes. Cell lines expressing major intestinal metabolic enzymes and transporters, such as CYP3A4, MDR1, MRP2, BCRP, PEPT1, OATP1B1, and OATP1B3, have been developed. Although the expression levels of some transporters have been examined, the protein levels remain to be further defined and experimental standards need to be set up to better interpret results with respect to *in vivo* impact. Interplay between intestinal enzymes and transporters also affects drug oral bioavailability. However, due to the lack of model systems, research into this effect is currently limited to the interplay between MDR1 and CYP3A4. Development of cell lines that coexpress other intestinal metabolic enzymes and transporters will facilitate these studies. RNAi technology has been used to knock out a particular transporter to improve assay selectivity of cell lines. Owing to the limited number of specific substrates and inhibitors for transporters, this technology can be used as an alternative strategy to identify and define substrates and inhibitors for transporters.

References

1 van Zanden, J.J., van der Woude, H., Vaessen, J., Usta, M., Wortelboer, H.M., Cnubben, N.H. and Rietjens, I.M. (2007) The effect of quercetin phase II metabolism on its MRP1 and MRP2 inhibiting potential. *Biochemical Pharmacology*, **74**, 345–351.

2 Nakanishi, T., Doyle, L.A., Hassel, B., Wei, Y., Bauer, K.S., Wu, S., Pumplin, D.W., Fang, H.B. and Ross, D.D. (2003) Functional characterization of human breast cancer resistance protein (BCRP, ABCG2) expressed in the oocytes of *Xenopus laevis*. *Molecular Pharmacology*, **64**, 1452–1462.

3 Gopal, E., Miyauchi, S., Martin, P.M., Ananth, S., Roon, P., Smith, S.B. and Ganapathy, V. (2007) Transport of nicotinate and structurally related compounds by human SMCT1 (SLC5A8) and its relevance to drug transport in the mammalian intestinal tract. *Pharmaceutical Research*, **24**, 575–584.

4 Cui, Y., König, J. and Keppler, D. (2001) Vectorial transport by double-transfected cells expressing the human uptake transporter SLC21A8 and the apical export pump ABCC2. *Molecular Pharmacology*, **60**, 934–943.

5 Morrow, C.S., Peklak-Scott, C., Bishwokarma, B., Kute, T.E., Smitherman, P.K. and Townsend, A.J. (2006) Multidrug resistance protein 1 (MRP1, ABCC1) mediates resistance to mitoxantrone via glutathione-dependent drug efflux. *Molecular Pharmacology*, **69**, 1499–1505.

6 Schmiedlin-Ren, P., Thummel, K.E., Fisher, J.M., Paine, M.F., Lown, K.S. and Watkins, P.B. (1997) Expression of enzymatically active CYP3A4 in Caco-2 cells grown in extracellular matrix-coated permeable supports in the presence of 1-alpha, 25-dihydroxyvitamin D3. *Molecular Pharmacology*, **51**, 741–754.

7 Engman, H.A., Lennernas, H., Taipalensuu, J., Otter, C., Leidvik, B. and Artursson, P. (2001) CYP3A4, CYP3A5 and MDR1 in human small and large intestine cell lines suitable for drug transport studies. *Journal of Pharmaceutical Sciences*, **90**, 1736–1751.

8 Magnarin, M., Morelli, M., Rosati, A., Bartoli, F., Candussio, L., Giraldi, T. and Decorti, G. (2004) Induction of proteins involved in multidrug resistance (P-glycoprotein, MRP1, MRP2, LRP) and of CYP 3A4 by rifampicin in LLC-PK1 cells. *European Journal of Pharmacology*, **483**, 19–28.

9 Shim, C.K., Cheon, E.P., Kang, K.W., Seo, K.S. and Han, H.K. (2007) Inhibition effect of flavonoids on monocarboxylate transporter 1 (MCT1) in Caco-2 cells. *The Journal of Pharmacy and Pharmacology*, **59**, 1515–1519.

10 Xia, C.Q., Liu, N., Yang, D., Miwa, G. and Gan, L.S. (2005) Expression, localization, and functional characteristics of breast cancer resistance protein in Caco-2 cells. *Drug Metabolism and Disposition: The Biological Fate of Chemicals*, **33**, 637–643.

11 Kimoto, E., Seki, S., Itagaki, S., Matsuura, M., Kobayashi, M., Hirano, T., Goto, Y., Tadano, K. and Iseki, K. (2007) Efflux transport of *N*-monodesethylamiodarone by the human intestinal cell-line Caco-2 cells. *Drug Metabolism and Pharmacokinetics*, **22**, 307–312.

12 Maeda, T., Takahashi, K., Ohtsu, N., Oguma, T., Ohnishi, T., Atsumi, R. and Tamai, I. (2007) Identification of influx transporter for the quinolone antibacterial agent levofloxacin. *Molecular Pharmacology*, **4**, 85–94.

13 Maubon, N., Le Vee, M., Fossati, L., Audry, M., Le Ferrec, E., Bolze, S. and Fardel, O. (2007) Analysis of drug transporter expression in human intestinal Caco-2 cells by real-time PCR. *Fundamental & Clinical Pharmacology*, **21**, 659–663.

14 Watanabe, T., Onuki, R., Yamashita, S., Taira, K. and Sugiyama, Y. (2005) Construction of a functional transporter analysis system using MDR1 knockdown Caco-2 cells. *Pharmaceutical Research*, **22**, 1287–1293.

15 Soars, M.G., Burchell, B. and Riley, R.J. (2002) *In vitro* analysis of human drug glucuronidation and prediction of *in vivo* metabolic clearance. *The Journal of Pharmacology and Experimental Therapeutics*, **301**, 382–390.

16 Zhang, L., Lin, G. and Zuo, Z. (2007) Involvement of UDP-glucuronosyltransferases in the extensive liver and intestinal first-pass metabolism of flavonoid baicalein. *Pharmaceutical Research*, **24**, 81–89.

17 Paine, M.F., Khalighi, M., Fisher, J.M., Shen, D.D., Kunze, K.L., Marsh, C.L., Perkins, J.D. and Thummel, K.E. (1997) Characterization of interintestinal and intraintestinal variations in human CYP3A-dependent metabolism. *The Journal of Pharmacology and Experimental Therapeutics*, **283**, 1552–1562.

18 Paine, M.F., Hart, H.L., Ludington, S.S., Haining, R.L., Rettie, A.E. and Zeldin, D.C. (2006) The human intestinal cytochrome P450 "pie". *Drug Metabolism and Disposition: The Biological Fate of Chemicals*, **34**, 880–886.

19 Paine, M.F., Schmiedlin-Ren, P. and Watkins, P.B. (1999) Cytochrome P-450 1A1 expression in human small bowel: interindividual variation and inhibition by ketoconazole. *Drug Metabolism and Disposition: The Biological Fate of Chemicals*, **27**, 360–364.

20 Brimer, C., Dalton, J.T., Zhu, Z., Schuetz, J., Yasuda, K., Vanin, E., Relling, M.V., Lu, Y. and Schuetz, E.G. (2000) Creation of polarized cells

coexpressing CYP3A4, NADPH cytochrome P450 reductase and MDR1/P-glycoprotein. *Pharmaceutical Research*, **17**, 803–810.

21 Crespi, C.L., Penman, B.W. and Hu, M. (1996) Development of Caco-2 cells expressing high levels of cDNA-derived cytochrome P4503A4. *Pharmaceutical Research*, **13**, 1635–1641.

22 Hu, M., Li, Y., Davitt, C.M., Huang, S.M., Thummel, K., Penman, B.W. and Crespi, C.L. (1999) Transport and metabolic characterization of Caco-2 cells expressing CYP3A4 and CYP3A4 plus oxidoreductase. *Pharmaceutical Research*, **16**, 1352–1359.

23 Crespi, C.L., Fox, L., Stocker, P., Hu, M. and Steimel, D.T. (2000) Analysis of transport and metabolism in cell monolayer systems that have been modified by cytochrome P4503A4 cDNA-expression. *European Journal of Pharmaceutical Sciences*, **12**, 63–68.

24 Cummins, C.L., Jacobsen, W., Christians, U. and Benet, L.Z. (2004) CYP3A4-transfected Caco-2 cells as a tool for understanding biochemical absorption barriers: studies with sirolimus and midazolam. *The Journal of Pharmacology and Experimental Therapeutics*, **308**, 143–155.

25 Cummins, C.L., Jacobsen, W. and Benet, L.Z. (2002) Unmasking the dynamic interplay between intestinal P-glycoprotein and CYP3A4. *The Journal of Pharmacology and Experimental Therapeutics*, **300**, 1036–1045.

26 Wu, C.Y. and Benet, L.Z. (2005) Predicting drug disposition via application of BCS: transport/absorption/elimination interplay and development of a biopharmaceutics drug disposition classification system. *Pharmaceutical Research*, **22**, 11–23.

27 Hilgendorf, C., Ahlin, G., Seithel, A., Artursson, P., Ungell, A.L. and Karlsson, J. (2007) Expression of thirty-six drug transporter genes in human intestine, liver, kidney, and organotypic cell lines. *Drug Metabolism and Disposition: The Biological Fate of Chemicals*, **35**, 1333–1340.

28 Berggren, S., Gall, C., Wollnitz, N., Ekelund, M., Karlbom, U., Hoogstraate, Schrenk, J.D. and Lennernäs, H. (2007) Gene and protein expression of P-glycoprotein, MRP1, MRP2, and CYP3A4 in the small and large human intestine. *Molecular Pharmacology*, **4**, 252–257.

29 Horio, M., Chin, K.V., Currier, S.J., Goldenberg, S., Williams, C., Pastan, I., Gottesman, M.M. and Handler, J. (1989) Transepithelial transport of drug by multidrug transporter in cultured Madin–Darby canine kidney cell epithelia. *The Journal of Biological Chemistry*, **264**, 14880–14884.

30 Tanigawara, Y., Okamura, N., Hirai, M., Yasuhara, M., Ueda, K., Kioka, N., Komano, T. and Hori, R. (1992) Transport of digoxin by human P-glycoprotein expressed in porcine kidney epithelial cell line (LLC-PK1). *The Journal of Pharmacology and Experimental Therapeutics*, **263**, 840–845.

31 Guo, A., Marinaro, W., Hu, P. and Sinko, P.J. (2002) Delineating the contribution of secretory transporters in the efflux of etoposide using Madin–Darby canine kidney (MDCK) cells overexpressing P-glycoprotein (Pgp), multidrug resistance-associate protein (MRP1) and canalicular multispecific organic anion transporter (cMOAT). *Drug Metabolism and Disposition: The Biological Fate of Chemicals*, **30**, 457–463.

32 Xiao, Y., Davidson, R., Smith, A., Pereira, D., Zhao, S., Soglia, J., Gebhard, D., de Morais, S. and Duignan, D.B. (2006) A 96-well efflux assay to identify ABCG2 substrates using a stably transfected MDCK II cell line. *Molecular Pharmacology*, **3**, 45–54.

33 Matsushima, S., Maeda, K., Kondo, C., Hirano, M., Sasaki, M., Suzuki, H. and Sugiyama, Y. (2005) Identification of the hepatic efflux transporters of organic anions using double-transfected Madin–Darby canine kidney II cells

expressing human organic anion-transporting polypeptide 1B1 (OATP1B1)/multidrug resistance-associated protein 2, OATP1B1/multidrug resistance 1, and OATP1B1/breast cancer resistance protein. *The Journal of Pharmacology and Experimental Therapeutics*, **314**, 1059–1067.

34 Kopplow, K., Letschert, K., König, J., Walter, B. and Keppler, D. (2005) Human hepatobiliary transport of organic anions analyzed by quadruple-transfected cells. *Molecular Pharmacology*, **68**, 1031–1038.

35 Kato, Y., Akhteruzzaman, S., Hisaka, A. and Sugiyama, Y. (1999) Hepatobiliary transport governs overall elimination of peptidic endothelin antagonists in rats. *The Journal of Pharmacology and Experimental Therapeutics*, **288**, 568–574.

36 Sasaki, M., Suzuki, H., Aoki, J., Ito, K., Meier, P.J. and Sugiyama, Y. (2004) Prediction of *in vivo* biliary clearance from the *in vitro* transcellular transport of organic anions across a double-transfected Madin–Darby canine kidney II monolayer expressing both rat organic anion transporting polypeptide 4 and multidrug resistance associated protein 2. *Molecular Pharmacology*, **66**, 450–459.

37 Abel, S., Beaumont, K.C., Crespi, C.L., Eve, M.D., Fox, L., Hyland, R., Jones, B.C., Muirhead, G.J., Smith, D.A., Venn, R.F. and Walker, D.K. (2001) Potential role of P-glycoprotein in the non-proportional pharmacokinetics of UK-343 664 in man. *Xenobiotica; The Fate of Foreign Compounds in Biological Systems*, **31**, 665–676.

38 Ekins, S., Kim, R.B., Leake, B.F., Dantzig, A.H., Schuetz, E.G., Lan, L.B., Yasuda, K., Shepard, R.L., Winter, M.A., Schuetz, J.D., Wikel, J.H. and Wrighton, S.A. (2002) Applications of three-dimensional quantitative structure–activity relationships of P-glycoprotein inhibitors and substrates. *Molecular Pharmacology*, **61**, 974–981.

39 Ganapathy, M.E., Huang, W., Wang, H., Ganapathy, V. and Leibach, F.H. (1998) Valacyclovir: a substrate for the intestinal and renal peptide transporters PEPT1 and PEPT2. *Biochemical and Biophysical Research Communication*, **246**, 470–475.

40 Ganapathy, M.E., Brandsch, M., Prasad, P.D., Ganapathy, V. and Leibach, F.H. (1995) Differential recognition of beta-lactam antibiotics by intestinal and renal peptide transporters, PEPT 1 and PEPT 2. *The Journal of Biological Chemistry*, **270**, 25672–25677.

41 Brandsch, M., Ganapathy, V. and Leibach, F.H. (1995) H(+)-peptide cotransport in Madin–Darby canine kidney cells: expression and calmodulin-dependent regulation. *The American Journal of Physiology*, **268**, F391–F397.

42 Sawada, K., Terada, T., Saito, H. and Inui, K. (2001) Distinct transport characteristics of basolateral peptide transporters between MDCK and Caco-2 cells. *Pflugers Archiv: European Journal of Physiology*, **443**, 31–37.

43 Irie, M., Terada, T., Sawada, K., Saito, H. and Inui, K. (2001) Recognition and transport characteristics of nonpeptidic compounds by basolateral peptide transporter in Caco-2 cells. *The Journal of Pharmacology and Experimental Therapeutics*, **298**, 711–717.

44 Balimane, P.V., Chong, S., Patel, K., Quan, Y., Timoszyk, J., Han, Y.H., Wang, B., Vig, B. and Faria, T.N. (2007) Peptide transporter substrate identification during permeability screening in drug discovery: comparison of transfected MDCK-hPepT1 cells to Caco-2 cells. *Archives of Pharmacal Research*, **30**, 507–518.

45 Han, H.K., Rhie, J.K., Oh, D.M., Saito, G., Hsu, C.P., Stewart, B.H. and Amidon, G.L. (1999) CHO/hPEPT1 cells overexpressing the human peptide transporter (hPEPT1) as an alternative *in vitro* model for peptidomimetic drugs. *Journal of Pharmaceutical Sciences*, **88**, 347–350.

46 Balakrishnan, A. and Polli, J.E. (2006) Apical sodium dependent bile acid transporter

(ASBT, SLC10A2): a potential prodrug target. *Molecular Pharmacology*, **3**, 223–230.

47 Balakrishnan, A., Sussman, D.J. and Polli, J.E. (2005) Development of stably transfected monolayer overexpressing the human apical sodium-dependent bile acid transporter (hASBT). *Pharmaceutical Research*, **22**, 1269–1280.

48 Gill, R.K., Saksena, S., Alrefai, W.A., Sarwar, Z., Goldstein, J.L., Carroll, R.E., Ramaswamy, K. and Dudeja, P.K. (2005) Expression and membrane localization of MCT isoforms along the length of the human intestine. *American Journal of Physiology. Cell Physiology*, **289**, C846–C852.

49 Takaishi, N., Yoshida, K., Satsu, H. and Shimizu, M. (2007) Transepithelial transport of alpha-lipoic acid across human intestinal Caco-2 cell monolayers. *Journal of Agricultural and Food Chemistry*, **55**, 5253–5259.

50 Martín-Venegas, R., Rodríguez-Lagunas, M.J., Geraert, P.A. and Ferrer, R. (2007) Monocarboxylate transporter 1 mediates DL-2-hydroxy-(4-methylthio)butanoic acid transport across the apical membrane of Caco-2 cell monolayers. *The Journal of Nutrition*, **137**, 49–54.

51 Glaeser, H., Bailey, D.G., Dresser, G.K., Gregor, J.C., Schwarz, U.I., McGrath, J.S., Jolicoeur, E., Lee, W., Leake, B.F., Tirona, R.G. and Kim, R.B. (2007) Intestinal drug transporter expression and the impact of grapefruit juice in humans. *Clinical Pharmacology and Therapeutics*, **81**, 362–370.

Part Four
Computational Approaches to Drug Absorption and Bioavailability

14
Calculated Molecular Properties and Multivariate Statistical Analysis

Ulf Norinder

Abbreviations

2D	Two dimensional
3D	Three dimensional
AD	Applicability domain
ADME	Absorption, distribution metabolism, and excretion
ADMET	Absorption, distribution metabolism, excretion, and toxicity
ANN	Artificial neural network
ARD	Automatic relevance determination
BCI	Bernard chemical information
BCUT	Burden, CAS, University of Texas descriptors
BNN	Bayesian neural network
C4.5	Decision trees using information entropy
CART	Classification and regression tree
Clog*P*	Calculated partition coefficient between octanol and water
CoMFA	Comparative molecular field analysis
CV	Cross-validation
DECORATE	Diverse ensemble creation by oppositional relabeling of artificial training examples
F_a	Fraction absorbed
FFD	Fractional factorial design
FIRM	Formal inference-based recursive modeling
FLAPs	Fingerprints for ligands and proteins
FNHS	Fractional negative hydrophobic surface area
FPHS	Fractional positive hydrophobic surface area
GAs	Genetic algorithms
GP	Genetic programming
G-REX	Genetic rule extraction
hERG	Human ether-a-go-go related gene
HMLP	Heuristic molecular lipophilicity potential

LDA	Linear discriminant analysis
LOO-CV	Leave-one-out cross-validation
LMO-CV	Leave-multiple-out cross-validation
MACC	Maximum auto- and cross-correlation
MIF	Molecular interaction field
MLP	Molecular lipophilicity potential
MLR	Multiple linear regression
MOE	Molecular operating environment
NN	Neural network
OD	Onion design
P-gp	P-Glycoprotein
PCA	Principal component analysis
RDS	Rule discovery system
PLS	Partial least square projection to latent structures
QSPR	Quantitative structure–property relationship
RNH	Relative hydrophilicity
RPH	Relative hydrophobicity
PNHS	Partial negative hydrophobic surface area
PPHS	Partial positive hydrophobic surface area
PSA	Polar surface area
QSAR	Quantitative structure–activity relationship
RP	Recursive partitioning
SFD	Space-filling design
SVM	Support vector machine
TPSA	Topological polar surface area
WDI	World Drug Index
WHIM	Weighted holistic invariant molecular descriptors
WNHS	Weighted negative hydrophobic surface area
WPHS	Weighted positive hydrophobic surface area

Symbols

$A\%$	Percentage absorbed
A	Abraham hydrogen-bond acidity parameter
B	Abraham hydrogen-bond basicity parameter
C_d	Hydrogen-bond donor factor
C_a	Hydrogen-bond acceptor factor
δ, δ^v	Kier–Hall molecular connectivity chi parameter
E	Abraham excess molar refraction parameter
$\log P$	$\log_{10}$ of partition coefficient between octanol and water
S	Dipolarity/polarizability solute–solvent interactions
V	McGowan characteristic volume
q^2	Cross-validated coefficient of determination
r^2	Coefficient of determination (correlation coefficient)

14.1 Introduction

To derive statistically good and predictive models, there are some aspects to consider. The investigated data set should have a reasonable spread with respect to continuous target values, for example, biological activities or some ADME-related property, of approximately three orders of magnitude or more, and the target values should also be reasonably well distributed. For deriving good and predictive classification models, the investigated classes should either be well balanced from the start, that is, the number of objects in each class are approximately the same, or should be balanced during the analysis by some appropriate weighting scheme. However, there are additional requirements that will need attention to consider a derived model robust with good forecasting ability. The investigated objects, for example, chemical structures, need to be well described for the statistical analysis to find adequate information among the collected independent variables (descriptors) to correlate to the corresponding dependent variable (target value). Today, there exist a large number of different descriptors as well as programs, for example, Dragon [1], Molconn-Z [2], MOE [3], Sybyl [4], and others, with which to calculate these variables. It is easy to rapidly calculate several thousands of descriptors for relatively large data set in the order of 10 k and upward. What kinds of descriptors are useful for modeling ADME properties? How correlated are the variables? Should 2D and/or 3D descriptors be utilized? Does the large magnitude of descriptors used has implications for the choice of statistical method or methods to be employed for analysis? What is the applicability domain (AD) of the derived model? How can this domain be quantified and used to advise users about the limitations of the model in question?

This chapter will try to answer some of these questions and investigate various approaches to derive statistically sound, robust, and predictive *in silico* models.

14.2 Calculated Molecular Descriptors

14.2.1 2D-Based Molecular Descriptors

Among the advantages with 2D-based descriptors are their rapid speed of computation for large sets of compounds and that they do not require 3D structures. Thus, these descriptors avoid the problem and compute times associated with 3D structure generation and conformational analysis, even though there are programs available that generate reliable 3D structures, for example, CORINA [5].

The 2D-based descriptors are sometimes divided into different types of descriptors such as constitutional, fragment, and functional group-based as well as topological descriptors.

14.2.1.1 Constitutional Descriptors

The constitutional descriptors are typically descriptors such as molecular weight, the number of various *x*-membered rings, the number of different types of atoms – for example, atoms of carbon, oxygen, nitrogen, and different halogens – and bonds, for example, single, double, triple, and aromatic. These kinds of descriptors have been used as one part of the structure description for modeling different ADMET end points [6–11]. Particularly, descriptors related to nitrogen and oxygen atoms have been found to be useful in deriving good ADME models since these descriptors capture the importance of hydrogen bonding for absorption and solvation processes. Another constitutional descriptor that has been frequently used is the number of rotatable bonds. This parameter is an attempt to easily obtain a crude estimation of entropy. In addition, incorporation of descriptors such as counts of various *x*-membered rings may provide important information regarding the influence of molecular self-association, for example, π–π interactions, in problems related to solubility [12].

A significant advantage of using constitutional descriptors is the ease of interpretation. It is straightforward for a researcher to understand the impact of these descriptors on derived statistical structure–property models.

14.2.1.2 Fragment- and Functional Group-Based Descriptors

The fragment and functional group based descriptors also represent a large and diverse number of available descriptors, and the division between these two sets of descriptors is rather fuzzy. These types of descriptors are also frequently called fingerprints, bits, or keys; for example, Scitegic fingerprints [13], MDL keys [14], and so on. This group of descriptors can vary significantly in the number of generated descriptors, the size of fragments identified, and the technique employed to store the descriptors. One may distinguish between two major approaches: a predefined set of patterns to be identified, also called a dictionary-based set, or a set of patterns that will vary depending upon the set of chemical structures that is under investigation. The former types of descriptors are generated using BCI fingerprints [15], Leadscope fingerprints [16], or MDL keys [17]. Many times user-defined fingerprints are of the same kind, for example, the Bursi alerts for toxicological screening [18].

The Leadscope fingerprints (the set contains some 27 k descriptors) vary markedly in size. These fingerprints cover structural patterns from small functional groups to rather large substructural moieties, whereas the Dragon functional group fingerprints (154 descriptors) [1] are restricted to identifying mostly small function groups, for example, ketones, amides carboxylic acids, esters, and alcohols. The descriptor sets generated using Daylight [19], Unity [4], or Scitegic fingerprints [13] represent the latter kinds of fingerprints, that is, the *in situ*-generated patterns. These fingerprints are usually "hashed" onto a fingerprint vector of predefined length, many times of lengths 512, 1024, or 2048, using a pseudorandom number generator. Owing to the hashing function, as well as the chosen size of the fingerprint bit vector, it is not guaranteed that different fingerprints would not be assigned to the same bit. This, in turn, means that the interpretability of such fingerprints can be lost. Nevertheless, these descriptors still contain important information for ADMET

modeling and may, many times, be quite useful for deriving statistical models with significant predictability [7–11, 20–22].

The general problem with using fingerprints resides in their binary nature, that is, either present or absent in a particular (sub)structure. Unlike a continuous variable where inter- or extrapolations are possible for new structures to be predicted by an existing statistical model, a new structure to be predicted by a model based on the binary fingerprints may contain a large number of unrecognized fragments. This, in turn, may, at worst, mean that the new compound is poorly predicted by the latter fingerprint-based models.

14.2.1.3 **Topological Descriptors**

Again, there are a large number of topological descriptors available (Table 14.1) that can be calculated from the 2D structure (graph) of a compound.

Some of the most widely used topological descriptors are the so-called Kier–Hall indices [23] that describe connectivity (^{m}Chi, $m = 1$–3, where m represents the summation over atoms, bond paths, or bond fragments) and shapes (^{m}Kappa, $m = 1$–3, where m represents the topological paths of length m). These indices are based on two parameters δ and δ^{v}, respectively, where the former parameter is the difference between the number of sigma electrons and the count of hydrogen atoms, while the latter is the difference between the number of valence electrons and the count of hydrogen atoms for the particular atom in question. Other indices that have been frequently used in ADMET modeling are the Wiener, Balaban, and Zagreb indices [24]. The Wiener index, for instance, is related to the half-sum of the bond path lengths between each atom in a molecule (the sum of all off-diagonal elements of the path distance matrix in a molecule).

Another set of topological descriptors that have been found to be important in ADMET modeling is the BCUT (Burden, Cas, University of Texas) descriptors [25], which are eigenvalue-based parameters. They are computed as the highest and lowest eigenvalues from the hydrogen-depleted 2D connectivity matrix of the structure, where the diagonal elements of the original BCUT parameters have information regarding atomic charge, polarizability, and hydrogen-bonding ability, respectively. A large number of different BCUT-type descriptors have been developed over the years and, for instance, the Dragon software [1] computes over a hundred of these kinds of indices. The disadvantage with these descriptors is that they, in many cases, are difficult to interpret in terms of how should the current structures be modified to obtain a compound with better properties for the investigated target, for example, absorption or solubility. However, the topological descriptors are quite useful for computational screening of large virtual libraries (brute force approach) when a good statistical model has been developed.

Another set of topological descriptors is the electrotopological state indices (E-state indices) developed by Kier and Hall [26, 27]. These descriptors are based on the topological state of a particular atom with corrections for electronic interactions due to other atoms in the structure. This methodology originally devised for nonhydrogen atoms only has been extended to also include E-state indices for hydrogen atoms [28] and to also include atom-type E-state indices, for

Table 14.1 Selected topological descriptors.

Topological descriptor
Information index on molecular size
Total information index of atomic composition
Mean information index on atomic composition
First Zagreb index M_1
First Zagreb index by valence vertex degrees
Second Zagreb index M_2
Second Zagreb index by valence vertex degrees
Quadratic index
Narumi simple topological index (log)
Narumi harmonic topological index
Narumi geometric topological index
Total structure connectivity index
Pogliani index
Ramification index
Polarity number
Logarithm of product row sums (PRSs)
Average vertex distance degree
Mean square distance index (Balaban)
Schultz molecular topological index (MTI)
Schultz MTI by valence vertex degrees
Gutman molecular topological index
Gutman MTI by valence vertex degrees
Xu index
Superpendentic index
Wiener W index
Mean Wiener index
Reciprocal distance Wiener-type index
Harary H index
Quasi-Wiener index (Kirchhoff number)
First Mohar index T_{I1}
Second Mohar index T_{I2}
Hyperdistance-path index
Reciprocal hyperdistance-path index
Detour index
Hyperdetour index
Reciprocal hyperdetour index
Distance/detour index
All-path Wiener index
Wiener-type index from *Z*-weighted distance matrix (Barysz matrix)
Wiener-type index from mass-weighted distance matrix
Wiener-type index from van der Waals-weighted distance matrix
Wiener-type index from electronegativity-weighted distance matrix
Wiener-type index from polarizability-weighted distance matrix
Balaban J index
Balaban-type index from *Z*-weighted distance matrix (Barysz matrix)
Balaban-type index from mass-weighted distance matrix
Balaban-type index from van der Waals-weighted distance matrix
Balaban-type index from electronegativity-weighted distance matrix

Table 14.1 (*Continued*)

Balaban-type index from polarizability-weighted distance matrix
Connectivity index chi-0
Connectivity index chi-1 (Randic connectivity index)
Connectivity index chi-2
Connectivity index chi-3
Connectivity index chi-4
Connectivity index chi-5
Average connectivity index chi-0
Average connectivity index chi-1
Average connectivity index chi-2
Average connectivity index chi-3

example, for methyl groups, hydroxy and keto oxygens, respectively, and the corresponding atom-type E-state sums for various groups, as well as for different hydrogens, for example, hydrogen-bond donors and acceptors. The type E-state sums related to groups of hydrogen atoms have been found to correlate well with hydrogen-bonding properties [29].

One significant difference between many other topological descriptors and the E-state parameters is that the latter indices are much easier to interpret and, thus, capable of answering the question "Which are the next molecules to make?" in a relatively straightforward manner. These two aspects (computational speed and interpretability) make these descriptors quite attractive both for e-screening purposes and for having an interpretable model with which to focus the virtual library generation and for further pharmaceutical investigations or work. The sum of hydrogen-bonding donor- and acceptor-related E-state descriptors is well correlated with the corresponding HYBOT parameters (see Section 14.2.3.2 for further details) with r^2 values between 0.8 and 0.95 [30].

14.2.2
3D Descriptors

The 3D descriptors described in this section are the weighted holistic invariant molecular (WHIM) descriptors, the Jurs descriptors, and the GRID-based VolSurf and Almond descriptors, as well as pharmacophore fingerprints.

14.2.2.1 WHIM Descriptors

The WHIM descriptors are based on statistical indices calculated on the projections of atoms along principal axes [31–34]. There are different types of WHIM descriptors with the aim to incorporate 3D information regarding size, shape, symmetry, and atom distributions independent of molecular alignments.

The WHIM algorithm performs a principal component analysis (PCA) on the mean centered Cartesian coordinates of the molecule from a weighted covariance matrix of the atomic coordinates. The weights of this matrix are such properties as atomic mass, van der Waals volume, Sanderson atomic electronegativity, atomic

Table 14.2 List of examples of WHIM descriptors.

L1u: first component size directional WHIM index/unweighted
L2u: second component size directional WHIM index/unweighted
L3u: third component size directional WHIM index/unweighted
L1m: first component size directional WHIM index/weighted by atomic masses
L2m: second component size directional WHIM index/weighted by atomic masses
L3m: third component size directional WHIM index/weighted by atomic masses
L1v: first component size directional WHIM index/weighted by atomic van der Waals volumes
L2v: second component size directional WHIM index/weighted by atomic van der Waals volumes
L3v: third component size directional WHIM index/weighted by atomic van der Waals volumes
L1e: first component size directional WHIM index/weighted by atomic Sanderson electronegativities
L2e: second component size directional WHIM index/weighted by atomic Sanderson electronegativities
L3e: third component size directional WHIM index/weighted by atomic Sanderson electronegativities
L1p: first component size directional WHIM index/weighted by atomic polarizabilities
L2p: second component size directional WHIM index/weighted by atomic polarizabilities
L3p: third component size directional WHIM index/weighted by atomic polarizabilities
P1p: first component shape directional WHIM index/weighted by atomic polarizabilities
P2p: second component shape directional WHIM index/weighted by atomic polarizabilities
Tu: *T* total size index/unweighted
Tm: *T* total size index/weighted by atomic masses
Tv: *T* total size index/weighted by atomic van der Waals volumes
Te: *T* total size index/weighted by atomic Sanderson electronegativities
Tp: *T* total size index/weighted by atomic polarizabilities
Ts: *T* total size index/weighted by atomic electrotopological states

polarizability, and electrotopological state indices (for a list of selected WHIM descriptors see Table 14.2).

14.2.2.2 **Jurs Descriptors**

The so-called Jurs descriptors are 3D surface descriptions related to various total and fractional defined surfaces. They can be divided into to two parts: one electronic [35] and one hydrophobic [36]. The former set of descriptors is generated from partial positive and negative surface areas, total charge as well as atomic positively and negatively charged weighted surface areas, and various differential and fractional charged partial surface areas of the molecule (see Table 14.3).

The second set of descriptors describes hydrophobic surface properties of a molecule. As with the first set, the second set contains similar partial hydrophobic and partial hydrophilic surface area descriptors (PPHS-*x* and PNHS-*x*, respectively), differences in partial surface area descriptors (FPHS-*x* and FNHS-*x*), as well as total surface area weighted descriptors (WPHS-*x* and WNHS-*x*). In addition, two descriptors assessing the most hydrophobic atom and the most hydrophilic atom on the overall lipophilicity are also described (RPH and RNH). The atom-based fractional log *P* contributions used for calculations are those of Wildman and Crippen [37] and

Table 14.3 List of selected electronic Jurs descriptors.

PPSA-1: partial positive surface area
PNSA-1: partial negative surface area
PPSA-2: total charge weighted PPSA
PNSA-2: total charge weighted PNSA
PPSA-3: atomic charge weighted PPSA
PNSA-3: atomic charge weighted PNSA
DPSA-1: difference in charged partial surface areas [(PPSA-1) – (PNSA-l)]
DPSA-2: difference in charged partial surface areas [(PPSA-2) – (PNSA-2)]
DPSA-3: difference in charged partial surface areas [(PPSA-3) – (PNSA-3)]
FPSA-1: fractional charged partial surface areas
FNSA-1: fractional charged partial surface areas
FPSA-2: fractional charged partial surface areas
FNSA-2: fractional charged partial surface areas
FPSA-3: fractional charged partial surface areas
FNSA-3: fractional charged partial surface areas
WPSA-1: surface-weighted charged partial surface areas
WNSA-1: surface-weighted charged partial surface areas
WPSA-2: surface-weighted charged partial surface areas
WNSA-2: surface-weighted charged partial surface areas
WPSA-3: surface-weighted charged partial surface areas
WNSA-3: surface-weighted charged partial surface areas
RPCG: relative positive charge
RNCG: relative negative charge
RPCS: relative positive charged surface area
RNCS: relative negative charged surface area

computed on the solvent-accessible surface area using the SAVOL program [38] with a probe radius of 1.5 Å.

The Jurs descriptors have been found useful in modeling ADMET properties such as human intestinal absorption [25, 39] and toxicity [40].

14.2.2.3 VolSurf and Almond Descriptors

VolSurf and Almond descriptors are based on results from molecular interaction fields (MIFs) but do not explicitly require the alignment of the structures under investigation as a first step in the analysis. Although VolSurf and Almond descriptors use the same source of information, that is, the computed GRID MIFs, they differ significantly with respect to their underlying approaches. The VolSurf method [41,42] is created with the aim of predicting pharmacokinetic properties, for example, blood–brain barrier permeation [43]. VolSurf descriptors summarize the MIF information related to the size and shape of the molecule under investigation as well as to the size and shape of the hydrophilic and hydrophobic regions and the balance between the two regions. Almond descriptors are designed to characterize pharmacodynamic properties such as protein–ligand interactions. Almond descriptors are primarily aimed at the identification of optimal interaction sites and the description of the geometrical relationship between such sites by using a default set of GRID probes: DRY (hydrophobic), O (carbonyl oxygen, hydrogen-bond acceptor),

and N1 (amide nitrogen, hydrogen-bond donor). A fixed number of GRID points from each MIF with respect to the GRID energy level and the internode distance between the two points are used. An autocorrelogram is generated via the MACC-2 (maximum auto- and cross-correlation) algorithm by storing only the highest pair-wise product of interaction energies between all pairs. The three default auto-correlograms are DRY–DRY (hydrophobic); O–O (hydrogen-bond donor); N1–N1 (hydrogen-bond acceptor). The three default cross-correlograms are DRY–O (hydrophobic–hydrogen-bond donor); DRY–N1 (hydrophobic–hydrogen-bond acceptor); O–N1 (hydrogen-bond donor–hydrogen-bond acceptor). These auto- and cross-correlograms are then used as descriptors. Almond descriptors have, so far, in the ADMET area primarily been used in P450 modeling [44–46].

14.2.2.4 **Pharmacophore Fingerprints**

Pharmacophores have been used for many years to derive models for understanding the common interaction patterns of ligands or their subsets. These pharmacophores have, subsequently, been used not only to design new structures with better target properties or devoid of such activities if so being the desired case, for example, hERG pharmacophores [47], but also to search 3D databases for new interesting entities or core structures. For a recent review on pharmacophores, see Ref. [48].

Pharmacophore fingerprints have also been used to assess the similarity of molecules from an interaction property point of view [49–51].

Pharmacophore fingerprints have typically so far been generated as three- or four-point pharmacophores spanning 0–15 (16) Å edges with increments of typically 2–3 Å. However, there are some issues to the generation of these fingerprints. First, how important is information of chirality, that is, is a three-point pharmacophore triangle sufficient or is the need for a four-point pharmacophore important for the set of studied compounds? This choice has considerable implications with respect to the number of fingerprints generated and stored for subsequent use for a typical set of structures. Second, is a conformational analysis required so that many conformations for a particular compound may map to the pharmacophores or will a single conformation be sufficient? For the latter case, should that conformation be selected from the conformational analysis and, if so, which conformations should be used? Perhaps, the lowest energy conformation should be used or some conformation of choice, for example, the one more closely related to the proposed bioactive conformation, is the best choice. Perhaps, a single conformation generated with a 3D generation program, for example, CORINA, is good enough for the problem at hand. If so, should that conformation be subjected to an energy minimization? Three-point pharmacophore triangles using conformational analysis (~10 k pharmacophores) with subsequent support vector machine (SVM)-based classification modeling for lead hopping purposes have been published by Saeh and coworkers [52]. Pharmacophore fingerprints have also been used for modeling the efflux transporter P-glycoprotein (P-gp) by Penzotti and coworkers [53]. In this work, a huge ensemble of fingerprints from all two-, three-, and four-point pharmacophores present in the conformers of the investigated compounds was generated. Even though the authors imposed a limit of at most two hydrophobic features for each generated

pharmacophore, the resulting pharmacophore bit length was approximately 12 million bits! Recently, an interesting approach using a combination of pharmacophore fingerprints and GRID MIFs (see Section 14.2.2.3) called FLAPs (fingerprints for ligands and proteins) has been developed where the combined knowledge of protein and ligand profiles is used [54].

14.2.3 Property-Based Descriptors

This section will cover a variety of descriptors related more to experimental physicochemical properties such as lipophilicity and hydrogen bonding.

14.2.3.1 log *P*

The calculated water/octanol partition coefficient (log *P*) is probably the most commonly used descriptor in structure–activity modeling. However, this well-known and widely used descriptor is not without computational difficulties. There exist quite a number of software programs for the prediction of log *P*, for example, CLOGP [55], KOWWIN [56], SciLogP/ULTRA [57], and ACD/logP [58], that employ different algorithms including experimental values of parent structures, that is, a substructure of the compound to be predicted, coupled with perturbation equations, that is, equations for corrections due to additional fragments in the investigated structure, and special correction factors due to, for instance, the proximity of other fragments, to more fragment-based approaches, where each fragment has a certain set of log *P* factors, and to rule-based approaches. This, in turn, means that a log *P* prediction for a particular compound may vary markedly using different programs. For two recent investigations of this issue, see Refs [59, 60]. In addition, a fact to be remembered is that log *P* is a composite variable constituted by the three underlying properties of molecular size, polarity/polarizability, and hydrogen bonding. This natural partitioning of the three factors, as it occurs in log *P*, may not always be optimal for deriving the best statistical model [61]. Instead, models employing separate descriptors for molecular size, polarity/polarizability, and hydrogen bonding may indeed have more reliable forecasting abilities.

Although log *P* is a scalar, there are 3D protocols designed to calculate log *P*. These approaches utilize the concept of molecular lipophilicity potentials (MLPs). Testa and coworkers introduced MLPs using distance-dependent functions calculated on the solvent-accessible surface area molecules [62]. They used fragment-based lipophilicity factors from Broto and coworkers [63] as well as from Ghose and Crippen [64] to compute the MLPs. Lately, Du and coworkers have introduced the concept of heuristic molecular lipophilicity potentials (HMLPs) [65] that describe certain aspects of molecular solvation. The HMLPs are based on quantum mechanical electrostatic potentials (ESPs) that are calculated on a formal molecular surface of a compound. The corresponding molecular lipophilicity potential for a particular point on the surface is then constructed by comparing the local electron density at that point with the ESP on the surrounding atoms. Du and coworkers have applied the HMLP approach to calculate log *P* values for some alcohols [65].

14.2.3.2 HYBOT Descriptors

Another set of property-based descriptors that have been quite useful in ADMET modeling is the HYBOT parameters. Raevsky and coworkers have collected a large database of thermodynamic data related to hydrogen bonding with which they have developed the HYBOT program [66]. HYBOT will compute hydrogen-bond donor (ΣC_d) and acceptor (ΣC_a) factors that describe the donor and acceptor strengths, respectively, of a compound. By using these two descriptors, many significant statistical models related to areas such as water solubility, log *P* estimations, Caco-2 permeability, human intestinal absorption, and human skin permeability have been developed [67–69]. The HYBOT parameters represent another interesting aspect of computational descriptors containing relevant information for calculating not only a qualitative measure of a particular property, for example, hydrogen bonding, but also a more quantitative one [66]. By using HYBOT parameters, it is possible to obtain information regarding the possible importance of various hydrogen-bonding patterns, for example, whether a few but strong hydrogen-bonding groups are more important for the investigated property than perhaps many but weaker such entities.

14.2.3.3 Abraham Descriptors

Abraham and coworkers have developed a general solvation equation

$$\mathrm{SP} = c + eE + sS + aA + bB + vV, \tag{14.1}$$

where the dependent variable, SP, is the target property in question and *E* is an excess molar refraction, *S* represents the dipolarity/polarizability solute–solvent interactions, *A* and *B* are the hydrogen-bond acidity and basicity, respectively, and represent the strength and number of H bonds formed by donor and acceptor groups, respectively, in solute–solvent interactions, and *V* is the McGowan characteristic volume. These five parameters (*E*, *S*, *A*, *B*, and *V*) constitute the Abraham descriptors. The solute – descriptors *A* and *B* are based on the theoretical cavity model of solute-solvent interactions and are widely applied in the prediction of a variety of properties, such as solubility [70], blood–brain partitioning [71], and skin permeability [72]. Again, the use of the Abraham descriptors allows a more detailed understanding of possible hydrogen-bonding patterns.

14.2.3.4 Polar Surface Area

A very useful property for predicting absorption is the polar surface area (PSA), usually defined as those parts of the van der Waals or solvent-accessible surface of a molecule that are associated with hydrogen-bond-accepting capability (e.g., N or O atoms) and hydrogen-bond-donating capability (e.g., NH or OH groups). Three types of PSAs have been used in ADME studies:

1. dynamic PSA (PSA_d) [73];
2. static PSA (PSA) [74]; and
3. two-dimensional (or topological) PSA (TPSA) [75].

The dynamic PSA, PSA_d, was developed by Palm *et al.* [73]. PSA_d is calculated by a Monte Carlo conformational search with subsequent energy minimization.

This generates a set of low-energy conformers where the van der Waals surface-based PSAs for all conformers are within 2.5 kcal/mol of the "global" minimum, that is, the lowest energy conformer found, are computed. The Boltzmann-weighted average of the calculated PSAs are then used as the PSA_d. Palm and coworkers found a good sigmoidal correlation ($r^2 = 0.94$) between PSA_d and percentage human absorbed ($A\%$) for 20 well-characterized drugs [73].

A major drawback of the PSA_d is, however, the rather time-consuming calculation, particularly the Monte Carlo conformational search, which makes PSA_d inappropriate for computational screening (e-screening) of large virtual libraries.

This prompted further development of the static PSA, originally proposed by van de Waterbeemd and Kansy [76], based on only one conformer. Although this simplification would save considerable computational time, it is not without complications since it raises the question: Which conformation should be used? Probably a low-energy conformation could be considered as a good estimation of the bioactive conformation. However, in some cases, some sort of conformational search, although short, has to be employed, and most of the advantage of using PSA instead of PSA_d would be lost. Fortunately, a single conformer generated directly from the 2D molecular structure without minimization can be used. This approximation does not compromise the excellent correlation with absorption previously found [77, 78]. This approach reduces the computational time to such a level so as to make PSA useful for *in silico* screening of virtual libraries. However, still a slight drawback of PSA is the generation of the 3D conformation. The problem is not related to the computational time but from a conformational point of view. No matter how well 2D and 3D conversion programs, such as CORINA, perform on an overall basis, the generation may, in some cases, result in unreasonable 3D structures. Thus, it would be even more favorable if this step could be circumvented or eliminated in some manner.

Ertl and coworkers [75] have developed such a method for generating a topological PSA (TPSA) based on 3D PSA values for 43 fragments resulting from an analysis of 34 810 compounds taken from the WDI database. The correlation between PSA and TPSA is very high ($r^2 = 0.98$).

A further simplification, avoiding even the use of 3D fragments, has been developed by Sherbukhin [79]. This method uses a 2D projection technique whereby the TPSA (TPSA-2D) is computed. The algorithm employed sums up atomic contributions of 2D-generated atom-based van der Waals spheres and subtracts buried surfaces where two atomic spheres intersect to make a bond.

One thing to bear in mind here is that conformational dependencies may bury parts of the PSA, thus resulting in an overestimation of the computed TPSA.

14.3 Statistical Methods

There are a large number of statistical techniques available to the researcher to relate the independent variables (descriptors) computed for the objects (structures) under investigation to the corresponding dependent variable (target value).

These techniques span the entire field from multiple linear regression (MLR)-type methods and various forms of neural network architectures to rule-based techniques of different kinds. These approaches also span from single models to multiple models, that is, consensus or ensemble modeling. Terms like machine learning and data or information fusion are also frequently encountered in this area of research, as well as the concepts of applicability domain and validation.

This section attempts to present some of the most common statistical techniques used today to derive statistically sound structure–activity or structure–property models with good predictive ability.

There are a number of important issues and possible trade-offs to be discussed in this section that, in principle, do not stand against each other but, in reality, often do, such as the balance between the interpretability versus robustness or predictability of the derived model, that is, transparent versus opaque models, white versus black box models, a well as whether to derive local versus more global models for a particular target in question. For a recent review of statistical methods, see Ref. [80].

There are many ways of characterizing different statistical machine-learning methods and protocols, but in this section, they will be organized into linear and nonlinear methods (even though the descriptor matrix they operate on may contain higher order terms and cross-terms) as well as rule-based and Bayesian methods.

14.3.1 Linear and Nonlinear Methods

14.3.1.1 Multiple Linear Regression

Multiple linear regression is a classic mathematical multivariate regression analysis technique [81] that has been applied to quantitative structure–property relationship (QSPR) modeling. There are a few aspects, with respect to statistical issues, that the researcher must be aware of when using MLR:

1. A general prerequisite that affects all statistical multivariate data analysis techniques is that each of the variables should be given equal chance to influence the outcome of the analysis. This can be achieved by scaling the variables in an appropriative way. One popular method for scaling variables is autoscaling whereby the variance of each variable is adjusted to 1.
2. MLR assumes each variable to be exact and relevant.
3. Strong co-linear variables must be eliminated by removing all but one of the strongly correlated variables. Otherwise, spurious chance correlation may result.
4. Some sort of estimation of the statistical "distance" to the overall model should be reported for each compound to provide an estimate of how much an intra- or extrapolation in multivariate descriptor space the prediction actually constitutes.

MLR has been applied extensively to problems related to various aspects predicting ADMET properties such as solubility, Caco-2 cells permeability, human intestinal

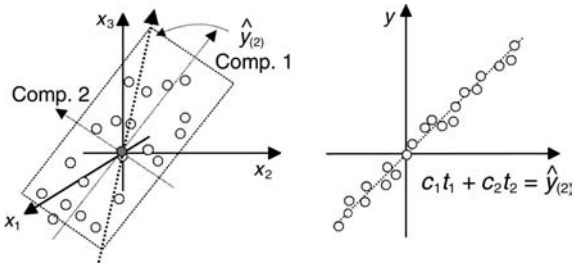

Figure 14.1 PLS of two components (picture reproduced with permission from the authors [125] and Umetrics, Inc.).

absorption, and blood–brain permeability, as well as for predicting metabolism. For a recent review, see Ref. [82].

14.3.1.2 **Partial Least Squares**

Partial least square projection to latent structures (PLS) [83] is a multivariate data analysis tool that has gained much attention during the past 10 years starting with the introduction of the 3D-QSAR method CoMFA [84]. PLS is a projection technique that uses latent variables (linear combinations of the original variables) to construct multidimensional projections while focusing on explaining as much as possible the information in the dependent variable and not among the descriptors used to describe the objects (compounds) under investigation (the independent variables) (Figure 14.1).

PLS differs from MLR in a number of ways:

1. The descriptors are not treated as exact and relevant but as consisting of two parts: one part related to the dependent variable and the other part unrelated (noise).
2. Strong correlations between relevant variables are not a problem in PLS, and all such variables can be kept in the analysis. In fact, the models derived using PLS become more stable with the inclusion of strongly correlated and relevant parameters.
3. The number of original descriptors may vastly exceed the number of compounds in the analysis (as opposed to MLR) since PLS uses only a few (usually less than 5–10) latent variables for the actual statistical analysis.
4. In PLS analysis, a "distance" to the overall model (distance-to-model), defined as the variance in the descriptors remaining after the analysis (residual standard deviation, RSD), is given for each predicted compound. This is an important piece of information that is presented to the researcher.

There are of course also some difficulties faced when using the PLS technique:

1. The number of latent variables (PLS components) has to be determined by some sort of validation technique, for example, cross-validation (CV) [85]. The PLS solution will coincide with the corresponding MLR solution when the number of latent variables becomes equal to the number of descriptors used in the analysis.

The validation technique, at the same time, also serves the purpose of avoiding overfitting of the model.

2. The possibility to use a very large number of descriptors, where many of them may not be particularly correlated with the dependent variable and thus represent large amounts of noise, must be considered with great care or otherwise the signal-to-noise ratio becomes too low for PLS to be able to create useful projections (latent variables).

14.3.1.3 Artificial Neural Networks

Artificial neural networks (ANNs) represent, as opposed to PLS and MLR, a nonlinear statistical analysis technique [86]. The most commonly used NN is of the feed-forward back-propagation type (Figure 14.2). As is the case of both PLS and MLR, there are a few aspects of NN to be considered when using this type of analysis technique:

1. The number of middle layers, hidden nodes, in an NN must be identified either through a particular choice or through an optimization procedure with careful monitoring of the predictive behavior of the derived model (see point 2).
2. NNs are well-known to overtrain, that is, to be able to explain a large portion of the variance of the dependent variable for the training set but to fail grossly to be able to predict a correct answer for the objects that are not part of the model (external test set). Overtraining of NNs can be avoided by setting aside a fixed number of compounds to validate the predictive ability of the NN model (validation set) as part of the NN training and stop when the predictive ability starts to deteriorate.
3. The interpretability of the derived NN model may be difficult to understand even though the influences of the descriptors on the derived model can be simulated. Guha and coworkers [87] have developed a two-step method for understanding the weights and biases in neural networks, in which first the neuron transform is linearized followed by a ranking scheme for the neurons.

NN methods have been used by Wessel and coworkers [39], Agatonovic-Kustrin *et al.* [8], and Ghuloum *et al.* [88] to model intestinal absorption.

14.3.1.4 Bayesian Neural Networks

Bayesian neural networks (BNNs) are an alternative to the more traditional ANNs. The main advantage with BNNs is that they are less prone to overtraining compared to ANNs. BNNs are based on Bayesian probabilistics for the network training. Network weights are determined by Bayesian inference. BNNs have been successfully used together with automatic relevance determination (ARD) for the selection of relevant descriptors to model aqueous solubility [89]. For a good review on BNNs, see Ref. [90].

14.3.1.5 Support Vector Machines

The Support vector machine technique is a relatively new method in the field of structure–property relationships. SVMs originated from the work of Vapnik *et al.* [91] and were originally applied to image analysis, text categorization, and

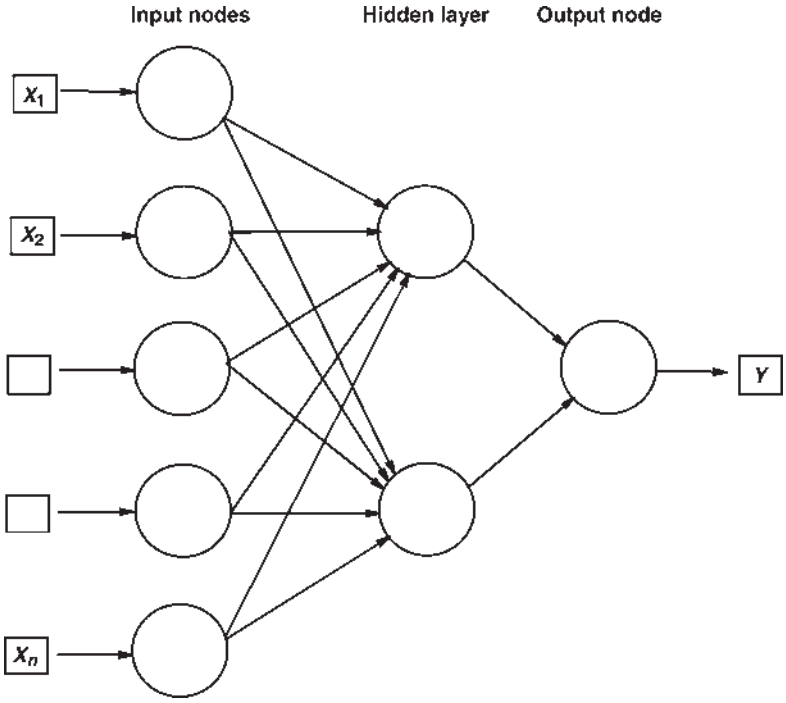

Figure 14.2 Simple scheme of an artificial neural network with one hidden layer.

character recognition [92]. Support vector machines have gained considerable interest in modeling ADMET properties during the last 5–6 years for, among other things, their robustness and forecasting abilities with respect to noisy data [93]. For a compilation of SVM applications in ADMET modeling, see Refs [94–96]. The basic idea of SVM technology is to construct a hyperplane that discriminates between the two classes of objects under investigation (binary SVM). The SVM algorithm maximizes the construction of a margin between the classes. SVMs use transformations of the original data for the successful construction of the margin (Figure 14.3).

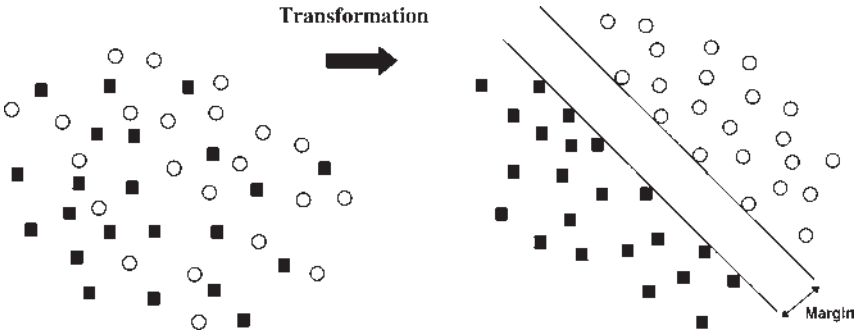

Figure 14.3 Basic principle of a support vector machine transformation for a two-class problem.

These transformations are executed by using so-called kernel functions. The kernel functions can be both linear and nonlinear in nature. The most commonly used kernel function is of the latter type and called the radial basis function (RBF). There are a number of parameters, for example, cost functions and various kernel settings, within the SVM applications that will affect the statistical quality of the derived SVM models. Optimization of those variables may prove to be productive in deriving models with improved performance [97]. The original SVM protocol was designed to separate two classes but has later been extended to also handle multiple classes and continuous data [80].

14.3.1.6 *k*-Nearest Neighbor Modeling

k-Nearest neighbor (kNN) modeling is based on the assumption of similarity, that is, similar compounds have similar target properties. In its simplest form, the method uses an unweighted distance measure, usually Euclidian distance, in chemical property space and from the *k*-nearest objects determines the target property or which class the object in question can be assigned to. There are, however, some aspects to highlight when using this approach:

1. Euclidian distances can, from a strict perspective, only be used for determining the distance between orthogonal variables. This is most often not the case for chemical descriptors. The problem of orthogonality can be handled in two ways: either compensate for the nonorthogonal behavior within the distance calculation, for example, use Mahalanobis distance instead [98] of an Euclidian distance or orthogonalize the variables, for example, by principal component analysis, prior to the Euclidian distance calculation.
2. All variables are treated equally importantly. It is unlikely that all the computed chemical properties for the compounds in the data set are of equal importance for the target property, for example, solubility, absorption, or metabolism.
3. The *k*-nearest neighbors are treated with equal weight with respect to determining the target property. This is of particular importance when estimating continuous properties. This aspect has been investigated by Shen *et al.* [99] where they used weighted distances to obtain better predictions for the target property.

14.3.1.7 Linear Discriminant Analysis

Linear discriminant analysis (LDA) is aimed at finding a linear combination of descriptors that best separate two or more classes of objects [100]. The resulting transformation (combination) may be used as a classifier to separate the classes. LDA is closely related to principal component analysis and partial least square discriminant analysis (PLS-DA) in that all three methods are aimed at identifying linear combinations of variables that best explain the data under investigation. However, LDA and PLS-DA, on one hand, explicitly attempt to model the difference between the classes of data whereas PCA, on the other hand, tries to extract common information for the problem at hand. The difference between LDA and PLS-DA is that LDA is a linear regression-like method whereas PLS-DA is a projection technique

(see Sections 14.3.1.1 and 14.3.1.2 for further details). Thus, for a two-class, two-descriptor problem (X_1 and X_2), the LDA description becomes

$$Y = c_1 \cdot X_1 + c_2 \cdot X_2. \tag{14.2}$$

The object of the LDA is to find values of the two constants c_1 and c_2, respectively, that separate the two classes expressed through the variable Y as, for instance, 1 and 2, respectively.

14.3.2 Partitioning Methods

14.3.2.1 Traditional Rule-Based Methods

The basic underlying idea with partitioning methods is to split, usually in a recursive, that is, repetitive, manner, the data set at hand into two or more groups, branches, thus creating a decision tree. The object is to create more and more homogeneous groups in the respective branches. There are several methods available for the construction of decision trees, for example, FIRM [101], CART [102], RDS [103], and C4.5 [104] (Figure 14.4).

As always, there are certain aspects to consider when developing a decision tree:

1. Overtraining: As with many other methods, decision trees are prone to overtraining if not monitored. The forecasting ability of the tree must be estimated by some, usually, internal validation method such as a validation set or through cross-validation. This will determine the depth and degree of branching of the derived tree.
2. Forecasting ability: Most decision tree methods are "greedy," that is, they split on the variable giving the best enhancement in group homogeneity according to

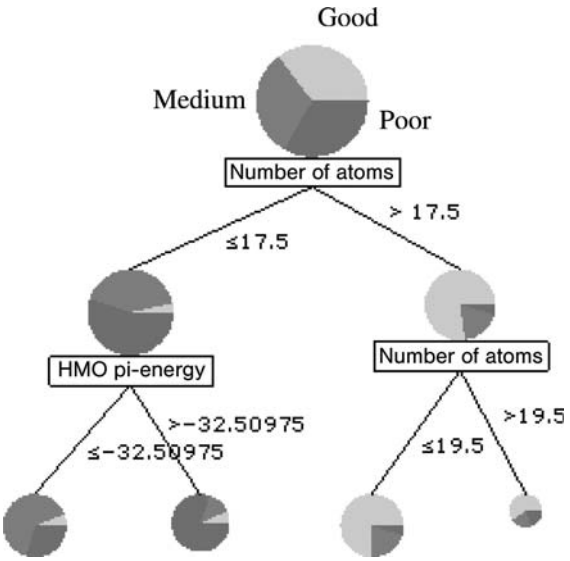

Figure 14.4 Simple decision tree with split points and terminal leaves.

some statistical test, such as the *t*- or *F*-test, at each split point. This may, however, not produce the model with the best predictive performance after model construction. Random selection of variables, that is, a subset, available for each split has been devised to overcome this situation.

Recursive partitioning has successfully been used to develop models for various ADMET properties, see Ref. [80], as well as for the elucidation of toxicological modes of action [103].

14.3.2.2 Rule-Based Methods Using Genetic Programming

Neural networks and genetic algorithms (GAs) have been used in QSAR applications for some time [105]. The main idea of genetic programming (GP) closely resembles that of the GA. Most GP applications use a tree-based representation and normally a genetic program has a tree-like construction consisting of functional nodes and terminal leaves (see Figure 14.5).

The algorithm G-REX uses crossover and mutation (see Figure 14.6), and the extraction strategy is based on genetic programming [106–109].

Crossover is very common, that is, around 85% of each new generation is created by crossover, whereas mutation is used less than 2% for generating new offsprings. One key property of G-REX is the option to directly balance accuracy against comprehensibility by using an appropriate fitness function. G-REX modeling often results in rather short and transparent models (see Chapter 15, Section 15.3.2.2: an example using genetic programming-based rule extraction).

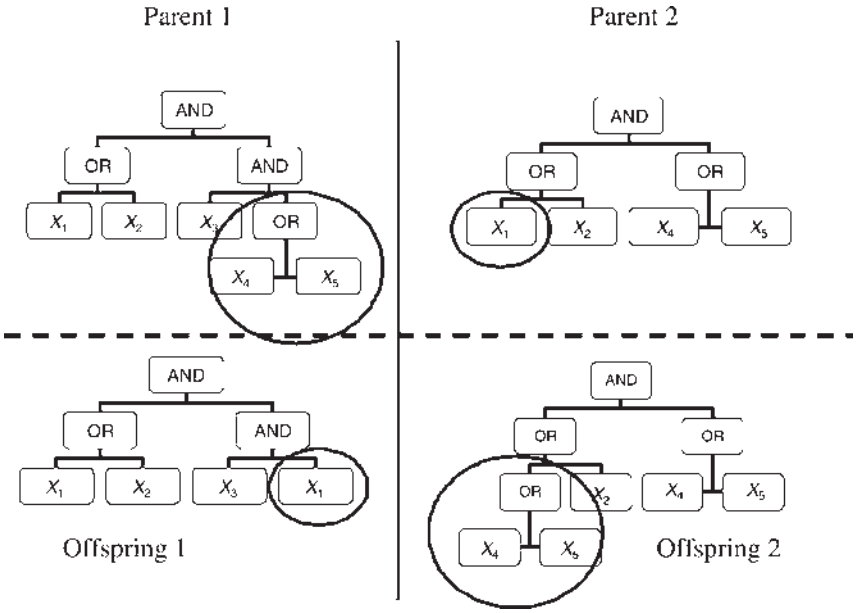

Figure 14.5 Principle of crossover in genetic programming (picture reproduced with permission from the author [109]).

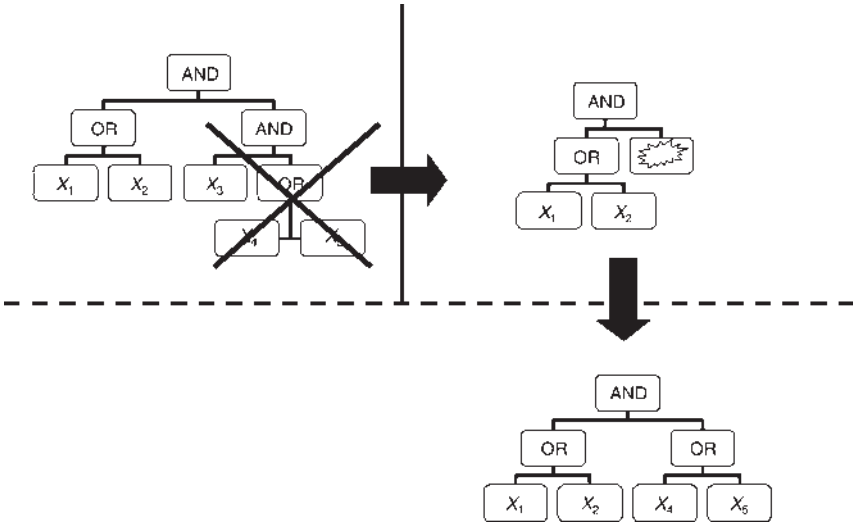

Figure 14.6 Principle of mutation in genetic programming (picture reproduced with permission from the author [109]).

14.3.3 Consensus and Ensemble Methods

Many times there is a trade-off between the transparency and the accuracy of the derived model for a particular target. In some cases, the transparency is the most important aspect as long as the derived model has acceptable predictive ability. These models are better suited to answer the question, "Which are the next compounds to investigate?" by understanding the underlying properties of deriving compounds with improved target properties. Other times the most important aspect of a derived *in silico* model is the accuracy and robustness with respect to its forecasting performance. For the latter cases, consensus, often also called ensemble, models may offer some attractive properties. Many times these kinds of models offer improved forecasting performance and robustness compared to an individual model for the target in question. There are several ways to construct consensus models with respect to the input variables, the statistical methods, and how the final prediction from the battery of models is derived. It should be noted that the two kinds of models, transparent versus more opaque, are not necessarily in conflict with each other. On the contrary, they may benefit from each other's existence in the following manner: One may use the more transparent models to focus the attention around certain areas (subspaces) in property space indicated to result in promising new entities. Once these areas have been identified, the more complex consensus model, sometimes requiring considerably longer time for computation, is employed to predict the target property in question at a higher level of accuracy and precision. However, it may sometimes be debatable whether or not the increase in performance really outweighs the added complexity [110].

The simplest and most straightforward way to employ consensus modeling is to use the same set of descriptors and statistical method (single method-descriptor set methods). Considerable time saving with respect to descriptor generation, that is, using only one set and not several different sets, can be achieved. In addition, using the same statistical approach may have a favorable effect on implementation of the consensus approach with respect to issues such as licenses and data format compatibility. Single method-descriptor set methods have been implemented in decision tree programs such as TreeNet [111] and RDS [112]. The approach actually consists of two selection parts. The training set for the various models of contributing to the ensemble is often selected using bagging (bootstrap aggregating). Then, at each split point for decision tree programs, the variables to be included in the model are also randomly chosen. Thus, a certain variation of the models of the ensemble is achieved that promotes predictive performance and robustness of the final ensemble. There are also approaches available to monitor and ensure a certain diversity of the derived ensembles with acceptable statistical quality. One such an approach is DECORATE (diverse ensemble creation by oppositional relabeling of artificial training examples) [113].

The obvious extension to single method-descriptor set methods is of course some combination of single or multiple methods using single or multiple descriptor sets.

Various forms of these combinations with an accuracy of the ensemble models better than the corresponding single reference have been reported [90, 114–119].

14.4 Applicability Domain

A very important aspect of statistical modeling is to determine the domain in which the model is defined with high significant reliability, called the applicability domain.

It is important to do this for several reasons:

1. To make the users of the model aware of the applicability and limitations of the present model.
2. To avoid the misuse of a model for forecasting of compounds outside the model's present statistical limits, which renders the model (and/or statistical technique as well as the parameterization) a false "bad reputation."
3. To be able to use extrapolations from the present model in a constructive manner to expand the model to cover a larger domain space.

However, many statistical modeling techniques do not, in an easy and straightforward way, by default, enable the estimation of whether a prediction is an interpolation to the model, thus rendering the prediction more credibility or an extrapolation to the model in which case the prediction must be evaluated with greater care. Furthermore, there are two aspects to the extrapolation problem: one structural and the other statistical. Considerable research has been devoted to the problem of ADs. For a recent compilation on this issue, see Ref. [120].

The structurally focused methods for defining ADs are related to a large extent with the independent variable (descriptor) side. These methods comprise techniques, such as

1. Range-based methods whereby the AD is defined solely on the ranges that the investigated descriptors of the training set, that is, the objects used to derive the model in question, span. If a new object to be predicted is within the range of all the model descriptors, then the object is within the AD of the model.
2. Distance-based methods whereby some kind of distance measure between the object to be predicted and the closest neighbor or neighbors of the training set defines the AD. Typical methods for distance-based measures are Euclidian and Mahalanobis distances. The difference between the two is that the former distance can only be used for determining the distance between orthogonal variables, whereas the latter method compensates for the nonorthogonal behavior (see further discussion in Section 14.3.1.6). In its simplest form, all descriptors are treated with equal importance while some more advanced methods use some kind of weighting scheme to increase accuracy and relevance of the distance measure, for example, by using the coefficients of the derived statistical model for modulating the influence of the descriptors.
3. Geometric methods where most definitions rest on defining the smallest convex area that covers the training set compounds in descriptor space. This method is also known as the convex hull method (Figure 14.7).

The statistically focused methods for defining ADs are related to information content of the investigated descriptors, for example, the variance of the descriptor matrix and calculate the amount of an unexplained variance for the training set objects (the model) and compare it with the corresponding amount for the new objects to be predicted. If the amount of unexplained variance for the new objects is much greater, typically more than the two standard deviations from the training set compounds (~95% confidence interval), the former objects are designated to be outside the AD of the model.

A constructive way of using the estimations of AD, and particularly extrapolations thereof, as mentioned under point 3, would be to include some of the predicted

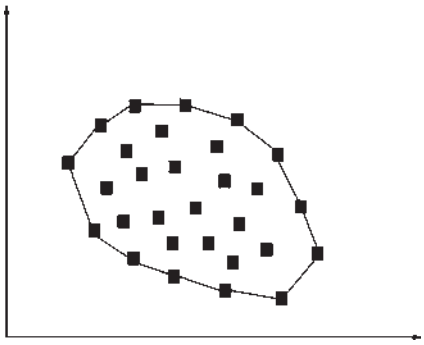

Figure 14.7 Schematic representation of the convex hull method for a two-parameter description.

compounds that are identified as outliers in later updates of the model thus increasing the AD of the new model.

14.5 Training and Test Set Selection and Model Validation

An integral part of deriving a statistically valid and predictive *in silico* model is the choice of training and test set, as well as the model validation. Without proper validation of the derived model, it is difficult to assess its statistical qualities and forecasting ability.

14.5.1 Training and Test Set Selection

There are several methods for designing the training set and test set, respectively. Most of them are dissimilarity based, that is, their aim is to select a training set as diverse as possible for the studied descriptor and target space. Some include the target variable, for example, biological activity, as part of the selection process so that a good spread in target space is also achieved. Lately, however, approaches focusing on local rather than global models have suggested the opposite strategy for the selection of the training set; that is, selecting a small set of similar compounds with respect to the new compound to be predicted and for each prediction, deriving a local statistical model on-the-fly, also known as lazy model [121–124]. The potential issues with lazar (lazy structure–activity relationships) methods are related to the underlying basic assumption of structure–activity relationships, namely, that similar molecules have similar activities. It is sometimes difficult to select a good representative set of similar training set compounds for which there is a sufficient spread in target value, for example, biological activity, and some investigations report that the local lazy model predicts worse than the corresponding global model [122].

For the purpose of selecting a diverse training set, one may use experimental design methods, for example, fractional factorial designs (FFDs) [125–128]. Using these methods, a training set with a good spread in the investigated properties (descriptors) can usually be selected. Since the nature of the FFDs is to select compounds at the edges of the investigated descriptor space and the user has considerable freedom of choice with respect to which compounds to include in the proposed FFD, the user must be aware that too extreme compounds should not form the majority of the compounds selected for the final training set. It is therefore also common to combine the FFDs with some compounds close to the center of the FFD. To avoid some of the above-mentioned problems with classical FFDs, a new type of designs called onion designs (ODs) has recently been developed [129]. The purpose of ODs is to achieve efficiency as well as controlled coverage of both the outer and the inner region of the descriptor space. The OD approach is based on combining several designs in layers. Thus, the compounds available are divided into subsets, or layers,

and a separate selection is performed on each subset. The selection technique in each layer can be of different kind, for example, FFDs or some space-filling design (SFD).

SFDs are aimed at creating a uniform distribution of compounds in descriptor space by selecting compounds as dissimilar as possible. A particular form of SFDs is the maximin technique designed by Marengo and Todeschini [130] whereby the desired number of training set compounds are selected by maximizing the shortest (minimum) distance in descriptor space between the chosen compounds. Again, if using Euclidian distance as the distance measure, orthogonality among the descriptors must be ensured. The authors have found that using a principal component analysis prior to the maximin selection addresses not only the descriptor orthogonality problem but also reduces the number of variables to be considered during the selection process. The latter is of interest since the method involves repetitive distance calculations between the compounds presently chosen and potential new compounds to be exchanged in order to maximize the shortest distance among the training set compounds. There are also sphere exclusion algorithms available for training and test set selection [131].

14.5.2 Model Validation

Some kind of model validation is necessary to determine the statistical quality with respect to forecasting target values of new compounds. There are typically three validation tests that should be performed:

- internal validation, for example, cross-validation [85];
- randomization of the target variable; and
- external test set predictions.

The internal validation is often performed through cross-validation whereby one, leave-on-one-out cross validation (LOO-CV), or several, leave-multiple-out cross validation (LMO-CV), compounds are removed from the training set. The remaining compounds of the training set are then used to derive a model with which the left-out compounds are predicted. Another set of compounds is then removed from the training set, a new model derived, and the new set of left-out compounds predicted. This procedure is continued until all compounds have been left out once. The computed measure of quality is the cross-validation squared correlation coefficient (q^2). While the normal squared correlation coefficient (r^2) can only assume values between 0 and 1, the cross-validation squared correlation coefficient can be both positive and negative. In fact, a value of zero for q^2 merely indicates that the model has used the average experimental value for all of the training set compounds as the predicted value for each test compound. Normally, values greater than 0.3 are recommended for a model to be considered as statistically sound, but it has been shown that values lower than 0.3 may be acceptable depending on the size of the data set [132]. The problem with LOO-CV methods is that they tend to overestimate the forecasting ability of the model when presented with new external compounds to be predicted. Also, LMO-CV methods have the same tendency, albeit

to a lower extent. A real danger with cross validation is through the combination with variable selection. When variable selection is applied and the computed q^2 is used to drive the variable selection, then the validation aspect of cross validation is lost and q^2 becomes an optimization function instead. By using this kind of approach, it is possible to fit random (white) noise with excellent statistical "quality" and respectable q^2 values (>0.5, unpublished result by the author). For further information regarding the predictive ability overestimation by the q^2 metric, see Ref. [133]. Variable randomization is another method for ensuring the reliability of models. In this method, the values of the target are randomly reassigned for training set compounds and then used to derive a new "model" [134]. After performing the randomization procedure sufficiently (more than 50–100 times), there should be clear difference between the model derived using true target values and the model derived using randomized target data. The most rigorous validation of a derived model is, however, through the use of an external test set, that is, data that have not been used for deriving the models. The use of external test sets is not without problems either. It is important that the test set also covers the applicability domain of the model to be evaluated in a good manner. There should be sufficient difference between training and test set compounds so that near-neighbor compounds are not in both sets. If that is the case, then the predictive ability of the derived model will most likely be significantly overestimated. The use of an external test set may, in some cases, be the only way, of the three validation procedures described here, to realize that the derived model is without any forecasting ability. For more details regarding model validation, see Ref. [135].

14.6 Future Outlook

The application of SAR and QSAR in modern discovery research to predict important properties, for example, solubility, absorption, and toxicity, of both small and large collections of (virtual) libraries, also known as "frontloading," forces not only the development of both more informative and more easily computed, for example, faster computed, molecular descriptors but also necessitates new statistical techniques to be used. For instance, the need for robust and predictive methods and models in virtual screening may infer the use of rather opaque consensus or ensemble methods, whereas transparent models are of value to understand the most important properties for the target in question and perhaps, at the same time, learn something about the mechanisms and/or processes at hand. Thus, one may envision the intertwined use of both these approaches, that is, transparent and opaque models, to enable better understanding as well as final precision and quality of predictions. The transparent models, with acceptable statistical quality, may then be utilized to drive virtual library generation to the most promising areas in chemical space, whereas the more complex and opaque models may then be applied for the final predictions to obtain the extra precision and robustness offered by these latter techniques.

Another important area of research is the "T" in *in silico* ADMET, that is, *in silico* toxicology, on which a lot of effort is already spent both in academia and in industry. The ADME area has seen substantial efforts during the past 10 years to obtain important understanding as well as to derive good models for solubility and absorption. The coming years will most likely see the same kind of attention for *in silico* toxicology. However, this new area of research is more demanding from a mechanistic point of view than that of solubility and absorption. Several mechanisms may come into play, even within analogous series of compounds, depending on what chemical functionalities are present in the molecule. Also, overall physicochemical parameters describing the entire structure may be less useful for modeling toxicology. Probably, structural fragments, toxicophores, will prove to be more important and useful descriptors and as descriptors capturing electronic properties of the investigated compounds. The use of such descriptors is most probably not a straightforward exercise either, to a certain extent depending upon the constitution of the structural fragments employed, since the chemical surrounding of a substructure, fragment, is important to ascertain whether the compound is likely to be toxic or not. Thus, a particular fragment may be identified as inducing toxicity in one compound but not in another. Many of the statistical methods employed today will have problems with such descriptors and will be unable to derive good statistical models. A possible way in the future is therefore to both derive new descriptor sets and use other statistical tools that take context dependency better into account.

References

1 http://www.talete.mi.it.

2 http://www.edusoft-lc.com/molconn.

3 http://www.chemcomp.com.

4 http://www.tripos.com.

5 http://www.molecular-networks.com.

6 Liu, H.X., Hu, R.J., Zhang, R.S., Yao, X.J., Liu, M.C., Hu, Z.D. and Fan, B.T. (2005) The prediction of human oral absorption for diffusion rate-limited drugs based on heuristic method and support vector machine. *Journal of Computer-Aided Molecular Design*, **19**, 33–46.

7 Bai, J.P.F., Utis, A., Crippen, G., He, H.-D., Fischer, V., Tullman, R., Yin, H.-Q., Hsu, C.-P., Jiang, L. and Hwang, K.-K. (2004) Use of classification regression tree in predicting oral absorption in humans. *Journal of Chemical Information and Computer Sciences*, **44**, 2061–2069.

8 Agatonovic-Kustrin, S., Beresford, R., Pauzi, A. and Yusof, M. (2001) Theoretically-derived molecular descriptors important in human intestinal absorption. *Journal of Pharmaceutical and Biomedical Analysis*, **25**, 227–237.

9 Klon, A.E., Lowrie, J.F. and Diller, D.J. (2006) Improved naive Bayesian modeling of numerical data for absorption, distribution, metabolism and excretion (ADME) property prediction. *Journal of Chemical Information and Modeling*, **46**, 1945–1956.

10 Zmuidinavicius, D., Didziapetris, R., Japertas, P., Avdeef, A. and Petrauskas, A. (2003) Classification structure–activity relations (C-SAR) in prediction of human intestinal absorption. *Journal of Pharmaceutical Sciences*, **92**, 621–633.

11 Klopman, G., Stefan, L.R. and Saiakhov, R.D. (2002) ADME evaluation. 2. A computer model for the prediction of intestinal absorption in humans. *European Journal of Pharmaceutical Sciences*, **17**, 253–263.

12 Lipinski, C.A., Lombardo, F., Dominy, B.W. and Feeney, P.J. (1997) Experimental and computational approaches to estimate solubility and permeability in drug discovery and development settings. *Advanced Drug Delivery Reviews*, **23**, 3–25.

13 http://www.scitegic.com.

14 Durant, J.L., Leland, B.A., Henry, D.R. and Nourse, J.G. (2002) Reoptimization of MDL keys for use in drug discovery. *Journal of Chemical Information and Computer Sciences*, **42**, 1273–1280.

15 http://www.digitalchemistry.co.uk.

16 http://www.leadscope.com.

17 http://www.mdl.com.

18 Kazius, J., McGuire, R. and Bursi, R. (2005) Derivation and validation of toxicophores for mutagenicity prediction. *Journal of Medicinal Chemistry*, **48**, 312–320.

19 http://www.daylight.com.

20 Niwa, T. (2003) General regression and probabilistic neural networks to predict human intestinal absorption with topological descriptors derived from two-dimensional chemical structures. *Journal of Chemical Information and Computer Sciences*, **43**, 113–119.

21 Pérez, M.A.C., Sanz, M.B., Torres, L.R., Ávalos, R.G., González, M.P. and Díaz, H.G. (2004) A topological sub-structural approach for predicting human intestinal absorption of drugs. *European Journal of Medicinal Chemistry*, **39**, 905–916.

22 Sun, H. (2004) A universal molecular descriptor system for prediction of logP, logS, logBB, and absorption. *Journal of Chemical Information and Computer Sciences*, **44**, 748–757.

23 Hall, L.H. and Kier, L.B. (1991) *The molecular connectivity chi indices and kappa shape indices in structure–property modelling, in Reviews of Computational Chemistry*, **Vol. 2** (eds D.B. Boyd and K. Lipkowitz), VCH Publishers, USA, pp. 367–422.

24 Downs, G.M. (2004) Molecular descriptors, in *Computational Medicinal Chemistry for Drug Discovery* (eds P. Bultinck, J.P. Tollenaere and H. de Winter), Marcel Dekker, USA, pp. 515–537.

25 Gunturi, S.B. and Narayanan, R. (2007) *In silico* ADME modeling 3: computational models to predict human intestinal absorption using sphere exclusion and kNN QSAR methods. *QSAR & Combinatorial Science*, **26**, 653–668.

26 Hall, L.H. and Kier, L.B. (1999) *Molecular Structure Description: The Electrotopological State*, Academic Press, USA.

27 Hall, L.H., Mohney, B. and Kier, L.B. (1991) The electrotopological state: structure information at the atomic level for molecular graphs. *Journal of Chemical Information and Computer Sciences*, **31**, 76–82.

28 Kellogg, G.E., Kier, L.B., Gaillard, P. and Hall, L.H. (1996) The e-state fields. Applications to 3D QSAR. *Journal of Computer-Aided Molecular Design*, **10**, 513–520.

29 Rose, K., Hall, L.H. and Kier, L.B. (2002) Modeling blood–brain barrier partitioning using the electrotopological state. *Journal of Chemical Information and Computer Sciences*, **42**, 651–666.

30 Stenberg, P., Norinder, U., Luthman, K. and Artursson, P. (2001) Experimental and computational screening models for the prediction of intestinal drug absorption. *Journal of Medicinal Chemistry*, **44**, 1927–1937.

31 Todeschini, R. and Grammatica, P. (1997) 3D-modelling and prediction by WHIM descriptors. Part 6. Application of WHIM descriptors in QSAR studies. *Quantitative Structure–Activity Relationships*, **16**, 120–125.

32 Todeschini, R., Grammatica, P., Marengo, E. and Provenzani, R. (1996)

Modeling and prediction by using WHIM descriptors in QSAR studies: submitochondrial particles (SMP) as toxicity biosensors of chlorophenols. *Chemosphere*, **33**, 71–79.

33 Todeschini, R., Lasagni, M. and Marengo, E. (1994) New molecular descriptors for 2D and 3D structures. Theory. *Journal of Chemometrics*, **8**, 263–272.

34 Todeschini, R., Vighi, M., Provenzani, R., Finzio, A. and Grammatica, P. (1996) Modeling and prediction by using whim descriptors in QSAR studies: toxicity of heterogeneous chemicals on *Daphnia magna*. *Chemosphere*, **32**, 1527–1545.

35 Stanton, D.T. and Jurs, P.C. (1990) Development and use of charged partial surface area structural descriptors in computer-assisted quantitative structure–property relationship studies. *Analytical Chemistry*, **62**, 2323–2329.

36 Stanton, D.T., Mattioni, B.E., Knittel, J.J. and Jurs, P.C. (2004) Development and use of hydrophobic surface area (HSA) descriptors for computer-assisted quantitative structure–activity and structure–property relationship studies. *Journal of Chemical Information and Computer Sciences*, **44**, 1010–1023.

37 Wildman, S.A. and Crippen, G.M. (1999) Prediction of physicochemical parameters by atomic contributions. *Journal of Chemical Information and Computer Sciences*, **39**, 868–873.

38 Pearlman, R.S. (1980) Molecular surface area and volumes and their use in structure/activity relationships, in *Physical Chemical Properties of Drugs* (eds S.H., Yalkowsky, A.A. Sinkula and S.C. Valvani), Marcel Dekker, USA, pp. 321–347.

39 Wessel, M.D., Jurs, P.C., Tolan, J.W. and Muskal, S.M. (1998) Prediction of human intestinal absorption of drug compounds from molecular structure. *Journal of Chemical Information and Computer Sciences*, **38**, 726–735.

40 Mazzatorta, P., Cronin, M.T.D. and Benfenati, E. (2006) A QSAR study of avian oral toxicity using support vector machines and genetic algorithms. *QSAR & Combinatorial Science*, **25**, 616–628.

41 Cruciani, G., Pastor, M. and Guba, W. (2000) VolSurf: a new tool for the pharmacokinetic optimization of lead compound. *European Journal of Pharmaceutical Sciences*, **11** (Suppl. 2), S29–S39.

42 Cruciani, G., Meniconi, M., Carosati, E., Zamora, I. and Mannhold, R. (2003) VOLSURF: a tool for drug ADME–properties prediction, in *Drug Bioavailability*, Vol. 18 (eds H. van de Waterbeemd, H. Lennernäs and P. Artursson), *Methods and Principles in Medicinal Chemistry*, Wiley-VCH, Germany, pp. 406–419.

43 Crivori, P., Cruciani, G., Carrupt, P.A. and Testa, B. (2000) Predicting blood-brain barrier permeation from three-dimensional molecular structure. *Journal of Medicinal Chemistry*, **43**, 2204–2216.

44 Crivori, P., Zamora, I., Speed, B., Orrenius, C. and Poggesi, I. (2004) Model based on GRID-derived descriptors for estimating CYP3A4 enzyme stability of potential drug candidates. *Journal of Computer-Aided Molecular Design*, **18**, 155–166.

45 Afzelius, L., Zamora, I., Masimirembwa, C.M., Karlen, A., Andersson, T.B., Mecucci, S., Baroni, M. and Cruciani, G. (2004) Conformer- and alignment-independent model for predicting structurally diverse competitive CYP2C9 inhibitors. *Journal of Medicinal Chemistry*, **47**, 907–914.

46 Afzelius, L., Masimirembwa, C.M., Karlen, A., Andersson, T.B. and Zamora, I. (2002) Discriminant and quantitative PLS analysis of competitive CYP2C9 inhibitors versus non-inhibitors using alignment independent GRIND descriptors. *Journal of Computer-Aided Molecular Design*, **16**, 443–458.

47 Aronov, A.M. and Goldman, B.B. (2004) A model for identifying hERG K^+ channel blockers. *Bioorganic and Medicinal Chemistry*, **12**, 2307–2315.

48 Drie, J.H. (2004) Pharmacophore discovery: a critical review, in *Computational Medicinal Chemistry for Drug Discovery* (ed. P. Bultinck), Marcel Dekker, USA, pp. 437–460.

49 Mason, J.S. and Pickett, S.D. (2003) Combinatorial library design, molecular similarity and diversity applications, in *Burger's Medicinal Chemistry and Drug Discovery 6* (ed. D.J. Abraham), John Wiley & Sons, Inc., USA, pp. 187–242.

50 Good, A.C., Mason, J.S. and Pickett, S.D. (2000) Pharmacophore pattern application in virtual screening, library design and QSAR, in *Methods and Principles in Medicinal Chemistry*, Vol. 10 (eds H.J. Bohm and G. Schneider), John Wiley & Sons, Inc., USA, pp. 131–159.

51 Mason, J.S., Morize, I., Menard, P.R., Cheney, D.L., Hulme, C.R. and Labaudiniere, R.F. (1999) New 4-point pharmacophore method for molecular similarity and diversity applications: overview of the method and applications, including a novel approach to the design of combinatorial libraries containing privileged substructures. *Journal of Medicinal Chemistry*, **42**, 3251–3264.

52 Saeh, J.C., Lyne, P.D., Takasaki, B.K. and Cosgrove, D.A. (2005) Lead hopping using SVM and 3D pharmacophore fingerprints. *Journal of Chemical Information and Modeling*, **45**, 1122–1133.

53 Penzotti, J.E., Lamb, M.L., Evensen, E. and Grootenhuis, P.D.J. (2002) A computational ensemble pharmacophore model for identifying substrates of P-glycoprotein. *Journal of Medicinal Chemistry*, **45**, 1737–1740.

54 Baroni, M., Cruciani, G., Sciabola, S., Perruccio, F. and Mason, J.S. (2007) A common reference framework for analyzing/comparing proteins and ligands. Fingerprints for ligands and proteins (FLAP): theory and application. *Journal of Chemical Information and Modeling*, **47**, 279–294.

55 http://www.biobyte.com.

56 http://www.syrres.com/esc/kowwin.htm.

57 http://www.scivision.com.

58 www.acdlabs.com.

59 Eros, D., Kövesdi, I., Orfi, L., Takács-Novák, K., Acsády, G. and Kéri, G. (2002) Reliability of logP predictions based on calculated molecular descriptors: a critical review. *Current Medicinal Chemistry*, **9**, 1819–1829.

60 Machatha, S.G. and Yalkowsky, S.H. (2005) Comparison of the octanol/water partition coefficients calculated by ClogP®, ACDlogP and KowWin® to experimentally determined values. *International Journal of Pharmaceutics*, **294**, 185–192.

61 Norinder, U. and Österberg, T. (2001) Theoretical calculation and prediction of drug transport processes using simple parameters and partial least squares projections to latent structures (PLS) statistics. The use of electrotopological state indices. *Journal of Pharmaceutical Sciences*, **90**, 1076–1084.

62 Testa, B., Carrupt, P.-A., Gaillard, P., Billois, F. and Weber, P. (1996) Lipophilicity in molecular modeling. *Pharmaceutical Research*, **13**, 335–343.

63 Broto, P., Moreau, G. and Van Dycke, C. (1984) Molecular structures: perception, autocorrelation descriptor and SAR studies. *European Journal of Medicinal Chemistry*, **19**, 61–70.

64 Ghose, A.K. and Crippen, G.M. (1986) Atomic physicochemical parameters for three-dimensional structure-directed quantitative structure–activity relationships. 1. Partition coefficients as a measure of hydrophobicity. *Journal of Computational Chemistry*, **7**, 565–577.

65 Du, Q., Liu, P.-J. and Mezey, P.G. (2005) Theoretical derivation of heuristic molecular lipophilicity potential: a quantum chemical description for

molecular solvation. *Journal of Chemical Information and Modeling*, **45**, 347–353.

66 Raevsky, O.A. (1997) Hydrogen bond estimation by means of HYBOT, in *Computer-Assisted Lead Finding and Optimisation* (eds H. van de Waterbeemd, B. Testa and G. Folkers), Verlag Helvetica Chimica Acta, Switzerland, pp. 367–378.

67 Raevsky, O.A., Schaper, K.-J., van de Waterbeemd, H. and McFarland, J. (1999) Hydrogen bond contribution to properties and activities of chemicals and drugs, in *Molecular Modeling and Prediction of Bioactivity* (eds K. Gundertofte and K. Jorgensen), Kluwer Academic/Plenum Publishers, USA, pp. 221–228.

68 McFarland, J.W., Raevsky, O.A. and Wilkerson, W.W. (1999) Hydrogen bond acceptor and donor factors, C_a and C_d: new QSAR descriptors, in *Molecular Modeling and Prediction of Bioactivity* (eds K. Gundertofte and K. Jorgensen), Kluwer Academic/Plenum Publishers, USA, pp. 280–281.

69 Raevsky, O.A., Schaper, K.-J., Artursson, P. and McFarland, J.W. (2002) A novel approach for prediction of intestinal absorption of drugs in humans based on hydrogen bond descriptors and structural similarity. *Quantitative Structure–Activity Relationships*, **20**, 402–413.

70 Abraham, M.H. and Le, J. (1999) The correlation and prediction of the solubility of compounds in water using an amended solvation energy relationship. *Journal of Pharmaceutical Sciences*, **88**, 868–880.

71 Abraham, M.H., Ibrahim, A., Zhao, Y. and Acree, W.E., Jr. (2006) A data base for partition of volatile organic compounds and drugs from blood/plasma/serum to brain, and an LFER analysis of the data. *Journal of Pharmaceutical Sciences*, **95**, 2091–2100.

72 Abraham, M.H. and Martins, F. (2004) Human skin permeation and partition: general linear free-energy relationship analyses. *Journal of Pharmaceutical Sciences*, **93**, 1508–1523.

73 Palm, K., Stenberg, P., Luthman, K. and Artursson, P. (1997) Polar molecular surface properties predict the intestinal absorption of drugs in humans. *Pharmaceutical Research*, **14**, 568–571.

74 Clark, D.E. (1999) Rapid calculation of polar surface area and its application to the prediction of transport phenomena. 1. Prediction of intestinal absorption. *Journal of Pharmaceutical Sciences*, **88**, 807–814.

75 Ertl, P., Rohde, B. and Selzer, P. (2000) Fast calculation of molecular polar surface area as a sum of fragment-based contributions and its application to the prediction of drug transport properties. *Journal of Medicinal Chemistry*, **43**, 3714–3717.

76 van de Waterbeemd, H. and Kansy, M. (1992) Hydrogen-bonding capacity and brain penetration. *Chimia*, **46**, 299–303.

77 Clark, D.E. and Pickett, S.D. (2000) Computational methods for the prediction of 'drug-likeness'. *Drug Discovery Today*, **5**, 49–58.

78 Clark, D.E. (2001) Prediction of intestinal absorption and blood–brain barrier penetration by computational methods. *Combinatorial Chemistry & High Throughput Screening*, **4**, 477–496.

79 Sherbukhin, V.V. (2002) Personal communication.

80 Fox, T. and Kriegl, J.M. (2006) Machine learning techniques for *in silico* modeling of drug metabolism. *Current Topics in Medicinal Chemistry*, **6**, 1579–1591.

81 Livingstone, D. (1995) *Data Analysis for Chemists Applications to QSAR and Chemical Product Design*, Oxford University Press, United Kingdom.

82 Lombardo, F., Gifford, E. and Shalaeva, M.Y. (2003) *In silico* ADME prediction: data, models, facts and myths. *Mini Reviews in Medicinal Chemistry*, **3**, 861–875.

83 Wold, S., Johansson, E. and Cocchi, M. (1993) PLS – partial least-squares projections to latent structures, in *3D QSAR in Drug Design* (ed. H. Kubinyi), ESCOM Science Publishers B.V., The Netherlands, pp. 523–550.

84 Cramer, R.D., Patterson, D.E. and Bunce, J.D. (1988) Comparative molecular field analysis (CoMFA). 1. Effect of shape on binding of steroids to carrier proteins. *Journal of the American Chemical Society*, **110**, 5959–5967.

85 Wold, S. (1979) Cross-validatory estimation of the number of components in factor and principal components models. *Technometrics*, **20**, 379–405.

86 Rojas, R. (1996) *Neural Networks – A Systematic Introduction*, Springer-Verlag, Germany.

87 Guha, R., Stanton, D.T. and Jurs, P.C. (2005) Interpreting computational neural network quantitative structure–activity relationship models: a detailed interpretation of the weights and biases. *Journal of Chemical Information and Modeling*, **45**, 1109–1121.

88 Ghuloum, A.M., Sage, C.R. and Jain, A.N. (2000) Molecular hashkeys: a novel method for molecular characterisation and its application for predicting important pharmaceutical properties of molecules. *Journal of Medicinal Chemistry*, **42**, 1739–1748.

89 Bruneau, P. (2001) Search for predictive generic model of aqueous solubility using Bayesian neural nets. *Journal of Chemical Information and Computer Sciences*, **41**, 1605–1616.

90 Gola, J., Obrezanova, O., Champness, E. and Segall, M. (2006) ADMET property prediction: the state of the art and current challenges. *QSAR & Combinatorial Science*, **25**, 1172–1180.

91 Vapnik, V.N. (1995) *The Nature of Statistical Learning Theory*, Springer, USA.

92 Hearst, M.A., Schölkopf, B., Dumais, S., Osuna, E. and Platt, J. (1998) Trends and controversies: support vector machines. *IEEE Intelligent Systems*, **13**, 18–28.

93 Czerminski, R., Yasri, A. and Hartsough, D. (2001) Use of support vector machine in pattern classification: application to QSAR studies. *Quantitative Structure–Activity Relationships*, **20**, 227–240.

94 Trotter, M.W.B. and Holden, S.B. (2003) Support vector machines for ADME property classification. *QSAR & Combinatorial Science*, **22**, 533–548.

95 Warmuth, M.K., Liao, J., Rätsch, G., Mathieson, M., Putta, S. and Lemmen, C. (2003) Active learning with support vector machines in the drug discovery process. *Journal of Chemical Information and Computer Sciences*, **43**, 667–673.

96 Barrett, S.J. and Langdon, W.B. (2006) Advances in the application of machine learning techniques in drug discovery, design and development, in *Applications of Soft Computing: Recent Trends* (*Advances in Soft Computing*) (eds A. Tiwari, J. Knowles, E. Avineri, K. Dahal and R. Roy), Springer, USA.

97 Norinder, U. (2003) Support vector machine models in drug design – applications to drug transport processes and QSAR using simplex optimisations and variable selection. *Neurocomputing*, **55**, 337–346.

98 De Maesschalck, R., Jouan-Rimbaud, D. and Massart, D.L. (2000) Tutorial. The Mahalanobis distance. *Chemometrics and Intelligent Laboratory Systems*, **50**, 1–18.

99 Shen, M., Xiao, Y., Golbraikh, A., Gombar, V.K. and Tropsha, A. (2003) Development and validation of *k*-Nearest-Neighbor QSPR models of metabolic, stability of drug candidates. *Journal of Medicinal Chemistry*, **46**, 3013–3020.

100 Li, Y., Jiang, J.-H., Chen, Z.-P., Xu, C.-J. and Yu, R.-Q. (1999) Robust linear discriminant analysis for chemical pattern recognition. *Journal of Chemometrics*, **13**, 3–13.

101 Hawkins, D.M. and Kass, G.V. (1982) Automatic interaction detection, in *Topics*

in Applied Multivariate Analysis (ed. D.M. Hawkins), Cambridge University Press, United Kingdom.

102 Breimann, L., Friedman, J.H., Olshen, R.A. and Stone, C.J. (1984) *Classification and Regression Trees*, Wadsworth, New York.

103 Norinder, U., Lidén, P. and Boström, H. (2006) Discrimination between modes of toxic action of phenols using rule based methods. *Molecular Diversity*, **10**, 207–212.

104 Quinlan, J.R. (1992) *C45 Programs for Machine Learning*, Morgan Kaufmann Publishers, USA.

105 Niculescu, S.P. (2003) Artificial neural networks and genetic algorithms in QSAR. *Journal of Molecular Structure* (*THEOCHEM*) , **622**, 71–83.

106 Johansson, U., König, R. and Niklasson, L. (2003) Rule extraction from trained neural networks using genetic programming. 13th International Conference on Artificial Neural Networks, Istanbul, Turkey, supplementary proceedings, pp. 13–16.

107 Johansson, U., Sönströd, C., König, R. and Niklasson, L. (2003) Neural networks and rule extraction for prediction and explanation in the marketing domain. The International Joint Conference on Neural Networks, IEEE Press, USA, Portland, OR, pp. 2866–2871.

108 Johansson, U., König, R. and Niklasson, L. (2004) The truth is in there – rule extraction from opaque models using genetic programming. 17th Florida Artificial Intelligence Research Symposium (FLAIRS) 04, AAAI Press, USA, Miami, FL, pp. 658–662.

109 Johansson, U. (2007) Obtaining accurate and comprehensible data mining models, PhD thesis, Institute of Technology, Linköping University.

110 Hewitt, M., Cronin, M.T.D., Madden, J.C., Rowe, P.H., Johnson, C., Obi, A. and Enoch, S.J. (2007) Consensus QSAR models: do the benefits outweigh the complexity? *Journal of Chemical Information and Modeling*, **47**, 1460–1468.

111 http://www.salfordsystems.com.

112 http://www.compumine.com.

113 Melville, P. and Mooney, R.J. (2005) Creating diversity in ensembles using artificial data. *Journal of Information Fusion (Special Issue on Diversity in Multiple Classifier Systems)*, **6**, 99–111.

114 O'Brien, S.E. and de Groot, M.J. (2005) Greater than the sum of its parts: combining models for useful ADMET prediction. *Journal of Medicinal Chemistry*, **48**, 1287–1291.

115 Votano, J.R., Parham, M., Hall, L.H., Kier, L.B., Oloff, S., Tropsha, A., Xie, Q. and Tong, W. (2004) Three new consensus QSAR models for the prediction of Ames genotoxicity. *Mutagenesis*, **19**, 365–377.

116 Manallack, D.T., Tehan, B.G., Gancia, E., Hudson, B.D., Ford, M.G., Livingstone, D.J., Whitley, D.C. and Pitt, W.R. (2003) A consensus neural network-based technique for discriminating soluble and poorly soluble compounds. *Journal of Chemical Information and Computer Sciences*, **43**, 674–679.

117 Merkwirth, C., Mauser, H., Schulz-Gasch, T., Roche, O., Stahl, M. and Lengauer, T. (2004) Ensemble methods for classification in cheminformatics. *Journal of Chemical Information and Computer Sciences*, **44**, 1971–1978.

118 Agrafiotis, D.K., Cedeno, W. and Lobanov, V.S. (2002) On the use of neural network ensembles in QSAR and QSPR. *Journal of Chemical Information and Computer Sciences*, **42**, 903–911.

119 van Rhee, A.M. (2003) Use of recursion forests in the sequential screening process: consensus selection by multiple recursion trees. *Journal of Chemical Information and Computer Sciences*, **43**, 941–948.

120 Netzeva, T.I., Worth, A.P., Aldenberg, T., Benigni, R., Cronin, M.T.D., Gramatica, P., Jaworska, J.S., Kahn, S., Klopman, G., Marchant, C.A., Myatt, G., Nikolova-Jeliazkova, N., Patlewicz, G.Y., Perkins, R., Roberts, D.W., Schultz, T.W.,

Stanton, D.T., van de Sandt, J.J.M., Tong, W., Veith, G. and Yang, C. (2005) Current status of methods for defining the applicability domain of (quantitative) structure–activity relationships. The report and recommendations of ECVAM workshop 521. *Alternatives to Laboratory Animals*, **33**, 155–173.

121 Zhang, H., Ando, H.Y., Chen, L. and Lee, P.H. (2007) On-the-fly selection of a training set for aqueous solubility prediction. *Molecular Pharmacology*, **4**, 489–497.

122 Guha, R., Dutta, D., Jurs, P.C. and Chen, T. (2006) Local lazy regression: making use of the neighborhood to improve QSAR predictions. *Journal of Chemical Information and Modeling*, **46**, 1836–1847.

123 Helma, C. (2006) Lazy structure–activity relationships (lazar) for the prediction of rodent carcinogenicity and Salmonella mutagenicity. *Molecular Diversity*, **10**, 147–158.

124 Zhang, S., Golbraikh, A., Oloff, S., Kohn, H. and Tropsha, A. (2006) A novel automated lazy learning QSAR (ALL-QSAR) approach: method development, applications, and virtual screening of chemical databases using validated ALL-QSAR models. *Journal of Chemical Information and Modeling*, **46**, 1984–1995.

125 Eriksson, L., Johansson, E., Kettaneh-Wold, N., Trygg, J., Wikström, C. and Wold, S. (2006) Multi- and Megavariate Data Analysis Part I: Basic Principles and Applications, 2nd edn, Umetrics.

126 Linusson, A., Gottfries, J., Olsson, T., Örnskov, E., Folestad, S., Nordén, B. and Wold, S. (2001) Statistical molecular design, parallel synthesis, and biological evaluation of a library of thrombin inhibitors. *Journal of Medicinal Chemistry*, **44**, 3424–3439.

127 Box, G.E.P., Hunter, W.G. and Hunter, J.S. (1978) *Statistics for Experimenters*, John Wiley & Sons, Inc., USA.

128 Lundstedt, T., Seifert, E., Abramo, L., Thelin, B., Nyström, A., Pettersen, J. and Bergman, R. (1998) Experimental design and optimisation. *Chemometrics and Intelligent Laboratory Systems*, **42**, 3–40.

129 Gottfries, J. and Wold, S. (2004) D-optimal onion designs in statistical molecular design. *Chemometrics and Intelligent Laboratory Systems*, **73**, 37–46.

130 Marengo, E. and Todeschini, R. (1992) A new algorithm for optimal distance-based experimental design. *Chemometrics and Intelligent Laboratory Systems*, **16**, 37–44.

131 Golbraikh, A., Shen, M., Xiao, Z., Xiao, Y.-D., Lee, K.-H. and Tropsha, A. (2003) Rational selection of training and test sets for the development of validated QSAR models. *Journal of Computer-Aided Molecular Design*, **17**, 241–253.

132 Clark, M. and Cramer, R.D., III (1993) The probability of chance correlation using partial least squares (PLS). *Quantitative Structure–Activity Relationships*, **12**, 137–145.

133 Golbraikh, A. and Tropsha, A. (2002) Beware of q2! *Journal of Molecular Graphics & Modelling*, **20**, 269–276.

134 van der Voet, H. (1994) Comparing the predictive accuracy of models using a simple randomization test. *Chemometrics and Intelligent Laboratory Systems*, **25**, 313–323.

135 Tropsha, A., Gramatica, P. and Gombar, V.K. (2003) The importance of being earnest: validation is the absolute essential for successful application and interpretation of QSPR models. *QSAR & Combinatorial Science*, **22**, 69–77.

15
Computational Absorption Prediction

Christel A.S. Bergström, Markus Haeberlein, and Ulf Norinder

Abbreviations

ADME	Absorption, distribution, metabolism, and excretion
ADMET	Absorption, distribution, metabolism, excretion, and toxicity
Alog*P*	Ghose–Crippen–Viswanadhan octanol–water partition coefficient
BCS	Biopharmaceutics Classification System
BCUT	Burden, CAS, University of Texas descriptors
CART	Classification and regression tree
Clog*P*	Calculated partition coefficient between octanol and water
CMR	Calculated molar refractivity
F_a	Fraction absorbed
FPSA	Fractional polar surface area
GP	Genetic programming
G-REX	Genetic rule extraction
GSE	General solubility equation
HBA	Hydrogen-bond acceptors
HBD	Hydrogen-bond donors
HIA	Human intestinal absorption
LDA	Linear discriminant analysis
LOO-CV	Leave-one-out cross-validation
Mlog*P*	Moriguchi log *P*
MV	Molar volume
MW	Molecular weight
nHBA	Number of hydrogen-bond acceptors
nHBD	Number of hydrogen-bond donors
NN	Neural network
NPSA	Nonpolar surface area
nRB	Number of rotatable bonds
PDR	Physician's desk reference
P-gp	P-glycoprotein

PLS	Partial least square projection to latent structures
PSA	Polar surface area
QSAR	Quantitative structure–activity relationship
RMSE	Root mean square error
ROC	Receiver-operating characteristic
RP	Recursive partitioning
SVM	Support vector machine
TOPS-MODE	TOPological Substructural Molecular Design
TPSA	Topological polar surface area

Symbols

2D	Two-dimensional
3D	Three-dimensional
A	Abraham hydrogen-bond acidity parameter
$\log D_{6.5}$	Logarithm of apparent partition coefficient at pH 6.5
$\log P$	Logarithm of partition coefficient between octanol and water
$\log S$	Logarithm of intrinsic solubility
N rule-of-5	Number of violations of the four rule-of-5 rules developed by Lipinski
r^2	Coefficient of determination (correlation coefficient)
q^2	Cross-validated coefficient of determination

15.1 Introduction

During the past 10 years starting with the publications of Lipinski and coworkers [1] and Palm and coworkers [2], a considerable amount of research has been performed to develop predictive computational models for intestinal absorption in humans. The purpose of these investigations has been to develop computationally fast and accurate models for *in silico* electronic screening of large virtual compound libraries.

This chapter will give a theoretical background of the oral absorption and then discuss the computational models that are based on the publicly available data sets. A short overview of the software for absorption prediction is also included in the discussion.

15.2 Descriptors Influencing Absorption

The intestinal wall is optimized to absorb fluids and nutrients while keeping away different xenobiotics. Which factors, from a theoretical point of view, are the most influential in intestinal absorption?

Let us assume passive diffusion as the main driving force for absorption. Passive diffusion can be calculated by applying Fick's first law to the flux through the intestinal wall. At each point i on the intestinal surface, the flux J_i is:

$$J_i = c_i P_i, \tag{15.1}$$

where c_i is the concentration of the drug at a point i and P_i is the permeability of the drug at the same point. Hence, the total mass m of absorbed drug at a time t can be written as:

$$m(t) = \int_0^t \iint_A c_i P_i \mathrm{d}A\mathrm{d}t, \tag{15.2}$$

where A is the total area of the intestinal tract. The fraction absorbed (F_a) is defined by the total mass absorbed divided by the given dose of the drug:

$$F_a = \frac{m(\infty)}{\text{Dose}}. \tag{15.3}$$

This brief simplified analysis shows that the absorption mainly depends on the concentration at the intestinal wall, the permeability of the drug, and the given dose [3]. Let us analyze these three factors further.

15.2.1 Solubility

The concentration of the drug at a point i at the intestinal wall depends on the dissolution rate and the gastrointestinal transit. The dissolution rate of a drug molecule is affected by the energy difference that arises when the compound dissolves with similar molecules in the crystal or the molecules of the formulation and instead forms bonds with the components in the intestinal fluid. If this process is related to a high-energy penalty, the dissolution rate of the compound will be low, whereas if the process releases energy, the dissolution rate will be high. The most common factor for drug molecules is that the dissolution process is related to an energy penalty of some extent. Some of the factors influencing the dissolution rate and the maximum solubility obtained in the intestinal fluid are the formulation, particle size, particle aggregation, pH in different segments of the intestine, food content, and physicochemical properties of the drug molecule. Considering these factors one can expect a large variation in the solubility for the same drug with different formulations in different subjects, for example, humans.

If we look at the physicochemical factors governing solubility, among the first identified were log P [4] and melting point [5, 6]. The lipophilicity is often calculated theoretically using, among other techniques, fragment-based approaches. It has lately become apparent that the log P is not always correctly calculated for new drug-like compounds, and for new AstraZeneca and Pfizer compounds, the root mean square error (RMSE) has been reported to be 0.84–1.46 on a log scale [7, 8]. Hence, the calculated (Clog$P$) value for such compounds becomes 7–29-fold falsely calculated.

Several approaches have been applied to predict the melting point, but all of them result in prediction errors of 35–45 °C [9, 10] and can therefore not be regarded as accurate enough to be included in solubility calculations. Hence, the prediction of solubility from the general solubility equation (GSE) established by Yalkowsky and coworkers [6] still requires the experimentally determined melting point. Other typical molecular descriptors included in solubility predictions are molecular size, hydrogen bonding, nonspecific van der Waals interactions, aromaticity, flexibility, and dipole moment [11–17].

15.2.2 Membrane Permeability

The other mechanistically important component for intestinal absorption is the actual passage over the cell membrane. Before reaching the cell membrane, the drug molecule needs to diffuse through the unstirred water layer. However, theoretical considerations suggest that in most cases this diffusion is not the rate-limiting step for permeability. When at the cell wall, there are a number of different mechanisms for which a compound can be transported across the cell barrier. The most important mechanisms are transcellular passive diffusion, paracellular diffusion, active transport with a transporter, and transcytosis (Figure 15.1). In addition, the drug can be metabolized in close connection to the luminal cell membrane by CYP3A4.

For a theoretical model, each mechanism has to be described in a different manner.

If we restrict ourselves to discuss transcellular diffusion, there are numerous theoretical approaches, which differ depending on the underlying assumptions. In general, permeability mainly depends on lipophilicity (log *P* or Clog*P*), molecular

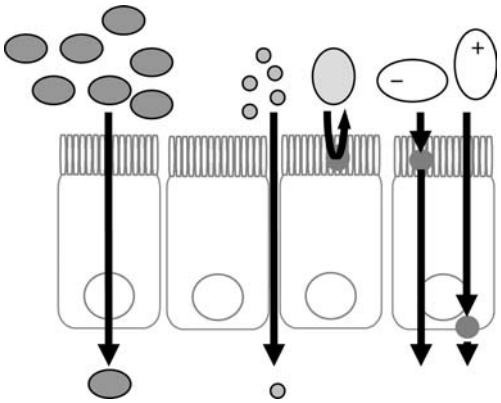

Figure 15.1 The following routes are available for permeating the intestinal wall (from the left-hand side): the transcellular route, mainly used by nonpolar and medium-sized molecules; the paracellular route, mainly used by polar and small molecules often bearing a net charge; and energy-dependent active transport processes, which efflux (secret) transporter substrates or influx (take up) transporter substrates. Each transport protein has its own substrate specificity.

weight (MW), and measures of hydrogen-bonding capacity or polarity [18]. If we use the findings from computational models on permeability measurements of cell lines, for example, Caco-2 cells, the following factors are among the most important: polar surface area (PSA), nonpolar surface area (NPSA) and/or lipophilicity, hydrogen-bond acceptors (HBA), hydrogen-bond donors (HBD), polarity (charge distribution), MW, size, shape, and degree of ionization [19–22].

Amidon *et al*. [3] devised a Biopharmaceutics Classification System (BCS), where they divided drugs into four different classes based on their solubility and permeability: class 1 (high solubility, high permeability), class 2 (low solubility, high permeability), class 3 (high solubility, low permeability), and class 4 (low solubility, low permeability); see also Chapter 19. The rate-limiting step to drug absorption and hence the factors affecting drug absorption will differ depending on which class the drug belongs to. For class 2, the rate-limiting step is dissolution, and the permeability plays a minor role. For class 3, however, the permeability is rate limiting and the dissolution has very little influence on the absorption. Given the above-mentioned considerations, it is difficult to believe that it would be possible to fit drugs from all four classes into one single model. However, it is worth to note that several molecular descriptors highly influence both permeability and solubility. For example, it has been suggested that the four BCS classes can be divided solely by considering the MW and PSA [23].

15.3
Computational Models of Oral Absorption

15.3.1
Quantitative Predictions of Oral Absorption

To date, a large number of models aiming at quantitative prediction of oral absorption are available, either published in scientific journals (Table 15.1) or included in commercial software (Table 15.2). These models are often based on human F_a data, also known as the human intestinal absorption (HIA), extracted from the literature. Original sources are generally clinical studies, the physician's desk reference (PDR) or product specifications. Occasionally, substitute parameters are used for absorption, one of the most commonly applied being the permeability in Caco-2 cell monolayers [24]. The Caco-2 cells originate from colon carcinoma, which when cultured *in vitro* easily form an intact monolayer mimicking the intestinal epithelium. The advantages with using such a system are obvious; for instance, a large number of compounds can easily be screened for their intestinal permeability at a low cost and without facing ethical restrictions. However, the disadvantages are also clear – the permeability obtained in the *in vitro* cell system reflects only the F_a after oral administration if the absorption of the compound is limited by permeability. Hence, for compounds that have poor solubility (BCS class 2 and 4) and/or stability issues and are subjected to active transport, such an *in vitro* surrogate marker for F_a is not applicable.

Table 15.1 Publications on quantitative models of human fraction absorbed.

Publication	Title	Data set (*n*)	Technique	RMSE test set	Descriptors
Raevsky *et al.*, *Quantitative Structure–Activity Relationships*, 2000 [34]	Quantitative estimation of drug absorption in humans for passively transported compounds on the basis of their physicochemical parameters	32	MLR, MNLR	n.a.	MW, log *D*, hydrogen-bond descriptors ($n = 5$)
Verma *et al.*, *Journal of Computer-Aided Molecular Design*, 2007	Comparative QSAR studies on PAMPA/modified PAMPA for high-throughput profiling of drug absorption potential with respect to Caco-2 cells and human intestinal absorption	68	MLR	n.a.[a]	Clog *P*, hydrogen-bond descriptors ($n = 3$)
Wessel *et al.*, *Journal of Chemical Information and Computer Sciences*, 1998 [25]	Prediction of human intestinal absorption of drug compounds from molecular structure	86	GANN	16% ($n = 10$)	Topological and electronical 2D, geometrical 3D ($n = 6$)
Agatonovic-Kustrin *et al.* *Journal of Pharmaceutical and Biomedical Analysis*, 2001	Theoretically derived molecular descriptors important in human intestinal absorption	86	GANN	17% ($n = 10$)	Constitutional, topological, chemical, geometrical, and quantum mechanical ($n = 15$)
Niwa, *Journal of Chemical Information and Computer Sciences*, 2003 [35]	Using general regression and probabilistic neural networks to predict human intestinal absorption with topological descriptors derived from two-dimensional chemical structures	86	GRNN	23% ($n = 10$)	CMR, Clog *P*, 2D topological descriptors ($n = 7$)

Deretey *et al.*, *Quantitative Structure–Activity Relationships*, 2002	Rapid prediction of human intestinal absorption	124	MNLR	17% ($n = 31$)	Clog *P*, hydrogen-bond descriptor ($n = 2$)
Abraham *et al.*, *European Journal of Medicinal Chemistry*, 2002	On the mechanism of the human intestinal absorption	127	MLR	n.a.	Abraham descriptors ($n = 5$)
Deconinck *et al.*, *Journal of Pharmaceutical and Biomedical Analysis*, 2005	Prediction of gastrointestinal absorption using multivariate adaptive regression splines	140	MARS	n.a.	2D and 3D descriptors from Dragon ($n = 9$)
Deconick *et al.*, *Journal of Pharmaceutical and Biomedical Analysis*, 2007	Exploration of the linear modeling techniques and their combination with multivariate adaptive regression splines to predict gastrointestinal absorption of drugs	141	PLS-MARS	n.a.	2D and 3D descriptors from Dragon ($n = 9$ PCs from the PLS analysis)
Zhao *et al.*, *Journal of Pharmaceutical Sciences*, 2001 [26]	Evaluation of human intestinal absorption data and subsequent derivation of a quantitative structure–activity (QSAR) with Abraham descriptors	169	MLR	14% ($n = 131$)	Abraham descriptors ($n = 5$)
Liu *et al.*, *Journal of Computer-Aided Molecular Design*, 2005	The prediction of human oral absorption for diffusion rate-limited drugs based on heuristic method and support vector machine	169	SVM	14% ($n = 56$)	CODESSA descriptors: constitutional, topological, electrostatic, geometrical, and quantum mechanical ($n = 5$)
Gunturi and Narayanan, *QSAR & Combinatorial Science*, 2007 [41]	*In silico* ADME modeling. 3. Computational models to predict human intestinal absorption using sphere exclusion and kNN QSAR methods	174	kNN-QSAR	9% ($n = 49$)[b]	Structural, physicochemical, geometrical, and topological ($n = 4$)

(*Continued*)

Table 15.1 (*Continued*)

Publication	Title	Data set (*n*)	Technique	RMSE test set	Descriptors
Iyer *et al.*, *Molecular Pharmaceutics*, 2007	Prediction and mechanistic interpretation of human oral drug absorption using MI-QSAR analysis	188	MLR	n.a.	2D and 3D solute descriptors ($n = 7$)
Zhao *et al.*, *Journal of Pharmaceutical Sciences*, 2002	Rate-limited steps of human oral absorption and QSAR studies	238	MLR, MNLR	n.a.[c]	Abraham descriptors ($n = 5$)
Klopman *et al.*, *European Journal of Pharmaceutical Sciences*, 2002 [31]	ADME evaluation. 2. A computer model for the prediction of intestinal absorption in humans	467	MLR	12% ($n = 50$)	Physicochemical descriptors group contribution approach ($n = 37$)
Votano *et al.*, *Molecular Diversity*, 2004 [27]	New predictors for several ADME/Tox properties: aqueous solubility, human oral absorption, and Ames genotoxicity using topological descriptors	612	ANN	16% ($n = 195$)	Clog *P*, PSA, and topological descriptors ($n = 10$)

Abbreviations used: multiple linear regression (MLR), multiple nonlinear regression (MNLR), genetic algorithm neural network (GANN), general regression neural network (GRNN), multivariate adaptive regression splines (MARS), partial least square projection to latent structures (PLS), support vector machine (SVM), *k*-nearest neighbor quantitative structure–activity relationship (*k*NN-QSAR), artificial neural network (ANN), root mean square error (RMSE).n.a., not applicable; the fraction-absorbed model has not been validated with a test set or the result of a validation is not given.

[a]The model was tested on 11 compounds and log F_a was used as response. Since several of the compounds were severely falsely predicted, our calculation of the RMSE of the test set was more than 100% indicating that the model cannot be used for predictions. The authors do not comment this in their paper.

[b]Based on model 1.

[c]Only a qualitative validation has been performed.

Table 15.2 Examples of commercial software available for computational prediction of human fraction absorbed and related properties.

Software	Company	Dissolution	Sol	Perm	Trp	Oral bioavailability	F_a	Other PK
ADME boxes/batches	Pharma Algorithms		•	•	•	•	•	•
Cerius[2]	Accelrys		•				•	•
Chem Silico modules	ChemSilico		•	•			•	•
KnowItAll ADME/Tox	Bio-Rad Laboratories		•	•		•	•	•
QikProp	Schrödinger		•	•				•
QMPRPlus	Simulations Plus		•	•			•	•

Bullets show properties predicted in each of the reported software. The following abbreviations are used: solubility (Sol), membrane permeability (Perm), transporters (Trp), human intestinal absorption (F_a), pharmacokinetic properties (PK).

15.3.1.1 Responses: Evaluations of Measurement of Fraction Absorbed

To obtain the responses, that is, the experimentally measured value for F_a, several different techniques have been applied. We will briefly go through the procedure performed in the establishment of three different data sets, namely, the "Wessel" data set [25], the "Zhao" data set [26], and the "Votano" data set [27]. These data sets were selected based on their repeated use in model development and/or their large size.

The first large data set for F_a prediction was created by Wessel and coworkers [25], who compiled F_a data for 86 compounds based on results found in 151 studies. Each reference was carefully reviewed to ensure that the value used was indeed the F_a data and not the absolute oral bioavailability, since the latter can be lower than the F_a. Furthermore, the data were controlled to not be dose-dependent or disease-dependent, that is, only results based on healthy volunteers were used. The 86 compounds were divided into a training set of 76 compounds and a test set of 10. The authors claimed that they included all poorly absorbed compounds available at the time for the construction of the data set. Furthermore, they did not include all highly absorbed compounds available with the intention to not let the highly absorbed compounds skew the data set and thereby affect the results of the modeling. Even though these precautions were taken, the final training set ($n = 76$) consisted of 49 compounds with more than 80% absorbed and 7 compounds below 20%. It has lately become apparent that some of the compounds included in the "Wessel" data set are substrates for active transporters and therefore the data set may not be optimal for F_a modeling. The clinical relevance of such active transport has though been debated in the literature, and many claim that active transporters in most cases do not affect the absorption rate in the intestine due to high concentrations of the drug available. However, for specific molecules, the active transport is the dominating uptake mechanism and is of pharmaceutical importance to some peptides, β-lactam

antibiotics, and ACE inhibitors [28]. Hence, the generalization that active transport does not have a significant effect on the uptake from the intestine can lead to significant false predictions of such molecules.

Zhao and colleagues [26] published a quantitative structure–activity relationship (QSAR) for F_a based on a data set of 241 compounds. From 244 papers, the following properties were recorded for the compounds:

- the absorption data;
- the oral or absolute bioavailability;
- the percentage of cumulative urinary excretion of unchanged drug and metabolites following oral and intravenous administration;
- the percentage of metabolites in urine or first-pass effect following oral and intravenous administration;
- the percentage of unchanged drug in urine following oral and intravenous administration;
- the percentage excretion of drug in bile following oral and intravenous administration;
- the percentage of cumulative excretion of drug in feces following oral and intravenous administration;
- total recovery of drug in urine and feces following oral and intravenous administration.

The information was thereafter used to sort the response into classes that depend on the quality of the data. This resulted in 169 compounds in the group sorted as having good or OK quality of the response data, which were divided into a training set of 38 compounds and a test set of 131 compounds. Out of these, 23 compounds of the training set had an F_a larger than 80%, and only 6 compounds had an F_a of less than 20%. The number of compounds for the test set was 96 displaying more than 80% absorbed, but only 2 compounds with fraction absorbed data less than 20%. This, together with the histogram of F_a for the data set, clearly shows that the "Zhao" data set is heavily skewed toward compounds with high fraction absorbed. The clear reason for this is that most marketed drugs already have been optimized for absorption, and hence troublemakers have failed during the development process. From a computational model development viewpoint, this results in the tools developed to be good at identifying a compound with good absorption, whereas it will be difficult to identify poorly absorbed compounds since this chemical space has not been well represented in the model development. The skewness of data sets used for prediction of oral absorption has also been identified and treated recently [29].

The largest data set we have found published for quantitative prediction of F_a is the data set treated by Votano and coworkers [27], who used a training set of 417 compounds and a test set of 195 compounds for model development and validation, respectively. The data came from several different sources [26, 30, 31], the PDR [32], and therapeutic drugs [33], and the compounds included were scrutinized to remove substances reported to be actively transported across the intestinal membrane. A true objective validation of this data set, however, cannot be performed, since the authors do not reveal the compounds included in the study. However, the authors state that a

large fraction of the compounds showed a high F_a. Only 25% of the compounds displayed an F_a value less than 60%, whereas 54% had an F_a value more than 80%. The authors divided the complete data set into three groups: two groups were formed through the use of a molecular weight cut-off rule, to handle paracellular ($\leq$251 Da) and transcellular ($\geq$252 Da) transport separately. Again, the compounds included in each cluster are not publicly available, making this effort of mechanistic modeling difficult to evaluate. Finally, a subset of 23 compounds carrying a formal positive charge was excluded from the two groups and modeled separately. The results from the three different models were thereafter combined, resulting in an RMSE of the training set of 11.5% and an $RMSE_{test\ set}$ of 15.9%. Of these compounds, 10 were not well predicted by the model, and these were probenecid, gilbornuride, indomethacin, meropenem, cymarin, piretanide, lodoxamide, etretinate, exemestane, and carbenoxolone. The authors could not find any chemical reason for the bad predictions (27–49% falsely predicted), but they speculate that the solubility may be a limiting factor for the absorption *in vivo*. The obtained "transcellular" model was based on lipophilicity, PSA, and other hydrogen-bond descriptors. Unfortunately, the authors do not reveal which descriptors were most important for the prediction of the "paracellular" data set and the 23 charged compounds, and therefore conclusions regarding absorption mechanisms based on molecular descriptors cannot be drawn.

15.3.1.2 Model Development: Data sets, Descriptors, Technologies, and Applicability

Quantitative predictions of oral absorption aim at returning an accurate percentage absorbed from the prediction. Going through the models published for prediction of F_a reveals that the size of the data sets used differs tremendously, from 32 compounds [34] to more than 600 [27] (Table 15.1). Depending on the size of the data set, and hence the volume and the density of the chemical space investigated, the obtained model will be more or less generally applicable. Small data sets as well as data sets including a large series of homologous structures are often generally less applicable than models based on larger and structurally diverse data sets.

Most commonly applied descriptors for the development of F_a models have different 2D and 3D properties. These are physicochemical, topological, electrostatical, or geometrical. Several different software programs for the calculation of these descriptors are available, which are rapid and allow several hundreds of descriptors to be calculated. Typical descriptors are discussed in detail in Section 14.2.

In Table 15.1, quantitative predictions of F_a published during the past 10 years are compiled. As can be seen, the problem of predicting F_a has been investigated using quite different statistical techniques, and a variety of linear and nonlinear methodologies have been applied. In general, the models predict the training sets within 10–15% range of the experimental value, even though the true accuracy is difficult to evaluate. To do so, the obtained models must be challenged with test sets composed of compounds that have not been included in the model development. This is not performed in all studies, sometimes due to the limitation of compounds available or selected for the study. However, when test sets have been used, the range of accuracy for the test set is within 9–23%. This indicates that there is a large uncertainty in the value of absorption obtained from the prediction, as a result of which a compound can

easily be falsely predicted by as much as 20% in absorption. Thus, there is a tendency to perform qualitative predictions, in which the percentage absorption is binned into classes such as low, intermediate, and high F_a. These investigations will be discussed in Section 15.3.2. However, we also note that quantitative models are sometimes recommended to be used more as a sorting tool than for the actual value resulting from the prediction. This is exemplified in the study performed by Niwa [35], who treated the "Wessel" data set with a general regression neural network (NN) and a probabilistic NN based on calculated molar refractivity (CMR), Clog*P*, and 2D topological descriptors. As a result of the general regression NN, the test set was predicted with an RMSE of 22.8%, indicating that the model is not really quantitatively reliable. When the same data set was used for classification purposes, the results improved, and 80% of the test set was correctly predicted (see further description of this study in Section 15.3.2). In this study, the effects of skewed data sets also became clear. A large majority of the responses had F_a values of more than 80%, as a result of which all the well-absorbed compounds were correctly sorted by the model whereas the poorly absorbed were partly misclassified.

15.3.2
Qualitative Predictions of Oral Absorption

15.3.2.1 Model Development: Data sets, Descriptors, Technologies, and Applicability

Owing to large uncertainties in measured F_a values as well as the uneven distribution of the poorly and well-absorbed compounds, it is rather common to derive qualitative *in silico* models for F_a instead of quantitative models (Table 15.3). For this purpose, the F_a (0–100%) is split (binned) into two or more classes. As always, there is a potential danger with binning continuous data since poor binning may disrupt the underlying data structure of a continuous variable.

Zmuidinavicius *et al*. [30] have used a compilation of compounds both from the "Zhao" and "Wessel" data sets and from some additional sources such as therapeutic drugs [33, 36, 37]. The data set covered over 1000 compounds. After questionable data and compounds influenced by active transport were removed, the data set consisted of 977 compounds. Unfortunately, the authors do not disclose more than a sample data set of some 200 compounds in their publication. The structures were described by properties such as Abraham descriptors (see Section 14.2.3.3), hydrogen-bonding parameters, log *P*, PSA, and the number of rotatable bonds (nRB). Structural descriptors of fragment-type were also used to characterize the investigated compounds. The authors divided the F_a absorption into two classes with "good" absorption defined as $F_a > 15\%$ and "poor" absorption defined as $F_a < 10\%$, respectively. A recursive partitioning (RP) approach was employed by the authors to derive a small set of rules, less than 10, which correctly explained ~94.2% of the data. The data set is, however, rather skewed with ~90% of the compounds belonging to the "good" class of compounds. Important parameters for determining the correct class were log *P*, PSA, and Abraham alpha (A) hydrogen-bond acidity parameter. From the publication, it is not possible to determine how the authors validated their model with respect to both internal cross-validation and external validation (see Section 14.5 for details of

Table 15.3 Publications on classification models of human fraction absorbed.

Publication	Title	Data set	Technique	Correct test set	Descriptors
Clark, *Journal of Pharmaceutical Sciences*, 1999	Rapid calculation of polar surface area and its application to the prediction of transport phenomena. 1. Prediction of intestinal absorption	94	SR	91% ($n = 74$)	PSA
Subramanian and Kitchen, *Journal of Molecular Modeling*, 2006	Computational approaches for modeling human intestinal absorption and permeability	121	SR	70%[a] ($n = 46$)	PSA
Deconinck *et al.*, *Journal of Pharmaceutical and Biomedical Analysis*, 2005 [46]	Classification of drugs in absorption classes using the classification and regression trees (CART) methodology	141	CART	85% ($n = 27$)	2D and 3D descriptors from Dragon, HyperChem, and ACDlabs ($n_{final} = 9$)
Sun, *Journal of Chemical Information and Computer Sciences*, 2004 [42]	A universal molecular descriptor system for prediction of log *P*, log *S*, log BB, and absorption	169	PLS-DA	n.a.	Atom types ($n_{final} = 3$ PCs from the PLS-DA analysis)
Wegner *et al.*, *Journal of Chemical Information and Computer Sciences*, 2004	Feature selection for descriptors based classification models. 2. Human intestinal absorption (F_a)	196	GA-SEC	n.a.	2D and 3D from several sources ($n_{final} = 10$–245)
Cabrera Perez *et al.*, *European Journal of Medicinal Chemistry*, 2004	A topological sub-structural approach for predicting human intestinal absorption of drugs	209	LDA	93%	TOPS-MODE ($n_{final} = 3$)
Egan *et al.*, *Journal of Medicinal Chemistry*, 2000	Prediction of drug absorption using multivariate statistics	234	Pattern recognition	n.a.	Clog *P*, PSA, MW

(*Continued*)

Table 15.3 (*Continued*)

Publication	Title	Data set	Technique	Correct test set	Descriptors
Klon *et al.*, *Journal of Chemical Information and Modeling*, 2006 [49]	Improved näve Bayesian modeling of numerical data for absorption, distribution, metabolism and excretion (ADME) property prediction	264	Näve Bayes with continuous numerical	81%	2D and 3D descriptors from Dragon ($n_{final} = 3$)
Zmuidinavicius *et al.*, *Journal of Pharmaceutical Sciences*, 2003 [30]	Classification structure–activity relations (C-SAR) in prediction of human intestinal absorption	977	HC and RP	n.a.	2D and 3D descriptors ($n_{final} = 2$–3)
Bai *et al.*, *Journal of Chemical Information and Computer Sciences*, 2004 [44]	Use of classification regression tree in predicting oral absorption in humans	1260	CART	65%[b]	2D and 3D descriptors ($n_{final} =$ n.s.)
Hou, *et al.*, *Journal of Chemical Information and Modeling*, 2007	Use of support vector machines in predicting oral absorption in humans	578	SVM	96.9% ($n = 98$)	log $D_{6.5}$, TPSA, nHBD, MW, MV, *N* rule-of-5 and N+

Abbreviations used: sigmoidal regression (SR), classification and regression trees (CART), partial least square projection to latent structure discrimination analysis (PLS-DA), genetic algorithms based on Shannon entropy cliques (GA-SEC), linear discriminant analysis (LDA), hierarchical clustering (HC), recursive partitioning (RP), topological substructural molecular design (TOPS-MODE). n.a., not applicable; the fraction-absorbed model has not been validated with a test set or the result of a validation is not given. n.s., not stated.

[a]Using a cutoff limit between poor and good absorption of 80%, and Equation 12.

[b]Six classes were used in this evaluation: 0–19, 20–31, 32–43, 44–59, 60–75, and 76–100%.

the importance of model validation). This makes the results obtained somewhat unreliable with respect to the forecasting ability of the derived model.

Pérez and coworkers [38] have used linear discriminant analysis (LDA) to develop a classification model for F_a. The data set studied is, in part, based on the "Zhao" data set but with additional compounds from Benet *et al*. [39] and consists of 209 compounds, which the authors divided into a training set and a test set of 82 and 127 compounds, respectively. The F_a was divided into three classes: highly ($F_a > 70\%$), moderately (F_a between 30 and 70%), and poorly ($F_a < 30\%$) absorbed compounds. The authors used a methodology called TOPS-MODE [40], which is based on the calculation of spectral moments of a bond matrix, whose entries are ones or zeros if the corresponding bonds are adjacent or nonadjacent. The diagonal elements of the bond matrix in this study were weighted by PSA, hydrophobicity, molar refraction, atomic charge, and atomic mass. This weighting aspect of the descriptor matrix (bond matrix) makes computed descriptors of the TOPS-MODE method similar to the ones obtained using the BCUT methodology (see Ref. [41] for further description of the BCUT method). The authors actually derived two models to be used sequentially. The purpose of the first model was to distinguish the poorly absorbed compounds from the highly and moderately absorbed ones while the second model was designed to do the opposite, that is, distinguish the highly absorbed compounds from the moderately and poorly absorbed ones. Pérez *et al*. performed extensive validation of their model apart from the training and test set selection mentioned above. They also conducted leave-one-out cross-validation (LOO-CV) on their training set and tested the derived model with an additional external test set of some 100 compounds. The predictive ability of the derived models with respect to both external and internal validation is impressive with accuracies of between 80 and 94% for the various validation sets. The authors found variables related to log *P*, PSA, the number of bonds in the molecules, and the size of the molecules to be important for discriminating the three absorption classes.

Sun [42] has also investigated the "Zhao" data set using atom-type descriptors, as the author derived two models – a 2-class model and a 3-class model. The three classes were defined as class 1 $F_a > 80\%$, class 2 $F_a = 20$–80%, and class 3 $F_a < 20\%$. For the 2-class model, the division between classes was set at 20%. The atom-type classification employed in this study was based upon identifying a particular type depending upon several factors, namely, its element, its aromaticity, its neighboring atoms, and whether the atom is in a ring or not. This atom classification scheme resulted in 218 different descriptors. Sun used partial least square projection to latent structures (PLS) [43] (see Section 14.3 for further details) as statistical engine for deriving the relationship and cross-validation as internal validation technique. For the 3-class model, the analysis resulted in a five-component model with a coefficient of determination (r^2) of 0.92 and a cross-validated coefficient of determination (q^2) of 0.79. The corresponding values for the 2-class case were 0.94 and 0.86, respectively. Unfortunately, Sun neither reports the accuracy of the predictions nor does the investigation use external validation for determining the forecasting ability of the derived model.

Bai *et al*. [44] investigated approximately 1260 drugs from the OraSpotter human pharmacokinetic database [45] using CART rule-based modeling. They

divided the F_a into six classes (0–0.19, 0.2–0.31, 0.32–0.43, 0.44–0.59, 0.6–0.75, and 0.76–1) and used 28 different molecular descriptors that included variables such as log *P*, number of HBDs and HBAs, MW, and PSA, as well as counts of some functional groups. The data set was randomly split into a training set and a test set consisting of 899 and 362 compounds, respectively. The accuracy was 65% for the prediction of the correct class and 80.4% accuracy within one class error. Furthermore, Bai and coworkers additionally tested three more diverse data sets that consisted of 67, 90, and 37 compounds and resulted in 85.1, 74.4, and 86.4% accuracy, respectively, within one class error. From the investigations, the authors concluded that the CART model performed better for high and low absorption but performed not so well for the intermediate classes between 0.32 and 0.59. As with most data sets, the data set used by Bai and coworkers was also skewed and had relatively few compounds in the intermediate range between 0.32 and 0.59. This may, in part, explain the somewhat poor predictive ability for this kind of compounds.

Deconinck *et al.* [46] have also used CART to model F_a for the "Zhao" data set. They investigated 141 compounds using both Dragon [47] and Hyperchem [48] descriptors (>1400 descriptors). The authors divided the F_a range into five classes: class 1, 0–25%; class 2, 26–50%; class 3, 51–70%; class 4, 71–90%; and class 5, more than 90%. For internal validation, a 10-fold cross-validatory procedure was employed. Deconinck and coworkers developed three models: the first, second, and third models were based on all available descriptors, all available 2D descriptors, and all available 3D descriptors, respectively. They found that the first model based on all descriptors performed best. Furthermore, the authors also found that the first five splits in the CART tree were defined by 2D descriptors. Thus, the investigation indicated that the rough classification of the compounds was performed by 2D descriptors and then refined, by additional splits in the model further down the tree, by 3D descriptors. The predictive power of the three models was tested with an external test set consisting of 27 compounds, that is, ∼20% of the size of the training set. The three models predicted the test with accuracies of 88.9, 85.2, and 77.8%, respectively. The data set used by Deconinck and coworkers is well documented so that other researchers may investigate the same data set.

Another study on the "Zhao" data set with some additional compounds was performed by Klon and coworkers [49]. After removing P-glycoprotein (P-gp) substrates and compounds for which human intestinal absorption was either not reported or could not be related to passive intestinal absorption, the data set consisted of 264 structures. The authors randomly assigned 75% of the compounds to the training set (205 entries) while the remaining compounds constituted the external test set (59 entries). Unfortunately, Klon *et al.* do not reveal the names or structures of the compounds included in the training and test sets, which makes it difficult for other researchers to verify or reinvestigate the data set in question. The authors used three different implementations of naïve Bayesian classifiers – one in-house-developed method and two commercially available [50, 51]. The former method uses a Gaussian approach while the latter two are based on a Laplacian implementation. The authors treated the F_a investigation as a binary classification

with three different cut-offs (90, 80, and 70%, respectively) for defining the high (above the cut-off) and the low (below the cut-off) absorbed compounds. The measure of performance by the derived models was also estimated in a somewhat different fashion compared to what is usually the case. Normally, accuracy is used as the criteria of how well the model performs. In this investigation, a well-known measure within the field of machine learning was used, namely, the receiver-operating characteristic (ROC) curve. The ROC curve is a measure of the models' sensitivity, that is, the ability to identify true positives, and specificity, that is, the ability to avoid false negatives. The area under the ROC curve serves as a measure of the predictive ability of the derived model. A value of 1.0 represents a perfect model that is able to discriminate perfectly between true positives and true negatives, while 0.5 is indicative of a model with random performance, that is, no predictive ability. The structures in the data set were described by three sets of descriptors: Dragon descriptors [47], Pipeline Pilot descriptors [51], and the ADME Profiler descriptors FPSA (a polar surface area descriptor) and Alog*P* (a calculated log *P* descriptor) [52]. Finally, the Dragon descriptors were selected so that only variables with an absolute correlation with F_a of 0.7 were retained. Also, pairwise highly correlated variables were removed keeping only one of the descriptors. After redundant descriptors were removed, only the hydrophilic factor (Hy), TPSA(NO), and the Moriguchi log *P* (Mlog*P*) remained. The Pipeline Pilot descriptors were an extended connectivity fingerprint with a neighborhood size of six bonds (FCFP_6), Alog*P*, MW, the number of hydrogen-bond donors (nHBD), the number of hydrogen-bond acceptors (nHBA), the number of rotatable bonds, and PSA defined by nitrogen and oxygen atoms (PSA(NO)). The authors found that the Gaussian implementation outperformed both the Pipeline Pilot and the binary QSAR implementations. The area under ROC curve varied from 0.70 using the FPSA and AlogP98 descriptors at the 90% cut-off for good absorption to 0.91 using the selected Dragon descriptors at 70% cut-off.

Hou and coworkers [53] have also investigated HIA using a data set of 578 compounds and support vector machine (SVM) technology. The data set studied in this work is a compilation from the Palm, Wessel, and Zhao data sets. Eleven different descriptors were used (topological polar surface area (TPSA), the octanol–water partitioning coefficient (log *P*), the apparent partition coefficient at pH 6.5 (log $D_{6.5}$), the number of violations of the four rule-of-5 rules developed by Lipinski (*N* rule-of-5), the number of hydrogen-bond donors and acceptors, the intrinsic solubility (log *S*), the number of rotatable bonds, the molar volume (MV), the molecular weight, and a binary indicator (N+) representing the existence of a positively charged N atom). The authors divided the data set into a 480-molecule training set and a 98-molecule test set. Ten SVM classification models were developed to investigate the impact of different individual molecular properties on F_a. The final model consisted of the seven parameters: log $D_{6.5}$, TPSA, nHBD, MW, MV, *N* rule-of-5, and N+. The overall correctness of the model is quite impressive: 97.8 and 94.5% of the good and poor classes, respectively, were correctly classified for the training set while for the test set, the model achieved corresponding accuracies of 97.8 and 100%, respectively.

15.3.2.2 An Example Using Genetic Programming-Based Rule Extraction

The example described here employs genetic programming (GP) (see further description of the method in Section 14.3.2.2) and the genetic rule extraction (G-REX) algorithm [54, 55].

We have used the data set published by Hou and coworkers [53]. The data set consists of 578 compounds. The compounds were divided into two classes depending upon the measured F_a value. Compounds with an F_a higher than 30% were assigned to class "high" while the remaining compounds were designated "low." The distribution of classes was, as is unfortunately the case for data sets of this kind, rather skewed with 407 compounds belonging to class "high" while only 73 compounds belonging to class "low." The training data were randomly divided into a training set and a validation set consisting of 380 and 100 compounds, respectively, and the classes were balanced internally by adding multiple copies of each object. The data set is available through Ref. [53]. Crossover and mutation for the genetic algorithm were set to 0.8 and 0.001, respectively. G-REX was applied and a rather simple model emerged (see Figure 15.2) with good fit and predictive ability. The actual model consists of four rules using parameters N+, N rule-of-5, log $D_{6.5}$, and MV (Figure 15.2).

In the external test set, the "high" and the "low" compounds were predicted with accuracies of 96.8 and 100%, respectively. The corresponding accuracies for the training set and the validation set are 93.1%, 93.3% and 96.6%, 100%, respectively. The G-REX technique applied in this study thus performed as good as the SVM model from the original study in Ref. [53] with respect to the external predictive ability. A possible advantage of the G-REX-derived model is the simplicity and transparency of the model that makes it quite attractive for further use.

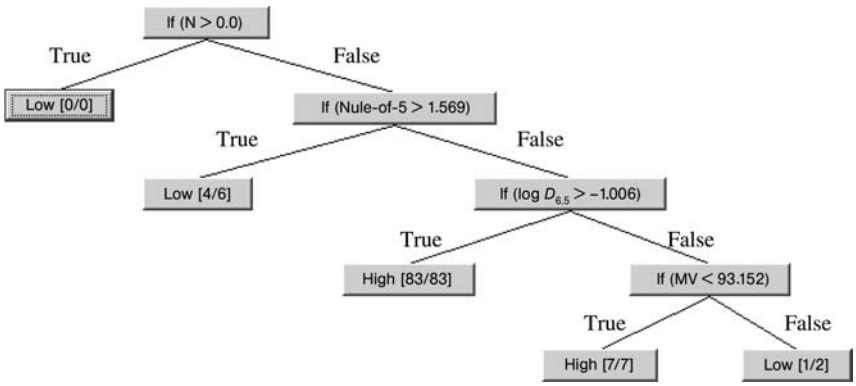

Figure 15.2 Genetic programming F_a classification model for the data set in Ref. [53]. Compounds with F_a higher than 30% were assigned to class "high" while the remaining compounds were designated "low."

15.3.3
Repeated Use of Data Sets

The available literature within the field of prediction of oral absorption reveals that the same literature data sets are repeatedly used. One of the most used data sets to date is the "Palm" data set [56], which is included in almost all large data sets, the "Wessel" data set [25], and the "Zhao" data set [26]. All of these are based on marketed drugs and hence are heavily skewed toward data reflecting good absorption. The scientific interest has been strongly directed toward which technique or which descriptor space is the best for obtaining models with good external predictivity, but it can be questioned how much more we can learn from these data sets. Can we use them to produce predictive models applicable to the drug discovery process of today? Can we use the results to predict the oral absorption of new lead structures? One way to improve the predictions and to make them applicable also for new drug structures is to go back to the experimental settings and produce response data for such compounds. Instead of using F_a data from traditionally used drugs, which are sometimes of intermediate quality, it may be more successful to model the major underlying mechanisms for absorption, for example, solubility and membrane permeation. These investigations can be performed on new chemicals and proof of concept can be performed in animal studies. To virtually predict human F_a of new chemical entities based on such *in vitro* and *in vivo* data with high accuracy for both poorly and well-absorbed compounds is one of the future scientific challenges in this area.

15.4
Software for Absorption Prediction

A large number of software programs are available for prediction of oral absorption and other pharmacokinetically relevant properties (Table 15.2). Is it possible to know beforehand which one to use? Evaluations to test the performance of the software are performed with the help of a standard data set. One such evaluation compared the performance of GastroPlus and iDEA, two simulation software, among others, for predicting oral absorption, and found them to perform quite equally [57]. One reason for this can be the issues discussed in Section 15.3, that is, the repeated use of data sets. It is likely that the training sets used for the model development are similar and hence the performance becomes similar. However, the training set used and the applicability domain for the models incorporated in the software are generally not stated and thus it becomes difficult to know beforehand which one to use. Therefore, the best way to decide which software to choose for future use is to evaluate several software programs for a selected test set representing the typical compounds that are to be predicted. By doing so, not only the accuracy of the software but also the user-friendliness of each program is included in the evaluation and the decision. Often the most predictive models are established in-house since these models are based on the chemical space of interest. However, the commercial software can be a good complement to such

in-house models in terms of investigating interactions between different processes and allow visualization of the complete absorption process.

15.5 Future Outlook

Frontloading of assessing ADME properties early in the discovery process has gained much importance during recent years and is now considered a routine. These efforts have significantly reduced the ADME-related attrition in the clinical phase.

For the frontloading process in early drug discovery to have an impact, the ADME properties have to be assessed on a large number of compounds already in the early lead generation phase. This has led to the development of high-capacity *in vitro* assays to model different aspects of the *in vivo* situation; for example, permeability is being approximated with the Caco-2 assay. The information gained from such assays has played an important role in the design of molecules with good ADME properties.

To have a higher impact on the decision-making process, the next step has been the heavy use of prediction models in the design stage before the molecules are synthesized. Ideally, the prediction models are based on more complex measures, such as F_a. The largest limitation of this initiative is the availability of such data, which is not likely to increase much in the near future. However, *in vitro* permeability and solubility values are being routinely measured on thousands of compounds. This gives the opportunity to generate more elaborate models and also to fine-tune them using technologies such as correction libraries [58]. Combining solubility and permeability models (and possibly models for active transport) can give a good estimate of oral absorption for a large number of compounds.

For the use of these models in the drug discovery phase, one can identify two scenarios:

1. *The lead generation (or hit-to-lead) phase:* In this phase, it is desirable to obtain predictions of a large number of molecules before any experimental measurements are feasible from a practical point of view. The predictions do not need to be limited to the hits found in a high-throughput screen but can also comprise large virtual libraries of possible follow-up compounds. This requires very fast models for which the prediction of each molecule is done in a fraction of a second. A necessary requirement for future models is therefore speed, which has to be combined with a quality that is acceptable. Another future requirement is the generation of good data analysis programs, which can handle and judge the impact of each prediction and make intelligent selection of which compounds will be most successful. In this step, it is most likely that other absorption, distribution, metabolism, elimination/excretion, and toxicity (ADMET) components will be included such as predictions of transporter interactions, distribution, enzymatic degradation, and toxicity.
2. *The lead optimization phase:* For the lead optimization phase, one can afford slightly more elaborate (and also probably slower) models if they have a significant

increase in predictability. However, calculation times above minutes for each molecule are still not desirable. Experimental data are more generally available in this phase of the drug discovery process and the compounds of interest can normally be assigned to one or several series. Therefore, local prediction models can be advantageous to use.

An increased use of models predicting oral absorption will not only reduce the ADME-related attrition in the clinic but also increase the speed of the discovery process. Even though the models can give a good estimate of the ADME properties of molecules, it is most likely that the *in silico* models of the future will be used in concert with *in vitro* and *in vivo* models to predict the complex ADME profile of compounds that have advanced to a later phase in the drug discovery process.

References

1 Lipinski, C.A., Lombardo, F., Dominy, B.W. and Feeney, P.J. (1997) Experimental and computational approaches to estimate solubility and permeability in drug discovery and development settings. *Drug Delivery Reviews*, **23**, 3–25.

2 Palm, K., Stenberg, P., Luthman, K. and Artursson, P. (1997) Polar molecular surface properties predict the intestinal absorption of drugs in humans. *Pharmaceutical Research*, **14**, 568–571.

3 Amidon, G.L., Lennernäs, H., Shah, V.P. and Crison, J.R. (1995) A theoretical basis for a biopharmaceutic drug classification: the correlation of *in vitro* drug product dissolution and *in vivo* bioavailability. *Pharmaceutical Research*, **12**, 413–420.

4 Hansch, C., Quinlan, J.E. and Lawrence, G.L. (1968) Linear free-energy relationship between partition coefficients and the aqueous solubility of organic liquids. *The Journal of Organic Chemistry*, **33**, 347–350.

5 Yalkowsky, S.H. and Valvani, S.C. (1980) Solubility and partitioning I: Solubility of nonelectrolytes in water. *Journal of Pharmaceutical Sciences*, **69**, 912–922.

6 Jain, N. and Yalkowsky, S.H. (2001) Estimation of the aqueous solubility I: Application to organic nonelectrolytes. *Journal of Pharmaceutical Sciences*, **90**, 234–252.

7 Tetko, I.V. and Bruneau, P. (2004) Application of AlogPS to predict 1-octanol/water distribution coefficients, log *P* and log *D*, of AstraZeneca in-house database. *Journal of Pharmaceutical Sciences*, **93**, 3103–3110.

8 Tetko, I.V. and Poda, G.I. (2004) Application of ALOGPS 2.1 to predict log *D* distribution coefficient for Pfizer propriety compounds. *Journal of Medicinal Chemistry*, **47**, 5601–5604.

9 Bergström, C.A.S., Norinder, U., Luthman, K. and Artursson, P. (2003) Molecular descriptors influencing melting point and their role in classification of solid drugs. *Journal of Chemical Information and Computer Sciences*, **43**, 1177–1185.

10 Karthikeyan, M., Glen, R.C. and Bender, A. (2005) General melting point prediction based on a diverse compound data set and artificial neural networks. *Journal of Chemical Information and Modeling*, **45**, 581–590.

11 Huuskonen, J., Salo, M. and Taskinen, J. (1997) Neural network modeling for estimation of the aqueous solubility of structurally related drugs. *Journal of Pharmaceutical Sciences*, **86**, 450–454.

12 Bruneau, P. (2001) Search for predictive generic model of aqueous solubility using Bayesian neural nets. *Journal of Chemical*

Information and Computer Sciences, **41**, 1605–1616.

13 Liu, R.F. and So, S.S. (2001) Development of quantitative structure–property relationship models for early ADME evaluation in drug discovery. 1. Aqueous solubility. *Journal of Chemical Information and Computer Sciences*, **41**, 1633–1639.

14 Livingstone, D.J., Ford, M.G., Huuskonen, J.J. and Salt, D.W. (2001) Simultaneous prediction of aqueous solubility and octanol/water partition coefficient based on descriptors derived from molecular structure. *Journal of Computer-Aided Molecular Design*, **15**, 741–752.

15 Bergström, C.A.S., Wassvik, C.M., Norinder, U., Luthman, K. and Artursson, P. (2004) Global and local computational models for aqueous solubility prediction of drug-like molecules. *Journal of Chemical Information and Computer Sciences*, **44**, 1477–1488.

16 Wassvik, C.M., Holmen, A.G., Bergström, C.A.S., Zamora, I. and Artursson, P. (2006) Contribution of solid-state properties to the aqueous solubility of drugs. *European Journal of Pharmaceutical Sciences*, **29**, 294–305.

17 Bergström, C.A.S., Wassvik, C.M., Johansson, K. and Hubatsch, I. (2007) Poorly soluble marketed drugs display solvation limited solubility. *Journal of Medicinal Chemistry*, **50**, 5858–5862.

18 Camenisch, G., Folkers, G. and van de Waterbeemd, H. (1996) Review of theoretical passive drug absorption models: historical background, recent developments and limitations. *Pharmaceutica Acta Helvetiae*, **71**, 309–327.

19 Abraham, M.H., Chadha, H.S. and Mitchell, R.C. (1995) The factors that influence skin penetration of solutes. *The Journal of Pharmacy and Pharmacology*, **47**, 8–16.

20 Palm, K., Luthman, K., Ungell, A.L., Strandlund, G. and Artursson, P. (1996) Correlation of drug absorption with molecular surface properties. *Journal of Pharmaceutical Sciences*, **85**, 32–39.

21 Norinder, U., Osterberg, T. and Artursson, P. (1997) Theoretical calculation and prediction of Caco-2 cell permeability using MolSurf parameterisation and PLS statistics. *Pharmaceutical Research*, **14**, 1786–1791.

22 Stenberg, P., Luthman, K., Ellens, H., Lee, C.P., Smith, P.L., Lago, A. and Elliott, J.D. (1999) Prediction of the intestinal absorption of endothelin receptor antagonists using three theoretical methods of increasing complexity. *Pharmaceutical Research*, **16**, 1520–1526.

23 van de Waterbeemd, H. (1998) The fundamental variables of the biopharmaceutics classification system (BCS): a commentary. *European Journal of Pharmaceutical Sciences*, **7**, 1–3.

24 Artursson, P. (1990) Epithelial transport of drugs in cell culture. I: A model for studying the passive diffusion of drugs over intestinal absorptive (Caco-2) cells. *Journal of Pharmaceutical Sciences*, **79**, 476–482.

25 Wessel, M.D., Jurs, P.C., Tolan, J.W. and Muskal, S.M. (1998) Prediction of human intestinal absorption of drug compounds from molecular structure. *Journal of Chemical Information and Computer Sciences*, **38**, 726–735.

26 Zhao, Y.H., Le, J., Abraham, M.H., Hersey, A., Eddershaw, P.J., Luscombe, C.N., Butina, D., Beck, G., Sherborne, B., Cooper, I., Platts, J.A. and Boutina, D. (2001) Evaluation of human intestinal absorption data and subsequent derivation of a quantitative structure–activity relationship (QSAR) with the Abraham descriptors. *Journal of Pharmaceutical Sciences*, **90**, 749–784.

27 Votano, J.R., Parham, M., Hall, L.H. and Kier, L.B. (2004) New predictors for several ADME/Tox properties: aqueous solubility, human oral absorption, and Ames genotoxicity using topological descriptors. *Molecular Diversity*, **8**, 379–391.

28 Yang, C.Y., Dantzig, A.H. and Pidgeon, C. (1999) Intestinal peptide transport systems

and oral drug availability. *Pharmaceutical Research*, **16**, 1331–1343.

29 Matsson, P., Bergström, C.A.S., Nagahara, N., Tavelin, S., Norinder, U. and Artursson, P. (2005) Exploring the role of different drug transport routes in permeability screening. *Journal of Medicinal Chemistry*, **48**, 604–613.

30 Zmuidinavicius, D., Didziapetris, R., Japertas, P., Avdeef, A. and Petrauskas, A. (2003) Classification structure–activity relations (C-SAR) in prediction of human intestinal absorption. *Journal of Pharmaceutical Sciences*, **92**, 621–633.

31 Klopman, G., Stefan, L.R. and Saiakhov, R.D. (2002) ADME evaluation. 2. A computer model for the prediction of intestinal absorption in humans. *European Journal of Pharmaceutical Sciences*, **17**, 253–263.

32 Physicians' Desk Reference (2003) 57th edn, Thomson Healthcare, USA.

33 Dollery, C. (1999) Therapeutic Drugs, 2nd edn, Churchill Livingstone, UK.

34 Raevsky, O.A., Fetisov, V.I., Trepalina, E.P., McFarland, J.W. and Schaper, K.-J. (2000) Quantitative estimation of drug absorption in humans for passively transported compounds on the basis of their physicochemical parameters. *Quantitative Structure–Activity Relationships*, **19**, 366–374.

35 Niwa, Y. (2003) Using general regression and probabilistic neural networks to predict human intestinal absorption with topological descriptors derived from two-dimensional chemical structures. *Journal of Chemical Information and Computer Sciences*, **43**, 113–119.

36 Physicians' Desk Reference (1994) 48th edn, Medical Economics Data Production Company, USA.

37 Physicians' Desk Reference (1997) 51th edn, Medical Economics Data Production Company, USA.

38 Pérez, M.A.C., Sanz, M.B., Torres, L.R., Ávalos, R.G., Pérez González, M. and Díaz, H.G. (2004) A topological sub-structural approach for predicting human intestinal absorption of drugs. *European Journal of Medicinal Chemistry*, **39**, 905–916.

39 Benet, L.Z., Øie, S. and Schwartz, J.B. (1996) Appendix II. Design and optimization of dosage regimens; pharmacokinetic data, in *Goodman and Gilman's The Pharmacological Basis of Therapeutics* (eds J.G. Hardman, L.E. Limbird, P.B. Molinoff and R.W. Ruddon), McGraw-Hill, New York, pp. 1712–1792.

40 Estrada, E. (1997) Spectral moments of the edge-adjacency matrix of molecular graphs. 2. Molecules containing heteroatoms and QSAR applications. *Journal of Chemical Information and Computer Sciences*, **37**, 320–328.

41 Gunturi, S.B. and Narayanan, R. (2007) *In silico* ADME modeling. 3. Computational models to predict human intestinal absorption using sphere exclusion and kNN QSAR methods. *QSAR & Combinatorial Science*, **26**, 653–668.

42 Sun, H. (2004) A universal molecular descriptor system for prediction of log *P*, log *S*, log BB, and absorption. *Journal of Chemical Information and Computer Sciences*, **44**, 748–757.

43 Wold, S., Johansson, E. and Cocchi, M. (1993) PLS: Partial least-squares projections to latent structures, in *3D QSAR in Drug Design* (ed. H. Kubinyi), ESCOM Science Publishers B.V., The Netherlands, pp. 523–550.

44 Bai, J.P.F., Utis, A., Crippen, G., He, H.-D., Fischer, V., Tullman, R., Yin, H.-Q., Hsu, C.-P., Jiang, L. and Hwang, K.-K. (2004) Use of classification regression tree in predicting oral absorption in humans. *Journal of Chemical Information and Computer Sciences*, **44**, 2061–2069.

45 ZyxBio LLC, Hudson.

46 Deconinck, E., Hancock, T., Coomans, D., Massart, D.L. and Vander Heyden, Y. (2005) Classification of drugs in absorption classes using the classification and regression trees (CART) methodology. *Journal of Pharmaceutical and Biomedical Analysis*, **39**, 91–103.

47 Todeschini, R., Consonni, V., Mauri, A. and Pavan, M.Dragon version 4.0, Talete srl.

48 http://www.hyper.com.

49 Klon, A.E., Lowrie, J.F. and Diller, D.J. (2006) Improved naïve Bayesian modeling of numerical data for absorption, distribution, metabolism and excretion (ADME) property prediction. *Journal of Chemical Information and Modeling*, **46**, 1945–1956.

50 MOE Molecular Operating Environment (2005 –2006) Chemical Computing Group, Inc., http://www.chemcomp.com.

51 Pipeline Pilot, version 5.1, SciTegic, Inc, http://www.scitegic.com.

52 Cheng, A., Diller, D.J., Dixon, S.L., Egan, W.J., Lauri, G. and Mertz, K.M., Jr (2002) Computation of the physio-chemical properties and data mining of large molecular collections. *Journal of Computational Chemistry*, **23**, 172–183.

53 Hou, T., Wang, J. and Li, Y. (2007) ADME evaluation in drug discovery. 8. The prediction of human intestinal absorption by a support vector machine. *Journal of Chemical Information and Modeling*, **47**, 2408–2415.

54 Johansson, U., Sönströd, C., König, R. and Niklasson, L. (2003) Neural networks and rule extraction for prediction and explanation in the marketing domain, in *The International Joint Conference on Neural Networks*, IEEE Press, Portland, OR, pp. 2866–2871.

55 Johansson, U. (2007) Obtaining accurate and comprehensible data mining models, PhD Thesis, Institute of Technology, Linköping University, (http://urn.kb.se/resolve?urn=urn:nbn:se:liu:diva-8881).

56 Palm, K., Luthman, K., Ungell, A.-L., Strandlund, G., Beigi, F., Lundahl, P. and Artursson, P. (1998) Evaluation of dynamic polar molecular surface area as predictor of drug absorption: comparison with other computational and experimental predictors. *Journal of Medicinal Chemistry*, **41**, 5382–5392.

57 Parrott, N. and Lave, T. (2002) Prediction of intestinal absorption: comparative assessment of GASTROPLUS and IDEA. *European Journal of Pharmaceutical Sciences*, **17**, 51–61.

58 Rodgers, S.L., Davis, A.M., Tomkinson, N.P. and van de Waterbeemd, H. (2007) QSAR modeling using automatically updating correction libraries: application to a human plasma protein binding model. *Journal of Chemical Information and Modeling*, **47**, 2401–2407.

16
In Silico Prediction of Human Bioavailability

David J. Livingstone and Han van de Waterbeemd

Abbreviations

ADME	Absorption, distribution, metabolism, and excretion
AFP	Adaptive fuzzy partitioning
ANN	Artificial neural network
CoMFA	Comparative molecular field analysis
MLR	Multiple linear regression
NCE	New chemical entity
PBPK	Physiologically-based pharmacokinetics
PK	Pharmacokinetics
QSAR	Quantitative structure–activity relationship
R&D	Research and development
SIMCA	Soft independent modeling of class analogy

Symbols

$A\%$	Percentage absorbed
AUC	Area under the curve
C_0	Concentration at time zero
Caco-2	Human colon adenocarcinoma cell line (used as absorption model)
CL	Clearance
CL_u	Unbound clearance
Dose	Administered dose
F	Bioavailability (expressed as fraction)
$F\%$	Percentage bioavailable
f_a	Fraction absorbed
f_g	Fraction escaping gut wall intestinal metabolism
f_u	Fraction unbound to plasma proteins
$\log D$	Logarithm of the distribution coefficient D (for ionized species)

$\log P$	Logarithm of the partition coefficient P
$t_{1/2}$	Half-life
V_d	Volume of distribution
V_{du}	Unbound volume of distribution

16.1 Introduction

To make it convenient to the patients and to increase compliance, most drugs are given orally. Therefore, high bioavailability is a key quest in most drug discovery projects. Low bioavailability usually results in undesired variability due to population differences. *In vitro* ADMET and safety profiling is now well established in drug discovery [1]. Often, oral bioavailability is assessed in the rat. However, this is not always predictive for bioavailability in human. Factors that influence oral drug bioavailability can be divided into physicochemical/biopharmaceutical and physiological/biological factors. The first group tends to be essentially species independent. Indeed, species differences in pH values change percentage ionization and hence molecular behavior. Biological factors are often different between species [2]. Early estimates of oral bioavailability can help to focus on most promising lead series and clinical candidates. To address bioavailability issues in a drug discovery project, a road map of experimentation and prediction has been proposed [3].

This chapter reviews some of the *in silico* attempts to predict oral bioavailability. However, bioavailability is a complex property, and various pros and cons of current quantitative structure–activity relationship (QSAR) based approaches will be discussed here. As an alternative, physiologically-based pharmacokinetic (PBPK) modeling is discussed as a promising approach to predict and simulate pharmacokinetics (PK), including estimating bioavailability.

In silico models of biological activity have been constructed in the discovery research departments of the pharmaceutical companies since the 1970s. Early adopters of the technologies built QSAR models of pharmacological response and even wrote molecular modeling software before integrated packages became commercially available. Expectations of the results that might be delivered by these approaches were high, partly as a result of the enthusiasm of the computational chemists and partly because of the acceptance of the ideas by medicinal chemists. The failure of these early attempts to deliver dramatic changes in the rate of discovery of new chemical entities (NCEs) led to disappointment and a decrease in popularity of these approaches over the next few years. Expectations have now reached a mature level, and computer-aided molecular design is an accepted part of the discovery process with the advantages and limitations of *in silico* modeling well understood [4].

The next major technological advance in drug discovery was the development of combinatorial chemistry [5] and high-throughput screening [6], which increased the number of compounds synthesized and tested by factors of hundreds or even

thousands. A decade after the widespread adoption of this approach, however, has seen little or no increase in the number of NCEs submitted to the regulatory authorities, despite the ever-increasing expenditure on pharmaceutical R&D. There has been much debate about the reasons for this apparent failure, but a general consensus of opinion at that time was that the primary cause is poor ADME (absorption, distribution, metabolism, and excretion) properties. Indeed, widely quoted reports conclude that as much as 40% of the failures of NCEs can be attributed to this cause [7–9]. In fact, these figures are now old data and the truer situation is probably as little as 10–15% [10, 11] but, nevertheless, there is still a considerable effort focussed on the optimization of ADME properties, and high-throughput methods are now being applied to generate ADME and toxicity information [12–14].

Various attrition analysis studies appeared in the literature, the one by Pfizer's Chris Lipinski being one of the most cited. He investigated a range of easily computable properties of compounds in the World Drug Index (WDI). Since these compounds are either marketed drugs or are currently in clinical trial, the properties common to these compounds define what we call now "drug-like" properties [86]. It was found that compounds tend to have poor oral absorption if their molecular weight (MW) is more than 500, calculated partition coefficient (Clog *P*) is more than 5, the number of hydrogen-bond acceptors (HBAs) is more than 10, and number of hydrogen-bond donors (HBDs) is more than 5 [15]. This was called the rule-of-5, since all key numbers are a multiple of 5. Many drugs are ionized at physiological pH values (pH 5.5–7.4) and to reflect this, a proposal was made to use log *D* instead of log *P* in drug-like filters [16]. Unfortunately, quite often the rule-of-5 is wrongly linked to bioavailability [17, 18]. Poor bioavailability can occur even for compounds with excellent oral absorption, if they have high first-pass liver clearance (CL). In Figure 16.1, the difference between oral absorption and bioavailability is

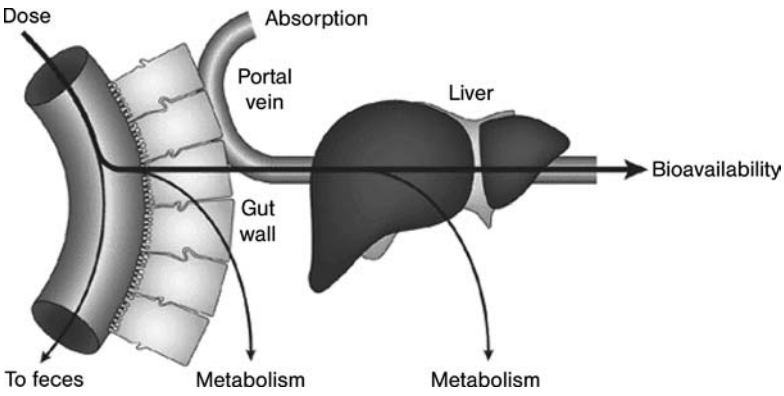

Figure 16.1 Definition of oral absorption (percentage of dose reaching the portal vein) and bioavailability (percentage of dose reaching the systemic circulation [50].

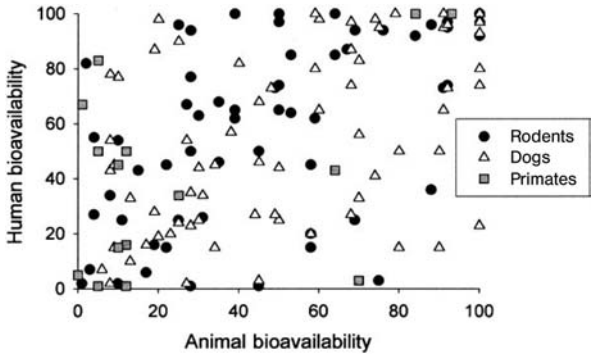

Figure 16.2 Plot of the absolute human bioavailability of various drugs versus their absolute bioavailability in primates, dogs, and rodents [19].

schematically presented. The key difference is metabolism (or clearance) and, for some compounds, the interaction with transporters.

Human bioavailability is often estimated by measuring bioavailability *in vivo* in several animal species and assuming humans are similar. Unfortunately, the direct use of measured animal bioavailability data is unlikely to be a good model of the human situation as shown in Figure 16.2, where data are plotted from Sietsema [19]. At first sight, it might appear that these experimental bioavailability measurements in animals are completely irrelevant for the prediction of human bioavailability, but the situation is not as bad as it first appears since what is plotted here are absolute bioavailability measurements. The lack of correlation between animal and human data is likely to be due to differences in physiology between the species, that is, to say differences in absorption, metabolism, plasma protein binding, and so on [20]. The use of absolute bioavailability data from animals to model the human data is equivalent to attempting to correlate all of the independent processes in the animal and simultaneously relate them to the corresponding processes in the humans [21]. This lack of direct correlation simply highlights the fact that bioavailability is a complex property as discussed in the next section. It should be noted that oral absorption compares often, but not always, much better between species [20, 51].

It should also be borne in mind that a complex biological property such as bioavailability is influenced by many factors as discussed in this chapter. The result is the considerable interindividual variability of about 15% standard deviation in observed bioavailability. The consequence of this is that any modeling approach cannot be better than this (Figure 16.3).

Another approach to human bioavailability estimation is based on *in vitro* data using Caco-2 as a measure of permeability and human liver microsomes for metabolism estimates. These data are combined in a graphical method to get a rough estimate of human oral bioavailability [22]. In principle, but not yet proven, this method could also be applied by using calculated permeability and metabolic stability.

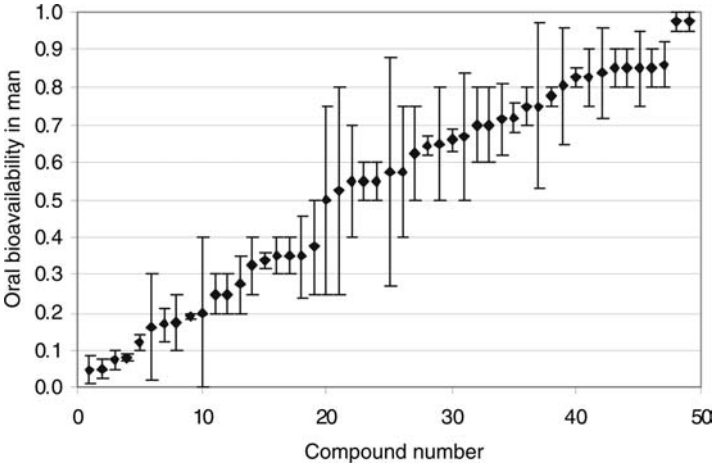

Figure 16.3 Interindividual variability in bioavailability [32].

16.2 Concepts of Pharmacokinetics and Role of Oral Bioavailability

Most drugs are given orally for reasons of convenience and compliance. Typically, a drug dissolves in the gastrointestinal tract, is absorbed through the gut wall, and then passes the liver to get in the blood circulation. The percentage of the dose reaching the systemic circulation is called bioavailability. From there, the drug will get distributed to various tissues and organs in the body. The extent of distribution will depend on the compound's structural and physicochemical properties. Some drugs may enter the brain and central nervous system (CNS) via the blood–brain barrier (BBB). Finally, the drug will bind to its molecular target, for example, a receptor or ion channel, and exert its desired action. A short summary of the key pharmacokinetic parameters is given here [23].

The volume of distribution (V_d) is a theoretical concept that connects the administered dose with the actual initial concentration (C_0) present in the circulation:

$$V_d = \frac{\text{Dose}}{C_0}. \tag{16.1}$$

Most drugs will bind to various tissues and in particular to proteins such as albumin in the blood. Since only the free (unbound) drug will bind to the molecular target, the concept of unbound volume of distribution (V_{du}) is used:

$$V_{du} = \frac{V_d}{f_u}, \tag{16.2}$$

where f_u is the fraction unbound to plasma proteins. Clearance of the drug from the body mainly takes place via the liver (hepatic clearance or metabolism and biliary excretion) and the kidney (renal excretion). By plotting the plasma concentration

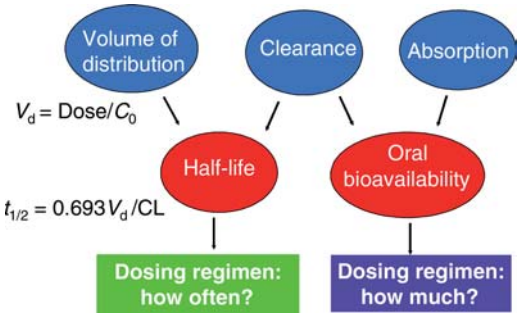

Figure 16.4 The key pharmacokinetic properties and their role in setting dose size and dose regimen [50].

against time, the area under the curve (AUC) relates to dose, bioavailability, and clearance [24]:

$$\text{AUC} = \frac{F \times \text{Dose}}{\text{CL}}. \tag{16.3}$$

The required dose can be estimated from the potency (e.g., IC_{50}) of the compound and the unbound clearance (CL_u):

$$\text{Dose} = \text{therapeutic concentration} \times \text{dose interval} \times \text{oral unbound clearance}. \tag{16.4}$$

The daily dose size is determined by the free (unbound) concentration of drug required for efficacy and not by plasma protein or tissue binding. Protein or tissue binding is important in the actual dosage regimen or frequency per day. The greater the binding the lower and more sustained the free drug concentrations are [23].

Half-life ($t_{1/2}$), the time taken for a drug concentration in the plasma to reduce by 50%, is a function of the clearance and volume of distribution and reflects how often a drug needs to be administered as shown in Figure 16.4:

$$t_{1/2} = \frac{0.693 V_d}{\text{CL}}. \tag{16.5}$$

16.3 *In Silico* QSAR Models of Oral Bioavailability

16.3.1 Prediction of Human Bioavailability

Quantitative structure–activity relationships have been used since the 1960s to model receptor and enzyme affinity, as well as physicochemical properties. The renewed interest in QSAR [25] arises from the recognition that an early prediction of ADMET properties ensures compound quality and avoids early development failure related to

ADME and safety/toxicity issues. Predictive models are therefore widely used in library design and profiling.

One of the earliest *in silico* models of human bioavailability was reported by Hirono and coworkers [26]. This study employed a set of 188 compounds that were classified as low (<50%), medium (50–89%), or well (>90%) absorbed and used a classification routine, fuzzy adaptive least squares, to generate discriminant functions. The molecules were described by their physicochemical properties and substructural descriptors, which meant that functional groups or substructures that enhanced bioavailability (e.g., saturated carbon atoms in side chains) or reduced it (e.g., aliphatic hydroxyl groups) could be identified. The performance varied between the three classes with the lowest success for the well-absorbed compounds, perhaps the most important group of the three.

Yoshida and Topliss published another classification study in 2000 [27]. This used a larger set of compounds ($n = 232$), classified into four classes, described by 15 substructural descriptors expected to be related to metabolism. The authors used in their work on bioavailability prediction a descriptor $\Delta\log D$ defined as the difference between the distribution coefficient at pH 6.5 (taken as pH of the small intestine) and at pH 7.4 (blood) for an ionizable species to reflect drug transport. The efficiency of this *in silico* system on a test set of 40 compounds was around 60%.

A model of bioavailability using a continuous measure was generated through stepwise regression and recursive partitioning to optimize the regression equations [28]. This study employed 591 compounds that were characterized by a large set (~600) of simple chemical substructure descriptors. Model efficiency was quite poor since the average R^2 value from 2000 random splits of the data into 80/20% training and test sets was 0.58. The model was also judged by comparison with predictions from the "rule-of-5" [15] (although this rule refers to oral absorption) and was shown to give a slight improvement over the false negative, 3 versus 5%, and false positive, 46 versus 53%, predictions. Some insights into the difficulty of modeling bioavailability may be gained by the complexity of the regression model, which involved 85 terms. Another linear regression approach using 169 compounds led to a regression model containing eight terms [29]. This study involved more complex descriptors, including some calculated by quantum mechanics, and gave a slight improvement in fit compared to the model reported by Andrews and coworkers.

These later two models of bioavailability as a continuous variable are linear since they used stepwise multiple linear regression (MLR) as the modeling tool. An obvious alternative, which may offer improved performance, is a nonlinear technique and such a model using an artificial neural network (ANN) was reported by Turner and colleagues [30]. This study employed 167 compounds characterized by several descriptor types, 1D, 2D, and 3D, and resulted in a 10-term model. Although the predictive performance was judged adequate, it was felt that the model was better able to differentiate qualitatively between poorly and highly bioavailable compounds.

Given the relatively poor performance of quantitative models, it is not surprising that other attempts to build *in silico* models of human bioavailability have concentrated on classification. Adaptive fuzzy partitioning (AFP) was applied for two sets of bioavailability data subdivided into four ranges of activity [31]. The best models using

the Yoshida and Topliss data [27] were able to predict correctly 75% of the validation set compounds. It was also shown that the predictive power increases when including more chemical diversity in the training set.

A genetic programming algorithm has been used to build models based on an automatic generation of substructural descriptors [32]. These models performed as good as other models based on classified data, so given the variety of descriptors tried and modeling techniques employed, this perhaps indicates that the problem in modeling human bioavailability lies in the data. This is not to say that there is anything wrong with the data but that it represents a summation of many different processes as discussed further in the next section.

Another approach is based on the combination of molecular interaction fields using the 3D-QSAR technique CoMFA and soft independent modeling of class analogy (SIMCA) [33]. Predictions were made for *F*% ranges by using the data sets from Refs [19, 27], with about 60% correctly classified.

Hou *et al*. compiled a database of human bioavailability for 768 compounds, which is publicly available [34]. These authors used a cutoff of 20% as acceptable. This can be questioned as *F*% up to about 30–40% can show considerable interindividual variability. It was concluded that *F*% of highly metabolized compounds cannot be well predicted from simple molecular descriptors as these do not encode for metabolism.

Martin proposed a "bioavailability score" based on several molecular properties including polar surface area (PSA), rule-of-5, and molecular charged state. With the descriptors used, this is an example aiming to estimate oral absorption and not bioavailability [19]; hence, the title of this work is misleading. A score was developed to assign the probability that a compound has an *F* more than 10% in the rat. We do not consider this as a meaningful cutoff. Better would be *F* more than 30% in man [30].

A cascade method was proposed using recursive partitioning and descriptors generated with a program called Algorithm Builder were used with a 800-compound training set [35]. Their predictions are 2-class models with *F*s less than and more than 30%, respectively. As parameters, they use a combination of solubility, pK_a, fractions ionized, human permeability, P-gp substrate specificity, physicochemical properties, and various structural descriptors. This is an attempt to model the components of bioavailability and then to integrate them into an overall prediction (see further in Section 16.4).

Using a data set of 577 compounds with experimental human bioavailability, a set of 42 bioavailability-boosting fragments was derived [36], although the general validity of these can be questioned without further proof of concept. These fragments were combined with other descriptors and with a genetic algorithm (GA), a set of 20 models for *F*% was obtained, and the final prediction was based on a consensus score ($r^2 = 0.55$, RMSE = 21.9%). In addition, an HQSAR (hologram QSAR) model (see also below) was derived from the same data set ($r^2 = 0.35$, RMSE = 26.4%). The combined consensus GA and HQSAR model works best ($r^2 = 0.62$, RMSE = 20.2%). This is a reasonable result in view of the fact that the standard error of the experimental data is 14.5%.

Molecular holograms are an extended form of fingerprints based on the 2D structures. An HQSAR model was derived for 250 compounds ($r^2 = 0.93$, $q^2 = 0.70$) and tested with 52 compounds ($r^2 = 0.85$) [37], which is a good result. The authors correctly point out some limitations of the model. Training is based on drugs, most compliant to the rule-of-5, and has no real solubility issues. The question therefore arises whether such model would be predictive for and pick out nondrug-like compounds.

A recent review gives a comprehensive survey of the state of the art in modeling human bioavailability [38]. Commercial software for the prediction of bioavailability using QSAR approaches include ADME Boxes [www.ap-algorithms.com], truPK [trupk.strandgenomics.com], and KnowItAll [www.knowittallcom].

16.3.2
Prediction of Animal Bioavailability

These models have all attempted to explain human bioavailability, which of course is our primary interest in drug design. Much data, however, have been measured in animals, particularly in the rat. Veber and colleagues at GSK have studied a set of 1100 compounds for which oral bioavailability in the rat was measured in-house [39]. The most important properties favorable for high oral bioavailability (in the rat) appear to be reduced molecular flexibility as measured by the number of rotatable bonds and low polar surface area. They conclude that these properties are in fact independent of the molecular weight. This would contradict the MW less than 500 rule as proposed by Lipinski in developing his rule-of-5 [15]. However, it was also found by others at Pharmacia that these results could not be generalized [40]. These authors reminded that property calculations can be algorithm dependent and that conclusions can be drug-class dependent; therefore, generalizations must be used with caution.

16.4
Prediction of the Components of Bioavailability

Oral *bioavailability* is a complex property. Many of the contributing factors are known (see Figure 16.4), but their cooperation is not always fully clear. Modeling of each of the more fundamental properties contributing to oral bioavailability will give more mechanistic insight. This might help the medicinal chemist to fine-tune the properties of a compound, which lead to poor bioavailability, while keeping the others in the right ballpark [41]. Fortunately, *in silico* models have been developed for many of these individual processes and, as the pharmaceutical industry continues to concentrate on these problems, better and more meaningful experimental tests are being developed leading to larger amounts of more accurate and reliable data. Reasonably successful models have been developed for several of the components shown in Figure 16.5. Many chapters in this book detail these approaches to understand properties contributing to bioavailability.

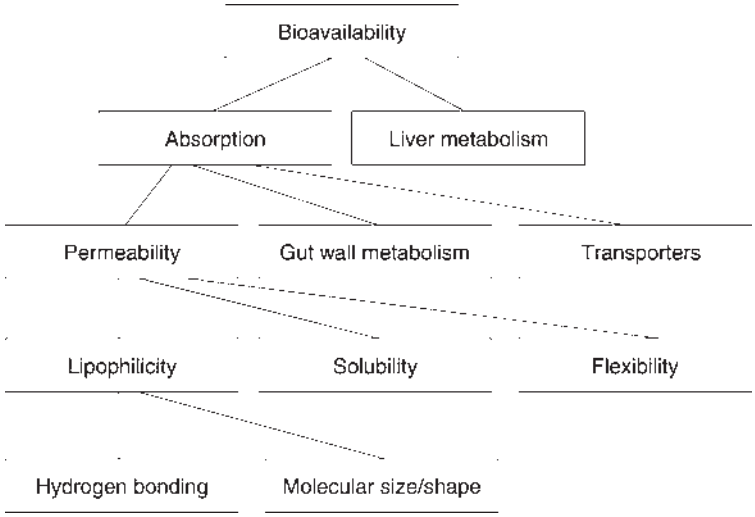

Figure 16.5 Bioavailability is a complex property, which can be unravelled into its more fundamental components [51].

Fundamental *physicochemical properties* (see Chapter 5) such as partition coefficient (log *P*) and distribution coefficient (log *D*) and pK_a are well predicted directly from chemical structure [42, 43]. Aqueous solubility may also be predicted reasonably well [44–46] (see Chapter 4), though there are warnings on the accuracy of solubility predictions for in-house pharmaceutical company compounds since these tend to be quite different chemical structures from those used to develop the commercial models [47].

Permeability is perhaps the most widely studied of the "biological" components of Figure 16.5 and as a result has led to a number of *in silico* models of this component [48]. There are various experimental systems designed to give some measure of permeability ranging in complexity from partition into liposomes to permeability across Caco-2 cells (see Chapter 7). *In silico* models of Caco-2 cell permeability have been constructed [49], but the question may be asked: "why model the model of human absorption?" [50]. It may be better to measure, and make models of, more fundamental factors that affect permeability.

There is considerable literature available on the prediction of oral *absorption* [51, 34] (see Chapter 15). One of the key problems is the lack of sufficient data to build robust predictive models.

Other components of bioavailability are also studied experimentally and in some cases *in silico* models have been developed for them. Examples include plasma protein binding [52], P-glycoprotein [53] (see Chapter 18) and other transporters [54] (see Chapter 10), and metabolism by cytochrome P450s [55, 56] (see Chapter 12).

Metabolism forms an important and probably least well-modeled part of the overall ADME process [57]. While metabolism/clearance may have a significant effect on oral bioavailability, it is clearly ultimately responsible for the fate of xenobiotics,

except those few that are excreted unchanged. To be able to produce reliable *in silico* models of the ADME properties of drugs, it will be necessary to understand and model the complex processes involved in metabolism. There is need to answer such questions as which enzyme is involved [58], what extent and rate, regioselectivity, or site of metabolism [59, 60], which metabolites are being formed [54, 55], are some of these reactive metabolites (which can cause toxic effects)? There are two main approaches to this problem: expert systems and computer-aided design. The expert system approach consists of a set of rules based on individual experience of how compounds are "dissected" by metabolism. The rules may be supplemented by physicochemical property calculations to apply some simple QSAR predictions. Examples of programs based on expert systems are MetabolExpert [61] and METEOR [62, 63]. The computer-aided design methods may be based on the properties of the ligands (QSAR) [64, 65] or on the structure of the enzyme (molecular modeling) [66–68].

This brief discussion of the components of bioavailability has shown that many of them are accessible experimentally and that *in silico* models may be built for the majority of them. Some recent reviews discuss the modeling of these components and other ADME processes [69–72]. It is by no means clear, however, and therefore remains a challenge as to how the individual components can easily be integrated into an overall prediction of oral bioavailability.

16.5 Using Physiological Modeling to Predict Oral Bioavailability

The concepts of pharmacokinetics come from classical compartmental modeling as described in Section 16.2. These compartments are not "real" compartments in any physical sense but rather virtual compartments that are required to make the modeling process work. The components of bioavailability and other parts of the whole ADME process are quite well understood, amenable to experimental measurements, and capable of *in silico* modeling as discussed in Section 16.3. The question remains, therefore, whether is it possible to link these pharmacokinetic concepts to the individual components and processes occurring in the body? The simple answer to this question is "yes, in principle," but the way to do this is by no means obvious. There is one approach, known as physiologically-based pharmacokinetic modeling, which is promising and increasingly used [73, 74]. PBPK modeling attempts to produce models that describe a system in physiological terms, in other words, the actual organs, blood flow, partition processes, and so on [75–77]. The information required for PBPK modeling is both chemical and biological as shown in Table 16.1.

This form of modeling is intellectually appealing since it is based on physiology, and thus there is a good scientific rationale to the process. Since it is based on physiology, it is possible to draw mechanistic conclusions and make quantitative predictions of disposition in various tissues. As a result, it being routinely applied in chemical risk assessment and can be judged as a standard methodology in this

Table 16.1 Information needs for PBPK models (adapted from Ref. [57]).

Chemical-specific data	Biological data
Partition coefficients	Anatomical dimensions
Metabolic rate constants	Organ blood flows
Elimination rate constants	Organ volumes
Molecular weight	Cardiac output
Aqueous solubility	Ventilation rate
Vapor pressure	Body mass
Permeability coefficients	Level of physical activity
Diffusion coefficients	Age
Protein-binding constants	Gender

field [78]. In drug research, most applications are performed in drug development where sufficient data are available to feed into the models. The ultimate bioavailability of a new drug considerably depends on formulation. The biopharmaceutical assessment is therefore an important part of the preclinical development program. The Biopharmaceutical Classification System (BCS) is one such tool used (see Chapter 19). Hurdles and critical parameters for oral bioavailability can be studied by using computer simulations, for example, GastroPlus [www.simulations-plus.com] [79] (see Chapter 17).

Unfortunately, the application of PBPK modeling in drug discovery so far has been very limited, and only a few studies have been reported [80, 81]. This is almost certainly due to the high data requirements, both chemical and biological, to produce these models. This sort of data is not normally collected as part of the regular drug discovery process and thus an investment in resources is required to produce it. Fortunately, some of the parameters required for PBPK modeling, for example, solubility, partition coefficients, uptake, and so on, can be estimated from *in silico* models, and so it looks set to become a more routine part of drug research [82].

Another way in which the components of bioavailability can be used, without the complexity of a formal PBPK model, is to link the components in an empirical but logical fashion. Two programs that demonstrated this, iDEA and pkEXPRESS, had modules to estimate oral bioavailability from Caco-2 and microsomal metabolic stability [83, 84]. Unfortunately, both products are no longer commercially available.

The principle for the bioavailability estimate is as follows [84]. Hepatic intrinsic clearance (CL_{int}) is measured in hepatocytes by measuring the half-life ($t_{1/2}$) in the following equation:

$$CL_{int} = \left(\frac{0.693}{t_{1/2}}\right) \times \left(\frac{\text{g liver}}{\text{kg body}}\right) \times \left(\frac{\text{ml incubation}}{\text{cells incubation}}\right) \times \left(\frac{\text{cells}}{\text{g liver}}\right). \quad (16.6)$$

The blood clearance can then be obtained through one of the several approaches, for example, the well-stirred model and fraction unbound ($f_{u,}$ obtained from plasma

protein binding) and the liver blood flow (Q, which for humans can be taken as 25 ml/min/kg [23]):

$$\mathrm{CL_b} = \frac{Q \times \mathrm{CL_{int}} \times f_u}{Q + \mathrm{CL_{int}} \times f_u}. \tag{16.7}$$

The hepatic extraction rate (E_H) is

$$E_H = \frac{\mathrm{CL_b}}{Q}. \tag{16.8}$$

The bioavailability (F), correcting for the fraction absorbed (f_a) and fraction escaping intestinal metabolism (f_g), is

$$F = f_a \times f_g \times (1 - E_H). \tag{16.9}$$

The fraction absorbed (f_a) is obtained from other measurements including solubility and permeability by using, for example, Caco-2 or PAMPA data [83], each of which in principle can also be predicted with a QSAR model (but see comment in 16.4).

More recent PBPK software packages such as SIMCYP [www.simcyp.com], PK-Sim [www.pk-sim.com], GastroPlus [www.simulations-plus.com], and Cloe PK [www.cyprotex.com] offer similar bioavailability estimation. It is clear that these approaches require more data input than just molecular structure as in QSAR models.

Integration of *in vitro* results and pharmacokinetic modeling is also used to assess the bioavailability of nutrients [85] using TNO's gastrointestinal model TIM [www.tno.nl/pharma].

16.6 Conclusions

The properties that are important for drug metabolism and pharmacokinetics (DMPK) are much better understood now than they were some 10 years ago [24]. Good progress has been made in recent years toward robust modeling of a number of pharmacokinetic properties and various aspects of human drug metabolism. More and good quality data have become available for some of the important end points. However, and unfortunately, some end points are by nature very complex. These include clearance and oral bioavailability.

It is possible to build *in silico* models of human bioavailability but while these may work well for certain classes of drugs, possibly because their bioavailability is dominated by one process such as uptake, it is unlikely that they will work well for all drugs. This may be improved by increasing quantities of data, but taking into consideration more classes of drugs may have just the opposite effect. The cause of these problems is clear since a small number of fundamental physicochemical

properties determine many of the components of bioavailability. Changes in these physicochemical properties may have quite different effects on individual components as we change from one drug class to another or, indeed, within a single class.

There is a choice of building in-house predictive models starting from literature and in-house bioavailability data. A wide range of QSAR tools are commercially or freely available. Alternatively, commercial packages can be used as discussed in this chapter.

Bioavailability is influenced by many properties, depending on the rate and the extent of absorption and systemic clearance. Each of these properties is impacted by physicochemical properties such as solubility, log *P*, log *D*, and pK_a. Absorption and metabolism are often governed by opposing factors. More lipophilic compounds tend to be more permeable, but solubility may also become a limiting factor. In addition, more lipophilic compounds will be more rapidly and extensively metabolized and will show increased toxicity liabilities [86].

Although formulation variables such as particle size and excipients have not been discussed here, they are highly relevant in practice. In addition, food can play an important role in oral absorption and thus bioavailability. Food may increase blood flow and thus limit the extent of first-pass effect. Bile secretion increases with food intake, which may enhance the solubility of lipophilic compounds. Attempts have been made to predict the effect of food on the extent of drug absorption [87]. Gastric emptying time is another factor, which depends on the type and the amount of food intake and physiopathology, among others.

Another approach to increase bioavailability via better absorption is using prodrugs (see Chapter 20).

It is therefore good to stress that bioavailability predictions can only be ballpark predictions in very early discovery stages, and they get better in later developments as *in silico* data can be mixed with *in vitro* and *in vivo* measurements [1].

References

1 Wang, J., Urban, L. and Bojanic, D. (2007) Maximising use of *in vitro* ADMET tools to predict *in vivo* bioavailability and safety. *Expert Opinion on Drug Metabolism and Toxicology*, **3**, 641–665.

2 Hurst, S., Loi, C.-M., Brodfuehrer, J. and El-Kattan, A. (2007) Impact of physiological, physicochemical and biopharmaceutical factors in absorption and metabolism mechanisms on the drug oral bioavailability of rats and humans. *Expert Opinion on Drug Metabolism and Toxicology*, **3**, 469–489.

3 Thomas, V.H., Bhattachar, S., Hitchingham, L., Zocharski, P., Naath, M., Surendran, N., Stoner, C.L. and El-Kattan, A. (2005) The road map to oral bioavailability: an industrial perspective. *Expert Opinion on Drug Metabolism and Toxicology*, **2**, 591–608.

4 Livingstone, D.J. and van de Waterbeemd, H. (2006) *In silico* models for human bioavailability, in *Virtual ADMET Assessment in Target Selection and Maturation* (eds B. Testa and L. Turski), IOS Press, Amsterdam, pp. 151–161.

5 Beck-Sickinger, A. and Weber, P. (2002) *Combinatorial Strategies in Biology and Chemistry*, John Wiley & Sons, Chichester, UK.

6 Dixon, G.K., Major, J.S. and Rice, M.J. (eds) (2000) *High Throughput Screening – The Next Generation*, Bios, Oxford, UK.

7 Kennedy, T. (1997) Managing the drug discovery/development interface. *Drug Discovery Today*, **2**, 436–444.

8 Lipper, R.A. (1999) How can we optimize selection of drug development candidates from many compounds at the discovery stage? *Modern Drug Discovery*, **2**, 55–60.

9 Venkatesh, S. and Lipper, R.A. (2000) Role of the development scientist in compound lead selection and optimization. *Journal of Pharmaceutical Sciences*, **89**, 145–154.

10 Forum, General Metrics (2001).

11 Kola, I. and Landis, J. (2004) Can the pharmaceutical industry reduce attrition rates? *Nature Reviews Drug Discovery*, **3**, 711–715.

12 Bertrand, M., Jackson, P. and Walther, B. (2000) Rapid assessment of drug metabolism in the drug discovery process. *European Journal of Pharmaceutical Sciences*, **11** (Suppl. 2), S61–S62.

13 Thompson, T.N. (2000) Early ADME in support of drug discovery: the role of metabolic stability studies. *Current Drug Metabolism*, **1**, 215–241.

14 Li, A.P. (2001) Screening for human ADME/Tox drug properties in drug discovery. *Drug Discovery Today*, **6**, 357–366.

15 Lipinski, C.A., Lombardo, F., Dominy, B.W. and Feeney, P.J. (1997) Experimental and computational approaches to estimate solubility and permeability in drug discovery and development settings. *Advanced Drug Delivery Reviews*, **23**, 3–25.

16 Bhai, S.K., Kassam, K., Peirson, I.G. and Pearl, G.M. (2007) The rule of five revisited: applying log *D* in place of log *P* in drug-likeness filters. *Molecular Pharmacology*, **4**, 556–560.

17 Hou, T., Wang, J., Zhang, W. and Xu, X. (2007) ADME evaluation in drug discovery. 7. Prediction of oral absorption by correlation and classification. *Journal of Chemical Information and Modeling*, **47**, 208–218.

18 Martin, Y.C. (2005) A bioavailability score. *Journal of Medicinal Chemistry*, **48**, 3164–3170.

19 Sietsema, W.K. (1989) The absolute oral bioavailability of selected drugs. *International Journal of Clinical Pharmacology, Therapy, and Toxicology*, **27**, 179–211.

20 Mandagere, A.K. and Jones, B. (2003) Prediction of bioavailability, in *Drug Bioavailability* (eds H. van de Waterbeemd, H. Lennernäs and P. Artursson), Wiley-VCH Verlag GmbH, Weinheim, pp. 444–460.

21 Grass, G.M. and Sinko, P.J. (2002) Physiologically-based pharmacokinetic simulation modelling. *Advanced Drug Delivery Reviews*, **54**, 433–451.

22 Mandagere, A.K., Thompson, T.N. and Hwang, K.K. (2002) Graphical model for estimating oral bioavailability of drugs in humans and other species from their Caco-2 permeability and *in vitro* liver enzyme metabolic stability rates. *Journal of Medicinal Chemistry*, **45**, 304–311.

23 Smith, D.A., van de Waterbeemd, H. and Walker, D.K. (2006) *Pharmacokinetics and Metabolism in Drug Design*, 2nd edn, Wiley-VCH Verlag GmbH, Weinheim.

24 van de Waterbeemd, H., Smith, D.A., Beaumont, K. and Walker, D.K. (2001) Property-based design: optimization of drug absorption and pharmacokinetics. *Journal of Medicinal Chemistry*, **44**, 1313–1333.

25 van de Waterbeemd, H. and Rose, S. (2008) Quantitative approaches to quantitative structure–activity relationships, in *The Practice of Medicinal Chemistry*, 3rd edn (ed. C.G. Wermuth), Elsevier, Amsterdam.

26 Hirono, S., Nakagome, I., Hirano, H., Matsushita, Y., Yoshi, F. and Moriguchi, I. (1994) Non-congeneric structure–pharmacokinetic property correlation studies using fuzzy adaptive least-squares: oral bioavailability. *Biological & Pharmaceutical Bulletin*, **17**, 306–309.

27 Yoshida, F. and Topliss, J.G. (2000) QSAR model for drug human oral bioavailability. *Journal of Medicinal Chemistry*, **43**, 2575–2585.

28 Andrews, C.W., Bennett, L. and Yu, L.X. (2000) Predicting human oral bioavailability of a compound: development of a novel quantitative structure–bioavailability relationship. *Pharmaceutical Research*, **17**, 639–644.

29 Turner, J.V., Glass, B.D. and Agatonovic-Kustrin, S. (2003) Prediction of drug bioavailability based on molecular structure. *Analytica Chimica Acta*, **485**, 89–102.

30 Turner, J.V., Maddalena, D.J. and Agatonovic-Kustrin, S. (2004) Bioavailability prediction based on molecular structure for a diverse series of drugs. *Pharmaceutical Research*, **21**, 68–82.

31 Pintore, M., van de Waterbeemd, H., Piclin, N. and Chrétien, J.R. (2003) Prediction of oral bioavailability by adaptive fuzzy partitioning. *European Journal of Medicinal Chemistry*, **38**, 427–431.

32 Bains, W., Gilbert, R., Sviridenko, L., Gascon, J.L., Scoffin, R., Birchall, K., Harvey, I. and Caldwell, J. (2002) Evolutionary computational methods to predict oral bioavailability QSPRs. *Current Opinion in Drug Discovery & Development*, **5**, 44–51.

33 Wolohan, P.R.N. and Clark, R.D. (2003) Predicting drug pharmacokinetic properties using molecular interaction fields and SIMCA. *Journal of Computer-Aided Molecular Design*, **17**, 65–76.

34 Hou, T., Wang, J., Zhang, W. and Xu, X. (2007) ADME evaluation in drug discovery. 6. Can oral bioavailability in humans be effectively predicted by simple molecular property-based rules? *Journal of Chemical Information and Modeling*, **47**, 460–463.

35 Japertas, P., Riauba, L., Zmuidinavicius, D., Didziapetris, R. and Petrauskas, A. (2003) Classification SAR in predicting oral bioavailability, in *Designing Drugs and Crop Protectants: Processes, Problems and Solutions* (eds M. Ford, D. Livingstone, J. Dearden and H. van de Waterbeemd), Blackwell, Oxford, pp. 229–230.

36 Wang, J., Krudy, G., Xie, X.-Q., Wu, C. and Holland, G. (2006) Genetic algorithm-optimized QSPR models for bioavailability, protein binding, and urinary excretion. *Journal of Chemical Information and Modeling*, **46**, 2674–2683.

37 Moda, T.L., Montanari, C.A. and Andricopulo, A.D. (2007) Hologram QSAR model for the prediction of human oral bioavailability. *Bioorganic and Medicinal Chemistry*, **15**, 7738–7745.

38 Turner, J.V. and Agatonovic-Kustrin, S. (2007) *In silico* prediction of oral bioavailability, in *ADME/Tox Approaches, Vol. 5* (eds B. Testa and H. van de Waterbeemd) in *Comprehensive Medicinal Chemistry*, 2nd edn, Elsevier, Oxford, pp. 699–724.

39 Veber, D.F., Johnson, S.R., Cheng, H.-Y., Smith, B.R., Ward, K.W. and Kopple, K.D. (2002) Molecular properties that influence the oral bioavailability of drug candidates. *Journal of Medicinal Chemistry*, **45**, 2615–2623.

40 Lu, J.J., Crimin, K., Goodwin, J.T., Crivori, P., Orrenius, C., Xing, L., Tandler, P.J., Vidmar, Th.J., Amore, B.M., Wilson, A.G.E., Stouten, P.F.W. and Burton, P.S. (2004) Influence of molecular flexibility and polar surface area metrics on oral bioavailability in the rat. *Journal of Medicinal Chemistry*, **47**, 6104–6107.

41 Clark, R.D. and Wolohan, P.R.N. (2003) Molecular design and bioavailability. *Current Topics in Medicinal Chemistry*, **3**, 1269–1288.

42 Livingstone, D.J. (2003) Theoretical property predictions. *Current Topics in Medicinal Chemistry*, **3**, 1171–1192.

43 Tetko, I.V. and Livingstone, D.J. (2007) Rule-based systems to predict lipophilicity, in *ADME/Tox Approaches*, Vol. 5 (eds B. Testa and H. van de Waterbeemd), in

Comprehensive Medicinal Chemistry, 2nd edn, Elsevier, Oxford, pp. 649–668.

44 Livingstone, D.J., Ford, M.G., Huuskonen, J.J. and Salt, D.W. (2001) Simultaneous prediction of aqueous solubility and octanol/water partition coefficient based on descriptors derived from molecular structure. *Journal of Computer-Aided Molecular Design*, **15**, 741–752.

45 Jorgensen, W.L. and Duffy, E.M. (2002) Prediction of drug solubility from structure. *Advanced Drug Delivery Reviews*, **54**, 355–366.

46 Manallack, D.T., Tehan, B.G., Gancia, E., Hudson, B.D., Ford, M.G., Livingstone, D.J., Whitley, D.C. and Pitt, W.R. (2003) A consensus neural network-based technique for discriminating soluble and insoluble compounds. *Journal of Chemical Information and Computer Sciences*, **43**, 674–679.

47 Morris, J.J. and Bruneau, P.P. (2000) Prediction of physicochemical properties, in *Virtual Screening for Bioactive Molecules* (eds H.J. Böhm and G. Schneider), John Wiley & Sons, Ltd, Chichester, pp. 33–58.

48 Egan, W.J. and Lauri, G. (2002) Prediction of intestinal permeability. *Advanced Drug Delivery Reviews*, **54**, 273–289.

49 Kulkarni, A., Yi, H. and Hopfinger, A.J. (2002) Predicting Caco-2 cell permeation coefficients of organic molecules using membrane-interaction QSAR analysis. *Journal of Chemical Information and Computer Sciences*, **42**, 331–342.

50 van de Waterbeemd, H. and Gifford, E. (2003) ADMET in silico modelling: towards prediction paradise? *Nature Reviews Drug Discovery*, **2**, 192–204.

51 van de Waterbeemd, H. (2007) *In silico* models to predict oral absorption, in *ADME/Tox Approaches*, Vol. 5 (eds B. Testa and H. van de Waterbeemd), in *Comprehensive Medicinal Chemistry*, 2nd edn, Elsevier, Oxford, pp. 669–698.

52 Kratochwil, N.A., Huber, W., Muller, F., Kansy, M. and Gerber, P.R. (2002) Predicting plasma protein binding of drugs: a new approach. *Biochemical Pharmacology*, **64**, 1355–1374.

53 Stouch, T.R. and Gudmundsson, O. (2002) Progress in understanding the structure–activity relationships of P-glycoprotein. *Advanced Drug Delivery Reviews*, **54**, 315–328.

54 Zhang, E.Y., Phelps, M.A., Cheng, C., Ekins, S. and Swaan, P.W. (2002) Modeling of active transport systems. *Advanced Drug Delivery Reviews*, **54**, 329–354.

55 Jones, J.P., Mysinger, M. and Korzekwa, K.R. (2002) Computational models for cytochrome P450: a predictive electronic model for aromatic oxidation and hydrogen atom abstraction. *Drug Metabolism and Disposition: The Biological Fate of Chemicals*, **30**, 7–12.

56 Arimoto, R. (2006) Computational models for predicting interactions with cytochrome P 450 enzyme. *Current Topics in Medicinal Chemistry*, **6**, 1609–1618.

57 Boobis, A., Gundert-Remy, U., Kremers, P., Macheras, P. and Pelkonen, O. (2002) *In silico* prediction of ADME and pharmacokinetics. Report of an expert meeting organized by COST B15. *European Journal of Pharmaceutical Sciences*, **17**, 183–193.

58 Terfloth, L., Bienfait, B. and Gasteiger, J. (2007) Ligand-based models for the isoform specificity of cytochrome P450 3A4, 2D6, and 2C9 substrates. *Journal of Chemical Information and Modeling*, **47**, 1688–1701.

59 Sheridan, R.P., Korzekwa, K.R., Torres, R.A. and Walker, M.J. (2007) Empirical regioselectivity models for human cytochromes P450 3A4, 2D6, and 2C9. *Journal of Medicinal Chemistry*, **50**, 3173–3184.

60 Afzelius, L., Hasselgren Arnby, C., Broo, A., Carlsson, L., Isaksson, C., Jurva, U., Kjellander, B., Kolmodin, K., Nilsson, K., Raubacher, F. and Weidolf, L. (2007) State-of-the-art tools for computational site of metabolism predictions: comparative analysis, mechanistical insights, and

future applications. *Drug Metabolism Reviews*, **39**, 61–86.

61 Ekins, S., Nikolsky, Y. and Nikolskaya, T. (2005) Techniques: application of systems biology to absorption, distribution, metabolism, excretion and toxicity. *Trends in Pharmacological Sciences*, **26**, 202–209.

62 Greene, N., Judson, P.N., Langowski, J.J. and Marchant, C.A. (1999) Knowledge-based expert systems for toxicity and metabolism prediction: DEREK, StAR and METEOR. *SAR and QSAR in Environmental Research*, **10**, 299–314.

63 Testa, B., Balmat, A.L., Long, A. and Judson, P. (2005) Predicting drug metabolism? An evaluation of the expert system METEOR. *Chemistry & Biodiversity*, **2**, 872–885.

64 Crivori, P., Zamora, I., Speed, B., Orrenius, C. and Poggesi, I. (2004) Model based on GRID-derived descriptors for estimating CYP3A4 enzyme stability of potential drug candidates. *Journal of Computer-Aided Molecular Design*, **18**, 155–166.

65 Ekins, S., de Groot, M.J. and Jones, J.P. (2001) Pharmacophore and three dimensional quantitative structure–activity relationship methods for modelling cytochrome P450 active sites. *Drug Metabolism and Disposition: The Biological Fate of Chemicals*, **29**, 936–944.

66 Crivori, P. and Poggesi, I. (2006) Computational approaches for predicting CYP-related metabolism properties in the screening of new drugs. *European Journal of Medicinal Chemistry*, **41**, 795–808.

67 Kuhn, B., Jacobsen, W., Christians, U., Benet, L.Z. and Kollman, P.A. (2001) Metabolism of sirolimus and its derivative everolimus by cytochrome P450 3A4: insights from docking, molecular dynamics and quantum chemical calculations. *Journal of Medicinal Chemistry*, **44**, 2027–2034.

68 Afzelius, L., Raubacher, F., Karlén, A., Jörgensen, F.S., Andersson, T.B., Masimirembwa, C. and Zamora, I. (2004) Structural analysis of CYP2C9 and CYP2C5 and an evaluation of commonly used molecular modelling techniques. *Drug Metabolism and Disposition: The Biological Fate of Chemicals*, **32**, 1–12.

69 Boyer, S. and Zamora, I. (2002) New methods in predictive metabolism. *Journal of Computer-Aided Molecular Design*, **16**, 403–413.

70 van de Waterbeemd, H. and Jones, B.C. (2003) Predicting oral absorption and bioavailability. *Progress in Medicinal Chemistry*, **41**, 1–59.

71 Stouch, T.R., Kenyon, J.R., Johnson, S.R., Chen, X.-Q., Doweyko, A. and Li, Y. (2003) *In silico* ADME/Tox: why models fail. *Journal of Computer-Aided Molecular Design*, **17**, 83–92.

72 Yamashita, F. and Hashida, M. (2004) *In silico* approaches for predicting ADME properties of drugs. *Drug Metabolism and Pharmacokinetics*, **19**, 327–338.

73 Mager, D.E. (2006) Quantitative structure–pharmacokinetic/pharmacodynamic relationships. *Advanced Drug Delivery Reviews*, **58**, 1326–1356.

74 De Buck, S.S., Sinha, V.K., Fenu, L.A., Nijsen, M.J., Mackie, C.E. and Gilissen, R.A.H.J. (2007) Prediction of human pharmacokinetics using physiologically-based modelling: a retrospective analysis of 26 clinically tested drugs. *Drug Metabolism and Disposition: The Biological Fate of Chemicals*, **35**, 1766–1780.

75 Theil, F.-P., Guentert, T.W., Haddad, S. and Poulin, P. (2003) Utility of physiologically-based pharmacokinetic models to drug development and rational drug discovery candidate selection. *Toxicology Letters*, **138**, 29–49.

76 Dickins, M. and van de Waterbeemd, H. (2004) Simulation models for drug disposition and drug interactions. *Drug Discovery Today: Biosilico*, **2**, 38–45.

77 Germani, M., Crivori, P., Rocchetti, M., Burton, P.S., Wilson, A.G.E., Smith, M.E. and Poggesi, I. (2007) Evaluation of a basic physiologically-based pharmacokinetic model for simulating

the first-time-in-animal study. *European Journal of Pharmaceutical Sciences*, **31**, 190–201.

78 Andersen, M.E. (1995) Physiologically-based pharmacokinetic (PBPK) models in the study of the disposition and biological effects of xenobiotics and drugs. *Toxicology Letters*, **82/83**, 341–348.

79 Kuentz, M., Nick, S., Parrott, N. and Röthlisberger, D. (2006) A strategy for preclinical formulation development using GastroPlus as pharmacokinetic simulation tool and a statistical screening design applied to a dog study. *European Journal of Pharmaceutical Sciences*, **27**, 91–99.

80 Kawai, R., Lemaire, M., Steimer, J.-L., Bruelisauer, A., Niederberger, W. and Rowland, M. (1994) Physiologically-based pharmacokinetic study on a cyclosporine derivative, SDZ IMM 125. *Journal of Pharmacokinetics and Biopharmaceutics*, **22**, 327–365.

81 Charnik, S.B., Kawai, R., Nefelman, J.R., Lemaire, M., Niederberger, W. and Sato, H. (1995) Perspectives in pharmacokinetics. Physiologically-based pharmacokinetic modeling as a tool for drug development. *Journal of Pharmacokinetics and Biopharmaceutics*, **23**, 231–235.

82 Leahy, D.E. (2003) Progress in simulation modelling for pharmacokinetics. *Current Topics in Medicinal Chemistry*, **3**, 1257–1268.

83 Stoner, C.L., Cleton, A., Johnson, K., Oh, D.-M., Hallak, H. Brodfuehrer, Surendran, N. and Han, H.-K. (2004) Integrated oral bioavailability projection using *in vitro* screening data as a selection tool in drug discovery. *International Journal of Pharmaceutics*, **269**, 241–249.

84 Cai, H., Stoner, C., Reddy, A., Freiwald, S., Smith, D., Winters, R., Stankovic, C. and Surendran, N. (2006) Evaluation of an integrated *in vitro – in silico* PBPK (physiologically-based pharmacokinetic) model to provide estimates of human bioavailability. *International Journal of Pharmaceutics*, **308**, 133–139.

85 Verwei, M., Freidig, A.P., Havenaar, R. and Groten, J.P. (2006) Predicted serum folate concentrations based on *in vitro* studies and kinetic modelling are consistent with measured folate concentrations in humans. *The Journal of Nutrition*, **136**, 3074–3078.

86 Leeson, P.D. and Springthorpe, B. (2007) The influence of drug-like concepts on decision-making in medicinal chemistry. *Nature Reviews Drug Discovery*, **6**, 881–890.

87 Gu, C.H., Li, H., Levons, J., Leatz, K., Gandhi, R.B., Raghavan, K. and Smith, R.L. (2007) Predicting effect of food on extent of drug absorption based on physicochemical properties. *Pharmaceutical Research*, **24**, 1118–1130.

17
Simulations of Absorption, Metabolism, and Bioavailability

Michael B. Bolger, Robert Fraczkiewicz, and Viera Lukacova

Abbreviations

ACAT	Advanced compartmental absorption and transit model
ADMET	Absorption, distribution, metabolism, excretion, and toxicity
Caco-2	Adenocarcinoma cell line derived from human colon
CAT	Compartmental absorption and transit model
EPA	Environmental Protection Agency
FDA	Food and Drug Administration
GI	Gastrointestinal
MRTD	Maximal recommended therapeutic dose
P-gp	P-Glycoprotein
PK	Pharmacokinetics
PBPK	Physiologically-based pharmacokinetics
RBA	Ratio of the estimated estrogen receptor-binding affinities for 17b-estradiol divided by the affinity estimated for the unknown molecule
TEER	Transcellular epithelial electrical resistance

Symbols

C_p	Plasma concentration
$\Delta\log P$	Difference between log *P* in octanol/water and log *D* at a given pH
HIA%	Percent human intestinal absorption across apical membrane of the enterocyte.
log *D*	Logarithm of the distribution coefficient, usually in octanol/water at a specified pH
log *P*	Logarithm of the partition coefficient, usually in octanol/water (for neutral species)
MW	Molecular weight

P_{app}	Apparent permeability
pK_a	Ionization constant in water
S_w	Solubility
SITT	Small intestinal transit time (3.3 h = 199 min)
V	Volume
V_{ss}	Volume at steady state

17.1 Introduction

Ever since this chapter was first published in 2002, there has been an explosion of awareness and research in the area of *in silico* methods for early assessment of absorption and bioavailability [1–5]. Physiologically-based mechanistic gastrointestinal simulation and physiologically-based pharmacokinetic (PBPK) models of absorption and distribution are now routinely used to identify and rank drug discovery candidates with regard to their absorption, distribution, metabolism, excretion, and toxicity (ADMET) properties [6–12]. Biopharmaceutical property inputs for such simulations can be derived from *in silico* estimations or *in vitro* experiments [13, 14]. The one property that still requires experimental data for quantitative estimation is metabolism. However, computational approaches have advanced rapidly in the last few years [15]. Formulation of development candidates can be enhanced by using this same type of simulation [16]. A new area for computational approaches to absorption and bioavailability is the application of systems biology [17, 18]. Finally, model-based drug development and clinical trial simulation technology have become a mainstay for regulatory agencies [19–22].

The observed oral bioavailability and biological activity of a particular therapeutic agent can be broken down into components that reflect delivery to the intestine, liberation from formulated product (gastric emptying, intestinal transit, pH, and food), absorption from the lumen (dissolution, lipophilicity, particle size, and active transport), intestinal and hepatic first-pass metabolism, distribution into tissues, and subsequent excretion, and toxicity (ADMET) [23]. This chapter will focus on *in silico* approaches that have demonstrated ability to save valuable resources in the drug discovery and development process. We will review some of the recent advances in physiologically-based pharmacokinetics and discuss our results in simulating GI absorption by using the advanced compartmental absorption and transit model (ACAT).

17.2 Background

For the purposes of GI simulation, it is important to distinguish absorption (transfer of drug from the lumen of the intestine across the apical membrane into the

enterocyte) from bioavailability (the fraction of administered dose that is available in the systemic circulation for interaction with the target tissue). Simulation of absorption and bioavailability must account for many factors that fall into three classes [24]. The first class represents physicochemical factors including pK_a, solubility, stability, diffusivity, lipophilicity, and salt forms. The second class comprises physiological factors including GI pH, gastric emptying, small and large bowel transit times, active transport and efflux, and gut wall and liver metabolism. The third class comprises formulation factors such as surface area, drug particle size and crystal form, and dosage forms such as solution, tablet, capsule, suspension, and modified release.

An early concept governing oral absorption of organic molecules was called the "pH-partition" hypothesis. Under this hypothesis, only the unionized form of ionizable molecules was thought to partition into the membranes of epithelial cells lining the GI tract [25, 26]. The contribution of pH to permeability and dissolution of solid dosage forms has been proven to be a critical factor, but ionized molecules have now been shown to be absorbed by a variety of mechanisms [27]. Ho and colleagues developed one of the most sophisticated early theoretical approaches to simulating drug absorption based on the diffusional transport of drugs across a compartmental membrane [28–30]. Their physical model consisted of a well-stirred bulk aqueous phase, an aqueous diffusion layer, and a heterogeneous lipid barrier composed of several compartments ending in a perfect sink. Their model represented the first example of the rigorous application of a physical model to the quantitative and mechanistic interpretation of *in vivo* absorption [31]. The simultaneous chemical equilibria and mass transfer of basic and acidic drugs were modeled and compared favorably to *in situ* measurements of intestinal, gastric, and rectal absorption in animals. The pH-partition theory was shown to be a limiting case of the more general model they developed. Because of its complexity, the diffusional mass transit model has not been widely used. In the 1980s, a simple and intuitive alternative approach based on a series of mixing tank compartments was developed [32]. Pharmacokinetic models incorporating discontinuous GI absorption from at least two absorption sites separated by N nonabsorbing sites have been used to explain the occurrence of double peaks in plasma concentration versus time (C_p–time) profiles for ranitidine and cimetidine [33]. A similar discontinuous oral absorption model based on two absorption compartments and two transit compartments was developed to explain the bioavailability of nucleoside analogues [34]. Amidon and Yu developed a compartmental absorption and transit model (CAT) of the GI tract based on seven equal transit time compartments [24]. Using a five-compartment GI simulation model, Norris *et al*. were able to estimate C_p–time profiles for ganciclovir [35, 36]. A physiologically-based segregated flow model (SFM) was developed to examine the influence of intestinal transport (absorption and exsorption), metabolism, flow, tissue-partitioning characteristics, and elimination in other organs on intestinal clearance, intestinal availability, and systemic bioavailability [37]. Using a completely different approach, a stochastic simulation of drug molecules moving through a cylinder of fixed radius with random geometric placement of dendritic-type virtual "villi" was able to accurately

account for the observed human SI transit time distribution [38, 39]. Ito *et al*. have developed a pharmacokinetic model for drug absorption that includes metabolism by CYP3A4 inside the epithelial cells, P-gp mediated efflux into the lumen, intracellular diffusion from the luminal side to the basal side, and subsequent permeation through the basal membrane [40]. As expected, they demonstrated that the fraction of dose into the portal vein was synergistically elevated by simultaneous inhibition of both CYP3A4 and P-gp. The Simcyp Consortium Project has compiled extensive demographic and physiological data to build virtual human populations and has demonstrated good prediction of *in vivo* pharmacokinetic profiles using *in vitro* data and a simulation approach similar to the CAT model [41]. In contrast to the compartmental absorption and transit model, others have developed a simulation of the GI tract modeled as a continuous tube with spatially varying properties and continuous plug flow with dispersion of drug molecules [42, 43].

We demonstrated the utility of GI absorption simulation based on the ACAT in predicting the impact of physiological and biochemical processes on oral drug bioavailability [44, 45].

The ACAT model is loosely based on the work of Amidon and Yu who found that seven equal transit time compartments are required to represent the observed cumulative frequency distribution for small intestine transit times [24]. Their original CAT was able to explain the oral plasma concentration profiles of atenolol [46].

17.3
Use of Rule-Based Computational Alerts in Early Discovery

17.3.1
Simple Rules for Drug Absorption (Druggability)

In silico ADMET profiling of compound libraries in early discovery has become a valuable addition to the research toolbox of computational and medicinal chemists. A computational alert was developed by Lipinski based on the physicochemical characteristics of approximately 90% of 2245 drugs with USAN names that have had clinical exposure found in the World Drug Index [47]. Most of these drugs have entered at least phase-II clinical trials. The rule-of-5 has had a significant impact on early drug discovery and has stimulated development of similar computational alerts [48–52]. Application of a computational alert to compound libraries prior to synthesis helps limit the requirement of *in vitro* testing to those compounds that are most likely to have "drug-like" characteristics.

We have developed a new set of rules, called "ADMET Risk," that contains cutoffs for human jejunal permeability, pH of a saturated solution of the drug in water, partial charge on H-bond donors and acceptors, an indicator variable for permanent cations, and a low-level cutoff for log *P*. The ADMET Risk rules and two-letter abbreviations are listed as follows:

LP $S + \log P < -1.006$
Pr $S + P_{\text{eff}} < 0.314$
pH $S + \text{pH} < 3.12$
Hd HBDCH > 1.34
Ha HBACH < −6.6
PC QuaAmine_>[N+]>0,

where $S + \log P$ represents Simulations Plus artificial neural network model of log P (octanol/water); $S + P_{\text{eff}}$ represents Simulations Plus predicted human jejunal effective permeability; $S + \text{pH}$ represents Simulations Plus estimation of the pH of a saturated solution of the drug in pure water; HBDCH represents partial charge on hydrogen-bond donors; HBACH represents partial charge on hydrogen-bond acceptors; and QuaAmine_>[N+] represents an indicator variable for the presence of quaternary amines, sulfonium cations, or diazonium cations.

All the descriptors and properties necessary to calculate ADMET Risk are generated by the software program ADMET Predictor (formerly called QMPRPlus) (Simulations Plus, Inc.). The current set of ADMET Predictor computational models for biopharmaceutical properties is listed below:

- multiprotic ionization constants (pK_a);
- log P ($\log_{10}$ of octanol–water partition coefficient for unionized molecules);
- log D ($\log_{10}$ of octanol–water distribution coefficient for all molecular species);
- effective permeability (human jejunum) (P_{eff}, cm/s $\times 10^4$);
- average effective permeability (entire small intestine) (P_{avg}, cm/s $\times 10^4$);
- MDCK cell monolayer permeability (P_{app}, nm/s);
- blood–brain barrier permeation (high, low, undecided)
- saturated aqueous solubility in pure water (mg/ml);
- saturated aqueous pH in pure water;
- saturated intrinsic solubility in pure water (mg/ml);
- saturated solubility at user-specified pH (mg/ml);
- salt solubility factor;
- diffusivity (diffusion coefficient, cm^2/s);
- molal volume (cm^3/mol);
- percentage unbound to blood plasma proteins (%);
- pharmacokinetic volume of distribution (l/kg);
- maximum recommended therapeutic dose (mg/kg/day);
- estrogen receptor toxicity;
- lethal acute toxicity against fathead minnow (mg/l/96 h);
- affinity toward hERG K^+ channel (a measure of cardiac toxicity);
- carcinogenicity in rats and mice;
- Ames mutagenicity in *Salmonella*;
- metabolism rate constants ($V_{\max}$, K_m) for five main CYP enzymes in human (1A2, 2C19, 2C9, 2D6, and 3A4);
- inhibition of HIV-1 integrase;
- simulated fraction absorbed in human.

These models are based on the calculation of 297 molecular descriptors obtained by parsing the 2D or 3D structures of drug molecules as represented either in SMILES string format or as ISIS-.RDF, .SDF, or .MOL file format (MDL Information Systems, Inc., http://www.mdli.com/). Molecular descriptor values are used as inputs to independent mathematical models to generate estimates for each of the biopharmaceutical properties listed above. Using these property estimates or experimentally determined properties as inputs to the ACAT model, drug molecules may be classified according to their ADMET qualities. While no computer program is able to estimate the exact experimental values for these properties, we have demonstrated that the estimated values generated by our method are sufficiently accurate to allow rank ordering of a large number of compounds for "overall ADMET quality." In fact, *in vitro* methods also fail to predict *in vivo* ADMET properties under certain conditions. We have found that the *in silico* methods are comparable to *in vitro* methods for predictive capability.

We tested the usefulness of these *in silico* biopharmaceutical properties in predicting the rank order of human intestinal absorption (HIA%). The percentage absorbed for 266 drug molecules was collected from various literature sources [53, 54]. These drugs are known to be absorbed by a number of mechanisms including passive transcellular, passive paracellular, and active transport mechanism and some were actively effluxed. Starting from three-dimensional structures calculated by CORINA (http://www2.ccc.uni-erlangen.de/software/corina/), we used ADMET Predictor to generate molecular descriptors, to estimate the biopharmaceutical properties, and to calculate the ADMET Risk values as described above.

Results from ADMET Predictor using a rule-based method were first ranked by the value of ADMET Risk and, within an ADMET Risk category (0–5), were ranked by increasing permeability (*in silico* estimate of human effective permeability). Table 17.1 lists the experimental HIA% and compares their rank order with the rank order predicted for 266 drugs using the rule-based method. We found a significant Spearman rank correlation coefficient of 0.70 ($p < 0.001$) when the rule-based method of predicting the rank order of oral faction absorbed was applied to 209 passively absorbed compounds. Figure 17.1 shows a plot of the experimental rank order compared with the ADMET Risk-based rank order method for 209 compounds that are known to be absorbed through a passive transcellular or paracellular route. It can be seen that there is a good correlation for the passively absorbed compounds. By contrast, Figure 17.2 shows a similar plot for the 43 compounds that are known to be absorbed by an active route or are known to be actively effluxed. For these compounds the correlation is nonexistent.

In a comparison between Lipinski's rules and the ADMET Risk, we have found that the "rule-of-5" accurately identifies only a fraction of the compounds that have experimental absorption less than 50%. This high false-positive result allows many of the poor compounds to go undetected. By contrast, the ADMET Risk identifies a much higher fraction of the unfavorable compounds in addition to many of the well-absorbed compounds.

ADMET Predictor was used to generate *in silico* estimates of log *P*, aqueous solubility, the pH of a saturated solution in water, partial charges on H-bond donors

Table 17.1 Table of 266 common drugs used in the comparison of rule-based ranking with mechanistic simulation-based ranking.

Name	HIA%	F_a rank	ADMET Risk	AR rank	Active transport	Smiles
AAFC	32	22	3	17	n/a	FC1N2C(=NC(=N)C=1)OC3C2OC(C3O)CO
Acarbose	2	9	4	1	n/a	O=CC(C(C(OC1OC(C(OC2OC(C(NC3C=C(C(O)C(O)C3O)CO)C(O)C2O)C)C(O)C1O)CO)C(O)CO)O)O
Acebutolol	80	50	0	79	n/a	C(=O)(c1c(OCC(O)CNC(C)C)ccc(NC(=O)CCC)c1)C
Acetaminophen	80	51	0	87	n/a	C(=O)(Nc1ccc(O)cc1)C
Acetylsalicylic acid	84	58	1	53	n/a	C(=O)(Oc1c(C(=O)O)cccc1)C
Acrivastine	88	39	0	46	n/a	C(c1nc(C=CC(=O)O)ccc1)(c2ccc(cc2)C)=CCN3CCCC3
Acyclovir	23	15	3	18	n/a	O=C1c2c(N=C(N1)N)n(cn2)COCCO
Adefovir	16	13	4	9	n/a	O=P(O)(O)COCCn1c2c(c(ncn2)N)nc1
Adriamycin	5	18	3	26	P-gp	C(=O)(C1(O)C(OC2OC(C(O)C(N)C2)C)Cc3c(c4C(=O)c5c(OC)cccc5C(=O)c4c(c3C1)O)O)CO
Allopurinol	90	151	0	143	Hypoxanthine	c12c(ncnc1[nH]nc2)O
Alpha-difluoromethylornithine	55	70	3	34	CAT1?	C(C(C(F)F)(CCCN)N)(=O)O
Alprazolam	90	49	0	71	n/a	Clc1cc2C(c3ccccc3)=NCc4nnc(n4-c2cc1)C
Alprenolol	93	81	0	121	n/a	O(c1c(cccc1)CC=C)CC(O)CNC(C)C
Amantadine	95	85	0	62	n/a	C12(N)CC3CC(C1)CC(C2)C3
Amiloride	50	65	1	91	n/a	C(=O)(c1c(nc(c(Cl)n1)N)N)NC(=N)N
Aminopyrine	100	123	0	113	n/a	N(C1C(=O)N(c2ccccc2)N(C=1C)C)(C)C
Amoxicillin	93	171	2	58	PepT1	C(=O)(C(c1ccc(O)cc1)N)NC2C(=O)N3C(C(=O)O)C(SC32)(C)C
Amphetamine	90	46	0	62	n/a	c1(ccccc1)CC(N)C
Amphotericin B	3	10	3	12	n/a	C(=O)(O)C1C2OC(O)(CC1O)CC(O)CC(O)C(O)CCC(O)CC(O)CC(=O)OC(C(C)O)C(C=CC=CC=CC=CC=CC=CC(OC3OC(C(O)C(C3O)N)C)C2)C)C)C

(*Continued*)

Table 17.1 (*Continued*)

Name	HIA%	F_a rank	ADMET Risk	AR rank	Active transport	Smiles
Ampicillin	62	84	2	60	PepT1	C(=O)(C(c1ccccc1)N)NC2C(=O)N3C(C(=O)O)C(SC32)(C)C
Amrinone	93	52	0	61	n/a	O=C1C(=CC(c2ccncc2)=CN1)N
Antipyrine	97	98	0	117	n/a	O=C1N(c2ccccc2)N(C(=C1)C)C
Ascorbic acid	35	23	4	11	n/a	O=C1C(=C(O)C(O1)C(O)CO)O
Atenolol	50	29	1	49	n/a	C(=O)(Cc1ccc(OCC(O)CNC(C)C)cc1)N
Atropine	98	58	0	37	n/a	C(=O)(OC1CC2N(C(C1)CC2)C)C(c3ccccc3)CO
Azithromycin	37	24	3	15	n/a	N(C1C(O)C(OC2C(O)(CC(CN(C(C(C(O)(C(OC(=O)C(C(OC3OC(C(C(OC)(C3)C)O)C)C2C)C)CC)C)O)C)C)C)OC(C1)C)(C)C
Azosemide	20	11	1	28	n/a	O=S(=O)(c1c(Cl)cc(c(-c2nnn[nH]2)c1)NCc3sccc3)N
Aztreonam	1	5	3	20	n/a	C(C(=O)NC1C(=O)N(S(=O)(=O)O)C1C)(=NOC(C(=O)O)(C)C)C2=CS=C(N2)N
Benazepril	37	14	0	52	n/a	C(=O)(OCC)C(NC1C(=O)N(c2c(cccc2)CC1)CC(=O)O)CCc3ccccc3
Benserazide	90	74	2	30	n/a	C(=O)(C(CO)N)NNCc1c(c(c(O)cc1)O)O
Benzylpenicillin	30	42	1	104	Intes. pept. carrier	C(=O)(NC1C(=O)N2C(C(=O)O)C(SC21)(C)C)Cc3ccccc3
Betaxolol	90	45	0	50	n/a	O(c1ccc(cc1)CCOCC2CC2)CC(O)CNC(C)C
Bornaprine	100	72	0	53	n/a	C(=O)(OCCCN(CC)CC)C1(c2ccccc2)C3CC(C1)CC3
Bretyliumtosylate	23	31	3	38	n/a	Brc1c(cccc1)C[N+](CC)(C)C
Bromazepam	84	59	0	100	n/a	O=C1Nc2c(C(c3ncccc3)=NC1)cc(Br)cc2
Bromocriptine	28	38	1	78	n/a	C(=O)(NC1(C(=O)N2C(O1)(O)C3N(C(=O)C2CC(C)C)CCC3)C(C)C)C4C=C5c6c7c(c(Br)[nH]c7ccc6)CC5N(C4)C
Bumetanide	96	189	1	100	Bile acid	C(=O)(c1cc(S(=O)(=O)N)c(Oc2ccccc2)c(NCCCC)c1)O
Bupropion	87	66	0	116	n/a	C(=O)(c1cc(Cl)ccc1)C(NC(C)(C)C)C
Caffeine	100	118	0	96	n/a	O=C1c2c(ncn2C)N(C(=O)N1C)C
Camazepam	100	134	0	130	n/a	C(N(C)C)(=O)OC1C(=O)N(c2c(C(c3ccccc3)=N1)cc(Cl)cc2)C

Capreomycin	50	63	4	8	n/a	C(=O)(NCC1C(=O)NC(C(=O)NC(C(=O)NCC(C(=O)NC(C(=O)N1)C)N)C2NC(=N)NCC2)=CNC(=O)N)CC(CCCN)N
Captopril	84	126	1	115	Intes. pept. carrier	C(=O)(N1C(C(=O)O)CCC1)C(CS)C
Carbamazepine	97	97	0	112	n/a	C(=O)(N1c2c(cccc2)CCc3c1cccc3)N
Carfecillin	99	207	0	147	Intes. pept. carrier	C(=O)(Oc1ccccc1)C(C(=O)NC2C(=O)N3C(C(=O)O)C(SC32)(C)C)c4ccccc4
Cefadroxil	100	220	2	61	Intes. pept. carrier	C(=O)(C1=C(CSC2N1C(=O)C2NC(=O)C(c3ccc(O)cc3)N)C)O
Cefatrizine	75	100	2	57	Intes. pept. carrier	C(=O)(C1=C(CSc2cnn[nH]2)CSC3N1C(=O)C3NC(=O)C(c4ccc(O)cc4)N)O
Cefetametpivoxil	47	26	1	48	n/a	C(C(=O)NC1C(=O)N2C(C(=O)OCOC(C(C)(C)C)=O)=C(CSC21)C)(=NOC)C3=CS=C(N3)N
Ceftizoxime	72	97	2	52	n/a	C(C(=O)NC1C(=O)N2C(C(=O)O)=CCSC21)(=NOC)C3=CSC(=N)N3
Ceftriaxone	1	6	2	29	n/a	C(C(=O)NC1C(=O)N2C(C(=O)O)=C(CSC3=NC(=O)C(=O)NN3C)CSC21)(=NOC)C4=CS=C(N4)N
Cefuroxime	1	3	4	5	n/a	C(C(=O)NC1C(=O)N2C(C(=O)O)=C(COC(=O)N)CSC21)(=NOC)c3occc3
Cefuroximeaxetil	44	56	2	41	n/a	C(C(=O)NC1C(=O)N2C(C(=O)OC(OC(=O)C)C)=C(COC(=O)N)CSC21)(=NOC)c3occc3
Cephalexin	100	224	2	62	PepT1	C(=O)(C1=C(CSC2N1C(=O)C2NC(=O)C(c3ccccc3)N)C)O
Chloramphenicol	90	78	1	59	n/a	C(=O)(C(Cl)Cl)NC(C(c1ccc([N+](=O)[O-])cc1)O)CO
Chlorothiazide	49	27	1	33	n/a	O=S(=O)(c1c(Cl)cc2c(S(=O)(=O)NC=N2)c1)N
Cicaprost	100	69	0	43	n/a	C(#CC1C(O)CC2C1CC(=CCOCC(=O)O)C2)C(C(CC#CCC)C)O
Cidofovir	3	4	5	1	n/a	O=P(O)(O)COC(CN1C(=O)NC(=CC1)N)CO
Cimetidine	64	22	1	19	n/a	C(#N)N=C(NCCSCC1=NC=NC1C)NC
Ciprofloxacin	69	24	2	14	n/a	C(=O)(C1C(=O)c2c(N(C=1)C3CC3)cc(c(F)c2)N4CCNCC4)O
Cisapride	100	116	0	91	n/a	C(=O)(c1c(OC)cc(c(Cl)c1)N)NC2C(OC)CN(CCCOc3ccc(F)cc3)CC2

(*Continued*)

Table 17.1 (*Continued*)

Name	HIA%	F_a rank	ADMET Risk	AR rank	Active transport	Smiles
Clofibrate	97	99	0	131	n/a	C(C(Oc1ccc(Cl)cc1)(C)C)(=O)OCC
Clonazepam	98	104	0	111	n/a	O=C1Nc2c(C(c3c(Cl)cccc3)=NC1)cc([N+](=O)[O-])cc2
Clonidine	95	92	0	110	n/a	N(c1c(Cl)cccc1Cl)=C2NCCN2
Codeine	95	86	0	64	n/a	O(c1c2c3c(cc1)CC4N(CCC35C(O2)C(O)C=CC54)C)C
Corticosterone	100	106	1	42	n/a	C(=O)(C1C2(C(C3C(C4(C(=CC(=O)CC4)CC3)C)C(O)C2)CC1)C)CO
Cromolyn sodium	0.4	2	2	44	n/a	C(=O)(C1Oc2c(C(=O)C=1)c(OCC(O)COc3c4C(=O)C=C(C(=O)O)Oc4ccc3)ccc2)O
Cycloserine	73	99	1	89	hPAT1	O=C1C(N)CON1
Cymarin	47	18	1	16	n/a	O=C1OCC(=C1)C2C3(C(O)(C4C(C5(C(O)(CC(OC6OC(C(O)C(OC)C6)C)CC5)CC4)C=O)CC3)CC2)C
Cyproterone acetate	100	109	0	67	n/a	C(=O)(OC1(C(=O)C)C2(C(C3C=C(Cl)C4C(C5C(C(=O)C=4)C5)(C3CC2)C)CC1)C)C
Desipramine	100	73	0	73	n/a	c12c(cccc1)CCc3c(N2CCCNC)cccc3
Dexamethasone	80	30	1	22	n/a	C(=O)(C1(C2(C(C3C(F)(C4(C(=CC(=O)C=C4)CC3)C)C(O)C2)CC1C)C)O)CO
Diazepam	100	131	0	127	n/a	O=C1N(c2c(C(c3ccccc3)=NC1)cc(Cl)cc2)C
Diclofenac	100	264	0	259	n/a	C(=O)(O)Cc1c(Nc2c(Cl)cccc2Cl)cccc1
Diflunisal	100	135	0	132	n/a	C(=O)(c1c(O)ccc(-c2c(F)cc(F)cc2)c1)O
Digoxin	81	33	3	6	OATP/P-gp	O=C1OCC(=C1)C2C3(C(O)(C4C(C5(C(CC(OC6OC(C(OC7OC(C(OC8OC(C(O)C(O)C8)C)C(O)C7)C)C(O)C6)C)CC5)CC4)C)CC3O)CC2)C
Dihydrocodeine	89	40	0	35	n/a	O(c1c2c3c(cc1)CC4N(CCC35C(O2)C(O)CCC54)C)C
Diltiazem	100	115	0	89	n/a	C(=O)(OC1C(=O)N(c2c(SC1c3ccc(OC)cc3)cccc2)CCN(C)C)C
Distigmine	8	7	3	12	n/a	C(N(CCCCCCN(C(=O)Oc1c[n+](ccc1)C)C)C)(=O)Oc2c[n+](ccc2)C

Disulfuram	97	55	0	57	n/a	C(N(CC)CC)(=S)SSC(N(CC)CC)=S
Doxorubicin	12	8	3	7	n/a	C(=O)(C1(O)Cc2c(c3C(=O)c4c(C(=O)c3c(c2C(OC5OC(C(O)C(N)C5)C)C1)O)c(OC)ccc4)O)CO
Enalapril	66	90	0	185	Intes. pept. carrier	C(=O)(OCC)C(NC(C(=O)N1C(C(=O)O)CCC1)C)CCc2ccccc2
Enalaprilat	25	16	2	26	n/a	C(=O)(N1C(C(=O)O)CCC1)C(NC(C(=O)O)CCc2ccccc2)C
Erythromycin	35	13	3	9	n/a	N(C1C(O)C(OC2C(O)(CC(C(=O)C(C(C(O)(C(OC(=O)C(C(OC3OC(C(C(OC)(C3)C)O)C)C2C)C)CC)C)O)C)C)C)OC(C1)C)(C)C
Ethambutol	80	52	1	57	n/a	C(NCCNC(CO)CC)(CO)CC
Ethinylestradiol	100	74	0	54	n/a	C(C1(C2(C(C3C(c4c(cc(O)cc4)CC3)CC2)CC1)C)O)#C
Etoposide	50	64	3	24	P-gp	O=C1OCC2C(OC3OC4C(OC(OC4)C)C(O)C3O)c5c(cc6c(OCO6)c5)C(c7cc(OC)c(c(OC)c7)O)C12
Famciclovir	77	47	0	61	n/a	C(=O)(OCC(COC(=O)C)CCn1c2c(nc1)cnc(n2)N)C
Famotidine	38	25	3	13	n/a	C(=NS(=O)(=O)N)(CCSCc1nc(N=C(N)N)sc1)N
Felbamate	90	42	1	26	n/a	C(=O)(OCC(c1ccccc1)COC(=O)N)N
Felodipine	88	69	0	83	n/a	C(=O)(OCC)C1=C(NC(=C(C(=O)OC)C1c2c(Cl)c(Cl)ccc2)C)C
Fenclofenac	100	136	0	133	n/a	C(=O)(O)Cc1c(Oc2c(Cl)cc(Cl)cc2)cccc1
Fenoterol	60	38	1	54	n/a	c1(C(O)CNC(Cc2ccc(O)cc2)C)cc(O)cc(O)c1
Flecainide	81	34	0	69	n/a	C(=O)(c1c(OCC(F)(F)F)ccc(OCC(F)(F)F)c1)NCC2NCCCC2
Fluconazole	95	53	0	51	n/a	C(c1c(F)cc(F)cc1)(O)(Cn2ncnc2)Cn3ncnc3
Flumazenil	95	89	0	77	n/a	C(=O)(OCC)C1=NCN2c3c(C(=O)N(CC12)C)cc(F)cc3
Fluoxetine	80	54	0	135	n/a	C(F)(F)(F)c1ccc(OC(c2ccccc2)CCNC)cc1
Fluvastatin	100	226	1	111	n/a	C(=O)(O)CC(O)CC(C=Cc1c(c2c(n1C(C)C)cccc2)-c3ccc(F)cc3)O
Foscarnet	17	14	3	21	n/a	C(=O)(P(=O)(O)O)O
Fosfomycin	31	21	3	14	n/a	O=P(O)(O)C1OC1C
Fosinopril	36	50	0	144	n/a	C(=O)(OC(OP(=O)(CC(=O)N1C(C(=O)O)CC(C2CCCCC2)C1)CCCCc3ccccc3)C(C)C)CC
Fosmidomycin	30	19	4	10	n/a	N(C=O)(O)CCCP(=O)(O)O

(*Continued*)

Table 17.1 (*Continued*)

Name	HIA%	F_a rank	ADMET Risk	AR rank	Active transport	Smiles
Furosemide	61	39	2	23	n/a	C(=O)(c1c(NCc2occc2)cc(Cl)c(S(=O)(=O)N)c1)O
Gabapentin	59	34	1	45	LAT1	C(=O)(O)CC1(CN)CCCCC1
Gallopamil	100	127	0	119	n/a	C(C(c1cc(OC)c(OC)c(OC)c1)(C(C)C)CCCN(CCc2cc(OC)c(OC)cc2)C)#N
Ganciclovir	3	5	3	8	n/a	O=C1c2c(N=C(N1)N)n(cn2)COC(CO)CO
Gentamicin	1	2	4	4	n/a	O(C1OC(C(NC)C)CCC1N)C2C(O)C(OC3OCC(O)(C(NC)C3O)C)C(N)CC2N
Gliclazide	65	42	1	35	n/a	C(=O)(NS(=O)(=O)c1ccc(cc1)C)NN2CC3C(C2)CCC3
Glipizide	100	105	1	34	n/a	C(=O)(c1ncc(nc1)C)NCCc2ccc(S(=O)(=O)NC(=O)NC3CCCCC3)cc2
Glyburide	100	71	0	34	n/a	C(=O)(c1c(OC)ccc(Cl)c1)NCCc2ccc(S(=O)(=O)NC(=O)NC3CCCCC3)cc2
Glycine	100	236	1	118	hPAT1	C(=O)(O)CN
Granisetron	100	113	0	82	n/a	C(=O)(c1c2c(n(n1)C)cccc2)NC3CC4N(C(C3)CCC4)C
Guanabenz	80	31	1	30	n/a	C(=N)(NN=Cc1c(Cl)cccc1Cl)N
Guanoxan	50	28	1	46	n/a	C(=N)(NCC1Oc2c(OC1)cccc2)N
Hydrochlorothiazide	65	23	2	13	n/a	O=S(=O)(c1c(Cl)cc2c(S(=O)(=O)NCN2)c1)N
Hydrocortisone	91	79	1	41	n/a	C(=O)(C1(C2(C(C3C(C4(C(=CC(=O)CC4)CC3)C)C(O)C2)CC1)C)O)CO
Ibuprofen	95	93	0	124	n/a	C(=O)(C(c1ccc(cc1)CC(C)C)C)O
Imipramine	100	133	0	129	n/a	N(CCCN1c2c(cccc2)CCc3c1cccc3)(C)C
Indapamide	97	96	0	95	n/a	C(=O)(c1cc(S(=O)(=O)N)c(Cl)cc1)NN2c3c(cccc3)CC2C
Indomethacin	100	124	0	114	n/a	C(=O)(c1ccc(Cl)cc1)n2c3c(c(c2C)CC(=O)O)cc(OC)cc3
Iothalamate sodium	1.9	8	1	58	n/a	C(=O)(c1c(I)c(C(=O)O)c(I)c(c1I)NC(=O)C)NC
Isoniazid	80	28	0	48	n/a	C(=O)(c1ccncc1)NN
Isoxicam	100	67	0	42	n/a	C(=O)(C1=C(c2c(S(=O)(=O)N1C)cccc2)O)NC3=CC(ON3)C

Isradipine	92	50	1	18	n/a	C(=O)(OC(C)C)C1=C(NC(=C(C(=O)OC)C1c2c3c(ccc2)NON3)C)C
Kanamycin	1	4	4	6	n/a	O(C1OC(C(O)C(C1O)N)CO)C2C(O)C(OC3OC(C(O)C(O)C3O)CN)C(N)CC2N
Ketoprofen	92	51	0	74	n/a	C(=O)(c1cc(C(C(=O)O)C)ccc1)c2ccccc2
Ketorolac	90	76	0	92	n/a	C(=O)(c1n2c(cc1)C(C(=O)O)CC2)c3ccccc3
K-Strophanthoside	16	12	4	4	n/a	O=C1OCC(=C1)C2C3(C(O)(C4C(C5(C(O)(CC(OC6OC(C(OC7OC(C(OC8OC(C(O)C(O)C8O)CO)C(O)C7O)CO)C(OC)C6)C)CC5)CC4)C=O)CC3)CC2)C
Labetalol	95	91	1	60	n/a	C(=O)(c1c(O)ccc(C(O)CNC(CCc2ccccc2)C)c1)N
Lactulose	0.6	2	4	8	n/a	O(C1OC(C(O)C(O)C1O)CO)C2C(C(OC2CO)(O)CO)O
Lamivudine	87	65	2	22	n/a	O=C1N(C2OC(SC2)CO)CC=C(N1)N
Lamotrigine	98	59	1	31	n/a	Clc1c(Cl)cccc1-c2c(nc(nn2)N)N
Lansoprazole	85	61	0	120	n/a	C(F)(F)(F)COc1c(c(ncc1)CS(=O)c2nc3c(cccc3)[nH]2)C
Leucine	100	247	1	127	B(0)AT2	C(=O)(C(CC(C)C)N)O
Levodopa	86	136	2	65	LAT1	C(=O)(C(Cc1cc(c(O)cc1)O)N)O
Levonorgestrel	100	75	0	45	n/a	C(C1(C2(C(C3C(C4C(=CC(=O)CC4)CC3)CC2)CC1)CC)O)#C
Lincomycin	28	17	2	24	n/a	C(=O)(NC(C(O)C)C1OC(SC)C(O)C(O)C1O)C2N(CC(CCC)C2)C
Lisinopril	28	37	2	46	Intes. pept. carrier	C(=O)(N1C(C(=O)O)CCC1)C(NC(C(=O)O)CCc2ccccc2)CCCCN
Loracarbef	100	232	2	64	Intes. pept. carrier	C(=O)(C1=C(Cl)CCC2N1C(=O)C2NC(=O)C(c3ccccc3)N)O
Lormetazepam	100	130	0	126	n/a	O=C1N(c2c(C(c3c(Cl)cccc3)=NC1O)cc(Cl)cc2)C
Lornoxicam	100	126	0	118	n/a	C(=O)(C1=C(C2C(S(=O)(=O)N1C)C=C(Cl)S=2)O)Nc3ncccc3
Lovastatin	10	21	0	150	OATP/P-gp	C(=O)(OC1C2C(C=CC(C2CCC3OC(=O)CC(O)C3)C)=CC(C1)C)C(CC)C
Mannitol	16	9	2	15	n/a	C(C(C(O)CO)O)(C(O)CO)O
Meloxicam	90	43	0	59	n/a	C(=O)(C1=C(c2c(S(=O)(=O)N1C)cccc2)O)Nc3ncc(s3)C
Mercaptoethanesulfonic acid	77	104	2	59	Influx?	O=S(=O)(O)CCS
Metaproterenol	44	17	1	25	n/a	c1(C(O)CNC(C)C)cc(O)cc(O)c1

(*Continued*)

Table 17.1 (*Continued*)

Name	HIA%	F_a rank	ADMET Risk	AR rank	Active transport	Smiles
Metformin	53	31	3	19	hOCT1/PMAT	C(N(C)C)(=N)NC(=N)N
Methadone	80	32	0	75	n/a	C(C(c1ccccc1)(c2ccccc2)CC(N(C)C)C)(=O)CC
Methotrexate	70	93	3	35	RFCP	C(=O)(c1ccc(N(Cc2nc3c(nc(nc3N)N)nc2)C)cc1)NC(C(=O)O)CCC(=O)O
Methyldopa	41	15	3	11	n/a	C(C(Cc1cc(c(O)cc1)O)(N)C)(=O)O
Methylprednisolone	82	56	1	40	n/a	C(=O)(C1(C2(C(C3C(C4(C(=CC(=O)C=C4)C(C3)C)C)C(O)C2)CC1)C)O)CO
Metolazone	64	41	0	72	n/a	O=S(=O)(c1c(Cl)cc2c(C(=O)N(c3c(cccc3)C)C(N2)C)c1)N
Metoprolol	95	90	0	102	n/a	O(c1ccc(cc1)CCOC)CC(O)CNC(C)C
Mexiletine	100	132	0	128	n/a	O(c1c(cccc1C)C)CC(N)C
Mibefradil	69	25	0	49	n/a	C(=O)(OC1(C(c2c(cc(F)cc2)CC1)C(Cl)C)CCN(CCCc3nc4c(cccc4)[nH]3)C)COC
Miconazole	25	34	0	263	P-gp	O(C(c1c(Cl)cc(Cl)cc1)Cn2cncc2)Cc3c(Cl)cc(Cl)cc3
Mifobate	82	57	0	136	n/a	O=P(OC(P(=O)(OC)OC)c1ccc(Cl)cc1)(OC)OC
Minoxidil	98	57	1	21	n/a	C1(=NC(N(C(=C1)N)O)N)N2CCCCC2
Morphine	85	37	0	36	n/a	c12c3c(O)ccc1CC4N(CCC25C(O3)C(O)C=CC54)C
Moxonidine	88	70	0	85	n/a	O(c1c(c(Cl)nc(n1)C)NC2=NCCN2)C
Nadolol	57	72	1	99	P-gp	C(NCC(O)COc1c2c(ccc1)CC(O)C(O)C2)(C)(C)C
Naloxone	91	80	0	68	n/a	O=C1C2C34c5c(c(O)ccc5CC(C3(O)CC1)N(CC=C)CC4)O2
Naproxen	99	61	0	72	n/a	C(=O)(C(c1cc2c(cc(OC)cc2)cc1)C)O
Nefazodone	100	129	0	125	n/a	O=C1N(C(=NN1CCCN2CCN(c3cc(Cl)ccc3)CC2)CC)CCOc4ccccc4
Neomycin	1	1	4	3	n/a	O(C1OC(C(OC2OC(C(O)C(O)C2N)CN)C1O)CO)C3C(OC4OC(C(O)C(O)C4N)CN)C(N)CC(C3O)N
Netivudine	28	18	2	28	n/a	C(#CC)C1C(=O)NC(=O)N(C=1)C2OC(C(O)C2O)CO
Nicotine	100	117	0	93	n/a	c1(cnccc1)C2N(CCC2)C

Nicotinic acid	88	141	1	83	Intes. active transport	C(=O)(c1cnccc1)O
Nisoldipine	90	44	0	41	n/a	C(=O)(OCC(C)C)C1=C(NC(=C(C(=O)OC)C1c2c([N+](=O)[O-])cccc2)C)C
Nitrendipine	88	68	0	71	n/a	C(=O)(OCC)C1=C(NC(=C(C(=O)OC)C1c2cc([N+](=O)[O-])ccc2)C)C
Nitrofurantoin	100	110	0	69	n/a	N(N1C(=O)NC(=O)C1)=Cc2oc([N+](=O)[O-])cc2
Nizatidine	90	150	1	71	OCT	C(=C[N+](=O)[O-])(NCCSCC1=CS=C(N1)CN(C)C)NC
Nordiazepam	99	63	0	65	n/a	O=C1Nc2c(C(c3ccccc3)=NC1)cc(Cl)cc2
Norfloxacin	71	95	1	87	P-gp	C(=O)(C1C(=O)c2c(N(C=1)CC)cc(c(F)c2)N3CCNCC3)O
Ofloxacin	100	64	1	17	n/a	C(=O)(C1C(=O)c2c3c(c(c(F)c2)N4CCN(CC4)C)OCC(N3C=1)C)O
Olanzapine	75	45	0	94	n/a	c12C(=Nc3c(cccc3)Nc1sc(c2)C)N4CCN(CC4)C
Olsalazine	24	32	1	109	n/a	C(=O)(c1c(O)ccc(N=Nc2cc(C(=O)O)c(O)cc2)c1)O
Omeprazole	80	29	0	58	n/a	O=S(c1nc2c(cc(OC)cc2)[nH]1)Cc3c(c(OC)c(cn3)C)C
Ondansetron	100	121	0	99	n/a	O=C1c2c3c(n(c2CCC1Cn4c(ncc4)C)C)cccc3
Ouabain	1.4	7	4	7	n/a	O=C1OCC(=C1)C2C3(C(O)(C4C(C5(C(O)(CC(OC6OC(C(O)C(O)C6O)C)CC5O)CC4)CO)C(O)C3)CC2)C
Oxatomide	100	125	0	115	n/a	O=C1N(c2c(cccc2)N1)CCCN3CCN(C(c4ccccc4)c5ccccc5)CC3
Oxazepam	89	41	0	66	n/a	O=C1C(N=C(c2c(ccc(Cl)c2)N1)c3ccccc3)O
Oxprenolol	95	54	0	63	n/a	O(c1c(OCC(O)CNC(C)C)cccc1)CC=C
Oxyfedrine	85	62	0	123	n/a	C(=O)(c1cc(OC)ccc1)CCNC(C(c2ccccc2)O)C
Pafenolol	29	40	1	92	n/a	C(=O)(NC(C)C)NCCc1ccc(OCC(O)CNC(C)C)cc1
Paromomycin	3	11	4	2	n/a	O(C1OC(C(OC2OC(C(O)C(O)C2N)CN)C1O)CO)C3C(OC4OC(C(O)C(O)C4N)CO)C(N)CC(C3O)N
Pefloxacin	95	87	0	65	n/a	C(=O)(C1C(=O)c2c(N(C=1)CC)cc(c(F)c2)N3CCN(CC3)C)O
Penicillin V	30	20	1	51	n/a	C(=O)(NC1C(=O)N2C(C(=O)O)C(SC21)(C)C)COc3ccccc3
Phenglutarimide	100	119	0	97	n/a	N(CCC1(C(=O)NC(=O)CC1)c2ccccc2)(CC)CC
Phenoxymethylpenicillin	59	77	1	106	Intes. pept. carrier	C(=O)(NC1C(=O)N2C(C(=O)O)C(SC21)(C)C)COc3ccccc3

(*Continued*)

Table 17.1 (*Continued*)

Name	HIA%	F_a rank	ADMET Risk	AR rank	Active transport	Smiles
Phenytoin	90	75	0	88	n/a	O=C1C(c2ccccc2)(c3ccccc3)NC(=O)N1
Pindolol	87	38	0	44	n/a	O(c1c2c(N=CC2)ccc1)CC(O)CNC(C)C
Pirbuterol	60	35	1	47	n/a	C(NCC(c1nc(c(O)cc1)CO)O)(C)(C)C
Pirenzepine	27	35	0	135	P-gp	C(=O)(N1c2c(cccn2)NC(=O)c3c1cccc3)CN4CCN(CC4)C
Piroxicam	100	68	0	56	n/a	C(=O)(C1=C(c2c(S(=O)(=O)N1C)cccc2)O)Nc3ncccc3
Piroximone	81	55	0	76	n/a	C(=O)(C1C(=NC(=O)N=1)CC)c2ccncc2
Practolol	95	88	0	75	n/a	C(=O)(Nc1ccc(OCC(O)CNC(C)C)cc1)C
Pravastatin	34	47	2	47	OATP	C(=O)(OC1C2C(C=CC(C2CCC(O)CC(O)CC(=O)O)C)=CC(O)C1)C(CC)C
Praziquantel	100	111	0	80	n/a	C(=O)(N1CC(=O)N2C(c3c(cccc3)CC2)C1)C4CCCCC4
Prazosin	86	64	0	74	n/a	C(=O)(c1occc1)N2CCN(c3nc4c(c(n3)N)cc(OC)c(OC)c4)CC2
Prednisolone	99	60	1	20	n/a	C(=O)(C1(C2(C(C3C(C4(C(=CC(=O)C=C4)CC3)C)C(O)C2)CC1)C)O)CO
Prefloxacin	100	108	0	66	n/a	C(=O)(C1C(=O)c2c(N(C=1)CC)cc(c(F)c2)N3CCN(CC3)C)O
Probenecid	100	128	0	122	n/a	C(=O)(c1ccc(S(N(CCC)CCC)(=O)=O)cc1)O
Progesterone	100	225	0	168	P-gp	C(=O)(C1C2(C(C3C(C4(C(=CC(=O)CC4)CC3)C)CC2)CC1)C)C
Propiverine	84	60	0	105	n/a	C(C(OCCC)(c1ccccc1)c2ccccc2)(=O)OC3CCN(CC3)C
Propranolol	99	62	0	67	n/a	O(c1c2c(ccc1)cccc2)CC(O)CNC(C)C
Propylthiouracil	76	46	0	78	n/a	c1(nc(O)cc(n1)CCC)S
Quinidine	81	120	0	184	P-gp	O(c1cc2c(nccc2C(O)C3N4CC(C=C)C(C3)CC4)cc1)C
Raffinose	0.3	1	4	5	n/a	O(C1(OC(C(O)C1O)CO)CO)C2OC(C(O)C(O)C2O)COC3OC(C(O)C(O)C3O)CO
Ranitidine	64	86	0	133	P-gp	C(=C[N+](=O)[O-])(NCCSCc1oc(cc1)CN(C)C)NC
Recainam	71	44	0	109	n/a	C(=O)(Nc1c(cccc1C)C)NCCCNC(C)C
Remikiren	10	22	1	113	n/a	C(=O)(C(NC(=O)C(CS(C(C)(C)C)C)(=O)=O)Cc1ccccc1)Cc2cnc[nH]2)NC(C(C(O)C3CC3)O)CC4CCCCC4

Reproterol	60	36	1	52	n/a	O=C1c2c(ncn2CCCNCC(c3cc(O)cc(O)c3)O)N(C(=O)N1C)C
Ribavirin	33	12	3	10	n/a	C(=O)(C1=NCN(C2OC(C(O)C2O)CO)N1)N
Rifabutine	53	30	3	16	n/a	C(=O)(OC1C(C(OC)C=COC2(C(=O)c3c4c(C(=O)C(=C5C4=NC6(N5)CCN(CC(C)C)CC6)NC(=O)C(=CC=CC(C(O)C(C(O)C1C)C)C)C)c(c(c3O2)C)O)C)C)C
Rimiterol	48	19	1	29	n/a	c1(c(O)ccc(C(O)C2NCCCC2)c1)O
Saccharin	88	67	2	25	n/a	O=C1c2c(S(=O)(=O)N1)cccc2
Salicylic acid	100	120	1	56	n/a	C(=O)(c1c(O)cccc1)O
Saquinavir	80	48	2	27	n/a	C(=O)(c1nc2c(cc1)cccc2)NC(C(=O)NC(C(O)CN3C(C(=O)NC(C)(C)C)CC4C(C3)CCCC4)Cc5ccccc5)CC(=O)N
Scopolamine	95	82	1	36	n/a	C(=O)(OC1CC2N(C(C3OC32)C1)C)C(c4ccccc4)CO
Sorivudine	82	123	2	56	Nucleoside?	O=C1C(C=CBr)=CN(C(=O)N1)C2OC(C(O)C2O)CO
Sotalol	95	84	1	38	n/a	O=S(=O)(Nc1ccc(C(O)CNC(C)C)cc1)C
Spironolactone	73	26	0	32	n/a	C(=O)(SC1C2C(C3(C(=CC(=O)CC3)C1)C)CCC4(C5(CC(=O)OC5)CCC42)C)C
Stavudine	100	66	0	40	n/a	O=C1C(=CN(C(=O)N1)C2OC(C=C2)CO)C
Streptomycin	1	3	4	1	n/a	C(=N)(NC1C(OC2OC(C(C=O)(O)C2OC3OC(C(O)C(O)C3NC)CO)C)C(O)C(O)C(NC(=N)N)C1O)N
Sudoxicam	100	122	0	104	n/a	C(=O)(C1=C(c2c(S(=O)(=O)N1C)cccc2)O)Nc3nccs3
Sulfamethoxazole	100	107	0	63	n/a	O=S(=O)(c1ccc(cc1)N)Nc2noc(c2)C
Sulfasalazine	59	33	1	43	n/a	C(=O)(c1c(O)ccc(N=Nc2ccc(S(=O)(=O)Nc3ncccc3)cc2)c1)O
Sulindac	90	47	0	64	n/a	C(=O)(O)CC1c2c(C(C=1C)=Cc3ccc(S(=O)C)cc3)ccc(F)c2
Sulpiride	44	16	0	38	n/a	C(=O)(c1c(OC)ccc(S(=O)(=O)N)c1)NCC2N(CC)CCC2
Sultopride	89	72	0	98	n/a	C(=O)(c1c(OC)ccc(S(=O)(=O)CC)c1)NCC2N(CC)CCC2
Sumatriptan	57	21	0	39	n/a	N(CCC1c2c(N=C1)ccc(c2)CS(=O)(=O)NC)(C)C
Telmisartan	90	48	0	70	n/a	C(=O)(c1c(-c2ccc(cc2)Cn3c4c(c(cc(-c5nc6c(n5C)cccc6)c4)C)nc3CCC)cccc1)O
Tenidap	89	71	0	73	n/a	C(=O)(N1C(=O)C(=C(c2sccc2)O)c3c1ccc(Cl)c3)N

(*Continued*)

Table 17.1 (*Continued*)

Name	HIA%	F_a rank	ADMET Risk	AR rank	Active transport	Smiles
Tenoxicam	100	65	0	60	n/a	C(=O)(C1=C(C2C(S(=O)(=O)N1C)C=CS=2)O)Nc3ncccc3
Terazosin	90	73	0	70	n/a	C(=O)(N1CCN(c2nc3c(c(n2)N)cc(OC)c(OC)c3)CC1)C4OCCC4
Terbinafine	80	53	0	134	n/a	C(#CC=CCN(Cc1c2c(ccc1)cccc2)C)C(C)(C)C
Terbutaline	62	40	1	44	n/a	C(NCC(c1cc(O)cc(O)c1)O)(C)(C)C
Testosterone	100	112	0	81	n/a	O=C1C=C2C(C3C(C4C(C(O)CC4)(CC3)C)CC2)(CC1)C
Theophylline	100	238	0	197	Active uptake?	O=C1c2c(nc[nH]2)N(C(=O)N1C)C
Thiacetazone	20	10	1	27	n/a	C(=O)(Nc1ccc(C=NNC(=S)N)cc1)C
Tiagabine	90	155	0	170	n/a	C(c1c(ccs1)C)(c2c(ccs2)C)=CCCN3CC(C(=O)O)CCC3
Timolol	95	83	1	37	n/a	C(NCC(O)COc1c(nsn1)N2CCOCC2)(C)(C)C
Tinidazole	100	114	0	86	n/a	O=S(=O)(CCn1c(ncc1[N+](=O)[O-])C)CC
Tolbutamide	85	36	0	33	n/a	C(=O)(NS(=O)(=O)c1ccc(cc1)C)NCCCC
Tolmesoxide	98	102	0	107	n/a	O=S(c1c(cc(OC)c(OC)c1)C)C
Topiramate	86	63	1	32	n/a	O=S(=O)(OCC12OC(OC1C3OC(OC3CO2)(C)C)(C)C)N
Torasemide	96	94	1	31	n/a	C(=O)(NS(=O)(=O)c1c(Nc2cc(ccc2)C)ccnc1)NC(C)C
Toremifene	100	137	0	137	n/a	C(=C(c1ccccc1)CCCl)(c2ccc(OCCN(C)C)cc2)c3ccccc3
Tramadol	90	77	0	106	n/a	N(CC1C(c2cc(OC)ccc2)(O)CCCC1)(C)C
Tranexamic acid	55	20	1	24	n/a	C(=O)(O)C1CCC(CN)CC1
Trapidil	96	95	0	101	n/a	N(C1n2c(N=C(C=1)C)ncn2)(CC)CC
Trimethoprim	97	191	1	112	RFCP?	O(c1c(OC)cc(cc1OC)Cc2c(nc(nc2)N)N)C
Trovofloxicin	37	52	0	132	MDR1 in bacteria	C(=O)(C1C(=O)c2c(nc(c(F)c2)N3CC4C(C4C3)N)N(c5c(F)cc(F)cc5)C=1)O
Urapidil	78	27	0	47	n/a	O=C1N(C(=O)C=C(N1C)NCCCN2CCN(c3c(OC)cccc3)CC2)C
Valproic acid	100	70	0	68	n/a	C(=O)(C(CCC)CCC)O
Venlafaxine	97	56	0	55	n/a	N(CC(c1ccc(OC)cc1)C2(O)CCCCC2)(C)C
Verapamil	100	258	0	250	P-gp	C(C(c1cc(OC)c(OC)cc1)(C(C)C)CCCN(CCc2cc(OC)c(OC)cc2)C)#N

Vigabatrin	58	32	1	50	n/a	C(=O)(O)CCC(C=C)N
Viloxazine	98	100	0	90	n/a	O(c1c(OCC)cccc1)CC2OCCNC2
Viomycin	85	35	4	2	n/a	C(=O)(NC1C(=O)NC(C(=O)NC(C(=O)NC(C(=O)NC1)C2NC(=N)NC(O)C2)=CNC(=O)N)CO)CO)CC(CCCN)N
Warfarin	98	101	0	103	n/a	C(=O)(CC(C1C(=O)Oc2c(C=1O)cccc2)c3ccccc3)C
Xamoterol	5	6	1	23	n/a	C(=O)(N1CCOCC1)NCCNCC(O)COc2ccc(O)cc2
Ximoprofen	98	103	0	108	n/a	C(=O)(C(c1ccc(cc1)C2CC(=NO)CCC2)C)O
Xipamide	70	43	1	55	n/a	C(=O)(c1c(O)cc(Cl)c(S(=O)(=O)N)c1)Nc2c(cccc2C)C
Zidovudine	100	214	0	131	Nucleoside	N(=[N+]=[N-])C1C(OC(N2C(=O)NC(=O)C(=C2)C)C1)CO
Ziprasidone	60	37	0	84	n/a	O=C1Nc2c(cc(c(Cl)c2)CCN3CCN(c4c5c(sn4)cccc5)CC3)C1
Zopiclone	80	49	1	39	n/a	C(=O)(OC1c2c(C(=O)N1c3ncc(Cl)cc3)nccn2)N4CCN(CC4)C

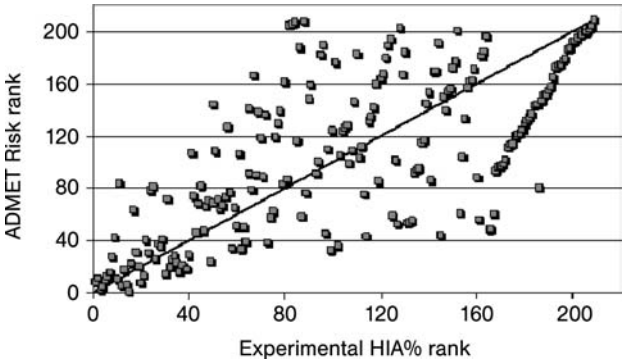

Figure 17.1 Correlation of rank order for ADMET Risk and human intestinal absorption (HIA%). The ADMET Risk score ranged from 0 to 5, with 5 being compounds with the greatest risk of having poor ADMET properties. Within a single ADMET Risk number, the compounds were ranked according to ascending estimated human jejunal permeability (ADMET Predictor, Simulations Plus, Inc.). Spearman rank correlation coefficient was 0.7 ($p < 0.001$).

and acceptors, and human jejunal permeability from 3D molecular structures. The predictive performance of Lipinski's original rule-of-5 [47] was compared with that of the ADMET Risk. A positive was defined as HIA% greater than or equal to 50%, and a negative was defined as less than or equal to 50%.

Both sets of rules correctly identified over 99% of the true positives. However, because of the liberal criteria found in Lipinski's rule-of-5, only 20% true negatives were predicted correctly whereas 80% were predicted as false positives. The default ADMET Risk rules predicted 64% of the true negatives and lowered the false positives to only 36%. Unlike the original rule-of-5, however, ADMET Risk marked one

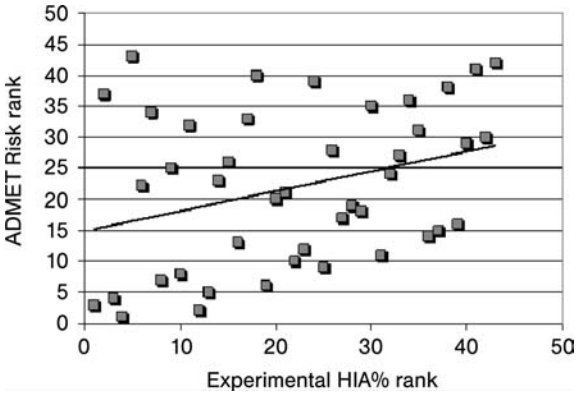

Figure 17.2 Correlation of rank order for 43 compounds that are known substrates for influx or efflux transporters. Spearman rank correlation coefficient was 0.3.

compound as a false negative – a result of more conservative rules. Rifabutine has $F_a = 53\%$ and was assigned an ADMET Risk score of 3, so it was right on the border of having poor ADMET properties. Thus, application of ultrahigh-throughput *in silico* estimation of biopharmaceutical properties to the generation of computational alerts has the potential to improve compound selection to those drug candidates that are likely to have less trouble in development.

17.3.2 Complex Rules That Include Toxicity

Computational alerts can be extended from having rules that predict absorption properties only to customized rules that include distribution and toxicity. Here, we will consider *in silico* models for four types of toxicity. When the "hits" in the ADME rules are combined with additional rules for estimated toxicity, we generate a more general computational "ADMET Risk."

Maximal recommended therapeutic dose (MRTD as defined by the US FDA) has been correlated with potential toxicity. Matthews *et al.* have reported *in silico* multicase models for MRTD [55]. According to their analysis, more toxic molecules will have MRTD values less than 2.7 mg/kg/day and less toxic molecules will have MRTD more than 4.99 mg/kg/day. If one builds an *in silico* model for MRTD, then a new rule can be added to the computational alert ADME rules described above.

The US Environmental Protection Agency (EPA) has released a number of toxicological databases on its Distributed Structure-Searchable Toxicity (DSSTox) database network. These databases make a tremendous resource for building *in silico* models of toxicity. The first toxicity we will consider from the EPA is for molecules that bind to the estrogen receptor and have the potential to produce endocrine disruption. The primary quantitative end point for this toxicity is a ratio of the estimated estrogen receptor-binding affinities for 17b-estradiol divided by the affinity estimated for the unknown molecule (RBA). A high value for the ratio (RBA > 1) would imply that the new molecule has a binding affinity for the estrogen receptor greater than estradiol. The EPA database contains 232 molecules with measured RBA values, and the median ratio is 0.02. Thus, half of the molecules would have ratios greater than 0.02 (more toxic), and half would have ratios less than 0.02 (less toxic). When a virtual screen is conducted on a set of new molecules, this RBA estimation would be a valuable addition to the overall ADMET Risk score.

When considering environmental chemicals, another important measure of toxicity is based on the EPA acute fathead minnow toxicity database. In this assay, 28–36-day-old fathead minnows are exposed to varying concentrations of a test molecule in a flow-through apparatus for 96 h [56]. The concentration of the organic chemical that produced 50% lethality (LD_{50}) was reported in the EPA database. The median LD_{50} from 586 molecules was 21.5 mg/l. This value could comprise another cutoff in a computational alert.

Rat carcinogenicity is another important measure of toxicity reported in one of the DSSTox databases. TD_{50} is the daily dose that will induce tumors in half of the test animals that would have remained tumor free at zero dose [57]. The median TD_{50}

from 265 compounds tested was 1.15 mg/kg/day. In screening for ADMET Risk, thus, one might be able to estimate if the new molecules were more or less carcinogenic than the most carcinogenic half of the molecules tested by the EPA.

The DSSTox web site also provides a database for *Salmonella* mutagenicity with 506 molecules approximately half of which are designated as positive for mutagenicity [57]. In addition, Simulations Plus, Inc., has a database with approximately 5000 molecules that covers 10 strains of bacterial mutagenesis.

Finally, we can consider the inhibition of human ether-a-go-go related gene (hERG) product, which encodes a voltage-gated potassium channel in the cardiac myocyte. Inhibition of the channel predisposes patients to long QT syndrome, the characteristic "Torsades de Pointes" arrhythmia, and sudden cardiac death. Several publications have reported the results of electrophysiological measurement of the hERG IC_{50} for a variety of drugs [58, 59]. In building a model for hERG IC_{50}, it is important to screen the data for a common target, preferably the expression of hERG on mammalian cells (HEK, CHO, COS, cardiac myocytes, and neuroblastoma cells). For 93 drugs, the median half-maximal inhibition of potassium channel current tested in patch clamp electrophysiological apparatus on mammalian cells expressing human ERG gene was 1.58 μM. This represents a reasonable cutoff for hERG toxicity.

Thus, an extension of the ADMET Risk rules to include toxicity would include

- MRTD values less than 2.7 mg/kg/day;
- RBA ratios more than 0.02;
- fathead minnow LD_{50} less than 21.5 mg/l;
- Positive prediction for *Salmonela* mutagenicity;
- hERG IC_{50} less than 1.58 μM.

17.4 Mechanistic Simulation (ACAT Models) in Early Discovery

We have developed a two-step procedure for the *in silico* screening of compound libraries based on biopharmaceutical property estimation linked to a mechanistic simulation of GI absorption. The first step involves biopharmaceutical property estimation by application of machine learning procedures to empirical data modeled with a set of molecular descriptors derived from 2D and 3D molecular structures. *In silico* methods were used to estimate such biopharmaceutical properties as effective human jejunal permeability, cell culture permeability, aqueous solubility, and molecular diffusivity. In the second step, differential equations for the advanced compartmental absorption and transit model were numerically integrated to determine the rate, extent, and approximate GI location of drug liberation (for controlled release), dissolution, and absorption. Figure 17.3 shows the schematic diagram of the ACAT model in which each one of the arrows represents an ordinary differential equation (ODE).

The form of the ACAT model implemented in GastroPlus describes the release, dissolution, luminal degradation (if any), metabolism, and absorption/exsorption of

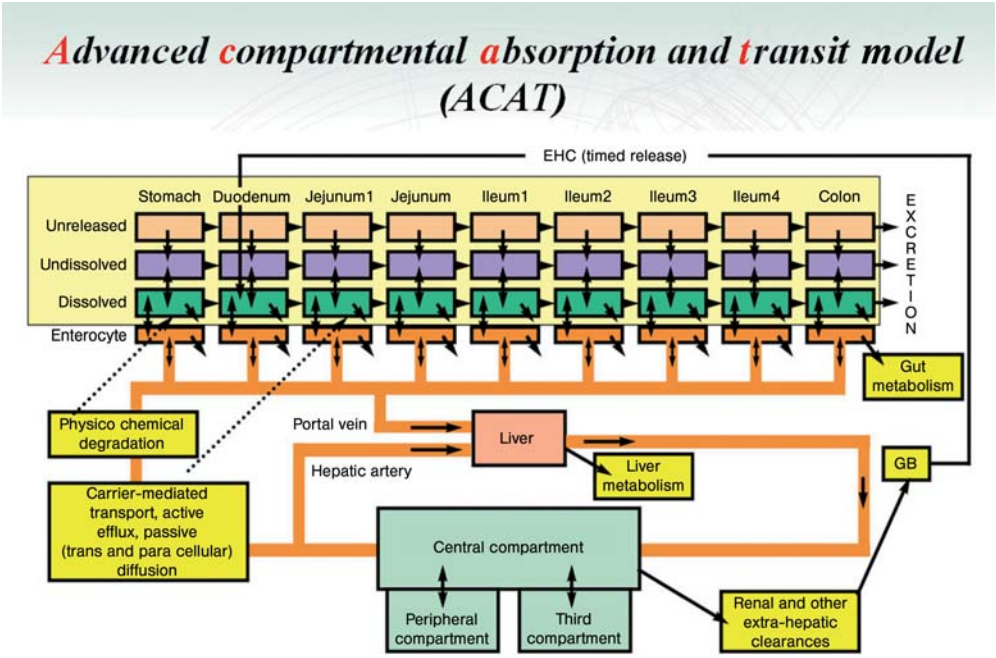

Figure 17.3 Schematic diagram of the advanced compartmental absorption and transit model as implemented in GastroPlus.

a drug as it transits through successive compartments. The kinetics associated with these processes is modeled by a system of coupled linear and nonlinear rate equations. The equations include the consideration of 6 states (unreleased, undissolved, dissolved, degraded, metabolized, and absorbed), 18 compartments (9 GI – 1 stomach, 6 small intestine, and 2 colon– and 9 enterocyte), 3 states of excreted material (unreleased, undissolved, and dissolved), and the amount of drug in up to 3 pharmacokinetic compartments (when pharmacokinetic parameters are available) or in a whole body physiologically-based pharmacokinetic model. The total amount of absorbed material is summed over the integrated amounts being absorbed/exsorbed from each absorption/transit compartment.

For example, the rate of change of dissolved drug concentration in a luminal GI compartment depends on six different processes: (1) transit of drug into a compartment, (2) transit of drug out of a compartment, (3) release of drug from the formulation in the compartment, (4) dissolution/precipitation of drug particles, (5) luminal degradation of the drug, and (6) absorption/exsorption of the drug . The timescale associated with luminal transit through a compartment is determined by a transfer rate constant, k_t, that is calculated as one divided by the mean transit time within the compartment. Transit times within each compartment are determined as the product of the physical volume of fluid in the compartment (milliliter) divided by the average fluid flow rate (ml/h). The timescale of the dissolution process is set by a

rate constant, k_d, that is computed from a drug's solubility (as a function of pH), its effective particle size, particle density, lumen concentration, diffusion coefficient, and the diffusion layer thickness (Equation 17.1). The timescale associated with the absorption process is set by a rate coefficient, k_a, that depends on the effective permeability of the drug (P_{eff}, units of cm/s) multiplied by an absorption scale factor (ASF with units of cm^{-1}) for each compartment (Equation 17.2). The nominal value of the ASF is the surface-to-volume ratio of the compartment, which reduces to 2/radius of the SI compartment. ASFs are adjusted from these nominal values to correct for the changes in permeability due to changing physiology along the GI tract; for example, absorption surface area, pH, tight junction gap width, and transport protein (influx or efflux) densities. The rates of absorption and exsorption depend on the concentration gradients across the apical and basolateral enterocyte membranes (Equations 17.3 and 17.4). The timescale for luminal degradation is set by a rate constant k_{Degrad} that is determined by interpolation from an input table of degradation rate (or half-life) versus pH and the pH in the compartment.

The system of differential equations is integrated using CVODE numerical integration package. CVODE is a solver for stiff and nonstiff ordinary differential equation systems [60]. The fraction of dose absorbed is calculated as the sum of all drug amounts crossing the apical membrane as a function of time, divided by the dose, or by the sum of all doses if multiple dosing is used.

$$k_{(i)d} = 3\gamma \frac{C_{S(i)} - C_{(i)L}}{\rho r_0 T}, \tag{17.1}$$

$$k'_{(i)a} = \alpha_{(i)} P_{eff(i)}, \tag{17.2}$$

$$\frac{\text{Absorption}}{\text{Exsorption}}_{(i)} = k'_{(i)a} V_{(i)} (C_{(i)L} - C_{(i)E}), \tag{17.3}$$

$$\text{Basolateral transfer}_{(i)} = k'_{(i)b} V_{(i)} (C_{(i)E} - C_p), \tag{17.4}$$

where $k_{(i)d}$ is dissolution rate constant for the ith compartment; $k'_{(i)a}$ is absorption rate coefficient for the ith compartment; $k'_{(i)b}$ is absorption rate coefficient specific for the basolateral membrane of the ith compartment; C_S is aqueous solubility at local pH; $C_{(i)L}$ is lumen concentration for the ith compartment; $C_{(i)E}$ is intracellular enterocyte concentration for the ith compartment; C_p is plasma central compartment concentration; $V_{(i)}$ is lumen volume of ith compartment; γ is molecular diffusion coefficient; ρ is drug particle density; r_0 is effective initial drug particle radius; T is diffusion layer thickness; $\alpha_{(i)}$ is compartmental absorption scale factor for ith compartment; and $P_{eff(i)}$ is human effective permeability for ith compartment.

As one part of our software validation, we tested the accuracy of GastroPlus simulation of fraction absorbed. Starting from two-dimensional structures, ADMET Predictor was used to generate the molecular descriptors and estimates of log P,

solubility, permeability, and diffusivity that were used in GI simulations. The extent of GI absorption for each drug was determined *in silico* using the ACAT model after making the following simplifying assumptions: (default dose (100 mg), particle radius (was adjusted to achieve 100% dissolution in 3.3 h), and human fasted physiology). The simulation results from GastroPlus were compared with literature values. The simplest assumption for the regional dependence of the rate of absorption (Equation 17.2) is that the compartmental absorption scale factor is equal to 2 divided by the radius of the small intestine and that this value of ASF is applied to all compounds equally.

17.4.1
Automatic Scaling of k_a' as a Function of P_{eff}, pH, log D, and GI Surface Area

The size and shape of a drug molecule, its acid and base dissociation constants, and the pH of the GI tract all influence the absorption rate constant for specific regions of the GI. Pade and coworkers measured the Caco-2 cellular permeability for a diverse set of acidic and basic drug molecules at two pH values [61]. They concluded that the permeability coefficient of the acidic drugs was greater at pH 5.4, whereas that of the basic drugs was greater at pH 7.2 and that the transcellular pathway was the favored pathway for most drugs, probably due to its larger accessible surface area. The paracellular permeability of the drugs depended on size and charge. The permeability of the drugs through the tight junctions decreased with increasing molecular size. Further, the pathway also appeared to be cation selective, with the positively charged cations of weak bases permeating the aqueous pores of the paracellular pathway at a faster rate than the negatively charged anions of weak acids. Thus, the extent to which the paracellular and transcellular routes are utilized in drug transport is influenced by the fraction of ionized and unionized species (which in turn depends on the pK_a of the drug and the pH of the solution), the intrinsic partition coefficient of the drug, and molecule size and charge.

Figure 17.4 is a representation of regional permeability coefficients of 19 drugs with different physicochemical properties determined by Ungell *et al*. by using excised segments from three regions of rat intestine: jejunum, ileum, and colon [62].

They observed a significant decrease in the permeability to hydrophilic drugs and a significant increase in the permeability for hydrophobic drugs aborally to the small intestine ($p < 0.0001$). Figure 17.4 illustrates that for hydrophilic drugs (low permeability and low log *D*), the ratio of colon: jejunal permeability was less than 1, whereas for hydrophobic drugs (higher permeability and higher log *D*), the ratio of colon: jejunal permeability was observed to be greater than 1. At certain pH values, the permeability of small hydrophilic drugs may have a large paracellular component [63], and it is well known that the transepithelial electrical resistance (TEER) of colon is much higher than that of the small intestine. TEER increases as the width of tight junctions decreases, and the tight junction width has been determined to be 0.75–0.8 nm in jejunum, 0.3–0.35 nm in ileum, and 0.2–0.25 nm in colon [64–67]. The narrower tight junctions in colon suggest that the paracellular transport will be much less significant in the colon, which helps to explain the lower ratio of colon:

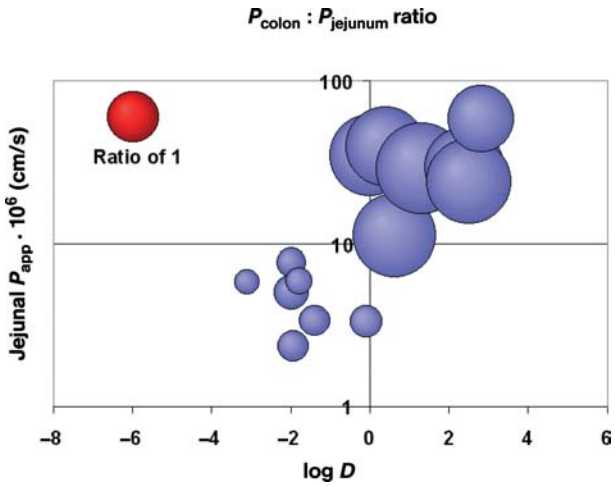

Figure 17.4 Relationship between distribution coefficient at pH = 7.4 and the intestinal permeability of jejunum, ileum, and colon. Data were collected from [62].

jejunal permeability for hydrophilic drugs. To our knowledge, a conclusive explanation for the increased colon permeability of drugs with high small intestine permeability is not yet available. We have used the ACAT model with experimental biopharmaceutical properties for a series of hydrophilic and hydrophobic drug molecules to calibrate a "log *D* model" that explains the observed rate and extent of absorption.

The mechanistic simulation ACAT model was modified to automatically account for the change in small intestinal and colon k_a' as a function of the local (pH-dependent) log *D* of the drug molecule. The rank order of HIA% from GastroPlus was directly compared with the rank order experimental HIA% with this correction for the log *D* of each molecule in each of the pH environments of the small intestine. The mechanistic simulation produced 82% of HIA% predictions within 25% of the experimental values.

17.4.2 Mechanistic Corrections for Active Transport and Efflux

Table 17.2 lists the 43 molecules used in this study that are known to be substrates for active transport or active efflux. The mechanistic ACAT model was modified to accommodate saturable uptake and efflux by using standard Michaelis–Menten equations. It was assumed that transporters responsible for active uptake of drug molecules from the lumen and active efflux from the enterocytes to the lumen were homogeneously dispersed within each luminal compartment and each corresponding enterocyte compartment, respectively. Equation 17.5 represents the

Table 17.2 Forty-three drugs with some evidence of active uptake or efflux.

Name	Influx/efflux	Reference	Name	Influx/efflux	References
Adriamycin	P-gp	[111]	Lovastatin	OATP/P-gp	[112–114]
Allopurinol	Hypoxanthine	[115]	Mercaptoethanesulfonic acid	Influx?	[116]
Alpha-difluoromethylornithine	CAT1?	[117]	Metformin	hOCT1/PMAT	[118]
Amoxicillin	PepT1 conc. dep.	[119]	Methotrexate	RFCP	[120]
Ampicillin	PepT1/2	[121]	Miconazole	P-gp	[122, 123]
Benzylpenicillin	Intes. pept. carrier	[119]	Nadolol	P-gp	[124]
Bumetanide	Bile acid	[125]	Nicotinic acid	Intes. active trans.	[126]
Captopril	Intes. pept. carrier	[127]	Nizatidine	OCT	[128]
Carfecillin	Intes. pept. carrier	[119]	Norfloxacin	P-gp	[129]
Cefadroxil	Intes. pept. carrier	[119]	Phenoxymethylpenicillin	Intes. pept. carrier	[130]
Cefatrizine	Intes. pept. carrier	[119]	Pirenzepine	P-gp	[131, 132]
Cephalexin	PepT1	[133]	Pravastatin	OATP	[134]
Cycloserine	hPAT1	[135, 136]	Progesterone	P-gp	[137]
Digoxin	OATP/P-gp	[138, 139]	Quinidine	P-gp	[140]
Enalapril	Intes. pept. carrier	[141]	Ranitidine	P-gp	[142]
Etoposide	P-gp	[140]	Sorivudine	Nucleoside?	Structural analogy to zidovudine
Gabapentin	LAT1	[143]	Theophylline	Active uptake?	[144]
Glycine	hPAT1	[145, 146]	Trimethoprim	RFCP?	[147, 148]
Leucine	B(0)AT2	[149]	Trovofloxicin	MDR1 in bacteria	[150]
Levodopa	LAT1	[151]	Verapamil	P-gp	[152]
Lisinopril	Intes. pept. carrier	[130]	Zidovudine	Nucleoside	[153]
Loracarbef	Intes. pept. carrier	[154, 155]			

overall mass balance for drug in the enterocyte compartment lining the intestinal wall:

$$\frac{dM_{ent(i)}}{dt} = ADR_{(i)} + ATR_{(i)} - BDR_{(i)} - GMR_{(i)}, \tag{17.5}$$

$$ATR = DF_{influx(i)} \frac{V_{max(influx)} C_i}{K_{m(influx)} + C_i} - DF_{efflux(i)} \frac{V_{max(efflux)} C_{ent(i)}}{K_{m(efflux)} + C_{ent(i)}}, \tag{17.6}$$

where $M_{ent(i)}$ is the mass of drug in the enterocyte compartment i; $ADR_{(i)}$ is the apical diffusion rate for ith compartment; $ATR_{(i)}$ is the apical transport rate for ith compartment; $BDR_{(i)}$ is the basolateral diffusion rate for ith compartment; $GMR_{(i)}$ is the gut metabolism rate for ith compartment; $DF_{influx(i)}$ is distribution factor for influx transporter in compartment i; $DF_{efflux(i)}$ is distribution factor for efflux transporter in compartment i; $V_{max(influx\ or\ efflux)}$ is the maximal velocity of the saturable transporter; $K_{m(influx\ or\ efflux)}$ is the Michaelis constant for the saturable transporter; C_i is the concentration of drug inside the lumen of the intestine; $C_{ent(i)}$ is the concentration of drug inside the enterocyte in compartment i.

Because the amounts and density of these transporters vary along the GI tract, it is necessary to introduce a correction factor for the varying transport rates in the different luminal and enterocyte compartments. Owing to the lack of experimental data for the regional distribution and Michaelis–Menten constants for each drug in Table 17.2, we fitted an intrinsic (concentration-independent) transport rate for each drug to closely approximate the experimental HIA%. Figure 17.5 shows a correlation

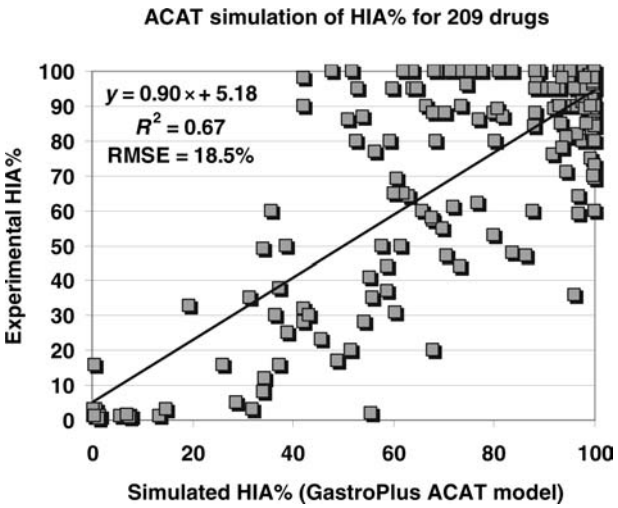

Figure 17.5 Correlation of experimental and simulated percentage absorbed. Percentage absorbed is defined as the percentage of the dose that crosses the apical membrane of the intestine. Percentage absorbed was simulated using the ACAT model as described in the text.

between the simulated HIA% and the experimental HIA% for 209 passively absorbed compounds.

17.4.3
PBPK and *In Silico* Estimation of Distribution

Prior to 2002, most studies published on physiologically-based pharmacokinetic models focused on the distribution and elimination of environmental toxins such as dioxin, styrene, and organic solvents [68–70]. PBPK models for drug molecules generally relied on tissue/plasma partition coefficients (K_{ps}) measured in rat [71–73]. The earliest models for calculation of tissue/plasma partition coefficients from structure were typical QSAR models developed from a database of empirical K_p values [74]. However, several years back, one group had already started a revolution in PBPK modeling with the introduction of a mechanistic model for tissue/plasma partition coefficients based on the tissue composition of neutral and phospholipids and volume fraction of water [75]. Years after the introduction of the tissue composition method, a comparison of methods for calculating K_p values observed that the mechanistic tissue composition methods worked well to estimate K_p values for volatile organic molecules [76]. However, the widespread use of these models for calculating drug distribution achieved great momentum from the work of Poulin and Theil [77–80]. Recent reviews and validation studies have confirmed the utility of PBPK modeling in early drug discovery [8, 10, 11, 81].

To address the inaccuracy of estimates for volume at steady state (V_{ss}) for strongly basic drug molecules, Rodgers and Rowland have proposed an extension to the tissue composition method that takes into account the volume fraction of acidic phospholipids. Presumably, the higher values of V_{ss} observed for these basic molecules is due to the interaction of the cationic state (at physiological pH) of the base with the anionic state of the acidic phospholipids [82–85]. Several commercial software programs are now extensively used in the pharmaceutical industry for PBPK modeling [86, 41, 87, 11].

17.5
Mechanistic Simulation of Bioavailability (Drug Development)

In addition to the mechanistic simulation of absorptive and secretive saturable carrier-mediated transport, we have developed a model of saturable metabolism for the gut and liver that simulates nonlinear responses in drug bioavailability and pharmacokinetics [44]. Hepatic extraction is modeled using a modified venous equilibrium model that is applicable under transient and nonlinear conditions. For drugs undergoing gut metabolism by the same enzymes responsible for liver metabolism (e.g., CYPs 3A4 and 2D6), gut metabolism kinetic parameters are scaled from liver metabolism parameters by scaling V_{max} by the ratios of the amounts of metabolizing enzymes in each of the intestinal enterocyte compartments relative to the liver. Significant work in identifying the distribution of CYP3A4 and CYP2D6

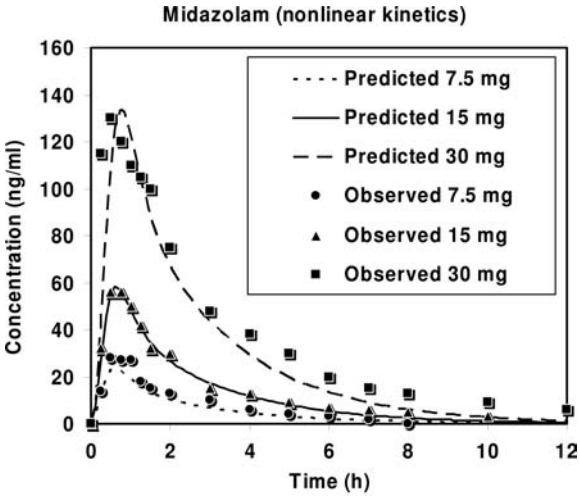

Figure 17.6 Experimental and simulated plasma concentration versus time profiles for three solution doses of midazolam. Data were collected from the literature [90].

isozymes in the gut has been done by Paine *et al.* and Madani *et al.*, respectively [88, 89], and their data were used in our simulations. We have validated the model against experimental data for drugs that undergo liver metabolism alone (propranolol and metoprolol), gut metabolism, and liver metabolism (midazolam), and efflux, gut metabolism, and liver metabolism (saquinavir).

We used *in vitro* kinetic constants obtained from homogenate or whole-cell experiments under controlled conditions and scaled the constants to the *in vivo* scenario by using appropriate physiological scale factors. Figure 17.6 shows our simulated results for absorption and metabolism of midazolam at three solution doses [90]. Midazolam is metabolized in the gut and liver by cytochrome 3A4, and Figure 17.6 shows the accurate simulation of the nonlinear dose dependence due to saturation of CYP3A4. Saquinavir is also metabolized in the gut and liver by 3A4, and it is also a substrate for efflux by P-glycoprotein. Figure 17.7 shows our simulated results for absorption and metabolism of saquinavir when dosed with and without grapefruit juice [91]. It can be seen that the simulation correctly predicts the increase in oral AUC and bioavailability when the drugs are dosed after the patient ingested grapefruit juice. It is well known that grapefruit juice is able to inhibit CYP3A4 metabolism in the gut by approximately 60% but not in the liver. Our results show that *in vitro* kinetic constants can be used to predict drug behavior *in vivo*, provided adequate data on enzyme distribution and activity are available, and that the *in vitro* method adequately measures the metabolic processes for the compound. The use of *in vitro* data from human liver microsomes, as was done for midazolam and saquinavir above, is adequate when the metabolism of the compound is well described by only phase-I processes that take place in microsomes. For compounds with significant phase-II metabolism, such as propranolol, microsomal measure-

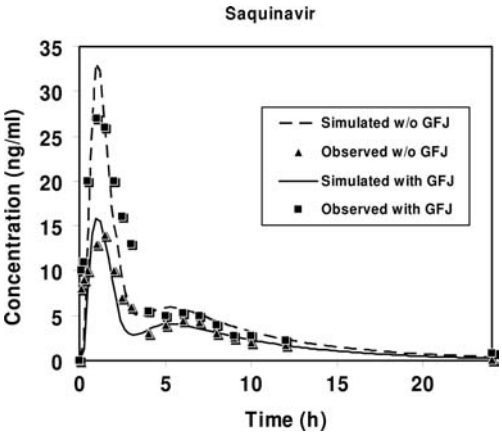

Figure 17.7 Experimental and simulated plasma concentration versus time profiles for a single dose of saquinavir administered with and without grape fruit juice [91].

ments will not reflect the entire metabolism, and clearance will be underpredicted. Data from hepatocytes can provide both phase-I and phase-II metabolism, and so the use of hepatocytes would be preferred when phase-II metabolism is involved. Even with the best of experimental data, factors such as interindividual variability in enzyme content and activity strongly limit the extension of predictions across different demographics.

More experimental information is needed regarding distribution and densities of metabolizing enzymes and efflux proteins in the GI tract. This information is crucial since dissolution and absorption are site dependent all along the GI tract. Knowledge of the variation in enzyme and efflux transporter amounts in the intestine and colon can also be used to design formulations with increased bioavailabilities by avoiding sites of high intestinal first pass and efflux. For example, the bioavailability of oxybutynin, a CYP3A4 substrate, is increased by modifying the formulation to release most of the drug in the distal GI [92]. Similarly, the bioavailability of a P-gp substrate might be increased by using a gastric-retentive formulation to release the drug in proximal GI where the P-gp density is relatively low. The influence of inhibitors and inducers of enzymes can be modeled by using appropriate scale factors to mimic changes in enzyme amounts, activity, and competitive inhibition. Similarly, drug–drug interactions can be modeled using the same techniques.

In spite of its limitations, the ACAT model combined with modeling of saturable processes has become a powerful tool in the study of oral absorption and pharmacokinetics. To our knowledge, it is the only tool that can translate *in vitro* data from early drug discovery experiments all the way to plasma concentration profiles and nonlinear dose-relationship predictions. As more experimental data become available, we believe that the model will become more comprehensive, and its predictive capabilities will be further enhanced.

17.5.1
Approaches to *In Silico* Estimation of Metabolism

In silico estimation of metabolism is still an area of intense study and development. Accurate prediction of intrinsic clearance is still not possible with the currently available methods [15]. Most of the progress in this area has been focused on the mixed function oxidase cytochrome P450 enzyme family. Advances in this area have been focused on three areas: (1) prediction of the cytochrome P450 (CYP) enzyme isotype that is responsible for the major metabolism, (2) prediction of the chemical site of a molecule that is most likely to undergo biotransformation by oxidative metabolism, and (3) structure-based docking studies of CYP enzyme substrate complexes .

Unsupervised machine learning based on the application of Kohonen self-organizing maps to groups of isotype-specific molecules has been applied to predict the CYP enzyme isotype involved in the major metabolism [93]. The same group used similar computational methods to estimate the catalytic K_m values for P450 substrates [94]. The most successful methods for predicting the P450 metabolism site utilize a method for calculation of the activation energy for homolytic cleavage of a C−H bond in the substrate [95–99]. Homolytic H atom abstraction is the rate-limiting step in P450 oxidative metabolism, and the C−H bonds with lowest activation energy are generally the sites of major metabolism for CYP enzymes such as 3A4 that has a large binding pocket that can easily accommodate the substrate in a variety of orientations. This method is less predictive for other CYP enzymes such as 2D6 or 2C9 that have a definite pharmacophore that helps orient the substrate so that oxidation can occur at carbons that have a higher activation energy for homolytic cleavage. A newer, empirical method for estimating the H-atom abstraction energy was shown to be more accurate than the classical methods based on semiempirical AM1 calculations [100, 101].

The availability of X-ray crystallographic structures and homology models of the CYP450 enzymes allows the application of structure-based methods to predict P450 metabolism [102–105]. Newer approaches that have promise in this area include hybrid methods that use an energy calculation with some knowledge of the steric interaction of a given CYP enzyme. Metasite, a software program, combines the calculation of H-atom abstraction energetics with a method based on a comparison between alignment-independent descriptors derived from GRID molecular interaction fields for the active site and a distance-based representation of the substrate [106, 107].

17.6
Regulatory Aspects of Modeling and Simulation (FDA Critical Path Initiative)

Pharmaceutical productivity has been falling and costs have been rising. In 2004, the US FDA introduced the Critical Path Initiative to modernize drug development by introducing advancements in genomics, modeling and simulation, and advanced

imaging [22, 108, 109, 20, 110]. One important use of such data will be to construct quantitative models of disease processes, incorporating what is known about biomarkers, clinical outcomes, and the effects of various interventions. These models can then be used for trial simulations to better design appropriate trials and clinical outcome measures. These methods have been dubbed "Model-Based Drug Development and have the potential to improve the success rate in regulatory approval [20]."

17.7 Conclusions

The application of ultrahigh-throughput *in silico* estimation of biopharmaceutical properties to generate rule-based computational alerts has the potential to improve compound selection for those drug candidates that are likely to have less trouble in development. Extension of purely *in silico* methods to the realm of mechanistic simulation further enhances our ability to predict the impact of physiological and biochemical processes on drug absorption and bioavailability. Quantitative prediction of metabolic rates is still a future goal, but great progress has been achieved in calculating substrate specificity, sites of metabolism, and relative binding interactions with metabolic enzymes. It remains to be seen if all of these innovations combined with clinical trial simulations and model-based drug development will lead to a faster and less expensive drug development.

References

1 Modi, S. (2003) Computational approaches to the understanding of ADMET properties and problems. *Drug Discovery Today*, **8** (14), 621–623.

2 van de Waterbeemd, H. and Gifford, E. (2003) ADMET *in silico* modelling: towards prediction paradise? *Nature Reviews. Drug Discovery*, **2** (3), 192–204.

3 Stoner, C.L., Gifford, E., Stankovic, C., Lepsy, C.S., Brodfuehrer, J., Prasad, J.V. and Surendran, N. (2004) Implementation of an ADME enabling selection and visualization tool for drug discovery. *Journal of Pharmaceutical Sciences*, **93** (5), 1131–1141.

4 Yamashita, F. and Hashida, M. (2004) *In silico* approaches for predicting ADME properties of drugs. *Drug Metabolism and Pharmacokinetics*, **19** (5), 327–338.

5 Balakin, K.V., Ivanenkov, Y.A., Savchuk, N.P., Ivashchenko, A.A. and Ekins, S. (2005) Comprehensive computational assessment of ADME properties using mapping techniques. *Current Drug Discovery Technologies*, **2** (2), 99–113.

6 Lupfert, C. and Reichel, A. (2005) Development and application of physiologically based pharmacokinetic-modeling tools to support drug discovery. *Chemistry & Biodiversity*, **2** (11), 1462–1486.

7 Cai, H., Stoner, C., Reddy, A., Freiwald, S., Smith, D., Winters, R., Stankovic, C. and Surendran, N. (2006) Evaluation of an integrated *in vitro–in silico* PBPK (physiologically based pharmacokinetic) model to provide estimates of human

bioavailability. *International Journal of Pharmaceutics*, **308** (1–2), 133–139.

8 Jones, H.M., Parrott, N., Jorga, K. and Lave, T. (2006) A novel strategy for physiologically based predictions of human pharmacokinetics. *Clinical Pharmacokinetics*, **45** (5), 511–542.

9 Jones, H.M., Parrott, N., Ohlenbusch, G. and Lave, T. (2006) Predicting pharmacokinetic food effects using biorelevant solubility media and physiologically based modelling. *Clinical Pharmacokinetics*, **45** (12), 1213–1226.

10 De Buck, S.S., Sinha, V.K., Fenu, L.A., Gilissen, R.A., Mackie, C.E. and Nijsen, M.J. (2007) The prediction of drug metabolism, tissue distribution, and bioavailability of 50 structurally diverse compounds in rat using mechanism-based absorption, distribution, and metabolism prediction tools. *Drug Metabolism and Disposition: The Biological Fate of Chemicals*, **35** (4), 649–659.

11 De Buck, S.S., Sinha, V.K., Fenu, L.A., Nijsen, M.J., Mackie, C.E. and Gilissen, R.A. (2007) Prediction of human pharmacokinetics using physiologically based modeling: a retrospective analysis of 26 clinically tested drugs. *Drug Metabolism and Disposition: The Biological Fate of Chemicals*, **35** (10), 1766–1780.

12 Rowland, M., Balant, L. and Peck, C. (2004) Physiologically based pharmacokinetics in drug development and regulatory science: a workshop report (Georgetown University, Washington, DC, May 29–30, 2002). *AAPS Journal*, **6** (1), E6.

13 Bolger, M.B., Fraczkiewicz, R. and Steere, B. (2006) *In silico* surrogates for vivo properties: profiling for ADME and toxicological behaviour, in *Exploiting Chemical Diversity for Drug Discovery* (eds P.A. Bartlett and M. Entzeroth), Royal Society of Chemistry, London, pp. 364–381.

14 Bolger, M.B., Fraczkiewicz, R., Entzeroth, M. and Steere, B. (2006) Concepts for *in vitro* profiling: Drug activity, selectivity, and liability, in *Exploiting Chemical Diversity for Drug Discovery* (eds P.A. Bartlett and M. Entzeroth), Royal Society of Chemistry, London, pp. 336–362.

15 Jolivette, L.J. and Ekins, S. (2007) Methods for predicting human drug metabolism. *Advances in Clinical Chemistry*, **43**, 131–176.

16 Haworth, I.S. (2006) Computational drug delivery. *Advanced Drug Delivery Reviews*, **58** (12–13), 1271–1273.

17 Ekins, S., Nikolsky, Y. and Nikolskaya, T. (2005) Techniques: application of systems biology to absorption, distribution, metabolism, excretion and toxicity. *Trends in Pharmacological Sciences*, **26** (4), 202–209.

18 Ekins, S. (2006) Systems-ADME/Tox: resources and network approaches. *Journal of Pharmacological and Toxicological Methods*, **53** (1), 38–66.

19 Powell, J.R. and Gobburu, J.V. (2007) Pharmacometrics at FDA: evolution and impact on decisions. *Clinical Pharmacology and Therapeutics*, **82** (1), 97–102.

20 Lalonde, R.L., Kowalski, K.G., Hutmacher, M.M., Ewy, W., Nichols, D.J., Milligan, P.A., Corrigan, B.W., Lockwood, P.A., Marshall, S.A., Benincosa, L.J., Tensfeldt, T.G., Parivar, K., Amantea, M., Glue, P., Koide, H. and Miller, R. (2007) Model-based drug development. *Clinical Pharmacology and Therapeutics*, **82** (1), 21–32.

21 Zhang, L., Sinha, V., Forgue, S.T., Callies, S., Ni, L., Peck, R. and Allerheiligen, S.R. (2006) Model-based drug development: the road to quantitative pharmacology. *Journal of Pharmacokinetics and Pharmacodynamics*, **33** (3), 369–393.

22 Miller, R., Ewy, W., Corrigan, B.W., Ouellet, D., Hermann, D., Kowalski, K.G., Lockwood, P., Koup, J.R., Donevan, S., El-Kattan, A., Li, C.S., Werth, J.L., Feltner, D.E. and Lalonde, R.L. (2005) How modeling and simulation have enhanced decision making in new drug

development. *Journal of Pharmacokinetics and Pharmacodynamics*, **32** (2), 185–197.

23 Hall, S.D., Thummel, K.E., Watkins, P.B., Lown, K.S., Benet, L.Z., Paine, M.F., Mayo, R.R., Turgeon, D.K., Bailey, D.G., Fontana, R.J. and Wrighton, S.A. (1999) Molecular and physical mechanisms of first-pass extraction. *Drug Metabolism and Disposition: The Biological Fate of Chemicals*, **27** (2), 161–166.

24 Yu, L.X., Lipka, E., Crison, J.R. and Amidon, G.L. (1996) Transport approaches to the biopharmaceutical design of oral drug delivery system: prediction of intestinal absorption. *Advanced Drug Delivery Reviews*, **19**, 359–376.

25 Jacobs, M.H. (1940) Some aspects of cell permeability to weak electrolytes. *Cold Spring Harbor Symposia on Quantitative Biology*, **8**, 30–39.

26 Hogben, C.A.M., Tocco, D.J., Brodie, B.B. and Schanker, L.S. (1959) On the mechanism of intestinal absorption of drugs. *The Journal of Pharmacology and Experimental Therapeutics*, **125**, 275–282.

27 Palm, K., Luthman, K., Ros, J., Grasjo, J. and Artursson, P. (1999) Effect of molecular charge on intestinal epithelial drug transport: pH-dependent transport of cationic drugs. *The Journal of Pharmacology and Experimental Therapeutics*, **291** (2), 435–443.

28 Suzuki, A., Higuchi, W.I. and Ho, N.F. (1970) Theoretical model studies of drug absorption and transport in the gastrointestinal tract. 2. *Journal of Pharmaceutical Sciences*, **59** (5), 651–659.

29 Suzuki, A., Higuchi, W.I. and Ho, N.F. (1970) Theoretical model studies of drug absorption and transport in the gastrointestinal tract.1. *Journal of Pharmaceutical Sciences*, **59** (5), 644–651.

30 Ho, N.F., Higuchi, W.I. and Turi, J. (1972) Theoretical model studies of drug absorption and transport in the GI tract. 3. *Journal of Pharmaceutical Sciences*, **61** (2), 192–197.

31 Ho, N.F. and Higuchi, W.I. (1971) Quantitative interpretation of *in vivo* buccal absorption of n-alkanoic acids by the physical model approach. *Journal of Pharmaceutical Sciences*, **60** (4), 537–541.

32 Dressman, J.B., Fleisher, D. and Amidon, G.L. (1984) Physicochemical model for dose-dependent drug absorption. *Journal of Pharmaceutical Sciences*, **73** (9), 1274–1279.

33 Suttle, A.B., Pollack, G.M. and Brouwer, K.L. (1992) Use of a pharmacokinetic model incorporating discontinuous gastrointestinal absorption to examine the occurrence of double peaks in oral concentration–time profiles. *Pharmaceutical Research*, **9** (3), 350–356.

34 Wright, J.D., Ma, T., Chu, C.K. and Boudinot, F.D. (1996) Discontinuous oral absorption pharmacokinetic model and bioavailability of 1-(2-fluoro-5-methyl-beta-L-arabinofuranosyl)uracil (L-FMAU) in rats. *Biopharmaceutics & Drug Disposition*, **17** (3), 197–207.

35 Grass, G.M. (1997) Simulation models to predict oral drug absorption from *in vitro* data. *Advanced Drug Delivery Reviews*, **23**, 199–219.

36 Norris, D.A., Leesman, G.D., Sinko, P.J. and Grass, G.M. (2000) Development of predictive pharmacokinetic simulation models for drug discovery. *Journal of Controlled Release*, **65** (1–2), 55–62.

37 Cong, D., Doherty, M. and Pang, K.S. (2000) A new physiologically based, segregated-f model to explain route-dependent intestinal metabolism. *Drug Metabolism and Disposition: The Biological Fate of Chemicals*, **28** (2), 224–235.

38 Kalampokis, A., Argyrakis, P. and Macheras, P. (1999) A heterogeneous tube model of intestinal drug absorption based on probabilistic concepts. *Pharmaceutical Research*, **16** (11), 1764–1769.

39 Kalampokis, A., Argyrakis, P. and Macheras, P. (1999) Heterogeneous tube model for the study of small intestinal

transit flow. *Pharmaceutical Research*, **16** (1), 87–91.

40 Ito, K., Kusuhara, H. and Sugiyama, Y. (1999) Effects of intestinal CYP3A4 and P-glycoprotein on oral drug absorption–theoretical approach. *Pharmaceutical Research*, **16** (2), 225–231.

41 Rostami-Hodjegan, A. and Tucker, G.T. (2007) Simulation and prediction of *in vivo* drug metabolism in human populations from *in vitro* data. *Nature Reviews. Drug Discovery*, **6** (2), 140–148.

42 Willmann, S., Schmitt, W., Keldenich, J. and Dressman, J.B. (2003) A physiologic model for simulating gastrointestinal flow and drug absorption in rats. *Pharmaceutical Research*, **20** (11), 1766–1771.

43 Willmann, S., Schmitt, W., Keldenich, J., Lippert, J. and Dressman, J.B. (2004) A physiological model for the estimation of the fraction dose absorbed in humans. *Journal of Medicinal Chemistry*, **47** (16), 4022–4031.

44 Agoram, B., Woltosz, W.S. and Bolger, M.B. (2001) Predicting the impact of physiological and biochemical processes on oral drug bioavailability. *Advanced Drug Delivery Reviews*, **50** (Suppl. 1) S41–S67.

45 Aarons, L., Karlsson, M.O., Mentre, F., Rombout, F., Steimer, J.L. and van Peer, A. (2001) Role of modelling and simulation in phase I drug development. *European Journal of Pharmaceutical Sciences*, **13** (2), 115–122.

46 Yu, L.X. and Amidon, G.L. (1999) A compartmental absorption and transit model for estimating oral drug absorption. *International Journal of Pharmaceutics*, **186** (2), 119–125.

47 Lipinski, C.A., Lombardo, F., Dominy, B.W. and Feeney, P.J. (1997) Experimental and computational approaches to estimate solubility and permeability in drug discovery and development settings. *Advanced Drug Delivery Reviews*, **23** (1–3), 3–25.

48 Andrews, C.W., Bennett, L. and Yu, L.X. (2000) Predicting human oral bioavailability of a compound: development of a novel quantitative structure–bioavailability relationship *Pharmaceutical Research*, **17** (6), 639–644.

49 Oprea, T.I. and Gottfries, J. (1999) Toward minimalistic modeling of oral drug absorption. *Journal of Molecular Graphics & Modelling*, **17** (5–6), 261–274, 329.

50 Stenberg, P., Luthman, K., Ellens, H., Lee, C.P., Smith, P.L., Lago, A., Elliott, J.D. and Artursson, P. (1999) Prediction of the intestinal absorption of endothelin receptor antagonists using three theoretical methods of increasing complexity. *Pharmaceutical Research*, **16** (10), 1520–1526.

51 Matter, H., Baringhaus, K.H., Naumann, T., Klabunde, T. and Pirard, B. (2001) Computational approaches towards the rational design of drug-like compound libraries. *Combinatorial Chemistry & High Throughput Screening*, **4** (6), 453–475.

52 Osterberg, T. and Norinder, U. (2000) Prediction of polar surface area and drug transport processes using simple parameters and PLS statistics. *Journal of Chemical Information and Computer Sciences*, **40** (6), 1408–1411.

53 Chiou, W.L. and Barve, A. (1998) Linear correlation of the fraction of oral dose absorbed of 64 drugs between humans and rats. *Pharmaceutical Research*, **15** (11), 1792–1795.

54 Zhao, Y.H., Le, J., Abraham, M.H., Hersey, A., Eddershaw, P.J., Luscombe, C.N., Butina, D., Beck, G., Sherborne, B., Cooper, I., Platts, J.A. and Boutina, D. (2001) Evaluation of human intestinal absorption data and subsequent derivation of a quantitative structure–activity relationship (QSAR) with the Abraham descriptors. *Journal of Pharmaceutical Sciences*, **90** (6), 749–784.

55 Matthews, E.J., Kruhlak, N.L., Benz, R.D. and Contrera, J.F. (2004) Assessment of the health effects of chemicals in humans: I. QSAR estimation of the maximum

recommended therapeutic dose (MRTD) and no effect level (NOEL) of organic chemicals based on clinical trial data. *Current Drug Discovery Technologies*, **1** (1), 61–76.

56 Russom, C.L., Bradbury, S.P., Broderius, S.J., Hammermeister, D.E. and Drummond, R.A. (1997) Predicting modes of toxic action from chemical structure: acute toxicity in the fathead minnow (*Pimephales promelas*). *Environmental Toxicology and Chemistry/SETAC*, **16** (5), 948–967.

57 Gold, L.S., Manley, N.B., Slone, T.H. and Rohrbach, L. (1999) Supplement to the Carcinogenic Potency Database (CPDB): results of animal bioassays published in the general literature in 1993 to 1994 and by the National Toxicology Program in 1995 to 1996. *Environmental Health Perspectives*, **107** (Suppl. 4) 527–600.

58 Bains, W., Basman, A. and White, C. (2004) HERG binding specificity and binding site structure: evidence from a fragment-based evolutionary computing SAR study. *Progress in Biophysics and Molecular Biology*, **86** (2), 205–233.

59 Keseru, G.M. (2003) Prediction of hERG potassium channel affinity by traditional and hologram qSAR methods. *Bioorganic & Medicinal Chemistry Letters*, **13** (16), 2773–2775.

60 Cohen, S.D. and Hindmarsh, A.C. (1996) CVODE, a stiff/nonstiff ODE solver in C. *Computers in Physics*, **10** (2), 138–143.

61 Pade, V. and Stavchansky, S. (1997) Estimation of the relative contribution of the transcellular and paracellular pathway to the transport of passively absorbed drugs in the Caco-2 cell culture model. *Pharmaceutical Research*, **14** (9), 1210–1215.

62 Ungell, A.L., Nylander, S., Bergstrand, S., Sjoberg, A. and Lennernäs, H. (1998) Membrane transport of drugs in different regions of the intestinal tract of the rat. *Journal of Pharmaceutical Sciences*, **87** (3), 360–366.

63 Adson, A., Burton, P.S., Raub, T.J., Barsuhn, C.L., Audus, K.L. and Ho, N.F. (1995) Passive diffusion of weak organic electrolytes across Caco-2 cell monolayers: uncoupling the contributions of hydrodynamic, transcellular, and paracellular barriers. *Journal of Pharmaceutical Sciences*, **84** (10), 1197–1204.

64 Fordtran, J.S., Rector, F.C., Jr. Ewton, M.F., Soter, N. and Kinney, J. (1965) Permeability characteristics of the human small intestine. *The Journal of Clinical Investigation*, **44** (12), 1935–1944.

65 Soergel, K.H., Whalen, G.E. and Harris, J.A. (1968) Passive movement of water and sodium across the human small intestinal mucosa. *Journal of Applied Physiology*, **24** (1), 40–48.

66 Artursson, P. and Karlsson, J. (1991) Correlation between oral drug absorption in humans and apparent drug permeability coefficients in human intestinal epithelial (Caco-2) cells. *Biochemical and Biophysical Research Communications*, **175** (3), 880–885.

67 Billich, C.O. and Levitan, R. (1969) Effects of sodium concentration and osmolality on water and electrolyte absorption form the intact human colon. *The Journal of Clinical Investigation*, **48** (7), 1336–1347.

68 Maruyama, W., Yoshida, K., Tanaka, T. and Nakanishi, J. (2002) Determination of tissue–blood partition coefficients for a physiological model for humans, and estimation of dioxin concentration in tissues. *Chemosphere*, **46** (7), 975–985.

69 Sarangapani, R., Teeguarden, J.G., Cruzan, G., Clewell, H.J. and Andersen, M.E. (2002) Physiologically based pharmacokinetic modeling of styrene and styrene oxide respiratory-tract dosimetry in rodents and humans. *Inhalation Toxicology*, **14** (8), 789–834.

70 Thrall, K.D., Soelberg, J.J., Weitz, K.K. and Woodstock, A.D. (2002) Development of a physiologically based pharmacokinetic model for methyl ethyl ketone in F344 rats. *Journal of Toxicology and*

Environmental Health. Part A, **65** (13), 881–896.

71 Nestorov, I.A., Aarons, L.J. and Rowland, M. (1997) Physiologically based pharmacokinetic modeling of a homologous series of barbiturates in the rat: a sensitivity analysis. *Journal of Pharmacokinetics and Biopharmaceutics*, **25** (4), 413–447.

72 Kawai, R., Lemaire, M., Steimer, J.L., Bruelisauer, A., Niederberger, W. and Rowland, M. (1994) Physiologically based pharmacokinetic study on a cyclosporin derivative, SDZ IMM 125. *Journal of Pharmacokinetics and Biopharmaceuticst*, **22** (5), 327–365.

73 Bjorkman, S., Wada, D.R., Berling, B.M. and Benoni, G. (2001) Prediction of the disposition of midazolam in surgical patients by a physiologically based pharmacokinetic model. *Journal of Pharmaceutical Sciences*, **90** (9), 1226–1241.

74 Fouchecourt, M.O., Beliveau, M. and Krishnan, K. (2001) Quantitative structure–pharmacokinetic relationship modelling. *The Science of the Total Environment*, **274** (1–3), 125–135.

75 Pelekis, M., Poulin, P. and Krishnan, K. (1995) An approach for incorporating tissue composition data into physiologically based pharmacokinetic models. *Toxicology and Industrial Health*, **11** (5), 511–522.

76 Payne, M.P. and Kenny, L.C. (2002) Comparison of models for the estimation of biological partition coefficients. *Journal of Toxicology and Environmental Health. Part A*, **65** (13), 897–931.

77 Poulin, P. and Theil, F.P. (2000) *A priori* prediction of tissue:plasma partition coefficients of drugs to facilitate the use of physiologically-based pharmacokinetic models in drug discovery. *Journal of Pharmaceutical Sciences*, **89** (1), 16–35.

78 Luttringer, O., Theil, F.P., Poulin, P., Schmitt-Hoffmann, A.H., Guentert, T.W. and Lave, T. (2003) Physiologically based pharmacokinetic (PBPK) modeling of disposition of epiroprim in humans. *Journal of Pharmaceutical Sciences*, **92** (10), 1990–2007.

79 Theil, F.P., Guentert, T.W., Haddad, S. and Poulin, P. (2003) Utility of physiologically based pharmacokinetic models to drug development and rational drug discovery candidate selection. *Toxicology Letters*, **138** (1–2), 29–49.

80 Poulin, P. and Theil, F.P. (2002) Prediction of pharmacokinetics prior to *in vivo* studies. II. Generic physiologically based pharmacokinetic models of drug disposition. *Journal of Pharmaceutical Sciences*, **91** (5), 1358–1370.

81 De Buck, S.S. and Mackie, C.E. (2007) Physiologically based approaches towards the prediction of pharmacokinetics: *in vitro–in vivo* extrapolation. *Expert Opinion on Drug Metabolism and Toxicology*, **3** (6), 865–878.

82 Rodgers, T., Leahy, D. and Rowland, M. (2005) Tissue distribution of basic drugs: accounting for enantiomeric, compound and regional differences amongst beta-blocking drugs in rat. *Journal of Pharmaceutical Sciences*, **94** (6), 1237–1248.

83 Rodgers, T., Leahy, D. and Rowland, M. (2005) Physiologically based pharmacokinetic modeling 1: predicting the tissue distribution of moderate-to-strong bases. *Journal of Pharmaceutical Sciences*, **94** (6), 1259–1276.

84 Rodgers, T. and Rowland, M. (2006) Physiologically based pharmacokinetic modelling 2: predicting the tissue distribution of acids, very weak bases, neutrals and zwitterions. *Journal of Pharmaceutical Sciences*, **95** (6), 1238–1257.

85 Rodgers, T. and Rowland, M. (2007) Mechanistic approaches to volume of distribution predictions: understanding the processes. *Pharmaceutical Research*, **24** (5), 918–933.

86 Brightman, F.A., Leahy, D.E., Searle, G.E. and Thomas, S. (2006) Application of a generic physiologically based

pharmacokinetic model to the estimation of xenobiotic levels in rat plasma. *Drug Metabolism and Disposition: The Biological Fate of Chemicals*, **34** (1), 84–93.

87 Willmann, S., Hohn, K., Edginton, A., Sevestre, M., Solodenko, J., Weiss, W., Lippert, J. and Schmitt, W. (2007) Development of a physiology-based whole-body population model for assessing the influence of individual variability on the pharmacokinetics of drugs. *Journal of Pharmacokinetics and Pharmacodynamics*, **34** (3), 401–431.

88 Paine, M.F., Khalighi, M., Fisher, J.M., Shen, D.D., Kunze, K.L., Marsh, C.L., Perkins, J.D. and Thummel, K.E. (1997) Characterization of interintestinal and intraintestinal variations in human CYP3A-dependent metabolism. *The Journal of Pharmacology and Experimental Therapeutics*, **283** (3), 1552–1562.

89 Madani, S., Paine, M.F., Lewis, L., Thummel, K.E. and Shen, D.D. (1999) Comparison of CYP2D6 content and metoprolol oxidation between microsomes isolated from human livers and small intestines. *Pharmaceutical Research*, **16** (8), 1199–1205.

90 Bornemann, L.D., Min, B.H., Crews, T., Rees, M.M., Blumenthal, H.P., Colburn, W.A. and Patel, I.H. (1985) Dose dependent pharmacokinetics of midazolam. *European Journal of Clinical Pharmacology*, **29** (1), 91–95.

91 Kupferschmidt, H.H., Fattinger, K.E., Ha, H.R., Follath, F. and Krahenbuhl, S. (1998) Grapefruit juice enhances the bioavailability of the HIV protease inhibitor saquinavir in man. *British Journal of Clinical Pharmacology*, **45** (4), 355–359.

92 Gupta, S.K. and Sathyan, G. (1999) Pharmacokinetics of an oral once-a-day controlled-release oxybutynin formulation compared with immediate-release oxybutynin. *Journal of Clinical Pharmacology*, **39** (3), 289–296.

93 Korolev, D., Balakin, K.V., Nikolsky, Y., Kirillov, E., Ivanenkov, Y.A., Savchuk, N.P., Ivashchenko, A.A. and Nikolskaya, T. (2003) Modeling of human cytochrome p450-mediated drug metabolism using unsupervised machine learning approach. *Journal of Medicinal Chemistry*, **46** (17), 3631–3643.

94 Balakin, K.V., Ekins, S., Bugrim, A., Ivanenkov, Y.A., Korolev, D., Nikolsky, Y.V., Skorenko, A.V., Ivashchenko, A.A., Savchuk, N.P. and Nikolskaya, T. (2004) Kohonen maps for prediction of binding to human cytochrome P450 3A4. *Drug Metabolism and Disposition: The Biological Fate of Chemicals*, **32** (10), 1183–1189.

95 Korzekwa, K.R., Jones, J.P. and Gillette, J.R. (1990) Theoretical studies on cytochrome P-450 mediated hydroxylation: a predictive model for hydrogen atom abstractions. *Journal of the American Chemical Society*, **112**, 7042–7046.

96 Korzekwa, K.R., Trager, W.F., Mancewicz, J. and Osawa, Y. (1993) Studies on the mechanism of aromatase and other cytochrome P450 mediated deformylation reactions. *The Journal of Steroid Biochemistry and Molecular Biology*, **44** (4–6), 367–373.

97 Korzekwa, K.R. and Jones, J.P. (1993) Predicting the cytochrome P450 mediated metabolism of xenobiotics. *Pharmacogenetics*, **3** (1), 1–18.

98 Jones, J.P. and Korzekwa, K.R. (1996) Predicting the rates and regioselectivity of reactions mediated by the P450 superfamily. *Methods in Enzymology*, **272**, 326–335.

99 Jones, J.P., Mysinger, M. and Korzekwa, K.R. (2002) Computational models for cytochrome P450: a predictive electronic model for aromatic oxidation and hydrogen atom abstraction. *Drug Metabolism and Disposition: The Biological Fate of Chemicals*, **30** (1), 7–12.

100 Singh, S.B., Shen, L.Q., Walker, M.J. and Sheridan, R.P. (2003) A model for predicting likely sites of CYP3A4-mediated metabolism on drug-like

molecules. *Journal of Medicinal Chemistry*, **46** (8), 1330–1306.

101 Sheridan, R.P., Korzekwa, K.R., Torres, R.A. and Walker, M.J. (2007) Empirical regioselectivity models for human cytochromes P450 3A4, 2D6, and 2C9. *Journal of Medicinal Chemistry*, **50** (14), 3173–3184.

102 de Groot, M.J., Vermeulen, N.P., Kramer, J.D., van Acker, F.A. and Donne-Op den Kelder, G.M. (1996) A three-dimensional protein model for human cytochrome P450 2D6 based on the crystal structures of P450 101, P450 102, and P450 108. *Chemical Research in Toxicology*, **9** (7), 1079–1091.

103 de Groot, M.J., Alex, A.A. and Jones, B.C. (2002) Development of a combined protein and pharmacophore model for cytochrome P450 2C9. *Journal of Medicinal Chemistry*, **45** (10), 1983–1993.

104 de Groot, M.J., Kirton, S.B. and Sutcliffe, M.J. (2004) *In silico* methods for predicting ligand binding determinants of cytochromes P450. *Current Topics in Medicinal Chemistry*, **4** (16), 1803–1824.

105 de Groot, M.J. (2006) Designing better drugs: predicting cytochrome P450 metabolism. *Drug Discovery Today*, **11** (13–14), 601–606.

106 Cruciani, G., Carosati, E., De Boeck, B., Ethirajulu, K., Mackie, C., Howe, T. and Vianello, R. (2005) MetaSite: understanding metabolism in human cytochromes from the perspective of the chemist. *Journal of Medicinal Chemistry*, **48** (22), 6970–6979.

107 Zamora, I., Afzelius, L. and Cruciani, G. (2003) Predicting drug metabolism: a site of metabolism prediction tool applied to the cytochrome P450 2C9. *Journal of Medicinal Chemistry*, **46** (12), 2313–2324.

108 O'Neill, R.T. (2006) FDA's critical path initiative: a perspective on contributions of biostatistics. *Biometrical Journal*, **48** (4), 559–564.

109 Woosley, R.L. and Cossman, J. (2007) Drug development and the FDA's critical path initiative. *Clinical Pharmacology and Therapeutics*, **81** (1), 129–133.

110 Woodcock, J. and Woosley, R. (2008) The FDA critical path initiative and its influence on new drug development. *Annual Review of Medicine*, **59**, 1–12.

111 Leonce, S., Pierre, A., Anstett, M., Perez, V., Genton, A., Bizzari, J.P. and Atassi, G. (1992) Effects of a new triazinoaminopiperidine derivative on adriamycin accumulation and retention in cells displaying P-glycoprotein-mediated multidrug resistance. *Biochemical Pharmacology*, **44** (9), 1707–1715.

112 Hsiang, B., Zhu, Y., Wang, Z., Wu, Y., Sasseville, V., Yang, W.P. and Kirchgessner, T.G. (1999) A novel human hepatic organic anion transporting polypeptide (OATP2). Identification of a liver-specific human organic anion transporting polypeptide and identification of rat and human hydroxymethylglutaryl-CoA reductase inhibitor transporters. *The Journal of Biological Chemistry*, **274** (52), 37161–37168.

113 Chen, C., Lin, J., Smolarek, T. and Tremaine, L. (2007) P-Glycoprotein has differential effects on the disposition of statin acid and lactone forms in mdr1a/b knockout and wild-type mice. *Drug Metabolism and Disposition: The Biological Fate of Chemicals*, **35** (10), 1725–1729.

114 Holtzman, C.W., Wiggins, B.S. and Spinler, S.A. (2006) Role of P-glycoprotein in statin drug interactions. *Pharmacotherapy*, **26** (11), 1601–1607.

115 de Koning, H.P. and Jarvis, S.M. (1997) Hypoxanthine uptake through a purine-selective nucleobase transporter in Trypanosoma brucei brucei procyclic cells is driven by protonmotive force. *European Journal of Biochemistry*, **247** (3), 1102–1110.

116 Balch, W.E. and Wolfe, R.S. (1979) Transport of coenzyme M (2-mercaptoethanesulfonic acid) in

methanobacterium ruminantium. *Journal of Bacteriology*, **137** (1), 264–273.

117 Shima, Y., Maeda, T., Aizawa, S., Tsuboi, I., Kobayashi, D., Kato, R. and Tamai, I. (2006) L-arginine import via cationic amino acid transporter CAT1 is essential for both differentiation and proliferation of erythrocytes. *Blood*, **107** (4), 1352–1356.

118 Zhou, M., Xia, L. and Wang, J. (2007) Metformin transport by a newly cloned proton-stimulated organic cation transporter (plasma membrane monoamine transporter) expressed in human intestine. *Drug Metabolism and Disposition: The Biological Fate of Chemicals*, **35** (10), 1956–1962.

119 Swaan, P.W. and Tukker, J.J. (1997) Molecular determinants of recognition for the intestinal peptide carrier. *Journal of Pharmaceutical Sciences*, **86** (5), 596–602.

120 Nagakubo, J., Tomimatsu, T., Kitajima, M., Takayama, H., Aimi, N. and Horie, T. (2001) Characteristics of transport of fluoresceinated methotrexate in rat small intestine. *Life Sciences*, **69** (7), 739–747.

121 Luckner, P. and Brandsch, M. (2005) Interaction of 31 beta-lactam antibiotics with the H+/peptide symporter PEPT2: analysis of affinity constants and comparison with PEPT1. *European Journal of Pharmaceutics and Biopharmaceutics*, **59** (1), 17–24.

122 Katiyar, S.K. and Edlind, T.D. (2001) Identification and expression of multidrug resistance-related ABC transporter genes in *Candida krusei*. *Medical Mycology*, **39** (1), 109–116.

123 Chang, C., Bahadduri, P.M., Polli, J.E., Swaan, P.W. and Ekins, S. (2006) Rapid identification of P-glycoprotein substrates and inhibitors. *Drug Metabolism and Disposition: The Biological Fate of Chemicals*, **34** (12), 1976–1984.

124 Terao, T., Hisanaga, E., Sai, Y., Tamai, I. and Tsuji, A. (1996) Active secretion of drugs from the small intestinal epithelium in rats by P-glycoprotein functioning as an absorption barrier. *The Journal of Pharmacy and Pharmacology*, **48** (10), 1083–1089.

125 Honscha, W., Schulz, K., Muller, D. and Petzinger, E. (1993) Two different mRNAs from rat liver code for the transport of bumetanide and taurocholate in *Xenopus laevis* oocytes. *European Journal of Pharmacology*, **246** (3), 227–232.

126 Sadoogh-Abasian, F. and Evered, D.F. (1980) Absorption of nicotinic acid and nicotinamide from rat small intestine *in vitro*. *Biochimica et Biophysica Acta*, **598** (2), 385–391.

127 Hu, M. and Amidon, G.L. (1988) Passive and carrier-mediated intestinal absorption components of captopril. *Journal of Pharmaceutical Sciences*, **77** (12), 1007–1011.

128 Nakamura, H., Sano, H., Yamazaki, M. and Sugiyama, Y. (1994) Carrier-mediated active transport of histamine H2 receptor antagonists, cimetidine and nizatidine, into isolated rat hepatocytes: contribution of type I system. *The Journal of Pharmacology and Experimental Therapeutics*, **269** (3), 1220–1227.

129 de Lange, E.C., Marchand, S., van den Berg, D., van der Sandt, I.C., de Boer, A.G., Delon, A., Bouquet, S. and Couet, W. (2000) *In vitro* and *in vivo* investigations on fluoroquinolones; effects of the P-glycoprotein efflux transporter on brain distribution of sparfloxacin. *European Journal of Pharmaceutical Sciences*, **12** (2), 85–93.

130 Swaan, P.W., Stehouwer, M.C. and Tukker, J.J. (1995) Molecular mechanism for the relative binding affinity to the intestinal peptide carrier. Comparison of three ACE-inhibitors: enalapril, enalaprilat, and lisinopril. *Biochimica et Biophysica Acta*, **1236** (1), 31–38.

131 Lauterbach, F. (1987) Intestinal permeation of nonquaternary amines: a study with telenzepine and pirenzepine in the isolated mucosa of guinea pig jejunum and colon. *The Journal of Pharmacology and Experimental Therapeutics*, **243** (3), 1121–1130.

132 Boulton, D.W., DeVane, C.L., Liston, H.L. and Markowitz, J.S. (2002) *In vitro* P-glycoprotein affinity for atypical and conventional antipsychotics. *Life Sciences*, **71** (2), 163–169.

133 Covitz, K.M., Amidon, G.L. and Sadee, W. (1996) Human dipeptide transporter, hPEPT1, stably transfected into Chinese hamster ovary cells. *Pharmaceutical Research*, **13** (11), 1631–1634.

134 Hatanaka, T. (2000) Clinical pharmacokinetics of pravastatin: mechanisms of pharmacokinetic events. *Clinical Pharmacokinetics*, **39** (6), 397–412.

135 Metzner, L., Neubert, K. and Brandsch, M. (2006) Substrate specificity of the amino acid transporter PAT1. *Amino Acids*, **31** (2), 111–117.

136 Anderson, C.M. and Thwaites, D.T. (2005) Indirect regulation of the intestinal H + -coupled amino acid transporter hPAT1 (SLC36A1). *Journal of Cellular Physiology*, **204** (2), 604–613.

137 van Kalken, C.K., Broxterman, H.J., Pinedo, H.M., Feller, N., Dekker, H., Lankelma, J. and Giaccone, G. (1993) Cortisol is transported by the multidrug resistance gene product P-glycoprotein. *British Journal of Cancer*, **67** (2), 284–289.

138 Yao, H.M. and Chiou, W.L. (2006) The complexity of intestinal absorption and exsorption of digoxin in rats. *International Journal of Pharmaceutics*, **322** (1–2), 79–86.

139 Lau, Y.Y., Wu, C.Y., Okochi, H. and Benet, L.Z. (2004) *Ex situ* inhibition of hepatic uptake and efflux significantly changes metabolism: hepatic enzyme–transporter interplay. *The Journal of Pharmacology and Experimental Therapeutics*, **308** (3), 1040–1045.

140 Makhey, V.D., Guo, A., Norris, D.A., Hu, P., Yan, J. and Sinko, P.J. (1998) Characterization of the regional intestinal kinetics of drug efflux in rat and human intestine and in Caco-2 cells. *Pharmaceutical Research*, **15** (8), 1160–1167.

141 Swaan, P.W. and Tukker, J.J. (1995) Carrier-mediated transport mechanism of foscarnet (trisodium phosphonoformate hexahydrate) in rat intestinal tissue. *The Journal of Pharmacology and Experimental Therapeutics*, **272** (1), 242–247.

142 Collett, A., Higgs, N.B., Sims, E., Rowland, M. and Warhurst, G. (1999) Modulation of the permeability of H2 receptor antagonists cimetidine and ranitidine by P-glycoprotein in rat intestine and the human colonic cell line Caco-2. *The Journal of Pharmacology and Experimental Therapeutics*, **288** (1), 171–178.

143 Uchino, H., Kanai, Y., Kim, D.K., Wempe, M.F., Chairoungdua, A., Morimoto, E., Anders, M.W. and Endou, H. (2002) Transport of amino acid-related compounds mediated by L-type amino acid transporter 1 (LAT1): insights into the mechanisms of substrate recognition. *Molecular Pharmacology*, **61** (4), 729–737.

144 Johansson, O., Lindberg, T., Melander, A. and Wahlin-Boll, E. (1985) Different effects of different nutrients on theophylline absorption in man. *Drug-Nutrient Interactions*, **3** (4), 205–211.

145 Metzner, L., Kottra, G., Neubert, K., Daniel, H. and Brandsch, M. (2005) Serotonin, L-tryptophan, and tryptamine are effective inhibitors of the amino acid transport system PAT1. *FASEB Journal*, **19** (11), 1468–1473.

146 Metzner, L. and Brandsch, M. (2006) Influence of a proton gradient on the transport kinetics of the H + /amino acid cotransporter PAT1 in Caco-2 cells. *European Journal of Pharmaceutics and Biopharmaceutics*, **63** (3), 360–364.

147 Lambie, D.G. and Johnson, R.H. (1985) Drugs and folate metabolism. *Drugs*, **30** (2), 145–155.

148 Zimmerman, J., Selhub, J. and Rosenberg, I.H. (1987) Competitive inhibition of folate absorption by dihydrofolate reductase inhibitors, trimethoprim and pyrimethamine. *The American Journal of Clinical Nutrition*, **46** (3), 518–522.

149 Broer, S. (2006) The SLC6 orphans are forming a family of amino acid transporters. *Neurochemistry International*, **48** (6–7), 559–567.

150 Zhang, L., Li, X.Z. and Poole, K. (2001) Fluoroquinolone susceptibilities of efflux-mediated multidrug-resistant *Pseudomonas aeruginosa*, *Stenotrophomonas maltophilia* and *Burkholderia cepacia*. *The Journal of Antimicrobial Chemotherapy*, **48** (4), 549–552.

151 Uchino, H., Kanai, Y., Kim do, K., Wempe, M.F., Chairoungdua, A., Morimoto, E., Anders, M.W. and Endou, H. (2002) Transport of amino acid-related compounds mediated by L-type amino acid transporter 1 (LAT1): insights into the mechanisms of substrate recognition. *Molecular Pharmacology*, **61** (4), 729–737.

152 Saitoh, H. and Aungst, B.J. (1995) Possible involvement of multiple P-glycoprotein-mediated efflux systems in the transport of verapamil and other organic cations across rat intestine. *Pharmaceutical Research*, **12** (9), 1304–1310.

153 Ngo, L.Y., Patil, S.D. and Unadkat, J.D. (2001) Ontogenic and longitudinal activity of Na(+)-nucleoside transporters in the human intestine. *American Journal of Physiology. Gastrointestinal and Liver Physiology*, **280** (3), G475–G481.

154 Wenzel, U., Thwaites, D.T. and Daniel, H. (1995) Stereoselective uptake of beta-lactam antibiotics by the intestinal peptide transporter. *British Journal of Pharmacology*, **116** (7), 3021–3027.

155 Hu, M., Chen, J., Zhu, Y., Dantzig, A.H., Stratford, R.E., Jr and Kuhfeld, M.T. (1994) Mechanism and kinetics of transcellular transport of a new beta-lactam antibiotic loracarbef across an intestinal epithelial membrane model system (Caco-2). *Pharmaceutical Research*, **11** (10), 1405–1413.

18
Toward Understanding P-Glycoprotein Structure–Activity Relationships

Anna Seelig

Abbreviations

ABC	ATP-binding cassette (transport protein)
ATP	Adenosine triphosphate
BBB	Blood–brain barrier
GRIND	Grid independent descriptors
IUPAC	International Union of Pure and Applied Chemistry
LDA	Linear discriminant analysis
MDR	Multidrug resistance
NBD	Nucleotide-binding domain
PCA	Principle component analysis
PLS-DA	Partial least square discriminant analysis
P-gp	P-Glycoprotein (MDR1, ABCB1)
(Q)SAR	(Quantitative) structure–activity relationship
Sav1866	ABC transporter from *Staphylococcus aureus*
SVM	Support vector machine
TMD	Transmembrane domain

Symbols

C_{Saq}	Substrate concentration in aqueous solution
K_1	Substrate concentration at half-maximum P-gp activation
K_2	Substrate concentration of at half-minimum P-gp activation
V_0	Basal P-gp activity in the absence of substrates
V_1	Maximum transporter activity
V_2	Minimum transporter activity
V_{Saq}	Transporter activity at a given substrate concentration in aqueous solution
k	Rate constant
$K_{tw(1)}$	Binding constant of a drug from water to the activating binding region of the transporter

$K_{tl(1)}$	Binding constant of a drug from the lipid phase to the inhibitory binding region of the transporter
K_{lw}	Lipid–water partition coefficient
$\Delta G^0_{tw(1)}$	Free energy of binding of a substrate from water to the activating binding region of the transporter
$\Delta G^0_{tl(1)}$	Free energy of binding of a substrate from the lipid phase to the activating binding region of the transporter
ΔG^0_{lw}	Free energy of partitioning of a substrate from water to the lipid membrane
J	Net flux
Φ	Passive flux
IC_{50}	Half-maximum (50%) inhibitory concentration

18.1 Introduction

P-Glycoprotein (P-gp/MDR1/ABCB1) is an efflux transporter of broad substrate specificity that is encoded by the multidrug resistance (MDR) 1 gene (*MDR1*) [1]. P-gp was first observed in multidrug resistant cancer cells [2]. It is also highly expressed in different plasma membrane barriers with protective functions, such as the intestinal barrier (IB) [3, 4], the blood–brain barrier (BBB) [3, 5], the placental barrier [6], and the blood–testis barrier [7], where it reduces or even prevents the absorption of a broad range of drugs and toxins (for review see Ref. [3, 8]). Recently, P-gp was detected in the nuclear membrane [9] where it contributes to an additional protection shell around the nucleus. P-gp not only prevents absorption but also plays a role in the excretion of drugs, toxins, and their metabolites, for example, in proximal tubules of the kidney and biliary ducts of the liver [3].

Cells can be induced to overexpress P-gp after exposure to a single agent (e.g., anticancer drugs, certain antibiotics, or food components) [10] or even after exposure to physical stress, such as X-ray [11], UV light irradiation [12], or heat shock [13]. Overexpression of P-gp leads to multidrug resistance, that is, to a resistance toward all drugs that are substrates for P-gp. The expression level of P-gp not only depends on the exposure of cells to various stimuli but also on genetic factors [14].

The same type of stimuli that induce MDR due to P-gp in human can also induce MDR in bacteria, parasites, and fungi by promoting the expression of related ABC transporters. MDR is detrimental not only for the treatment of cancers (for review see Ref. [15]), but also for the treatment of bacterial [16], parasitic [17], and fungal [18] diseases and can be considered as a general problem for pharmacotherapy.

18.1.1 Similarity Between P-gp and Other ABC Transporters

*A*TP-*b*inding *c*assette transport proteins (ABCs) are phylogenetically highly conserved and transport a large variety of compounds across cell membranes. The 48 human ABC transporters are grouped into seven subfamilies (A–G) according to

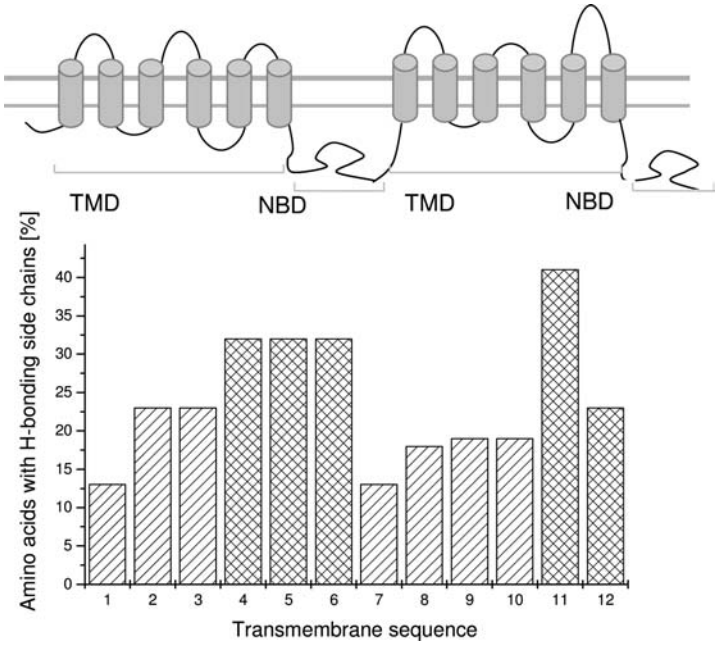

Figure 18.1 The putative transmembrane domains of P-gp derived from hydropathy plots. Hydropathy analyses search for all clusters of about 20–22 amino acids in a protein, which are hydrophobic enough to form a transmembrane sequence. Upper panel: P-gp in a 2D model derived from hydropathy plots comprises two halves each consisting of six putative α-helices (gray tubes) (TMDs) followed by a nucleotide-binding domain. Lower panel: the percentage of hydrogen-bond donor side chains in the putative transmembrane sequences of P-gp. The crosshatched putative α-helices are known to be especially important for binding and transport of substrates (updated version of Figure 18.3 in Ref. [26]).

similarities in their amino acid sequences [19]. On the basis of hydropathy plots, most human ABC transporters are predicted to consist of two homologous parts, each consisting of a transmembrane domain (TMD) and a cytosolic nucleotide-binding domain (NBD) coupled by a cytosolic linker region. P-gp (MDR1/ABCB1) (Figure 18.1) is the best studied example.

Some transporters (e.g., BCRP/ABCG2) are half-transporters (with one TMD comprising six transmembrane α-helices and one cytosolic NBD) that only function as homodimers, like the prokaryotic ABC transporter (e.g., Sav1866). Other members (e.g., ABCC1, ABCC2, ABCC3, ABCC6, and ABCC10) exhibit an additional amino-terminal TMD [20]. Despite these variations, overlapping substrate specificity has been observed, for example, between P-gp/ABCB1and MRP1/ABCC1 [21] as well as between P-gp/ABCB1 and BCRP/ABCG2 [22].

Like many membrane proteins, P-gp (170 kDa) has been recalcitrant to crystallization. So far, only a low-resolution (~8 Å) structure from two-dimensional crystals of P-glycoprotein trapped in the nucleotide-bound state has been obtained by electron microscopy [23]. A high-resolution crystal structure is available for a homologous

bacterial ABC transporter, Sav1866 (64.9 kDa). It was also crystallized in the nucleotide-bound state [24, 25] and was found to be a homodimer, formed from two TMD units, each consisting of six transmembrane α-helices.

18.1.2 Why P-gp Is Special

P-gp differs from many well-characterized membrane transporters such as sugar or amino acid transporters. First, it transports not one specific class of compounds but an intriguing number of chemically unrelated drugs, toxins, and metabolites (see, e.g., Ref. [26]). Second, it seems to exhibit not one single well-defined binding site but several binding sites [1, 27, 28]. The different binding sites may not even be well-defined, lock–key-type binding sites but may constitute a binding region that is occupied only transiently [21]. Third, P-gp recognizes its substrates not when they are dissolved in aqueous phase but when they are dissolved in the lipid membrane [29]; more precisely, when the substrates are dissolved in the membrane leaflet facing the cytosol [30, 31]. This implies that binding occurs in two consecutive binding steps, partitioning from water into lipid followed by partitioning from lipid into the P-gp-binding region. The membrane concentration of the substrate thus determines the P-gp activity [32].

In silico methods that are able to predict quantitative aspects of the interaction of a substrate with P-gp would be of great value. So far, modeling was applied mainly to lock–key-type reactions taking place in aqueous solution. The structural diversity and lipid solubility of P-gp substrates and the fact that their encounter with the transporter takes place in the lipid membrane and not in aqueous solution are new challenges for *in silico* predictions. Since all *in silico* models are based on experimental data, we first provide a short introduction to various P-gp assays and discuss their underlying principles (18.2). Secondly, we summarize the different *in silico* approaches (18.3), and, lastly, we discuss the parameters that are most relevant for the different *in silico* models (18.4).

18.2 Measurement of P-gp Function

Different assays are used to monitor the function of P-gp such as (i) ATPase assays; (ii) drug transport assays across confluent, polarized cell monolayers; and (iii) competition assays with reference substrates. The different assays address different functional aspects of P-gp.

18.2.1 P-gp ATPase Activity Assay

P-gp ATPase activity is measured using either inside-out cellular vesicles of MDR1-transfected cells or reconstituted proteoliposomes. In both types of systems, NBDs

are oriented at least partially toward the extravesicular side, and ATP hydrolysis can therefore be monitored with a colorimetric [33–35] or a coupled enzyme assay [36].

For cells *in vitro*, glycolysis is the main metabolic pathway and yields one molecule of lactic acid per molecule of ATP synthesized; the lactic acid leaves the cell as a waste product. At steady state, the rate of ATP synthesis corresponds to the rate of ATP hydrolysis and can therefore be monitored in living MDR1-transfected cells by measuring the rate of lactic acid extrusion by the cell. Lactic acid extrusion can be measured either by a spectroscopic approach [37] or by recording the extracellular acidification rate (ECAR) in NIH-MDR1-G185 cells [32, 38] with a micro-pH meter based on silicon chip technology (Cytosensor microphysiometer) [39]. A graphical representation of these assays is shown in Figure 18.2.

P-gp shows a basal ATPase activity in the absence of exogenous compounds; on addition of drugs, the ATPase activity can increase or decrease. Drug-induced inorganic phosphate release [33–35] or ECAR [32] shows a bell-shaped dependence on the drug concentration (log scale), first increasing to a maximum and then decreasing at high concentrations (Figure 18.3). Both equimolar (e.g., Ref. [40]) and equitoxic (e.g., Refs [41, 42]) concentrations have been used to classify compounds as substrates, modulators, or inhibitors. The fact that the same drugs can either activate or inhibit P-gp depending on the assay concentration (Figure 18.3) may explain the numerous inconsistencies in the classification of drugs with respect to their effects on P-gp.

Different models have been used to analyze P-gp activity profiles [32–34]. Here, we describe the modified Michaelis–Menten equation proposed by Litman *et al.* [33]. It

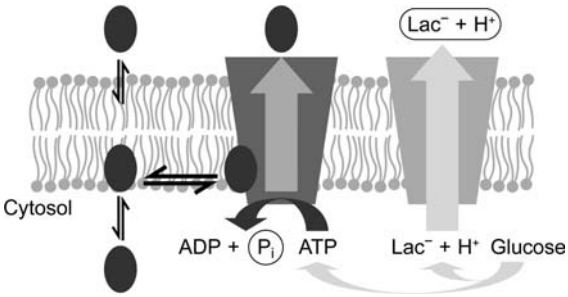

Figure 18.2 ATPase assays: In living cells, the drug first partitions into the extracellular leaflet of the plasma membrane and then crosses the membrane by passive diffusion. Once the drug reaches the cytosolic membrane leaflet, it either escapes to the cytosol or is captured by P-gp (indicated in dark gray). The diffusion process, that is, passive influx, can vary by several orders of magnitude. If the drug is bound by P-gp (which is more likely if diffusion through the intracellular leaflet is slow), it can be exported out of the cell at the expense of ATP hydrolysis. ATP in cultured cells is produced via glycolysis; whereby an equimolar amount of lactic acid is formed, which leaves the cell as a waste product, and dissociates extracellularly to lactate and a proton. This can be monitored with a Cytosensor as an extracellular acidification rate. Cytosensor assays are performed under steady-state conditions. In contrast, in inside-out plasma membrane vesicles, the drug first partitions into the cytosolic leaflet of the plasma membrane. P-gp activation can be measured by monitoring inorganic phosphate released by ATPase activity using a colorimetric assay.

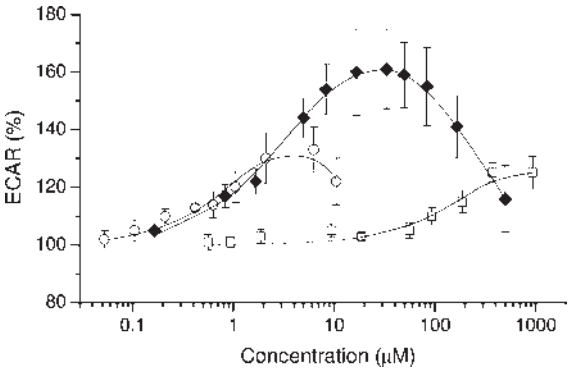

Figure 18.3 P-gp activity profiles measured with living MDR1-transfected cells as a function of drug concentration. The extracellular acidification rate is expressed as a percentage of the basal rate (100%): verapamil is represented by lozenges, lidocaine by open squares, and trifluopromazine by open circles. (Data are taken from Ref. [32].)

assumes activation with one substrate molecule, S, bound, and inhibition with two substrate molecules bound to P-gp as described by Scheme 18.1:

$$\mathrm{T + ATP + S \underset{k_{-1}}{\overset{k_1}{\rightleftharpoons}} T(ATP)S + S \underset{k_{-2}}{\overset{k_2}{\rightleftharpoons}} T(ATP)S_2 \overset{k''}{\rightarrow} T(ADP) + 2S_{rel} + P_i + H^+}$$
$$\mathrm{\downarrow k'}$$
$$\mathrm{T(ADP) + P_i + H^+ + S_{rel}}$$

Scheme 18.1

T(ATP)S and T(ATP)S_2 are transporter–ATP complexes with one and two substrate molecules bound, respectively; T(ADP) is the transporter–ADP complex; P_i inorganic phosphate; S_{rel} is the substrate molecule flipped to the outer leaflet or released extracellularly; k_1, k_{-1}, and k_2, k_{-2} are the rate constants of the first and the second substrate binding steps, respectively; and k' and k'' the rate constants of the catalytic steps. For this model, the rate of ATP hydrolysis is a function of the P-gp-stimulating drug concentration:

$$V_{Saq} = \frac{K_1 K_2 V_0 + K_2 V_1 C_{Saq} + V_2 C_{Saq}^2}{K_1 K_2 + K_2 C_{Saq} + C_{Saq}^2}, \tag{18.1}$$

where V_{Saq} is the rate of P_i release as a function of the substrate concentration in solution, C_{Saq}; V_0 is the basal activity in the absence of substrate; V_1 is the maximal ATPase rate that is achieved only when the inhibitory second step is negligible; V_2 is the minimal rate at infinite substrate concentration and lower than V_1; K_1 is the drug concentration at half-maximum activation, that is, $V_1/2$; K_2, the drug concentration at half-minimum activation, that is, $V_2/2$. At low drug concentrations, Equation 18.1 simplifies to the Michaelis–Menten equation. The catalytic rate constant (k') corresponds to $V_1/[T_0]$, where $[T_0]$ is the transporter concentration.

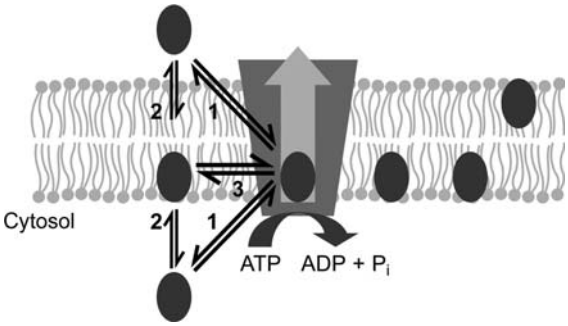

Figure 18.4 Binding from water to the transporter (1) is divided into two steps: membrane partitioning (2) and transporter binding (3). These processes are fast and can be considered (to a first approximation) as equilibrium processes in inside-out vesicles as well as in cells under steady-state conditions in a Cytosensor: this is indicated by the double arrows. The free energy of binding of the drug from water to the transporter ($\Delta G^0_{tw(1)}$) was derived from ATPase assays, and the free energy of binding of the drug from water to the lipid membrane (ΔG^0_{lw}) was derived from surface activity measurements or from isothermal titration calorimetry. The free energy of binding of the drug from the lipid membrane to the transporter (ΔG^0_{tl}) is not directly accessible by experiment but can be estimated as the difference between the two free energies $\Delta G^0_{tw(1)}$ and ΔG^0_{lw} (see Equation 18.3).

Evidence for a direct correlation between the turnover number for vinblastine-stimulated ATP hydrolysis and vinblastine transport rate was provided by Ambudkar and Stein [43]. Since compounds that interact with P-gp often exhibit a high lipid–water partition coefficient and can cross the lipid bilayer by passive diffusion, the stoichiometry between ATP hydrolysis and drug transport is difficult to assess. Using a permanently charged spin-labeled analogue of verapamil that cannot cross the membrane by passive diffusion [44], a direct correlation between ATP hydrolysis and drug transport was demonstrated [45].

18.2.1.1 Quantification of Substrate–Transporter Interactions

Substrate binding from water to the transporter can be described as a two-step binding process [32] as illustrated in Figure 18.4.

ATPase activation experiments are performed under steady-state conditions, and the catalytic rate (rate constant, $k_1 \approx 1\text{–}5\ s^{-1}$) of P-gp is much slower than the rates of drug and ATP binding. Hence, the concentration at half-maximum activation (K_1) can be considered as the dissociation constant and $1/K_1$ as the binding constant of a drug to the activating binding region of the transporter ($K_{tw(1)}$) to a first approximation. The binding constant of the drug to the transporter ($K_{tw(1)}$) can then be expressed as the product of the lipid–water partition coefficient (K_{lw}) and the binding constant of the substrate from the lipid membrane to the activating binding site of the transporter ($K_{tl(1)}$),

$$\frac{1}{K_1} \cong K_{tw(1)} \cong K_{tl(1)} \cdot K_{lw}. \tag{18.2}$$

This leads to the free energy relationship,

$$\Delta G^0_{tw(1)} \cong \Delta G^0_{tl(1)} + \Delta G^0_{lw}, \tag{18.3}$$

where the superscript zero refers to a biological standard state (pH 7.4 and 37 °C). The free energy of substrates binding from water to the transporter, $\Delta G^0_{tw(1)}$, and the free energy of partitioning into the lipid membrane, ΔG^0_{lw}, are defined as

$$\Delta G^0_{tw(1)} \cong -RT\ln(C_w K_{tw(1)}) \tag{18.4}$$

and

$$\Delta G^0_{lw} = -RT\ln(C_w K_{lw}), \tag{18.5}$$

respectively, where C_w (55.3 mol/l) corresponds to the molar concentration of water at 37 °C. Analogous equations can be formulated for the binding constant, $K_{tw(2)}$, and the free energy of binding, $\Delta G^0_{tw(2)}$, to the second binding region as outlined previously [32]. The more negative the free energy of binding is, the higher is the binding affinity to the transporter. For 15 drugs [32], the free energy of drug partitioning from water to the lipid membrane, ΔG^0_{lw}, was somewhat more negative than the free energy of drug binding from the lipid phase to the transporter, $\Delta G^0_{tl(1)}$. However, the variation in $\Delta G^0_{tl(1)}$ was more pronounced (~fourfold) than that in ΔG^0_{lw} (~1.5 fold) as shown in Figure 18.5.

18.2.1.2 Relationship between Substrate–Transporter Affinity and Rate of Transport

As seen in Figure 18.6, the maximal extent of P-gp ATPase stimulation, which correlates with the rate of intrinsic transport, $\ln k_1$, decreases as the affinity of drugs to the transporter increases or as the free energy of binding, $\Delta G^0_{tw(1)}$, decreases. Molecules with low affinity are thus transported more rapidly and tend to be smaller (Figure 18.7).

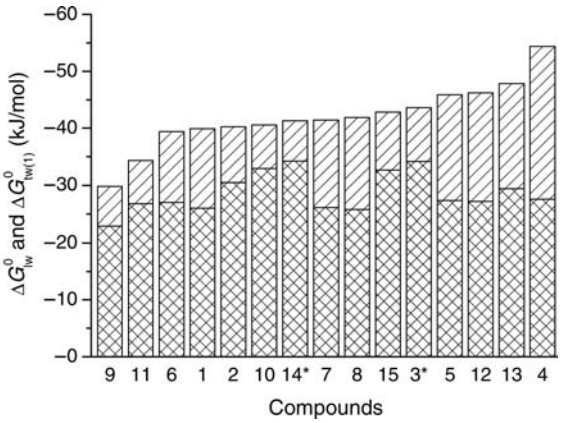

Figure 18.5 The free energy of drug binding from water to the activating binding region of P-gp ($\Delta G^0_{tw(1)}$) (hatched and cross-hatched bars) in comparison to the free energy of drug partitioning from water to the lipid membrane (ΔG^0_{lw}) (cross-hatched bars). The difference between $\Delta G^0_{tw(1)}$ and ΔG^0_{lw} represents the free energy of drug binding from lipid membrane to the transporter ($\Delta G^0_{tl(1)}$) (hatched bar). Amitriptyline (1), chlorpromazine (2), *cis*-flupenthixol (3), cyclosporin A (4), daunorubicin (5), dibucaine (6), diltiazem (7), glivec (8), lidocaine (9) progesterone (10), promazine (11), verapamil (12), reserpine (13), trifluoperazine (14), and trifluopromazine (15) measured at pH 7.4 and 37 °C. (Data are taken from Ref. [32].)

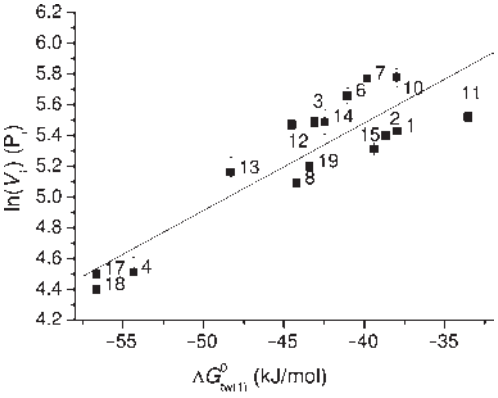

Figure 18.6 Correlation between the logarithm of the maximum P-gp activity ($\ln V_1$) obtained from phosphate release measurements at pH 7.0 (37 °C) and the free energy of drug binding from water to transporter ($\Delta G^0_{tw(1)}$). The maximum activity of P-gp (V_1) is expressed as a percentage of the basal rates taken as 100%. Data are presented as average of two to 15 measurements. The solid line is a linear regression to the data with a slope 0.06 ± 0.01 and an intercept 7.76 ± 0.34 ($R^2 = 0.79$). Compounds are as in Figure 18.5 (1–15); daunorubicin (5), and lidocaine (9) were excluded from the fit due to experimental problems; extra data for OC144-093 (17), PSC-833 (18), and vinblastine (19) (data taken from Ref. [35]).

In summary, ATP hydrolysis by P-gp correlates well with the intrinsic rate of substrate transport. A complete characterization of the interaction of a compound with P-gp is obtained by measuring the ATPase activity as a function of concentration. The rate of intrinsic substrate transport first increases with increasing concentration, reaches a maximum, and decreases again at high concentrations. The rate of intrinsic transport by P-gp depends not only on the substrate concentration but also on its affinity to the transporter; substrates with high affinities for P-gp are transported more slowly than those with low affinities.

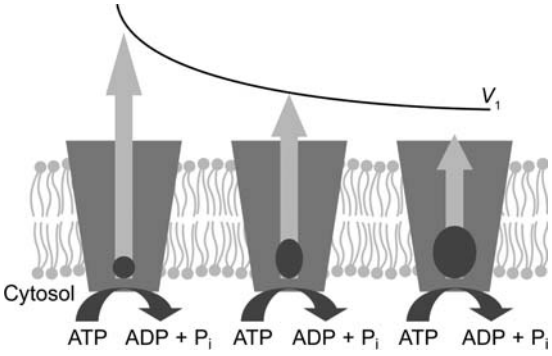

Figure 18.7 Intrinsic transport by P-gp. P-gp transports drugs at different rates. Small drugs often have a lower affinity to the transporter and are transported more rapidly (at least at low concentrations when only one drug is bound) than larger drugs with higher affinity.

18.2.2 Transport Assays

P-gp-specific transport is often assayed with confluent monolayers of polarized epithelial cells transfected with the MDR1 gene (e.g., kidney cells) using radioactively labeled compounds [46]. Instead of MDR1-transfected cells, Caco-2 cell lines have been used [47]. Caco-2 cells can express a number of different transporters, including P-gp, and thus show activities typical of all transporters. To assess transport, basolateral-to-apical flux ($J_{B\rightarrow A}$) is generally compared with apical-to-basolateral flux ($J_{A\rightarrow B}$) of a compound across the confluent cell monolayer using identical initial compound concentrations in the donor compartments (Figure 18.8) (see e.g., Ref. [48]). If P-gp or other efflux transporters are present in the basolateral membrane, the basolateral-to-apical flux ($J_{B\rightarrow A}$) is enhanced and the apical-to-basolateral flux is reduced resulting in a flux ratio

$$\frac{J_{B\rightarrow A}}{J_{A\rightarrow B}} > 1. \tag{18.6}$$

As illustrated in Figure 18.8, the net flux (J) across a membrane is the sum of passive and active transport processes. To estimate the net flux across a membrane, the following simplifying assumptions are made. The net flux ($J_{B\rightarrow A}$) from the basolateral to the apical side of the membrane is assumed to be the sum of the passive flux ($\Phi_{B\rightarrow A}$) plus the active transport rate ($+V$), and the net flux from the apical to the basolateral side ($J_{A\rightarrow B}$) is the sum of the passive flux ($\Phi_{A\rightarrow B}$) less the active transport rate ($-V$):

$$J_{B\rightarrow A} = \Phi_{B\rightarrow A} + V, \tag{18.7}$$

$$J_{A\rightarrow B} = \Phi_{A\rightarrow B} - V. \tag{18.8}$$

To illustrate the role of passive influx in transport assays, we plotted the flux ratio $J_{B\rightarrow A}/J_{A\rightarrow B}$ as a function of the passive flux (Φ). Passive flux varies enormously

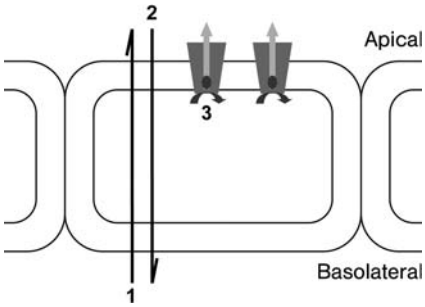

Figure 18.8 Transport processes across a confluent cell monolayer of P-gp-expressing cells. The flux from the basolateral to the apical side of the membrane ($J_{B\rightarrow A}$) is the sum of the passive flux ($\Phi_{B\rightarrow A}$) (black arrow 1) plus an active efflux component (V) (light gray arrow 3). The flux from the apical to the basolateral side of the membrane ($J_{A\rightarrow B}$) is the sum of the passive flux ($\Phi_{A\rightarrow B}$) (black arrow 2) and an active efflux component ($-V$) (light gray arrow 3).

(from about 10^{12} to less than 10^6 molecules/s/cell). It decreases exponentially with increasing cross-sectional area (A_D) and the charge (pK_a) of the molecule. Further factors that influence the passive flux are the lateral membrane packing density (π_M), which depends on the lipid composition, and the pH of the solution [49]. In contrast, active efflux varies by less than one order of magnitude for a given cell line (see Figure 18.6) [50]. Major factors influencing active efflux are the drug concentration (Equation 18.1) (see also Ref. [51]) and the expression level of P-gp.

Passive flux $|\Phi|$ is orders of magnitude higher than active efflux $|V|$ for small drugs (intrinsic substrates) and is therefore "masked" in assays (Figure 18.9). As the passive flux tends to decrease strongly with molecular size and the intrinsic transport tends to decrease only slightly [49, 50], membrane-specific limiting cross-sectional areas (A_D) can be defined for drug permeation and have been reported for the blood–brain barrier [52] and the intestinal barrier [53].

In summary, assays with confluent cell monolayers reveal the net flux (J) that is the result of passive and active transport processes. Substrate transport is observable only if the magnitude of passive flux $|\Phi|$ is similar to that of active efflux $|V|$ but is "masked" if the passive flux is significantly higher than active efflux. Since the passive flux decreases exponentially with the cross-sectional area (A_D) and the ionization status (pK_a), these two parameters dominate the flux, or the apparent transport, across a cell

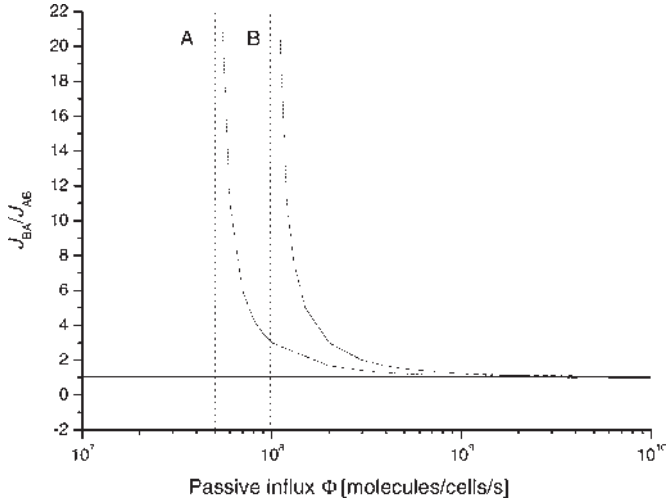

Figure 18.9 Transport across confluent cell monolayers depends on many parameters (see Section 20.2.2). The quotient $J_{B\to A}/J_{A\to B}$ is plotted as a function of the passive influx (Φ). It was assumed that $\Phi_{B\to A}$ and $\Phi_{A\to B}$ are identical. Active export was taken as $V = 5 \times 10^7$ molecules/cell/s (A) or $V = 1 \times 10^8$ molecules/cell/s (B). If the passive flux $|\Phi|$ is high, active transport by P-gp is masked, leading to flux ratio $J_{B\to A}/J_{A\to B}$ close to 1; if the flux $|\Phi|$ is similar to the rate of active transport $|V|$, then $J_{B\to A}/J_{A\to B} > 1$; if the passive flux $|\Phi|$ is very low (lower limits indicated by dotted lines), the quotient cannot be determined experimentally because all substrate molecules that then permeate the plasma membrane are exported again and none are able to permeate into the cytosol. (Data are taken from Ref. [49].)

layer. Compounds that are determined as substrates in transport assays are called apparent substrates to distinguish them from intrinsic substrates determined by ATPase assays.

18.2.3 Competition Assays

The most frequently used competition assays are the calcein–AM [54–56] and the cytotoxicity assays (e.g., performed with doxorubicin) [41, 42], carried out with living cells expressing P-gp. Calcein–AM as well as doxorubicin is used as reference substrates for P-gp as their concentrations in the cytosol are reduced by its action. If a second compound that competes for the transporter P-gp is added to the cell, the reference substrates accumulate above control levels in the cytosol in a concentration-dependent manner up to a maximal value. The more effective the competing agent, the larger is the increase in cytosolic concentration of the reference substrates. In the case of the calcein–AM that is hydrolyzed as soon as it reaches the cytosol, the fluorescent hydrolysis product, calcein, is assayed by fluorescence spectroscopy. The inhibitory potencies of compounds are measured as half-inhibitory constants, K_I.

In the case of the cytotoxin doxorubicin, its concentration in the cytosol is generally estimated via the incumbent cytotoxicity, which reduces cell growth rates. Defined concentrations of doxorubicin inhibit growth of the MDR-expressing cells by 50 or 20% (IC_{50} or IC_{20} values). When P-gp is inhibited by a competing drug, lower concentrations of doxorubicin are required to cause the same level of toxicity; hence, drug potencies are expressed as effect–concentration ratio or MDR ratio.

$$\text{MDR ratio} = \frac{IC_{50}(\text{cytotoxic drug alone})}{IC_{50}(\text{cytotoxic drug} + \text{modulator})}. \tag{18.9}$$

In summary, competition assays yield information on the affinity of a drug to the transporter relative to the affinity of a reference substrate, for example, calcein–AM or doxorubicin. The higher the affinity of a drug for P-gp (or the more negative the free energy of binding to P-gp), the greater is the ability to suppress efflux of a reference substrate.

18.3 Predictive *In Silico* Models

Different prediction models have been reported including (i) pharmacophore models that take into account structural features, (ii) linear discriminant models that do not consider structural features, (iii) a modular-binding approach, and (iv) rule-based approaches. The focus of the following discussion is to identify the most important descriptors in the different approaches and relate them to the physicochemical parameters determined in the different P-gp assays.

18.3.1
Introduction to Structure–Activity Relationship

Structure–activity relationship (SAR) studies are based on the assumption that similar molecules elicit similar activities in a lock/key-type manner. Quantitative structure–activity relationships (QSARs) correlate the extent of a change in a biological response (e.g., activity) elicited by a specific compound with its physicochemical and/or its structural properties,

$$\text{activity} = f(\text{physical} - \text{chemical parameters and/or structural properties}). \tag{18.10}$$

Individual physicochemical parameters are also called molecular descriptors, and the net structural properties describe a pharmacophore. According to IUPAC, a pharmacophore is defined as the ensemble of steric and electronic features that is necessary to ensure interactions with a specific biological target and that induces or blocks its biological response.

QSAR modeling has been successfully applied for elucidating the stereochemical features relevant for the function of small ligands binding to an acceptor in a lock/key-type mechanism in aqueous solution. For such a process, the following assumptions are appropriate: (i) the modeled conformation is the bioactive one (i.e., the pharmacophore); (ii) the binding site and/or mode is the same for all modeled compounds; (iii) interactions between the drug and the binding site are mainly due to enthalpic processes such as van der Waals interactions; and (iv) solvent or membrane effects are negligible [57].

Extending QSAR models to P-gp is nontrivial since no high-resolution structure of P-gp is available yet [23]. In addition, the binding site or binding region is not well defined, but is most likely large and flexible [58]; as it is located in the interior membrane, electrostatic and hydrogen-bond interactions are more specific and stronger than van der Waals interactions, due to the low dielectric constant of the environment [32]. Substrates have extremely diverse and flexible structure [59]. A further difficulty arises from the complexity of the biological data used as the basis for QSAR or SAR. Generally, data from transport or competition assays are used, although the underlying principles are more complex than in ATPase assays.

18.3.2
3D-QSAR Pharmacophore Models

Examples of pharmacophore models are discussed in this chapter. The earlier models are primarily based on competition assays whereas the newer models are rather based on transport assays.

On the basis of competition assays, Pajeva and Wiese [60] proposed pharmacophores with different interaction points with the transporter using the program GASP (Tripos software). GASP elucidates pharmacophore models while allowing ligand flexibility, without requiring prior knowledge of pharmacophore elements or constraints. The pharmacophore model consists of two hydrophobic points, three

hydrogen-bond acceptor points, and one hydrogen-bond donor point. In this model, the affinity of the substrate to the transporter depends on the number of pharmacophore points per substrate and thus allows for variable binding to the transporter.

Ekins *et al.* built QSAR models using Catalyst software to rank and predict inhibitors for P-gp substrate transport. In their first attempt, four different pharmacophores were derived from the analysis of inhibitors of digoxin transport, vinblastine binding, or intracellular accumulation of vinblastine and calcein [61]. These data were then combined with experiments using verapamil as inhibitor and led to the construction of a unique pharmacophore consisting of one hydrogen-bond acceptor, one aromatic ring, and two hydrophobic centers [62].

Langer *et al.* [63] used a training set of propafenone-type MDR modulators tested with a daunorubicin competition assay and developed a pharmacophore for P-gp inhibition using Catalyst software. The pharmacophore features identified by this model were one hydrogen-bond acceptor, one hydrophobic area, two aromatic centers, and (iv) one positively ionizable group.

On the basis of transport data, Penzotti *et al.* [64] constructed and validated a model for recognizing P-gp transport substrates. The model consists of an ensemble of 100 two-, three-, and four-point pharmacophores. The "point pharmacophores" were selected from the following descriptors: hydrogen-bond acceptors, hydrogen-bond donors, hydrophobic centers, negative and positive charges, aromatic groups, and the associated six interfeature distances. Together, these were assumed to describe the various chemotypes that interact with P-gp.

Cianchetta *et al.* [65] selected compounds from Caco-2 cell transport assays and investigated them for their ability to inhibit calcein–AM efflux. Using GRIND (*gr*id *in*dependent *d*escriptors), they then proposed a unique pharmacophore containing two hydrophobic groups separated by 16.5 Å and two hydrogen-bond acceptor groups separated by 11.5 Å. Moreover, they observed that the dimensions of the molecule play a significant role for substrate transport.

Applying supervised machine learning techniques, Li *et al.* [66] proposed a model that differentiates substrates from nonsubstrates of P-gp based on a simple tree using nine distinct pharmacophores. Four-point 3D pharmacophores were employed to increase the amount of shape information and resolution and possessed the ability to distinguish chirality. Relevant features were hydrogen-bond acceptors, hydrophobicity indices, and a cationic charge.

18.3.3
Linear Discriminant Models

Linear discriminant analysis (LDA) is used in statistics and machine learning methods to find the best linear combination of descriptors that distinguish two or more classes of objects or events, and, in the present case, to distinguish between substrates and nonsubstrates of P-gp. A linear classifier achieves this by making a classification decision based on the value of the linear combination of descriptors.

The linear discriminant models applied to P-gp [67, 68] are essentially based on data from transport assays. Several methods such as the support vector machine

approach (SVM) [69], principle component analysis (PCA) [69], partial least square discriminant analysis (PLS-DA) [70, 71], or the machine learning approach (neural network) [70, 72] are derived from related principles. Svetnik *et al*. [73] used boosting tree or bagging tree techniques for P-gp substrate classification, each of which consists of a sequence of about 100 tree classifiers based on 1522 binarized atom pair descriptors. The investigation was performed with the transport data set of Penzotti *et al*. [64] and it revealed that when chlorine and fluorine substitutions enhanced permeability [74] they also lowered the tendency of a compound to be effluxed by P-gp. All these procedures start with a very large number of general descriptors that are then reduced to lower numbers of essential ones; size- and charge-related parameters dominate again.

18.3.4
Modular Binding Approach

To get the broadest possible information on the nature of P-gp/substrate interactions, we chose data from all types of assays and analyzed 3D structures by visual inspection. Chemically very diverse compounds known to interact (or not to interact) with P-gp were analyzed, with their molecular weight ranging from approximately 250 to 1250. The only recognition elements found in all compounds interacting with P-gp were hydrogen-bond acceptor groups. Patterns with two hydrogen-bond acceptors with a spatial separation of 2.5 ± 0.3 Å (type I units) were observed in all P-gp substrates. In addition, patterns with three hydrogen-bond acceptor groups with a spatial separation of the outer two acceptor groups of 4.6 ± 0.6 Å or two hydrogen-bond acceptor groups with a spatial separation of 4.6 ± 0.6 Å (type II units) were observed in many substrates and all inducers of P-gp [21, 26]. Hydrogen-bond acceptor patterns were therefore suggested to serve as binding modules interacting with the hydrogen-bond donor-rich transmembrane domains of P-gp.

In lipid environments, exhibiting a low dielectric constant, the hydrogen-bonding interactions are stronger and more specific than van der Waals interactions. It was therefore suggested that the measured total free energy of binding of a drug from the lipid membrane to the transporter $\Delta G^0_{\mathrm{tl}(1)}$ is the sum of the free energies, $\Delta G^0_{\mathrm{H}i}$, of the individual hydrogen bonds formed between the substrate and the transporter [26, 75]

$$\Delta G^0_{\mathrm{tl}(1)} \approx \sum_{i=1}^{n} \Delta G^0_{\mathrm{H}i}. \tag{18.11}$$

To test this hypothesis, the experimentally determined free energy of binding to P-gp, $\Delta G^0_{\mathrm{tl}(1)}$, for a given drug was divided by the number of possible hydrogen bonds formed thus yielding the free energy per hydrogen bond of $\Delta G^0_{\mathrm{H}i} \approx -2.5\ \mathrm{kJ}/mol$ as a lower limit. This value is in good agreement with expectations [32]. Combining Equations 18.3 and 18.11, the free energy of binding of a substrate from water to the transporter can then be estimated as

$$\Delta G^0_{\mathrm{tw}(1)} \approx \sum_{i=1}^{n} \Delta G^0_{\mathrm{H}i} + \Delta G^0_{\mathrm{lw}}. \tag{18.12}$$

The requirement to bind to P-gp is thus the ability to partition into the inner lipid leaflet and to carry hydrogen-bond acceptor groups (arranged in type I or type II units).

18.3.5 Rule-Based Approaches

One of the first and most cited rule-based approaches is the "rule-5" by Lipinski [76], which predicts whether a compound will be absorbed from the intestinal tract, that is, cross the intestinal barrier. Although transporters are not explicitly mentioned, they play a role in intestinal absorption. "Lipinski's rule-of-5" states that, in general, a well-absorbed drug violates no more than one of the following criteria: no more than five hydrogen-bond donors (i.e., nitrogen or oxygen atoms with one or more hydrogen atoms); not more than 10 hydrogen-bond acceptors (nitrogen or oxygen atoms); molecular weight below 500 Da; and an octanol–water partition coefficient (log P) below 5.

An approach that is related to the "rule-of-5" was proposed by Didziapetris *et al.* [77] to predict whether a drug is a substrate for P-glycoprotein. On the basis of transcellular transport experiments, they suggested that compounds with more than eight oxygen and nitrogen atoms, molecular weights above 400 Da, and acidic pK_a more than 4 are likely to be P-glycoprotein substrates; compounds with less than four oxygen and nitrogen atoms, molecular weights below 400 Da, and pK_a less than 8 are likely to be nonsubstrates.

The cross-sectional area, A_D, of a compound oriented in an amphiphilic gradient such as the air–water or lipid–water interface has been shown to be even more reliable for permeability predictions than the molecular weight [52]. For BBB permeation, the limiting cross-sectional area, A_D, was determined as $A_D \approx 73$ Å^2, and the limiting ionization constants, pK_as, for bases and acids were determined as 9 and 4, respectively [52]. For intestinal barrier permeation, the limiting cross-sectional area was assessed as $A_D \approx 100$ Å^2, and the limiting ionization constants (pK_as) for bases as 9 and for acids as 2 [53]. In this approach, the role of P-gp is again implicit [49].

To predict membrane barrier permeation *in silico*, we developed an algorithm that determines the molecular axis of amphiphilicity and the cross-sectional area, A_{Dcalc}, perpendicular to this axis. Starting with the conformational ensemble of each molecule, the three-dimensional membrane-binding conformation was determined as the one with the smallest cross-sectional area, A_{DcalcM}, and the strongest amphiphilicity. The calculated cross-sectional areas, A_{DcalcM}, were then correlated with the calculated octanol–water distribution coefficients, log $D_{7.4}$, of the 55 compounds with known abilities to permeate the blood–brain barrier, to predict the probability of blood–brain barrier permeation. The limiting cross-sectional area was $A_{DcalcM} = 70$ Å^2, and the optimal range of octanol–water distribution coefficients was $-1.4 \leq \log D_{7.4} < 5.0$. The correlation was validated with an independent set of 43 compounds with known abilities to permeate the blood–brain barrier and yielded a prediction accuracy of 86% [59].

18.4 Discussion

We now compare the main descriptors obtained from the different *in silico* models (Section 18.3) with the physicochemical parameters that allow a quantitative description of the different aspects of P-gp transport (Section 18.2).

18.4.1 Prediction of Substrate-P-gp Interactions

Most pharmacophore models for P-gp substrate prediction have similar predictive accuracies. All three-dimensional pharmacophores use similar features such as size-related parameters, hydrogen-bond acceptors, hydrophobicity parameters, aromatic rings, and ionizable groups. Thereby size- and charge-related parameters and hydrogen-bond acceptor groups were generally considered as the most relevant descriptors. Despite these agreements, the resulting pharmacophores showed no similarity at all, raising the question whether three-dimensional lock/key-type pharmacophores are appropriate for P-gp. Moreover, it is difficult to envisage how a single pharmacophore could account for the different affinities of drugs to the transporter. Variable binding affinities can, however, only be explained with modular binding approaches.

18.4.2 Prediction of ATPase Activity or Intrinsic Transport

The binding affinity of a substrate to P-gp seems to directly influence the rate of transport as seen in Figure 18.6. ATPase activity (or the intrinsic transport rate by P-gp) decreases with increasing binding affinities of substrates to the transporter. Rather accurate predictions are possible assuming modular binding [26, 32, 78] using Equation 18.12 [79]. The modular binding principles also allow the prediction of the extent of competition between different substrates for binding P-gp (see Ref. [79]).

18.4.3 Prediction of Transport (i.e., Apparent Transport)

Pharmacophore models, linear discriminate models, and rule-based models agree with respect to the relevance of size and charge for transport by P-gp and also agree with experimental investigations [80]. This is also consistent with the analysis of net influx (Section 18.2.2), which shows that increasing size (or cross-sectional area) and/or charge of the molecule diminishes the rate of diffusion that in turn unmasks active transport rates [49]. It can thus be concluded that compounds that are large, have hydrogen-bond acceptors, and are cationic are likely to be apparent substrates for P-gp. Large molecules with hydrogen-bond acceptor groups are also at risk when being effluxed by transporters with overlapping substrate specificities.

18.4.4 Prediction of Competition

Hydrogen-bond acceptor groups and size-related descriptors are also dominant in QSAR models predicting P-gp inhibitors on the basis of competition assays. However, substrate–transporter interactions are most likely not determined by the size of the substrate as such, but rather by a concomitant increase in residues that can undergo specific interactions with the transmembrane sequences of P-gp (for details see Ref. [32]). A good estimate of the competitive potential of compounds is possible on the basis of the total hydrogen-bond acceptor strength alone, if the lipid-binding properties of the compounds are comparable [35, 81].

18.4.5 Conclusions

Considerable effort has been put into the development of *in silico* methods that predict apparent transport by P-gp and competition for P-gp-binding sites. The models cited include pharmacophore, linear discriminant and rule-based models, respectively, and a modular binding approach. The first three *in silico* models are strongly based on transport assays that are very complex and determine apparent rather than intrinsic transport rates by P-gp. Although the different models discussed are very diverse, they nevertheless agree with respect to the relevance of size and charge of the molecule for apparent transport; they also agree on the relevance of hydrogen-bond acceptor groups as recognition elements for P-gp. However, they disagree greatly with respect to the proposed structural arrangement of recognition elements. At present, only the modular binding approach that considers small hydrogen-bond acceptor patterns as binding modules allows modeling the different binding affinities of the enormously diverse intrinsic substrates for P-gp. Translation of the results obtained from these investigations into the synthesis of new ligands or into an optimization of known ligands could lead to a reduction of MDR.

References

1 Gottesman, M.M. and Ambudkar, S.V. (2001) Overview: ABC transporters and human disease. *Journal of Bioenergetics and Biomembranes*, **33**, 453–458.

2 Juranka, P.F., Zastawny, R.L. and Ling, V. (1989) P-Glycoprotein: multidrug-resistance and a superfamily of membrane-associated transport proteins. *FASEB Journal*, **3**, 2583–2592.

3 Cordon-Cardo, C., O'Brien, J.P., Boccia, J., Casals, D., Bertino, J.R. and Melamed, M.R. (1990) Expression of the multidrug resistance gene product (P-glycoprotein) in human normal and tumor tissues. *The Journal of Histochemistry and Cytochemistry*, **38**, 1277–1287.

4 Mukhopadhyay, T., Batsakis, J.G. and Kuo, M.T. (1988) Expression of the mdr (P-glycoprotein) gene in Chinese hamster digestive tracts. *Journal of the National Cancer Institute*, **80**, 269–275.

5 Thiebaut, F., Tsuruo, T., Hamada, H., Gottesman, M.M., Pastan, I. and Willingham, M.C. (1989)

Immunohistochemical localization in normal tissues of different epitopes in the multidrug transport protein P170: evidence for localization in brain capillaries and crossreactivity of one antibody with a muscle protein. *The Journal of Histochemistry and Cytochemistry*, **37**, 159–164.

6 Smit, J.W., Huisman, M.T., van Tellingen, O., Wiltshire, H.R. and Schinkel, A.H. (1999) Absence or pharmacological blocking of placental P-glycoprotein profoundly increases fetal drug exposure. *The Journal of Clinical Investigation*, **104**, 1441–1447.

7 Holash, J.A., Harik, S.I., Perry, G. and Stewart, P.A. (1993) Barrier properties of testis microvessels. *Proceedings of the National Academy of Sciences of the United States of America*, **90**, 11069–11073.

8 Sarkadi, B., Muller, M. and Hollo, Z. (1996) The multidrug transporters – proteins of an ancient immune system. *Immunology Letters*, **54**, 215–219.

9 Calcabrini, A., Meschini, S., Stringaro, A., Cianfriglia, M., Arancia, G. and Molinari, A. (2000) Detection of P-glycoprotein in the nuclear envelope of multidrug resistant cells. *The Histochemical Journal*, **32**, 599–606.

10 Endicott, J.A. and Ling, V. (1989) The biochemistry of P-glycoprotein-mediated multidrug resistance. *Annual Review of Biochemistry*, **58**, 137–171.

11 McClean, S., Hosking, L.K. and Hill, B.T. (1993) Dominant expression of multiple drug resistance after *in vitro* X-irradiation exposure in intraspecific Chinese hamster ovary hybrid cells. *Journal of the National Cancer Institute*, **85**, 48–53.

12 Uchiumi, T., Kohno, K., Tanimura, H., Matsuo, K., Sato, S., Uchida, Y. and Kuwano, M. (1993) Enhanced expression of the human multidrug resistance 1 gene in response to UV light irradiation. *Cell Growth & Differentiation: The Molecular Biology Journal of the American Association for Cancer Research*, **4**, 147–157.

13 Chin, K.V., Tanaka, S., Darlington, G., Pastan, I. and Gottesman, M.M. (1990) Heat shock and arsenite increase expression of the multidrug resistance (MDR1) gene in human renal carcinoma cells. *The Journal of Biological Chemistry*, **265**, 221–226.

14 Sauna, Z.E., Kim, I.W. and Ambudkar, S.V. (2007) Genomics and the mechanism of P-glycoprotein (ABCB1). *Journal of Bioenergetics and Biomembranes*, **39**, 481–487.

15 Gottesman, M.M., Fojo, T. and Bates, S.E. (2002) Multidrug resistance in cancer: role of ATP-dependent transporters. *Nature Reviews Cancer*, **2**, 48–58.

16 Van Bambeke, F.B.E. and Tulkens, P.M. (2000) Antibiotic efflux pumps. *Biochemical Pharmacology*, **60**, 457–470.

17 Borst, P. and Ouellette, M. (1995) New mechanisms of drug resistance in parasitic protozoa. *Annual Review of Microbiology*, **49**, 427–460.

18 Wolfger, H., Mamnun, Y.M. and Kuchler, K. (2001) Fungal ABC proteins: pleiotropic drug resistance, stress response and cellular detoxification. *Research in Microbiology*, **152**, 375–389.

19 Dean, M. and Annilo, T. (2005) Evolution of the ATP-binding cassette (ABC) transporter superfamily in vertebrates. *Annual Review of Genomics and Human Genetics*, **6**, 123–142.

20 Haimeur, A., Conseil, G., Deeley, R.G. and Cole, S.P. (2004) The MRP-related and BCRP/ABCG2 multidrug resistance proteins: biology, substrate specificity and regulation. *Current Drug Metabolism*, **5**, 21–53.

21 Seelig, A., Blatter, X.L. and Wohnsland, F. (2000) Substrate recognition by P-glycoprotein and the multidrug resistance-associated protein MRP1: a comparison. *International Journal of Clinical Pharmacology and Therapeutics*, **38**, 111–121.

22 Matsson, P., Englund, G., Ahlin, G., Bergstrom, C.A., Norinder, U. and Artursson, P. (2007) A global drug

inhibition pattern for the human ATP-binding cassette transporter breast cancer resistance protein (ABCG2). *The Journal of Pharmacology and Experimental Therapeutics*, **323**, 19–30.

23 Rosenberg, M.F., Callaghan, R., Modok, S., Higgins, C.F. and Ford, R.C. (2005) Three-dimensional structure of P-glycoprotein: the transmembrane regions adopt an asymmetric configuration in the nucleotide-bound state. *The Journal of Biological Chemistry*, **280**, 2857–2862.

24 Dawson, R.J. and Locher, K.P. (2006) Structure of a bacterial multidrug ABC transporter. *Nature*, **443**, 180–185.

25 Dawson, R.J. and Locher, K.P. (2007) Structure of the multidrug ABC transporter Sav1866 from *Staphylococcus aureus* in complex with AMP-PNP. *FEBS Letters*, **581**, 935–938.

26 Seelig, A. (1998) A general pattern for substrate recognition by P-glycoprotein. *European Journal of Biochemistry*, **251**, 252–261.

27 Dey, S., Ramachandra, M., Pastan, I., Gottesman, M.M. and Ambudkar, S.V. (1997) Evidence for two nonidentical drug-interaction sites in the human P-glycoprotein. *Proceedings of the National Academy of Sciences of the United States of America*, **94**, 10594–10599.

28 Martin, C., Berridge, G., Higgins, C.F., Mistry, P., Charlton, P. and Callaghan, R. (2000) Communication between multiple drug binding sites on P-glycoprotein. *Molecular Pharmacology*, **58**, 624–632.

29 Raviv, Y., Pollard, H.B., Bruggemann, E.P., Pastan, I. and Gottesman, M.M. (1990) Photosensitized labeling of a functional multidrug transporter in living drug-resistant tumor cells. *The Journal of Biological Chemistry*, **265**, 3975–3980.

30 Chen, Y., Pant, A.C. and Simon, S.M. (2001) P-glycoprotein does not reduce substrate concentration from the extracellular leaflet of the plasma membrane in living cells. *Cancer Research*, **61**, 7763–7769.

31 Shapiro, A.B. and Ling, V. (1997) Extraction of Hoechst 33342 from the cytoplasmic leaflet of the plasma membrane by P-glycoprotein. *European Journal of Biochemistry*, **250**, 122–129.

32 Gatlik-Landwojtowicz, E., Aanismaa, P. and Seelig, A. (2006) Quantification and characterization of P-glycoprotein–substrate interactions. *Biochemistry*, **45**, 3020–3032.

33 Litman, T., Zeuthen, T., Skovsgaard, T. and Stein, W.D. (1997) Structure–activity relationships of P-glycoprotein interacting drugs: kinetic characterization of their effects on ATPase activity. *Biochimica et Biophysica Acta*, **1361**, 159–168.

34 Al-Shawi, M.K., Polar, M.K., Omote, H. and Figler, R.A. (2003) Transition state analysis of the coupling of drug transport to ATP hydrolysis by P-glycoprotein. *The Journal of Biological Chemistry*, **278**, 52629–52640.

35 Aanismaa, P. and Seelig, A. (2007) P-Glycoprotein kinetics measured in plasma membrane vesicles and living cells. *Biochemistry*, **46**, 3394–3404.

36 Garrigues, A., Nugier, J., Orlowski, S. and Ezan, E. (2002) A high-throughput screening microplate test for the interaction of drugs with P-glycoprotein. *Analytical Biochemistry*, **305**, 106–114.

37 Broxterman, H.J., Pinedo, H.M., Kuiper, C.M., Schuurhuis, G.J. and Lankelma, J. (1989) Glycolysis in P-glycoprotein-overexpressing human tumor cell lines. Effects of resistance-modifying agents. *FEBS Letters*, **247**, 405–410.

38 Gatlik-Landwojtowicz, E., Aanismaa, P. and Seelig, A. (2004) The rate of P-glycoprotein activation depends on the metabolic state of the cell. *Biochemistry*, **43**, 14840–14851.

39 McConnell, H.M., Owicki, J.C., Parce, J.W., Miller, D.L., Baxter, G.T., Wada, H.G. and Pitchford, S. (1992) The cytosensor microphysiometer: biological applications of silicon technology. *Science*, **257**, 1906–1912.

40 Polli, J.W., Wring, S.A., Humphreys, J.E., Huang, L., Morgan, J.B., Webster, L.O. and Serabjit-Singh, C.S. (2001) Rational use of *in vitro* P-glycoprotein assays in drug discovery. *The Journal of Pharmacology and Experimental Therapeutics*, **299**, 620–628.

41 Ford, J.M., Prozialeck, W.C. and Hait, W.N. (1989) Structural features determining activity of phenothiazines and related drugs for inhibition of cell growth and reversal of multidrug resistance. *Molecular Pharmacology*, **35**, 105–115.

42 Toffoli, G., Simone, F., Corona, G., Raschack, M., Cappelletto, B., Gigante, M. and Boiocchi, M. (1995) Structure–activity relationship of verapamil analogs and reversal of multidrug resistance. *Biochemical Pharmacology*, **50**, 1245–1255.

43 Ambudkar, S.V., Cardarelli, C.O., Pashinsky, I. and Stein, W.D. (1997) Relation between the turnover number for vinblastine transport and for vinblastine-stimulated ATP hydrolysis by human P-glycoprotein. *The Journal of Biological Chemistry*, **272**, 21160–21166.

44 Saparov, S.M., Antonenko, Y.N. and Pohl, P. (2006) A new model of weak acid permeation through membranes revisited: does Overton still rule? *Biophysical Journal*, **90** (11), L86–L88.

45 Omote, H. and Al-Shawi, M.K. (2002) A novel electron paramagnetic resonance approach to determine the mechanism of drug transport by P-glycoprotein. *The Journal of Biological Chemistry*, **277**, 45688–45694.

46 Schinkel, A.H., Wagenaar, E., van Deemter, L., Mol, C.A. and Borst, P. (1995) Absence of the mdr1a P-glycoprotein in mice affects tissue distribution and pharmacokinetics of dexamethasone, digoxin, and cyclosporin A. *The Journal of Clinical Investigation*, **96**, 1698–1705.

47 Anderle, P., Niederer, E., Rubas, W., Hilgendorf, C., Spahn-Langguth, H., Wunderli-Allenspach, H., Merkle, H.P. and Langguth, P. (1998) P-Glycoprotein (P-gp) mediated efflux in Caco-2 cell monolayers: the influence of culturing conditions and drug exposure on P-gp expression levels. *Journal of Pharmaceutical Sciences*, **87**, 757–762.

48 Schwab, D., Fischer, H., Tabatabaei, A., Poli, S. and Huwyler, J. (2003) Comparison of *in vitro* P-glycoprotein screening assays: recommendations for their use in drug discovery. *Journal of Medicinal Chemistry*, **46**, 1716–1725.

49 Seelig, A. (2007) The role of size and charge for blood–brain barrier permeation of drugs and fatty acids. *Journal of Molecular Neuroscience*, **33**, 32–41.

50 Seelig, A. and Gatlik-Landwojtowicz, E. (2005) Inhibitors of multidrug efflux transporters: their membrane and protein interactions. *Mini Reviews in Medicinal Chemistry*, **5**, 135–151.

51 Hochman, J.H., Yamazaki, M., Ohe, T. and Lin, J.H. (2002) Evaluation of drug interactions with P-glycoprotein in drug discovery: *in vitro* assessment of the potential for drug–drug interactions with P-glycoprotein. *Current Drug Metabolism*, **3**, 257–273.

52 Fischer, H., Gottschlich, R. and Seelig, A. (1998) Blood–brain barrier permeation: molecular parameters governing passive diffusion. *The Journal of Membrane Biology*, **165**, 201–211.

53 Fischer, H., Seelig, A., Chou, R.C. and van de Waterbeemd, J. (1997) The difference between the diffusion through the blood–brain barrier and the gastro-intestinal membrane. 4th International Conference on Drug Absorption, Edinborough.

54 Hollo, Z., Homolya, L., Davis, C.W. and Sarkadi, B. (1994) Calcein accumulation as a fluorometric functional assay of the multidrug transporter. *Biochimica et Biophysica Acta*, **1191**, 384–388.

55 Essodaigui, M., Broxterman, H.J. and Garnier-Suillerot, A. (1998) Kinetic analysis of calcein and calcein–acetoxymethylester efflux mediated by the multidrug resistance protein and P-glycoprotein. *Biochemistry*, **37**, 2243–2250.

56 Fricker, G. (2002) Drug transport across the blood–brain barrier, in *Pharmacokinetic Challenges in Drug Discovery*, Vol. 37 (eds O. Pelkonen, A. Baumann and A. Reichel), Springer, pp. 139–154.

57 Ekins, S., Waller, C.L., Swaan, P.W., Cruciani, G., Wrighton, S.A. and Wikel, J.H. (2000) Progress in predicting human ADME parameters *in silico*. *Journal of Pharmacological and Toxicological Methods*, **44**, 251–272.

58 Ekins, S., Ecker, G.F., Chiba, P. and Swaan, P.W. (2007) Future directions for drug transporter modelling. *Xenobiotica; The Fate of Foreign Compounds in Biological Systems*, **37**, 1152–1170.

59 Gerebtzoff, G. and Seelig, A. (2006) *In silico* prediction of blood–brain barrier permeation using the calculated molecular cross-sectional area as main parameter. *Journal of Chemical Information and Modeling*, **46**, 2638–2650.

60 Pajeva, I.K. and Wiese, M. (2002) Pharmacophore model of drugs involved in P-glycoprotein multidrug resistance: explanation of structural variety (hypothesis). *Journal of Medicinal Chemistry*, **45**, 5671–5686.

61 Ekins, S., Kim, R.B., Leake, B.F., Dantzig, A.H., Schuetz, E.G., Lan, L.B., Yasuda, K., Shepard, R.L., Winter, M.A., Schuetz, J.D., Wikel, J.H. and Wrighton, S.A. (2002) Three-dimensional quantitative structure–activity relationships of inhibitors of P-glycoprotein. *Molecular Pharmacology*, **61**, 964–973.

62 Ekins, S., Kim, R.B., Leake, B.F., Dantzig, A.H., Schuetz, E.G., Lan, L.B., Yasuda, K., Shepard, R.L., Winter, M.A., Schuetz, J.D., Wikel, J.H. and Wrighton, S.A. (2002) Application of three-dimensional quantitative structure–activity relationships of P-glycoprotein inhibitors and substrates. *Molecular Pharmacology*, **61**, 974–981.

63 Langer, T., Eder, M., Hoffmann, R.D., Chiba, P. and Ecker, G.F. (2004) Lead identification for modulators of multidrug resistance based on *in silico* screening with a pharmacophoric feature model. *Archiv der Pharmazie*, **337**, 317–327.

64 Penzotti, J.E., Lamb, M.L., Evensen, E. and Grootenhuis, P.D. (2002) A computational ensemble pharmacophore model for identifying substrates of P-glycoprotein. *Journal of Medicinal Chemistry*, **45**, 1737–1740.

65 Cianchetta, G., Singleton, R.W., Zhang, M., Wildgoose, M., Giesing, D., Fravolini, A., Cruciani, G. and Vaz, R.J. (2005) A pharmacophore hypothesis for P-glycoprotein substrate recognition using GRIND-based 3D-QSAR. *Journal of Medicinal Chemistry*, **48**, 2927–2935.

66 Li, W.X., Li, L., Eksterowicz, J., Ling, X.B. and Cardozo, M. (2007) Significance analysis and multiple pharmacophore models for differentiating P-glycoprotein substrates. *Journal of Chemical Information and Modeling*, **47**, 2429–2438.

67 Gombar, V.K., Polli, J.W., Humphreys, J.E., Wring, S.A. and Serabjit-Singh, C.S. (2004) Predicting P-glycoprotein substrates by a quantitative structure–activity relationship model. *Journal of Pharmaceutical Sciences*, **93**, 957–968.

68 Cabrera, M.A., Gonzalez, I., Fernandez, C., Navarro, C. and Bermejo, M. (2006) A topological substructural approach for the prediction of P-glycoprotein substrates. *Journal of Pharmaceutical Sciences*, **95**, 589–606.

69 Xue, Y., Yap, C.W., Sun, L.Z., Cao, Z.W., Wang, J.F. and Chen, Y.Z. (2004) Prediction of P-glycoprotein substrates by a support vector machine approach. *Journal of Chemical Information and Computer Sciences*, **44**, 1497–1505.

70 Crivori, P., Reinach, B., Pezzetta, D. and Poggesi, I. (2006) Computational models for identifying potential P-glycoprotein substrates and inhibitors. *Molecular Pharmaceutics*, **3**, 33.

71 Li, Y., Wang, Y.-H., Yang, L., Zhang, S.-W., Liu, C.-H. and Yang, S.-L. (2005) Comparison of steroid substrates and

inhibitors of P-glycoprotein by 3D-QSAR analysis. *Journal of Molecular Structure*, **733**, 111–118.

72 Wang, Y.H., Li, Y., Yang, S.L. and Yang, L. (2005) Classification of substrates and inhibitors of P-glycoprotein using unsupervised machine learning approach. *Journal of Chemical Information and Modeling*, **45**, 750–757.

73 Svetnik, V., Wang, T., Tong, C., Liaw, A., Sheridan, R.P. and Song, Q. (2005) Boosting: an ensemble learning tool for compound classification and QSAR modeling. *Journal of Chemical Information and Modeling*, **45**, 786–799.

74 Gerebtzoff, G., Li-Blatter, X., Fischer, H., Frentzel, A. and Seelig, A. (2004) Halogenation of drugs enhances membrane binding and permeation. *Chembiochem: A European Journal of Chemical Biology*, **5**, 676–684.

75 Ecker, G., Huber, M., Schmid, D. and Chiba, P. (1999) The importance of a nitrogen atom in modulators of multidrug resistance. *Molecular Pharmacology*, **56**, 791–796.

76 Lipinski, C.A., Lombardo, F., Dominy, B.W. and Feeney, P.J. (1997) Experimental and computational approaches to estimate solubility and permeability in drug discovery and development settings. *Advanced Drug Delivery Reviews*, **23**, 3–25.

77 Didziapetris, R., Japertas, P., Avdeef, A. and Petrauskas, A. (2003) Classification analysis of P-glycoprotein substrate specificity. *Journal of Drug Targeting*, **11**, 391–406.

78 Sauna, Z.E., Andrus, M.B., Turner, T.M. and Ambudkar, S.V. (2004) Biochemical basis of polyvalency as a strategy for enhancing the efficacy of P-glycoprotein (ABCB1) modulators: stipiamide homodimers separated with defined-length spacers reverse drug efflux with greater efficacy. *Biochemistry*, **43**, 2262–2271.

79 Seelig, A. and Gerebtzoff, G. (2006) Enhancement of drug absorption by noncharged detergents through membrane and P-glycoprotein binding. *Expert Opinion on Drug Metabolism & Toxicology*, **2**, 733–752.

80 van de Waterbeemd, H., Camenisch, G., Folkers, G., Chretien, J.R. and Raevsky, O.A. (1998) Estimation of blood–brain barrier crossing of drugs using molecular size and shape, and H-bonding descriptors. *Journal of Drug Targeting*, **6**, 151–165.

81 Seelig, A. and Landwojtowicz, E. (2000) Structure–activity relationship of P-glycoprotein substrates and modifiers. *European Journal of Pharmaceutical Sciences*, **12**, 31–40.

Part Five
Drug Development Issues

19
Application of the Biopharmaceutics Classification System Now and in the Future

Bertil Abrahamsson and Hans Lennernäs

Abbreviations

ANDA	Abbreviated new drug application
BCRP	Breast cancer-resistant protein
BCS	Biopharmaceutics Classification System
CYP3A4	Cytochrome P450 3A4
EMEA	European Medical Evaluation Agency
ER	Extended release
FDA	Food and Drug Administration
GI	Gastrointestinal
HBD	Number of hydrogen-bond donors
hPepT1	Oligopeptide carrier for di- and tripeptides
ICH	International Committee of Harmonization
IR	Immediate release
IVIVC	*In vitro*/*in vivo* correlation
MCT	Monocarboxylic acid cotransporter
MRP	Multidrug-resistant protein family
NDA	New drug application
P-gp	P-Glycoprotein
PSA	Polar molecular surface area
SR	Solubilization ratio

Symbols

CL_{int}	Intrinsic clearance
Clog *P*	Logarithm of the calculated octanol/water partition coefficient (for neutral species)
E_G	Gut wall extraction
E_H	Hepatic extraction
F	Bioavailability

f_a	Fraction dose absorbed
f_u	Fraction drug unbound in plasma
log $D_{6.5}$	Logarithm of the distribution coefficient in octanol/water at pH 6.5
MW	Molecular weight
P_{eff}	Effective intestinal permeability
Q_h	Hepatic blood flow

19.1 Introduction

Almost all of the 50 most sold drug products in the US and European markets are administered orally (Figure 19.1). Significant drug absorption and appropriate drug delivery are prerequisites for successful oral treatment of diseases. Through retrospective analysis, the reasons behind failures in the development of oral drugs for the market have been poor pharmacokinetic properties, lack of efficacy, safety issues, and marketing, as shown in Figure 19.2 [1–3]. Among the pharmacokinetic aspects, a low and highly variable bioavailability, that is, the amount of drug that reaches the plasma compartment, is indeed considered to be the main reason for stopping the further development of the pharmaceutical product [3]. It is not surprising that pharmacokinetics is crucial for a successful drug development since the plasma drug levels are related in various ways to the effects at the sites of pharmacological and toxicological actions (pharmacodynamics) (Figure 19.3).

It is also well recognized that the design and composition of the pharmaceutical dosage form may have an important impact on the bioavailability and hence the therapeutic outcome of a drug product. This includes both intentional effects such as altered drug absorption rates by modified-release formulations or increased bioavailability for dosage forms including absorption-enhancing principles and undesirable effects such as reduction of the amount of drug reaching the systemic circulation as a result of poor product design. Consequently, bioavailability also reflects the pharmaceutical product quality and *in vivo* performance for oral dosage forms. This has to be considered in the development of generic products, which

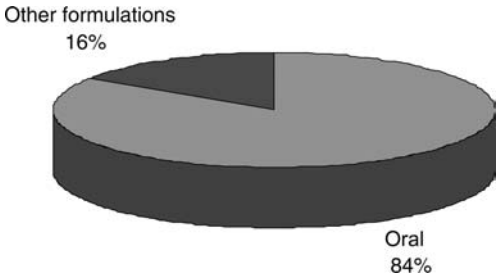

Figure 19.1 Percent sales of orally administered drugs for the 50 most sold products in the United States and Europe (from IMS Health 2001).

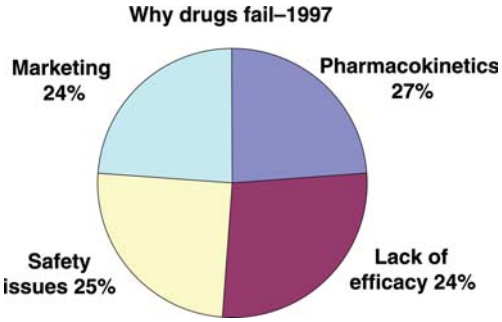

Figure 19.2 The reasons why clinical development of drugs are sometimes terminated and the drug does not reach the market are due to safety issues, marketing reasons, lack of efficacy, and/or pharmacokinetics/bioavailability (from Dr Lawrence Lesko, FDA Regulatory Standards: BA/BE & PK/PD; in Strategies for Oral Drug Delivery, Lake Tahoe, USA, March 6–10, 2000).

should be interchangeable with the original product and provide the same clinical outcome, or when formulations and manufacturing processes are changed during clinical development or for a marketed product. *In vivo* investigations comparing the bioavailability of two formulations of the same drug with the aim to verify sufficient similarity from a clinical perspective for a "new" versus an "old" formulation are called bioequivalence studies.

Successful development of pharmaceutical products for oral use requires identification of the rate-limiting step(s) of the intestinal absorption process of the drug. This will aid in the selection of suitable candidate molecules for drug development as well as in the design of a dosage form. Biopharmaceutical investigations are needed to obtain the necessary understanding of the intestinal absorption process. The rate and extent of drug absorption (f_a) from a solid dosage form during its transit through the

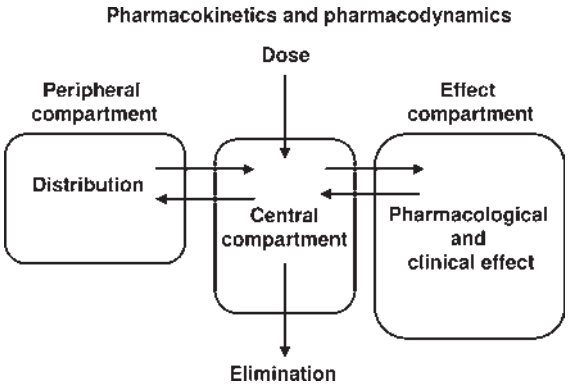

Figure 19.3 A schematic drawing of the relation between pharmacokinetics and pharmacodynamics to better understand the action of drugs.

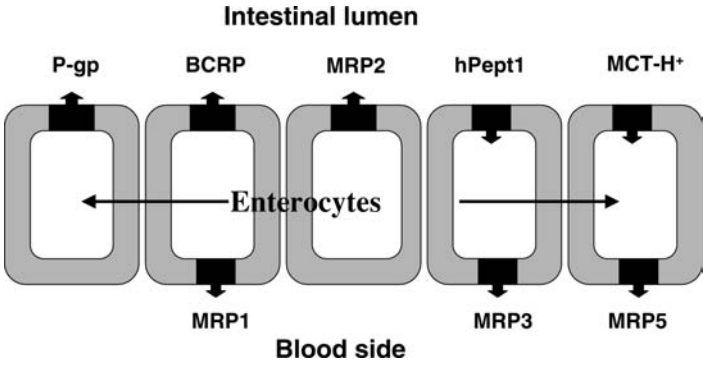

Figure 19.4 The intestinal permeability of drugs *in vivo* is the total transport parameter that may be affected by several parallel transport mechanisms in both absorptive and secretory directions. A few of the most important transport proteins that may be involved in the intestinal transport of drugs and their metabolites across intestinal epithelial membrane barriers in humans are displayed. P-gp, glycoprotein; BCRP, breast cancer-resistant protein; MRP1-5, multidrug-resistant protein family; hPepT1, oligopeptide carrier for di- and tripeptides; MCT-$H^{(+)}$, monocarboxylic acid cotransporter.

small and large intestines include several steps: drug release and dissolution, potential stability and binding issues in the lumen, transit time, and effective intestinal permeability (P_{eff}) [4, 5]. The transport of a drug across the intestinal barrier (P_{eff}) may be complex and involve multiple transport mechanisms as illustrated in Figure 19.4. For instance, the transport measured is a consequence of parallel processes in the absorptive directions such as passive diffusion and carrier-mediated uptake through proteins such as oligopeptide (PepT1), monocarboxylic cotransporter (MCT-H^+) amino acid transporters, and others [6–9]. Today, there is also evidence that transport in the secretory directions through various efflux proteins may restrict both the rate and extent of intestinal absorption. The following efflux proteins are located in the human intestine: P-glycoprotein, multidrug-resistant protein family (MRP-family 1–6), and breast cancer-resistant protein (BCRP) [10]. However, many efflux transport substrates show complete intestinal absorption, and the pharmacokinetics is superimposable with increasing dose [11–13].

In many cases, the intestinal P_{eff} is considered to be the rate-limiting step in the overall absorption process, and this poor intestinal permeability of drugs constitutes a major bottleneck in the successful development of candidate drugs [2, 5, 14–16]. However, in drug discovery today, several new pharmacological targets, for instance, intracellular receptors, and the use of high-throughput techniques, including permeability screens, have brought more lipophilic compounds into drug development [2, 14]. Novel candidate drugs will therefore often be poorly soluble in water [2, 14]. This could limit the bioavailability to an extent that endangers successful product development though poor permeability could be expected to be less of an issue for these molecules. However, several formulation principles are available that could be applied to increase dissolution and solubility. Thus, drug molecules with a favorable pharmacological profile but poor biopharmaceutical properties could thereby sometimes be

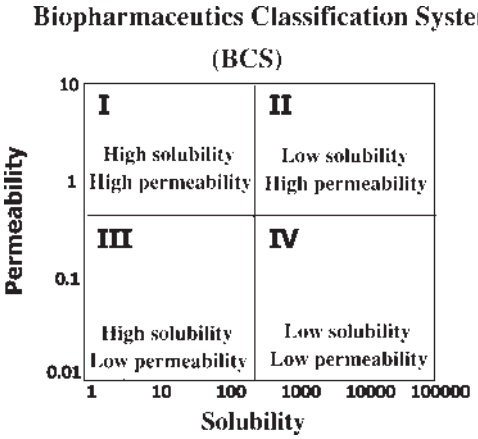

Figure 19.5 The Biopharmaceutics Classification System provides a scientific basis for predicting intestinal drug absorption and for identifying the rate-limiting step based on primary biopharmaceutical properties such as solubility and effective intestinal permeability (P_{eff}). The BCS divides drugs into four different classes based on their solubility and intestinal permeability. Drug regulation aspects related to *in vivo* performance of pharmaceutical dosage forms have been the driving force in the development of BCS. Guidance for industry based on BCS mainly clarifies when bioavailability/bioequivalence studies can be replaced by *in vitro* bioequivalence testing (www.fda.gov/cder/guidance/3618fnl.htm).

saved from development failures and turned into useful pharmaceutical products. Such a reliance on formulations that reduce the shortcomings of the pure active drug is more controversial for poor permeability drugs, for which the use of permeation enhancers to increase P_{eff} has been described, but this is still more of an explorative research area than an established tool in product development.

The Biopharmaceutics Classification System (BCS) provides a scientific basis for predicting intestinal drug absorption and identifying the rate-limiting step on the basis of primary biopharmaceutical properties such as solubility and effective intestinal permeability (P_{eff}) [4, 17, 18]. The BCS divides drugs into four different classes on the basis of their solubility and intestinal permeability (Figure 19.5). Drug regulation aspects related to *in vivo* performance of pharmaceutical dosage forms have been the driving force in the development of BCS. Guidance for industry based on BCS mainly clarifies when bioavailability/bioequivalence (BA/BE) studies can be replaced by *in vitro* bioequivalence testing [17, 19].

The aim of this chapter is to describe the BCS and the science behind BCS and to discuss its use in the development of oral pharmaceutical products from both regulatory and nonregulatory aspects.

19.2
Definition of Absorption and Bioavailability of Drugs Following Oral Administration

The general definition of the bioavailability (F) of a drug following oral administration is the rate at and extent to which a pharmacological active drug reaches the systemic

circulation. The bioavailability (F) of a compound is a consequence of several processes shown in Equation 19.1:

$$F = f_a \cdot (1-E_G) \cdot (1-E_H), \tag{19.1}$$

where the extent of absorption (f_a) includes all processes from dissolution of the solid dosage form to the intestinal transport of the drug into the intestinal tissue, that is, across the apical membrane of the enterocyte. This is the general definition of the extent of absorption and does not include the metabolic first-pass effect in the gut (E_G) and/or metabolism/biliary excretion in the liver (E_H) [4, 5].

The rate (mass/time) and fractional extent of drug absorption (mass/dose $= f_a$) from the intestinal lumen *in vivo* at any time t is schematically shown in Equation 19.2 [4]:

$$\frac{M(t)}{\text{dose}} = \int_0^t \iiint A \cdot P_{\text{eff}} \cdot C_{\text{lumen}} \cdot \mathrm{d}A\, \mathrm{d}t, \tag{19.2}$$

where A is the available intestinal surface area, P_{eff} is the average value of the effective intestinal permeability along the intestinal region where absorption occurs, and C_{lumen} is the free concentration of the drug in the lumen from the corresponding intestinal part [4, 20]. Several processes such as dissolution rate, degradation, metabolism, and binding in the gastrointestinal tract affect the free drug concentration in the lumen.

19.3 Dissolution and Solubility

Dissolution of a drug molecule into the GI fluids is a prerequisite for drug absorption since the permeability of particulate material over the GI mucosa is negligible in the context of oral drug bioavailability. The dissolution process could thereby affect both the rate and extent of oral drug absorption. The use of high-throughput techniques in the modern drug discovery process brings more lipophilic compounds into drug development [2, 14]. This means that drug dissolution in the gastrointestinal fluids has become increasingly important to be considered in the design, development, and optimization of a solid oral drug product.

Drug dissolution is the dynamic process by which solid material is dissolved in a solvent and is characterized by a rate (amount/time), whereas solubility describes an equilibrium state, where the maximal amount of drug per volume unit is dissolved.

The solubility, as well as the dissolution, in a water solution depends on factors such as pH and contents of salts and surfactants.

The solubility is most often experimentally determined from the drug concentration in the liquid phase after adding excessive amounts of a solid drug substance to the test medium. This apparent solubility is affected by the solid-state properties of the drug, for example, polymorphs, solvates, impurities, and amorphous content. An equilibrium with the thermodynamically most stable solid-state form, being the least

soluble, should eventually be reached. This could, however, be a very slow process requiring several days. More short-term supersaturation phenomena may also occur; that is, the measured solubility is much higher than the true saturation solubility during an initial phase before precipitation occurs from the supersaturated solution and an equilibrium can be reached. Thus, although solubility is a simple concept, it is far from being unproblematic to obtain robust data because of the indicated time dependence and effects of differences in solid-state properties as well as other sources of experimental variability.

The dissolution of drugs has been described by the Noyes–Whitney equation and later modified by Nernst and Brunner [21, 22]:

$$\frac{dX}{dt} = \frac{AD}{h(C_s - X_d/V)}, \tag{19.3}$$

where dX/dt is the dissolution rate in terms of mass X per unit time t, A is the available surface area of the solid drug, D is the drug diffusion coefficient, h is the effective diffusion boundary layer thickness, C_s is the saturation solubility of the drug in the test medium, X_d is the amount of drug already in solution, and V is the volume of fluid in the lumen available for dissolution. The dissolution rate is not an inherent property for a drug substance and will vary with the solid-state properties such as particles size, degree of crystallinity, and crystal form.

The drug dissolution rate could be determined by dispersing the powder in a test medium under suitable agitation or by studying the dissolution for a constant surface area by using the rotating-disk method (Figure 19.6). The latter method should be the technique of choice, except when studies of the effect of particle size are of special relevance. The rotating-disk method, which is described in the United State Pharmacopeia, has the advantage of providing very well-defined hydrodynamic test

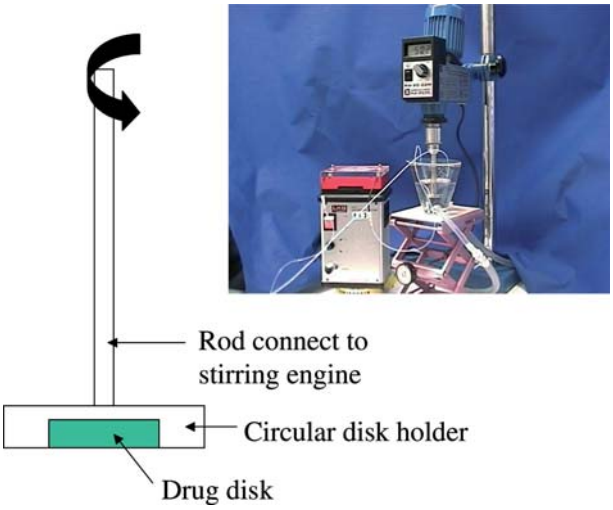

Figure 19.6 A schematic drawing and photo of the rotating-disk method.

conditions and a known drug surface area, which reduces the risk for artifacts and allows for accurate comparisons of data obtained for different drugs, in different labs. In addition, the test conditions in the rotating-disk method also allow for more mechanistic evaluations of the dissolution process, such as determination of the drug diffusion coefficient and estimation of an intrinsic dissolution rate, being independent of hydrodynamic conditions [23].

The solubility as well as the dissolution rate in the GI tract is affected by several physiological factors, which have to be taken into account when predicting the influence of drug dissolution on the oral bioavailability. These include physicochemical properties of the GI fluids, agitation provided by the GI motility, and available volumes of GI fluids. The *in vivo* situation is highly complex and depends, for example, on the nutritional status. The conditions also differ in different regions within the GI tract. Human GI juices have been characterized after both fasting and fed conditions by measuring aspiration through tubes [24, 25]. A summary of the most important variables for the fasting and fed states is given in Table 19.1. In addition to these main effects, the GI conditions of relevance for drug dissolution may also be affected by other cyclic variations, diurnal effects, diseases, age, and concomitant medications [22].

A summary of how physiological factors affect the dissolution rate is given in Table 19.2. More extensive characterizations of human gastrointestinal fluids, during both fasting and fed conditions, have been performed with respect to components and physicochemical parameters of relevance for drug dissolution [26, 27] The effective surface area will be affected by the wetting properties of the bile acids and other surface-active agents in the GI tract. The diffusivity of a drug molecule in the intestinal juice will be altered by changes in viscosity induced, for instance, by meal components. An increased dissolution rate could be obtained at more intense intestinal motility patterns or increased flow rates [22]. The effect on the dissolution of a low-solubility compound of different hydrodynamic conditions, being relevant

Table 19.1 Summary of physiological GI characteristics in fasting and fed state of importance for drug dissolution and solubility.

	Fasting	**Fed**
Stomach		
• Fluid volume (ml)	50–100	Up to 1000 ml
• pH	1–2	2–5
• Ionic strength	0.10	Varying
• Motility pattern/intensity	Cyclic/low–high	Continuous/high
• Surface tension (mN/m)	40	Often lower than fasting
• Osmolarity (mOsm)	hyposmotic	hyperosmotic
Upper small intestine		
• Flow rate (ml/min)	0.6–1.2	2.0–4.2
• pH	5.5–6.5	Similar
• Bile acids (mm)	4–6	10–40
• Ionic strength	0.16	0.16

Table 19.2 Physicochemical and physiological parameters important to drug dissolution in the gastrointestinal tract [22].

Factor	Physicochemical parameter	Physiological parameter
Surface area of drug (A)	Particle size, wettability	Surfactants in gastric juice and bile
Diffusivity of drug (D)	Molecular size	Viscosity of luminal contents
Boundary layer thickness (h)		Motility patterns and flow rate
Solubility (C_s)	Hydrophilicity, crystal structure, solubilization	pH, buffer capacity, bile, food components
Amount of drug already dissolved (C_t)		Permeability
Volume of solvent available (C_t)		Secretions, coadministered fluids

With kind permission from Kluwer Academic Publishers.

for the fasting and fed states, was recently investigated in an *in vivo* study [28]. It was found that the hydrodynamic conditions significantly affected both rate and extent of bioavailability for slowly dissolving unmilled drug particles whereas for more rapidly dissolving micronized drug substances no effect was detected. The lack of influence of agitation on dissolution of small (radius $\sim$<5 μm) primary drug particles is in accordance with the theoretical work by Nielsen [29]. The lack of influence by different degrees of stirring on dissolution of small particles in contrast to the reverse for latter particles has also been observed in *in vitro* dissolution experiments [30]. The saturation solubility in the GI fluids could be affected by several factors such as pH, solubilization by bile acids, or dissolution in lipid food components [31]. The pH, which varies according to region as well as food intake, is a key factor for proteolytic drugs with pK_a values within or close to the physiological pH interval. The bile concentrations increase after food intake, and mixed micelles with nutritional lipids are formed. However, significantly enhanced solubility due to solubilization can be achieved already under fasting conditions. An example of the dramatic increase in solubility due to solubilization by bile components is given in Figure 19.7. The solubilization by bile acids increases by increased drug lipophilicity. An empirical algorithm for the solubilization ratio (SR) of drugs in bile acids has been developed (Equation 19.4), which indicates that for drugs with a log $P < 2$ no solubility improvement should be expected [32]. In a pharmacokinetic database of a total of 472 drugs, it was found that 235 drugs (50%) had a log P value higher than 2, which means that this process applies to a large part of the clinically used drugs [33].

$$\log \mathrm{SR} = 2.09 + 0.64 \log P. \tag{19.4}$$

The micellar solubilization of drugs in the small intestine is increased not only due to the higher bile acid secretion induced by a meal but also by lipid components of nutritional origin, such as fatty acids and monoglycerides. The solubility of six drugs

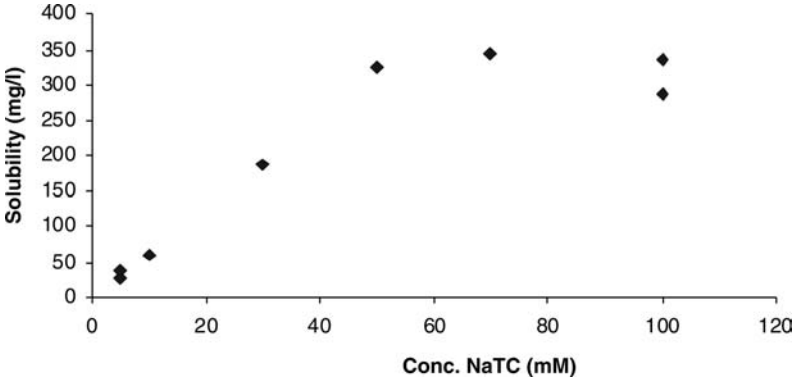

Figure 19.7 Solubility of a very poorly soluble drug, candersartan cilexitil, at different concentrations of bile acid/lecithin (2.5 : 1).

was increased 3–30 times in the fed compared to the fasting state in human intestinal fluid [34].

The amount of drug in solution, which will affect the drug dissolution rate at "nonsink conditions," is dependent on the available volume that is controlled by oral intake, secretions, and water flux over the GI wall. For instance, it has been approximated that the physiological volume of the small intestine varies from 50 to 1100 ml, with an average of 500 ml in the fasting state [4, 18]. A more recent study quantifying free water in the small intestine in man by the use of magnetic resonance imaging found liquid volumes of around only 100 ml [35]. It should also be realized that the small intestine is not a water-filled tube and that the fluids are irregularly located in pockets. The drug concentration in the intestinal lumen is not only a function of dissolution and available volumes but also dependent on the drug permeability, which will be of special importance when the drug levels in the intestine approach the saturation level.

It should, however, be noted that it is almost impossible to fully predict the *in vivo* dissolution rate because of the many factors involved, of which several have not yet been completely characterized. The introduction of new study techniques to directly follow drug dissolution *in vivo* in the human intestine should therefore be of importance [36, 37]. For example, *in vivo* dissolution studies, on the basis of the intestinal perfusate samples, discriminated between the dissolution rates of the two different particle sizes of spironolactone. In addition, dissolution rates of carbamazepine obtained *in vitro* were significantly slower than the direct *in vivo* measurements obtained from the perfusion method. The higher *in vivo* dissolution rate was probably due to the efficient sink conditions provided by the high permeability of carbamazepine [36, 37].

It is highly desirable in drug discovery and early drug development to predict the influence of the drug dissolution on oral absorption on the basis of rather simple measurements of dissolution or solubility [2, 14]. The primary variable for judgments of *in vivo* absorption is the dissolution rate rather than the solubility. Drug dissolution can be the rate-limiting step in the absorption process and thereby affect the rate of

Table 19.3 Proposed limits of drug dissolution on solubility to avoid absorption problems.

Factor	Limit	Reference
Solubility at pH 1–7	>10 mg/ml at all pH	[33]
Solubility at pH 1–8 and dose	Complete dose dissolved in 250 ml at all pH	[4]
Water solubility	>0.1 mg/ml	[32]
Dissolution rate at pH 1–7	>1 mg/min/cm^2 (0.1–1 mg/nm/cm^2 borderline) at all pH values	[33]

bioavailability, and, often more importantly, it can also limit the extent of bioavailability when the dissolution rate is too slow to provide complete dissolution within the absorptive region(s) of the GI tract. However, most often solubility data are more readily available than dissolution rates for a drug candidate, especially in early phases when only minute amounts of drug are available, preventing accurate dissolution rate determinations. Consequently, predictions of *in vivo* effects on absorption caused by poor dissolution must often be made on the basis of solubility data rather than dissolution rate. This can theoretically be justified by the direct proportionality between dissolution rate and solubility under "sink conditions" according to Equation 19.3. A list of proposed criteria to be used to avoid absorption problems caused by poor dissolution is given in Table 19.3 [4, 38, 39] and further discussed below. A solubility in water of $\geq$10 mg/ml in the pH range 1–7 has been proposed as an acceptance limit to avoid absorption problems, while another suggestion is that drugs with water solubilities less than 0.1 mg/ml often lead to dissolution limitations of absorption. It should be noted that these arbitrary limits may be conservative; that is, the bioavailability of drugs with even lower solubility may not always be limited by drug dissolution. For example, a drug with much lower solubility, such as felodipine (0.001 mg/ml), provides complete absorption when administered in an appropriate solid dosage form [40]. This may be explained by both successful application of dissolution-enhancing formulation principles and more favorable drug solubility *in vivo* owing to the presence of solubilizing agents such as bile acids.

The BCS provides another model for biopharmaceutical interpretation of solubility data. Two different classes of drugs have been identified on the basis of the drug solubility as outlined in Figure 19.5, that is, high and low solubilities. If the administered dose is completely dissolved in the fluids in the stomach, which is assumed to be 250 ml (50 ml basal level in stomach plus administration of the solid dose with 200 ml of water), the drug is classified as a "high-solubility drug" [4, 17]. Such a good solubility should be obtained within a range of pH 1–8 to cover all possible conditions in a patient and to exclude the risk of precipitation in the small intestine because of the generally higher pH there than in the stomach. Drug absorption is expected to be independent of drug dissolution for drugs that fulfill this requirement, since the total amount of the drug will be in solution before entering the major absorptive area in the small intestine and the rate of absorption will then be determined by the gastric emptying of fluids. Such "highly soluble drugs" are

advantageous in pharmaceutical development since no dissolution-enhancing principles are needed, and the process parameters that could affect drug particle form and size are generally not critical formulation factors. However, many low-solubility drugs according to BCS have been developed into clinically useful products, that is, this classification is hardly useful as a screening criterion in drug discovery.

A special case in dissolution-limited bioavailability occurs when the assumption of "sink condition" *in vivo* fails, that is, the drug concentration in the intestine is close to the saturation solubility. Class IV compounds, according to BCS, are most prone to this situation because of the combination of low solubility and low permeability, but it could also happen for class II compounds, depending primarily on the ratio between dose and solubility. Non "sink conditions" *in vivo* lead to less than proportional increases of bioavailability for increased doses. This is illustrated in Figure 19.8, where the fraction of drug absorbed has been simulated by the use of a compartmental absorption and intestinal transit model [41] for different doses and for different permeabilities of a low-solubility aprotic compound. Although the lowest permeability in this example is still within the range of high permeability according to the BCS, the fraction absorbed could vary between just a small percentage to complete uptake for a low-solubility compound (1 µg/ml) at a fixed dose just as a function of the permeability. Similarly, the dose level would also be a critical determinant of the amount absorbed for a given permeability and solubility. Thus, it is crucial in evaluating dissolution/solubility effects on bioavailability to consider these effects not in isolation but together with permeability and dose, as is the case in the BCS.

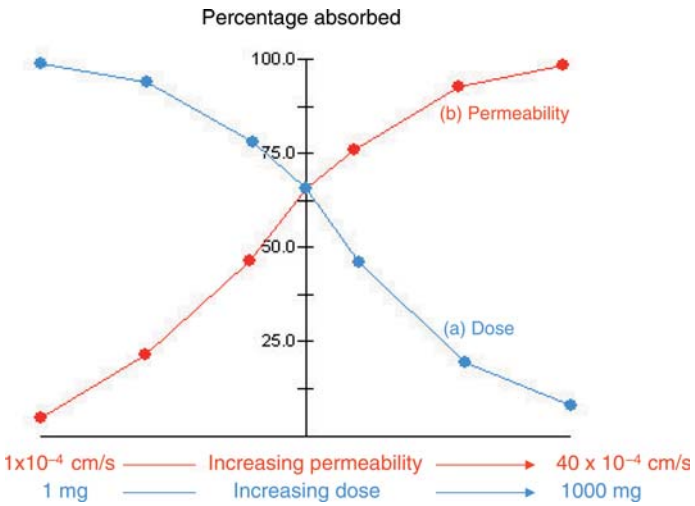

Figure 19.8 Fraction drug absorbed predicted by Gastroplus (SimulationPlus, Lancaster, CA, USA) for oral administrations of a poorly soluble (1 µg/ml), aprotic drug at (a) different doses with a constant, high permeability (4×10^{-4} cm/s) and (b) different permeabilities with a constant dose (100 mg).

19.4
The Effective Intestinal Permeability (P_{eff})

The intestinal permeability (P_{eff}) is a major determinant of fraction drug absorbed and quantitatively represents the principal membrane transport coefficient of the intestinal mucosa of a drug, which is possible to use regardless of the transport mechanism across mucosa [4, 5, 42]. The different transport mechanisms by which a drug may be transported across the intestinal barrier are displayed in Figure 19.4. There are different approaches to predicting and measuring intestinal permeability as summarized in Figure 19.9. Most *in vitro* models, such as cell monolayers (Caco-2 model) and excised tissue segment in a diffusion chamber (Ussing model), are based on the appearance of the drug on the serosal (basolateral) side. The measured *in vitro* P_{app} includes drug transport across the apical cell membrane, cytosol, and basolateral membrane for cell monolayers, as well as the interstitial fluid and connective tissue for the Ussing chamber model [20]. Consequently, such a definition also includes gut first-pass metabolism that may occur in the cytosol of the enterocyte (for instance, by CYP P450 isoenzymes and cytosolic localized peptidases). The activity of these intracellular enzymes will particularly influence the appearance rate of the drug on the basolateral side (i.e., in the portal vein *in vivo*). Thus, it may be useful to switch on and off genes coding for intestinal CYP3A4 in the Caco-2 model [43]. Another, and probably more accurate, definition suggests that the intestinal epithelial P_{eff} for most drugs reflects the transport across the apical membrane of the enterocyte [4, 5, 42]. This view is valid for most drugs that are absorbed by passive diffusion and/or carrier-mediated transport. Recently, it has also been reported that passive transcellular

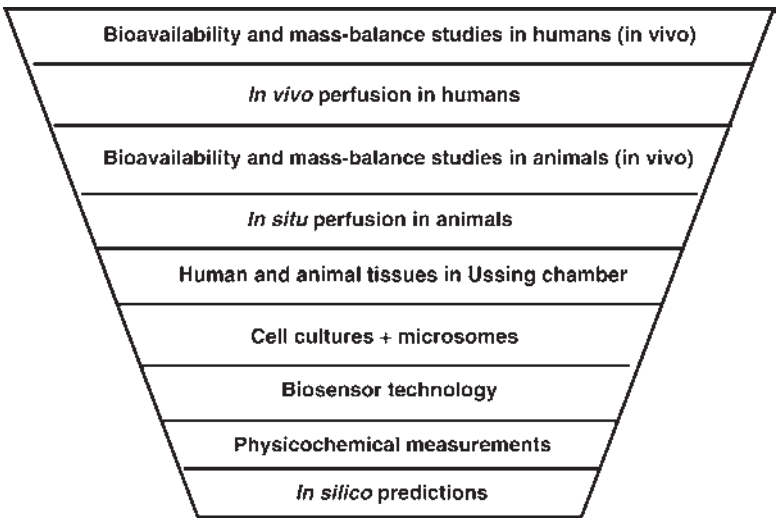

Figure 19.9 A short overview, from *in silico* to *in vivo* in humans, of the methods available to investigate and predict fraction dose absorbed and bioavailability following oral dosing.

permeability across epithelial cells is determined by the largest resistance, which is the apical epithelial membrane [43, 44]. Accordingly, intestinal permeability represents the transport of compounds into the enterocyte's cytosol [4, 5, 42]. This view is certainly the case for passive transcellular diffusion across the apical membrane, which is considered to be rate limiting. Intestinal perfusion models of the animal and human intestine are often based on the disappearance of the drug from the perfused gut lumen. Interestingly, results from single-pass perfusion of both rat and human small intestines have been shown to predict fraction dose absorbed in humans with high accuracy [5, 20, 45].

The BCS is based on a human *in vivo* permeability (P_{eff}) database of about 20 different drugs. This database was established by using the Loc-I-Gut technique, an *in vivo* single-pass perfusion technique, in the human proximal jejunum [46]. This region of the proximal small intestine is where the major absorption of most drugs takes place when they are given in immediate-release (IR) dosage form. These *in vivo* values of P_{eff} have been used to establish a correlation between measured *in vivo* permeability and fraction dose absorbed in humans for soluble drugs as shown in Figure 19.10. This fundamental *in vivo* correlation between permeability and fraction of dose absorbed has established *in vitro–in vivo* correlations (IVIVCs) between human *in vivo* jejunal P_{eff} and permeabilities from animal tissues or cell cultures [5, 20, 46–48]. Model correlations based on *in vivo* permeability data will be very useful when preclinical models are developed and validated regarding predictions of human intestinal absorption. They are also important for the development of theoretical models (*in silico*) where intestinal drug absorption is predicted from

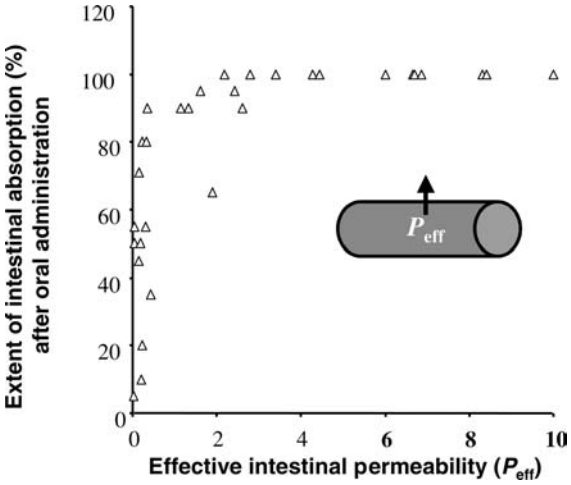

Figure 19.10 Human *in vivo* permeability values (P_{eff}) can be determined by the use of a single-pass perfusion technique (Loc-I-Gut) in humans. These human P_{eff} values have been excellently correlated to fraction dose absorbed (f_a) of oral doses for a large number of drugs from different pharmacological classes, which consequently are representing structural diversity.

molecular structure [2, 16, 49]. Altogether, they provide tools that might be very helpful in classifying drugs according to the BCS and consequently contribute to the regulatory evaluation of both bioavailability and bioequivalence [4, 18, 50].

According to the FDA BCS guidelines, measurements of the permeability and fraction dose absorbed of a drug can be made by mass balance, absolute bioavailability, or intestinal perfusion methods. The intestinal permeability of a drug can be determined by (1) *in vivo* intestinal perfusion in man [46]; (2) *in vivo* or *in situ* perfusion of a suitable animal model [45]; (3) *in vitro* transport across excised human or animal tissues [48, 51]; and (4) *in vitro* transport across epithelial cell monolayer [52] (www.fda.gov/cder/guidance/3618fnl.htm). When applying any of these models, it is crucial to understand the main transport mechanisms and metabolic route and characterization of the activity of the transporter/enzyme involved. It is well recognized that carrier-mediated processes in Caco-2 cells are considerably lower than those *in vivo* [20, 47, 53]. Therefore, it is crucial to extrapolate *in vitro* cell culture data to the *in vivo* situation with great care [18, 20, 47, 53]. This is especially important when carrier-mediated processes are involved, which has been made evident by a recent study showing significant differences in gene expression levels for transporters, channels, and metabolizing enzymes in Caco-2 cells compared to human duodenum [53]. If an animal model is used, potential species difference has to be considered [18, 20, 50].

The human *in vivo* permeability for various drugs is one of the cornerstones in the BCS, and their correlation with fraction dose absorbed and permeability values from other permeability models mentioned above would make it feasible to classify drugs according to the BCS and to define bioequivalence regulation for pharmaceutical product approval. These human *in vivo* P_{eff} were determined with a regional double-balloon perfusion approach (Loc-I-Gut), which is described shortly below (Figure 19.11). The tube was introduced through the mouth after an application of a local anesthetic (lidocaine) to the throat. The position of the tube was checked by fluoroscopy, and the perfused segment was located in the proximal part of the jejunum. Once the perfusion tube was in place, the two balloons were inflated with approximately 26–30 ml of air creating a 10 cm long segment. The jejunal segment was then rinsed with isotonic saline (37 °C) for at least 20 min, and a flow rate of 2.0 ml/min was most often applied. A more extensive description of this intestinal perfusion technique is published elsewhere [46, 54].

Jejunal P_{eff} and other variables were calculated from the steady-state level in the perfusate leaving the intestinal segment. We have reported earlier that a well-mixed model best describes the hydrodynamics within the perfused jejunal segment, and P_{eff} is calculated according to Equation 19.5:

$$P_{eff} = \frac{Q_{in} \cdot (C_{in} - C_{out})}{C_{out} \cdot 2\pi r L}, \tag{19.5}$$

where Q_{in} is the inlet perfusate rate, C_{in} and C_{out} are the inlet and outlet perfusate concentrations of the drug, respectively, r is the radius ($r = 1.75$ cm), and L is the length of the jejunal segment (10 cm) [46, 55].

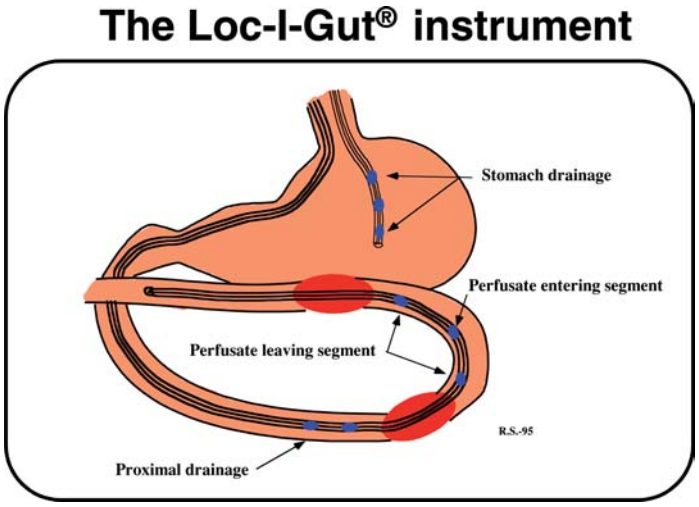

Figure 19.11 Loc-I-Gut is a perfusion technique for the proximal region of the human jejunum. The multichannel tube is 175 cm long and is made of polyvinyl chloride with an external diameter of 5.3 mm. It contains six channels and is provided distally with two 40 mm long, elongated latex balloons, placed 10 cm apart each separately connected to one of the smaller channels. The two wider channels in the center of the tube are for infusion and aspiration of perfusate. The two remaining peripheral smaller channels are used for administration of marker substances and/or for drainage. At the distal end of the tube is a tungsten weight attached in order to facilitate passage of the tube into the jejunum. The balloons are filled with air when the proximal balloon has passed the ligament of Treitz. Gastric suction is obtained by a separate tube. ^{14}C-PEG 4000 is used as a volume marker to detect water flux across the intestinal barrier.

The jejunal perfusion approach generates data, which may be used to predict absorption/bioavailability and to establish *in vivo–in vitro* correlation even for extended-release (ER) products. If a drug is transported mainly by passive diffusion and has a jejunal P_{eff} higher than that for metoprolol (1.5×10^{-4} cm/s = high-permeability compound), it can be expected to be completely absorbed throughout the small and large intestines [5, 51].

Predictions of human *in vivo* permeability can be made with a particularly high degree of accuracy in all preclinical models for drugs with passive diffusion as their main mechanism. It is only the dog model that seems to low-permeability (passively) drugs more efficiently than both humans and rats [5, 20]. Special care must be taken for drugs that are absorbed by a carrier-mediated transport mechanism as the main mechanism. It has been shown that absorptive carriers, such as the oligopeptide and amino acids carriers, have a low functional activity because of low protein expression in the Caco-2 model [7, 18, 47, 56, 57]. For these drugs, a scaling factor has to be developed and introduced, otherwise the *in vivo* permeability will be underestimated. This low expression is not surprising, since preliminary gene chip assays have reported that the Caco-2 cells have about 40% of the genes turned on compared to the normal gene expression in the human small intestine. Carrier-mediated absorption

by the oligopeptide carrier and the amino acid transport family in rats has not shown a significant species difference [7, 20, 45, 53, 56, 58–61, 90].

It is important to recognize that the *in vitro* permeability obtained in cell monolayers (such as Caco-2 models) should be considered as a qualitative rather than quantitative value. Especially poor are the predictions of fraction dose absorbed for carrier-mediated drugs with low Caco-2 permeability and predictions of high fraction dose absorbed in humans [7, 20, 47, 53, 56, 62]. However, it is possible to establish a reasonable good *in vitro–in vivo* correlation when passive diffusion is the dominating absorption mechanism.

19.5 Luminal Degradation and Binding

Degradation and formation of nonabsorbable drug complexes in the intestinal lumen is the third factor, in addition to dissolution and permeability, which could affect fraction absorption. Limitations of bioavailability due to these factors seem to be less frequent compared to the two other main factors. Regulatory guidelines for BCS-based biowaivers still ask for *in vitro* studies of luminal degradation in relevant test media whereas specific binding studies are not required [17].

The acidic environment in the stomach could degrade some substances. For example, the proton pump inhibitor omeprazol has a half-life of less than 5 min at pH 1, whereas it is practically stable in the intestinal pH range. Such limitations can be handled by the use of properly designed modified-release formulations with enteric coating, which protects the drug from the acid, as is the case for omeprazol [63]. Reverse forms of pH-dependent drug degradation could also occur, that is, the drug is stable at lower pH but has significant degradation at close to neutral pH.

Drugs may also undergo hydrolysis by intestinal esterases (hydrolases), more specifically carboxylesterases (EC 3.1.1.1) in the intestinal lumen and at the brush border membrane [64, 65]. It has been demonstrated that the intestinal hydrolase activity in humans was closer to that of the rat than the dog or Caco-2 cells [66]. They used six propranolol ester prodrugs and *p*-nitrophenylacetate as substrates and found that hydrolase activity was ranked in the order human > rat $\gg$ Caco-2 cells > dog for intestinal microsomes. The rank order in hydrolase activity for the intestinal cytosolic fraction was rat > Caco-2 cells = human > dog. The hydrolase activity toward *p*-nitrophenylacetate and tenofovir disoproxil has also been reported in various intestinal segments from rats, pigs, and humans. The enzyme activity in intestinal homogenates was found to be both site specific (duodenum $\geq$ jejunum > ileum > colon) and species dependent (rat > man > pig).

The bacteria in the intestinal tract exert is another well-known source for luminal drug degradation [67]. This is only important for the colon region since the luminal concentration of bacteria is 10^4–10^9 higher in the colon compared with that in the small intestine. Thus, this aspect is only relevant for drugs that reach this region as a result of, for example, poor permeability, slow dissolution, or delivery by modified-release formulations. It is predominantly hydrolytic and also includes other reductive

Table 19.4 Drug degradation reactions by intestinal bacteria.

Enzyme	Reaction	Representative substrate
Hydrolysis		
Amidase	Cleavage of amides of carboxylic acids	Methotrexate
Decarboxylase	Decarboxylation of amino acids and simple phenolic acids, primarily *p*-hydroxylated	L-Dopa, tyrosine
Dehydroxylase	Dehydroxylation of C- and N-hydroxy groups	Bile acids, *N*-hydroxyfluorenylacetamide
Esterase	Cleavage of esters of carboxylic acids	Acetyldigoxin
Glucuronidase	Cleavage of β-glucuronides of alcohols and phenols	Estradiol-3-glucuronides, morphine glucuronide
Glucosidase	Cleavage of β-glucosides of alcohols and phenols	Cycasin, rutin
Nitrase	Cleavage of nitrates	Pentaerythriol trinitrate
Sulfatase	Cleavage of *O*-sulfates and sulfamates	Cyclamate, amygdalin, estrone sulfate
Reduction		
Alcohol dehydrogenase	Reduction of aldehydes	Benzylaldehydes
Azoreductase	Reductive cleavage of azo compounds	Food dyes, sulfasalazine
Hydrogenase	Reduction of carbonyl groups, aliphatic double bonds	Unsaturated fatty acids, estrone
Nitroreductase	Reduction of aromatic and heterocyclic nitro compounds, nitrosamine formation	*p*-Nitrobenzoic acids, chloramphenic metronidazol, nitrazepam
N-oxide reductase	Removal of oxygen from N-oxides	4-Nitroquinolone-1-oxide, nicotine-*N*-oxide
Sulfoxide reductase	Removal of oxygen from sulfoxides	Sulfinpyrazone
Other reactions		
Aromatization	Quinic acid	
D-Demethylation	Biochanin A	
Dealkylation	3,4,5-Trimethoxycinnamic acid	
Deamination	Amino acids	
Dehalogenation	DDT	

reactions that are mediated by the bacterial enzymes. A list of the most prominent types of enzymes, reactions, and examples of substrates is given in Table 19.4 [61, 68]. The effectiveness of this process has been exemplified by the use of *in vitro* incubation studies showing rapid drug degradation [70].

Reduced absorption due to complex formation or other interactions between drugs and intestinal components leading to poor absorption has been described in a few cases. One example is the precipitation of cationic drugs as a result of very poorly soluble salts with bile acids, which has been reported for several compounds [31].

Another well-known example is the complex formation between tetracycline and calcium as a result of chelation after administration of the drug together with milk. It has also been shown that protease inhibitor drugs can bind very strongly to enzymes secreted by the pancreas [71].

Interactions between drugs in the lumen and intestinal components are generally a poorly studied area, and it is difficult to discriminate on the basis of *in vivo* data such effects from other factors affecting absorption. In addition, evidence for *in vivo* relevance of available *in vitro* methods is very sparse.

19.6
The Biopharmaceutics Classification System

19.6.1
Regulatory Aspects

19.6.1.1 Present Situation

BCS has been primarily developed for regulatory applications though its use has been extended beyond this area as discussed in more detail below. The aim of BCS in a regulatory context is to provide a basis for replacing certain bioequivalence studies by equally or more accurate *in vitro* dissolution tests. This could reduce costs and time in the development process as well as reduce unnecessary drug exposure in healthy volunteers, which is normally the study population in bioequivalence studies.

Numerous bioequivalence studies are presently being conducted for NDAs of new compounds, in supplementary NDAs for new indications and line extensions, in ANDAs of generic products, and in applications for scale-up and postapproval changes. For example, NDA bioequivalence studies may be required for comparing different clinical formulations in pivotal clinical trials and products aimed for market. The complexity and number of studies required are often boosted by the fact that several dose strengths might be included in the development process. In addition, bioequivalence documentation may also be needed for comparing blinded and original comparator products in clinical trials. Thus, an NDA typically contains a multitude of bioequivalence studies.

The BCS was first applied in a regulatory context in the US FDA guidelines for SUPAC's of oral immediate-release formulations [51]. More recently, guidelines for applying BCS in NDAs and ANDAs have been finalized by both FDA and the European agency, EMEA [17, 19]. In addition, the BCS principles are also included in ICH guidelines for requirements of *in vitro* dissolution testing as a quality control in manufacturing [73] and the recent WHO guidance on waiving *in vivo* BE studies for oral immediate-release formulations of essential medicines [74].

The BCS classes are defined as follows: Class I. High Solubility (S) – High P_{eff}; Class II. Low S – High P_{eff}; Class III. High S – Low P_{eff}; Class IV. Low S – Low P_{eff}. A drug is considered as highly permeable when the extent of absorption is complete in humans, defined by the US FDA as being more than 90%, whereas EMEA requires

"complete" absorption [17, 19]. This could be determined by any of these study methods:

- absolute bioavailability in humans (in case of no first-pass metabolism);
- mass balance studies in humans with the help of radiolabeled drug;
- determination of P_{eff} in humans by the "Loc-I-Gut method" and applying the correlation between P_{eff} and fraction absorbed presented in Figure 19.10;
- determination of P_{eff} in any animal *in vivo* perfusion or *in vitro* permeation method that provides a solid correlation to the fraction dose absorbed in humans for a predefined set of drug substances. Special consideration has to be given to indications of carrier-mediated transport across the intestinal membrane, in both the secretory and absorptive directions.

A compound can be classified as a high-solubility drug if the highest strength can be dissolved in 250 ml buffer at all pH values within range of pH 1–8. This criterion is applied by both the European and US guidelines [17, 19].

BCS is primarily used in this context to identify the substances that are suitable for *in vitro* bioequivalence testing, which in the United States is preceded by a request to the authority to gain a biowaiver, that is, an acceptance for replacing an *in vivo* study with *in vitro* dissolution testing. It is presently only oral IR formulations of class I compounds, that is, highly soluble/highly permeable drugs, for which such an option is available. Additional criteria for allowance of *in vitro* bioequivalence testing are that the drug stability in the GI fluids must be verified and it should also be a non-narrow therapeutic index drug. If these criteria are fulfilled, test and reference products can be compared by *in vitro* dissolution testing and deemed bioequivalent but achieved only when sufficiently similar results are obtained. The *in vitro* dissolution testing should be done at three different pH values within the physiological range, typically pH 1, 4, and 6.8. The product dissolution must be complete (>85%) within 30 min in order to utilize the *in vitro* bioequivalence route. The underlying rationale for this demand on product performance is to ascertain that drug dissolution is fast enough as not to become the rate-limiting step. It is assumed that gastric emptying will control the absorption rate for class I substances in products with such a fast dissolution and no effect on bioavailability will be obtained for different dissolution profile within acceptance limits. This has also been verified *in vivo* by studying metoprolol tablets with different *in vitro* release profiles [75].

The difference between a test (T) and a reference (R) product should be evaluated by use of the f_2-test (see Equation 19.6), where $f_2 > 50$ is the required limit for equivalence. This limit corresponds to an average difference in the amount dissolved at different times (t) of less than 10%. If the dissolution is very rapid, that is, complete dissolution within 15 min, the f_2-testing is not necessary.

$$f_2 = 50 \log \left[\left(1 + \frac{1}{n} \sum_{t=1}^{n} (R_t - T_t)^2 \right)^{-0.5} \times 100 \right]. \tag{19.6}$$

In addition to the *in vitro* testing, the test and reference products must not contain excipients that could modify drug absorption in any way except for dissolution effects. For example, the potential for permeability-enhancing effects by surface-active agents, sometimes included in solid formulations, has been identified as one potential concern. Furthermore, the effect on gastrointestinal transit by large amounts of sugars has been highlighted as another issue [18, 76].

19.6.1.2 Potential Future Extensions

The application of BCS in a regulatory context has gained acceptance and is now used in both NDAs and ANDAs [81]. However, one important limitation of the present application of BCS is that class I substances are quite rare in pharmaceutical development. It has also been recognized that the present application represents a deliberately conservative approach, and proposals for extensions have been discussed since the original publication of BCS. For example, it was suggested that the requirement of the highest pH for the solubility measurements could be changed from 7.5 to 6.8 since the latter one is more relevant for the pH in the stomach and upper small intestine [18]. This revision would thus somewhat relax the requirements for basic drugs. Another proposal in the paper by Yu to reduce the high-permeability definition from 90 to 85% fraction absorption-based observations that many drugs are considered completely absorbed provides experimental values below 90%, that is, 90% seems to be a too rigid a criterion considering the precision of the experimental methods. More radical developments are also fairly well supported like allowing biowaivers for very rapidly dissolving class III drugs, at least for those with intermediate permeability [81]. Since the majority of drugs in drug development today most probably are class II drugs, the greatest benefits to be gained should be sought in this area. Support has been expressed for allowing biowaivers especially for acidic class II drugs that have a high solubility at intestinal pH, thereby assuring a rapid and complete dissolution in the upper part of the small intestine [81]. An additional prerequisite for biowaivers of class II drugs would be to provide assurance of *in vivo* predictability of *in vitro* dissolution methods to be used as a surrogate for *in vivo* bioequivalence studies.

19.6.2 Drug Development Aspects

BCS has primarily been developed for regulatory applications. However, it has also several other implications in the drug development process and has gained a wide recognition within the research-based industry. The importance of drug dissolution in the GI tract and permeability over the gut wall in the oral absorption process has been well known since the 1960s, but the research carried out to constitute the BCS has provided new quantitative data of importance for drug development, so far especially within the area of drug permeability. Another merit of the BCS in a development context is that it provides very clear and easily applied rules to determine the rate-limiting factor in the drug

absorption process. Thereby, BCS has implications in the selection of candidate drugs for full development, predictions, and elucidations of food interactions, choice of formulation principle including suitability for oral ER administration, and the possibility for *in vitro*/*in vivo* correlations in dissolution testing of solid formulations. Most of these aspects will be discussed and exemplified in further detail below.

19.6.2.1 **Selection of Candidate Drugs**

Permeability and solubility are of key importance in the selection of candidate drugs for development [2]. Molecules with too low permeability and/or solubility will provide low and variable bioavailability, which increases the risk that a clinically useful product cannot be developed. Experimental methods and relevant acceptance criteria regarding permeability and solubility are needed in the early drug discovery process. Such procedures have also been introduced in the industry, including solubility screens using turbidimetric measurements and automatic permeability screens based on the Caco-2 cell model. Computational approaches have also been developed for permeability and solubility determinations [72, 77, 78]. If further refinement can be achieved for such methods leading to improved predictions, it may be possible in the future to displace cell-based permeability screens and early solubility estimates. It has even been suggested that BCS can be further developed toward consideration of true fundamental molecular properties for membrane permeability, as well as for drug solubility [91].

Selection of candidates that fulfill the BCS requirement of high permeability/high solubility (class I) almost guarantees the absence of failures due to poor absorption by the oral route. However, these limits are generally too conservative to use as an acceptance criterion since many useful drugs can be found in class II–III and even class IV. First, a class I drug is expected to provide complete absorption, whereas a certain reduction in bioavailability due to permeability or solubility, as well as due to other reasons (e.g., first-pass metabolism), is generally acceptable. A summary of the different factors that have to be taken into account when defining more relevant acceptance criteria is as follows:

- acceptability of a low and highly variable bioavailability depending on
  –medical need
  –width of therapeutic window
  –potency
  –substance manufacturing costs
- potential for poor *in vivo* predictability of early permeability and solubility characterizations as a result of, for example,
  –active transport across the gut wall
  –high paracellular transport through gut wall
  –*in vivo* solubilization by bile salt micelles
- possibilities to use formulation approaches that improve bioavailability, for example,

–dissolution and solubility enhancement
–permeation enhancers.

Thus, BCS points out some important variables in the screening of drug candidates though the proposed limits are less useful as acceptance criteria in a drug discovery context.

19.6.2.2 **Choice of Formulation Principle**

Oral dosage forms are often developed under time constraints and preferably by an efficient use of available resources. One way to reduce time and increase efficiency could be to minimize the number of different formulations included in different stages of clinical development. The BCS could be used as a framework to decide which types of formulation should be suitable for a certain compound.

If a drug is classified as having low solubility, it is obvious that bioavailability properties could be improved by the use of formulation principles that increase the dissolution rate and/or drug solubility. There are a number of different principles of varying complexity to achieve such improvements, ranging from selecting a suitable solid-state form or salt to the use of technologically more advanced formulation principles. Although their application could be limited by several practical factors such as poor drug stability, excessive size because of the need for large amounts of excipients in relation to the dose, technical manufacturing problems, and the high cost of goods, it is believed that many poorly soluble compounds with good pharmacological properties could be "saved" by such approaches. A list of different formulation principles for oral solid formulations including modifications of the drug substance form is given below.

Substance form:

- salt – choose most water soluble;
- crystal form – select the most soluble polymorph/anhydrate, if possible, from stability and technical points of view;
- amorphous form – provide the most rapid dissolution and the most often increased solubility by supersaturation, but practical usefulness is limited by stability issues including transformation of solid-state form;
- size reduction by milling/micronization – increase surface area in contact with dissolution medium.

Formulation approaches for solids:

- addition of wetting agents;
- solid solutions/eutectic mixtures;
- cyclodextrin complexes;
- lipid systems such as oils/emulsions/microemulsions/self-emulsifying systems in capsules;
- nanoparticles.

This list illustrates the numerous pharmaceutical possibilities to handle bioavailability problems due to low solubility. This is a continuously developing area

exemplified by more recent developments, such as self-emulsifying lipid systems and nanoparticles.

The optimal formulation should provide such a good dissolution and/or solubility that this step is no longer the rate-limiting step in the absorption process, that is, a situation comparable with the one for class I drugs. The obvious approach for reaching this goal is to formulate the drug as a solution that maintains the drug in solution even after mixing and dilution with the gastric fluids. However, such formulations are generally not feasible to use as drug products, where solid formulations such as tablets and capsules are strongly preferred. Absorption properties similar to a solution may, however, be obtained for a solid formulation of poorly soluble drugs in case of successful application of dissolution-enhancing principles.

Another important decision in oral formulation development where BCS could provide guidance is the start of an oral extended-release development. ER formulations could significantly improve the clinical usefulness of a drug substance by reducing the peak-to-trough ratio of drug levels in the body and the need for less frequent dosing. However, not all drugs that would benefit from ER delivery are suitable candidates because of unfavorable absorption properties. Solubility and permeability are crucial factors to consider before making a decision to embark on an ER development program.

The realization of the desirable clinical advantages most often requires a duration of drug release of 12–24 h. Thus, since the transit of formulations through the small intestine is 3–4 h, a significant part of the dose will be delivered to the colon, and the absorption of the drug over almost the entire GI tract is a prerequisite. Class I drugs, having both good solubility and good permeability, should therefore be the best candidates for ER development. Several well-documented ER formulations are also based on class I compounds such as metoprol but class II drugs are also frequently used. For example, felodipine ER tablets provide an example where a low-solubility compound is included in a useful ER product. Felodipine, which has water solubility in the physiological pH range of about 1 μg/ml, is possible to administer as a once-daily product in doses up to at least 10 mg without any reduced bioavailability compared to an oral solution [40]. Such a successful performance is indeed dependent on the use of a dissolution-enhancing formulation principle where the drug is given in a solubilized form.

A special consideration can be made regarding classification of low-solubility compounds in ER forms. The standard classification is based on the idea that the drug should be completely dissolved in the gastric fluids, which has been estimated to be 250 ml. However, this way of classifying drugs may be less relevant for ER formulations since only a very small part of the dose is made available for dissolution in the stomach. The dose is generally spread over the entire GI tract making the effective water volume available as a dissolution medium for the drug probably larger than the 250 ml used in the original BCS. Furthermore, the drug permeability of these compounds is often much faster than the drug release, further preventing solubility limitations for class II drugs in ER formulations. Thus, this gives a further explanation of the relative frequent abundance of class II drugs developed as ER

products, and if BCS is to be applied to ER formulations in the future, a different classification criterion regarding solubility may be needed.

The permeability classification of a drug according to BCS, based on theoretical considerations, should be very useful as a criterion for selecting a drug as an ER formulation. A classification of a drug as a low-permeability compound means that the drug is not completely absorbed after oral administration of a solution or an IR tablet. A certain amount of drug for such compounds is clearly delivered to the colon, and the permeability in the colon is so poor that a significant part of the dose passes through the entire colon without being absorbed. This implies that the permeability in the colon is very slow, preventing any significant drug absorption. Using rat intestinal and colonic tissues in an Ussing chamber, it has also been shown *in vitro* that the permeability of class III–IV drugs is even slower in the colon than in the small intestine, whereas class I–II drugs show a slightly higher permeability in the colon when passive diffusion is the dominating mechanism [52]. This permeability pattern has also been shown to be relevant for small and large intestinal specimens from humans when the Ussing chamber model [79] is applied. Consequently, it will not be possible to control the rate of absorption by an ER formulation for low-permeability drugs. In addition, a large part of the dose will not be absorbed, leading to a low and uneven variability. This is exemplified in ER tablets of amoxicillin. This high-solubility drug is classified as a low P_{eff}, even if it is transported across the intestinal barrier via the oligopeptide carrier (PepT1) [62]. Essentially no absorption occurred for an ER tablet when it entered the colon as determined by gamma scintigraphy [80].

19.6.2.3 *In Vitro/In Vivo* Correlation

In vitro dissolution testing is an important tool in the development of solid drug products as well as in batch quality controls. The aim of the test is to see that the drug is appropriately dissolved in the GI tract and made available for absorption. It is therefore highly desirable that the *in vitro* tests provide data that correlate to the *in vivo* situation. However, attainment of IVIVC has often failed, and the concept of IVIVC has been challenged.

The BCS could be used as a framework for predictions when IVIVC could be expected for solid immediate-release products as summarized in Table 19.5. It is

Table 19.5 Expectations for *in vitro/in vivo* correlations for IR products based on BCS.

Class	IVIVC expectations
I. High *S*/High P_{eff}	No IVIVC until product dissolution becomes slower than gastric emptying
II. Low *S*/High P_{eff}	IVIVC should be possible to establish provided that *in vitro* relevant dissolution test method is used and drug absorption is limited by dissolution rate rather than saturation solubility
III. High *S*/Low P_{eff}	No IVIVC until product dissolution becomes slower than intestinal permeability
IV. Low *S*/Low P_{eff}	Low chance for IVIVC

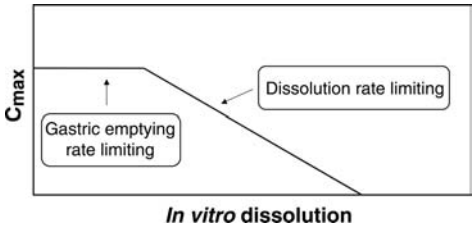

Figure 19.12 Principal level *C in vitro/in vivo* correlation for IR formulation of class I substance.

important to realize that the *in vitro* dissolution test only models the release and dissolution of the active drug substance from the formulation and it is only when these processes are rate limiting in the absorption process that IVIVC can be expected. In the case of class I drugs, the complete dose will be dissolved already in the stomach and, provided that the absorption over the gut wall is negligible, the gastric emptying of the dissolved drug will be the rate-limiting step. This is clearly not a factor that is included in the *in vitro* dissolution test. Thus, no IVIVC should be expected for class I drugs as long as the release of drug is faster than the gastric emptying. The half-life of gastric emptying of fluids in the fasting state is normally about 10 min though this could vary because of several factors such as the timing of drug administration in relation to gastric motility phase and fluid volume [84]. The relationship between *in vitro* dissolution, described as the time to dissolve half of the dose (t50%), and the peak plasma concentration (C_{max}) for a fictive class I drug is exemplified in Figure 19.12. This type of *in vitro/in vivo* relationship should only be expected for variables that are influenced by the absorption rate, whereas variables reflecting the extent of bioavailability, for example, AUC, should be independent of dissolution rate.

Class II drugs, that is, low-solubility/high-permeability compounds, are expected to have a dissolution-limited absorption. Thus, for these kinds of drugs, an IVIVC should be possible to establish by use of a well-designed *in vitro* dissolution test. One way to investigate and establish such a correlation is to study formulations containing drug particles with different surface areas. An example of such a study is given in Figure 19.13a and b, where *in vitro* dissolution and plasma concentration–time profiles are given for administration of tablets containing drug substance with two different mean particle sizes. The mean reduction of about 30% in C_{max} for the larger particles was predicted in this case by a somewhat slower dissolution *in vitro*.

Two cases could be identified for class II drugs when the establishment of simple IVIVCs is not feasible. First, there are a number of formulation principles that could enhance the dissolution rate and solubility of low-solubility compounds as discussed above. It may be possible to achieve such a rapid and complete dissolution of a class II drug that the gastric emptying becomes the rate-limiting step, that is, the bioavailability of the solid dosage forms equals that of an oral solution. Thus, in such a case, the prerequisites for IVIVC will be identical to the situation for class I drugs; that is, no correlation will be obtained as long as the dissolution rate is significantly faster than the gastric emptying.

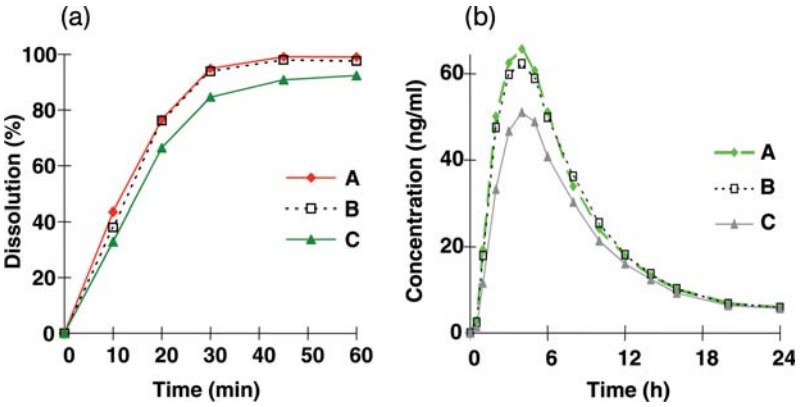

Figure 19.13 Mean (a) *in vitro* dissolution and (b) human plasma concentrations for candersartan cilexitil tablets containing drug particles with three different mean particle diameters (A, 3.9 μm; B, 5.7 μm; C, 9.1 μm).

The second case when IVIVC is not likely for class II drugs is the situation where the absorption is limited by the saturation solubility in the GI tract rather than the dissolution rate, as discussed in more detail above. In this situation, the drug concentration in the GI tract will be close to the saturation solubility and changes of the dissolution rate will not affect the plasma concentration profile and the *in vivo* bioavailability. Standard *in vitro* dissolution tests are carried out under "sink conditions," that is, at concentrations well below the saturation solubility. Thus, only effects related to dissolution rate can be predicted *in vitro*. If more physiologically relevant dissolution media are used, which not necessarily provides "sink conditions," the possibility for IVIVC could be improved as indicated by recent work using simulated intestinal medium [85].

The absorption of class III drugs is limited by their permeability over the intestinal wall. Thus, since this process is not at all modeled by the classical *in vitro* dissolution test, no IVIVC should be expected. When the drug dissolution becomes slower than the gastric emptying, a reduction of the extent of bioavailability will be found in slower dissolution rates because the time when the drug is available for permeation over the gut wall in the small intestine will then be reduced. Thus, the same type of relationship can be expected between bioavailability and *in vitro* dissolution as shown in Figure 19.12 for a class I drug.

19.6.2.4 **Food–Drug Interactions**

Alterations of bioavailability due to a concomitant food intake can have serious implications for the clinical usefulness of a drug, and it is therefore beneficial to predict such effects at an early stage. However, this is not easily done because of the multitude of factors involved in food–drug interactions including physicochemical effects such as increased solubility and binding to secretory or food components; physiological effects in the GI tract such as altered flow rates and gastric emptying;

Table 19.6 Most likely food effects on bioavailability for BCS class I–IV drugs.

BCS class	Absorption effect by food	Possible mechanism
I	Reduced rate but same extent	Slower gastric emptying
II	Increased extent	Increased solubility and first-pass metabolism
III	Reduced extent	Reduced intestinal drug concentrations
IV	Increased extent	See class II

mechanical effects on formulations due to different motility patterns; permeability effects due to interactions with active transporters; or effects on the membrane and altered first-pass metabolism. A more extensive review of different mechanisms for food–drug interactions in the absorption step including formulation factors can be found elsewhere [86].

The BCS can be used as a framework for predictions and to set up hypotheses for mechanisms of food effects related to permeability, solubility, and gastric emptying as outlined in Table 19.6. This was supported by a review of food interactions including more than 90 drugs, which showed a clear relationship between BCS class and direction of food interactions [82]. The prediction of food effects was possible to further improve by grouping drugs regarding maximal absorbable dose in relation to clinical dose, dose in relation to solubility (dose number), and lipophilicity (log *D*) [82]. The most severe cases of food interactions due to factors considered in BCS are generally found in the group of poorly soluble compounds given in high doses, that is, those that approach the saturation solubility in the GI tract. For such compounds, such as griseofulvin, the extent of bioavailability has been reported to increase up to five times by food and dosing recommendations requiring concomitant intake of the drug with a meal [31]. The saturation solubility will be significantly improved by food as a result of solubilization in mixed micelles, including bile acids, lecithin, and monoglycerides obtained from the dietary fat intake, and dissolution into emulsified nutritional lipids. Thus, the amount of drug available for absorption will significantly increase. A further contributing effect to an increased bioavailability could be the increased fluid volume in the stomach after a meal, that is, allowing an increased amount of drug that could be dissolved in comparison with the fasting situation. The increase in bioavailability for class II drugs after intake together with food that should be attributed not only to dissolution effects but also to reduction in first-pass metabolism, for example, because of the increased blood flow.

For highly permeable, poorly soluble drugs given in lower doses, the dissolution rate rather than the saturation solubility is the limiting factor. An increase in dissolution rate as a result of *in vivo* solubilization mediated by food intake could theoretically be obtained, but this is not always found *in vivo*. For example, food does not affect the rate and extent of bioavailability for candersartan cilexitil, a very poorly soluble compound [87]. An *in vitro* dissolution and solubility study of this compound

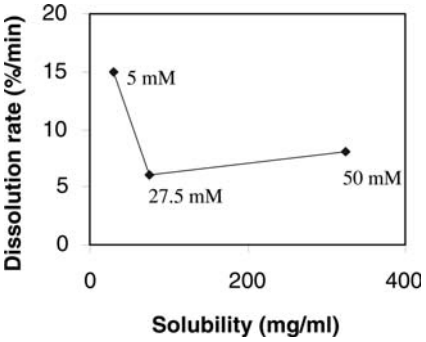

Figure 19.14 *In vitro* dissolution rate versus saturation solubility for candersartan cilexitil in different concentrations of sodium taurocholate:lecithin ratio (2.5 : 1).

in simulated intestinal media provided a potential explanation. It was revealed that the solubility was increased as a function of bile concentration as expected whereas the dissolution rate was not increased by the higher bile concentrations being representative for the fed state (see Figure 19.14). Thus, although intestinal solubility most often will be increased in the fed state for class II drugs, this will not always lead to a more rapid dissolution.

For class I drugs, a slower rate of absorption could be expected after concomitant intake with food as a result of the decreased gastric emptying rate induced by a meal. The gastric emptying in the fed state varies significantly depending on the meal composition, including factors such as energy content, osmolality, and pH. A gastric emptying half-life of about 45 min has been reported for fluids when measured under nonfasting conditions [88]. In addition to the meal composition, the extent of the reduction and delay in peak plasma concentration induced by food for a class I drug will also be influenced by the plasma concentration half-life; that is, food effects will be more pronounced for drugs with a shorter half-life.

Class III drugs will generally be less susceptible to both gastric emptying effects caused by slow permeability as well as solubility effects caused by the high solubility already under fasting conditions. However, the extent of bioavailability is often reduced for class III drug. Mechanisms behind this effect have not yet been clearly verified. One explanation could be the dilution of dissolved drug due to fluid intake and secretion decreasing the driving force for passive intestinal permeability. Another potential source for interactions between food components and low-permeability drugs could occur for drugs that are actively transported in the intestine, especially if nutritional carriers are involved. The two most important nutrient absorption carriers for drugs are the oligopeptide carrier (hPepT1) and the amino acid transport family. These carrier proteins have a high transport capacity in the human small intestine, and they seem less likely to be involved in direct food–drug interactions, unless high doses are given together with a protein rich meal. The nutritional status could also cause transcriptional activation of the PepT1 gene by selective amino acids and dipeptides in the diet [90]. It has also been reported that the

Table 19.7 Proposed role of BCS in assuring clinical performance by dissolution testing within QbD.

BCS class	Dissolution testing requirements
I	Dissolution within 30 min at most discriminating conditions
II	Dissolution acceptance limits validated by bioavailability data of formulation variants
III	Dissolution within 15 min at most discriminating conditions
IV	As II or III if shown to behave *in vivo* as class II or III drug, respectively, otherwise *in vivo* BE

integrated response to a certain stimuli may increase PepT1 activity by translocation from a preformed cytoplasm pool [58].

19.6.2.5 Quality by Design

Quality by design (QbD) has recently been introduced in pharmaceutical product development in a regulatory context [83], and the process for implementing such concepts in the drug development and approval process is presently ongoing. This has the potential to allow for a more flexible regulatory approach where, for example, postapproval changes can be introduced without prior approval and end product batch testing can be replaced by in-process monitoring. This is based on understanding and optimization of how design of a product and its manufacturing process are affecting product quality. Good pharmaceutical quality represents an acceptable low risk of failing to achieve the desired clinical attributes. Thus, adding restrictions to manufacturing beyond what can be motivated by clinical quality brings no benefits but only additional costs.

QbD therefore brings the need to link clinical product performance to critical manufacturing attributes. It is not desirable to do *in vivo* bioavailability studies to evaluate all pharmaceutical factors potentially influencing drug absorption, but *in vitro* dissolution must be used as a surrogate. BCS could provide a platform for establishing clinical relevance by *in vitro* dissolution. However, the application of BCS might need to be further developed in context of QbD compared to the bioequivalence area to take benefit of the higher level of understanding that is implied by utilizing QbD concepts. A proposal for using BCS in context of QbD is outlined in Table 19.7 [89].

19.7 Conclusions

In this chapter, we have discussed and emphasized the importance of the fundamental factors in BCS, solubility, and intestinal permeability for oral drug absorption. The main regulatory impact today is the use of BCS as a framework for identifying drugs for which *in vitro* dissolution testing could replace *in vivo* studies to determine bioequivalence. Extensions of this approach to cases other than IR formulations of

the rather rare class I drugs would significantly enhance the impact of BCS [18]. However, product quality assurance must not be jeopardized, and a brief discussion illustrated the possible difficulties involved if BCS were extended, for example, to oral ER products. Finally, we emphasize the great use of BCS as a simple tool in early drug development to determine the rate-limiting step in the oral absorption process.

References

1 Venkatesh, S. and Lipper, R.A. (2000) Role of the development scientist in compound lead selection and optimization. *Journal of Pharmaceutical Sciences*, **89**, 145–154.

2 van de Waterbeemd, H., Smith, D.A., Beaumont, K. and Walker, D.K. (2001) Property-based design: optimization of drug absorption and pharmacokinetics. *Journal of Medicinal Chemistry*, **44**, 1313–1333.

3 Prentis, R.A., Lis, Y. and Walker, S.R. (1988) Pharmaceutical innovation by the seven UK-owned pharmaceutical companies (1964–1985). *British Journal of Clinical Pharmacology*, **25**, 387–396.

4 Amidon, G.L., Lennernäs, H., Shah, V.P. and Crison, J.R. (1995) A theoretical basis for a biopharmaceutic drug classification: the correlation of *in vitro* drug product dissolution and *in vivo* bioavailability. *Pharmaceutical Research*, **12**, 413–420.

5 Lennernäs, H. (1998) Human intestinal permeability. *Journal of Pharmaceutical Sciences*, **87**, 403–410.

6 Benet, L.Z., Wu, C.Y., Hebert, M.F. and Wacher, V.J. (1996) Intestinal drug metabolism and antitransport processes: potential paradigm shift in oral drug delivery. *Journal of Controlled Release*, **39**, 139–143.

7 Chu, X.Y., Sanchez-Castano, G.P., Higaki, K., Oh, D.M., Hsu, C.P. *et al.* (2001) Correlation between epithelial cell permeability of cephalexin and expression of intestinal oligopeptide transporter. *The Journal of Pharmacology and Experimental Therapeutics*, **299**, 575–582.

8 Jonker, J.W., Smit, J.W., Brinkhuis, R.F., Maliepaard, M., Beijnen, J.H. *et al.* (2000) Role of breast cancer resistance protein in the bioavailability and fetal penetration of topotecan. *Journal of the National Cancer Institute*, **92**, 1651–1656.

9 Greiner, B., Eichelbaum, M., Fritz, P., Kreichgauer, H.P., von Richter, O. *et al.* (1999) The role of intestinal P-glycoprotein in the interaction of digoxin and rifampin. *The Journal of Clinical Investigation*, **104**, 147–153.

10 Fricker, G. and Miller, D.S. (2002) Relevance of multidrug resistance proteins for intestinal drug absorption *in vitro* and *in vivo*. *Pharmacology & Toxicology*, **90**, 5–13.

11 Sandstrom, R., Karlsson, A., Knutson, L. and Lennernäs, H. (1998) Jejunal absorption and metabolism of *R*/*S*-verapamil in humans. *Pharmaceutical Research*, **15**, 856–862.

12 Lindahl, A., Sandstrom, R., Ungell, A.L., Abrahamsson, B., Knutson, T.W. *et al.* (1996) Jejunal permeability and hepatic extraction of fluvastatin in humans. *Clinical Pharmacology and Therapeutics*, **60**, 493–503.

13 Chiou, W.L., Chung, S.M., Wu, T.C. and Ma, C. (2001) A comprehensive account on the role of efflux transporters in the gastrointestinal absorption of 13 commonly used substrate drugs in humans. *International Journal of Clinical Pharmacology and Therapeutics*, **39**, 93–101.

14 Lipinski, C.A., Lombardo, F., Dominy, B.W. and Feeney, P.J. (2001) Experimental and computational approaches to estimate solubility and permeability in drug discovery and

development settings. *Advanced Drug Delivery Reviews*, **46**, 3–26.

15 Mandagere, A.K., Thompson, T.N. and Hwang, K.K. (2002) Graphical model for estimating oral bioavailability of drugs in humans and other species from their Caco-2 permeability and *in vitro* liver enzyme metabolic stability rates. *Journal of Medicinal Chemistry*, **45**, 304–311.

16 Winiwarter, S., Bonham, N.M., Ax, F., Hallberg, A., Lennernäs, H. *et al.* (1998) Correlation of human jejunal permeability (*in vivo*) of drugs with experimentally and theoretically derived parameters. A multivariate data analysis approach. *Journal of Medicinal Chemistry*, **41**, 4939–4949.

17 CDER (2000) Waiver of *in vivo* bioavailability and bioequivalence studies for immediate-release solid oral dosage forms based on a biopharmaceutics classification system. Food and Drug Administration.

18 Yu, L.X., Amidon, G.L., Polli, J.E., Zhao, H., Mehta, M.U. *et al.* (2002) Biopharmaceutics classification system: the scientific basis for biowaiver extensions. *Pharmaceutical Research*, **19**, 921–925.

19 CPMP (2001) Note for guidance on the investigation of bioavailability and bioequivalence (CPMP/EWP/QWP/1401/98). The European Agency for the Evaluation of Medicinal Products.

20 Lennernäs, H. (1997) Human jejunal effective permeability and its correlation with preclinical drug absorption models. *The Journal of Pharmacy and Pharmacology*, **49**, 627–638.

21 Nernst, W. and Brunner, E. (1904) Theorie der Reaktionsgeschwindigkeit in heterogenen Systemen. *Zeitschrift für Physikalische Chemie*, **47**, 52–110.

22 Dressman, J.B., Amidon, G.L., Reppas, C. and Shah, V.P. (1998) Dissolution testing as a prognostic tool for oral drug absorption: immediate release dosage forms. *Pharmaceutical Research*, **15**, 11–22.

23 Nicklasson, M., Brodin, A. and Sundelof, L.-O. (1985) Studies of some characteristics of molecular dissolution kinetics from rotating discs. *International Journal of Pharmaceutics*, **23**, 97–108.

24 Hernell, O., Staggers, J.E. and Carey, M.C. (1990) Physical–chemical behavior of dietary and biliary lipids during intestinal digestion and absorption. 2. Phase analysis and aggregation states of luminal lipids during duodenal fat digestion in healthy adult human beings. *Biochemistry*, **29**, 2041–2056.

25 Lindahl, A., Ungell, A.L., Knutson, L. and Lennernäs, H. (1997) Characterization of fluids from the stomach and proximal jejunum in men and women. *Pharmaceutical Research*, **14**, 497–502.

26 Persson, E., Nilsson, R., Hansson, G., Löfgren, L., Abrahamsson, B., Knutsson, L. and Lennernäs, H. (2006) Investigation of the dynamic secretory *in vivo* response of a dietary meal in human proximal small intestine. *Pharmaceutical Research*, **23**, 742–751.

27 Kalantzi, L., Goumas, K., Kalioras, V., Abrahamsson, B., Dressman, J.B. and Reppas, C. (2006) Characterization of the human upper gastrointestinal contents under conditions simulating bioavailability/bioequivalence studies. *Pharmaceutical Research*, **23**, 165–176.

28 Scholz, A., Abrahamsson, B., Diebold, S.M., Kostewicz, E., Polentarutti, B.I. *et al.* (2002) Influence of hydrodynamics and particle size on the absorption of felodipine in labradors. *Pharmaceutical Research*, **19**, 42–46.

29 Nielsen, A. (1961) Diffusional controlled growth of a moving sphere. The kinetics of crystal growth in potassium perchlorate precipitation. *The Journal of Physical Chemistry*, **65**, 46–49.

30 Sheng, J.J., Sirois, P.J., Dressman, J.B. and Amidon, G.L. (2008) Particle diffusional layer thickness in a USP dissolution apparatus. II: a combined function of particle size and paddle speed. *Journal of Pharmaceutical Sciences*, in press.

31 Charman, W.N., Porter, C.J., Mithani, S. and Dressman, J.B. (1997) Physiochemical and physiological mechanisms for the effects of food on drug absorption: the role of lipids and pH. *Journal of Pharmaceutical Sciences*, **86**, 269–282.

32 Mithani, S.D., Bakatselou, V., TenHoor, C.N. and Dressman, J.B. (1996) Estimation of the increase in solubility of drugs as a function of bile salt concentration. *Pharmaceutical Research*, **13**, 163–167.

33 Jack, D.B. (1992) *Handbook of Clinical Pharmacokinetic Data*, Macmillan Publishers Ltd, Basingtoke.

34 Persson, E., Gustafsson, A.S., Carlsson, A., Knutsson, L., Hanisch, G., Lennernäs, H. and Abrahamsson, B. (2005) The effects of food on the dissolution of poorly soluble drugs in human and in model small intestinal fluids. *Pharmaceutical Research*, **22**, 2141–2151.

35 Schiller, C., Frohlich, C.-P., Giessmann, T., Siegmund, W., Monnikes, H., Hosten, N. and Weitschies, W. (2005) Intestinal fluid volumes and transit of dosage forms as assessed by magnetic resonance imaging. *Alimentary Pharmacology & Therapeutics*, **22**, 971–979.

36 Bonlokke, L., Christensen, F.N., Knutson, L., Kristensen, H.G. and Lennernäs, H. (1997) A new approach for direct *in vivo* dissolution studies of poorly soluble drugs. *Pharmaceutical Research*, **14**, 1490–1492.

37 Bonlokke, L., Hovgaard, L., Kristensen, H.G., Knutson, L. and Lennernäs, H. (2001) Direct estimation of the *in vivo* dissolution of spironolactone, in two particle size ranges, using the single-pass perfusion technique (Loc-I-Gut) in humans. *European Journal of Pharmaceutical Sciences*, **12**, 239–250.

38 Horter, D. and Dressman, J.B. (1997) Influence of physicochemical properties on dissolution of drugs in the gastrointestinal tract. *Advanced Drug Delivery Reviews*, **25**, 3–14.

39 Kaplan, S.A. (1972) Biopharmaceutical considerations in drug formulation and design and evaluation. *Drug Metabolism Reviews*, **1**, 15–34.

40 Wingstrand, K., Abrahamsson, B. and Edgar, B. (1990) Bioavailability from felodipine extended-release tablets with different dissolution properties. *International Journal of Pharmaceutics*, **60**, 151–156.

41 Agoram, B., Woltosz, W.S. and Bolger, M.B. (2001) Predicting the impact of physiological and biochemical processes on oral drug bioavailability. *Advanced Drug Delivery Reviews*, **50 (**Suppl. 1), S41–S67.

42 Csáky, T.Z. (1984) Methods for investigation of intestinal permeability, in *Pharmacology of Intestinal Permeability I*, Springer, Berlin, pp. 91–112.

43 Engman, H.A., Lennernäs, H., Taipalensuu, J., Otter, C., Leidvik, B. *et al.* (2001) CYP3A4, CYP3A5, and MDR1 in human small and large intestinal cell lines suitable for drug transport studies. *Journal of Pharmaceutical Sciences*, **90**, 1736–1751.

44 Lande, M.B., Priver, N.A. and Zeidel, M.L. (1994) Determinants of apical membrane permeabilities of barrier epithelia. *The American Journal of Physiology*, **267**, C367–C374.

45 Lande, M.B., Donovan, J.M. and Zeidel, M.L. (1995) The relationship between membrane fluidity and permeabilities to water, solutes, ammonia, and protons. *The Journal of General Physiology*, **106**, 67–84.

46 Fagerholm, U., Johansson, M. and Lennernäs, H. (1996) Comparison between permeability coefficients in rat and human jejunum. *Pharmaceutical Research*, **13**, 1336–1342.

47 Lennernäs, H., Ahrenstedt, O., Hallgren, R., Knutson, L., Ryde, M. *et al.* (1992) Regional jejunal perfusion, a new *in vivo* approach to study oral drug absorption in man. *Pharmaceutical Research*, **9**, 1243–1251.

48 Lennernäs, H., Palm, K., Fagerholm, U. and Artursson, P. (1996) Comparison between active and passive drug transport in human intestinal epithelial (Caco-2)

cells *in vitro* and human jejunum *in vivo*. *International Journal of Pharmaceutics*, **127**, 103–107.

49 Lennernäs, H., Nylander, S. and Ungell, A.L. (1997) Jejunal permeability: a comparison between the Ussing chamber technique and the single-pass perfusion in humans. *Pharmaceutical Research*, **14**, 667–671.

50 Palm, K., Stenberg, P., Luthman, K. and Artursson, P. (1997) Polar molecular surface properties predict the intestinal absorption of drugs in humans. *Pharmaceutical Research*, **14**, 568–571.

51 CDER Guidance for Industry (1995) SUPAC-IR: immediate-release solid oral dosage forms: scale-up and post-approval changes: chemistry, manufacturing and controls, *in vitro* dissolution testing, and *in vivo* bioequivalence documentation. US Food and Drug Administration.

52 Ungell, A.L., Nylander, S., Bergstrand, S., Sjoberg, A. and Lennernäs, H. (1998) Membrane transport of drugs in different regions of the intestinal tract of the rat. *Journal of Pharmaceutical Sciences*, **87**, 360–366.

53 Artursson, P. (1990) Epithelial transport of drugs in cell culture. I. A model for studying the passive diffusion of drugs over intestinal absorptive (Caco-2) cells. *Journal of Pharmaceutical Sciences*, **79**, 476–482.

54 Sun, D., Lennernäs, H., Welage, L.S., Barnett, J., Landowaki, C.P. *et al.* (2002) A comparison of human and Caco-2 gene expression profiles for 12,000 genes and the permeabilities of 26 drugs in the human intestine and Caco-2 cells. *Pharmaceutical Research*, **19**, 1398–1413.

55 Knutson, L., Odlind, B. and Hallgren, R. (1989) A new technique for segmental jejunal perfusion in man. *The American Journal of Gastroenterology*, **84**, 1278–1284.

56 Lennernäs, H., Lee, I.D., Fagerholm, U. and Amidon, G.L. (1997) A residence-time distribution analysis of the hydrodynamics within the intestine in man during a regional single-pass perfusion with Loc-I-Gut: *in-vivo* permeability estimation. *The Journal of Pharmacy and Pharmacology*, **49**, 682–686.

57 Steffansen, B., Lepist, E.I., Taub, M.E., Larsen, B.D., Frokjaer, S. *et al.* (1999) Stability, metabolism and transport of D-Asp(OBzl)-Ala – a model prodrug with affinity for the oligopeptide transporter. *European Journal of Pharmaceutical Sciences*, **8**, 67–73.

58 Thamotharan, M., Bawani, S.Z., Zhou, X. and Adibi, S.A. (1999) Hormonal regulation of oligopeptide transporter pept-1 in a human intestinal cell line. *The American Journal of Physiology*, **276**, C821–C826.

59 Amidon, G.L., Sinko, P.J. and Fleisher, D. (1988) Estimating human oral fraction dose absorbed: a correlation using rat intestinal membrane permeability for passive and carrier-mediated compounds. *Pharmaceutical Research*, **5**, 651–654.

60 Sinko, P.J., Leesman, G.D. and Amidon, G.L. (1991) Predicting fraction dose absorbed in humans using a macroscopic mass balance approach. *Pharmaceutical Research*, **8**, 979–988.

61 Oh, D.M., Sinko, P.J. and Amidon, G.L. (1993) Characterization of the oral absorption of some beta-lactams: effect of the alpha-amino side chain group. *Journal of Pharmaceutical Sciences*, **82**, 897–900.

62 Lennernäs, H., Knutson, L., Knutson, T., Hussain, A., Lesko, L. *et al.* (2002) The effect of amiloride on the *in vivo* effective permeability of amoxicillin in human jejunum: experience from a regional perfusion technique. *European Journal of Pharmaceutical Sciences*, **15**, 271–277.

63 Pilbrant, A. and Cederberg, C. (1985) Development of an oral formulation of omeprazole. *Scandinavian Journal of Gastroenterology. Supplement*, **108**, 113–120.

64 Inoue, M., Morikawa, M., Tsuboi, M. and Sugiura, M. (1979) Species difference and characterization of intestinal esterase on

the hydrolyzing activity of ester-type drugs. *Japanese Journal of Pharmacology*, **29**, 9–16.

65 Inoue, M., Morikawa, M., Tsuboi, M., Ito, Y. and Sugiura, M. (1980) Comparative study of human intestinal and hepatic esterases as related to enzymatic properties and hydrolyzing activity for ester-type drugs. *Japanese Journal of Pharmacology*, **30**, 529–535.

66 Yoshigae, Y., Imai, T., Horita, A., Matsukane, H. and Otagiri, M. (1998) Species differences in stereoselective hydrolase activity in intestinal mucosa. *Pharmaceutical Research*, **15**, 626–631.

67 Faigle, J.W. (1993) Drug metabolism in the colon wall and lumen, in *Colonic Drug Absorption and Metabolism*, Marcel Dekker Inc, Tübingen, pp. 29–54.

68 Goldin, B.R. (1990) Intestinal microflora: metabolism of drugs and carcinogens. *Annals of Medicine*, **22**, 43–48.

69 Scheline, R.R. (1973) Metabolism of foreign compounds by gastrointestinal microorganisms. *Pharmacological Reviews*, **25**, 451–532.

70 Basit, A.W. and Lacey, L.F. (2001) Colonic metabolism of ranitidine: implications for its delivery and absorption. *International Journal of Pharmaceutics*, **227**, 157–165.

71 Sjostrom, M., Lindfors, L. and Ungell, A.L. (1999) Inhibition of binding of an enzymatically stable thrombin inhibitor to lumenal proteases as an additional mechanism of intestinal absorption enhancement. *Pharmaceutical Research*, **16**, 74–79.

72 Bergstrom, C.A., Norinder, U., Luthman, K. and Artursson, P. (2002) Experimental and computational screening models for prediction of aqueous drug solubility. *Pharmaceutical Research*, **19**, 182–188.

73 WHO (2006) Proposal to waive *in vivo* bioequivalence requirements for WHO Model List of Essential Medicines: immediate-release, solid oral dosage forms. Technical Report Series, No. 937, 40th Report, Annex 8 of WHO Expert Committee on Specifications for Pharmaceutical Preparations.

74 The European Agency for the Evaluation of Medicinal Products (1999) ICH Topic Q6A, Step 4: Note for Guidance Specifications: Test Procedures and Acceptance Criteria for New Drug Substances and New Drug Products: Chemical Substances (CPMP/ICH/367/96 – adopted November 99).

75 Rekhi, G.S., Eddington, N.D., Fossler, M.J., Schwartz, P., Lesko, L.J. *et al*. (1997) Evaluation of *in vitro* release rate and *in vivo* absorption characteristics of four metoprolol tartrate immediate-release tablet formulations. *Pharmaceutical Development and Technology*, **2**, 11–24.

76 Adkin, D.A., Davis, S.S., Sparrow, R.A., Huckle, P.D., Phillips, A.J. *et al*. (1995) The effects of pharmaceutical excipients on small intestinal transit. *British Journal of Clinical Pharmacology*, **39**, 381–387.

77 Stenberg, P., Norinder, U., Luthman, K. and Artursson, P. (2001) Experimental and computational screening models for the prediction of intestinal drug absorption. *Journal of Medicinal Chemistry*, **44**, 1927–1937.

78 Yang, G., Ran, Y. and Yalkowsky, S.H. (2002) Prediction of the aqueous solubility: comparison of the general solubility equation and the method using an amended solvation energy relationship. *Journal of Pharmaceutical Sciences*, **91**, 517–533.

79 Berggren, S., Lennernäs, P., Ekelund, M., Westrom, B., Hoogstraate, J. *et al*. (2003) Regional transport and metabolism of ropivacaine and its CYP 3A4 metabolite PPX in human intestine. *Journal of Pharmacy and Pharmacology*, **55**, 963–972.

80 Gottfries, J., Svenheden, A., Alpsten, M., Bake, B., Larsson, A. *et al*. (1996) Gastrointestinal transit of amoxicillin modified-release tablets and a placebo tablet including pharmacokinetic assessments of

amoxicillin. *Scandinavian Journal of Gastroenterology*, **31**, 49–53.

81 Polli, E., Abrahamsson, B.S.I., Yu, L.X., Amidon, G.L., Baldoni, J.M., Cook, J.A., Fackler, P., Hartauer, K., Johnston, G., Krill, S.L., Lipper, R.A., Malick, W.A., Shah, V.P., Sun, D., Winkle, H.N., Wu, Y. and Zhang, H. (2008) Summary Workshop Report: bioequivalence, biopharmaceutics classification system, and beyond. *AAPS Journal*, in press.

82 Gu, C.-H., Li, H., Levons, J., Lentz, K., Gandhi, R.B., Raghavan, K. and Smith, R.L. (2007) Predicting effect of food on extent of drug absorption based on physicochemical properties. *Pharmaceutical Research*, **24**, 1118–1130.

83 International Committee of Harmonisation of Technical Requirements for Registration of Pharmaceuticals for Human Use (2003) Q8: Pharmaceutical Development.

84 Oberle, R.L., Chen, T.S., Lloyd, C., Barnett, J.L., Owyang, C. *et al*. (1990) The influence of the interdigestive migrating myoelectric complex on the gastric emptying of liquids. *Gastroenterology*, **99**, 1275–1282.

85 Kostewicz, E.S., Brauns, U., Becker, R. and Dressman, J.B. (2002) Forecasting the oral absorption behavior of poorly soluble weak bases using solubility and dissolution studies in biorelevant media. *Pharmaceutical Research*, **19**, 345–349.

86 Fleisher, D., Li, C., Zhou, Y., Pao, L.H. and Karim, A. (1999) Drug, meal and formulation interactions influencing drug absorption after oral administration. Clinical implications. *Clinical Pharmacokinetics*, **36**, 233–254.

87 Gleiter, C.H. and Morike, K.E. (2002) Clinical pharmacokinetics of candesartan. *Clinical Pharmacokinetics*, **41**, 7–17.

88 Ziessman, H.A., Fahey, F.H. and Collen, M.J. (1992) Biphasic solid and liquid gastric emptying in normal controls and diabetics using continuous acquisition in LAO view. *Digestive Diseases and Sciences*, **37**, 744–750.

89 Dickinson, P., Lee, W.W., Stott, P., Behn, S., Townsend, A., Smart, J., Ghahramani, P., Hammett, T., Billett, L., Gibb, R. and Abrahamsson, B. (2008) Clinical Relevance of Dissolution Testing in Quality by Design. *AAPS Journal*, in press.

90 Shiraga, T., Miyamoto, K., Tanaka, H., Yamamoto, H., Taketani, Y. *et al*. (1999) Cellular and molecular mechanisms of dietary regulation on rat intestinal H^+/peptide transporter PepT1. *Gastroenterology*, **116**, 354–362.

91 van de Waterbeemd, H. (1998) The fundamental variables of the biopharmaceutic classification system (BCS): a commentary. *European Journal of Pharmaceutical Sciences*, **7**, 1–3.

20
Prodrugs

Bernard Testa

Abbreviations

CYP	Cytochrome P450
DEPT	Directed enzyme-prodrug therapies
5-FU	5-Fluorouracil
PEG	Polyethylene glycol

20.1
Introduction

The concepts and examples presented here are meant to clarify the objectives of a prodrug strategy, to exemplify the major chemical moieties used in prodrug design, and to illustrate the biochemical pathways involved in prodrug activation (i.e., hydrolysis, oxidation, or reduction). More detailed information can be found in a number of reviews [1–15].

What makes prodrugs different from other drugs is the fact that they are devoid of intrinsic pharmacological activity. Thus, the simplest and clearest definition is the one given in 1958 by Adrien Albert [16], who coined the term. In a modified form, the definition reads

> *Prodrugs are chemicals with little or no pharmacological activity, undergoing biotransformation to a therapeutically active metabolite.*

The complete opposites of prodrugs are thus drugs whose metabolites make no contribution to the desired therapeutic effects, for example, oxazepam. However, prodrugs should not be confused (as is too often the case) with drugs that are intrinsically active, though they are transformed into one or more active metabolites. In this case, two or more active agents will contribute to the observed clinical response in proportions that depend on differences in pharmacological activities, in compartmentalization, and in time profiles. Examples include cisplatin (which is chemically transformed to the monoaqua and diaqua species), morphine and its

6-*O*-glucuronide, diazepam (which is N-demethylated to nordiazepam), and codeine (which is O-demethylated to morphine).

It is also important to distinguish prodrugs from soft drugs [17, 18] defined as "biologically active compounds (drugs) characterized by a predictable and fast *in vivo* metabolism to inactive and nontoxic moieties, after they have achieved their therapeutic role." An example is afforded by the short-acting β-blocker esmolol, whose half-life of hydrolysis in human blood at pH 7.4 and 37 °C is 23 min [19].

20.2 Why Prodrugs?

Although many prodrug studies in the literature bring useful information on activation mechanisms and structure–metabolism relation, they do not appear to address a genuine clinical need. In contrast, many other studies do attempt to improve some properties of a marketed drug or a drug candidate under development. As detailed below, the target properties to be improved (i.e., the objectives) may be pharmaceutical, pharmacokinetic, or pharmacodynamic. A summary of these objectives is presented in Table 20.1.

20.2.1 Pharmaceutical Objectives

Pharmaceutical scientists are often faced with serious formulation problems resulting from poor solubility, insufficient chemical stability, or poor organoleptic properties such as bitterness that affect patients' compliance. While pharmaceutical technology can sometimes solve such problems, success may be difficult and time

Table 20.1 Objectives of a prodrug strategy.

A. Pharmaceutical objectives		**Relation with**
A1. Improved solubility		B1
A2. Improved chemical stability		B5 and C2
A3. Improved taste and odor	Improved	
A4. Decreased pain and irritation	acceptability	B5
B. Pharmacokinetic objectives		
B1. Improved oral absorption	Improved	A1, B3, and B4
B2. Decreased presystemic metabolism	bioavailability	B4 and C1
B3. Improved absorption by nonoral routes		B1
B4. Improved time profile (often increased duration of action)		B1, B2, and C1
B5. Tissue-selective delivery		A2, A4, C1, and C2
C. Pharmacodynamic objectives		
C1. Masking of a reactive agent to improve its therapeutic index		B2, B4, B5, and C2
C2. *In situ* activation of a cytotoxic agent		A2, B5, and C1

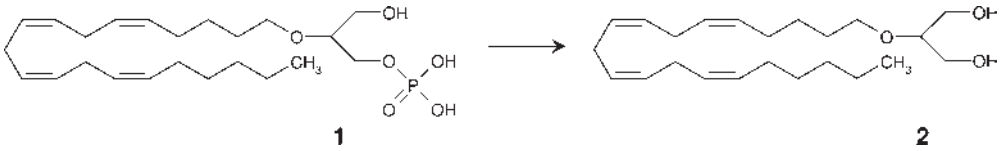

Figure 20.1 Noladin ether (**2**), a cannabinoid CB1 receptor agonist, and its monophosphate prodrug (**1**) [22, 23].

consuming to achieve. Project leaders may thus prefer to take advantage of a prodrug strategy and hope on an early solution. For example, medicinal chemists may consider the derivatization of phenols or alcohols by phosphate esterification to achieve greater solubility, although precipitation or absorption problems may result from premature hydrolysis [20], or the phosphate prodrug may even be too polar to allow good bioavailability [21]. A promising example of phosphorylation in prodrug design involves the endocannabinoid noladin ether (**2** in Figure 20.1). This cannabinoid CB1 receptor agonist reduces intraocular pressure, but its pharmacological profiling and pharmaceutical development are hindered by a poor aqueous solubility. Its monophosphate (**1** in Figure 20.1) and diphosphate esters increased the water solubility of noladin ether more than 40 000-fold. They showed high stability against chemical hydrolysis, yet were rapidly hydrolyzed by alkaline phosphatase and liver homogenates to the parent drug [22, 23]. Hydrolysis in 4% cornea homogenates was also fast. When tested *in vivo* in rabbits, the monophosphate ester (**2**) was very effective in reducing intraocular pressure.

Interestingly, increasing solubility is a pharmacokinetic as well as a pharmaceutical objective. Indeed, and as made explicit in the Biopharmaceutics Classification Scheme (BCS) [24], solubility is one of the main factors influencing oral absorption and hence oral bioavailability.

20.2.2 Pharmacokinetic Objectives

The need to improve the oral bioavailability of a drug or a candidate is one of the pharmacokinetic objectives in prodrug research, and it is currently the most important one. This can be achieved by improving the oral absorption of the drug and/or by decreasing its presystemic metabolism. Other pharmacokinetic objectives are to improve absorption by parenteral (nonenteral, e.g., dermal, ocular) routes, to lengthen the duration of action of the drug by slow metabolic release, and finally achieve the organ/tissue-selective delivery of an active agent. Some of these objectives are exemplified below with clinically successful prodrugs.

Achieving an improved oral absorption by a prodrug strategy is a frequent rationale in marketed prodrugs [5], as aptly illustrated with neuraminidase inhibitors of therapeutic value against type A and B influenza in humans [25]. Here, target-oriented rational design has led to highly hydrophilic agents that are not absorbed orally. One of the two current drugs is zanamivir (**3** in Figure 20.2), a highly hydrophilic drug administered in aerosol form. The other active agent is Ro-64-0802 (**5**), which also shows very high *in vitro* inhibitory efficacy toward the enzyme but low oral

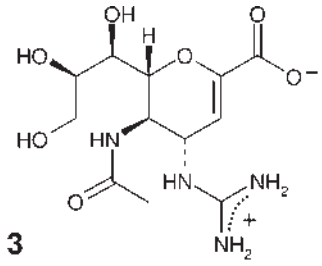

3

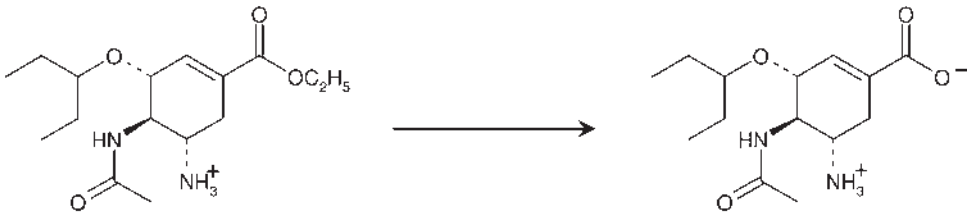

4 5

Figure 20.2 Structure of neuraminidase inhibitors used against type A and B influenza in humans, namely, the drug zanamivir (**3**) and the prodrug oseltamivir (**4**) whose active agent is Ro-64-0802 (**5**) [25, 26].

bioavailability because of its high polarity [26]. To circumvent this problem, Ro-64-0802 has been developed and marketed as oseltamivir, its ethyl ester prodrug (**4**). Following intestinal absorption, the prodrug undergoes rapid enzymatic hydrolysis and produces high and sustained plasma levels of the active agent. As demonstrated by this example, the prodrug concept may thus be a valuable alternative to disentangle pharmacokinetic and pharmacodynamic optimization.

A slow-release pharmaceutical formulation is the most frequent method used when the objective is to prolong the duration of action of a given drug. However, there are examples of a prodrug strategy complementing a slow-release formulation, as exemplified by injectable depot formulations of esters of steroid hormones. A conceptually different and particularly elegant approach to slow metabolic release has been achieved with bambuterol (**6** in Figure 20.3), a prodrug of the β_2-adrenoreceptor agonist terbutaline (**7**) [27, 28]. Bambuterol is activated to terbutaline by hydrolysis in blood serum and by monooxygenase-catalyzed oxidation in the liver, lung, and other tissues. The hydrolysis reaction is catalyzed by cholinesterase (butyrylcholinesterase, EC 3.1.1.8). Following a first burst of terbutaline release, the enzyme is inhibited by covalent attachment of the dimethylcarbamate moiety (Me_2N-CO-), resulting in a potent and slowly reversible inhibition of cholinesterase. In clinical terms and when compared with terbutaline 5 mg taken three times

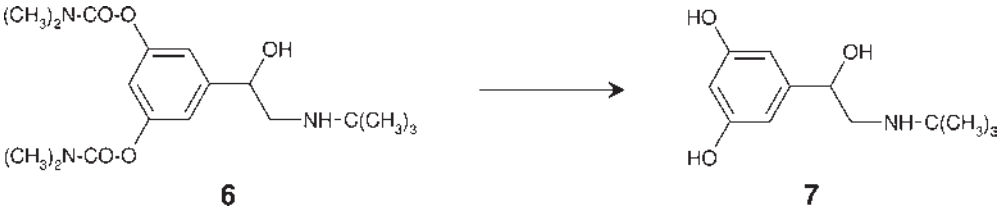

Figure 20.3 Structure of terbutaline (**7**) and its prodrug bambuterol (**6**) [27, 28].

daily, bambuterol 20 mg taken once daily provided smooth and sustained plasma levels of terbutaline and a greater symptomatic relief of asthma with a lower incidence of side effects.

A pharmacokinetic objective of great current interest is the organ- or tissue-selective delivery of a given drug, in other words, the search for the "magic bullet." A clinically significant example is that of capecitabine (**8** in Figure 20.4), a multistep, orally active prodrug of the antitumor drug 5-fluorouracil [29, 30]. Capecitabine is well absorbed orally and undergoes three activation steps resulting in high tumor concentrations of the active drug. It is first hydrolyzed by liver carboxylesterase (reaction **a**), the resulting metabolite being a carbamic acid that spontaneously decarboxylates (reaction **b**) to 5′-deoxy-5-fluorocytidine (**9**). The enzyme cytidine

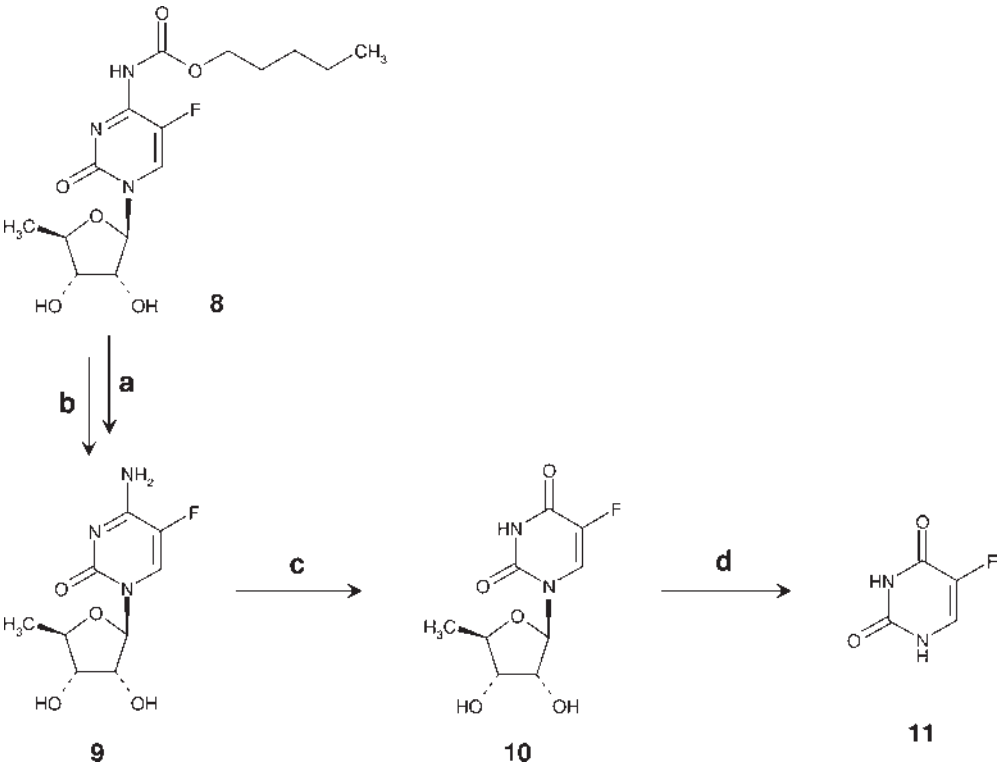

Figure 20.4 Stepwise activation of capecitabine (**8**) to the antitumor drug 5-fluorouracil (**11**) [29, 30].

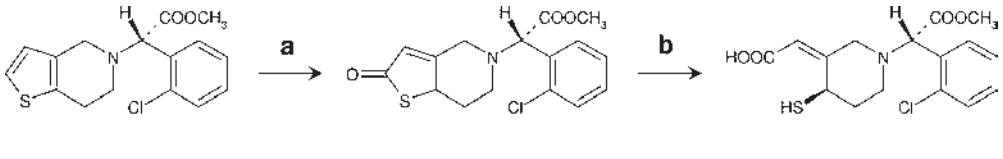

12 13 14

Figure 20.5 Metabolic activation of clopidogrel (**12**) in humans. A small part of a dose is activated by CYP3A to 2-oxo-clopidogrel (**13**), followed by hydrolytic ring opening to the active agent, a highly reactive thiol metabolite (**14**) that irreversibly antagonizes platelet ADP receptors via a covalent S–S bridge [31, 32].

deaminase, which is present in the liver and tumors, then transforms 5′-deoxy-5-fluorocytidine into 5′-deoxy-5-fluorouridine (reaction **c** and compound **10**). Transformation into 5-fluorouracil (reaction **d** and compound **11**) is catalyzed by thymidine phosphorylase and occurs selectively in tumor cells. Capecitabine is of great interest in the present context, since it affords an impressive gain in therapeutic benefits compared to 5-FU as a result of its oral bioavailability and a relatively selective activation in and delivery to tumors.

20.2.3 Pharmacodynamic Objectives

In simple terms, pharmacodynamic objectives are synonymous with decreasing systemic toxicity. Two such cases are mentioned in Table 20.1 and are illustrated here. The masking of a reactive agent to improve its therapeutic index is aptly exemplified by the successful antiaggregating agent clopidogrel (**12** in Figure 20.5). This compound was known to be inactive without activation, but its metabolism and molecular mechanism of action remained poorly understood for years. In other words, clopidogrel should be considered as a fortuitous prodrug. The compound is of further interest among prodrugs in that its major metabolic route in humans (about 85% of a dose) is indeed one of hydrolysis, but this reaction leads to an inactive acid. In contrast, clopidogrel is activated by cytochromes P450 3A in a two-step sequence. The CYP-catalyzed reaction first oxidizes clopidogrel to 2-oxo-clopidogrel (**13**). This is followed by a rapid cleavage of the cyclic thioester to a highly reactive thiol metabolite (**14**) that irreversibly antagonizes platelet ADP receptors via a covalent S–S bridge [31, 32]. Interestingly, the same activation mechanism appears to account for the potent and irreversible inhibition of human CYP2B6 by clopidogrel [33], again demonstrating the high reactivity of the thiol metabolite.

In situ activation to a cytotoxic agent is part of the well-known mechanism of action of the antibacterial and antiparasitic nitroarenes such as metronidazol. This concept is now intensively investigated in the search for more selective antitumor agents [34–36]. Given that tumor cells have a greater reductive capacity than normal cells, various chemical strategies are being explored to design hypoxia-activated prodrugs of cytotoxic agents. Thus, the bioreductive antitumor agent tirapazamine (**15** in Figure 20.6) is seemingly the best studied drug candidate in this class [37, 38].

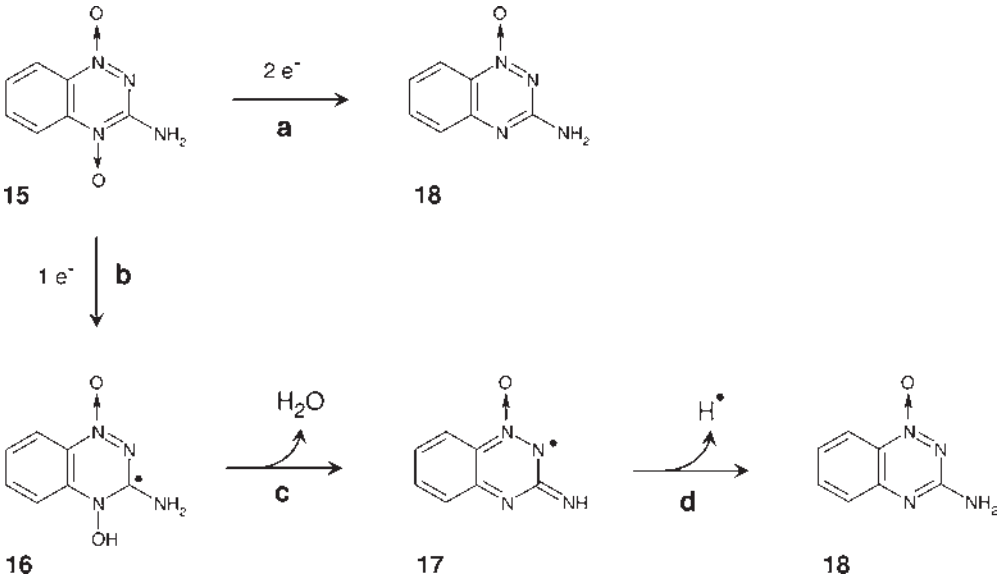

Figure 20.6 The hypoxia-selective antitumor agent tirapazamine **15**. Reaction **a**: reductive inactivation by two-electron steps catalyzed by quinone reductase (the first two-electron step being shown here). Reaction **b**: reductive activation (one-electron step catalyzed by cytochrome P450 reductase). Reaction **c**: dehydration to yield the reactive radical **17**, which abstracts a hydrogen radical from DNA [37, 38].

Tirapazamine is inactivated by two-electron reduction steps catalyzed by quinone reductase, yielding first the mono-*N*-oxide (reaction **a** and compound **18**). In contrast, it is activated to a cytotoxic nitroxide (**16**) by a one-electron reduction catalyzed by NADPH-cytochrome P450 reductase (reaction **b**). This delocalized radical loses one molecule of water to yield a reactive radical (reaction **c** and compound **17**). Radical **17** can then abstract one hydrogen radical from DNA (reaction **d** and compound **18**), leading to DNA breaks and cytotoxicity. In summary, both inactivation and activation involve reduction reactions, but cytotoxicity will depend on the relative levels of quinone reductase and CYP reductase in hypoxic cells.

20.3 How Prodrugs?

20.3.1 Types of Prodrugs

A useful way to classify prodrugs is the one based on chemical arguments. Thus, medicinal chemists find it useful to distinguish between four major classes of prodrugs, namely,

Table 20.2 Examples of common and less common carrier groups used in prodrug design.

Prodrug types	Generic structure(s)
Prodrugs of active carboxylic acids	
Simple alkyl or aryl esters	R-CO-O-R′
Alkyl esters containing an amino or amido group, or another functionality	For example, R-CO-O-(CH2)$_n$-NR′R″ or R-CO-O-(CH$_2$)$_n$-CO-NR′R″
(Acyloxy)methyl or (acyloxy)ethyl esters	For example, R-CO-O-CH$_2$-O-CO-R″
Esters of diacylaminopropan-2-ols	For example, R-CO-O-CH(CH$_2$-NH-COR′)$_2$
N,*N*-Dialkyl hydroxylamino derivatives	R-CO-O-NR′R″
Amides of amino acids	R-CO-NH-CH(R′)-COOH
Prodrugs of active alcohols or phenols	
Esters of carboxylic acids	R-O-CO-R′
Esters of ring-substituted aromatic acids	R-O-CO-aryl
Monoesters of diacids	For example, R-O-CO-(CH$_2$)$_n$-COOH
Esters of α-amino acids or other amino acids	For example, R-O-CO-CH(NH$_2$)R′
Carbonates or carbamates	For example, R-O-CO-O-R′ or R-O-CO-NR′R″
(Acyloxy)methyl or (acyloxy)ethyl ethers	For example, R-O-CH$_2$-O-CO-R′
(Alkoxycarbonyloxy)methyl or (alkoxycarbonyloxy)ethyl ethers	For example, R-O-CH$_2$-O-CO-O-R′ or R-O-CH(CH$_3$)-O-CO-O-R′
O-Glycosides	R-O-sugar
Phosphates or sulfates	R-O-PO(OR′)(OR″) or R-O-SO$_3$H
Prodrugs of active amines or amides	
Amides formed from acyl groups	RR′N-CO-R″
Amides of amino acids or peptides	RR′N-CO-CHR″-NHR″
Simple or structurally complex carbamates	RR′N-CO-O-R″ or for example, RR′N-CO-O-CH(R″)-O-CO-R″
N-Mannich bases	For example, RR′N-CH$_2$-NR″R″
O-Mannich bases	For example, RR′N-CH$_2$-O-CO-R″
Cyclic Mannich bases	For example, oxazolidines
Imines (Schiff bases)	RN=CH-NR′R″
Azo conjugates	R-N=N-R′

- Carrier-linked prodrugs, in which the active agent (the drug) is linked to a carrier (also known as a promoiety) and whose activation in most cases occurs by hydrolysis (esters, amides, imines, etc.). These are the most frequently encountered prodrugs and examples can be found in Figures 20.1–20.4. There also exist a limited number of carrier-linked prodrugs whose activation occurs by oxidation or reduction. A list of prodrug types derivatized with selected promoieties can be found in Table 20.2.
- Bioprecursors are distinguished from prodrugs by the lack of a promoiety, yet can be activated by oxidation (see Figure 20.5), reduction (see Figure 20.6), or hydrolysis (e.g., lactone opening) [14].
- Macromolecular prodrugs, where the carrier is a macromolecule such as a PEG (polyethylene glycol) [39].

- Directed enzyme-prodrug therapies (DEPTs), which are prodrugs derived from biotechnology [1, 4, 40–44]. These are highly specialized biochemical strategies that would require separate treatment. They include

  -drug–antibody conjugates where the carrier is an antibody raised against tumor cells, as in antibody-directed enzyme prodrug therapies (ADEPTs);

  -gene-directed enzyme prodrug therapies (GDEPTs).

20.3.2
Hurdles in Prodrug Research

This chapter has focused on carrier-linked prodrugs and bioprecursors, which remain by far the largest groups of prodrugs in use. Indeed, of the 1562 different active substances marketed in Germany in 2002, 6.9% were prodrugs, with one-half of these being activated by hydrolytic cleavage of a promoiety, and one-quarter being bioprecursors [3].

After discussing the objectives of prodrug research, one cannot ignore the difficulties involved. Indeed, developing prodrugs involves additional work in synthesis, physicochemical profiling, pharmacokinetic profiling, and toxicological assessment [3]. Two major challenges are biological variability and toxicity potential. The challenge of biological variety results principally from the huge number and evolutionary diversity of enzymes involved in xenobiotic metabolism. Inter- and intraspecies differences in the nature of these enzymes, as well as many other differences such as the nature and level of transporters, may render prodrug optimization difficult to predict and achieve. The high level of carboxylesterases in the plasma of rodents but not in the plasma of other mammals is but one example of a biological difference that may affect the rate and site of activation of some prodrug esters. A chemical strategy developed by medicinal chemists to overcome the problem of biological variety is the development of prodrugs activated by nonenzymatic hydrolysis, for example, imines, Mannich bases, (2-oxo-1,3-dioxol-4-yl)methyl esters, or oxazolidines. A more promising approach appears to be the two-step activation of carrier-linked prodrugs, involving first a relative facile enzymatic hydrolysis to unmask a nucleophilic group, followed by a nonenzymatic, intramolecular nucleophilic substitution and cyclization [1–4, 8, 45].

A second challenge is the toxicity potential of some prodrugs, namely, a toxic metabolite formed from the promoiety or a reactive metabolic intermediate generated during the activation of some bioprecursors. The former case is illustrated by the liberation of formaldehyde, as seen with Mannich bases or some double esters [1, 4]. The latter case involves a very few known examples of failed bioprecursors whose activation was via a reactive and toxic intermediate. Thus, arylacetylenes were examined as potential bioprecursors of nonsteroidal anti-inflammatory agents [1]. Although the nature of the final (and stable) metabolite (an arylacetic acid) was known, researchers at the time were not aware that the metabolic pathway involved an intermediate and highly reactive ketene.

20.4 Conclusions

The prodrug concept has allowed some apparently intractable pharmaceutical, pharmacokinetic, or pharmacodynamic problems to be overcome [4]. But there is more, since the objectives discussed above are often intertwined. Thus, an improved solubility can greatly facilitate oral absorption, while improving the chemical stability of an active agent can allow tissue-selective delivery and even lead to its *in situ* activation. As a result, medicinal chemists and biochemists in prodrug research should be aware that the behavior of their prodrug candidates may differ from that of the parent drug in ways that go beyond the original pharmaceutical, pharmacokinetic, or pharmacodynamic objectives being pursued.

A large number of prodrug examples published in the literature are clear cases of *post hoc* research that never advanced to development. In contrast, the examples presented above illustrate how well-designed or even fortuitous prodrugs allow to achieve medicinal objectives that remain out of reach of the active drug. Indeed, a prodrug approach is most fruitful when a traditional hit or lead optimization fails because the structural conditions for activity (i.e., the pharmacophore) are incompatible with the target pharmaceutical, pharmacokinetic, or pharmacodynamic properties. In other words, the gap between activity and other drug-like properties may be of such a nature that only a prodrug strategy can bridge it [1, 2].

References

1 Testa, B. (2007) Prodrug objectives and design, in *ADME-Tox Approaches*, Vol. 5 (eds B. Testa and H. van de Waterbeemd), in *Comprehensive Medicinal Chemistry II* (series eds J.B. Taylor and D.J. Triggle), Elsevier, Oxford, UK, pp. 1009–1041.

2 Testa, B. (2004) Prodrug research: futile or fertile? *Biochemical Pharmacology*, **68**, 2097–2106.

3 Ettmayer, P., Amidon, G., Clement, B. and Testa, B. (2004) Lessons learned from marketed and investigational prodrugs. *Journal of Medicinal Chemistry*, **47**, 2393–2404.

4 Testa, B. and Mayer, J.M. (2003) *Hydrolysis in Drug and Prodrug Metabolism – Chemistry, Biochemistry and Enzymology*, Wiley-VHCA, Zurich.

5 Beaumont, K., Webster, R., Gardner, I. and Dack, K. (2003) Design of ester prodrugs to enhance oral absorption of poorly permeable compounds: challenges to the discovery scientist. *Current Drug Metabolism*, **4**, 461–485.

6 Testa, B. and Soine, W. (2003) Principles of drug metabolism, in *Burger's Medicinal Chemistry and Drug Discovery*, Vol. 2, 6th edn (ed. D.J. Abraham), Wiley-Interscience, Hoboken, NJ, pp. 431–498.

7 Testa, B. and Mayer, J.M. (2001) Concepts in prodrug design to overcome pharmacokinetic problems, in *Pharmacokinetic Optimization in Drug Research: Biological, Physicochemical and Computational Strategies* (eds B. Testa, H. van de Waterbeemd, G. Folkers and R. Guy), Wiley-VHCA, Zurich, pp. 85–95.

8 Wang, W., Jiang, J., Ballard, C.E. and Wang, B. (1999) Prodrug approaches in the improved delivery of peptide drugs. *Current Pharmaceutical Design*, **5**, 265–287.

9 Lee, H.J., You, Z., Ko, D.H. and McLean, H.M. (1998) Recent advances in prodrugs and antedrugs. *Current Opinion in Drug Discovery & Development*, **1**, 235–244.

10 Bradley, D.A. (1996) Prodrugs for improved CNS delivery. *Advanced Drug Delivery Reviews*, **19**, 171–202.

11 Testa, B. and Caldwell, J. (1996) Prodrugs revisited – the "ad hoc" approach as a complement to ligand design. *Medicinal Research Reviews*, **16**, 233–241.

12 Waller, D.G. and George, C.F. (1989) Prodrugs. *British Journal of Clinical Pharmacology*, **28**, 497–507.

13 Stella, V.J., Charman, W.N.A. and Naringrekar, V.H. (1985) Prodrugs – do they have advantages in clinical practice? *Drugs*, **29**, 455–473.

14 Wermuth, C.G. (1984) Designing prodrugs and bioprecursors, in *Drug Design: Fact or Fantasy?* (eds G. Jolles and K.R.H. Woolridge), Academic Press, London, pp. 47–72.

15 Harper, N.J. (1962) Drug latentiation, in *Progress in Drug Research*, Vol. 4 (eds E. Jucker), Birkhäuser, Basel, pp. 221–294.

16 Albert, A. (1958) Chemical aspects of selective toxicity. *Nature*, **182**, 421–422.

17 Bodor, N. and Buchwald, P. (2000) Soft drug design: general principles and recent applications. *Medicinal Research Reviews*, **20**, 58–101.

18 Bodor, N. (1984) Novel approaches to the design of safer drugs: soft drugs and site-specific chemical delivery systems, in *Advances in Drug Research*, Vol. 13 (ed. B. Testa), Academic Press, London, pp. 255–331.

19 Benfield, P. and Sorkin, E.M. (1987) Esmolol: a preliminary review of its pharmacodynamic and pharmacokinetic properties, and therapeutic efficacy. *Drugs*, **33**, 392–412.

20 Heimbach, T., Oh, D.M., Li, L.Y., Rodriguez-Hornedo, N., Garcia, G. and Fleisher, D. (2003) Enzyme-mediated precipitation of parent drug from their phosphate prodrugs. *International Journal of Pharmaceutics*, **26**, 81–92.

21 Heimbach, T., Oh, D.M., Li, L.Y., Forsberg, M., Savolainen, J., Leppänen, J., Matsunaga, Y., Flynn, G. and Fleisher, D. (2003) Absorption rate limit considerations for oral phosphate prodrugs. *Pharmaceutical Research*, **20**, 848–856.

22 Juntunen, J., Vepsäläinen, J., Niemi, R., Laine, K. and Järvinen, T. (2003) Synthesis, *in vitro* evaluation, and intraocular pressure effects of water-soluble prodrugs of endocannabinoid noladin ether. *Journal of Medicinal Chemistry*, **46**, 5083–5086.

23 Juntunen, J., Järvinen, T. and Niemi, R. (2005) *In-vitro* corneal permeation of cannabinoids and their water-soluble phosphate ester prodrugs. *Journal of Pharmacy and Pharmacology*, **57**, 1153–1157.

24 Amidon, G.L., Lennernäs, H., Shah, V.P. and Crison, J.R. (1995) A theoretical basis for a biopharmaceutic drug classification: the correlation of *in vitro* drug product dissolution and *in vivo* bioavailability. *Pharmaceutical Research*, **12**, 413–420.

25 Oxford, J.S. and Lambkin, R. (1998) Targeting influenza virus neuraminidase – a new strategy for antiviral therapy. *Drug Discovery Today*, **3**, 448–456.

26 Lew, W., Chen, X. and Kim, C.U. (2000) Discovery and development of GS 4104 (oseltamivir): an orally active influenza neuraminidase inhibitor. *Current Medicinal Chemistry*, **7**, 663–672.

27 Svensson, L.Å. and Tunek, A. (1988) The design and bioactivation of presystematically stable prodrugs. *Drug Metabolism Reviews*, **19**, 165–194.

28 Persson, G., Pahlm, O. and Gnosspelius, Y. (1995) Oral bambuterol versus terbutaline in patients with asthma. *Current Therapeutic Research*, **56**, 457–465.

29 Tsukamoto, Y., Kato, Y., Ura, M., Horii, I., Ishitsuka, H., Kusuhara, K. and Sugiyama, Y. (2001) A physiologically based pharmacokinetic analysis of capecitabine, a triple prodrug of 5-FU, in

humans: the mechanism for tumor-selective accumulation of 5-FU. *Pharmaceutical Research*, **18**, 1190–1202.

30 Hwang, J.J. and Marshall, J.L. (2002) Capecitabine: fulfilling the promise of oral chemotherapy. *Expert Opinion on Pharmacotherapy*, **3**, 733–743.

31 Savi, P., Pereillo, J.M., Uzabiaga, M.F., Combalbert, J., Picard, C., Maffrand, J.P., Pascal, M. and Herbert, J.M. (2000) Identification and biological activity of the active metabolite of clopidogrel. *Thrombosis and Haemostasis*, **84**, 891–896.

32 Clarke, T.A. and Waskell, L.A. (2003) The metabolism of clopidogrel is catalyzed by human cytochrome P450 3A and is inhibited by atorvastatin. *Drug Metabolism and Disposition: The Biological Fate of Chemicals*, **31**, 53–59.

33 Richter, T., Mürdter, T.E., Heinkele, G., Pleiss, J., Tatzel, S., Schwab, M., Eichelbaum, M. and Zanger, U.M. (2004) Potent mechanism-based inhibition of human CYP2B6 by clopidogrel and ticlopidine. *Journal of Pharmacology and Experimental Therapeutics*, **308**, 189–197.

34 Denny, W.A. (2005) Hypoxia-activated anticancer drugs. *Expert Opinion on Therapeutic Patents*, **15**, 635–646.

35 Denny, W.A. (2003) Synthetic DNA-targeted chemotherapeutic agents and related tumor-activated prodrugs, in *Burger's Medicinal Chemistry and Drug Discovery*, Vol. 5, 6th edn (ed. D.J. Abraham), Wiley-Interscience, Hoboken, NJ, pp. 51–105.

36 Dubowchik, G.M. and Walker, M.A. (1999) Receptor-mediated and enzyme-dependent targeting of cytotoxic anticancer drugs. *Pharmacology & Therapeutics*, **83**, 67–123.

37 Riley, R.J. and Workman, P. (1992) Enzymology of the reduction of the potent benzotriazine-di-*N*-oxide hypoxic cell cytotoxin SR 4233 (WIN 59075) by NAD(P)H: (quinone acceptor) oxidoreductase (EC 1.6.99.2) purified from Walker 256 rat tumour cells. *Biochemical Pharmacology*, **43**, 167–174.

38 Anderson, R.F., Shinde, S.S., Hay, M.P., Gamage, S.A. and Denny, W.A. (2003) Activation of 3-amino-1,2,4-benzotriazine 1,4-dioxide antitumor agents to oxidizing species following their one-electron reduction. *Journal of the American Chemical Society*, **125**, 748–756.

39 Veronese, F.M. and Pasut, G. (2007) Drug-polymer conjugates, in *ADME-Tox Approaches*, Vol. 5 (eds B. Testa and H. van de Waterbeemd), in *Comprehensive Medicinal Chemistry II* (series eds J.B. Taylor and D.J. Triggle), Elsevier, Oxford, UK, pp. 1043–1068.

40 Niculescu-Duvaz, I., Friedlos, F., Niculescu-Duvaz, D., Davies, L. and Springer, C.J. (1999) Prodrugs for antibody- and gene-directed enzyme prodrug therapies (ADEPT and GDEPT). *Anti-Cancer Drug Design*, **14**, 517–538.

41 Cassidy, J. (2000) Polymer-directed enzyme prodrug therapy. *Drug News & Perspectives*, **13**, 477–480.

42 Springer, C.J. and Niculescu-Duvaz, I. (2000) Prodrug-activating systems in suicide gene therapy. *The Journal of Clinical Investigation*, **105**, 1161–1167.

43 HariKrishna, D. Raghu Ram Rao, A. and Krishna, D.R. (2003) Selective activation of anthracycline prodrugs for use in conjunction with ADEPT. *Drug News & Perspectives*, **16**, 309–318.

44 Davies, L.C., Friedlos, F., Hedley, D., Martin, J., Ogilvie, L.M., Scanlon, I.J. and Springer, C.J. (2005) Novel fluorinated prodrugs for activation by carboxypeptidase G2 showing good *in vivo* antitumor activity in gene-directed enzyme prodrug therapy. *Journal of Medicinal Chemistry*, **48**, 5321–5328.

45 Testa, B. and Mayer, J.M. (1998) Design of intramolecularly activated prodrugs. *Drug Metabolism Reviews*, **30**, 787–807.

21
Modern Delivery Strategies: Physiological Considerations for Orally Administered Medications

Clive G. Wilson and Werner Weitschies

Abbreviations

BMI	Body mass index
[^{51}Cr]-EDTA	Chromium-51 labeled ethylenediamine-tetraacetic acid
CYP3A4	Cytochrome P450, 3A4 isozyme
GI	Gastrointestinal
IMMC	Interdigestive migrating motor complex
MMC	Migrating motor complex
PEG	Polyethylene glycol
q.d.s.	Four times a day
SITT	Small intestinal transit time (h)
t.d.s.	Three times a day
WGTT	Whole-gut transit time (h)

Symbols

AUC	Area under the plasma concentration–time profile (mg h/l)
Cmax	Maximum concentration reached in the concentration profile
[^{111}In]	Indium-111
t_{50}	Time for 50% emptying of the stomach (h)
t_{max}	Time for maximum concentration (h)
[^{99m}Tc]	Technetium-99m

21.1 Introduction

The control of physiological processes to achieve reliable plasma concentration–time profiles following oral drug administration is a key goal in therapy. At the investigational level, it would allow the scientist to use manageable numbers of volunteers in

appropriately powered tests to proceed with formulation development and at the medicinal level, it might allow more consistent outcomes. The weasel word "might" is important here, since disease and/or concomitant medication may alter transit, pH, disposition, metabolism, and clearance in a manner unforeseen in the original clinical trials. The opposite scenario can also happen, with patients showing consistent blood level–time curves and studies in *volunteer cohorts* yielding huge differences in AUC and C_{max}. More generally, the issue relates to erratic blood levels with patients or volunteers grouped into "poor" and "good" absorbers or those with troughs in the profile. At this stage, there is usually a frantic appeal to the formulator to come up with a strategy to solve the problem. This will result in futile endeavors if the phenomenon is related to a physiological process that was not controlled in the trial providing the anomalous results. This state of affairs occurs because the impact of some elements of physiological processes, particularly those relevant to drug absorption, are poorly appreciated and physicians and pharmaceutical scientists have failed to reach a common perspective.

In our view, physiological and pathophysiological factors have to be considered hand-in-hand with pharmaceutical and physicochemical issues in the exploitation of modern drug delivery strategies. In this chapter, attempts have been made to illustrate this point from the perspective of clinical pharmacology, drawing on examples largely from imaging, patient, and volunteer studies conducted by us and our colleagues. To make the task manageable, we will confine our analysis to the oral route, although similar consideration could be applied to any mode of delivery.

21.2 The Targets

For most drugs, the limitations to delivery are defined in terms of solubility and permeability. The solubility issues are addressed by various means including selection of an amorphous form where appropriate, reduction in particle size, and the use of cosolvents. For permeability problems, a mechanism to increase flux by altering the membrane/microenvironment conditions or even a simple increase in concentration gradient might achieve the goal. Examples of design strategies include the use of absorption enhancers and formulations designed to keep the drug in the upper gastrointestinal (GI) tract, which may achieve reduction of first-pass effect (buccal), increased solubility in acid (stomach), or avoidance of degradation in the colon. When the compound selected is problematic in terms of both solubility and permeability, the number of permutations becomes almost infinite, especially when juggling with the added dimensions of dose and plasma half-life. In general, the desired outcomes could be listed as in Table 21.1.

The gastrointestinal tract is conveniently divided into a number of areas, primarily on the basis of morphology and function. For most pharmaceutical purposes, we can group the target tissues into three regions: the upper, mid- and lower gastrointestinal tract.

Table 21.1 Desired outcomes of targeted treatments at various regions of the gut.

Region	Objective	Strategy	Issues
Buccal	Avoid first pass	Adhere to buccal mucosa (prophylaxis)	Taste
		OR	Saliva (some drugs cause dry mouth)
		Sublingual (immediate)	Potency (has to be high)
			Talking, eating, drinking
	Increase flux	Open tight junctions	Irritancy
	Increase convenience	Use fast-dissolving system	Will not have equivalent profile to simple IR systems
Esophagus	Ensure transit	Adjust tablet shape, coating	Surface area/weight ratio
	Avoid sticking	Stand up, take with water	(How much? When?) Age, previous Rx, posture
Stomach	Promote rapid absorption	Control intrinsic dissolution	*In vitro*/*in vivo* correlation
		Control emptying	Fed/fasting effects
	Prevent degradation	Enteric coat	Achlorhydria in elderly (especially Japanese)
	Extend absorption (in intestine)	Float, swell, adhere	Posture
			Rate of degradation after delivery, bezoars
			Food effects, gastric inhomogeneity
			Disease effects
Intestine	Extend exposure	Adhere to villus tip	Access?
		Promote Peyer's patch uptake	Wall–lumen mixing
	Increase absorption	Decrease P-glycoprotein efflux	Timing
		Block Cytochrome P450 3A	Concomitant administration
		Open tight junctions	Unselective
	Utilize lymphatic system	Increase absorption of lipophiles	Food effects persist for longer than 24 h
	Increase exposure	Target with coated preparation	Variability in transit and pH
		Utilize bacterial fermentation	Variability, disease effects?
		Increase surface area of preparation	Stirring, dispersion available water, gas, time of dosing

21.3 The Upper GI Tract: Mouth and Esophagus

The surface tissue of the mouth is squamous epithelium, and the cells lining the cheek are dead and enucleated. The effective permeability barrier is quoted as between 10^{-9} and 10^{-5} cm/s due in part to the activity of membrane coating granules

positioned near superficial tissues. These granules, after fusion with the plasma membrane, empty their contents into the intercellular space [1] like mortar around bricks, and the principal mechanism of drug entry is diffusion [2]. The liquid phase is provided by saliva and therefore any disease or treatment that affects production of saliva may alter distribution of drugs within the buccal cavity.

The three main areas of development over the last decade have been in smoking cessation, pain control, testosterone replacement, and to some less significant extent, novel formulations. A recent review by Smart [3] summarizes these latter directions in reformulation. Buccal delivery remains an area of interest for most companies, particularly for niche products, where conventional oral medication does not provide sufficiently faster onset of action or where treatment may be discontinuous.

Clearance of drugs from the buccal mucosa is generally slow, which may reflect high nonspecific binding in the tissue: plasma morphine concentrations, for example, decline more slowly than that of an intramuscular site and may be used with advantage to extend the period of analgesia [4, 5]. Oddly enough, Gordon [6] has concluded that morphine is not absorbed faster sublingually than when swallowed. Diffusion through the tissue can be improved for many drugs by manipulating lipophilicity (prodrug or pH control) to increase partitioning into the tissue. A simple application of this concept can be seen in the development of nicotine formulations where raising buccal pH increases the flux significantly, producing a rise in drug absorption from nicotine formulations held in the mouth [7, 8].

Utilizing absorption enhancers in this area is probably more benign than elsewhere in the gastrointestinal tract. The maximum size of a buccal patch that would be acceptable to a patient has been defined as >15 cm^2 (or more usually between 0.5 and 3 cm^2), and Hoogstraate and colleagues [9] have commented that an absorption enhancer would therefore probably be necessary to keep buccal patches to a desirable size. Commonly employed enhancers such as fatty acids, synthetic surfactants (sodium dodecyl sulfate), and natural surfactants (bile salts) have appeared in many experimental formulations and polymer salts. Chitosan glutamate, for example, enhances the solubility of nifedipine [10]. In addition, the small area for delivery dictates that the drug must be potent and although the buccal mucosa is less hostile with regard to peptidase and other enzymatic activity, it may be necessary to incorporate enzyme inhibitors as excipients in the formulation.

Although gels can be used to increase contact and promote absorption [11], the requirement for unidirectional delivery cannot be met by simple systems, and release of actives from erodible matrices are influenced by physiological abrasion from the cheek surfaces by talking. Novel systems for oral delivery have been extensively investigated by Hoogstraate, and others have reviewed developments in the field including melatonin delivery and low molecular weight heparin in the Cydot system [9]. In pain management, Gordon [12] has reviewed a number of novel transmucosal and transdermal systems including the effervescent fentanyl tablet designed for the control of breakthrough pain using the effervescent system to produce local pH shifts. The drug is rapidly absorbed with a peak concentration achieved 40 min after dosing with a

complex triexponential clearance at high doses [13]. Later investigations showed that t_{max} was not related to mouth dwell time [14].

Fast-dissolving formulations (flash dispersing) are not primarily intended for buccal delivery; the issue here is that they may be taken without water. This causes an important difference in performance relative to ordinary immediate-release products, especially if the drug is in suspension. If the material is swallowed dry, it may adhere to the fundus area of the stomach, where the amount of shear is low. This causes a significant fraction of the material to be retained resulting in tailing of the absorption phase and an apparently decreased AUC as the material is released over several hours.

21.3.1 Swallowing the Bitter Pill...

It is commonly assumed that swallowed dosage forms pass without hindrance into the stomach unless an underlying esophageal condition is present. However, it has been shown that esophageal transit of capsules or tablets is strongly influenced by the volume of the coswallowed water and the body position [15, 16].

Radiological studies of an asymptomatic group of 56 patients (mean age 83) showed that a normal pattern of deglutition was present in only 16% of the patients and 63% of this population experienced difficulty in swallowing [17]. To assist the swallowing of a tablet, patients are instructed to take a dosage form in an upright position with plenty of water. It might be expected that simple encouragement and education could encourage compliance. In practice, when patients are presented with a 240 ml glass of water and instructed to swallow a tablet "according to normal practice," they imbibe only two to three mouthfuls (between 50 and 100 ml). Radiological studies conducted back in the mid-1980s concluded that the effect of taking diazepam with either 10 or 50 ml water made little difference to absorption, although 20% of the study group showed delayed absorption irrespective of volume imbibed [18]. In our studies, the effects of small volumes of water (30 or 50 ml) on the esophageal clearance of either a small, uncoated circular tablet or film-coated oval tablet were compared [19]. Clearance of the oval tablet was significantly faster and stasis occurred in 5 instances with the uncoated tablet versus zero in the same 28 patients taking the film-coated oval tablet.

Deliberate attempts to adhere to the esophagus have been made to treat ulcer sites in esophagus and stomach, for example, with sucralfate [20]. These data suggested that acid-activated sucralfate showed high retention in man, and separate supporting data were obtained in the dog. Unfortunately, a later study failed to confirm this observation in the clinic [21]. The explanation for visible coating in the dog is probably related to the angle of the esophagus. The development of an esophageal bandage based on graft polymers that possess mucoadhesive and thermosetting properties was investigated in our laboratory and some limited success was achieved as shown in Figure 21.1 [22]. However, the issue of starting temperature and heat transfer during mouth-hold and deglutition proved to be problematic.

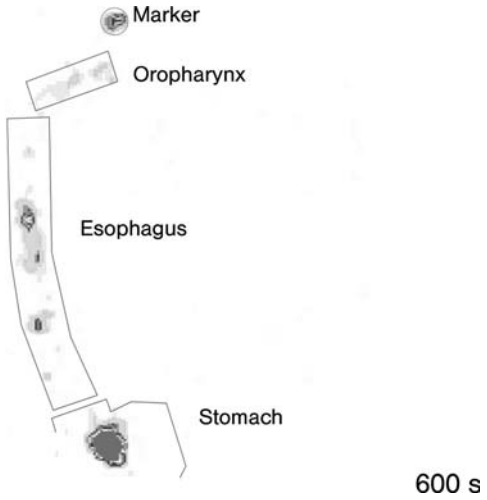

Figure 21.1 Scintiscan of [^{99m}Tc]-labeled "Smartgel," 10 min after administration showing material adhering in mid-esophagus.

21.4
Mid-GI Tract: Stomach and Intestine

The stomach provides a reservoir allowing food to be made available to the small intestine at a rate that is controlled by the complex system of the brain–gut axis. To do this, the food contents are churned with acid and enzymes, which begins the digestive process. There is essentially no absorption of food components from the stomach. The same holds true for drug substances. Even the highly permeable, small-molecule ethanol is only poorly absorbed from the stomach [23]. The early stage of digestion allows the duodenum to sample the contents and adjust the gastroduodenal pressure difference to regulate the supply of calories. These function impacts explain some of the characteristics of the first part of the intestine (i) that absorption will be extremely efficient and (ii) transit will be very rapid to allow modulation by further food intake.

21.4.1
Gastric Inhomogeneity

For the most part, the resting pH of the stomach is close to 2 than 1 and during feeding, the meal causes a transient rise to 4–5 depending on the volume and nature of the meal consumed. The fundus undergoes receptive relaxation to allow the proximal stomach to accommodate the food mass: in the distal stomach, the food is triturated to form chyme that is ejected into the duodenum in spurts of 2–5 ml. The division of function causes significant inhomogeneity in the conditions of the stomach, as the proximal stomach is more stagnant and the number of parietal cells is much less in the fundal area [24].

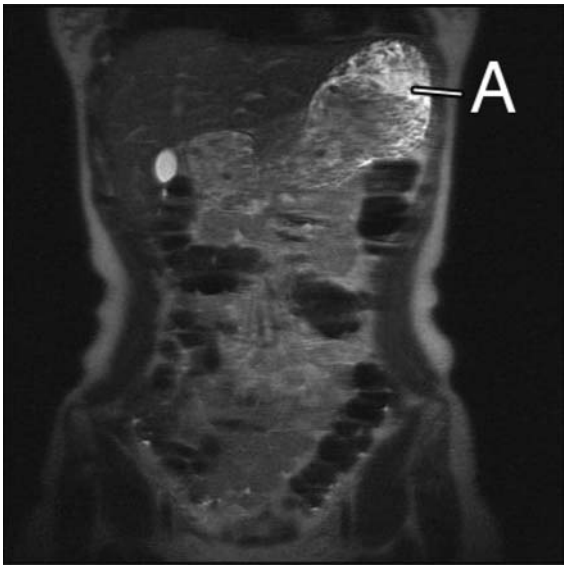

Figure 21.2 T2-weighted image showing water in the fundus when the subject is recumbent [47].

The stomach is not rigid and, as a predominately muscular structure, changes shape on filling. The upper part of the stomach (the fundus) undergoes receptive relaxation to accommodate the ingested food that is kneaded at the bottom of the stomach (the pyloric region). In the upright position when visualized with X-ray contrast, the stomach has classically a fishhook shape, but on lying down, the fundal area falls into the abdomen and becomes the lowest part. In the T2-weighted MRI image in Figure 21.1, the subject is lying on the back and the water appears brightest in the image. Thus, posture will influence the relative distribution in the stomach strongly (Figure 21.2).

Stratification of gastric contents is also evident when an upright posture is adopted. For example, if a raft-forming alginate-based antacid formulation is taken after a meal, with the subject upright or seated, the formulation may be retained in the upper stomach by a mixture of flotation and stratification provided there is sufficient gas generated to increase buoyancy. The timing of the dosing of the formulation relative to the meal is quite critical. When taken after a meal, an almagate-based preparation Flot-Coat was demonstrated to reside in the stomach on top of the meal and empty from the stomach more slowly than the food. The time for 50% of the Flot-Coat granulate to empty was more than 4.5 h compared to 2.3 h for the meal. The standard granulate mixed and emptied with the digestible solid phase of the meal, with 50% emptying in 1.7 h [25].

Mixing in the stomach and the intragastric distribution result from postural and motility effects, which are strongly influenced by the type of the meal. The effects of functional separation into an upper, low-motility reservoir and a lower grinding chamber can be shown by differences in absorption rates according to the sequence

of administration relative to meal intake. For water-soluble drugs given in liquid meal, the substance will be uniformly distributed within about 40 to 80 min; however, this is not the case for drug intake after solid meals [26, 27]. The currently unsolved problem of the inhomogeneity of intragastric distribution is, in our experience, a major source of unwanted food effects after administration of ER products (dose dumping), erratic blood levels with class II substances, and a mostly ignored critical issue of many current concepts for gastroretentive delivery systems [28]. The influence of this effect is nicely shown with data obtained following administration of extended release formulation of amoxicillin and clavulanate (Augmentin XR). In the prescribed information, it is advised that Augmentin XR has to be taken at the beginning of a meal. The formulation was labeled with small amounts of magnetite to permit imaging of the position and the rate of disintegration by magnetic moment imaging. Intake under fasting conditions led to a decreased amoxicillin absorption and intake after the meal resulted in a decreased clavanulate absorption. These differences were the result of early gastric emptying of the tablets in case of fasting administration and prolonged intragastric residence in case of administration after the meal. Early gastric emptying causes a reduced absorption of amoxicillin due to its absorption window in the upper GI tract and long intragastric residence results in a poor bioavailability of clavulanic acid due to acid-catalyzed hydrolysis [29].

In response to food, the parietal cells secrete acid that will be moved upward by contractions of the pylorus. In an individual with an incompetent cardiac sphincter, this can result in a reflux of acid into the esophagus. To assess food and acid reflux, patients are provided with a refluxogenic meal, after which the reflux of technetium-99m-labeled food and acid appearance in the esophagus are monitored using ambulatory pH and radioisotope telemetry [30]. Using this technique, the reflux of acid and food was noted to be quite separate events and consistent with a mechanism by which acid can move around the food mass. This related to another observation during the reformulation of paracetamol (acetaminophen) into both fast-acting and sustained-acting preparations. Gamma scintigraphy was utilized to examine the emptying of a novel paracetamol formulation in the fed and fasting state. In the fasting state, we expected to be able to show faster dissolution of the formulation and a consequent increased rate of gastric emptying. This we were able to do; however, we also found that the novel formulation showed faster gastric emptying in the fed state. The scintiscans in Figure 21.3 indicate that the phenomenon is probably due to rapid dissolution and movement of the formulation around the food mass in the stomach [31]. It is known that liquid and solids empty the stomach at different rates, although the significance of the discrete boundary phase has been ignored.

It is well established that a meal containing sufficient fat will stratify. By using MRI, several investigators have been able to show the appearance of a fat layer on the fundal gastric contents after a fatty meal. In this situation, the inhibitory effects of fats are reduced, since the fat must be homogenized, emulsified, and presented to the duodenal receptors before an action is initiated. If a suitable substrate for dispersion of fat is provided (i.e., minced beef), the inhibitory effects of fats on the rate of gastric emptying are increased. This indicates that significant differences in intragastric distribution of fat occur after eating a meal [32].

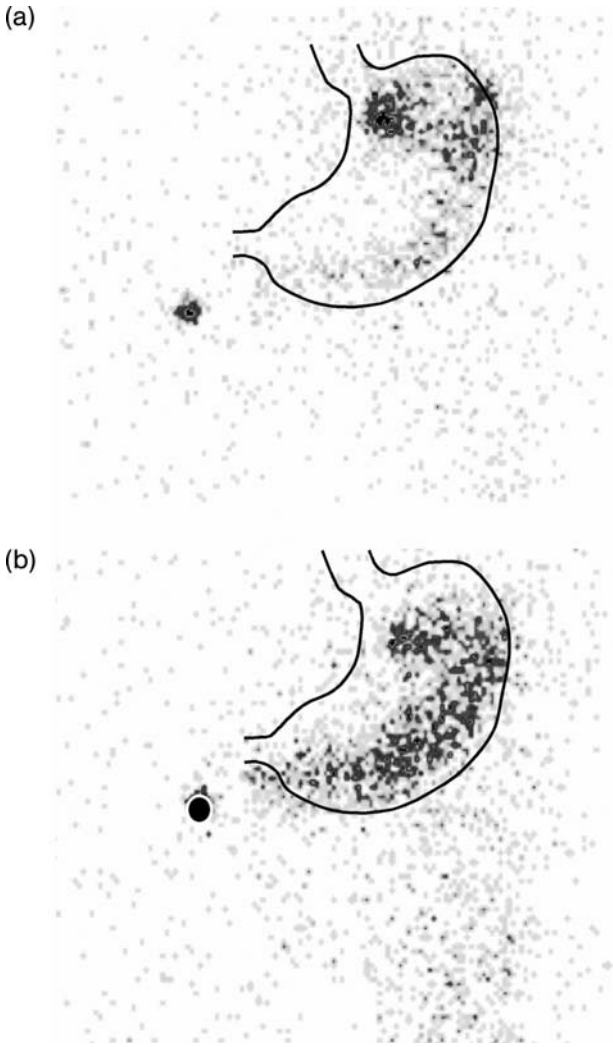

Figure 21.3 (a and b) The start of a sequence of static views of a radiolabeled paracetamol tablet. In frame (a), the tablet has started to dissolve and the released drug and radioactivity move along the greater curvature of the stomach. In frame (b), antral mixing has started to move the label and the drug into the food mass in the pyloric antrum.

21.4.2 Gastric Emptying

The rate of gastric emptying under fed conditions is controlled by the energy content of the meal, the energy requirement of the body, and feedback mechanisms including the ileal brake mechanism [33, 34]. Furthermore, the rate of gastric emptying of

nondisintegrating systems under fed conditions is also influenced by particle size. For food components, the mean emptying rate depends on the caloric content as described in the classical studies of Hunt and colleagues [35]. As a consequence, the emptying of drug substances from the stomach in the digestive phase depends on three main factors: the gastric emptying rate of the meal, the intragastric distribution of the drug, and the particle size of the formulation. In clinical food effect studies, a serving of a high-caloric (1000 kcal), high-fat (50% of calories) breakfast is administered before the drug formulation [36] resulting in very long gastric residence times. In our experience, this huge and unnatural food load for small individuals will cause large physiological effects, and typical volunteers with body weights less than 80 kg will not have completely emptied a test high-fat breakfast even when lunch is served 4–6 h later.

There has been an intensive effort to determine a distinct upper size limit with regard to particle emptying under fed conditions for years. This concept was mainly driven by the hypothesis that the pylorus acts under fed conditions as a filter with a fixed effective aperture of about 2 mm This concept is not valid. Gastric emptying is the result of a coordinative function of pyloric opening and antral contractions, producing what is known as gastric sieving [37]. Owing to the involvement of sedimentation processes, the particle size of withdrawn (retropulsed) material is a function of meal viscosity and particle density [38].

In the elderly, subtle changes in emptying are seen and distinct trends are hard to elucidate [39]. There is an increased incidence of reflux associated with slow esophageal clearing, probably associated with weaker peristaltic contractions and the presence of muscular abnormalities such as hiatus hernia. The MMC complex is maintained until the eighth or ninth decade of life with clear propagation of phase-III activity suggesting that short-range intrinsic intestinal nervous pathways are maintained [40]. Studies on aging laboratory animals suggest that neurons are lost from the myenteric plexus, particularly the nonadrenergic pathway of the proximal jejunum, but plasticity and adaptation of the human bowel compensate to preserve motility. Thus, diseases normally associated with abnormal motility such as bacterial overgrowth are not primarily a reflection of normal aging. The clearest evidence for aging effects are seen with regard to the emptying of mixed meals and in the slower gastric emptying of the liquid phase suggesting changes in the motility of the fundus [41], although fasting and postprandial antral motility remains normal [42].

Gender – or, more particularly, the menstrual cycle – has also been mentioned as a significant influence on the whole-gut transit. Madsen and colleagues carried out a study to elucidate the influences of gender, age, and body mass index (BMI) on gastrointestinal transit times using a meal containing [^{99m}Tc]-labeled cellulose as a fiber and 2–3 mm [^{111}In]-labeled plastic particles. Seventeen healthy young and sixteen healthy older subjects (eight men, eight women) were studied. All transit variables were unaffected by gender. The older subjects had a slower mean colonic transit time of radiolabeled plastic particles than the young subjects ($p < 0.05$), while BMI affected the gastric emptying of fiber but not other gastrointestinal variables [43]. In another study comparing young and elderly males, which employed ultrasonographic and radiographic techniques to measure transit, no age-related effect could be determined [44].

According to a survey of the literature conducted by Baron and colleagues between 1963 and 1992, there appears to be a reduction in the rate of small-bowel and colonic transit during pregnancy [45]. Gastrointestinal symptoms were reported predominantly as abdominal bloating and constipation. These effects are mediated by progesterone, with estrogen probably acting as a primer.

21.4.3
Small Intestinal Transit Patterns

Small intestinal transit of nondisintegrating dosage forms as well as chyme is extremely discontinuous and characterized by phases of rest and short episodes of transport. In Figure 21.4, the velocity profile of an enteric-coated tablet from ingestion until disintegration (141 min postadministration) is shown. The postulation that the small intestine is a tube filled with fluid allowing the transit dosage forms in a continuous movement is completely misleading [46]. Nonabsorbable materials including fibers or modified release dosage forms usually gather in the terminal small ileum together with remaining fluid. Generally, the contents by the end of the small intestine are a homogeneous mass unlike the very high heterogeneity of the stomach contents.

After intake of the next meal, motility is increased and the contents of the terminal ileum are transported into the ascending colon, a mechanism known as the gastroileocecal reflex [47, 48]. Small intestinal transit time (SITT) of nondissolving dosage forms in humans is reported to be usually quite constant with a mean transit time of about 3 h. This mean small intestinal transit time of solids depends on the interval between dosing of the medication and the serving of the next meal, illustrating the strong influence of the gastroileocecal reflex. Accordingly, the scheme of food administration after dosing of the medication is of major influence on small intestinal transit times.

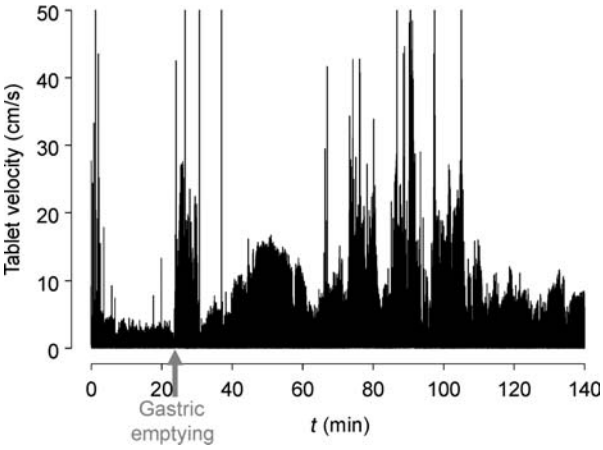

Figure 21.4 Velocity profile of an enteric-coated tablet from ingestion until disintegration in the small intestine (gastric emptying at 24 min).

21.4.4
Modulation of Transit to Prolong the Absorption Phase

Adhesion and slowing intestinal transit are two mechanisms that have been proposed to extend the absorption phase of drugs, particularly if colonic permeability is poor. Our real-time measurements of the transit of formulations along the GI tract elegantly demonstrate that during the initial phases of transit through the duodenum and jejunum, the formulation is swept forward in a series of pulsatile movements that would leave little opportunity for adhesion in the upper gut in the fasting state [28].

It is well appreciated that dietary fat retards proximal gastrointestinal transit. Since absorption of fats is generally complete in the healthy gut by the distal ileum, the colon epithelium is not equipped to process fats and excess load leads to steattorhea.

The role of lipids on absorption has been extensively reviewed by Porter and Charman [49, 50]. The influences are diverse and include effects on lumenal drug solubility, altering the metabolic and barrier function of the intestinal wall, stimulating lymphatic transport, and a reduction in gastric transit, thereby increasing the time available for dissolution.

21.4.5
Absorption Enhancement

As mentioned earlier, treatments that transiently open up intercellular gaps increase absorption significantly. In the villus, the loss of apical cells may cause large gaps at the tip, allowing drug to enter through the lymphatic spaces. Prolonged insult leads to an alteration of the goblet cell/enterocyte ratio and a histological phenomenon known as goblet cell capping. This effect can be seen after quite short exposures with high concentrations of low molecular weight polyethylene glycol [51] and is a response to osmotic stress.

As pointed out by Baluom and colleagues, absorption enhancers are efficient in small body cavities such as the nasal and the rectum [52]. In the fed state, the issues of dilution during gastric mixing would probably obviate the possibility of interaction between the dispersed phase and the small intestine. Using a perfused rat model, the authors showed that a synchronized administration of an absorption enhancer (sodium decanoate) is required for optimal absorption of a poorly absorbed drug (cefazoline) and that levels of the enhancer need to be sustained rather than high.

The finding that grapefruit juice can increase the bioavailability of certain drugs, by reducing presystemic intestinal metabolism, led to interest in the area of "food–drug interactions." It has been suggested that this could be exploited to increase bioavailability, especially for poorly soluble compounds. Interest focused particularly on the effects of the grapefruit flavonoid, naringin, and the furanocoumarin, 6′,7′- dihydroxybergamottin on the activity of intestinal CYP3A4. Given that P-gp and canalicular multispecific organic anion transporters are involved in the intestinal absorption and biliary excretion of a wide range of drugs and metabolites, it is reasonable to

suspect that furanocoumarins may alter drug disposition in humans [53]. Wagner and colleagues [54], in a review of food effects on intestinal drug efflux, have recently suggested that the effect of grapefruit juice is likely to be due to the inhibition of intestinal P-glycoprotein rather than metabolism. Recent reviews suggest that the influence of grapefruit juice is controversial with activation or inhibition of P-gp being noted, although the inhibitory action on intestinal rather than hepatic CYP3A4 is clearly established [55].

Animal data suggest that dietary salt modulates the expression of renal CYPs. Darbar and colleagues [56] extended this observation to suggest that intestinal CYP3A may be similarly modulated by dietary salt. They studied the effects of dietary salt on the kinetics of quinidine on normal volunteers, each given high-salt (400 mEq/day) and low-salt (10 mEq/day) diets for 7–10 days. They found that plasma concentrations after oral quinidine were significantly lower during the high-salt phase, with the difference between the two treatments attributable to changes within the first 1–4 h.

The possibility of exploiting excipient effects, particularly of the nonionic detergents, such as Tween 80 or Pluronic, has been of interest to several laboratories. The data suggest that a strategy based on bioavailability enhancement for drugs undergoing intestinal secretion might be valid with the caveats general to absorption enhancers. The effects are evident with model peptides and with cyclosporin, whose bioavailability is increased in normal subjects when the drug is coadministered with D-α-tocophenylpolyethylene glycol 1000 succinate [57].

21.5
The Lower GI Tract: The Colon

At the end of the small intestine, deposition is almost complete and there is no need for intestinal secretions to aid assimilation. The principal role of the colon is to resorb water and reclaim sodium, which it does very efficiently; for every 2 l of water entering the colon, the residual water in the stools will be less than 200 ml.

The material that arrives in the colon will contain cellulosic materials from the vegetables in the diet, which cannot be broken by the intestinal secretions. In the cecum, a bacterial ecosystem digests the soluble, fermentable carbohydrates to yield short-chain fatty acids that are assimilated into the systemic circulation by the colon, together with vitamin K released from the plant material. Carbon dioxide release is also a fermentation product, and if the redox potential is sufficiently low, bacteria can produce methane and hydrogen, which can be detected in the breath particularly after the ingestion of pulses. In the upright position, the gas will rise to the transverse colon: an adult produces approximately 2–3 l/day of which most is exchanged through the lungs. The accumulation is illustrated in Figure 21.5.

The average bacterial load of the colon has been estimated at just over 200 g (equivalent to approximately 35 g dry weight). Water available for dissolution is maximal in the ascending colon and 1.5–2 l of water enters from the terminal small intestine each day. The amount of water present varies, being maximal in the period

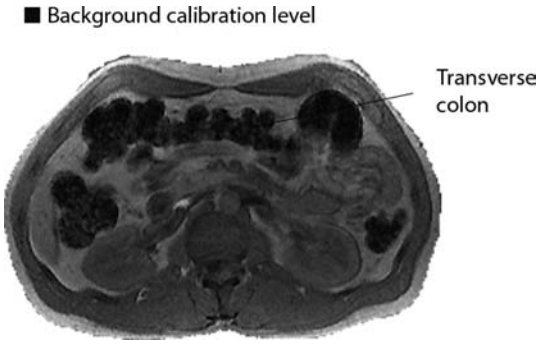

Figure 21.5 Accumulation of gas in the transverse colon illustrated by MRI.

4–8 h after ingestion of a meal. In the morning, the colon is often empty, and any material remaining in the ascending colon is slowly cleared. Thus, availability of water appears to be very small. In a recent MRI study conducted by one of the authors, the total water content of the colon was determined at about 10–15 ml [46]. These estimates have been recently confirmed by direct cecal sampling by a collaboration between Reppas, Dressman, and colleagues. The consequences of this poor availability of water or colon drug targeting or extended release systems must be carefully considered.

21.5.1 Colonic Transit

The data available concerning the movement through the gut were previously confined to measurements of whole-gut transit time until gamma scintigraphy became a routine tool in pharmaceutical research. Both the stomach and the colon can be identified unambiguously in planar images, allowing the contribution of colonic absorption in the plasma-concentration–time profile to be assessed in each individual. Table 21.2 shows colonic transit of single-unit dosage forms when dosed at different times of the day.

There is a large variability in the data, but in general, units administered prior to retiring for the night have a slower colonic transit than those dosed in the morning, which is in agreement with the pattern of electrical and contractile activity measured by

Table 21.2 Colonic transit times (h) of single unit dosage forms [37].

Colon region	Time of dosing			
	Morning fasting	Morning light breakfast	Morning heavy	Evening breakfast
Ascending	3.6 ± 1.2	2.5 ± 1.5	4.8 ± 3.9	8.9 ± 4.0
Transverse	5.6 ± 2.9	—	—	11.3 ± 3.2

several workers [58–61]. Only a proportion of the colon will be usable for drug delivery, unless prepared by irrigation, and the useful sites will generally include the cecum and ascending and transverse colon. The length of time available for drug release in these regions of the gut, and the influence of formulation variables (size, shape, and density) on transit in "normal" and pathophysiological conditions, is therefore of great interest to pharmaceutical scientists. There are conflicting values in the literature regarding transit from cecum to splenic flexure; for example, in a study quantifying the change in geometric center in normal and slow transit, the value was approximately 15 h in normal subjects and 52 h in patients with slow colonic transit [62].

Gamma scintigraphy was used to compare the colonic transit rate of different sizes of nondisintegrating radiolabeled model dosage forms in healthy subjects. In the first study, colonic transit of radiolabeled capsules, volume 0.3–1.8 cm^3 and density 0.7–1.5 g/cm^3, were monitored in 18 healthy subjects. The capsules were administered after an overnight fast and entered the colon, on an average, 5 h after dosing. Transit rates through the proximal colon were independent of capsule density. Effects due to capsule volume were small compared to intersubject variations in transit rates. Within 10 h of entering the colon, 80% of the units had reached the splenic flexure [63].

By administering both sizes of formulation simultaneously, a better discrimination of relative transit of the two phases can be made. In a cohort of 22 healthy young volunteers, an enteric-coated capsule was administered, which contained tablets ([^{99m}Tc]-labeled; 5 or 8.4 mm in diameter) together with pellets ([^{111}In]-labeled 0.2 mm ion-exchange resin particles). The unit delivered the radiopharmaceuticals simultaneously to the ileocecal junction [64]. Under controlled conditions, no difference was observed between the rate of transit through the ascending colon of 0.2 mm particles versus 5 mm tablets or 0.2 mm particles versus 8.4 mm tablets. The mean period of residence of 50% of the administered 0.2 mm particles in the ascending colon was 11.0 ± 4.0 h.

Adkin and colleagues compared transit of 3, 6, and 12 mm nondisintegrating [^{111}In]-labeled tablets in eight healthy male volunteers. The transit of tablets through the ileocecal junction was unaffected by tablet size. All tablets entered into the colon as a bolus. The 3 and 6 mm tablets were retained in the ascending colon for the longest period of time [65].

21.5.2 Time of Dosing

The time of dosing is an important parameter with regard to the whole-gut transit of nondisintegrating formulations. Sathyan and colleagues [66] have noted that an analysis of 1163 administrations of OROS devices showed a bimodal distribution clustered at 12 and 36 h following nighttime dosing and 24 and 48 h after morning dosing. After nighttime dosing, a monolithic device will be propulsed forward during the strong contractile activity on waking and rising, but may not move far enough to be excreted. Our own data show that, subsequent to the mass movement in the first hour of rising, propulsive movements are weak until sometime after the lunchtime meal has been ingested [67].

21.5.3
Modulating Colonic Water

In our early attempts at producing models of diarrheal predominant disease, it was found that the administration of the laxative lactulose provided a useful and reversible simulation of altered colonic hydrodynamics such as might be seen in colitis. Lactulose is used therapeutically to manage a number of conditions including hepatic encephalopathy, constipation, and salmonellosis. This semisynthetic disaccharide is neither metabolized nor absorbed in the normal small intestine, but may undergo bacterial fermentation in the colon to short-chain fatty acids and gases. Major consequences include a fall in pH and a change in the composition and metabolic activity of the colonic flora [68]. The changes provoked by lactulose are sensitive to fiber supplementation [69] and can be reversed by codeine [70].

In the experiments with enteric-coated tablet plus pellet preparations [64], a second leg was conducted in which a preparation containing 5 mm tablets and 0.2 mm resin was administered after laxative treatment. Following lactulose dosing, there was a significant acceleration in colonic transit and the ascending-colon residence time of the 0.2 mm resin was significantly shorter than that for the 5 mm tablets, though the magnitude of the effect was small.

In later experiments, stool water content was modulated and the influence of luminal water content on the absorption from the distal gut of either quinine (a transcellular probe) or [^{51}Cr]-EDTA (a paracellular probe) was observed. Absorption of these probe markers from a timed-release delivery system was determined following treatment with lactulose 20 ml t.d.s. (increasing water content) or codeine 30 g q.d.s. (decreasing water content) and compared with control untreated values. Lactulose accelerated ascending-colon transit, increased stool water, caused greater dispersion of released material, and enhanced the absorption of the quinine compared to control. Conversely, codeine slowed down ascending colon, reduced stool water content, and also tended to diminish absorption. More distal release resulted in less absorption in the control arm, whereas lactulose enhanced drug absorption from the distal gut [71]. An interesting finding was that a proportion of the asymptomatic normal volunteers showed higher than expected urinary recoveries of [^{51}Cr]-EDTA (5–10% of dose) suggesting an increased paracellular permeability.

Other workers have shown that the increased fluid load produced by an osmotic laxative results in redistribution of colonic contents. Since the distal colon is considered to be mainly a conduit without extensive storage function, Hammer and colleagues considered whether the capacity of the colon to retain fluid might be relevant in compensating for increased fluid loads and preventing diarrhea. Changes in distribution following cecal infusion of an iso-osmotic solution labeled with [^{99m}Tc]-DTPA containing polyethylene glycol (PEG; 500 ml) were compared with changes following infusion of an equal amount of readily absorbable electrolyte solution. After the osmotic load, fecal output was increased significantly ($p < 0.05$), but whole-colonic transit after PEG infusion was not different from transit after the

electrolyte solution ($p > 0.05$), indicating that the distal colon is able to manage nonabsorbable fluid volumes to a large extent [72].

21.6 Pathophysiological Effects on Transit

Active left-sided colitis is often resistant to topical therapy, and resolution may only be achieved by administration of systemic therapy. Twenty-two volunteers and ten patients were recruited for a clinical trial in which they received morning doses of a Eudragit-coated capsules containing [^{111}In]-labeled resin pellets [73]. At day 4 into the regime at steady state, the relative distribution of the marker was measured in the ascending, transverse, descending, and rectosigmoid colon. The results showed that colonic distribution among healthy subjects was asymmetric, with two-thirds of the administered dose in the proximal colon and one-third in the distal colon. In the patients, this difference was even more pronounced, with only one-tenth of the administered dose in the distal segment.

Rapid transit through this region suggests that the area is empty of colonic contents most of the time, and so the opportunity for topical treatment is consequently limited. If the exposure to a drug such as mesalazine is calculated on the basis of these data, the results show that treatment is probably inadequate. For example, the dose per day is approximately 3 g (800–1200 mg, t.d.s.), and therefore in active disease, the effective dose would be about 300 mg on the basis of this regimen. Doses of between 500 and 1000 mg are often given as an enema, but these doses are more effectively delivered and not sequestered within a viscous, partially dehydrated stool, as would be the case following oral administration. Modern "gold standard" treatment suggests that a combined oral and rectal dosing strategy is the most efficacious method of using this drug.

Although discrete effects of diseases are often noted by studying a single parameter such as gastric emptying, the effects of pathophysiological conditions, once established, are usually evident throughout the gut. Mollen and colleagues attempted to describe the motor activity of the upper gastrointestinal tract in patients with slow-transit constipation using perfusion manometry. Orocecal transit time was found to be similar between patients and controls, but esophageal motility was abnormal in 5 out of 18 patients and gastric emptying was abnormal in 8 out of 15 patients. These data support the case that disorders of upper gut motility occur frequently in patients with slow-transit constipation [74]. Gattuso studied 10 young patients with idiopathic megarectum using radiographic and scintigraphic methods. All patients had a dilated large bowel, with no radiographic evidence of upper gut dilation. Gastric emptying was normal in four patients and abnormally slow in six, which suggested that this bowel condition might be reflected in a disturbance of upper gut function. Both radioisotope scans and radio-opaque marker studies showed abnormal colonic transit, and regions of delay corresponded with the region of dilated bowel [75].

Studies in dogs have shown that postoperative ileus following surgery resolves an initial phase of weak irregular, nonpropagating contractions of the gastrointestinal tract, followed by transmission of the contractions from the upper gut to the lower gastrointestinal tract. Tsukamoto [76] found that recovery from postoperative ileus was aided by a change in the pattern of gastrointestinal motility in which contractions were transmitted from the stomach to the lower gastrointestinal tract, like an interdigestive migrating contraction. Bouchoucha characterized colonic transit time in 30 healthy subjects and in 43 patients with inflammatory bowel disease using X-ray opaque markers. The response to food was different in the two populations: in controls, the cecum and ascending colon emptied and filled the distal bowel, whereas in patients, only the splenic flexure and left transverse colon emptied. Movement through both the right and the left colon in patients was observed to be much slower than that in controls, both before and after a meal [77].

Patients with anxiety and depression often have bowel symptoms. Gorad and colleagues compared 21 psychiatric outpatients with generalized anxiety disorders and depression with an equal number of healthy controls. Whole-gut transit time (WGTT) was found to be shorter in patients with anxiety (mean 14 h; range 6–29 h) than in either those with depression (mean 49 h; range 35–71 h; $p < 0.001$) or controls (mean 42 h; range 10–68 h; $p < 0.001$). In patients with anxiety, orocecal transit time (measured using the lactulose hydrogen breath test) was shorter than in patients with depression and also shorter than in controls. The authors concluded that anxiety is associated with increased bowel frequency, while depressed patients tend to be constipated; taken together, these data strongly suggested that mood has an effect on intestinal motor function [78]. Bennett and colleagues [79] concluded that male hypochondriacs had normal intestinal transit, whereas elderly females with depressive illness were more likely to have both colonic and gastric stasis.

Among several disease conditions that affect gastric emptying, diabetes is probably the most extensively studied. Folwaczny and colleagues used scintigraphy to examine esophageal transit and gastric emptying and a metal-detector test to determine large bowel motility in patients with type I and type II diabetes. These authors concluded that both gastric emptying and large bowel transit were affected by both conditions [80].

The alteration of transit by disease, or a change produced by hydrodynamic factors such as diarrhea, will be highly significant for sophisticated zero-order release formulations such as osmotic pumps. For the pumps, inadequate retention may occur in some patients, perhaps leading to less optimal clinical outcome. Even in normal subjects, the range of intestinal transit time can be extreme; for example, the median gastrointestinal transit time for both oxprenolol and metoprolol OROS drug delivery systems has been reported as 27.4 h, with individual times ranging from 5.1 to 58.3 h [81].

Hammer [82] conducted an experiment in which volunteers received either autologous blood or egg white by duodenal intubation to simulate the condition of upper gastrointestinal bleeding. [^{99m}Tc]-DTPA was added to each infusion and arrival at, and clearance from, the colon was recorded. At 4 h after the start of blood infusion, a median of 30% of counts was observed in the transverse colon compared to 0% after

egg white administration; small intestinal transit was unaffected. Although it had been established that bleeding alters gastric motility, this demonstration for the first time that haem-containing proteins have a significant effect on proximal bowel motility.

21.7
Pathophysiological Effects on Permeability

Inflammation leads to changes in permeability of large and polar molecules, which forms the basis of diagnostic tests such as urinary recovery of [^{51}Cr]-EDTA after oral administration. Evidence for increased permeability to very large molecules and small particles in humans is limited, although in an experimental model of colitis in the rat, Lamprecht [83] demonstrated significant uptake of 100 nm-sized particles compared to controls.

21.8
pH

The pH changes of the gut are obvious triggers for the delivery of drug from enteric-coated preparations, in particular, tablets used for the delivery of topical agents in the treatment of bowel disease. Sasaki and coworkers measured pH profiles in the gut in patients with Crohn's disease by using a pH-sensitive radiotelemetry capsule as it traveled from the stomach to the cecum. Gastrointestinal pH profiles measured in four patients with left-sided Crohn's disease were similar to those in four gender- and age-matched control subjects. In contrast, colonic luminal pH profiles in both right and left colon in active or quiescent Crohn's disease showed more coarse fluctuations, with significantly lower values than were seen in controls [84].

The bulk luminal pH is heavily affected by the fermentation of carbohydrates to short-chain fatty acids; however, near the colonic mucosa, the pH rises and changes in the bulk pH have little effect on the epithelial microclimate. Bicarbonate/chloride exchange is partly responsible for raising the pH against the challenge posed by the high colonic p_{CO_2} and the acid production by fermentation. The mucus has been shown to contain a distinct carbonic anhydrase, produced by epithelial tissues that help to carefully regulate the thick unstirred layer of the colonic epithelium.

Many patients with Crohn's disease undergo an ileocecal resection, which might be expected to influence small intestinal pH and transit time. A "radiopill" technique (similar to that of Sasaki *et al.*) was used by Fallingborg and colleagues [85] to examine intraluminal pH and transit time in ileocecally resected Crohn's disease patients. These data were compared with those obtained from 13 healthy volunteers. The mean SITT was significantly shorter in patients than in controls (5.2 and 8.0 h, respectively). However, although the pH levels of the small intestine were identical in patients and controls, cecal pH was 0.9 pH units higher in resected Crohn's disease patients, and the period when the pH was elevated above 5.5 was significantly shorter in patients than in controls [86].

21.9 Conclusions

In summary, it is emphasized that disease conditions may result in changed physiological parameters that could strongly influence the effectiveness of orally administered medications. Changes in patterns of motility, pH, and amount of water available for dispersion and dissolution may be significant for patients compared to the "normal" population. On this basis, it seems appropriate to completely investigate the impact of a target disease – whether it is diabetes, inflammatory bowel disease, or irritable bowel syndrome – on the deposition of drug from the candidate delivery system. Neglect of these issues might lead to suboptimal therapy and a waste of healthcare resources.

References

1 Matolsky, A.G. and Parakkal, P.F. (1985) Membrane coating granules of keratinising epithelia. *The Journal of Cell Biology*, **24**, 297–307.

2 Salamat-Miller, N., Chittchang, M. and Johnson, T.P. (2005) The use of mucoadhesive polymers in buccal drug delivery. *Advanced Drug Delivery Reviews*, **57**, 1666–1691.

3 Smart, J.D. (2005) Buccal Drug Delivery. *Expert Opinion in Drug Delivery*, **2**, 507–517.

4 Bell, M.D.D., Murray, G.R., Mishra, P., Calvey, T.N., Weldon, B.D. and Williams, N.E. (1985) Buccal morphine: a new route for analgesia. *Lancet*, **1**, 71–73.

5 McElnay, J.C. and Hughes, C.M. (2002) Drug delivery: buccal route, in *Encyclopaedia of Pharmaceutical Technology* (ed. J. Swarbrick), Marcel Dekker, New York, pp. 800–810.

6 Gordon, D.B. (2006) Oral transmucosal fentanyl citrate for cancer breakthrough pain: a review. *Oncology Nursing Forum*, **33**, 257–264.

7 Squier, C.A. (1986) Penetration of nicotine and nitroso-nornicotine across porcine oral mucosa. *Journal of Applied Toxicology*, **6**, 123–128.

8 Adrian, C.A., Olin, H.B.D., Dalhoff, K. and Jacobsen, J. (2006) *In vivo* human buccal permeability of nicotine. *International Journal of Pharmaceutics*, **311**, 196–202.

9 Hoogstraate, J., Benes, J., Burgaud, S., Horriere, F. and Seyler, I. (2001) Oral trans-mucosal drug delivery, in *Drug Delivery and Targeting* (eds A.M. Hillery, A.W. Lloyd and J. Swarbrick), Taylor & Francis, London, pp. 186–206.

10 Portero, A., Remuñán-López, C. and Vila-Jato, J.L. (1998) Effect of chitosan and chitosan glutamate enhancing the dissolution properties of the poorly water soluble drug nifedipine. *International Journal of Pharmaceutics*, **175**, 75–78.

11 Uzunoglu, B., Senel, S., Hincal, A.A., Ozalp, M. and Wilson, C.G. (2000) Formulation of a bioadhesive bilayered buccal tablet of natamycin for oral candidiasis. *Proceedings of the International Symposium on Control Related Bioactive Materials*, **27**, 8205.

12 Gordon, D.B. (2007) New opioid formulations and delivery systems. *Pain Management Nursing*, **8**, S6–S13.

13 Darwish, M., Kirby, M., Robertson, P., Jr, Tracewell, W. and Jiang, J.G. (2006) Pharmacokinetic properties of fentanyl effervescent buccal tablets: a phase I, open-label, crossover study of single-dose 100, 200, 400, and 800 microg in healthy adult

volunteers. *Clinical Therapeutics*, **28**, 707–714.

14 Darwish, M., Kirby, M. and Jiang, J.G. (2007) Effect of buccal dwell time on the pharmacokinetic profile of fentanyl buccal tablet. *Expert Opinion on Pharmacotherapy*, **8**, 2011–2016.

15 Gallo, S.H., Mcclave, A., Makk, L.J. and Looney, S.W. (1996) Standardization of clinical criteria required for use of the 12.5 millimeter barium tablet in evaluating esophageal lumenal patency. *Gastrointestinal Endoscopy*, **44**, 181–184.

16 Osmanoglou, E., Van Der Voort, I.R., Fach, K., Kosch, O., Bach, D., Hartmann, V., Strenzke, A., Weitschies, W., Wiedenmann, B., Trahms, L. and Mönnikes, H. (2004) Oesophageal transport of solid dosage forms depends on body position, swallowing volume and pharyngeal propulsion velocity. *Neurogastroenterology and Motility*, **16**, 547–556.

17 Ekeberg, O. and Feinberg, M.J. (1991) Altered swallowing function in elderly patients without dysphagia: radiologic findings in 56 cases. *American Journal of roentgenology*, **156**, 1181–1184.

18 Richards, D.G., Mcpherson, J.J., Evans, K.T. and Rosen, M. (1986) Effects of volume of water taken with diazepam tablets on absorption. *British Journal of Anaesthesia*, **58**, 41–44.

19 Perkins, A.C., Wilson, C.G., Frier, M., Blackshaw, P.E., Dansereau, R.J., Vincent, R., wenderoth, D., Hathaway, S., Li, Z. and Spiller, R.C. (2001) The use of scintigraphy to demonstrate the rapid esophageal transit of the oval film-coated placebo risedronate tablet compared to a round uncoated placebo tablet when administered with minimal volumes of water. *International Journal of Pharmaceutics*, **222**, 295–303.

20 Hardy, J.G., Hooper, G., Ravelli, G., Steed, K.P. and Wilding, I.R. (1993) A comparison of the gastric retention of a sucralfate gel and a sucralfate suspension. *European Journal of Pharmaceutics and Biopharmaceutics*, **39**, 70–74.

21 Dansereau, R.J., Dansereau, R.N. and Mcrorie, J.W. (1999) Scintigraphic study of oesophageal transit and retention, in *Nuclear Medicine in Pharmaceutical Research* (eds A.C. Perkins and M. Frier), Taylor & Francis, London, pp. 57–69.

22 Potts, A.M., Wilson, C.G., Stevens, H.N.E., Dobrozsi, D.J., Washington, N., Frier, M. and Perkins, A.C. (2000) Oesophageal bandaging: a new opportunity for thermosetting polymers. *STP Pharma Sciences*, **10**, 293–301.

23 Holt, S. (1981) Observations on the relation between alcohol absorption and the rate of gastric emptying. *Canadian Medical Association Journal*, **124**, 267–277.

24 Wilson, C.G. (1999) Gastrointestinal transit and drug absorption, in *Oral drug Absorption* (eds J.D. Dressman and H. Lennernas), Marcel Dekker, New York, pp. 7–15.

25 Washington, N., Steed, K.P. and Wilson, C.G. (1992) Evaluation of a sustained release formulation of the antacid almagate. *European Journal of Gastroenterology and Hepatology*, **4**, 495–500.

26 O'reilly, S., Wilson, C.G. and Hardy, J.G. (1987) The influence of food on gastric emptying of multiparticulate dosage forms. *International Journal of Pharmaceutics*, **34**, 213–216.

27 Faas, H., Steingoetter, A., Feinle, C., Rades, T., Lengsfeld, H., Boesiger, P., Fried, M. and Schwizer, W. (2002) Effects of meal consistency and ingested fluid volume on the intragastric distribution of a drug model in humans: a magnetic resonance imaging study. *Alimentary Pharmacology & Therapeutics*, **16**, 217–224.

28 Weitschies, W., Wedemeyer, R.S., Kosch, O., Fach, K., Nagel, S., Söderlind, E., Trahms, L., Abrahamsson, B. and Mönnikes, H. (2005) Impact of the intragastric location of extended release

tablets on food interactions. *Journal of Controlled Release*, **28**, 375–385.

29 Weitschies, W., Friedrich, C., Wedemeyer, R.S., Schmidtmann, M., Kosch, O., Kinzig, M., Trahms, L., Sörgel, F., Siegmund, W., Horkovics-Kovats, S., Schwarz, F., Raneburger, J. and Mönnikes, H. (2008) Bioavailability of amoxicillin and clavulanic acid from extended release tablets depends on intragastric tablet deposition and gastric emptying. *European Journal of Pharmaceutics and Biopharmaceutics*, DOI: 10.1016/j. ejpb. 2008.05.011.

30 Washington, N., Moss, H.A., Washington, C. and Wilson, C.G. (1993) Non-invasive detection of gastro-oesophageal reflux using an ambulatory system. *Gut*, **34**, 1482–1486.

31 Kelly, K., O'mahony, B., Lindsay, B., Jones, T., Grattan, T.J., Rostami-Hodjegan, A., Stevens, H.N.E. and Wilson, C.G. (2003) Comparison of the rates of disintegration, gastric emptying and drug absorption, following administration of a new and a conventional paracetamol formulation, using gamma scintigraphy. *Pharmaceutical Research*, **20**, 1668–1673.

32 Edelbroek, M., Horowitz, M., Maddox, A. and Bellen, J. (1992) Gastric emptying and intragastric distribution of oil in the presence of a liquid or a solid meal. *Journal of Nuclear Medicine*, **33**, 1283–1290.

33 Hellström, P.M., Grybäck, P. and Jacobsson, H. (2006) The physiology of gastric emptying. *Best Practices & Research. Clinical Anaesthesiology*, **20**, 397–407.

34 Cuche, G., Cuber, J.C. and Malbert, C.H. (2000) Ileal short-chain fatty acids inhibit gastric motility by a humoral pathway. *American Journal of Physiology. Gastrointestinal and Liver Physiology*, **279**, G925–G930.

35 Hunt, J.N. and Stubbs, D. (1975) The volume and energy content of meals as determinants of gastric emptying. *The Journal of Physiology*, **245**, 209–225.

36 U.S. Department of Health and Human Services, Food and Drug Administration, Center for Drug Evaluation and Research (CDER). Guidance for Industry: Food-Effect Bioavailability and Fed Bioequivalence Studies, December 2002.

37 Ramkumar, D. and Schulze, K.S. (2005) The pylorus. *Neurogastroenterology and Motility*, **17** (Suppl. 1), 22–30.

38 Marciani, L., Gowland, P.A., Fillery-Travis, A., Manoj, P., Wright, J., Smith, A., Young, P., Moore, R. and Spiller, R.C. (2001) Assessment of antral grinding of a model solid meal with echo-planar imaging. *American Journal of Physiology. Gastrointestinal and Liver Physiology*, **280**, G844–G849.

39 Orr, W.C. and Chen, C.L. (2002) Aging and neural control of the GI tract. IV. Clinical and physiological aspects of gastrointestinal motility and aging. *American Journal of Physiology. Gastrointestinal and Liver Physiology*, **283**, G1226–G1231.

40 Bortolotti, M., Frada, G.J.R., Barbagallo-Sangiogi, G. and Labo, G. (1984) Interdigestive gastroduodenal motor activity in the elderly (Abstract). *Gut*, **25**, A1320.

41 Evans, M.A., Trigg, S.E.J., Cheung, M., Boe, G.A. and Creasey, H. (1981) Gastric emptying rates in the elderly: implication for drug therapy. *Journal of the American Geriatrics Society*, **29**, 201–205.

42 Fich, A., Camilleri, M. and Phillips, S.F. (1989) Effect of age on human gastric and small bowel motility. *Journal of Clinical Gastroenterology*, **11**, 416–420.

43 Madsen, J.L. (1992) Effects of gender, age, and body mass index on gastrointestinal transit times. *Digestive Diseases and Sciences*, **37**, 1548–1553.

44 Brogna, A., Ferrara, R., Bucceri, A.M., Lanteri, E. and Catalano, F. (1999) Influence of aging on gastrointestinal transit time: an ultrasonographic and radiologic study. *Investigative Radiology*, **34**, 357–359.

45 Baron, T.H., Ramirez, B. and Richter, J.E. (1993) Gastrointestinal motility disorders during pregnancy. *Annals of Internal Medicine*, **118**, 366–375.

46 Schiller, C., Fröhlich, C.P., Giessmann, T., Siegmund, W., Mönnikes, H., Hosten, N. and Weitschies, W. (2005) Intestinal fluid volumes and transit of dosage forms as assessed by magnetic resonance imaging. *Alimentary Pharmacology & Therapeutics*, **22**, 971–979.

47 Spiller, R.C., Brown, M.L. and Phillips, S.F. (1987) Emptying of the terminal ileum in intact humans. Influence of meal residue and ileal motility. *Gastroenterology*, **92**, 724–729.

48 Dinning, P.G., Bampton, P.A., Kennedy, M.L., Kajimoto, T., Lubowski, D.Z., De Carle, D.J. and Cook, I.J. (1999) Basal pressure patterns and reflexive motor responses in the human ileocolonic junction. *The American Journal of Physiology*, **276**, G331–G340.

49 Charman, W.N., Porter, C.J.H., Mithani, S. and Dressman, J.B. (1997) Physicochemical and physiological mechanisms for the effects of food on drug absorption: the role of lipids and pH. *Journal of Pharmaceutical Sciences*, **86**, 269–282.

50 Porter, C.J.H. and Charman, W.N. (2001) *In vitro* assessment of oral lipid based formulations. *Advanced Drug Delivery Reviews*, **50**, S127–S147.

51 Bryan, A.J., Kaur, R., Robinson, G., Thomas, N.W. and Wilson, C.G. (1980) Histological and physiological studies on the intestine of the rat exposed to solutions of Myrj 52 and PEG 2000. *International Journal of Pharmaceutics*, **7**, 145–156.

52 Baluom, M., Friedman, M. and Rubinstein, A. (1998) The importance of intestinal residence time of absorption enhancer on drug absorption and implication on formulative considerations. *International Journal of Pharmaceutics*, **176**, 21–30.

53 Evans, A.M. (2000) Influence of dietary components on the gastrointestinal metabolism and transport of drugs. *Therapeutic Drug Monitoring*, **22**, 131–136.

54 Wagner, D., Spahn-Langguth, H., Hanafy, A., Koggel, A. and Langguth, P. (2001) Intestinal drug efflux: formulation and food effects. *Advanced Drug Delivery Reviews*, **50**, S13–S31.

55 Kiani, J. and Imam, S.Z. (2007) Medicinal importance of grapefruit juice and its interaction with various drugs. *Nutrition Journal*, **6**, 33.

56 Darbar, D., Dellorto, S., Morike, K., Wilkinson, G.R. and Roden, D.M. (1997) Dietary salt increases first-pass elimination of oral quinidine. *Clinical Pharmacology and Therapeutics*, **61**, 292–300.

57 Chang, T., Benet, L.Z. and Herbert, M.F. (1996) The effect of water-soluble vitamin E on cyclosporine kinetics in healthy volunteers. *Clinical Pharmacology and Therapeutics*, **59**, 297–303.

58 Frexinos, J., Bueno, L. and Fioramonti, J. (1985) Diurnal changes in myoelectrical spiking activity of the human colon. *Gastroenterology*, **88**, 1104–1110.

59 Narducci, F., Bassotti, G., Gaburri, M. and Morelli, A. (1987) Twenty four hour manometric recording of colonic motor activity in healthy man. *Gut*, **28**, 17–25.

60 Bassotti, G., Crowell, M.D. and Whitehead, W.E. (1993) Contractile activity of the human colon: lessons from 24 hour studies. *Gut*, **34**, 129–133.

61 Bassotti, G., Iantorno, G., Fiorella, S., Bustos-Fernandez, L. and Bilder, C.R. (1999) Colonic motility in man: features in normal subjects and in patients with chronic idiopathic constipation. *The American Journal of Gastroenterology*, **94**, 1760–1770.

62 Cook, B.J., Lim, E., Cook, D., Hughes, J., Chow, C.W., Stanton, M.P., Bidarkar, S.S., Southwell, B.R. and Hutson, J.M. (2005) Radionuclear transit to assess sites of delay in large bowel transit in children with chronic idiopathic constipation. *Journal of Pediatric Surgery*, **40**, 478–483.

63 Parker, G., Wilson, C.G. and Hardy, J.G. (1988) The effect of capsule size and density on transit through the proximal colon. *The Journal of Pharmacy and Pharmacology*, **40**, 376–377.

64 Watts, P.J., Barrow, L., Steed, K.P., Wilson, C.G., Spiller, R.C., Melia, C.D. and Davies, M.C. (1992) The transit rate of different-sized model dosage forms through the human colon and the effects of a lactulose-induced catharsis. *International Journal of Pharmaceutics*, **87**, 215–221.

65 Adkin, D.A., Davis, S.S., Sparrow, R.A. and Wilding, I.R. (1993) Colonic transit of different sized tablets in healthy-subjects. *Journal of Controlled Release*, **23**, 147–156.

66 Sathyan, G., Hwang, S. and Gupta, S.K. (2000) Effect of dosing time on the total intestinal transit time of non-disintegrating systems. *International Journal of Pharmaceutics*, **204**, 47–51.

67 Hebden, J.M., Gilchrist, P.J., Blackshaw, E., Frier, M.E., Perkins, A.C., Wilson, C.G. and Spiller, R.C. (1999) Night-time quiescence and morning activation in the human colon: effect on transit of dispersed versus large single unit formulations. *European Journal of Gastroenterology & Hepatology*, **11**, 1379–1385.

68 Huchzermeyer, H. and Schumann, C. (1997) Lactulose: a multifaceted substance. *Zeitschrift fur Gastroenterologie*, **35**, 945–955.

69 Barrow, L., Steed, K.P., Spiller, R.C., Watts, P.J., Melia, C.D., Davies, M.C. and Wilson, C.G. (1992) Scintigraphic demonstration of accelerated proximal colon transit by lactulose and its modification by gelling agents. *Gastroentrology*, **103**, 1167–1173.

70 Barrow, L., Steed, K.P., Spiller, R.C., Maskell, N.A., Brown, J.K., Watts, P.J., Melia, C.D., Davies, M.C. and Wilson, C.G. (1993) Quantitative, noninvasive assessment of antidiarrheal actions of codeine using an experimental-model of diarrhea in man. *Digestive Diseases and Sciences*, **38**, 996–1003.

71 Hebden, J.M., Gilchrist, P.J., Perkins, A.C., Wilson, C.G. and Spiller, R.C. (1999) Stool water content and colonic drug absorption: contrasting effects of lactulose and codeine. *Pharmaceutical Research*, **16**, 1254–1259.

72 Hammer, J., Pruckmayer, M., Bergmann, H., Kletter, K. and Gangl, A. (1997) The distal colon provides reserve storage capacity during colonic fluid overload. *Gut*, **41**, 658–663.

73 Hebden, J.M., Perkins, A.C., Frier, M., Wilson, C.G. and Spiller, R.C. (2000) Limited exposure of left colon to daily dosed oral formulations in active distal ulcerative colitis: exploration of poor response to treatment? *Alimentary Pharmacology & Therapeutics*, **14**, 155–161.

74 Mollen, R.M.G.H., Hopman, W.P.M., Kuijpers, H.H.C. and Jansen, J.B.M.J. (1999) Abnormalities of upper gut motility in patients with slow-transit constipation. *European Journal of Gastroenterology & Hepatology*, **11**, 701–708.

75 Gattuso, J.M., Kamm, M.A., Morris, G. and Britton, K.E. (1996) Gastrointestinal transit in patients with idiopathic megarectum. *Diseases of the Colon & Rectum*, **39**, 1044–1050.

76 Tsukamoto, K., Mizutani, M., Yamano, M. and Suzuki, T. (1999) The relationship between gastrointestinal transit and motility in dogs with postoperative ileus. *Biological & Pharmaceutical Bulletin*, **22**, 1366–1371.

77 Bouchoucha, M.L., Dorval, E., Arhan, P., Devroede, G. and Arsac, M. (1999) Patterns of normal colorectal transit time in healthy subjects and in patients with an irritable bowel syndrome (IBS). *Gastroenterology*, **116**, G4192.

78 Gorard, D.A., Gomborone, J.E., Libby, G.W. and Farthing, M.J.G. (1996) Intestinal transit in anxiety and depression. *Gut*, **39**, 551–555.

79 Bennett, E.J., Evans, P., Scott, A.M., Badcock, C.A., Shuter, B., Hoschl, R., Tennant, C.C. and Kellow, J.E. (2000) Psychological and sex features of delayed gut transit in functional gastrointestinal disorders. *Gut*, **46**, 83–87.

80 Folwaczny, C., Hundegger, K., Volger, C., Sorodoc, J., Kuhn, M., Tatsch, K., Landgraf,

R. and Karbach, U. (1995) Measurement of transit disorders in different gastrointestinal segments of patients with diabetes-mellitus in relation to duration and severity of the disease by use of the metal-detector test. *Zeitschrift fur Gastroenterologie*, **33**, 517–526.

81 Grundy, J.S. and Foster, R.T. (1996) The nifedipine gastrointestinal therapeutic system (GITS): evaluation of pharmaceutical, pharmacokinetic and pharmacological properties. *Clinical Pharmacokinetics*, **30**, 28–5160.

82 Hammer, J., Lang, K. and Kletter, K. (1998) Accelerated right colonic emptying after simulated upper gut hemorrhage. *The American Journal of Gastroenterology*, **93**, 628–631.

83 Lamprecht, A. Schafer, U. and Lehr, C.M. (2001) Size dependency of nanoparticle deposition in the inflamed colon in inflammatory bowel disease: *in vivo* results from the rat. *Journal of Controlled Release*, **72**, 235–237.

84 Sasaki, Y., Hada, R., Nakajima, H., Fukuda, S. and Munakata, A. (1997) Improved localizing method of radiopill in measurement of entire gastrointestinal pH profiles: colonic luminal pH in normal subjects and patients with Crohn's disease. *The American Journal of Gastroenterology*, **92**, 114–118.

85 Fallingborg, J., Pedersen, F. and Jacobsen, B.A. (1998) Small intestinal transit time and intraluminal pH in ileocecal resected patients with Crohn's disease. *Digestive Diseases and Sciences*, **43**, 702–705.

86 Kleinke, T., Wagner, S., John, H., Hewett-Emmett, D., Parkkila, S., Forssmann, W.-G. and Gros, G. (2005) A distinct carbonic anhydrase in the mucus of the colon of humans and other mammals. *The Journal of Experimental Biology*, **208**, 487–496.

22
Nanotechnology for Improved Drug Bioavailability

Marjo Yliperttula and Arto Urtti

Abbreviations

AUC	Area under the curve
BCS	Biopharmaceutical Classification System
CMC	Critical micelle concentration
DNA	Deoxyribonucleic acid
FDA	Food and Drug Administration
i.v.	Intravenous
PEG	Polyethylene glycol
SEAP	Secreted alkaline phosphatase
siRNA	Small interfering ribonucleic acid

Symbols

3D	Three-dimensional
CD44	Membrane receptor for the hyaluronan uptake into the cells

22.1 Introduction

Nanotechnology is one of the major fields of current pharmaceutical research. This field is strongly related to drug delivery and targeting, because nanosized drug delivery systems are able to modify the pharmacokinetics significantly. Based on the most common definition, nanotechnology is dealing with structures of below 1 μm. At very small sizes, material has peculiar physical chemical properties that are distinct from the macroscopic properties of the same matter. In pharmaceutical nanotechnology, these physical distinctions are not the main point. Rather, pharmaceutical nanotechnology aims to generate structural units below 1 μm and, most importantly, these particulates should have controlled functionalities that improve drug delivery.

Bioavailability is a parameter that defines the fraction of the dose that enters the "site of action." In general, bioavailability refers to the *systemic bioavailability*. After per oral drug administration, the systemic bioavailability is always 0–100%, and the extent of bioavailability is determined by comparing the AUC values of the drug concentration in plasma versus time curves after oral and intravenous (i.v.) (100% bioavailability) drug administration [1]. There are some cases in which systemic bioavailability is improved with nanotechnology (e.g., nanocrystals). However, the main emphasis in the design of nanosystems is to improve *local bioavailability*. For example, nanotechnology is used to increase drug or gene delivery into the diseased target tissue, for example, vessel wall, tumor, or brain [2]. Another therapeutic goal is to improve the therapeutic index. Doxorubicin liposomes are a good example [3]. The drug as such is cardiotoxic as a solution, but liposomal doxorubicin avoids the toxicity by maintaining the free drug concentration in the blood stream at low level. Because the liposomes are preferentially distributed to the tumor tissue, the overall therapeutic index and efficacy of the treatment are improved.

Nanotechnology is a timely topic in pharmaceutical science and there are good reasons for that. *First*, in drug discovery, the solubility of new chemical entities shows historically a declining trend. In fact, poor water solubility has become one of the major problems that limit the systemic drug bioavailability. Nanosizing has been used to improve the rate of dissolution, and sometimes this method results in improved drug absorption after oral dosing [4]. *Second*, some target sites of drug treatment are difficult to reach. For example, narrow therapeutic index is a problem in anticancer drug treatment, as these drugs have serious adverse effects. If the doses could be reduced in association with improved drug delivery to the tumors, the extent of side effects would also be reduced. Other difficult targets include the brain and the posterior segment of the eye. *Third*, emerging biotechnological pharmacologically active compounds require nanotechnology-based drug delivery. This is because biotechnological drugs, such as peptides, proteins, oligonucleotides, and DNA, have large molecular weight, and they are not able to distribute in the body as small molecules do. The task is further complicated by the susceptibility of these drugs to enzymatic degradation by peptidases and nucleases. In many cases, the target sites are intracellular (e.g., siRNA, transcription factors, and DNA), and the delivery system should protect the drug from these enzymes and shuttle it to intracellular target sites [5]. In this case, the goal is to improve bioavailability in the cellular target organelles of the diseased tissue. In fact, the progress of these therapeutic approaches depends on the possibility to efficiently deliver these compounds to the target sites. In the case of gene medicines, it is straightforward to find the drug (i.e., DNA or siRNA sequence) after biological basic research on the mechanisms of the disease. However, drug delivery becomes the limiting factor.

Nanotechnologists are constructing new smart materials at an increasing pace. It is, however, important to realize that only a small part of the invented materials is applicable in medicine due to the limiting issues of toxicology and materials safety. Nanotoxicology has gained a lot of publicity, but the most serious safety issues are related to the technical use of nanoparticles and to the unintentional exposure to these materials [6]. Nanopharmaceuticals must be tested in preclinical toxicological tests and in clinical studies. Therefore, these products are not expected to have more

safety problems than regular pharmaceutical products after their acceptance for the clinical use.

In this chapter, we describe different nanotechnological systems for drug delivery and their potential applications for improved systemic and local bioavailability. The chapter is an overview that hopefully guides the interested reader to the more detailed texts on this issue.

22.2 Nanotechnological Systems in Drug Delivery

Nanotechnological systems have a particle size in the nanometer scale (1–1000 nm). In general, these systems can be divided into top-to-down and bottom-to-top systems. The first category includes nanosystems that are made by processing larger particles to smaller units. For example, drug nanocrystals are produced by milling larger particles to nanosize [4]. Bottom-to-top systems are constructed from molecules that adhere to each other thereby forming associated structures in the nanoscale. These systems are based on the principles of self-assembly and they have particular advantage of spontaneous formation and functional versatility.

22.2.1 Classification of the Technologies

The following paragraphs briefly describe the main categories of nanostructures that are relevant in drug delivery. The main points are compiled in Table 22.1.

22.2.1.1 Nanocrystals

Nanocrystals are small drug particles, usually about 100 nm in diameter, which are produced by milling drug particles in the presence of surfactant. Eventually, the

Table 22.1 Classification of nanotechnological drug delivery systems.

Class	Approximate size range (nm)	Applications	Clinical status
Nanocrystals	100–200	Dissolution enhancement	Accepted
Dendrimers	5–10	Drug targeting	Experimental
Nanoparticulates			
Liposomal	50–500	Intravenous drug delivery	Accepted
		Localized drug delivery	Experimental
Micelles	10	Drug delivery, solubilization (i.v.)	Accepted
Albumin	130	Intravenous drug delivery	Accepted
Polymeric	100–200	Drug delivery	Experimental
Peptide vesicles	10–100	Drug delivery	Experimental
Targeted nanoparticles	10–200	Site-specific drug delivery	Experimental
Nucleic acid complexes	50–200	DNA and siRNA delivery	Experimental

surfactant will cover the surface of the drug nanocrystals [4]. The main use of such particles is in the field of dissolution enhancement. Poorly soluble drugs (BCS class III and IV) show typically very slow dissolution, and, for that reason, they do not dissolve adequately during the passage of the tablet in the small intestine (typical transit time is 3 h). According to the law of Noyes and Whitney that is already more than 100 years old, increased surface area of the powder increases the rate of dissolution. From the bioavailability point of view, the increased dissolution rate is meaningless for most of the class I and class II compounds because their entire dose would dissolve anyway rapidly. In the case of class III and class IV compounds, the rate of drug dissolution can make a great difference. This was shown early in the case of digoxin when the importance of digoxin particle size on bioavailability was demonstrated [7]. There is indeed clear rationale for the use of nanocrystals in oral drug delivery.

22.2.1.2 **Self-Assembling Nanoparticulates**

Self-assembled nanoparticulates comprise various kinds of polymeric, peptide-based, and lipoidal systems. The rationale for their pharmaceutical use is to incorporate the drug into the system and thereby modify its solubility or delivery.

Self-assembled delivery systems form spontaneously in water solution when the structural component is added to water. Amphiphilic compounds form such structures and the features of the resulting nanostructures depend on the molecular properties of the amphiphile. Typically, these systems have a critical association concentration (e.g., critical micelle concentration (CMC)). Below this concentration, the compound exists as individual molecules (monomers) and orient toward the surface of water. Above the critical concentration self-associated structures are formed. The relative sizes of the polar head group and nonpolar chains determine the critical association concentration and morphology of the resulting structures. Micelles are formed by surfactants that have relatively large head groups compared to their nonpolar ends. Lamellar phases (i.e., liposomes) are formed when the both ends are of similar size. Tubular hexagonal phases result from the self-association of the molecules with small polar group relative to the wide hydrophobic end of the molecule. Lipid-like amphiphilic molecules can adopt various 3D structural orientations, which have been summarized earlier.

In addition to lipid-like molecules, polymers can also form self-assembling particulates [8]. As expected, the amphiphilic polymers do form polymeric micelles with polar part orienting towards the surface of the particle and the hydrophobic part orienting towards the core of the particle. Also, in this case, different complicated self-assembled structures can be tailored by using block copolymers with regular blocks of monomer units; but, only the simpler ones have been investigated so far in the context of drug delivery.

Biological molecules do show regularity at the level that is not obtained with synthetic polymers. Protein folding is a perfect example, but it is not yet well understood. Therefore, protein-based 3D drug delivery systems are difficult to design. However, small peptides with amphiphilic structure (e.g., V_6K, where six valines form hydrophobic part and lysine is the hydrophilic end group) can assemble

to form vesicles or tubes [9]. Peptides with regular repeating units may also self-assemble to fiber structures [10]. DNA, RNA, and oligonucleotides are versatile materials due to their ability to exactly recognize the complimentary sequences. Nanotechnologists have tailored even smiley-shaped DNA nanostructures. The self-assembling peptides and DNA-based nanostructures have only sparsely been explored in the field of drug delivery.

The size of the self-assembled amphiphilic structures varies from about 10 nm to a micron scale. Micelles are smaller than the vesicles, because they do not have internal aqueous core, and the wall is monolayer, not bilayer like in the liposomes.

22.2.1.3 **Processed Nanoparticulates**

Polymeric nanoparticles and nanocapsules are usually based on processing [11]. The processing may involve dispersion of the polymer solution in the dispersed organic phase in the continuous water phase and subsequent precipitation of the polymer by changes in the solvent composition. Nanoparticulates can be produced also by spraying techniques, including electrospraying [12]. The most commonly used materials include polylactide and polyglycolide and their copolymers. They are FDA-approved biodegradable materials with safe degradation products.

22.2.1.4 **Single-Molecule-Based Nanocarriers**

In the aforementioned cases, each particle contains typically at least thousands of molecules that are bound to each other by secondary chemical forces. The progress of chemistry since 1990s has provided a new class of materials, the dendrimers [13]. They are dendritic structures that are synthesized in generations around a core molecule that serves as a starting point. Large dendrimers may have even 10 generations, which means that it has 10 layers of dendritic structures in onion-like conformation. The simple dendrimers have spherical shape and they are much more monodisperse than most other synthetic polymers. Dendrimers are interesting materials for drug delivery purposes. They have been used for DNA and oligonucleotide delivery [14], but the dendritic shape as such does not provide improved properties compared to similar chemistry (poly-L-lysine) but linear or branched shape [15].

22.2.2
Pharmaceutical Properties of Nanotechnological Formulations

22.2.2.1 **Drug-Loading Capacity**

Drug-loading capacity of the system defines the dose of drug per individual particle. In principle, solid drug nanoparticle has the maximal loading capacity because it is nearly 100% drug. Drug nanocrystals have been mostly used for dissolution enhancement. In this context, the surface area per milligram of drug is the key parameter and this is defined by the particle size. For intracellular drug delivery and targeting, solid nanoparticles of pure drug have rarely been used. Abraxane is a paclitaxel product that is administered intravenously [16]. It contains drug crystals associated with albumin, but this is not a delivery system for intracellular drug

delivery, rather an approach to improve the drug dissolution after injection. The size of individual albumin molecules is 4–6 nm, whereas the paclitaxel-containing albumin nanoparticles are about 130 nm in diameter.

Vesicular systems can encapsulate both hydrophilic and hydrophobic drugs. They are localized either in the membrane (lipophilic) or in the aqueous core (hydrophilic) of the delivery system. In general, the micellar systems (surfactant or polymer based) are useful for the loading of hydrophobic drugs. Importantly, the size of the vesicular systems, such as liposomes, is in the range of 100–500 nm, and micellar systems are in the range of 5–10 nm. In terms of volume and drug-loading capacity per particle, this is a huge difference because the particle volume is proportional to the $(\text{radius})^3$ of the particle. Tenfold difference in the radius means thousandfold difference in the volume. Therefore, drug dose that is delivered per particle upon endocytosis is much bigger with larger particles than with the small micellar structures. However, the smaller micellar particles more easily gain access to the tissues because they can more easily extravasate from the blood circulation to the tissues.

Drug loading into nanoparticles can also depend on charge. For example, efficient loading of negatively charged nucleic acid-based drugs into the positively charged micelles, liposomes, or dissolved polymers is achieved by electrostatic binding [17]. This results in the formation of a new nanoparticle complex and disruption of the original liposomal or micellar structure.

22.2.2.2 **Processing**

The processing of the nanoparticulate structures is out of the scope of this chapter. It is important, however, to notice that in some cases the nanoparticulates may form spontaneously and drug is partitioned to the nanoparticulate structure by simple mixing. However, loading of hydrophilic drugs into liposomes requires reverse-phase evaporation or other processing methods, and likewise drug encapsulation into the polymeric nanoparticles often requires special processing. These factors depend on the drug and carrier properties and they are designed case by case.

22.2.2.3 **Biological Stability**

Biological stability of nanoparticles is an important determinant of their applications. The stability depends on the nanoparticle class.

In the case of self-assembling nanoparticulates, the critical association concentration affects their behavior. If the critical concentration of the amphiphile is high, the concentration may decrease after intravenous injection below the critical value thereby resulting in the dissociation of the particles [18]. This is the reason why surfactant-based micelles, with CMC in the millimolar range, are not useful as intravenous drug targeting vehicles as they do not retain their integrity long enough to enable improved target site bioavailability. Such micelles are, however, useful in solubilization of the drug to avoid the drug-induced irritation. If micellar drug solution is applied to extravascular site with limited dilution upon administration, the self-associated micelles may remain intact and enable localized drug delivery (e.g., in the skin).

Phospholipids have low CMC values in the nanomolar range. Therefore, this class of nanoparticulates is more suitable for intravenous administration, because the

phospholipid concentration remains above CMC even after i.v. injection. Thus, liposomal products are successful in the intravenous delivery of anticancer agents and the liposomes do not disintegrate in the blood circulation. Owing to their integrity, normal phospholipid liposomes are too stable for transdermal drug delivery. After their application on the skin, the liposomes stay on the skin surface and do not facilitate drug delivery across the skin. Only special classes of lipids, fusogenic hexagonal phase forming lipids such as DOPE or lysophospholipids, are able to fuse to the skin lipids and facilitate transdermal drug delivery by permeabilizing the skin barrier [19].

Polymeric micelles have critical association concentrations that can be modified by the polymer structures. The critical concentrations are lower than those in the case of surfactant-based micelles enabling the stability of the polymeric micelles in the circulation [18]. Polymeric micelles have been used successfully for drug targeting intravenously.

Typically, the processed polymeric nanoparticles are stable in the blood stream and elsewhere in the body [20]. Their degradation and drug release are determined by the chemical degradation rate of the polymer such as poly(lactide) and poly(glycolide). Such nanoparticles can be used for site-specific intracellular drug delivery if they have targeting moieties on the surface.

22.3 Delivery via Nanotechnologies

22.3.1 Delivery Aspects at Cellular Level

In principle, the nanotechnological systems could facilitate the overcoming of the biological barriers at tissue and cell levels.

Nanoparticulates may get across the *tissue barriers* depending on the type of the delivery system and tissue boundary (Figure 22.1). The size of the nanoparticulates is relatively large compared to the size of small molecular weight drugs. In tight epithelial and endothelial tissue linings, the size of the paracellular penetration pathway is about 2–3 nm [21]. This is clearly smaller than the size of the nanocarriers (10–1000 nm). Only some metallic nanoparticles, such as gold nanoparticles, can be in the size range that should allow paracellular penetration across tight epithelia. Current nanosystems do not fuse with the cell membranes either, and therefore, the only possible mechanism for crossing the tight epithelial and endothelial barriers is by transcytosis (Figure 22.1a) [22]. This process requires specific docking on the cell surface receptor, subsequent transcytosis, and release from the basolateral side of the membrane. Without specific cell biological mechanisms, the nanoparticulate systems are not useful in drug delivery across tight junction containing membranes, such as small intestinal wall, cornea, blood–brain barrier, and nasal epithelium.

There are several tissue boundaries in the body with more leaky character. For example, the vascular endothelium in the liver and spleen allows passage of even

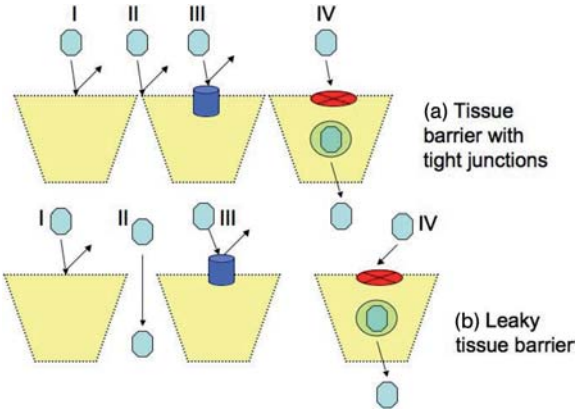

Figure 22.1 Nanoparticulate-mediated drug delivery across the tight (a) and leaky (b) tissue barriers. In the case of nanocrystals and drug solubilization systems, the dissolution rate is increased and free drug permeates across the tissue barrier with the appropriate mechanism. The nanoparticulate-bound drug behaves differently. The nanoparticulates are too large for the direct transcellular permeation across the cells' walls (I), for the paracellular diffusion through the tight tissue boundaries (a-II), and for the active transport by membrane transporters (III). The tight tissue boundaries include the intestinal wall, skin, cornea, conjunctiva, blood–brain barrier, placental barrier, and blood–retina barrier. In leaky tissue boundaries (e.g. fenestrated endothelia, sinusoidal vessels, and tissue boundaries disrupted by the disease states such as inflammation), the nanoparticulates may pass the barrier by paracellular permeation. In specific cases, receptor-mediated transcytosis may be possible (IV), but in this case specific recognition and transport mechanisms must be utilized.

micrometer-scale particles, and tumor vasculature can be extravasated by nanoparticulates of 200 nm and smaller (Figure 22.1b). In addition, many localized tissues such as vitreous in the eye or coronary vessel walls allow nanoparticulate diffusion after local administration.

In the case of *intracellular targeting* of the nanoparticulates, it is important to consider the intracellular target organelle, nanoparticle type, and characteristics of the cell (Figure 22.2). Nanoparticulates are simply too large to diffuse across cell membranes. They may, however, enter the cells via endocytic mechanisms [23]. These mechanisms involve binding of the nanoparticles to the cell surface and subsequent invagination of the cell membrane and formation of the endosomal vesicle (Figures 22.1 and 22.2). The size of the nanoparticle is important in this process. Only a few specialized professional phagocytic cells, such as macrophages and retinal pigment epithelium, are able to engulf large micrometer-sized particles [24]. Most cell types can endocytose only nanoparticles that are less than 200 nm in diameter. Endocytosis can be a receptor-mediated specific process, a nonspecific fluid-phase process, or an adherence-based process.

The endosomes can be further divided into clathrin-coated pits and caveolae [25]. The former is acidified and they deliver their contents to the lysosomes. Depending on the case, lysosomal delivery can be beneficial or vice versa. Nanosystems can be designed to release the drug resulting from the action of specific lysosomal enzymatic

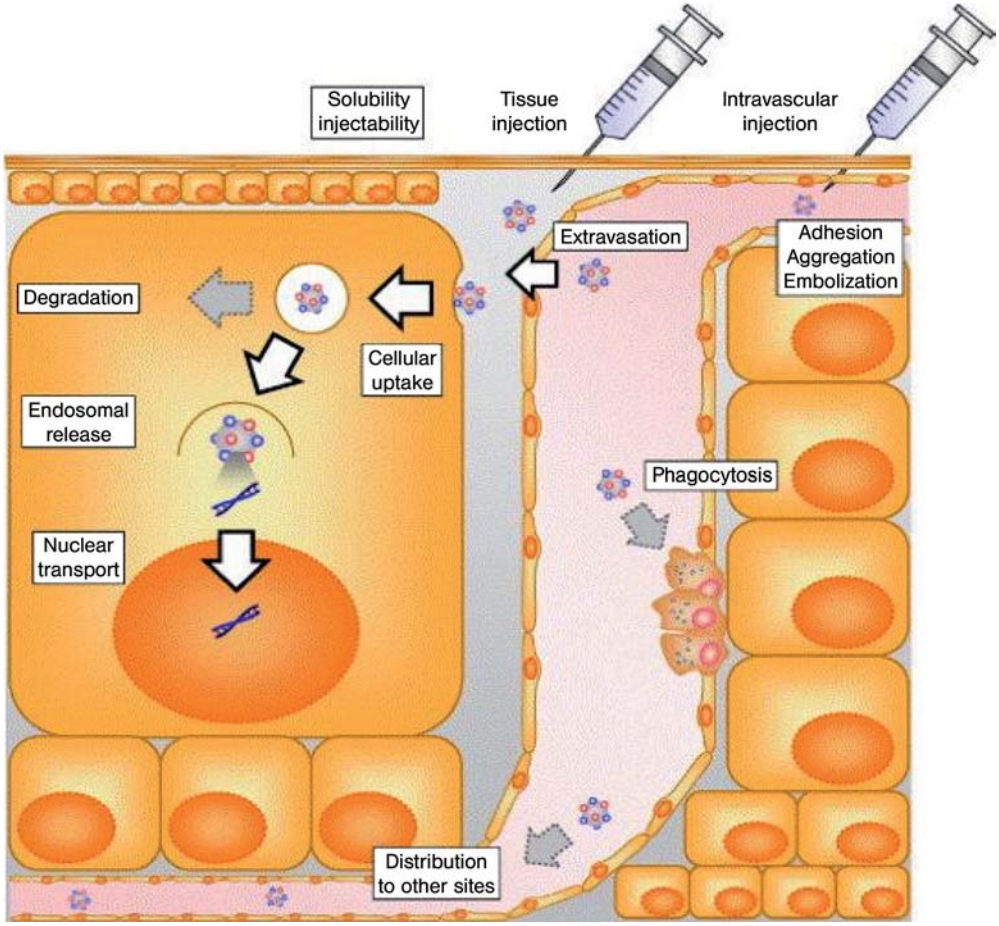

Figure 22.2 Fates of nanoparticulates after i.v. injection and local administration to the target tissue. After i.v. injection, the particles should avoid aggregation and embolization to avoid entrapment into the lung capillaries. Kuppfer cells of the liver phagocytose major part of the nanoparticulate dose (illustrated on the right), but this may be slowed down by nanoparticulate surface modifications. In the target tissue (on the left), the nanosystem should enter the vascular endothelial cells, if they are the target cells, like in the case of neovascularization. Otherwise, they should escape from the vasculature, dock to the target cell surface, and internalize into the target cells by endocytosis. Depending on the case, the intracellular target may be cytosolic, lysosomal, nuclear, or elsewhere. With the exception of the lysosomal targets, the nanoparticulates should escape from the endosomes and enter the cytoplasm (e.g., siRNA) or nucleus (e.g., DNA). The nanoparticulates may be injected or given directly to the tissue of interest. Then, the barriers of Kupffer cells and vascular walls are avoided. The issues of cellular uptake and intracellular kinetics are relevant also in this case. This figure is taken from Ref. [43].

cleavage. In this case, the drug as such should be resistant to the acidic lysosomal pH and the catalytic activity in this organelle. In many cases, the lysosomal delivery should be avoided, and the drug ought to escape from the endosomes to the cytoplasm before entering the lysosomes. The escape can be facilitated with special

design of the nanoparticulates. For example, the acidification in the endosomes (from pH 7.4 to 5.5) and reducing environment can be utilized as triggering mechanisms that allow nanoparticulate activation and endosomal escape [26]. Membrane-active peptides, pH-sensitive lipids, and reducing polymer structures with disulfide bridges have been utilized as nanoparticulate components for this purpose.

Cytoplasm is an important target for siRNA and antisense oligonucleotides whereas transcription factors and plasmid DNA should be delivered into the nucleus (Figure 22.2). Cytoplasm is a highly viscous medium where passive diffusion of nanoparticles, and macromolecules are very slow [27]. It is very appealing to search for the means by which the nanoparticulate transport in the cytoplasm and delivery into the nucleus can be maximized [28]. Specific nuclear localizing peptides have been attached to the nanoparticulates for the nuclear delivery but their efficacy is still not adequate [29].

22.3.2
Nanosystems for Improved Oral Drug Bioavailability

The steps in oral drug absorption have been described in detail elsewhere in this book. The preceding discussion about the cellular interactions of the nanoparticulates suggests that the nanoparticles are not physically optimal for drug delivery across the relatively tight intestinal wall (Figure 22.1). Rather, other mechanisms are more viable. *First*, the nanoparticulates can be used to improve drug dissolution especially in the case of BCS class III and class IV compounds. This can be accomplished by making pure drug nanocrystals, as discussed above. Another alternative is to use self-assembling structures, such as self-emulsifying systems, to solubilize the poorly soluble drugs [30]. These techniques have shown some improvement in systemic bioavailability after oral drug administration. *Second*, the retention time of the particles in the intestine can be prolonged by adhering the particles to the gut wall. This approach involves the use of lectin moieties at the particle surface. Lectin binds to carbohydrates on the gut wall and generates higher localized drug concentration next to the intestinal wall thereby increasing drug absorption [31]. *Third*, the transcytosis mechanism can be used [22]. As far as the third approach is concerned, only vitamin B-12 utilizes transcytosis in its absorption [32]; otherwise, this approach has not been successful. It is difficult to obtain high enough permeation through the intestinal wall with this mechanism.

It is important to realize that in the first and second option, the local concentration of the free drug is increased by the nanosystems. The drug may be absorbed by passive diffusion or active transport, but it is not specifically carried by the nanoparticulates.

22.3.3
Nanosystems for Improved Local Drug Bioavailability

Improved local tissue-specific bioavailability can be reached either by systemic administration intravenously or by localized direct injection in the vicinity of the target tissue (Figure 22.2).

The local administration of the nanoparticles can be used either to increase the retention at the site of administration or to control the drug release. Intravitreal drug administration into the eye is an interesting example. If a small molecular weight drug is administered in the form of water solution to the vitreous, the concentration decreases rapidly, because the drug diffuses to the systemic circulation across the blood–retina barrier or via the anterior chamber [33]. Therefore, the drug concentration profile in the vitreous shows rapid decline after initial high concentration peak. When the drug is administered in the liposomes, prolonged concentration profile is obtained due to the hindered permeation of the liposomes across the barriers. Thus, nanoparticulates modulate the concentration profile of the free drug in the vitreous by removing the high-peak concentration and by prolonging the retention in the vitreous. Similar principles are applicable to many other sites of localized injections: nanoparticulates increase drug retention at the site of injection and modify the concentration profile toward controlled release profile (e.g., at the surgical sites).

If cell-specific targeting is sought, the nanoparticle should bear appropriate ligands on its surface to recognize the cell of interest. This was exemplified by recent study with nanoparticulates that recognize CD44 receptors responsible for internalization of hyaluronic acid-coated DNA complexes [34]. Lipid–DNA nanoparticulates were also able to transfect corneal epithelial cell surface that released the encoded protein to the basolateral side of the epithelium [35]. As such, the protein would not diffuse through the tight junctions on the corneal epithelial surface (Figure 22.3). This

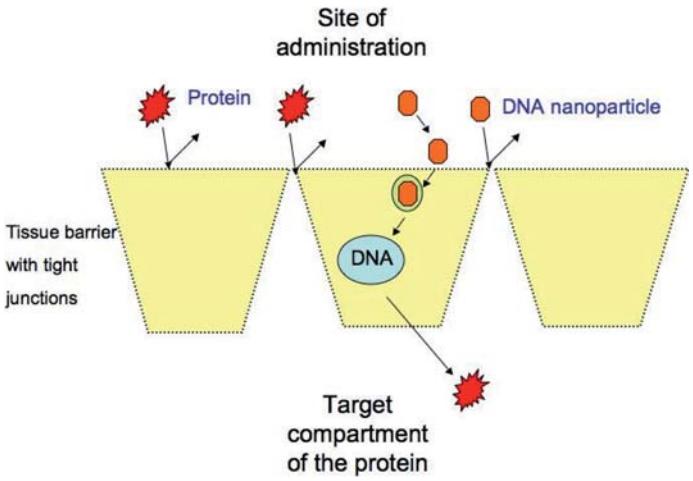

Figure 22.3 Epithelial cells can be transfected to serve as secreting platform of the therapeutic protein. Protein as such does not permeate across the tissue boundary. The nanoparticulates that encode the protein also cannot permeate the epithelial barrier, but they can internalize to the outer most all layer of the epithelium. These cells are transfected and subsequently secrete the therapeutic protein to the basolateral target compartment. This principle of circumventing the apical tight junctions was demonstrated recently in the eye [35]. DNA nanoparticulates were administered to the tear side of the cornea and the transgene product, SEAP, was secreted to the anterior chamber of the eye.

method circumvents the tight epithelial barrier by transfecting the surface cells to secrete the therapeutic protein to the other side of the barrier.

The systemic i.v. administration can be used for targeted localized drug delivery with nanosystems (Figure 22.2). This is particularly appealing in the case of cancer medications, because these drugs cause serious adverse effects at therapeutic doses [36]. In addition, the metastases are difficult to treat with local injections. Therefore, most nanoparticulate studies dealing with systemic administration are directed to the cancer treatments. This approach is not an easy one, because a major fraction of the nanoparticulate dose is captured by Kuppfer cells in the liver (Figure 22.2). The half-life of the particles in the circulation is increased by the "stealth" coating of the particles. Polyethylene glycol (PEG) moieties on the nanoparticulate (polymeric micelle, liposome, polymeric nanoparticle, and DNA complexes) surface prevent the adherence of plasma proteins on the surface. Therefore, the Kuppfer cells do not recognize these particles and long retention times in plasma (1–2 days) are achieved. Eventually, a large fraction of these particles ends up in the liver as well, albeit at a slower rate. The particles must extravasate from the blood circulation, and PEG-coated nanosystems have a higher probability of extravasation in the tumors due to their leaky vasculature. Thereafter, the cell-level issues (see above) determine the fate and therapeutic efficacy of the nanoparticulate systems (Figure 22.2).

Systemic administration of drugs in the form of nanoparticulates intravenously has been widely studied. Currently, there are some liposomal anticancer and antifungal medications in clinical use. These products show relative increase in drug bioavailability in the target sites. They are not, however, active targeting systems with recognition ligands on the surface.

22.4
Key Issues and Future Prospects

The delivery of drugs to difficult-to-reach targets, such as brain and tumors, remains a major challenge. Biotechnological drugs, such as gene medicines and some proteins, need improved nanotechnological formulations for their intracellular delivery. Design of such delivery systems requires interplay between the delivery system and the biological machinery to reach the therapeutic goals. Viruses have evolved to use the cells for their own purposes and in doing so they deliver their genetic cargo into the target cells in elegant ways. Successful functional mimicking of biological self-assembling nanostructures is essential to the progress in this field.

Another important future issue in the field of drug delivery nanotechnology is the use of smart responsive materials and small devices based on such materials. The materials may take into account the human physiology by releasing the drug at needed rate at the right time. These systems are also applicable in the design, fabrication, and use of advanced nanobiosystems for cellular integration and tissue engineering. The opportunities exist for the use of functional biomaterials and therapeutic drug targeting and delivery systems that combine both biological and

engineering aspects of drug delivery [37], like in the case of the off-water fabrication and surface modification device consisting of asymmetric 3D SU-8 microparticles for drug delivery and tissue engineering [38].

Nanoparticulate systems can be designed to bear multiple components and functions, including activation at the target site or by external signal (e.g., light or magnetic field) [39, 40]. Such future trends would also involve the use of new types of nanomaterials, such as carbon nanotubes [41] and functionalized metallic nanoparticles [42]. Taking the safety issues into account is an imperative, as many nanomaterials for the technical purposes do not meet the criteria that are required for pharmaceutical materials. Anyway, it is likely that the current research investments in the fields of nanomedicine and pharmaceutical nanotechnology will lead to improved drug therapies by improving the drug bioavailability at the target site.

References

1 Rowland, M. and Tozer, T. (1995) *In Clinical Pharmacokinetics, Concepts and Applications*, Lippincott, USA.

2 Turunen, M.P., Hiltunen, M.O., Ruponen, M., Virkamäki, L., Szoka, F.C., Urtti, A. and Ylä-Herttuala, S. (1999) Efficient adventitial gene delivery to rabbit carotid artery with cationic polymer–plasmid complexes. *Gene Therapy*, **6**, 6–11.

3 Allen, T.M., Cheng, W.W.K., Hare, J.I. and Laginha, K.M. (2006) Pharmacokinetics and pharmacodynamics of lipidic nano-particles in cancer. *Anti-Cancer Agents in Medicinal Chemistry*, **6**, 513–523.

4 Merisko-Liversidge, E., Liversidge, G.C. and Cooper, E.R. (2003) Nanosizing: a formulation approach for poorly-water-soluble compounds. *European Journal of Pharmaceutical Sciences*, **18**, 113–120.

5 Liu, F. and Huang, L. (2002) Development of non-viral vectors for systemic gene delivery. *Journal of Controlled Release*, **78**, 259–266.

6 Stern, S.T. and McNeil, S.E. (2008) Nanotechnology safety concerns revisited. *Toxicological Sciences*, **101**, 4–21.

7 Shaw, T.R.D. and Carless, J.E. (1974) The effect of particle size on the absorption of digoxin. *European Journal of Clinical Pharmacology*, **7**, 269–273.

8 Kataoka, K., Harada, A. and Nagasaki, Y. (2001) Block copolymer micelles for drug delivery: design, characterization and biological significance. *Advanced Drug Delivery Reviews*, **47**, 113–131.

9 van Hell, A.J., Costa, C.I.C.A., Flesch, F.M., Sutter, M., Jiskoot, W., Crommelin, D.J.A., Hennink, W.E. and Mastrobattista, E. (2007) Self-assembly of recombinant amphiphilic oligopeptides into vesicles. *Biomacromolecules*, **8**, 2753–2761.

10 Hosseinkhani, H., Hosseinkhani, M. and Kobayashi, H. (2006) Design of tissue-engineered nanoscaffold through self-assembly of peptide amphiphile. *Journal of Bioactive and Compatible Polymers*, **21**, 277–296.

11 Galindo-Rodríguez, S.A., Puel, F., Briançon, S., Allémann, E., Doelker, E. and Fessi, H. (2005) Comparative scale-up of three methods for producing ibuprofen-loaded nanoparticles. *European Journal of Pharmaceutical Sciences*, **25**, 357–367.

12 Jaworek, A. (2007) Micro- and nanoparticle production by electrospraying. *Powder Technology*, **176**, 18–35.

13 Liu, M. and Fréchet, J.M.J. (1999) Designing dendrimers for drug delivery.

Pharmaceutical Science & Technology Today, **2**, 393–401.

14 Tang, M.X. and Szoka, F.C. (1997) The influence of polymer structure on the interactions of cationic polymers with DNA and morphology of the resulting complexes. *Gene Therapy*, **4**, 823–832.

15 Männistö, M., Vanderkerken, S., Toncheva, V., Ruponen, M., Elomaa, M., Schacht, E.H. and Urtti, A. (2002) Structure–activity relations of poly(L-lysines): effects of pegylation and molecular shape on physicochemical and biological properties in gene delivery. *Journal of Controlled Release*, **83**, 169–182.

16 Gradishar, W.J. (2006) Albumin-bound paclitaxel: a next-generation taxane. *Expert Opinion on Pharmacotherapy*, **7**, 1041–1053.

17 Hyvönen, Z., Plotniece, A., Reine, I., Checavichus, B., Duburs, G. and Urtti, A. (2000) Novel cationic amphiphilic 1,4-dihydropyridine derivatives for DNA delivery. *Biochimica et Biophysica Acta*, **1509**, 451–466.

18 Torchilin, V.P. (2001) Structure and design of polymeric surfactant-based drug delivery systems. *Journal of Controlled Release*, **73**, 137–172.

19 Kirjavainen, M., Urtti, A., Jääskeläinen, I., Suhonen, T.M., Paronen, P., Valjakka, R., Kiesvaara, J. and Mönkkönen, J. (1996) Interaction of liposomes with human skin *in vitro*: the influence of lipid structure. *Biochimica et Biophysica Acta*, **1304**, 179–189.

20 Stolnik, S., Illum, L. and Davis, S.S. (1995) Long circulating microparticulate drug carriers. *Advanced Drug Delivery Reviews*, **16**, 195–214.

21 Hämäläinen, K.M., Kontturi, K., Murtomäki, L., Auriola, S. and Urtti, A. (1997) Estimation of pore size and porosity of biomembranes from permeability measurements of polyethylene glycols using an effusion-like approach. *Journal of Controlled Release*, **49**, 97–104.

22 Kreuter, J. (2001) Nanoparticulate systems for brain delivery of drugs. *Advanced Drug Delivery Reviews*, **47**, 65–81.

23 Panyam, J. and Labhasetwar, V. (2003) Dynamics of endocytosis and exocytosis of poly(D,L-lactide-*co*-glycolide) nanoparticles in vascular smooth muscle cells. *Pharmaceutical Research*, **20**, 212–220.

24 Tuovinen, L., Ruhanen, E., Kinnarinen, T., Rönkkö, S., Pelkonen, J., Urtti, A., Peltonen, S. and Järvinen, K. (2004) Starch acetate microparticles for drug delivery into retinal pigment epithelium. *Journal of Controlled Release*, **98**, 407–413.

25 Lai, S.K., Hida, K., Man, S.T., Chen, C., Machamer, C., Schroer, T.A. and Hanes, J. (2007) Privileged delivery of polymer nanoparticles to the perinuclear region of live cells via a non-clathrin, non-degradative pathway. *Biomaterials*, **28**, 2876–2884.

26 Jääskeläinen, I., Lappalainen, K., Honkakoski, P. and Urtti, A. (2004) Requirements for delivery of active antisense oligonucleotides into cells via lipid carriers. *Methods in Enzymology*, **387**, 210–230.

27 Lukacs, G.L., Haggie, P., Seksek, O., Lechardeur, D., Freedman, N. and Verkman, A.S. (2000) Size-dependent DNA mobility in cytoplasm and nucleus. *Journal of Biological Chemistry*, **275**, 1625–1629.

28 Eguchi, A., Furusawa, H., Yamamoto, A., Akuta, T., Hasegawa, M., Okahata, Y. and Nakanishi, M. (2005) Optimization of nuclear localization signal for nuclear transport of DNA-encapsulating particle. *Journal of Controlled Release*, **104**, 507–519.

29 van der Aa, M.A.E.M., Koning, G.A., d'Oliveira, C., Oosting, R.S., Wilschut, K.J., Hennink, W.E. and Crommelin, D.J.A. (2005) An NLS peptide covalently linked to linear DNA does not enhance transfection efficiency of cationic polymer based gene delivery systems. *Journal of Gene Medicine*, **7**, 208–217.

30 Pouton, C.W. (2006) Formulation of poorly water-soluble drugs for oral administration: physicochemical and physiological issues and the lipid formulation classification system. *European Journal of Pharmaceutical Sciences*, **29**, 278–287.

31 Gabor, F., Bogner, E., Weissenboeck, A. and Wirth, M. (2004) The lectin–cell interaction and its implications to intestinal lectin-mediated drug delivery. *Advanced Drug Delivery Reviews*, **56**, 459–480.

32 Bose, S., Kalra, S., Yammani, R.R., Ahuja, R. and Seetharam, B. (2007) Plasma membrane delivery, endocytosis and turnover of transcobalamin receptor in polarized human intestinal epithelial cells. *Journal of Physiology*, **581**, 457–466.

33 Barza, M., Stuart, M. and Szoka, F. (1987) Effect of size and lipid composition on the pharmacokinetics of intravitreal liposomes. *Investigative Ophthalmology & Visual Science*, **28**, 893–900.

34 Hornof, M., Fuente, M., Hallikainen, M., Tammi, R. and Urtti, A. (2008) Low molecular weight hyaluronan shielding of DNA/PEI polyplexes facilitates CD44 receptor mediated uptake in human corneal epithelial cells. *Journal of Gene Medicine*, **10**, 70–80.

35 Toropainen, E., Hornof, M., Kaarniranta, K. and Urtti, A. (2007) Corneal epithelium as a platform for secretion of transgene products after transfection with liposomal gene eyedrops. *The Journal of Gene Medicine*, **9**, 208–216.

36 Northfelt, D.W., Martin, F.J., Working, P., Volberding, P.A., Russell, J., Newman, M., Amantea, M.A. and Kaplan, L.D. (1996) Doxorubicin encapsulated in liposomes containing surface-bound polyethylene glycol: pharmacokinetics, tumor localization, and safety in patients with AIDS-related Kaposi's sarcoma. *Journal of Clinical Pharmacology*, **36**, 55–63.

37 Saltzman, M. and Desai, T. (2006) Drug delivery in the BME curricula. *Annals of Biomedical Engineering*, **34**, 270–275.

38 Tao, S.L., Popat, K. and Desai, T.A. (2006) Off-water fabrication and surface modification of asymmetric 3D SU-8 microparticles. *Nature Protocols*, **1**, 3153–3158.

39 Paasonen, L., Laaksonen, T., Johans, C., Yliperttula, M., Kontturi, K. and Urtti, A. (2007) Gold nanoparticles enable selective light induced drug release from liposomes. *Journal of Controlled Release*, **122**, 86–93.

40 Derfus, A.M., Von Maltzahn, G., Harris, T.J., Duza, T., Vecchio, K.S., Ruoslahti, E. and Bhatia, S.N. (2007) Remotely triggered release from magnetic nanoparticles. *Advanced Materials*, **19**, 3932–3936.

41 Kam, N.W.S., O'Connell, M., Wisdom, J.A. and Dai, H. (2005) Carbon nanotubes as multifunctional biological transporters and near-infrared agents for selective cancer cell destruction. *Proceedings of the National Academy of Sciences of the United States of America*, **102**, 11600–11605.

42 West, J.L. and Halas, N.J. (2003) Engineered nanomaterials for biophotonics applications: improving sensing, imaging, and therapeutics. *Annual Review of Biomedical Engineering*, **5**, 285–292.

43 Nishikawa, M., Takakura, Y. and Hashida, M. (2005) Theoretical considerations involving the pharmacokinetics of plasmid DNA. *Advanced Drug Delivery Reviews*, **57**, 675–688.

Index